Diagnostic Imaging

Guidelines 2021

Japan Radiological Society

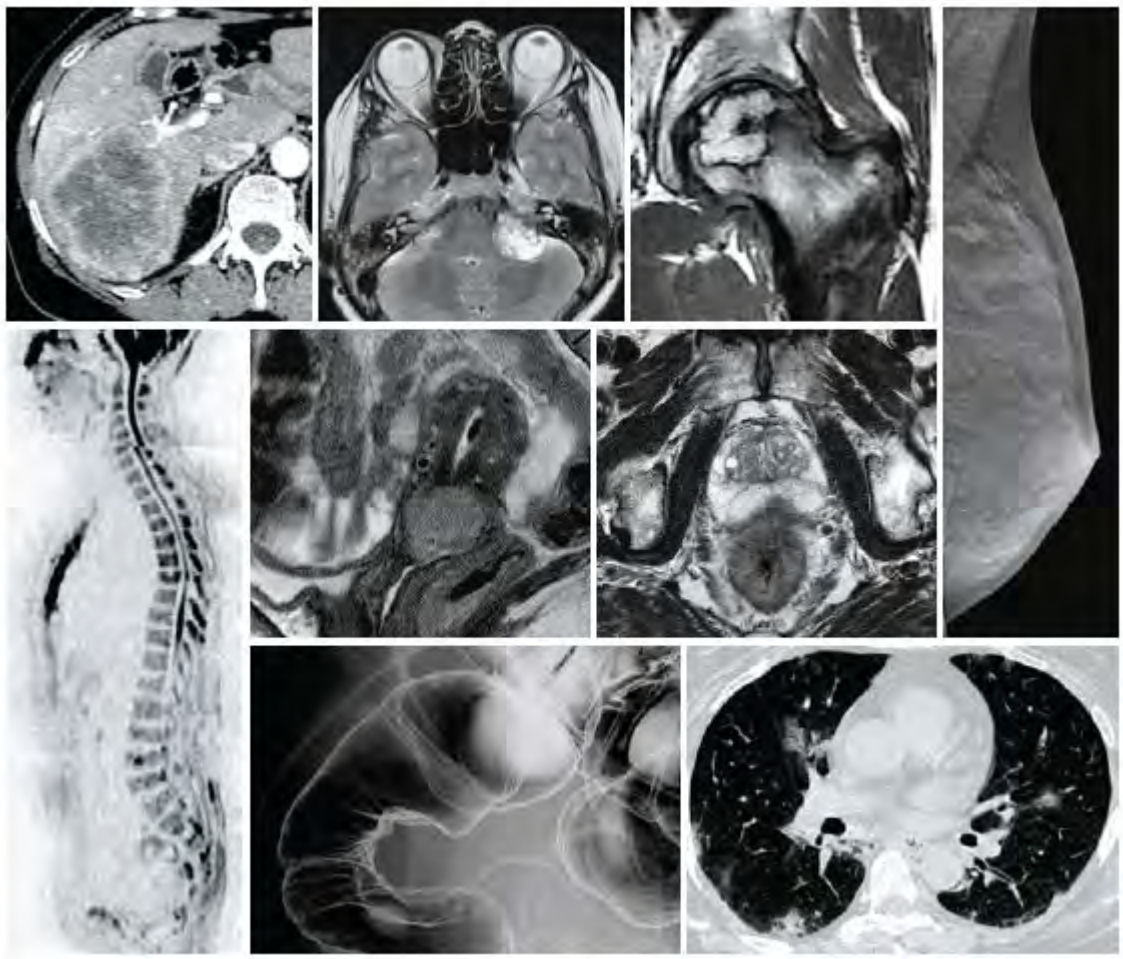

Kanehara & Co., Ltd.

Introduction

The purpose of the diagnostic imaging guidelines is to ensure that medical care that uses diagnostic imaging is justified, optimized, performed effectively and efficiently, grounded in science to the greatest extent possible, and that its outcome is beneficial to the patient. Since the 2013 edition, the guidelines have been provided in the form of clinical questions (CQs) and recommendation grades for the different fields. Progress in diagnostic imaging has been rapid, and immediately after the 2016 edition was published, work on the next revision began. The current revision was made possible through the efforts of all members of the guidelines committee, particularly the committee chair, Dr. Murayama.

The previous belief about medical research was that the level of evidence from randomized, controlled studies was high, whereas the level of evidence from diagnostic imaging tended to be weak because it was based on cross-sectional studies. Moreover, evidence from imaging procedures for which multicenter, randomized, controlled studies could be performed and that used technology that was already widely used (somewhat older) was considered stronger than evidence from clearly superior, cutting-edge, imaging procedures (e.g., in detecting stroke, CT had stronger evidence than diffusion-weighted MRI). In the rapidly advancing field of diagnostic imaging, this left the impression of being removed from the current reality. Consequently, the Grades of Recommendation Assessment, Development and Evaluation (GRADE) system has been incorporated for the first time to bring the guidelines in line with reality.

Although the target audience for the 2016 edition of the guidelines was mainly diagnostic radiology specialists, the target audience of the present guidelines is general practitioners, who order imaging procedures. Japan has the highest number of CT and MRI systems per capita. On the one hand is the view that the government and citizenry understand the importance of diagnostic imaging, and it is therefore widely used. On the other is the criticism that there is often inadequate justification for imaging procedures, as indicated by the fact that CT exposure in Japan is the highest in the world, and that CT needs to be used appropriately. The number of radiologists per capita is smaller in Japan than in other countries, suggesting that diagnostic imaging guidelines aimed at the general practitioner could play a major role in encouraging the appropriate use of imaging procedures.

A questionnaire survey of radiologists at a training facility for radiology specialists on compliance with the 2016 edition of the diagnostic imaging guidelines showed that, although many procedures were performed according to the recommendations, a considerable number of tests that were not recommended were also performed (Fig.; Kumamaru KK et al: Jpn J Radiol 35: 648-659, 2017). It is hoped that these general practitioner-oriented guidelines will be used widely, and that imaging procedures will be used appropriately, leading not only to improvements in the quality of medical care and outcomes for patients, but also appropriate restraints on medical costs.

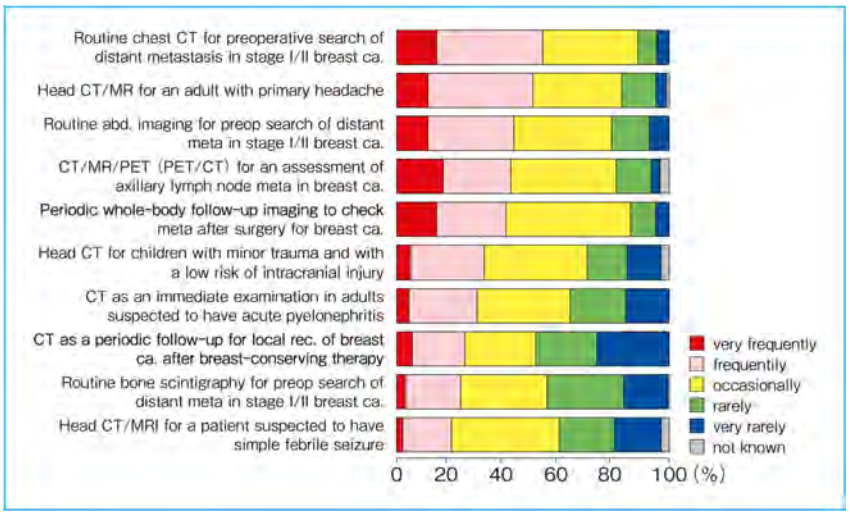

Figure Frequency of non-recommended imaging procedures
(Japan Radiological Society appropriate-use survey, 2017)

September 2021
Shigeki Aoki
President, Japan Radiological Society

Formulation of the 2021 Diagnostic Imaging Guidelines

As with the previous edition (2016 edition), I was appointed a committee chair and engaged in formulating the guidelines. In the 5 years since the previous edition was published, there have been several developments that have had a major impact on the context in which clinical practice guidelines are developed. First, to ensure consistency among the guidelines proposed by the various academic societies, the Japanese Association of Medical Sciences established a clinical practice guidelines management committee, and the societies were required to coordinate their efforts in developing clinical practice guidelines. One aspect of this was disclosing any conflicts of interest on the part of committee members who develop clinical practice guidelines and setting forth a policy stipulating that individuals with commercial conflicts of interests in excess of what is allowed should not serve as a chairperson or member of a guidelines development committee. With regard to the present guidelines, the Japan Radiological Society was notified of the presence or absence of any conflicts of interest held by the individuals who developed the guidelines, and this information was publicly disclosed on the society's website. Another aspect was consolidating the target readership of the clinical practice guidelines. During management committee meetings, the decision was made to target the guidelines at physicians belonging to key academic societies. The previous edition of the diagnostic imaging guidelines was aimed at diagnostic radiology specialists and was developed to serve as a guide for radiologists who provide advice on the usefulness of an imaging procedure when one was requested in the clinical setting. However, the present edition is aimed at physicians affiliated with key academic societies and was developed to serve as a guide when requesting an imaging procedure. In other words, the previous guideline has been changed to information that is more suitable for the medical treatment site.

Moreover, in the previous edition, the recommendation grades took into account evidence-based medicine (EBM) levels based on the MINDS Manual for Guideline Development 2007. For the present edition, a 4-step assessment was performed incorporating the GRADE system (explained in Overview section 2, Preparing the Diagnostic Imaging Guidelines) for the clinical questions (CQs), based on the MINDS Manual for Guideline Development 2017. In the previous edition, grade C1, "procedure recommended, although there is no scientific basis for performing it," was the most common grade, and this was limited to assessments indicating that the procedure could be performed because adequate evidence was lacking. In the present edition, many of these assessments were changed to "weakly recommended" under the GRADE system. In brief, this was because it enabled the assessments to reflect not only the evidence, but also the clinical importance of the procedure.

The many physicians on the subcommittees for the different fields expended considerable effort in developing the present guidelines, starting with the numerous training sessions on the GRADE system held at the headquarters of the Medical Information Distribution Service (MINDS) and extending to development of the background questions (BQs), clinical questions (CQs), and future research questions

(FQs) for each field. In addition, the physicians on the central committee, particularly Dr. Masako Kataoka of Kyoto University and Dr. Yuko Iraha of the University of the Ryukyus, oversaw all aspects of the preparation of the guidelines, from inception to publication. Furthermore, assistance was provided through the publication stage by the physicians who served as advisors, those from other academic societies who provided assessments as outside committee members, and many other physicians. We are deeply grateful to everyone involved.

September 2021

Sadayuki Murayama

Chair, Clinical Practice Guidelines Committee, Japan Radiological Society

Overview of the 2021 Diagnostic Imaging Guidelines

1 Purpose of the guidelines

The purpose of these guidelines is to help ensure that medical care that uses diagnostic imaging is provided effectively, efficiently, and in a manner that benefits the patient in terms of outcomes. The guidelines are based on evidence-based medicine (EBM; i.e., using the latest and best evidence in making diagnostic imaging decisions for the individual patient in a conscientious, clear, and prudent manner) related to diagnostic imaging performed in a variety of fields. Indications for diagnostic imaging and the effectiveness of diagnostic imaging, particularly standard imaging methods, are discussed in detail.

2 Revisions

The diagnostic imaging guidelines were prepared based on EBM methods by the Japanese College of Radiology in 2003 and as a joint project by the Japan Radiological Society and Japanese College of Radiology in 2007 and 2013. Since the 2016 edition ("previous edition" below), the Japan Radiological Society has assumed responsibility for the project and prepared the guidelines based on the MINDS Manual for Guideline Development 2007. The 2021 edition ("present edition" below) represents a major revision that, based on the MINDS Manual for Guideline Development 2017,[2)] incorporates the GRADE system.[3)] The standard imaging methods for each field were updated with the addition of the 3T-MRI and 64-row CT imaging methods. Moreover, in addition to the 9 fields covered in the previous edition, new sections were created for the fields of pediatrics and hematology. Through the previous edition, the target audience was diagnostic imaging specialists. However, the present edition was created with physicians affiliated with key academic societies in mind.

3 Intended users

In developing the present edition, an effort was made to ensure that the content is easy to use for physicians affiliated with the key academic societies, as well as for those who specialize in diagnostic imaging (specialists). It was also intended as a reference for paramedical staff such as radiology technologists.

4 Usage notes

The guidelines strictly represent the guidance considered standard when they were developed. They do not regulate actual medical practice, and they should be used flexibly and in a manner that takes into account the healthcare environment (personnel, experience, facilities, etc.) and the individual patient.

Although the academic society assumes responsibility for the content of the guidelines, responsibility for treatment outcomes lies with those directly providing the medical care. Neither the Japan Radiological Society nor the members of the guidelines development committee bear any responsibility for such outcomes. Use of the guidelines as examination criteria for health insurance or as reference material in medical practice disputes or medical lawsuits would be an obvious deviation from the purpose of clinical practice guidelines.

5 Organization of the present edition and the formulation process

As was mentioned above, the first edition of these guidelines was published in 2003, and revisions have since been made as appropriate. The guidelines, which cover all areas where diagnostic imaging is used, are organized according to 11 fields (14 fields when the digestive organs field is subclassified): neuroradiology, head and neck, chest, cardiovascular, digestive organs (liver, hepatobiliary, pancreas, and gastrointestinal tract), uroradiology, obstetrics and gynecology, breast, musculoskeletal, pediatrics, and hematology. Since the previous edition, the organization responsible for preparing and revising the guidelines has been the Japan Radiological Society, with the society's standing diagnostic imaging guidelines committee actually preparing and revising the guidelines. The guidelines committee consists of central committee members who coordinate and assist in all fields and 14 subcommittees, one for each field.

In implementing the present revision, new committee members were appointed, and the work began in April 2018. At the first guidelines committee meeting (April 2018), the decision was made to prepare the guidelines based on the GRADE system,[3)] which was recommended by the EBM promotion program (MINDS) being implemented by the Japan Council for Quality Health Care. Subsequently, through May 2019, approximately 100 committee members participated in on-demand seminars on preparing clinical practice guidelines organized by MINDS, where they learned about the process of preparing CQs using the GRADE system. At the fourth meeting of the guidelines committee (June 2019), it was decided that each subcommittee would reorganize the 171 CQs of the previous edition by dividing them into CQs, BQs, and FQs and retaining or discarding items or creating new CQs, BQs, and FQs as necessary (see Overview section 2, Developing the diagnostic imaging guidelines). The final CQs, BQs, and FQs for each area were determined by the fifth meeting of the guidelines committee (October 2019). The members of each subcommittee responsible for BQs and FQs began writing, adding articles published through June 2019 to the cited references. However, if an article published after June 2019 provided important findings that were related to a recommendation grade, it was added as appropriate at the discretion of the subcommittee members. The previous edition provided the evidence level proposed by the Oxford EBM Centre for each cited reference. In the present edition, however, because the quality of evidence grade based on the GRADE system[3)] was used (see next section 6), the evidence level for each cited reference was not indicated to avoid confusion. CQ-related literature searches were performed

using the PubMed database, with the assistance of the Japan Medical Library Association. The period searched was January 1, 2016 to June 30, 2019. If the search results were inadequate, the search queries were modified, and additional searches were performed by each subcommittee. The subcommittee members responsible for systematic reviews (SRs) of the CQs selected by each subcommittee participated in an SR workshop for the radiological society (February 2020) organized by Cochrane Japan in order to gain an understanding of the specific tasks involved in SRs. Substantive SR work began in August 2020, when the Japan Medical Library Association finished collecting literature. Between January 2021 and March 2021, the subcommittees met to determine recommendation grades (all meetings held online due to the coronavirus pandemic) and decided on the grade for each CQ. The designated subcommittee members wrote the CQ explanations based on these decisions.

6 Strength of Recommendation, quality of evidence grade (strength), and agreement rate based on the GRADE system

The recommendation strength in the present edition determined the degree to which a procedure was recommended. It was based not only on the scientific evidence presented in the previous edition, but also factors such as the balance between the benefits and harms that result from intervention in routine clinical practice, the consistency of the patients' wishes, and economic considerations. The strength of the evidence was rated on a 4-step scale according to the MINDS Manual for Guideline Development 2017,[2)] with the Clinical Practice Guidelines for Breast cancer 2018 used as a reference (Table 1).[4)] The strength ratings roughly correspond to the recommendation grades of A, B, C1, C2, and D that were used through the previous edition. In the text of the recommendations, the quality of the evidence was indicated according to 4 steps: high, moderate, low, and very low (Table 2). For all of the outcomes specified for each CQ, the recommendation is considered strong in proportion to the strength of the overall evidence. Conversely, the recommendation is considered weak in proportion to the weakness of the evidence. The quality of evidence reflects the extent to which our confidence in an estimate of the effect is adequate to support a particular recommendation.

The reason for indicating the agreement rates (%) in the meetings held to determine recommendations is that a recommendation grade of "weakly recommended," for example, would have different implications if the agreement rate were 100% than if it were 73%. The authors hope that the users will understand that a small number of panel members were leaning toward strongly recommending the procedure or toward weakly recommending not performing it, and to refer to it as useful information in actual diagnostic intervention. In addition, knowing whether the decision was made with a single vote or if agreement was reached after multiple votes enables the user to understand whether there are differences of opinion. In other words, when shared decision-making is practiced in the clinical setting, it would be preferable to share with the patient the fact that there are differences of opinion among specialists before determining the ultimate means of intervention. If agreement was not reached after 3

votes, “agreement not reached” was indicated for the agreement rate. Because the agreement rate indicates where opinions diverged, the authors hope that the users will refer to such information in determining the means of intervention.

Table 1. Strength of Recommendation

Recommendation Strength	Recommendation Text	Recommendation Grade in Previous Edition
1	Strongly recommend performing	A
2	Weakly recommend performing	B, C1
3	Weakly recommend not performing	C2
4	Strongly recommend not performing	D

When both performing and not performing were difficult to recommend, “no recommendation” was indicated.

Table 2. Quality of Evidence Grades (strength) for a recommendation

A: High	We are very confident that the true effect lies close to that of the estimate of the effect.
B: Moderate	We are moderately confident in the effect estimate.
C: Low	Our confidence in the effect estimate is limited.
D: Very Low	We have very little confidence in the effect estimate.

7 Third-party evaluations

In implementing the present revision, third-party evaluations were obtained by sending a draft indicating the standard imaging methods, BQs, CQs, and FQs for each field to the academic societies listed in the third-party evaluation list provided below. For the previous edition, a post-publication third-party evaluation was obtained from MINDS, and a post-publication third-party evaluation will continue to be obtained from MINDS for each revision.

8 Funding sources

The Japan Radiological Society bears the entire cost of preparing and revising these guidelines; no outside funding is provided.

9 Conflicts of interest (COIs)

Publication of these guidelines is approved by the Japan Radiological Society, and the society bears the entire cost of preparing and revising the guidelines. No outside funding whatsoever, such as grants or research funding, has been accepted. In accordance with the society’s COI rules, the conflict-of-

interest status of all committee members involved in preparing the guidelines (members of the central committee and subcommittees and outside committee members) was determined for the previous 3 years. When voting took place in meetings to determine recommendations, the members self-reported any COIs (economic or academic). If a member was disqualified due to a COI, the member abstained from voting on that CQ in an effort to avoid biased opinions. The COI status of each committee member is indicated on the Japan Radiological Society website (http://www.radiology.jp/).

10 Future plans

The guidelines will be published in print by Kanehara & Co., Ltd. and subsequently released on the Japan Radiological Society website.

1) MINDS Clinical Practice Guidelines Selection Working Group, Ed.-in chief: MINDS Manual for Guideline Development 2007. Igaku-Shoin Ltd., 2007.
2) Kojimahara N, et al., Ed.: MINDS Manual for Guideline Development 2017. Japan Council for Quality Health Care, 2017.
3) GRADE: The grading of recommendations assessment, development and evaluation (https://www.gradeworkinggroup.org)
4) The Japanese Breast cancer Society Clinical Practice Guidelines for Breast cancer 2018

Guidelines Development Committee Members

Indicated in Japanese syllabary order for each field

Central committee

Sadayuki Murayama	University of the Ryukyus【Chair】
Yuko Iraha	University of the Ryukyus
Masahiro Okada	Nihon University
Yasushi Kaji	Dokkyo Medical University
Masako Kataoka	Kyoto University
Kanako Kumamaru	Juntendo University
Kei Takase	Tohoku University
Hiromitsu Hayashi	Nippon Medical School
Naoko Mori	Tohoku University
Yohei Morishita	Tohoku University
Yasuyuki Yamashita	Kumamoto University

Overview authors

Noriko Aida	Kanagawa Children's Medical Center
Kazuko Ohno	Kyoto College of Medical Science
Masako Kataoka	Kyoto University
Yasuo Takehara	Nagoya University
Yasuo Nakajima	St.Marianna Univ. School of Medicine
Hiromitsu Hayashi	Nippon Medical School
Yoshiyuki Watanabe	Shiga University of Medical Science

Subcommittees by field

Neuroradiology

Toshinori Hirai	Kumamoto University【Chair】
Kazunari Ishii	Kindai University
Hiroshi Oba	Teikyo University
Mitsunori Kanagaki	Hyogo Prefectural Amagasaki General Medical Center
Kohsuke Kudo	Hokkaido University
Noriko Sato	National Center of Neurology and Psychiatry
Yuki Shinohara	Akita Research Institute of Brain and Blood Vessels
Toshiaki Taoka	Nagoya University
Masayuki Maeda	Mie University
Harushi Mori	Jichi Medical University
Kei Yamada	Kyoto Prefectural University of Medicine
Yoshiyuki Watanabe	Shiga University of Medical Science

Head and Neck

Hiroki Kato	Gifu University【Chair】
Ryutaro Ukisu	Kitasato University
Hiroya Ojiri	The Jikei University School of Medicine
Nobuo Kashiwagi	Osaka University
Naoko Saito	Juntendo University
Akira Baba	The Jikei University School of Medicine
Takashi Hiyama	National Cancer Center Hospital East
Akifumi Fujita	Haga Red Cross Hospital
Daisuke Yunaiyama	Tokyo Medical University Hachioji Medical Center

Chest

Kazuto Ashizawa	Nagasaki University【Chair】
Tae Iwasawa	Kanagawa Cardiovascular and Respiratory Center
Katsunori Oikado	The Cancer Institute Hospital of JFCR
Katsuya Kato	Kawasaki Medical School General Medical Center
Takeshi Kamitani	Kyushu University
Suzushi Kusano	Hitachi Health Care Center
Shuji Sakai	Tokyo Women's Medical University
Hiromitsu Sumikawa	Kinki-Chuo Chest Medical Center
Nobuyuki Tanaka	Yamaguchi-Ube Medical Center
Shin Tsutsui	Nagasaki University
Takahiko Nakazono	Saga University
Hideyuki Hayashi	Isahaya General Hospital
Shin Matsuoka	St. Marianna University School of Medicine
Hidetake Yabuuchi	Kyushu University

Cardiovascular

Norihiko Yoshimura	Niigata City General Hospital【Chair】
Masaki Ishida	Mie University
Daisuke Utsunomiya	Yokohama City University
Hideki Ota	Tohoku University
Seitaro Oda	Kumamoto University
Kakuya Kitagawa	Mie University
Kido Masafumi	Kumamoto University
Akira Kurata	Shikoku Cancer Center
Eijun Sueyoshi	Nagasaki University
Fuminari Tatsugami	Hiroshima University
Ryoichi Tanaka	Iwate Medical University
Yuki Tanabe	Ehime University
Seiji Tomiguchi	Japanese Red Cross Society Kumamoto Health Care Centaer
Yoshitake Yamada	Keio University
Kenichi Yokoyama	Kyorin University
Kunihiro Yoshioka	Iwate Medical University

Digestive organs: Liver

Utaroh Motosugi	Kofu-Kyoritsu Hospital【Chair】
Masaaki Akahane	International University of Health and Welfare
Shintaro Ichikawa	Hamamatsu University School of Medicine
Tomoaki Ichikawa	Gunma University
Kazuhiko Ueda	The Cancer Institute Hospital of JFCR
Hiromitsu Onishi	Osaka University
Satoshi Kobayashi	Kanazawa University
Tomoko Hyodo	Kindai University
Masakazu Hirakawa	Kyushu University Beppu Hospital
Satoshi Funayama	University of Yamanashi
Masatoshi Hori	Kobe University
Hiroyuki Morisaka	University of Yamanashi
Akira Yamada	Shinshu University
Takeshi Yoshikawa	Hyogo Cancer Center

Digestive organs: Hepatobiliary

Satoshi Goshima	Hamamatsu University School of Medicine【Chair】
Azusa Kitao	Kanazawa University
Hiroshi Kondo	Teikyo University
Katsuhiro Sano	Juntendo University
Keitaro Sofue	Kobe University
Masakatsu Tsurusaki	Kindai University
Tatsuyuki Tonan	Kurume University
Yuko Nakamura	Hiroshima University
Akihiro Nishie	Kyushu University
Hiroki Haradome	Kitasato University
Atsushi Higaki	Kawasaki Medical School
Yasunari Fujinaga	Shinshu University
Norihide Yoneda	Kanazawa University
Kengo Yoshimitsu	Fukuoka University

Digestive organs: Pancreas

Hiroyuki Irie	Saga University【Chair】
Kousei Ishigami	Kyushu University
Dai Inoue	Kanazawa University
Nakamura Shinichi	Amakusa Medical Center
Shunro Matsumoto	Almeida Memorial Hospital
Haruo Watanabe	Chuno Kosei Hospital

Digestive organs: Gastrointestinal

Daisuke Tsurumaru	Kyushu University【Chair】
Masanori Imuta	Kumamoto University
Narumi Taguchi	Tamana Central Hospital
Yusuke Nishimuta	Kyushu Cancer Center
Mototaka Miyake	National Cancer Center Hospital

Obstetrics / Gynecology

Yumiko Oishi Tanaka	Cancer Institute Hospital of Japanese Foundation for Cancer Research【Chair】
Mina Asatani	Niigata Cancer Center Hospital
Yoshiko Ueno	Kobe University
Yuka Okajima	
Yuki Kamishima	Medical Imaging Sakae
Satomi Kitai	The Jikei University School of Medicine
Eito Kozawa	Saitama Medical University
Junko Takahama	Higashiosaka City Medical Center
Mayumi Takeuchi	Tokushima University
Megumi Takewa	Nara Prefecture Seiwa Medical Center
Ayako Tamura	Tokyo-Kita Medical Center
Takahiro Tsuboyama	Osaka University
Yuji Nakamoto	Kyoto University
Shinya Fujii	Tottori University
Yukiko Honda	Hiroshima University
Kenji Matsuzaki	Tokushima Bunri University
Tomoko Manabe	Ito Municipal Hospital

Uroradiology

Satoru Takahashi	Kobe University【Chair】
Yuki Arita	Keio University
Hirotoshi Ito	Kajiicho Medical Imaging Center
Yoshimitsu Ohgiya	Showa University
Kazuhiro Kitajima	Hyogo College of Medicine
Tatsuya Gomi	Toho University Ohashi Medical Center
Hiroshi Juri	Osaka Medical and Pharmaceutical University
Masahiro Jinzaki	Keio University
Hiroshi Shinmoto	National Defense Medical College
Mitsuru Takeuchi	Radiolonet Tokai
Nobuyuki Takeyama	Showa University Fujigaoka Hospital
Tsutomu Tamada	Kawasaki Medical School
Go Nakai	Osaka Medical and Pharmaceutical University
Atsushi Nakamoto	Osaka University
Yoshihiko Fukukura	Kagoshima University
Yukiko Honda	Hiroshima University
Nagaaki Marugami	Nara Medical University
Jiro Munechika	Showa University
Kaori Yamada	Japanese Red Cross Society Kyoto Daiichi Hospital
Akira Yamamoto	Kawasaki Medical School
Kotaro Yoshida	Kanazawa University
Rika Yoshida	Shimane University
Takeshi Yoshizako	Shimane University

Breast

Ichiro Isomoto	St. Francis Hospital【Chair】
Setsuko Ishihara	Okayama Saiseikai General Hospital
Mari Kikuchi	Cancer Institute Hospital of Japanese Foundation for Cancer Research
Kazunori Kubota	Dokkyo Medical University Saitama Medical Center
Mariko Goto	Kyoto Prefectural University of Medicine
Hiroko Satake	Nagoya University
Misaki Shiraiwa	Kagawa Prefectural Central Hospital
Hiroshi Nakahara	Sagara Hospital Miyazaki
Ritsuko Fujimitsu	Itoshima Medical Association Hospital
Satoshi Honda	Tokyo Metropolitan Toshima Hospital
Shuichi Monzawa	Shinko Hospital
Sachiko Yuen	Shinko Hospital

Musculoskeletal

Takatoshi Aoki	University of Occupational and Environmental Health【Chair】
Nozomi Oki	Nagasaki University
Shuji Nagata	Kurume University
Tamotsu Kamishima	Hokkaido University
Yasuhiro Kawahara	Sasebo Kyosai Hospital
Kaoru Kitsukawa	St. Marianna University
Shoichiro Takao	Tokushima University
Waka Nakata	Jichi Children's Medical Center Tochigi
Katsuyuki Nakanishi	Osaka International Cancer Institute
Taiki Nozaki	St Luke's International Hospital
Eiji Fukuniwa	PICTORU Izumo Diagnostic Imaging Office
Hajime Fujimoto	Chiba University Hospital

Pediatric

Eiji Oguma	Saitama Children's Medical Center【Chair】
Noriko Aida	Kanagawa Children's Medical Center
Yoshinobu Akasaka	Hyogo Prefectural Kobe Children's Hospital
Kumiko Ando	Kobe City Medical Center General Hospital
Mayuki Uchiyama	The Jikei University School of Medicine
Tatsuo Kono	Tokyo Metropolitan Children's Medical Center
Yutaka Tanami	Saitama Children's Medical Center
Chihiro Tani	Hiroshima City Hospital
Yoshiyuki Tsutsumi	National Center for Child Health and Development
Motoo Nakagawa	Nagoya City University
Masanori Nishikawa	Osaka Women's and Children's Hospital
Kumiko Nozawa	Kanagawa Children's Medical Center
Yuta Fujii	Kanagawa Children's Medical Center
Rieko Furukawa	Jichi Children's Medical Center Tochigi
Takahiro Hosokawa	Saitama Children's Medical Center
Mikiko Miyasaka	National Center for Child Health and Development
Osamu Miyazaki	National Center for Child Health and Development

Nuclear Medicine and Hematology

Ukihide Tateishi	Tokyo Medical and Dental University【Chair】
Kazunari Ishii	Kindai University
Hiroshi Ito	Fukushima Medical University
Tomohiro Kaneta	University of Tsukuba
Takashi Kudo	Nagasaki University
Seiji Kurata	Kurume University
Mitsuaki Tatsumi	Osaka University
Yoshihiro Nishiyama	Kagawa University
Kota Yokoyama	Tokyo Medical and Dental University

Advisors

Takeo Nakayama	Kyoto University

Japan Medical Library Association

Shinichi Abe

Yu Ootani

Third-Party Evaluators

In implementing the present revision, third-party evaluations were obtained by sending a draft indicating the standard imaging methods, BQs, CQs, and FQs for each field to the academic societies listed below. We are deeply indebted to the physicians who were involved in this effort.

The Japan Neurosurgical Society.

Japanese society of neurology

Japanese Society of OtoRhinoLaryngology-Head and Neck Surgery

Japan Society for Head and Neck Cancer

The Japanese Circulation Society

The Japanese Society for Vascular Surgery

The Japanese Respiratory Society

The Japan Lung Cancer Society

The Japan Society of Hepatology

Japan Liver Cancer Association

Japan Biliary Association

Japan Pancreas Society

The Japanese Urological Association

Japanese Breast Cancer Society

The Japanese Orthopaedic Association

The Japan Society of Gynecologic Oncology

The Japan Society of Obstetrics and Gynecology

Japan Pediatric Society

The Japanese Society of Child Neurology

The Japanese Society of Pediatric Surgeons

Japanese Society of Hematology

(legal status omitted)

Table of Contents

3 Chest

4 Cardiovascular

5 Digestive Organs

10 Pediatric

11 Nuclear Medicine and Hematology

Abbreviations

Abbreviation	Full Term in English
ADC	apparent diffusion coefficient
AUC	area under the curve * Unless otherwise indicated, the AUC is obtained from ROC analysis in this guideline.
BQ	background question
CHESS	chemical-shift selective
CI	confidence interval
CQ	clinical question
CT	computed tomography
CTA	computed tomography angiography
EOB-MRI	Gd-EOB-DTPA enhanced MRI
EPI	echo planar imaging
ERCP	endoscopic retrograde cholangiopancreatography
ERP	endoscopic retrograde pancreatography
ETL	echo train length
EUS	endoscopic ultrasonography
FA	flip angle
FDG	fluorodeoxyglucose
FLAIR	fluid attenuated inversion recovery
FOV	field of view
FQ	future research question
FSE	fast spin echo
Gd-EOB-DTPA	gadolinium ethoxy-benzyl diethylene triamine penta-acetic acid
GRE	gradient echo
HASTE	half-Fourier single-shot turbo spin echo
HRCT	high-resolution computed tomography
HU	Hounsfield unit
IR	inversion recovery
MDCT	multi-detector row CT
MIBG	meta-iodobenzylguanidine
MIP	maximum intensity projection
MPR	multi planar reconstruction
MRA	magnetic resonance angiography
MRCP	magnetic resonance cholangiopancreatography

Abbreviation	Full Term in English
MRI	magnetic resonance imaging
NEX	number of excitations
PET	positron emission tomography * Unless otherwise indicated, ^{18}F-FDG is used for PET and PET/CT in this guideline.
ROC	receiver operating characteristic
SAR	specific absorption rate
SE	spin echo
SNR	signal-to-noise ratio
SPAIR	spectral attenuated inversion recovery
SPECT	single photon emission computed tomography
SPIR	spectral inversion recovery
SROC	summary receiver operating characteristic
SSFP	steady-state free precession
SSFSE	single shot fast spin echo
STIR	short TI inversion recovery
SUV	standardized uptake value
T	tesla
TE	echo time
TR	repetition time
VR	volume rendering
WL	window level
WW	window width

General Remarks

1 Evidence-Based Imaging Test Selection

Introduction

One approach to clinical diagnosis is the probabilistic approach (hypothetico-deductive method). With this approach, diagnosis involves establishing a pre-test probability for each differential diagnosis based on a clinical evaluation (history of present illness and physical findings), then calculating a post-test probability based on the test results. These steps constitute the procedure for evidence-based diagnostic procedures, and much has been written about them in recent years.[1-3] The approach of diagnostic inference is also currently becoming more widely adopted and being practiced by medical students and during the training of medical residents. It is hoped that diagnostic imaging and test selection based on theory will be practiced by many clinicians in the future and result in optimal and rapid diagnosis.

Evidence-based imaging test selection

The concept of testing and treatment thresholds is used in determining whether a test is indicated (Fig. 1). This is the idea that a test is first indicated if the diagnosis or treatment plan would change based on the test results. Before a test is requested, it is important to estimate the pre-test probability, gain an understanding of the characteristics of the test to be requested, and consider whether the test is indicated by taking into account factors such as whether a decision to begin treatment will be made and whether a differential diagnosis can be excluded based on the results. This will likely reduce the number of unnecessary screening tests and confirmatory tests performed just to be safe. Test or treatment thresholds vary greatly depending on the risk of procedures, (high thresholds for highly invasive tests and treatments, low thresholds for tests and treatments that are easy to administer, inexpensive, and minimally invasive). Consequently, whether a test is indicated is based on whether the diagnosis or treatment will change depending on the test results. As a specific example, consider coronary artery CT. If the patient is a young adult with no risk factors and no symptoms suggestive of ischemic heart disease (pre-test probability close to 0) but is concerned about angina pectoris and wishes to have a CT test, considering the radiation exposure from coronary artery CT, the possibility of an adverse reaction to the contrast agent, and the cost of the test, the risks of testing would outweigh the benefits, and the test would therefore not be indicated. On the other hand, if the patient had anginal pain, and angina pectoris was suspected based on electrocardiography, percutaneous coronary intervention (PCI) would be indicated regardless of the CT results (treatment threshold is exceeded). A CT test would therefore be unnecessary, because a catheter intervention ought to be selected from the outset. Thus, coronary artery CT would be most strongly indicated for patients at moderate risk.

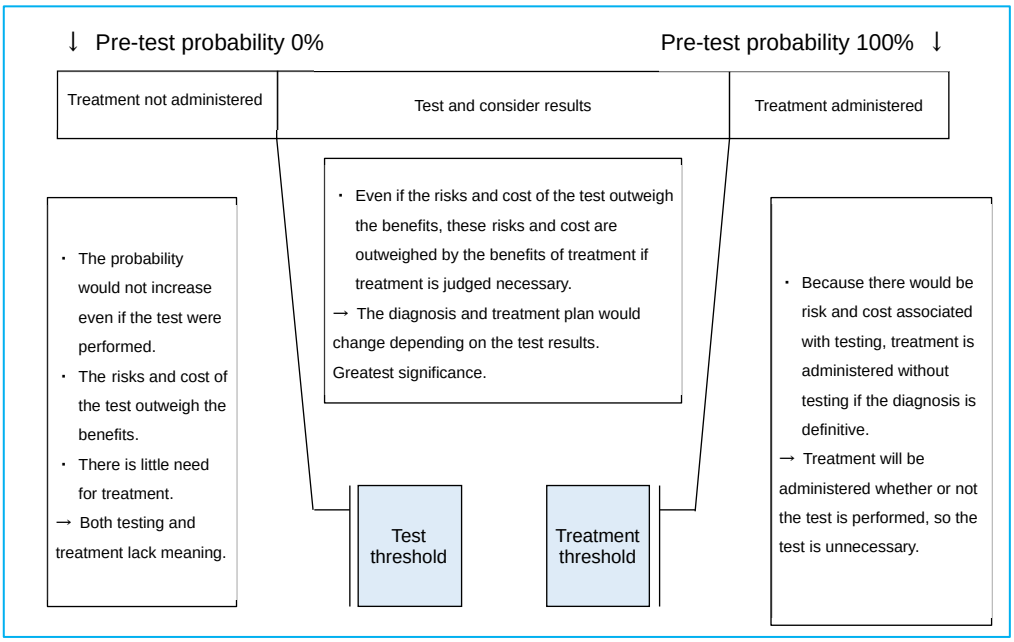

Figure 1. Test and treatment thresholds

The Japanese Circulation Society's diagnostic guidelines for chronic coronary artery disease (2018 revised edition) indicate the testing recommendation grades for each condition.[4)] However, many of the items are assigned a recommendation class of III (not useful; see table), and whether a test is indicated needs to be considered according to the condition (recommendation classes: I. there is evidence or a broad consensus that the procedure or treatment is effective and useful; II. the evidence and opinions regarding the effectiveness and usefulness of the procedure or treatment are inconsistent; IIa. based on the evidence and opinions, it is highly likely that the procedure or treatment is effective and useful; IIb. the effectiveness and usefulness of the procedure or treatment are not well established by the evidence and opinions; III. the procedure or treatment is not effective or useful, and there is evidence or a broad consensus that it is occasionally harmful.)

Diagnostics is the process through definitive diagnosis in patients undergoing initial examination. Currently, many imaging procedures are performed as a treatment adjunct (e.g., surgery support) and to evaluate treatment efficacy; these procedures need to be considered separately from those performed for initial diagnosis.

Table Recommendations and evidence levels for coronary artery CT

1) If asymptomatic

	Recommendation Class	Evidence Level	MINDS Recommendation Grade	MINDS Evidence Classification
Risk stratification based on coronary artery calcium score (CACS)				
No chest pain, low CAD risk group	III	C	C2	VI
No chest pain, moderate CAD risk group	II a	A	B	II
No chest pain, high CAD risk group	II a	A	B	II
Stenotic vessel(s) detected by X-ray CT				
No chest pain, low CAD risk group	III	C	C2	VI
No chest pain, moderate CAD risk group	III	C	C2	VI
No chest pain, high CAD risk group	II b	C	C1	VI

2) If angina pectoris or CAD suspected based on clinical presentation

	Recommendation Class	Evidence Level	MINDS Recommendation Grade	MINDS Evidence Classification
Stenotic vessel(s) detected by X-ray CT				
If chest pain is present, low CAD risk group, and exercise is difficult or exercise ECG is difficult to evaluate	I	A	A	I
If chest pain is present, moderate CAD risk group, and exercise is difficult or exercise ECG is difficult to evaluate	I	A	A	I
If chest pain is present, high CAD risk group, and exercise is difficult or exercise ECG is difficult to evaluate	II a	B	B	II
If coronary spastic angina is strongly suspected	III	C	C2	VI
If unstable angina/non-ST-elevation myocardial infarction is suspected				
Low-to-moderate risk group (no ECG changes, blood chemistry tests negative)	II a	B	A	II
High-risk group (ECG changes present, blood chemistry tests positive)	III	C	D	VI

3) Combination with other tests

	Recommendation Class	Evidence Level	MINDS Recommendation Grade	MINDS Evidence Classification
Coronary artery CT as a combined test				
If exercise ECG evaluation is difficult	I	A	B	III
When stress MPI indicates mild perfusion abnormality or is difficult to evaluate	II a	B	B	III
Myocardial ischemia detected by stress CTP				
When coronary artery CT is difficult to evaluate or indicates stenosis of moderate or greater severity	II a	B	B	II
Myocardial ischemia diagnosed by stress CTP alone	II a	B	B	II
Infarct imaging by late imaging				

As alternative method if SPECT or MRI cannot be performed	II b	C	C1	IVa

4) Other scenarios in combination with other tests

	Recommendation Class	Evidence Level	MINDS Recommendation Grade	MINDS Evidence Classification
Examination for coronary lesions as cause of heart failure	II b	B	C2	VI
Follow-up after revascularization				
Post-CABG evaluation	II a	B	B	I
Post-PCI (> 3-mm stent)	II a	B	B	IVa
Post-PCI (≤ 3-mm stent)	II b	B	D	IVa
Evaluation of sites of percutaneous old balloon angioplasty (POBA), directional coronary atherectomy (DCA), or rotablator treatment	II a	B	C1	VI
Preoperative evaluation for cardiac great vessel surgery	II a	B	B	IVb
Preoperative evaluation for noncardiac surgery	II b	C	C2	IVb
Kawasaki disease coronary lesion (aneurysm)	II a	C	C1	IVb
Congenital coronary artery malformation	I	B	B	I
Screening test during health checkup	III	C	C2	VI

Japanese Circulation Society: JCS 2018 Guideline on Diagnosis of Chronic Coronary Heart Diseases, https://www.j-circ.or.jp/cms/wp-content/uploads/2020/02/JCS2018_yamagishi_tamaki.pdf (accessed on July 1, 2020)
http://www.j-circ.or.jp/cms/wp-content/uploads/

In addition, one approach for reducing unnecessary tests is to promulgate clinical prediction rules concerning test indications. Specific examples include the Canadian Assessment of Tomography for Childhood Head injury (CATCH rule)[5] for determining whether CT is indicated for childhood head injuries and the Ottawa Ankle Rules[6] for minor trauma. If numerous clinical studies are conducted using these clinical prediction rules, and studies that provide strong evidence accumulate, it may become possible to use the rules effectively to limit the number of patients who require tests. In Japan, few studies of clinical prediction rules have been conducted. It is expected that many such studies will be conducted and evidence accumulated in the future.

Evidence-based differential diagnosis

This method involves estimating the pre-test probability based on symptoms and physical findings and calculating the post-test probability based on the test results. That calculation is performed as shown below using the likelihood ratio for each test.

post-test odds[*1] = pre-test odds × likelihood ratio[*2]

[*1] Odds: The ratio of the probability of an event happening to that of a different event. It is calculated as follows: odds = probability / (1−probability). For a probability of 10%, the odds would be 0.1 / (1−0.1) = 0.101. For a probability of 50%, the odds would be 0.5 / (1−0.5) = 1.

[*2] Likelihood ratio: expresses how many fold a positive test result increases the pre-test odds to reach the post-test odds. It is calculated as follows: likelihood ratio = sensitivity / (1−specificity).

In considering a differential diagnosis, it is important to understand whether the pre-test probability (odds) can be correctly predicted and the characteristics of the test. Broadly speaking, the characteristics of tests are of the following 2 types, and their use needs to be distinguished according to the circumstances, such as when a definitive diagnosis or diagnosis of exclusion is desired.

Sensitive/negative rule out (SnNout): If the result of a highly sensitive test is negative, the condition can be ruled out.

Specific/positive rule in (SpPin): If the result of a test with high specificity is positive, it can be considered definitive.

If the likelihood ratio for a test is ≥ 10 or ≤ 0.1, the result will be a large and often conclusive change from the pre-test probability to the post-test probability. The likelihood ratio for a test with sensitivity and specificity of 90% each would be calculated as follows: likelihood ratio = 0.9 / (1−0.9) = 9. Therefore, a test with equal or greater sensitivity and specificity would be highly useful in differential diagnosis. Conversely, in the case of a test with a low likelihood ratio, a result based on the pre-test probability is often the only result, and the characteristics and purpose of the test must therefore be carefully considered.

In diagnostic imaging, a high diagnostic accuracy rate is required for diseases in which a diagnosis is established based on imaging findings (e.g., aneurysm, artery dissection), regardless of the pre-test probability.

New tests

As advances are made in diagnostic imaging systems, the number of new tests and imaging methods is increasing by the day. The relationship between the new tests and existing tests was summarized by Bossuyt et al., as shown in Fig. 2.[7)]

As the figure indicates, the circumstances in which a new test emerges and the number of tests does not increase are the replacement or triage scenarios, which effectively reduce the number of subsequent tests. Currently, many new tests are thought to be add-on tests. Although it is important to increase findings with new tests, clinical studies are needed in order to accumulate the evidence needed to determine whether performing new tests reduces the number of other tests.

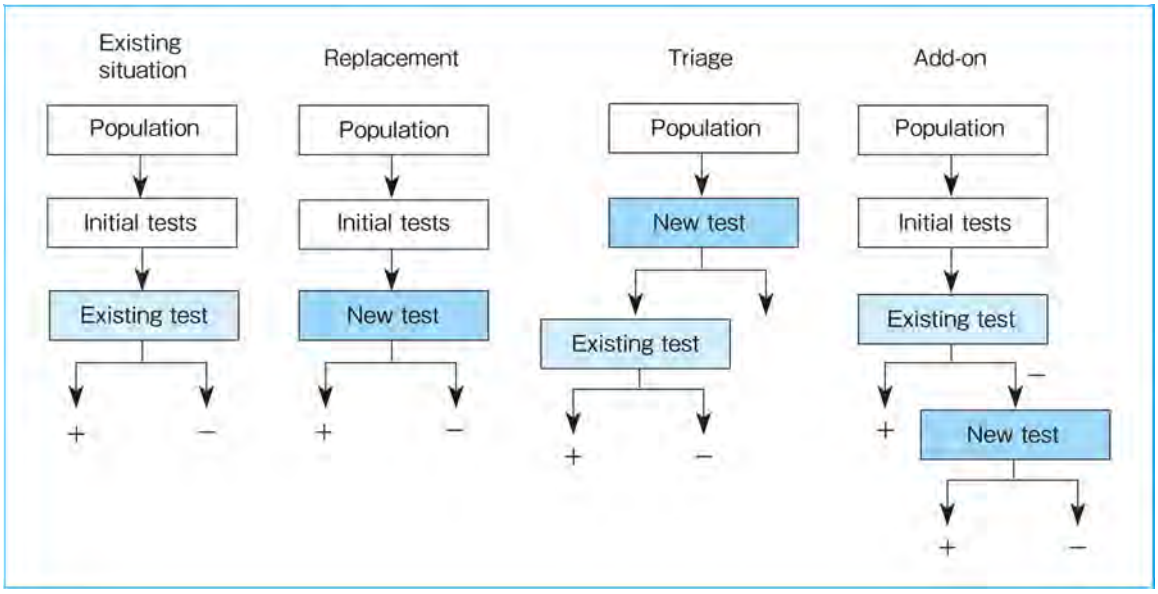

Figure 2. Relationships between indications for new tests and existing tests (excerpted from reference 7).

Secondary source materials used as references

1) Guyatt GH, et al. User's Guides to the Medical Literature: A Manual for Evidence-Based Clinical Practice, 2nd Ed. Toppan Media, 2010.
2) Scott DC, et al. Symptom to Diagnosis: An Evidence-Based Guide, 3rd Ed. Nikkei BP Shuppan Center, 2007.
3) Noguchi Y. Secrets of Diagnostic Reasoning. Japan Medical Journal, 2019.
4) Guideline on Diagnosis of Chronic Coronary Heart Diseases joint research group: JCS 2018 Guideline on Diagnosis of Chronic Coronary Heart Diseases. Japanese Circulation Society, 2019.
5) Osmond MH et al: CATCH: a clinical decision rule for the use of computed tomography in children with minor head injury. CMAJ 182 (4): 341-348, 2010
6) Bachmann LM et al: Accuracy of Ottawa ankle rules to exclude fractures of the ankle and mid-foot: systematic review. BMJ 326 (7386): 417, 2003
7) Bossuyt PM et al: Comparative accuracy: assessing new tests against existing diagnostic pathways. BMJ 332 (7549): 1089-1092, 2006

2 Developing Diagnostic Imaging Guidelines

The concept behind the new clinical practice guidelines

As indicated in the preface of the guidelines, the present diagnostic imaging guidelines were developed based on the MINDS Guide for developing Clinical Practice Guidelines issued in and after 2014.[1,2] The method used to develop clinical practice guidelines has advanced continuously. A significant difference from the previous method is the introduction of the GRADE (grading of recommendations assessment, development and evaluation) system, a relatively new method of guideline development.[3] In the current version, we changed the target audience from board-certified diagnostic radiologist specialists to general practitioners, who order imaging procedures.

Moreover, the definition of clinical practice guidelines shifted from "systematically developed statements to assist practitioner and patient decisions about appropriate health care for specific clinical circumstances"[4] to "statements that include recommendations, intended to optimize patient care, that are informed by a systematic review of evidence and an assessment of the benefits and harms of alternative care options." Thus, this definition clarified several key concepts such as the SR, overall evaluation, and balancing benefits and harms.[1] In the area of therapeutic options, guideline development based on the GRADE system has been established, while in the diagnostic options, guideline development is still in its early days with trials and errors. A small number of GRADE-based clinical practice guidelines, such as the clinical practice guidelines for breast cancer (diagnosis and epidemiology volumes) were used as references[5].

Forming clinical questions (CQs)

The CQs represent important points for decision-making by patients and healthcare personnel (more accurately, determine key clinical issues, and extract the components of questions that should be addressed) that consist of the following components.

- P: The patient situation, population, or problem of interest
- I/C: The main intervention and a comparison intervention
- O: The clinical outcome (benefits and harms)

The new method of guideline development emphasizes the balance between benefit and harm.[1,2] Benefit refers to the anticipated effectiveness. Examples of harm include adverse events, the cost burden, and the physical and mental burden. Outcome encompasses both benefit and harm.

The previous diagnostic imaging guidelines (2016 edition) included a total of 171 CQs. Because it would be difficult to re-examine all of the CQs based on the new method, and because they included indisputable

information that could be regarded as standard and questions that, although important, had little supporting evidence, we decided to follow the above-mentioned clinical practice guidelines for breast cancer and organize the CQs of the previous edition accordingly. Questions that could be regarded as standard information and test methods were classified as background questions (BQs), and those for which there were insufficient data to raise them as CQs, but that were considered important issues for the future, were classified as future research questions (FQs). The remaining CQs were controversial ones. For these CQs, quantitative or qualitative SRs were performed based on evidence, and recommendations were determined after voting took place in the panel meeting. This process was conducted at the start of the development of the guidelines and then repeated during the course of the work. Depending on the amount and consistency of the evidence obtained, original CQs were changed to FQs.

An SR is a comprehensive review of the research that pertains to CQs, in which studies of the same type are summarized, analyzed, and integrated while risk of bias is assessed. The steps involved evaluating the individual studies, then evaluating the summarized results as the body of evidence.

Appraisal of diagnostic imaging studies

Under the conventional view focusing on treatment research of the primary source of evidence, evidence from randomized, clinical trials (RCTs) was considered the strongest, and that from cross-sectional studies, which many studies of diagnostic imaging are classified, was regarded as relatively weak. With the new method of developing guidelines, secondary studies such as properly performed meta-analyses are given higher standing. Those showing a high probability of effectiveness and a large effect are considered correct, and if multiple studies show an effect in the same direction, the findings are regarded as having a high probability of being correct. The fact that cross-sectional studies are not considered to be of lower quality can be considered an advantage for the field of diagnostic imaging.

The steps to a recommendation

The steps involved in developing clinical practice guidelines are indicated in Fig. 1. For the CQs, an SR plays an important role. In the SR, a comprehensive review of the research is performed, and studies of the same type are analyzed and integrated while bias is assessed.

The SR involves a rigorous standardized comprehensive search and critical appraisal of peer-reviewed articles related to specific health problems (clinical questions). The evidence based on an SR is superior to that based on individual studies because: (1) the risk of bias is reduced; (2) suitable to see overall trends and variability; and (3) the evidence level is higher than with individual studies. However, it should be kept in mind that these advantages depend on the quality of the articles used. An SR is not always the same as a meta-analysis. A meta-analysis refers to a statistical method of integrating data from multiple studies and the article written following this method, alternatively referred to as a quantitative SR. It is an effective

method when the individual studies, even if small, show a similar trend, and significant differences are seen when the data from the studies are integrated. It is also useful for detecting publication bias, which occurs when only studies with positive results are published. However, integrating the data is meaningless if the number of studies is small, with small sample sizes, with wide variability, or with studies of inconsistent quality. In such cases, the more appropriate method is a qualitative SR, in which no meta-analysis is performed, but rather the data from each original study are shown and summarized.

1. Procedure for performing an SR

The SR process can be divided into the 4 steps shown in Fig. 2 (1) to (4) below.

① Literature search and screening

The literature search was based on PubMed and used sources such as the Cochrane Database, and the guidelines of relevant academic societies in Japan and other countries were used as secondary sources. Because keywords related to articles on diagnostic imaging do not necessarily have a high rate of coverage by MeSH terms, concurrent hand searches of citations from guidelines and reviews were also performed in parallel. The individuals in each field subcommittee who were responsible for CQs and SRs selected the CQs, example search queries, keywords, and important articles, supported by the specialist from the Japan Medical Library Association in performing a comprehensive literature search, which yielded a list of several hundred references. The individuals responsible for SRs then reviewed the titles and abstracts and narrowed down the candidate articles

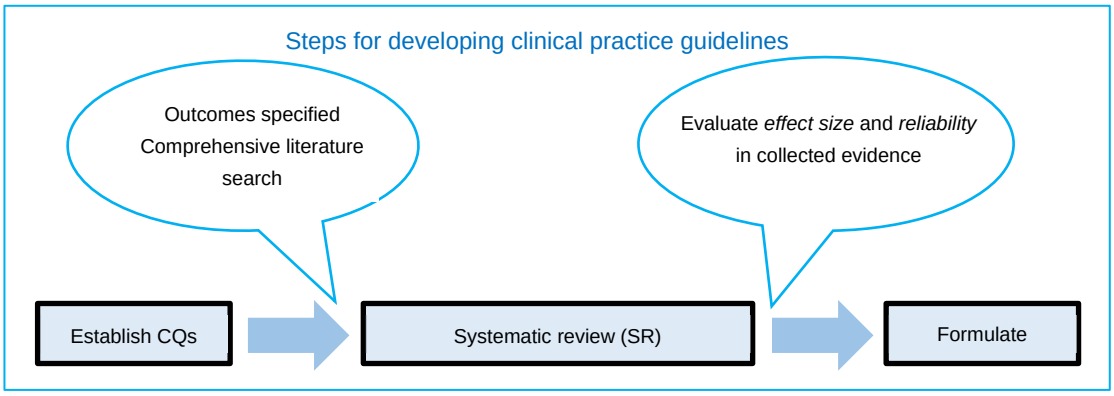

Figure 1. Steps for developing clinical practice guidelines

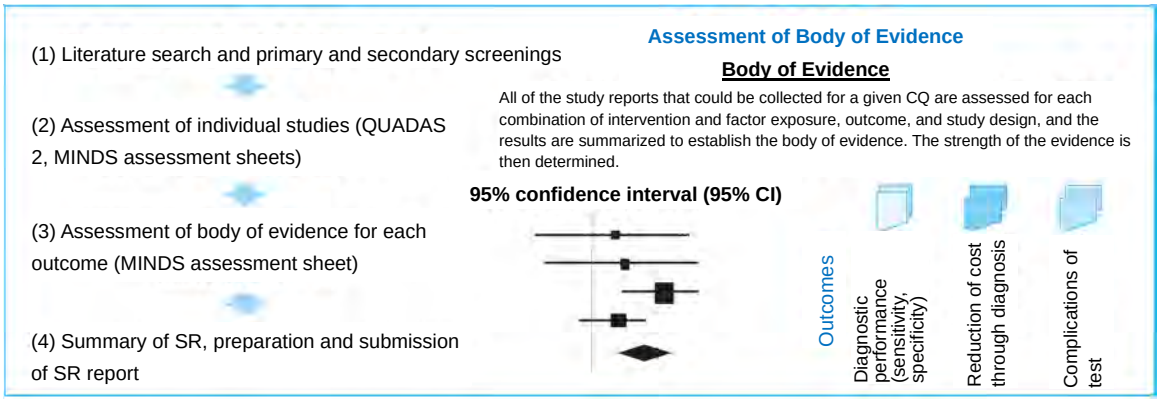

Figure 2. The 4 steps of the SR process

② Assessment of individual studies

The assessment of individual studies involves reading each article and assessing the reliability of the evidence. The evaluated points are as follows:

- Risk of bias: e.g., selection bias;
- Indirectness = external validity/generalizability: Differences between study populations (e.g., original CQ concerns the Japanese population, and the evidence is data from the American population); Inconsistency: variability seen in effect depending on the report;
- Imprecision: small sample size and wide confidence intervals;
- Other types of bias: e.g., publication bias.

Using the QUADAS 2 assessment sheet (revised tool for the Quality Assessment of Diagnostic Accuracy Studies 2)[6], these points were assessed for the individual studies, and the results were recorded on a sheet for individual studies, shown below (Fig. 3).[7]

③ Assessment of the body of evidence

This process involves assessing the evidence for each outcome while referring to the assessment sheets for individual studies. Although many of the main items also apply to individual studies, the main points of this assessment are those such as the consistency of the outcomes. If necessary, a meta-analysis is performed, and the results for the integrated data are examined for any significant differences.

④ SR report preparation

An SR report is written in light of the above-mentioned results. The report is prepared according to the template provided on the MINDS website.

2. Formulating recommendations

The summarized recommendations are formulated with reference to the SR report. In the case of a CQ, the aim at this stage is to form a consensus regarding the final recommendation. During this process, a panel meeting is held to gain an understanding of the report and ask questions, and assess the balance of benefits and harms (Fig. 4). However, different from the previous conference system, methods for determining the recommendation by a vote, such as the Delphi process, which more fairly reflects the opinions held, are currently being promulgated. In this way, recommendations are finally determined at the 4 levels indicated below.

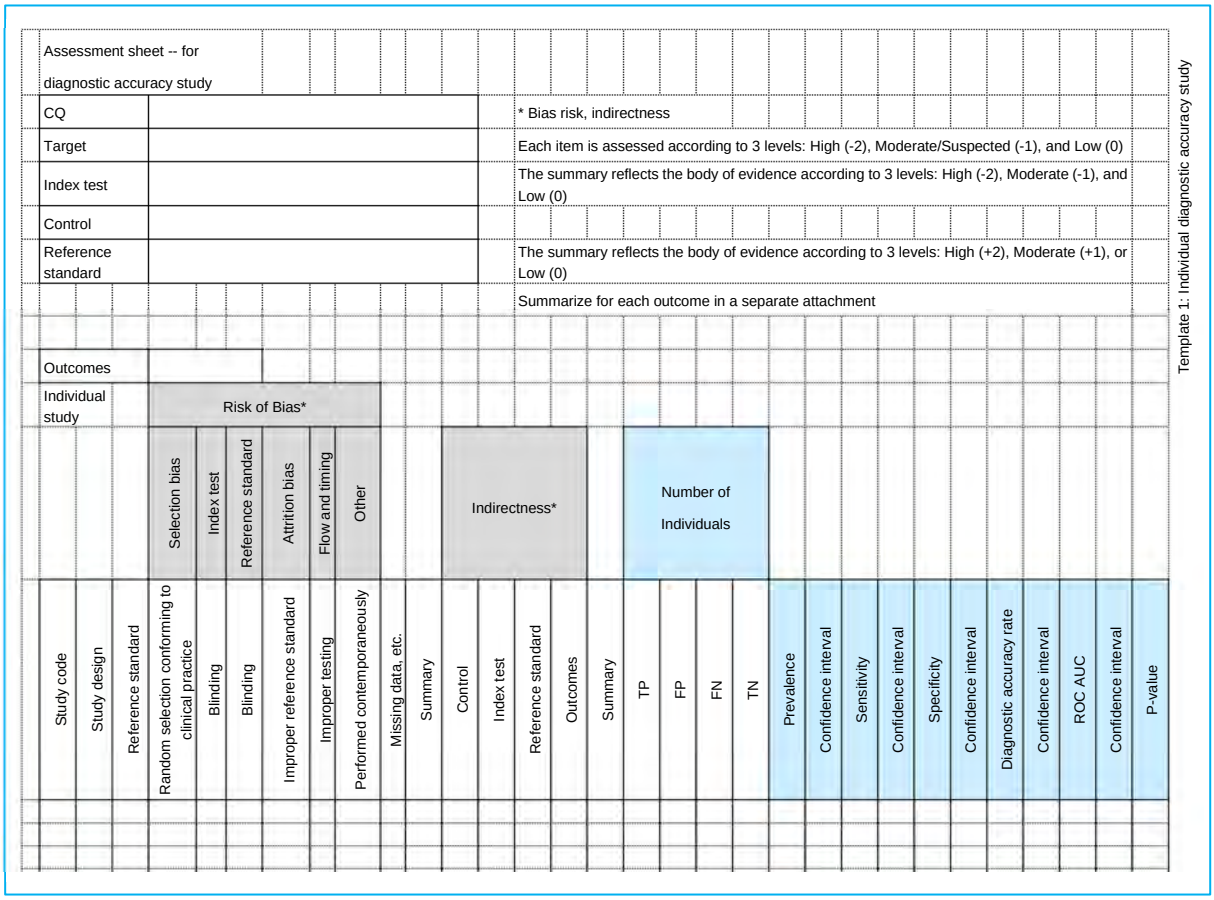

Figure 3. Individual study assessment sheet

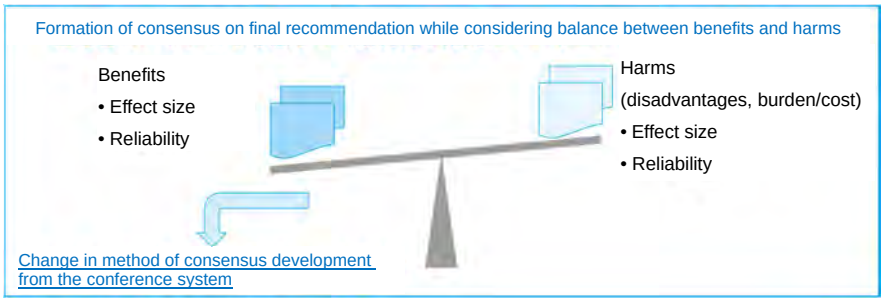

Figure 4. Determination of recommendation that takes into account balance between benefits and harms

- Strong recommendation: perform
- Weak recommendation: perform
- Weak recommendation: do not perform
- Strong recommendation: do not perform

Purpose of panel meeting

Based on the results of the SR conducted for the CQ, a statement of the following form is established: “performing XX is strongly/weakly recommended.” Following discussion, an anonymous vote is ultimately taken. In view of the specialized nature of each field, voting on the diagnostic imaging guidelines was conducted at the level of the subcommittee for each field. In addition, 1 or 2 general practitioners associated with each field (non-diagnostic radiologists) were asked to participate in the discussions so that adequate consideration was given to comprehensibility and validity from the perspective of the clinician. Specifically, the following provisions were adhered to during the process.

1. Voter requirements

(1) Qualified as a voter (varies depending on the CQ)

• Not a committee member involved in the SR

• Outside committee member

(2) Unqualified as voters (varies depending on the CQ)

• An individual involved in the SR

• An individual with a COI (including academic COIs)

2. Requirements for a meeting to serve as a venue for discussion to establish recommendation (“panel meeting” below)

The participants are voters, non-voters, and the individual(s) who developed the SR (in the case of multiple individuals, one can participate as a representative). The meeting can be held online.

3. Panel meeting

A common understanding of the SR results is established, and any unclarified issues are resolved. Aspects such as any negative effects and social impacts of the test not covered in the SR are also discussed. After the meeting concludes, an anonymous vote is taken.

- If either choice (perform/do not perform) receives half or more of the vote, and the other choice receives less than 20% of the vote, the former choice is recommended.
- If agreement of 70% or greater is reached in the vote, the strength of the recommendation is determined.
- If agreement of 70% or greater is not reached, the results are announced, and a revote is taken.
- Up to 2 revotes are taken. If that is insufficient to come to a decision, the judgement is “no recommendation.”

Due to restrictions on mobility related to the COVID-19 pandemic, all meetings related to the 23 CQs in 8 areas on the current revision were held online, in accordance with the above-mentioned provision. Outside committee members also participated. In fact it was easier to adjust the schedule online. Although the meetings placed heavy demands on the field committee chairs and the individuals in charge of SRs, they allowed the views of outside committee members to be heard directly, allowing these views to be reflected when preparing the text of the recommendations.

Acknowledgments

Finally, many experts provided advice during the development of the present guidelines, which used a new method that incorporated the GRADE system. Specifically, they were the individuals indicated below. We are deeply grateful for their assistance.

Takeo Nakayama and Yoshihito Goto, Department of Health Informatics, Kyoto University School of Public Health

Toshio Morizane and other experts from MINDS

Norio Watanabe, Yuki Kataoka, and other experts from Cochrane Japan

Hiroji Iwata and Takayoshi Uematsu from the Japanese Breast cancer Society

The experts responsible for the guidelines of the Japan Society of Clinical Oncology

Secondary source materials used as references

1) Kojimahara N, et al., Ed.: Minds Manual Developing Committee ed. Minds Manual for Guideline Development 2017 Tokyo: Japan Council for Quality Health Care, 2017.
2) Fukui T, Yamaguchi N, Ed.-in chief: MINDS Manual for Guideline Development 2014. Igaku-Shoin Ltd., 2014.
3) Balshem H, et al: GRADE guidelines: 3. Rating the quality of evidence. J Clin Epidemiol 64: 401-406, 2011
4) MINDS Clinical Practice Guidelines Selection Working Group, Ed.-in-chief: MINDS Manual for Guideline Development 2007. Igaku-Shoin Ltd., 2007.
5) The Japanese Breast cancer Society Clinical Practice Guidelines for Breast cancer 2018
6) Quadas 2 (https://www.bristol.ac.uk/population-health-sciences/projects/quadas/quadas-2/)

7) Morizane T, et al.: Minds Manual for Guideline Development, Special Contribution 5. Developing Clinical Practice Guidelines (CPGs) for Diagnosis. Japan Council for Quality Health Care, 2015 (see https://minds.jcqhc.or.jp/s/guidance_special_articles5_1, January 5, 2021).

3 CT and MRI in the Radiological and Medical Services in Japan

The efficiency of healthcare services in Japan

When the quality of medical services in Japan is measured by international rankings, I am probably not the only one who is embarrassed by the magnitude of variation in the ranking among items. Medical services in Japan have made remarkable achievements in mean life expectancy and in the infant mortality rate, which are among the best in the world. People's access to medical services is generally satisfactory. Despite some regional differences, patients in urban regions can access any medical organization's department at a low cost. Such superficial achievements are often cited as grounds for justification of the status quo, but favorably evaluating the whole based on selected items with good results permanently denies opportunities to reform weaknesses. In reality, data that question the efficiency of medical services in Japan are abundant. First, concerning the cost, the number of visits to medical facilities per patient is the highest in Japan (Fig. 1). It has the highest number of hospital beds (Fig. 2),[Footnote1] and the cost of drug prescriptions as a percentage of medical expenditures is in the higher bracket (Fig. 3). In terms of the number of CT/MRI systems per capita, Japan ranks 1st in the world, towering above other countries (Fig. 4A, B). As a result, it has been noted that medical radiation exposure is conspicuously high among the OECD member countries (discussed later). On the other hand, the number of CT/MRI tests per system is the lowest among the Group of Seven industrialized nations.[2)] If Japan's total medical expenditure per population is still relatively low despite such inefficiency (Fig. 5), it would be natural to think that it is due to low unit prices of medical services.

Problems that the status quo causes for Japanese society

As observed above, there seem to be inefficient areas in medical services in Japan that need improvement. Then, what effects do such weaknesses exert on medical services in Japan? Regarding radiological and medical services, this question boils down to an increase in medical radiation exposure, delay of implementation of necessary examinations, and deterioration of the clinical skill of physicians in various clinical departments. Because of the good access to medical services, outpatient clinics of medical organizations (particularly those of middle-sized or large hospitals) are always crowded beyond the capacity of physicians assigned to outpatient care, allowing the mocking phrase, "waiting for 2 hours, treated in 5 minutes". I would venture to say, taking the risk of being misunderstood, that the low cost of each visit is a cause of the high frequency of patient consultations (i.e., high patient-regulated

Footnote 1: Despite having the largest number of hospital beds, Japan encountered problems in coping with severe pneumonia related to the COVID-19 pandemic in spring 2020, because the number of beds available for acute care, particularly in ICUs, was less than half the number in the United States and Germany.[1)]

demand).[Footnote2] Patients' preference for large hospitals and the lowest number of physicians among OECD countries contribute to this situation as well (Fig. 6). As a result, in outpatient clinics, each physician must see 30 or sometimes 50 patients until evening without even taking a break for lunch. An outpatient physician is required to reach some conclusion about the diagnosis and treatment within 10 minutes for each patient on the initial visit. The physician performs a medical interview and physical examinations, determines an examination plan, explains the plan to the patient, obtains consent, explains the results to the patient coming back after the examinations, shows possible diagnoses, explains the treatments, obtains consent, and performs them all within 10 minutes. The fact that medical actions are performed in Japan in such a short time can never be understood by physicians in Western countries. If the situation is explained to them, they would reply that it is impossible to make a diagnosis and prescribe treatment in such a short time (without mistakes). Patients demand an increasingly higher quality of medical services, so their tolerance for medical errors is diminishing. Physicians inevitably rely on diagnostic imaging modalities such as CT and MRI to quickly reach some conclusion or treatment plan without overlooking any pathologies. The physicians are also prompted to eliminate buds of medical errors, though their possibility may be low, by resorting to broadly targeted treatments, such as the prophylactic administration of anti-influenza virus agents or antibiotics even when spontaneous cure is expected. The same prescriptions are continued for patients on revisits, and follow-up examinations are repeated without carefully talking to the patients or re-evaluating their medications. Thus, radiological investigations, which are originally supportive diagnostic procedures, have been transformed into low-cost automatic diagnostic devices in busy outpatient clinics. The medical fee reimbursement system may also be promoting orders based on "conditioned reflexes," not based on a well-thought-out medical plan. The fees for outpatient care are paid on a fee-for-service basis, and payments are made even when a physician orders examinations without carefully evaluating their indications, possibly contributing to an increase in examinations that are unlikely to be necessary. However, if such practice becomes routine, the waiting time for necessary examinations is prolonged. If the number of tests performed increases, outpatient visits would further increase. That is because, as the testing load increases, the radiology department and the diagnostic radiologists become extremely busy. Consequently, wait times for tests increase, test reports are delayed, and patients are notified of the test results during a return visit at a later date. Particularly in the last ten years, rapid advances have been seen in the increases in the number of detector rows in CT systems and the speed of MRI systems.[Footnote3)] Consequently, the number of images produced per patient has increased exponentially, while the number of diagnostic radiologists has increased only linearly.[5)] If a test is performed with no

---

Footnote 2: Due to the COVID-19 pandemic in spring 2020, people were asked to refrain from seeking nonessential and non-urgent medical care. During this period and for several months after, the number of patients seeking outpatient treatment at clinics and medical institutions throughout the country dropped sharply, resulting in economic difficulties.[3)] This suggests that a form of the medical fee system that can sustain healthcare during such times needs to be explored by calculating the number of outpatients that would normally be expected to use a facility.

Footnote 3: In the 5 years from 2013 to 2017, 6,103 CT systems were newly installed in Japan. However, less than 2.2% were systems with detectors having ≤ 16 rows. During the same 5-year period, 2,632 MRI systems were installed, but only 16% had a magnetic field strength of < 1.5 T.[4)] Thus, the CT and MRI systems newly installed in the previous 5 years were largely high-performance systems that are capable of high-speed imaging.

consideration given to whether it was indicated, the diagnostic radiologist must at least glance through all of the images before arriving at a diagnosis of “no finding” or “normal.” In addition, for diagnostic devices to be constantly available, even minor medical facilities are required to install them. This increases the number of CT/MRI devices, and the installation of devices in excessive numbers leads to a low utilization level and poor maintenance. Efforts to increase the degree of utilization under such circumstances result in hospital-induced demand, i.e., the use of devices in patients for whom the examination may be unnecessary and even for the general public.

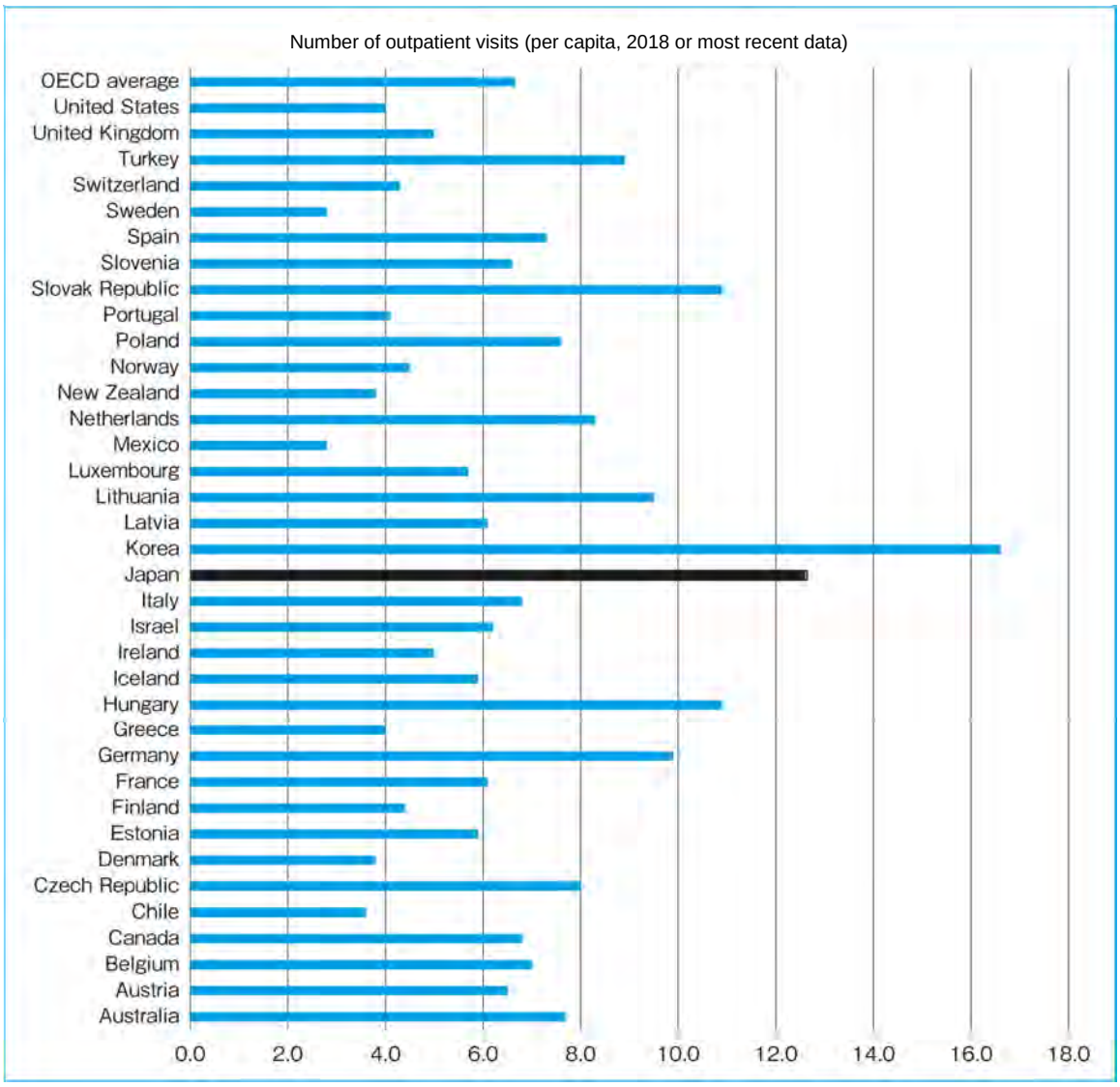

Figure 1. Number of outpatient visits per capita (OECD Health Statistics 2018 or most recent data)

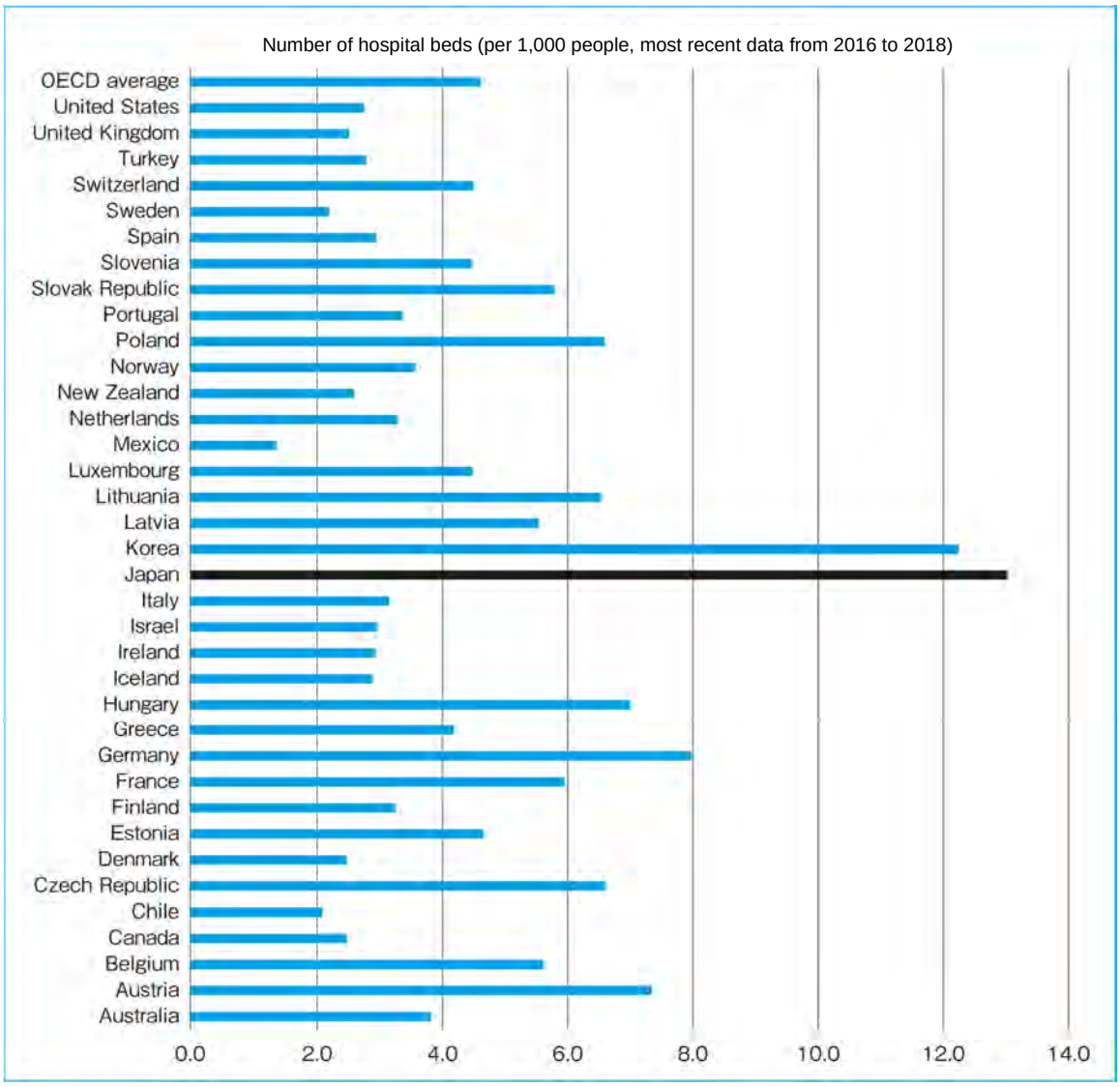

Figure 2. Number of beds per 1,000 people (OECD Health Statistics 2018 or most recent data)

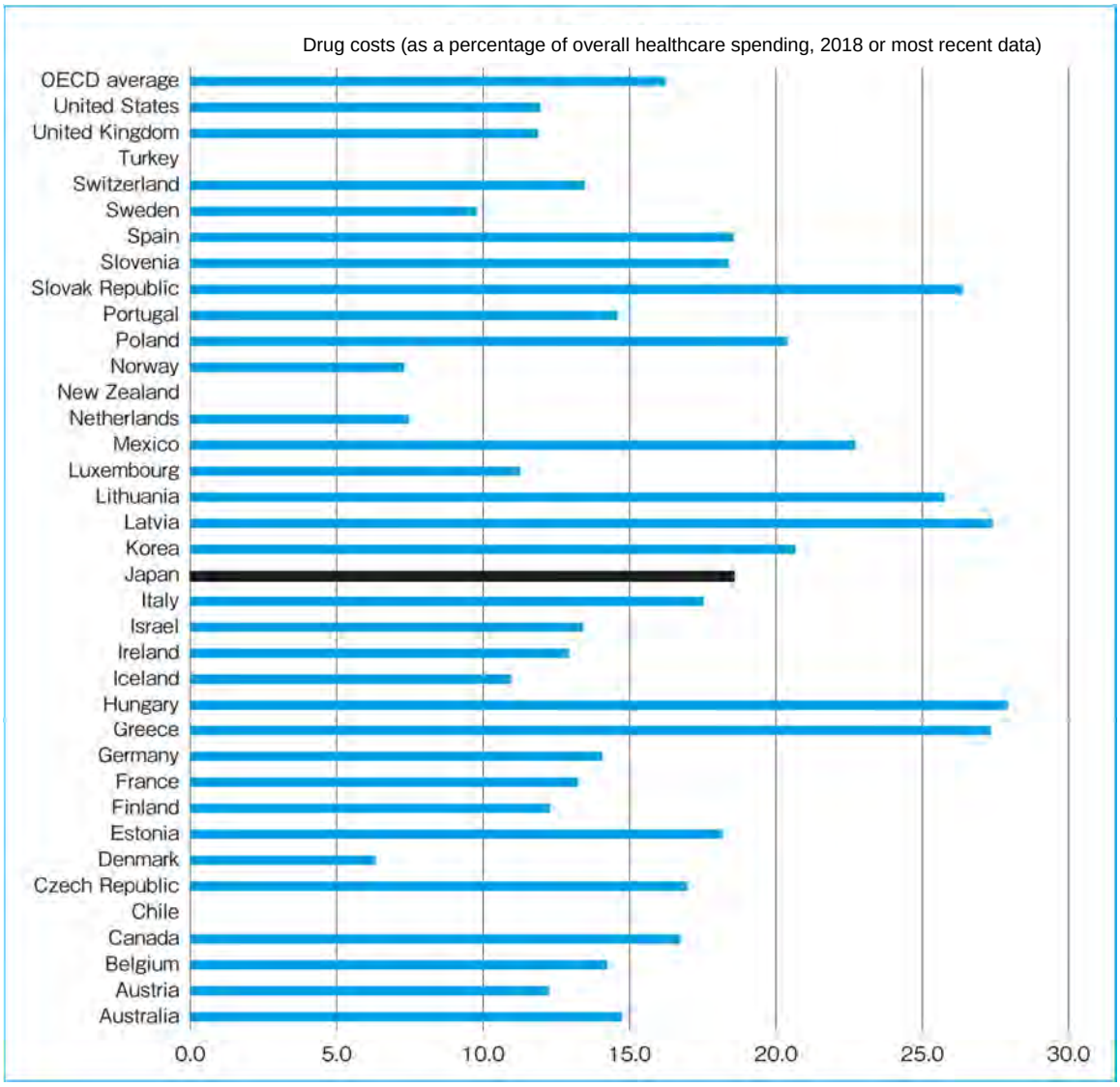

Figure 3. Expenditures for drugs and medical expendables (%; relative to total medical expenditures, 2018 or latest)

“Assembly-line”-like orders for CT/MRI and failed communications

In recent years, physicians in some departments have failed to read radiology reports or have not passed on information satisfactorily, resulting in delays that have left patients with advanced diseases. Thirty-seven such incidents were reported between January 2015 and March 2018 alone.[6)] Factors contributing to this problem include poor communication by healthcare professionals and the overwhelming increase in the volume of information provided by CT and MRI tests. The information provided in radiology reports is wide-ranging and sometimes goes beyond the specialties of the departments that request tests. In cases where the results reported are not anticipated at the time of the orders or beyond the understanding of the specialty, it can be surmised that there will be an incident involving an inadequate response by the

requesting physician who falls short or poor information transfer between the relevant specialties. However, although such incidents cannot be eliminated, they can be gradually decreased through measures such as introducing an IT system to handle unread radiology reports and adding a new unit to monitor this as a hospital function. More than half of the national university hospitals have already implemented such efforts or are considering doing so.[7)] There may be opportunities to arrange conditions in the future toward a policy whereby the attending physician shares all chart information, including radiology reports, with the patient so they can double-check each other, as in the United States. However, it will be necessary to thoroughly consider the misunderstandings and other harmful effects that could arise if patients obtain reports that are still in a form intended for healthcare professionals.

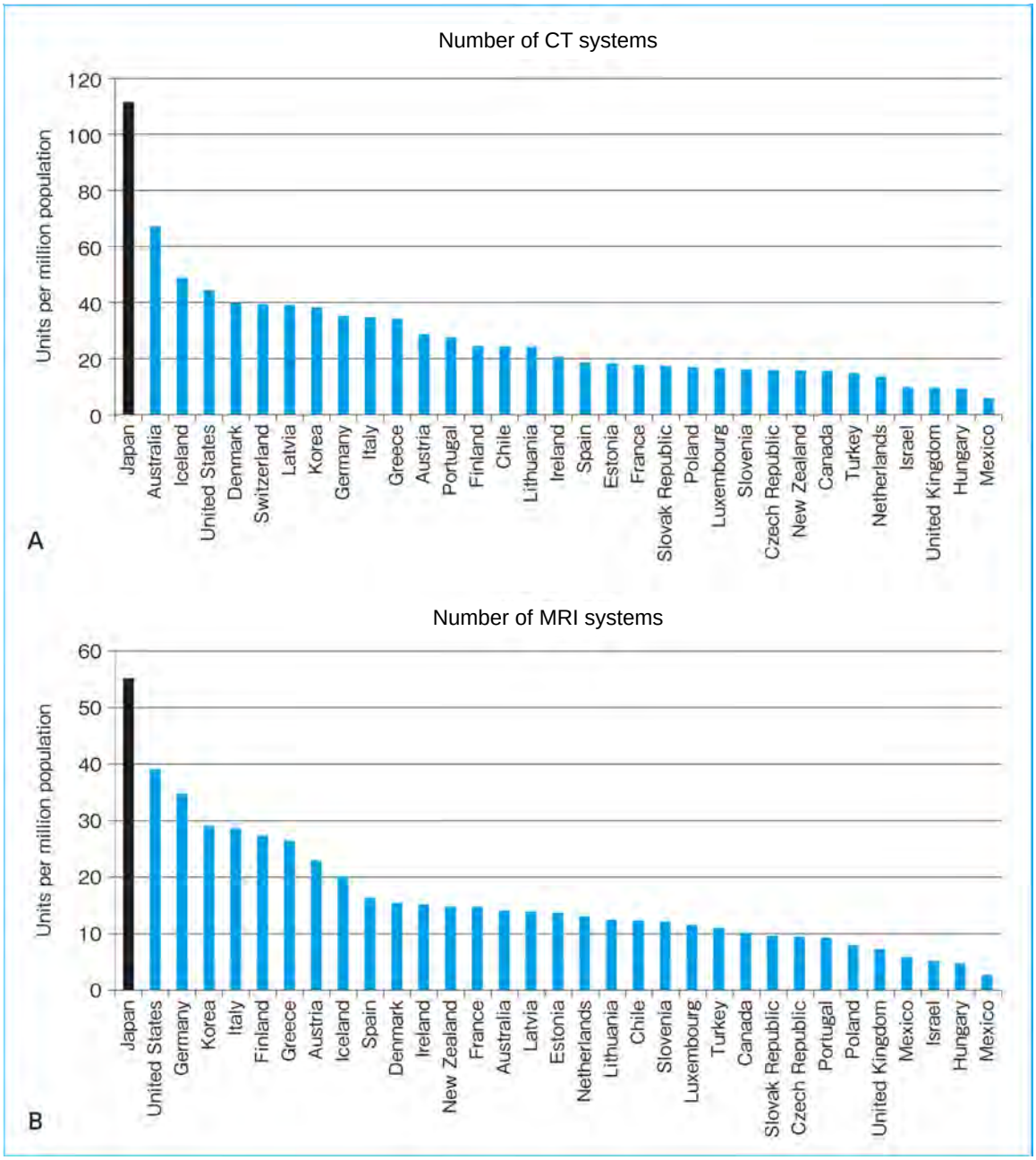

Figure 4. Numbers of installed CT (A) and MRI (B) devices (OECD Health Statistics 2018 or most recent data)

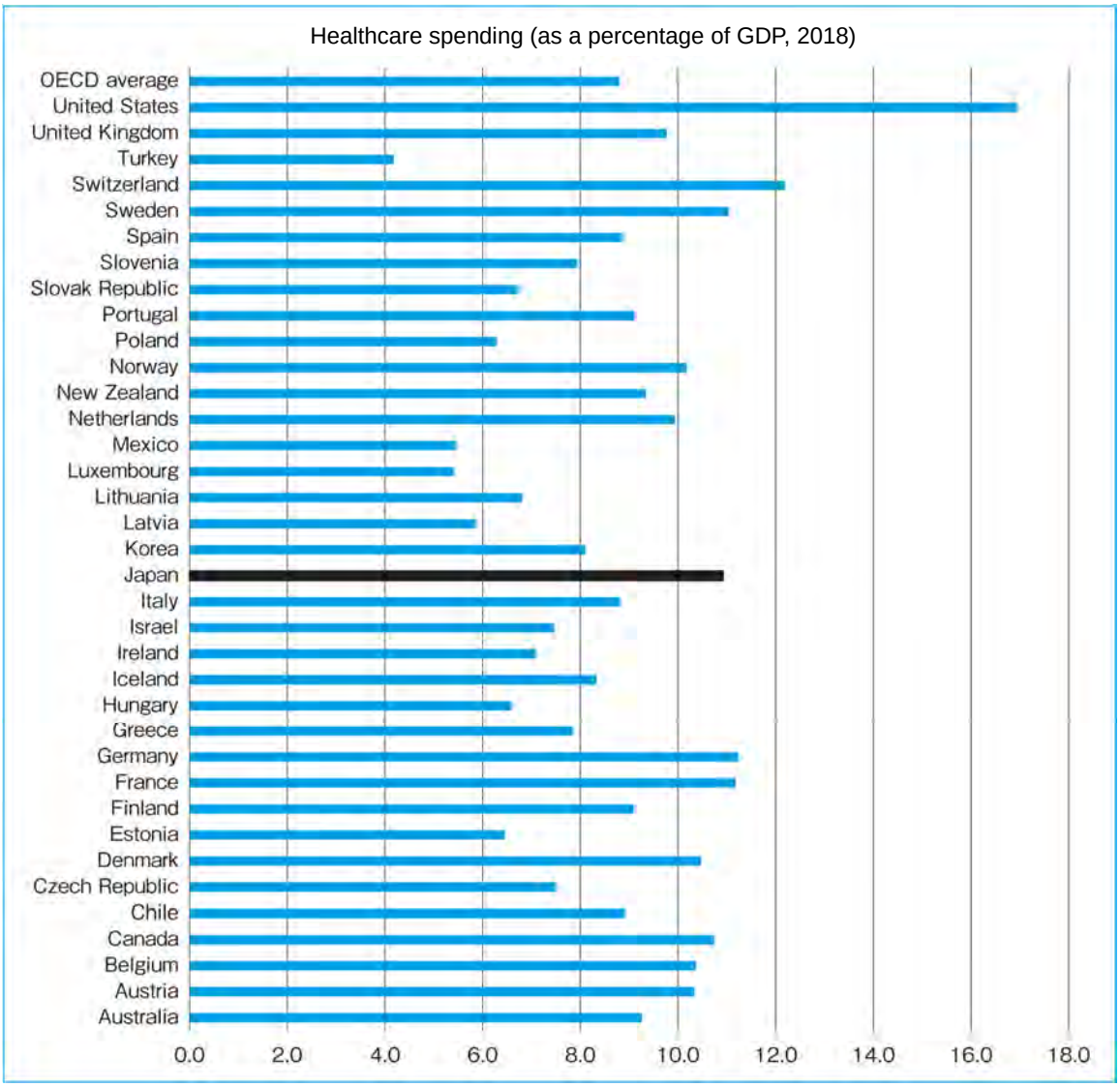

Figure 5. Medical expenditures (relative to GDP) (OECD Health Statistics 2018 or most recent data)

The trap of cost increases due to uniform control of medical fees and the necessity of redistribution of resources for improvements in efficiency

As observed above, efficiency cannot be improved as expected from attempts to reduce costs by across-the-board cuts of medical fees. This paradox is the “trap of cost increases due to uniform control of medical fees.” Unquestionably, the national budget allocated to medical services is limited, and state finance is critical due to long-standing economic stagnation. If such uncontrolled increases in the number of imaging examinations continue, the government would reasonably be tempted to cut the budget for diagnostic imaging uniformly. Indeed, fees for CT and MRI examinations have been repeatedly cut at each revision of fees for medical services. However, many studies in Japan and abroad have demonstrated that the policy to reduce reimbursement of medical fees universally is a double-edged sword that ironically

invites increases in medical costs by provoking demand.[8-10)] In Japan, such uniform reduction of fees for examinations and drugs is accompanied by the risk of promoting excessive use of drugs and diagnostic tools, including CT. If wasteful medical expenditures are difficult to eradicate in Japan, the medical administration may be caught in the “trap of cost increases due to uniform control of medical fees.” In taking measures to improve the efficiency of medical services, it is necessary to evaluate the causes of the excessive use of drugs and diagnostic devices as mentioned above and to remove fundamental reasons. In advanced countries such as Japan, the days when the efficiency of medical services was measured simply in terms of quantity are gone. We are in the era of quality-oriented assessment of medical services. Regarding radiological and medical services, policies ensure the highest payment when: (1) based on appropriate testing indications, (2) a roadmap to mildly invasive and accurate diagnoses with minimum radiation exposure is drawn by a specialist in diagnostic imaging; (3) a suitable system that has undergone quality control (QC) is used to (4) perform testing based on an appropriate testing plan; (5) a qualified diagnostic radiologist performs an appropriate diagnosis; (6) treatment is administered based on that diagnosis; and (7) the patient is rehabilitated through the shortest process possible. This will likely require a redistribution of healthcare resources to provide appropriate incentives for such practices.

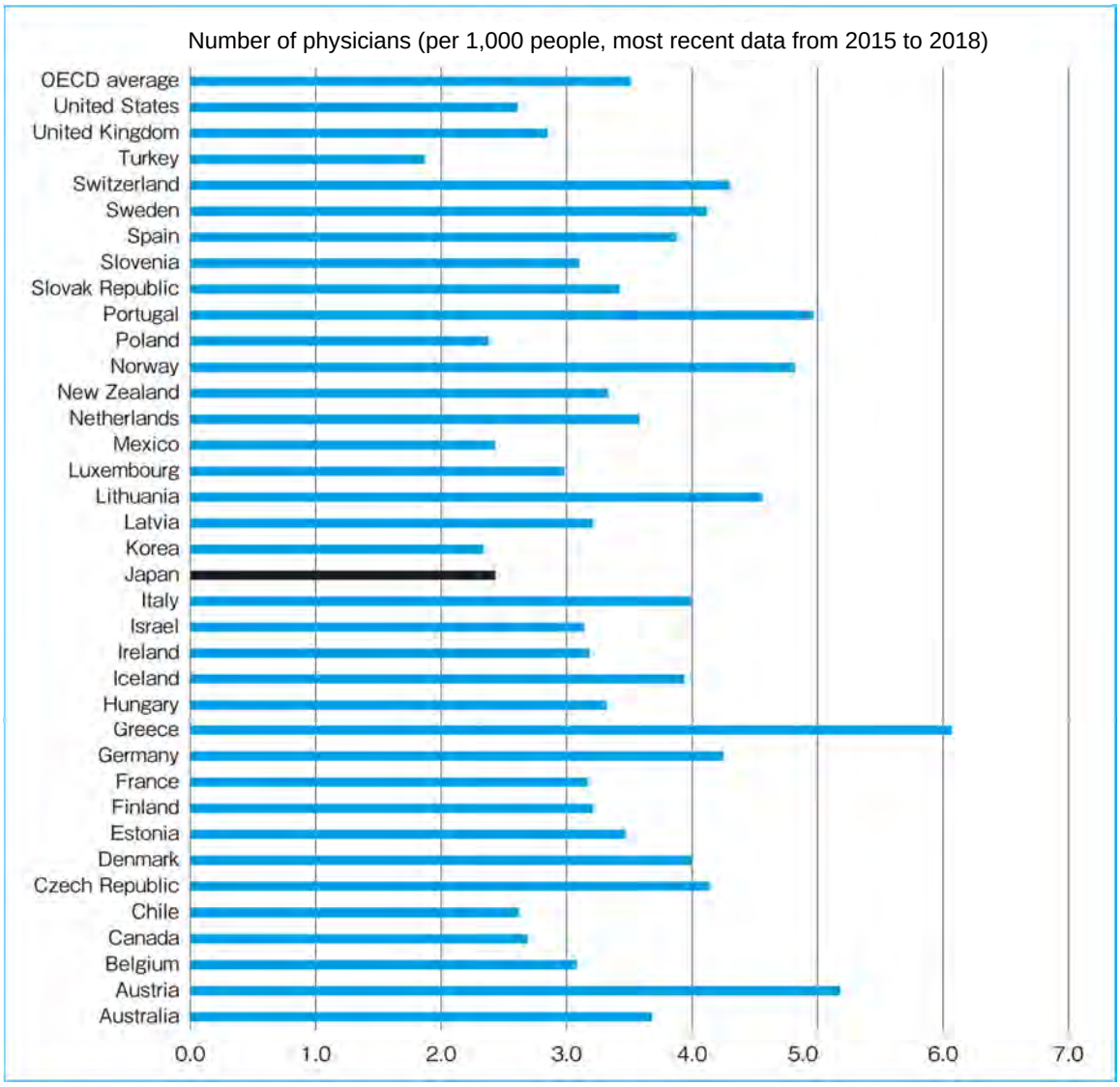

Figure 6. Number of physicians per 1,000 people (OECD Health Statistics 2018 or most recent data)

Excessive examinations and increases in medical radiation exposure

The proper use of diagnostic imaging by physicians is highly desirable from the perspective of the diagnostic radiologist. Needless to say, the use of radiation, particularly in CT, has contributed significantly to improving the public's health. However, the overuse of radiation for the aforementioned reasons and tests performed using obsolete imaging systems or based on flawed testing plans may also have adverse effects on healthcare. An article by de González et al. published in *The Lancet* in 2004 showed that diagnostic X-ray use in Japan was the highest among OECD-member nations, and that the risk of developing cancer was also increased.[11)] The article received front-page newspaper coverage,[12)] causing anxiety about medical radiation exposure in members of the public. In response to the public's reaction, a symposium on medical radiation exposure was held at the 63rd General Conference of the Japan

Radiological Society in 2004. The results were summarized in the chairperson's statement.[13] Following the Fukushima nuclear power plant accident in Japan, the public's concern about the health hazards of low-dose radiation exposure increased further. Consequently, with the assistance of international institutions and organizations, diagnostic reference levels (DRLs) for optimizing radiological protection in medicine were released to the public in 2015 to implement evidence-based radiation protection.[14] The establishment of DRLs by countries is now becoming a requirement of medical radioprotection internationally. In 2017, the Science Council of Japan (Radiology and Clinical Testing Subcommittee of the Clinical Medicine Committee) published proposals to reduce medical radiation exposure from CT tests. The points raised expanded on the 2004 statement of the Japan Radiological Society and advocated for the following. A redoubling of our constant effort is needed to bring about these changes.

(1) To monitor the status of CT practice in Japan and facilitate the use of DRLs

(2) To promote radiation protection training

(3) To clarify the indications for CT examinations

(4) To develop low-radiation-dose, high-performance CT systems to replace conventional ones

Conclusion

Medical services in Japan, which appear to be making considerable achievements at a low cost, also have weak areas and may be improved further by their correction. If radiological and medical services account for a large part of this inefficiency, we are bound to be more serious about improving the situation.

Secondary source materials used as references

1) Ministry of Health, Labour and Welfare, Health Policy Bureau: International Comparison of Hospital Bed Counts in ICUs, etc. (https://www.mhlw.go.jp/content/10900000/000627782.pdf), 2020.
2) OECD Health Statistics (https://stats.oecd.org/index.aspx?DataSetCode=HEALTH_STAT).
3) Japan Hospital Association, All Japan Hospital Association, Japanese Association of Medical care Corporations: Emergency survey on the status of hospital management with the spread of COVID-19 (bulletin), May 18, 2020 (http://www.hospital.or.jp/pdf/06_20200518_01.pdf), 2020.
4) Central Social Insurance Medical Council: 427th general meeting data: Medium-term outlook for the medical engineering equipment market and manufacturer market share by function, 2019.
5) Ministry of Health, Labour and Welfare: 2018 Physician, Dentist, and Pharmacist Statistics (https://www.mhlw.go.jp/toukei/list/33-20c.html), 2019. (https://www.mhlw.go.jp/toukei/list/33-20c.html), 2019.
6) Japan Council for Quality Health Care: Project to Collect Medical Near-Miss/Adverse Event Information, Medical Safety Information No. 138: Inadequate Checks Concerning Diagnostic Imaging Reports (2nd Follow-up Report), 2018.
7) National University Radiation Division Meeting, Medical Safety Subcommittee: 2019 Medical Safety Subcommittee Survey Report (1), 2019.
8) Hsiao WC: "Marketization" - the illusory magic pill. Health Econ 3: 351-357, 1994.
9) Grytten J, et al: Supplier inducement in a public health care system. J Health Econ 14(2): 207-229, 1995.
10) Yamada T: Examination of the physician-induced demand hypothesis using national health insurance payment data. Quarterly of Social Security Research 38(1): 39-51, 2002.
11) de González AB, Darby S: Risk of cancer from diagnostic X-rays: estimates for the UK and 14 other countries. Lancet 31: 345-351, 2004.
12) Diagnostic Radiation Exposure the Cause in 3.2% of Cancer, Yomiuri Shimbun, February 10, 2004, page 1, 2004.

13) Sasaki Y: Considering CT radiation exposure and carcinogenesis: What those involved with radiation in Japan ought to do. New Medicine in Japan 31(9): 45-48, 2004.
14) Diagnostic Reference Levels Based on Latest Surveys in Japan (http://www.radher.jp/J-RIME/report/DRLhoukokusyo.pdf). (for the new report; http://www.radher.jp/J-RIME/report/japanDRL2020_jp.pdf).

4 Contrast Media Safety

Summary of the 2018 Guidelines on the Use of Iodinated Contrast Media in Patients with Kidney Disease

Introduction

Diagnostic imaging using iodinated contrast media is an essential type of test in routine clinical practice and yields an abundance of useful information. However, the use of contrast media in patients with decreased renal function carries a risk of contrast-induced nephropathy (CIN), making guidelines for such use necessary. Consequently, the 2012 Guidelines on the Use of Iodinated Contrast Media in Patients with Kidney Disease were jointly published by 3 academic societies: the Japan Radiological Society, which represents the specialists who use contrast media; the Japanese Circulation Society; and the Japanese Society of Nephrology, which represents the specialists who treat kidney disease.[1)]

Although the guidelines have been widely used, a number of new study results were reported 5 years after the guidelines were published. In addition, contrast-related guidelines in Europe and the United States were revised, and the 2016 Kidney Disease: Improving Global Outcomes (KDIGO) Clinical Practice Guideline for Acute Kidney Injury (AKI) was published for kidney disease that meets the diagnostic criteria for AKI.[2)] Consequently, the 3 Japanese societies jointly revised their previous guidelines and released the 2018 Guidelines on the Use of Iodinated Contrast Media in Patients with Kidney Disease.[3)]

Because the previous version of the guidelines, published in 2012, were developed according to the methods recommended in the 2007 edition of the MINDS guidelines, any revisions of the previous CQs were developed according to the methods recommended in those guidelines. Some CQs and newly added CQs were developed according to the methods recommended in the 2014 and 2017 editions of the Minds Manual for Guideline Development.[4,5)] Consequently, it should be kept in mind that the 2018 guidelines use a mix of 2 types of evidence and methods of assessing recommendations.

This document excerpts and lists strongly radiology-related CQs and their answers from the 2018 Guidelines on the Use of Iodinated Contrast Media in Patients with Kidney Disease.

Definition of contrast-induced nephropathy

○ **How is contrast-induced nephropathy (CIN) diagnosed?**

CIN is generally diagnosed if the serum creatinine (SCr) level increases by ≥ 0.5 mg/dL or ≥ 25% from the previous level within 72 hours after administration of an iodinated contrast medium. Because CIN is a type of AKI, it is also evaluated using the diagnostic criteria for AKI. Based on the KDIGO diagnostic criteria for AKI, CIN is diagnosed in the following cases: the SCr level increases by ≥ 0.3 mg/dL from the previous level within 48 hours after iodinated contrast medium administration; the SCr level increases ≥

1.5-fold from a baseline value determined within the previous 7 days or the predicted baseline value; or urine volume decreases to < 0.5 mL/kg/h for 6 hours.

Rather than remaining constant, renal function is affected by diet, exercise, and changes in body fluid volume, and drugs that inhibit renal tubular secretion of creatinine increase the SCr level. In addition, increased SCr levels are seen due to creatinine absorption resulting from the ingestion of cooked meat and supplements that contain creatinine. Consequently, the following points should be kept in mind.

(1) Diurnal variations in SCr levels of approximately 10% may occur.
(2) SCr levels increase with vigorous exercise or ingestion of large amounts of meat and decrease when protein intake is restricted.
(3) Cimetidine and trimethoprim may reduce renal tubular creatinine excretion and increase SCr levels.

Risks and patient evaluations

(1) Are patients with chronic kidney disease (CKD) at increased risk of CIN?
CKD (eGFR < 60 mL/min/1.73 m^2) is a risk factor for CIN. However, the risk of CIN varies depending on the route of contrast medium administration and the patient's condition.

(2) Does aging increase the risk of CIN?
Aging is a CIN risk factor.

(3) Does diabetes mellitus increase the risk of CIN?
Diabetes mellitus with CKD (eGFR < 60 mL/min/1.73 m^2) is a risk factor for CIN. However, whether diabetes mellitus in the absence of CKD is a CIN risk factor is unclear.

(4) Does continued use of a diuretic increase the risk of CIN?
It is unclear whether continuing to take an oral diuretic increases the risk of CIN.

(5) Does the prophylactic use of a diuretic increase the risk of CIN?
The prophylactic use of a diuretic does increase the risk of CIN and is therefore not recommended.

(6) Does biguanide increase the risk of lactic acidosis?
A transient decrease in renal function resulting from administration of an iodinated contrast medium poses a risk of lactic acidosis. If an iodinated contrast medium is administered, it is recommended that appropriate measures, such as temporarily withdrawing biguanide antidiabetic drugs, be taken after considering the CIN risk, except during an emergency test.

(7) Is the risk of CIN increased by having a single kidney?
The evidence that having a single kidney increases the risk of CIN as compared with having 2 kidneys is unclear.

Types of contrast media

(1) Is there a difference between iso-osmolar and low-osmolar contrast media with respect to the risk of CIN?

No difference has been seen between iso-osmolar and low-osmolar contrast media with respect to the frequency of CIN.

(2) Are there differences between different types of low-osmolar contrast media with respect to the risk of CIN?

Although no definite conclusions have been drawn regarding the risk of CIN with different types of low-osmolar contrast media, no differences in CIN frequency have been reported to date.

(3) Does invasive contrast medium administration (intraarterial) increase the risk of CIN more than non-invasive administration (intravenous)?

There is currently no evidence that intraarterial contrast medium administration is an independent risk factor for CIN. However, there have been many reports of a higher incidence of CIN with invasive (intraarterial) administration than with non-invasive (intravenous) administration. Because differences in the patients' underlying diseases (e.g., diabetes mellitus and chronic nephropathy) may be behind these reports, careful administration that takes into account factors such as the patient's underlying disease is required, particularly when performing invasive (intraarterial) administration.

Testing and treatment with intraarterial contrast media administration

(1) How can one differentiate between decreased renal function caused by CIN and that caused by cholesterol embolization?

Although decreased renal function caused by CIN can usually be differentiated from that caused by cholesterol embolization based on symptoms and test findings, such differentiation can occasionally be difficult.

(2) Does CIN increase cardiovascular events?

The incidence of cardiovascular events is high in patients with CIN.

Tests using intravenous contrast media administration

(1) Is there an increased risk of CIN resulting from contrast CT in CKD patients?

The likelihood of CIN occurring after contrast medium administration is low in CKD patients with an eGFR $\geq$ 30 mL/min/1.73 m^2. Even with an eGFR $\geq$ 30 mL/min/1.73 m^2, however, it is important to thoroughly evaluate CIN risk factors. When performing contrast CT in a CKD patient with an eGFR < 30 mL/min/1.73 m^2, it is recommended that considerations such as the risk of CIN be explained to the patient and that appropriate precautions be taken as necessary.

(2) Is there an increased risk of CIN resulting from contrast CT in intensive care patients or patients receiving emergency outpatient care?

There is little evidence of an increased risk of CIN resulting from contrast CT in intensive care patients or patients receiving emergency outpatient care. However, these patients have a high risk of AKI regardless of whether they are administered a contrast medium. It is therefore recommended that such patients be given a thorough explanation regarding AKI and CIN and that appropriate precautions be taken when contrast CT is performed.

(3) Does reducing the dose of contrast medium used in contrast CT reduce the risk of CIN?

Reducing the dose of contrast medium used in contrast CT may reduce the risk of CIN. Particularly in patients at high risk of CIN, use of the lowest dose of contrast medium that will preserve diagnostic performance is recommended.

(4) Is there a recommended imaging method to use when the dose of contrast medium used in contrast CT is reduced

When the contrast medium dose is reduced, it is recommended that low-tube-voltage imaging and iterative reconstruction be used in combination in facilities where this is possible.

(5) Does repeating contrast CT testing in a short period of time increase the risk of CIN?

Repeating contrast CT in a short period of time (24 to 48 hours) is not recommended because the risk of CIN may increase.

Preventing CIN: fluid infusion

(1) Is physiological saline administration recommended to prevent CIN?

Administering physiological saline intravenously before and after a contrast study is recommended to prevent CIN in patients with CKD, who are at risk of CIN.

In terms of effectiveness in preventing CIN, a 0.9% physiological saline solution, which is an isotonic infusion, is superior to 0.45% physiological saline, a hypotonic infusion. Consequently, the use of an isotonic infusion is recommended.

(2) Is drinking water recommended to prevent CIN?

There is insufficient evidence regarding whether drinking water alone has an inhibitory effect on CIN comparable to that of intravenous fluid infusion. To prevent CIN, substantial measure such as fluid infusion is recommended more highly than hydration with drinking water alone.

(3) Is sodium bicarbonate (baking soda) administration recommended to prevent CIN?

Because sodium bicarbonate (baking soda) administration may inhibit CIN, administration of baking soda solution is recommended when infusion time is limited. When administering sodium bicarbonate (baking soda), use an isotonic preparation.

Preventing CIN: hemodiafiltration

○ Is hemodiafiltration recommended after contrast medium administration to prevent CIN?

The use of hemodiafiltration after contrast medium administration to prevent CIN does not reduce the risk of CIN and is therefore not recommended. It is particularly recommended that hemodialysis not be performed.

Treatment of CIN

(1) Is administration of a loop diuretic recommended to treat CIN?

The evidence that loop diuretic administration to treat CIN inhibits the progression of renal dysfunction is weak, and such administration may instead be deleterious. It is therefore not recommended.

(2) Is fluid therapy recommended to treat CIN?

Fluid therapy to treat CIN is not recommended except when a decrease in body fluid volume is seen.

(3) Is acute blood purification therapy recommended to treat CIN?

There is no evidence that acute blood purification therapy administered after the onset of CIN improves the prognosis of renal function. It is therefore not recommended to improve the prognosis of renal function.

Acute blood purification therapy is strongly recommended as a lifesaving measure if the patient's general condition is strikingly poor as a result of abnormal fluid volume or an electrolyte or acid-base imbalance. This is not limited to AKI resulting from CIN. The timing of the start of blood purification therapy should be determined after broadly considering the patient's clinical status and pathophysiology.

Secondary source materials used as references

1) Japanese Society of Nephrology, et. al., Ed: 2012 Guidelines on the Use of Iodinated Contrast Media in Patients with Kidney Disease. Tokyo Igakusha, 2012.
2) Acute Kidney Injury (AKI) Clinical Practice Guidelines Committee, Ed: 2016 AKI Clinical Practice Guidelines. Tokyo Igakusha, 2016.
3) Japanese Society of Nephrology, et. al., Ed: 2018 Guidelines on the Use of Iodinated Contrast Media in Patients with Kidney Disease. Tokyo Igakusha, 2018.
4) Fukui T, Yamaguchi N, Ed.-in chief; Morizane T, Ed.: Minds Manual for Guideline Development 2014. Igaku-Shoin Ltd., 2017.
5) Kojimahara N, et al., Ed.: Minds Manual for Guideline Development 2017. Japan Council for Quality Health Care, 2017.

5 Effects of Medical Radiation Exposure in Diagnostic Imaging and of Electromagnetic Fields in MRI

Introduction

Because ionizing radiation and electromagnetic fields (nonionizing radiation) have biological effects, diagnostic imaging is a medical practice associated with invasiveness. All healthcare practitioners should recognize this and perform these tests with the aim of maximizing their benefits for the patient.

Medical radiation exposure in diagnostic imaging

1. Fundamental views

Because the ionizing radiation used in diagnostic imaging has biological effects, the appropriate principles of radiological protection must be strictly adhered to, even though the purpose of the testing is its effective medical use. The 3 principles of radioprotection are justification, optimization, and dose limit. However, setting dose limits for patients could constrain radiological and medical services by, for example, limiting testing and interventional radiology (IVR) procedures, thereby undermining the benefits to the patient. Consequently, radiological protection is addressed based on the principles of justification and optimization.[1)] Moreover, the physician bears responsibility for the practice of radiological and medical services and is therefore obligated to ensure safety. The Enforcement Regulations on the Medical Care Act (Order of the Ministry of Health and Welfare), the revision of which went to effect in April 2020, requires each facility with X-ray systems to formulate policies for the safe use of radiation for patients and to strengthen its safety management. Stronger steps need be taken to address radiation safety, using for reference the Guidelines for Safety Management Systems Concerned with Radiation for Medical Use and Reference Material for Guidelines on the Safe Use of Radiation for Medical Use, which were published by the Japanese Society of Radiation (http://www.radiology.jp/member_info/guideline).

The justification principle in radiation medicine means that the benefits obtained from radiation use outstrip the risks of radiation exposure. The optimization principle means that unnecessary radiation exposure is avoided during justified uses of radiation medicine, that the doses used ensure maximum benefit to the patient, and that this takes place in an environment that fosters a culture of safety.

Methods of justification and optimization in diagnostic imaging are described in specific terms below. To justify exposing a patient to radiation, an indication for testing or IVR is needed, and the patient’s consent must be obtained. Optimization means ensuring that imaging radiation doses and radiopharmaceutical doses take into account the diagnostic reference levels (DRLs) (www.radher.jp/J-RIME/report/JapanDRL2020_jp.pdf) indicated for each clinical practice guideline or

procedure and maximize the benefit to the individual patient. The procedures for managing patient radiation exposure in accordance with these principles are (1) to (4) below (Fig. 1).

(1) Conclude that a radiological test or IVR, such as CT or nuclear medicine, is medically essential.
(2) Based on the medical records, confirm that the procedure does not duplicate another procedure.
(3) The patient understands the need for the test or IVR and consents to it.
(4) The test is performed using imaging conditions and a dose appropriate to the circumstances of the individual patient.

Needless to say, these points are premised on the performance of quality assurance/quality control (QA/QC) for the system, with the assistance of radiology technologists. When attempting to reduce the radiation dose, one should pay attention to ensuring that lesions are well visualized and that the image quality is such that it does not place undue demands on the diagnostic radiologist, who performs many diagnostic imaging studies on a daily basis. In addition, if the radiopharmaceutical used in a nuclear medicine test is excreted through the urinary tract, encouraging the patient to urinate frequently will directly reduce the patient's radiation dose.

2. Classifications of radiation exposure

In the field of radioprotection, radiation exposure is classified as medical, occupational, and public exposure. In addition to the exposure of the patient himself or herself, which was discussed in the preceding paragraph, medical radiation exposure includes the exposure of family members and caregivers as a result of providing care for a patient and the exposure of subjects who volunteer for biomedical research. Although no regulatory dose limits for medical radiation exposure have been established, a dose of ≤ 5 mSv during a single treatment period has been indicated in notifications as a reference standard for those who provide care for patients.[2)] Although such reference levels are referred to collectively as dose constraints, they lack the enforceability of dose limits. Dose constraints can be determined to suit the circumstances of the individual. For example, when considering the return home of a pediatric patient who has received internal radiation therapy, consideration of the patient's mental anxiety from spending time separated from family members should take precedence over ensuring strict compliance with the dose constraints for the family members.

Volunteers for biomedical research are essential for the advancement of medicine. During drug development, the pharmacokinetics of the drug must be understood, and when a diagnostic imaging system is developed, it is finally evaluated by imaging volunteers. When a study is begun, effort is made to ensure not only compliance with clinical ethics, but also to ensure that the principles of justification and optimization are adhered to in using radiation. Although dose constraints have not been specifically defined, it would be desirable for the Japan Radiological Society to formulate a radioprotection proposal for diagnostic imaging based on the proposal set forth for the radioprotection of biomedical research volunteers

by the Radiological Protection Committee of the Japanese Society of Nuclear Medicine (http://www.jsnm.org/archives/649). The targets are generally participants in clinical trials, clinical studies, and clinical research in patients. However, when used to compare accuracy with that of other new testing methods, in addition to dose controls, specific limits on the number of tests (number of subjects) are needed. For studies involving healthy volunteer subjects, the ages of the participants and their previous participation in studies must be taken into account. The use of pregnant women and children as subjects should be avoided unless absolutely necessary. When the subjects are volunteer patients, testing should be limited to methods that are expected to directly or indirectly benefit the individual participants.

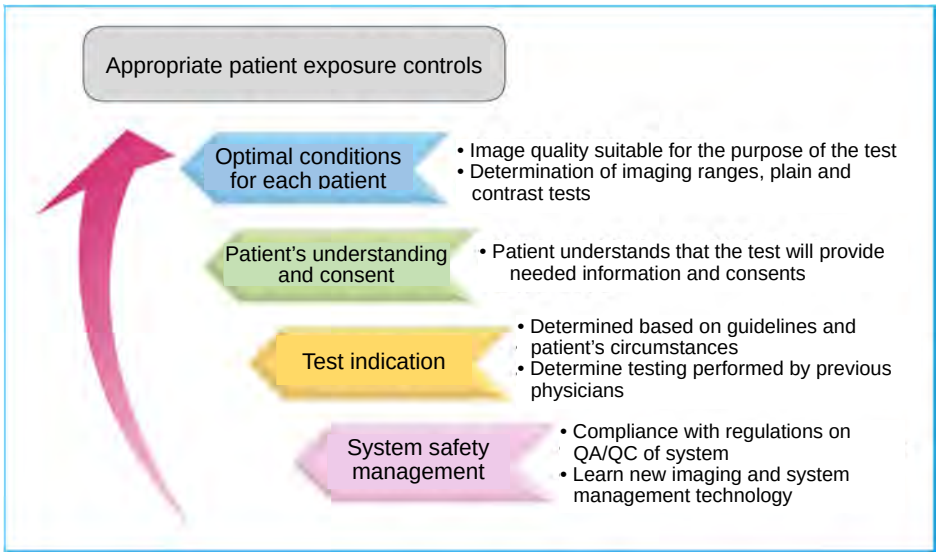

Figure 1. Principles of medical radiation exposure management

The optimal dose for lesion detection and disease treatment is managed for each patient. It is important to train healthcare staff to be able to implement these steps with an awareness of radiation safety.

3. Dose evaluation

To evaluate the dose of medical radiation exposure in diagnostic imaging, the index generally used for each testing method is used. For general imaging and fluoroscopy, the entrance surface dose for the patient's skin (units: mGy) is used. For CT, the CT dose index volume (CTDIvol, units: mGy) and dose length product (DLP, units: mGy·cm) are used. In nuclear medicine, the administered radioactivity dose (units: MBq) is used. In nuclear medicine, the dose can be determined before testing. However, it is difficult to measure radiographic indices for each patient. Consequently, in compliance with the medical safety quality controls and training stipulated in the Enforcement Regulations on the Medical Care Act, the accuracy of the index values displayed by systems is ensured through periodic training in dose measurement using the established methods and in operating skills.[3)]

If radiation exposure from a radiation source will occur, the effective dose used in radiological protection is evaluated in advance at the planning stage and used for safety considerations. It is also used as a regulatory value, such as a dose limit, to determine whether safety was ensured after the plan was

implemented. However, although the International Commission on Radiation Protection (ICRP) recommends using the effective dose as the basic radiation protection dose, it has also stated that it should not be used to retrospectively estimate the risk of probabilistic effects for specific individuals or for epidemiological evaluation of physical exposure.[1)] The biggest reason for this is that the risk of carcinogenic probabilistic effects, which is the basis of the tissue weighting factor, largely depends on age and sex. To evaluate medical exposure risk, use of the doses absorbed by the individual tissues and organs (units: Gy) that are irradiated has been proposed. Although the effective dose is easy to determine and has been used in many medical reports that compare doses, its accepted use in medicine is limited to evaluations in the following cases: (1) a different diagnostic test or IVR procedure is used; (2) a similar technology or procedure is used in a different hospital or country; or (3) different technologies are used for the same medical test. The fact that cancer risk depends largely on age and sex also must be considered in these cases. After the accident at the Fukushima Daiichi Nuclear Power Plant, the mass media reported the results of various tests using the effective dose and often erroneously compared it with the exposure dose of residents, which created confusion among patients. Rigor therefore needs to be applied when using the effective dose.

Effects of electromagnetic fields in MRI

With MRI, the effects of static magnetic fields and electromagnetic radiation are taken into account. In environments with extremely strong static magnetic fields, symptoms such as erythrocyte deformation and, in individuals who move back and forth between locations with electromagnetic radiation, lightheadedness occur. However, these changes do not occur with the use of systems with a magnet strength ≤ 3 T, which are the systems used in routine medical care. The specific absorption rate (SAR) is considered an effect of the electromagnetic radiation in MRI. The SAR refers to the radiofrequency power that is absorbed by the body per unit mass (W/kg), and it is associated with increases in core temperature. It is proportional to the square of the magnetic field strength, the square of the high-frequency magnetic field strength, the radiofrequency (RF) pulse duty cycle, the square of the radius of the cross-section of the patient, and the electrical conductivity of tissues (largely affected by the brain, blood, liver, and cerebrospinal fluid, slightly by adipose tissue and bone marrow). As in the case of the absorbed dose for X-ray examinations, the SAR is an index than cannot be measured in the course of routine medical care. It is therefore determined using the operating modes that are displayed by the system for each imaging condition and guaranteed by the manufacturer (normal, the first-level controlled, and second-level controlled operating modes). The standard is to use imaging conditions within the normal operating mode to ensure safety and allow no possibility of causing physiological stress to the patient. However, when a system ≥ 3 T is used and image quality is sought, the first-level controlled operating mode, which is defined as a mode that could cause extreme physiological stress in the patient, may easily be reached. This is addressed by considering what is clinically necessary and changing the imaging condition settings so that, for example, the smallest possible flip angle (FA) is used, the number of slices is limited, and the repetition time (TR) is increased.

For MRI examinations in pregnant women, the possible developmental effects of increasing SAR, such as developmental delay in the fetus, are considered, rather than the risk of pediatric cancer or teratogenicity, as in the case of ionizing radiation. However, there have been almost no findings that provide a basis for determining safety and risk with systems of ≤ 4 T.[4] Consequently, the view of the Japanese Society for Magnetic Resonance in Medicine is that, if nonionizing radiation imaging other than MRI (ultrasound) is considered inadequate, and MRI testing is considered so essential that it is used as an alternative to ionizing radiation imaging (e.g., X-ray and CT), then there is no obstacle to performing MRI in pregnant women. When an MRI test is medically necessary, it is performed after it has been confirmed that the patient has been given accurate information about the test and has agreed to it.

MRI carries a risk of burns resulting from conduction currents (eddy currents) on the body surface, and steps must therefore be taken to avoid creating a circuit (loop) that facilitates current flow. When water from sweating functions as a conductor, burn incidents have been reported in which the cause was resistance to conduction currents (eddy currents) that occurred as a result of point contact of the bore, coil, or part of the subject's body. Thus, a lack of knowledge regarding the electromagnetic field environment often leads directly to a medical accident. Engaging in continuous training that, as part of the education and training stipulated in the Enforcement Regulations on the Medical Care Act, emphasizes safety so that precautions are taken when a system is operated is the most effective means of avoiding the effects of electromagnetic radiation.

All healthcare practitioners must recognize the risks of core temperature increases and eddy current formation on the body surface that are associated with the electromagnetic field of MRI, and exercise judgement that conforms to the diagnostic radiology principles of justification and optimization for imaging conditions that exceed those of the normal operating mode.

Conclusion

The use of radiation and radioactive materials has contributed to advances in fields ranging from medicine to manufacturing to agriculture. These are the results of effectively using the properties of radiation that give it its ability to sterilize, alter the links between molecules, induce cellular mutagenicity, and damage tissue. When using it, however, effort must be made to use it safely by taking appropriate radiation protection measures based on the knowledge that radiation and radioactive materials are carcinogenic in humans.[1]

Secondary source materials used as references

1) Japan Radioisotope Association, Ed.: Radiation protection in medicine. ICRP Publication 105, 2011.
2) Health Policy Bureau Guidance No. 1108-2: Concerning the departure of patients administered radiopharmaceuticals, 2010.

3) Health Policy Bureau Guidance 0612, Health Policy Bureau Notification 0612-1: Important points for operations involved in ensuring the safety of medical devices, 2018.
4) ACOG committee on obstetric practice: ACOG committee opinion: No 723, 2017 Guidelines for diagnostic imaging during pregnancy and lactation. Obstant Gynecol 130: e210-e216, 2017.

6 The Medical Accident Investigation System and Radiological and Medical Services

Introduction

The Medical Accident Investigation System was included in the revised Medical Care Act as a measure to prevent medical accidents and took effect in October 2015. When an accident occurs, the medical institution carries out an internal investigation and reports the accident to the Medical Accident Investigation and Support Center, a private third-party agency. The center then performs a case analysis and conducts an investigation to prevent recurrence. The center forms technical analysis committees to address the various circumstances that cause in-hospital deaths, organizes and analyzes accident information, and prepares written proposals for prevention of recurrence of medical accidents. As of 2020, the center had published recommendations for 12 items (Table 1). One such set of proposals, based on an analysis of deaths related to diagnostic imaging in emergency medicine, was compiled as proposal set no. 8 in April 2019.[1)] In the present document, that proposal is analyzed from the perspective of a radiologist. There is also an additional note regarding radiological and medical services other than emergency diagnostic imaging, especially interventional radiology (IR), which is related to the Medical Accidents Investigation System.

Table 1. Proposals for prevention of recurrence of medical accidents

No. 1	Analysis of deaths related to complications of central venous puncture: Part 1
No. 2	Analysis of deaths related to acute pulmonary thromboembolism
No. 3	Analysis of deaths related to injection-induced anaphylaxis
No. 4	Analysis of deaths related to early post-tracheotomy dislodgement or aberration of a tracheostomy tube
No. 5	Analysis of deaths related to laparoscopic cholecystectomy
No. 6	Analysis of deaths related to nasogastric intubation performed for nutrient administration
No. 7	Analysis of deaths related to non-positive pressure ventilation (NPPV) and tracheostomy positive-pressure ventilation (TPPV) in general and long-term care units
No. 8	Analysis of deaths related to diagnostic imaging in emergency medicine
No. 9	Analysis of deaths related to head injuries caused by falls occurring during hospitalization
No. 10	Analysis of deaths related to pretreatment for procedures such as colonoscopy
No. 11	Analysis of deaths related to liver biopsy
No. 12	Analysis of deaths related to thoracentesis

Proposals based on analysis of deaths related to diagnostic imaging in emergency medicine

The analysis included 12 patients who were concluded to have died without having undergone proper diagnostic imaging and interpretation or having received an appropriate clinical decision. They were among 15 patients whose deaths were suspected of being related to emergency diagnostic imaging and whose cases were analyzed in detail. These 15 patients were selected from 851 hospital internal investigation

reports filed between October 2015 and October 2018. The analysis results were compiled as 6 proposals (Table 2).

Table 2. Proposals based on an analysis of deaths related to diagnostic imaging in emergency medicine

Proposal 1	Significance of imaging procedures in emergency medicine and key findings
Proposal 2	Information-sharing when an imaging procedure is requested
Proposal 3	Checking images acquired for emergency outpatient care
Proposal 4	Additional imaging procedures and judgments regarding hospitalization or returning home
Proposal 5	Checking diagnostic imaging reports and incidental findings
Proposal 6	Establishing adequate in-hospital systems

1. Specific proposals and their explanations

(1) Proposal 1: Significance of imaging procedures in emergency medicine and key findings

With emergency medicine imaging procedures, interpreting radiographic images with urgent, life-threatening diseases (killer diseases) in mind is more important than making a definitive diagnosis. Pay particular attention to imaging findings of slight bleeding due to a head injury, impending rupture of aortic aneurysm and aortic dissection, and the appearance of free gas from intestinal perforation.

Diagnostic radiologists are required to detect subtle findings of the killer diseases mentioned above. Image interpretation during an emergency requires a proactive approach to detecting such findings, regardless of the clinical presentation. It requires recognizing that detecting killer diseases outside the purview of the attending physician is the responsibility of the diagnostic radiologist.

(2) Proposal 2: Information-sharing when an imaging procedure is requested

Physicians who request imaging procedures should share information with radiology technologists and radiologists by clearly indicating on the request form about the patient's clinical symptoms and suspected disorder and any specific disorders they wish to rule out.

Although this proposal is mainly concerned with sharing information with radiology technologists, it also applies to radiologists responsible for emergency image interpretation. Naturally, information-sharing does not mean a unidirectional flow of information from the attending physician to the radiology department. It also requires radiologists to convey information about highly urgent findings. In addition, the following points must be confirmed: that the images have subsequently been examined in detail, such as on the following morning; and a final diagnostic imaging report has been prepared and that information on any incidental findings of the type referred to in proposal 5 has been shared.

(3) Proposal 3: Checking images acquired for emergency outpatient care

Not just the attending physician, but rather multiple physicians, including senior staff and radiologists, check the images from their own perspective and share information on the findings. If a radiology technologist can detect urgent findings during the radiological procedure in an emergency outpatient clinic,

he or she promptly provides this information to the interpreting physician. Using information communication technology (ICT) to obtain interpretations from outside radiologists is also useful.

In relation to this proposal, there have been cases in which a radiologist in an outside hospital was not notified despite the presence of a remote diagnosis system for emergency image interpretation in the hospital, and an important finding was overlooked as a result. Remote diagnosis systems have begun to be adopted by medical institutions, along with a lack of familiarity with such systems. Cases have been reported in which the radiologist, who is normally busy with interpretations in daily work, was not contacted out of a reluctance to wake him or her up late at night with an interpretation request. To avoid this systemic error, both the emergency physician and the hospital should understand that mistakes in emergency diagnostic imaging carry a significant risk of medical accidents. The radiologists have an important role in making the hospital system work.

(4) Proposal 4: Additional imaging procedures and judgments regarding hospitalization or returning home

If killer diseases cannot be ruled out based on the initial imaging procedure, additional procedures such as non-contrast CT and contrast CT are performed. Continue with adequate imaging diagnosis until such diseases are definitively ruled out. It is important that healthcare personnel share information on any symptoms observed during this time.

In the emergency care setting, it is recommended that having a single individual decide whether a patient should return home be avoided to the extent possible and that a radiologist be consulted about imaging. There have been 2 cases in which new findings emerged after the patient was sent home, but unfortunately the information was not shared, resulting in the patient's death. These cases showed the importance of information-sharing among healthcare personnel, particularly the importance of radiologists sharing information with attending physicians.

(5) Proposal 5: Checking diagnostic imaging reports and incidental findings

An individual is designated to take responsibility for ensuring that the diagnostic imaging reports that are prepared following emergency care can be checked. With regard to abnormal findings detected incidentally in testing not performed as the initial test (incidental findings), it is important that those that need to be addressed by the attending physician be communicated by a radiologist.

In 2018, cases in which lung cancer was missed because diagnostic imaging reports were neglected stirred controversy and prompted discussions about creating report-checking systems. In 2 of these emergency cases, reports that were issued at a later date had not been shared. Details regarding report-checking will be left to other articles. However, in the emergency medicine setting, radiologists need to adopt a posture of actively sharing information.

(6) Proposal 6: Establishing adequate in-hospital systems

The following systems are established: a system of training in the differentiation of killer diseases in emergency medicine; a support system for attending physicians working in emergency medicine; and a system that can ascertain whether diagnostic imaging reports that contain important findings are checked and the response to such reports. It is hoped that these systems will foster a culture in which all healthcare personnel are proactively involved in the safety of imaging procedures and accurate diagnosis.

This proposal and proposal 1 are the most important proposals. Based on a thorough understanding of the fact that emergency medicine is an extremely busy environment where important imaging findings can easily be overlooked, medical, radiology, medical information, and medical safety departments need to collaborate in establishing systems suitable for the circumstances at each facility.[2)]

2. Expectations (suggestions) for organizations such as academic societies and companies

These proposals include requests for support and leadership from organizations such as academic societies and companies with respect to the challenges related to emergency diagnostic imaging that medical institutions address. First, with regard to training in emergency diagnostic imaging, the involvement of the Japan Radiological Society and Japanese Association for Acute Medicine is needed in sharing the importance of emergency diagnostic imaging and promoting training in this area. In the area of undergraduate education, the Ministry of Education, Culture, Sports, Science and Technology needs to add training in explaining imaging findings that involve killer diseases to the learning objectives for diagnosis and treatment using radiation of its medical education model and core curriculum. In addition, as a safety measure for electronic medical records systems, a mechanism for checking diagnostic imaging reports needs to be made a standard feature. Finally, progress in developing diagnostic imaging support systems using artificial intelligence, an examination of the effectiveness of emergency interpretation by diagnostic radiology specialists, and a move toward revising medical fees are recommended. Several reports have summarized how clinical decisions for acute abdomen have changed based on a radiologist's CT report.[3-5)] Amid the demand for value-based medicine, it is hoped that the importance of emergency diagnostic imaging, in the sense that it increases the value of radiological and medical services, will be recognized.

Medical accident investigation other than emergency diagnostic imaging in radiological and medical services

The matters examined in medical accident investigations conducted for radiological and medical services are not limited to emergency diagnostic imaging, but also concern regular radiographic interpretation. In addition, interventional radiology (IR), like a surgical procedure, always carries the potential for a fatal medical accident. It requires responses that differ from those for normal diagnostic radiology work. These include providing the patients and their families with information appropriate for a selected IR procedure, determining whether a procedure is indicated based on shared decision-making agreed to by consent,

providing a postoperative explanation, and establishing a record of the procedure in the manner of operative notes. IR is an important branch of radiological and medical services that can contribute greatly to the entire hospital as a means of avoiding circumstances that can result from medical accidents, such as postoperative accidents and obstetrical hemorrhage. It is important for attending physicians in each department to recognize the efficacy of IR, and this entails establishing an in-house system as described above in Proposal 6 for emergency diagnostic imaging. On the other hand, with salvage therapy by IR, whose purpose is lifesaving, there is the risk of occasionally giving the attending physician and the patient's family unrealistic expectations and pushing ahead with a hopeless procedure. If a case is considered difficult, it is essential that decisions not be made by a single individual, but rather that the indications always be examined by multiple eyes and decisions made calmly.

Summary

Eliminating loss of life caused by a lack of accurate diagnostic imaging is the mission of the radiologist. The whole point of emergency diagnostic imaging is to effectively use information possessed by the attending physician, the radiology technologist taking the images, and the nurses managing the patient and to provide the treatment team with information that is directly linked to treatment. Although it is important to seek to strengthen the systemic aspects of the hospital as a whole, as was described in the proposal section, it is more important to first seek to change how emergency diagnostic imaging is viewed within the radiology department.

Secondary source materials used as references

1) Medical Accident Investigation and Support Center, Ed.: Proposals to Prevent Medical Accident Recurrences (8th edition): Analysis of deaths involving diagnostic imaging in emergency medicine. Japan Medical Safety Research Organization, 2019 (https://www.medsafe.or.jp/modules/advocacy/index.php?content_id=1#teigen008).
2) Health Insurance Bureau Notification No. 0430-1: Promoting team medicine through medical staff collaboration and coordination (https://www.mhlw.go.jp/topics/2013/02/dl/tp0215-01-09d.pdf).
3) Max P et al: Impact of abdominal CT on the management of patients presenting to the emergency department with acute abdominal pain. AJR Am J Roentgenol 174: 1391-1396, 2000.
4) Suzuki T: Usefulness of CT tests for diagnosing patients with acute abdomen. Journal of Abdominal Emergency Medicine 30(7): 875-881, 2010.
5) Bagheri-Hariri S et al: Abdominal and pelvic CT scan interpretation of emergency medicine physicians compared with radiologists' report and its impact on patients' outcome. Emerg Radiol 24: 675-680, 2017.

7 Views and Procedures for Pediatric Diagnostic Imaging

Introduction

Unlike adults, children change in both somatotype and normal appearance as they develop. They also differ from adults in the types and frequencies of illnesses that affect them. Consequently, knowledge of children and how to accommodate them is needed for imaging procedures and required of physicians and diagnostic radiologists involved in pediatric care. The discussion in these guidelines focuses on imaging procedures for children that involve radiation exposure. In addition, because imaging procedures in children often require sedation, ensuring safety during examination is also important.

Reducing radiation exposure in imaging procedures of children: Justification and optimization

Needless to say, children have more years of life remaining than adults, and they are therefore more sensitive to the various invasive effects of imaging procedures; thus, more attention must be given to the principles of justification and optimization for children than for adults. A factor that clearly affects children more than adults is the cancer risk associated with radiation exposure, and the type of procedure that results in the highest radiation exposure, number of examinations, and total dose from diagnostic imaging is CT. Although there was no evidence that cancer risk increases with low-dose exposure with CT in the past, a succession of articles has recently been published reporting an increased risk of various types of cancer resulting from CT radiation exposure in children.[1-4] Although the risk for individuals is by no means high, there is clearly an increase in the overall risk of cancer. The diagnostic radiologist should take this seriously and make an effort to justify and optimize CT studies in children.

1. Justifying imaging procedures in children

A report from Europe, where the rate at which CT is controlled by radiologists is considered appreciably higher than in Japan, indicated that 30% of pediatric CT examinations are either unnecessary or could be replaced by a study that does not use radiation (typically ultrasound and MRI).[5] Guidelines are useful for judging the justifiability of an imaging study,[5] and the present guidelines should also be useful for that purpose.

Based on the concept that communication between various disciplines and the patients and their family members is essential for reducing radiation exposure in pediatric diagnostic imaging, the World Health Organization (WHO) compiled a booklet. A Japanese-language version of it (Figure)[6,7] was created by the Japan Network for Research and Information on Medical Exposure (J-RIME), a body formed by relevant academic societies and organizations, particularly the National Institutes for Quantum Science and

Technology and the Japan Radiological Society. Communication among diagnostic radiologists, the physicians requesting imaging procedures, and the patients and their family members is necessary for justification. Before requesting a study, the requesting physician needs to ask himself or herself whether the examination has already been performed, whether it will affect patient management, whether it is truly necessary, whether it is necessary now, whether it is the optimal examination, and whether he or she has clearly explained the need for the examination to the diagnostic radiologist. In Europe and the United States, guidelines for the requesting physician have also been created. In Japan, training and awareness in this area are inadequate, and it is likely almost always the diagnostic radiologist who asks the above questions of the requesting physician. However, a pediatric imaging procedure cannot be justified without making that effort. Although it is the requesting physician who first determines that an examination is indicated, determining whether it is justified is the most important job of the diagnostic radiologist. The diagnostic radiologist's job is not only to interpret images. Particularly for children, the diagnostic radiologist should try to justify testing by thoroughly considering the examination indication, communicating with the requesting physician, and considering whether to perform the examination and whether the information can be obtained by ultrasound or MRI. It is helpful to have as many regular opportunities as possible to talk to requesting physicians, such as during conferences.

Figure. Booklets on communication for radiation risks prepared by the WHO and J-RIME

2. Optimization of pediatric imaging procedures: Reducing exposure and optimal use of contrast media

Optimization of pediatric imaging is undertaken based on the ALARA (as low as reasonably achievable) principle.[8] The WHO has stated in reports that optimization requires communication among diagnosticians, technicians, and medical physicists.[6,7] The move toward reducing exposure doses has gained momentum in Japan in recent years, with J-RIME releasing a revised version of the Diagnostic Reference Levels in Japan (2020 edition).[9] The diagnostic reference levels (DRLs) for pediatric CT are shown in the table below. Because there are differences in facility size, localities, personnel, and the performance of the CT systems that can be used, DRLs are not dose limits. Depending on the procedure, the values can be exceeded if clinically necessary. However, they are indices that enable the identification of facilities that use unusually

high doses or levels that are the same as those used for adults, thereby encouraging optimization. The purpose of DRLs is optimization, not simply dose reduction. Adequate diagnostic information for pediatric CT can usually be obtained with single-phase imaging (e.g., generally non-contrast CT alone for emergency head CT, single-phase contrast alone for usual truncal CT). At facilities that specialize in pediatric care, examinations may be performed at dose settings that exceed the DRLs if necessary, and arterial phase imaging may be added. However, these are performed as the result of optimization for the diagnostic information required by the diagnostician. Moreover, DRLs are indices for facilitating exposure dose optimization and do not take image quality into account at all. Due to concern over exposure, imaging in children is often performed at a dose so low that sufficient information cannot be obtained, and multi-phasic CT imaging is frequently performed with a low single dose, but according to the protocol for each organ in adults. However, even if an examination has been justified, it just results in needless exposure if it cannot provide the necessary information. In addition, it should be recognized that, even if the CT dose index volume (CTDIvol) is below the DRL, the dose length product (DLP) increases 2- or 3-fold if multi-phasic imaging is performed unnecessarily, which is far from optimal. The very fact that the imaging procedures are being performed in children, who are sensitively affected by radiation exposure, means that it is the duty of the diagnostic radiologist to make the best possible use of his or her knowledge.

Table　Diagnostic reference levels in pediatric CT[9)]

Classified by age group

	< 1 year old		1 to < 5 years old		5 to < 10 years old		10 to < 15 years old	
	$CTDI_{vol}$ mGy	DLP mGy･cm	$CTDI_{vol}$ mGy	DLP mGy･cm	$CTDI_{vol}$ mGy	DLP mGy･cm	$CTDI_{vol}$ mGy	DLP mGy･cm
Head	30	480	40	660	55	850	60	1,000
Chest	6 (3)	140 (70)	8 (4)	190 (95)	13 (6.5)	350 (175)	13 (6.5)	460 (230)
Abdomen	10 (5)	220 (110)	12 (6)	380 (190)	15 (7.5)	530 (265)	18 (9)	900 (450)

Classification by weight

	< 5 kg		5 to < 15 kg		15 to < 30 kg		30 to < 50 kg	
	$CTDI_{vol}$ mGy	DLP mGy･cm	$CTDI_{vol}$ mGy	DLP mGy･cm	$CTDI_{vol}$ mGy	DLP mGy･cm	$CTDI_{vol}$ mGy	DLP mGy･cm
Chest	5 (2.5)	76 (38)	9 (4.5)	122 (61)	11 (5.5)	310 (155)	13 (6.5)	450 (225)
Abdomen	5 (2.5)	130 (65)	12 (6)	330 (165)	13 (6.5)	610 (305)	16 (8)	720 (360)

Note 1) Values for a 16-cm phantom shown; values based on a 32-cm phantom also given in parentheses.
Note 2) Imaging range for abdomen extends from the upper abdomen to the pelvic region.

(Japan Network for Research and Information on Medical Exposure (J-RIME): Diagnostic Reference Levels in Japan, 2020 edition, p5, 2020 http://www.radher.jp/J-RIME/report/JapanDRL2020_jp.pdf)

The appropriate use of contrast media is also important for the optimization of diagnostic imaging. With both CT and MRI, additional information may be obtained using contrast media. However, contrast media result in adverse reactions, and gadolinium contrast media deposition has recently been shown to occur in human tissue.[10,11] Therefore, an important responsibility of the diagnostic radiologist is to rigorously determine whether contrast media use is necessary. At present, the only adverse event in humans reported in association with tissue deposition of free gadolinium from contrast media has been nephrogenic systemic fibrosis (NSF). However, because gadolinium contrast media were first marketed only 35 years ago, the indications for its use should be more rigorously considered for children, who have more years yet to live. See section 4, Contrast Media Safety, for information on safety and precautions.

Safety measures for children in diagnostic imaging

The radiologists responsible for clinical care in the diagnostic imaging department puts in place safety measures for adverse reactions to contrast media, but ensuring the safety of pediatric patients who are sedated for an imaging procedure is also important. In MRI laboratories, a strong magnetic field is always present, requiring that measures be taken to address emergencies, including measures to prevent secondary accidents. A helpful reference source is the 2020 edition of the Joint Recommendation on Sedation during MRI Examination by the Japan Pediatric Society, the Japanese Society of Pediatric Anesthesiology, and the Japanese Society of Pediatric Radiology.[12] Preparing the facilities (e.g., plumbing), monitors, and emergency items in various sizes tailored to the different physique of children in diagnostic imaging departments and establishing emergency backup systems are also useful measures for addressing adverse reactions to contrast media.

Conclusion

Imaging procedures must not be performed thoughtlessly in children, who still have long to live. Inappropriate imaging test occurs because justification and optimization are not properly performed. Making use of our knowledge as pediatric or diagnostic imaging specialists and mutually cooperating to perform the necessary examinations safely and under optimal conditions is the duty and responsibility of those of us involved in healthcare.

Secondary source materials used as references

1) Brenner D et al: Estimated risks of radiation-induced fatal cancer from pediatric CT. AJR Am J Roentgenol 176: 289-296, 2001.
2) Pearce MS et al: Radiation exposure from CT scans in childhood and subsequent risk of leukaemia and brain tumours: a retrospective cohort study. Lancet 380: 499-505, 2012.

3) Miglioretti DL et al: The use of computed tomography in pediatrics and the associated radiation exposure and estimated cancer risk. JAMA Pediatr 167(8): 700-707, 2013.
4) Mathews JD et al: Cancer risk in 680 000 people exposed to computed tomography scans in childhood or adolescence: data linkage study of 11 million Australians. BMJ 346: f2360, 2013.
5) Rutger AJ et al: Multidetector CT in children: current concepts and dose reduction strategies. Pediatr Radiol 40: 1324-1344, 2010.
6) WHO: Radiation risk communication in paediatric imaging: Global Initiative on Radiation Safety in Health Care Settings Workshop Report (http://www.who.int/ionizing_radiation/medical_exposure/Bonn_Workshop_Risk_Communication_Report01.pdf).
7) National Institutes for Quantum Science and Technology, Japan Network for Research and Information on Medical Exposure (J-RIME): Communicating Radiation Risks in Pediatric Imaging: information to support health care discussions about benefit and risk (https://www.qst.go.jp/uploaded/attachment/17113.pdf).
8) The ALARA (as low as reasonably achievable) concept in pediatric CT intelligent dose reduction: multidisciplinary conference organized by the Society of Pediatric Radiology. Pediatr Radiol 32: 217-313, 2002.
9) Japan Network for Research and Information on Medical Exposure (J-RIME): Diagnostic Reference Levels in Japan (2020 edition) (http://www.radher.jp/J-RIME/report/Japan-DRL2020_jp.pdf).
10) Kanda T et al: Gadolinium-based contrast agent accumulates in the brain even in subjects without severe renal dysfunction: evaluation of autopsy brain specimens with inductively coupled plasma mass spectroscopy. Radiology 276(1): 228-232, 2015.
11) Murata N et al: Gadolinium tissue deposition in brain and bone. Magn Reson Imaging 34(10): 1359-1365, 2016.
12) Japan Pediatric Society, the Japanese Society of Pediatric Anesthesiology, and the Japanese Society of Pediatric Radiology: Joint proposal on sedation during MRI tests (February 23, 2020 edition). The Journal of the Japan Pediatric Society 124(4): 771-805, 2020 (http://www.jspr-net.jp/information/data/MRI_20200223.pdf).

1
Neuroradiology

Standard Imaging Methods for the Brain and Nervous System

Introduction

MRI provides better contrast resolution than CT, and because there are no artifacts from bone, it is an excellent modality for visualizing central nervous system lesions. It is therefore the first-line choice of diagnostic imaging methods for many diseases of the head. CT is given priority if there are concerns about MRI use, such as when the patient has a device incompatible with MRI or is in poor general condition, or when evaluating a bone lesion or calcification, as well as in the case of acute brain hemorrhage or head trauma. Compared with CT, MRI is highly useful in diseases such as the following: inflammatory diseases, including demyelinating diseases such as multiple sclerosis; degenerative and metabolic diseases; congenital malformations; brainstem and spinal cord lesions; meningeal dissemination; axonal injury resulting from head trauma; and sellar lesions. MRI is in general highly useful for brain tumors, subacute and chronic cerebrovascular disorders, and bone marrow changes. In addition to morphological information, MRI can provide functional information on aspects such as water molecule diffusion, blood flow, and metabolism. SPECT and PET, which use radioactive tracers, are useful for the functional evaluation of aspects such as blood flow and metabolism.

Basic methods of head MRI

Routine MRI of the head is generally performed with a slice thickness of approximately 5 mm and involves T1-weighted and T2-weighted imaging and fluid-attenuation inversion recovery (FLAIR) imaging (or proton density-weighted imaging). In addition, because diffusion-weighted imaging can be performed in a short time and provides a large amount of information, it can also be included in routine imaging. The reference plane for transverse imaging is generally the AC-PC line (line joining the anterior and posterior commissures). Depending on the location to be imaged and the purpose of the examination, images such as coronal and sagittal images, thin-slice images, and 3D images are selected in addition. For example, coronal and sagittal images provide useful information for the cranial base, sellar, and high convexity regions.

Evaluation of contrast enhancement by contrast medium administration is necessary to determine whether the blood-brain barrier (BBB) has failed due to a lesion and whether the lesion has a solid component. If a tumor or inflammation is suspected, use of a contrast medium is considered to determine whether a tumor or inflammation is present and perform differential diagnosis. MRI is superior to CT for evaluating contrast enhancement in such a condition.

1. T1-weighted imaging

Spin echo (SE) sequences are commonly used for T1-weighted imaging, but images can also be acquired with gradient echo (GRE) sequences. Items that show hyperintensity in T1-weighted images include hemorrhagic components, fluids with high protein concentration, fat components, and melanin. The presence of a fat component can be confirmed if it is suppressed by fat suppression when hyperintense in T1-weighted images. Calcification shows hyperintensity in T1-weighted images as the result of surface effects occurring with supplementation of water molecules by sponge-like calcification foci. However, whether they show hyperintensity depends on the status of the calcification foci.

Contrast enhancement resulting from contrast medium administration is generally evaluated using pre-contrast and post-contrast T1-weighted images. When a lesion shows hyperintensity in pre-contrast T1-weighted images, contrast enhancement can be readily evaluated by pre-contrast and post-contrast image subtraction. In the orbit and cranial base, the fat signal interferes with assessment of contrast enhancement resulting from the contrast medium, and fat suppression is therefore used concurrently. To detect pituitary microadenomas and diagnose other pituitary lesions, dynamic imaging using thin slices (approximately 3-mm-thick) and rapid contrast medium injection is useful.

2. T2-weighted imaging

T2-weighted imaging is typically performed using a fast spin echo (FSE) sequence. T2-weighted imaging is essential for detecting brain parenchymal lesions and evaluating lesion characteristics, such as cysts, necrosis, and hemorrhage, and the extent of lesion progression. The characteristics represented by marked hyperintensity are mainly those of components such as fluid (cysts, mucous components, blood components) and cartilaginous components. Because many 180° pulses are used with FSE, the susceptibility effect decreases, reducing the ability to detect hemorrhage. $T2^{*}$-weighted imaging and susceptibility-weighted imaging (SWI) are useful for detecting small hemorrhages.

3. FLAIR imaging

With FLAIR imaging, lesions generally show hyperintensity, and cerebrospinal fluid is suppressed. It is therefore useful for detecting brain lesions that are in contact with cerebrospinal fluid. It is also useful for detecting lesions in cerebrospinal fluid, such as subarachnoid hemorrhage. However, a shortcoming of FLAIR imaging is that cerebrospinal fluid artifacts are readily apparent with 2D imaging. It should also be noted that its ability to visualize lesions in deep gray matter and the brain stem/cerebellum is inferior to that of T2-weighted imaging. Evaluation in combination with T1-weighted and T2-weighted imaging is often useful for diagnosis. For example, evaluations that combine these 3 types of imaging are useful for differentiating among old lacunar infarcts, white matter lesions, and perivascular spaces.

Basic methods of head CT

Multidetector CT enables an extensive area to be imaged at high spatial resolution. It also allows rapid imaging and improves temporal resolution, enabling CT angiography (CTA) to be performed and cerebral perfusion images to be acquired. It generally enables 0.5 to 0.6-mm isotropic volume data to be obtained over an extensive range. Image reconstruction methods such as multiplanar reformation (MPR), maximum intensity projection (MIP), and volume rendering (VR) techniques are also useful for diagnosis.

● Imaging methods used when stroke is suspected

① CT

CT can be performed easily and in a short time and is generally performed first to exclude intracranial hemorrhage. Hemorrhage and signs of early ischemia are evaluated with non-contrast CT (NCCT). Adding CTA is useful for identifying cerebrovascular lesions.

② MRI

In addition to routine imaging of the head, diffusion-weighted imaging, T2*-weighted imaging, and MRA are generally performed. Depending on the patient's condition, the MRI examination may be discontinued before its completion. Consequently, examinations are performed in sequential order, beginning with the most important imaging methods. In acute brain infarction, diffusion-weighted imaging and MRA are particularly important and should be performed early. If acute brain infarction is suspected, the following types of imaging should commonly be performed.

(1) Diffusion-weighted imaging
(2) MRA
(3) FLAIR imaging
(4) T2*-weighted imaging (SWI)
(5) T2-weighted imaging
(6) T1-weighted imaging

Intravascular hyperintensity is often seen in occluded blood vessels with FLAIR imaging, making it useful for diagnosing such occlusion (Fig. 1). In addition, because FLAIR imaging suppresses the cerebrospinal fluid signal, it is often helpful for diagnosing subarachnoid hemorrhage. T2*-weighted imaging is an effective means of detecting brain hemorrhage. An example of an MRI protocol is shown in Table 1.

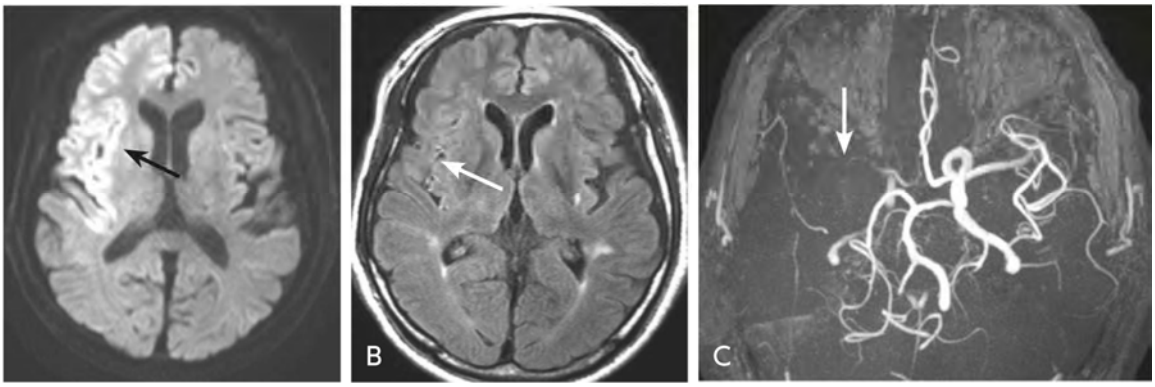

Figure 1. Acute cerebral infarction (MRI)

A: Diffusion-weighted image shows an area of hyperintensity in the right frontal lobe and insula (→).
B: FLAIR image demonstrates a hyperintense blood vessel in the right Sylvian fissure (→).
C: MRA shows decreased visualization of the right middle cerebral artery, indicating occlusive changes (→).

Table 1. An example of a MRI protocol for brain ischemia (3T system, 8-channel head coil)

Imaging Method	Sequence	TR/TE	Slice thickness	Other
Diffusion-weighted imaging	SE-EPI	3,200/60 ms	5 mm	
MRA	GRE	20/3.5 ms	0.5 mm	Time-of-flight method
FLAIR imaging	IR	10,000/120 ms	5 mm	
T2*-weighted imaging	GRE	570/40 ms	5 mm	
T2-weighted imaging	FSE	3,500/80 ms	5 mm	
T1-weighted imaging	FSE	450/10 ms	5 mm	

Note: Diffusion-weighted imaging and MRA are particularly important in evaluating acute cerebral infarction and are therefore performed early.

● Imaging methods in head trauma

① CT

CT is useful in acute head trauma. Specifically, it is useful for evaluating intracranial hemorrhage, cerebral contusion, and skull fracture. Helical imaging allows observation in multiple planes and is useful for determining the relationships among bone, brain, and hemorrhage.

② MRI

The types of MRI sequences indicated below are commonly performed when the main target condition is head trauma.

(1) T1-weighted imaging
(2) T2-weighted imaging
(3) FLAIR imaging
(4) T2*-weighted imaging (SWI)
(5) Diffusion-weighted imaging

These imaging methods are considered useful for diagnosing acute epidural/subdural hematoma, traumatic subarachnoid hemorrhage, cerebral contusion, and diffuse axonal injury (DAI) (Fig. 2). An example of a typical MRI protocol is shown in Table 2.

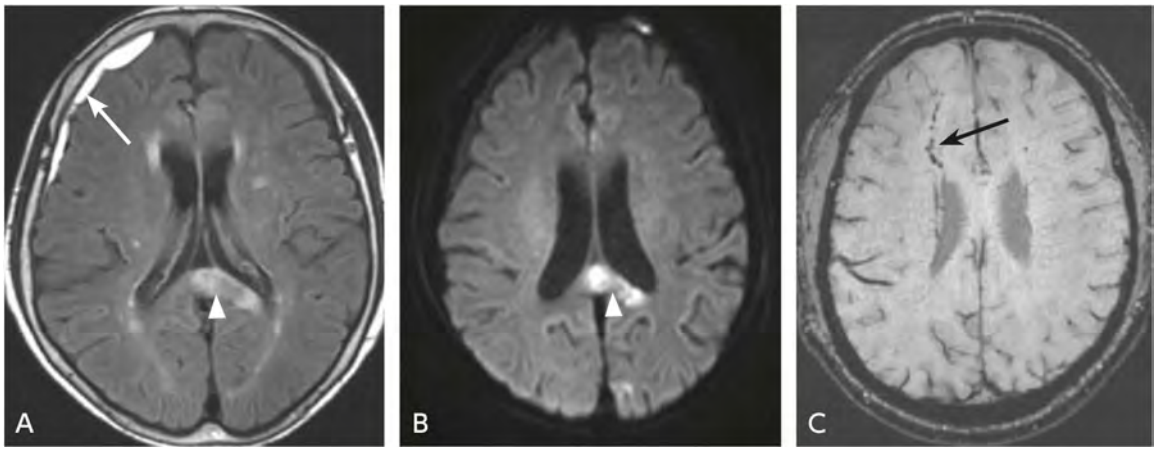

Figure 2. Subdural hematoma and axonal injury (MRI)

A: FLAIR image shows a subdural hematoma on the cortical surface of the right frontal lobe (→), and a lesion in the splenium of the corpus callosum that appears to be an axonal injury (▷).
B: Diffusion-weighted image depicts a hyperintense lesion in the splenium of the corpus callosum, likely axonal injury (▷).
C: SWI shows small hypointense areas in the right frontal lobe white matter, suggestive of an axonal injury (→).

Table 2. An example of a MRI protocol for head trauma (3T system, 8-channel head coil)

Imaging Method	Sequence	TR/TE	Slice Thickness	Other
T1-weighted imaging	SE	450/10 ms	5 mm	
T2-weighted imaging	FSE	3,800/80 ms	5 mm	Sagittal and coronal planes both useful
FLAIR imaging	IR	10,000/120 ms	5 mm	Sagittal and coronal planes both useful
$T2^*$-weighted imaging	GRE	570/40 ms	5 mm	
(SWI)	(GRE)	(27/20 ms)	(2 mm)	
Diffusion-weighted imaging	SE-EPI	3,200/60 ms	5 mm	

Note: SWI can be substituted for $T2^*$-weighted imaging.

Cerebral blood flow scintigraphy

The following are used as radiopharmaceuticals for cerebral blood flow scintigraphy: ^{99m}Tc-ethyl cysteinate dimer (^{99m}Tc-ECD), ^{99m}Tc-hexamethyl propylene amine oxime (^{99m}Tc-HMPAO), and N-isopropyl-p-I-123-iodoamphetamine (^{123}I-IMP). The radiopharmaceutical is administered by intravenous injection with the patient at rest in bed with eyes closed. The patient remains at rest until imaging is performed. Imaging begins 5 to 10 minutes after administration of ^{99m}Tc-ECD or ^{99m}Tc-HMPAO and 30 to 40 minutes after ^{123}I-IMP administration. If the objective is dynamic analysis or cerebral blood flow quantitation, dynamic acquisition is performed in addition to normal imaging. The use of a gamma camera

equipped with a high-resolution collimator for low-energy imaging is recommended. The 2008 nuclear medicine diagnostic guidelines should be referred to regarding stress testing, cerebral blood flow measurement, and statistical image analysis.

PET in epilepsy

1. Test procedure

The patient is intravenously administered ^{18}F-FDG while at rest in the supine position with eyes closed. The dose used is adjusted as appropriate depending on the type of system used and the patient's age and weight. The patient lies at rest for 40 to 60 minutes after administration, and a PET or PET/CT system is used to perform emission and transmission scans (in the case of PET) or CT imaging (in the case of PET/CT) of the head. Data should be acquired for 10 minutes in 3D mode with administration of 185 MBq.

2. Important points for testing

① Pretreatment

The patient is fasted for at least 4 to 5 hours before the examination. Only water intake is permitted during this time (no sugar intake). Because uptake by the brain decreases if the patient's blood glucose level is high, blood glucose is checked immediately before ^{18}F-FDG administration. In addition, cerebral metabolism is altered by neuronal activity. The patient is therefore asked to try to remain at rest for 30 minutes before ^{18}F-FDG administration, and ^{18}F-FDG is administered with the patient supine with eyes closed. To the extent possible, the patient remains at rest on the bed until the examination begins.

② Points to note regarding the measurements

Because the distribution of radioactivity in the brain changes over time after ^{18}F-FDG administration, the timing of the imaging must be consistent. Up to approximately 40 minutes after ^{18}F-FDG administration, the imaging is affected by cerebral blood flow. Consequently, in the case of a single scan, imaging should be performed at approximately 60 minutes, taking into account attenuation and the examination waiting time. Steps should be taken to prevent head movement during imaging to avoid misregistration between the transmission scan and CT data using absorption correction and emission data.

Secondary source materials used as references

1) Miki Y, et al. Head MRI: Imaging protocol and latest 3T MRI findings. Japanese Journal of Magnetic Resonance in Medicine 27:156-165, 2007.
2) Sasaki M, et al. Discriminating between silent cerebral infarction and deep white matter hyperintensity using combinations of three types of magnetic resonance images: a multicenter observer performance study. Neuroradiology 50: 753-758, 2008
3) ASIST-JAPAN Committee to Formulate Clinical Practice Guidelines, Ed.: 2007 Clinical Practice Guidelines for Diagnostic Imaging of Acute cerebral infarction, Nankodo, 2007.
4) Latchaw RE, et al. Recommendations for imaging of acute ischemic stroke: a scientific statement from the American Heart Association. Stroke 40: 3646-3678, 2009
5) Essig M, et al. MR imaging of neoplastic central nervous system lesions: review and recommendations for current practice. AJNR Am J Neuro Radiol 33: 803-817, 2012

6) Hirai T, et al. Protocol for routine brain imaging with 3T MRI. Japanese Journal of Magnetic Resonance in Medicine 28: 244-254, 2008.
7) Japanese Society of Nuclear Medicine, Ed.: Nuclear Medicine Diagnostic Guidelines. Japanese Society of Nuclear Medicine, 2008.
8) Japanese Society of Nuclear Medicine, Ed.: 2020 FDG-PET and PET/CT Diagnostic Guidelines. (http://jsnm.org/archives/4372/)
9) Japanese Society of Nuclear Medicine, Ed.: Japanese Consensus Guidelines for Pediatric Nuclear Medicine. (http://jsnm.org/archives/4675/)

BQ 1 Which imaging examinations are recommended to diagnose subarachnoid hemorrhage?

Statement

The most useful imaging examination is non-contrast CT (NCCT). If diagnosis is difficult with NCCT, MRI can be considered. When subarachnoid hemorrhage is strongly suspected based on clinical findings, even if no significant findings are obtained with CT or MRI, lumbar puncture should be performed.

Background

The vast majority of headache is primary headache, such as tension headache and migraine headache. However, conditions for which an early response is extremely important, such as subarachnoid hemorrhage, are also included in this category. The main cause of non-traumatic subarachnoid hemorrhage is rupture of a cerebral aneurysm. Although CT is generally used for diagnosis in the acute phase, false-negatives are obtained with CT in some cases of subarachnoid hemorrhage (Fig. A). Lumbar puncture is therefore considered necessary. Some studies have shown that MRI, particularly FLAIR imaging, is more useful than CT for detecting subarachnoid hemorrhage (Fig. B). The advantages and shortcomings of each are outlined below.

Explanation

NCCT is the standard imaging examination for subarachnoid hemorrhage.[1)] In a study of 3,132 patients who underwent CT within 6 hours after the onset of symptoms to exclude subarachnoid hemorrhage, radiologists were able to detect it with sensitivity and specificity of 100%.[2)] However, the hemorrhage detection rate is affected by the severity of the hemorrhage and the time since it occurred. CT sensitivity has been found to decrease over time, with sensitivity of 98% to 100% within 12 hours after the onset of symptoms, 93% at 24 hours, 85% at 5 days, 57% to 85% at 6 days, and 50% at 1 week.[3-7)] Confirmation by lumbar puncture is therefore desirable 5 or more days after onset. In some cases, cerebral ventriculomegaly, particularly of the inferior horn of the lateral ventricle, may be the only finding.

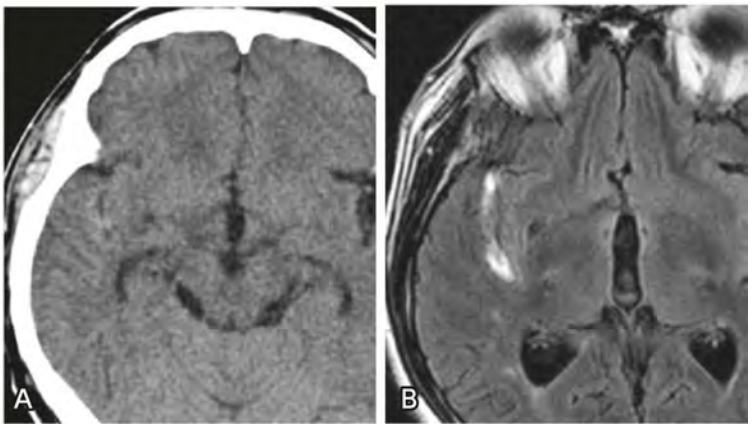

Figure. Subarachnoid hemorrhage

A: NCCT on the day of onset: The right Sylvian fissure is indistinct compared with the left and shows slightly high attenuation.

B: MR (FLAIR imaging) at 1 week after onset: Hyperintensity is seen in the right Sylvian fissure, where an abnormality was seen on CT, indicating a subarachnoid hemorrhage.

MRI (FLAIR, proton density-weighted, and T2*-weighted imaging) is also useful for diagnosing subarachnoid hemorrhage. An investigation using a 1.5T system involving 22 patients found that the sensitivity of FLAIR imaging, T2*-weighted imaging, and CT was 100%, 90.9%, and 91%, respectively, up to 5 days after onset. Subsequently, the sensitivity of FLAIR imaging and CT decreased to 33.3% and 45%, respectively, whereas that of T2*-weighted imaging increased to 100%.[8)] Similarly, in an investigation using a 1.5T system involving 41 patients, the sensitivity of T2*-weighted and FLAIR imaging was 94% and 81%, respectively, up to 4 days after onset and 100% and 75% from 5 to 14 days after onset.[9)] Although FLAIR imaging is useful in the acute phase, its sensitivity decreases over time, and the addition of T2*-weighted imaging to FLAIR imaging is necessary for the subacute phase. However, distinguishing between old and new subarachnoid hemorrhages may be difficult with T2*-weighted imaging.

The rate of subarachnoid hemorrhage misdiagnosis in the acute outpatient setting has been reported to range from 5% to 12%,[10, 11)] and the main cause of misdiagnosis was that NCCT was not performed.[6)] Moreover, one-fourth of patients with subarachnoid hemorrhage do not have headache, and approximately half have no neurological abnormalities.[1)] If the patient's symptoms are mild at onset, and there is little bleeding (bleeding referred to as a sentinel bleed or warning leak), the condition cannot be diagnosed even if CT is performed.[12-14)] In a prospective, cohort study of 592 neurologically normal patients with non-traumatic acute headache up to 14 days after the onset of symptoms, the sensitivity and specificity of CT in detecting subarachnoid hemorrhage were 90% and 99%, respectively. If CT was negative and lumbar puncture was added, the sensitivity and specificity (100% and 67%, respectively) were found to be sufficient to exclude subarachnoid hemorrhage.[14)]

In an investigation including 12 patients with subarachnoid hemorrhage diagnosed by lumbar puncture that could not be diagnosed by CT, false negatives were obtained for 10 patients who underwent FLAIR imaging with a 1.5T system (FLAIR imaging performed within 2 days after CT for 10 patients and within 1

week for 2 patients). Thus, subarachnoid hemorrhage that could not be detected by CT was also difficult to detect with FLAIR imaging. Consequently, FLAIR imaging could not substitute for lumbar puncture.[15] Moreover, with FLAIR imaging, the cerebral sulci and cisterns may show hyperintensity due not only to subarachnoid hemorrhage, but also due to conditions such as meningitis, meningeal dissemination, acute cerebral infarction, moyamoya disease, venous thrombosis, oxygen administration, intravenous anesthesia with propofol, and artifacts.[16] The basilar cistern is particularly susceptible to ghost artifacts resulting from pulsation of the cerebrospinal fluid. Consequently, the interpretation of subarachnoid hemorrhage with FLAIR imaging requires caution.

Search keywords and secondary sources used as references

PubMed was searched using the following keywords: subarachnoid hemorrhage, subarachnoid haemorrhage, MRI, CT, fluid attenuated inversion recovery, and FLAIR. The search was limited to the article titles, and articles related to diagnosis were used in the review. The period searched was through May 2020.

References

1) Bederson JB et al: Guidelines for the management of aneurysmal subarachnoid hemorrhage: a statement for healthcare professionals from a Special Writing Group of the Stroke Council, American Heart Association. Stroke 40: 994-1025, 2009
2) Perry JJ et al: Sensitivity of computed tomography performed within six hours of onset of headache for diagnosis of subarachnoid haemorrhage: prospective cohort study. BMJ 343: 4277, 2011
3) Van der Wee N et al: Detection of subarachnoid haemorrhage on early CT: is lumbar puncture still needed after a negative scan? J Neurol Neurosurg Psychiatry 58: 357-359, 1995
4) Sames TA et al: Sensitivity of new-generation computed tomography in subarachnoid hemorrhage. Acad Emerg Med 3: 16-20, 1996
5) Sidman R et al: Subarachnoid hemorrhage diagnosis: lumbar puncture is still needed when the computed tomography scan is normal. Acad Emerg Med 3: 827-831, 1996
6) Morgenstern LB et al: Worst headache and subarachnoid hemorrhage: prospective, modern computed tomography and spinal fluid analysis. Ann Emerg Med 32: 297-304, 1998
7) Gijn J et al: The time course of aneurysmal haemorrhage on computed tomograms. Neuroradiology 23: 153-156, 1982
8) Yuan MK et al: Detection of subarachnoid hemorrhage at acute and subacute/chronic stages: comparison of four magnetic resonance imaging pulse sequences and computed tomography. J Chin Med Assoc 68: 131-137, 2005
9) Mitchell P et al: Detection of subarachnoid haemorrhage with magnetic resonance imaging. J Neurol Neurosurg Psychiatry 70: 205-211, 2001
10) Vermeulen MJ et al: Missed diagnosis of subarachnoid hemorrhage in the emergency department. Stroke 38: 1216-1221, 2007
11) van Gijn J et al: Subarachnoid haemorrhage: diagnosis, causes and management. Brain 124: 249-278, 2001
12) Kowalski RG et al: Initial misdiagnosis and outcome after subarachnoid hemorrhage. JAMA 291: 866-869, 2004
13) Tong DM et al: Predictors of the subarachnoid hemorrhage of a negative CT scan. Stroke 41: e566-567, 2010
14) Perry JJ et al: Is the combination of negative computed tomography result and negative lumbar puncture result sufficient to rule out subarachnoid hemorrhage? Ann Emerg Med 51: 707-713, 2008
15) Mohamed M et al: Fluid-attenuated inversion recovery MR imaging and subarachnoid hemorrhage: not a panacea. AJNR 25: 545-550, 2004
16) Maeda M et al: Abnormal hyperintensity within the subarachnoid space evaluated by fluid-attenuated inversion-recovery MR imaging: a spectrum of central nervous system diseases. Eur Radiol 13: L192-L201, 2003

BQ 2 Which imaging examinations are recommended to diagnose acute intracerebral hemorrhage?

Statement

Non-contrast CT (NCCT) is strongly recommended to evaluate the presence or absence of intracerebral hemorrhage.

Background

NCCT has generally been used to diagnose stroke due to its high detection performance for brain hemorrhage and its versatility. However, with the increased availability of MRI, settings in which MRI is used to diagnose stroke have increased in Japan (Fig.). However, it is unclear whether MRI can substitute for NCCT in diagnosing acute intracerebral hemorrhage. The diagnostic performance of NCCT and MRI to diagnose acute intracerebral hemorrhage was examined.

Explanation

1. CT

Intracerebral hemorrhage accounts for approximately 20% of strokes, and the presence or absence of intracranial hemorrhage is important for determining stroke treatment. Although there have been studies of the sensitivity and specificity of CT for subarachnoid hemorrhage that have used the lumbar puncture test as the reference standard, reports comparing early CT with surgery and autopsy results in intracerebral hemorrhage are limited to reports from the 1970s.[1, 2] Thus, there is insufficient evidence regarding the sensitivity and specificity of NCCT in diagnosing acute intracerebral hemorrhage. Nevertheless, NCCT has been accepted as the first choice for detecting acute cerebral hemorrhage, and it is now widely used for this purpose.[3-5] It should be noted, however, that the detection performance of CT with respect to intracerebral hemorrhage is also affected by factors such as the time from onset, the site and size of the hemorrhage, and the hematocrit concentration.

2. MRI

There have been few studies that have compared MRI methods for detecting intracerebral hemorrhage.[6] Consequently, there is insufficient evidence regarding which MRI method is the best. With the change from oxyhemoglobin to deoxyhemoglobin after hemorrhage, acute hemorrhage shows a signal ranging from isointense to mildly hyperintense in T1-weighted images and from hyperintense to hypointense in T2-weighted and diffusion-weighted images. In $T2^{*}$-weighted images (GRE), oxyhemoglobin shows a signal ranging from isointense to hyperintense, whereas deoxyhemoglobin, because it is a paramagnet, shows strong hypointensity due to the susceptibility effect. T2*-weighted imaging is therefore considered useful for diagnosing acute hemorrhage.[5]

In a retrospective study of 43 patients with hemorrhagic stroke and 43 patients with nonhemorrhagic stroke (41 patients with arterial cerebral infarction and 2 with transient ischemic attack), the sensitivity and specificity of T2*-weighted imaging were 100% and 95% to 97.5%, respectively. Chronic hemorrhage was concluded to be acute hemorrhage in 1 patient based on T2*-weighted imaging.[6] In a prospective investigation involving 217 patients with stroke, acute intracerebral hemorrhage was seen in 12 patients, and the sensitivity and specificity of T2*-weighted imaging [diffusion-weighted imaging (b-value = 0) performed when image quality was poor with T2*-weighted imaging] for acute intracerebral hemorrhage, with NCCT used as the reference standard, were 83% and 100%, respectively.[7]

In a study of 200 patients with suspected stroke within 6 hours of onset, acute hemorrhage was seen in 25 patients on both CT and MRI. Acute hemorrhages were seen only on MRI in 4 patients, and all were hemorrhagic changes in an ischemic area. Acute hemorrhages were identified only on CT in 3 patients. With MRI, they were diagnosed as old hematomas. Although a small subarachnoid hemorrhage was detected on CT in 1 patient, it was not identified on MRI. In 52 patients, chronic hemorrhage was seen only on MRI and was difficult to identify with CT. The inter-reader agreement rate for acute hemorrhage was higher with CT.[8]

The diagnostic performance of MRI was examined in 62 patients with acute cerebral hemorrhage within 6 hours of onset, with NCCT used as the reference standard. With diagnosis by physicians skilled in the diagnostic imaging of stroke, the sensitivity and specificity of MRI were both 100%.[5] However, the diagnostic accuracy of MRI in diagnosing hemorrhage differs depending on the experience of the diagnostician. Skill is therefore required to diagnose acute cerebral hemorrhage by MRI.[5] If the time of onset is unclear or the MRI assessment is uncertain, it is important to obtain confirmation by CT.

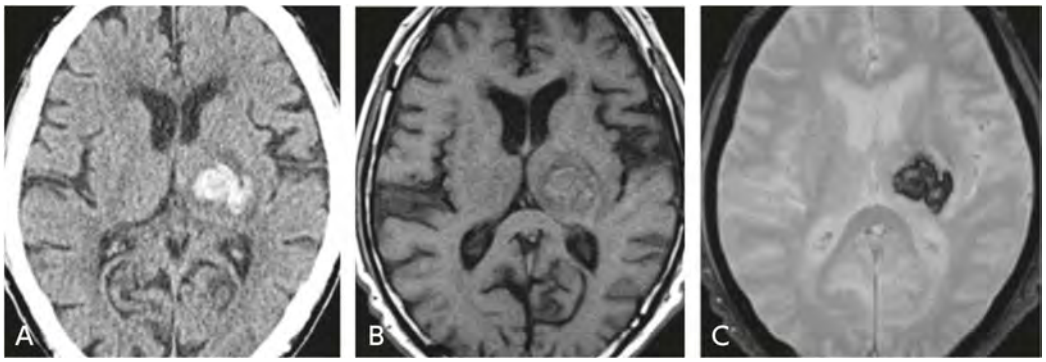

Figure. Acute thalamic hemorrhage 3 hours after onset

A: NCCT: High-attenuation hemorrhage is seen in the left thalamus.

B: MRI, T1-weighted image: The area shows non-homogeneous hyperintensity, and acute hemorrhage is suspected.

C: MRI, T2*-weighted image: The area shows strong hypointensity due to the presence of deoxyhemoglobin.

There is currently no evidence that MRI is superior to CT for evaluating acute intracerebral hemorrhage, though many reports indicate that they perform equally well in this role. Particularly in severe cases, measures such as limiting physical activity of the patient and biomonitoring during the examination should be considered.[7]

Search keywords and secondary sources used as references

PubMed was searched using the following keywords: CT, MRI, imaging, stroke, hemorrhage, guideline, and systematic review.

In addition, the following were referenced as secondary sources.

1) Salmela MB et al: ACR Appropriateness Criteria®: cerebrovascular disease. J Am Coll Radiol 5S: S34-S61, 2017
2) Brazzelli M et al: Magnetic resonance imaging versus computed tomography for detection of acute vascular lesions in patients presenting with stroke symptoms. Cochrane Database Syst Rev (4): CD007424, 2009
3) Goyal MS et al: Hyperacute ischemic stroke in adults. Kelly A et al (eds.): Evidence-based emergency imaging. Springer, pp.91-112, 2018
4) Hemphill JC 3rd et al: Guidelines for the Management of Spontaneous Intracerebral hemorrhage: a guideline for healthcare professionals from the American Heart Association/American Stroke Association. Stroke. 46: 2032-2060, 2015

References

1) Paxton R and Ambrose J: The EMI scanner: a brief review of the first 650 patients. Br J Radiol 47: 530-565, 1974
2) Jacobs L et al: Autopsy correlations of computerized tomography: experience with 6,000 CT scans. Neurology 26: 1111-1118, 1976
3) Hacke W et al: Randomised double-blind placebo-controlled trial of thrombolytic therapy with intravenous alteplase in acute ischaemic stroke (ECASS II): Second European-Australasian Acute Stroke Study Investigators. Lancet 352: 1245-1251, 1998
4) Berkhemer OA et al: A randomized trial of intraarterial treatment for acute ischemic stroke. N Engl J Med. 372: 11-20, 2015
5) Fiebach JB et al: Stroke magnetic resonance imaging is accurate in hyperacute intracerebral hemorrhage: a multicenter study on the validity of stroke imaging. Stroke 35: 502-506, 2004
6) Oppenheim C et al: Comparison of five MR sequences for the detection of acute intracranial hemorrhage. Cerebrovasc Dis 20: 388-394, 2005
7) Chalela JA et al: Magnetic resonance imaging and computed tomography in emergency assessment of patients with suspected acute stroke: a prospective comparison. Lancet 369: 293-298, 2007
8) Kidwell CS et al: Comparison of MRI and CT for detection of acute intracerebral hemorrhage. JAMA 292: 1823-1830, 2004

BQ 3 Which imaging examinations are recommended to determine whether reperfusion therapy is indicated for patients with acute cerebral infarction?

Statement

Diagnostic imaging by CT or MRI is essential for determining whether reperfusion therapy is indicated. Note, however, that they are imaging examinations whose use should be minimized and should not delay the start of treatment.

We recommended the use of noncontrast CT (NCCT) for excluding hemorrhage.

We also recommended regional evaluation of early ischemic changes (EICs) with NCCT using the Alberta Stroke Program Early CT Score (ASPECTS) for determining whether thrombolytic therapy is indicated and predicting prognosis.

MRI provides information similar to CT in evaluating hemorrhage, and diffusion-weighted imaging (DWI) is more sensitive than CT in detecting ischemic lesions. The use of MRI, with attention paid to safety, is therefore recommended.

If mechanical thrombectomy within 6 hours after onset is considered, it is recommended that the site of vascular occlusion be examined by CTA or MRA.

DWI-FLAIR mismatch is useful for estimating the time of onset in patients for whom the onset time is unknown. DWI and FLAIR imaging are therefore recommended in such cases.

Ischemic core evaluation using diffusion-weighted or CT perfusion images and ischemic penumbra (perfusion-core mismatch) evaluation using CT/MR perfusion images are considered useful for determining whether mechanical thrombectomy is indicated for patients 6-24 hours after onset. Their use is therefore recommended.

Background

In 2005, intravenous therapy with recombinant tissue plasminogen activator (rt-PA, alteplase) for acute cerebral infarction within 3 hours of onset became covered by national health insurance in Japan. The coverage was expanded to include acute cerebral infarction within 4.5 hours of onset in 2012. Subsequently, thrombus removal by catheterization was shown to be effective in cases of internal carotid artery or proximal middle cerebral artery occlusion.[1-6] In recent years, there have been reports of the indications for intravenous rt-PA therapy for acute cerebral infarction with an unknown time of onset[7] and on the expansion of the time during which thrombectomy is indicated.[8, 9] This discussion summarizes the evidence regarding the usefulness of diagnostic imaging in determining whether thrombolysis and thrombectomy are indicated, with a focus on NCCT and MRI.

Explanation

To predict the efficacy of thrombolytic therapy, it is important to evaluate the region that would be saved (ischemic penumbra) by recanalization. The revised version of the guidelines for appropriate treatment calls for the use of diagnostic imaging with NCCT or MRI to exclude intracranial hemorrhage and determine whether EICs (Fig.1) are present.

NCCT is excellent for detecting acute intracranial hemorrhage and highly useful for diagnosing intracranial hemorrhage by exclusion. EIC evaluation by CT has in the past been performed by assessing whether the extent of EICs is ≤ 1/3 of the territory of the middle cerebral artery (MCA, the 1/3 MCA rule).[10, 11] However, EICs and territory assessment have not been clearly defined, and there is variability between readers.[12] ASPECTS is therefore currently in general use. ASPECTS (Fig. 2) divides the MCA territory into 10 regions, and EICs in each region are evaluated and scored by subtracting from a perfect score of 10 points. It is a relatively easy method of assessment, and it has higher interrater agreement rate than the 1/3 MCA rule.[13] The relationships of ASPECTS with functional prognosis and the mortality rate have been examined.[14, 15] However, both methods of evaluation are limited to the MCA territory, and there has been insufficient examination of the scoring, such as the fact that the distribution of scores is the same regardless of the localization of brain function. Moreover, there have been reports indicating that these methods of evaluation are not useful for treatment selection.[15, 16] Thus, there are limitations to evaluating the ischemic penumbra by NCCT alone when assessing whether thrombolytic therapy is indicated.

Figure 1. Early ischemic changes (EICs)

CT 2.5 hours after onset: Loss of the insular ribbon (→) and loss of gray-white differentiation (►) are seen. Obscuring of the lentiform nucleus, loss of the insular ribbon, loss of gray-white differentiation, and effacement of the cortical sulci are known EICs.

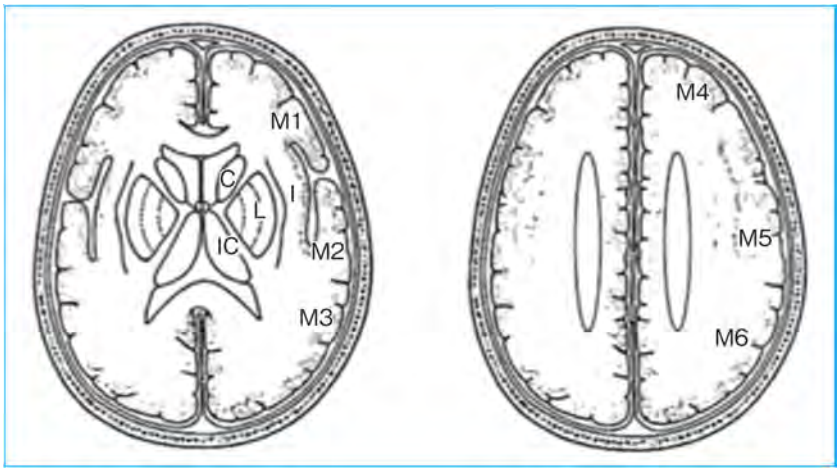

Figure 2. ASPECTS study form (taken from secondary source 4 with permission)

The unilateral middle cerebral artery territory is divided into 10 regions, and each region is evaluated for the presence or absence of EICs, which are scored by subtraction. A score of 10 points is assigned if EICs are completely absent, and the score is 0 points if EICs are seen in all MCA regions.

C: area of the head of the caudate nucleus; L: lentiform nucleus; IC: posterior limb of the internal capsule; I: insular cortex; M1 to M3: middle cerebral artery territory, basal ganglia level; M4 to M6: middle cerebral artery territory, corona radiata level.

An advantage of MRI is that diffusion-weighted images can be obtained (Fig. 3). In some cases, faint hyperintensity on diffusion-weighted images is reversible. Although the significance of this has not been established, it enables infarcts to be distinctly visualized from an early stage, with little inter-reader variability. It is also excellent for detecting small lesions of the brain stem, cerebellum, cortex, and subcortex. Consequently, the diagnostic performance of (DWI) with respect to acute cerebral infarction is considered high. A method of evaluation that matches areas of hyperintensity in DWI with ASPECTS (DWI-ASPECTS) is used to evaluate EICs. The scores obtained with DWI-ASPECTS are approximately 1 point lower than those obtained by CT. Although the scores obtained with both methods are good predictors of posttreatment symptomatic cerebral hemorrhage and functional prognosis after 3 months, DWI-ASPECTS has been found to be superior.[17)]

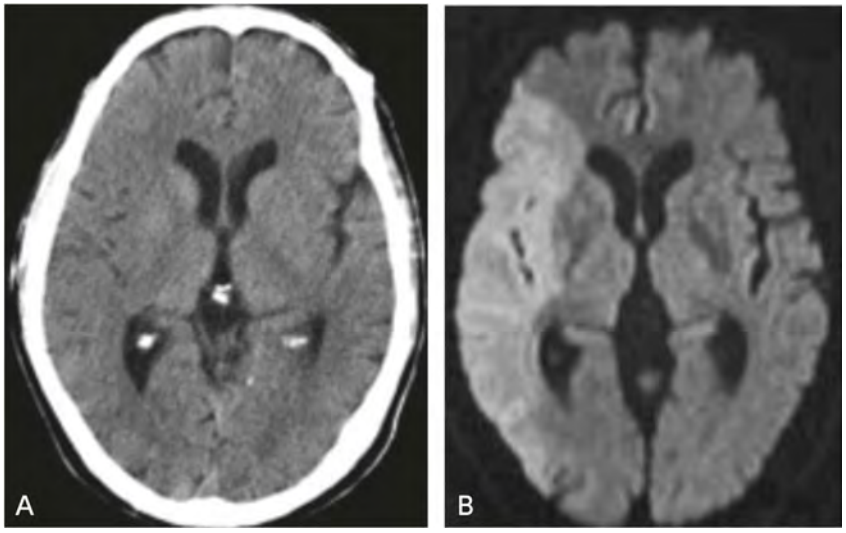

Figure 3. Patient with acute cerebral infarction

A: CT 50 minutes after onset, B: MRI 1 hour and 10 minutes after onset (diffusion-weighted image)
During hospitalization for heart failure, acute cerebral infarction occurred with consciousness disturbance and left hemiplegia. National Institutes of Health Stroke Scale (NIHSS) score of 29 points at onset.
EICs seen extensively in the right hemisphere on both CT and MRI (diffusion-weighted imaging). However, the extent of ischemia is more clearly identifiable with MRI. ASPECTS score of 3 points on both CT and MRI. Watchful waiting was adopted because rt-PA was not indicated. CT the next day showed clear hypodensity in the same region.

The detection performance of MRI is also high in acute intracranial hemorrhage (see the section on brain hemorrhage for details). In particular, susceptibility-weighted imaging such as T2*-weighted imaging is excellent for detecting microbleeds (MBs). However, the basis for using the presence of MBs as the criterion for careful administration of thrombolytic therapy is weak.

Moreover, it has been reported that, if the ischemic lesion is hyperintense on diffusion-weighted images, but does not show hyperintensity on FLAIR images (DWI-FLAIR mismatch), it can be estimated that the patient is within 4.5 hours after stroke onset.[18] An RCT called WAKE-UP, published in 2018, showed that intravenous rt-PA therapy was useful in patients with DWI-FLAIR mismatch for whom the time of onset was unknown.[7]

Endovascular thrombectomy is strongly recommended for patients within 6 hours of onset and with acute occlusion of the internal carotid artery (ICA) or proximal MCA (M1) for whom intravenous rt-PA therapy is indicated by an ASPECTS score ≥ 6 points and NIHSS score ≥ 6 points on head CT or diffusion-weighted images. In 2018, 2 RCTs, the DAWN and DEFUSE 3 trials, reported that thrombectomy was useful for acute occlusion of the ICA or M1 area occurring more than 6 hours from the time last known well.[8, 9] In Japan, it is recommended that thrombectomy begin within 16 hours for patients with a modified Rankin Scale (mRS) score of 0 or 1 before onset, an NIHSS score ≥ 10 points, and a DWI-ASPECTS score ≥ 7 points, and within 24 hours for patients judged to have a mismatch between the ischemic core volume on CT perfusion images or diffusion-weighted images and neurological symptoms or the delayed perfusion area in perfusion images.

Although identification of a vascular lesion is not essential for intravenous rt-PA therapy, evaluation of intracranial vessels by CTA or MRA is necessary if endovascular therapy is considered. However, intravenous therapy should be given priority in patients for whom intravenous rt-PA therapy is indicated, and the start of therapy should not be delayed by additional examinations. In other countries, CTA is often the first choice for diagnosing occluded vessels.[6] CTA can be used to evaluate thrombus size as the area of contrast deficit, as well as the site of an occlusion. CTA imaging in multiple time phases has been reported to enable collateral blood flow to be evaluated and to provide an estimate of the extent of the ischemic core.[3] MRA is also useful for evaluating occluded blood vessels. Compared with other countries, its use in acute cerebral infarction is particularly common in Japan, where MRI is frequently performed. An advantage of MRA is its low invasiveness, due to the fact that a contrast agent is not used, and no radiation exposure is involved. Another advantage is that it enables the extent of the ischemic core to be evaluated by DWI almost simultaneously during a sequence of MRI examinations. Because slow blood flow results in poor visualization, careful interpretation of the images is needed.

Perfusion imaging with CT involves rapidly injecting an iodinated contrast medium intravenously and performing continuous scanning to acquire images of cerebral perfusion. MRI methods of perfusion imaging are dynamic susceptibility contrast, which involves rapid intravenous injection of a gadolinium contrast agent, and arterial spin labeling (ASL), which does not use a contrast agent. However, only a limited number of facilities can use ASL, and its adoption has been slow. Recent RCTs in acute cerebral infarction have included trials that have measured pretreatment ischemic core volume using cerebral blood flow (CBF) on CT perfusion images.[2, 4, 8, 9] In an RCT that examined the period beginning from 6 hours after onset, not only the ischemic core volume, but also the extent of the delayed perfusion area based on Tmax was measured on CT/MR perfusion images. Whether endovascular thrombectomy was indicated was determined with the mismatch region considered the salvageable region.[9] Thus, the number of studies that used perfusion images to determine whether reperfusion therapy is indicated has been increasing, and most of the published RCTs from other countries have used automated analysis software called RAPID™ (Rapid AI). Software that can rapidly measure ischemic core volumes, delayed perfusion areas, and mismatch regions, such as RAPID™, has not yet been widely adopted in Japan. Care must therefore be exercised in determining whether reperfusion therapy is indicated for individual patients.

Search keywords and secondary sources used as references

PubMed was searched using the following keywords: acute ischemia, thrombolysis, thrombectomy, brain, CT, and MRI.

In addition, the following were referenced as secondary sources.

1) Working Group on Revised Guidelines for Intravenous Thrombolysis, Committee for Medical Improvement and Social Insurance in Stroke, Japan Stroke Society, Ed.: Guidelines for Appropriate Intravenous Thrombolytic Therapy (rt-PA), 3rd Edition. Japanese Journal of Stroke 41:205-245, 2019.
2) Japan Stroke Society, et al., Ed.: Guidelines for the Appropriate Use of Percutaneous Transluminal Thrombectomy Devices, 4th Edition. Japan Stroke Society, Japan Neurosurgical Society, Japanese Society for Neuroendovascular Therapy, 2020.
3) Powers WJ et al: Guidelines for the early management of patients with acute ischemic stroke: 2019 update to the 2018 guidelines for the early management of acute ischemic stroke: a guideline for healthcare professionals from the American Heart Association / American Stroke Association. Stroke 50: e344-e418, 2019
4) Barber PA et al: Validity and reliability of a quantitative computed tomography score in predicting outcome of hyperacute stroke before thrombolytic therapy. ASPECTS Study Group. Alberta Stroke Programme Early CT Score. Lancet 355: 1670-1674, 2000

References

1) Berkhemer OA et al: MR CLEAN investigators: a randomized trial of intraarterial treatment for acute ischemic stroke. N Engl J Med 372: 11-20, 2015
2) Campbell BC et al: EXTEND-IA investigators: endovascular therapy for ischemic stroke with perfusion-imaging selection. N Engl J Med 372: 1009-1018, 2015
3) Goyal M et al: ESCAPE trial investigators: randomized assessment of rapid endovascular treatment of ischemic stroke. N Engl J Med 372: 1019-1030, 2015
4) Saver JL et al: SWIFT PRIME investigators: Stent-retriever thrombectomy after intravenous t-PA vs. t-PA alone in stroke. N Engl J Med 372: 2285-2295, 2015
5) Jovin TG et al: REVASCAT trial investigators: thrombectomy within 8 hours after symptom onset in ischemic stroke. N Engl J Med 372: 2296-2306, 2015
6) Goyal M et al: HERMES collaborators: endovascular thrombectomy after large-vessel ischaemic stroke: a meta-analysis of individual patient data from five randomised trials. Lancet 387: 1723-1731, 2016
7) Thomalla G et al: WAKE-UP investigators: MRI-guided thrombolysis for stroke with unknown time of onset. N Engl J Med 379: 611-622, 2018
8) Nogueira RG et al: DAWN trial investigators: thrombectomy 6 to 24 hours after stroke with a mismatch between deficit and infarct. N Engl J Med 378: 11-21, 2018
9) Albers GW et al: DEFUSE 3 investigators: thrombectomy for stroke at 6 to 16 hours with selection by perfusion imaging. N Engl J Med 378: 708-718, 2018
10) von Kummer R et al: Acute stroke: usefulness of early CT findings before thrombolytic therapy. Radiology 205: 327-333, 1997
11) Hacke W et al: Randomised double-blind placebo-controlled trial of thrombolytic therapy with intravenous alteplase in acute ischaemic stroke (ECASS II): Second European-Australasian Acute Stroke Study Investigators. Lancet 352: 1245-1251, 1998
12) Grotta JC et al: Agreement and variability in the interpretation of early CT changes in stroke patients qualifying for intravenous rtPA therapy. Stroke 30: 1528-1533, 1999
13) Pexman JH et al: Use of the Alberta Stroke Program Early CT Score (ASPECTS) for assessing CT scans in patients with acute stroke. AJNR Am J Neuroradiol 22: 1534-1542, 2001
14) Hill MD et al: Selection of acute ischemic stroke patients for intra-arterial thrombolysis with pro-urokinase by using ASPECTS. Stroke 34: 1925-1931, 2003
15) Demchuk AM et al: Importance of early ischemic computed tomography changes using ASPECTS in NINDS rtPA Stroke Study. Stroke 36: 2110-2115, 2005
16) Patel SC et al: Lack of clinical significance of early ischemic changes on computed tomography in acute stroke. JAMA 286: 2830-2838, 2001
17) Nezu T et al: Early ischemic change on CT versus diffusion-weighted imaging for patients with stroke receiving intravenous recombinant tissue-type plasminogen activator therapy: stroke acute management with urgent risk-factor assessment and improvement (SAMURAI) rt-PA registry. Stroke 42: 2196-2200, 2011
18) Thomalla G et al: DWI-FLAIR mismatch for the identification of patients with acute ischaemic stroke within 4.5 h of symptom onset (PRE-FLAIR): a multicentre observational study. Lancet Neurol 10: 978-986, 2011

BQ 4 Is MRI recommended for diagnosing diffuse axonal injury (DAI)?

Statement

Detailed examination by MRI is recommended when DAI is suspected.

Background

With prolonged consciousness disturbance following head trauma, CT findings may be weak. DAI is suspected when there is a discrepancy like this between the neurological symptoms and CT findings or when traumatic subarachnoid hemorrhage or intraventricular hemorrhage is seen on CT.[1)] In such cases, detailed examination by MRI is often performed. Various imaging methods have been reported to be useful for evaluating such cases by MRI. The lesion detection performance of MRI in head trauma and its usefulness for evaluating neurological prognosis are summarized below.

Explanation

1. CT and MRI

For the diagnosis of brain hemorrhage, cerebral contusion, and DAI occurring with head trauma, MRI provides higher contrast resolution and superior diagnostic performance than CT.[2-6)] DAI in particular is often not detected by CT and normal MRI imaging such as T1- and T2-weighted imaging, and caution is therefore required in its diagnosis.[4-6)] Dionei et al. compared CT and MRI in 55 patients with head trauma and found that T2- and T2*-weighted and FLAIR MRI were significantly superior to CT for lesion detection in acute subdural hematoma, traumatic subarachnoid hemorrhage, cerebral contusion, and DAI.[2)]

2. FLAIR and diffusion-weighted imaging

Of the general imaging methods, FLAIR and diffusion-weighted imaging are excellent for lesion detection in conditions such as non-hemorrhagic DAI. In a retrospective examination of 56 patients by Ashikaga et al. that compared evaluation with FLAIR and T2-weighted images, FLAIR imaging was significantly superior for detecting DAI, cerebral contusion, and subdural hematoma, its detection performance being equal to or better than that of T2-weighted imaging in all patients.[7)] In a retrospective examination of 36 patients by Kinoshita et al. that compared the detection performance of FLAIR and diffusion-weighted imaging with respect to DAI, the evaluations were comparable, suggesting that FLAIR and diffusion-weighted imaging are useful in this role.[8)]

3. T2*- and susceptibility-weighted imaging

DAI is often associated with microscopic hemorrhagic lesions, and T2*- and susceptibility-weighted imaging, which strongly reflect differences in susceptibility, are useful for its diagnosis. Compared with other imaging methods, T2*-weighted imaging provides higher detection performance for DAI and is

superior for detecting microscopic lesions.[9, 10] In an investigation of 66 patients with head trauma, Scheid et al. reported that normal T2-weighted imaging detected DAI at a total of 233 locations, whereas T2*-weighted imaging detected it at 608 locations. Thus, the detection performance of T2*-weighted imaging was significantly better than that of normal T2-weighted imaging.[10] In a comparison of T2*-weighted imaging and SWI with respect to the number of DAIs detected in 7 patients with severe head trauma, Tong et al. reported that T2*-weighted imaging detected DAI at a mean of 28.8 ± 8 locations per patient, whereas SWI detected DAI at a mean of 134 ± 27 locations. Thus, the detection performance of SWI was significantly better than that of T2*-weighted imaging (Fig.).[11] In addition, SWI has detected microscopic petechiae in the brain parenchyma of individuals who regularly sustain mild head trauma, such as boxers, suggesting that it can also detect microscopic DAI in diagnosing head trauma.[12]

4. Neurological prognosis evaluation

With regard to neurological prognosis based on DAI and the Glasgow Coma Scale, the number of lesions detected with T2*-weighted imaging has been found not to be correlated with the prognosis.[10] However, an increase in the number of lesions detected with SWI has been found to be correlated with prognosis in terms of indices such as prolongation of consciousness disturbance.[13, 14] SWI is recommended if feasible.

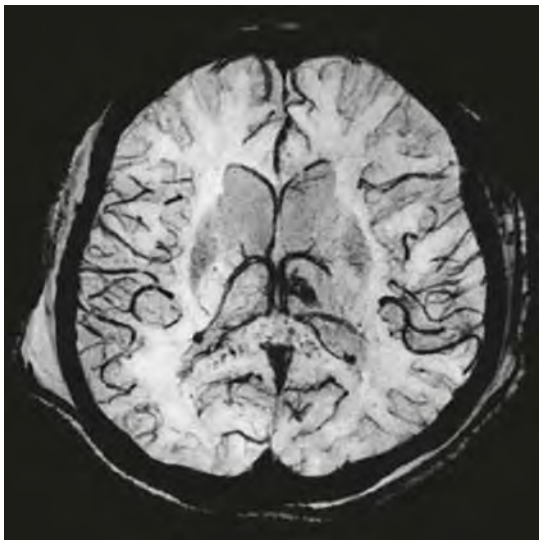

Figure. Patient with prolonged consciousness disturbance following a traffic accident (MRI)

SWI: Multiple punctiform hypointensities are seen in the splenium of the corpus callosum, and DAI was diagnosed.

Search keywords and secondary sources used as references

PubMed was searched using the following keywords: brain contusion, diffuse axonal injury, hemorrhage, and MRI.

References

1) Vieira GFR et al: Early computed tomography for acute post-traumatic diffuse axonal injury: a systematic review. Neuroradiology 2020 Mar 4
2) Dionei FS et al: Clinical application of magnetic resonance in acute traumatic brain injury. Arq Neuropsiquiatr 66: 53-58, 2008
3) Yokota H et al: Significance of magnetic resonance imaging in acute head injury. J Trauma 31: 351-357, 1991
4) Mittl RL et al: Prevalence of MR evidence of diffuse axonal injury in patients with mild head injury and normal head CT findings. AJNR Am J Neuroradiol 15: 1583-1589, 1994
5) Paterakis K et al: Outcome of patients with diffuse axonal injury: the significance and prognostic value of MRI in the acute phase. J Trauma 49: 1071-1075, 2000
6) Chelly H et al: Diffuse axonal injury in patients with head injuries: an epidemiologic and prognosis study of 124 cases. J Trauma 71: 838-846, 2011
7) Ashikaga R et al: MRI of head injury using FLAIR. Neuroradiology 39: 239-242, 1997
8) Kinoshita T et al: Conspicuity of diffuse axonal injury lesions on diffusion-weighted MR imaging. Eur J Radiol 56: 5-11, 2005
9) Scheid R et al: Comparative magnetic resonance imaging at 1.5 and 3 tesla for the evaluation of traumatic microbleeds. J Neurotrauma 24: 1811-1816, 2007
10) Scheid R et al: Diffuse axonal injury associated with chronic traumatic brain injury: evidence from T2*-weighted gradient-echo imaging at 3T. AJNR Am J Neuroradiol 24: 1049-1056, 2003
11) Tong KA et al: Hemorrhagic shearing lesions in children and adolecents with posttraumatic diffuse axonal injury: improved detection and initial results. Radiology 227: 332-339, 2003
12) Hasiloglu ZI et al: Cerebral microhemorrhages detected by susceptibility-weighted imaging in amateur boxers. AJNR Am J Neuroradiol 32: 99-102, 2011
13) Tong KA et al: Diffuse axonal injury in children: clinical correlation with hemorrhgic lesions. Ann Neurol 56: 36-50, 2004
14) Jing Z et al: Hemorrhagic shearing lesions associated with diffuse axonal injury: application of T2 star-angiography sequence in the detection and clinical correlation. Br J Neurosurg 25: 596-605, 2011

BQ 5 Are CT and MRI recommended for diagnosing primary headache in adults?

Statement

CT and MRI are of very little use for primary headache not associated with a neurological deficit, and their use is therefore not recommended for this purpose. However, CT and MRI may be useful for atypical headache, headache that does not fit a specific definition, thunderclap headache, and trigeminal autonomic cephalalgia, and its use can be considered for such conditions.

Background

The 3rd edition of the International Classification of Headache Disorders (ICHD-3), published by the International Headache Society (IHS), broadly categorizes headache as primary and secondary headaches and cephalalgias as central/primary facial pain and other types of headache (secondary source 1). Primary headache is classified as migraine headache, tension headache, cluster headache and other trigeminal autonomic cephalalgia, and other types of headache. Secondary headache encompasses headache associated with a variety of conditions, such as trauma, vascular disorders, non-vascular intracranial disorders, infection, and psychiatric disorders. ICHD-3 added reversible cerebral vasoconstriction syndrome (RCVS) to the secondary headache disorders. Primary headache and chronic headache are generally treated as synonymous, and their diagnosis centers on a detailed examination of medical history and neurological findings. The role of neuroimaging is considered small. In the clinical setting, however, CT or MRI is often performed before a headache is classified, and it therefore cannot be said that assessment of primary headache is common. For this discussion, the usefulness of diagnostic neuroimaging for primary headache was examined.

Explanation

The only studies that have examined the usefulness of neuroimaging for primary headache have been observational studies such as cohort and case-control studies. Its usefulness is therefore estimated based on the results of those studies. In 1985, Joseph et al. examined 48 patients who underwent CT or MRI for headache and reported that brain tumors were seen in 5 patients, and an arteriovenous malformation was seen in 1 patient.[1)] Of these patients with abnormal imaging findings, 5 showed neurological abnormalities, and 1 had an unclassifiable type of headache referred to as exertional headache. In an investigation of 100,800 patients with adult migraine headache, Weingarten et al. reported that, among patients with chronic headache with no symptoms of a neurological deficit, the detection rate of patients who required surgical treatment was approximately 0.01% with CT.[2)] In 1994, the American Academy of Neurology published diagnostic neuroimaging guidelines for patients with headache not associated with symptoms of a neurological deficit (secondary source 2). The recommendation in those guidelines was based on an

investigation by Fishberg, which was also published in 1994.[3] Fishberg reviewed 17 articles published between 1974 and 1991 and examined the findings from a total of 897 CT and MRI examinations performed in patients with migraine headache. Only 4 patients (0.4%) showed abnormalities that required treatment: 3 patients with brain tumors and 1 with an arteriovenous fistula. Based on these findings, the guidelines indicated that there was little need for neuroimaging examinations in patients with typical migraine headache. However, they also mentioned that organic disease that requires treatment may actually be present and indicated that CT or MRI may be indicated if the patient has atypical headache, a history of convulsions, or symptoms of a neurological deficit. In 2004, based on an examination of the literature, Sandrini et al. published guidelines on the usefulness of neurological and neuroimaging examinations in patients with non-acute headache (secondary source 3). The guidelines were revised and the 2nd edition published in 2010 (secondary source 4). The revised edition cited a prospective study by Sempere et al. of 1,876 patients with non-acute headache.[4] All of the patients in that study underwent CT or MRI. Significant organic disease was seen in only 1.2%, and intracranial disease was seen in only 0.9% of patients with headache not associated with symptoms of a neurological deficit. Based on this investigation, the authors concluded that the frequency of intracranial disease is low in patients with headache, and that the factors that can predict such cases are neurological findings, clinical course, and the history of the present illness. In 2005, Tsushima et al. examined MRI images of 306 patients with chronic headache not associated with symptoms of a neurological deficit.[5] They saw no abnormal findings in 169 patients and mild abnormalities in 135, and significant organic abnormalities were seen in only 2 patients (0.7%): pituitary adenoma and chronic subdural hematoma in 1 patient each. Thus, the literature consistently shows that imaging for chronic headache not associated with symptoms of a neurological deficit is of little use. However, the reports also indicate that imaging is to a certain extent necessary for atypical headache and headache that does not fit a specific definition. A recent report of a population-based study indicated that the presence of migraine headaches in women is a risk factor for deep white matter lesions. In addition, migraine headache associated with aura has been found to increase the risk of asymptomatic ischemic brain lesions.[6, 7] However, no causal relationship has been shown between detected lesions and headache, and further investigation is needed. Willbrink et al. examined 56 reports of patients with trigeminal autonomic cephalalgia, which is characterized by frequent, short-lasting headache attacks that are associated with unilateral autonomic symptoms of the face. They found that many of the patients had secondary causes associated with organic lesions such as brain tumors and vascular lesions.[8] Based on this finding, they concluded that neuroimaging is indicated when trigeminal autonomic cephalalgia is suspected based on an appropriate assessment. Besides routine cranial MRI, additional imaging should be performed as needed to evaluate the cervical blood vessels and the parasellar and paranasal sinus areas.

Search keywords and secondary sources used as references

PubMed was searched using the following keywords: chronic headache, diagnostic imaging, guideline, migraine, and cephalalgia.

In addition, the following were referenced as secondary sources.

1) Japanese Headache Classification Committee, Japanese Headache Society, Translation: International Classification of Headache Disorders, 3rd Edition. Igaku Shoin, 2018.
2) Practice parameter: the utility of neuroimaging in the evaluation of headache in patients with normal neurologic examinations (summary statement): report of the quality standards subcommittee of the American Academy of Neurology. Neurology 44: 1353-1354, 1994
3) Sandrini G et al: Neurophysiological tests and neuroimaging procedures in non-acute headache: guidelines and recommendations. Eur J Neurol 11: 217-224, 2004
4) Sandrini G et al: Neurophysiological tests and neuroimaging procedures in non-acute headache, 2nd ed. Eur J Neurol 18: 373-381, 2011

References

1) Joseph R et al: Intracranial space-occupying lesions in attending a migraine clinic. Practitioner 229: 477-481, 1985
2) Weingarten S et al: The effectiveness of cerebral imaging in the diagnosis of chronic headache. Arch Intern Med 152: 2457-2462, 1992
3) Fishberg BM: The utility of neuroimaging in the evaluation of headache in patients with normal neurologic examinations. Neurology 44: 1191-1197, 1994
4) Sempere AP et al: Neuroimaging in the evaluation of patients with non-acute headache. Cephalgia 25: 30-35, 2005
5) Tsushima Y, Endo K: MR imaging in the evaluation of chronic or recurrent headache. Radiology 235: 575-579, 2005
6) Swartz RH, Kern RZ: Migraine is associated with magnetic resonance imaging white matter abnormalities: a metaanalysis. Arch Neurol 61: 1366-1368, 2004
7) ETMinan M et al: Risk of ischemic stroke in people with migraine: systematic review and meta-analysis of observational studies. Bmj 330: 63, 2005
8) Wilbrink LA et al: Neuroimaging in trigeminal autonomic cephalgias: when, how, and of what ? Curr Opin Neurol 22: 247-253, 2009

BQ 6 Which imaging examinations are recommended to diagnose temporal lobe epilepsy?

Statement

MRI is the first-choice imaging modality for diagnosing temporal lobe epilepsy, and its use is therefore recommended for this purpose.

CT is less sensitive than MRI for detecting culprit lesions. However, it is useful for detecting calcification, and its use can be considered.

To identify epileptic foci for surgery, functional imaging is recommended, such as cerebral blood flow SPECT or glucose metabolism PET performed during a non-seizure period and cerebral blood flow SPECT performed during a seizure.

Background

Epileptogenic lesions in temporal lobe epilepsy are varied and include conditions such as hippocampal (amygdaloid) sclerosis, focal cortical dysplasia (FCD), tumors, vascular malformations, trauma, and pathological inflammatory changes such as limbic encephalitis and herpes simplex encephalitis. The importance of diagnostic imaging lies in the localization and qualitative diagnosis of these epileptogenic lesions. Moreover, for surgical treatment, the addition of functional neuroimaging using nuclear medicine examinations is recommended to identify epileptic foci. For this discussion, the usefulness of functional neuroimaging using nuclear medicine examinations was also examined.

Explanation

1. CT

Few studies have evaluated the usefulness of CT in detecting epileptogenic lesions. A retrospective study in children that included a comparison with MRI found that the sensitivity of CT for the culprit lesion was 31%, lower than that of MRI, at 64%.[1)] However, additional screening by CT may be useful when a pathological change associated with tissue calcification is suspected, as in the case of tumors and cavernous angiomas. Focal cortical dysplasia (FCD) type IIb was reported to be an area of high density on CT, which was thought to reflect a rich density of balloon cells.[2)] In addition, CT is selected when the patient's condition is poor; MRI cannot be performed due to the presence of a device such as a pacemaker; or there is a finding suggestive of increased intracranial pressure, such as intracranial hemorrhage, and surgical treatment is considered if possible.

2. MRI

MRI is recommended, along with electroencephalography, as a routine examination for epilepsy. For epilepsy diagnosis, appropriate imaging with high spatial resolution and contrast is important.

Consequently, 3T MRI is recommended. Recommended sequences include high-resolution 3D T1-weighted imaging and 2D T2-weighted/FLAIR imaging (transverse and coronal planes). High-resolution 3D T1-weighted imaging should be performed with thin slices (≤ 1 mm) if possible and should be used to examine cerebral cortical morphology in fine detail.[3] For coronal imaging, imaging is performed in the plane orthogonal to the long axis of the hippocampus and must include the tip of the temporal lobe, which may be associated with an abnormal signal (Fig.). For 2D, a slice thickness of 3 mm is recommended (2 mm for infants). The 3D double inversion recovery (DIR) sequence, which suppresses the signal not only for cerebrospinal fluid, but also for white matter, is excellent for visualizing slight abnormal signal intensity in subcortical white matter.[4] $T2^*$-weighted or susceptibility-weighted imaging (SWI) is added if a vascular malformation, such as a cavernous angioma or arteriovenous malformation, or trauma or a tumor associated with hemorrhage is suspected. In addition, contrast-enhanced imaging is added if a nascent tumor is suspected.

3. SPECT

The tracers ^{99m}Tc-ethyl cysteinate dimer (^{99m}Tc-ECD) and ^{99m}Tc-hexamethyl-propylene amine oxime (^{99m}Tc-HMPAO) are taken up by the brain approximately 30 seconds after contrast medium administration. This is not true of ^{123}I-N-isopropyl-p-iodoamphetamine (IMP). Consequently, radiopharmaceuticals with the former 2 tracers are generally used when locating epileptic foci. Blood flow is decreased in foci on SPECT performed during a non-seizure period and increased on SPECT performed during a seizure. Sensitivity for identifying foci in temporal lobe epilepsy is ≤ 50% with SPECT performed during a non-seizure period. In contrast, it is a high 70% to 90% with SPECT performed during a seizure.[5] Moreover, subtraction of ictal SPECT-coregistered MRI (SISCOM), which involves subtracting SPECT images acquired during non-seizure periods from those acquired during seizures and superimposing them on MR images, is considered the best method for detecting foci.[6]

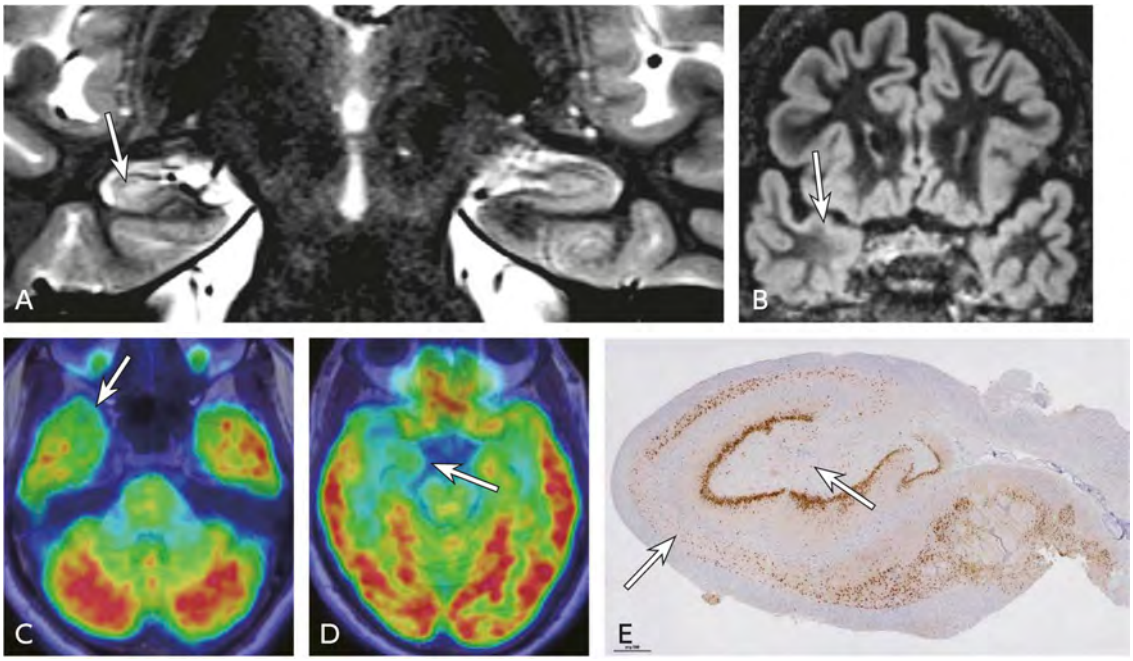

Figure. Right hippocampal sclerosis

A: MRI, T2-weighted coronal image; B: MRI, DIR coronal image
C, D: FDG-PET; E: Anti-NeuN immunostaining, right hippocampus
F: Anti-NeuN immunostaining, tip of the right temporal lobe
The patient was a woman in her 50s. Right temporal lobe epilepsy first occurred when she was 18 years old.
The right hippocampus is atrophied. On T2-weighted MRI, it shows hyperintensity, and the laminar structure is indistinct. In particular, strong hyperintensity is seen in regions C1 and C4 (A →). With the MR DIR sequence, the signal of the white matter at the tip of the right temporal lobe is higher than that of the contralateral side (B →). This may indicate changes secondary to epilepsy or a complication of FCD. In the FDG-PET images, decreased glucose metabolism is present not only in the interior of the right temporal lobe, but it also extends to the tip and lateral area (C, D →). The pathological appearance of the right hippocampus shows neuronal loss in regions C1, C3, and C4 (E →) with NeuN staining of the neurons, indicating hippocampal sclerosis type 1. This pathological finding corresponds well with the MRI findings (A). The pathology of the tip of the right temporal lobe is not associated with disturbance of the 6-layer laminar structure (F), and no complicating FCD is seen, indicating it resulted from secondary changes.

4. PET

FDG-PET assessment of glucose metabolism has long been used to identify epileptic foci in the temporal lobe.[5)] Although uptake at the site of a focus decreases during non-seizure periods, the decrease is more extensive than the focus site (Fig.). One study found no significant difference in post-temporal lobectomy prognosis between a group of patients with negative MRI and positive FDG-PET findings (decreased temporal lobe uptake) and a group with a positive MRI finding (hippocampal sclerosis),[7)] indicating that FDG-PET was useful.

Search keywords and secondary sources used as references

PubMed was searched using the following keywords: CT, MRI, SPECT, PET, temporal lobe, and epilepsy.

In addition, the following was referenced as a secondary source.

1) Japanese Society of Neurology, Ed.: Clinical Practice Guidelines for Epilepsy 2018. Igaku Shoin, 2018.

References

1) Sinclair DB: Pathology and neuroimaging in pediatric temporal lobectomy for intractable epilepsy. Pedia Neurosurg 35: 239-246, 2001
2) Kimura Y: Radiologic and pathologic features of the transmantle sign in focal cortical dysplasia: the T1 signal is useful for differentiating subtypes. AJNR Am J Neuroradiol 40: 1060-1066, 2019
3) Ahmed R: Utility of additional dedicated high-resolution 3T MRI in children with medically refractory focal epilepsy. Epilepsy Res 143: 113-119, 2018
4) Rugg-Gunn FJ: Imaging the neocortex in epilepsy with double inversion recovery imaging. Neuroimage 31 (1): 39-50, 2006
5) Kumar A, Chugani HT: The role of radionuclide imaging in epilepsy, part 1: sporadic temporal and extratemporal lobe epilepsy. J Nucl Med 54 (10): 1775-1781, 2013
6) O'Brien TJ et al: Subtraction ictal SPECT co-registered to MRI improves clinical usefulness of SPECT in localizing the surgical seizure focus. Neurology 50: 445-454, 1998
7) Carla LK: Surgical outcome in PET-positive, MRI-negative patients with temporal lobe epilepsy. Epilepsia 53 (2): 342-348, 2012

BQ 7 Are MRI and cerebral blood flow SPECT recommended to diagnose Alzheimer's disease (AD)?

Statement

MRI can detect the medial temporal lobe atrophy that is characteristic of AD, and it is also useful for diagnosing diseases that result in cognitive impairment other than AD. It is therefore recommended.

Cerebral blood flow SPECT can visualize the decreased blood flow in the bilateral temporoparietal lobes and posterior cingulate gyrus/precuneus that is characteristic of AD and is therefore recommended.

Background

The prevalence of dementia is increasing throughout the world, and the increase in mild dementia, particularly AD, is becoming a social problem in Japan, which has entered an era of extreme population aging. This BQ summarizes the evidence regarding the usefulness of MRI, cerebral blood flow SPECT, and PET in diagnosing AD.

Explanation

Advances in diagnostic imaging technology have made it possible to detect the mild cerebral atrophy and decreases in blood flow and metabolism that occur in dementia. Consequently, the role played by diagnostic imaging in AD diagnosis has changed from an adjunctive one of excluding dementing disorders other than AD to being an important method that supports early AD diagnosis. Assessment of cerebral volume and blood flow and glucose metabolism by statistical image analysis or amyloid PET provides high diagnostic accuracy in predicting conversion from mild cognitive impairment (MCI) to AD and is regarded as clinically important.

1. MRI

Beginning early in AD, a decrease in the number of neurons in the medial temporal lobe is seen, resulting in cerebral parenchymal atrophy (Fig. 1). A meta-analysis of 12 investigations that evaluated medial temporal lobe atrophy with MRI showed sensitivity and specificity of 85% and 88%, respectively, in differentiating patients with AD from healthy individuals.[1)] Based on statistical image analysis using voxel-based morphometry (VBM), atrophy was seen in areas such as the posterior cingulate gyrus/precuneus, fusiform gyrus, and medial frontal lobe in AD, in addition to the medial temporal lobe (hippocampus, entorhinal area).[2)] However, caution is required because the sites of atrophy differ depending on the patient's age at onset (with onset at a young age, medial temporal lobe atrophy is mild, and parietal lobe atrophy is pronounced).[3)] The use of special software had previously been required for VBM analysis. Since 2006, however, the voxel-based specific regional analysis system for AD (VSRAD®) has been available for use in Japan. The diagnostic accuracy rate of VBM analysis with the

hippocampus/entorhinal area as the region of interest was 87.8%.[4] In clinical use, however, VBM cannot be used alone, but rather must always be used as an adjunct to interpretation of the original image. MR examinations other than morphological diagnosis that have been shown to be useful are ^{1}H-MR spectroscopy and diffusion tensor imaging, which reflect changes in brain tissue in AD. In differentiating AD patients from healthy individuals, the sensitivity and specificity of ^{1}H-MR spectroscopy based on the myo-inositol/N-acetyl aspartate ratio (MI/NAA) have been reported to be 83% and 98%, respectively.[5] With diffusion tensor imaging, a decrease in diffusion anisotropy in the limbic system and uncinate bundle has been found to be characteristic.[6] However, these methods have not reached the stage of routine clinical use. The use of arterial spin labeling (ASL) in differential diagnosis by acquiring non-contrast cerebral blood flow images with MRI has been attempted.[7] However, this too has not reached the stage of routine clinical use. Methods of AD diagnosis by artificial intelligence using deep learning have also been developed in recent years, but they have not reached the stage of routine clinical use.

2. Blood flow SPECT

Compared with healthy individuals of similar age, individuals with AD have decreased blood flow in the temporoparietal association cortex and posterior cingulate gyrus/precuneus, and cerebral blood flow SPECT can detect it (Fig. 2). In a large, prospective study, the sensitivity and specificity of cerebral blood flow SPECT in differentiating individuals with AD from healthy individuals were 89% and 80%, respectively.[8] When cerebral blood flow SPECT was compared with standard clinical diagnosis, the sensitivity of cerebral blood flow SPECT was lower (74% vs. 81%), but its specificity was higher (91% vs. 70%). Methods of statistical image analysis that have been widely adopted in the clinical setting and are used as diagnostic aids include medi+FALCON®, which uses three-dimensional stereotactic surface projection (3D-SSP), and the easy Z-score imaging system (eZIS®), which uses statistical parametric mapping (SPM). Furthermore, the sensitivity and specificity of cerebral blood flow SPECT in differentiating AD from other dementing disorders (frontotemporal dementia, vascular dementia) range from 70% to 79%, indicating that blood flow SPECT is also useful for differentiating AD from dementing disorders other than AD.[9]

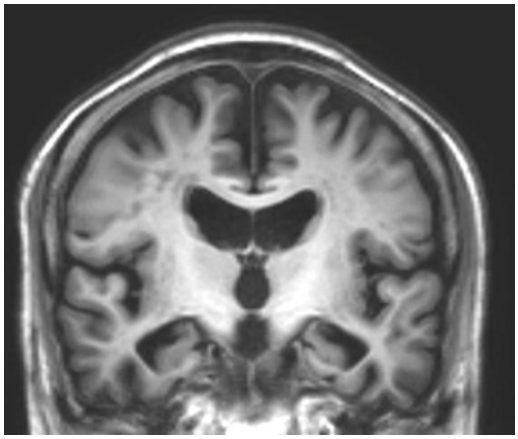

Figure 1. Alzheimer's-type dementia (1)

MRI, T1-weighted coronal image: Atrophy of the bilateral medial temporal lobes (hippocampus, parahippocampal gyri) is seen.

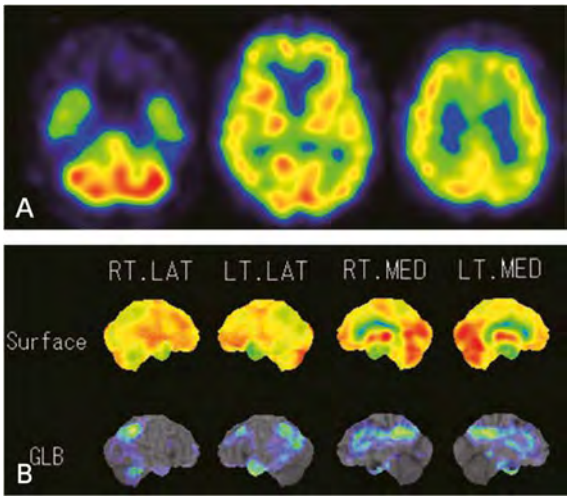

Figure 2. Alzheimer's-type dementia (2)

A: Cerebral blood flow SPECT (^{123}I-IMP, axial image)
B: Statistical image analysis (3D-SSP image)
Decreased blood flow is seen in disease-specific regions (posterior cingulate gyrus/precuneus, temporoparietal association cortex).

3. PET (^{18}F-FDG PET, amyloid PET, tau PET)

The use of PET for AD is not covered by national health insurance in Japan (FDG-PET is being performed under Advanced Medical Care Category B, pharmaceutical approval has been received for 3 devices to synthesize ^{18}F-labeled amyloid PET agents and 2 delivery agents, and the results will be reported with the aim of insurance coverage). However, it has been reported to be useful in diagnosing AD and differentiating it from other types of degenerative dementia.[10, 11] FDG-PET can detect decreases in glucose metabolism in the temporoparietal association cortex and posterior cingulate gyrus/precuneus in AD more sensitively than cerebral blood flow SPECT. The sensitivity and specificity of FDG-PET in differentiating individuals with AD from healthy individuals range from 86% to 96% and from 80% to 90%, respectively, its diagnostic performance in this role being superior to that of blood flow SPECT.[12-14] The use of statistical image analysis methods such as 3D stereotactic surface projection (3D-SSP) further improves diagnostic accuracy (sensitivity, 95% to 97%; specificity, 100%).[15] Amyloid PET shows amyloid beta-protein accumulation in the brain in AD (senile plaque formation). Reports on ^{18}F-labeled amyloid PET have increased in recent years, particularly reports on the use of ^{11}C-Pittsburgh compound-B (PiB). Although its diagnostic sensitivity is high,[16] amyloid beta-protein accumulation is also seen in some healthy elderly individuals (10% to 30%), in non-AD types of degenerative dementia, such as Lewy body dementia, and in cerebral amyloid angiopathy. Consequently, the presence of amyloid deposits does not necessarily indicate AD.[11, 17] Because the half-life of ^{11}C is a very short 20 minutes, efforts are currently underway to have diagnostic agents labeled with ^{18}F, which has a long half-life, covered by national health insurance so that they can be used in routine clinical practice.[15] For tau PET, which shows tau protein

deposition, next-generation tau PET agents are currently being developed, and their clinical application is expected.[18)]

Search keywords and secondary sources used as references

PubMed was searched using the following keywords: Alzheimer's disease, diagnosis, MRI, SPECT, and PET. The search was limited to investigations described by the following terms: meta-analysis, practice guideline, randomized controlled trial, and review.

In addition, the following were referenced as secondary sources.

1) Japanese Society of Neurology, Ed.: Clinical Practice Guidelines for Dementing disorders 2017. Igaku Shoin, 2017.

References

1) Scheitens P et al: Structural magnetic resonance imaging in the practical assessment of dementia: beyond exclusion. Lancet Neurol 1: 13-21, 2002
2) Karas GB et al: A comprehensive study of gray matter loss in patients with Alzheimer's disease using optimized voxel-based morphometry. Neuroimage 18: 895-907, 2003
3) Ishii K et al. Voxel-based morphometric comparison between early- and late-onset mild Alzheimer's disease and assessment of diagnostic performance of z score images. AJNR Am J Neuroradiol. 26: 333-340, 2005
4) Hirata Y et al: Voxel-based morphometry to discriminate early Alzheimer's disease from controls. Neurosci Lett 15: 269-274, 2005
5) Shonk TK et al: Probable Alzheimer disease: diagnosis with proton MR spectroscopy. Radiology 195: 65-72, 1995
6) Nakata Y et al: Tract-specific analysis for investigation of Alzheimer disease: a brief review. Jpn J Radiol 28: 494-501, 2010
7) Wolk DA et al: Arterial spin labeling MRI: an emerging biomarker for Alzheimer's disease and other neurodegenerative conditions. Curr Opin Neurol 25: 421-428, 2012
8) Jobst KA et al: Accurate prediction of histologically confirmed Alzheimer's disease and the differential diagnosis of dementia: the use of NINCDS-ADRDA and DSM-III-R criteria, SPECT, X-ray CT, and Apo E4 in medial temporal lobe dementias: Oxford Project to Investigate Memory and Aging. Int Psychogeriatr 10: 271-302, 1998
9) Dougall NJ et al: Systematic review of the diagnostic accuracy of ^{99m}Tc-HMPAO-SPECT in dementia. Am J Geriatr Psychiatry 12: 554-570, 2004
10) Nasrallah IM et al: Multimodality imaging of Alzheimer disease and other neurodegenerative dementias. J Nucl Med 55: 2003-2011, 2014
11) Ishii K: PET Approaches for diagnosis of dementia. AJNR Am J Neuroradiol 35: 2030-2038, 2014
12) Zakzanis KK et al: A meta-analysis of structural and functional brain imaging in dementia of the Alzheimer's type: a neuroimaging profile. Neuropsychol Rev 13: 1-18, 2003
13) Patwardhan MB et al: Alzheimer disease: operating characteristics of PET-a meta-analysis. Radiology 231: 73-80, 2004
14) Bohnen NI et al: Effectiveness and safety of ^{18}F-FDG PET in the evaluation of dementia: a review of the recent literature. J Nucl Med 53: 59-71, 2012
15) Minoshima S et al: A diagnostic approach in Alzheimer's disease using three dimensional-stereotactic surface projections of fluorine-18-FDG PET. J Nucl Med 36: 1238-1248, 1995
16) Edison P et al: Amyloid, hypometabolism, and cognition in Alzheimer disease: an [11C] PIB and [18F] FDG PET study. Neurology 13: 501-508, 2007
17) Jack CR Jr et al: Serial PIB and MRI in normal, mild cognitive impairment and Alzheimer's disease: implications for sequence of pathological events in Alzheimer's disease. Brain 132 (Pt 5): 1355-1365, 2009
18) Matsuda H et al: Neuroimaging of Alzheimer's disease: focus on amyloid and tau PET. Jpn J Radiol 37: 735-749, 2019

BQ 8 Which imaging examinations are recommended when an intracranial space-occupying lesion is suspected based on the patient's subacute and chronic clinical course?

Statement

MRI is recommended.

CT is recommended if an urgent response is required in circumstances where MRI cannot be promptly performed.

Background

CT and MRI are widely used to diagnose intracranial space-occupying lesions. However, there is no clear indicator of which examination should be given priority. Following is a summary of the evidence regarding the usefulness of CT and MRI for intracranial space-occupying lesions with a subacute or chronic course other than stroke and traumatic lesions.

Explanation

For nearly all abnormal intracranial findings, the sensitivity of MRI is comparable to or greater than that of CT.[1-6)]

MRI provides even better contrast resolution and visualization of details than CT, and it allows imaging to be performed in any arbitrary plane. It is also excellent for detecting lesions associated with no clinical symptoms.[1, 2, 5-8)] Furthermore, MRI is excellent for visualizing areas surrounded by bone, enabling more accurate evaluation of lesions in the posterior cranial fossa, brain stem, and middle cranial fossa than can be performed with CT (Fig.).[2, 9-11)] In particular, MRI is superior to CT for evaluating the status of structures near lesions of the sellar and suprasellar areas, such as the optic nerve, optic chiasm, and internal carotid artery.[7, 8)] On the other hand, CT is better for detecting calcification in lesions and evaluating associated bone changes.[1, 10, 12)]

A review that compared MRI with other modalities, including CT, found that, although MRI affected the treatment strategy, it did not have a major effect on quality of life (QOL).[2)] Although dramatic advances in CT and MRI hardware have been made in the past 30 years, CT still allows imaging to be performed in a shorter time than MRI in nearly all cases. Moreover, MRI is more expensive than CT and, depending on the circumstances of the individual facilities, MRI examinations often cannot be performed expeditiously. CT is adequate for detecting large intracranial masses and hemorrhage of the type that requires immediate intervention.[1-3)] In addition, MRI requires caution regarding the fact that some internal metal products are contraindications for MRI, as typified by the pacemaker. On the other hand, since CT involves radiation exposure, unnecessary examinations should not be performed.

The use of an iodinated contrast agent in CT and of a gadolinium contrast agent in MRI is useful for improving the ability to detect intracranial neoplasms and to determine the overall appearance of lesions.[1, 13-16] In general, contrast-enhanced MRI is superior to contrast-enhanced CT with respect to the ability to detect and visualize lesions. Many intracranial neoplasms are observed more distinctly with contrast-enhanced MRI than with contrast-enhanced CT, such as primary intraaxial brain tumor and metastatic neoplasms, typified by gliomas, as well as meningiomas and schwannomas. This makes contrast-enhanced MRI useful for evaluating the extent of lesion progression (Fig.).[1, 2, 16-20] Particularly for brain metastasis and meningeal dissemination, the detection rate of contrast-enhanced MRI is higher than that of contrast-enhanced CT according to many reports.[3, 16-18, 20] Contrast-enhanced MRI is therefore recommended for detailed examination of intracranial masses using a contrast agent.

However, large meningiomas and schwannomas often can also be evaluated with non-contrast MRI.[13] Moreover, it should be noted that not all intracranial neoplasms exhibit contrast enhancement.

Search keywords and secondary sources used as references

PubMed was searched using keywords such as the following: brain, intracranial, central nervous system, tumor or neoplasm or mass or occupying, CT, MR, and sensitivity or specificity. In selecting articles to use, preference was given to articles with large sample sizes and strong evidence.

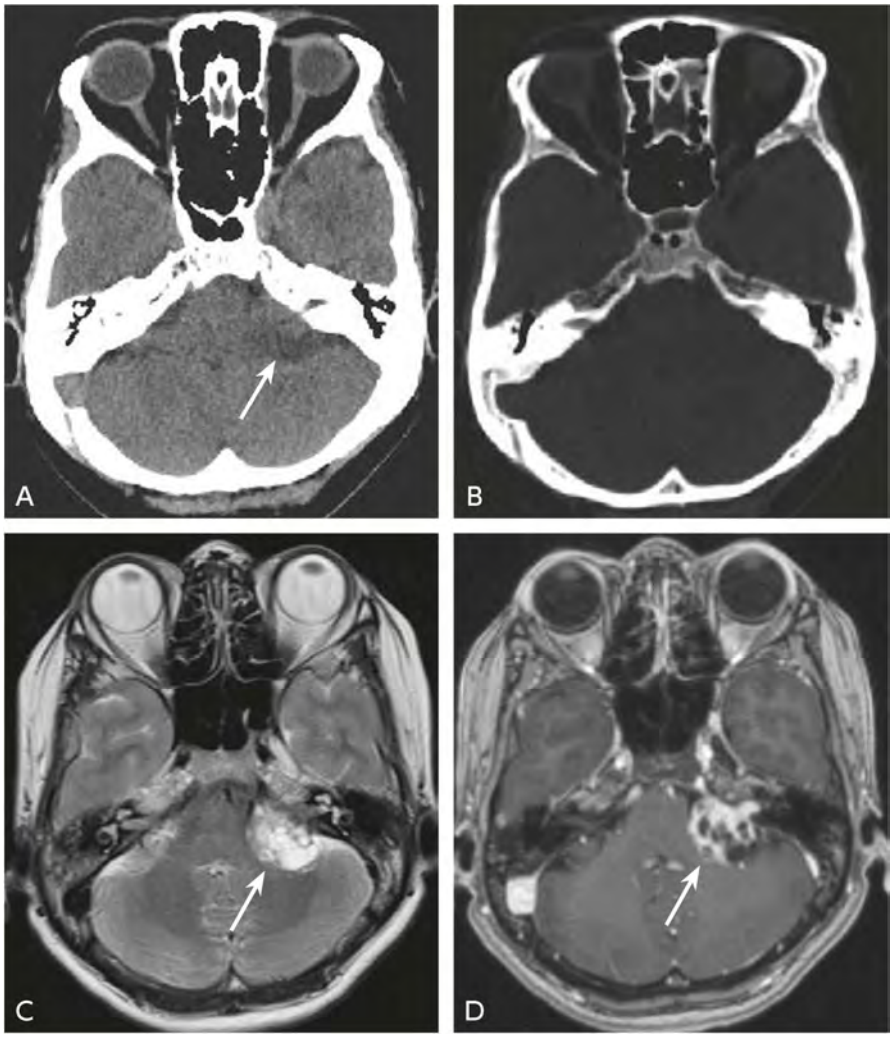

Figure. Left acoustic schwannoma

A: NCCT; B: NCCT, bone imaging conditions; C: MRI, T2-weighted image; D: MRI, contrast-enhanced T1-weighted image. Both CT and MRI enable the presence of the mass to be established (→). However, the overall appearance of the lesion is clearest with contrast-enhanced MRI. The enlargement of the left internal auditory canal is indistinct even on CT under bone imaging conditions.

In addition, the following was referenced as a secondary source.

1) Medina LS, Blackmore C (eds.): Evidence-based imaging: optimizing imaging in patient care. Springer, 2011

References

1) Hutter A et al: Brain neoplasms: epidemiology, diagnosis, and prospects for cost-effective imaging. Neuroimaging Clin N Am 13: 237-250, 2003
2) Kent DL et al: The clinical efficacy of magnetic resonance imaging in neuroimaging. Ann Intern Med 120: 856-871, 1994
3) Medina LS et al: Adults and children with headache: evidence-based diagnostic evaluation. Neuroimaging Clin N Am 13: 225-235, 2003
4) Kucharczyk W et al: Central nervous system tumors in children: detection by magnetic resonance imaging. Radiology 155: 131-136, 1985
5) Price AC et al: Primary glioma: diagnosis with magnetic resonance imaging. J Comput Tomogr 10: 325-334, 1986
6) Orrison WW et al: Comparison of CT, low-field-strength MR imaging, and high-field-strength MR imaging: work in progress. Radiology 181: 121-127, 1991

7) Lee BC et al: Sellar and juxtasellar lesion detection with MR. Radiology 157: 143-147, 1985
8) Karnaze MG et al: Suprasellar lesions: evaluation with MR imaging. Radiology 161: 77-82, 1986
9) Lee BC et al: MR imaging of brainstem tumors. AJNR Am J Neuroradiol 6: 159-163, 1985
10) Barloon TJ et al: Lesions involving the fourth ventricle evaluated by CT and MR: a comparative study. Magn Reson Imaging 7: 635-642, 1989
11) Loneragan R et al: Magnetic resonance imaging evaluation of cerebellopontine angle tumours. Australas Radiol 33: 47-55, 1989
12) Schubeus P et al: Intracranial meningiomas: how frequent are indicative findings in CT and MRI ? Neuroradiology 32: 467-473, 1990
13) Felix R et al: Brain tumors: MR imaging with gadolinium-DTPA. Radiology 156: 681-688, 1985
14) Haughton VM et al: Sensitivity of Gd-DTPA-enhanced MR imaging of benign extraaxial tumors. Radiology 166: 829-833, 1988
15) Elster AD et al: Is Gd-DTPA required for routine cranial MR imaging ? Radiology 173: 231-238, 1989
16) Sze G et al: Detection of brain metastases: comparison of contrast-enhanced MR with unenhanced MR and enhanced CT. AJNR Am J Nueroradiol 11: 785-791, 1990
17) Sze G et al: MR imaging of the cranial meninges with emphasis on contrast enhancement and meningeal carcinomatosis. AJR Am J Roentogenol 153: 1039-1049, 1989
18) Chamberlain MC et al: Leptomeningeal metastasis: a comparison of gadolinium-enhanced MR and contrast-enhanced CT of the brain. Neurology 40: 435-438, 1990
19) Schörner W et al: Intracranial meningiomas: comparison of plain and contrast-enhanced examinations in CT and MRI. Neuroradiology 32: 12-18, 1990
20) Davis P et al: Diagnosis of cerebral metastases: double-dose delayed CT vs contrast-enhanced MR imaging. AJNR Am J Neuroradiol 12: 293-300, 1991

BQ 9 Which imaging examinations are recommended to detect metastatic brain tumors?

Statement

Contrast-enhanced MRI is strongly recommended to detect metastatic brain tumors.

Background

In cancer-bearing patients, whether brain metastasis has occurred is important for determining a treatment strategy. In addition to detecting brain metastatic foci, it is important to accurately determine their number, size, and location to select a treatment. CT and MRI have often been used for this evaluation. With the increase in concern over healthcare resources, an emphasis on avoiding unnecessary examinations has recently emerged. In addition, FDG-PET is becoming ever more widely adopted. For this BQ, the question of which imaging examination should be the first choice for detecting metastatic brain tumors was examined, including an assessment of whether to screen for metastatic brain tumors in cancer-bearing patients.

Explanation

Reports investigating the usefulness of imaging studies for metastatic brain tumors are limited to observational studies, such as cohort studies and case-control studies. Their usefulness is therefore evaluated based on the results of those studies.

Many comparative studies of CT and MRI for the detection of metastatic brain tumors have been conducted since the late 1980s.[1-4] With a normal contrast medium dose, contrast-enhanced MRI detected more metastatic foci than contrast-enhanced CT.[2] Even when compared with contrast-enhanced CT using a double dose of contrast medium, normal contrast-enhanced MRI provided higher detection performance.[3] A comparison of the detection performance of contrast-enhanced CT, T1-weighted and T2-weighted imaging, and contrast-enhanced MRI using the normal contrast dose and triple dose found that the number of metastatic foci detected was highest with MRI using the triple contrast dose, followed in descending order by MRI using the normal contrast dose, contrast-enhanced CT, and T2-weighted and pre-contrast T1-weighted imaging. MRI using the triple contrast dose was significantly better than the other methods, the differences being particularly striking in the detection of metastatic foci $\leq$ 5 mm in size.[4] These reports consistently showed the superiority of contrast-enhanced MRI. Consequently, contrast-enhanced MRI, rather than contrast-enhanced CT, is the imaging examination recommended for detecting metastatic brain tumors.

The contrast medium dose, timing of the imaging, magnetic field strength, and the imaging method used have been examined as factors affecting the performance of contrast-enhanced MRI in detecting lesions.

With regard to the contrast medium dose, several reports indicate that sensitivity for detecting metastatic foci is improved with a triple dose of gadolinium contrast medium.[4-6] Using a 1.5T system, an investigation examined the effects of contrast medium dose and the time from contrast medium administration to imaging on visualization performance with respect to metastatic foci ≤ 10 mm in size. The results showed that contrast dose had the strongest effect on the detection of small lesions. A comparison of immediate-post-administration images showed that, compared with the normal contrast dose, approximately 3 times as many metastatic foci were detected with a triple dose. Moreover, with images acquired immediately after administration of contrast at a triple dose, more metastatic foci were detected than with images acquired 20 minutes after administration of the normal contrast dose.[5] An examination of metastatic foci < 5 mm in size showed that, with administration of a triple dose, detection performance was significantly better than with administration of the normal dose. This was true for both 1.5T and 3T systems.[6] On the other hand, a prospective investigation using a 1.5T system in patients suspected of having metastatic brain tumors found that administration of a triple dose of contrast medium was associated with an increase in false positives and was not useful for any of the patients. It was concluded that the use of a triple dose should be limited to patients with ambiguous findings with the normal dose or when a single metastasis is seen with the normal dose.[7] In Japan, additional administration of up to a double dose of gadoteridol is approved for patients suspected of having metastatic brain tumors for whom visualization with a single administration is judged to be inadequate. Although a single administration of a double dose of gadoteridol has been found to improve visualization compared with additional divided administration of a double dose of gadoteridol,[8] the latter has been approved in Japan. Thus, although administration of double and triple doses of contrast has been considered useful, important issues have been raised. Nephrogenic systemic fibrosis (NSF) is a well-known serious adverse reaction to gadolinium contrast media.[9] In addition, intracerebral deposition of gadolinium contrast media has been identified, although no clinical symptoms have been observed as a result.[10] Based on these considerations, even with a single administration, renal function should be evaluated when contrast media are used, and they should be administered carefully. In Japan, contrast-enhanced MRI is normally performed to detect metastatic brain tumors using a single dose of gadolinium contrast medium. The above findings indicate that additional administration of up to a double dose of gadoteridol is desirable in patients whose findings with a single dose are ambiguous, or if a single metastasis is seen with a single dose.

With regard to timing of the imaging, in the above-mentioned study of metastatic foci ≤ 10 mm in size that used a 1.5T system, although contrast medium dose had the strongest effect on the detection of small lesions, detection performance of small lesions was higher approximately 20 minutes after contrast medium administration than immediately after.[5] Improved detection performance at 7 to 10 minutes after administration compared with immediately after was also noted in the investigation of a single double-dose described above.[8] The above findings indicate that, even with administration of a single dose of contrast medium, improved detection of metastatic brain tumors is likely if the time after administration until imaging is appropriately selected.

With regard to magnetic field strength, an investigation comparing metastatic foci detection performance with a triple dose and normal dose using 3T and 1.5T systems found that performance was highest with the 3-fold dose using the 3T system. Moreover, with either dose, detection of metastatic foci < 5 mm in size was the best with the 3T system.[6] In addition, an increase in the contrast-noise ratio of metastatic brain tumors was reported with a 3T system compared with a 1.5T system.[11] These findings indicate that the use of a 3T system results in improved detection performance with respect to metastatic brain tumors.

With regard to imaging methods, 3D imaging has been found to be useful.[8, 12-14] Differentiation from blood vessel signals is often problematic, particularly for detecting small metastatic foci. However, with 3D high-speed SE using a variable flip angle (VISTA, CUBE, SPACE), blood vessels signals often decrease, facilitating detection and diagnosis of metastatic foci.[15] With contrast-enhanced FLAIR imaging, although metastasis detection sensitivity is low with this method alone, blood vessel signals are low. Consequently, the addition of another imaging method to contrast-enhanced MRI facilitates the differentiation of small metastatic foci and blood vessels.[16] In addition, excellent visualization of metastasis to the pia mater has been reported with contrast-enhanced FLAIR imaging.[17] The presence or absence of pia mater lesions is important information for determining a strategy for treatments such as stereotactic radiation therapy.

FDG-PET/CT is used for whole-body metastasis screening. Although there have been few systematic investigations regarding brain metastasis, in a prospective study of 104 patients with lung cancer, 100 metastatic brain tumor lesions were detected by contrast-enhanced MRI, whereas just 17 lesions were detected with FDG-PET/CT. Moreover, the patient-based sensitivity, specificity, true positive rate, and true negative rate with FDG-PET/CT were 27.3%, 97.6%, 75.0%, and 83.3%, respectively.[18] On the other hand, by expanding the imaging range of FDG-PET/CT whole-body screening to include the brain, brain metastasis may be detected by chance. In a retrospective investigation of 227 patients with lung cancer, brain metastasis was detected by chance in 5 patients.[19] In a study in 1,000 cancer-bearing patients, expanding the imaging range to include the head resulted in detection of brain metastasis by chance in 13 patients.[20] These findings indicate that, though the sensitivity of FDG-PET/CT alone is low for detecting metastatic brain tumors, expanding the imaging range to include the brain during whole-body screening may enable such tumors to be detected by chance.

With the increasing concern about healthcare costs, the need for imaging examinations to screen for metastatic brain tumors in cancer-bearing patients has also been evaluated. Although lung cancer is the primary tumor most commonly responsible for metastatic brain tumors, the guidelines for non-small cell lung cancer developed by the National Comprehensive Cancer Network (NCCN) of the United States recommend brain MRI screening for metastasis in stages II to IV, but they indicate that it is optional in stage Ib, whereas screening by routine brain MRI is not recommended in stage Ia. Supporting this approach, an investigation in 1,751 patients with non-small cell lung cancer found that the incidence of metastatic brain tumors was 0.5% in stage T1 and 0.7% in stage N0.[21] Moreover, in an examination of pretreatment MRI in 109 patients with lung cancer with pure ground-glass nodules, no metastatic brain tumors were detected.[22] These findings indicate that imaging examinations to screen for metastatic brain tumors are unnecessary in stage Ia lung cancer.

Search keywords and secondary sources used as references

PubMed was searched using the following keywords: brain metastasis, CT, and MRI.

In addition, the following was referenced as a secondary source.

1) David S et al: NCCN Guidelines®: non-small cell lung cancer Ver 2. 2021. National Comprehensive Cancer Network, 2021

References

1) Russell EJ et al: Multiple cerebral metastases: detectability with Gd-DTPA-enhanced MR imaging. Radiology 165 (3): 609-617, 1987
2) Sze G et al: Detection of brain metastases: comparison of contrast-enhanced MR with unenhanced MR and enhanced CT. AJNR Am J Neuroradiol 11 (4): 785-791, 1990
3) Davis PC et al: Diagnosis of cerebral metastases: double-dose delayed CT vs contrast-enhanced MR imaging. AJNR Am J Neuroradiol 12 (2): 293-300, 1991
4) Akeson et al: Brain metastases: comparison of gadodiamide injection-enhanced MR imaging at standard and high dose, contrast-enhanced CT and non-contrast-enhanced MR imaging. Acta Radiologica 36 (3): 300-306, 1995
5) Yuh WT et al: The effect of contrast dose, imaging time, and lesion size in the MR detection of intracerebral metastasis. AJNR Am J Neuroradiol 16 (2): 373-380, 1995
6) Ba-Ssalamah A et al: Effect of contrast dose and field strength in the magnetic resonance detection of brain metastases. Invest Radiol 38 (7): 415-422, 2003
7) Sze G et al: Comparison of single- and triple-dose contrast material in the MR screening of brain metastases. AJNR Am J Neuroradiol 19 (5): 821-828, 1998
8) Ochi T et al: Comparison between two separate injections and a single injection of double-dose contrast medium for contrast-enhanced MR imaging of metastatic brain tumors. Magn Reson Med Sc 3 (4): 221-229, 2014
9) Wang Y et al: Incidence of nephrogenic systemic fibrosis after adoption of restrictive gadolinium-based contrast agent guidelines. Radiology 260 (1): 105-111, 2011
10) Kanda T et al: High signal intensity in the dentate nucleus and globus pallidus on unenhanced T1-weighted MR images: relationship with increasing cumulative dose of a gadolinium-based contrast material. Radiology 270 (3): 834-841, 2014
11) Krautmacher C et al: Brain tumors: full- and half-dose contrast-enhanced MR imaging at 3.0 T compared with 1.5 T: initial experience. Radiology 237 (3): 1014-1019, 2005
12) Kakeda S et al: Detection of brain metastasis at 3T: comparison among SE, IR-FSE and 3D-GRE sequences. Eur Radiol 17 (9): 2345-2351, 2007
13) Kato Y et al: Usefulness of contrast-enhanced T1-weighted sampling perfection with application-optimized contrasts by using different flip angle evolutions in detection of small brain metastasis at 3T MR imaging: comparison with magnetization-prepared rapid acquisition of gradient echo imaging. AJNR Am J Neuroradiol 30 (5): 923-929, 2009
14) Nagao E et al: 3D turbo spin-echo sequence with motion-sensitized driven-equilibrium preparation for detection of brain metastases on 3T MR imaging. AJNR Am J Neuroradiol 32 (4): 664-670, 2011
15) Komada T et al: Contrast-enhanced MR imaging of metastatic brain tumor at 3 tesla: utility of T1-weighted SPACE compared with 2D spin echo and 3D gradient echo sequence. Magn Reson Med Sci 7 (1): 13-21, 2008
16) Terae S et al: Contrast-enhanced FLAIR imaging in combination with pre- and postcontrast magnetization transfer T1-weighted imaging: usefulness in the evaluation of brain metastases. J Magn Reson Imaging 25 (3): 479-487, 2007
17) Fukuoka H et al: Comparison of the added value of contrast-enhanced 3D fluid-attenuated inversion recovery and magnetization-prepared rapid acquisition of gradient echo sequences in relation to conventional postcontrast T1-weighted images for the evaluation of leptomeningeal diseases at 3T. AJNR Am J Neuroradiol 31 (5): 868-873, 2010
18) Krüger S et al: Brain metastasis in lung cancer. Comparison of cerebral MRI and ^{18}F-FDG-PET/CT for diagnosis in the initial staging. Nucl Med 50 (3): 101-106, 2011
19) Nia ES et al: Incidence of brain metastases on follow-up (18) F-FDG PET/CT scans of non-small cell lung cancer patients: should we include the brain? J Nucl Med Technol 45 (3): 193-197, 2017
20) Abdelmalik AG et al: The incremental added value of including the head in (18) F-FDG PET/CT imaging for cancer patients. Front ncol 3: 71, 2013
21) Diaz ME et al: Non-small cell lung cancer brain metastasis screening in the era of positron emission tomography-CT staging: current practice and outcomes. J Med imaging Rad Oncol 62 (3): 383-388, 2018
22) Cho H et al: Pure ground glass nodular adenocarcinomas: are preoperative positron emission tomography/computed tomography and brain magnetic resonance imaging useful or necessary ? J Thorac Cardiovasc Surg 150 (3): 514-520, 2015

2
Head and Neck

Standard Imaging Methods for Head and Neck

Introduction

Unless otherwise indicated, the following applies both to CT and MRI of the head and neck.

① The standard CT slice thickness is ≤ 3 mm regardless of the conditions.

② Reconstructed CT images are generated for the transverse plane with soft tissue and bone conditions and for the coronal and/or sagittal plane as needed.

③ For contrast-enhanced CT, either 100 mL or twice the patient's weight in mL of a nonionic contrast agent at a concentration of 240 to 300 mgI/mL is intravenously injected at a rate of 2 to 3 mL/second, and imaging is performed 50 to 70 seconds later. For CTA, a high-concentration contrast medium is used.

④ MRI slice thickness is 3 mm, and the slice gap is 1 mm. Although an FOV of 160 to 180 mm is the standard for local evaluation, decreases in the SNR should be taken into account, and the optimal imaging conditions for each system used.

⑤ With contrast-enhanced MRI, a gadolinium contrast medium is administered intravenously at a dose equal to the patient's weight (kg) multiplied by 0.1 mmol/kg, and imaging is performed.

⑥ MRI is generally more suitable for the local evaluation of head and neck cancer. However, contrast-enhanced CT is suitable for the hypopharynx and larynx.

⑦ Fat-suppressed contrast-enhanced 3D T1-weighted imaging [CUBE (GE), SPACE (Siemens), VISTA (Philips), MPV (Canon Medical Systems), iso FSE (Hitachi)] is used for purposes such as evaluating the detailed lesion distribution and diagnosing perineural spread, and reconstruction allows observations in any arbitrary plane. Although not indicated in the examples of protocols, it can be considered as needed.

⑧ There are a variety of imaging methods for fat suppression, with differences in the suppressive effect depending on the system and imaging method used. It is important to use them as needed based on the advantages and shortcomings of each.

Orbit and optic nerve

1. Overview

CT is suitable for screening for conditions such as proptosis, oculomotor dysfunction, double vision, visual impairment, trauma, foreign bodies, inflammation, and tumors. MRI is sensitive for purposes such as detecting small lesions, hemorrhage, and melanin pigment associated with malignant melanoma of the eyeball. Tumors and inflammation of the optic nerve or orbit are good indications for contrast-enhanced MRI. When optic nerve and intracranial lesions are suspected based on the presence of a condition such as neuromyelitis optica, MRI is also very useful because it can evaluate these lesions in a single examination

(Fig. 1). Screening for intraorbital foreign bodies is first performed by CT, and evaluation by MRI is useful if the presence of metal is ruled out by CT.[1, 2)]

2. Detailed discussion

① CT (Table 1)

(1) Non-contrast CT is standard, but contrast-enhanced imaging is performed if inflammation or a tumor is present. Non-contrast CT is also useful for pathological changes associated with calcification, such as venous malformation and retinoblastoma.

(2) The imaging range should sufficiently include the orbit.

(3) Thin slices approximately 1-mm thick can be tried for observation of foreign bodies or orbital fractures.

② MRI (Table 2)

(1) Using a head coil, imaging is performed over a range that includes the orbit and cavernous sinus.

(2) Caution is required regarding eye-movement artifacts; imaging is performed with the patient at rest with eyes closed.

(3) Contrast-enhanced imaging is performed for tumors and inflammation. If contrast-enhanced imaging cannot be performed, fat-suppressed T2-weighted, STIR, or diffusion-weighted imaging may be informative.

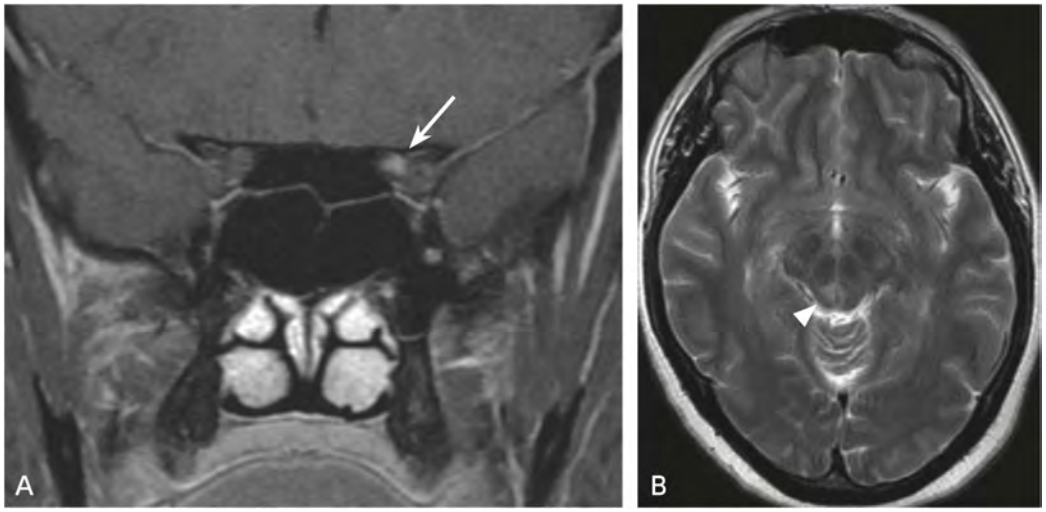

Figure 1. Neuromyelitis optica

A: Orbital MRI, fat-suppressed, contrast-enhanced T1-weighted coronal image; B: Head MRI performed at the same time, T2-weighted transverse image

Contrast enhancement of the left optical nerve is seen in A (→). An area of faint hyperintensity is seen in the periphery of the cerebral aqueduct (▷), consistent with neuromyelitis optica.

Table 1. Examples of protocols for the orbit: 64-row MDCT system

Imaging Range	Reconstruction Function	Scan Slice Thickness	Reconstruction Slice Thickness	Reconstruction Slice Interval	FOV	WW/WL	Image Processing
From the superior margin of the dentition to 1 cm cranial to the supraorbital margin	For soft tissue	≤ 0.625 mm	≤ 2 mm	Same as at left	160 mm	350/30	Coronal plane Sagittal plane added as appropriate
Same as above	For bone	≤ 0.625 mm	≤ 2 mm	Same as at left	160 mm	4,000/500	Coronal plane Sagittal plane added as appropriate

Note 1: The imaging dose is selected by taking into account radiation exposure of the lens, and selective dose-reduction mechanisms are aggressively used.
Note 2: If the patient has no teeth, imaging is performed 1 cm caudal to the inferior margin of the hard palate in reference to the lateral view of the image used to determine location.

Table 2. Examples of orbit sequences: 3T MRI system, head coil

Imaging Method	Sequence	TR/TE	Slice Thickness	Other
① T2-weighted/transverse	FSE	4,000/85 ms	3 mm	The entire brain is imaged if a demyelinating disease such as NMO* is suspected.
② Fat-suppressed T2-weighted/coronal	FSE	4,000/85 ms	3 mm	Changed to coronal STIR if fat suppression is poor due to the effect of a metal object, etc.
③ T1 weighted/transverse	SE	400/10 ms	3 mm	
④ Fat-suppressed T1-weighted/coronal	FSE	479/12.3 ms	3 mm	
⑤ Diffusion-weighted	EPI	6,500/55.3 ms	3 mm	The entire brain is imaged and an ADC map generated if a demyelinating disease such as NMO* is suspected.
⑥ Fat-suppressed, contrast-enhanced T1-weighted/transverse	FSE	479/12.3 ms	3 mm	
⑦ Fat-suppressed, contrast-enhanced T1-weighted/coronal	FSE	479/12.3 ms	3 mm	Changed to DIXON contrast-enhanced T1-weighted coronal if fat suppression is poor due to effect of a metal object, etc.

Note 1: Imaging performed at rest with eyes closed
*NMO: neuromyelitis optica

(4) Attention should be paid to decreases in the SNR if artifacts caused by an item such as a dental prosthetic are prominent with fat-suppressed T2-weighted imaging, and STIR imaging is used instead.

(5) Note that makeup occasionally results in artifacts and hinders diagnostic imaging.

(6) Diffusion-weighted imaging may be useful in diagnosing conditions such as malignant lymphoma, orbital cellulitis, IgG4-related disease, retinoblastoma, optic neuritis, lacrimal gland tumors, and epidermoid cysts.[3)]

Nasal cavity and paranasal sinuses

1. Overview

The nasal cavity and paranasal sinuses are a complex mix of pneumatic space, bone, and soft tissue, which show good tissue contrast on CT. CT provides higher spatial resolution than MRI and is also excellent for visualizing small soft tissue lesions in pneumatic space and minor bone erosion. In chronic sinusitis, CT is good for showing items such as the affected area, normal variants of the nasal cavity and paranasal sinuses, as well as sinusitis complications, and therefore plays an important role in determining a procedure for endoscopic sinus surgery (ESS). In conditions such as eosinophilic sinusitis and allergic fungal rhinosinusitis, allergic mucin in affected sinuses shows high attenuation on CT. Changes such as polyps, cysts, mucosal thickening, and tumors show similar soft tissue attenuation on CT. MRI is useful for differentiating between these soft-tissue lesions and changes such as granulomatous lesions and mycotic infections, and tumors of the nasal cavity and paranasal sinuses are particularly good indications for MRI (Fig. 2). Contrast-enhanced MRI shows tumor and inflammation localization and intracranial extension well. CT is the first choice imaging modality for bone fractures, including those of the nasal cavity and paranasal sinuses.[4-6)]

2. Detailed discussion

① CT (Table 3)

(1) A plain examination is used for screening. Contrast-enhanced imaging is performed for tumors.

(2) The imaging range sufficiently includes the nasal cavity and paranasal sinuses.

(3) Observation in the coronal and transverse planes is standard.

(4) The addition of sagittal plane images is useful for observations such as those of the drainage route and normal variants of the paranasal sinuses and the course of the anterior and posterior ethmoidal arteries.

(5) In the nasal cavity and paranasal sinuses, bone and pneumatic space adjoin in a complex fashion, making them susceptible to artifacts caused by partial volume effects. Consequently, a slice thickness of ≤ 2 mm is used.

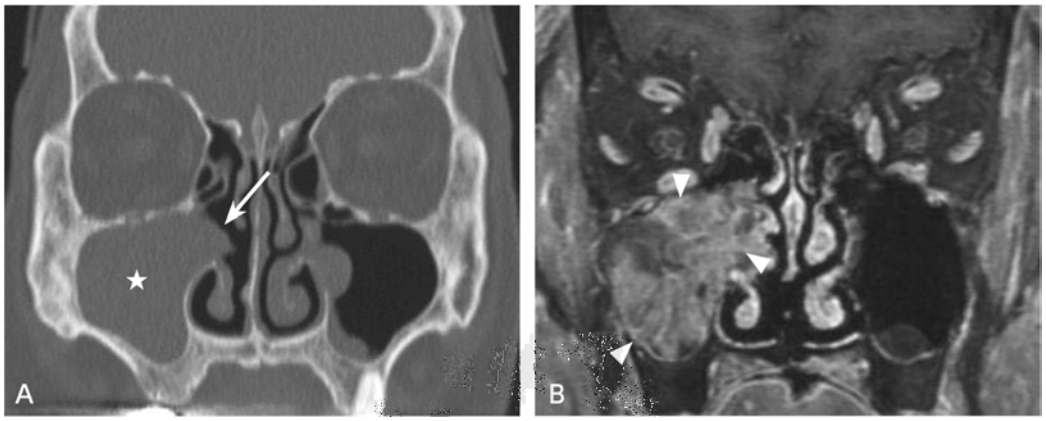

Figure 2. Inverted papilloma

A: Non-contrast CT, bone algorithm, coronal image; B: MRI, fat-suppressed, contrast-enhanced, T1-weighted coronal image
In A, soft tissue attenuation is seen in the right maxillary antrum (☆), and the maxillary infundibulum is widened (→). In B, convoluted solid masses are seen in the area from the right maxillary antrum to the middle meatus (▷), which is typical for inverted papilloma.

Table 3. Examples of protocols for the nasal cavity and paranasal sinuses: 64-row MDCT system

Imaging Range	Reconstruction Function	Scan Slice Thickness	Reconstruction Slice Thickness	Reconstruction Slice Interval	FOV	WW/WL	Image Processing
From the inferior margin of the dentition to 1 cm cranial to the superior margin of the frontal sinus	For soft tissue	≤ 0.625 mm	≤ 2 mm	Same as at left	160 mm	350/30	Coronal plane Sagittal plane added as appropriate
Same as above	For bone	≤ 0.625 mm	≤ 2 mm	Same as at left	160 mm	4,000/500	Coronal plane Sagittal plane added as appropriate

Note 1: The imaging dose is selected by taking into account radiation exposure of the lens, and selective dose-reduction mechanisms are aggressively used.
Note 2: If the patient has no teeth, imaging is performed 1 cm caudal to the inferior margin of the hard palate in reference to the lateral view of the image used to determine location.

Table 4. Examples of sequences for the nasal cavity and paranasal sinuses: 3T MRI system, head and neck coil

Imaging Method	Sequence	TR/TE	Slice Thickness	Other
① T2-weighted/transverse	FSE	4,000/85 ms	3 mm	
② T1-weighted/transverse	SE	480/10 ms	3 mm	
③ Fat-suppressed, T2-weighted/coronal	FSE	4,000/85 ms	3 mm	
④T1-weighted/coronal	SE	480/10 ms	3 mm	
⑤ Diffusion-weighted	EPI	6,000/55.3 ms	3 mm	STIR, ADC mapping
⑥ Contrast-enhanced, T1-weighted/transverse	SE	480/10 ms	3 mm	
⑦ Fat-suppressed, contrast-enhanced, T1-weighted/coronal	FSE	667/7.8 ms	3 mm	

Note: STIR is used as the method of fat suppression in diffusion-weighted imaging in view of the poor fat suppression that results from magnetic field non-uniformity.

② MRI (Table 4)

(1) A head and neck coil is used for imaging, and the imaging range includes the nasal cavity and paranasal sinuses sufficiently.

(2) Areas near pneumatic spaces are prone to susceptibility artifacts. Particular attention should be paid to decreased image quality with fat suppression.

(3) Contrast-enhanced imaging is performed for tumors and inflammation.

(4) Attention should be paid to decreases in the SNR if artifacts caused by an item such as a dental prosthetic are prominent with fat-suppressed T2-weighted imaging, and STIR imaging is used instead.

(5) Diffusion-weighted imaging is useful for purposes such as determining whether a sinonasal tumor is benign or malignant and qualitatively diagnosing conditions such as malignant lymphoma. Because of the large amount of airspace, however, diffusion-weighted imaging is prone to susceptibility artifacts, which often makes the evaluation of small lesions particularly difficult.

Oral cavity

1. Overview

In this region, oral cavity cancer, typified by tongue cancer, abscesses, and inflammatory diseases such as osteomyelitis are important. CT is useful for evaluating aspects such as tumor extension, bone invasion, and lymph node metastasis in oral cavity cancer. However, metal artifacts caused by dental treatment often interfere with diagnosis. Gold is the metal most commonly used in dental care in Japan, and there are far fewer metal artifacts with MRI than with CT.[7)] Contrast-enhanced MRI shows the tumor extension of oral cavity cancer well and is the first-choice imaging modality (Fig. 3). Contrast-enhanced CT is used for evaluation if MRI is contraindicated. Diagnostic imaging of inflammatory disease of the oral cavity region is a good indication for contrast-enhanced CT.[8, 9)] ^{18}F-FDG PET sensitively detects oral cavity cancer and metastatic lymph nodes and is also useful for screening for distant metastasis. PET should be used if postoperative recurrence or metastasis is suspected, but no lesions are clearly seen on CT or MRI. With regard to its indications, however, careful judgement based on CT and MRI findings is required.[10-12)]

2. Detailed discussion

① Standard CT imaging method when inflammation is suspected

(1) Contrast-enhanced CT is performed.

(2) Abscesses may broadly progress vertically. Imaging is performed from the skull base to the superior mediastinum. If an abscess is present, additional imaging of the chest is performed.

(3) Bone algorithm is always added for dental caries and osteomyelitis.

② Standard imaging methods when a tumor is suspected

(1) CT

(A) CT is suitable for evaluating tumor extension, maxillary invasion, and cervical lymph node metastasis in oral cavity cancer.

(B) Contrast-enhanced CT is performed.

(2) MRI (Table 5)

(A) MRI shows the relationship between tumors and the deep lingual muscles well and thus contributes to accurate T-staging.

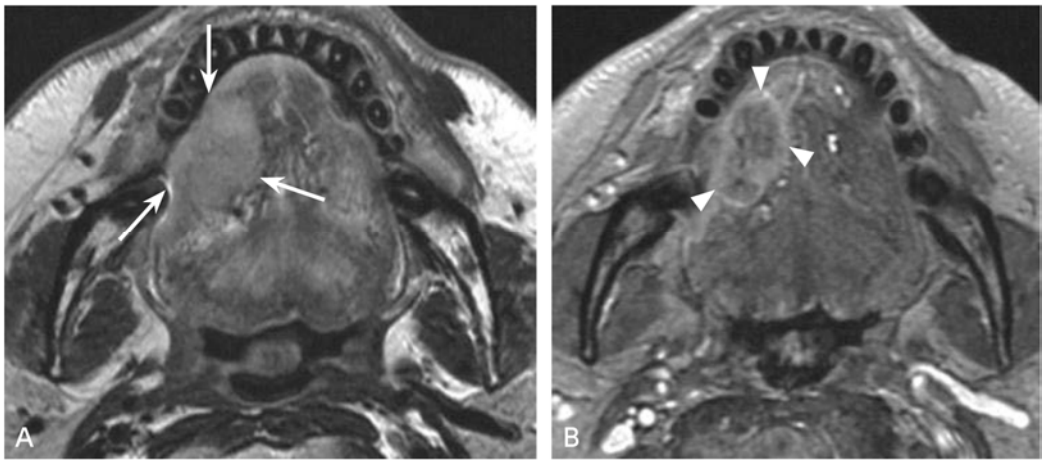

Figure 3. Tongue cancer

A: MRI, T2-weighted image; B: MRI, fat-suppressed, contrast-enhanced, T1-weighted image
In A, a mass with an irregular border that is nearly isointense with muscle is seen on the right margin of the tongue (→). In B, strong contrast enhancement is seen at the margin of the mass (▷).

Table 5. Examples of sequences for the oral cavity: 3T MRI system, head and neck coil

Imaging Method	Sequence	TR/TE	Slice Thickness	Other
① T2-weighted/transverse	FSE	4,000/85 ms	3 mm	
② T1-weighted/transverse	SE	480/10 ms	3 mm	
③ T2-weighted/coronal	FSE	4,000/85 ms	3 mm	
④T1-weighted/coronal	SE	480/10 ms	3 mm	
⑤ Diffusion-weighted	EPI	6,000/55.3 ms	3 mm	STIR, ADC mapping
⑥ Contrast-enhanced, T1-weighted/transverse	SE	480/10 ms	3 mm	
⑦ Fat-suppressed, contrast-enhanced, T1-weighted/transverse or coronal	FSE	667/7.8 ms	3 mm	

Note 1: The examinee is asked to take small breaths, minimize tongue movement, and appropriately refrain from swallowing.
Note 2: STIR is used as the method of fat suppression in diffusion-weighted imaging in view of the poor fat suppression that results from magnetic field non-uniformity.

(B) Imaging is performed using a head and neck coil, and the imaging range includes the area from the soft palate to the floor of the mouth sufficiently.

(C) Tongue movement and swallowing during imaging result in image quality deterioration. The patient is asked to minimize these movements.

Temporal bone

1. Overview

CT is often performed for conditions such as conductive hearing loss, chronic otitis media, mastoiditis, cholesteatoma, congenital hearing disorder, and facial paralysis and middle ear disorder/inner ear disorder

resulting from bone fracture. CT is good for showing the bone structure of the temporal bone and bone changes resulting from lesions (Fig. 4A).[13] MRI is performed after CT for detailed examination. It enables the characterization of soft tissue lesions and the observation of structures such as the facial and auditory nerves.

2. Detailed discussion

① CT (Table 6)

(1) Non-contrast CT can be considered standard. Contrast-enhanced imaging is performed for tumors.

(2) Tomograms with a thickness of ≤ 1 mm are generated using bone algorithm.

(3) The plane parallel to the hard palate is considered the transverse plane, and images in this plane are displayed together with coronal plane images, which are acquired in the plane perpendicular to the transverse plane.

② MRI (Table 7)

(1) T1- and T2-weighted transverse images are acquired. Contrast-enhanced imaging is also necessary for tumors.

(2) A slice thickness of 2 mm is ideal. However, care is needed because a decreased SNR interferes with diagnosis. The imaging conditions are therefore optimized for the system used.

(3) SSFP (e.g., FIEST-C, CISS, balanced FFE) enables the inner ear to be observed at high spatial resolution.

(4) Diffusion-weighted imaging with reduced susceptibility artifacts is useful for diagnosing cholesteatoma (Fig. 4B).

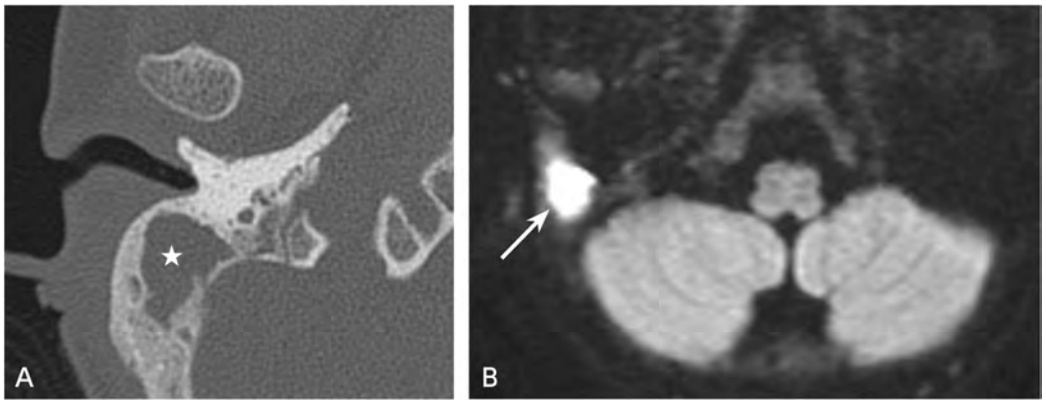

Figure 4. Right cholesteatoma

A: Non-contrast CT, bone algorithm; B: MRI, diffusion-weighted image

In A, no bony partition of the right mastoid air cells is seen, the soft tissue density is full, and there is associated bone erosion at the margin (☆). In B, the lesion shows distinct hyperintensity, consistent with cholesteatoma.

Table 6. Example protocol for the temporal bone: 64-row MDCT system

Imaging Range	Reconstruction Function	Scan Slice Thickness	Reconstruction Slice Thickness	Reconstruction Slice Interval	FOV	WW/WL	Image Processing
From the inferior margin of the mastoid air cells to 1 cm cranial to the petrous apex	For bone	≤ 0.625 mm	≤ 1 mm	Same as at left	≤ 100 mm	4,000/500	Coronal plane, sagittal plane added as appropriate Reconstruction enlarged separately for left and right Soft tissue algorithm added as appropriate

Note: An imaging plane that excludes the lens from the imaging range is selected.

Table 7. Examples of temporal bone sequences: 3T MRI system, head coil

Imaging Method	Sequence	TR/TE	Slice Thickness	Other
① T2-weighted/transverse	FSE	4,000/85 ms	2 to 3 mm	
② T1-weighted/transverse	SE	480/10 ms	2 to 3 mm	
③ T2-/T1-weighted/transverse	Balanced SSFP*	4.6/2.2 ms	1 mm	MPR generated 3D T2-weighted transverse imaging also feasible
④ Diffusion-weighted	EPI**	6,000/55.3 ms	3 mm	STIR, ADC mapping
⑤ Contrast-enhanced, T1-weighted/transverse	SE	480/10 ms	3 mm	Coronal plane added as appropriate
⑥ Contrast-enhanced, T1-weighted/transverse	3D FSPGR***	8.3/3.3 ms	1 mm	

Note: STIR is used as the method of fat suppression in diffusion-weighted imaging in view of the poor fat suppression that results from magnetic field non-uniformity.

*FIESTA-C/FIESTA (GE), CISS/True FISP (Siemens), Balanced FFE (Philips), True SSFP (Canon Medical Systems), balanced SARGE (Hitachi)

**EPI diffusion-weighted imaging is prone to susceptibility artifacts, particularly in areas of the temporal bone where air is prevalent. Consequently, if imaging can be performed, non-EPI diffusion-weighted imaging is preferable.

***FSPGR: fast spoiled gradient echo

Salivary glands

1. Overview

If salivary calculus is suspected clinically, this is a good indication for CT. MRI is more sensitive than CT for salivary gland inflammation. In salivary gland tumors, MRI is also superior to CT both for identifying the presence of lesions and diagnosing them qualitatively. Contrast-enhanced MRI with concomitant fat suppression is particularly useful for evaluating perineural spread. The change in contrast enhancement over time with dynamic contrast-enhanced MRI of parotid tumors and diffusion-weighted imaging with the measurement of ADC values can aid in differentiating benign from malignant parotid masses, particularly pleomorphic adenomas.[14, 15])

2. Detailed discussion

① CT

(1) Salivary calculus itself can be diagnosed with non-contrast CT. If contrast-enhanced CT is performed for a purpose such as evaluating associated sialadenitis, nearly all salivary calculi can be detected with the bone algorithm of contrast-enhanced CT.[16] To reduce radiation exposure, care should therefore be exercised in deciding whether to perform non-contrast CT (before contrast-enhanced imaging).

(2) Salivary calculus in the salivary duct may not be observable due to artifacts caused by dental prosthetics. The addition of plain radiography is useful.

② MRI (Table 8)

(1) A head and neck coil is used for imaging.

(2) Contrast-enhanced imaging is performed for tumors and inflammation.

(3) Fat-suppressed T2-weighted and STIR imaging may also be instructive for diagnosis.

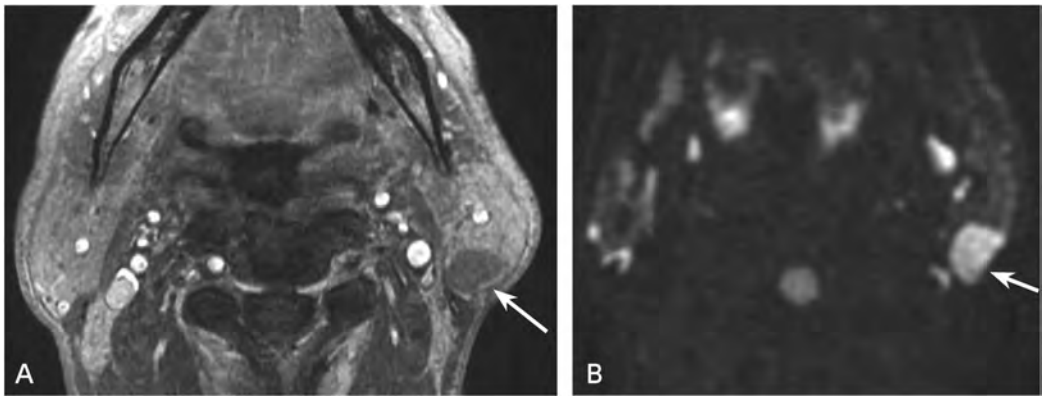

Figure 5. Warthin's tumor of the left parotid gland

A: MRI, fat-suppressed, contrast-enhanced, T1-weighted image; B: MRI, diffusion-weighted image
In A, a mass with distinct borders and uniform characteristics is seen in the lower dorsal region of the left parotid gland (→). In B, the mass shows hyperintensity (→). The ADC value is 0.80×10^{-3} mm^2/s. Although the findings are suggestive of a Warthin's tumor, caution is required in differentiating it from malignancy.

Table 8. Examples of sequences for the salivary gland: 3T MRI system, head and neck coil

Imaging Method	Sequence	TR/TE	Slice Thickness	Other
① T2-weighted/transverse	FSE	4,000/85 ms	3 mm	
② T1-weighted/transverse	SE	480/10 ms	3 mm	
③ STIR/coronal	STIR	8,800/60 ms	3 mm	
④ Fat-suppressed T1-weighted/coronal*	FSE	667/7.8 ms	3 mm	Imaging performed over a range that includes the cavernous sinus/the course of V3**
⑤ Diffusion-weighted	EPI	6,000/55.3 ms	3 mm	STIR, ADC mapping
⑥ Contrast-enhanced, T1-weighted/transverse (multiphase imaging)	3D FSPGR	5.6/2.7 ms	3 mm	Imaging at pre-injection and 30, 60, 90, 120, and 180 seconds after injection
⑦ Contrast-enhanced T1-weighted/transverse	SE	480/10 ms	3 mm	Coronal plane added as appropriate
⑧ Fat-suppressed, contrast-enhanced T1-weighted/coronal*	FSE	667/7.8 ms	3 mm	Imaging performed over a range that includes the cavernous sinus/the course of V3**

Note 1: The examinee is asked to take small breaths, minimize tongue movement, and appropriately refrain from swallowing.
Note: STIR is used as the method of fat suppression in diffusion-weighted imaging in view of the poor fat suppression that results from magnetic field non-uniformity.
*CHESS recommended
**V3: 3rd branch of the trigeminal nerve

(4) Diffusion-weighted imaging may be useful for determining whether a salivary gland tumor is benign or malignant and for diagnosing it qualitatively. However, because the ADC values of Warthin's tumors, which are benign, are low, overlap is seen between the ADC values of benign and malignant tumors (Fig. 5).

Upper and middle pharynx

1. Overview

Inflammatory disease of the upper and middle pharynx is a good indication for contrast-enhanced CT. MRI is the first choice of imaging examinations for nasopharyngeal tumors. It is useful for differentiating from malignant lymphoma and adenoid hypertrophy, and it allows the extent of tumor extension to be determined in detail. CT sensitively detects subtle changes in the cortex of bone resulting from tumor invasion. If bone invasion is suspected based on MRI, it is important to compare the findings with those of CT during diagnosis (Fig. 6). In oropharyngeal cancer, diagnosis is susceptible to interference by artifacts caused by dental prosthetics (Fig. 7). MRI is the first choice because suprahyoid cervical lymph node metastasis is often difficult to detect on CT. PET is recommended when differentiating recurrence/metastasis and posttreatment change is difficult with CT or MRI.[11, 12, 17)]

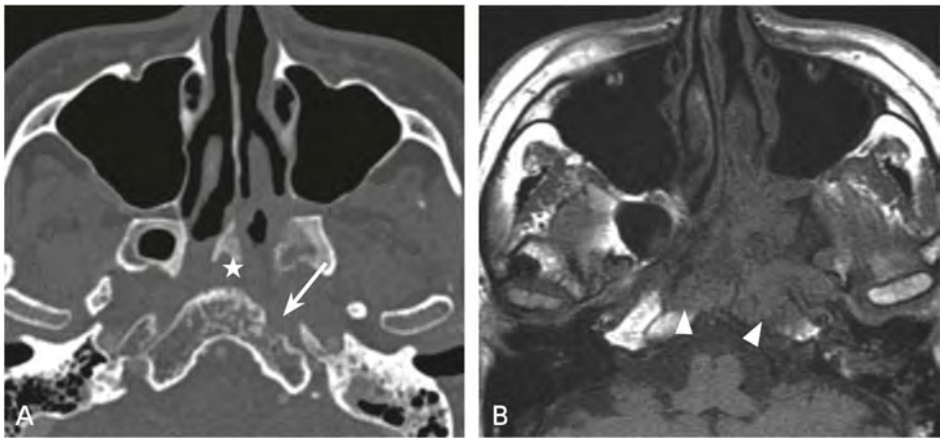

Figure 6. Cranial base invasion of nasopharyngeal cancer

A: Non-contrast CT, bone algorithm; B: MRI, T1-weighted image

In A, the bony cortex of the anterior margin of the clivus, which adjoins the neoplastic area (☆), is ruptured (→). In B, the bone marrow of the clivus shows hypointensity (▷), a finding indicative of extensive bone marrow infiltration.

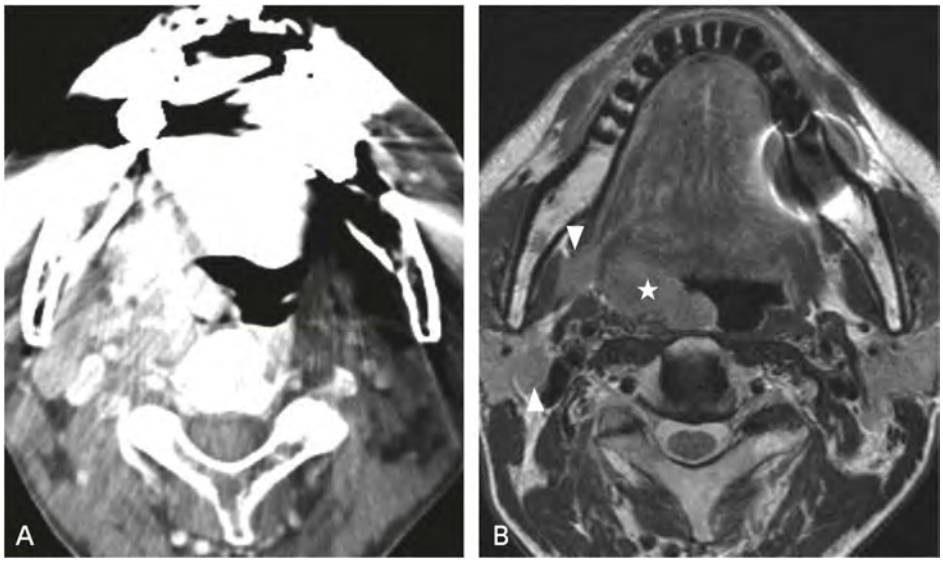

Figure 7. Oropharyngeal cancer and lymph node metastasis

A: Contrast-enhanced CT; B: MRI, contrast-enhanced T1-weighted image

In A, extensive artifacts are present, mainly in the oral cavity, due to a dental prosthetic. Consequently, the tumor cannot be identified. In B, a tumorous lesion is seen in the right palatine tonsil (☆), and a metastatic lymph node (▷) can be clearly observed along with the peripheral soft tissue.

2. Detailed discussion

① CT (Table 9)

(1) Contrast-enhanced CT imaging is performed from the skull base to the superior mediastinum.

(2) Coronal imaging with bone algorithm is useful for evaluating the skull base, and sagittal imaging is useful for observing the retropharyngeal space.

Table 9. Examples of protocols for the upper and middle pharynx: 64-row MDCT system

Imaging Range	Reconstruction Function	Scan Slice Thickness	Reconstruction Slice Thickness	Reconstruction Slice Interval	FOV	WW/WL	Image Processing
From the posterior clinoid process to the inferior extremity of the sternoclavicular joint	For soft tissue	≤ 1.25 mm	≤ 3 mm	Same as at left	160 mm	350/30	Sagittal and coronal planes added as appropriate
Same as above	For bone	≤ 1.25 mm	≤ 3 mm	Same as at left	160 mm	4,000/500	Sagittal and coronal planes added as appropriate

Note 1: Imaging performed under resting respiration
Note 2: Imaging range selected in reference to lateral view of image used to determine location

Table 10. Examples of sequences for the upper and middle pharynx: 3T MRI system, head and neck coil

Imaging Method	Sequence	TR/TE	Slice Thickness	Other
① T2-weighted/transverse	FSE	4,000/85 ms	3 mm	
② T1-weighted/transverse	SE	480/10 ms	3 mm	
③ Fat-suppressed T1-weighted/transverse*	FSE	667/7.8 ms	3 mm	
④ Fat-suppressed T2-weighted/coronal	FSE	4,000/85 ms	3 mm	
⑤ Diffusion-weighted	EPI	6,000/55.3 ms	3 mm	STIR, ADC mapping
⑥ Contrast-enhanced T1-weighted/transverse	SE	480/10 ms	3 mm	Coronal and sagittal planes added as appropriate
⑦ Fat-suppressed, contrast-enhanced T1-weighted/transverse*	FSE	667/7.8 ms	3 mm	

*CHESS recommended

② MRI (Table 10)

(1) A head and neck coil is used for imaging, which is performed over a range that includes the orbit and cavernous sinuses.

(2) Contrast-enhanced imaging is performed for tumors and inflammation.

(3) To obtain good-quality images, the examinee is asked to refrain from coughing or swallowing and to avoid moving his or her tongue as much as possible.

(4) MRI is good for visualizing changes such as tumor soft tissue invasion, bone marrow infiltration, and perineural spread.

Hypopharynx, larynx, and thyroid gland

1. Overview

Non-contrast CT is suitable for detecting foreign bodies such as fish bones. Otolaryngologic emergencies, such as acute epiglottitis and retropharyngeal abscess, are good indications for contrast-enhanced CT.[1, 7] The vast majority of laryngeal cancers and hypopharyngeal cancers are diagnosed before diagnostic imaging is performed. Consequently, the main role of diagnostic imaging is to assess the tumor extension and lymph node metastasis. Artifacts caused by movements such as breathing and swallowing result in poor evaluations with MRI. Contrast-enhanced CT should therefore be given priority (Fig. 8). CT and MRI are performed for thyroid tumors to diagnose the spread of lesions beyond the thyroid gland and to determine the presence or absence of invasion of adjacent organs, such as the trachea, esophagus, and blood vessels, and lymph node metastasis.[18, 19]

2. Detailed discussion

① CT (Table 11)

(1) Non-contrast CT is standard, but contrast-enhanced imaging is necessary if inflammation or a tumor is present.

(2) The imaging range is from the skull base to the superior mediastinum.

(3) Breath-holding is not required during imaging.

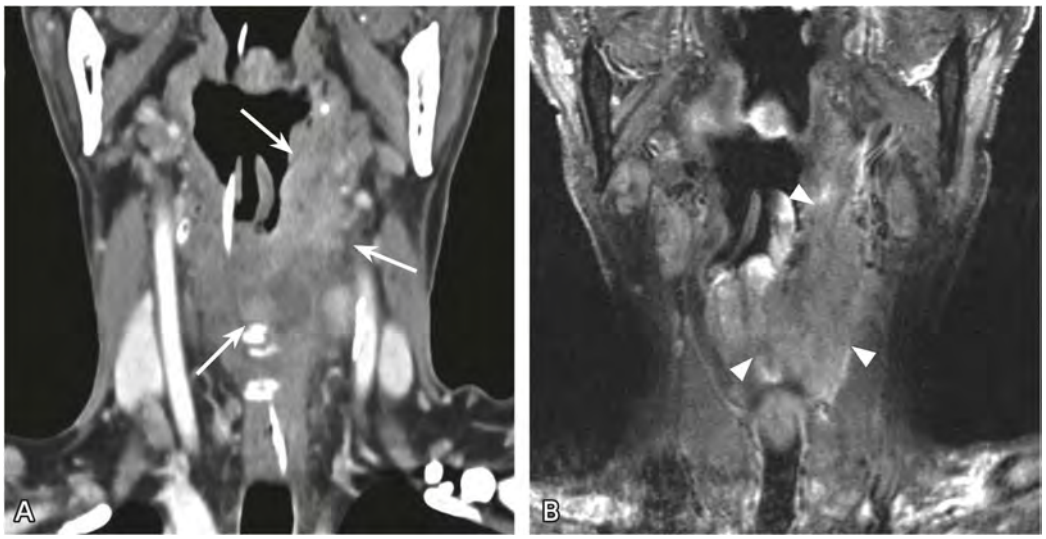

Figure 8. Hypopharyngeal cancer

A: Contrast-enhanced CT, coronal reconstructed image; B: MRI, fat-suppressed, contrast-enhanced, T1-weighted, coronal image

In A, a neoplastic area with non-uniform characteristics is seen progressing hypopharynx anteriorly and superiorly (→). In B, a tumor can be identified (▷). However, there is a marked deterioration in image quality, particularly near pneumatic spaces, resulting from body movement and susceptibility artifacts.

Table 11. Examples of protocols for the hypopharynx and larynx: 64-row MDCT system

Imaging Range	Reconstruction Function	Scan Slice Thickness	Reconstruction Slice Thickness	Reconstruction Slice Interval	FOV	WW/WL	Image Processing
From the posterior clinoid process to the inferior extremity of the sternoclavicular joint	For soft tissue	≤ 1.25 mm	≤ 3 mm	Same as at left	160 mm	350/30	Sagittal or coronal plane and bone algorithm added as appropriate

Note 1: Imaging performed under resting respiration

Note 2: For the thyroid gland, the imaging range extends from the superior margin of the nasopharynx to the inferior extremity of the tracheal bifurcation.

Table 12. Examples of sequences for the hypopharynx and larynx: 3T MRI system, head and neck coil

Imaging Method	Sequence	TR/TE	Slice Thickness	Other
① T2-weighted/transverse	FSE	4,000/85 ms	3 mm	
② T1-weighted/transverse	SE	480/10 ms	3 mm	
③ Fat-suppressed T1-weighted/transverse*	FSE	667/7.8 ms	3 mm	
④ Fat-suppressed T2-weighted/coronal	FSE	4,000/85 ms	3 mm	
⑤ Diffusion-weighted	EPI	6,000/55.3 ms	3 mm	STIR, ADC mapping
⑥ Contrast-enhanced T1-weighted/transverse	SE	480/10 ms	3 mm	Coronal plane added as appropriate
⑦ Fat-suppressed, contrast-enhanced T1-weighted/transverse*	FSE	667/7.8 ms	3 mm	

*CHESS recommended

② MRI (Table 12)

(1) A head and neck coil is used for imaging.

(2) MRI is almost always performed to evaluate local tumor extension not evaluable by CT.

(3) The imaging range is limited to the region of interest, and specifying a smaller FOV is therefore important.

(4) Detailed examination by MRI is useful if invasion of an anterior vertebral muscle/vertebral body is suspected.

Cervical lymph nodes

1. Overview

When observed by CT and MRI, cervical lymph nodes at levels IB (submandibular nodes) and II (superior internal jugular nodes) with a maximum diameter of < 15 mm, minimum diameter of < 11 mm, and other cervical lymph nodes with a minimum diameter of < 10 mm are treated as normal lymph nodes, and larger lymph nodes are treated as enlarged. Rouviere's lymph nodes with a long-axis diameter of ≥ 8 mm and short-axis diameter of ≥ 6 mm are treated as enlarged lymph nodes.[21)] At all sites, central necrosis and indistinct borders are considered pathological findings.[22)]

With CT, contrast-enhanced imaging is essential. If a contrast-enhanced examination cannot be performed, an alternative modality such as MRI or ultrasonography is considered. Contrast-enhanced imaging is also the rule with MRI. Diffusion-weighted imaging and ADC mapping may be useful for distinguishing between benign and malignant lesions. With contrast-enhanced CT and MRI, indistinct structures derived from hilar fat tissue and changes in the attenuation value or signal inside a node due to central necrosis are examined as possible pathological findings regardless of size.[23-25)]

2. Detailed discussion

① CT

A contrast-enhanced examination is standard.

(1) The CT imaging range is from the skull base to the aortic arch.

(2) Coronal plane images are generated by multiplanar reconstruction, with sagittal images added as necessary.

② MRI (Table 13)

(1) A head and neck coil is used for imaging.

(2) T1-weighted imaging, T2-weighted imaging, and contrast-enhanced T1-weighted imaging are standard.

(3) Fat-suppressed T2-weighted imaging is useful for lymph node internal characterization, particularly the detection of colliquative necrosis.

(4) With regard to imaging planes, transverse plane imaging is standard, and coronal imaging is added as necessary.

(5) When fat-suppressed, contrast-enhanced, T1-weighted imaging is performed, non-fat-suppressed, non-contrast-enhanced, T1-weighted imaging is also performed in view of the effects of susceptibility artifacts.

(6) Diffusion-weighted imaging is useful for detecting cervical lymph nodes and diagnosing conditions such as malignant lymphoma.

Table 13. Examples of sequences for the cervical lymph nodes: 3T MRI system, head and neck coil

Imaging Method	Sequence	TR/TE	Slice Thickness	Other
① T2-weighted/transverse	FSE	4,000/85 ms	3 mm	
② T1-weighted/transverse	SE	480/10 ms	3 mm	
③ Fat-suppressed T1-weighted/transverse*	FSE	667/7.8 ms	3 mm	
④ Fat-suppressed T2-weighted/coronal	FSE	4,000/85 ms	3 mm	
⑤ Diffusion-weighted	EPI	6,000/55.3 ms	3 mm	STIR, ADC mapping
⑥ Contrast-enhanced, T1-weighted/transverse	SE	480/10 ms	3 mm	Coronal plane added as appropriate
⑦ Fat-suppressed, contrast-enhanced, T1-weighted/transverse*	FSE	667/7.8 ms	3 mm	

*CHESS recommended

^{18}F-FDG PET/CT imaging[26)]

1. Procedure

^{18}F-FDG is administered intravenously. The dose used is adjusted appropriately depending on the type of system used and the patient's age and weight. Blood glucose is measured immediately before the test. Sixty minutes after administration, whole-body CT and PET imaging is performed using a PET/CT system. Late-phase imaging from 2 hours onward is added as necessary.

2. Important points for testing

As pretreatment, the patient is fasted for at least 4 hours. When the blood glucose level is high, and in some patients with diabetes mellitus, tumor ^{18}F-FDG uptake may decrease, and background uptake may increase, reducing detection performance. In addition, background uptake by tissue such as muscle increases after insulin administration.

Uptake by skeletal muscle increases from before to after ^{18}F-FDG administration, particularly with post-administration exercise (muscular tension and contraction). Consequently, the patient remains at rest after administration.

Because ^{18}F-FDG is excreted mainly by urinary excretion, the patient is asked to urinate immediately before the test, which reduces intravesical radioactivity. Radiation exposure is also reduced by encouraging water intake/diuresis.

Together with an evaluation by visual assessment, the level of uptake is semi-quantitatively evaluated using the standardized uptake value (SUV), which is the uptake ratio for the dose per unit body weight.

Secondary source materials used as references

1) Capps EF et al: Emergency imaging assessment of acute, nontraumatic conditions of the head and neck. Radiographics 30: 1335-1352, 2010
2) Winegar BA et al: Imaging of orbital trauma and emergent non-traumatic conditions. Neuroimaging Clin N Am 25: 439-456, 2015
3) Bhatt N et al: Role of diffusion-weighted imaging in head and neck lesions: pictorial review. Neuroradiol J 30: 356-369, 2017
4) Mafee MF et al: Imaging of rhinosinusitis and its complications: plain film, CT, and MRI. Clin Rev Allergy Immunol 30: 165-186, 2006
5) Hähnel S et al: Relative value of MR imaging as compared with CT in the diagnosis of inflammatory paranasal sinus disease. Radiology 210: 171-176, 1999
6) Aribandi M et al: Imaging features of invasive and noninvasive fungal sinusitis: a review. Radiographics 27: 1283-1296, 2007
7) Kaneda T et al: Dental bur fragments causing metal artifacts on MR images. AJNR AM J Neuroradiol 19: 317-319, 1998
8) McKellop JA et al: Emergency head & neck imaging: infections and inflammatory processes. Neuroimaging Clin N Am 20: 651-661, 2010
9) Lam P et al: Correlating MRI and histologic tumor thickness in the assessment of oral tongue cancer. AJR Am J Roentgenol 182: 803-808, 2004
10) Tomura N et al: Irradiated carcinoma of the tongue: correlation of MR imaging findings with pathology. AJR AM J Roentgenol 178: 705-710, 2002
11) Dammann F et al: Rational diagnosis of squamous cell carcinoma of the head and neck region: comparative evaluation of CT, MRI, and ^{18}FDG PET. AJR Am J Roentgenol 184: 1326-1331, 2005
12) Yoon DY et al: CT, MR, US, ^{18}F-FDG PET/CT, and their combined use for the assessment of cervical lymph node metastases in squamous cell carcinoma of the head and neck. Eur Radiol 19: 634-642, 2009
13) Jager L et al: CT of the normal temporal bone: comparison of multi– and single–detector row CT. Radiology 23: 133-141, 2005

14) Yabuuchi H et al: Salivary gland tumors: diagnostic value of gadolinium-enhanced dynamic MR imaging with histopathologic correlation. Radiology 226: 345-354, 2003
15) Eida S et al: Apparent diffusion coefficient mapping of salivary gland tumors: prediction of the benignancy and malignancy. AJNR Am J Neuroradiol 28: 116-121, 2007
16) Purcell YM et al: The diagnostic accuracy of contrast-enhanced CT of the neck for the investigation of sialolithiasis. AJNR Am J Neuroradiol 8: 2161-2166, 2017
17) Khalek AA et al: MRI and CT of Nasopharyngeal Carcinoma. AJR Am J Roentgenol 198: 11-18, 2012
18) Becker M et al: Neoplastic invasion of the laryngeal cartilage: comparison of MR imaging and CT with histopathologic correlation. Radiology 194: 661-669, 1995
19) Weber AL et al: The thyroid and parathyroid glands. CT and MR imaging and correlation with pathology and clinical findings. Radiol Clin North Am 38: 1105-1129, 2000
20) Gleeson M et al: Management of lateral neck masses in adults. BMJ 320: 1521-1524, 2000
21) Zhang GY et al: Radiologic criteria of retropharyngeal lymph node metastasis in nasopharyngeal carcinoma treated with radiation therapy. Radiology 255: 605–612, 2010
22) Curtin HD et al: Comparison of CT and MR imaging in staging of neck metastases. Radiology 207: 123-130, 1998
23) Sumi M et al: Diagnostic performance of MRI relative to CT for metastatic nodes of head and neck squamous cell carcinomas. J Magn Reson Imaging 26: 1626-1633, 2007
24) Nakamura T et al: Nodal imaging in the neck: recent advances in US, CT and MR imaging of metastatic nodes. Eur Radiol 17: 1235-1241, 2007
25) Wang J et al: Head and neck lesions: cholerization with diffusion-weighted echo-planar MR imaging. Radiology 220: 621-630, 2001
26) Japanese Society of Nuclear Medicine, Ed.: 2018 FDG PET and PET/CT Diagnostic Guidelines. Japanese Society of Nuclear Medicine, 2018.

BQ 10 Is CT recommended for adult sinusitis?

Statement

CT is usually unnecessary for uncomplicated acute sinusitis. CT imaging is recommended in the following cases: whether sinusitis is present needs to be determined and the cause identified; an intraorbital or intracranial complication is suspected; surgery is considered; or the presence of a tumorous lesion is suspected.

Background

In the outpatient setting, occasions on which paranasal sinus plain radiography is performed for patients complaining of paranasal sinus-related symptoms are decreasing, and CT is becoming the standard imaging examination. MRI may be added if complications are suspected. The evidence that such an examination process is appropriate is described below.

Explanation

Uncomplicated acute sinusitis is diagnosed based on symptoms, clinical course, and intranasal findings, and imaging examinations are usually unnecessary.[1)] In a comparison of endoscopy and plain radiography, Berger et al. found that the diagnostic performance of the 2 examinations was comparable, and they recommended endoscopy as the first choice.[2)] A negative endoscopy examination or the presence of strong symptoms may be an indication for an imaging examination. Outpatient examinations are screening tests, and high sensitivity is required. However, the sensitivity of plain radiography is low. Consequently, CT is the standard when imaging is indicated for acute sinusitis.[3-5)]

The sensitivity and specificity of plain radiography for chronic sinusitis are also lower than the sensitivity and specificity of endoscopy.[6)] CT is excellent for bone evaluation and can readily be used to evaluate mucosal thickening. It is therefore the standard examination for sinusitis.[4, 5, 7-10)] CT can also be used to evaluate conditions such as anatomical variations that cause sinusitis, odontogenic maxillary sinusitis, and fungal sinusitis.[4, 11)] Consequently, when CT can be performed, it is recommended that plain radiography be omitted, and that CT be performed from the start.[12)] In preoperative evaluations before endoscopic surgery, CT is excellent for visualizing important anatomical structures (e.g., the air cell/osteomeatal unit, ethmoidal foramen, optic canal, and internal carotid artery), and its use is recommended for this purpose.[1, 4, 8, 12)] Although there is insufficient evidence regarding the usefulness of a contrast medium, such use is unnecessary in chronic sinusitis, but it can be considered if a tumor is suspected. Cone-beam CT is a method of CT by which X-rays are emitted in a conical pattern and detected by a 2-dimensional detector. Cone-beam CT was commercialized in 2001. Compared with multi-row detector CT, it is inexpensive, compact, and involves a low radiation dose. Consequently, it can be a potent

tool for diagnosing sinusitis. However, it provides low tissue contrast, making it unsuitable for evaluating soft tissue lesions, such as those seen with the spread of inflammation outside the sinus.[13, 14)]

With MRI, bone visualization is inferior to that provided by CT, and the imaging takes time. MRI is therefore unlikely to be the first imaging examination used for sinusitis.[7, 8)] However, MRI provides better tissue contrast than CT and is therefore recommended when inflammation is suspected of having spread intracranially and intraorbitally.[1, 4, 8, 9)] If invasive fungal sinusitis is suspected, MRI should be considered to evaluate the spread of inflammation to outside the sinus. In addition, MRI facilitates the differentiation of fluid accumulation and tumors. It is therefore also useful when a tumorous legion such as papilloma or cancer is suspected of being the cause of sinusitis.[7, 10, 11)] When an intracranial/intraorbital complication or tumor is suspected, fat-suppressed, contrast-enhanced T1-weighted imaging is preferred.

In summary, diagnostic imaging is unnecessary for uncomplicated acute sinusitis. Plain radiography can be considered in circumstances where CT cannot be performed. However, scientific evidence of its usefulness for diagnosis has not been established. CT imaging is recommended as the standard examination in the following cases: whether sinusitis is present needs to be determined and the cause identified; an intraorbital or intracranial complication is suspected; surgery is considered; or the presence of a tumorous lesion is suspected. MRI is recommended when intracranial or intraorbital complications, a tumorous lesion, or invasive fungal sinusitis is suspected.

Search keywords and secondary sources used as references

PubMed was searched using the following keywords: plain radiography, paranasal sinus, CT, and MRI. The period searched was through the end of June 2019.

In addition, the following was referenced as a secondary source.

1) Kirsch CFE et al: ACR Appropriateness Criteria®: sinonasal disease. J Am Coll Radiol 14: S550-S559, 2017

References

1) Orlandi RR et al: International consensus statement on allergy and rhinology: rhinosinusitis. Int Forum Allergy Rhinol 6: S22-209, 2016
2) Berger G et al: Endoscopy versus radiography for the diagnosis of acute bacterial rhinosinusitis. Eur Arch Otorhinolaryngol 262: 416-422, 2005
3) Burke TF et al: Comparison of sinus x-rays with computed tomography scans in acute sinusitis. Acad Emerg Med 1: 235-239, 1994
4) Yousem DM: Imaging of sinonasal inflammatory disease. Radiology 188: 303-314, 1993
5) Aalokken TM et al: Conventional sinus radiography compared with CT in the diagnosis of acute sinusitis. Dentomaxillofac Radiol 32: 60-62, 2003
6) Srivastava M et al: Comparative evaluation of chronic rhinosinusitis patients by conventional radiography, computed tomography and diagnostic nasal endoscopy (DNE). Indian J Otolaryngol Head Neck Surg 68: 173-178, 2016
7) Bachert C et al: ICON: chronic rhinosinusitis. World Allergy Organ J 7: 25, 2014
8) Hahnel S et al: Relative value of MR imaging as compared with CT in the diagnosis of inflammatory paranasal sinus disease. Radiology 210: 171-176, 1999
9) Younis RT et al: The role of computed tomography and magnetic resonance imaging in patients with sinusitis with complications. Laryngoscope 112: 224-229, 2002
10) Wang PP et al: Endoscopic treatment of isolated sphenoid sinus disease in children. Ear Nose Throat J 98: 425-430, 2019
11) Ikeda K et al: Unilateral sinonasal disease without bone destruction: differential diagnosis using diagnostic imaging and endonasal endoscopic biopsy. Arch Otolaryngol Head Neck Surg 123: 198-200, 1997

12) Kaluskar SK et al: The role of CT in functional endoscopic sinus surgery. Rhinology 31: 49-52, 1993
13) Al AJ et al: Cone beam CT paranasal sinuses versus standard multidetector and low dose multidetector CT studies. Am J Otolaryngol 37: 59-64, 2016
14) Fakhran S et al: Comparison of simulated cone beam computed tomography to conventional helical computed tomography for imaging of rhinosinusitis. Laryngoscope 124: 2002-2006, 2014

BQ 11 Is MRI recommended for determining the T stage of head and neck cancer?

Statement

The strength with which MRI is recommended for the T staging of head and neck cancer varies depending on the subsite. It is recommended for nasopharyngeal and oropharyngeal cancer, but it is not strongly recommended for laryngeal or hypopharyngeal cancer.

Background

The most accurate possible staging by diagnostic imaging is required to determine an appropriate treatment plan for head and neck cancer. With diagnostic imaging for the T staging of head and neck cancer, MRI is thought to provide diagnostic performance comparable to that of CT. However, the recommendation grade for MRI varies depending on the subsite. MRI is clearly superior for evaluating nasopharyngeal cancer, oral cavity cancer, or oropharyngeal cancer (particularly in patients for whom evaluation by CT is difficult due to artifacts). However, in laryngeal and hypopharyngeal cancer, due to low temporal resolution, image quality deterioration resulting from body movements such as breathing and swallowing is problematic. The basis for the statement regarding nasopharyngeal, oropharyngeal, oral cavity, laryngeal, and hypopharyngeal cancer in the BQ is summarized in the following.

Explanation

A meta-analysis found that MRI showed higher accuracy than CT in the T staging of nasopharyngeal cancer,[1)] and MRI is strongly recommended for this purpose.[1-3)] With its high tissue contrast, MRI is also superior to CT for evaluating extension to the adjacent pharyngeal space, cranial base, intracranial area, and sphenoid sinus.[2)] MRI shows high sensitivity and specificity for skull base invasion (particularly high sensitivity compared with CT).[4)] MRI is also superior to CT in the evaluation of intracranial invasion.[5)] In addition, MRI is useful for evaluating the involvement of areas such as anterior vertebral muscle (T2), cervical vertebrae and pterygoid process (T3), and parotid gland (T4), which were items added in the 6th edition of the General Rules for Clinical Studies on Head and Neck Cancer (secondary source 1).

In oral cavity cancer, MRI is superior to CT for evaluating soft tissue and bone marrow infiltration.[6-10)] MRI is generally superior to CT for visualizing soft tissue and is little affected by artifacts from metal in the oral cavity. It is therefore recommended for evaluating the tumor extension of the primary lesion.[6, 8, 10, 11)] Tongue cancer is the most common form of oral cavity cancer in Japan, and the depth of invasion (DOI) is important for the T staging of tongue cancer. MRI has shown a strong correlation with pathological DOI, and the DOI measured with T2- and T1-weighted imaging has been found to be 2 to 3 mm deeper than the pathological DOI.[12-14)] In evaluating jaw bone invasion in lower gingival cancer, MRI is more sensitive but less specific than CT,[8, 9, 15-18)] and its diagnostic accuracy rate is comparable to that of CT.[17)] CT is useful

for evaluating bone cortex invasion and MRI for evaluating invasion of the bone marrow.[11] MRI is more accurate than CT for evaluating soft tissue and bone invasion in oropharyngeal cancer anatomically adjacent to the oral cavity, [6, 7] and it is little affected by artifacts from metal in the oral cavity. MRI is therefore recommended for this purpose.

From the perspectives of test efficiency, cost-effectiveness, and diagnostic accuracy, CT is the first choice for T staging in hypopharyngeal and laryngeal cancers. Although taking MRI findings into account has been found to enable more accurate T staging,[19, 20] the diagnostic accuracy rates of CT and MRI have been found not to differ significantly.[19, 20] Although MRI is used for T staging in clinical practice, detailed evaluation with MRI is often difficult due to susceptibility artifacts caused by adjacent air. CT is always performed in patients with advanced disease and suspected cartilage invasion corresponding to stage T3 or T4a. However, no reported investigations have compared the diagnostic performance of CT alone and CT combined with MRI. For CT, the reported sensitivity and specificity for cartilage invasion have ranged from 0.50 to 0.96 and from 0.60 to 1.00, respectively.[20-25] For MRI, they have ranged from 0.88 to 1.00 and from 0.75 to 1.00, respectively.[20-22, 24, 26-28] Thus, MRI and CT are comparable in specificity, and MRI is higher in sensitivity than CT. However, if cartilage invasion can be definitively ruled out by CT, the addition of MRI is unnecessary. If cartilage invasion is suspected based on CT, MRI is not strongly recommended in view of its low test efficiency. The addition of MRI is considered only if definitively diagnosing cartilage invasion is difficult with CT and affects treatment selection. High sensitivity and specificity have been reported for both MRI and CT in the evaluation of pre-epiglottic and paraglottic space invasion corresponding to stage T3.[20, 29] However, the high sensitivity of MRI can result in overestimates in early stage glottic cancer.[22] Overestimation of paraglottic space invasion resulting from inflammatory changes is also a problem for MRI.[30, 31] Consequently, CT is the standard choice. For anterior vertebral space invasion corresponding to state T4b, the negative predictive values of both MRI and CT are high, and both therefore contribute to preoperative evaluation.[32] In thyroid gland invasion corresponding to stage T4a, false-positives are common with MRI, and it therefore lacks reliability.[33]

Search keywords and secondary sources used as references

PubMed was searched using the following keywords: head and neck cancer, stage, nasopharyngeal carcinoma, oral cavity carcinoma, imaging, oropharyngeal carcinoma, laryngeal cancer, and hypopharyngeal carcinoma.

In addition, the following was referenced as a secondary source.

1) The General Rules for Clinical Studies on Head and Neck Cancer 2019, The 6th Edition, Revised Version

References

1) Chen WS et al: Comparison of MRI, CT and ^{18}F-FDG PET/CT in the diagnosis of local and metastatic of nasopharyngeal carcinomas: an updated meta analysis of clinical studies. Am J Transl Res 8 (11): 4532-4547, 2016
2) Ng SH et al: Staging of untreated nasopharyngeal carcinoma with PET/CT: comparison with conventional imaging work-up. Eur J Nucl Med Mol Imaging 36 (1): 12-22, 2009

3) King AD et al: Primary nasopharyngeal carcinoma: diagnostic accuracy of MR imaging versus that of endoscopy and endoscopic biopsy. Radiology 258 (2): 531-537, 2011
4) Zhang SX et al: Comparison of SPECT/CT, MRI and CT in diagnosis of skull base bone invasion in nasopharyngeal carcinoma. Biomed Mater Eng 24 (1): 1117-1124, 2014
5) Chung NN et al: Impact of magnetic resonance imaging versus CT on nasopharyngeal carcinoma: primary tumor target delineation for radiotherapy. Head Neck 26 (3): 241-246, 2004
6) Leslie A et al: Staging of squamous cell carcinoma of the oral cavity and oropharynx: a comparison of MRI and CT in T- and N-staging. J Comput Assist Tomogr 23 (1): 43-49, 1999
7) Bolzoni A et al: Diagnostic accuracy of magnetic resonance imaging in the assessment of mandibular involvement in oral-oropharyngeal squamous cell carcinoma: a prospective study. Arch Otolaryngol Head Neck Surg 130 (7): 837-843, 2004
8) Wiener E et al: Comparison of 16-slice MSCT and MRI in the assessment of squamous cell carcinoma of the oral cavity. Eur J Radiol 58 (1): 113-118, 2006
9) Dammann F et al: Rational diagnosis of squamous cell carcinoma of the head and neck region: comparative evaluation of CT, MRI, and 18FDG PET. AJR Am J Roentgenol 184 (4): 1326-1331, 2005
10) Pérez MGS et al: Utility of imaging techniques in the diagnosis of oral cancer. J Craniomaxillofac Surg 43 (9): 1880-1894, 2015
11) Sigal R et al: CT and MR imaging of squamous cell carcinoma of the tongue and floor of the mouth. Radiographics 16 (4): 787-810, 1996
12) Baba A et al: Magnetic resonance imaging findings of styloglossus and hyoglossus muscle invasion: relationship to depth of invasion and clinical significance as a predictor of advisability of elective neck dissection in node negative oral tongue cancer. Eur J Radiol 118: 19-24, 2019
13) Baba A et al: Undetectability of oral tongue cancer on magnetic resonance imaging: clinical significance as a predictor to avoid unnecessary elective neck dissection in node negative patients. Dentomaxillofac Radiol 48 (3): 20180272, 2019
14) Murakami R et al: Reliability of MRI-derived depth of invasion of oral tongue cancer. Acad Radiol S1076-6332 (18): 30423-30429, 2018
15) van den Brekel MW et al: Assessment of tumour invasion into the mandible: the value of different imaging techniques. Eur Radiol 8 (9): 1552-1557, 1998
16) Vidiri A et al: Multi-detector row computed tomography (MDCT) and magnetic resonance imaging (MRI) in the evaluation of the mandibular invasion by squamous cell carcinomas (SCC) of the oral cavity: correlation with pathological data. J Exp Clin Cancer Res 17 (29): 73, 2010
17) Uribe S et al: Accuracy of imaging methods for detection of bone tissue invasion in patients with oral squamous cell carcinoma. Dentomaxillofac Radiol 42 (6): 20120346, 2013
18) Suzuki N et al: Diagnostic abilities of 3T MRI for assessing mandibular invasion of squamous cell carcinoma in the oral cavity: comparison with 64-row multidetector CT. Dentomaxillofac Radiol 48 (4): 20180311, 2019
19) Zbären P et al: Pretherapeutic staging of hypopharyngeal carcinoma: clinical findings, computed tomography, and magnetic resonance imaging compared with histopathologic evaluation. Arch Otolaryngol Head Neck Surg 123 (9): 908-913, 1997
20) Zbären P et al: Staging of laryngeal cancer: endoscopy, computed tomography and magnetic resonance versus histopathology. Eur Arch Otorhinolaryngol 254: S117-S122, 1997
21) Becker M et al: Neoplastic invasion of the laryngeal cartilage: comparison of MR imaging and CT with histopathologic correlation. Radiology 194 (3): 661-669, 1995
22) Allegra E et al: Early glottic cancer: role of MRI in the preoperative staging. Biomed Res Int 2014: 890385, 2014
23) Dankbaar JW et al: Detection of cartilage invasion in laryngeal carcinoma with dynamic contrast-enhanced CT: laryngoscope Investig. Otolaryngol 2 (6): 373–379, 2017
24) Castelijns JA et al: Invasion of laryngeal cartilage by cancer: comparison of CT and MR imaging. Radiology 167 (1): 199–206, 1988
25) Li B et al: Overstaging of cartilage invasion by multidetector CT scan for laryngeal cancer and its potential effect on the use of organ preservation with chemoradiation. Br J Radiol 84 (997): 64–69, 2011
26) Becker M et al: Neoplastic invasion of laryngeal cartilage: reassessment of criteria for diagnosis at MR imaging. Radiology 249 (2): 551-559, 2008
27) Preda L et al: Diagnostic accuracy of surface coil MRI in assessing cartilaginous invasion in laryngeal tumours: Do we need contrast-agent administration? Eur Radiol 27 (11): 4690–4698, 2017
28) Kuno H et al: Comparison of MR imaging and dual-energy CT for the evaluation of cartilage invasion by laryngeal and hypopharyngeal squamous cell carcinoma. AJNR Am J Neuroradiol 39 (3): 524–531, 2018
29) Loevner LA et al: Can radiologists accurately predict preepiglottic space invasion with MR imaging? AJR Am J Roentgenol 169 (6): 1681-1687, 1997
30) Banko B et al: Diagnostic significance of magnetic resonance imaging in preoperative evaluation of patients with laryngeal tumors. Eur Arch Otorhinolaryngol 268 (11): 1617-1623, 2011

31) Banko B et al: MRI in evaluation of neoplastic invasion into preepiglottic and paraglottic space. Auris Nasus Larynx 41 (5): 471-474, 2014
32) Imre A et al: Prevertebral space invasion in head and neck cancer: negative predictive value of imaging techniques. Ann Otol Rhinol Laryngol 124 (5): 378-383, 2015
33) Kinshuck AJ et al: Accuracy of magnetic resonance imaging in diagnosing thyroicd cartilage and thyroid gland invasion by squamous cell carcinoma in laryngectomy patients. J Laryngol Otol 126 (3): 302-306, 2012

BQ 12 Is CT recommended for determining the N stage of head and neck cancer?

Statement

CT is the standard examination and recommended for determining the N stage of head and neck cancer.

Background

The N staging of head and neck cancer is important for determining a treatment strategy and predicting prognosis. Diagnosing cervical lymph node metastasis involves evaluating size, morphology, and internal and margin characteristics. Modalities such as ultrasound, CT, MRI, and PET are used for this purpose, and each has advantages and disadvantages. The basis of CT's rank as a first-line standard examination for the N staging of head and neck cancer is summarized below.

Explanation

Various imaging modalities are used to diagnose cervical lymph node metastasis in head and neck squamous cell carcinoma. Curtin et al. reported comparable sensitivity and specificity for CT and MRI in detecting lymph node metastasis.[1)] A meta-analysis by Wu et al. showed that, in a comparison of MRI and CT, sensitivity was 67.4% and 64.2%, respectively, and specificity was 78.7% and 75.4%, respectively. In a comparison of MRI and PET, sensitivity was 66.5% and 66.2%, respectively, and specificity was 76.6% and 81.4%, respectively. They reported finding no significant differences between the modalities.[2)]

In the morphological diagnosis of cervical lymph node metastasis, aspects such as lymph node size, morphology, internal characteristics, and margin characteristics must be evaluated.[3)] Various criteria are used to assess lymph node metastasis size. However, the following criteria are generally used: one in which a maximum cross-sectional diameter of 15 mm for the superior internal jugular nodes and submandibular nodes and ≥ 10 mm for the other lymph nodes is considered significant and another in which a minimum cross-sectional diameter of 11 mm for the superior internal jugular nodes and ≥ 10 mm for the other nodes is considered significant. Adding information on morphology and internal and margin characteristics to these criteria increases sensitivity and diagnostic performance. Consequently, evaluation by contrast-enhanced CT is required when possible, except in patients with a contrast medium allergy or decreased kidney function (dialysis patients excluded).

Internal non-uniformity, such as that resulting from necrosis in a lymph node, is the imaging finding with the highest specificity, and evaluation by MRI, which provides high tissue contrast, is considered useful for detecting such non-uniformity. King et al. found MRI to be comparable to contrast-enhanced CT with respect to its performance in detecting nodal necrosis with lymph node metastasis of head and neck cancer.[4)] Sumi et al. reported that, when used to evaluate internal characteristics such as cancer foci, necrosis, and keratinization seen in metastatic foci with lymph node metastasis of head and neck cancer,

MRI was superior to contrast-enhanced CT for metastatic small lymph nodes with a short-axis diameter of < 10 mm.[5] Apparent diffusion coefficient (ADC) values for lymph node enlargement obtained in MRI diffusion-weighted imaging have been found to be useful for benign-malignant differentiation of lymph nodes. Moreover, ADC values for lymph node metastasis have been found to be significantly lower than those for benign lymph node enlargement.[6] In addition, a meta-analysis regarding lymph node metastasis differentiation found that quantitative assessment using ADC values aided in diagnosis.[7] These results indicate that there is room to consider the addition of MRI for determining the N stage of head and neck cancer in patients who cannot undergo contrast-enhanced CT. It should be noted, however, that MRI image quality and the values used in quantitative assessments depend on the systems and imaging methods used at each facility.

Ultrasound and PET/CT have also been reported to be useful for diagnosing lymph node metastasis in head and neck cancer.[3, 8] However, contrast-enhanced CT enables images of high spatial resolution to be obtained over an extensive range in a short time. It is therefore often performed both to evaluate primary lesions and to screen for distant metastasis. It is therefore appropriate to consider contrast-enhanced CT the standard for determining the N stage of head and neck cancer.

Search keywords and secondary sources used as references

PubMed was searched using the following keywords: cervical lymph node metastasis, head and neck cancer, CT, MRI, and PET/CT. The period searched was through the end of June 2019.

References

1) Curtin HD et al: Comparison of ct and mr imaging in staging of neck metastases. Radiology 207: 123-130, 1998
2) Wu LM et al: Value of magnetic resonance imaging for nodal staging in patients with head and neck squamous cell carcinoma: a meta-analysis. Acad Radiol 19: 331-340, 2012
3) Nakamura T et al: Nodal imaging in the neck: recent advances in us, ct and mr imaging of metastatic nodes. Eur Radiol 17: 1235-1241, 2007
4) King AD et al: Necrosis in metastatic neck nodes: diagnostic accuracy of CT, MR imaging, and us. Radiology 230: 720-726, 2004
5) Sumi M et al: Diagnostic performance of MRI relative to ct for metastatic nodes of head and neck squamous cell carcinomas. J Magn Reson Imaging 26: 1626-1633, 2007
6) Vandecaveye V et al: Head and neck squamous cell carcinoma: value of diffusion-weighted mr imaging for nodal staging. Radiology 251: 134-146, 2009
7) Payabvash S et al: Differentiation of lymphomatous, metastatic, and non-malignant lymphadenopathy in the neck with quantitative diffusion-weighted imaging: Systematic review and meta-analysis. Neuroradiology 61: 897-910, 2019
8) Liao LJ et al: Detection of cervical lymph node metastasis in head and neck cancer patients with clinically n0 neck-a meta-analysis comparing different imaging modalities. BMC Cancer 12: 236, 2012

BQ 13 Is PET recommended for determining the M stage of head and neck cancer?

Statement

PET is the standard examination and recommended for determining the M stage of head and neck cancer.

Background

The number of facilities that perform PET for the preoperative staging of head and neck cancer is increasing, and it is becoming established as an essential modality, particularly for performing highly accurate staging. The basis for considering PET useful for determining the M stage of head and neck cancer is summarized in the following.

Explanation

The importance of PET is that it can easily perform whole-body screening, and its strength is therefore particularly evident in determining the M stage. It is generally performed in patients for whom staging and the diagnosis of metastasis and recurrence cannot be definitively established with other examinations and diagnostic imaging modalities. However, given the usefulness of visual diagnosis with PET, it is also generally recommended for determining the M stage of head and neck cancer. In an investigation of staging and treatment plan changes in 52 patients with head and neck squamous cell carcinoma by Jorgenson et al., the addition of PET/CT to CT/MRI resulted in TNM stage changes in 0.0%, 23.1%, and 3.8%, respectively, and changes in stage and treatment plan in 9.6% and 5.8%, respectively.[1)] However, there have been warnings that PET/CT delays the start of treatment and increases its cost. In addition, the performance of FDG-PET/CT in detecting distant metastasis and simultaneous cancer in patients with laryngeal cancer, oral cavity cancer, and pharyngeal cancer was reported to be significantly better than that of chest radiography combined with head and neck CT.[2)] Similarly, the performance of FDG-PET/CT in detecting distant metastasis and simultaneous cancer in patients with laryngeal cancer, oral cavity cancer, and pharyngeal cancer was significantly better than that of chest radiography combined with cervical MRI and chest CT combined with cervical MRI.[3)] Since FDG-PET/CT came into clinical use, the frequency of distant metastasis detection has increased. Moreover, FDG-PET/CT is considered useful in screening for simultaneous cancer, which has a stronger effect on prognosis than the primary cancer.

Lymph node metastasis can also be evaluated with PET/CT. A meta-analysis by Kim et al. of 18 articles on diagnostic performance for lymph node metastasis with the addition of PET/CT in patients with clinical N0 (cN0) head and neck squamous cell carcinoma found that sensitivity and specificity were 58% and 87%, respectively, in a patient-based analysis, 67% and 85%, respectively, in a neck side-based analysis, and 53% and 97%, respectively, in a level-based analysis. The authors therefore concluded that PET/CT is an examination with excellent specificity.[4)] Li et al. performed a meta-analysis of 8 articles and reported the

following regarding diagnostic performance with the addition of PET/CT in patients with cN0.[5] Sensitivity, specificity, the odds ratio, positive likelihood ratio, and negative likelihood ratio were, respectively, 0.61 (95% CI, 52% to 69%), 0.74 (95% CI, 68% to 78%), 9.62 (95% CI, 2.49 to 37.22), 3.22 (95% CI, 1.55 to 6.71), and 0.42 (95% CI, 0.24 to 0.37). The authors indicated that, although the diagnostic performance of PET/CT was not better than that of CT/MRI, that was attributable to the high heterogeneity of the study designs.[5] In an investigation by Lee et al. in 39 patients with head and neck squamous cell carcinoma, the sensitivity of PET/CT, CT/MRI, and PET/CT combined with CT/MRI for disease classified as cN0 based on palpation was 65.7%, 57.1%, and 65.7%, respectively. The authors concluded that there were no significant differences in sensitivity between the imaging methods.[6] Although there is debate regarding the usefulness of PET/CT in patients with cN0, it should be combined with other modalities to comprehensively evaluate the lymph nodes.

Search keywords and secondary sources used as references

PubMed was searched using the following keywords: head and neck cancer and PET/CT. The period searched was from June 2015 to the end of June 2019.

References

1) Jorgensen JB et al: Impact of PET/CT on staging and treatment of advanced head and neck squamous cell carcinoma. Otolaryngol Head Neck Surg 160: 261-266, 2019
2) Kim Y et al: Chest radiography or chest CT plus head and neck CT versus 18F-FDG PET/CT for detection of distant metastasis and synchronous cancer in patients with head and neck cancer. Oral Oncol 88: 109-114, 2019
3) Rohde M et al: Head-to-head comparison of chest X-ray/head and neck MRI, chest CT/head and neck MRI, and 18F-FDG PET/CT for detection of distant metastases and synchronous cancer in oral, pharyngeal, and laryngeal cancer. J Nucl Med 58: 1919-1924, 2017
4) Kim SJ et al: Diagnostic accuracy of F-18 FDG PET or PET/CT for detection of lymph node metastasis in clinically node negative head and neck cancer patients；a systematic review and meta-analysis. Am J Otolaryngol 40: 297-305, 2019
5) Li XY et al: The role of ^{18}F-FDG PET/CT for detecting nodal metastases in cN0 head neck cancer patients: a meta-analysis. J Clin Otorhinolaryngol Head Neck Surg 32: 700-704, 2018
6) Lee HJ et al: ^{18}F-FDG PET-CT as a supplement to CT/MRI for detection of nodal metastasis in hypopharyngeal SCC with palpably negative neck. Laryngoscope 125: 1607-1612, 2015

BQ 14 Are CT and MRI recommended for the post-treatment follow-up of head and neck cancer?

Statement

CT and MRI are the standard examinations and are recommended for the post-treatment follow-up of head and neck cancer.

Background

Treatments for head and neck cancer include surgery, radiation therapy, and chemoradiotherapy. The optimal treatment is selected according to the primary site, pathological diagnosis, and disease stage. Early detection of post-treatment recurrence is an important prognostic factor. However, methods of follow-up vary between facilities, and the diagnostic imaging modalities that are selected are also varied. The reasons why CT and MRI are the standard examinations for post-treatment follow-up of head and neck cancer are summarized below.

Explanation

In post-treatment follow-up of head and neck cancer, adequately determining postoperative status by inspection or endoscopy alone is often difficult, and imaging modalities such as CT or MRI are necessary for the early detection of recurrence. Recurrence after treatment for head and neck cancer nearly always occurs within 2 years after the treatment.[1, 2)] The 2019 edition of the NCCN guidelines for head and neck cancer recommend periodic examination once every 1 to 3 months in the first year after surgery, once every 2 to 6 months in the 2nd year, once every 4 to 8 months in the 3rd to 5th years, and subsequently once a year. In addition, they recommend performing the baseline imaging examination for follow-up within 6 months after treatment.

After radiation therapy or chemoradiotherapy for head and neck cancer, the treatment response of the primary tumor and cervical lymph node metastases is evaluated, and whether to perform resection for the residual tumors or neck dissection is determined. According to the NCCN guidelines, inspection is performed 4 to 8 weeks after radiation therapy or chemoradiotherapy. If an increase in size or the presence of residual tumors is suspected for the primary tumor and cervical lymph node metastases, CT, MRI, or PET is performed. If a treatment response is seen, either CT or MRI at 8 to 12 weeks or PET at 12 weeks or later is recommended. If residual cervical lymph node metastases are seen with these examinations, neck dissection should be performed. If the PET examination is negative, the likelihood of residual tumors is low, and subsequent imaging is not recommended.

With regard to the imaging examinations used at baseline and during follow-up, although contrast-enhanced CT is generally used, contrast-enhanced MRI is useful for tumors near the skull base, such as nasopharyngeal and paranasal sinus tumors, salivary gland tumors, and tumors suggestive of bone

marrow, skull base, intracranial invasion or perineural spread.[1, 3] The baseline examination should be performed at a time when postoperative reactions such as edema and inflammation have subsided and no recurrence is seen. CT and MRI are generally performed 6 to 8 weeks after treatment.[1, 4]

Many investigations of the performance of CT and MRI in diagnosing recurrence and residual tumors have used ADC values obtained by diffusion-weighted MRI. The ADC values for recurrence and residual tumors are significantly lower than those for postoperative scar tissue, and their reported sensitivity and specificity have ranged from 90.1% to 94% and from 82.5% to 83.3%, respectively.[5, 6] Consequently, the addition of diffusion-weighted imaging to normal morphological imaging enables more accurate internal characterization of lesions.

In addition, many investigations have used PET, which has been reported to be an excellent examination for diagnosing recurrence and residual tumors. The sensitivity and specificity of PET have ranged from 72.3% to 92% and from 82.3% to 87%, respectively.[7, 8] However, a disadvantage of PET is the high rate of false positives early after treatment completion due to conditions such as edema and inflammation. Although the timing of PET varies somewhat depending on the report, 12 weeks after treatment or later is considered preferable. Although PET is useful for diagnosing recurrence and residual tumors, it poses problems for follow-up, such as problems related to its indications, timing, intervals, cost-effectiveness, and radiation exposure. Consequently, it can be considered when diagnosis proves difficult with CT or MRI.

Search keywords and secondary sources used as references

PubMed was searched using the following keywords: head and neck cancer, post treatment, follow up, diagnostic imaging, CT, and MRI. The period searched was through the end of June 2019.

In addition, the following was referenced as a secondary source.

1) Pfister DG: NCCN Guidelines®: head and neck cancers Ver 3. 2021. National Comprehensive Cancer Network, 2021

References

1) Manikantan K et al: Making sense of post–treatment surveillance in head and neck cancer: when and what of follow-up. Cancer Treat Rev 35: 744-753, 2009
2) Liu G et al: Post-therapeutic surveillance schedule for oral cancer: is there agreement? Oral Maxillofac Surg 16: 327-340, 2012
3) Mukherji SK et al: Evaluation of head and neck squamous cell carcinoma after treatment. AJNR Am J Neuroradiol 24: 1743-6, 2003
4) Lell M et al: Head and neck tumor: imaging recurrent tumor and post-therapeutic change with CT and MRI. Eur J Radiol 33: 239-247, 2000
5) Vaid S et al: Differentiating recurrent tumors from post-treatment changes in head and neck cancers: dose diffusion-weighted MRI solve the eternal dilemma? Clin Radiol 72: 74-83, 2017
6) Jajodia A et al: Value of diffusion MR imaging in differentiation of recurrent head and neck malignancies from post treatment changes. Oral Oncol 96: 89-96, 2019
7) Sheikhbahaei S et al: Diagnostic accuracy of follow-up FDG PET or PET/CT in patients with head and neck cancer after definitive treatment: a systematic review and meta-analysis. AJR Am J Roentgenol 205: 629-639, 2015
8) Cheung PK et al: Detecting residual/recurrent head neck squamous cell carcinomas using PET or PET/CT: systematic review and meta-analysis. Otolaryngol Head Neck Surg 154: 421-432, 2016

BQ 15 Is MRI recommended for the qualitative diagnosis of parotid tumors?

Statement

MRI is the standard examination and recommended for the qualitative diagnosis of parotid tumors.

Background

Approximately 80% of parotid tumors are benign, and ≥ 90% of those are pleomorphic adenomas and Warthin's tumors. Consequently, in addition to broad categorization as benign and malignant, differentiating pleomorphic adenomas (resection is recommended, including the capsule) and Warthin's tumors (enucleation or watchful waiting is sufficient) is important in diagnosing parotid tumors. Ultrasound-guided fine-needle aspiration cytology (FNAC) is an established diagnostic method with a diagnostic accuracy rate higher than 85%. However, diagnosing tumors located in the deep lobe is difficult with FNAC, and there is a risk of tumor seeding and infarction associated with the technique. Consequently, MRI, which is noninvasive and provides excellent tissue contrast, is widely used for the qualitative diagnosis of parotid tumors. The reasons why MRI is the standard imaging examination for the qualitative diagnosis of parotid tumors are summarized below.

Explanation

The main findings suggestive of malignant tumors with conventional MRI, which does not include diffusion-weighted imaging or dynamic contrast-enhanced MRI, are indistinct margin characteristics and lower signal intensity than the parotid gland tissue on T2-weighted images.[1)] The former finding overlaps with that for inflammatory masses, and the latter overlaps with that for Warthin's tumor. However, comparisons with FNAC have shown their diagnostic accuracy rates to be comparable.[2, 3)] A meta-analysis by Liang et al. found that sensitivity and specificity, as measures of diagnostic performance in differentiating benign and malignant lesions based on conventional MRI findings, were 76% and 83%, respectively. Adding the ADC values of diffusion-weighted imaging and the time-signal intensity curve (TIC) analysis of dynamic contrast-enhanced MRI to conventional MRI increased sensitivity and specificity to 86% and 90%, respectively.[4)] With diffusion-weighted imaging, which is incorporated as the standard imaging method in this guideline (p. 76), the ADC values of pleomorphic adenomas are significantly higher than those of malignant tumors and Warthin's tumors, which is useful for differential diagnosis. However, the ADC values for Warthin's tumors and malignant tumors overlap.[5-7)] The TIC patterns often seen with dynamic contrast-enhanced MRI are a gradual increase for pleomorphic adenomas, a rapid increase and rapid decrease (peak reached within 120 seconds and washout rate of ≥ 30% after 300 seconds) for Warthin's tumors, and a rapid increase and gradual decrease for malignant tumors. These patterns are useful for differentiating benign from malignant tumors and diagnosing Warthin's tumors.[6, 7)]

With perfusion imaging using arterial spin labeling (ASL), which does not require a contrast medium, the tumor-to-parotid gland signal intensity ratio of Warthin's tumors is higher than of malignant tumors and of pleomorphic adenomas, which is useful for diagnosing Warthin's tumor.[8] Classic observations such as lobulated shape for pleomorphic adenomas and inferior pole and multiple bilateral occurrences in the parotid glands for Warthin's tumors are also important in clinical practice.

With regard to CT, because its tissue contrast is low, it is lacking in usefulness with respect to the qualitative diagnosis of parotid tumors. However, CT is useful when diagnosing extent is required, as in the case of lymph node metastasis or bone cortex invasion.[9] Fat-suppressed, contrast-enhanced, T1-weighted imaging is recommended for evaluating perineural spread along nerves such as the 3rd branch of the trigeminal nerve (mandibular nerve) or facial nerve.[9]

It is therefore appropriate to consider MRI the standard examination for the qualitative diagnosis of parotid tumors.

Search keywords and secondary sources used as references

PubMed was searched using the following keywords: MRI, parotid, and diagnostic accuracy. A filter was applied to limit the search to English-language reports with human subjects. The period searched was from January 1, 2005 to December 31, 2019. Hits were obtained for 55 articles, which were screened based on their titles and abstracts. The full text of 17 articles was then evaluated. Of these, 8 articles were used as reference articles for MRI diagnosis. In addition, a search was performed using "parotid gland" and "imaging review" as the keywords, with a filter applied that limited the search to review articles in English, and the resulting articles were used.

References

1) Christe A et al: MR imaging of parotid tumors: typical lesion characteristics in MR imaging improve discrimination between benign and malignant disease. AJNR Am J Neuroradiol 32: 1202-1207, 2011
2) Inohara H et al: The role of fine-needle aspiration cytology and magnetic resonance imaging in the management of parotid mass lesions. Acta Otolaryngol 128: 1152-1158, 2008
3) Paris J et al: Preoperative diagnostic values of fine-needle cytology and MRI in parotid gland tumors. Eur Arch Otorhinolaryngol 262: 27-31, 2005
4) Liang YY et al: Diagnostic accuracy of magnetic resonance imaging techniques for parotid tumors, a systematic review and meta-analysis. Clin Imaging 52: 36-43, 2018
5) Eida S et al: Apparent diffusion coefficient mapping of salivary gland tumors: prediction of the benignancy and malignancy. AJNR Am J Neuroradiol 28: 116-121, 2007
6) Yabuuchi H et al: Parotid gland tumors: can addition of diffusion-weighted MR imaging to dynamic contrast-enhanced MR imaging improve diagnostic accuracy in characterization ? Radiology 249: 909-916, 2008
7) Tao X et al: The value of combining conventional, diffusion-weighted and dynamic contrast-enhanced MR imaging for the diagnosis of parotid gland tumours. Dentomaxillofac Radiol 46: 20160434, 2017
8) Kato H et al: Perfusion imaging of parotid gland tumours: usefulness of arterial spin labeling for differentiating Warthin's tumours. Eur Radiol 25: 3247-3254, 2015
9) Abdel Razek AAK, Mukherji SK: State-of-the-art imaging of salivary gland tumors. Neuroimaging Clin N Am 28: 303-317, 2018

BQ 16 Is I-131 internal radiation therapy recommended in young patients with thyroid carcinoma?

Statement

I-131 internal radiation therapy is safe, useful, and recommended in young patients with thyroid carcinoma.

Background

Slightly less than 15% of well-differentiated thyroid carcinomas occur in individuals aged 18 years or less. It is often more advanced in prepubescent patients than in adolescents, and the recurrence rate is higher in prepubescent patients than in adult patients. The usefulness of I-131 internal radiation therapy in young patients with thyroid carcinoma was examined.

Explanation

I-131 internal radiation therapy is widely used in young patients after total thyroidectomy. It has been found to be useful for treating residual tumors and thyroid bed ablation.[1-5)] Although adverse reactions such as nausea, vomiting, and mild bone marrow suppression may occur, internal radiation therapy particularly for lesions up to 1 cm in diameter at intervals of 6 to 12 months for a total dose of 18.5 to 37 GBq (500 to 100 mCi) is considered a relatively safe treatment.[2)] However, there have been almost no reports of studies comparing it with a group that has not received internal radiation therapy. In addition, because there may be a risk of secondary carcinogenesis resulting from the radiation exposure, periodic follow-up is considered necessary.[3-5)]

Search keywords and secondary sources used as references

PubMed was searched using the following keywords: differentiated, thyroid carcinoma, radioiodine, therapy, and childhood. Five articles were selected from the results.

References

1) Gao YC, Lu HK: Outcome after high-dose radioiodine therapy for advanced differentiated thyroid carcinoma in childhood. Endocr Res 34 (4): 121-129, 2009
2) Kumagai A et al: Childhood thyroid cancers and radioactive iodine therapy: necessity of precautious radiation health risk management. Endocr J 54 (6): 839-847, 2007
3) Handkiewicz-Junak D et al: Total thyroidectomy and adjuvant radioiodine treatment independently decrease locoregional recurrence risk in childhood and adolescent differentiated thyroid cancer. J Nucl Med 48 (6): 879-888, 2007
4) Jarzab B et al: Juvenile differentiated thyroid carcinoma and the role of radioiodine in its treatment: a qualitative review. J Endocr Relat Cancer 12 (4): 773-803, 2005
5) Chow SM et al: Differentiated thyroid carcinoma in childhood and adolescence-clinical course and role of radioiodine. Pediatr Blood Cancer 42 (2): 176-183, 2004

3
Chest

Standard Imaging Methods for Chest

Chest radiography

1. Imaging method

The digital imaging systems currently used at nearly all facilities, such as flat-panel detectors and computed radiography systems, perform histogram analysis. Consequently, the radiation dose affects image quality without affecting the photographic density of the images. It has been reported that, although the increase in noise that results from a moderate reduction in dose reduces image quality, it has little effect on diagnostic performance. It is, therefore, appropriate to set the imaging conditions (radiation dose) to a level comparable to or lower than used for conventional film-screen imaging.

2. Image processing

With chest radiography that uses a digital imaging system, images of high diagnostic value need to be obtained through appropriate image processing, such as the use of gradients, frequencies, dynamic range reduction, and denoising.

3. Soft copy display requirements

According to the Guidelines for Handling Digital Images, 3rd Edition,[1)] a compliant liquid-crystal monitor is one that has a resolution of 1 megapixel or greater and satisfies the requirements for control grade 1 of the Guidelines for Quality Control of Monitors for Displaying Medical Images (JESRAX-0093-*B^{-2017}) of the Japan Medical Imaging and Radiological Systems Industries Association.[2)]

Computed tomography (CT)

1. Imaging method

For the performance required of a computed tomography (CT) system to diagnose diseases of the thoracic region, imaging with a high-resolution computed tomography (HRCT) system (Figs. 1A and 6A), early-phase imaging using bolus injection of a contrast medium (Fig. 6B), and a multidetector computer tomography (MDCT) system equipped with a multi-row detector that can withstand clinical use is desirable. The imaging method used depends largely on the performance of the CT system. Continuous scanning from the apex to the base of the lungs is generally recommended. Although a slice thickness of 5 mm is widely used, CT with intermediate slice thicknesses of 3 to 5 mm is used concurrently as needed. Adequate breath-holding is required during scanning.

2. High-resolution CT (HRCT)

HRCT imaging uses thin collimation. "Thin" is usually considered ≤ 2 mm. A high-spatial-frequency algorithm is used in reconstruction (Figs. 1A and 6A). The methods used are one that involves re-imaging of only the necessary sites and another that involves first performing continuous thin-collimation CT imaging of all lung fields by MDCT, then creating images of intermediate slice thickness by reconstruction.

① Imaging of diffuse lung disease

An imaging based on the method of Goddard is widely used in emphysema and chronic obstructive pulmonary disease (COPD). Specifically, the method involves HRCT imaging at the level of the aortic arch, tracheal bifurcation and 1 to 2 cm above either the left or right upper diaphragm and performing a visual assessment.[3] In pulmonary fibrosis, assessment at 1 to 2-cm intervals with a collimation thickness of 1 to 2 mm is commonly performed. Recently, a method involving the imaging of all lung fields by continuous thin-collimation CT using ≥ 16-row MDCT has been used for emphysema volumetry.[4] Expiratory imaging, as well as inspiratory imaging, is useful for purposes such as the qualitative diagnosis of obstructive pulmonary disease (see BQ 19).[5]

② Imaging method for pulmonary nodules

An imaging method based on HRCT is used. At the image reconstruction stage, coronal images (Fig. 1B), sagittal images, and target images of the nodules (FOV, approximately 20 cm) are generated as needed. Not only can nodules be qualitatively assessed, but quantitative changes in nodules over time can be assessed by volumetry.[6]

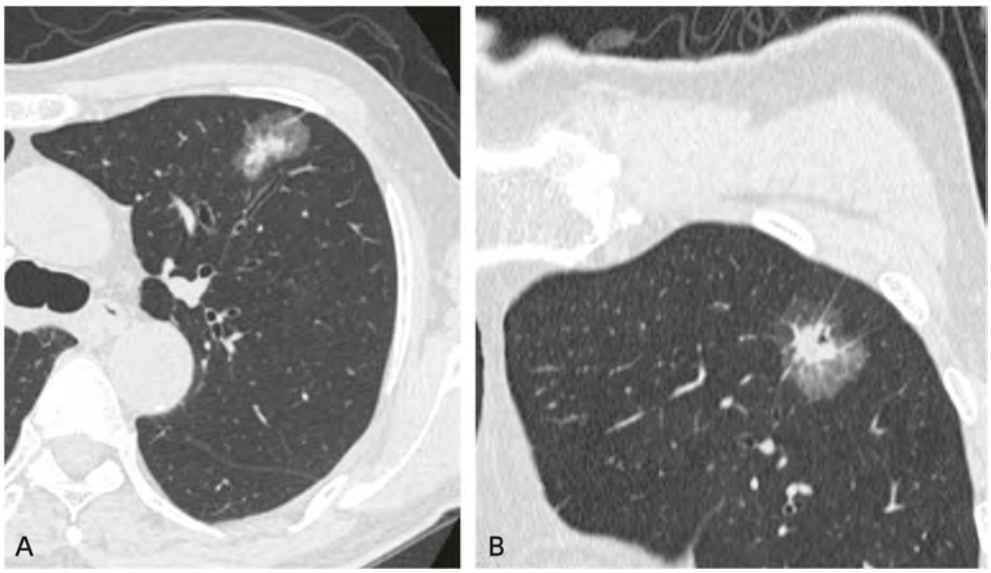

Figure 1. Invasive lung adenocarcinoma

A: HRCT, transverse image: A part-solid nodule with a whole-tumor diameter of 28 mm and solid-component diameter of 15 mm is seen in the left upper lobe.

B: HRCT, coronal reconstructed image: The whole-tumor diameter is 29 mm, and the solid-component diameter is 11 mm.

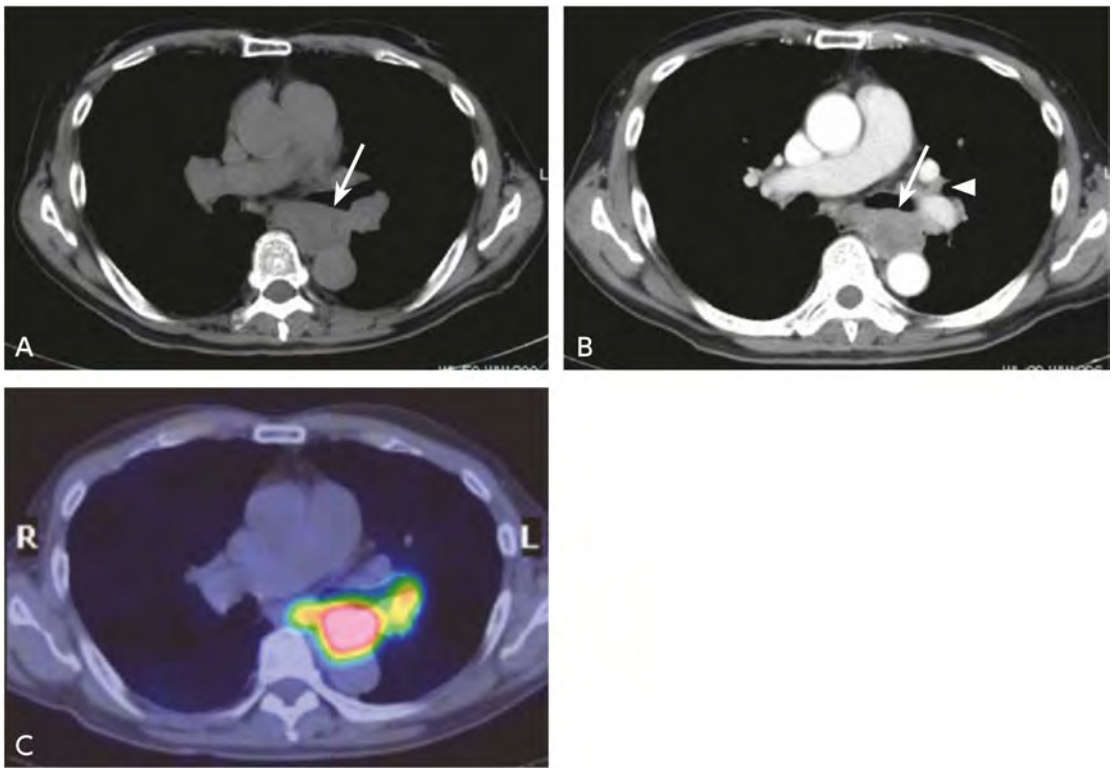

Figure 2. Hilar and mediastinal lymph node metastases of lung cancer

(c-T2N3M0, stage III B)

A: Non-contrast-enhanced CT, transverse image: Lymph node enlargement is seen dorsal to the left main bronchus and ventral to the descending aorta (⇨).

B: Contrast-enhanced CT, transverse image: The relationship between the enlarged lymph nodes and surrounding blood vessels is clearly seen (⇨). Left hilar lymph node enlargement is also suspected (▷).

C: FDG-PET/CT, transverse image: Accumulation consistent with enlarged lymph nodes is seen.

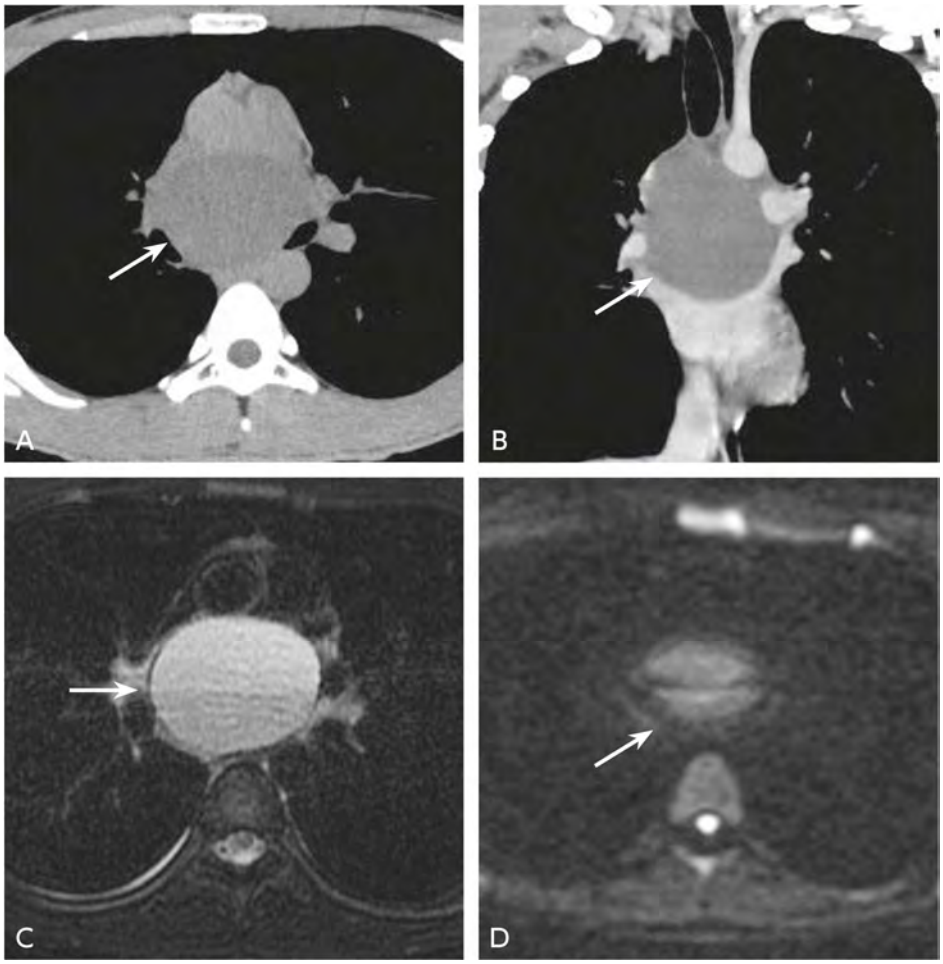

Figure 3. Bronchogenic cyst

A: Non-contrast-enhanced CT, transverse image: A mass with distinct borders is seen below the tracheal bifurcation. The mass is homogeneous and shows slightly higher attenuation than water (→).

B: Contrast-enhanced CT, coronal reconstructed image: Contrast enhancement is not seen in the mass (→).

C: MRI, fat-suppressed T2-weighted transverse image: The mass shows hyperintensity, and a fluid-fluid level (→) is seen in the mass.

D: MRI, diffusion-weighted transverse image, b-value = 1,000 s/mm^2: The mass shows slight hyperintensity (→).

3. Reducing the patient's radiation exposure

Although filtered back projection (FBP) has been used in CT for image reconstruction in the past, recent years have seen the emergence of systems that enable iterative reconstruction methods, which provide excellent noise reduction. Low-dose imaging and iterative reconstruction methods have made it possible to perform CT examinations with doses previously not considered feasible. For the thoracic region, image quality has been found to be comparable with 120-mA FBP imaging and 60-mA imaging using iterative reconstruction.[7)] The use of low-dose imaging using systems capable of iterative reconstruction methods should be emphasized in the future to reduce radiation exposure.

4. Display conditions

Window settings (WSs) of approximately 30 to 50 HU for window level (WL) and 250 to 400 HU for window width (WW) (mediastinum WS) are appropriate for observing soft tissue such as the mediastinum. Window settings of approximately -500 to -700 HU for WL and 1,200 to 2,000 HU for the WW (lung WS) are suitable when observing the lungs. Except in special cases, images are displayed using the pair of conditions for the mediastinum and lungs. The standard algorithm is used in reconstruction in the mediastinum WS, and reconstruction that accentuates the high-spatial-frequency algorithm is used in reconstruction in the lung WS.

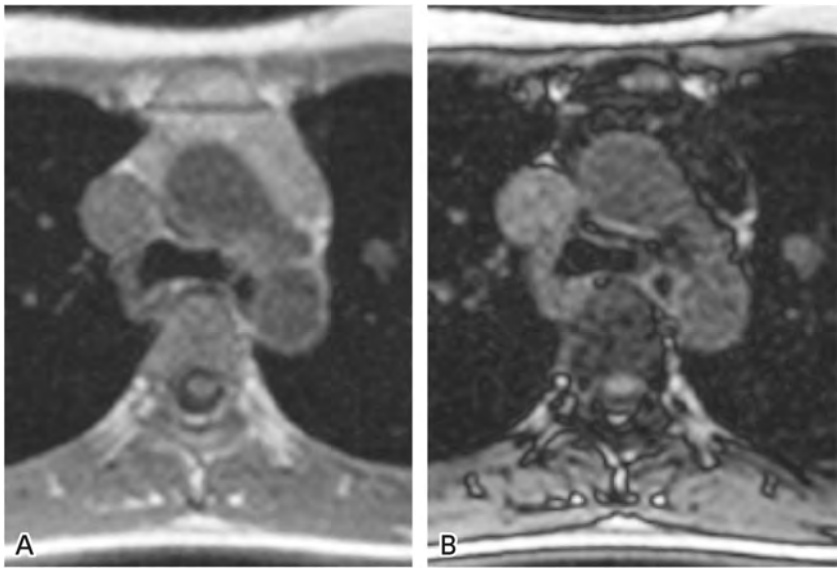

Figure 4. Thymic hyperplasia

A: MRI, GRE T1-weighted in-phase image, TR/163, TE/4.6, FA/75: The anterior mediastinal mass shows slightly higher signal intensity than muscle.

B: MRI, GRE T1-weighted opposed-phase image, TR/163, TE/2.3, FA/75: As compared with the in-phase image, a homogeneous signal decrease is seen in the mass.

5. Contrast imaging examinations

Automatic injectors are now widely used for bolus injections, with a total contrast medium dose of ≤ 100 mL and an injection rate of approximately 1 to 5 mL/s (Figs. 2B and 6B).[8] To obtain good contrast enhancement over an extensive area, effort is needed to substantially improve temporal resolution by using an automatic injector in combination with MDCT. Perfusion imaging using dual-energy CT has recently been reported to be useful (Fig. 6C).[9]

Magnetic resonance imaging (MRI)

1. Imaging method

Although imaging with a high-performance system with a strong magnetic field is preferable, artifacts caused by differences in magnetic susceptibility are always a problem for lung imaging. The thoracic region is prone to artifacts caused by heartbeats, blood flow in the great vessels, and breathing and is therefore an unfavorable location for MRI examination. However, these artifacts can be reduced by ECG and pulse-wave gating, respiratory gating and breath-holding, and the application of a presaturation pulse.

T1-weighted imaging and T2-weighted imaging are standard, and transverse images are usually acquired (Figs. 3C and 3D). However, coronal and sagittal images are also acquired for lung apex lesions (e.g., superior sulcus tumors), lung base lesions (e.g., diaphragmatic invasion of a malignancy), and mediastinal and chest wall lesions. A slice thickness of 5 to 8 mm is commonly used. A matrix size of $\geq 256 \times 192$ is preferred. The method called fast-spin echo (FSE), which has a short imaging duration, is generally used. Gradient echo (GRE) is used in MRA and cine imaging. The use of diffusion-weighted imaging has been examined for distinguishing between benign and malignant lesions and for diagnosing mediastinal lymph node metastasis in lung cancer and mediastinal tumors (Fig. 3D). However, there is poor reproducibility between MRI systems in determining an ADC cutoff, and this remains a challenge. Lesion blood flow status and the extent of progression can be evaluated by post-contrast T1-weighted imaging. However, depending on the location of the lesion, the evaluation may be more useful when combined with fat-suppressed imaging. In addition, chemical shift imaging has been reported to be effective for distinguishing thymic hyperplasia from thymoma. With this method, because protons in water and fat resonate at different frequencies, signals that strengthen each other (in phase) and signals that cancel each other (opposed phase) are generated, and changes in signal intensity are observed. In thymic hyperplasia, which is high in fat content, a decreased signal is seen in opposed-phase images. The imaging method mainly involves the use of GRE, with images acquired by increasing and decreasing the echo time (Figs. 4 and 5).[10)]

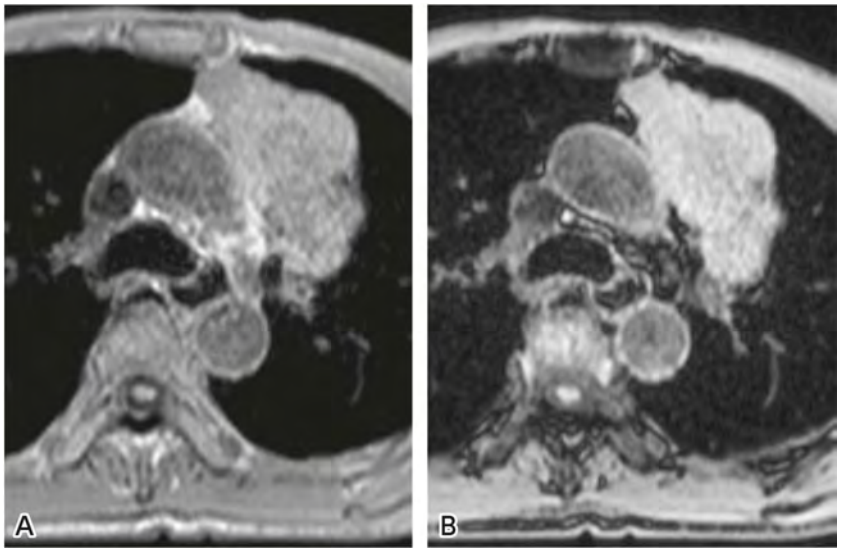

Figure 5. Thymoma

A: MRI, GRE T1-weighted in-phase image, TR/225, TE/4.6, FA/70: The anterior mediastinal mass shows slightly higher signal intensity than muscle.
B: MRI, GRE T1-weighted opposed-phase image, TR/225, TE/2.3, FA/70: No change in the signal of the mass is seen.

Nuclear medicine imaging

1. Pulmonary perfusion scintigraphy ^{99m}TC-macroaggregated albumin (^{99m}Tc-MAA)

In general, the patient lies supine at rest, the injection syringe is shaken immediately before intravenous infusion, and ^{99m}Tc-MAA is slowly injected intravenously at a dose of 111 to 185 MBq as the patient takes 2 to 3 deep breaths. Beginning 5 minutes after injection, images are acquired from 6 angles (or 8 with the addition of left and right anterior oblique), frontal (Fig. 6E), posterior, left and right lateral, and left and right posterior oblique, using a gamma camera equipped with a low-energy general-purpose (or high-resolution) collimator. It can also be imaged in combination with SPECT.

2. Ventilation scintigraphy (^{81m}Kr)

Imaging is generally performed with the patient sitting with his or her back to a gamma camera equipped with a medium- (or low-medium-) energy collimator. When ^{81m}Kr gas is used, humidified oxygen or air is passed through a generator at a flow rate of approximately 0.3 to 3.0 L/min. The patient then inhales the ^{81m}Kr gas that emerges through a mask or similar device, and imaging is performed. Because the physical half-life of ^{81m}Kr is a short 13 seconds, repeated imaging can be performed without the need for special equipment, and it can be performed from many angles (Figs. 6D and 6E). Ventilation scintigraphy is highly clinically useful in pulmonary thromboembolism, which is visualized as a defect only on perfusion scintigraphy when pulmonary blood flow scintigraphy and ventilation scintigraphy are performed concurrently.

3. ^{18}F-Fluorodeoxyglucose (^{18}F-FDG) PET and PET/CT imaging

For 2D data acquisition, 185 to 444 MBq (3 to 7 MBq/kg) of FDG are administered intravenously; for 3D data acquisition, 111 to 259 MBq (2 to 5 MBq/kg) are administered. The dose is adjusted as appropriate depending on the equipment used and the patient's age and weight. Approximately 60 minutes after administration, a PET or PET/CT system is used to perform a whole-body emission scan. A transmission scan (in the case of PET) or CT imaging (in the case of PET/CT; Fig. 2C) is also performed. Delayed-phase imaging is added as necessary.

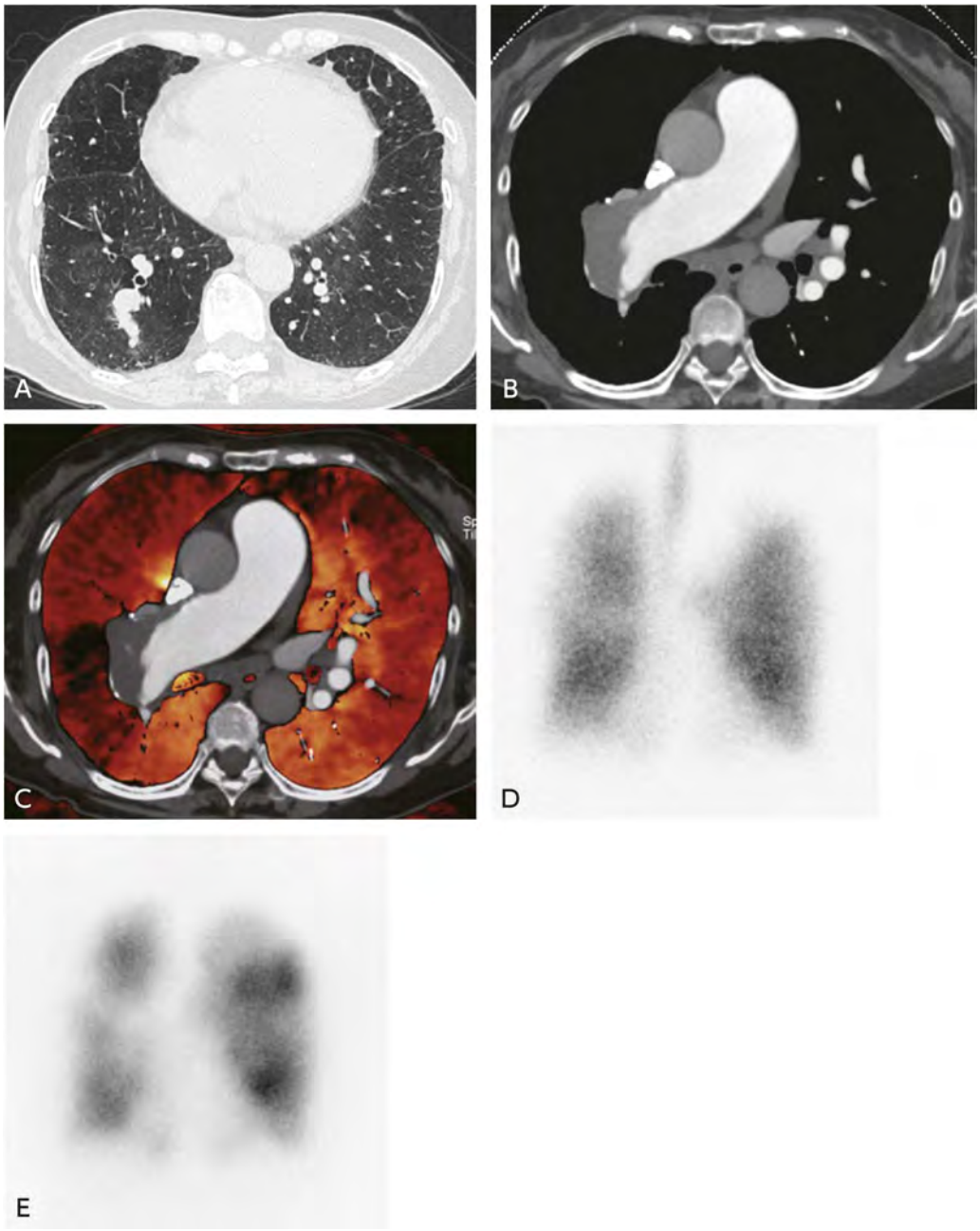

Figure 6. Chronic thromboembolic pulmonary hypertension

A: HRCT, transverse image: The lung attenuation shows an inhomogeneous mosaic pattern.
B: Contrast-enhanced CT, arterial phase, transverse image: The pulmonary arteries are markedly dilated, and a large thrombus is seen in the right pulmonary artery.
C: Contrast-enhanced CT, perfusion image: Blood flow in the lungs appears inhomogeneous, and areas of perfusion defects are seen.
D: Pulmonary ventilation scintigraphy (^{81m}Kr): Accumulation defects are not seen in either lung.
E: Pulmonary perfusion scintigraphy (^{99m}Tc-MAA): Multiple defects are seen in both lungs.

Secondary sources used as references

1) Japan Radiological Society, Ed.: Guidelines for Handling Digital Images, 3rd Edition. Japan Radiological Society, 2015.
2) Japan Medical Imaging and Radiological Systems Industries Association, Ed.: Guidelines for Quality Control of Monitors for Displaying Medical Images, revised on July 20, 2017. Japan Medical Imaging and Radiological Systems Industries Association, 2017.
3) Nishimura M et al: Annual change in pulmonary function and clinical phenotype in chronic obstructive pulmonary disease. Am J Respir Crit Care Med 185: 44-52, 2012
4) Akira M et al: Quantitative CT in chronic obstructive pulmonary disease: inspiratory and expiratory assessment. AJR Am J Roentgenol 192: 267-272, 2009
5) Matsuoka S et al: Quantitative assessment of air trapping in chronic obstructive pulmonary disease using inspiratory and expiratory volumetric MDCT. AJR Am J Roentgenol 190: 762-769, 2008
6) van Klaveren RJ et al: Management of lung nodules detected by volume CT scanning. N Engl J Med 361: 2221-2229, 2009
7) Yamashiro T et al: Adaptive iterative dose reduction using three dimensional processing (AIDR3D) improves chest CT image quality and reduces radiation exposure. PLoS One 9: e105735, 2014
8) Yi CA et al: Efficacy of helical dynamic CT versus integrated PET/CT for detection of mediastinal nodal metastasis in non-small cell lung cancer. AJR Am J Roentgenol 188: 318-325, 2007
9) Le Faivre J et al: Impact of CT perfusion imaging on the assessment of peripheral chronic pulmonary thoromboembolism: clinical experience in 62 patients. Eur Radiology 26: 4011-4020, 2016
10) Inaoka T et al: Thymic hyperplasia and thymus gland tumors: differentiation with chemical shift MR imaging. Radiology 243: 869-876, 2007
11) Bajc M et al: EANM guidelines for ventilation/perfusion scintigraphy: part 1. pulmonary imaging with ventilation/perfusion single photon emission tomography. Eur J Nucl Med Mol Imaging 36: 1356-1370, 2009

CQ 1 Is CT recommended for the differential diagnosis of adult community-acquired pneumonia and non-infectious diseases?

Recommendation

CT is weakly recommended for the differential diagnosis of adult community-acquired pneumonia and non-infectious diseases.

Recommendation strength: 2, strength of evidence: D (very weak), agreement rate: 100% (15/15)

Background

There are a variety of lung diseases that must be differentiated from community-acquired pneumonia. Examples in immunocompetent individuals include pulmonary edema, eosinophilic pneumonia (EP), hypersensitivity pneumonitis, idiopathic interstitial pneumonia, and drug-induced lung disorders.[1)] In addition to these, several pathologies are possible in immunodeficient individuals, such as opportunistic infections and changes caused by malignancies.[2)] The role of CT was examined in the differential diagnosis of community-acquired pneumonia and these non-infectious diseases, particularly acute respiratory disorders, which appear as diffuse lung opacities.

Explanation

There is considerable overlap in the chest radiography findings of community-acquired pneumonia and diffuse lung disease, and no findings are considered disease-specific. However, it has been reported that the addition of CT, particularly HRCT, may provide new information (Figs. 1 and 2).[3-5)]

An investigation of the use of CT in patients with community-acquired pneumonia who required hospitalization found it useful for detecting lesion cavities and masses not detected by chest radiography and for excluding masses suspected of being present based on chest radiography.[3)] Although its usefulness does not extend as far as differentiating from infectious pneumonia, it has been found to be useful to some extent for diagnosis by exclusion or revealing important findings. A survey of pulmonologists was conducted to examine the status of HRCT use and its usefulness in diffuse lung disease.[4)] Of the valid responses received from the 230 physicians surveyed, 67% to 89% indicated that HRCT was useful in diagnosing diseases such as idiopathic interstitial pneumonia, EP, Langerhans cell histiocytosis, lymphangioleiomyomatosis, and bronchiectasis.

Figure 1. *Mycoplasma pneumoniae* pneumonia (man in his 40s)

HRCT: Centrilobular branching opacities and nodules (→), acinar to lobular ground-glass opacities and consolidations (►) are seen in the right upper and lower lobes. Bronchovascular bundle thickening is also prominent.

Figure 2. Non-fibrotic (subacute) hypersensitivity pneumonitis (man in his 60s)

HRCT: Centrilobular ground-glass opacities are seen diffusely. A low-attenuation area (→) caused by air-trapping is seen in the periphery of S3. No centrilobular branching opacities are seen.

Five of the articles describing investigations of the use of HRCT to differentiate between infectious and non-infectious diseases indicated that there are several common distinguishing features in images.[2, 6-9)] An investigation of acute lung parenchymal lesions in immunocompetent individuals found that the most important finding for distinguishing infectious from non-infectious disease was centrilobular nodules,[6)] which are typically not seen in non-infectious diseases other than hypersensitivity pneumonitis. Other findings specific to infection were the presence of segmental distribution and wedge-shaped consolidation associated with the segmental bronchi. The sensitivity of these findings was 83% for infectious disease and 94% for non-infectious disease.[6)] An examination of a group with multiple consolidations seen on chest radiography found that important HRCT findings for distinguishing infectious from non-infectious disease were a centrilobular branching structure caused by centrilobular nodules and endobronchial mucus plugs.[7)] Neither the centrilobular branching structure nor a tree-in-bud appearance is seen in non-infectious lung diseases such as hypersensitivity pneumonitis, emphysema, obstructive bronchiolitis, and cryptogenic organizing pneumonia.[8, 9)] An examination of the diagnostic rate for various diseases in a group of immunodeficient patients who did not have acquired immune deficiency syndrome and who developed acute lung injuries,[2)] including infection, showed variability in the diagnostic rate depending on the disease, with sensitivity ranging from 27% to 100% and positive predictive value ranging from 25% to 100%. HRCT findings frequently seen in bacterial pneumonia include centrilobular lesions and lesions of secondary lobules, and the CT halo sign and cavities tend to be common in mycosis and tuberculosis. Malignancies included leukemia, malignant lymphoma, and lymphangitis carcinomatosa, with

bronchovascular bundle thickening, nodules, and lymph node enlargement frequently seen in these diseases. An examination of differentiation between infectious pneumonia and invasive mucinous adenocarcinoma mimicking pneumonia found that bronchial wall thickening proximal to a lesion and pleural thickening adjacent to a lesion were findings suggestive of infectious pneumonia.[10)]

Although not differentiation based on imaging, examples of the purposes for which CT is useful include determining locations for alveolar lavage fluid collection, transbronchial lung biopsy, and surgical biopsy, which may contribute to the differentiation of pneumonia and non-infectious disease.

Although the above findings are insufficient scientific evidence to establish that CT is effective in this role, there are HRCT findings that are relatively characteristic of community-acquired pneumonia and non-infectious disease, making their differentiation possible to some extent, which may aid in determining a treatment plan. It was therefore concluded that CT can be weakly recommended for the differential diagnosis of adult community-acquired pneumonia and non-infectious diseases.

Search keywords and secondary sources

PubMed was searched using the following keywords: pneumonia and computed tomography.

References

1) Shorr AF et al: Pulmonary infiltrates in the non-HIV-infected immunocompromised patient: etiologies, diagnostic strategies, and outcomes. Chest 125: 260-271, 2004
2) Emoto T et al: HRCT findings of pulmonary complications in non-AIDS immunocompromised patients: are they useful in differential diagnosis? Radiat Med 21: 7-15, 2003
3) Beall DP et al: Utilization of computed tomography in patients hospitalized with community-acquired pneumonia. Maryland Med J 47: 182-187, 1998
4) Scatarige JC et al: Utility of high-resolution CT for management of diffuse lung disease: results of a survey of U.S. pulmonary physicians. Acad Radiol 10: 167-175, 2003
5) Tanaka N et al: Community-acquired pneumonia: a correlative study between chest radiographic and HRCT findings. Jpn J Radiol 33: 317-328, 2015
6) Tomiyama N et al: Acute parenchymal lung disease in immunocompetent patients: diagnostic accuracy of high-resolution CT. AJR Am J Roentgenol 174: 1745-1750, 2000
7) Johkoh T et al: Usefulness of high-resolution CT for differential diagnosis of multi-focal pulmonary consolidation. Radiat Med 14: 139-146, 1996
8) Aquino SL et al: Tree-in-bud pattern: frequency and significance on thin-section CT. J Comput Assist Tomogr 20: 594-599, 1996
9) Okada F et al: Clinical/pathological correlations in 553 patients with primary centrilobular findings on high-resolution CT scan of the thorax. Chest 132: 1939-1948, 2007
10) Kim TH et al: Differential CT features of infectious pneumonia versus bronchioloalveolar carcinoma (BAC)mimicking pneumonia. Eur Radiol 16: 1763-1768, 2006

BQ 17 Is CT recommended for differentiating between bacterial pneumonia and atypical pneumonia?

Statement

CT is recommended for differentiating between *Streptococcus pneumoniae* pneumonia and *Mycoplasma pneumoniae* pneumonia. Although evidence for its usefulness in the case of other prophlogistic microorganisms is limited, their CT characteristics have been established to some degree.

Background

The guidelines of the Japanese Respiratory Society recommend that atypical pneumonias be screened from among the community-acquired pneumonias and treated early. The usefulness of CT for distinguishing between bacterial pneumonia and atypical pneumonias in adults was examined.

Explanation

The main CT findings examined were those of *Streptococcus pneumoniae* pneumonia (Fig. 1), the most common type of bacterial pneumonia, and frequently occurring atypical pneumonias (*Mycoplasma pneumoniae* pneumonia, *Chlamydophila pneumoniae* pneumonia, and influenza virus pneumonia; Fig. 2). The characteristics of the findings have been established to some extent for *Streptococcus pneumoniae* pneumonia, *Mycoplasma pneumoniae* pneumonia, and influenza virus pneumonia.

Tanaka et al. compared the CT findings of 18 patients with bacterial pneumonia and 14 patients with atypical pneumonia.[1)] Centrilobular shadows, acinar shadows, air space consolidations, and ground-glass opacities with lobular distribution were seen more frequently in atypical pneumonia than in bacterial pneumonia. An investigation by Nambu et al. (24 patients with *Chlamydophila pneumoniae* pneumonia, 30 patients with *Mycoplasma pneumoniae* pneumonia, 41 patients with *Streptococcus pneumoniae* pneumonia) showed that findings of bronchovascular bundle thickening and centrilobular nodules were more frequent in *Mycoplasma pneumoniae* pneumonia and *Chlamydophila pneumoniae* pneumonia than in *Streptococcus pneumoniae* pneumonia.[2)]

An investigation by Reittner et al. of CT findings in a total of 114 patients, comprising 35 patients with bacterial pneumonia, 28 with *Mycoplasma pneumoniae* pneumonia, and 9 with viral pneumonia, found a higher frequency of centrilobular nodules in *Mycoplasma pneumoniae* pneumonia and viral pneumonia than in bacterial pneumonia, with no consolidation seen in viral pneumonia.[3)] Ito et al. examined bacterial pneumonia in 94 patients (including 65 patients with *Streptococcus pneumoniae* pneumonia) and atypical pneumonia in 31 patients (including 20 patients with *Mycoplasma pneumoniae* pneumonia and 7 with *Chlamydophila pneumoniae* pneumonia).[4)] Centrilobular nodules, bronchovascular bundle thickening, and lobular ground-glass opacities were seen significantly more frequently in atypical pneumonia, making these

findings useful for differentiating atypical pneumonia from bacterial pneumonia. However, distinguishing *Chlamydophila pneumoniae* pneumonia from bacterial pneumonia was difficult.

Figure 1. *Streptococcus pneumoniae* pneumonia

HRCT, transverse image: Consolidation and ground-glass opacities associated with air bronchograms are seen in the right lower lobe. Bronchial wall thickening is unremarkable.

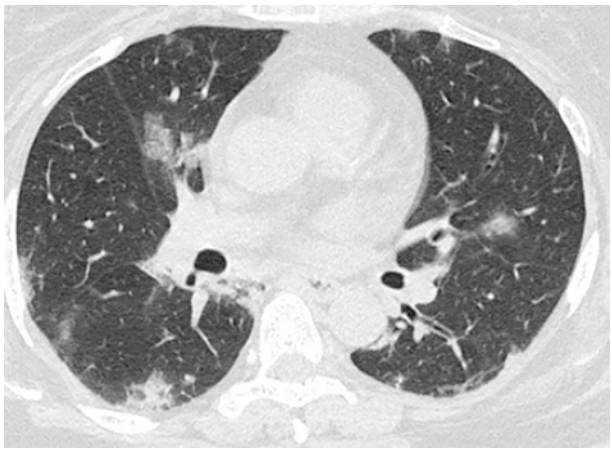

Figure 2. Influenza virus pneumonia

HRCT, transverse image: Multiple ground-glass opacities and consolidations are seen in both lungs, with intralobular reticular opacities seen in the ground-glass opacities.

Investigations by Miyashita et al. (64 patients with *Mycoplasma pneumoniae* pneumonia and 68 with *Streptococcus pneumoniae* pneumonia)[5] and Nei et al. (36 patients with *Mycoplasma pneumoniae* pneumonia and 52 with community-acquired pneumonia, including 20 with *Streptococcus pneumoniae* pneumonia)[6] found bronchial wall thickening and centrilobular nodules at significantly higher frequencies in *Mycoplasma pneumoniae* pneumonia. There are other, similar reports of CT findings in *Streptococcus pneumoniae* pneumonia and *Mycoplasma pneumoniae* pneumonia, indicating that findings of bronchial wall thickening and centrilobular nodules are useful for distinguishing between these two conditions.

There have been few summary reports of the imaging findings for *Chlamydophila pneumoniae* pneumonia. As compared with *Mycoplasma pneumoniae* pneumonia, bronchial wall thickening and centrilobular nodules are seen less frequently in *Chlamydophila pneumoniae* pneumonia, whereas lobular ground-glass opacities and lobular consolidation are seen more frequently.[7] However, differentiation from *Streptococcus pneumoniae* pneumonia is considered difficult.[4]

With regard to influenza virus pneumonia, summary reports of seasonal and novel influenza viruses have indicated that intralobular reticular opacities are frequently seen in these conditions.[8-10] Ono et al. compared CT findings in seasonal influenza virus pneumonia (30 patients) and *Streptococcus pneumoniae* pneumonia (71 patients).[11] Ground-glass opacities and reticular opacities were frequently seen in influenza

virus pneumonia, and consolidation, intrabronchial mucus plugs, and centrilobular nodules were common in *Streptococcus pneumoniae* pneumonia. Significant differences were seen for each finding.

Fujita et al. examined the CT findings of 12 patients with virus-associated pneumonia and found segmental consolidation in patients with mixed infections with bacterial pneumonia, which distinguished them from pure viral pneumonia.[8)] In an examination of the CT findings of 93 patients with viral pneumonia and 22 patients with bacterial pneumonia, Miller et al. frequently observed diffuse ground-glass opacities or consolidation in bacterial pneumonia.[12)]

Numerous reports have described findings similar to those seen in influenza virus pneumonias in other viral pneumonias such as adenoviral pneumonia. CT may therefore be useful for distinguishing viral pneumonia from bacterial pneumonia.[3, 8)]

Search keywords and secondary sources

PubMed was searched using the following keywords: pneumonia and computed tomography.

In addition, the following were referenced as secondary sources.

1) Japanese Respiratory Society, Ed.: 2017 Guidelines for the Management of Community-acquired Pneumonia. Japanese Respiratory Society, 2017.
2) Japan Radiological Society, Japanese College of Radiology, Ed.: 2007 Diagnostic Imaging Guidelines for Adult Community-acquired Pneumonia, Japan Radiological Society, 2007.
3) Murayama S: CT diagnosis of lung infections. Tuberculosis 77: 79-86, 2002.
4) Murata K, et al.: CT appearance of respiratory tract infections. Nippon Acta Radiologica 59: 371-379, 1999.
5) Ashizawa K: Bacterial pneumonia. Japanese Journal of Clinical Medicine 28: 231-234, 2007.
6) Tanaka H, et al.: CT appearance of mycoplasma pneumonia lesions. Japanese Journal of Clinical Radiology 30: 979-986, 1985.

References

1) Tanaka N et al: High resolution CT findings in community-acuired pneumomonia. J Comput Assist Tomogr 20: 600- 608, 1996
2) Nambu A et al: Chlamydia pneumoniae: comparison with findings of mycoplasma pneumoniae and streptococcus pneumoniae at thin-section CT. Radiology 238: 330-338, 2006
3) Reittner P et al: Pneumonia: high-resolution CT findings in 114 patients. Eur Radiol 13: 515-521, 2003
4) Ito I et al: Differentiation of bacterial and non-bacterial community-acuired pneumomonia by thin-section computed tomography. Eur J Radiol 72: 388-395, 2009
5) Miyashita N et al: Radiographic features of mycoplasma pneumoniae pneumonia: differential diagnosis and performance timing. BMC Med Imaging 9: 7, 2009
6) Nei T et al: Mycoplasma pneumoniae pneumonia: differential diagnosis by computerized tomography. Intern Med 46: 1083-1087, 2007
7) Okada F et al: Chlamydia pneumoniae pneumonia mycoplasma pneumoniae pneumonia: comparison of clinical finfings and CT findings. J Comput Assist Tomogr 29: 626-632, 2005
8) Fujita J et al: Chest CT findings of influenza virus- associated pneuonia in 12 adult patients. Influenza Other Respi Viruses 1: 183-187, 2007
9) Agarwal PP et al: Chest radiographic and CT findings in novel swine-origin influenza A (H1N1) virus (S-OIV) infection. AJR Am J Roentgenol 193: 1488-1493, 2009
10) Marchiori E et al: High resolution computed tomography findings from adult patients with influenza A (H1N1) virus-associated pneumonia. Eur J Radiol 74: 93-98, 2010
11) Ono A et al: A comparative study of thin-section CT findings between seasonal influenza virus pneumonia and Streptococcus pneumoniae pneumonia. Br J Radiol 87: 20140051, 2014
12) Miller WT Jr et al: CT of viral lower respiratory tract infestions in adults: comparison among viral organisms and between viral and bacterial infections. AJR Am J Roentgenol 197: 1088-1095, 2011

BQ 18 Is CT recommended for diagnosing pneumoconiosis?

Statement

CT is useful and recommended for determining the distribution and extent of pneumoconiosis lesions and diagnosing complications.

Background

Under the Pneumoconiosis Law in Japan, chest radiography plays the central role in the diagnosis of pneumoconiosis, and its severity is determined according to the PR classification for chest radiography. Clinically, however, CT findings are used complementarily in diagnosis.

Explanation

In silicosis, CT has been reported to provide excellent detection of coalescence and large opacities.[1)] CT has also been found to improve the rate of inter-reader agreement on findings.[2)] In patients who exhibit small granular opacities classified as type-p opacities on chest radiography, the addition of HRCT improves the rate of detection of granular opacities themselves[3)] and makes it possible to determine whether granular opacities are actually present, or if the findings indicate peribronchiolar fibrosis alone,[4)] enabling more accurate PR classification.

In the case of asbestosis, diagnosis is difficult with chest radiography of general lung lesions alone when severe pleural plaques are present, and the combined use of CT is therefore considered advisable.[5)] A subpleural curvilinear shadow (SCLS) is a characteristic CT finding in asbestosis (Fig.) and is observed frequently in patients with this disease.[6)] Such findings of mild fibrosis are not visualizable without CT and therefore require it.

Figure. Asbestosis

HRCT, transverse image: A linear shadow that follows the pleura is seen immediately below the upper dorsal pleura, and findings suggestive of aggregated partially granular opacities are seen. This is the typical appearance of SCLSs seen in asbestosis.

Search keywords and secondary sources

PubMed was searched using the following keywords: CT, pneumoconiosis, silicosis, asbestosis, and PR classification.

References

1) Remy-Jardin M et al: Coal worker's pneumoconiosis: CT assessment in exposed workers and correlation with radiographic findings. Radiology 177 (2): 363-371, 1990
2) Antao VC et al: High-resolution CT in silicosis: correlation with radiographic findings and functional impairment. J Compt Assist Tomo; 29 (3): 350-356, 2005
3) Begin R et al: Computed tomography scan in the early detection of silicosis. Am Rev Resp Dis 144 (3 Pt 1): 697-705, 1991
4) Akira M et al: Radiographic type p pneumoconiosis: high-resolution CT. Radiology 171 (1): 117-123, 1989
5) Friedman AC et al: Asbestos-related pleural disease and asbestosis: a comparison of CT and chest radiography. AJR Am J Roentgenol 150 (2): 269-275, 1988
6) Yoshimura H et al: Pulmonary asbestosis: CT study of subpleural curvilinear shadow. Radiology 158 (3): 653-658, 1986

FQ 1 Is CT recommended for diagnosing the severity of chronic obstructive pulmonary disease (COPD)?

Statement

Although CT is not required to diagnose the severity of COPD, there is scientific evidence supporting its usefulness in this role.

Background

The severity of COPD is determined comprehensively based on respiratory symptoms, spirometric classification, and/or risk of exacerbation. CT is not required (secondary sources 1 and 2). However, the structural abnormalities on CT, such as the extent of emphysema, peripheral airway narrowing, and a decrease in the pulmonary vascular bed, are correlated with airflow limitation on spirometry, acute COPD exacerbation, and patients' prognosis.

Explanation

Emphysema is defined as a region of low attenuation not bounded by a visible wall on CT. Visual assessment of low-attenuation areas is a simple method for evaluating emphysema extent on CT.[1, 2] Recently, computer-based quantification has been increasingly used. The ratio of low-attenuation area on CT (LAA%) is widely used as a measure of emphysema extent.[3] The mean CT attenuation values of the whole lung,[4] the Hounsfield Unit (HU) points below 15% of the voxels (Perc15),[5] are also useful measures. A previous study reported that a lower Perc15 value was significantly related to a greater decline in FEV1.[6] Moreover, quantitative evaluations of emphysematous lung based on artificial intelligence were found to be correlated with patient prognosis.[7]

A histological analysis of surgical specimens showed that COPD severity is associated with bronchial wall thickening and lumen narrowing.[8] Various methods of computer measurement on CT have been proposed for evaluating the airways [airway wall area,[9] percent airway wall area corrected for total airway area (WA%),[10] peak attenuation of the bronchial wall,[11] and intrathoracic airway volume measurement[12]].

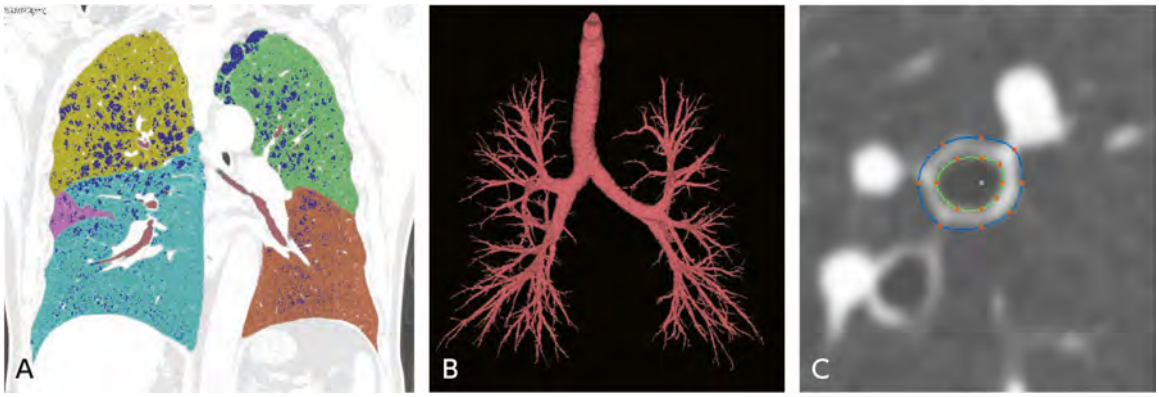

Figure. Examples of CT quantitative evaluation of COPD

The patient was a man in his 70s.

A: Quantitative measurement of emphysema (areas with ≤ -950 HU shown in blue), B: Extraction of bronchial tree, C: Measurement of bronchial wall area (WA%)

Expiratory CT is useful for evaluating emphysematous lung and airway lesions (see BQ 19).

A method using the percent cross-sectional area of small pulmonary vessels (% CSA < 5) has been proposed to evaluate vascular lesions. A % CSA < 5 has been found to be highly correlated with LAA% (r = -0.83)[13] and to be strongly correlated with mean pulmonary arterial pressure measured by right heart catheterization in patients with COPD.[14] The diameter of the main pulmonary artery on CT is a predictive factor for acute exacerbation of COPD.[15]

COPD severity should be evaluated comprehensively based on not only spirometry, but also exercise tolerance, nutritional status, and systemic comorbidities. Morphological evaluation of the erector spinae muscles by CT also correlates with prognosis.[16]

Search keywords and secondary sources

PubMed was searched using the keywords "COPD" and "CT," and 3,230 articles were retrieved, of which 16 were cited.

In addition, the following were referenced as secondary sources.

1) Global strategy for the diagnosis, management, and prevention of chronic obstructive pulmonary disease 2020 REPORT, 2020
2) Japanese Respiratory Society, Ed.: 2018 Guidelines for the Diagnosis and Treatment of Chronic Obstructive Pulmonary Disease (COPD), 5th Edition. Medical Review, 2018.

References

1) Lynch DA et al: CT-based visual classification of emphysema: association with mortality in the COPDGene study. Radiology 288 (3): 859-866, 2018
2) Goddard PR et al: Computed tomography in pulmonary emphysema. Clin Radiol 33 (4): 379-387, 1982
3) Gevenois PA et al: Comparison of computed density and macroscopic morphometry in pulmonary emphysema. Am J Respir Crit Care Med 152 (2): 653-657, 1995
4) Camiciottoli G et al: Spirometrically gated high-resolution CT findings in COPD: lung attenuation vs lung function and dyspnea severity. Chest 129 (3): 558-564, 2006

5) Mohamed Hoesein FA et al: CT-quantified emphysema in male heavy smokers: association with lung function decline. Thorax 66 (9): 782-787, 2011
6) Lowe KE et al: COPDGene ((R)) 2019: Redefining the diagnosis of chronic obstructive pulmonary disease: Chronic Obstr Pulm Dis 6 (5): 384-399, 2019
7) Humphries SM et al: Deep learning enables automatic classification of emphysema pattern at CT. Radiology 294 (2): 434-444, 2020
8) Hogg JC et al: The nature of small-airway obstruction in chronic obstructive pulmonary disease. N Engl J Med 350 (26): 2645-2653, 2004
9) Nakano Y et al: Computed tomographic measurements of airway dimensions and emphysema in smokers: correlation with lung function. Am J Respir Crit Care Med 162 (3 Pt 1): 1102-1108, 2000
10) Berger P et al: Airway wall thickness in cigarette smokers: quantitative thin-section CT assessment. Radiology 235 (3): 1055-1064, 2005
11) Yamashiro T et al: Quantitative assessment of bronchial wall attenuation with thin-section CT: an indicator of airflow limitation in chronic obstructive pulmonary disease. AJR Am J Roentgenol 195 (2): 363-9, 2010
12) Tanabe N et al: Associations of airway tree to lung volume ratio on computed tomography with lung function and symptoms in chronic obstructive pulmonary disease. Respir Res 20 (1): 77, 2019
13) Matsuoka S et al: The relationship between small pulmonary vascular alteration and aortic atherosclerosis in chronic obstructive pulmonary disease: quantitative CT analysis. Acad Radiol 18 (1): 40-46, 2011
14) Matsuoka S et al: Pulmonary hypertension and computed tomography measurement of small pulmonary vessels in severe emphysema. Am J Respir Crit Care Med 181 (3): 218-225, 2010
15) Wells JM et al: Pulmonary arterial enlargement and acute exacerbations of COPD. N Engl J Med 367 (10): 913-921, 2012
16) Tanimura K et al: Quantitative assessment of erector spinae muscles in patients with chronic obstructive pulmonary disease: novel chest computed tomography-derived index for prognosis. Ann Am Thorac Soc 13 (3): 334-341, 2016

BQ 19 Is expiratory CT recommended for the diagnosis of obstructive pulmonary disease?

Statement

Although scientific evidence is lacking, the use of expiratory CT can be considered after reduction of radiation exposure.

Background

Expiratory CT is basically used as a technique for functional respiratory imaging for research purposes, such as evaluating air trapping and the collapse of the trachea and bronchi that occur during expiration as a result of obstruction caused by peripheral airway stenosis in bronchial asthma and COPD. Whether expiratory CT is useful for the diagnosis of obstructive pulmonary disease was evaluated.

Explanation

As indicated in references such as the GOLD documents and the Japanese Respiratory Society's guidelines for the diagnosis and treatment of COPD (secondary sources 1 and 2), CT is not considered essential for diagnosing obstructive pulmonary disease. Fundamental to the diagnosis of obstructive pulmonary disease is respiratory function testing. That is, CT is unnecessary for the actual diagnosis of various obstructive pulmonary diseases. However, even the above-mentioned guidelines indicate that CT is useful in cases such as when morphological differentiation from other diseases is required or to detect mild emphysematous lesions. There also have been no reports indicating that expiratory CT is necessary for the actual diagnosis of various obstructive pulmonary diseases. However, as a technique for functional respiratory imaging of conditions such as air trapping (Fig.) and the collapse of the trachea and bronchi in obstructive pulmonary disease, expiratory CT may be used in the clinical setting to plan treatment and evaluate treatment efficacy. Therefore, the use of expiratory CT imaging may be desirable depending on the purpose.

Typical uses of expiratory CT in obstructive pulmonary disease include ① evaluating air trapping, ② evaluating airway collapse, ③ quantitatively evaluating emphysematous lesions, and ④ diagnosing obstructive pulmonary disease that appears normal on inspiratory CT, but abnormal on expiratory CT.

1. Evaluating air trapping and respiratory function with expiratory CT

The methods used to evaluate air trapping with expiratory CT include using the lung density threshold and mean lung density. The severity of air trapping seen with either method in various obstructive pulmonary diseases has been found to be correlated with the severity of airflow limitation indicated by respiratory function tests.[1-3] However, air trapping is also seen in healthy individuals and must therefore be interpreted carefully.[4]

2. Evaluating collapse of the trachea and bronchi and pulmonary function with expiratory CT

Collapse of the bronchi is evaluated based on the changes in the luminal areas of the segmental, subsegmental, and sub-subsegmental bronchi as compared with inspiratory CT. The ratio of the luminal area during inspiration versus the luminal area during expiration was found to be correlated with the severity of the airflow limitation in patients with COPD, with this trend being the strongest for peripheral sub-subsegmental bronchi.[5)]

3. Evaluating emphysematous lesions with expiratory CT

A tendency for expiratory CT to underestimate emphysema severity has been identified,[6)] and inspiratory CT has been found to be superior to expiratory CT for quantitatively evaluating emphysematous lesions.[7)]

4. Obstructive diseases with normal inspiratory CT and abnormal expiratory CT findings

Typical obstructive diseases with normal inspiratory CT and abnormal expiratory CT findings include bronchiolitis obliterans and bronchial asthma. There is evidence suggesting that expiratory CT may enable milder abnormalities to be detected at an early stage in these diseases.[6)] In particular, expiratory CT has been found to be useful for diagnosing bronchiolitis obliterans syndrome, which occurs in lung transplants, with sensitivity of 83% and specificity of 89%.[8)]

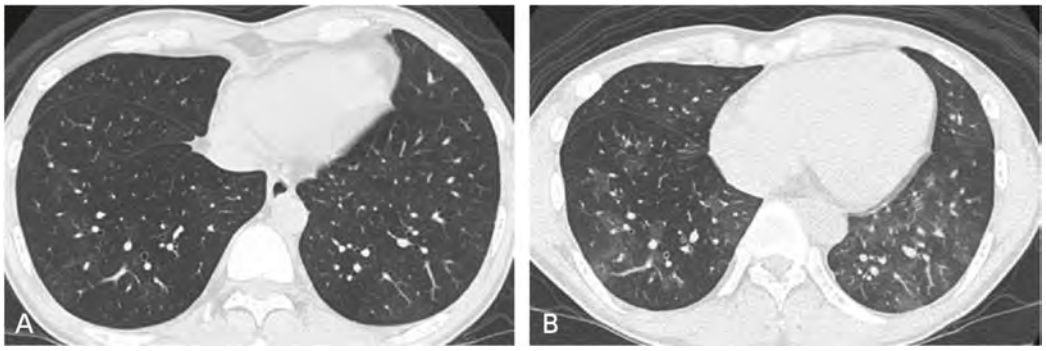

Figure. Bronchiolitis obliterans syndrome

A: Inspiratory CT, B: Expiratory CT

A region of air trapping that shows no increase in density with expiratory CT is accentuated.

The imaging protocol used for expiratory CT must reduce radiation exposure. Although the inter-reader agreement rate and confidence in image evaluations decrease in proportion to decreases in the tube current, reducing the current to 20 mAs has been found to not be problematic.[9)]

Search keywords and secondary sources

PubMed was searched for the period from January 1985 through March 2020 using the following keywords: CT, expiratory, and expiration.

In addition, the following were referenced as secondary sources.

1) Global Initiative for Chronic Obstructive Lung Disease (GOLD): Global strategy for diagnosis, management, and prevention of COPD (2019 Report)
2) Japanese Respiratory Society, Ed.: 2018 Guidelines for the Diagnosis and Treatment of Chronic Obstructive Pulmonary Disease (COPD), 5th Edition. Medical Review, 2018.

References

1) Lamers RJ et al: Chronic obstructive pulmonary disease: evaluation with spirometrically controlled CT lung densitometry. Radiology 193: 109-113, 1994
2) Arakawa H et al: Air trapping on expiratory high-resolution CT scans in the absence of inspiratory scan abnormalities: correlation with pulmonary function tests and differential diagnosis. AJR Am J Roentgenol 170: 1349-1353, 1998
3) Matsuoka S et al: Quantitative assessment of air trapping in chronic obstructive pulmonary disease using inspiratory and expiratory volumetric MDCT. AJR Am J Roentgenol 190: 762-769, 2008
4) Tanaka N et al: Air trapping at CT: high prevalence in asymptomatic subjects with normal pulmonary function. Radiology 227: 776-785, 2003
5) Matsuoka S et al: Airway dimensions at inspiratory and expiratory multisection CT in chronic obstructive pulmonary disease: correlation with airflow limitation. Radiology 248: 1042-1049, 2008
6) Nishimura K et al: Comparison of different computed tomography scanning methods for quantifying emphysema. J Thorac Imaging 13: 193-198, 1998
7) Gevenois PA et al: Pulmonary emphysema: quantitative CT during expiration. Radiology 199: 825-829, 1996
8) Bankier AA et al: Bronchiolitis obliterans syndrome in heart-lung transplant recipients: diagnosis with expiratory CT. Radiology 218: 533-539, 2001
9) Bankier AA et al: Air trapping: comparison of standard-dose and simulated low-dose thin-section CT techniques. Radiology 242: 898-906, 2007

BQ 20 Is HRCT recommended for diagnosing idiopathic pulmonary fibrosis (IPF)?

Statement

HRCT is an essential test for diagnosing IPF and is therefore recommended.

Background

IPF is an idiopathic interstitial pneumonia that typically presents the usual interstitial pneumonia (UIP) pattern on CT. CT is now essential for diagnosing IPF, and a multidisciplinary discussion (MDD) that combines CT findings with clinical and pathological findings is fundamental to diagnosis.

Explanation

IPF is an idiopathic interstitial pneumonia that presents the UIP imaging pattern. Because its CT findings are distinctive, the usefulness of CT in the diagnosis of IPF has long been recognized. Moreover, CT has been found to be superior even to chest radiography in diagnostic performance and correlation with clinical severity.[1, 2)]

A characteristic CT finding in IPF is bibasilar-predominant honeycombing (Fig.), and the IPF diagnostic accuracy rate is extremely high when typical findings are seen. The 2019 IPF diagnostic guidelines, the most recent guidelines, divided CT findings into 4 classifications, UIP pattern, probable UIP, indeterminate for UIP, and alternative diagnosis, and they recommended that IPF be diagnosed based on an MDD that combines clinical and pathological findings. Patients who show the UIP pattern on CT and have no clinical findings inconsistent with IPF can be diagnosed with IPF without making a pathological diagnosis.[1)] CT is also important for diagnosing interstitial pneumonias in general. A retrospective study found that CT findings changed ≥ 50% of the initial diagnoses made by internists.[3)] A separate investigation found that the diagnostic concordance rate for multiple clinicians was a κ value of 0.41 for diagnosis by HRCT alone. The rate increased to 0.51 when the CT findings were augmented with clinical information and to 0.67 when a radiologist was included. It increased further, to 0.75, with the addition of pathological diagnosis and to 0.85 with the consensus diagnosis of a clinician, radiologist, and pathologist.[4)] However, many patients do not show the typical UIP pattern on CT. An examination of HRCT findings in patients clinically diagnosed with IPF found that 34% had the typical definite UIP pattern with honeycomb lung; 36% did not have honeycomb lung, but had findings consistent with UIP, which is suggestive of IPF; and 30% had findings suggestive of an alternative diagnosis to UIP.[5)] The rate of inter-reader agreement on honeycomb lung, which is important for diagnosing the UIP pattern, is not very high, with κ values ranging from 0.40 to 0.58.[6)] This is related to the low rate of agreement on the classification of CT findings. The rates of inter-reader agreement on UIP classification in reports that used the previous (2013) classification were moderate, with κ values ranging from 0.48 to 0.52.[8)]

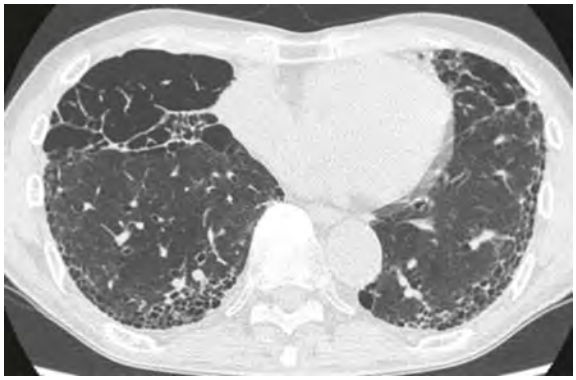

Figure. IPF

HRCT, transverse image: Reticular opacities and honeycomb lung are seen predominantly in the bilateral basilar subpleural regions.

CT is used for prognostic assessment, as well as diagnosis. The observed extent of traction bronchiectasis has been reported to be linked to prognosis in IPF.[5)] CT also plays an important role in IPF follow-up. Reticular and ground-glass opacities and honeycomb lung increase during the clinical course of IPF.[9)] Acute exacerbation and lung cancer occur occasionally and are important prognostic factors in IPF.[10)] Depending on the CT pattern, acute exacerbation is divided into peripheral, diffuse, and multifocal patterns. The multifocal pattern has been reported to have a significantly better prognosis than the other patterns.[11)]

In addition to being essential for IPF diagnosis, CT is important for evaluating its status and stage of its clinical course.

Search keywords and secondary sources

PubMed was searched using the following keywords: CT, usual interstitial pneumonias, imaging, and idiopathic pulmonary fibrosis.

In addition, the following were referenced as secondary sources.

1) Raghu G et al: Diagnosis of Idiopathic pulmonary fibrosis: an official ATS/ERS/JRS/ALAT clinical practice guideline. Am J Respir Crit Care Med 198 (5): e44-e68, 2018
2) Travis WD et al: An official American Thoracic Society/European Respiratory Society statement: update of the international multidisciplinary classification of the idiopathic interstitial pneumonias. Am J Respir Crit Care Med 188 (6): 733-748, 2013

References

1) Mathieson JR et al: Chronic diffuse infiltrative lung disease: comparison of diagnostic accuracy of CT and chest radiography. Radiology 171 (1): 111-116, 1989
2) Staples CA et al: Usual interstitial pneumonia: correlation of CT with clinical, functional, and radiologic findings. Radiology 162 (2): 377-381, 1987
4) Aziz ZA et al: Interstitial lung disease: effects of thin-section CT on clinical decision making. Radiology 238 (2): 725-733, 2006
5) Flaherty KR et al: Idiopathic interstitial pneumonia: what is the effect of a multidisciplinary approach to diagnosis? Am J Respir Crit Care Med 170 (8): 904-910, 2004
6) Sumikawa H et al: Computed tomography findings in pathological usual interstitial pneumonia: relationship to survival. Am J Respir Crit Care Med 177 (4): 433-439, 2008
7) Watadani T et al: Interobserver variability in the CT assessment of honeycombing in the lungs. Radiology 266 (3): 936-944, 2013

8) Walsh SL et al: Interobserver agreement for the ATS/ERS/JRS/ALAT criteria for a UIP pattern on CT. Thorax 71 (1): 45-51, 2016
9) Hartman TE et al: Disease progression in usual interstitial pneumonia compared with desquamative interstitial pneumonia. Assessment with serial CT. Chest 110 (2): 378-382, 1996
10) Natsuizaka M et al: Epidemiologic survey of Japanese patients with idiopathic pulmonary fibrosis and investigation of ethnic differences. Am J Respir Crit Care Med 190 (7): 773-779, 2014
11) Akira M et al: CT findings during phase of accelerated deterioration in patients with idiopathic pulmonary fibrosis. AJR Am J Roentgenol 168 (1): 79-83, 1997

BQ 21 Is HRCT recommended for differentiating among collagen vascular diseases?

Statement

There is a good deal of overlap between the HRCT findings for lung lesions in various collagen vascular diseases, which makes it difficult to find clear differences in the findings. However, differentiation is possible to some extent if characteristic findings are observed.

Background

The treatment strategy and prognosis for collagen vascular disease lesions of the lungs vary with the type of collagen vascular disease. Moreover, collagen vascular disease preceded by lung lesions is somewhat frequent. Identifying the collagen vascular disease may therefore be difficult initially. The question of whether the type of collagen vascular disease present can be inferred based on the HRCT findings for lung lesions was examined, and the findings are outlined below.

Explanation

Few articles have examined the differences in HRCT findings depending on the type of collagen vascular disease [rheumatoid arthritis (RA), systemic sclerosis (SSc), polymyositis/dermatomyositis (PM/DM), mixed connective tissue disease (MCTD), primary Sjögren's syndrome (pSjS), and systemic lupus erythematosus (SLE)]. One article compared the findings for RA, SSc, PM/DM, pSjS, and MCTD.[1)] Another compared the findings for all of the diseases: RA, SSc, PM/DM, pSjS, MCTD, and SLE.[2)] The report by Daimon et al. focused on collagen vascular disease lesions in the lungs in 49 patients who were found to have nonspecific interstitial pneumonia (NSIP) pattern based on surgical biopsy. The type of collagen vascular disease was inferred in 22 of the 49 patients (45%). Diagnostic accuracy for the various collagen vascular diseases varied widely depending on the type of disease: RA, 47%; SSc, 38%; PM/DM, 61%; pSjS, 25%; and MCTD, 0%.[1)] The authors concluded that diagnosis was possible to some extent if typical findings were observed, such as intralobular reticular opacities in SSc and subpleural linear opacities in PM/DM. Tanaka et al. compared collagen vascular disease lesions of the lungs in 187 patients (RA, 55 patients; SSc, 50 patients; PM/DM, 46 patients; MCTD, 15 patients; pSjS, 11 patients; and SLE, 10 patients) using multivariate analysis and the chi-squared test. They found that, compared with other collagen vascular diseases, findings of honeycombing and traction bronchiectasis were more frequent for RA lung lesions; lymph node enlargement, esophageal dilatation, and extensive ground-glass attenuation (GGA) were more frequent for SSc lung lesions; and consolidation and the absence of honeycombing were more frequent for PM/DM lung lesions.[2)] For the other 3 collagen vascular diseases, the only differences detected were chi-squared test results showing that GGA along the bronchovascular bundle and consolidation were more frequent findings for pSjS and SLE lung lesions than for the other collagen

vascular diseases.[2)] RA, SSc, and PM/DM have characteristic findings that differ from those of the other collagen vascular diseases and these characteristic findings may contribute to differentiation.

As mentioned above, few articles have compared the characteristics of the various collagen vascular diseases systematically. Differentiation is therefore currently attempted by means of an analysis that takes into account reports of the CT findings for these diseases.[3-15)]

Airway lesions are seen frequently in RA, and bronchial dilatation, bronchiolitis obliterans, and follicular bronchiolitis (FB) are observed with moderate frequency.[3)] Reflecting these conditions, mosaic perfusion and centrilobular opacities (air trapping) are observed on CT.[3, 4)] In interstitial pneumonia, the usual interstitial pneumonia (UIP) and NSIP patterns are seen with roughly equal frequency,[6)] and the organizing pneumonia (OP) pattern is seen occasionally.[3, 6, 7)] The most recent articles have reported that the greatest number of patients with RA show the UIP pattern.[7-9)] Reflecting these findings, ground-glass and reticular opacities and consolidation are seen on HRCT, and honeycombing is more prominent than in other collagen vascular diseases.[3, 6)]

In SSc, the NSIP pattern is the most common pathologically. Reflecting this, overlapping of fine reticular opacities in dorsal and subpleural GGAs is characteristic and associated with traction bronchiectasis. The findings more closely resemble those seen in idiopathic NSIP than they do those seen in IPF or UIP.[3, 10)]

Figure. Dermatomyositis (DM)-related lung disease

(NSIP pattern + OP pattern)

HRCT, transverse image: GGAs are seen immediately below the pleura and along the bronchi in the bilateral lower lung fields, and the internal bronchi are dilated (traction bronchiectasis). Mixed consolidation is also present, and bandlike opacities are seen parallel to the pleura.

In PM/DM, findings of overlapping GGAs and consolidation are seen predominantly in the lower lung field, in addition to subpleural linear or bandlike opacities, reflecting the NSIP and OP patterns, which are frequent pathological findings in these conditions.[11, 12)] Characteristics of PM/DM are more frequent consolidation and less frequent honeycombing compared with other collagen vascular diseases (Fig.).[3, 11, 12)] In patients with DM who do not exhibit muscle symptoms (amyopathic DM, or ADM), rapidly progressing

interstitial pneumonia may be seen.[13] If the findings described above are seen in such patients, caution should be exercised clinically regarding the presence of ADM.

In MCTD, the UIP or NSIP pattern has been seen pathologically,[3, 14] and findings such as GGAs, consolidation, honeycombing, and centrilobular nodular opacities have been reported.[14]

In pSjS, as in RA, airway lesions such as FB are frequent, and centrilobular opacities and the tree-in-bud pattern are seen.[15] The interstitial pneumonias, including lymphocytic interstitial pneumonia (LIP), NSIP, and UIP have been reported, with centrilobular opacities and cyst formation being characteristics of LIP.[3, 15]

In SLE, acute lupus pneumonitis and diffuse alveolar hemorrhage are important complications,[3] with diffuse or patchy GGAs or consolidation seen in both conditions.

Collagen vascular disease lung lesions are diverse, and the NSIP pattern is the most frequent pattern for such lesions. Consequently, GGAs are a frequent finding on HRCT, and identifying differences between collagen vascular diseases is difficult. However, RA and pSjS are suggested by airway lesions, RA by prominent honeycombing, SSc by GGAs with internal reticular opacities, and PM/DM by peripheral consolidation or consolidation along the bronchi. Thus, the type of collagen vascular disease can be inferred.

Search keywords and secondary sources

In addition to the previous literature, articles were identified by searching PubMed using the following keywords: CT (tomography, X-ray computed), lung, collagen vascular disease, and connective tissue disease. In addition, the following keywords related to the various collagen vascular diseases were used: rheumatoid arthritis, scleroderma, polymyositis, dermatomyositis, mixed connective tissue disease, primary Sjogren syndrome, and systemic lupus erythematosus. The period searched was from September 1, 2015 to June 30, 2019.

References

1) Daimon T et al: Nonspecific interstitial pneumonia associated with collagen vascular disease: analysis of CT features to distinguish the various types. Intern Med 48: 753-761, 2009
2) Tanaka N et al: HRCT findings of collagen vascular disease-related interstitial pneumonia (CVD-IP): a comparative study among individual underlying diseases. Clin Radiol 73: 833.e831-833.e810, 2018
3) Lynch DA: Lung disease related to collagen vascular disease. J Thorac Imaging 24: 299-309, 2009
4) Jokerst C et al: An overview of collagen vascular disease-associated interstitial lung disease. Semin Roentgenol 50: 31-39, 2015
5) Chung MH et al: Airway obstruction in rheumatoid arthritis: CT manifestations, correlated with pulmonary function testing. Yonsei Med J 45: 443-452, 2004
6) Tanaka N et al: Rheumatoid arthritis-related lung diseases: CT findings. Radiology 232: 81-91, 2004
7) Kelly CA et al: Rheumatoid arthritis-related interstitial lung disease: associations, prognostic factors and physiological and radiological characteristics: a large multicentre UK study. Rheumatology 53: 1676-1682, 2014
8) Assayag D et al: Rheumatoid arthritis-associated interstitial lung disease: radiologic identification of usual interstitial pneumonia pattern. Radiology 270: 583-588, 2014
9) Chansakul T et al: Intra-thoracic rheumatoid arthritis: Imaging spectrum of typical findings and treatment related complications. Eur J Radiol 84: 1981-1991, 2015

10) Desai SR et al: CT features of lung disease in patients with systemic sclerosis: comparison with idiopathic pulmonary fibrosis and nonspecific interstitial pneumonia. Radiology 232: 560-567, 2004
11) Ikezoe J et al: High-resolution CT findings of lung disease in patients with polymyositis and dermatomyositis. J Thorac Imaging 11: 250-259, 1996
12) Mino M et al: Pulmonary involvement in polymyositis and dermatomyositis: sequential evaluation with CT. AJR Am J Roentgenol 169: 83-87, 1997
13) Tanizawa K et al: HRCT features of interstitial lung disease in dermatomyositis with anti-CADM-140 antibody. Respir Med 105: 1380-1387, 2011
14) Kozuka T et al: Pulmonary involvement in mixed connective tissue disease: high-resolution CT findings in 41 patients. J Thorac Imaging 16: 94-98, 2001
15) Taouli B et al: Thin-section chest CT findings of primary Sjogren's syndrome: correlation with pulmonary function. Eur Radiol 12: 1504-1511, 2002

BQ 22 Is HRCT recommended for diagnosing drug-induced lung injury?

Statement

CT is the standard method for diagnosing drug-induced lung injury, although there is little definitive scientific evidence to support such use.

Background

There is no reliable non-invasive method for clinically diagnosing drug-induced lung injury. The diagnosis is determined by a comprehensive assessment that includes clinical evaluation, imaging, and pathology. The roles of CT include confirming that there are findings consistent with a drug-induced lung injury, differentiating from other diseases, and evaluating the status of the condition when drug administration is discontinued and resumed.

Explanation

Although there is little definitive evidence that CT is useful for diagnosing drug-induced lung injury, it has become indispensable for diagnosing such disorders in the actual clinical setting. There is no reliable non-invasive method for clinically diagnosing drug-induced lung injury. The diagnosis needs to be determined by a comprehensive assessment that includes clinical information, such as the patient's medical history and clinical course, and testing and pathology findings. The diagnostic criteria for a drug-induced lung injury include ① ingestion of a drug that could cause the disorder, ② reports that the clinical disease type is attributable to a drug, ③ the exclusion of other causative diseases, ④ improvement of the condition with discontinuation of the drug, and ⑤ worsening when administration is resumed.[1)] The roles of CT in examining these criteria include: determining whether the imaging findings are consistent with those for previously reported drug-induced lung injury (criterion ②); differentiating from other types of lesions, such as those resulting from infection, pulmonary edema, and worsening of underlying disease (criterion ③); evaluating any improvement in opacities resulting from discontinuation of the drug (criterion ④); and evaluating any worsening of opacities resulting from the resumption of drug administration (criterion ⑤). CT is also used to evaluate the presence or absence of lung lesions before a drug is administered. A survey study concerning the drug gefitinib found that the presence of chronic interstitial pneumonia and ≤ 50% normal lung on CT were risk factors for a drug-induced lung injury.[4)]

The imaging findings for drug-induced lung injury are extremely varied. Typical findings include extensive bilateral ground-glass opacities or infiltrative shadows, which may be associated with interlobular wall thickening and intralobular reticular opacities. The findings are classified according to imaging pattern, using expressions that indicate the imaging pattern of the idiopathic lung disease, such as hypersensitivity pneumonitis (HP)-like, eosinophilic pneumonia (EP)-like, organizing pneumonia (OP)-like, nonspecific interstitial pneumonia (NSIP)-like, and diffuse alveolar damage (DAD)-like patterns. It should be noted

that, unlike the original diseases, the radiology-pathology correlations for these imaging pattern classifications have not been adequately examined. An examination of CT and pathology in 20 patients with drug-induced lung injury found that the 2 diagnoses agreed for only 9 patients (45%).[3] However, correlations are seen between imaging patterns and prognosis. The DAD-type imaging pattern indicates a serious lung disorder and suggests a poor prognosis.[4] With drugs such as m-TOR inhibitors, patients may have no subjective symptoms and only abnormal CT findings.[2] Other types of drug-induced lung injury that have been reported include the appearance of peritumoral infiltrative shadows and ground-glass opacities (peritumoral infiltration) caused by immune checkpoint inhibitors,[5] and the radiation recall phenomenon, in which acute inflammation occurs in the previously treated radiation field when chemotherapy is administered after radiotherapy.[6]

Figure. Pembrolizumab-induced lung injury

HRCT, transverse image: Consolidation and ground-glass opacities are seen predominantly in the bilateral periphery. They show an OP-like imaging pattern.

To summarize, the roles of CT in drug-induced lung injury include ① assessing disease present before drug administration, such as chronic interstitial pneumonia, ② confirming the onset of a lung disorder, ③ differentiating from other conditions, ④ predicting prognosis, and ⑤ evaluating treatment efficacy. CT is therefore considered clinically useful in drug-induced lung injury.

Search keywords and secondary sources

PubMed was searched using the keyword “pneumonitis drug,” and 46,491 articles were retrieved, of which 6 were cited.

In addition, the following was referenced as a secondary source.

1) Japanese Respiratory Society, Ed.: 2018 Guide for the Diagnosis and Treatment of Drug-induced Lung Injury, 2nd Edition. Medical Review, 2018.

References

1) Camus P et al: Interstitial lung disease induced by drugs and radiation. Respiration 71: 301-326, 2004
2) White DA et al: Noninfectious pneumonitis after everolimus therapy for advanced renal cell carcinoma. Am J Respir Crit Care Med 182: 396-403, 2010
3) Cleverley JR et al: Drug-induced lung disease: high-resolution CT and histological findings. Clin Radiol 57: 292-299, 2002
4) Inoue A et al: Severe acute interstitial pneumonia and gefitinib. Lancet 361: 137-139, 2003
5) Baba T et al: Radiologic features of pneumonitis associated with nivolumab in non-small-cell lung cancer and malignant melanoma. Future Oncol 15: 1911-1920, 2019
6) Ding X et al: Radiation recall pneumonitis induced by chemotherapy after thoracic radiotherapy for lung cancer. Rad Oncol 6: 24, 2011

FQ 2 Is CT recommended for diagnosing acute respiratory distress syndrome (ARDS)?

Statement

Although CT is not essential for diagnosing ARDS, it is useful for this purpose, and there is scientific evidence supporting its use.

Background

The presence of bilateral lung opacities on chest radiography is the criterion for the diagnosis of ARDS. Although CT is not essential for diagnosis, its diagnostic performance is higher than that of chest radiography, and it is useful for pathological evaluation.

Explanation

ARDS was first identified in a report by Ashbaugh et al. in 1967. Since then, the presence of bilateral diffuse infiltrative shadows on chest radiography has been regarded as being a characteristic of ARDS.[1)] The diagnostic criteria referred to as the Berlin Definition, developed in 2012, are currently widely used. They are: PaO_2/FiO_2 (arterial blood oxygen pressure/fraction of inspired oxygen) ≤ 300 mmHg; onset within 1 week; the presence of bilateral opacities on chest radiography not fully explained by pleural effusion, atelectasis, or nodules; and the exclusion of pulmonary edema due to heart failure or fluid infusion (secondary source 1). The use of CT in the diagnostic criteria was considered, but deferred, and CT was ultimately designated for use as an adjunct diagnostic test. The reasons given for this were the risk of moving critically ill patients to perform imaging and the fact that CT imaging is not available globally, as it is in Japan. Consequently, although CT is not essential for diagnosing ARDS, it is recommended that it be considered when possible causes such as pleural effusion, atelectasis, and nodules cannot be excluded by chest radiography; when an opacity cannot be definitively attributed to ARDS; or when differentiation from other diseases is necessary. The diagnostic performance of chest radiography in ARDS is inferior to that of CT. In a study that examined chest radiography in patients with ARDS diagnosed using CT, sensitivity was 0.73, specificity was 0.70, and the positive and negative predictive values were 0.88 and 0.47, respectively.[2)]

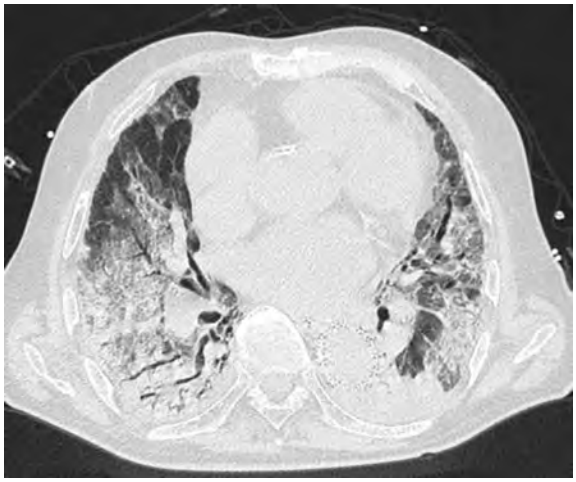

Figure. ARDS

HRCT, transverse image: Extensive ground-glass opacities, consolidation, and bronchodilatation are seen in both lungs. A homogeneous distribution associated with normal regions is seen predominantly dorsally.

CT can be used not only for ARDS diagnosis, but also for purposes such as predicting the causal and pathological condition s and prognosis and detecting complications. The causes of ARDS can be broadly divided into direct lung injury (e.g., pneumonia, aspiration, lung injury) and indirect lung injury (e.g., sepsis, nonthoracic trauma), and CT is useful for differentiating between them. With direct lung injury, ground-glass opacities and consolidation seen on CT tend to be distributed asymmetrically between the left and right lungs. With indirect lung injury, ground-glass opacities tend to be distributed symmetrically between the lungs.[3)] CT findings predictive of pathological conditions have been found to accurately reflect the advanced stages of DAD, pathological findings in ARDS. Ground-glass opacities and infiltrative shadows without traction bronchiectasis have been found to indicate the exudative or early proliferative phase. Ground-glass opacities and infiltrative shadows with traction bronchiectasis have been found to indicate the proliferative and fibrotic phases.[4)] With regard to predicting prognosis, a study of patients with ARDS that scored fibroproliferative CT findings found that they were independent predictors of prognosis and responsiveness to treatment and were related to the need for long-term mechanical ventilation.[5)] A separate study found that abnormal shadows in ≥ 80% of the lung field, a right atrium to left atrium ratio of ≥ 1, and the appearance of varicoid traction bronchiectasis on CT were adverse prognostic factors in ARDS.[6)] Complications such as pneumomediastinum, pneumothorax, and subcutaneous emphysema occur frequently with the use of positive-pressure ventilation in ARDS. Complications such as atelectasis, pneumonia, and abscess also occur and may be detected by CT.[7)]

As indicated above, CT is not essential, but it is useful for diagnosing ARDS. It is also clinically important for purposes other than diagnosis.

Search keywords and secondary sources

PubMed was searched using the following keywords: acute respiratory distress syndrome and CT. A total of 831 articles were retrieved, of which 7 were cited.

In addition, the following were referenced as secondary sources.

1) Ranieri VM et al: Acute respiratory distress syndrome: the Berlin definition. Jama 307 (23): 2526-2533, 2012
2) Japanese Respiratory Society et al., Ed.: 2016 Guidelines for the Diagnosis and Treatment of ARDS. Sogo Igaku Sha, 2016.

References

1) Ashbaugh DG et al: Acute respiratory distress in adults. Lancet 2 (7511): 319-323, 1967
2) Figueroa-Casas JB et al: Accuracy of the chest radiograph to identify bilateral pulmonary infiltrates consistent with the diagnosis of acute respiratory distress syndrome using computed tomography as reference standard. J Crit Care 28 (4): 352-357, 2013
3) Goodman LR et al: Adult respiratory distress syndrome due to pulmonary and extrapulmonary causes: CT, clinical, and functional correlations. Radiology 213 (2): 545-552, 1999
4) Ichikado K: High-resolution computed tomography findings of acute respiratory distress syndrome, acute interstitial pneumonia, and acute exacerbation of idiopathic pulmonary fibrosis. Seminars in ultrasound, CT, and MRI 35 (1): 39-46, 2014
5) Ichikado K et al: Fibroproliferative changes on high-resolution CT in the acute respiratory distress syndrome predict mortality and ventilator dependency: a prospective observational cohort study. BMJ open 2 (2): e000545, 2012
6) Chung JH et al: CT predictors of mortality in pathology confirmed ARDS. Eur Radiol 21 (4): 730-737, 2011
7) Gattinoni L et al: The role of CT-scan studies for the diagnosis and therapy of acute respiratory distress syndrome. Clin Chest Med 27 (4): 559-570, 2006

BQ 23 Is chest radiography recommended for lung cancer screening?

Statement

Although scientific evidence is lacking, chest radiography is now widely used in Japan for lung cancer screening, and its use in conjunction with adequate quality control can be considered.

Background

The lung cancer mortality rate in Japan is increasing, and lung cancer has been the leading cause of death among males since the late 1990s. The statistics for 2018 show that there were 74,328 deaths from lung cancer among males and females combined, and the number is said to be further increasing. Chest radiography is used for tuberculosis screening in Japan, as well as for lung cancer screening (Fig.). However, this practice is viewed unfavorably in some other countries. The following provides background, such as the results and interpretations of randomized, controlled studies conducted in other countries and case-control studies in Japan, and it summarizes the basis for the statement given in answer to this BQ.

Explanation

During the 1970s, two large, randomized, controlled studies were conducted in Europe and the United States to examine the effectiveness of the combined use of chest radiography and sputum cytology in reducing lung cancer mortality among smokers. However, no significant reduction in mortality was seen in either study.[1, 2)] A subsequent examination of long-term prognosis found that, although some patients in the group that underwent screening had a good prognosis, the group showed no reduction in mortality.[3)]

No randomized, controlled studies have been conducted in Japan. However, case-control studies in Japan reported reductions of 20% to 60% in lung cancer mortality when the chest radiography screening used for tuberculosis was applied to lung cancer screening.[4-7)] Chest radiography is widely used in Japan for lung cancer screening based on these results.

The Mayo Lung Project, which was conducted before these other studies, was the subject of controversy regarding the control group and study methods used. One point of controversy was the fact that the group designated as the screening intervention group underwent chest radiography and sputum cytology once every 4 months, whereas the non-intervention group underwent these procedures annually. A 2004 meta-analysis, which excluded reports from Japan because they were case-control studies, focused on the analysis of randomized, controlled studies and found no reduction in mortality with screening.[8)]

Against this backdrop, a study examined the effectiveness of screening for 4 types of cancer (prostate, lung, colorectal, and ovarian; PLCO study), including lung cancer, in reducing mortality. The study found no difference in mortality between the intervention group, which underwent chest radiography once a year for a total of 4 examinations, and the non-intervention group, which did not undergo screening, after follow-up for 13 years.[9)] Questions have been raised about the results of this study. For example,

re-analysis of the screening methods and conclusions showed the screening to be effective. Other questions have concerned aspects such as the initial observation period specified and a change in the follow-up period. Moreover, it has been noted that randomized, controlled studies of screening are not always conducted with strong quality control. The problems noted include low compliance (the proportion of subjects for whom screening is recommended who actually undergo screening) and high contamination (subjects for whom screening is recommended who undergo it at a different location).[10] Articles from Europe and the United States have noted a variety of problems with the randomized, controlled studies that have been conducted, including the Mayo Lung Project and PLCO studies.[11]

Although scientific evidence is lacking, lung cancer screening by chest radiography is now widely performed in Japan. Based on the above considerations, such screening can be considered if adequate quality control is implemented.

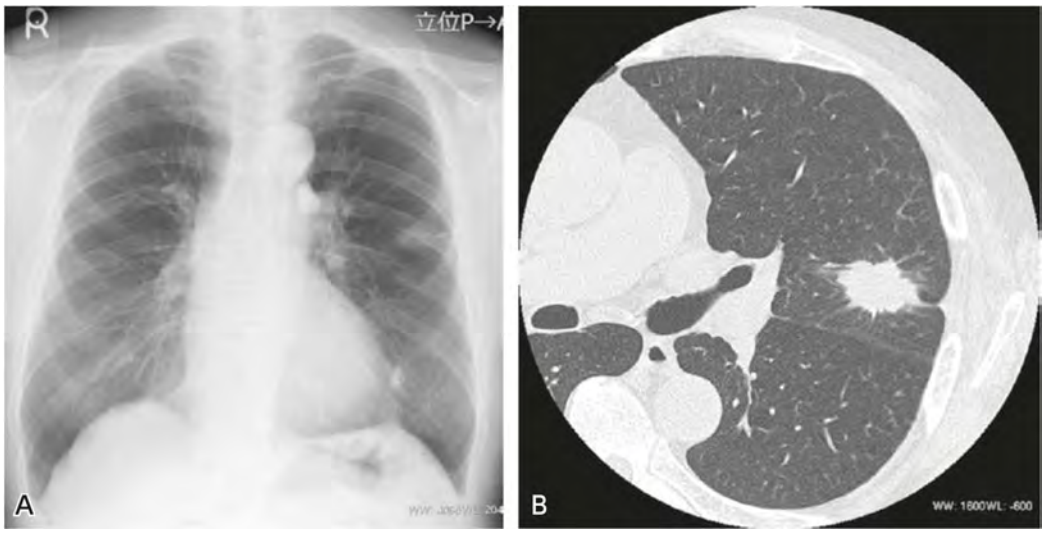

Figure. Primary lung squamous cell carcinoma found on screening (pT2aN0M0, stage IB)

The patient was an asymptomatic man in his 70s.

A: Chest radiography: An irregular marginal nodule, 3 cm in diameter, is seen in the lateral left middle lung. A linear opacity continuous with the pleura is also seen.

B: HRCT, transverse image: An irregular marginal nodule associated with indrawn pleura is seen in the dorsal left upper lobe.

Search keywords and secondary sources

PubMed was searched using the following keywords: lung cancer, screening, and chest radiograph.

In addition, the following was referenced as a secondary source.

1) Tomotaka S: New evidence regarding lung cancer screening and interpretation of that evidence: PLCO. Journal of the Japanese Association For Cancer Detection And Diagnosis 20: 156-159, 2012.

References

1) Fontana RS et al: Lung cancer screening: the Mayo Program. J Occup Med 28: 746-750, 1986
2) Kubik A et al: Lung cancer detection: results of a randomized prospective study in Czechoslovakia. Cancer 57: 2427-2437, 1986
3) Marcus PM et al: Lung cancer mortality in the Mayo Lung Project: impact of extended follow-up. J Nati Cancer lnst 92: 1308-1316, 2000

4) Nishii K et al: A case-control study of lung cancer screening in Okayama prefecture, Japan. Lung Cancer 34: 325-332, 2001
5) Nakayama T et al: An evaluation of chest X-ray screening for lung cancer in Gunma prefecture, Japan: a population-based case-control study. Eur J Cancer 38: 1380-1387, 2002
6) Tsukada H et al: An evaluation of screening for lung cancer in Niigata prefecture, Japan: a population-based case-control study. Br J Cancer85: 1326-1331, 2001
7) Sagawa M et al: A case–control study for evaluating the efficacy of mass screening program for lung cancer in Miyagi prefecture, Japan. Cancer 92: 588-594, 2001
8) Manser RL et al: Screening for lung cancer: The Cochrane Collaboration. 1-18, 2004
9) Oken MM et al: Screening by chest radiograph and lung cancer mortality: the prostate, lung colorectal, and ovarian (PLCO) randomized trial. JAMA 306: 1865-1873, 2011
10) Sagawa M et al: Revised recommendation (2010 edition) on lung cancer screening in “lung cancer clinical practice guidelines” of the Japanese lung cancer society. JJLC 52: 938-942, 2012
11) Strauss GM et al: Chest X-ray screening for lung cancer: overdiagnosis, endpoints, and randomized population trials. J Surg Oncol 108: 294-300, 2013

CQ 2 Is low-dose CT recommended for lung cancer screening?

Recommendation

Low-dose CT is strongly recommended for population-based screening of the high-risk group (men and women aged ≥ 50 years, smoking index ≥ 600)

Recommendation strength: 1, strength of evidence: strong (A), agreement rate: 100% (15/15)

Low-dose CT is weakly recommended for opportunistic screening of the non-high-risk group.

Recommendation strength: 2, strength of evidence: weak (C), agreement rate: 93% (14/15)

Background

Until recently, lung cancer screening using low-dose CT (LDCT) was performed on a limited basis as opportunistic screening rather than population-based screening, because there was insufficient evidence of its effectiveness in reducing mortality. Recently, however, LDCT screening was found to reduce lung cancer mortality in two large, randomized, controlled studies.

Explanation

1. Indirect evidence (detection rate, 5- and 10-year survival rates)

In studies by Sobue et al.,[1] Sone et al.,[2] Nawa et al.,[3] and Yoshimura et al.[4] in Japan and by the International Early Lung cancer Action Program (I-ELCAP),[5] the detection rate for stage I lung cancer with LDCT screening was found to be high, ranging from 75% to 100% on initial screening and from 79% to 100% with repeated screening.

Sobue et al. reported that the 5-year survival rate for detected lung cancer was 76.2% for that detected on initial screening and 64.9% for that detected with repeated screening.[1] Nawa et al. reported rates of 91% and 84% for initial and repeated screening, respectively. Moreover, their analysis showed female sex, nonsmoking, small tumor diameter, and non-solid morphology to be factors contributing to a high survival rate.[6] The I-ELCAP investigators reported that the 10-year survival rate was 80% for all patients with lung cancer detected on screening and 88% for those with stage I lung cancer.[7]

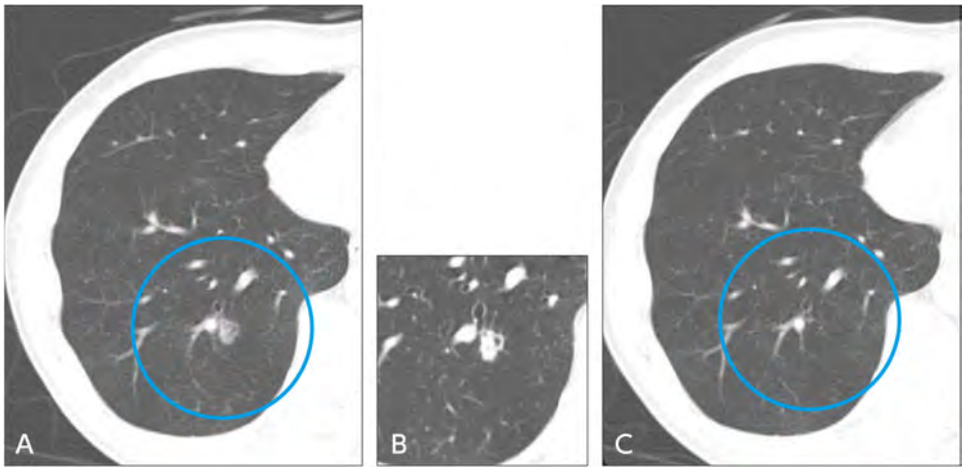

Figure 1. Lung cancer detected by LDCT screening: high-risk group

60-year-old man. Current smoker, 20 cigarettes/day × 40 years (smoking index, 800 = 40 pack-years). Squamous cell carcinoma, pT1N0M0.
A: MDCT at detection (tube current, 25 mAs), B: Thin-section CT on same day (tube current, 150 mAs)
C: MDCT 1 year prior (tube current, 25 mAs)

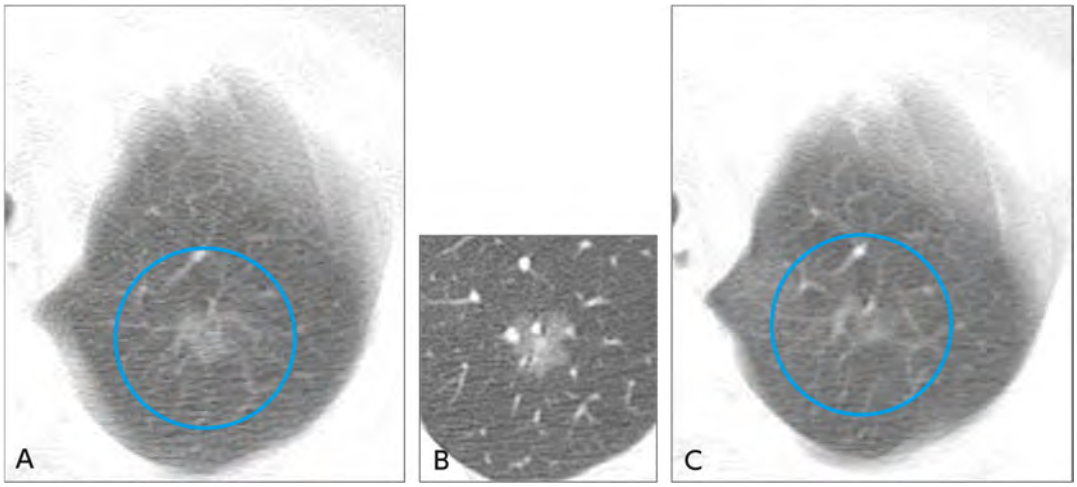

Figure 2. Lung cancer detected by LDCT screening: non-high-risk group

The patient was a woman in her 50s. Nonsmoker. Well-differentiated adenocarcinoma, pT1N0M0.
A: Single-slice CT at detection (tube current, 25 mAs), B: Thin-section CT on same day (tube current, 150 mAs)
C: 36 months prior (tube current, 50 mAs)

2. Direct evidence

① High-risk group

In 2011, the National Lung Screening Trial, a large, randomized, controlled study conducted in the United States, reported that, with LDCT screening in a high-risk group (smoking index ≥ 600 = 30 pack-years) aged 55 to 74 years, there were 2.47 deaths per 1,000 person-years, compared with 3.09 deaths per 1,000 person-years in a group that underwent chest radiography, a relative reduction in mortality of 20% (95% CI, 6.8 to 26.7, p = 0.004).[8)] In the Dutch-Belgian lung cancer screening trial (NELSON), a

large, randomized, controlled study that was conducted in Europe, 15,789 individuals aged 50 to 74 years with a history of smoking (smoking index ≥ 300 = 15 pack-years) were randomly assigned to a group that underwent LDCT screening or to an unscreened group. The results of the study, which were reported in 2020, showed that the relative risk of death from lung cancer was 0.76 in the LDCT screening group, significantly lower than in the unscreened group.[9)]

② Non-high-risk group

There have been no reports of a large study with a randomized, controlled design on LDCT screening that has included non-high-risk group patients. However, a cohort study in Japan using sequential observations suggested that LDCT screening that included the non-high-risk group reduced lung cancer mortality. Nawa et al. analyzed an LDCT screening group (25,385 individuals) between 50 and 59 years old through 2009 in Hitachi, Ibaraki Prefecture (population 199,218 in 2009, according to the national census).[10)] Nonsmokers accounted for 54% of those screened. Although 210 individuals were eventually diagnosed with lung cancer, the standardized mortality ratio (SMR) for the city of Hitachi as a whole was comparable to that of the nation as a whole during the period before the introduction of LDCT screening (1995 to 1999), and, early after its introduction (2000 to 2004), the ratio was 24% lower (SMR = 0.76; 95% CI, 0.67 to 0.86) after introduction (2005 to 2009), indicating that LDCT screening that included the non-high-risk group was effective.

Currently underway is the Japanese Randomized Trial for Evaluating the Efficacy of Low-dose Thoracic CT Screening for Lung cancer (JECS study),which is being conducted by the Working Group on Randomized, Controlled Studies for the Application of Lung cancer Screening Using Low-Dose CT of the Innovative Cancer Medical Application Research Project of the Japan Agency for Medical Research and Development. The study is a randomized, controlled investigation of LDCT screening in nonsmokers and smokers with a smoking index of < 600 (30 pack-years), aged ≥ 50 years and ≤ 70 years, and the results are awaited.[11, 12)]

As the above discussion indicates, large, randomized, controlled studies have found reductions in lung cancer mortality in the high-risk group with the use of LDCT in lung cancer screening. It was therefore concluded that its use can be recommended for population-based screening involving comprehensive assessment. However, the actual implementation of screening requires a nationwide system and facilities that can accommodate it, and a variety of problems remain to be solved. Moreover, there is a lack of scientific evidence that LDCT screening reduces mortality in the non-high-risk group, and it therefore cannot be recommended for population-based screening of this group. However, its use in opportunistic screening is permissible if the fact that its effectiveness is unclear and disadvantages such as overdiagnosis and radiation exposure are first explained appropriately. It was therefore concluded that its use in opportunistic screening involving comprehensive assessment can be weakly recommended.

Remarks

CT under non-low-dose imaging conditions must not be used in the screening of healthy individuals in either the high-risk or non-high-risk group. In addition, to ensure the appropriate implementation of LDCT lung cancer screening, it is important to give careful consideration to the individuals to be screened, radiation exposure management, screening criteria, quality control, informed consent regarding the benefits and disadvantages of screening, and conditions of screening providers. This is the stated view of the Japanese Society of CT Screening. Appropriate imaging and reconstruction conditions are needed to manage radiation exposure. In recent years, however, the clinical use of methods such as iterative approximation for image reconstruction has advanced with increases in computational speed. Consequently, further decreases in dose and improvements in image quality are anticipated for lung cancer CT screening.

Search keywords and secondary sources

PubMed and MEDLINE were searched using the following keywords: lung cancer, screening, low-dose, reduced dose, CT, sensitivity, specificity, mortality, and risk factor.

In addition, the following were referenced as secondary sources.

1) Ministry of Health, Labour and Welfare grant-in-aid, Working Group on Research to Establish Suitable Methods of Cancer Screening and its Evaluation: Guidelines for lung cancer screening based on efficacy evaluation, 2006.
2) Joint committee on lung cancer screening using low-dose CT: Guide for lung cancer screening using low-dose CT—database to support interpretation training/lung cancer CT screening, KANEHARA & Co., 2005.

References

1) Sobue T et al: Screening for lung cancer with low-dose helical computer tomography: anti-lung cancer association project. J Clin Oncol 20 (4): 911-920,2002
2) Sone S et al: Results of three-year mass screening programme for lung cancer using mobile low-dose spiral computed tomography scanner. Br J Cancer 84 (1): 25-32,2001
3) Nawa T et al: Lung cancer screening using low-dose spiral CT: results of baseline and 1-year follow-up studies. Chest 122 (1): 15–20 2002
4) Yoshimura A, et al.: Pilot study of primary screening for lung cancer using low-dose helical CT. Japanese Journal of Lung Cancer 40(2): 99-105, 2000.
5) Henschke CI et al: Early lung cancer action project: initial findings on repeat screening. Cancer 92 (1): 153-159, 2001
6) Nawa T et al: Long-term prognosis of patients with lung cancer detection on low-dose chest computed tomography screening. Lung Cancer 75: 197-202, 2012
7) The International Early Lung Cancer Action Program Investigators: Survival of patients with stage Ⅰ lung cancer detected on CT screening. N Engl J Med 355: 1763–1771, 2006
8) The National Lung Screening Trial Research Team: Reduced lung-cancer mortality with low-dose computed tomographic screening. N Engl J Med 365: 395-409, 2011
9) de Koning HJ et al: Reduced lung-cancer mortality with volume CT screening in a randomized trial. New Eng J Med 382: 503-513, 2020
10) Nawa T et al: A decrease in lung cancer mortality following the introduction of low-dose chest CT screening in Hitachi, Japan. Lung Cancer 78: 225–228, 2012
11) Sagawa M et al: A randomized controlled trial on the efficacy of thoracic CT screening for lung cancer in non-smokers and smokers of ＜30 pack-years aged 50-64 years (JECS Study): ressearch design. Jpn J Clin Oncol 42 (12): 1219-1221, 2012
12) Working Group on Randomized, Controlled Studies for the Application of Lung Cancer Screening Using Low-Dose CT, Innovative Cancer Medical Application Research Project, Japan Agency for Medical Research and Development: Controlled study of lung cancer CT screening—JECS study (http://www.jecs-study.jp/index.html).

BQ 24 Which imaging examinations are recommended for the differential diagnosis of benign and malignant lung nodules?

Statement

Because it enables micromorphology to be evaluated, HRCT is considered a standard test for the differential diagnosis of benign and malignant lung nodules.

With the use of contrast-enhanced CT for the differential diagnosis of benign and malignant lung nodules, the information obtained is increased not only by visually assessing enhancement, but also by measuring the change in density within the nodules.

Background

Lung nodules detected by chest radiography or CT during lung cancer screening and follow-up observations for other diseases are currently addressed by first performing HRCT and comprehensively assessing features such as the size of the nodule, the nature of its margins, its degree of enhancement, its internal structure, and the status of the surrounding lung tissue. Whether to perform invasive tests such as bronchoscopy and percutaneous biopsy is then determined. However, there is no objective standard for interpreting morphology, and interpretations may therefore differ depending on the diagnosing physician. Moreover, even if invasive testing is not performed, change over time is determined by follow-up observation. In recent years, the assessment of malignancy by measuring the volume-doubling time of lung nodules has been applied clinically. For differential diagnosis using contrast-enhanced CT, the degree of enhancement before and after contrast-enhanced imaging and the enhancement pattern in dynamic studies are also analyzed.

Explanation

1. HRCT

Many studies have compared HRCT and pathology findings,[1, 2] and HRCT is elucidating the histological background of attributes of the margins and interior of nodules (Fig.). However, the interpretation of HRCT findings is performed using subjective criteria that depend on the reader; no objective criteria for benign and malignant lesions have been established. Consequently, the fact that the criteria used vary from study to study has been noted to be problematic. As a result, large variability has been seen in sensitivity and specificity depending on the tissue type and attributes of the nodules included in studies and on the status of the surrounding lung tissue.[3-6] The current approach to the non-invasive differential diagnosis of solitary lung nodules is to first determine their size by HRCT, with follow-up 1 year later for nodules < 5 mm in diameter and 3 months later for those ≥ 5 mm and < 10 mm in diameter. If a growth trend is seen, the

approach shifts to invasive testing. For nodules ≥ 10 mm in diameter, FDG-PET is performed concomitantly, and highly invasive testing is recommended based on the results.[7)]

If a lung nodule is detected by chance in an asymptomatic patient, a helical HRCT scan can be performed to measure its volume. In this way, the volume-doubling time of nodules can also be calculated based on the interval between 2 CT scans performed sequentially. The volume-doubling time is also calculated with this type of quantitative method when there appears to be no change visually in short-term follow-up observations, and this method has begun to be used when the volume-doubling time is brief, based on a cutoff of 400 days, and malignancy is considered a possibility.[8)]

2. Contrast-enhanced CT

Contrast enhancement is stronger in malignant nodules than in benign nodules. Consequently, a method of differentiating benign from malignant nodules was examined by establishing a cutoff for the difference in the CT numbers of noncalcified lung nodules before and after administration of an iodine contrast medium. The results of this multicenter study showed that when malignant nodules were defined as those with contrast enhancement of ≥ 15 HU and benign nodules as those with contrast enhancement of < 15 HU, sensitivity and specificity were 98% and 58%, respectively.[9)] Based on these results, contrast enhancement of < 15 HU on contrast-enhanced CT strongly suggests that the nodule is benign. However, if contrast enhancement is ≥ 15 HU, it may be attributable to a disease such as organizing pneumonia (OP), and a benign condition therefore cannot be ruled out. A meta-analysis of studies of benign-malignant differentiation using dynamic contrast-enhanced CT found that sensitivity and specificity in differentiating benign and malignant lung nodules ranged from 88% to 97% and from 68% to 97%, respectively. These results were comparable to those for contrast-enhanced CT, indicating that further improvement in diagnostic performance cannot be expected with dynamic contrast-enhanced CT.[10)]

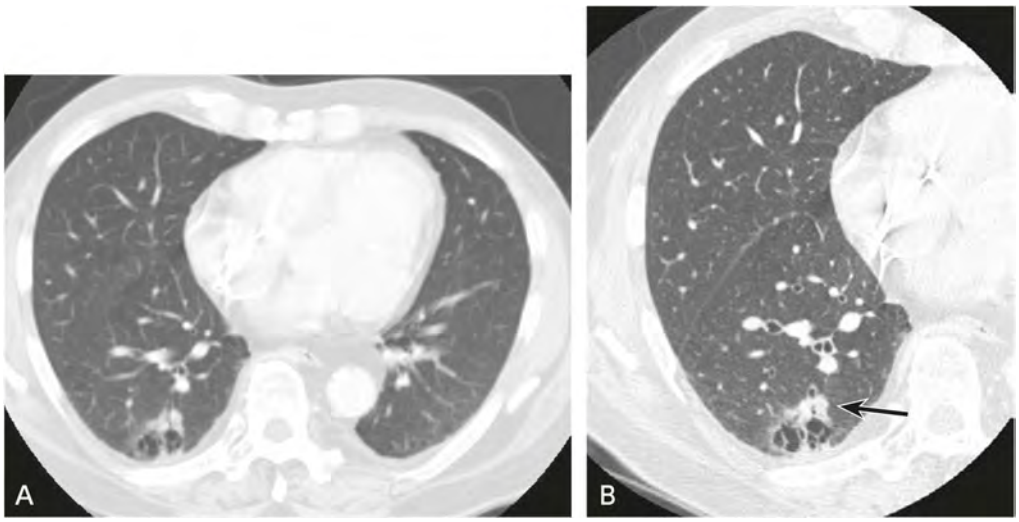

Figure. Assessment of lung nodule attributes using HRCT

A: CT, FOV includes both lungs, slice thickness of 5 mm: The presence of a small number of solid lesions on the margin of a cystic lesion in the dorsal right lower lobe is suspected, but determining their attributes is difficult.

B: HRCT, FOV limited to 1 lung, slice thickness of 1.3 mm: A distinct border (→) is seen between the normal lung and the lesions on the margin of the cystic lesion in the dorsal right lower lobe, a finding suggestive of lung cancer. Adenocarcinoma was diagnosed on resection.

Search keywords and secondary sources

PubMed was searched using the following keywords: lung nodule, differential diagnosis, and CT.

In addition, the following were referenced as secondary sources.

1) David S et al: NCCN Guidelines®: non-small cell lung cancer Ver 2. 2021. National Comprehensive Cancer Network, 2021
2) Silvestri GA et al: Methods for staging non-small cell lung cancer: diagnosis and management of lung cancer, 3rd ed: American College of Chest Physicians evidence-based clinical practice guidelines. Chest 143 (5): e211S-250S, 2013
3) Japan Lung Cancer Society, Ed.: 2020 Guidelines for the Diagnosis and Treatment of Lung Cancer: Includes Malignant Pleural Mesothelioma and Thymic Tumors. KANEHARA & Co., 2021.
4) MacMahon H et al: Guidelines for management of small pulmonary nodules detected on CT scans: a statement from the Fleischner Society. Radiology 237: 395-400, 2005

References

1) Aoki T et al: Evolution of peripheral lung adenocarcinomas: CT findings correlated with histology and tumor doubling time. AJR Am J Roentgenol 174: 763-768, 2000
2) Furuya K et al: New classification of small pulmonary nodules by margin characteristics on high-resolution CT. Acta Radiol 40: 496-504, 1999
3) Zwirewich CV et al: Solitary pulmonary nodule: high-resolution CT and radiologic-pathologic correlation. Radiology 179: 469-476, 1991
4) Seemann MD et al: Usefulness of morphological characteristics for the differentiation of benign from malignant solitary pulmonary lesions using HRCT. Eur Radiol 9: 409-417, 1999
5) Takanashi N et al: The diagnostic accuracy of a solitary pulmonary nodule, using thin-section high resolution CT. Lung Cancer 13: 105-112, 1995
6) Sakai S et al: Lung cancer associated with diffuse pulmonary fibrosis: CT-pathologic correlation. J Thorac Imaging 18: 67-71, 2003
7) Winer-Muram HT et al: The solitary pulmonary nodule. Radiology 239: 34-49, 2006
8) van Klaveren RJ et al: Management of lung nodules detected by volume CT scanning. N Engl J Med 361: 2221-2229, 2009
9) Swensen SJ et al: Lung nodule enhancement at CT: multicenter study. Radiology 214: 73-80, 2000
10) Cronin P et al: Solitary pulmonary nodules: meta-analytic comparison of cross-sectional imaging modalities for diagnosis of malignancy. Radiology 246: 772-782, 2008

CQ 3 Is FDG-PET/CT recommended for the differential diagnosis of benign and malignant lung nodules?

Recommendation

FDG-PET/CT is weakly recommended for the differential diagnosis of benign and malignant lung nodules.

Recommendation strength: 2, strength of evidence: weak (C), agreement rate: 100% (15/15)

Background

FDG-PET/CT, which can now be performed at many facilities, provides information on the glucose metabolism of lung nodules, in addition to enabling the interpretation of morphology by CT. This additional information can improve the accuracy of benign-malignant differentiation.

Explanation

FDG-PET/CT is used to diagnose the benign or malignant nature of lung nodules based on their level of glucose metabolism. Its diagnostic performance has been shown to be superior to that of CT and MRI in many studies (Fig.).[1-6] The standardized uptake value (SUV), which is used as a semi-quantitative index, is affected by factors such as the type of PET system and imaging method used, the patient's blood glucose level, and lesion localization (lung apex or base). Consequently, a cutoff is established and used for benign-malignant differentiation, which is a limitation. Benign-malignant differentiation using the SUV alone is therefore not recommended in routine clinical practice. Moreover, the volume effect is known to be strong in relatively small tumors with FDG-PET/CT. Consequently, the diagnostic performance of FDG-PET/CT is markedly lower for nodules < 10 mm in diameter. It is therefore recommended that it be used for benign-malignant differentiation of lesions ≥ 10 mm in diameter. Histologically, false negatives are known to occur for tumors such as those in the moderately malignant group, tumors with alveolar epithelial replacement growth, mucin-producing tumors, and tumors with strong central scar formation that are ≥ 10 mm in diameter. On the other hand, false positives are known to occur for some granulomatous inflammatory nodules, such as tuberculomas and cryptococcosis nodules.[7, 8] Current PET/CT involves performing thin-layer CT imaging and fusing it with PET images. Consequently, the CT images are of high diagnostic value. The radiation dose that the examinee is exposed to can be kept to a low level, which means the test has little adverse effect on the examinee. Thus, a comprehensive diagnosis can be performed by adding the information on glucose metabolism obtained by FDG-PET to the morphological diagnosis obtained by thin-layer CT.

FDG-PET/CT is more expensive than other tests. Based on the above considerations, however, the net benefits are commensurate with the cost if its use is limited to nodules ≥ 10 mm in diameter, for which benign-malignant differentiation is difficult with HRCT. It was therefore concluded that FDG-PET/CT can be weakly recommended for the differential diagnosis of benign and malignant lung nodules.

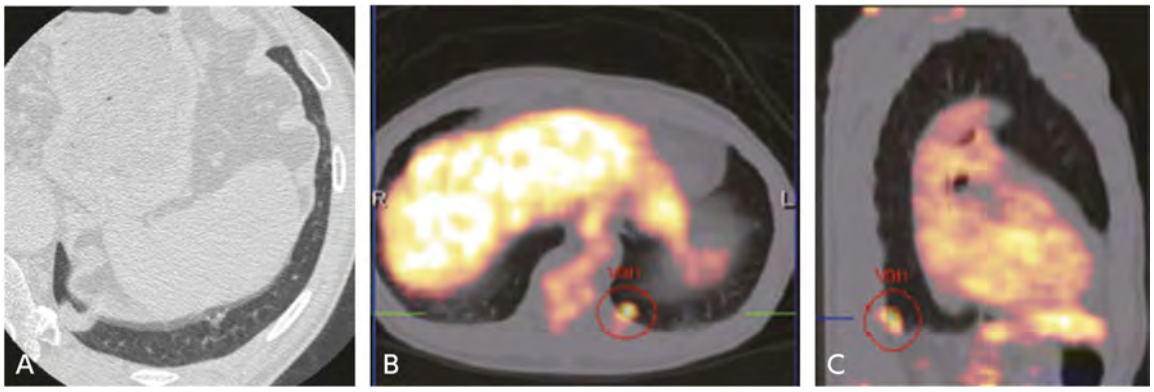

Figure. Lung squamous cell carcinoma

A: HRCT, slice thickness of 0.6 mm: A nodule with distinct margins is seen in the left lung base. There is no accompanying tendency for lobulation or spicula, and benign-malignant diagnosis is difficult.
B, C: FDG-PET/CT performed 10 days after A (B: transverse image, C: sagittal image): SUV max of 2.43 for the nodule in the left lung base. Comprehensive diagnosis that included HRCT was performed, and malignancy was more strongly suspected. Squamous cell carcinoma was diagnosed on resection.

Search keywords and secondary sources

PubMed was searched using the following keywords: pulmonary nodule, differential diagnosis, FDG-PET, and PET/CT.

In addition, the following was referenced as a secondary source.

1) Japan Lung Cancer Society, Ed.: Guidelines for Diagnosis and Treatment of the Lung Cancer/Malignant Pleural Mesothelioma/Thymic Tumors 2020. KANEHARA & Co., 2021.

References

1) Cronin P et al: Solitary pulmonary nodules: meta-analytic comparison of cross-sectional imaging modalities for diagnosis of malignancy. Radiology 246: 772-782, 2008
2) Lowe VJ et al: Prospective investigation of PET in lung nodules. J Clin Oncol 16: 1075-1084, 1998
3) Gould MK et al: Accuracy of positron emissioon tomography for diagnosis of pulmonary nodules and mass lesions: a meta-analysis. JAMA 285: 914-924, 2001
4) Fletcher JW et al: A comparison of the diagnostic accuracy of 18F-FDG PET and CT in the characterization of solitary pulmonary nodules. J Nucl Med 49: 179-185, 2008
5) Basso Dias A et al: Fluorine 18-FDG PET/CT and diffusion-weighted MRI for malignant versus benign pulmonary lesions: a meta-analysis. Radiology 290: 525-534, 2019
6) Hou S et al: Combination of positron emission tomography/computed tomography and chest thin-layer high-resolution computed tomography for evaluation of pulmonary nodules: correlation with imaging features, maximum standardized uptake value, and pathology. Medicine 97: 31, 2018
7) Kim SK et al: Accuracy of PET/CT in characterization of solitary pulmonary lesions. J Nucl Med 48: 214-220, 2007
8) Nomori H et al: Evaluation of 18F fluorodeoxyglucose (FDG) PET scanning for pulmonary nodules less than 3 cm in diameter, with special reference to the CT images. Lung Cancer 45: 19-27, 2004

BQ 25 Is CT recommended for determining the T stage of lung cancer?

Statement

There is strong scientific evidence for the use of CT to determine the T stage of lung cancer, and it is the standard test for this purpose.

Background

The usefulness of CT for determining the T stage of lung cancer before treatment was examined, and the findings are summarized below.

Explanation

CT is essential for accurately measuring the tumor diameter component of the T stage. Reconstructed coronal images and sagittal images are particularly useful for tumors that are long in the cranial-caudal direction (Fig.). They are also useful for determining the presence or absence of atelectasis and postobstructive pneumonia, whether there has been invasion of neighboring structures, and the extent of invasion of the central bronchi.[1-3] Although there are no significant differences between CT and MRI with respect to sensitivity and specificity in differentiating stages T0 to T2 and T3 to T4 (CT: 63% and 84%, respectively; MRI: 56% and 80%, respectively), MRI is superior to CT for assessing mediastinal invasion.[1] MRI has been reported to be superior to CT for determining the presence or absence and extent of invasion of the chest wall, vertebral bodies, brachial plexus, subclavian arteries and veins, and mediastinum.[1, 4-6] There have been an especially large number of reports indicating that it is useful for pulmonary apical tumors (Pancoast tumors).[4, 5] MRI is recommended when CT shows no obvious masses in the chest wall or costal bone destruction present, and the diagnosis is indeterminate with CT.

However, there have been no prospective studies comparing sagittal and coronal reconstruction CT and MRI using isotropic data obtained by MDCT. In diagnosing invasion of the interlobar pleura, chest wall, and mediastinum, the diagnostic accuracy of MDCT reconstructed sagittal images with a slice thickness of 1.25 mm has been reported to be significantly higher than that of CT with a slice thickness of 5 mm.[7] However, it has not been compared with MRI, and MRI therefore cannot be definitively concluded to be superior.

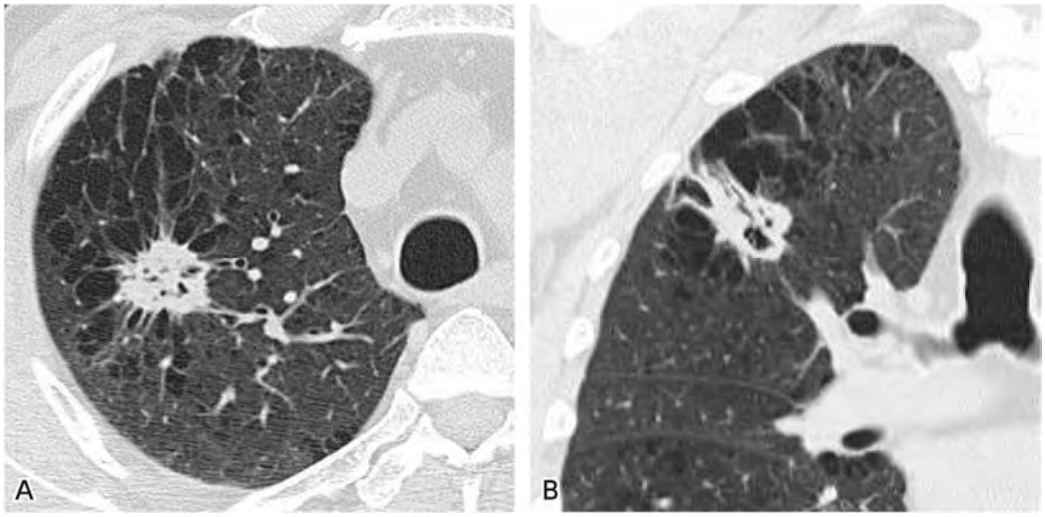

Figure. Primary lung cancer (pT2bN0M0, stage IIA)

A: HRCT, transverse image: Maximum diameter is 28 mm (> 2 cm, ≤ 3 cm, cT1c).

B: HRCT, coronal reconstructed image: The morphology of the tumor features a long length from top to bottom and a maximum diameter of 48 mm (> 4 cm, ≤ 5 cm), and the tumor was judged to be stage cT2b.

Search keywords and secondary sources

PubMed was searched using the following keywords: lung cancer, T-factor, invasion, and CT.

In addition, the following were referenced as secondary sources.

1) David S: NCCN Guidelines®: non-small cell lung cancer Ver 2. 2021. National Comprehensive Cancer Network, 2021
2) Silvestri GA et al: Methods for staging non-small cell lung cancer: diagnosis and management of lung cancer, 3rd ed: American College of Chest Physicians evidence-based clinical practice guidelines. Chest 143 (5): e211S-250S, 2013
3) Gaga M et al: An official American Thoracic Society/European Respiratory Society Statement: The role of the pulmonologist in the diagnosis and management of lung cancer. Am J Respir Crit Care Med 188 (4): 503-507, 2013

References

1) Webb WR et al: CT and MR imaging in staging non-small cell bronchogenic carcinoma: report of the Radiologic Diagnostic Oncology Group. Radiology 178: 705-713, 1991
2) White PG et al: Preoperative staging of carcinoma of the bronchus: can computed tomographic scanning reliably identify stage III tumours? Thorax 49 (10): 951-957, 1994
3) Herman SJ et al: Mediastinal invasion by bronchogenic carcinoma: CT signs. Radiology 190 (3): 841-846, 1994
4) Rapoport S et al: Brachial plexus: correlation of MR imaging with CT and pathologic findings. Radiology 167: 161-165, 1988
5) Laissy JP et al: Assessment of vascular involvement with magnetic resonance angiography (MRA) in Pancoast syndrome. Magn Reson Imaging 13 (4): 523, 1995
6) Tang W et al: The presurgical T staging of non-small cell lung cancer: efficacy comparison of 64-MDCT and 3.0 T MRI. Cancer Imaging 15 (1): 14, 2015
7) Higashino T et al: Thin-section multiplanar reformats from multidetector-row CT data: utility for assessment of regional tumor extent in non-small cell lung cancer. Eur J Radiol 56 (1): 48-55, 2005

CQ 4 Is MRI recommended for determining the T stage of lung cancer?

Recommendation

MRI is weakly recommended for determining the T stage of lung cancer when diagnosis of invasion of the chest wall, pericardium, brachial plexus, diaphragm/mediastinum/heart/great vessels, and vertebral bodies (T3 to T4) by CT is indeterminate.

Recommendation strength: 2, strength of evidence: weak (C), agreement rate: 93% (14/15)

Background

Accurate measurement of ground-glass opacities and the solid-component diameter and accurate diagnosis of invasion from the main bronchus to the tracheal bifurcation are required for determining the Tis, T1, and T2 components of the T stage of lung cancer. Consequently, diagnosis is performed using CT.

MRI has been reported to be superior to CT for determining the T3 and T4 components for the presence or absence and extent of invasion of the chest wall, pericardium, brachial plexus, diaphragm, heart, great vessels, and vertebral bodies. There have been an especially large number of reports indicating that it is useful for pulmonary apical tumors (Pancoast tumors).[1-3] Moreover, cine-MRI using respiratory motion has been reported to be useful for diagnosing involvement of the chest wall, mediastinum, heart, and great vessels.[4] If the chest wall, mediastinum, heart, and great vessels can be observed to move separately from the tumor, invasion of these structures can be ruled out (Fig. 1). MRI is indicated when there is extensive contact between a tumor and mediastinal structures such as the chest wall and great vessels and invasion is suspected on CT. To answer the question, Is MRI recommended for determining the T stage of lung cancer?, a systematic review was performed, and the diagnostic performance of MRI and CT was compared.

Explanation

In conducting this systematic review, diagnostic accuracy, sensitivity, specificity, cost, and contrast media adverse reactions were selected as outcome variables. Using the keywords indicated below, a literature search was performed for studies that compared the diagnostic performance of MRI and CT in determining the T stage in adults suspected of having lung cancer. There were no articles relevant to cost and contrast media adverse reactions. The 3 articles discussed below were relevant to the comparison of the diagnostic accuracy, sensitivity, and specificity of MRI and CT in determining the T stage.[5-7]

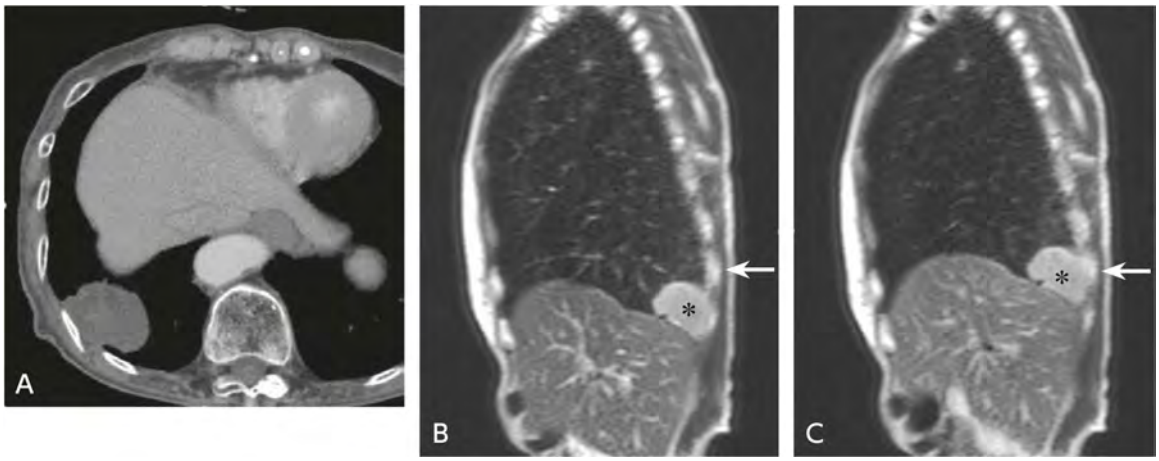

Figure 1. Primary lung cancer (Sq, cT1cN0M0, Stage IA3)

The patient was a woman in her 70s.

A: Chest CT: An irregular marginal solid nodule with a long-axis diameter of 2.6 cm is seen in the dorsal right lower lobe. Although it has extensive contact with the right 10th rib, there is no apparent rib destruction or involvement of the chest wall.

B, C: Respiratory dynamic MRI (B: inspiratory phase, C: expiratory phase): The tumor (*) slides in relation to the right 10th rib (←) on inspiration.

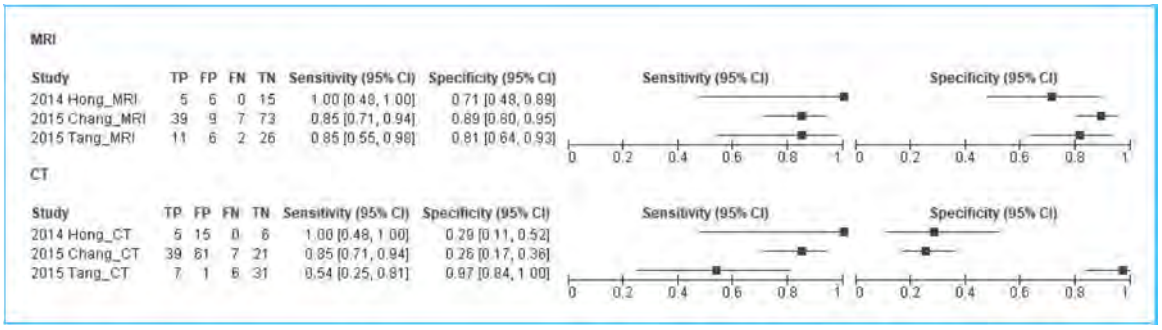

Figure 2. Meta-analysis results

In all 3 reports, the patients were selected consecutively, and no patient attrition bias was seen. With regard to index test (MRI) interpretation in the 3 articles, there may have been flow bias between facilities. Although blinding was used, none of the reports indicated whether the reference standard (pathological diagnosis) was interpreted without index test (MRI) information, and 2 of the 3 reports did not indicate the interval between the index test (MRI) and the control test (CT). The MRI methods and diagnostic criteria were not uniform (mixture of contrast-enhanced dynamic MRI and respiratory dynamic MRI), and the studies examined were a mix of prospective and retrospective studies.

Tang et al. compared T stage diagnostic performance in 45 consecutive patients diagnosed with non-small cell lung cancer who prospectively underwent contrast-enhanced dynamic MRI and contrast-enhanced CT within 1 week.[5] The criteria in the assessment of chest wall invasion were contact between the mass and chest wall > 3 cm, the presence of an obtuse angle contact between the mass and chest wall, extension of the mass into the chest wall, loss of the extra-pleural fat plane, or rib destruction.

The following criteria were used in the identification of mediastinal invasion: extensive contact between the mass and mediastinum; pleural and pericardial thickening; contact of ≥ 180 degrees between the mass and mediastinal great vessels; and loss of the fat plane between the mass and the mediastinal structures. Sensitivity and specificity for stages T3 and T4 were 85% and 91%, respectively, with MRI and 69% and 97%, respectively, with CT. Although the differences were not statistically significant, MRI showed superior sensitivity. Because this was a prospective study in consecutive patients, it included patients with chest wall and great vessel involvement that was not obvious on CT (32/45 patients with stages T1 and T2). Specificity was therefore high for both: 91% (29/32) for MRI and 97% (31/32) for CT.

Hong et al. compared the presence or absence of great vessel involvement (whether stage T4) observed by respiratory dynamic MRI and contrast-enhanced CT. Sensitivity and specificity were 100% and 71%, respectively, with MRI and 100% and 29%, respectively, with CT; the MRI specificity was statistically significantly superior.[6)] Similarly, Chang et al. compared the presence or absence of chest wall and great vessel involvement (whether stage T3 or T4) observed by respiratory/contrast-enhanced dynamic MRI and contrast-enhanced CT. Sensitivity and specificity were 85% and 89%, respectively, with MRI and 85% and 26%, respectively, with CT; the MRI specificity was statistically significantly superior.[7)]

In a meta-analysis of these 3 articles (Fig. 2), the pooled sensitivity, pooled specificity, AUC of the symmetric summary receiver-operating characteristic curve (SROC), and pooled diagnostic odds ratio were 86%, 84%, 0.92, and 36.9, respectively, for MRI and 80%, 43%, 0.80, and 5.7, respectively, for CT. No tests for significant differences were performed due to the small number of articles. However, MRI was superior to CT in all of these measures.

However, 2 of the 3 studies were retrospective studies, and MRI was not performed in patients with apparent invasion or no apparent chest wall or great vessel involvement.[6, 7)] Thus, patient selection bias was present in these studies. Based on the above considerations, it was concluded that MRI can be weakly recommended for determining the T stage of lung cancer, on condition that it be used in patients with an indeterminate T3/T4 diagnosis.

Search keywords and secondary sources

PubMed was searched using the following keywords: lung, pulmonary, neoplasms, magnetic resonance imaging, MRI, cancer, invasiveness, invasion, neoplasm invasion, staging, and neoplasm staging. The period searched was through June 2020; hits were obtained for 278 articles.

References

1) Webb WR et al: CT and MR imaging in staging non-small cell bronchogenic carcinoma: report of the Radiologic Diagnostic Oncology Group. Radiology 178: 705-713, 1991
2) Rapoport S et al: Brachial plexus: correlation of MR imaging with CT and pathologic findings. Radiology 167: 161-165, 1988
3) Laissy JP et al: Assessment of vascular involvement with magnetic resonance angiography (MRA) in Pancoast syndrome. Magn Reson Imaging 13 (4): 523, 1995
4) Sakai S et al: Bronchogenic carcinoma invasion of the chest wall: evaluation with dynamic cine MRI during breathing. J Comput Assist Tomogr 21 (4): 595-600, 1997

5) Tang W et al: The presurgical T staging of non-small cell lung cancer: efficacy comparison of 64-MDCT and 3.0 T MRI. Cancer Imaging 15 (1): 14, 2015
6) Hong YJ et al: Respiratory dynamic magnetic resonance imaging for determining aortic invasion of thoracic neoplasms. J Thorac Cardiovasc Surg 148 (2): 644-650, 2014
7) Chang S et al: Usefulness of thin-section single-shot turbo spin echo with half-Fourier acquisition in evaluation of local invasion of lung cancer. J Magn Reson Imaging 41 (3): 747-754, 2015

CQ 5 Is MRI recommended for diagnosing lymph node metastasis of lung cancer?

Recommendation

MRI is weakly recommended for diagnosing lymph node metastasis of lung cancer.

Recommendation strength: 2, strength of evidence: weak (C), agreement rate: 73.3% (11/15)

Background

CT is an essential test not only for determining the T stage, but also for determining the anatomical location of lymph nodes (lymph node mapping) for N stage determination. However, the diagnostic performance of FDG-PET is higher than that of CT in determining the presence or absence of metastasis (N0 or N1/2/3), and FDG-PET is therefore more widely used for this purpose. Moreover, as advances have been made in MRI technology, it has also been reported to be useful for N-staging. A systematic review was conducted to examine and compare the diagnostic performance of MRI and FDG-PET/CT in detecting lymph node metastasis.

Explanation

With CT, a short-axis diameter of ≥ 1 cm is often used as the criterion for enlargement, and its sensitivity and specificity range from 52% to 75% and 66% to 88%, respectively. These are inferior to the sensitivity and specificity of PET, which range from 83% to 91% and 86% to 92%, respectively.[1-3] A meta-analysis of 36 articles on FDG-PET/CT reported pooled sensitivity and specificity of 72% and 91%, respectively, in an examination of lymph node diagnostic performance for each patient.[4] FDG-PET/CT was therefore recommended for N stage determination.

In recent years, there have been many reports indicating that MRI is useful for N-staging. Short-inversion-time inversion-recovery turbo-spin-echo (STIR turbo SE) imaging and diffusion-weighted imaging have been used for this purpose, with the diagnostic performance of short-inversion-time inversion-recovery (STIR) imaging found to be superior to that of FDG-PET/CT, and FDG-PET/CT and diffusion-weighted imaging found to be comparable in diagnostic performance (Fig. 1).[5] Since 2016, three meta-analyses of the diagnostic performance of MRI in N-staging have been reported in major radiology journals.[6-8] The sensitivity and specificity of MRI for each patient in the 3 meta-analyses were high: 68% and 92%, 87% and 88%, and 72% and 97%, respectively. The article by Shen et al., which compared the diagnostic performance of MRI and FDG-PET/CT, reported sensitivity and specificity of 72% and 97%, respectively, for MRI and 65% and 93%, respectively, for FDG-PET/CT. Thus, although the differences were not statistically significant, a trend toward higher sensitivity and specificity was seen with MRI.[8]

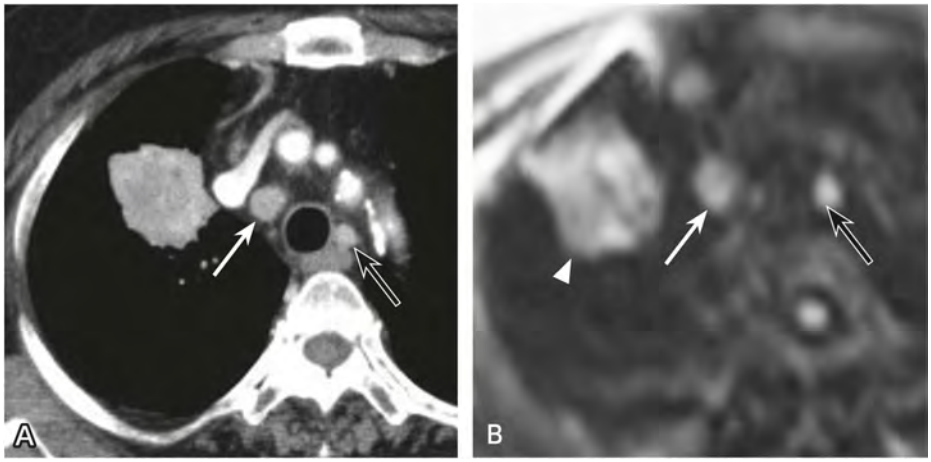

Figure 1. Lung cancer (cT2aN3M1b, stage IV)

A: Contrast-enhanced CT: An enlarged right lower paratracheal lymph node (#4R), with a short-axis diameter of > 1 cm, is seen (⇨). Also seen is a left lower paratracheal lymph node (#4L) with a short-axis diameter of < 1 cm.
B: MRI, diffusion-weighted imaging, b-value = 1,000 s/mm^2: The primary lesion in the right upper lobe (▷) and the #4R (⇨) and #4L (→) lymph nodes all show hyperintensity.

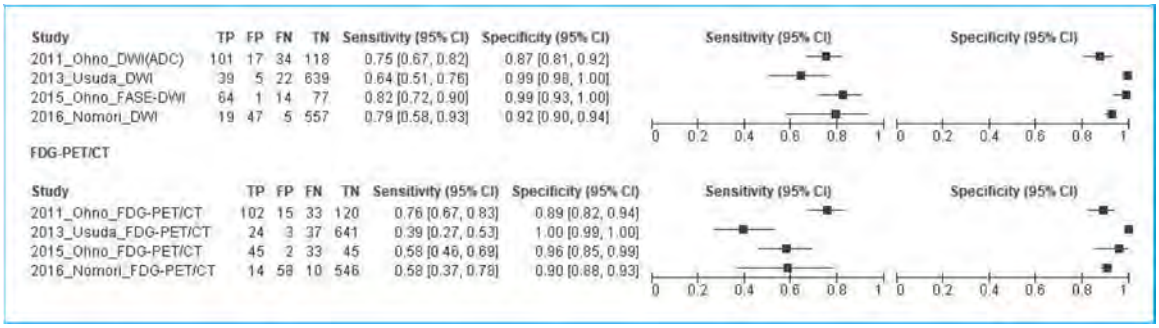

Figure 2. Meta-analysis results

Only one of these meta-analyses compared the diagnostic performance of MRI and FDG-PET/CT by collecting and analyzing reports published between 2003 and 2014.[8)] The MRI imaging method used is generally diffusion-weighted imaging; the use of STIR is reported by only certain institutions. Consequently, included in the search performed for the present systematic review were new reports published since 2015 that compared the diagnostic performance of diffusion-weighted imaging and FDG-PET/CT with respect to N stage determination. In addition, diagnostic accuracy, sensitivity, specificity, and cost were specified as outcome variables. Using the keywords indicated below, a literature search was performed for studies that compared the diagnostic performance of MRI (diffusion-weighted imaging) and the sensitivity and specificity of FDG-PET/CT in determining the N stage in adults suspected of having lung cancer. There were no articles relevant to cost. The four articles indicated below were relevant.[5, 9-11)]

The patients were selected consecutively, and no patient attrition bias was seen. With regard to index test (MRI) interpretation, there was a risk of bias. Although blinding was used, none of the reports indicated whether the reference standard (pathological diagnosis) was interpreted without index test (MRI) information. Moreover, the reports did not indicate the interval between the index test (MRI) and the control test (FDG-PET/CT). Consequently, there may have been flow bias between facilities. The results for diagnostic performance showed that the pooled sensitivity, pooled specificity, AUC of SROC, and pooled diagnostic odds ratio were 75%, 95%, 0.84, and 55.9, respectively, for MRI and 62%, 95%, 0.84, and 34.9, respectively, for FDG-PET/CT. No tests for significant differences were performed due to the small number of articles. However, a trend toward higher values for pooled sensitivity and the pooled diagnostic odds ratio was seen for MRI (Fig. 2).

As in the 3 meta-analyses mentioned above, the results of this meta-analysis showed that MRI provided high diagnostic performance. Additional advantages include the absence of radiation exposure and its lower cost compared with FDG-PET/CT. However, the N and M stages of lung cancer can be simultaneously determined during FDG-PET/CT, and it is an essential test for staging. Moreover, problems with MRI remain, such as standardizing the imaging and evaluation methods to use MRI as the standard imaging method and the fact that performing MRI in the brief period before surgery is difficult at some facilities. Based on the above considerations, it was concluded that MRI can be weakly recommended for diagnosing lymph node metastasis of lung cancer.

Search keywords and secondary sources used as references

PubMed was searched using the following keywords: lung, pulmonary, neoplasms, magnetic resonance imaging, MRI, lymph nodes, metastasis, lymphatic metastasis, and neoplasm metastasis. The period searched was through June 2020; hits were obtained for 78 articles.

References

1) McLuod TC et al: Bronchogenic carcinoma: analysis of staging in the mediastinum with CT by correlative lymph node mapping and sampling. Radiology 182 (2): 319-323, 1992
2) Birim O et al: Meta-analysis of positron emission tomographic and computed tomographic imaging in detecting mediastinal lymph node metastases in nonsmall cell lung cancer. Ann Thorac Surg 79 (1): 375-382, 2005
3) van Tinteren H et al: Effectiveness of positron emission tomography in the preoperative assessment of patients with suspected non-small-cell lung cancer: the PLUS multicentre randomised trial. Lancet 359 (9315): 1388-1393, 2002
4) Wu Y et al: Diagnostic value of fluorine 18 fluorodeoxyglucose positron emission tomography/computed tomography for the detection of metastases in nonsmall-cell lung cancer patients. Int J Cancer 132 (2): E37–E47, 2013
5) Ohno Y et al: N stage disease in patients with non-small cell lung cancer: efficacy of quantitative and qualitative assessment with STIR turbo spin-echo imaging, diffusion-weighted MR imaging, and fluorodeoxyglucose PET/CT. Radiology 261 (2): 605-615, 2011
6) Shen G et al: Performance of DWI in the nodal characterization and assessment of lung cancer: a meta-analysis. AJR Am J Roentgenol 206 (2): 283-290, 2016
7) Peerlings J et al: The diagnostic value of MR imaging in determining the lymph node status of patients with non-small cell lung xancer: a meta-analysis. Radiology 281 (1): 86-98, 2016
8) Shen G et al: Comparison of 18F-FDG PET/CT and DWI for detection of mediastinal nodal metastasis in non-small cell lung cancer: a meta-analysis. PLoS One 12 (3): e0173104, 2017

9) Usuda K et al: Advantages of diffusion-weighted imaging over positron emission tomography-computed tomography in assessment of hilar and mediastinal lymph node in lung cancer. Ann Surg Oncol 20 (5): 1676-1683, 2013
10) Ohno Y et al: Diffusion-weighted MR imaging using FASE sequence for 3T MR system: preliminary comparison of capability for N-stage assessment by means of diffusion-weighted MR imaging using EPI sequence, STIR FASE imaging and FDG PET/CT for non-small cell lung cancer patients. Eur J Radiol 84 (11): 2321-2331, 2015
11) Nomori H et al: Diffusion-weighted imaging can correctly identify false-positive lymph nodes on positron emission tomography in non-small cell lung cancer. Surg Today 46 (10): 1146-1151, 2016

BQ 26 Is PET recommended for N and M staging of lung cancer?

Statement

PET is recommended for N and M staging of lung cancer.

Background

PET is a modality that involves administering a positron-emitting isotope, imaging its biodistribution, and performing a diagnosis based on the distribution and kinetics of the tracer. Features of FDG-PET include its ① high detection sensitivity, ② good resolution, and ③ ability to correct for absorption in the body. It is used together with CT for lung cancer staging. FDG-PET and FDG-PET/CT are also recommended for lung cancer staging in the guidelines of the National Cancer Comprehensive Network (NCCN) and the American College of Chest Physicians (ACCP) and as the official statement of the American Thoracic Society/European Respiratory Society (ATS/ERS).

Explanation

1. N stage determination

The most important factor in the staging of lung cancer, particularly preoperative staging, is determining the mediastinal lymph node (N2) stage. The advantages of FDG-PET include its ① high detection sensitivity, ② good resolution, and ③ ability to correct for absorption in the body. However, for determining the mediastinal lymph node (N2) stage, it has 4 drawbacks: ① the lack of a diagnostic cutoff based on a semi-quantitative index; ② limited resolution of 7 to 10 mm; ③ weak uptake in well-differentiated, low-grade tumors; and ④ false positives due to inflammation. There have been numerous reports of N2 staging with FDG-PET.[1-3] Silvestri et al. reviewed 44 studies of mediastinal lymph node (N2) staging published between 1994 and 2006.[4] An SROC analysis of data for 2,865 patients with lung cancer showed sensitivity of 74% (95% CI, 69% to 79%) and specificity of 85% (95% CI, 82% to 88%). The results indicated that although FDG-PET/CT is more accurate than CT for mediastinal lymph node (N2) staging, it is not perfect. Mediastinal lymph node (N2) staging with FDG-PET is particularly important in patients predicted to have clinical stage IB to IIIB disease. If an abnormal finding is obtained by FDG-PET, a preoperative investigation of the lymph node diagnosis is recommended by means such as endobronchial ultrasonography (EBUS), thoracoscopy, or mediastinoscopy.

Taking into account the fact that the resolution limit of FDG-PET is 7 to 10 mm, Gould et al. performed a meta-analysis of only lymph node lesions that enlarged to ≥ 10 mm.[5] FDG-PET sensitivity and specificity were 100% and 78%, respectively. In a similar analysis of lymph nodes < 10 mm in size, sensitivity and specificity were 82% and 93%, respectively, indicating that false-negative results are obtained with FDG-PET in approximately 20% of patients. The results of a randomized, controlled,

multicenter study using FDG-PET/CT conducted by Fischer et al. showed sensitivity and specificity of 95% and 85%, respectively, an improvement on the data for FDG-PET.[6)]

2. M stage determination

With M staging of lung cancer by FDG-PET, unexpected metastasis is seen in 10% to 20% of patients.[4)] Although the clinical impact of this is strong, most of the data were obtained in small, single-center, prospective studies. The problems with using FDG-PET for M staging include ① non-standardized evaluation methods, ② the handling of brain metastasis, ③ the method of confirmation used when FDG-PET is negative, and ④ the contribution to patient prognosis. Li et al. examined the sensitivity of FDG-PET in the M staging of lung cancer in a meta-analysis of 9 studies and found that its sensitivity and specificity were 93% and 96%, respectively.[7)] In a meta-analysis of 10 studies, Yu et al. examined the sensitivity of FDG-PET/CT in the M staging of non-small cell lung cancer and found that its sensitivity and specificity were 81% and 96%, respectively.[8)] An examination by organ of metastasis found that the diagnostic sensitivity of FDG-PET for brain metastasis was only 60%, and that MRI was the most accurate modality for determining the extent of small lesions and tumors.[4)] Although diagnostic accuracy for liver metastasis ranges from 92% to 100%, the amount of relevant data is considered inadequate.[9,10)] FDG-PET sensitivity and specificity for bone metastasis have both been reported to be ≥ 90%. Moreover, the accuracy of FDG-PET in detecting bone metastasis has been found to be higher than that of both MRI and bone scintigraphy.[11, 12)] On the other hand, it is known to produce false negatives for the osteoblastic bone metastasis characteristic of breast or prostate cancer. Although its diagnostic accuracy for adrenal metastasis is 100%, the amount of relevant data is inadequate. Because accumulation by small nodules several mm in size is underestimated, lung and pleural metastases need to be determined by diagnostic chest CT.

Figure. Lung cancer and multiple metastases

FDG-PET/CT fusion imaging: In addition to the primary tumor in the right lung, abnormal accumulation (→) is seen in the right lung, mediastinal lymph nodes, and right adrenal gland.

Search keywords and secondary sources

PubMed, the Cochrane Library database, and the National Guideline Clearing House database were searched using the following keywords: lung cancer, bronchogenic carcinoma, staging, PET, PET/CT, and FDG. Important articles with high-level medical evidence were used in the review.

In addition, the following were referenced as secondary sources.

1) David S: NCCN Guidelines®: non-small cell lung cancer Ver 5. 2021. National Comprehensive Cancer Network, 2020
2) Silvestri GA et al: Methods for staging non-small cell lung cancer: diagnosis and management of lung cancer, 3rd ed: American College of Chest Physicians evidence-based clinical practice guidelines. Chest 143 (5): e211S-250S, 2013
3) Gaga M et al: An official American Thoracic Society/European Respiratory Society Statement: the role of the pulmonologist in the diagnosis and management of lung cancer. Am J Respir Crit Care Med 188 (4): 503-507, 2013

References

1) De Wever W et al: Integrated PET/CT in the staging of nonsmall cell lung cancer: technical aspects and clinical integration. Eur Respir J 33: 201-212, 2009
2) Antoch G et al: Non-small cell lung cancer: dual –modality PET/CT in preoperative staging. Radiology 229: 526-533, 2003
3) Lardinois D et al: Staging of non-small-cell lung cancer with integrated positron-emission tomography and computed tomography. N Engl J Med 348: 2500-2507, 2003
4) Silvestri GA et al: Noninvasive staging of non-small cell lung cancer: ACCP evidenced-based clinical practice guidelines, 2nd ed. Chest 132: 178S-201S, 2007
5) Gould MK et al: Test performance of positron emission tomography and computed tomography for mediastinal staging in patients with non-small-cell lung cancer: a meta-analysis. Ann Intern Med 139: 879-892, 2003
6) Fischer BM et al: Preoperative staging of lung cancer with combined PET-CT. N Engl J Med 361: 32-39, 2009
7) Li J et al: Meta-analysis: accuracy of 18FDG PET-CT for distant metastasis staging in lung cancer patients. Surg Oncol 22: 151-155, 2013
8) Yu B et al: Clinical usefulness of ^{18}F-FDG-PET/CT for the detection of distant metastases in patients with non-small cell lung cancer at initial staging: a meta-analysis. Cancer Management and Research 10: 1859-1864, 2018

9) Cerfolio RJ et al: The accuracy of integrated PET-CT compared with dedicated PET alone for the staging of patients with non-small cell lung cancer. Ann Thorac Surg 78: 1017-1023, 2004
10) Fischer BM et al: A prospective study of PET/CT in initial staging of small-cell lung cancer: comparison with CT, bone scintigraphy and bone marrow analysis. Ann Oncol 18: 338-345, 2007
11) Qu X et al: A meta-analysis of ^{18}FDG-PET-CT, ^{18}FDG-PET, MRI and bone scintigraphy for diagnosis of bone metastases in patients with lung cancer. Eur J Radiol 81: 1007-1015, 2012
12) Chang MC et al: Meta-analysis: comparison of F-18 fluorodeoxyglucose-positron emission tomography and bone scintigraphy in the detection of bone metastasis in patients with lung cancer. Acad Radiol 19: 349-357, 2012

BQ 27 Is contrast-enhanced cranial MRI recommended for diagnosing brain metastasis of lung cancer?

Statement

There is strong scientific evidence for the use of contrast-enhanced cranial MRI for diagnosing brain metastasis of lung cancer, and it is the standard test for this purpose. However, it can be omitted for non-small cell lung cancer that shows pure ground-glass nodules (GGNs) or part-solid nodules with a solid-component diameter of ≤ 1 cm on CT, because there is little possibility of brain metastasis in such cases.

Background

The brain is the organ where distant metastasis from lung cancer most frequently occurs. Consequently, the diagnosis of brain metastasis is important. The diagnostic performance of contrast-enhanced MRI in detecting brain metastasis was examined by comparison with contrast-enhanced CT, and the findings are summarized below.

Explanation

Contrast-enhanced MRI has been found to detect brain lesions with higher sensitivity and to detect more and smaller metastases than non-contrast MRI, contrast-enhanced CT, and non-contrast CT.[1, 2] This is attributed to factors such as the fact that contrast-enhanced MRI provides higher density resolution and greater contrast medium enhancement than CT and has no bone artifacts (Fig.). However, although the detection rate of contrast-enhanced MRI is higher than that of contrast-enhanced CT, and contrast-enhanced MRI can detect smaller metastases, it has also been found that there was no significant difference between these modalities with respect to mean survival time or the 2-year survival rate.[3]

A meta-analysis of 18 reports compared clinical evaluation and CT with respect to brain metastasis in 1,830 patients with non-small cell lung cancer. In the 9 reports that were limited to patients without clinical symptoms, the median prevalence of brain metastasis was 3%, and the median negative predictive value was 97%. In the 9 reports that included both patients with and without clinical symptoms, the median rate of brain metastasis was 14%, sensitivity was 76%, and specificity was 82%. On the other hand, in a study of brain metastasis detection in small cell lung carcinoma, the detection rate with MRI (24%) was higher than with CT (10%), and all of the patients found to have brain metastasis by CT were symptomatic. However, 11% of the patients found to have brain metastasis by MRI were asymptomatic.[4]

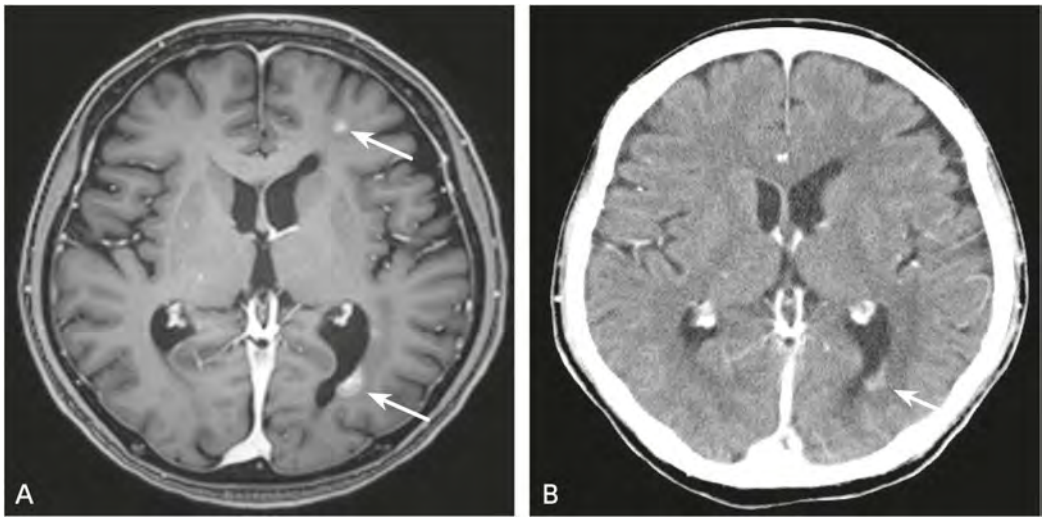

Figure. Multiple brain metastases of lung cancer (cT2aN2M1c, stage IVB)

A: Contrast-enhanced MRI: Hyperintense nodules are seen at 2 sites (→) in the left frontal and left parietal lobes.
B: Contrast-enhanced CT: Although the hyperintense region in the left parietal lobe (→) is identifiable, the lesion in the left frontal lobe is difficult to identify with CT alone.

The 3rd edition of the ACCP guidelines recommend that brain MRI be performed in patients with clinical stage I or II non-small cell lung cancer if CNS signs and symptoms are observed clinically. This is because the percentage of patients found to be positive for brain metastasis is low, at 3%, and the negative predictive value of brain MRI is extremely high in patients who are negative for brain metastasis on clinical evaluation. Another factor in this recommendation is cost-effectiveness. However, patients with asymptomatic brain metastasis have been found to have a better prognosis than patients with symptomatic brain metastasis.[5)] Consequently, the NCCN guidelines (NSCLC, version 3, 2020) recommend cranial MRI in patients with non-small cell lung cancer ≥ stage II (optional for stage IB) regardless of symptoms in order to enable asymptomatic brain metastasis to be detected and treated early. In view of the high prevalence of brain metastasis in asymptomatic small cell lung carcinoma, cranial MRI is recommended for all such patients, whether the disease is localized or advanced (SCLC, version 2, 2018). However, a histological diagnosis is often not obtained at the stage of preoperative staging, and contrast-enhanced cranial MRI is therefore recommended for all lung cancer staging.

However, there have been numerous reports that brain metastasis almost never occurs in adenocarcinoma that shows predominant ground-glass opacities and lepidic growth on CT.[4-6)] Sakurai et al. reported that all of the 25 patients with bronchioloalveolar carcinomas ≤ 3 cm that they examined had stage T1N0M0 disease.[6)] Cho et al. found that, of 109 patients with adenocarcinomas that showed pure GGNs on CT who underwent preoperative MRI, only 1 had brain metastasis 30 months after surgery (1/109, 0.9%).[7)] Suzuki et al. showed that, in patients whose primary lesions were GGNs ≤ 2 cm in size with a consolidation ratio of ≤ 25%, the cancer was also noninvasive pathologically, and there was very little distant metastasis.[8)] Brain imaging can therefore be omitted in non-small cell lung cancer that shows pure GGNs and part-solid nodules with a solid-component diameter of ≤ 1 cm on CT, because there is little possibility of brain

metastasis in such cases. If contrast-enhanced MRI cannot be performed for a reason such as the presence of an electronic device or metal in the patient's body, contrast-enhanced CT is considered appropriate.

Search keywords and secondary sources

PubMed was searched using the following keywords: lung cancer, brain metastasis, MRI, and CT.

In addition, the following were referenced as secondary sources.

1) David S: NCCN Guidelines®: non-small cell lung cancer Ver 3. 2020. National Comprehensive Cancer Network, 2020
2) David S: NCCN Guidelines®: small cell lung cancer Ver 2. 2018. National Comprehensive Cancer Network, 2018
3) Silvestri GA et al: Methods for staging non-small cell lung cancer: diagnosis and management of lung cancer, 3rd ed: American College of Chest Physicians evidence-based clinical practice guidelines. Chest 143 (5): e211S-250S, 2013
4) Gaga M et al: An official American Thoracic Society/European Respiratory Society Statement: the role of the pulmonologist in the diagnosis and management of lung cancer. Am J Respir Crit Care Med 188 (4): 503-507, 2013
5) Japan Lung Cancer Society, Ed.: Guidelines for Diagnosis and Treatment of the Lung Cancer/Malignant Pleural Mesothelioma/Thymic Tumors 2020. KANEHARA & Co., 2021.

References

1) Davis PC et al: Diagnosis of cerebral metastases: double-dose delayed CT vs contrast-enhanced MR imaging. AJNR Am J Neuroradiol 12 (2): 293-300, 1991
2) Akeson P et al: Brain metastases-comparison of gadodiamide injection-enhanced MR imaging at standard and high dose, contrast-enhanced CT and non-contrast-enhanced MR imaging. Acta Radiol 36 (3): 300-306, 1995
3) Yokoi K et al: Detection of brain metastasis in potentially operable non-small cell lung cancer. Chest 115 (3): 714-719, 1999
4) Seute T et al: Detection of brain metastases from small cell lung cancer: consequences of changing imaging techniques (CT versus MRI). Cancer 112 (8): 1827-1834, 2008
5) Sánchez de Cos J et al: Non-small cell lung cancer and silent brain metastasis: survival and prognostic factors. Lung Cancer 63 (1): 140-145, 2009
6) Sakurai H et al: Bronchioloalveolar carcinoma of the lung 3 centimeters or less in diameter: a prognostic assessment. Ann Thorac Surg 78 (5): 1728-1733, 2004
7) Cho H et al: Pure ground glass nodular adenocarcinomas: are preoperative positron emission tomography/computed tomography and brain magnetic resonance imaging useful or necessary? J Thorac Cardiovasc Surg 150 (3): 514-520, 2015
8) Suzuki K et al: A prospective radiological study of thin-section computed tomography to predict pathological noninvasiveness in peripheral clinical IA lung cancer (Japan Clinical Oncology Group 0201). J Thorac Oncol 6 (4): 751-756, 2011

BQ 28 Is bone scintigraphy recommended for diagnosing bone metastasis of lung cancer?

Statement

Although scientific evidence supporting the use of bone scintigraphy to diagnose bone metastasis is lacking, its use can be considered, particularly when bone metastasis is suspected clinically and FDG-PET cannot be performed.

Background

Diagnosing bone metastasis during the initial examination for primary lung cancer is important for prognosis prediction and treatment selection. Screening for bone metastasis previously involved bone scintigraphy. Recently, however, bone scintigraphy is being replaced by FDG-PET. FDG-PET and FDG-PET/CT are also recommended for lung cancer staging in the NCCN and ACCP guidelines and as the official statenebt of the ATS/ERS. That is because the sensitivity of FDG-PET is comparable to the sensitivity of bone scintigraphy,[1-3] whereas accumulation in bone scintigraphy is increased by factors such as trauma, infection, and joint disease, resulting in low specificity. Conversely, the advantages of bone scintigraphy are its short test duration, and the fact that it results in fewer false-negatives for osteoblastic bone metastasis than FDG-PET. Bone scintigraphy and FDG-PET were compared with respect to their performance in diagnosing bone metastasis of primary lung cancer, and the findings are summarized below.

Explanation

In a meta-analysis of 8 articles (723 patients), the sensitivity and specificity of bone scintigraphy for bone metastasis were 82% and 62%, respectively, in primary lung cancer patients with a mean prevalence of 20%. Thus, the specificity of bone scintigraphy was found to be somewhat low. However, a separate meta-analysis of 17 articles (2,940 patients), comprising 9 on FDG-PET/CT, 6 on FDG-PET, 6 on MRI, and 16 on bone scintigraphy, found sensitivity and specificity of 92% and 98%, 87% and 94%, 77% and 92%, and 86% and 88%, respectively. Moreover, the odd ratios for FDG-PET/CT (449.17) and FDG-PET (118.25) were significantly higher than those for MRI (38.27) and bone scintigraphy (63.37).[1] A meta-analysis of 7 articles found that the sensitivity and specificity of either FDG-PET/CT or FDG-PET and bone scintigraphy for bone metastasis were 93%, 95%, 87%, and 82%, respectively, on a per-patient basis (1,746 patients). On a per-lesion basis (1,263 lesions), sensitivity and specificity were 93%, 92%, 91%, and 57%, respectively.[3]

FDG-PET is recommended for staging in the NCCN and ACCP guidelines and as the official statement of the ATS/ERS. The ACCP guidelines state that bone scintigraphy can be used as an alternative to FDG-PET if it cannot be performed.

Search keywords and secondary sources

PubMed was searched using the following keywords: lung cancer, bone metastases, bone scintigraphy, and PET. Important articles with high-level medical evidence were used in the review.

In addition, the following were referenced as secondary sources.

1) David S: NCCN Guidelines®: non-small cell lung cancer Ver 2. 2021. National Comprehensive Cancer Network, 2021
2) David S: NCCN Guidelines®: small cell lung cancer Ver 2. 2021. National Comprehensive Cancer Network, 2021
3) Silvestri GA et al: Methods for staging non-small cell lung cancer: diagnosis and management of lung cancer, 3rd ed: American College of Chest Physicians evidence-based clinical practice guidelines. Chest 143 (5): e211S-250S, 2013
4) Gaga M et al: An official American Thoracic Society/European Respiratory Society Statement: the role of the pulmonologist in the diagnosis and management of lung cancer. Am J Respir Crit Care Med 188 (4): 503-507, 2013

Figure. Lung cancer and multiple bone metastases

Bone scintigraphy, frontal view: Abnormal accumulation is seen in a right rib and the right ilium, right femur, and right patella (→).

References

1) Qu X et al: A meta-analysis of ^{18}FDG-PET-CT, ^{18}FDG-PET, MRI and bone scintigraphy for diagnosis of bone metastases in patients with lung cancer. Eur J Radiol 81: 1007-1015, 2012
2) Chang MC et al: Meta-analysis: comparison of F-18 fluorodeoxyglucose-positron emission tomography and bone scintigraphy in the detection of bone metastasis in patients with lung cancer. Acad Radiol 19: 349-357, 2012
3) Schirrmeister H et al: Omission of bone scanning according to staging guidelines leads to futile therapy in non-small cel lung cancer. Eur J Nucl Med Mol Imaging 31: 964-968, 2004

BQ 29 Is PET recommended for detecting lung cancer recurrence?

Statement

PET is useful and recommended for detecting lung cancer recurrence. In some cases, tumor markers may be elevated, but a lesion at a site where recurrence is difficult to identify only by morphological diagnostic imaging using a modality such as CT and MRI may be detectable using PET.

Background

Lung cancer recurrence is usually detected using a morphological imaging modality such as CT or MRI. PET using FDG is a functional imaging method for imaging glucose metabolism that may be even more useful than diagnostic imaging based on conventional morphological diagnosis. This section summarizes the literature on the usefulness of PET for detecting lung cancer recurrence.

Explanation

Periodic morphological diagnostic imaging and examination of changes in tumor marker levels are the main methods used to detect lung cancer recurrence. However, in some cases, it is difficult to distinguish between postoperative changes and local recurrence with chest CT (Fig.). It can also be difficult to identify the site of recurrence based on tumor marker elevation alone, and detection may complicated by false positives.

Investigations of the diagnostic accuracy of PET/CT and PET with respect to the posttreatment recurrence of non-small cell lung cancer have reported sensitivity ranging from 81% to 100%, specificity of 77% to 98%, and diagnostic accuracy rates of 88% to 97%, indicating its usefulness in detecting recurrence.[1-11)] In examinations of patients suspected of having a recurrence based on elevated tumor marker carcinoembryonic antigen (CEA) levels and other clinical findings, the diagnostic accuracy rates of PET and PET/CT ranged from 90% to 95%,[2-6)] higher than the diagnostic accuracy rate of CT (50%), and confidence in the diagnosis was also better.[3)] On the other hand, examinations of postoperative patients with asymptomatic non-small cell lung cancer found that PET/CT identified recurrence in 18% to 38% of patients.[7, 8)]

In some cases, determining and differentiating local recurrence can be difficult with morphological diagnostic imaging by CT because pulmonary fibrosis occurs after stereotactic radiation therapy. With PET/CT, however, recurrence can be distinguished from fibrotic inflammation based on accumulation strength and shape.[12-14)]

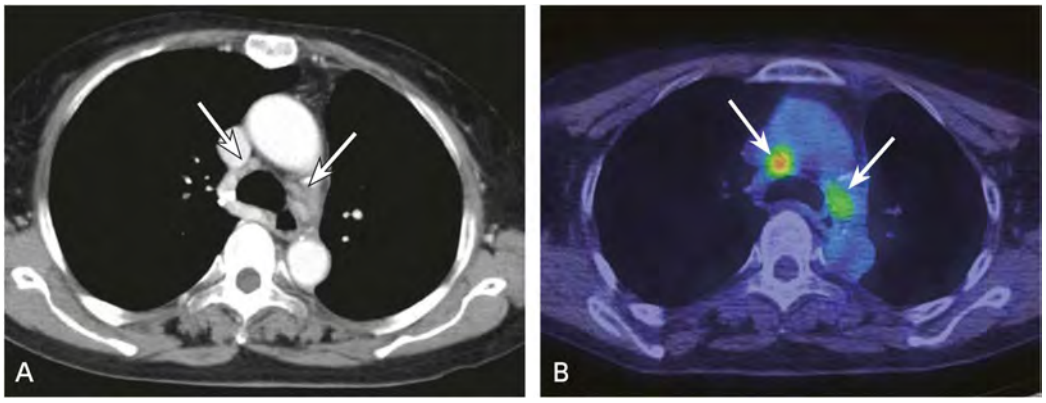

Figure. Screening for recurrence performed due to CEA elevation after surgery for right lower lobe, ALK fusion gene-positive lung cancer.

A: Contrast-enhanced CT, transverse image; B: PET/CT fusion imaging, transverse image
Although only small mediastinal lymph nodes are seen on contrast-enhanced CT, FDG accumulation (SUVmax = 3.8 to 5.7, →) is subsequently seen on PET/CT, suggesting recurrence. Alectinib administration was started, CEA decreased over time, and a reduction in the size of the mediastinal lymph nodes was seen (not shown).

An investigation of the use of PET/CT to examine recurrence and residual neoplasms following treatment for non-small cell lung cancer found that the examination resulted in treatment resumption in 20% of patients, a change of treatment in 6%, and treatment discontinuation in 2%. Thus, PET/CT resulted in a change in the treatment plan for 28% of the patients as a whole.[15)]

Although there have been very few reports of studies of the usefulness of PET in detecting small cell lung carcinoma recurrence, the results of one such study were similar to those obtained for non-small cell lung cancer: sensitivity of 100%, specificity of 80%, and a diagnostic accuracy rate of 92%.[16)] In an investigation of the use of PET to evaluate posttreatment recurrence and residual neoplasms, changes such as a change in the type of treatment and treatment resumption were made in the treatment plans of approximately half of the patients as a result of the evaluation.[17)]

Recurrent lung cancer lesions are not limited to a single location, but they can be present in multiple organs. PET, which can be used to evaluate the whole body, is therefore highly useful for detecting such lesions. Moreover, because the specificity of PET is also high, the likelihood of recurrence can be concluded to be low if the results of PET are negative, permitting follow-up to be carried out without performing other tests.

Search keywords and secondary sources

PubMed was searched using the following keywords: FDG, PET, lung cancer, and recurrence. The period searched was from 2015 to June 2019, and there were no new studies that ought to have been selected for review.

In addition, the following was referenced as a secondary source.

1) Japanese Society of Nuclear Medicine Subcommittee, Respiratory Nuclear Medicine Research Group, Ed.: Respiratory Nuclear Medicine Diagnostic (Clinical Practice) Guidelines, 2nd Edition. Japanese Society of Nuclear Medicine, 2015.

References

1) He YQ et al: Diagnostic efficacy of PET and PET/CT for recurrent lung cancer: a meta-analysis. Acta Radiol 55: 309-317, 2014
2) Opoka L et al: Assessment of recurrence of non-small cell lung cancer after therapy using CT and Integrated PET/CT. Pneumonol Alergol Pol 81: 214-220, 2013
3) Jiménez-Bonilla JF et al: Diagnosis of recurrence and assessment of post-recurrence survival in patients with extracranial non-small cell lung cancer evaluated by 18F-FDG PET/CT. Lung Cancer 81: 71-76, 2013
4) Isobe K et al: Usefulness of fluoro-2-deoxyglucose positron emission tomography for investigating unexplained rising carcinoembryonic antigen levels that occur during the postoperative surveillance of lung cancer patients. Int J Clin Oncol 14: 497-501, 2009
5) Keidar Z et al: PET/CT using 18F-FDG in suspected lung cancer recurrence: diagnostic value and impact on patient management. J Nucl Med 45: 1640-1646, 2004
6) Hellwig D et al: Diagnostic performance and prognostic impact of FDG-PET in suspected recurrence of surgically treated non-small cell lung cancer. Eur J Nucl Med Mol Imaging 33: 13-21, 2006
7) Toba H et al: 18F-fluorodeoxyglucose positron emission tomography/computed tomography is useful in postoperative follow-up of asymptomatic non-small-cell lung cancer patients. Interact Cardiovasc Thorac Surg 15: 859-864, 2012
8) Cho S, Lee EB: A follow-up of integrated positron emission tomography/computed tomography after curative resection of non-small cell lung cancer in asymptomatic patients. J Thorac Cardiovasc Surg 139: 1447-1451, 2010
9) Takenaka D et al: Integrated FDG-PET/CT vs. standard radiological examinations: comparison of capability for assessment of postoperative recurrence in non-small cell lung cancer patients. Eur J Radiol 74: 458-464, 2010
10) Kanzaki R et al: Clinical value of F18-fluorodeoxyglucose positron emission tomography-computed tomography in patients with non-small cell lung cancer after potentially curative surgery: experience with 241 patients. Interact Cardiovasc Thorac Surg 10: 1009-1014, 2010
11) Onishi Y et al: Non-small cell carcinoma: comparison of postoperative intra- and extrathoracic recurrence assessment capability of qualitatively and/or quantitatively assessed FDG-PET/CT and standard radiological examinations. Eur J Radiol 79: 473-479, 2011
12) Takeda A et al: Evaluation for local failure by 18F-FDG PET/CT in comparison with CT findings after stereotactic body radiotherapy (SBRT) for localized non-small-cell lung cancer. Lung Cancer. 79: 248-253, 2013
13) Zhang X et al: Positron emission tomography for assessing local failure after stereotactic body radiotherapy for non-small-cell lung cancer. Int J Radiat Oncol Biol Phys 83: 1558-1565, 2012
14) Nakajima N et al: Differentiation of tumor recurrence from radiation-induced pulmonary fibrosis after stereotactic ablative radiotherapy for lung cancer: characterization of 18F-FDG PET/CT findings. Ann Nucl Med 27: 261-270, 2013
15) Marcus C et al: 18F-FDG PET/CT and lung cancer: value of fourth and subsequent posttherapy follow-up scans for patient management. J Nucl Med 56: 204-208, 2015
16) Zhao DS et al: 18F-fluorodeoxyglucose positron emission tomography in small-cell lung cancer. Semin Nucl Med 32: 272-275, 2002
17) Blum R et al: Impact of positron emission tomography on the management of patients with small-cell lung cancer: preliminary experience. Am J Clin Oncol 27: 164-171, 2004

BQ 30 Is MRI recommended for diagnosing mediastinal tumors?

Statement

MRI is useful for diagnosing cystic tumors of the mediastinum and may also provide additional information about the internal attributes of solid tumors of the mediastinum. It is also highly useful and recommended for diagnosing tumors of the posterior mediastinum.

Background

CT is often used for diagnostic imaging of mediastinal tumors, and MRI is subsequently added in some cases. However, the necessity and usefulness of MRI in this role have not been adequately examined. Although few reports have directly compared the diagnostic performance of CT and MRI in diagnosing mediastinal tumors, several reports have indicated that MRI is useful for this purpose. Consequently, the usefulness of MRI in diagnosing mediastinal tumors was examined, and the findings are summarized below.

Explanation

The sites of mediastinal tumor development are chiefly classified as the anterior, middle, and posterior mediastinum. In addition, the tumors are broadly classified as cystic or solid tumors according to their internal attributes. When discussing the usefulness of MRI, it is necessary to consider the sites of development and internal attributes. There have been very few reports that have directly compared the usefulness of CT and MRI in evaluating mediastinal tumors. In an investigation of the diagnostic performance of CT and MRI in anterior mediastinal tumors, the diagnostic accuracy of CT and MRI was 83% and 84%, respectively, for thymomas; 38% and 13% for thymic carcinomas; 58% and 38% for teratomas; 35% and 27% for malignant germ cell tumors; and 55% and 43% for malignant lymphomas.[1)] Thus, the diagnostic performance of CT was comparable or superior to that of MRI in these solid anterior mediastinal tumors. Moreover, CT was significantly better than MRI in diagnosing teratomas.

Cystic mediastinal lesions, such as thymic cysts, bronchial cysts, and esophageal cysts, are known to show a variety of densities and signals on non-contrast CT and T1-weighted MRI images due to hemorrhage and protein content,[2)] making differentiation from solid tumors difficult. However, in the report mentioned above, the diagnostic performance of MRI (diagnostic accuracy, 71%) was significantly higher than that of CT (46%) for the diagnosis of thymic cysts.[1)] In an examination of the use of diffusion-weighted imaging to differentiate solid from cystic tumors of the mediastinum, the ADC values were significantly higher for cystic tumors than for solid tumors.[3)] Particularly when a contrast medium cannot be used, MRI can readily distinguish between cystic and solid tumors. Cystic teratomas, abscesses, and lesions that contain viscous fluids such as blood may show hyperintensity on diffusion-weighted imaging, and the ADC value may be relatively low. The signal intensities and ADC values of T1- and

T2-weighted images and diffusion-weighted images vary depending on the attributes of the intracystic fluid. Consequently, it may be possible to obtain additional information about the nature of the intracystic fluid by comprehensively evaluating each sequence.

In a report that compared the visualizability of various CT and MRI findings for thymic epithelial tumors, the visualization rate with CT and MRI was 18% and 75%, respectively, for the peritumoral capsule, 13% and 43% for intratumoral septa, and 5% and 17% for intratumoral hemorrhage. Thus, visualizability was significantly better with MRI. Moreover, visualization by MRI of a fibrous septum that divided the tumor or a capsule surrounding the tumor was found to be suggestive of a low-risk thymoma (Fig.).[4)] An examination of MRI findings and the WHO histological classifications of thymic epithelial tumors found that type A thymomas were often smaller than those of other tissue types, encapsulated, had a distinct border, and were round masses with smooth margins. It also found that thymic carcinomas were often internally inhomogeneous on T2-weighted images, frequently showed hypointense areas that reflected fibrous components in the lesion, and were often associated with mediastinal lymph node enlargement.[5)] Because CT and MRI are comparable for evaluating great vessel invasion of thymic epithelial tumors,[4)] MRI can be used for this purpose when contrast-enhanced CT cannot be performed for a reason such as iodine allergy. An investigation of the use of dynamic contrast-enhanced MRI for thymic epithelial tumors found that enhancement peaked early in noninvasive thymomas, while a late peak with a pattern of gradually increasing enhancement was seen in invasive thymomas and thymic carcinomas with an abundant intratumoral fibrous component.[6)] An investigation of the differentiation of thymic epithelial tumors, malignant lymphomas, and malignant germ cell tumors reported that a pattern of early enhancement and late washout on dynamic contrast-enhanced MRI was a characteristic of thymic epithelial tumors, while a pattern of gradually increasing enhancement was seen in malignant lymphomas and malignant germ cell tumors.[7)] An investigation of the differentiation of benign and malignant solid tumors of the mediastinum using diffusion-weighted imaging found that the ADC values of malignant tumors were lower than those of benign tumors.[8)] Particularly low ADC values have been reported for malignant lymphoma, reflecting high cell density.[8, 9)] Investigations of diffusion-weighted imaging for thymic epithelial tumors showed that ADC values were lower for high-risk thymomas and thymic carcinomas than for low-risk thymomas and also lower for advanced tumors of Masaoka stages III and IV than for early-stage tumors of stages I and II.[10, 11)] The use of diffusion-weighted imaging may provide additional information for the qualitative diagnosis of mediastinal tumors and the evaluation of their malignancy.

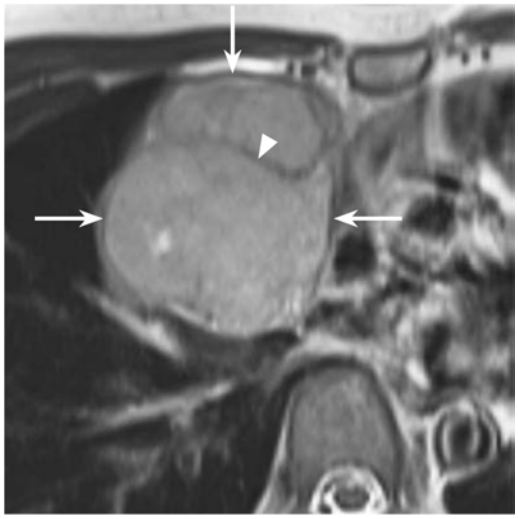

Figure. Low-risk thymoma (type AB thymoma)

MRI, T2-weighted transverse image: A lobulated mass with a distinct border and smooth margin is seen in the right anterior mediastinum. The entire circumference of the mass is covered with a hypointense capsule (→), and a hypointense septum (▷) that appears to divide the tumor interior is also seen.

In thymic hyperplasia, fat is often interposed between the thymic tissues, and the signal intensity is lower with opposed-phase chemical shift imaging (CSI) by MRI than with in-phase imaging. This has been found to be useful for differentiating from tumorous lesions such as thymomas.[12] A study examining the differentiation of thymoma from normal thymus and thymic hyperplasia in patients with myasthenia gravis found MRI to be superior to CT. The diagnostic accuracy rate of CT and MRI in a qualitative evaluation based on factors such as morphology and other attributes was 86.7% and 96.6%, respectively. Moreover, the diagnostic accuracy rate in a quantitative evaluation using non-contrast CT density and CSI signal changes was 75% and 98.9%, respectively.[13]

Nearly all tumors that develop in the posterior mediastinum are neurogenic tumors such as schwannomas, neurofibromas, ganglioneuromas, neuroblastomas, and paragangliomas, and MRI is useful for evaluating the relationships between tumors and structures such as nerves and intervertebral foramina.[14] In recent years, multiplanar reconstruction (MPR) has made it possible to easily perform evaluations using coronal and sagittal CT images, and the predominance of MRI is fading. However, an advantage of MRI is the high tissue contrast it provides, even with non-contrast-enhanced imaging. There have no reports that have compared the usefulness of CT and MRI in evaluating posterior mediastinal tumors.

Search keywords and secondary sources used as references

PubMed was searched using the following keywords: MRI, thymoma, thymic epithelial tumor, thymic hyperplasia, lymphoma, germ cell tumor, neurogenic tumor, mediastinum, and mediastinal tumor.

In addition, the following were referenced as secondary sources.

1) Japan Lung Cancer Society, Ed.: Guidelines for Diagnosis and Treatment of the Lung Cancer/Malignant Pleural Mesothelioma/Thymic Tumors 2020. KANEHARA & Co., 2021.

References

1) Tomiyama N et al: Anterior mediastinal tumors: diagnostic accuracy of CT and MRI. Eur J Radiol 69: 280-288, 2009
2) Murayama S et al: Signal intensity characteristics of mediastinal cystic masses on T1-weighted MRI. J Comput Assist Tomogr 19: 188-191, 1995
3) Shin KE et al: Diffusion-weighted MRI for distinguishing non-neoplastic cysts from solid masses in the mediastinum: problem-solving in mediastinal masses of indeterminate internal characteristics on CT. Eur Radiol 24: 677-684, 2014
4) Sadohara J et al: Thymic epithelial tumors: comparison of CT and MR imaging findings of low-risk thymomas, high-risk thymomas, and thymic carcinomas. Eur J Radiol 60: 70-79, 2006
5) Inoue A et al: MR imaging of thymic epithelial tumors: correlation with World Health Organization classification. Radiat Med 24: 171-181, 2006
6) Sakai S et al: Differential diagnosis between thymoma and non-thymoma by dynamic MR imaging. Acta Radiol 43: 262-268, 2002
7) Yabuuchi H et al: Anterior mediastinal solid tumours in adults: characterisation using dynamic contrast-enhanced MRI, diffusion-weighted MRI, and FDG-PET/CT. Clin Radiol 70: 1289-1298, 2015
8) Razek AA et al: Assessment of mediastinal tumors with diffusion-weighted single-shot echo-planar MRI. J Magn Reson Imaging 30: 535-540, 2009
9) Zhang W et al: A whole-tumor histogram analysis of apparent diffusion coefficient maps for differentiating thymic carcinoma from lymphoma. Korean J Radiol 19: 358-365, 2018
10) Abdel Razek AA et al: Diffusion-weighted MR imaging in thymic epithelial tumors: correlation with World Health Organization classification and clinical staging. Radiology 273: 268-275, 2014
11) Priola AM et al: Diffusion-weighted magnetic resonance imaging of thymoma: ability of the apparent diffusion coefficient in predicting the World Health Organization (WHO)classification and the Masaoka-Koga staging system and its prognostic significance on disease-free survival. Eur Radiol 26: 2126-2138, 2016
12) Inaoka T et al: Thymic hyperplasia and thymus gland tumors: differentiation with chemical shift MR imaging. Radiology 243: 869-876, 2007
13) Priola AM et al: Comparison of CT and chemical-shift MRI for differentiating thymoma from non-thymomatous conditions in myasthenia gravis: value of qualitative and quantitative assessment. Clin Radiol 71: e157-169, 2016
14) Sakai F et al: Intrathoracic neurogenic tumors: MR-pathologic correlation. AJR Am J Roentgenol 159: 279-283, 1992

BQ 31 Is CT recommended for distinguishing benign from malignant pleural lesions?

Statement

CT is useful for distinguishing benign from malignant pleural lesions and provides information that can be used to decide whether to perform thoracocentesis or thoracoscopy. Although it has limitations in detecting malignant disease, the use of contrast-enhanced CT is recommended.

Background

Pleural lesions are often asymptomatic, and detection by diagnostic imaging is important, However, the use of chest radiography to detect such lesions has limitations. The usefulness of differential diagnosis between benign and malignant tumors by CT was examined.

Explanation

Distinguishing pleural lesions from intrapulmonary lesions is not necessarily easy by chest radiography, and CT is therefore performed to diagnose pleural lesions. CT can provide information such as the extent and morphology of pleural lesions, their level of intrathoracic growth, and the presence or absence of bone destruction and chest wall invasion.

CT is considered capable of distinguishing between benign and malignant pleural lesions in the vast majority of cases. A 1990 retrospective study of CT in 74 patients with diffuse pleural disease (39 with malignant disease, 35 with benign disease; contrast media used except in those with asbestos exposure) used the following 4 parameters for diagnosis: ① circumferential/rind pleural involvement; ② nodular pleural thickening; ③ parietal pleural thickening greater than 1 cm; and ④ mediastinal pleural lesions. The results showed specificity of 100%, 94%, 94% and 88%, respectively, and sensitivity of 41%, 51%, 36%, and 56%, respectively. Moreover, the presence of 1 or more of these parameters enabled diagnosis in 28 of the 39 patients with malignancies.[1)] In a 2001 prospective study of contrast-enhanced chest CT in 40 patients with pleural effusion that used diagnostic criteria similar to those used in the study described above, evaluation of the pleural surface (nodular or irregular) enabled diagnosis in 28 of the 32 patients with malignant disease and all 8 patients with benign disease (sensitivity, 84%; specificity, 100%). The study found that circumferential pleural involvement/pleural rind was seen with nearly equal frequency in benign and malignant lesions and was, therefore, an unreliable finding.[2)] A 2002 retrospective study of the use of contrast-enhanced CT in 215 patients with pleural disease included 99 with malignant pleural mesothelioma (MPM), 39 with metastatic pleural disease (MPD), 32 with tuberculous pleurisy, 26 with empyema, and 19 with asbestos-related advanced benign pleural disease (ARBPD). Circumferential/rind pleural involvement was seen in 70% with MPM, 15% with MPD, 9% with tuberculous pleurisy, 5% with ARBPD, and none of the patients with empyema. Nodular pleural thickening was seen in 48% with MPM

and 13% with MPD; it was not seen with tuberculous pleurisy or empyema, but was seen in 16% with ARBPD. Pleural thickening greater than 1 cm was observed in 59% with MPM, 17% with MPD, 75% with tuberculous pleurisy, 61% with empyema, and 53% with ARBPD. Pleural thickening greater than 1 cm is therefore considered unreliable as a diagnostic finding. Mediastinal pleural lesions were found in 85% with MPM, 33% with MPD, 22% with tuberculous pleurisy, 12% with empyema, and 16% with ARBPD.[3)] A 2005 investigation of 146 patients (59 patients with malignant disease and 87 with benign disease) used similar diagnostic criteria: ① pleural nodularity; ② pleural rind; ③ pleural thickening greater than 1 cm; and ④ mediastinal pleural involvement. The results showed specificity of 97%, 97%, 85%, and 87%, respectively, and sensitivity of 37%, 22%, 31%, and 35%, respectively. Thus, low sensitivity was seen.[4)] Findings from evaluations of the pleural surface (nodular or irregular) and the presence of mediastinal pleural lesions are particularly reliable findings, and circumferential pleural involvement/pleural rind and parietal pleural thickening greater than 1 cm are findings with high specificity that can be used for reference depending on the circumstances (Figs. 1 and 2). However, all of the studies indicate that sensitivity is limited to a certain extent. A contrast medium should be used.

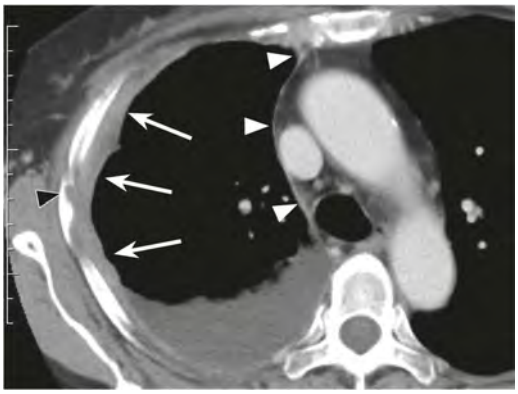

Figure 1. Malignant pleural mesothelioma

Contrast-enhanced CT, transverse image: Irregular parietal pleural thickening (11 mm, →) and pleural effusion are seen, accompanied by mediastinal pleural lesions (▷) and rib invasion (►).

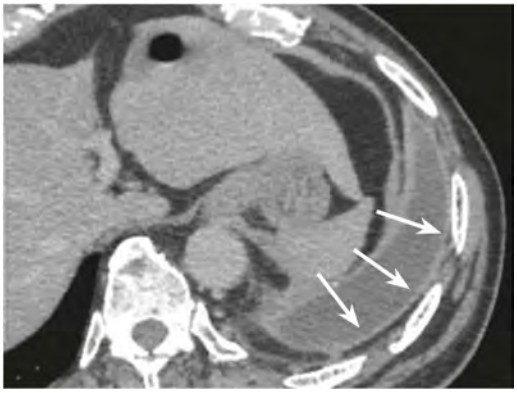

Figure 2. Tuberculous pleurisy

Contrast-enhanced CT, transverse image: Smooth parietal pleural thickening (4 mm, →) and pleural effusion are seen.

In a retrospective study of 370 patients who underwent thoracoscopy (211 patients with malignant disease and 159 with benign disease), sensitivity was 68% for CT reports of imaging performed before thoracoscopy that indicated malignant disease, and specificity was 78% for reports that indicated benign disease. Moreover, the positive predictive value was 80%, and the negative predictive value was only 65% for reports that indicated malignant disease.[5)]

Malignant pleural disease is often present even in the absence of CT findings indicating malignancy. It is therefore difficult to exclude malignancy based on CT alone.[4, 5)] Even in the absence of CT findings indicating malignancy, the possibility of clinical malignancy should be considered, and the appropriate means of thorough examination by thoracocentesis or thoracoscopy selected.

Search keywords and secondary sources

PubMed was searched using the following keywords: pleural tumor, pleural mesothelioma, differential diagnosis, and CT.

In addition, the following were referenced as secondary sources.

1) Japan Lung Cancer Society, Ed.: Guidelines for Diagnosis and Treatment of the Lung Cancer/Malignant Pleural Mesothelioma/Thymic Tumors 2018. KANEHARA & Co., 2018.

References

1) Leung AN et al: CT in differential diagnosis of diffuse pleural disease. AJR Am J Roentgenol 154 (3): 487-492, 1990
2) Traill ZC et al: Thoracic computed tomography in patients with suspected malignant pleural effusions. Clin Radiol 56 (3): 193-196, 2001
3) Metintas M et al: Computed tomography features in malignant pleural mesothelioma and other commonly seen pleural diseases. Eur J Radiol 41 (1): 1-9, 2002
4) Yilmaz U et al: CT in differential diagnosis of benign and malignant pleural disease. Monaldi Arch Chest Dis 63 (1): 17-22, 2005
5) Hallifax RJ et al: Role of CT in assessing pleural malignancy prior to thoracoscopy. Thorax 70 (2): 192-193, 2015

BQ 32 Is PET/CT recommended for diagnosing malignant pleural mesothelioma?

Statement

Although PET/CT has limitations for determining the degree of progression of primary tumors, it is useful for diagnosing lymph node and distant metastases, for patients considering surgical resection, and those with suspected posttreatment metastasis or recurrence.

Background

Malignant pleural mesothelioma has been shown to be closely associated with asbestos exposure, and it is a malignancy with an extremely poor prognosis. There is concern that the number of patients with this disease in Japan will increase between 2020 and 2030. The reasons for its poor prognosis include the fact that no method of early detection or standard treatment has been established.

PET/CT has been established to be useful for clinical staging malignancies and diagnosing metastasis and recurrence. However, malignant pleural mesothelioma is a relatively rare disease, and most of the reported studies on the usefulness of PET/CT in diagnosing it have been single-center studies. Moreover, there have been few systematic reviews or meta-analyses of the relevant literature.[1, 2] This section summarizes the literature on the usefulness of PET/CT in clinically staging malignant pleural mesothelioma and diagnosing its metastasis and recurrence.

Explanation

Diagnostic imaging plays a major role in diagnosing malignant pleural mesothelioma and evaluating the response to treatment. One aspect of this role, clinical staging, is important for its strong influence on treatment strategy. The most commonly used staging classification for this disease is currently TNM staging established by the International Mesothelioma Interest Group.

Diagnostic imaging modalities such as CT, MRI, and PET/CT are used as appropriate to determine the clinical stage. CT may in some cases underestimate changes such as chest wall invasion and mediastinal lymph node metastasis. However, it is widely available and offers excellent cost-effectiveness. It is therefore often the first choice for the diagnostic imaging of malignant pleural mesothelioma. PET/CT is considered effective for purposes such as detecting unforeseen distant metastasis that cannot be identified with the normal diagnostic imaging methods, and it can aid in selecting an appropriate treatment.

1. Usefulness of PET/CT in clinical staging

① T stage

Accurate T staging is vital for the surgical resection of a tumor. Particularly important is differentiating between T3 tumors, which are resectable even when locally advanced, and T4 tumors, which are unresectable when locally advanced. However, microinvasion of the abdominal cavity by tumors can occur transdiaphragmatically, making it difficult to accurately determine the degree of progression with either CT or PET/CT.[3)]

The reported sensitivity of PET/CT in T4 diagnosis ranges from 67% to 78%, and identifying transdiaphragmatic invasion of the abdominal cavity and invasion of the pericardium was found to be difficult with PET/CT.[4, 5)] Thoracoscopy or laparoscopy should be considered if diagnostic imaging suggests that lesions may have spread to the contralateral side of the thoracic cavity or abdominal cavity.

② N stage

Mediastinal lymph node metastasis of malignant pleural mesothelioma is an adverse prognostic factor. In evaluating hilar or mediastinal lymph node metastasis using CT, a lymph node with a short-axis diameter of ≥ 1 cm is often considered positive. Examination of the diagnostic performance of CT in evaluating mediastinal lymph node metastasis showed that sensitivity and specificity were 60% and 71%, respectively, and mediastinal lymph node diagnostic performance with MRI was comparable to the diagnostic performance with CT.

The reported sensitivity, specificity, and diagnostic accuracy rate of PET/CT in mediastinal lymph node diagnosis (N2) ranged from 11% to 50%, 78% to 93%, and 59% to 66%, respectively, which resulted in part from false negatives for micrometastasis and false positives caused by inflammation. Thus PET/CT has certain limitations in diagnosing hilar or mediastinal lymph node metastasis.[4-6)] However, in a comparative investigation of CT, PET, PET/CT, and MRI in operable (stage II and III) malignant pleural mesothelioma conducted by Plathow et al., the diagnostic accuracy rate of PET/CT was the highest obtained.[7)]

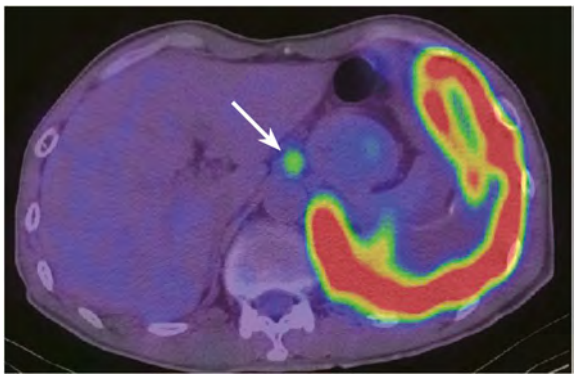

Figure. Malignant pleural mesothelioma

PET/CT fusion image, transverse image: FDG accumulation consistent with left pleural lesions is seen. FDG accumulation is also seen in an abdominal lymph node (→), suggesting lymph node metastasis.

③ M stage

Distant metastasis of malignant pleural mesothelioma occurs as unifocal or multifocal metastases in areas such as the brain, lungs, liver, adrenal glands, abdominal lymph nodes, and bones (Fig.). Erasmus et al. reported that extrathoracic metastasis that could not be identified with normal diagnostic imaging was detectable by PET/CT in 24% of patients.[4] Thus, PET/CT is useful for improving the accuracy of distant metastasis diagnosis and, therefore, may contribute to identifying patients who are candidates for surgery and inhibiting early postoperative recurrence.

2. Usefulness of PET/CT in diagnosing posttreatment metastasis and recurrence

Examination of the diagnostic performance of PET/CT with respect to local recurrence and distant metastasis occurring after treatment has shown sensitivity and specificity of 94% to 98% and 75% to 100%, respectively. PET/CT is highly useful when there are signs of malignant pleural mesothelioma recurrence, and recurrence and metastasis cannot be determined with other methods of diagnostic imaging.[8, 9]

Search keywords and secondary sources

PubMed was searched using the following keywords: mesothelioma, PET, and CT. The period searched was from 2015 to June 2019, and there were no new studies that should have been selected for review.

In addition, the following were referenced as secondary sources.

1) David S: NCCN Guidelines®: non-small cell lung cancer Ver 5. 2021. National Comprehensive Cancer Network, 2021
2) David S: NCCN Guidelines®: small cell lung cancer Ver 2. 2021. National Comprehensive Cancer Network, 2021

References

1) Basu S et al: Current evidence base of FDG-PET/CT imaging in the clinical management of malignant pleural mesothelioma: emerging significance of image segmentation and global disease assessment. Mol Imaging Biol 13: 801-811, 2011
2) Zahid I et al: What is the best way to diagnose and stage malignant pleural mesothelioma? Interact Cardiovasc Thorac Surg 12: 254-259, 2011
3) Wilcox BE et al: Utility of integrated computed tomography-positron emission tomography for selection of operable malignant pleural mesothelioma. Clin Lung Cancer 10: 244-248, 2009
4) Erasmus JJ et al: Integrated computed tomography-positron emission tomography in patients with potentially resectable malignant pleural mesothelioma: staging implications. Thorac Cardiovasc Surg 129: 1364-1370, 2005
5) Sørensen JB et al: Preoperative staging of mesothelioma by 18F-fluoro-2-deoxy-D-glucose positron emission tomography/computed tomography fused imaging and mediastinoscopy compared to pathological findings after extrapleural pneumonectomy. Eur J Cardiothorac Surg 34: 1090-1096, 2008
6) Pilling J et al: Integrated positron emission tomography-computed tomography does not accurately stage intrathoracic disease of patients undergoing trimodality therapy for malignant pleural mesothelioma. Thorac Cardiovasc Surg 58: 215-219, 2010
7) Plathow C et al: Computed tomography, positron emission tomography, positron emission tomography/computed tomography, and magnetic resonance imaging for staging of limited pleural mesothelioma: initial results. Invest Radiol 43: 737-744, 2008
8) Tan C et al: Role of integrated 18-fluorodeoxyglucose position emission tomography-computed tomography in patients surveillance after multimodality therapy of malignant pleural mesothelioma. J Thorac Oncol 5: 385-388, 2010
9) Gerbaudo VH et al: FDG PET/CT patterns of treatment failure of malignant pleural mesothelioma: relationship to histologic type, treatment algorithm, and survival. Eur J Nucl Med Mol Imaging 38: 810-821, 2011

4
Cardiovascular

Standard Imaging Methods for the Cardiovascular Region

A CT

Overview

1. Imaging and image reconstruction methods using ECG gating

The purpose of cardiac CT is often to evaluate the coronary arteries. Computed tomography angiography (CTA) and calcification scoring of the coronary arteries are performed for this purpose (Fig. 1). There are also various other applications of cardiac CT, such as myocardial wall motion evaluation (functional evaluation), tumor evaluation, and evaluation for atrial fibrillation ablation therapy.

Advancements in CT systems are important for the development of cardiac CT examination. The imaging method used varies depending on the type of equipment used, such as wide-detector (256 to 320 rows) MDCT, dual-source CT, and 64-row MDCT systems. This discussion focuses on cardiac CT using 64-row MDCT systems, the most widely available and basic type.

With the temporal resolution of CT, imaging of the heart while it is beating results in motion artifacts, which prevents accurate depiction of the structures of the heart, particularly the coronary arteries. In the mid-diastolic phase of the cardiac cycle (corresponding to 70% to 80% of the R-R interval), there is a period in which the heart moves slowly, and this brief period is used in coronary CTA. For example, if the heart rate is stable at approximately 60 beats per minute, 1 beat occurs per second, so the mid-diastolic phase lasts approximately 0.2 seconds. To accurately identify this brief period, ECG triggering or gating is required with cardiac CT. However, if the heart rate is high, imaging during systole (approximately 40% of the R-R interval) is often more appropriate than imaging during diastole. Because better image quality can generally be obtained with a low heart rate, it is important to control the heart rate using a beta-blocker (beta-1 selective). The beta-blocker is administered orally 1 hour before the test, by intravenous injection 5 minutes before the test, or both orally and intravenously. The optimal heart rate is below 60 beats per minute.

To obtain CT images, data for at least a half rotation plus the cone angle (half data) are required. In cardiac CT, reconstructing images from data for 1 rotation (full data) results in image quality improvement commensurate with the volume of data (image noise is reduced). However, cardiac motion greatly affects image quality, making it difficult to evaluate the coronary arteries. Consequently, image reconstruction in cardiac CT is performed based on half data (half reconstruction) to improve the temporal resolution. Split reconstruction (segment reconstruction and multisector reconstruction), wherein half data are obtained from the data for multiple heartbeats, is also used and may further increase the temporal resolution.

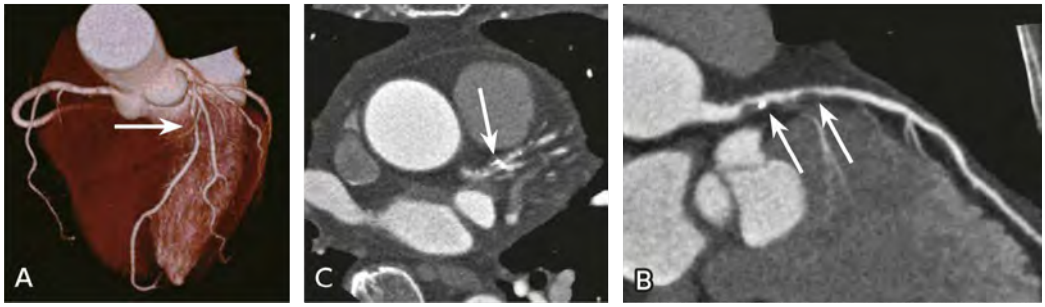

Figure 1. Coronary artery evaluation by cardiac CT

A: Volume rendering (VR) image; B: Original image, transverse; C: Curved MPR image
Severe stenosis resulting from a plaque with calcification is seen proximally in a coronary artery (left anterior descending artery).

There are two methods of ECG-gated CT. One is prospective ECG-gated scanning (ECG triggering), in which imaging is performed only during the ECG phase in which the pre-specified coronary artery motion is still (generally the mid-diastolic phase). The other method is retrospective ECG-gated reconstruction. With this method, data are acquired for all ECG phases, and image reconstruction is performed later by extracting images of interest for the cardiac standstill phase from the data. With 64-row MDCT, the extent that can be scanned at one time is limited to 3 to 4 cm, and cardiac CT images are generally acquired by retrospective ECG-gated reconstruction, which results in increased radiation exposure.

In recent years, wide-detector MDCT, which can allow high-speed rotation and cover the entire heart, and dual-source CT, which provides twice the temporal resolution, have also become widely used, and the use of prospective ECG-gated scanning has increased. These methods hold promise for reduced radiation exposure and high image quality.

2. Cardiac CT pretreatment, imaging, and contrast imaging protocols

Prospective ECG-gated scanning is generally performed for calcification scoring. Reconstruction is performed using a tube voltage of 120 kVp and a slice thickness of 2.5 to 3 mm. Tube current is determined according to body type to minimize radiation exposure, which should be approximately 1 to 2 mSv. Using dose modulation (Auto mA), image noise (SD) of 20 HU is commonly targeted.

With coronary CTA, breath-holding is practiced before the test. This is to prevent deviation from the imaging range, inhibit blurring caused by respiratory motion, and determine the changes in heart rate that occur during breath-holding. Physiologically, the heart rate often decreases during breath-holding. Therefore, depending on the circumstances, the dose of the intravenous beta-blocker used for coronary CTA can be reduced or its use avoided. Conversely, heart rate sometimes increases with breath-holding, and this information is useful for selecting the imaging and reconstruction methods. In addition, a nitrate preparation is recommended to dilate the coronary arteries and allow for more detailed coronary artery evaluation. However, because nitrate use generally increases the heart rate, it should be observed after a nitrate preparation is used.

For coronary CTA, an indwelling needle (20 G) is placed in the antecubital vein, and the contrast medium is injected using a dual-head automatic injector. The needle is attached to an extension tube and 3-way stopcock fitted with a syringe containing physiologic saline, and the apparatus can be flushed with contrast medium and physiologic saline. The 3-way stopcock is convenient for administering an injectable beta-blocker before the test. A high-concentration nonionic iodine contrast medium (350 to 370 mgI/mL) is used. Rapid injection is recommended, with an injection rate of 25 mgI/kg/s (fractional dose) considered standard.

Bolus tracking or test injection is used to determine the scan timing. With bolus tracking, a single-slice dynamic scan is performed before the actual scan, and the CT number in the blood vessel (aorta) is monitored in real time. When the target CT number is reached, the scan starts after a predefined time delay. The test injection method involves bolus injection of a small amount of contrast medium (10 to 20 mL) and measuring the contrast arrival time and time to peak contrast concentration from a single-slice dynamic scan to determine the timing of the actual scan.

Detailed discussion

1. Evaluating coronary artery lesions

A coronary artery calcification index (Agatston score) is calculated for the calcification score. The calcification score is useful for evaluating the risk associated with coronary artery lesions. For evaluating coronary lesions over time, maintaining consistent imaging conditions is important.

Coronary CTA provides particularly high sensitivity and negative predictive value for evaluating anatomical coronary artery stenosis. It plays a central role in current cardiovascular medicine as a noninvasive test for ischemic heart disease. It is useful for evaluating not only the severity of coronary artery stenosis, but also the characteristics of coronary artery plaques themselves (Fig. 2). It is also used for purposes such as evaluating coronary artery aneurysms associated with conditions such as Kawasaki disease, coronary artery malformation, and coronary artery bypass grafts (Fig. 3) and for evaluation after coronary stent placement (Fig. 4). However, coronary artery stent evaluations are affected by a number of factors, such as the stent material, coexisting calcification, and motion artifacts. Consequently, stents ≥ 3 mm in diameter that have been placed proximally in coronary arteries are indicated for stent evaluation at present.

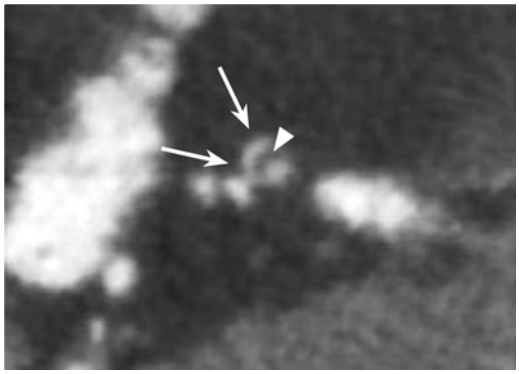

Figure 2. Evaluation of the characteristics of a coronary artery plaque (coronary CTA)

Short-axis MPR image of a coronary artery: A central necrotic core (hypodense component: ▷) and enhancement of the plaque margin (→) are seen. Referred to as a napkin-ring sign, it is a finding that indicates an unstable plaque.

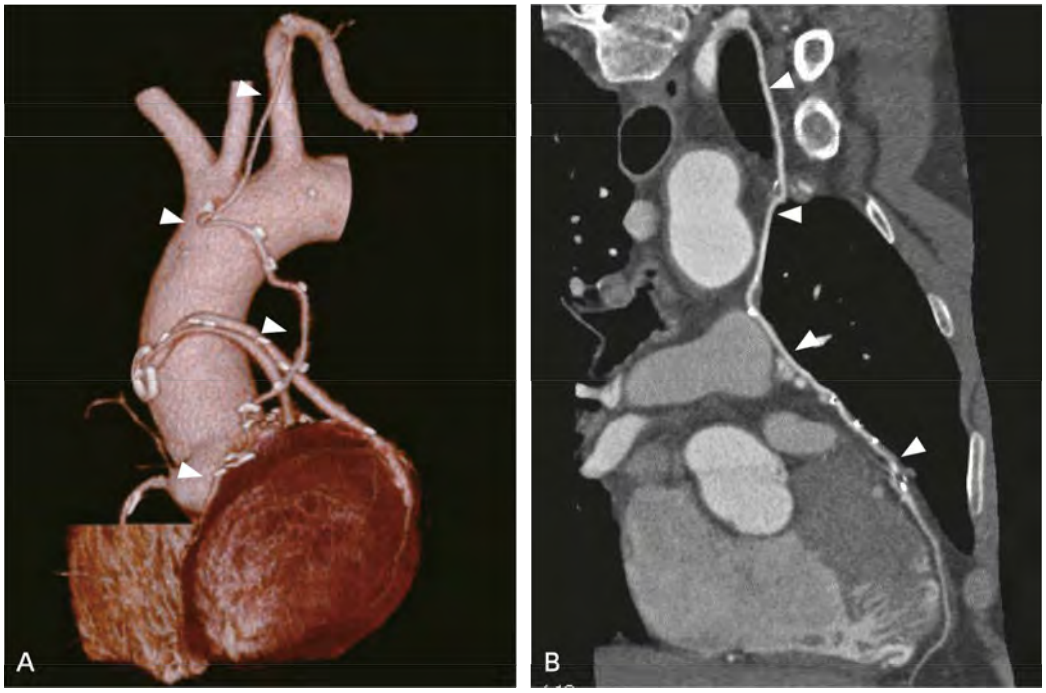

Figure 3. Evaluation of a graft after coronary artery bypass surgery (coronary CTA)

A: VR image, B: curved MPR image

Following coronary artery bypass surgery, the coronary artery (left anterior descending) is anastomosed to the left internal thoracic artery (▷). In addition, a diagonal branch and the circumflex artery are anastomosed, with the greater saphenous vein used as a graft.

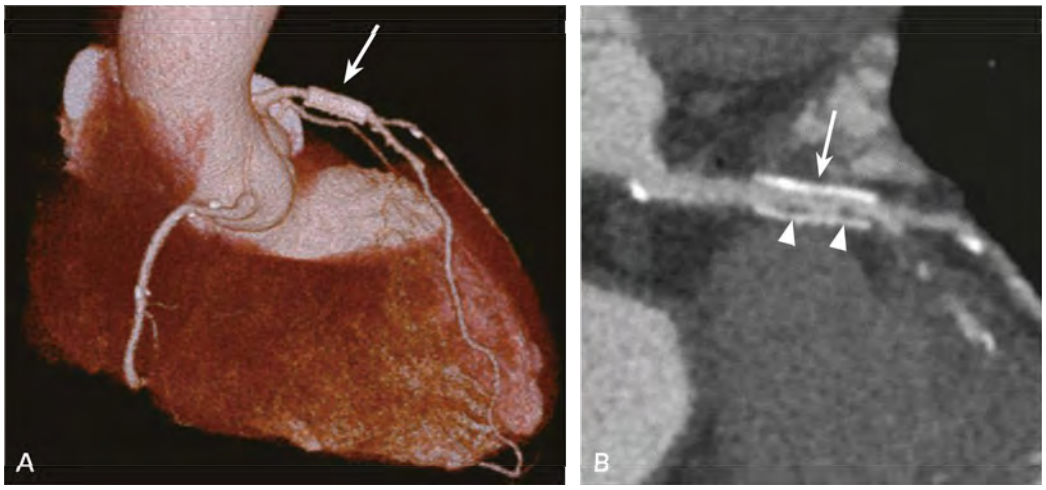

Figure 4. Evaluation after coronary stent placement (coronary CTA)

A: VR image, B: curved MPR image

A stent has been placed (→) proximally in the coronary artery (left anterior descending). Although the stent is patent, a hypodense component is seen in the lumen, suggestive of restenosis (▷).

2. Evaluating myocardial ischemia

The severity of anatomical coronary artery stenosis is not always consistent with that of a coronary lesion that induces hemodynamic myocardial ischemia. The methods used to evaluate functional stenosis by CT are myocardial CT perfusion imaging using pharmacological stress and fractional flow reserve CT (FFR-CT). Myocardial CT perfusion has disadvantages such as increased radiation exposure and a long test duration. However, an advantage is that it enables myocardial blood flow to be evaluated directly, and recent advances in CT systems and imaging technology have significantly reduced radiation exposure. FFR-CT is a simulation technique that estimates the myocardial fractional flow reserve (FFR) based on coronary CTA data.

3. Other cardiac evaluations

Coronary CT is also used to evaluate the location and size of the heart and blood vessels, fatty degeneration of the myocardium, cardiac tumors, valves, ventricle walls, the pericardium, and pericardial effusion accumulation. Appropriate indications for contrast-enhanced CT include evaluating intracardiac thrombus, cardiac tumors, pericardial and pericardiac lesions (inflammation and tumors), and congenital heart disease. With retrospective ECG-gated reconstruction, images can be acquired continuously in all ECG phases, enabling cardiac function, wall motion, and valve dynamics to be evaluated.

B MRI

Cardiac MRI

1. Overview

Cardiac MRI is an excellent noninvasive diagnostic modality for obtaining a wide variety of information, such as cardiac function, myocardial blood flow, myocardial viability, and coronary artery disease. Cardiac MRI enables all such essential information to be obtained with a single examination (so called one-stop shopping). However, the examination time is long and places a burden on the patient. Consequently, in actual practice, the appropriate imaging sequence is often selected according to the target disease or condition, and the purpose of the examination.[8, 9)]

① MR scanner and field strength considerations

Cardiac MRI always requires high temporal resolution to overcome the effects of heartbeats and respiratory motion. Use of a high-performance system is therefore necessary. Although systems with a magnetic field strength of 1.5T are most commonly used for cardiac MRI, examinations can also be performed with 3T systems. With 3T systems, sequences such as perfusion MRI and late gadolinium enhancement are beneficial for improving the signal-to-noise ratio (SNR). However, balanced steady-state free precession (bSSFP) imaging, a sequence used in cine MRI, is prone to problematic artifacts such as dark banding artifacts and flow artifacts, necessitating careful shimming.[10)]

② Specific surface coil and ECG-gating

A multi-element (typically ≥ 8 elements) surface coil for cardiac use is recommended. This allows improved temporal resolution using parallel imaging. ECG gating is typically used concurrently while acquiring images. Electrical signals should be collected in 3 dimensions with vector electrocardiography.

③ Reference cross-sections

In an actual examination, imaging is performed according to several reference cross-sections. As with other tomographic imaging methods such as echocardiography, the reference cross-sections make it easy to compare the results obtained using common cross-sections. Basic cross-sections include short-axis images of the left and right ventricles, perpendicular long-axis images of the left and right ventricles, horizontal long-axis images, 4-chamber long-axis images, 3-chamber long-axis images of the left ventricle, and long-axis images of the right ventricular outflow tract (RVOT).

2. Detailed discussion

① Cine imaging

Cine imaging can evaluate cardiac wall motion and function. It is currently the method that provides the most accurate and reproducible evaluations.[11)] The bSSFP sequence is used for cine imaging. With 3T systems, however, GRE is considered if artifacts become problematic.

When evaluating left ventricular structure and function, acquisition of left ventricle short-axis images from the mitral valve to the apex (Fig. 5A) is fundamental, and the images are used to measure left ventricular volume. In addition, horizontal long-axis images, 4-chamber long-axis images (Fig. 5B), perpendicular long-axis images of the left ventricle (Fig. 5C), and 3-chamber long-axis images of the left ventricle (Fig. 5D) are acquired and evaluated.

To evaluate right ventricular structure and function, right ventricle short-axis images are used. However, axial images can be used to measure right ventricular volume.[10] In addition, perpendicular long-axis images of the right ventricle and long-axis images of the RVOT are acquired and evaluated.

If evaluating interventricular interactions or performing conventional cine imaging is difficult (e.g., due to arrhythmias, breath-holding difficulty), real-time cine imaging can be used. However, it should be noted that the accuracy of quantitative evaluations may be lower due to the low temporal resolution.

It has recently become possible to quantitatively evaluate myocardial strain from conventional cine imaging images using the feature tracking method. This has been found to be useful for early diagnosis and outcome prediction in myocardial ischemia and many cardiomyopathies, and it is used as an optional technique.[12]

② First pass perfusion

Myocardial perfusion imaging involves intravenous bolus injection of gadolinium contrast medium and evaluating myocardial blood flow based on first-pass hemodynamics. It is used to diagnose myocardial ischemia.[13] It has high detectability to diagnose ischemia and is excellent for diagnosing subendocardial ischemia and severe 3-vessel disease, which are difficult to diagnose with conventional SPECT.[14]

The pulse sequences are typically saturation recovery (SR) imaging with bSSFP, GRE, or GRE-EPI hybrid read out. Left ventricle short-axis images (at least 3 slices per heartbeat) are acquired, with images acquired for every heartbeat. Coronary vasodilators such as adenosine, ATP, and dipyridamole are normally used in evaluating ischemia.

③ Late gadolinium enhancement (LGE)

With this technique, image acquisition is performed after gadolinium contrast medium is injected intravenously, when the concentration of contrast in the blood and extracellular fluid reaches equilibrium. The reduction in myocardial cell volume and myocardial fibrosis (increased extracellular fluid fraction) are then evaluated.[15] LGE MRI makes it possible to visualize myocardial lesions with high reproducibility. It has been shown to be useful for differential diagnosis and prognosis assessment in a variety of diseases, such as cardiomyopathy, myocarditis, and ischemic heart disease, in particular.[16]

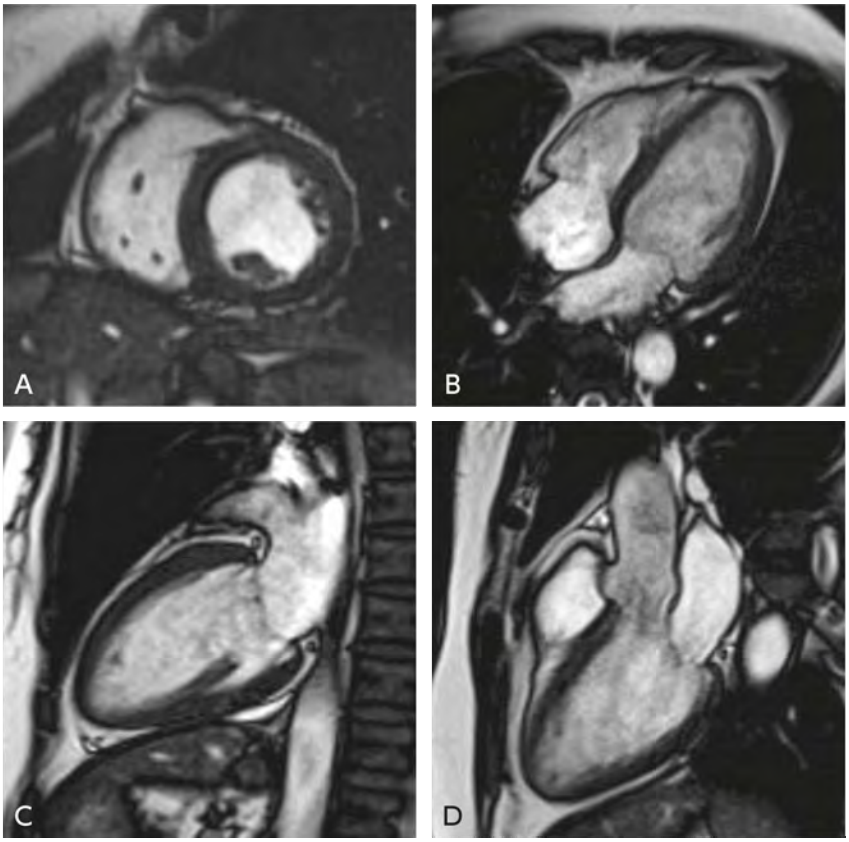

Figure 5. Cine imaging (bSSFP sequence) in a healthy individual

A: Left ventricle short-axis image, B: 4-chamber long-axis image, C: Perpendicular long-axis images of the left ventricle, D: 3-chamber long-axis image of the left ventricle

When adequate breath-holding is possible, the pulse sequences are a 2D IR GRE, 2D IR bSSFP, phase–sensitive IR (PSIR), or 3D sequence.[10] If the patient has an arrhythmia or difficulty with breath-holding, a single-shot bSSFP sequence is used.

Specifying an appropriate time of inversion (TI) nulls the signal intensity of normal myocardium, enabling a lesion to be visualized as a distinct hyperintensity (Fig. 6).

LGE is performed after waiting for at least 10 minutes after gadolinium contrast medium injection. However, if the dose of contrast medium is low, LGE is performed less than 10 minutes after injection; otherwise, adequate lesion visualization cannot be obtained.

④ Coronary MRA

Coronary MRA is used mainly to evaluate coronary artery morphology in the case of coronary artery malformation or coronary artery aneurysms associated with Kawasaki disease, or when a contrast medium cannot be used.[8] It has the advantages that it can be performed without the use of a contrast medium or radiation exposure. However, its spatial resolution does not equal that of X-ray coronary angiography or coronary CTA.

The 3D sequence, which images the entire heart at once, is commonly used. Imaging is performed under free-breathing conditions in combination with respiratory gating (navigator echo method), which is highly accurate.[17, 18] If respiratory gating cannot be used, or poor imaging quality is obtained, breath-hold imaging is also considered. Blood vessel visualization can also be improved using a gadolinium contrast medium.

⑤ Blood flow measurement

MRI is used to evaluate blood flow status and intracardiac shunts in valvular heart disease, aortic disease, and congenital heart disease. In coronary artery disease, it is also used to evaluate blood flow in coronary arteries and bypass grafts, and to determine coronary flow reserve by measuring blood flow in the coronary sinus.[8]

Figure 6. Late gadolinium enhancement (3D IR GRE sequence) of myocardial infarction (old infarct)

A: Left ventricle short-axis image, B: 4-chamber long-axis image, C: Perpendicular long-axis image of the left ventricle
Contrast enhancement is seen in an infarct centered on the region from the anterior wall of the left ventricle to the interventricular septum (→).

The sequence most commonly used to measure blood flow is phase contrast cine GRE with the flow encoding set perpendicular to the imaging plane. With phase contrast MRI, phase contrast images are obtained in addition to normal magnitude images, and the signal of phase contrast images is proportional to blood flow velocity.

Four-dimensional flow MRI, which can perform 3D measurements in multiple planes and enable serial observations, has become widely available in recent years, and its use is considered whenever possible.[19]

⑥ Advanced tissue characterization

Methods used to evaluate myocardial characteristics include T1 mapping, T2 mapping, T2-weighted imaging, and T2*mapping.[10,20] This area is a rapidly developing field, and the imaging methods that can be used vary between manufacturers and systems. It should be noted that the normal values vary depending on the facility, system, and sequence used.[20]

MRI and MRA of the aorta and peripheral vasculature

1. Overview

The main purpose of MRI and MRA in the aorta and peripheral vasculature is to evaluate lumen diameter and hemodynamics in combination with vessel wall assessment.[21] The MRA is categorized as contrast-enhanced MRA, which is performed with intravenous injection of gadolinium contrast medium, and non-contrast-enhanced MRA, which is performed without the contrast medium.[22] Contrast-enhanced MRA is little affected by blood flow velocity, enabling highly reproducible images to be obtained in a short time. However, it has been shown to be associated with a risk of nephrogenic systemic fibrosis (NSF) in patients with severe nephropathy, and its use has declined in recent years with advances in non-contrast-enhanced MRA imaging methods. Cine MRI and methods that involve the intravenous bolus injection of contrast medium are used to evaluate hemodynamics. Imaging methods such as SE are used to evaluate the vessel walls. Recently, however, the method called plaque imaging, the purpose of which is to perform qualitative plaque assessment, has been introduced into practical use, particularly for evaluating the carotid arteries.[23]

2. Detailed discussion

① Contrast-enhanced MRA

Contrast-enhanced MRA uses the T1 attenuation effect of blood to visualize the vessel lumen as a hyperintensity with gadolinium contrast medium. A fast 3D GRE sequence is typically used. Its strengths are that it is little affected by blood flow velocity or direction or by turbulence, and it enables extensive imaging in a relatively short time.[24] Following an intravenous bolus of contrast medium, hemodynamics is observed by continuously collecting multiphase data using imaging techniques with high temporal resolution.

② Non-contrast-enhanced MRA

Typical imaging methods are time-of-flight (TOF) sequences, which use the blood influx effect, and phase contrast (PC) sequences, which reflect the spin phase contrast of blood flow. However, PC sequences are used only for the evaluation of function that reflects phase information. TOF sequences comprise 3D TOF and 2D TOF sequences. The former are used mainly for arteries with high blood flow velocity that require high spatial resolution, such as the craniocervical arteries. The latter are appropriate for blood flow visualization in vessels with low flow rates, such as the arteries and veins of the extremities. Recently, ECG-gated 3D fast SE sequences (Fig. 7) and bSSFP sequences are also being used (Fig. 8A). ECG-gated 3D fast SE sequences use the differences in the blood flow patterns in systole and diastole determined using ECG gating. The bSSFP sequences reflect T2/T1 contrast and visualize the blood as hyperintensity.[25]

③ MRI

SE and fast SE sequences are commonly used. Blood flow in the lumen and the characteristics of the vessel wall can be clearly visualized without using a contrast medium. The imaging time is generally long,

and the images are susceptible to respiratory artifacts and signals from turbulence and slow blood flow. To suppress blood flow signals and prevent artifacts, the black blood sequence, which uses a double IR pulse, is used (Fig. 8B).[26)]

Numerous sequences have been proposed for plaque imaging, and it has not been standardized. In essence, however, blood flow signals are suppressed using double saturation pulses or a double IR pulse, and features such as intraplaque hemorrhage and the fibrous components of plaques are evaluated.[23)]

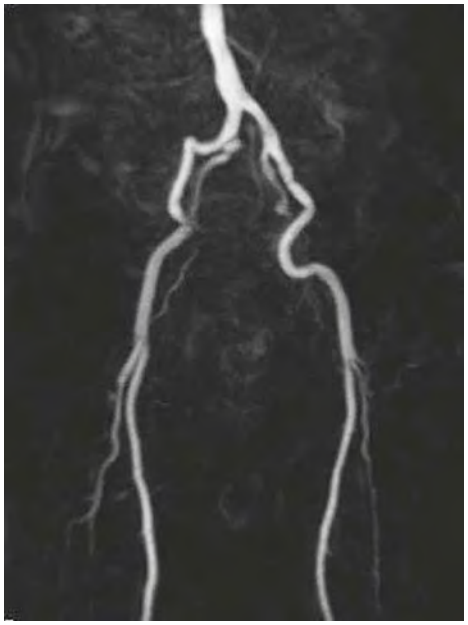

Figure 7. Non-contrast-enhanced MRA from the pelvis to femoral region in arteriosclerosis obliterans (ECG-gated 3D fast SE sequence)

Extended tortuosity is seen in the iliac artery. However, no apparent occlusion or significant stenosis is seen in the visualized extent.

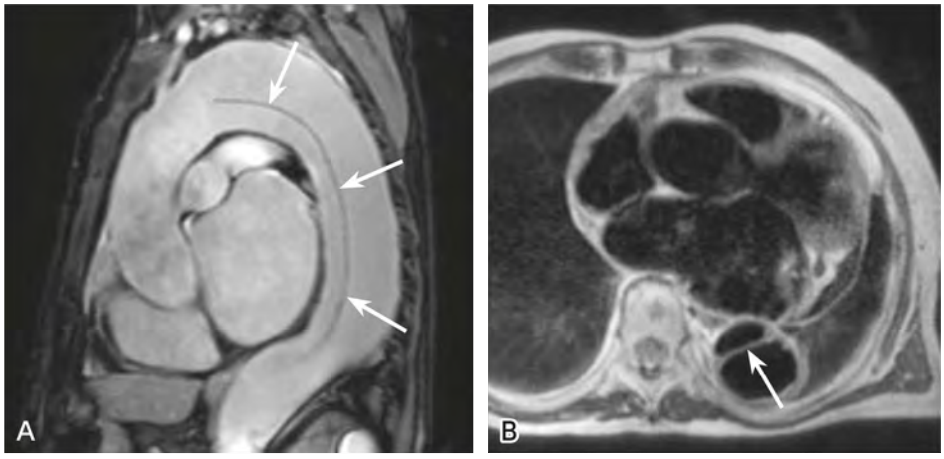

Figure 8. Non-contrast-enhanced MRI (MRA) of a communicating aortic dissection

A: bSSFP sequence, sagittal image; B: Black blood sequence, transverse image
The flap is clearly visualized (→).

C Angiography

Overview

With the development of noninvasive imaging modalities such as CT, MRI, and ultrasonography, angiography is being used less frequently as definitive diagnostic imaging in the cardiovascular region. Although cardiac catheterization (coronary angiography) remains a gold standard for examining coronary artery disease, the role of angiography is shifting to that of a therapeutic adjunct for the great vessels and peripheral vessels. However, angiography has some advantages not provided by other modalities, and it is therefore important to understand and take advantage of its features.

1. Features of angiography

Vascular structure and territory can be imaged in detail with angiography by selectively administering contrast medium to the vessel of interest. Imaging was initially performed using X-ray film in single shots. In addition to real-time fluoroscopy, continuous imaging by automatic film exchange became possible. Subsequently, the manual subtraction method was proposed, in which two X-ray films were used to perform imaging before and after contrast medium administration, and this particularly came to be used for cranial angiography.

Since digital image data became available, serial imaging and semi-automatic subtraction methods have become widely used. In particular, the subtraction technique, which is called digital subtraction angiography (DSA), is commonly used in thoracic and abdominal angiography.

Spatial and temporal resolutions are generally higher than with other imaging modalities. However, this procedure is highly invasive because selective imaging requires the use of a catheter. Imaging can also be performed with intravenous contrast agents, but resolution is reduced in areas of low contrast medium concentration. Consequently, selective imaging with transarterial contrast medium injection is normally performed.

Imaging frame rates of up to 15 to 30 fps can be selected, although this depends on the system. Taking into account radiation exposure, imaging with the minimum frame rate required for the pathology is recommended.

The direction and velocity of blood flow can be qualitatively evaluated by observing angiograms in video form. However, areas not filled with contrast medium are difficult to evaluate.

2. Classification according to imaging method

In recent systems, digitization of the image takes place, and the signal detectors have shifted from acquisition with a charge-coupled device (CCD) via an image intensifier to flat-panel X-ray sensors (Fig. 9).

① Digital angiography (DA, Fig. 10)

Digital angiography images are provided as projection images similar to those of X-ray fluoroscopy. Because the contrast of X-ray density is projected, not only the contrast medium, but also high-density structures such as bone and low-density structures such as the lungs are visualized simultaneously. For this reason, analog imaging suffers from image quality deterioration due to halation and insufficient radiation dose, but digitization has improved these problems and reduced radiation dose. A typical example of the use of DA in the cardiovascular region is coronary angiography. DA enables imaging to be performed while moving the table to follow the flow of contrast medium.

The imaging conditions vary depending on the patient's body type and location of imaging and the purpose of the test. For non-pediatric patients, frame rates of ≤ 15 fps are commonly used.

② Digital subtraction angiography (DSA) (Fig. 11)

DSA uses the difference between images before and after administration of contrast medium to selectively display contrast-enhanced areas[27]. The signal intensity of areas not filled with contrast is nulled by subtraction processing, and these areas are not visualized. Therefore, even in areas where the background X-ray transmittance is not uniform, which are difficult to observe with normal imaging, lesions can be easily observed by improving the contrast between lesions and healthy areas. Furthermore, DSA can visualize even slight changes in contrast, making it suitable for detailed diagnosis. However, object motion is rendered as artifacts, so the heartbeat, gastrointestinal peristalsis, and poor breath-holding can be problematic.

As with DA, the imaging conditions used depend on the patient and the purpose of the imaging procedure. However, radiation exposure tends to be higher than with DA, so selection of appropriate imaging conditions is important.

(1) DSA using a fixed table

A wide field of view is selected to image large blood vessels, and a narrow field of view is selected to magnify organs and lesions for selective angiography. Because the size of the field of view that can be selected depends on the system, it is important to select a system suitable for the purpose of the imaging procedure.

Figure 9. Flat-panel vascular imaging system

Pictured is a biplane system that uses flat-panel detectors. The small volume of the detectors somewhat reduces the limitations on aspects such as imaging angles. However, the imaging angles that can be used vary depending on the size of the panels.

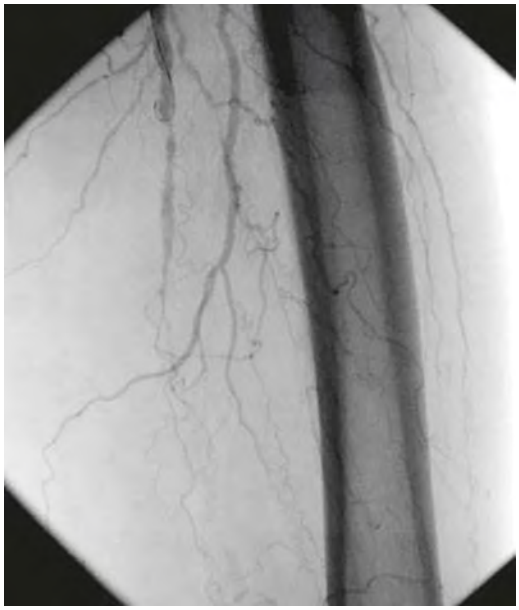

Figure 10. Digital angiography (DA)

Contrast-enhanced arteries and part of the femur are seen. The image is comparable to images obtained by normal fluoroscopic imaging.

Figure 11. Digital subtraction angiography (DSA)

A subtraction image of the same location shown in Fig. 10. The background is visualized homogeneously as a result of subtraction processing, so that only the contrast-enhanced arteries are observed, enabling details to be evaluated.

(2) DSA using a moving table

Used mainly to image a long extent such as the arteries of the lower extremities, this method is called stepping DSA[28, 29] or bolus chase DSA.[30] Because a long area is imaged with a single administration of contrast medium, the contrast medium dose and radiation exposure can be reduced. However, it should be noted that this imaging method is not available on all systems.

(3) Rotational angiography[31-33)]

This method enables the structure of vessels to be determined in 3 dimensions by rotating the arm of the angiography system around the subject, with the table fixed, and performing continuous imaging from multiple angles. This is also called cone-beam CT (CBCT). Observations can be carried from unlimited projection angles using reconstructed images. Examples of such use include examining the neck of an aneurysm and visualization of overlapping branch vessels. This method is commonly used for cerebral angiography. Recently, however, this method has been applied to abdominal angiography, such as hepatic arteriography, to provide information on three-dimensional vascular anatomy during interventional radiology (IVR) to assess feeding vessels of target lesions. Subtraction processing is also often used to improve observation precision.

3. Applications of angiography for the heart and great vessels

Due to its invasiveness, angiography is of limited use and is rarely used for simple diagnostic purposes. Although angiography is the gold standard for diagnosing coronary artery disease, it is advisable to carefully consider the risk of disease before choosing any imaging procedure. In recent years, screening use of coronary CT prior to percutaneous coronary intervention (PCI) has become common, and as a result, angiography tends to be used for treatment rather than diagnosis.

Examining the great vessels does not require as much spatial resolution as coronary artery imaging, and the role of angiography is limited, because information about vessel walls, plaques, and mural thrombi is important for understanding pathophysiology and cannot be assessed by angiography. However, depending on the status of the patient and disease, evaluation by angiography, which provides excellent selective visualization of vessels and spatial resolution, is required in cases such as when endovascular therapy is immediately implemented.

4. Typical diseases for which angiography is performed

① Aortic aneurysm

Because noninvasive evaluation by CT,[34)] ultrasonography,[35)] and MRI is widely performed, the use of angiography is limited for purposes such as performing an evaluation just before stent-graft insertion.

② Aortic dissection

In the acute phase, there is a risk that catheter insertion or rapid injection of contrast medium will exacerbate the condition. Consequently, angiography is currently not used for aortic dissection, and initial diagnosis is commonly performed by ultrasonography or CT.[36, 37)] The indications for angiography are considered to be limited to uses such as stent-graft insertion to occlude entry or to dilate the true lumen and branch stenoses.

③ Vasculitis

Vasculitis-related disorders such as Takayasu's arteritis and inflammatory aortic aneurysm are diagnosed mainly by CT and MRI.[38-42] Determining the condition of the vessel wall is particularly important in vasculitis, and angiography is unsuitable for initial diagnosis. Moreover, fragility of the vessel wall is common in vasculitis-related conditions such as vascular Behçet's disease, and the invasiveness of catheter insertion risks exacerbation. Consequently, the use of angiography must be considered carefully.

④ Pulmonary thromboembolism

As is the case with other disorders, pulmonary thromboembolism is diagnosed by means such as contrast-enhanced CT,[43] and angiography is rarely used for its diagnosis. However, it is used for purposes such as preoperative evaluation for transcatheter thrombus aspiration and thrombolysis and in chronic pulmonary thromboembolism.

⑤ Arteriosclerosis obliterans

Angiography is performed for this condition when surgery or endovascular therapy is planned. As in other vascular pathologies, the actual diagnosis of the disease is commonly performed by CT or MRI. However, if the artery wall is severely calcified, or lesions are severe, it is important to determine the patency of collaterals and vessels below the arteries of the lower extremities, and angiography may therefore be selected.

⑥ Acute arterial occlusion

Although the opportunities to use ultrasonography and CT for acute arterial occlusion are increasing, angiography is still selected to definitively determine the location of the embolism, the extent of the occlusion, and the patency of peripheral vessels. Angiography may also be performed intraoperatively.

Depending on the healthcare facility's approach and the patient's condition, transcatheter thrombus aspiration or thrombolysis may be performed, and angiography is concurrently used in such cases.

⑦ Thromboangiitis obliterans (Buerger's disease)

The estimated age of onset is in the 30s and 40s, and the condition is common in male smokers.[44] However, the bulk of the patients are aged 45 to 55 years, suggesting that the age of onset is increasing. The collaterals that develop in association with peripheral vascular occlusion have a characteristic tortuous appearance. Corkscrew-shaped collaterals develop,[45, 46] and characteristic findings such as standing waves[45] are seen on angiography, making it of high diagnostic value. However, these findings can also often be observed on CT and MRI, and the use of angiography for diagnostic purposes is waning**.**

D Nuclear cardiology

Overview

The introduction of new image reconstruction methods with spatial resolution recovery and noise suppression and dedicated cardiac gamma cameras with special semiconductor detectors (CZT) has made it possible to reduce patient radiation exposure (Table 1) during Nuclear cardiology imaging.[47, 48] The following practices are recommended to reduce radiation exposure during myocardial perfusion SPECT imaging (SPECT-MPI): low-dose ^{99m}Tc imaging, stress-only imaging with a ^{99m}Tc tracer, calculating the dose based on the body mass index (BMI), reducing artifacts by attenuation correction, and avoiding the use of ^{201}Tl alone and dual-isotope imaging with both ^{99m}Tc and ^{201}Tl.[49, 50] However, a weakness of ^{99m}Tc agents is that they accumulate at higher levels in the digestive tract than ^{201}Tl.[50] Using a cardiac-dedicated CZT gamma camera and the latest reconstruction methods, imaging can also be performed with a ^{201}Tl agent at a low dose.[47] Consequently, the radionuclide to be used should be selected by taking into account both the characteristics of the 2 radionuclides and the equipment at each facility. As the development of ^{18}F myocardial perfusion agents progresses, PET myocardial perfusion imaging (PET-MPI) is also expected to become an option in the future.[49, 50]

Table 1. Low-dose testing with the use of new image reconstruction methods or new cardiac-dedicated gamma cameras

Protocol	1st Acquisition			2nd Acquisition			Total Effective Dose (mSv)	Stress Only (effective dose: mSv)
	Stress/Rest	Dose Administered, MBq (mCi)	Effective Dose (mSv)	Stress/Rest	Dose Administered, MBq (mCi)	Effective Dose (mSv)		
^{99m}Tc 1-Day Protocol								
Stress/Rest	Stress	148–222 (4–6)	1.0–1.5	Rest	444–666 (12–18)	3.5–5.2	4.6–6.7	1.0–1.5
Rest/Stress	Rest	148–222 (4–6)	1.2–1.7	Stress	444–666 (12–18)	3.0–4.5	4.2–6.3	n/a
^{99m}Tc 2-Day Protocol								
Stress/Rest	Stress	148–222 (4–6)	1.0–1.5	Rest	148–222 (4–6)	1.2–1.7	2.2–3.3	1.0–1.5
Rest/Stress	Rest	148–222 (4–6)	1.2–1.7	Stress	148–222 (4–6)	1.0–1.5	2.2–3.3	n/a
^{201}Tl								
Stress/Redistribution	Stress	48.1–66.6 (1.3–1.8)	5.7–7.9	n/a	n/a	n/a	5.7–7.9	n/a
Dual radionuclides (^{201}Tl/^{99m}Tc)								
^{201}Tl rest/^{99m}Tc stress	Rest	48.1–66.6 (1.3–1.8)	5.7–7.9	Stress	148–222 (4–6)	1.0–1.5	6.7–9.4	n/a
^{201}Tl stress/^{99m}Tc rest	Stress	48.1–66.6 (1.3–1.8)	5.7–7.9	Rest	148–222 (4–6)	1.2–1.7	6.9–9.6	5.7–7.9

n/a: not applicable

Effective dose of ^{99m}Tc: Mean dose for ^{99m}Tc-MIBI and ^{99m}Tc-tetrofosmin. The tissue weighting factors (weightings) of ICRP publication 103 were used to calculate the effective doses.

Aside from myocardial perfusion imaging, ^{123}I-MIBG is used for prognosis prediction in heart failure. It is also used to diagnose Parkinson's disease and Lewy body dementia.[50, 51] Recently, bone scintigraphy agents (^{99m}Tc-pyrophosphate in Japan) have been used to diagnose cardiac amyloidosis,[52] and ^{18}F-FDG has been used to diagnose cardiac sarcoidosis.[53] It is recommended that nuclear cardiology imaging be optimized for the individual patient with respect to aspects such as indications and dose.[48] The following discussion focuses on standard imaging methods for nuclear cardiology testing.

Detailed discussion

1. Myocardial perfusion SPECT imaging methods (SPECT-MPI)

① Features of myocardial perfusion agents

The agent ^{201}Tl is a monovalent cation that, like potassium, is taken up by the myocardium by active transport and has a high first-pass extraction fraction (85%). A feature of ^{201}Tl is that its washout from the myocardium begins 10 to 15 minutes after administration.[47] Its washout over time is slower in ischemic myocardium than in normal or infarcted myocardium. Consequently, in delayed images, redistribution is

seen in ischemic myocardium, but not in infarcted myocardium (Fig. 12). The ^{99m}Tc agents [^{99m}Tc-methoxyisobutylisonitrile (MIBI) and ^{99m}Tc-tetrofosmin] are fat-soluble and passively taken up by the myocardium in proportion to blood flow. Within the myocardium, they are voltage-dependently sequestered in the mitochondrial inner membrane as monovalent cations.[47] However, their first-pass extraction fractions are lower than of ^{201}Tl, and they are not washed out over time.[47] Consequently, to distinguish ischemic from infarcted myocardium, they must be administered twice, once under stress and once at rest.

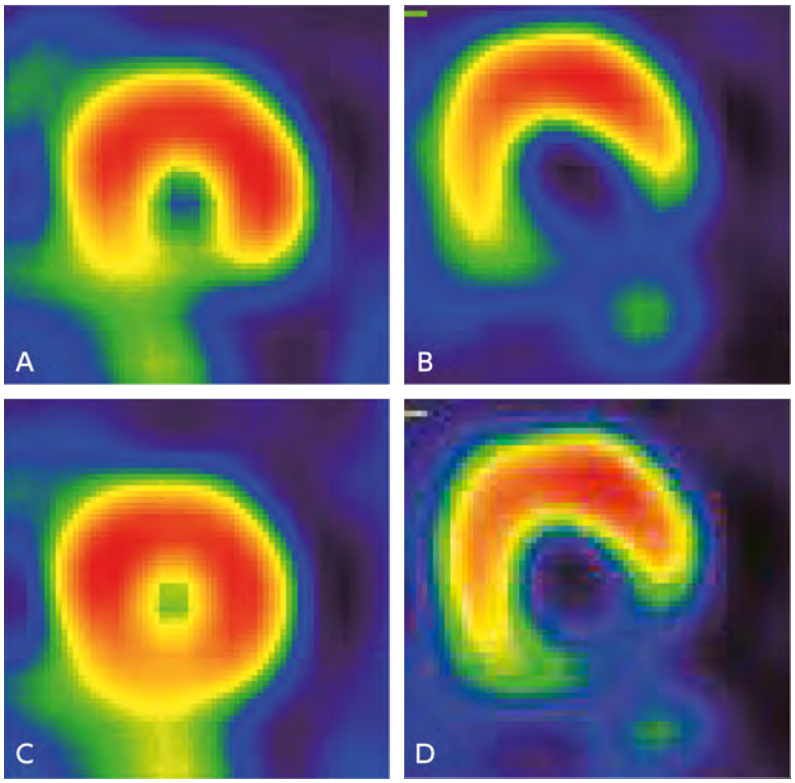

Figure 12. Ischemic and infarcted myocardium (^{201}Tl stress myocardial perfusion SPECT)

A, B: Stress image; C, D: Delayed image; A, C: Ischemic myocardium; B, D: Infarcted myocardium
In ischemic myocardium, decreased blood flow is seen in the inferior wall in the stress image (A), and redistribution is seen in the inferior wall in the delayed image (C). In infarcted myocardium, a perfusion defect is seen from the inferior wall to part of the lateral wall in the stress image (B), but redistribution is not seen in the delayed image (D).

② Stress methods

Exercise stress is applied in multiple steps using a treadmill or bicycle ergometer. Because diagnostic performance decreases if the exercise load is inadequate, the target workload is 85% of the predicted maximum heart rate. The myocardial perfusion agent is administered during maximum stress, and the stress is discontinued 60 to 90 seconds after administration. Adenosine is generally used for pharmacological stress. Adenosine is administered continuously over 6 minutes at a rate of 0.12 mg/kg/min, and the myocardial perfusion agent is administered 3 minutes after the start of adenosine administration. Because

caffeine is an adenosine antagonist, its ingestion is prohibited for 12 hours before adenosine administration. Regadenoson, a newly developed selective adenosine A_{2A} receptor agonist, enables stress to be applied with a single intravenous injection.[47] However, it has not been introduced in Japan.

③ Myocardial perfusion SPECT imaging

Table 2 summarizes the main recommendations of level IIa or higher for nuclear cardiology imaging provided in the JCS 2018 Guideline on Diagnosis of Chronic Coronary Heart Diseases,[50] along with the MINDS recommendation grades.

Because stress electrocardiography is performed first, the guidelines indicate that a good indication for myocardial perfusion SPECT is when ECG evaluation is difficult or there is an abnormal finding on ECG. It is considered useful for diagnosis when the pre-test probability is moderate or greater with typical chest pain. However, coronary CT angiography is also currently recommended if CT can be performed. Whether to perform coronary CT angiography or nuclear cardiology imaging first for diagnosis is not always clear. The most recent guidelines of the European Society of Cardiology (ESC) recommend that a pretest ECG be used to evaluate the risk of coronary artery disease rather than for diagnosis and that coronary CT angiography, with its high negative likelihood ratio, be used for exclusion of coronary artery disease in groups at low risk. In groups at high risk of coronary artery disease, the guideline recommends that nuclear cardiology imaging be used for definitive diagnosis because of its high positive likelihood ratio.[54] In addition, nuclear cardiology imaging has been shown to be useful for prognosis prediction in patients at moderate risk of coronary artery disease, although this is not indicated in the table.[54]

Table 2. Recommendation classes and MINDS recommendation grades for the main nuclear cardiology imaging

Item	Recommendation Class	Recommendation Grade
Myocardial perfusion SPECT (^{201}Tl, ^{99m}Tc-MIBI, ^{99m}Tc-tetrofosmin)		
Patients for whom ECG evaluation is difficult (limited to pharmacological stress in conditions such as complete left bundle branch block and ventricular pacing)	I	B
Abnormal stress ECG	I	B
Moderate or higher pre-test probability and typical anginal pain	I	B
Presence of residual ischemia from known coronary artery disease and regional diagnosis to be performed	I	B
For regional diagnosis of myocardial infarction	I	B
To determine whether coronary revascularization indicated	I	B
Patient with moderate or higher pre-test probability or atypical chest pain and coronary artery calcium score (CACS) ≥ 400	IIa	C1
To perform functional stenosis assessment of moderately severe (40% to 75%) stenotic lesion	IIa	C1
To evaluate treatment efficacy	IIa	C1
When performing pharmacological stress test because exercise stress cannot be used, although pre-test probability is moderate or higher	IIa	C1
Cardiac sympathetic innervation (^{123}I-MIBG)		
Prognostic assessment of ischemic heart failure	IIa	B
Myocardial fatty acid metabolism ($_{123}$I-beta-methyl-p-iodophenyl-pentadecanoic acid, BMIPP)		
Cardiomyopathy ischemia diagnosis and prognostic assessment/risk stratification	I	B
Myocardial ischemia diagnosis, prognostic assessment/risk stratification, vasospastic angina diagnosis	IIa	B
Myocardial glucose metabolism (^{18}F-FDG, myocardial viability evaluation)		
In patients with coronary artery disease and severe left ventricular dysfunction, to evaluate prognosis and the extent of myocardium that may recover with coronary revascularization or for heart transplant.	I	B
Performed in patients with myocardium with a fixed perfusion defect of moderate or greater severity or patients with an inconclusive diagnosis based on other tests.	I	B
Myocardial perfusion PET (^{13}N-ammonia)		
Diagnosing coronary artery disease in patients with a moderate to high pre-test probability	I	A
Risk stratification and prognostic assessment based on ischemia and amount of infarcted myocardium	I	A
Risk stratification and prognostic assessment based on quantitative analysis of myocardial perfusion	I	A
Risk stratification and prognostic assessment based on analysis of left ventricular function using ECG gating	IIa	B
Detecting left main disease and severe multivessel disease by quantitative analysis of myocardial perfusion	IIa	B

Recommendation classes

I: There is evidence or a broad consensus that the procedure or treatment is effective and useful.

IIa: Based on the evidence and opinions, it is highly likely that the procedure or treatment is effective and useful.

MINDS recommendation grades

A: Procedure strongly recommended, since there is strong scientific basis for performing it.

B: Procedure recommended, since there is scientific basis for performing it.

C1: Procedure recommended, although there is no scientific basis for performing it.

2. Imaging methods for myocardial perfusion PET

The myocardial perfusion agents for PET include ^{82}Rb, ^{15}O-water, and ^{13}N-ammonia (NH_3). In Japan, only ^{13}N-ammonia is covered by national health insurance.[50] ^{13}N-ammonia is taken up by the myocardium by passive diffusion or as monovalent ammonia ions by active transport via the sodium-potassium pump. The ^{13}N-ammonia that is taken up by the myocardium is incorporated into the amino acid pool as ^{13}N-glutamine, where it accumulates.[50, 55] ^{13}N has a relatively long half-life of 10 minutes, and its short positron range enables visual assessments to be performed with good image quality. Moreover, it has a good first-pass extraction fraction of 80%, enabling myocardial perfusion and coronary flow reserve (myocardial perfusion reserve) to be evaluated quantitatively by compartment analysis. Stress is applied pharmacologically, and data for compartment analysis are collected by dynamic imaging (dynamic PET) in list mode. However, because a cyclotron is required, the facilities where it can be performed are limited. ^{18}F-flurpiridaz, the most recently developed agent, has a shorter positron range than ^{13}N and a high first-pass extraction fraction of ≥ 90%. Consequently, it is superior to ^{13}N-ammonia with respect to image quality and quantitative evaluation.[56] Moreover, its long half-life of 110 minutes enables exercise stress testing to be performed, and because it can be supplied by delivery, it offers the advantage of enabling any PET facility to perform the test. Furthermore, because redistribution is observed, testing can be performed using the same test protocol used for ^{201}Tl.[56, 57] It is an agent whose future clinical introduction is eagerly awaited.

3. Myocardial metabolic imaging methods

The energy metabolism of the myocardium is mainly provided by fatty acids in the fasted state and glucose postprandially or during ischemia. The ^{123}I-labeled fatty acid analog ^{123}I-BMIPP is used to evaluate fatty acid metabolism, and ^{18}F-FDG is used to evaluate glucose metabolism. Although ^{123}I-BMIPP is taken up by the myocardium as a fatty acid, it is sequestered in the triglyceride pool without undergoing beta-oxidation, and it reflects the status of fatty acid utilization and the size of the triglyceride pool. ^{18}F-FDG is taken up by the myocardium by active transport via the glucose transporters (GLUT) and converted to ^{18}F-FDG-phosphate by hexokinase. It is not metabolized subsequently and is therefore sequestered in the myocardium. Clinically, ^{123}I-BMIPP is useful for diagnosing acute coronary syndrome (unstable angina) and predicting cardiovascular events in patients with chronic kidney disease (CKD) (cardiomyopathy, Table 2). ^{123}I-BMIPP is also used to evaluate myocardial viability during myocardial perfusion imaging and aspects such as myocardial damage in hypertrophic cardiomyopathy.[50] ^{18}F-FDG is used to evaluate myocardial viability.[50, 55]

① ^{18}F-FDG imaging methods

Because GLUT4 is insulin-dependent, an insulin clamp, which involves the combined use of glucose loading and insulin, is used to evaluate the viability of the myocardium. Imaging is generally performed 45 to 60 minutes after administration of 5 to 15 mCi (185 to 555 MBq) of ^{18}F-FDG. Data are collected in static or list mode over an imaging duration of 10 to 30 minutes. Images are reconstructed using the iterative

reconstruction or FBP method with a slice thickness of 2 to 4 mm. Myocardial viability is evaluated in conjunction with myocardial perfusion imaging. The myocardium can be concluded to be viable in an area of decreased myocardial perfusion if ^{18}F-FDG accumulation is observed.[55] Fasting is required as preparation to evaluate inflammatory disorders such as sarcoidosis.[55]

② ^{123}I-BMIPP imaging methods

With the patient fasted and at rest, 3 to 4 mCi (111 to 148 MBq) of ^{123}I-BMIPP are injected intravenously, and SPECT is performed 20 to 30 minutes later. A symmetrical energy window with a width of 20% centering on an energy peak of 159 keV is specified, and data are collected with a 180-degree circular orbit from 45 degrees RAO to 45 degrees LPO. Imaging data are collected from 32 angles using a 64 × 64 matrix for 30 to 45 seconds per angle. The collimators used include low-energy high-resolution (LEHR), extended low-energy general purpose (ELEGP), and medium-energy general purpose (MEGP) collimators. With Anger type gamma cameras, simultaneous dual-isotope imaging in combination with ^{201}Tl has been performed to simultaneously evaluate myocardial perfusion.[50] However, CZT gamma cameras provide superior energy resolution, making simultaneous dual isotope collection with the myocardial perfusion agent ^{99m}Tc possible as well.[58] It should be noted, however, that simultaneous dual-isotope collection requires crosstalk correction and increases the radiation exposure.

4. Cardiac sympathetic imaging

^{123}I-MIBG is used for cardiac sympathetic imaging. Unlike noradrenaline, ^{123}I-MIBG is not metabolized by enzymes such as the monoamine oxidases. However, like noradrenaline, it is taken into the presynaptic nerves by the uptake-1 transporter, enabling accumulation in the cardiac sympathetic preganglionic fibers to be imaged. Regions of interest are specified for the heart (H) and mediastinum (M) in frontal planar images, and the heart/mediastinum ratio (H/M ratio) and washout rate are calculated. In patients with heart failure in which cardiac function is decreased, including those with concomitant coronary artery disease, the late-phase images' H/M ratios and washout rate are both useful indices as predictors for cardiac events.[50]

^{123}I-MIBG imaging methods

In preparation for imaging, antidepressants, antipsychotics, and calcium channel blockers, which affect ^{123}I-MIBG accumulation, are withdrawn for 24 hours. In Japan, a variety of collimators are used, as is the case with ^{123}I-BMIPP, 111 MBq of ^{123}I-MIBG is administered, and frontal planar images and myocardial SPECT images are acquired approximately 15 to 30 minutes (early-phase images) and 3 to 4 hours (late-phase images) after administration.[50] Also in Japan, the H/M ratio is calculated using software that converts each measured value to the value obtained with a MEGP collimator, which makes it possible to compare H/M ratios obtained with different collimators and systems.[59]

Secondary source materials used as references

1) Hecht HS et al: Journal of Cardiovascular Computed Tomography 2016 SCCT/STR guidelines for coronary artery calcium scoring of noncontrast noncardiac chest CT scans: a report of the Society of Cardiovascular Computed Tomography and Society of Thoracic Radiology. J Cardiovasc Comput Tomogr 11: 74-84, 2017
2) Halliburton SS et al: SCCT guidelines on radiation dose and dose-optimization strategies in cardiovascular CT 5: 198-224, 2011
3) Taylor AJ et al: ACCF/SCCT/ACR/AHA/ASE/ASNC/NASCI/SCAI/SCMR 2010 Appropriate Use Criteria for cardiac computed tomography. J Cardiovasc Comput Tomogr 4: 407.e1-407.e33, 2010
4) Abbara S et al: SCCT guidelines for the performance and acquisition of coronary computed tomographic angiography: a report of the Society of Cardiovascular Computed Tomography Guidelines Committee endorsed by the North American Society for Cardiovascular Imaging (NASCI). J Cardiovasc Comput Tomogr 10: 435-449, 2016
5) Utsunomiya D et al: Relationship between diverse patient body size- and image acquisition-related factors, and quantitative and qualitative image quality in coronary computed tomography angiography: a multicenter observational study. Jpn J Radio 34: 548-55, 2016
6) Gonzalez JA et al: Meta-analysis of diagnostic performance of coronary computed tomography angiography, computed tomography perfusion, and computed tomography-fractional flow reserve in functional myocardial ischemia assessment versus invasive fractional flow reserve. Am J Cardiol 116: 1469-1478, 2015
7) Nørgaard BL et al: Diagnostic performance of noninvasive fractional flow reserve derived from coronary computed tomography angiography in suspected coronary artery disease: The NXT trial (Analysis of Coronary Blood Flow Using CT Angiography: Next Steps). J Am Coll Cardiol 63: 1145-1155, 2014
8) Japanese Circulation Society, et al. Ed.: JCS 2018 Guideline on Diagnosis of Chronic Coronary Heart Diseases. Japanese Circulation Society, 2018.
9) Japanese Circulation Society, et al. Ed.: 2010 Guidelines on Selection Criteria for Testing Methods for Diagnosis and Pathology Identification in Chronic Ischemic Heart Disease. Japanese Circulation Society (JSC 2010), 2010.
10) Kramer CM et al: Society for Cardiovascular Magnetic Resonance Board of Trustees Task Force on Standardized Protocols.: standardized cardiovascular magnetic resonance (CMR) protocols 2020 update. J Cardiovasc Magn Reson 15, doi: 10.1186/s12968-020-00607-1/2020
11) Axel L, Dougherty L: Heart wall motion: improved method of spatial modulation of magnetization for MR imaging. Radiology 172: 349-350, 1989
12) Eitel I et al: Cardiac magnetic resonance myocardial feature tracking for optimized prediction of cardiovascular events following myocardial infarction. JACC Cardiovasc Imaging 11: 1433-1444, 2018
13) Nagel E et al: Magnetic resonance perfusion measurements for the noninvasive detection of coronary artery disease. Circulation 108: 432-437, 2003
14) Schwitter J et al: MR-IMPACT: comparison of perfusion-cardiac magnetic resonance with single-photon emission computed tomography for the detection of coronary artery disease in a multicentre, multivendor, randomized trial. Eur Heart J 29: 480-489, 2008
15) Wagner A et al: Contrast-enhanced MRI and routine single photon emission computed tomography (SPECT) perfusion imaging for detection of subendocardial myocardial infarcts: an imaging study. Lancet 361: 374-379, 2003
16) Kim RJ et al: The use of contrast-enhanced magnetic resonance imaging to identify reversible myocardial dysfunction. N Eng J Med 343: 1445-1453, 2000
17) Weber OM et al: Whole-heart steady-state free precession coronary artery magnetic resonance angiography. Magn Reson Med 50: 1223-1228, 2003
18) Sakuma H et al: Assessment of the entire coronary artery tree with total study time of less than 30 minutes using whole heart coronary magnetic resonance angiography. Radiology 237: 316-321, 2005
19) Dyverfeldt P et al: 4D flow cardiovascular magnetic resonance consensus statement. J Cardiovasc Magn 17: 72, 2015
20) Roujol S et al: Accuracy, precision, and reproducibility of four T1 mapping sequences: a head-to-head comparison of MOLLI, ShMOLLI, SASHA, and SAPPHIRE. Radiology 272: 683-689, 2014
21) Japanese Circulation Society, et al. Ed.: Guidelines for the Diagnosis and Treatment of Cardiovascular Disease (2010 report of the joint working group), 2011 Guideline on Diagnosis and Treatment of Aortic Aneurysm and Aortic Dissection. Japanese Circulation Society, 2011.
22) Prince MR: Gadolinium-enhanced MR aortography. Radiology 191: 155-164, 1994
23) Makris GC et al: Advances in MRI for the evaluation of carotid atherosclerosis. B J Radiol 88: 20140208, 2015
24) Ho KY et al: Peripheral vascular tree stenosis; evaluation with moving-bed infusion-tracking MR angiography. Radiology 206: 683-692, 1998
25) Miyazaki M et al: Non-contrast enhanced MR angiography using 3D ECG synchronized half-Fourier fast spin echo. JMRI 12: 776-783, 2000
26) Simonetti OP et al: “Black blood T2-weighted inversion-recovery MR imaging of the heart. Radiology 199: 49-57, 1996
27) Meaney TF et al: Digital subtraction angiography of the human cardiovascular system. AJR Am J Roentgenol 135 (6): 1153-1160, 1980
28) Malden ES et al: Peripheral vascular disease: evaluation with stepping DSA and conventional screen-film angiography. Radiology 191 (1): 149-153, 1994

29) Fink U et al: Peripheral DSA with automated stepping. Eur J Radiol 13 (1): 50-54, 1991
30) Foley WD et al: Digital subtraction angiography of the extremities using table translation. Radiolog 157 (1): 255-258, 1985
31) Kumazaki T: Development of a new digital angiography system--improvement of rotational angiography and three dimensional image display. Nihon Igaku Hoshasen Gakkai Zasshi 51 (9): 1068-1077, 1991
32) Heautot JF et al: Analysis of cerebrovascular diseases by a new 3-dimensional computerised X-ray angiography system. Neuroradiology 40 (4): 203-209, 1998
33) Wiesent K et al: Enhanced 3-D-reconstruction algorithm for C-arm systems suitable for interventional procedures. IEEE Trans Med Imaging 19 (5): 391-403, 2000
34) Buscaglia LC et al: Use of CT scan in the diagnosis of abdominal aortic aneurysms. J Comput Tomogr 4 (3): 197-200, 1980
35) Wheeler WE et al: Angiography and ultrasonography: a comparative study of abdominal aortic aneurysms. AJR Am J Roentgenol 126 (1): 95-100, 1976
36) Godwin JD et al: Evaluation of dissections and aneurysms of the thoracic aorta by conventional and dynamic CT scanning. Radiology 136 (1): 125-133, 1980
37) Heiberg E et al: CT findings in thoracic aortic dissection. AJR Am J Roentgenol 136 (1): 13-17, 1981
38) Tennant WG et al: Radiologic investigation of abdominal aortic aneurysm disease: comparison of three modalities in staging and the detection of inflammatory change. J Vasc Surg 17 (4): 703-709, 1993
39) Arrive L et al: Inflammatory aneurysms of the abdominal aorta: CT findings. AJR Am J Roentgenol 165 (6): 1481-1484, 1995
40) Iino M et al: Sensitivity and specificity of CT in the diagnosis of inflammatory abdominal aortic aneurysms. J Comput Assist Tomogr 26 (6): 1006-1012, 2002
41) Gotway MB et al: Imaging findings in Takayasu's arteritis. AJR Am J Roentgenol 184 (6): 1945-1950, 2005
42) Matsunaga N et al: Takayasu arteritis: MR manifestations and diagnosis of acute and chronic phase. J Magn Reson Imaging 8 (2): 406-414, 1998
43) Katz DS et al: Combined CT venography and pulmonary angiography: a comprehensive review. Radiographics 22: S3-S19 (S20-S14), 2002
44) Mills JL: Buerger's disease in the 21st century: diagnosis, clinical features, and therapy. Semin Vasc Surg 16 (3): 179-189, 2003
45) Hagen B, Lohse S: Clinical and radiologic aspects of Buerger's disease. Cardiovasc Intervent Radiol 7 (6): 283-293, 1984
46) Suzuki S et al: Buerger's disease (thromboangiitis obliterans): an analysis of the arteriograms of 119 cases. Clin Radiol 33 (2): 235-240, 1982
47) Henzlova MJ et al: ASNC imaging guidelines for SPECT nuclear cardiology procedures: stress, protocols, and tracers. J Nucl Cardiol 23: 606-639, 2016
48) Dorbala S et al: Single photon emission computed tomography (SPECT) myocardial perfusion imaging guidelines: instrumentation, acquisition, processing, and interpretation. J Nucl Cardiol. 25: 1784-1846, 2018
49) Gimelli A et al: Strategies for radiation dose reduction in nuclear cardiology and cardiac computed tomography imaging: a report from the European Association of Cardiovascular Imaging (EACVI), Committee of European Association of Nuclear Medicine (EANM), and the European Society of Cardiovascular Radiology (ESCR). Eur Heart J 39: 286-296, 2018
50) Yamagishi M, et al.: JCS 2018 Guideline on Diagnosis of Chronic Coronary Heart Diseases. JCS, 2018.
51) Travin MI et al: How do we establish cardiac sympathetic nervous system imaging with ^{123}I-MIBG in clinical practice? perspectives and lessons from Japan and the US. J Nucl Cardiol 26: 1434-1451. 2019
52) Dorbala S et al: ASNC/AHA/ASE/EANM/HFSA/ISA/SCMR/SNMMI expert consensus recommendations for multimodality imaging in cardiac amyloidosis: part 1 of 2-evidence base and standardized methods of imaging. J Nucl Cardiol 26: 2065- 2123. 2019
53) Slart RHJA et al: A joint procedural position statement on imaging in cardiac sarcoidosis: from The Cardiovascular and Inflammation & Infection Committees of European Association of Nuclear Medicine, The European Association of Cardiovascular Imaging, and the American Society of Nuclear Cardiology. J Nucl Cardiol. 25: 298-319, 2018
54) Saraste A et al: Imaging in ESC clinical guidelines: chronic coronary syndromes. Eur Heart J 20: 1187-1197, 2019
55) Dilsizian V et al: ASNC imaging guidelines/SNMMI procedure standard for positron emission tomography (PET) nuclear cardiology procedures. J Nucl Cardiol 23: 1187-1226, 2016
56) Werner RA et al: Moving into the next era of PET myocardial perfusion imaging: introduction of novel ^{18}F-labeled tracers. Int J Cardiovasc Imaging 35: 569-577, 2019
57) Higuchi T et al: A new ^{18}F-labeled myovcardial PET tracer: myocardial uptake after permanent and transient coronary occlusion in rats. J Nucl Med 49: 1715-1722, 2008
58) Yamada Y et al: Feasibility of simultaneous ^{99m}Tc-tetrofosmin and ^{123}I-BMIPP dual-tracer imaging with cadmium-zinc-tellulide detectors in patients undergoing primary coronary intervention for acute myocardial infarction. J Nucl Cardiol: DOI: 10.1007/s 12350-018-01585-9, 2019
59) Nakajima K et al: Multicenter cross-calibration of I-123metaiodobenzylguanidine heart-to-mediastinum ratios to overcome camera-collimator variations. J Nucl Cardiol 21: 970-978, 2014

CQ 6 When ≥ 64-row MDCT is used to investigate acute pulmonary thromboembolism, is simultaneous CT venography recommended?

Recommendation

Although CT venography (CTV) should not be uniformly performed with CT pulmonary angiography (CTPA) that is performed to investigate acute pulmonary thromboembolism, the combined use of CTV is considered when the lower extremities cannot be adequately observed by ultrasonography and when the risk of acute pulmonary thromboembolism is high.

Recommendation strength: none, strength of evidence: weak (C), agreement rate: agreement not reached

Background

The addition of CTV to CTPA improves diagnostic performance in acute pulmonary thromboembolism, according to a large study of ≤ 16-row MDCT.[1)] It is not clear whether CTV is also needed with ≥ 64-row MDCT or whether the addition of CTV is useful for determining a treatment strategy and contributes to prognosis improvement. The addition of CTV necessitates increased X-ray exposure and an increase in the dose of contrast medium. Consequently, the benefits and drawbacks need to be considered.

Explanation

Acute pulmonary thromboembolism requires prompt and accurate diagnosis. The diagnostic test is selected based on the pre-test probability (clinical probability). With a low to moderate clinical probability, CTPA is recommended to exclude acute pulmonary thromboembolism. With a moderate to high clinical probability, it is recommended to confirm acute pulmonary thromboembolism (secondary source 1). CTPA is now used as the reference standard for acute pulmonary embolism diagnosis, instead of direct catheter pulmonary angiography.

In a multicenter, prospective study that examined the diagnostic performance of CTPA using ≤ 16-row MDCT [Prospective Investigation of Pulmonary Embolism Diagnosis (PIOPED) II trial], sensitivity and specificity were 83% and 96%, respectively. When simultaneous CTV was added, sensitivity and specificity improved to 90% and 95%, respectively. However, the availability of ≥ 64-row MDCT has increased in recent years. Consequently, high diagnostic performance can be expected with CTPA alone. The number of studies that have examined whether the addition of CTV to CTPA using ≥ 64-row MDCT contributes to improved diagnostic performance in acute pulmonary thromboembolism (venous thromboembolism) is limited.[2, 3)] Consequently, there is a lack of evidence supporting the clinical utility of additional CTV.

The embolic source in ≥ 90% of patients with acute pulmonary thromboembolism is the deep veins of the lower extremities. Evaluation of the lower extremity deep venous thrombus is therefore necessary to determine a treatment strategy. The first-line imaging examination for evaluating lower extremity deep venous thrombus is ultrasonography of the lower extremities, which provides high diagnostic performance. Deep vein thrombosis that is localized in the pelvis is difficult to evaluate by ultrasound, and evaluation by CTV may be useful in this case. However, such cases are very rare.[4, 5)] Consequently, information obtained by CTV alone in the diagnosis of deep vein thrombosis is limited. The addition of CTV allows for incidental findings in the pelvis and lower extremities (e.g., tumors, abscesses, aneurysms), which may assist in determining a treatment strategy. However, this occurs infrequently, and the usefulness of CTV in this role is therefore limited.[6)]

The addition of CTV is accompanied by increased X-ray and contrast medium doses. Ultrasonography of the lower extremities should therefore generally be given priority in diagnosing deep vein thrombosis, and the use of CTV should be limited to cases in which evaluation of the lower extremities by ultrasonography is difficult (secondary sources 2 to 5). The addition of CTV to CTPA may enable ultrasonography of the lower extremities to be omitted in the following cases, thereby shortening the diagnostic process and aiding in promptly determining a treatment strategy: ultrasonography of the lower extremities cannot be properly performed at the facility; circumstances make it difficult to perform (e.g. postoperative site or a cast is in place); image evaluation by ultrasonography is difficult; or the patient is in a highly urgent condition (e.g., condition unstable or high risk).[7)] However, the effects of adding CTV on healthcare management and prognosis have not been adequately investigated, which makes it difficult to comment on its usefulness.

None of the guidelines on acute pulmonary thromboembolism and deep vein thrombosis published in Japan or other countries recommend routinely adding CTV to CTPA. The view expressed in these guidelines is that the addition of CTV does not provide benefits commensurate with the increases in X-ray exposure and contrast medium dose, and that there is little evidence supporting the aggressive use of CTV (secondary sources 1-3, 6). The present guidelines also do not recommend the uniform use of CTV in combination with CTPA. However, it may assist in promptly determining a treatment strategy when adequate observation by lower extremity ultrasonography is not feasible or in high-risk patients. It was therefore concluded that concomitant CTV should remain an option after its benefits and drawbacks have been individually considered.

Search keywords and secondary sources used as references

PubMed was searched using the following keywords: deep vein thrombosis, deep venous thrombosis, venography, angiography, computed tomography angiography, pulmonary embolism, pulmonary thromboembolism, and venous thromboembolism.

In addition, the following were referenced as secondary sources.

1) Konstantinides SV et al: 2019 ESC guidelines for the diagnosis and management of acute pulmonary embolism developed in collaboration with the European Respiratory Society (ERS). Eur Heart J 41: 543-603, 2020

2) Mazzolai L et al. Diagnosis and management of acute deep vein thrombosis: a joint consensus document from The European Society of Cardiology working groups of aorta and peripheral vascular diseases and pulmonary circulation and right ventricular function. Eur Heart J 39: 4208-4218, 2018
3) Hanley M et al: ACR Appropriateness Criteria®: suspected lower extremity deep vein thrombosis. J Am Coll Radiol 15: S413-s417, 2018
4) Ito M, et al.: 2017 Guidelines for Diagnosis, Treatment and Prevention of Pulmonary Thromboembolism and Deep Vein Thrombosis. Japanese Circulation Society, 2017.
5) Japan Radiological Society, Ed.: 2016 Diagnostic Imaging Guideline. KANEHARA & Co., 2016.
6) Kirsch J et al: ACR Appropriateness Criteria®: acute chest pain-suspected pulmonary embolism. J Am Coll Radiol 14: S2-S12, 2017

References

1) Stein PD et al: Multidetector computed tomography for acute pulmonary embolism. N Engl J Med 354: 2317-2327, 2006
2) Nazaroglu H et al: 64-MDCT pulmonary angiography and CT venography in the diagnosis of thromboembolic disease. AJR Am J Roentgenol 192: 654-661, 2009
3) Stein PD et al: CT venous phase venography with 64-detector CT angiography in the diagnosis of acute pulmonary embolism. Clin Appl Thromb Hemost 16: 422-429, 2010
4) Reichert M et al: Venous thromboembolism: additional diagnostic value and radiation dose of pelvic CT venography in patients with suspected pulmonary embolism. Eur J Radiol 80: 50-53, 2011
5) Kalva SP et al: Venous thromboembolism: indirect CT venography during CT pulmonary angiography--should the pelvis be imaged? Radiology 246: 605-611, 2008
6) Douek P et al: Impact of CT venography added to CT pulmonary angiography for the detection of deep venous thrombosis and relevant incidental CT findings. Eur J Radiol 133: 109388, 2020
7) Salvolini L et al: Suspected pulmonary embolism and deep venous thrombosis: a comprehensive MDCT diagnosis in the acute clinical setting. Eur J Radiol 65: 340-349, 2008

CQ 7 Is functional testing with FFR-CT recommended if intermediate stenosis is seen by coronary CTA performed for effort angina?

Recommendation

FFR-CT is weakly recommended as a functional test if intermediate stenosis is seen on coronary CTA performed to investigate effort angina.

Recommendation strength: 2, strength of evidence: weak (A), agreement rate: 80% (8/10)

Background

Fractional flow reserve (FFR) is a well-established test for determining the indication for coronary revascularization, but it requires pharmacological stress for each individual lesion. FFR derived from coronary CT angiography (FFR-CT) offers the advantage of evaluating the severity of myocardial ischemia for each diseased vessel assessable by coronary CTA without additional testing. However, the usefulness of coronary CTA in intermediate stenosis (30% to 70%) has not been adequately evaluated.

Explanation

In the diagnostic algorithm for chronic coronary artery disease, coronary CTA holds an important role as a noninvasive test, on a par with stress electrocardiography and stress myocardial perfusion imaging. However, coronary CTA is useful for excluding significant coronary artery stenoses (≥ 50%), it is known to be inadequate for identifying obstructive coronary artery disease (CAD) requiring treatment. The invasive FFR is a well-established diagnostic examination for determining the indication for coronary revascularization, but it requires pharmacological stress-loading for each individual lesion. FFR-CT is a method of evaluation used to estimate the severity of myocardial ischemia for each diseased vessel (FFR). It does so using 3D data from coronary CTA and applying the fundamentals of computational fluid dynamics and cardiovascular physiology to hypothetically calculate pharmacological stress conditions.

For this CQ, we searched for studies that evaluated the diagnostic performance of coronary CTA (lesions of ≥ 50% stenosis) and FFR-CT (≤ 0.80) with respect to obstructive CAD (invasive FFR ≤ 0.80) in patients who had undergone coronary CTA for suspected effort angina. We explored the CADs with stenosis severity of 30% to 70% on coronary CTA, which are difficult to manage after testing. We reviewed seven studies, consisting of five prospective and two retrospective studies and evaluated a total of 1,701 vessels as the study population.[1-7)] The studies were uniform with respect to entry requirements such as the intervals between CT and FFR tests, the definition of intermediate stenosis (30% to 70%), endpoint blinding, and outcome condition (invasive FFR ≤ 0.80).

The results of a quantitative meta-analysis of these studies are shown in Table 1. Sensitivity ranged from 0.34 to 0.90 for coronary CTA [pooled sensitivity, 0.71 (95% CI, 0.40 to 0.91)] and from 0.59 to 0.95 for FFR-CT [pooled sensitivity, 0.86 (95% CI, 0.83 to 0.91)]. Thus, the sensitivity of FFR-CT was

comparatively stable and high. Specificity ranged from 0.21 to 0.87 for coronary CTA [pooled specificity, 0.49 (95% CI, 0.18 to 0.81)] and from 0.59 to 0.95 for FFR-CT [pooled specificity, 0.80 (95% CI, 0.77 to 0.83)]. Thus, the specificity of FFR-CT also showed a trend toward being comparatively high. As compared with coronary CTA, FFR-CT had a higher positive likelihood ratio (PLR) [pooled PLR, 4.07 (95% CI, 2.49 to 6.66) vs. 1.24 (95% CI, 1.02 to 1.51)], a lower negative likelihood ratio (NLR) [pooled NLR, 0.18 (95% CI, 0.11 to 0.27) vs. 0.65 (95% CI, 0.45 to 0.93)], and a higher diagnostic odds ratio (DOR) [pooled DOR, 26.52 (95% CI, 10.42 to 67.49) vs. 2.30 (95% CI, 1.30 to 4.07)]. The area under the curve (AUC) of the summary receiver operating characteristic (SROC) was also larger for FFR-CT than for coronary CTA (Fig. 1, 0.9183 vs. 0.6487).

References 1 to 3 and 6 were studies that used analysis software made by HeartFlow. The remaining 3 studies used different computational algorithms to calculate FFR-CT (in Japan, only HeartFlow FFR-CT is reimbursed under national health insurance).[4, 5, 7)] Previous studies have shown that FFR-CT improved the diagnostic performance of identifying obstructive CAD compared to coronary CTA alone, applying the same cutoff value.[8)] In the systematic review for this CQ, the inconsistency of the results for the sensitivity of coronary CTA (I-square = 90.3%) and specificity (I-square = 96.1%) and for the sensitivity of FFR-CT (I-square = 92.9%) must be considered in the assessment.

Table. Diagnostic performance of coronary CTA (≥ 50%) and FFR-CT (≤ 0.80) for vessels diagnosed as having intermediate stenosis (30% to 70% stenosis) by coronary CTA

	Number of Vessels	Number of Lesions	Sensitivity [95% CI]	Specificity [95% CI]	PLR [95% CI]	NLR [95% CI]	DOR [95% CI]
CCTA (≥ 50%)							
Min 2012[1)]	66	31	0.90 [0.74-0.98]	0.26 [0.13-0.43]	1.22 [0.97-1.53]	0.38 [0.11-1.27]	3.2 [0.79-13.25]
Nakazato 2013[2)]	150	35	0.34 [0.19-0.52]	0.72 [0.63-0.80]	1.23 [0.71-2.13]	0.91 [0.70-1.19]	1.35 [0.60-3.04]
Coenen 2015[4)]	144	63	0.83 [0.71-0.91]	0.21 [0.13-0.31]	1.05 [0.89-1.23]	0.83 [0.42-1.65]	1.26 [0.54-2.92]
Donnelly 2018[5)]	60	21	0.52 [0.30-0.74]	0.87 [0.73-0.96]	4.09 [1.64-10.20]	0.55 [0.34-0.87]	7.48 [2.10-26.65]
Tang 2020[7)]	299	76	0.84 [0.74-0.92]	0.35 [0.28-0.41]	1.29 [1.12-1.47]	0.46 [0.27-0.79]	2.81 [1.43-5.53]
pooled	719	226	0.71 [0.40-0.91]	0.49 [0.18-0.81]	1.24 [1.02-1.51]	0.65 [0.45-0.93]	2.30 [1.30-4.07]
FFR-CT (≤ 0.80)							
Min 2012[1)]	66	31	0.9 [0.74-0.98]	0.83 [0.66-0.93]	5.27 [2.52-11.01]	0.18 [0.04-0.35]	45.11 [10.27-198.1]
Nakazato 2013[2)]	150	35	0.74 [0.57-0.88]	0.67 [0.58-0.75]	2.25 [1.62-3.11]	0.38 [0.22-0.68]	5.85 [2.50-13.72]
Nørgaard 2014[3)]	234	34	0.82 [0.66-0.93]	0.86 [0.80-0.90]	5.68 [3.92-8.23]	0.21 [0.10-0.43]	27.52 [10.48-72.27]
Coenen 2015[4)]	144	63	0.87 [0.77-0.94]	0.59 [0.48-0.70]	2.14 [1.62-2.83]	0.21 [0.11-0.42]	10.00 [4.22-23.73]
Donnelly 2018[5)]	60	21	0.91 [0.70-0.99]	0.72 [0.55-0.85]	3.21 [1.91-5.39]	0.13 [0.04-0.50]	24.18 [4.81-121.6]
Driessen 2019[6)]	118	50	0.96 [0.86-1.00]	0.66 [0.54-0.77]	2.84 [2.03-3.98]	0.06 [0.02-0.24]	46.96 [10.47-210.7]
Tang 2020[7)]	299	76	0.88 [0.79-0.94]	0.95 [0.91-0.98]	17.87 [9.99-31.99]	0.13 [0.07-0.23]	143.5 [57.02-361.0]
pooled	1071	310	0.87 [0.83-0.91]	0.80 [0.77-0.83]	4.07 [2.49-6.66]	0.18 [0.11-0.27]	26.52 [10.42-67.49]

Note: Invasive FFR ≤ 0.80 considered as reference standard.

FFR-CT can detect coronary lesions that require treatment with high diagnostic accuracy and without the need for additional testing (Fig. 2). In its expert consensus, the Society of Cardiovascular Computed Tomography of the United States stated that FFR-CT evaluation may optimize further examination after coronary CTA diagnosis and may help with decision-making in strategies for patients with severe single-vessel disease or multivessel disease that includes intermediate stenoses (secondary source 1).

However, the medical remuneration points for FFR-CT provided under the national health insurance system are not necessarily reasonable compared to coronary CTA. Consequently, if the clinical indication for FFR-CT as an additional test is not adequately considered, the number of FFR-CT analyses could increase and strain the economics of healthcare. Of course, we should know that FFR-CT may be affected

by a variety of factors, such as CT image quality, coronary artery calcification, and patient-related factors.[9-11] The healthcare policies have allowed the use of FFR-CT analysis in the approved hospitals that can appropriately operate and evaluate coronary CTA, to avoid increases in medical costs. The Japanese Circulation Society (JCS) working group recently collaborated with related academic societies and proposed the appropriate use criteria for FFR-CT. The appropriate use criteria stipulate details such as the facility requirements established by the relevant societies and the use of FFR-CT only for CAD with ≥ 50% stenosis on coronary CTA (secondary source 2). The Japanese Circulation Society's 2018 Guideline on Diagnosis of Chronic Coronary Heart Diseases took into account guidelines on the appropriate use of FFR-CT and the status of its use in Japan and provided recommendations for its clinical use that are of recommendation class IIb and evidence level B (MINDS recommendation grade B and evidence classification II; secondary source 3).

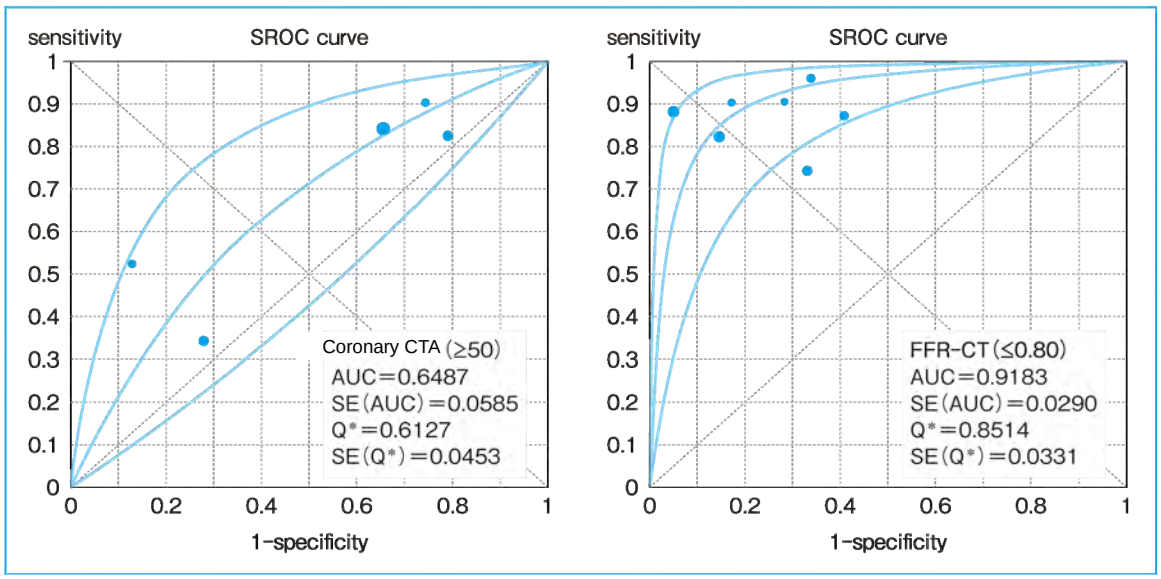

Figure 1. SROCs for coronary CTA (≥ 50%) and FFR-CT (≤ 0.80)

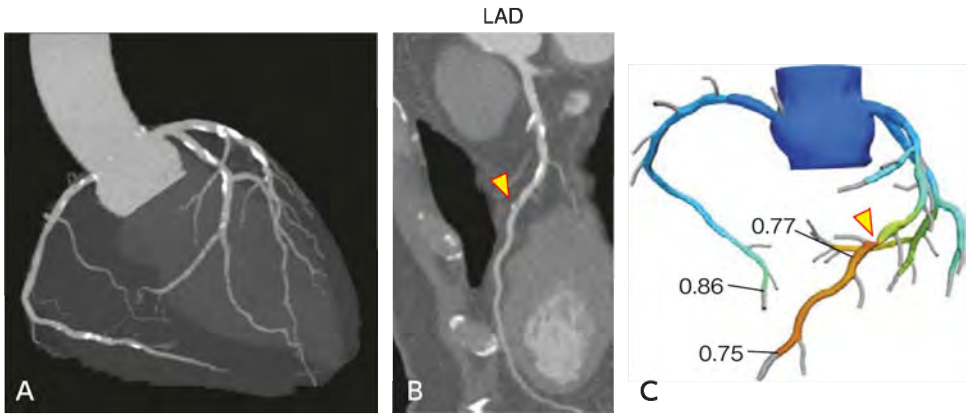

Figure 2. Clinical case with additional FFR-CT analysis

The patient was a man in his 60s. Multiple moderate stenoses are seen in the left anterior descending artery (LAD) on coronary CTA. An FFR-CT analysis was therefore performed (A, B). An FFR-CT value of 0.77 was obtained for the distal stenotic lesion with minor calcification in the distal LAD (C).

Some studies and systematic reviews have found that FFR-CT values near 0.8 had a grey zone of diagnostic accuracy with wide confidence intervals, false positives, and false negatives.[12, 13] The current appropriate use criteria in Japan allow FFR-CT only to assess CAD with stenosis ≥ 50% on coronary CTA. Consequently, the present meta-analyses, including some vessels with 30% to 49% stenosis, may not be optimal for this CQ. A previous study reported that approximately 80% of vessels with stenosis of 30% to 49% have an FFR-CT value > 0.8.[14] In this regard, it may be necessary to consider that the evaluation of FFR-CT diagnostic performance in the systematic review conducted for this CQ is a slight underestimate. In addition, a point to keep in mind when using FFR-CT clinically is that the national healthcare insurance system will not cover part of the medical costs for the downstream tests after FFR-CT analysis according to the supplementary items for clinical use of FFR-CT. For instance, this regulation will be applied when the cases undergo FFR-CT analysis, invasive FFR, and stress MPI using nuclear or magnetic resonance imaging in a series of further investigations for obstructive CAD.

Search keywords and secondary sources used as references

PubMed was searched using the following keywords: computed tomography, fractional flow reserve, FFR, intermediate stenosis, myocardial, coronary computed tomographic, coronary CT, stenosis, computed tomography angiography, and sensitivity.

In addition, the following were referenced as secondary sources.

1) Narula N et al: SCCT 2021 expert consensus document on coronary computed tomographic angiography: a report of the Society of Cardiovascular Computed Tomography. J Cardiovasc Comput Tomogr. S1934-5925: 30473-30471, 2021
2) Japanese Circulation Society Task Force Committee: Guidelines on the Appropriate Use of FFRCT, revised on December 1, 2018. Japanese Circulation Society, 2018.
3) Japanese Circulation Society, Ed.: Guidelines for the diagnosis and treatment of cardiovascular disease: JCS 2018 Guideline on Diagnosis of Chronic Coronary Heart Diseases. Japanese Circulation Society, 2009.

References

1) Min JK et al: Usefulness of noninvasive fractional flow reserve computed from coronary computed tomographic angiograms for intermediate stenoses confirmed by quantitative coronary angiography. Am J Cardiol 110: 971-976, 2012
2) Nakazato R et al: Noninvasive fractional flow reserve derived from computed tomography angiography for coronary lesions of intermediate stenosis severity: results from the DeFACTO study. Circ Cardiovasc Imaging 6: 881-889, 2013
3) Nørgaard BL et al: Diagnostic performance of noninvasive fractional flow reserve derived from coronary computed tomography angiography in suspected coronary artery disease: the NXT trial (analysis of coronary blood flow using CT angiography: next steps). J Am Coll Cardiol 63: 1145-1155, 2014
4) Coenen A et al: Fractional flow reserve computed from noninvasive CT angiography data: diagnostic performance of an on-site clinician-operated computational fluid dynamics algorithm. Radiology 274: 674-83, 2015
5) Donnelly PM et al: Experience with an on-site coronary computed tomography-derived fractional flow reserve algorithm for the assessment of intermediate coronary stenoses. Am J Cardiol 121: 9-13, 2018
6) Driessen RS et al: Comparison of coronary computed tomography angiography, fractional flow reserve, and perfusion imaging for ischemia diagnosis. J Am Coll Cardiol Img 73: 161-173, 2019
7) Tang CX et al: CT FFR for ischemia-specific CAD with a new computational fluid dynamics algorithm: a chinese multicenter study. JACC Cardiovasc Imaging: 13: 980-990, 2020
8) Zhuang B et al: Computed tomography angiography-derived fractional flow reserve (CT-FFR) for the detection of myocardial ischemia with invasive fractional flow reserve as reference: systematic review and meta-analysis. Eur Radiol.30: 712-725, 2020

9) Nørgaard BL et al: Influence of coronary calcification on the diagnostic performance of CT angiography derived FFR in coronary artery disease: a substudy of the NXT trial. JACC Cardiovasc Imaging 8: 1045-1055, 2015
10) Takx AP et al: Sublingual nitroglycerin administration in coronary computed tomography angiography: a systematic review. Eur Radiol. 25: 3536-42, 2015
11) Coenen A et al: Coronary CT angiography derived fractional flow reserve: Methodology and evaluation of a point of care algorithm. J Cardiovasc Comput Tomogr 10: 105-113, 2016
12) Cook CM et al: Diagnostic accuracy of computed tomography-derived fractional flow reserve: a systematic review. JAMA Cardiol 2: 803-810, 2017
13) Coenen A et al: Diagnostic accuracy of a machine-learning approach to coronary computed tomographic angiography-based fractional flow reserve: result from the MACHINE consortium. Circ Cardiovasc Imaging 11: e007217, 2018
14) Kitabata H et al: Incidence and predictors of lesion-specific ischemia by FFR CT: learnings from the international ADVANCE registry. J Cardiovasc Comput Tomogr 12: 95-100, 2018

CQ 8 Is MRI T1 mapping recommended for diagnosing left ventricular hypertrophy?

Recommendation

MRI T1 mapping is weakly recommended for diagnosing left ventricular hypertrophy.

Recommendation strength: 2, strength of evidence: weak (C), agreement rate: 83% (10/12)

Background

The diseases that result in left ventricular hypertrophy are varied, but mainly include cardiomyopathy, such as hypertrophic cardiomyopathy, Fabry disease, cardiac amyloidosis, and hypertensive heart disease. Cine MRI and late gadolinium enhanced (LGE) MRI are imaging modalities with established evidence levels for the diagnosis of cardiomyopathy. However, in patients with suspected cardiomyopathy and left ventricular hypertrophy, there are limits to the ability of those conventional cardiac MRI techniques alone to diagnose the cause of left ventricular hypertrophy. Consequently, the systematic review conducted for this CQ examined whether T1 mapping with conventional cine MRI or LGE MRI provides added value in diagnosing the underlying etiology of left ventricular hypertrophy in patients with suspected cardiomyopathy and left ventricular hypertrophy.

Explanation

In preparing the recommendation for this CQ, the following 3 outcomes were specified with regard to whether T1 mapping with conventional cine MRI or LGE MRI provides added value in diagnosing the underlying etiology of left ventricular hypertrophy in patients with suspected cardiomyopathy and left ventricular hypertrophy: diagnosis of cardiac amyloidosis; differentiation between hypertrophic cardiomyopathy and hypertensive cardiac hypertrophy; and differentiation between Fabry disease and hypertrophic cardiomyopathy.

Three studies that examined cardiac amyloidosis consistently found strikingly high myocardial T1 values in cardiac amyloidosis and that myocardial T1 was therefore of high diagnostic value.[1-3)] In a case-control study, Karamitsos et al. performed T1 mapping using the shortened modified look-locker inversion recovery (ShMOLLI) (1.5T) in 53 patients with AL amyloidosis (with no cardiac involvement, n = 14; with possible cardiac involvement, n = 11; and with definite cardiac involvement, n = 28), 17 patients with aortic stenosis, and 36 healthy individuals.[1)] The results showed that myocardial T1 values were significantly higher in patients with cardiac amyloidosis than in healthy individuals (1,140 ± 61 ms vs. 958 ± 20 ms, $p < 0.001$). In a receiver-operating characteristic (ROC) curve analysis of these patient groups, those suspected of having cardiac amyloidosis and those with cardiac amyloidosis were considered positive for cardiac amyloidosis, and the remainder were considered negative. The resulting AUC was 0.97 ($p < 0.0001$), and the cutoff was 1,020 ms. In a case-control study by Fontana et al., T1 mapping using ShMOLLI (1.5T) was

performed in patients with transthyretin (ATTR) cardiac amyloidosis (n = 85), healthy individuals with a transthyretin gene abnormality (n = 8), patients with light-chain (AL) cardiac amyloidosis (n = 79), patients with hypertrophic cardiomyopathy (n = 46), and healthy individuals (n = 52).[2] The study found that myocardial T1 values were significantly higher in patients with ATTR cardiac amyloidosis than in those with hypertrophic cardiomyopathy or healthy individuals (1,097 ± 43 ms, 1,026 ± 64 ms, and 967 ± 34 ms, respectively; $p < 0.0001$ for both differences). Moreover, diagnostic performance with respect to hypertrophic cardiomyopathy was comparably high for both AL cardiac amyloidosis and ATTR cardiac amyloidosis [The AUC for diagnostic performance was 0.84 (95% CI, 0.76 to 0.92) in accurately differentiating between AL cardiac amyloidosis and hypertrophic cardiomyopathy and 0.85 (95% CI, 0.77 to 0.92) in accurately differentiating between ATTR cardiac amyloidosis and hypertrophic cardiomyopathy; $p < 0.0001$ for both]. A large cohort study by Baggiano et al. involving patients with suspected cardiac amyloidosis (n = 868) found that myocardial T1 values (modified look-locker inversion recovery (MOLLI), 1.5T) were significantly higher in patients whose final diagnosis was cardiac amyloidosis (n = 441) than in the other patients (n = 427; 1,149 ± 63 ms vs. 1,038 ± 50 ms, $p < 0.001$).[3] An ROC analysis showed the diagnostic accuracy of myocardial T1 for cardiac amyloidosis to be high (AUC = 0.93). When myocardial T1 was < 1,036 ms, cardiac amyloidosis could be excluded with a negative predictive value of 98%; when myocardial T1 was ≥ 1,164 ms, cardiac amyloidosis could be diagnosed with a positive predictive value of 98%. The same study found the diagnostic performance of myocardial T1 in cardiac amyloidosis to be significantly higher than that of indices obtained with conventional cine MRI and delayed contrast-enhanced MRI. Moreover, a between-groups comparison according to the presence or absence of left ventricular hypertrophy showed no difference in the diagnostic performance of myocardial T1 in cardiac amyloidosis ($p = 0.35$).

With regard to distinguishing between hypertrophic cardiomyopathy and hypertensive cardiac hypertrophy, a case-control study by Hinojar et al. was included in the review.[4] In that study, T1 mapping was performed using MOLLI (3.0T) in patients with hypertrophic cardiomyopathy (n = 95), hypertensive cardiac hypertrophy (n = 69), hypertrophic cardiomyopathy genotype positive/phenotype negative (n = 23), and healthy individuals (n = 23). Myocardial T1 values were significantly higher in hypertrophic cardiomyopathy than in hypertensive cardiac hypertrophy (1,169 ± 41 ms vs. 1,058 ± 29 ms, $p < 0.05$). Moreover, myocardial T1 showed extremely high sensitivity and specificity in distinguishing between hypertrophic cardiomyopathy and hypertensive cardiac hypertrophy, with sensitivity of 96% (95% CI, 87% to 99%) and specificity of 98% (95% CI, 92% to 100%).

Two case-control studies concerned with distinguishing between Fabry disease and hypertrophic cardiomyopathy were included in the review.[5, 6] They found the low myocardial T1 values seen in Fabry disease to be of high diagnostic value. Karur et al. performed T1 mapping using MOLLI (3.0T) in patients with Fabry disease (n = 30) and hypertrophic cardiomyopathy (n = 30).[5] They found myocardial T1 values to be significantly lower in Fabry disease than in hypertrophic cardiomyopathy (1,161 ± 47 ms vs 1,296 ± 55 ms, $p < 0.001$). Using a cutoff of 1,220 ms, Fabry disease could be distinguished from hypertrophic

cardiomyopathy with sensitivity and specificity of 97% and 93%, respectively. Debore et al. performed T1 mapping using MOLLI (1.5T) in patients with Fabry disease (n = 17) and hypertrophic cardiomyopathy (n = 36) and healthy individuals (n = 70).[6] The results showed that myocardial T1 was significantly lower in patients with Fabry disease (891 ± 49 ms) than in those with hypertrophic cardiomyopathy (995 ± 34 ms) and healthy controls (966 ± 27 ms; $p < 0.001$ for both). Moreover, using a cutoff of 940 ms, Fabry disease could be distinguished from hypertrophic cardiomyopathy with sensitivity and specificity of 88% and 92%, respectively.

A problem common to the above studies included in the review is that the results shown are those obtained with an optimal threshold value for each group of study subjects, and it is unclear whether they are applicable to other facilities. In addition, the studies did not examine the added value to cine MRI and LGE MRI in differentiating between hypertrophic cardiomyopathy and hypertensive cardiac hypertrophy and between Fabry disease and hypertrophic cardiomyopathy.[4-6] Furthermore, the patients included in the studies that examined cardiac amyloidosis diagnosis and the differentiation of Fabry disease and hypertrophic cardiomyopathy did not always have left ventricular hypertrophy.[1, 2, 5, 6] Based on the above considerations, it was concluded that the evidence that it is useful to add T1 mapping to MRI in patients with left ventricular hypertrophy is weak. However, the addition of T1 mapping is likely to improve diagnostic accuracy in cardiac amyloidosis and Fabry disease and could greatly affect treatment strategy decisions. Moreover, T1 mapping is not invasive and does not clearly increase the cost of testing, aside from prolonging test duration to a certain extent. In view of these considerations, it is weakly recommended that T1 mapping be performed.

Search keywords and secondary sources used as references

PubMed was searched using the following keywords: hypertrophy, left ventricular, LVH, hypertrophies, hypertrophic cardiomyopathy, cardiomyopathy, hypertrophic, Fabry disease, immunoglobulin light-chain amyloidosis, hereditary amyloidosis, amyloidosis, familial, late gadolinium enhancement, magnetic resonance imaging, T1, T1 map, and T1 mapping. Eighty-two articles were extracted. A systematic review was conducted, and 6 articles that clearly indicated sensitivity and specificity were ultimately included.

References

1) Karamitsos TD et al: Noncontrast T1 mapping for the diagnosis of cardiac amyloidosis. JACC Cardiovasc Imaging 6: 488-497, 2013
2) Fontana M et al: Native T1 mapping in transthyretin amyloidosis. JACC Cardiovasc Imaging: 157-165, 2014
3) Baggiano A et al: Noncontrast magnetic resonance for the diagnosis of cardiac amyloidosis. JACC Cardiovasc Imaging 13: 69-80, 2020
4) Hinojar R et al: T1 mapping in discrimination of hypertrophic phenotypes: hypertensive heart disease and hypertrophic cardiomyopathy: findings from the international T1 multicenter cardiovascular magnetic resonance study. Circ Cardiovasc Imaging 8: e003285, 2015
5) Karur GR et al: Use of myocardial T1 mapping at 3.0 T to differentiate Anderson-Fabry disease from hypertrophic cardiomyopathy. Radiology 288: 398-406, 2018
6) Deborde E et al: Differentiation between Fabry disease and hypertrophic cardiomyopathy with cardiac T1 mapping. Diagn Interv Imaging 101: 59-67, 2020

BQ 33 Are CT and MRI recommended for diagnosing Takayasu's arteritis?

Statement

Contrast-enhanced CT is useful and recommended.

If contrast-enhanced CT is difficult to implement, MRI, which provides comparable diagnostic performance, is recommended. MRI, which does not involve radiation exposure, is preferable for long-term follow-up observation.

Background

Pathological diagnosis is rarely performed for the definitive diagnosis of Takayasu arteritis. It is generally diagnosed through a comprehensive assessment of factors such as imaging findings, the patient's clinical course, and test findings. Diagnostic imaging plays a particularly important role in diagnosing this condition. Accurate diagnostic imaging makes it possible to diagnose the condition early and begin appropriate treatment.

Explanation

Takayasu arteritis is a nonspecific, idiopathic vasculitis that affects elastic vessels such as the aorta, its major branches, and the pulmonary artery. It is common in Japan and other Asian countries and commonly occurs in young to middle-aged women. The patients it affects are often included in a patient group with fever of unknown origin. When young women present with complaints of fever and malaise, it is important to keep Takayasu arteritis in mind during differential diagnosis.

1. Diagnostic overview

The diagnostic criteria for Japan [Guidelines for Management of Vasculitis Syndrome (JCS 2017)] state that definitive diagnosis centers on diagnostic imaging (CT, MRI ultrasound, PET/CT, chest radiography, and angiography; secondary source 1). The morphology of the aorta and its main branches can be adequately evaluated with recent CT and MRI systems, and these modalities are recommended for the initial evaluation of Takayasu arteritis (secondary source 2).

Takayasu arteritis is associated with the following characteristic diagnostic imaging findings, and its diagnosis can be considered definitive if one or more of the symptoms indicated in the guidelines are present: multiple or diffuse hypertrophic, stenotic (including occlusions), or dilated lesions (including aneurysms) in the aorta and/or its primary branches. However, the following conditions must be excluded for definitive diagnosis: ① arteriosclerosis, ② a congenital vascular anomaly, ③ inflammatory abdominal aortic aneurysm, ④ infected aneurysm, ⑤ syphilitic aortitis, ⑥ giant cell arteritis (temporal arteritis), ⑦ vascular Behçet's disease, and ⑧ IgG4-related disease.

2. Usefulness of CT and MRI in the acute phase

The previous gold standard for diagnostic imaging of this condition was digital subtraction angiography (DSA).[1)] However, although DSA is an excellent method of evaluating the vessel lumen for conditions such as stenosis and dilatation, it is not suitable for evaluating the wall thickening without luminal changes that is seen in the acute phase. Consequently, the initial diagnosis of Takayasu arteritis is now almost always performed by CT and MRI. Thickening of the full circumference of the aortic wall is a characteristic of the acute phase. On non-contrast CT, the thickened aortic wall is seen as a hyperintensity area. In the late phase of contrast-enhanced CT, nearly homogeneous enhancement is seen in the thickened wall. However, double-ring-shaped enhancement may be seen on careful observation.[2-6)] This double-ring-shaped enhancement is called the double ring-like sign. The outer layer of contrast enhancement is thought to reflect inflammatory changes associated with angiogenesis of the vascular media and adventitia. The inner layer, which shows weak contrast enhancement, is thought to correspond to mucinous and gelatinous swelling of the intima. The frequency of pulmonary artery lesions in this condition is relatively high, approximately 70% to 80%. Consequently, its presence or absence may be the deciding factor in differentiating Takayasu arteritis from other diseases. Attention must therefore also be paid to pulmonary artery wall thickening and contrast enhancement in the acute phase.[6)] Similar acute-phase wall thickening and enhancement are also seen on contrast-enhanced MRI. Consequently, MRI, which does not involve radiation exposure, is useful for evaluating treatment efficacy and long-term follow-up observation.[7-9)] If Takayasu arteritis is diagnosed and corticosteroid therapy is started in this phase, improvement in arterial wall thickening is likely. However, nonspecific inflammatory findings such as fever of unknown origin are often the only changes seen clinically, and it is often not appropriately diagnosed.

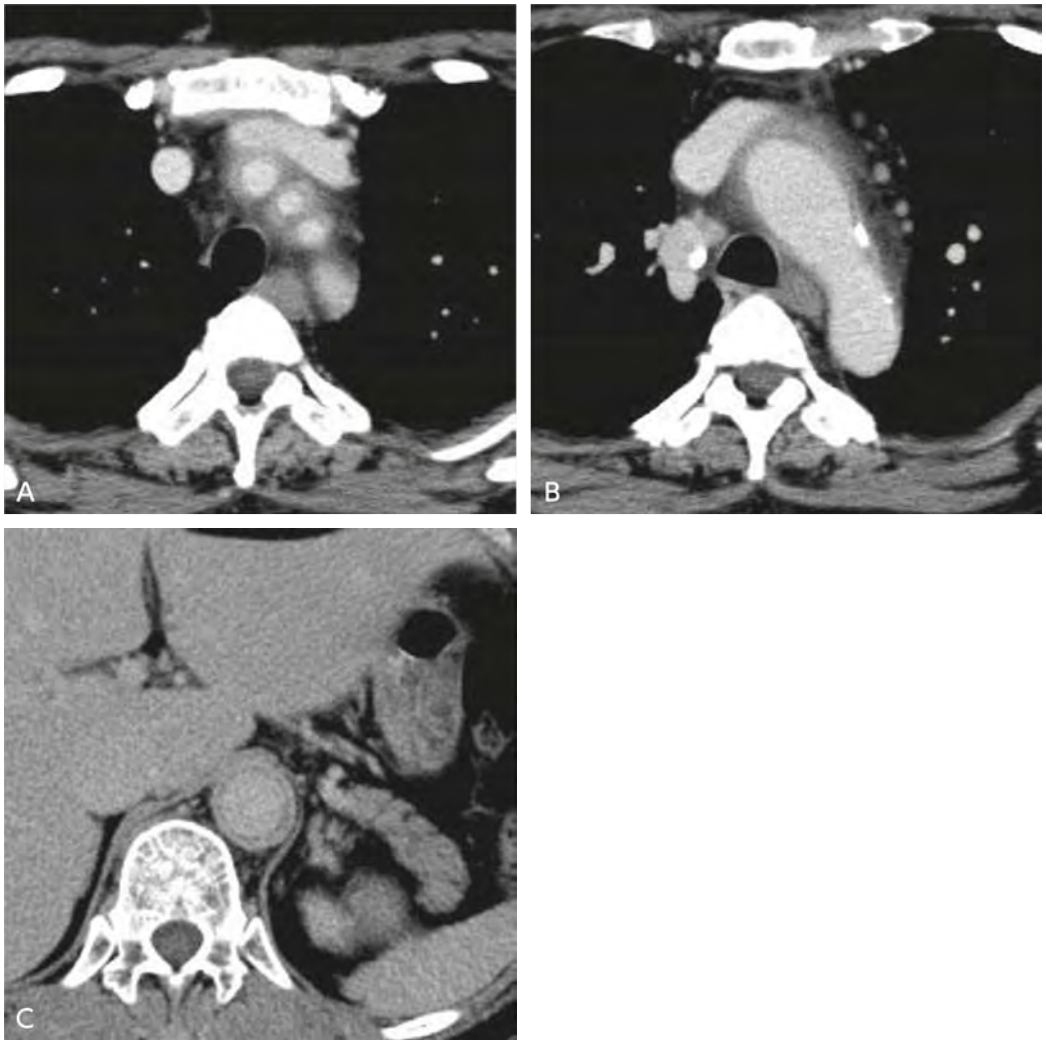

Figure 1. Takayasu arteritis (acute phase: woman in her 40s)

A to C: Contrast-enhanced CT, late phase: Wall thickening and contrast enhancement are seen in the aortic arch, the aortic arch branches, and the junction of the thoracoabdominal aorta. Although contrast enhancement is seen in the outer part of the thickened wall, contrast enhancement of the inner part is weak and shows double-ring-shaped enhancement (double ring-like sign).

Beginning in April 2018, ^{18}F-FDG PET and PET/CT testing became available at some PET facilities under national health insurance coverage for patients with large-vessel vasculitis in which lesion localization or activity could not be determined with other tests. Because ^{18}F-FDG accumulates in areas of active inflammation, its accumulation in great vessels is a useful finding for diagnosing Takayasu arteritis.[10] In addition, the level of ^{18}F-FDG accumulation is correlated with the clinical activity level of Takayasu arteritis.[10]

3. Usefulness of CT and MRI in the chronic phase

Common vascular diseases in the chronic phase are stenosis resulting from reactive intimal thickening and occlusive disease. However, dilated lesions and arterial aneurysms develop when there is severe

vascular smooth muscle cell necrosis or destruction of the elastic fiber layer and mild scarring. Stenotic lesions are commonly seen in vessels such as the left subclavian artery, left common carotid artery, descending thoracic aorta, and abdominal aorta. Collateral circulation develops as a result of stenotic lesions.[5, 6)] Dilated lesions are commonly seen in the ascending aorta, aortic arch, and brachiocephalic artery. Dilation, stenosis, and occlusive lesions of the aorta and its branches can be visualized well by CTA and MRA and are now rarely evaluated by DSA.[3, 11-13)] Sensitivity and specificity of 100% and 100%, respectively, for MRA and 95% and 100% for CT have been reported when DSA is used as the gold standard.[5, 13)] It has also been reported that CTA and MRA can be used to evaluate pulmonary artery stenosis and occlusion, suggesting that they can be used instead of pulmonary blood flow scintigraphy.[14)]

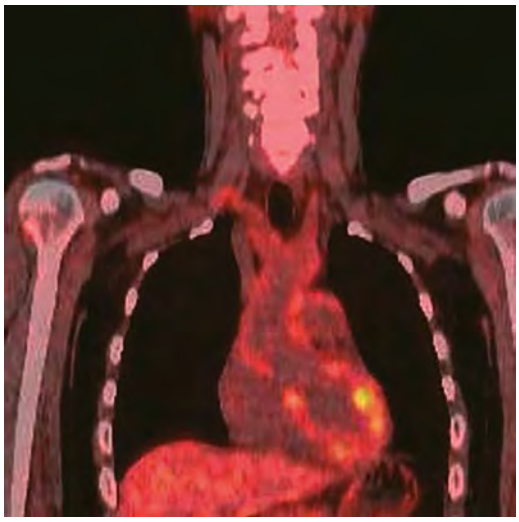

Figure 2. Takayasu arteritis (acute phase: woman in her 20s)

^{18}F-FDG PET/CT fusion image: Accumulation is seen in the walls of the thoracic aorta, its branches, and the pulmonary artery. The findings are suggestive of active inflammation.

Figure 3. Takayasu arteritis (chronic phase: woman in her 50s)

Contrast-enhanced CT, MIP image: Striking calcification is seen in the aortic arch. Occlusion of the aortic branches and marked collateral development are seen.

Conditions that define the prognosis of Takayasu arteritis include the following: ① hypertension resulting from the renal artery coarctation or atypical aortic coarctation; ② congestive heart failure resulting from aortic valve insufficiency; ③ ischemic heart disease resulting from coronary artery lesions; and ④ aneurysm rupture. When a complication involving the aorta is present, the 15-year survival rate decreases to 66%. Consequently, to improve the life expectancy of patients, appropriate medical treatment of these conditions must be administered from an early stage, and appropriate surgical treatment is required for patients with severe disease. Recently, CT has also been found to be useful for evaluating coronary artery disease in Takayasu arteritis.[15, 16)]

Search keywords and secondary sources used as references

PubMed was searched using the following keywords: Takayasu arteritis, CT, and MRI.

In addition, the following were referenced as secondary sources.

1) Joint Working Group on Guidelines for the Diagnosis and Treatment of Cardiovascular Disease, Ed.: 2017 Guidelines for Management of Vasculitis Syndrome. Japanese Circulation Society, 2017.
2) Hiratzka LF et al: ACCF/AHA/AATS/ACR/ASA/SCA/SCAI/SIR/STS/SVM guidelines for the diagnosis and management of patients with thoracic aortic disease: executive summary. J Am Coll Cardiol 55: 1509-1544, 2010

References

1) Yamato M et al: Takayasu arteritis: radiographic end angiographic findings in 59 patients. Radiology 161 (2): 329-334, 1986
2) Park JH: Conventional and CT angiographic diagnosis of Takayasu arteritis. Int J Cardiol 54 (suppl): S165-S171, 1996
3) Park JH et al: Takayasu arteritis evaluation of mural changes in the aorta and pulmonary artery with CT angiography. Radiology 196: 89-93, 1995
4) Shama S el al: Morphologic mural changes in the aorta revealed by CT in patients with nonspecific aortoarteritis (Takayasu arteritis). AJR Am J Roentgenol 167: 1321-1325, 1996
5) Yamada I et al: Takayasu arteritis evaluation of the thoracic aorta with CT angiography. Radiology 209: 103-109, 1998
6) Matsunaga N et al: Takayasu arteritis protean radiologic manifestations and diagnosis. Radiographics 17: 579-597,1997
7)Tso E et al Takayasu arteritis utility and limitation of magnetic resonance imaging in diagnosis and treatment. Arthritis Rheum 46: 1634-1612, 2002
8) Choe YH et al: Takayasu's arteritis assessment of disease activity with contrast-enhanced MR imaging. AJR Am J Roentgenol 175: 505-51, 2002
9) Yamada I et al: Takayasu arteritis evaluation with MR imaging. Rad iology 188: 89-94, 1993
10) Soussan M et al: Management of large-vessel vasculitis with FDG-PET: a systematic literature review and metaanalysis. Medicine (Baltimore) 94: e622, 2015)
11) Kumar S et al: Takayasu's arteritis evaluation with three-dimensional time-of-flight MR angiography. Eur Radiol 7: 44-50, 1997
12) Nastri MV et al: Gadolinium-enhanced three-dimensional MR angiography of Takayasu arteritis. Radiographies 24: 773-778, 2004
13) Yamada I et al: Takayasu arteritis diagnosis with breath-hold contrast-enhanced three-dimensional MR angiography. J Magn Reson Imaging 11: 481-487, 2000
14) Sueyoshi E et al: Diagnosis of perfusion abnormality of the pulmonary artery in Takayasu's arteritis using contrast-enhance MR perfusion imaging. Eur Radiol 16 1551-1556, 2006
15) Soto ME et al: Coronary OCT angiography of Takayasu arteritis. J Am Coll Cardiol 4: 1531-1540, 2011
16) Kang EJ et al: Takayasu arteritis assessment of coronary arterial abnormalities with 128 section dual-source CT angiography of the coronary arteries and aorta. Radiology 270: 74-81, 2014

BQ 34 Are CT and MRI recommended to determine whether TAVI/TAVR is anatomically indicated for aortic stenosis?

Statement

There is evidence that CT is useful for determining whether TAVI/TAVR is anatomically indicated, and it is therefore recommended. The usefulness of MRI has not yet been established.

Background

Aortic stenosis is a condition in which narrowing of the aortic valve obstructs blood flow from the left ventricle to the ascending aorta. The presence of stenosis is suggested when peak velocity through the aortic valve is > 2 m/s, and severe disease is defined as a peak velocity of > 4 m/s and an aortic valve area of < 1.0 cm^2 (secondary source 1). The rate of aortic stenosis morbidity is high in elderly individuals. A meta-analysis of studies conducted in Europe and the United States (n = 9,723) estimated the prevalence of aortic stenosis to be 12.4% and the prevalence of severe aortic stenosis to be 3.4% in the general population of individuals aged ≥ 75 years.[1)]

Transcatheter aortic valve implantation (TAVI) and transcatheter aortic valve replacement (TAVR) are treatments first performed in France in 2002.[2)] Since then, they have been accepted as alternatives to surgical aortic valve replacement in patients for whom surgery is contraindicated and those at high surgical risk, and they have become progressively more widely implemented in recent years.[3-5)] A 2013 meta-analysis estimated that TAVI/TAVR was indicated for approximately 290,000 patients in Europe and the United States (approximately 190,000 in the Europe and 100,000 in North America), and that it was newly indicated for approximately 27,000 patients annually (approximately 18,000 annually in Europe and 9,000 annually in North America).[1)] As of March 2020, the main devices used in Japan are the balloon-expandable SAPIEN 3 bioprosthetic valve (Edwards Lifesciences) and the self-expanding Evolut™ PRO system (Medtronic; Fig. 1). A transfemoral approach is generally selected (Fig. 2A). However, if this route is not feasible because of the patient's background, a transapical (Fig. 2B), transsubclavian, or transaortic (Fig. 2C) approach is selected.

Figure 1. Prosthetic valves used in TAVI/TAVR

A: Balloon-expandable SAPIEN 3 (provided by Edwards Lifesciences)
B: Self-expanding Evolut™ PRO (provided by Medtronic Japan)

Explanation

To select the appropriate bioprosthetic valve size for TAVI/TAVR, the aortic valve annulus must be accurately measured. If the bioprosthetic valve is too large for the annulus, rupture may occur, and this is often fatal.[4)] Conversely, bioprosthetic valves that are too small for the annulus have been found to increase the frequency of perivalvular aortic regurgitation and adversely affect outcomes.[6-8)] In the evaluation performed before TAVI/TAVR, the diameter of the aortic valve annulus has historically been measured by performing aortography, transthoracic echocardiography, or transesophageal echocardiography. However, measurements are often discrepant.[9, 10)] The reason these 2-dimensional tests have major limitations is that the aortic valve annulus is elliptical rather than circular.[9, 10)] With 2D echocardiography, the diameter is generally measured near the short-axis diameter of the elliptical annulus. Consequently, the diameter measured with 3D CT is greater than that obtained with echocardiography. The use of CT measurement to select valve size has been reported to reduce post-TAVI/TAVR aortic valve regurgitation, as compared with size selection based on echocardiography.[11)] CT is currently the gold standard for measuring the diameter of the aortic valve annulus.[5)]

Moreover, in pre-TAVI/TAVR examinations, CT provides useful information about access routes, including the apex and vasculature from the aortic root to the bilateral common femoral artery. Together with the patient background characteristics, this information plays an important role in selecting a transfemoral (Fig. 2A), transapical (Fig. 2B), or other approach.[4, 5)] Furthermore, the projection image orthogonal to the aortic valve, i.e., the perpendicular view during TAVI/TAVR procedure/contrast imaging (Fig. 3), can be estimated from pre-TAVI/TAVR CT images,[4, 5)] enabling the contrast medium dose to be reduced during the TAVI/TAVR procedure.

Based on the above considerations, CT is recommended to determine whether TAVI/TAVR is anatomically indicated in patients with aortic stenosis.[4, 5)]

The usefulness of MRI for determining whether TAVI/TAVR is anatomically indicated has not yet been established.

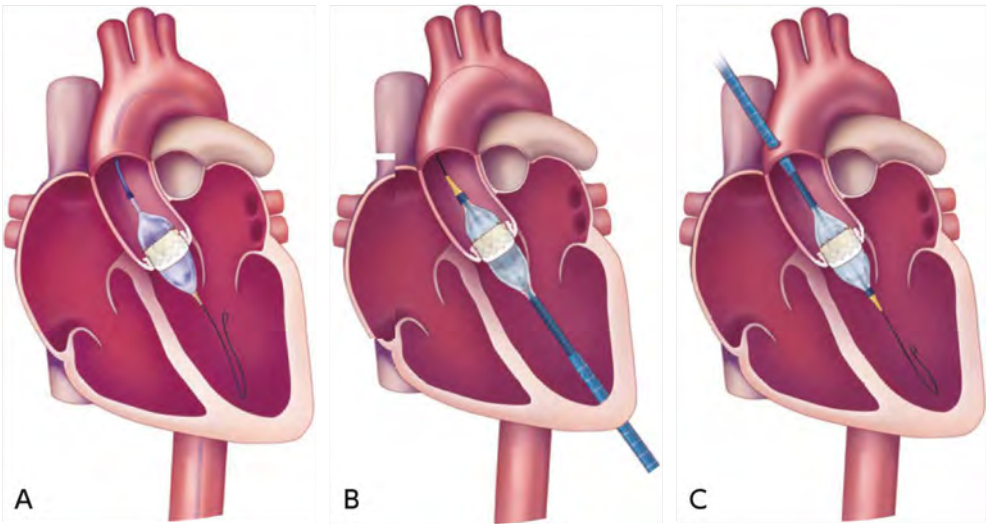

Figure 2. Various approaches for TAVI/TAVR

A: Transfemoral approach, B: Transapical approach, C: Transaortic approach
(provided by Edwards Lifesciences)

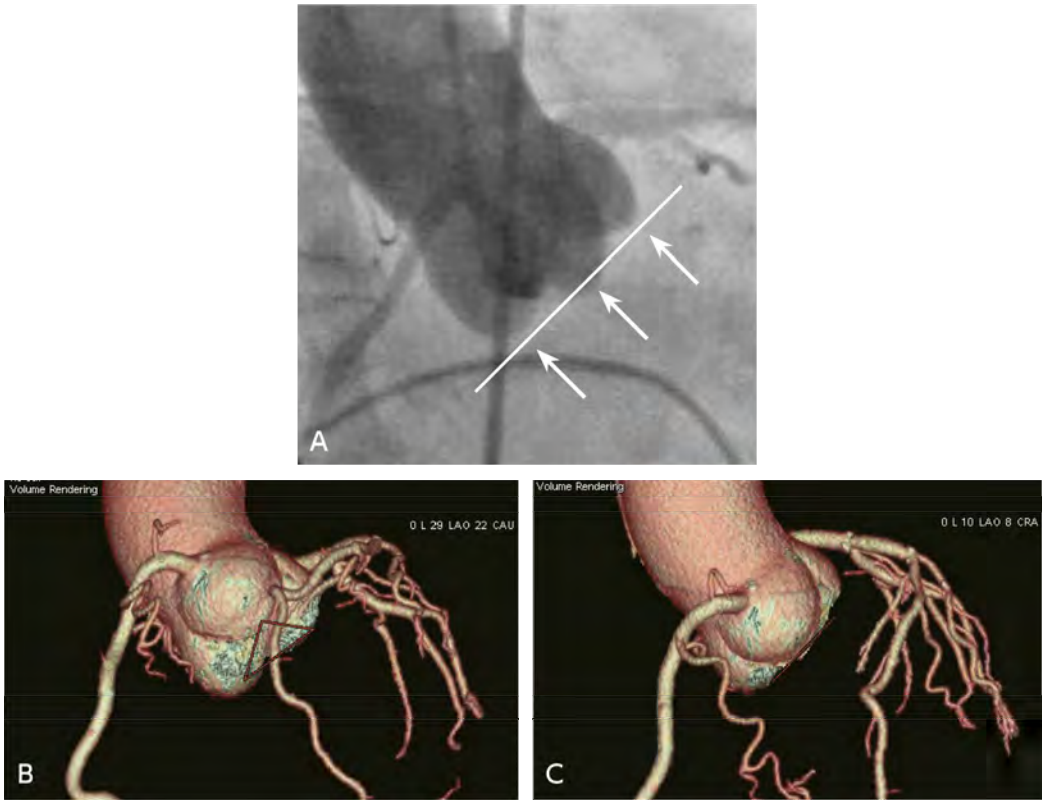

Figure 3. Pre-TAVI/TAVR CT estimate on the perpendicular view during TAVI/TAVR procedure/contrast imaging.

Search keywords and secondary sources used as references

PubMed was searched using the following keywords: aortic stenosis, transcatheter aortic value implantation, and transcatheter aortic valve replacement.

In addition, the following was referenced as a secondary source.

1) Nishimura RA et al: 2014 AHA/ACC guideline for the management of patients with valvular heart disease: a report of the American College of Cardiology/American Heart Association Task Force on Practice Guidelines. Circulation 129 (23):

References

1) Osnabrugge RL et al: Aortic stenosis in the elderly: disease prevalence and number of candidates for transcatheter aortic valve replacement: a meta-analysis and modeling study. J Am Coll Cardiol 62 (11): 1002-1012, 2013
2) Cribier A et al: Percutaneous transcatheter implantation of an aortic valve prosthesis for calcific aortic stenosis: first human case description. Circulation 106 (24): 3006-3008, 2002
3) Holmes DR et al: 2012 ACCF/AATS/SCAI/STS expert consensus document on transcatheter aortic valve replacement. J Am Coll Cardiol 59 (13): 1200-1254, 2012
4) Achenbach S et al: SCCT expert consensus document on computed tomography imaging before transcatheter aortic valve implantation (TAVI)/transcatheter aortic valve replacement (TAVR). J Cardiovasc Comput Tomogr 6 (6): 366-380, 2012
5) Blanke P et al: Computed tomography imaging in the context of transcatheter aortic valve implantation (TAVI)/transcatheter aortic valve replacement (TAVR): an expert consensus document of The Society of Cardiovascular Computed Tomography. JACC Cardiovasc Imaging 12 (1): 1-24, 2019
6) Gilard M et al: Registry of transcatheter aortic-valve implantation in high-risk patients. N Engl J Med 366 (18): 1705-1715, 2012
7) Sinning JM et al: Aortic regurgitation index defines severity of peri-prosthetic regurgitation and predicts outcome in patients after transcatheter aortic valve implantation. J Am Coll Cardiol 59 (13): 1134-1141, 2012

8) Kodali SK et al: Two-year outcomes after transcatheter or surgical aortic-valve replacement. N Engl J Med 366 (18): 1686-1695, 2012
9) Altiok E et al: Comparison of two-dimensional and three-dimensional imaging techniques for measurement of aortic annulus diameters before transcatheter aortic valve implantation. Heart (British Cardiac Society) 97 (19): 1578-1584, 2011
10) Ng AC et al: Comparison of aortic root dimensions and geometries before and after transcatheter aortic valve implantation by 2-and 3-dimensional transesophageal echocardiography and multislice computed tomography. Circulation Cardiovascular imaging 3 (1): 94-102, 2010
11) Jilaihawi H et al: Cross-sectional computed tomographic assessment improves accuracy of aortic annular sizing for transcatheter aortic valve replacement and reduces the incidence of paravalvular aortic regurgitation. J Am Coll Cardiol 59 (14): 1275-1286, 2012

FQ 3 Is preoperative identification of the artery of Adamkiewicz recommended before open repair or endovascular repair of a thoracic aortic aneurysm or thoracoabdominal aortic aneurysm?

Statement

There is a tendency to recommend identification of the artery of Adamkiewicz as a preoperative examination, although the evidence is not sufficient in the case of open repair.

Although the evidence is also insufficient in the case of endovascular repair, identification of the artery can be considered in cases if the critical zone is to be covered or in patients whose aortic pathologies require extensive coverage.

Background

One of the most serious complications in patients undergoing thoracic descending aortic aneurysm and thoracoabdominal aortic aneurysm repair is spinal cord ischemia. Preoperative identification of the artery of Adamkiewicz using CT or MRI can help prevent postoperative spinal cord injury.

Explanation

In the thoracolumbar spinal cord, the feeding artery of the anterior spinal artery is the great anterior radiculomedullary artery, also known as the artery of Adamkiewicz, with a diameter of approximately 1 mm. This artery supplies the lower one-third of the spinal cord, commonly originating between the 8th intercostal artery and the 1st lumbar artery.[1)]

The distal portion of the artery of Adamkiewicz and the anterior spinal artery form a “hairpin turn” configuration. This characteristic morphology is an important landmark when identifying the artery of Adamkiewicz on CT or MRI. Although invasive angiography was previously performed for identification of the artery of Adamkiewicz,[2)] CT and MRI are now usually used. In a meta-analysis, the visualization rates of CT and MRI were found to be 88.1% and 88.3%, respectively.[3)] On the other hand, there are still few studies examining whether preoperative identification of the artery of Adamkiewicz prevents postoperative spinal cord ischemia. We will discuss open repair and endovascular repair separately.

In the case of open repair, a multicenter, retrospective cohort study of more than 2,000 patients in Japan (JASPAR study) has been reported.

The results showed that, in open repair for aortic segments involving the origin of the artery of Adamkiewicz, having no reconstruction of the artery of Adamkiewicz was a significant risk factor for postoperative spinal cord ischemia (odds ratio 2.79, 95% CI, 1.14 to 6.79, $p = 0.024$).[4)] There have been several reports from single centers. Hyodoh et al. found a significant difference ($p < 0.01$) in the incidence

of postoperative spinal cord ischemia in 50 patients in the group operated with identification of the artery of Adamkiewicz and in the group operated without identification ($p < 0.01$). [5)]

Preoperative identification of the artery of Adamkiewicz in combination with other spinal cord protection methods has also been reported. Tanaka et al. reported the usefulness of selective reconstruction of the identified intercostal artery from which the artery of Adamkiewicz originated and hypothermia.[6)] Similarly, Furukawa et al. showed that selective perfusion and reconstruction of identified segmental arteries were useful.[7)] In addition, Ogino et al. and Nijenhuis et al. reported that preoperative identification of the artery of Adamkiewicz in combination with motor-evoked potentials was useful.[8, 9)]

As described above, although the evidence is not sufficient, identification of the artery of Adamkiewicz tends to be recommended as a preoperative examination for open repair. (secondary source 1).

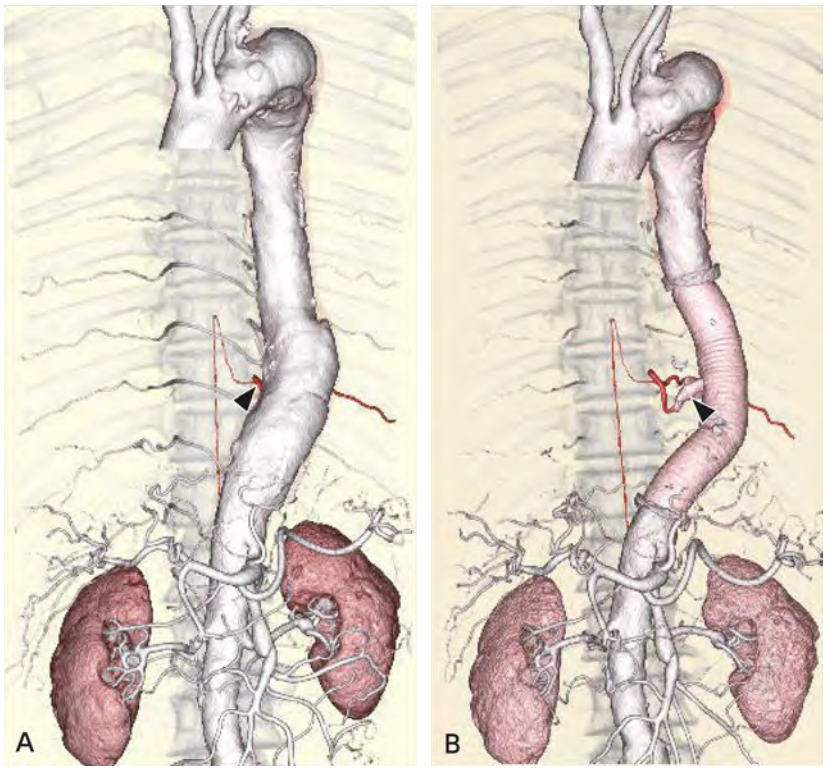

Figure. Preoperative identification of the artery of Adamkiewicz

A: Preoperative contrast-enhanced CT, VR image; B: Postoperative contrast-enhanced CT, VR image
The patient was a man in his 60s. DeBakey type IIIb dissecting aortic aneurysm. Preoperative CT shows the artery of Adamkiewicz originating from the left 10th intercostal artery (A►). The prosthetic graft replacement of the descending aorta and reconstruction of the left 10th intercostal artery (B►) were performed. Spinal cord ischemia did not occur postoperatively.

The incidence of spinal cord ischemia is lower with endovascular repair than with open repair. Moreover, the above-mentioned JASPAR study did not prove the usefulness of preoperative identification of the artery of Adamkiewicz in the case of endovascular repair.[4)] On the other hand, some studies have reported the usefulness of preoperative identification. Kamada et al. reported a single-center, retrospective study of 74

cases that showed that no spinal cord ischemia occurred in the group treated with preoperative identification of the artery of Adamkiewicz, but it did occur in 23.8% of those in a group for which the artery of Adamkiewicz was not identified preoperatively.[10] Matsuda et al. also reported that preoperative identification of the artery of Adamkiewicz was useful in determining the landing zones for stent grafts.[11] Furthermore, it has been shown that occlusion of the artery of Adamkiewicz by a stent-graft is a risk factor for spinal cord ischemia in patients whose thoracic aortas require extensive coverage.[12]

As the above findings indicate, although the evidence is insufficient in the case of endovascular repair, identification of the artery of Adamkiewicz can be considered in cases if the critical zone where the artery of Adamkiewicz frequently originates is to be covered or the repair length is long.

Although either CT or MRI can be selected for the examination, CT is generally easier to perform. Usually, CT is the first choice, and MRI is recommended for use in cases in which CT was not satisfactory for identification.[13] However, visualization of the artery of Adamkiewicz may be affected by the performance of the CT or MRI system. So, it is important to understand the characteristics of the equipment used at each institution before selecting an examination method.

Search keywords and secondary sources used as references

PubMed was searched using the following keywords: aortic aneurysm, Adamkiewicz, surgery or repair, TEVAR, complication, and spinal cord ischemia. The period searched was from January 1, 2009 to June 30, 2019; hits were obtained for 70 articles. Articles obtained by a hand search were also used.

In addition, the following was referenced as a secondary source.

1) Ogino H, et al.: 2020 Guideline on Diagnosis and Treatment of Aortic Aneurysm and Aortic Dissection. Japanese Circulation Society, 2020.

References

1) Koshino T et al: Does the Adamkiewicz artery originate from the larger segmental arteries? J Thorac Cardiovasc Surg 117 (5): 898-905, 1999
2) Kieffer E et al: Spinal cord arteriography: a safe adjunct before descending thoracic or thoracoabdominal aortic aneurysmectomy. J Vasc Surg 35 (2): 262-268, 2002
3) Taterra D et al: Artery of Adamkiewicz: a meta-analysis of anatomical characteristics. Neuroradioloty 61 (8): 869-880, 2019
4) Tanaka H et al: The impact of preoperative identification of the Adamkiewicz artery on descending and thoracoabdominal aortic repair. J Thorac Cardiovasc Surg 151 (1): 122-128, 2016
5) Hyodoh H et al: Usefulness of preoperative detection of artery of Adamkiewicz with dynamic contrast-enhanced MR angiography. Radiology 236 (3): 1004-1009, 2005
6) Tanaka H et al: Recent thoraco-abdominal aortic repair outcomes using moderate-to-deep hypothermia combined with targeted reconstruction of the Adamkiewicz artery†. Interact Cardiovasc Thorac Surg 20 (5): 605-610, 2015
7) Furukawa K et al: Operative strategy for descending and thoracoabdominal aneurysm repair with preoperative demonstration of the Adamkiewicz artery. Ann Thorac Surg 90 (6): 1840-1846, 2010
8) Ogino H et al: Combined use of Adamkiewicz artery demonstration and motor-evoked potentials in descending and thoracoabdominal repair. Ann Thorac Surg 82 (2): 592-596, 2006
9) Nijenhuis RJ et al: Magnetic resonance angiography and neuromonitoring to assess spinal cord blood supply in thoracic and thoracoabdominal aortic aneurysm surgery. J Vasc Surg 45 (1): 71-77, 2007
10) Kamada T et al: Strategy for thoracic endovascular aortic repair based on collateral circulation to the artery of Adamkiewicz. Surg Today 46 (9): 1024-1030, 2016

11) Matsuda H et al: Multidisciplinary approach to prevent spinal cord ischemia after thoracic endovascular aneurysm repair for distal descending aorta. Ann Thorac Surg 90 (2): 561-565, 2010
12) Matsuda H et al: Spinal cord injury is not negligible after TEVAR for lower descending aorta. Eur J Vasc Endovasc Surg 39 (2): 179-186, 2010
13) Takagi H et al: Identifying the Adamkiewicz artery using 3-T time-resolved magnetic resonance angiography: its role in addition to multidetector computed tomography angiography. Jpn J Radiol 33 (12): 749-756, 2015

BQ 35 Is nuclear medicine testing recommended for diagnosis and elucidation of pathology in patients with chronic heart failure?

Statement

Nuclear medicine testing has been shown to be highly accurate in noninvasively differentiating between chronic heart failure etiologies, and there is sufficient evidence to support its use in determining treatment. Moreover, there is abundant evidence of its usefulness in risk stratification and prognosis prediction, and it is therefore recommended for these purposes.

Background

Although ischemic heart disease is considered the typical disease in which chronic heart failure is manifested, other causes of heart failure include heart valve disease, cardiomyopathy, hypertensive heart disease, and congenital heart disease. The usefulness of echocardiography diagnosis of morphological abnormalities has long been established. However, differentiating ischemic heart failure from non-ischemic heart failure is occasionally difficult. Although coronary angiography is useful for diagnosing ischemic heart disease, it is invasive. A non-invasive method of diagnosis is needed.

The left ventricular ejection fraction (LVEF), end-diastolic volume (EDV), and end-systolic volume (ESV) are used to assess the severity of chronic heart failure and predict prognosis. However, their accuracy as prognostic factors is low, at least in the case of cardiomyopathy. In recent years, signs such as the presence of decreased right ventricular function and pulmonary hypertension and cardiac sympathetic abnormalities have drawn attention as factors for predicting prognosis.

The first half of this section describes nuclear medicine testing for pathology differentiation. The second half describes nuclear medicine testing for prognostic assessment.

Explanation

1. Pathology differentiation

Heart failure has a variety of causes, and treatment strategies vary greatly depending on whether it is ischemic heart failure or another type, making differentiation important. Stress perfusion SPECT is useful for diagnosing ischemia. In a study of 164 patients with chronic heart failure, Danias et al., using the total defect score with stress, reported sensitivity and specificity of 87% and 63%, respectively, for this modality.[1)]

In Japan, ^{123}I-beta-methyl-p-iodophenyl-pentadecanoic acid (BMIPP) myocardial scintigraphy is widely used as a method that does not involve stress, and its use in diagnosing both ischemic and non-ischemic disease has been investigated.[2, 3)] In recent years, the mismatch score for dual-isotope scintigraphy with BMIPP and ^{201}Tl (TL) accumulation has been used to differentiate between ischemic cardiomyopathy and dilated cardiomyopathy (Fig. 1). In an examination of 501 consecutive patients, Abe et al. reported

sensitivity and specificity of 84% and 83%, respectively, with this method. Thus, there appears to be sufficient evidence to support the use of this approach in actual clinical practice.[3)]

In recent years, cardiac amyloidosis has attracted attention as a cause of heart failure in elderly individuals, particularly heart failure with preserved left ventricular ejection fraction–(HFpEF). Recent studies have shown that cardiac amyloidosis is not a rare disorder. The amyloids that are related to heart disease are mainly AL amyloid, which is derived from the immunoglobulin light chain, and ATTR amyloid, which is caused by a transthyretin abnormality. The prognosis varies greatly with these 2 amyloids. The diagnostic agent ^{99m}Tc-pyrophosphate (PYP), which is used to diagnose acute myocardial infarction, has been found to accumulate in ATTR amyloid specifically (Fig. 2),[4)] and it is becoming a standard method of diagnosis in other countries. In a study of 171 patients at 3 centers, examination of its diagnostic accuracy showed sensitivity and specificity of 91% and 92%, respectively.[5)]

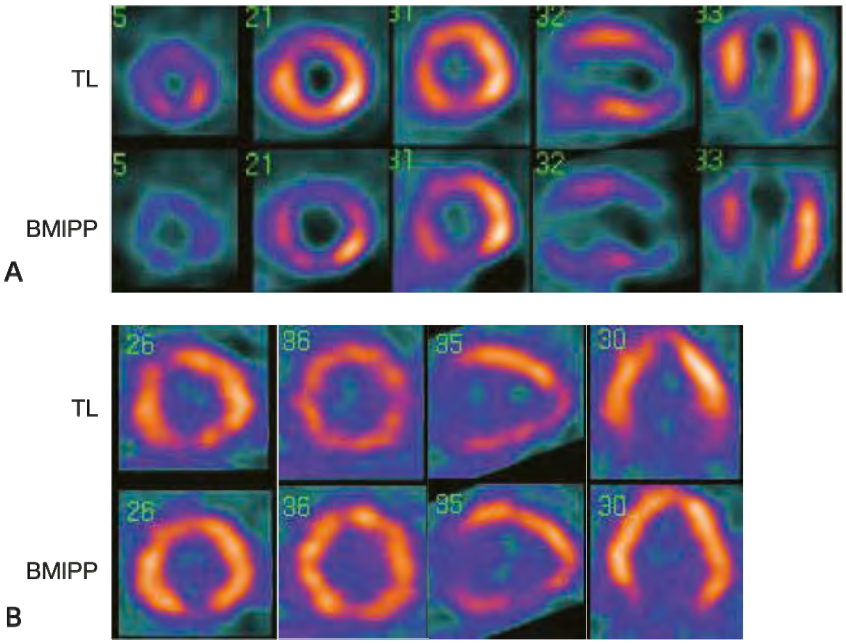

Figure 1. Simultaneous dual-isotope SPECT with TL and BMIPP, short axis, long axis image

A: Ischemic cardiomyopathy, B: Dilated cardiomyopathy
In A, a severe BMIPP defect is present from the anterior wall to the apex and inferoposterior wall. The defect is more severe than with TL. The patient's LVEF was 27%, and 3-vessel disease was seen by coronary angiography. In B, no apparent accumulation defect is seen with either tracer. These are typical findings for dilated cardiomyopathy.

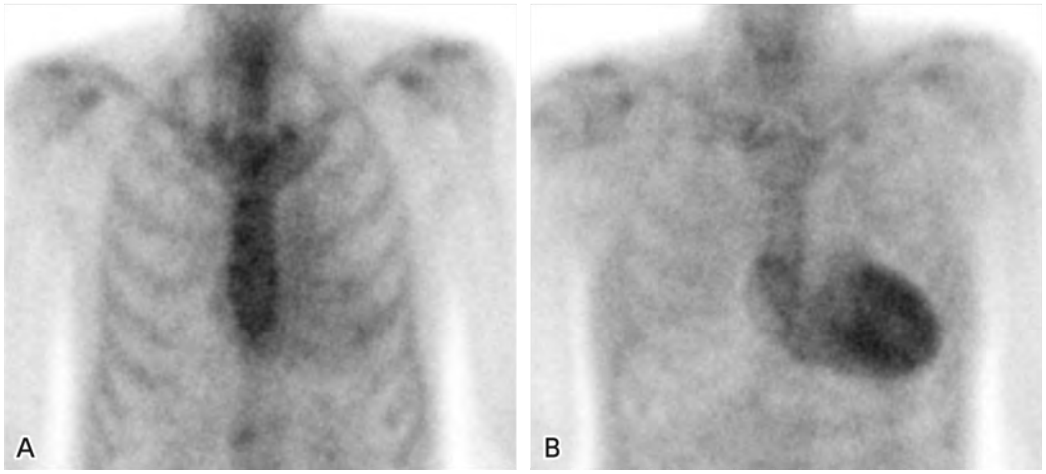

Figure 2. PYP scintigraphy in patients with heart failure and marked left ventricular hypertrophy, frontal view, planar image

A: Patient amyloid-negative on myocardial biopsy, B: Patient with ATTR cardiac amyloidosis
Clear myocardial accumulation is seen in the patient with ATTR cardiac amyloidosis. The heart to contralateral lung ratio (H/CL ratio) is 1.40 for the amyloid-negative patient and 2.02 for the patient with ATTR cardiac amyloidosis.

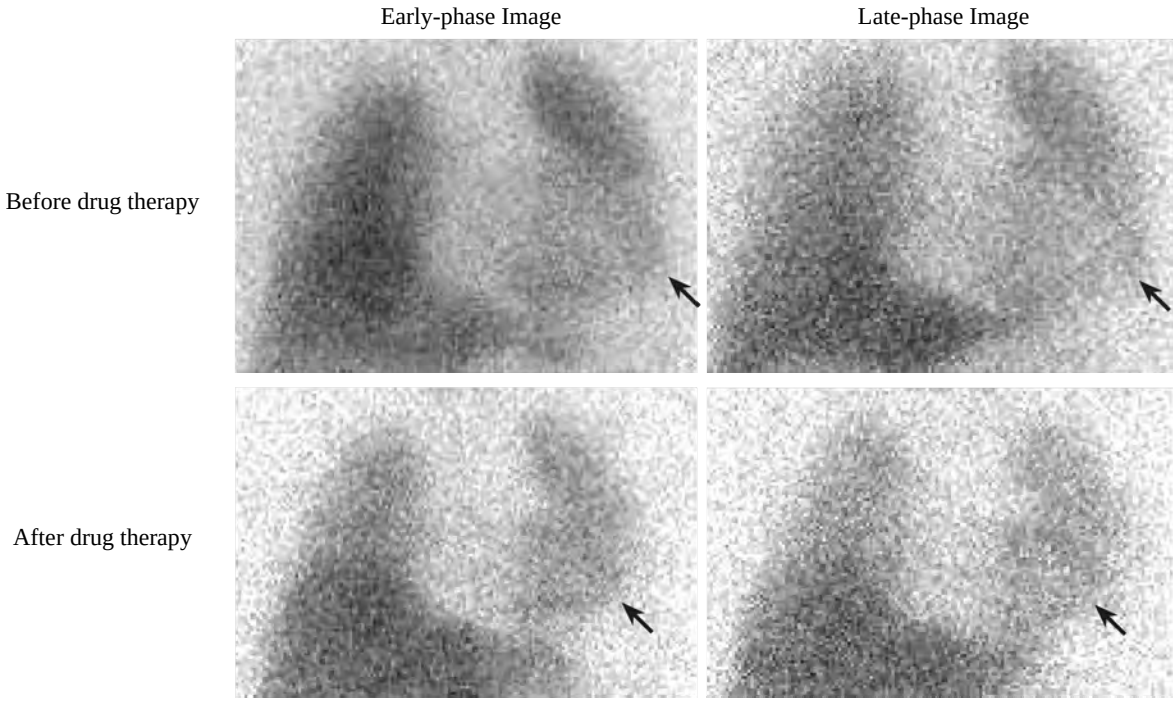

Figure 3. MIBG myocardium scintigraphy in a patient with dilated cardiomyopathy, frontal view, planar image

In the top row, the heart-to-mediastinum uptake ratio (H/M ratio) is low (1.53) in the late-phase image acquired before drug therapy. The patient was judged to have severe heart failure. After 6 months of drug therapy with a beta-blocker and ACE inhibitor, the left ventricle has decreased in size, and the H/M ratio has improved to 2.20 (→).

2. Prognostic assessment

As a compensatory mechanism for the decreased pumping function of the heart in chronic heart failure, the sympathetic nervous system and humoral factors are activated. However, their excessive activation can trigger catecholamine-induced myocardial damage and fatal arrhythmias. Monitoring of sympathetic function is therefore considered an effective means of assessing the relationship to myocardial damage and treatment efficacy. ^{123}I-MIBG (MIBG) is a catecholamine analog that enables imaging of catecholamine kinetics in sympathetic nerve endings. Early-phase imaging is normally performed 15 minutes after its intravenous injection, and late-phase imaging is performed 4 hours after intravenous injection. The H/M uptake ratio and washout rate (WR) at 4 hours are then calculated. Numerous studies have found that the lower the late-phase H/M ratio and the higher the WR, the poorer the prognosis (Fig. 2). A meta-analysis of 2-year[6] and 5-year[7] outcomes in the multicenter ADMIRE study conducted in Europe and the United States and reports from 6 facilities in Japan[8] showed that the MIBG late-phase H/M ratio reflected prognosis with high accuracy. Moreover, an examination of 116 patients for whom an implantable cardioverter defibrillator (ICD) was indicated found that, when the extent of the defect seen on MIBG late-phase SPECT images was large, the rates of appropriate ICD therapy and cardiac death increased significantly.[9] However, it should be noted that technical standardization is essential for H/M measurement.[10]

Although small in number, studies have also found BMIPP to be useful for prognosis prediction. Zavadovsky et al. found BMIPP to be better than perfusion scintigraphy for predicting response to cardiac resynchronization therapy in dilated cardiomyopathy.[11] In an examination of 804 patients with HFpEF without ischemia, Hashimoto et al. found the BMIPP defect score to be useful for prognosis stratification. With regard to cardiac amyloidosis prognosis prediction using PYP, it has been reported that prognosis stratification can be performed using a heart-to-contralateral lung ratio (H/CL ratio) of 1.6 as the cutoff[12] (Fig. 3).

Search keywords and secondary sources used as references

PubMed was searched using the following keywords: BMIPP, MIBG, PYP, heart failure, prognosis, cardiomyopathy, cardiac amyloidosis, and prognosis.

In addition, the following were referenced as secondary sources.

1) Japanese Circulation Society, Ed.: 2010 Guidelines for Clinical Use of Cardiac Nuclear Medicine (JCS 2010). Japanese Circulation Society, 2010.
2) Dorbala S et al: ASNC/AHA/ASE/EANM/HFSA/ISA/SCMR/SNMMI expert consensus recommendations for multimodality imaging in cardiac amyloidosis: Part 1 of 2-evidence base and standardized methods of imaging. J Nucl Cardiol 26: 2065-2123. 2019
3) Bokhari S et al: Standardization of ^{99m}Technetium pyrophosphate imaging methodology to diagnose TTR cardiac amyloidosis. J Nucl Cardiol 25: 181-190, 2018

References

1) Danias PG et al: Usefulness of electrocardiographic-gated stress technetium-99 m sestamibi single-photon emission computed tomography to differentiate ischemic from nonischemic cardiomyopathy. Am J Cardiol 94: 14-19, 2004
2) Ishida Y et al: Myocardial imaging with 123I-BMIPP in patients with congestive heart failure. Int J Card Imaging 15: 71-77, 1999
3) Abe H et al: Non-invasive diagnosis of coronary artery disease by ^{123}I-BMIPP/^{201}TlCl dual myocardial SPECT in patients with heart failure. Int J Cardiol 176: 969-974, 2014
4) Bokhari S et al: ^{99m}Tc-pyrophosphate scintigraphy for differentiating light-chain cardiac amyloidosis from the transthyretin-related familial and senile cardiac amyloidoses. Circ Cardiovasc Imaging 6: 195-201, 2013
5) Castano A et al: multicenter study of planar technetium 99 m pyrophosphate cardiac imaging: predicting survival for patients with ATTR cardiac amyloidosis. JAMA Cardiol 1: 880-889, 2016
6) Jacobson AF et al: Myocardial iodine-123 meta-iodobenzylguanidine imaging and cardiac events in heart failure. Results of the prospective ADMIRE-HF (AdreView Myocardial Imaging for Risk Evaluation in Heart Failure) study. J Am Coll Cardiol 55: 2212-2221, 2010
7) Agostini D et al: Prognostic usefulness of planar ^{123}I-MIBG scintigraphic images of myocardial sympathetic innervation in congestive heart failure: follow-up data from ADMIRE-HF. J Nucl Cardiol, 2019
8) Nakata T et al: A pooled analysis of multicenter cohort studies of ^{123}I-mIBG imaging of sympathetic innervation for assessment of long-term prognosis in heart failure. JACC Cardiovasc Imaging 6: 772-784, 2013
9) Boogers MJ et al: Cardiac sympathetic denervation assessed with 123-iodine metaiodobenzylguanidine imaging predicts ventricular arrhythmias in implantable cardioverter-defibrillator patients. J Am Coll Cardiol 55: 2769-2777, 2010
10) Nakajima K et al: Normal values and standardization of parameters in nuclear cardiology: Japanese Society of Nuclear Medicine working group database. Ann Nucl Med 30: 188-199, 2016
11) Zavadovsky KV et al: Perfusion and metabolic scintigraphy with ^{123}I-BMIPP in prognosis of cardiac resynchronization therapy in patients with dilated cardiomyopathy. Ann Nucl Med 30: 325-333, 2016
12) Hashimoto H et al: Prognostic value of 123I-BMIPP SPECT in patients with nonischemic heart failure with preserved ejection fraction. J Nucl Med 59: 259-265, 2018

5
Digestive Organs

Standard Imaging Methods for Digestive Organs (liver)

A Imaging of the liver

CT

Dynamic studies, in which contrast medium is rapidly injected and multiphase imaging that includes the arterial phase is performed, are essential to differentiate liver tumors, detect hypervascular tumors such as hepatocellular carcinoma, and stage malignancies.[1-3] Portal venous phase contrast-enhanced CT is typically performed for purposes such as watchful waiting of patients with malignant tumors. It is recommended that, with CT image reconstruction, diagnostic interpretation be performed with a slice thickness of ≤ 5 mm using a computer viewer.

1. Non-contrast CT (Fig. 1)

Although the diagnostic performance of non-contrast CT in liver tumors is limited, it is performed to examine fat and calcification in tumors and changes in the CT numbers for the liver parenchyma as a result of conditions such as fatty liver and hemosiderosis and to evaluate contrast enhancement in tumors by comparison with contrast-enhanced CT. Moreover, metastatic liver tumors that become obscure after contrast-enhanced CT are therefore identifiable only by CT performed before contrast-enhanced CT. Contrast tends to persist in liver lesions with non-contrast CT if observations during interpretation are performed using a narrow window width (WW) of 200 to 250 HU and a window level (WL) of 30 to 40 HU.

2. Contrast-enhanced CT

① Imaging method

(1) Contrast medium dose

The contrast medium dose administered is 520 to 600 mgI per kg body weight (1.73 to 2 mL per kg with a contrast concentration of 300 mgI/mL).

(2) Contrast medium injection

Multiphase contrast-enhanced CT: An injection rate that provides for a contrast medium injection time of approximately 30 seconds is used.

Normal contrast-enhanced CT: The contrast medium is generally injected at a rate of ≥ 2 mL/s (Maximum contrast enhancement of the liver depends on the iodine dose, not on the injection rate.).

② Multiphase contrast-enhanced CT (Figs. 1 and 2)

(1) Imaging phases

Late arterial phase imaging is essential to differentiate liver tumors and diagnose hypervascular tumors such as hepatocellular carcinoma, and multiphase imaging of 2 or 3 phases is performed for these purposes using combinations of the late arterial phase, portal venous phase, and equilibrium phase.

(2) Timing of imaging for each time phase

Late arterial phase: Start imaging at the time of contrast media injection + 5 to 10 seconds. To adjust for individual differences in the time needed for the contrast medium to reach the abdomen, the use of bolus tracking is recommended, with imaging started 20 to 25 seconds after the CT number of the aorta increases to 100 HU.

Portal venous phase: Approximately 70 seconds after the start of contrast medium injection.

Equilibrium phase: Approximately 180 seconds after the start of contrast medium injection.

③ Normal contrast-enhanced CT

Imaging is performed in the above-mentioned portal venous phase (timing of imaging is 70 to 90 seconds after the start of injection).

With regard to the contrast medium dose, the optimal dose for portal venous phase images was investigated. It is often considered that an increase of 50 HU in liver contrast enhancement is needed to detect liver lesions in the portal venous phase, and the iodine dose per kg body weight needed to obtain this 50-HU increase has been reported to be 521 mgI if chronic liver disease is not present.[4, 5] Moreover, an iodine dose of ≥ 600 mgI per kg body weight is considered necessary to produce adequate contrast enhancement in areas such as the liver, portal vein, pancreas, and aorta.[6] In obese patients, who have a high body fat percentage, it has been noted that determining the contrast medium dose based on body weight tends to result in an excessive iodine dose. Determining the dose based on lean body mass has been reported to be useful in such patients.[7, 8]

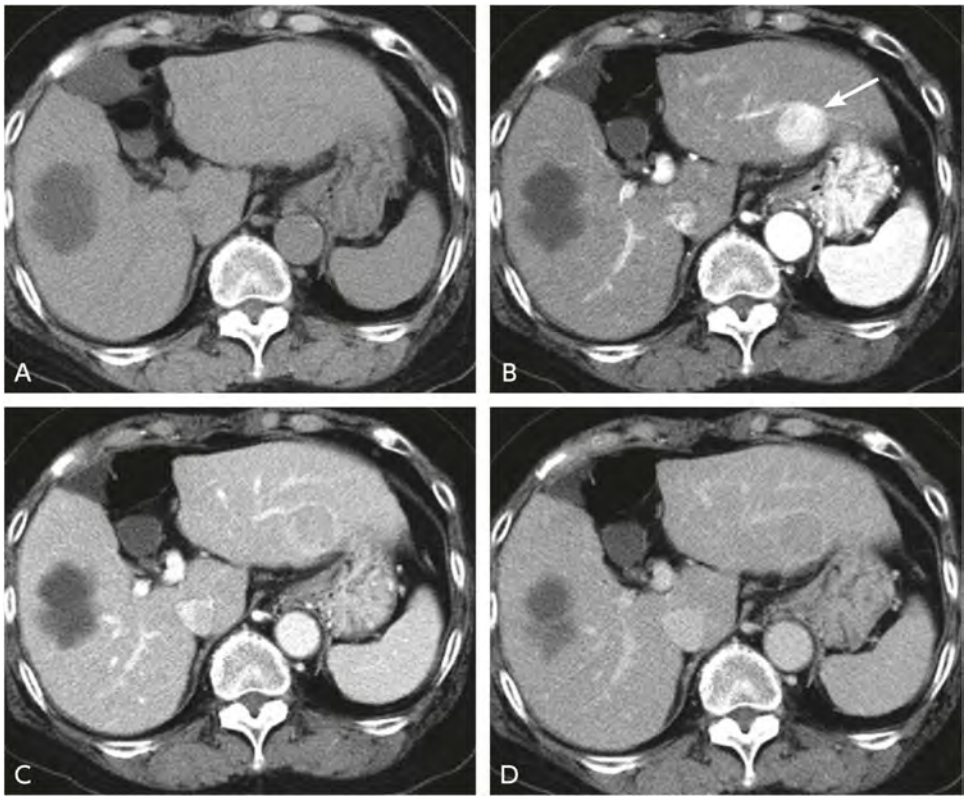

Figure 1. Multiphase contrast-enhanced CT (moderately differentiated hepatocellular carcinoma)

A: Before contrast imaging, B: Late arterial phase, C: Portal venous phase, D: Equilibrium phase
Hepatocellular carcinoma (→) of a liver with S2 steatosis is well visualized in the arterial phase, and the capsule is visualized in the equilibrium phase.

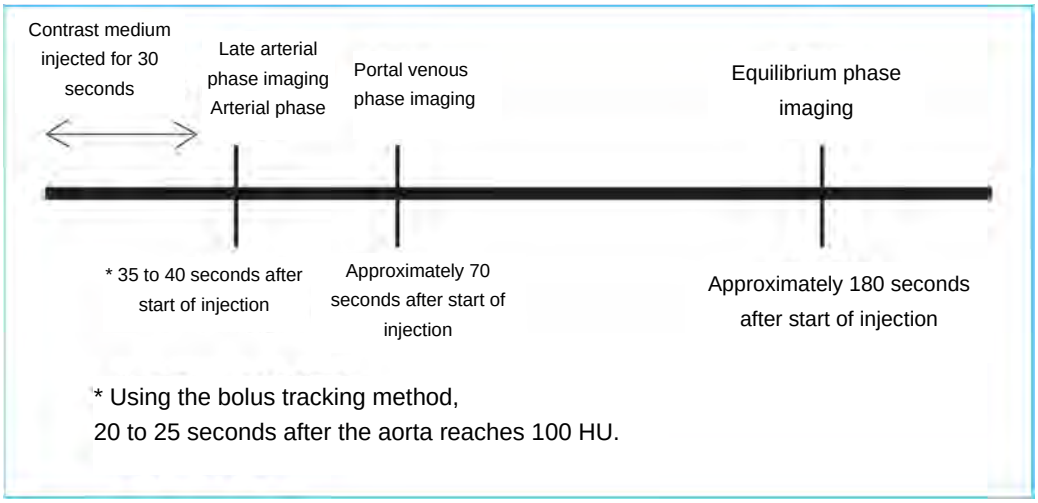

Figure 2. Standard multiphase contrast-enhanced CT imaging method

The contrast medium dose is 520 to 600 mgI per kg body weight (1.73 to 2 mL/kg with a 300 mgI/mL preparation). The late arterial phase is essential, and it is combined with the portal venous and equilibrium phases to perform 2- or 3-phase multiphase imaging.

In determining the contrast medium injection rate, an injection dose per unit time (mL/s) is used. Using a fast injection rate to administer a higher dose of iodine per unit time, arterial contrast enhancement increases, which is advantageous for visualizing hypervascular tumors.[9] Similar arterial contrast enhancement can be expected with the use of a high-concentration contrast medium (350 to 370 mgI/mL). However, if the contrast medium injection time varies with the patient's weight, the optimal timing of CT imaging will also vary. Consequently, rather than using a fixed injection rate, it is more reasonable to use a fixed injection time to enable the timing of the imaging to remain constant.[10]

In classifying the timing of multiphase CT imaging of the liver, the early and late arterial phases are classified as early phases, and the portal venous and equilibrium phases (delayed phase) are classified as transitional phases. Hepatocellular carcinoma is often hypervascular, and visualizing its enhancement during the late arterial phase and washout and capsular enhancement during the transitional phases is therefore important for its detection and qualitative diagnosis.[11] As a transitional phase, the portal venous phase is useful for evaluating tumor invasion of the portal and hepatic veins, and adding the equilibrium phase improves diagnostic performance in hepatocellular carcinoma.[12]

With regard to the timing of late arterial phase imaging, imaging of the liver begins at the contrast medium injection time + 5 to 10 seconds.[13] Thus, if contrast medium is injected for 30 seconds, imaging of the liver begins 35 to 40 seconds after the start of intravenous injection. However, a method that establishes fixed timing for imaging in this way may result in inappropriate timing due to individual differences in the time required for the contrast medium to reach the abdominal arteries. Particularly for patients in whom contrast medium reaches the abdomen slowly due to heart disease, imaging may begin too early, and sufficient contrast medium may not have reached the tumor from the hepatic artery in time for imaging. To adjust for such individual differences in imaging timing, the bolus tracking method is recommended. With this method, monitoring imaging of the abdomen is performed after the start of contrast medium injection, and imaging of the liver is started after the contrast medium is confirmed to have reached the abdominal aorta. With the use of the bolus tracking method, imaging of the liver is generally started 20 to 25 seconds after the CT number of the abdominal aorta reaches 100 HU. Similarly, the time needed for the contrast medium to reach the abdominal aorta can also be measured by the test injection method. With this method, a small amount of contrast medium is injected as a test, and the abdomen is continuously imaged. Portal venous phase imaging is performed approximately 70 seconds after the start of contrast medium injection, and equilibrium phase imaging is performed approximately 3 minutes after the start of injection.

In hypovascular liver tumors such as liver metastases, contrast peaks in the portal venous phase, when contrast enhancement of the liver is at its maximum. The maximum contrast enhancement of the liver in the portal venous phase depends on the iodine dose administered, not on the contrast medium injection rate. Consequently, for imaging in the portal venous phase only, rapid injection of the contrast medium is not necessary, and an injection rate of $\geq$ 2 mL/s is generally used. For interpretation and diagnosis, CT images reconstructed with a slice thickness of $\leq$ 5 mm and interpretation using a computer viewer is preferable.[14]

Ultrasound (Table 1, Figs. 3 and 4)

In January 2007, health insurance coverage began for a perflubutane preparation, Sonazoid®, a second-generation contrast medium for ultrasound. From the perspectives of cost and minimal invasiveness, normal ultrasonography is very useful for screening, and contrast-enhanced ultrasonography is also very useful for visualization, differentiation, and treatment efficacy evaluation. However, contrast-enhanced ultrasonography is burdensome with respect to examination time and labor intensiveness, and it is therefore considered a test not for screening, but for detailed examinations.

The imaging protocol involves imaging in the arterial-dominant phase, which is equivalent to the arterial phase of CT, after intravenous injection of 0.010 mL/kg of contrast medium, then subsequently imaging in the portal venous-dominant phase, which is equivalent to the portal venous phase of CT, in order to evaluate tumor arterial blood flow. After 10 minutes of imaging, the contrast medium is taken up by the liver parenchyma (Kupffer cells), and imaging is performed in the Kupffer phase, during which the liver parenchyma is hyperechoic. Hepatocellular carcinoma is visualized as hypoechoic in this phase because it contains no Kupffer cells, making it highly visualizable. Administration of additional contrast medium at this point enables arterial blood flow and hemodynamics to be evaluated for lesions first visualized in the Kupffer phase and facilitates differentiation and treatment efficacy evaluation.[15)]

Table 1. Ultrasound example

Contrast medium: bolus injection of 0.010 mL/kg of Sonazoid® (Daiichi-Sankyo)
Frequencies used: 4 MHz, 6.5 MHz
MI value: 0.2
Focal point: 1 point (depth: approximately 10 cm)
Frame rate: 10 to 14 Hz

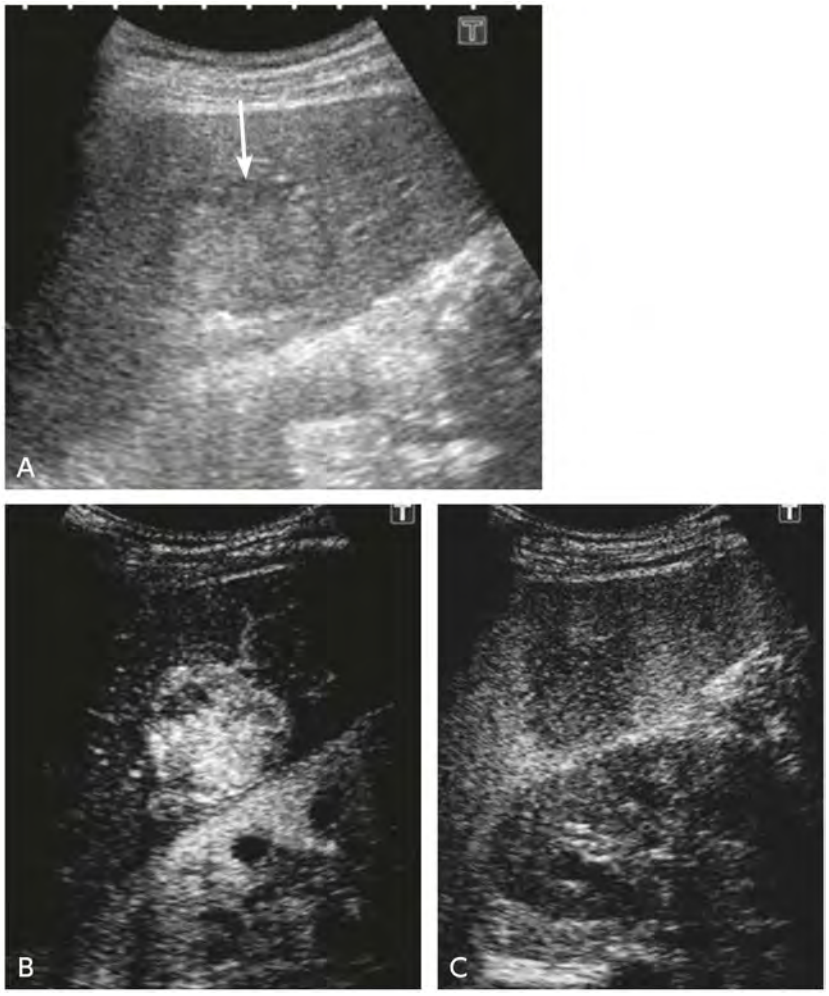

Figure 3. Ultrasound images (moderately differentiated hepatocellular carcinoma)

A: B-mode ultrasound image; B: perflubutane contrast-enhanced ultrasound image, arterial-dominant phase;
C: perflubutane contrast-enhanced ultrasound image, Kupffer phase
With perflubutane contrast-enhanced ultrasonography, enhancement of hepatocellular carcinoma (→) is seen in the arterial-dominant phase, and the hepatocellular carcinoma is hypoechoic in the Kupffer phase.

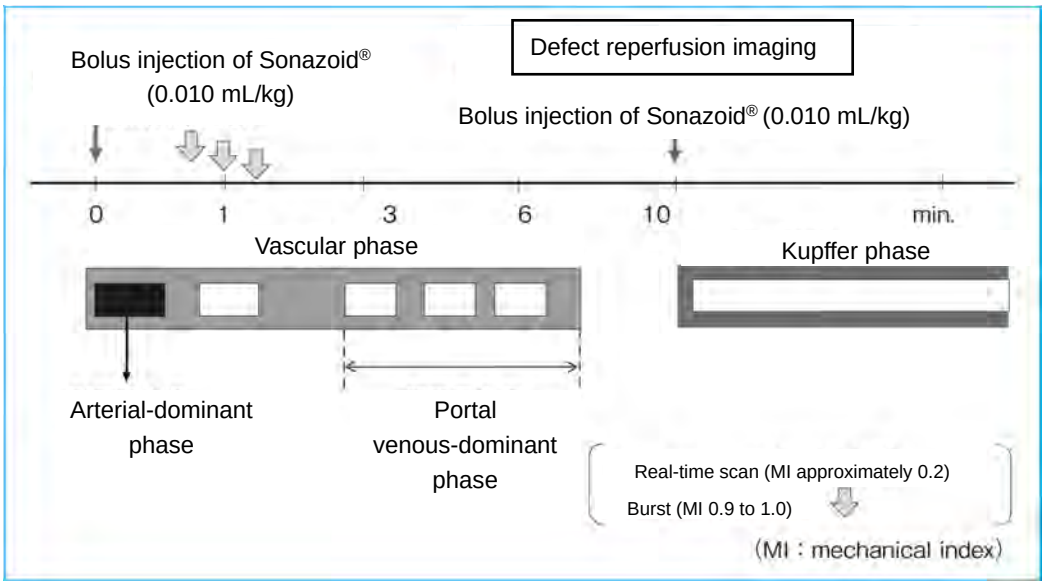

Figure 4. Basic imaging method using Sonazoid® (longitudinal section image)

MRI

Phased array coils are used for liver MRI diagnosis. Although non-contrast MRI and Gd-EOB-DTPA (EOB/Primovist®) contrast-enhanced MRI are often performed to diagnose liver tumors, imaging using an extracellular fluid gadolinium contrast medium or, when a gadolinium contrast medium is contraindicated, imaging using a superparamagnetic iron oxide (SPIO, Resovist®) contrast medium is performed when only blood flow information is needed. Diagnostic interpretation using a slice thickness of ≤ 5 mm and a computer viewer is recommended.

1. Non-contrast MRI (Fig. 5)

Imaging according to the following sequences is recommended, generally by transverse plane imaging.

① T1-weighted images: Breath-hold in-phase and out-of-phase (opposed phase) GRE images are essential.

② T2-weighted images (essential): Acquisition of respiratory-gated, fat-suppressed, FSE-T2-weighted and breath-hold SSFSE (HASTE), T2-weighted images is recommended. The addition of heavy T2-weighted imaging with a TE of ≥ 150 ms is useful for differentiating cysts and hemangiomas with long T2 values and malignancies.

③ Diffusion-weighted images (recommended): Imaging is performed using the echo-planar imaging (EPI) technique. The b-value is typically ≥ 400 s/mm^2.

④ Steady-state coherent image (sequence names: True FISP, balanced FFE, FIESTA, True SSFP; recommended): Concurrent fat suppression is also recommended.

2. Gd-EOB-DTPA contrast-enhanced MRI (EOB-MRI, Figs. 6 and 7)

Dynamic studies and hepatobiliary phase imaging are performed by Gd-EOB-DTPA contrast-enhanced imaging. To shorten the length of MRI tests, a Gd-EOB-DTPA dynamic study is performed after non-contrast MRI (T1-weighted imaging) and before hepatobiliary phase imaging are performed; T2-weighted imaging, diffusion-weighted imaging, and steady-state coherent imaging may also be performed.[16)]

① Imaging method

Contrast medium dose: 0.1 mL/kg of Gd-EOB-DTPA.

Contrast medium injection method: The Gd-EOB-DTPA dose is small, and rapid injection is unnecessary.[17)] As in CT, with varying injection times, the optimal timing of imaging differs between individuals. Consequently, as with CT, a constant injection time can be used by adjusting the injection time or diluting the contrast medium.[18)] Because the contrast medium dose is small, a saline chaser is essential.

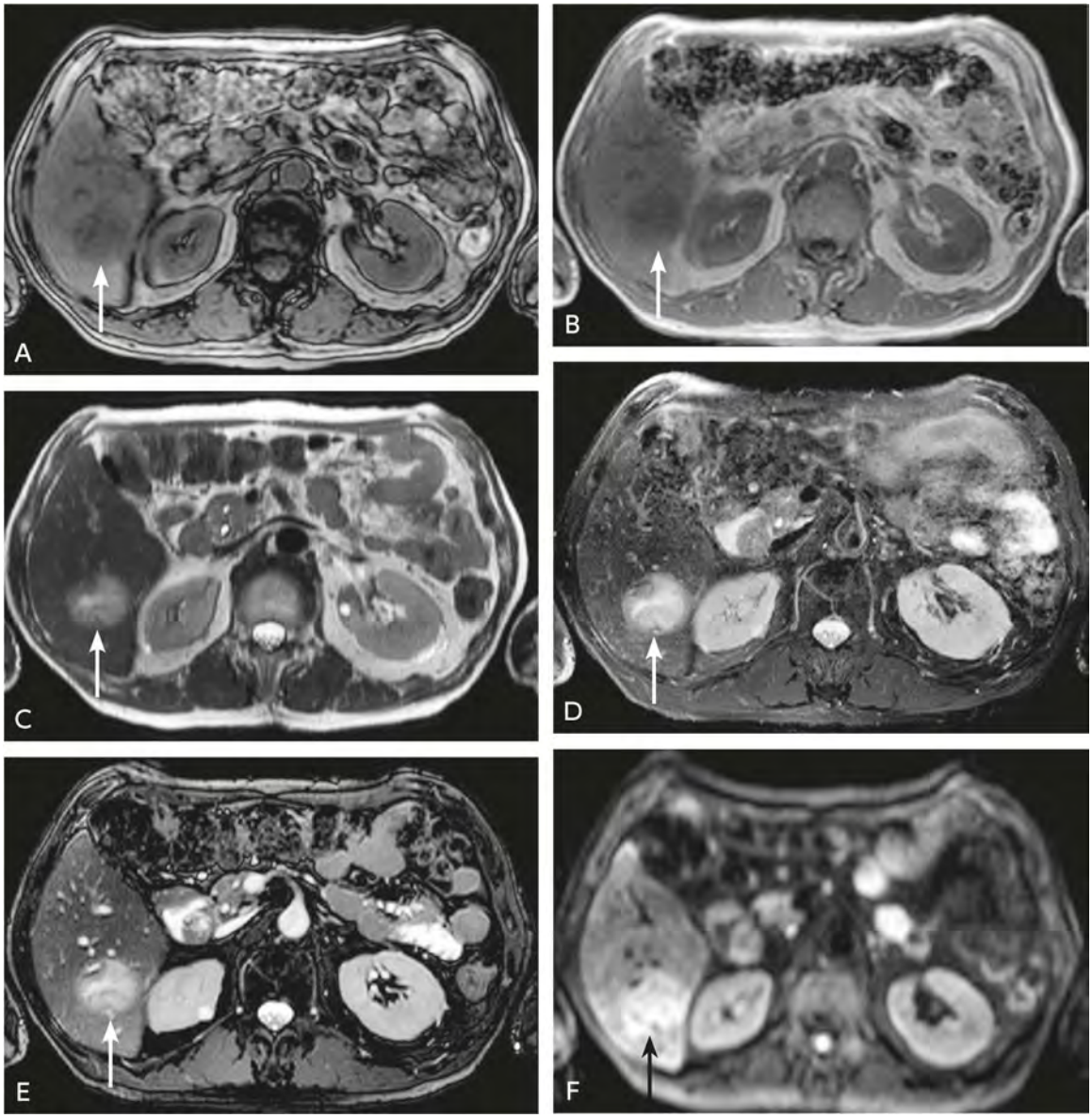

Figure 5. Non-contrast MRI (moderately differentiated hepatocellular carcinoma)

A: T1-weighted (opposed phase, GE imaging); B: T1-weighted (in phase, GRE imaging);
C: T2-weighted (breath-hold, HASTE imaging); D: Fat-suppressed, T2-weighted (respiratory-gated, FSE imaging);
E: Fat-suppressed, 3D balanced (FFE imaging); F: Diffusion-weighted imaging
Hepatocellular carcinoma (→) is visualized as a low-signal area with T1-weighted imaging and as a high-signal area with T2-weighted and diffusion-weighted imaging.

② Imaging method

(1) Imaging sequence

Fat-suppressed, T1-weighted, 3D GRE imaging is recommended.

(2) Slice thickness

A thickness of ≤ 5 mm is recommended.

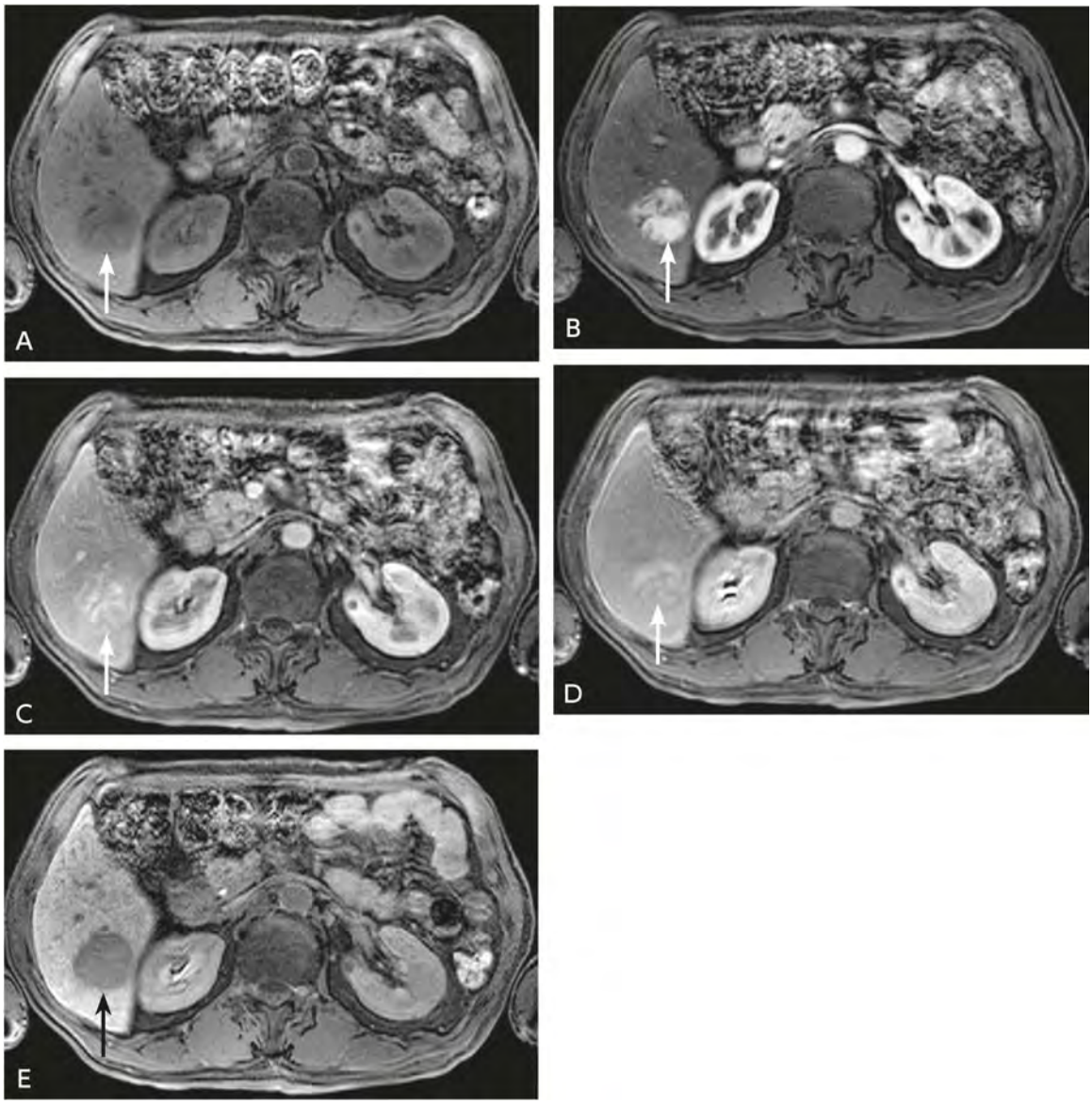

Figure 6. EOB-MRI (moderately differentiated hepatocellular carcinoma)

Fat-suppressed, T1-weighted (3D GRE imaging)
(A: Before contrast-enhanced imaging, B: arterial phase, C: portal venous phase, D: transitional phase, E: hepatobiliary phase
Hepatocellular carcinoma (→) is enhanced during the arterial phase and visualized as a low-signal area during the hepatobiliary phase due to decreased contrast medium uptake.

(3) Imaging plane

Transverse plane imaging. In the hepatobiliary phase, the addition of coronal and sagittal imaging is recommended.

(4) Imaging timing

Arterial phase: The bolus tracking method is recommended for determining the timing of imaging. Using the arrival of the contrast medium in the abdomen or descending aorta as the trigger, arterial phase imaging is performed so that the center of k-space occurs approximately 15 to 20 seconds after the trigger.[19] When fixed imaging timing is used, imaging is performed so that the center of k-space occurs approximately 30 seconds after the start of injection. For the portal venous phase, it is approximately 70 seconds after the start of contrast medium injection.

Transitional phase: 2 to 3 minutes after contrast medium injection.

Hepatobiliary phase: Beginning from 20 minutes after contrast medium injection. In patients with good liver function and imaging of the liver parenchyma, imaging can be performed at approximately 15 minutes after injection.

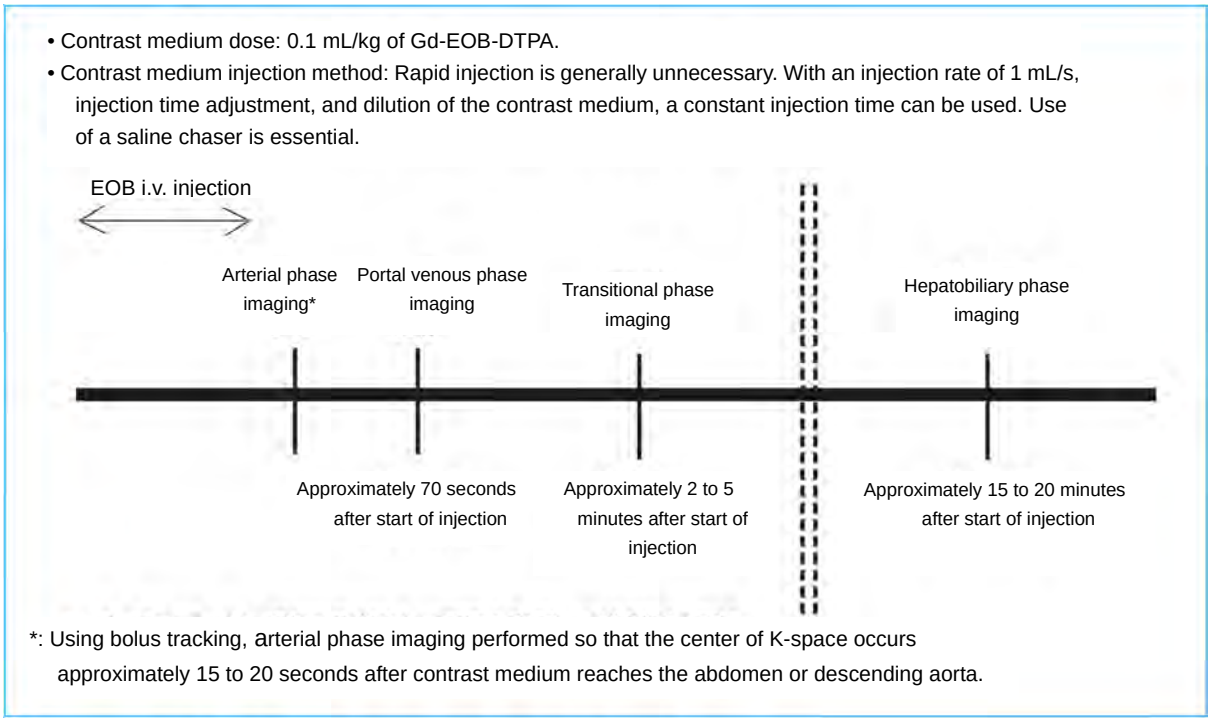

Figure 7. Standard EOB-MRI imaging method

3. Dynamic MRI using an extracellular gadolinium contrast medium

After non-contrast MRI imaging is performed, pre-contrast, arterial-phase, portal venous phase, and equilibrium-phase imaging is performed by the same method as used for the above-mentioned EOB-MRI imaging. A contrast medium dose of 0.2 mL/kg is used.

4. Superparamagnetic iron oxide (SPIO) MRI imaging (SPIO-MRI)

Imaging is performed beginning 10 minutes after intravenous administration of a 0.45 mg/kg (8 μmol/kg) iron dose. The following imaging sequences are recommended.

① Long TE-GRE imaging (TE ≥ 8 ms; transverse, sagittal, and coronal plane imaging recommended)

② Fat-suppressed, respiratory-gated, T2-weighted, FSE, transverse plane imaging

In addition, diffusion-weighted imaging and steady-state coherent imaging can be added.

Hepatocellular carcinoma generally appears as a low-signal area on T1-weighted images. However, some highly differentiated hepatocellular carcinomas appear as a high-signal area on T1-weighted images. Breath-hold in-phase and out-of-phase (opposed phase) GRE imaging is performed as T1-weighted imaging. Fat deposits in tissue appear as high-signal areas on in-phase imaging and areas of decreased signal intensity on out-of-phase imaging, enabling fatty degeneration of hepatocellular carcinoma to be observed. This is also useful for differentiating tumors and focal fat deposits.

Liver malignancies generally appear as high-signal areas on T2-weighted images. Although approximately 95% of hepatocellular carcinomas have been found to appear as high-signal areas on T2-weighted images, highly differentiated carcinomas may appear as areas of isointensity.[20] Respiratory-gated, fat-suppressed FSE T2-weighted imaging is useful for detecting hepatocellular carcinoma.[21, 22] Although the breath-hold SSFSE (HASTE) method is an inferior method for hepatocellular carcinoma detection because the T2 value of hepatocellular carcinoma is not very long, it enables visualization as a high signal of cysts and hemangiomas, which have long T2 values, and is useful for their differentiation.[22] Heavily T2-weighted imaging with a long TE of ≥ 150 ms is particularly useful for differentiating hemangiomas, cysts, and malignancies.[23]

Diffusion-weighted imaging is considered useful for detecting metastatic liver tumors.[24] Although it is inferior to contrast-enhanced MRI for detecting hepatocellular carcinoma, and its ability to detect hepatocellular carcinoma is limited,[25] it is useful in cases where a contrast study cannot be performed.

Steady-state coherent imaging enables blood flow and quiescent fluids to be visualized as a high signal in images that reflect T2/T1 contrast. Because it enables non-contrast-enhanced visualization of the portal vein, hepatic vein, and bile duct, it is useful for diagnosing vascular and bile duct invasion of hepatocellular carcinoma. Concurrent use of fat suppression is recommended.

As contrast-enhanced MRI tests to diagnose hepatocellular carcinoma, dynamic studies using extracellular gadolinium contrast media which, as in the case of CT, permit blood flow evaluation and contrast studies using SPIO contrast media, which are liver-specific and taken up by Kupffer cells, have been performed in the past. Currently, however, except in cases where a gadolinium contrast medium cannot be used, blood flow evaluations based on dynamic studies using Gd-EOB-DTPA contrast media and evaluations based on hepatocyte function determined by hepatobiliary phase imaging are recommended.

Standardization of diagnostic imaging terminology

Standardization of diagnostic imaging terminology for liver-related fields has been proposed for the American College of Radiology's reporting and data system (RAD) project. For the liver imaging reporting and data system (LI-RADS), the time phases for contrast-enhanced ultrasound (Lumason, Sonovue, Definity), dynamic CT, and dynamic MRI are defined as follows (for more information, see the American College of Radiology website).

Arterial phase (contrast-enhanced ultrasound, contrast-enhanced CT, and MRI): The time phase of post-contrast imaging in which the hepatic artery is completely enhanced and the hepatic veins (antegrade flow) are not enhanced more than the liver parenchyma.

Portal venous phase (contrast-enhanced ultrasound, contrast-enhanced CT, and MRI): The time phase of post-contrast imaging in which the portal and hepatic veins are enhanced more than the liver parenchyma and the images are acquired no more than 2 minutes after injection of a contrast agent.

Equilibrium phase (same as delayed phase; contrast-enhanced CT, and MRI using an extracellular gadolinium contrast medium): The time phase of post-contrast imaging in which the portal and hepatic veins are enhanced more than the liver parenchyma and the images are acquired at least 2 minutes after injection of a contrast agent.

Transitional phase (EOB-MRI): A time phase in which the signal intensities of the liver vessels and liver parenchyma are comparable in imaging performed after the arterial phase of contrast-enhanced MRI using a liver-specific contrast medium (a time phase between the portal venous and hepatobiliary phases).

Hepatobiliary phase (EOB-MRI): A time phase in which a liver-specific contrast medium is fully taken up by hepatocytes and excreted by the biliary system.

Standard imaging methods (gallbladder and bile duct)

B Imaging of the gallbladder and bile duct

Introduction

Although ultrasound is generally first used as a screening evaluation of the biliary system, there are regions that are difficult to visualize, such as the lower bile duct. Consequently, the use of CT or MRI is often necessary for close examination. The biliary system occupies an anatomically small region, and high spatial resolution is therefore needed to evaluate lesions that develop in this region. CT, which provides excellent spatial resolution and enables imaging to be performed over a broad area in a short time, is normally the first-line modality. However, MRI, with its excellent contrast resolution, is useful in cases such as when visualization of the biliary system as a whole is important.

CT

A slice thickness thinner than that used for the liver is recommended (at least approximately 2 mm). Imaging is performed using a thinner slice thickness (≤ 1 mm) if the objective is vascular reconstruction similar to that used for the liver. The imaging method and timing are the same as for the liver protocol. An example imaging protocol is shown in Table 2.

1. Imaging method used when the presence of calculus is suspected

The plain phase plays the central role in determining whether a calculus is present (Fig. 8A).[26] This is because it is sometimes difficult to distinguish faint calcified calculi from enhanced surrounding tissue on contrast-enhanced imaging (Fig. 8B). The portal venous-dominant phase is useful for evaluating the extent and severity of associated inflammation or complications such as abscesses. There has also been a report indicating that portal venous phase imaging alone is sufficient to diagnose calculi.[27]

Table 2. CT protocol [for 64-row multidetector computed tomography (MDCT)]

Tube voltage: 120 kVp, current: auto mAs
Image SD: 10/5 mm reconstruction
Detector: 0.5 mm × 64 or 1 mm × 32
Table speed: 26.5 mm/rot
Imaging timing: Trigger of 150 HU enhancement for arteries (early arterial phase); imaging performed for arterial-dominant phase 20 seconds later, for portal venous-dominant phase 60 seconds later; and for equilibrium phase 240 seconds later.
Collimation: 0.5 mm or 1 mm, Slice thickness: 1 or 2 mm
Contrast medium concentration: 300 to 370 mgI/mL (equivalent to 600 mgI/kg)
Injection time: 30 seconds, Needle: 20-G indwelling needle

2. Imaging method used if a tumor is suspected

In addition to qualitative diagnosis, imaging is often performed in 3 phases: plain, arterial-dominant, and portal venous-dominant phases. The arterial-dominant phase is useful for evaluating lesion vascularity and determining vascular anatomy. The portal venous phase, because it allows sufficient enhancement of the surrounding blood vessels and their related tissues, is useful for evaluating the extent of tumors. In addition, the equilibrium phase is useful for tumor characterization (persistent and delayed enhancement of adenocarcinoma, the most common type).[28, 29] Images reconstructed by multiplanar reconstruction (MPR) or coronal planar reconstruction (CPR) are useful for evaluating longitudinal progression of bile duct cancer, and their proactive use is recommended.[29]

○ Drip-infusion-cholangiography CT (DIC-CT)

Non-contrast CT of the entire liver is performed approximately 1 hour after intravenous injection of meglumine iotroxate. To determine the anatomy of the biliary system, it is assumed that reconstruction is performed by maximum intensity projection (MIP) or volume rendering (VR), and imaging and

reconstruction are therefore performed with a slice thickness of ≥ 1 mm.[30] Meglumine iotroxate is an iodine contrast medium for DIC, and its use was temporarily halted due to its numerous adverse reactions. However, its use was partially revived with the emergence of DIC-CT. When using it, greater attention should be paid to adverse reactions than when using regular iodine contrast media. In patients with normal liver function and no biliary dilatation, meglumine iotroxate can enable the biliary system anatomy to be determined at high spatial resolution. In the presence of impaired liver function, excretion of contrast medium into the biliary tract becomes impaired, resulting in poor visualization. Caution is therefore required in such cases.

MRI

MRI is indicated in cases such as the following: when there are doubts about a diagnosis based on dynamic CT by MDCT (a calculus that is completely isodense on CT may occur in rare cases); to evaluate the biliary tract as a whole; to evaluate cystic lesions; or if the patient has an iodine allergy.

1. Imaging method used when the presence of calculus is suspected

Magnetic resonance cholangiopancreatography (MRCP) has an important role as a sequence. The two imaging methods used for MRCP are a single-slice 2D method using thick slices 4 to 8 cm in thickness (Fig. 8C) and a 2D or 3D multislice method. The 3D multislice method has a long imaging time, and it is performed over several minutes, using respiratory gating or diaphragm navigation.[31] If the 3D multislice method is successful, high-resolution images of the biliary tract as a whole can be obtained by MIP (Fig. 8B), and examination of the original images can yield detailed information (Fig. 8E). Consequently, this method alone is sufficient. However, depending on the respiratory status of the patient, it may not always be successful, and imaging using a 2D method (single slice or multislice) under breath-hold is also recommended as a backup measure. A point to be noted during evaluations is that a small calculus that is completely surrounded by bile will, in principle, not be displayed in an MIP image (regardless of whether 2D or 3D) when observed from any angle. Consequently, the original image is always checked. A related point is that, with the 2D method using thick slices, areas with calculi are readily observed as areas of signal attenuation. In addition, normal T1-weighted and T2-weighted imaging is added, and diffusion-weighted imaging is also added if possible to detect any incidentalomas. Moreover, because some calculi (particularly intrahepatic bile duct stones) may appear as high-signal areas on T1-weighted images,[32] the addition of high-resolution, fat-suppressed, 3D T1-weighted imaging is also desirable (Fig. 8F). Balanced sequences enable imaging with a high signal-to-noise ratio to be performed in a short time and can therefore also be added as an option in cases where breath-holding is difficult (Fig. 8G). A contrast study is unnecessary as long as there are no comorbidities such as tumors. Examples of imaging protocols are shown in Table 3.

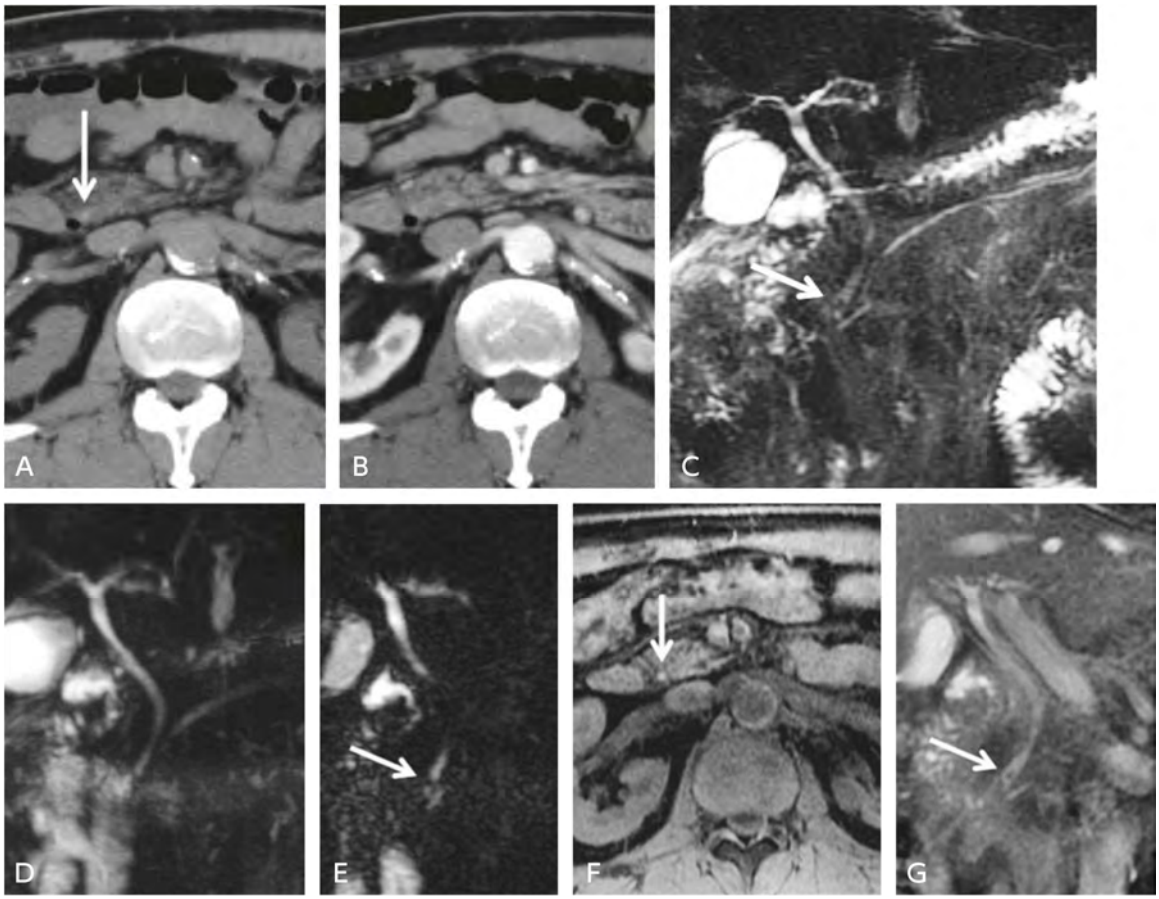

Figure 8. Calculus at the lower end of the common bile duct

A: Non-contrast CT: Small calculus barely visible (→).
B: Contrast-enhanced CT: Pancreatic parenchyma is enhanced, making it difficult to identify the calculus.
C: 2D single-shot, thick-slice MRCP: The calculus is visible (→).
D: 3D MRCP (MIP image): Intestinal fluid may obscure the calculus, making it difficult to identify with this image alone.
E: 3D MRCP (original image): The calculus is visible (→).
F: 3D MRI (T1-weighted, transverse image): The calculus is clearly visualized as a high-signal area (→).
G: Balanced sequence: The calculus is visible (→).

○ Oral contrast media

Oral contrast media that use manganese or iron preparations contribute to improved MRCP image quality by inhibiting the signal from excess fluid accumulated in the gastrointestinal tract. However, when evaluation of the papillary region is required due to conditions such as pancreaticobiliary maljunction, the presence of a sufficient amount of fluid in the duodenum can facilitate interpretation. Moreover, although rare, in the case of sphincter of Oddi dysfunction following papillotomy or a similar procedure, the contrast medium may reflux into the bile duct, preventing evaluation of this area. Care is thus required in this regard.[33] Therefore, rather than administering an oral contrast medium to all patients from the beginning, the recommended protocol is to first perform thick-slice 2D MRCP imaging in 3 to 5 directions and administer an oral contrast medium after determining whether one is needed (Table 3).

Table 3. Examples of MRCP protocols (1.5-T system, phased array coil)

Imaging Method	Sequence	TR/TE	Slice Thickness/ Interval, etc.	Other
(1) 2D MRCP/coronal plane, oblique coronal plane	Breath-hold, fat-suppressed, FSE	∞/800 (ETL approximately 256)	4 to 8 cm	3 to 5 directions, liver and pancreas included
(2) T1/T2-weighted/coronal plane	Breath-hold balanced sequence	3.5/1.8	6 to 4/0 mm	Optional
Oral contrast medium administered as needed				
(3) T2-weighted/transverse plane	FSE	∞/320 (ETL approximately 93)	5 to 6/0 mm	Extent: liver to papilla
(4) T1-weighted/transverse plane	Breath-hold 2D GRE (dual echo)	250/2.3 & 4.2	5 to 6/0 mm	Optional Extent: liver to papilla
(5) T1-weighted/transverse plane	Breath-hold, fat-suppressed 3D GRE or respiratory-gated, fat-suppressed 2D SE	4.3/2.1 (flip angle, 15°) 250/5.5 (flip angle, 70° to 90°)	4/-2 mm	Extent: liver to papilla
(6) 3D MRCP/coronal plane or 2D MRCP	Fat-suppressed FSE	1,300/650 (ETL approximately 124) ∞/87 (ETL 128)	2/-1 mm 5 to 6/0 mm	Evaluated using MIP and original image, with liver and pancreas included

Table 4. Examples of biliary system contrast-enhanced MRI protocols (including MRCP)

Imaging Method	Sequence	TR/TE	Slice Thickness/ Interval, etc.	Other
(7) 2D MRCP/coronal plane, oblique coronal plane	Breath-hold, fat-suppressed FSE	∞/800 (ETL approximately 256)	4 to 8 cm	3 to 5 directions, liver and pancreas included
(1) T1/T2-weighted imaging/coronal plane	Breath-hold balanced sequence	3.5/1.8	6 to 4/0 mm	Optional
(2) T2-weighted/transverse plane	2D FSE	∞/120 (ETL approximately 80)	5 to 6/0 mm	Extent: liver to papilla
(3) T1-weighted/transverse plane	Breath-hold 2D GRE (dual echo)	150/2.3 & 4.2 (flip angle, 70° to 90°)	6/0 mm	Extent: liver to papilla
(4) T1-weighted/transverse plane	Respiratory-gated, fat-suppressed 2D EPI	250/5.5 (flip angle, 70° to 90°)	6/0 mm	Optional Extent: liver to papilla
(5) Diffusion weighted/transverse plane	Free-breathing, fat-suppressed 2D EPI	5,000/65 (b-value = 0, 800 to 1,000 s/mm^2)	5 to 6/0 mm	
(6) Dynamic MRI/transverse plane or oblique	Breath-hold fat-suppressed 3D GRE or breath-hold, fat-suppressed 2D GE	4.3/2.1 flip angle, 15°) 150/4 flip angle, 70° to 90°)	4/-2 mm 5 to 6/0 mm	Extent: liver to papilla Plane determined to suit tumor
Oral contrast medium administered as needed				
(7) 3D MRCP/coronal plane or 2D MRCP	Fat-suppressed 3D FSE	1,300/650 (ETL approximately 124) ∞/87 (ETL 128)	2/-1 mm 5 to 6/0 mm	Evaluated using MIP and original image, liver and pancreas included

2. Imaging method used when a tumor is suspected

Dynamic MRI is performed in the arterial-dominant and portal venous phases and through the equilibrium phase,[34] with the use of high spatial resolution (≤ 3 to 4 mm thickness) 3D T1-weighted imaging recommended. If 3D imaging cannot be performed, the general orientation of the lesion is first determined by means such as single-shot 2D MRCP. Multislice dynamic 2D T1-weighted imaging is then performed in the optimal direction for visualizing the lesion. Examples of imaging protocols are shown in Table 4.

○ Oral contrast medium administration during dynamic MRI and MRCP and its timing

Because an oral contrast medium shortens T1, the presence of such a medium during dynamic MRI imaging can not only make it difficult to evaluate the intestinal tract itself, but artifacts from peristalsis can also produce noise in the periphery and make it difficult to evaluate enhancement of biliary tract lesions. On the other hand, the gadolinium preparations used in dynamic imaging shorten T2 of the background after intravenous injection and are useful for improving MRCP image quality. Consequently, it has also been suggested that MRCP should be performed as needed after oral contrast medium administration following the completion of dynamic imaging (Table 4).

Standard imaging methods (pancreas)

C Imaging of the pancreas

Introduction

If pancreatic disease is suspected, ultrasonography is first performed for screening. Although ultrasonography is useful for evaluating dilatation of the main pancreatic duct and detecting lesions at the junction of the head and body of the pancreas, the scope of observation can be limited by gas in the gastrointestinal tract. Multidetector CT (MDCT) provides excellent spatial resolution and enables imaging to be performed with thin sections. It is therefore considered the most useful test for pancreatic disease. If a pancreatic tumor is suspected, dynamic contrast-enhanced CT is recommended, except in patients for whom contrast media are contraindicated. MRI provides excellent contrast resolution, and new information can be obtained by combining it with ultrasound and CT. For example, MRI is superior even to CT for detecting cystic lesions. Moreover, MRCP enables the overall appearance and dilatation and stenosis of the main pancreatic duct, gallbladder, and biliary tract to be evaluated more easily than with CT. MRI is therefore recommended when an abnormality is suspected based on ultrasonography or CT.

CT (Fig. 9)

As with the biliary system, it is recommended that CT of the pancreas be performed with thinner section thickness (1 to 3 mm) than used for the liver. When the aim is to create 3D-reconstruction images, imaging is performed with even thinner section thickness (0.5 to 1.25 mm), and the data are stored on the image server. An MDCT imaging protocol (example) for pancreatic tumors is shown in Table 5.

1. Imaging method used when a pancreatic tumor such as pancreatic cancer is suspected

After unenhanced CT (which is optional), a high-concentration contrast medium is injected over a standardized period of 30 seconds, and dynamic contrast-enhanced CT is performed for 4 phases: the early arterial phase, late arterial phase (pancreatic parenchyma phase), portal venous phase, and equilibrium phase (≥ 180 seconds). The extent of the imaging in the arterial phase is from the liver to the pancreas or kidney. In the portal venous and equilibrium phases, imaging is performed from the liver to the pelvis so that changes such as peritoneal metastasis are not overlooked.

Imaging in the early arterial phase is performed to evaluate the arterial anatomy and create CT angiography. The late arterial phase, also called the pancreatic parenchymal phase, is the optimal phase to demonstrate pancreatic cancer because the normal pancreatic parenchyma shows peak contrast enhancement. Pancreatic cancer, which is hypovascular, appears as a hypodense lesion and contrasts highly with the normal pancreatic parenchyma. Liver metastasis and portal venous tumor invasion are evaluated in the portal venous phase. In the equilibrium phase, pancreatic cancer, which has an abundant fibrous stroma, undergoes delayed enhancement. Evaluating the contrast enhancement pattern from the arterial phase to the equilibrium phase is useful for the differential diagnosis of pancreatic mass lesions. Because liver metastases of pancreatic cancer occasionally show AP shunt-like enhancement, attention should be paid to the presence or absence of early enhancement of the liver parenchyma in the late arterial phase. In addition, MPR is useful for preoperatively evaluating peripancreatic arterial and venous anatomy and vascular invasion.

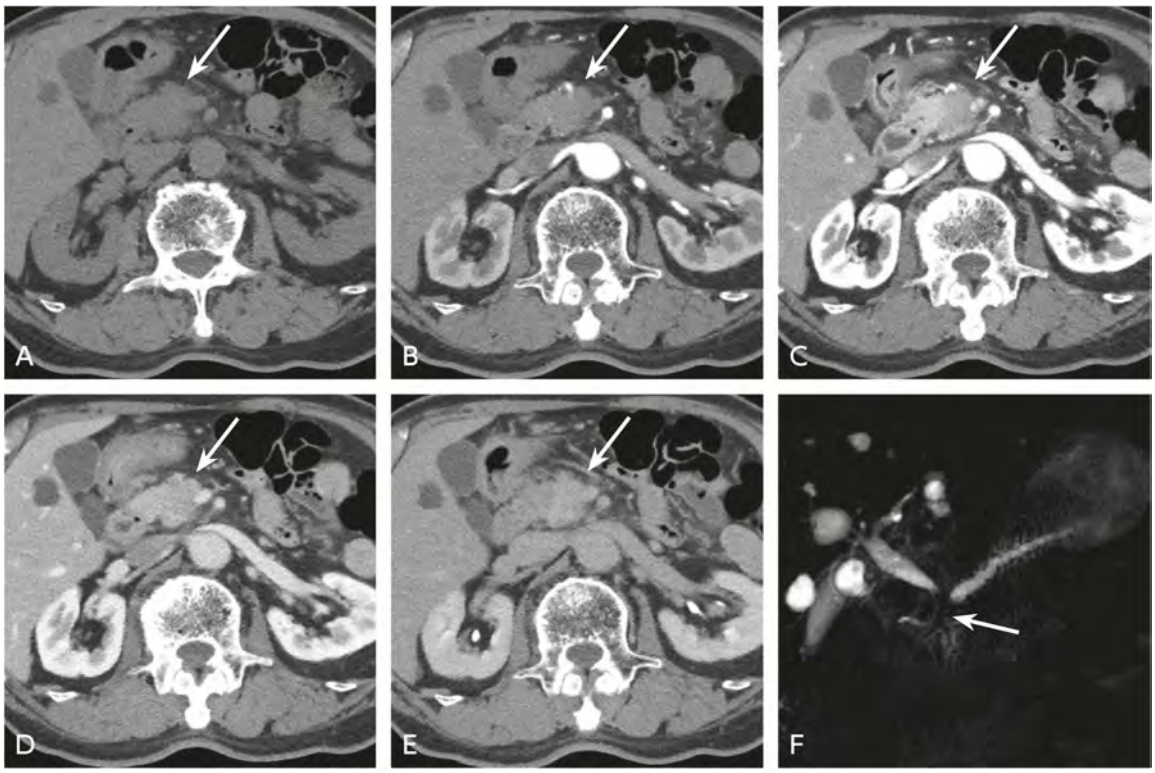

Figure 9. Dynamic CT and MRCP of pancreatic head cancer

A: unenhanced CT, B to E: dynamic CT, B: early arterial phase, C: late arterial phase (pancreatic parenchymal phase), D: portal venous phase, E: equilibrium phase, F: 2D thick-slab MRCP (breath-hold)
Pancreatic head cancer (→) is hypovascular and shows hypodensity, and it is most distinct in the late arterial phase I of dynamic CT. Pancreatic cancer undergoes delayed enhancement, and, in this example, it shows isodensity with the surrounding pancreatic parenchyma in the portal venous phase (D) and faint hyperdensity in the equilibrium phase (E). With MRCP, occlusion and upstream dilatation of the main pancreatic duct and common bile duct are seen as a result of pancreatic head cancer.

Table 5. MDCT imaging protocol (example) for pancreatic tumors

	Sites of Imaging	Imaging Start Time	Section Thickness
Unenhanced (pre-contrast)	Liver to kidney		3 mm 1 mm
Early arterial phase*	Liver to kidney	CT number increase of +100 HU for descending aorta	3 mm 1 mm
Late arterial phase (pancreatic parenchyma phase)	Liver to kidney	45 seconds after start of administration	3 mm 1 mm
Portal venous phase	Liver to kidney	60 seconds after start of administration	3 mm 1 mm
Equilibrium phase imaging	Liver to pelvis	240 seconds after start of administration	3 mm 1 mm

Contrast medium: 600 MgI/kg (100 mL high concentration syringe maximum)
Contrast media injection time: 30 seconds
* Using the bolus tracking method

For follow-up CT, attention should be paid to reducing radiation exposure, and phases considered unnecessary should be omitted as appropriate.

2. Imaging method used when pancreatitis is suspected

Imaging is performed in 4 phases: non-contrast CT and dynamic contrast-enhanced CT in the late arterial phase (pancreatic parenchymal phase), portal venous phase, and equilibrium phase (≥ 180 seconds after injection). Non-contrast CT is useful for diagnosing conditions such as hemorrhagic changes associated with calcification and fat necrosis of the pancreas and the choledocholithiasis that cause pancreatitis. The CT grade of acute pancreatitis is determined by contrast-enhanced CT. The arterial phase is useful for diagnosing a pseudoaneurysm, which is occasionally seen in pancreatitis associated with a pancreatic pseudocyst. Moreover, because acute pancreatitis may occur due to a pancreatic neoplasm such as pancreatic cancer, the presence or absence of tumors can also be evaluated in the arterial phase. The portal venous phase is useful for diagnosing venous thrombosis and venous stenosis associated with pancreatitis.

With regard to watchful waiting in pancreatitis, repeating dynamic contrast-enhanced CT is of little significance for a brief period of watchful waiting, and consideration is given to imaging mainly in the portal venous phase and adding other phases to suit the objectives.

MRI (Figs. 9 and 10)

An example of an MRI imaging protocol for pancreatic tumors is shown in Table 6.

The MRI imaging protocol for pancreatic disease involves a basic sequence of T2-weighted, T1-weighted plus diffusion-weighted images and MRCP (3D and 2D). Dynamic contrast-enhanced MRI is also performed as needed. T2-weighted images are combined with fat suppression as appropriate, obtaining both in-phase and out-of-phase (opposed-phase) T1-weighted images. In-phase and out-of-phase

T1-weighted images and their subtraction images are useful for diagnosing focal fatty replacement. With diffusion-weighted images, imaging is performed using b-values of 0 s/mm^2 and approximately 800 s/mm^2 or 1,000 s/mm^2, and an apparent diffusion coefficient (ADC) map is generated.

MRCP consists of 2D and 3D images, and the MIP images and original MRCP images are used for diagnosis. Erratic breathing during respiratory-gated 3D MRCP can result in poor-quality images that are unevaluable. It is therefore preferable to also perform breath-hold MRCP to ensure that good image quality is obtained. Single-shot fast-spin echo (SSFE) T2-weighted imaging provides the advantages of not only clear visualization of the pancreatic duct and biliary tract, but also visualization of solid organs such as the liver and pancreas and changes such as tumors at the same time, adding coronal and oblique coronal plane imaging as appropriate.

In fat-suppressed T1-weighted images acquired before contrast-enhanced imaging, the signal for normal pancreatic parenchyma is a high signal intensity. Therefore, the signal decreases if a tumor, fibrosis, or inflammation is present. If a contrast medium is not used, close attention is paid to the pancreas signal in fat-suppressed T1-weighted images. In addition, bleeding often results from the fat necrosis associated with severe acute pancreatitis. Hemorrhagic fat necrosis in or near the pancreas appears as a high signal intensity on fat-suppressed T1-weighted images, which facilitates diagnosis. However, a point that should be noted with fat-suppressed T1-weighted imaging is that the use of an oral contrast medium (high signal intensity on T1-weighted images) on MRCP narrows the dynamic range, reducing the contrast between lesions and the pancreas.

For dynamic MRI, which involves the rapid injection of an extracellular gadolinium contrast medium, 3D GRE (field echo), which provides high spatial resolution, is recommended. It also enables reconstructed images in the coronal and sagittal planes to be generated from the transverse plane images. Dynamic MRI that uses fat suppression provides better lesion contrast. Because MRI provides excellent contrast resolution, MRI and dynamic contrast-enhanced MRI may be useful in detecting even poorly defined lesions on dynamic CT.

Screening for liver metastases is important for patients in whom pancreatic cancer is suspected. Gd-EOB-DTPA (EOB/Primovist®) may be used to exclude liver metastases. An advantage of EOB-MRI is that it enables the presence or absence of pancreatic lesions and liver metastases to be evaluated at the same time. A disadvantage, however, is that if MRCP imaging is also performed, it must be performed before contrast-enhanced imaging, which lengthens the duration of testing.

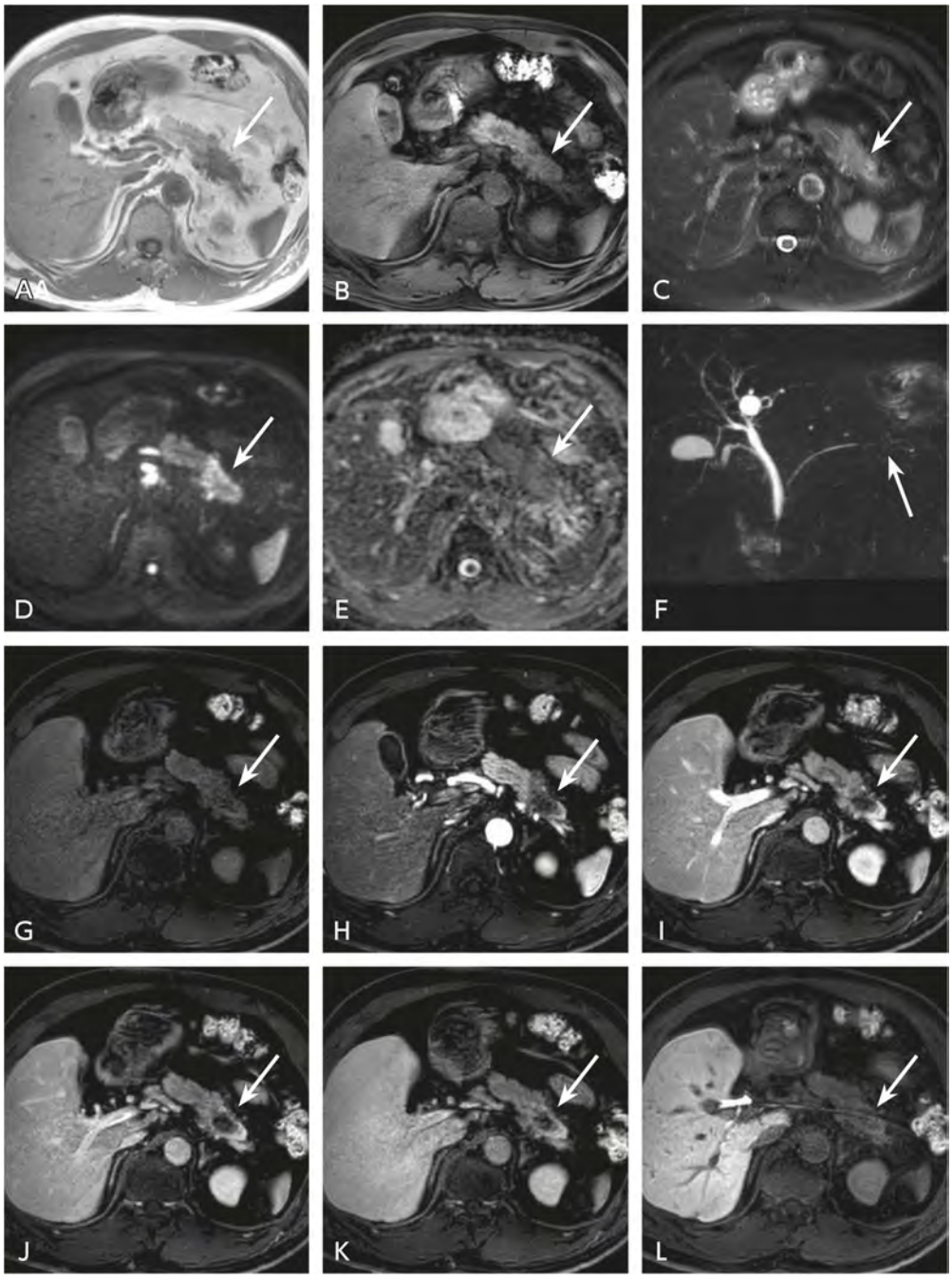

Figure 10. MRI of pancreatic tail cancer

A: T1-weighted image (in phase); B: fat-suppressed T1-weighted image; C: fat-suppressed T2-weighted image; D: diffusion-weighted image (b-value = 1,000 s/mm^2); E: ADC map; F: MRCP (3D, respiratory gated); G to K: EOB-MRI (G: before contrast-enhanced imaging, H: arterial phase, I: arterial phase + 30 seconds, J: arterial phase + 90 seconds, K: arterial phase + 180 seconds); L: hepatobiliary phase (20 minutes after injection)

Pancreatic tail cancer (→) shows a low signal intensity on T1-weighted images (A and B) and a high signal intensity on the T2-weighted image (C). On the diffusion-weighted image (D), it shows a high signal intensity mainly at the lesion margins. With MRCP (F), an obstruction of the main pancreatic duct is seen at the site of the tumor. In the arterial phase of dynamic MRI (H), the tumor is seen to be hypovascular, with enhancement seen mainly in the margins in the 2nd and 3rd phases (I and J) of the arterial phase. Persistent faint contrast enhancement is also seen in the tumor margins on the hepatobiliary phase (K).

Table 6. Pancreatic tumor MRI protocols (example)

Sequence	Plane	2D or 3D	FOV (mm)	Slice Thickness (mm)	Gap (mm)	Number of slices	Breathing
Balanced sequence	Coronal	2D	380	6	1	16	Breath-hold
Fat-suppressed T2-weighted images *	Transverse	2D	380	5	1	25	Breath-hold
T1-weighted images, in/out		2D	380	5	1	25	Breath-hold
Fat-suppressed T1-weighted images **		3D	380	6	–	25	Breath-hold
Diffusion-weighted images (EPI)		2D	380	5	1	25	Diaphragmatic gating
MRCP	Coronal (radial)	2D	300	10	–	10	Breath-hold
MRCP	Coronal	2D	300	4	0	22	Breath-hold
MRCP	Transverse	2D	300	4	0	20	Breath-hold
MRCP	Coronal	3D	300	2 (reconstruction, 1 mm)	–	80	Respiratory-gated
Fat-suppressed T1-weighted images	Transverse (dynamic)	3D	380	3 (reconstruction, 1.5 mm)	–	133	Breath-hold
Fat-suppressed T1-weighted images	Transverse (delay)	3D	380	6	–	25	Breath-hold

* Breath-hold T2-weighted images and MRCP are single-shot T2-weighted images.

**T1-weighted images acquired using GRE.

Standard imaging methods (gastrointestinal tract)

D Imaging of the gastrointestinal tract

Introduction

Gastrointestinal tract imaging using barium sulfate has traditionally been used in Japan as a major diagnostic imaging examination of the gastrointestinal tract, with the indications covering from screening to preoperative work-up. In recent years, however, remarkable advances in endoscopy have allowed endoscopy to be the main modality for both diagnostic and therapeutic endoscopies from the esophagus to the rectum. Currently, the main roles of gastrointestinal tract imaging have become defining the location and extent of lesions and evaluating critical features such as luminal stenosis, deformity, or fistula formation before and after treatment (chemo/chemoradiotherapy). The indications and techniques vary depending on the organ (Table 7). Specifically for the large bowel, CT colonography (CTC) has been developed thanks to advances in the technologies of CT equipment and applications, and it is widely accepted in clinical practice. There are several kinds of three-dimensional (3D) viewing options, including virtual enema, virtual endoscopy, and computed tomography angiography (CTA), which can be produced

by a single CT examination and provide useful anatomical information about colorectal cancer before surgery. In 2012, the revised medical service fees included an additional amount for CT colonography as a test for patients with suspected colorectal malignancies.

Gastrointestinal imaging (Fig. 11)

Basically, barium sulfate is used as a contrast agent under fluoroscopy to screen the gastrointestinal tract from the pharynx and esophagus to the rectum and anus. The use of low-viscosity barium sulfate at a high concentration of approximately 200% W/V is the basic procedure for the upper gastrointestinal tract, whereas agglutination-resistant barium at a concentration of less than half is used in the lower gastrointestinal tract. An aqueous iodine contrast medium can be an alternative for cases with suspected gastrointestinal perforation or obstruction (note that the aqueous iodine contrast medium is contraindicated for patients with suspected aspiration because of pulmonary toxicity). The test requires an empty gastrointestinal tract, and an anticholinergic agent or glucagon is injected intramuscularly to inhibit secretion and peristalsis, unless motility is being evaluated. A simple test can evaluate lesion location, luminal deformity and stenosis, fistula formation, and motility of the gastrointestinal tract. In addition, distending the gastrointestinal tract with a gas, called double-contrast technique, enables extremely detailed examination of radiological features. Carbon dioxide gas is administered using effervescent granules taken orally or air via a nasal catheter to distend the esophagus, stomach, duodenum, and small bowel. Air is administered via a transanal balloon catheter to distend the large bowel.

Table 7. Main indications for gastrointestinal tract contrast-enhanced imaging

	Indication
Esophagus	Esophageal cancer, achalasia (including similar conditions)
Stomach	Gastric cancer, screening/gastric cancer examinations
Duodenum	Duodenal tumor (adenoma, carcinoma, duodenal papillary neoplasm)
Small bowel	Inflammatory bowel disease (e.g., Crohn’s disease)
Large bowel	Colorectal cancer, inflammatory bowel disease (e.g., ulcerative colitis)
Other	After surgery

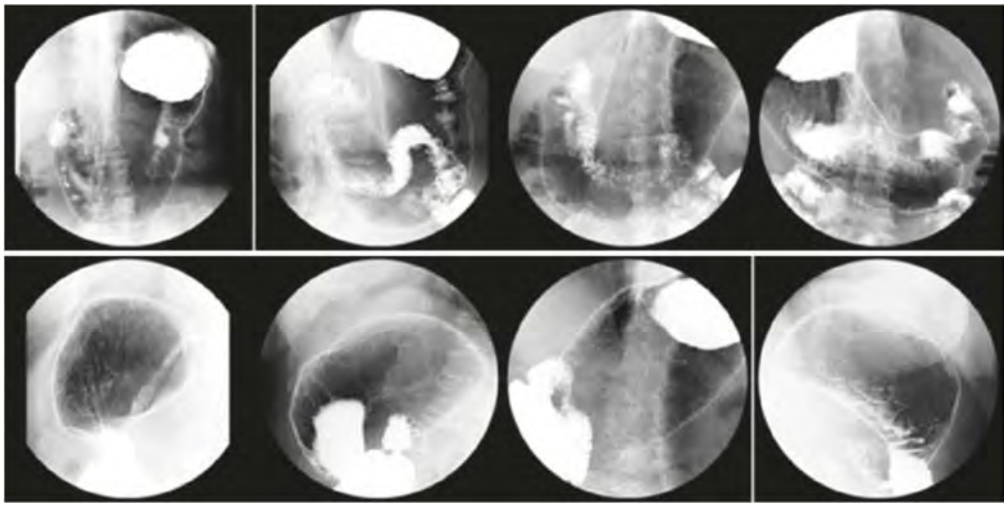

Figure 11. Examples of gastrointestinal series

Basic imaging method for population-based screening of the Japanese Society of Gastrointestinal Cancer Screening, 8 patient positions, using 150 mL of 200% W/V low-viscosity barium sulfate

1. Upper gastrointestinal tract imaging (Upper GI series)

Preparation: Fasting for at least 12 hours. Injection of an anticholinergic agent or glucagon immediately before the test.

Oropharynx and hypopharynx: Not mandatory but helpful in some situations. A small amount of contrast medium administered orally is enough to observe the first part of an upper gastrointestinal series. The dilution and amount of contrast medium and the patient's posture in drinking it (no jaw lift) should be considered depending on the patient's condition, such as risk of aspiration.[35)]

Esophagus: Mainly to evaluate neoplastic lesions. Use of a nasogastric tube is desirable to visualize a lesion better. Esophageal distension can be obtained by injection of contrast medium via the tube, followed by addition of air, which is the best imaging condition for close evaluation. Basically, the location and extent of a lesion are estimated on the frontal view, and the invasion depth of the lesion is estimated indirectly by lateral deformity or extensibility on the lateral view. Serial radiography covering the entire process (contrast medium passing through the esophagus) offers desirable images rather than one shot.

Stomach and duodenum: For the stomach, the Japanese Society of Gastrointestinal Cancer Screening recommends a standard imaging method covering the entire stomach using the double-contrast technique (references 2 to 6 and Fig. 12) as a screening test.[36-40)] Preoperative evaluation of a neoplastic lesion is also possible with this technique. Use of a nasogastric tube is desirable to visualize a lesion better. Gastric distension can be obtained by an adequate amount of contrast medium followed by air via the tube, which offers good image quality for close evaluation. Basically, the location and extent of a lesion are estimated

on the frontal view, and the invasion depth of the lesion is estimated indirectly by lateral deformity and extensibility on the lateral view (Fig. 12). For the duodenum, a special technique is applied (distal to the duodenal bulb), called hypotonic duodenography. It involves fixing a balloon in place at the duodenal bulb and injecting the contrast medium under an intravenous antispasmodic agent and delivering air. However, it involves a high degree of technical difficulty and requires skill.

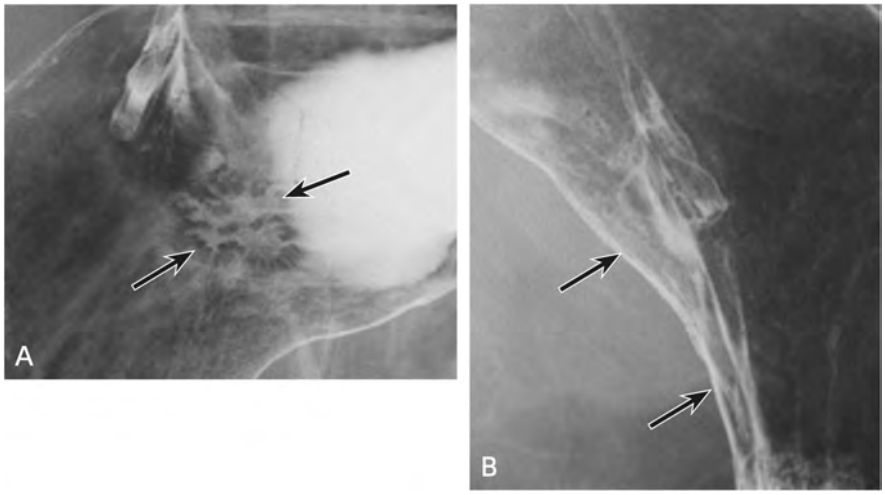

Figure 12. Early gastric cancer (T1a, tubular adenocarcinoma)

A: Upper gastrointestinal series (frontal view): The lesion shows slight depression on the posterior wall of the upper gastric body, indicating type 0-IIc gastric cancer (→).
B: Upper gastrointestinal series (lateral view): The lesion shows no lateral deformity, indicating mucosal cancer with no submucosal invasion (→).

2. Lower gastrointestinal tract imaging

Small bowel: A simple examination as a latter part of an upper gastrointestinal series called small bowel follow-through is used as a screening test. A special examination called small bowel enteroclysis is used to evaluate inflammatory bowel disease such as Crohn's disease or, occasionally, malignancies. An oral laxative is administered the day before the examination. Balloon probe insertion (the tip is placed distal to the ligament of Treitz under fluoroscopic guidance) is desirable to administer the appropriate amount of contrast medium and air. Sufficient distension of the small bowel is required for the double-contrast technique to accurately evaluate the lesions. To avoid overlap within the pelvis during imaging, compression, positional changes, and longitudinal observation are implemented.

Large bowel (Barium enema): Preparation includes a low-residue diet and laxative (modified Brown's method) on the day before the test or a combination of a low-residue diet the day before the test and an intestinal lavage agent on the day of the test. An anticholinergic agent or glucagon is injected intramuscularly immediately before the test. Following a contrast medium enema, air is delivered, and

double-contrast visualization of the entire colon is attempted in at least 2 directions. Basically, the location and extent of a lesion are estimated on the frontal view, and invasion depth of the lesion is estimated indirectly by lateral deformity and extensibility on the lateral view. Use of an aqueous iodine contrast medium should be considered for a case with possible intestinal perforation or obstruction.

CT

CT is used as a preoperative test for gastrointestinal tract malignancies mainly to evaluate lymph node involvement and distant metastases. Evaluation of the primary lesion is also possible depending on its size and spread. A thoracoabdominal scan using single-phase contrast-enhanced CT is common to scan from the lung to the pelvis. Multiphase contrast-enhanced CT including the arterial phase is helpful to visualize vessels for preoperative mapping. Gastrointestinal tract distention is required to evaluate the primary lesion at the same examination as well. The stomach is distended by administration of carbon dioxide gas (effervescent granules) taken orally. The large bowel is distended by carbon dioxide gas via a transanal catheter after preparation using a laxative agent, which technique is called CT colonography (CTC).

Example of CTC in colorectal cancer before surgery (Fig. 13)

Procedure: Administration of 2 to 3 L of carbon dioxide gas under monitoring of the amount and pressure via a transanal catheter. An antispasmodic agent may be intramuscularly injected as needed.

Scan: Three-phase (arterial, portal venous, and equilibrium phases) scanned data are loaded to the workstation for 3D reconstruction.

Protocol (CTC＋CT arterial portography): Tube voltage, 120 K; tube current, AEC; rotation time, 0.5 seconds; slice thickness, 0.5 mm; high-speed pitch used, 1.0,100 rows. CTC + CTA 370 mg/mL of contrast medium, injection pressure 4 mL/s (saline chaser), with bolus tracking technique, 30 seconds after CTA imaging.

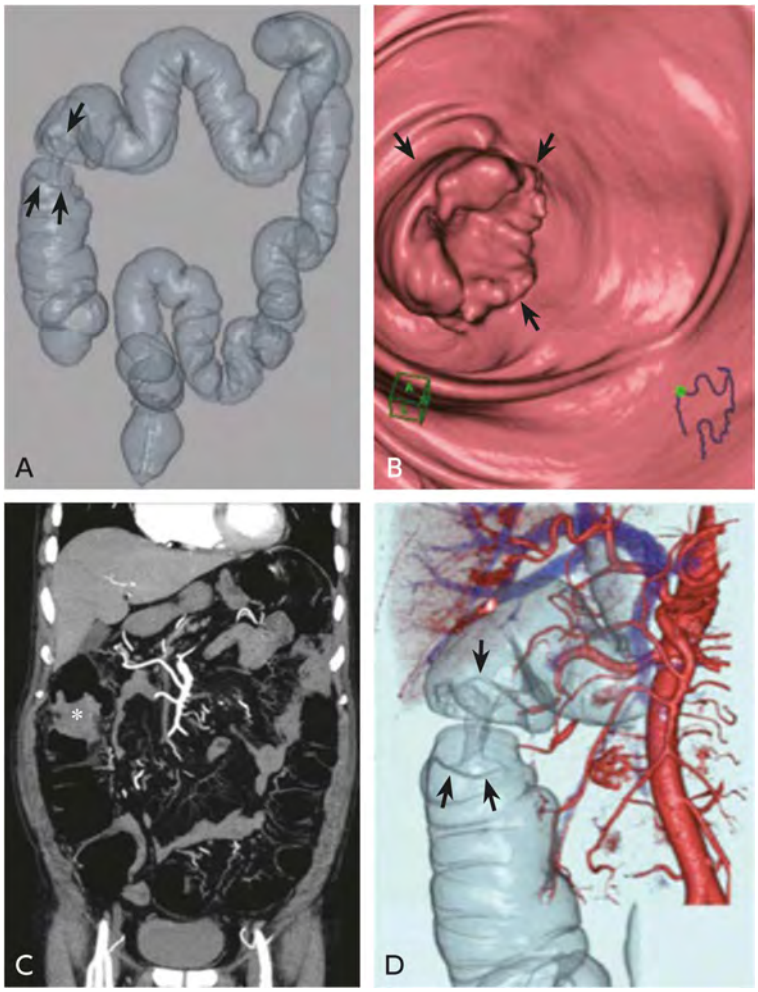

Figure 13. CTC of ascending colon cancer

A: Virtual enema, B: virtual endoscopy, C: 2D MIP (coronal plane), D: CTC + CTA (arterial phase + portal venous phase)
The photographs show type 2 colon cancer locating in the ascending colon (→).

References

1) Fujita M et al: Comparison between conventional and spiral CT in patients with hypervascular hepatocellular carcinoma. Eur J Radiol 18: 134-136, 1994
2) Ito K et al: Multislice dynamic MRI of hepatic tumors. J Comput Assist Tomogr 17: 390-396, 1993
3) Kihara Y et al: Optimal timing for delineation of hepatocellular carcinoma in dynamic CT. J Comput Assist Tomogr 17: 719-722, 1993
4) Heiken JP et al: dynamic incremental CT: effect of volume and concentration of contrast material and patient weight on hepatic enhancement. Radiology 195: 353-357, 1995
5) Brink JA et al: Hepatic spiral CT: reduction of dose of intravenous contrast material. Radiology 197: 83-88, 1995
6) Yamashita Y et al: Abdominal helical CT: evaluation of optimal doses of intrasvenous contrast material: a prospective randomized study. Radiology 216: 718-723, 2000
7) Kondo H et al: Aortic and hepatic enhancement at multidetector CT: evaluation of optimal iodine dose determined by lean body weight. Eur J Radiol 80: e273-277, 2011
8) Kondo H et al: Body size indexes for optimizing iodine dose for aortic and hepatic enhancement at multidetector CT: comparison of total body weight, lean body weight, and blood volume. Radiology 254: 163-169, 2010
9) Kim T et al: Effects of injection rates of contrast material on arterial phase hepatic CT imaging. AJR Am J Roentgenol 171: 429-432, 1998

10) Awai K, Hori S: Effect of contrast injection protocol with dose tailored to patient weight and fixed injection duration on aortic and hepatic enhancement at multidetector-row helical CT. Eur Radiol 13: 2155-2160, 2003
11) Baron RL et al: Hepatocellular carcinoma: evaluation with biphasic, contrast-enhanced, helical CT. Radiology 199: 505-511, 1996
12) Iannaccone R et al: Hepatocellular carcinoma: role of unenhanced and delayed phase multi-detector row helical CT in patients with cirrhosis. Radiology 234: 460-467, 2005
13) Murakami T et al: Evaluation of optimal timing of arterial phase imaging for the detection of hypervascular hepatocellular carcinoma by using triple arterial phase imaging with multidetector-row helical computed tomography. Invest Radiol 38:497-503, 2003
14) Kawata S et al: Multidetector CT: diagnostic impact of slice thickness on detection of hypervascular hepatocellular carcinoma. AJR Am J Roentgenol 179: 61-66, 2002
15) Kudo M et al.: Proposal for new Sonazoid contrast-enhanced ultrasonography technology to support hepatocellular carcinoma treatment: the usefulness of defect reperfusion imaging. Kanzo 48: 299-301, 2007.
16) Kim YK et al: Detection and characterization of focal hepatic tumors: a comparison of T2-weighted MR images before and after the administration of gadoxectic acidJ Magn Reson Imaging 30: 437-443, 2009
17) Zech CJ et al: Vascular enhancement in early dynamic liver MR imaging in an animal model: comparison of two injection regimen and two different doses Gd-EOB-DTPA (gadoxetic acid) with standard Gd-DTPA. Invest Radiol 44: 305-310, 2009
18) Motosugi U et al: Dilution method of gadolinium ethoxybenzyl diethylenetriaminepentaacetic acid (Gd-EOB-DTPA)-enhanced magnetic resonance imaging (MRI). J Magn Reson Imaging 30: 849-854, 2009
19) Kagawa Y et al: Optimal scanning protocol of arterial dominant phase for hypervascular hepatocellular carcinoma with gadoliniumethoxybenzyl-diethylenetriamine pentaacetic acid-enhanced MR. J Magn Reson Imaging 33: 864-872, 2011
20) Kadoya M et al: Hepatocellular carcinoma: correlation of MR imaging and histopathologic findings. Radiology 183: 819-825, 1992
21) Kanematsu M et al: Focal hepatic lesion detection: comparison of four fat-suppressed T2-weighted MR imaging pulse sequences. Radiology 211: 363-371, 1999
22) Hori M et al: Single breath-hold T2-weighted MR imaging of the liver: value of single-shot fast spin-echo and multishot spinecho echoplanar imaging. AJR Am J Roentgenol 174: 1423-1431, 2000
23) McFarland EG et al: Hepatic hemangiomas and malignant tumors: improved differentiation with heavily T2-weighted conventional spin-echo MR imaging. Radiology 193: 43-47, 1994
24) Nasu K et al: Hepatic metastases: diffusion-weighted sensitivity-encoding versus SPIO-enhanced MR imaging. Radiology 239: 122-130, 2006
25) Park MS et al: Hepatocellular carcinoma: detection with diffusion-weighted versus contrast-enhanced magnetic resonance imaging in pretransplant patients. Hepatology 56: 140-148, 2012
26) Anderson SW et al: Accuracy of MDCT in the diagnosis of choledocholithiasis. AJR Am J Roentgenol 187: 174-180, 2006
27) Chung WS et al: Diagnostic accuracy of multidetector-row computed tomography for common bile duct calculi: is it necessary to add non-contrast-enhanced images to contrast-enhanced images? J Comput Assist Tomogr 31: 508-512, 2007
28) Ogawa H et al: CT findings of intraductal papillary neoplasm of the bile duct: assessment with multiphase contrast-enhanced examination using multi-detector CT. Clin Radiol 67: 224-231, 2012
29) Kakihara D et al: Usefulness of the long-axis and short-axis reformatted images of multidetector-row CT in evaluating T-factor of the surgically resected pancreaticobiliary malignancies. Eur J Radiol 63: 96-104, 2007
30) Kitami M et al: Heterogeneity of subvesical ducts or the ducts of Luschka: a study using drip-infusion cholangiography-computed tomography in patients and cadaver specimens. World J Surg 29: 217-223, 2005
31) Choi JY et al: Magnetic resonance pancreatography: comparison of two- and three-dimensional sequences for assessment of intraductal papillary mucinous neoplasm of the pancreas. Eur Radiol 19: 2163-2170, 2009
32) Safar F et al: Magnetic resonance T1 gradient-echo imaging in hepatolithiasis. Abdom Imaging 30: 297-302, 2005
33) Sugita R, Nomiya T: Disappearance of the common bile duct signal caused by oral negative contrast agent on MR cholangiopancreatography. J Comput Assist Tomogr 26: 448-450, 2002
34) Yoshimitsu K et al: Magnetic resonance differentiation between T2 and T1 gallbladder carcinoma: significance of subserosal enhancement on the delayed phase dynamic study. Magn Reson Imaging 30: 854-859, 2012
35) Shibuya D: Procedural accidents in gastric mass surveys using indirect X-ray examination. Journal of Gastrointestinal Cancer Screening 44: 251-257, 2006.

36) Imamura K: Evaluation of new standard method of gastric photofluorography. Journal of Gastrointestinal Cancer Screening 45: 309-316, 2007.
37) Shimizu K: Examination of transition to a new method of gastric photofluorography: Focus on early cancer detection rates. Journal of Gastrointestinal Cancer Screening 47: 35-42, 2009.
38) Higashiyama K: Evaluation of the accuracy of gastric and colon cancer screening based on comparisons with community cancer registries: Measurement of sensitivity and specificity. Journal of Gastrointestinal Cancer Screening 48: 429-435, 2010.
39) Yamamoto K et al: Diagnostic validity of high-density barium sulfate in gastric cancer screening: follow-up of screenees by record linkage with the Osaka Cancer Registry. J Epidemiol 20: 287-294, 2010
40) Japanese Society of Gastrointestinal Cancer Screening, Committee on Accuracy Management of Gastric Cancer Screening, Ed.: 2011 Revised Guidelines on New Methods of Gastric Radiography. Igaku-Shoin Ltd., 2011.

BQ 36 Which imaging examinations are recommended for hepatocellular carcinoma screening in patients with chronic liver disease?

Statement

Abdominal ultrasonography at intervals of 3 to 6 months is the main recommendation.

For patients in an ultra-high-risk group, the additional use of EOB-MRI or abdominal dynamic contrast-enhanced CT every 6 months to 1 year is considered.

Background

Although hepatitis B virus (HBV), hepatitis C virus (HCV), and lifestyle play major roles as causes of hepatocellular carcinoma, hepatitis B incidence has leveled off, hepatitis C incidence is declining, and non-B and non-C hepatitis, including steatohepatitis, is increasing (secondary source 1). A reduction in cancer incidence has been seen with a sustained virologic response (SVR) in patients with chronic hepatitis B who were taking nucleoside analogs and with antiviral agents in patients with chronic hepatitis C. However, these patients are acknowledged to be at considerable risk of cancer. Consequently, patients with chronic type C or B liver disease and patients with nonviral liver cirrhosis are considered candidates for periodic screening for hepatocellular carcinoma. Particularly in patients with liver cirrhosis, which is a group at ultra-high risk for cancer, screening based on tumor markers and diagnostic imaging increases the opportunity for curative treatment due to early detection of hepatocellular carcinoma and may contribute to improved prognosis.[1)]

Explanation

1. Abdominal ultrasonography at 3- to 6-month intervals

Ultrasonography is easy to perform, minimally invasive, and inexpensive, and it is therefore widely used in hepatocellular carcinoma screening of groups at high and ultra-high risk of hepatocellular carcinoma. A randomized, controlled trial (RCT) found that periodic surveillance for hepatocellular carcinoma may improve prognosis.[1)] In addition, surveillance intervals were compared in 2 RCTs. A trial that compared 3- and 6-month intervals for ultrasonographic surveillance of patients with liver cirrhosis found no significant difference with respect to the primary endpoint, the incidence of hepatocellular carcinoma ≤ 30 mm in size, and no difference in overall survival.[2)] A trial that compared 4- and 12-month intervals found that, although more patients with tumors ≤ 2 cm in size were detected with 4-month intervals, no significant difference in 4-year survival was seen.[3)] Although the likelihood of detecting tumors shows small increases as the screening intervals shorten, the cost increases. These guidelines adhere to the established recommendations for Japan: screening by ultrasonography is recommended every 6 months for the high-risk group (chronic

hepatitis) and every 3 to 4 months for the ultra-high-risk group (patients with liver cirrhosis). At present, however, no literature that provides strong evidence regarding screening intervals has been identified.

2. Concurrent use of dynamic contrast-enhanced MRI using Gd-EOB-DTPA or dynamic CT

If ultrasound detects nodules or the patient is in an ultra-high-risk group, differential diagnosis of the nodules and further investigation of hepatocellular carcinoma are carried out by dynamic CT or MRI using an extracellular gadolinium contrast medium or by dynamic MRI using a hepatocyte-specific contrast medium (Gd-EOB-DTPA, EOB/Primovist®; EOB-MRI). In patients for whom CT and MRI contrast media are contraindicated, perflubutane (Sonazoid®) contrast-enhanced ultrasound is recommended. If ultrasound visualization is poor, dynamic CT/MRI imaging may be performed for surveillance and nodule detection. CQ2 of the 2017 guidelines for the diagnosis and treatment of liver cancer asked, "Who are the candidates for surveillance and how is it conducted?" The response was the following strong recommendation: "Patients with chronic type C or B liver disease and patients with nonviral liver cirrhosis are candidates for periodic hepatocellular carcinoma screening. The screening mainly involves abdominal ultrasonography and tumor marker measurement at 3- to 6-month intervals. Concurrent dynamic CT or dynamic MRI is also considered for patients in an ultra-high-risk group, such as patients with liver cirrhosis (secondary source 2)." In an RCT that compared the usefulness of abdominal ultrasonography performed every 6 months with that of annual contrast-enhanced CT in 163 patients with compensated liver cirrhosis, detection sensitivity and specificity for hepatocellular carcinoma in the study population, which had an annual cancer incidence of 6.6%, were 71.4% and 97.5%, respectively, in the abdominal ultrasonography group and 66.7% and 94.4%, respectively, in the CT group. Thus, superior sensitivity was seen in the group that underwent abdominal ultrasonography every 6 months. Moreover, testing costs were lower in this group. No reports on the usefulness of combining dynamic contrast-enhanced CT with ultrasonography for imaging screening have been identified. However, the concurrent use of CT or MRI approximately once a year for hepatocellular carcinoma (HCC) screening is common in ultra-high-risk groups, which have a high pre-test probability of the presence of HCC.

Many studies that have compared dynamic CT and EOB-MRI with respect to HCC detection sensitivity have reported EOB-MRI to be superior in this regard. In a multicenter study of diagnostic performance in HCC ≤ 2 cm in diameter, detection sensitivity for HCC showed a trend toward greater sensitivity with EOB-MRI (≤ 10 mm: 38.0% to 55.4%, 10 to 20 mm: 71.1% to 87.3%) than with dynamic CT (≤ 10 mm: 26.1% to 47.3%, 10 to 20 mm: 65.7% to 78.4%).[4)] The report attributed this to the usefulness of the hepatobiliary phase. One study found that the diagnostic performance of EOB-MRI did not differ from that of ultrasound or dynamic CT without the hepatobiliary phase, but it was greater when the hepatobiliary phase was added.[5)] The superiority of EOB-MRI in HCC diagnosis is particularly pronounced in the detection of mainly small lesions ≤ 2 cm in size and early (hypovascular) HCC.[6)] A meta-analysis of HCC detection with dynamic CT and EOB-MRI found higher sensitivity and diagnostic accuracy with EOB-MRI

than with dynamic CT, and that the differences were particularly marked for HCC lesions smaller than 2 cm.[7)]

With regard to the use of EOB-MRI in HCC screening, EOB-MRI was found to be more cost-effective than MRI using extracellular gadolinium contrast medium and CT in HCC-related diagnosis and treatment of patients with hepatitis and liver cirrhosis in Japan.[8)] Moreover, in the surveillance of patients with liver cirrhosis, EOB-MRI was found to provide a higher detection rate and result in fewer false-positives than other modalities.[9)] However, there has been limited reporting on the usefulness of EOB-MRI in screening, and no literature on the usefulness of its combined use with ultrasonography has been identified. In addition, dynamic MRI using extracellular gadolinium contrast media and EOB-MRI have been reported to be comparable with respect to HCC diagnostic accuracy. Consequently, EOB-MRI cannot be regarded as absolutely superior. One factor in this is poor contrast with HCC due to poor Gd-EOB-DTPA uptake in non-cancerous areas resulting from hepatic dysfunction.[10, 11)] Caution is therefore required when using EOB-MRI in patients with liver cirrhosis.

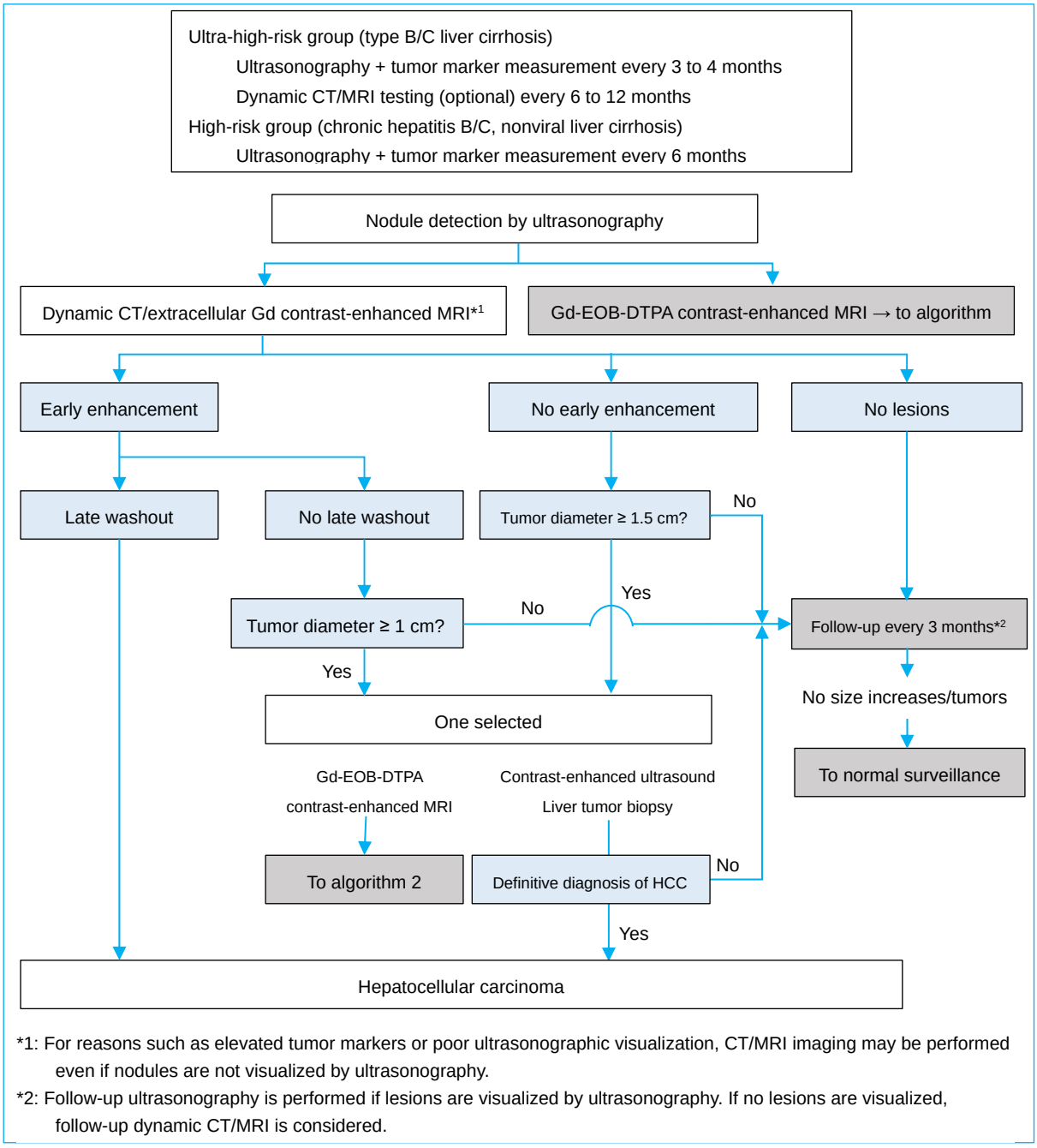

*1: For reasons such as elevated tumor markers or poor ultrasonographic visualization, CT/MRI imaging may be performed even if nodules are not visualized by ultrasonography.

*2: Follow-up ultrasonography is performed if lesions are visualized by ultrasonography. If no lesions are visualized, follow-up dynamic CT/MRI is considered.

Figure 1. Hepatocellular carcinoma diagnostic algorithm 1

Jointly prepared by the Japan Radiological Society and the Japan Society of Hepatology. Copyright held by the Japan Society of Hepatology. The same algorithm was presented in the 2021 Guidelines for the Diagnosis and Treatment of Liver Cancer.

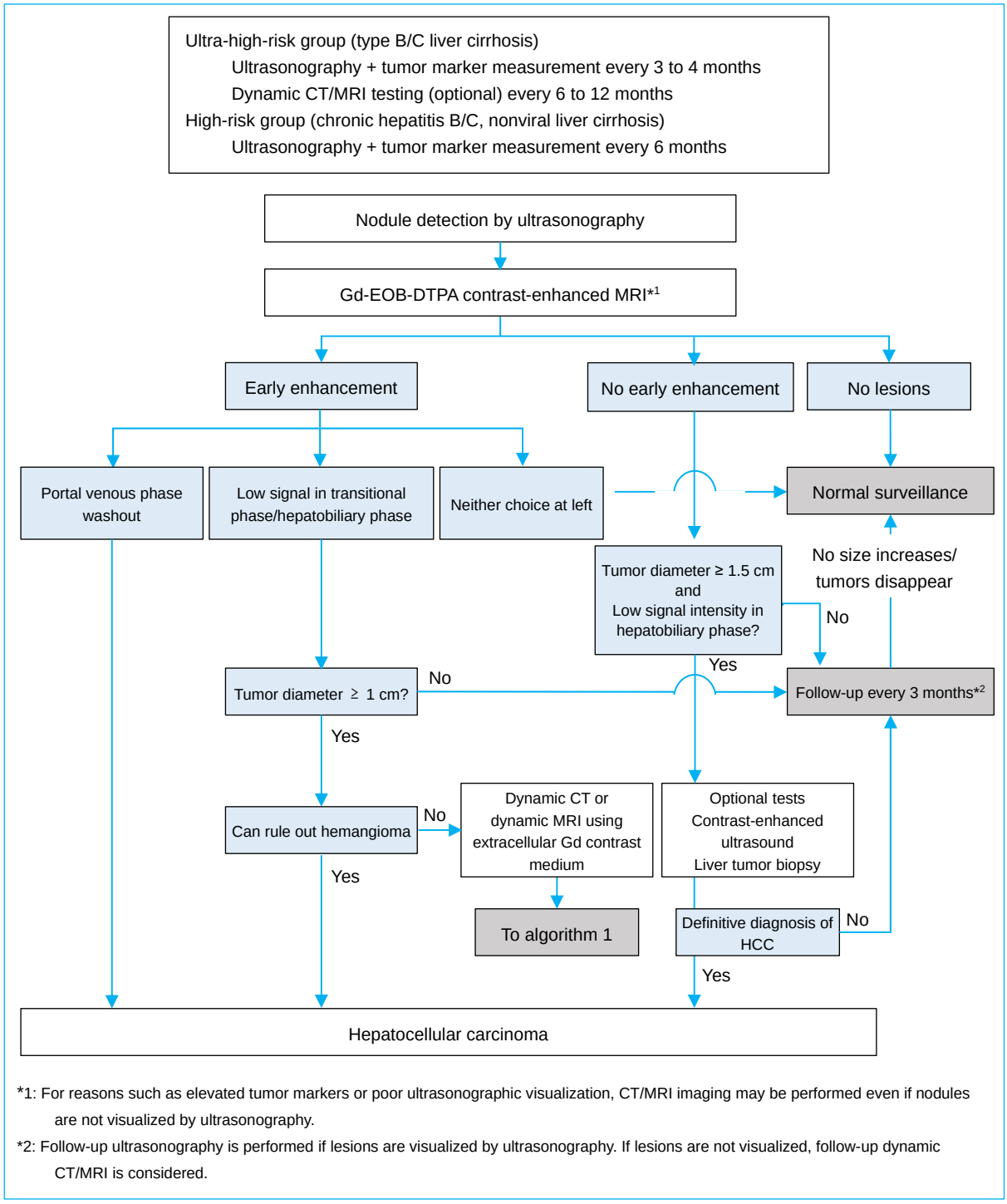

Figure 2. Hepatocellular carcinoma diagnostic algorithm 2

Jointly prepared by the Japan Radiological Society and the Japan Society of Hepatology. Copyright held by the Japan Society of Hepatology. The same algorithm was presented in the 2021 guidelines for the diagnosis and treatment of liver cancer.

3. Perflubutane (Sonazoid®) contrast-enhanced ultrasonography

An examination of the diagnostic performance of perflubutane contrast-enhanced ultrasonography found a trend toward greater detection sensitivity for HCC lesions ≤ 2 cm in size with perflubutane contrast-enhanced ultrasound (67.6%) and EOB-MRI (76.5%) than with dynamic CT (52.9%), though the differences were not significant.[10] In addition, detection performance with respect to hypovascular well-differentiated HCC was found to be greater with EOB-MRI than with perflubutane contrast-enhanced ultrasonography. This was reported to be related to the fact that perflubutane uptake decreases later than Gd-EOB-DTPA uptake in early HCC during the process of multistep carcinogenesis.[8] On the other hand, perflubutane contrast-enhanced ultrasonography enables blood flow to be evaluated in real time and is excellent for evaluating nodule blood flow. It is therefore considered useful as a diagnostic imaging modality that complements EOB-MRI. Perflubutane contrast-enhanced ultrasonography is not widely used clinically. This is due to the lack of skilled operators and the complexity of the procedure, in addition to the fact that it has disadvantages specific to ultrasonography (extensive dead space makes whole-liver evaluation difficult, limited objectivity of findings). It is therefore not well suited as a test to be performed next in patients with suspected intrahepatic lesions based on ultrasonography. However, in view of the fact that it offers the advantage of the greatest sensitivity to slight nodule hypervascularization, it is recommended for diagnosis in patients for whom hypervascularization detection is difficult and important, as in the case of well-differentiated HCC (including early HCC).

4. Summary

The main modality for HCC screening based on imaging is ultrasonography performed every 3 to 6 months, with consideration given to the concurrent use of EOB-MRI and dynamic contrast-enhanced CT, which provide high diagnostic performance. However, in view of the fact that the cost of EOB-MRI testing is 8 to 9 times the cost of abdominal ultrasound, it may be unlikely that the increased cost is offset by the increase in survival time. Moreover, the MRI systems used in the studies cited in this document were high-performance MRI systems, and the diagnostic performance of lower-performance MRI systems may be poorer. It should also be noted that the diagnostic performance of EOB-MRI is lower in patients with poor liver function or obstructive jaundice. Careful judgement is therefore required regarding the concurrent use of EOB-MRI. In view of the fact that high-performance MRI systems are not widely available, the current reality is that ultrasound and dynamic CT must be relied on for imaging screening.

Search keywords and secondary sources

PubMed was searched for the period through October 2019 using the keywords HCC, US, CT, MRI, screening, Sonazoid, and EOB. Thirteen articles were selected from the search results. The selected articles concerned HCC imaging screening, with a focus on comparisons of diagnostic performance. In addition, 2 articles identified in a hand search were included, for a final total of 15 articles used.

In addition, the following were referenced as secondary sources

1) JSH, Ed.: 2015 Liver Cancer White Paper. JSH, 2015.
2) JSH HCC Guidelines 2017, Revised Version

References

1) Zhang BH et al: Randomized controlled trial of screening for hepatocellularcar-cinoma. J Cancer Res Clin Oncol 130: 417-422, 2014
2) Trinchet JC et al: Ultrasonographic surveillance of hepatocellular carcinoma in cirrhosis: a randomized trial comparing 3-and 6-month periodicities. Hepatology 54: 1987-1997, 2011
3) Wang JH et al: Hepatocellular carcinoma surveillanceat4vs.12month intervals for patients with chronic viral hepatitis: a randomized study in community. Am J Gastroenterol 108: 416-424, 2013
4) Ichikawa T et al: Detection and characterization of focal liver lesions: a Japanese phase III, multicenter comparison between gadoxetic acid disodium-enhanced magnetic resonance imaging and contrast-enhanced computed tomography predominantly in patients with hepatocellular carcinoma and chronic liver disease. Invest Radiol 45: 133-141, 2010
5) Di Martino M et al: Hepatocellular carcinoma in cirrhotic patients: prospective comparison of US, CT and MR imaging. Eur Radiol 23: 887-896, 2013
6) Sano K et al: Imaging study of early hepatocellular carcinoma: usefulness of gadoxetic acid-enhanced MR imaging. Radiology 261: 834-844, 2011
7) Li J et al: The diagnostic performance of gadoxetic acid disodium-enhanced magnetic resonance imaging and contrast-enhanced multi-detector computed tomography in detecting hepatocellular carcinoma: a meta-analysis of eight prospective studies. Eur Radiol 29: 6519–6528, 2019
8) Ohama H et al: Imaging sinazoid-enhanced ultrasonography in multistep hepatocarcinogenesis: comparison with Gd-EOBDTPA enhanced MRI. J Gastroenterol 49: 1081-1093, 2014
9) Kim SY et al: MRI with liver-specific contrast for surveillance of patients with cirrhosis at high risk of hepatocellular carcinoma. JAMA Onco. 3: 456–463, 2017
10) Ayuso C et al: Prospective evaluation of gadoxetic acid magnetic resonance for the diagnosis of hepatocellular carcinoma in newly detected nodules ≤ 2 cm in cirrhosis. Liver Int 39: 1281–1291, 2019
11) Semaan S et al: Hepatocellular carcinoma detection in liver cirrhosis: diagnostic performance of contrast-enhanced CT vs. MRI with extracellular contrast vs. gadoxetic acid. Eur Radiol 30: 1020–1030, 2020

CQ 9 Is EOB-MRI recommended to differentiate HCC from hemangioma for lesions that show hypervascularity but no washout in patients with chronic liver disease?

Recommendation

Not performing EOB-MRI is weakly recommended.

Recommendation strength: 2, strength of evidence: weak (C), agreement rate: 80% (8/10)

CQ 10 Is EOB-MRI recommended to differentiate from hypervascular pseudolesions for lesions that show hypervascularity but no washout in patients with chronic liver disease?

Recommendation

Performing EOB-MRI is weakly recommended.

Recommendation strength: 2, strength of evidence: weak (C), agreement rate: 100% (10/10)

Background

In patients with chronic liver disease, a typical HCC imaging finding with a test that uses an extracellular contrast medium, such as contrast-enhanced CT, is a lesion that shows arterial phase enhancement and washout from the portal venous phase to the equilibrium phase. Even with HCC, however, there are cases in which washout is not clearly seen, making differentiation from hemangioma and hypervascular pseudolesions problematic. Although HCC is malignant, hemangiomas and hypervascular pseudolesions are benign. It is therefore clinically important to accurately differentiate between them with imaging.

Explanation

1. Is EOB-MRI recommended to differentiate HCC from hemangioma?

With EOB-MRI, lesions other than HCC also show strong enhancement in the arterial-dominant phase and show low signal intensity compared with the surrounding liver tissue from the transitional phase to the hepatobiliary phase. Referred to as a pseudo-washout appearance, it often poses problems for distinguishing high-flow hemangiomas, where the nodules as a whole show strong enhancement during early contrast imaging, from small HCC. However, no randomized studies have yet been conducted to prospectively examine the ability of EOB-MRI to differentiate hemangioma from HCC. Consequently, the retrospective, observational studies that have examined differentiation of these 2 conditions are summarized below.

In a study that used EOB-MRI to examine 50 nodules in 43 patients with high-flow hemangiomas that exhibited a pseudo-washout appearance and 113 nodules in 62 patients with hypervascular small HCC (all lesions less than 20 mm in diameter), Nam et al. found that the ADC determined from diffusion-weighted images and the contrast-to-noise ratio (CNR) determined from T2-weighted images were significantly higher for the high-flow hemangiomas than for the hypervascular small HCCs. The area under the receiver-operating characteristic curve (AUROC) for the ability to distinguish hemangioma from HCC was 0.995 (95% CI, 0.969 to 1.000; sensitivity, 98%; specificity, 97.3%) using the ADC, which was significantly better than the AUROC of 0.915 (95% CI, 0.861 to 0.953) obtained using the CNR from T2-weighted images. On the other hand, the ability to distinguish hemangioma from HCC was also high with qualitative visual assessment (AUROC, 0.988 to 0.999; sensitivity, 90% to 94%; specificity, 98.2% to 100%), with high interrater agreement (κ-value, 0.80).[1)]

Similarly, Choi et al. used EOB-MRI with concurrent intravoxel incoherent motion (IVIM) diffusion-weighted imaging to examine 20 hemangioma nodules, 91 HCC nodules, 27 intrahepatic cholangiocarcinoma nodules, 9 mixed liver cancer nodules, 9 metastatic liver cancer nodules, and 5 nodules of other types, for a total of 161 nodules in 161 patients (all lesions at least 20 mm in diameter). They reported that hemangiomas and liver malignancies differed significantly with respect to the molecular diffusion coefficient (Dslow) for ADC and IVIM, and that the AUROC for the ability to discriminate between hemangioma and liver malignancies was 0.907 (95% CI, 0.850 to 0.948; sensitivity, 90.0%; specificity, 80.9%) for ADC and 0.933 (95% CI, 0.882 to 0.967; sensitivity, 95.0%; specificity, 83.8%) for Dslow. On the other hand, no significant differences in ADC and Dslow were seen between liver malignancies, indicating that combining diffusion-weighted imaging with EOB-MRI is likely to improve the ability to distinguish HCC from hepatic hemangioma, but also the ability to distinguish it from other liver malignancies.[2)]

Although there has not yet been sufficient investigation of the use of EOB-MRI to distinguish HCC from hemangioma, the above findings indicate that combining it with diffusion-weighted imaging may provide clinically adequate diagnostic performance. However, when used to distinguish between such lesions, there have been no investigations that have compared the diagnostic performance of EOB-MRI combined with diffusion-weighted imaging with the diagnostic performance of other modalities (e.g., ultrasound, extracellular contrast-enhanced MRI).

2. Is EOB-MRI recommended for differentiating from hypervascular pseudolesions?

In patients with chronic liver disease, hypervascular pseudolesions are often observed in extracellular contrast-enhanced imaging examination such as contrast-enhanced CT due to changes such as the hyperplastic nodules seen with AP shunt development and in heavy users of alcohol. These are rarely definitively diagnosed pathologically, but rather it is considered appropriate to lump them together as hypervascular pseudolesions clinically. No RCTs have been identified that have used EOB-MRI for direct comparisons with respect to HCC and hypervascular pseudolesion imaging findings and differentiation.

Consequently, the retrospective, observational studies that have examined differentiation between HCC and hypervascular pseudolesions are summarized below.

In a study that examined 28 hypervascular hyperplastic nodules and 29 hypervascular HCC lesions ≤ 3 cm in size in patients with alcoholic liver cirrhosis, low-intensity to isointense signal intensity was seen in diffusion-weighted images in nodules ≤ 16 mm in size, with no washout seen in either the portal venous phase or the transitional phase or both. These 3 variables were independent predictors of hypervascular hyperplastic nodules. When 2 of these 3 variables were seen, the diagnostic performance for hypervascular hyperplastic nodules was as follows: sensitivity, 92.9% (26/28); specificity, 75.9% (22/29); and diagnostic accuracy, 84.2% (48/57). When all 3 variables were seen, diagnostic performance was as follows: sensitivity, 60.7% (17/28); specificity, 100% (29/29); and diagnostic accuracy, 80.7% (46/57).[3)]

In an investigation that examined 28 benign nodules comprising hemangiomas (11 lesions), AP shunts (15 lesions), and nonspecific benign lesions (2 lesions), and 111 HCC lesions, the indices of the diagnostic performance of EOB-MRI for HCC were sensitivity of 95% (107/111) and specificity of 96% (27/28) for reader 1 and sensitivity of 95% (106/111) and specificity of 96% (27/28) for reader 2. The indices of the diagnostic performance of dynamic CT for HCC were sensitivity of 84% (95/111) and specificity of 100% (28/28) for reader 1 and sensitivity of 89% (99/111) and specificity of 100% (28/28) for reader 2. Thus, for reader 1, sensitivity was higher with EOB-MRI than with dynamic CT ($p = 0.005$). No significant difference in sensitivity ($p = 0.052$) was seen between the modalities for reader 2 or in specificity for readers 1 and 2 ($p = 0.317$ for both).[4)]

In an investigation that examined 32 hypervascular pseudolesions with nodular morphology (mean size, 11.5 mm) and 123 hypervascular HCC lesions (mean size, 16.4 mm), the HCC lesions, as compared with the pseudolesions, were significantly larger, a significantly higher proportion showed high signal intensity on T2-weighted and diffusion-weighted images, and a significantly higher proportion showed low signal intensity during the hepatobiliary phase ($p < 0.0001$). The signal intensity ratio for the lesions and parenchyma in the hepatobiliary phase was significantly lower for the HCC lesions. Using a cutoff of 0.84, sensitivity was 91% (112/123), and specificity was 91% (29/32). In addition, when a high-intensity signal in a diffusion-weighted image was used as the diagnostic criterion for HCC lesions and hypervascular pseudolesions, sensitivity was 67% (83/123), and specificity was 100% (32/32).[5)]

An investigation that examined 53 hypervascular pseudolesions and 44 HCC lesions ≤ 2 cm in size compared the diagnostic performance of EOB-MRI (diagnostic criteria were arterial phase enhancement and low signal intensity in the hepatobiliary phase) and dynamic CT (diagnostic criteria were arterial phase enhancement and low signal intensity in the equilibrium phase) based on independent 5-point scale assessments by 2 raters. The results showed that EOB-MRI provided higher sensitivity than dynamic CT, with no significant difference in specificity [Reader 1 (EOB-MRI vs. CT): sensitivity, 93.9% (31/33) vs. 54.5% (18/33), $p = 0.001$; specificity, 92.6% (25/27) vs. 96.3% (26/27), $p = 1$. Reader 2: sensitivity, 90.9% (30/33) vs. 54.5% (18/33) $p = 0.0018$; specificity, 92.6% (25/27) vs. 96.3% (26/27), $p = 1$]. No significant

differences in the Az value were seen [Reader 1: 0.975 vs. 0.892 (p = 0.069), Reader 2: 0.966 vs. 0.888 (p = 0.106)].[6)]

In an investigation that examined 52 nodular lesions ≤ 1 cm in size that showed arterial phase enhancement and low signal intensity in the hepatobiliary phase (30 malignant lesions and 22 benign lesions), no washout was seen in 16.7% of the HCC lesions (5/30) and 50% of the benign lesions (11/22). That is, 16 nodules were lesions without washout, which indicates hypervascularity. Of these, 11 nodules [68.8% (11/16)] were benign, and 5 [31.3% (5/16)] were HCC lesions. Thus, the absence of washout was more frequent in benign lesions.[7)]

Although there has been insufficient examination of the use of EOB-MRI to distinguish between HCC and hypervascular pseudolesions, the above findings indicate that lesions that are hypervascular but do not show washout are more often benign lesions than HCC, and that EOB-MRI exhibits high diagnostic performance in distinguishing between such lesions. However, no definitive evidence has been shown that EOB-MRI is non-inferior or superior to other modalities (e.g., contrast-enhanced ultrasound, contrast-enhanced MRI using extracellular gadolinium contrast media) when used to distinguish between such lesions, and this remains a topic for future investigation.

Search keywords and secondary sources

PubMed was searched for articles on distinguishing HCC from hemangioma using the following keywords: hemangioma, gadoxetic acid, EOB, liver cancer, hepatic cancer, malignancy, and hepatocellular carcinoma. Of the 19 articles extracted, 2 were cited.

PubMed was searched for articles on distinguishing HCC from hypervascular pseudolesions using the following keywords: hepatic, liver, hypervascular, pseudo lesion, pseudo-lesion, benign, gadoxetic acid, EOB, and hepatocyte-specific. Of the 49 articles extracted, 3 were cited. In addition, 2 second-hand citations from these 3 articles were cited, for a total of 5 articles cited.

References

1) Nam SJ et al: High-flow haemangiomas versus hypervascular hepatocellular carcinoma showing “pseudo-washout” on gadoxetic acid-enhanced hepatic MRI: value of diffusion-weighted imaging in the differential diagnosis of small lesions. Clin Radiol 72: 247-254, 2017
2) Choi IY et al: Intravoxel incoherent motion diffusion-weighted imaging for characterizing focal hepatic lesions: correlation with lesion enhancement. J Magn Reson Imaging 45: 1589-1598, 2017
3) Choi IY et al: Value of gadoxetic acid-enhanced MRI and diffusion-weighted imaging in the differentiation of hypervascular hyperplastic nodule from small (＜3 cm) hypervascular hepatocellular carcinoma in patients with alcoholic liver cirrhosis: a retrospective case-control study. J Magn Reson Imaging 51: 70-80, 2020
4) Chen M et al: Added value of a gadoxetic acid-enhanced Hepatocyte-phase image to the LI-RADS system for diagnosing hepatocellular carcinoma. Magn Reson Med Sci 15: 49-59, 2016
5) Motosugi U et al: Distinguishing hypervascular pseudolesions of the liver from hypervascular hepatocellular carcinomas with gadoxetic acid-enhanced MR imaging. Radiology 256: 151-158, 2010
6) Sun HY et al: Gadoxetic acid-enhanced magnetic resonance imaging for differentiating small hepatocellular carcinomas (＜ or ＝2 cm in diameter) from arterial enhancing pseudolesions: special emphasis on hepatobiliary phase imaging. Invest Radiol 96-103, 2010
7) Park CJ et al: Management of subcentimetre arterially enhancing and hepatobiliary hypointense lesions on gadoxetic acid-enhanced MRI in patients at risk for HCC. Eur Radiol 28: 1476-1484, 2018

CQ 11 Is EOB-MRI recommended for diagnosing non-hypervascular lesions in patients with chronic liver disease?

Recommendation

Performing EOB-MRI is strongly recommended.

Recommendation strength: 1, strength of evidence: moderate (B), agreement rate: 100% (11/11)

CQ 12 Is periodic follow-up recommended for diagnosing non-hypervascular lesions in patients with chronic liver disease?

Recommendation

Follow-up using EOB-MRI (or dynamic CT) is strongly recommended.

Recommendation strength: 1, strength of evidence: moderate (B), agreement rate: 100% (11/11)

Background

With contrast-enhanced imaging in patients with chronic liver disease, the detection of nodules that do not exhibit hypervascularity and lack normal hepatocellular function on perflubutane contrast-enhanced ultrasound or EOB-MRI increases in the arterial phase, and these nodules are known to include HCC precursor lesions.

There have been many reports of the hypervascularization (malignant transformation) of non-hypervascular lesions since the retrospective investigation by Kumada et al. in 2011.[1)] However, the names used for these lesions are not established and vary depending on the article. Those that show low signal intensity in the hepatobiliary phase of EOB-MRI are readily detected, and the hepatobiliary phase imaging mechanism suggests a risk of malignant transformation. Consequently, the term “hepatobiliary phase hypointense nodule without arterial phase hyperenhancement” was proposed by the Liver Imaging Reporting and Data System (LI-RADS) HBA Working Group.[2)] In Japan, lesions that do not show early enhancement are also called “hypovascular lesions.” They include a considerable number of lesions that are in the process of multistage cancer development and are on the borderline between hypervascularity and hypovascularity. In view of the fact that early enhancement detection performance varies depending on the modality, the term “non-hypervascular lesions” is considered appropriate.

Explanation

1. Is EOB-MRI recommended for diagnosing non-hypervascular lesions in patients with chronic liver disease?

Among non-hypervascular nodules that show low signal intensity in the hepatobiliary phase of EOB-MRI, 44% are advanced HCC, 20% early HCC, 27.5% high-grade dysplastic nodules, and 8% low-grade dysplastic nodules and regenerative nodules.[3] Although there is selection bias, it should be noted that this includes advanced HCC, which obviously should be considered a target for treatment.

Many studies of diagnostic performance in non-hypervascular nodules, which show low signal intensity in the hepatobiliary phase of EOB-MRI, examined nodules that were detectable in the hepatobiliary phase, and there is insufficient evidence concerning diagnostic performance in nodules that could not be detected in the hepatobiliary phase. Of the non-hypervascular nodules detected in the hepatobiliary phase of EOB-MRI, 35% are also detectable by contrast-enhanced CT.[4] Because the rate of detection of non-hypervascular nodules with contrast-enhanced CT is relatively low, EOB-MRI is useful for detecting such nodules.

The diagnostic performance of each modality in HCC (≤ 2 cm in size) was found to be 53% for contrast-enhanced CT, 68% for contrast-enhanced ultrasound, 77% for EOB-MRI, and 88% for CT angiography.[5] In some cases, nodules are diagnosed as non-hypervascular using 1 modality, but visualized as hypervascular when re-examined using another modality. For example, 33% of HCC nodules determined to be non-hypervascular based on CT and MRI were diagnosed as hypervascular by contrast-enhanced ultrasound.[6] Consequently, it is preferable for non-hypervascularity to be diagnosed using multiple modalities.

The significance of detecting non-hypervascular nodules using EOB-MRI and its contribution to prognosis remain unclear based on the above findings. However, EOB-MRI tends to be an excellent modality for detecting non-hypervascular nodules, and its use in mapping hepatocellular lesions in the liver in patients with chronic liver disease is therefore recommended. It should be noted that non-hypervascular nodules that show low signal intensity in the hepatobiliary phase of EOB-MRI include not only early HCC and dysplastic nodules that subsequently undergo hypervascularization, but also advanced HCC. Differentiation needs to proceed carefully by also considering the findings obtained with other modalities.

2. Is periodic follow-up recommended for diagnosing non-hypervascular lesions in patients with chronic liver disease?

Periodic imaging procedures to screen for HCC are recommended for patients with chronic liver disease. It is therefore difficult to imagine that a non-hypervascular lesion found in the liver of a patient with chronic liver disease would be neglected and follow-up not performed. In addition, no RCTs have been identified that examined whether biopsy and/or treatment should be performed after a non-hypervascular lesion is discovered and of the effectiveness of biopsy and treatment in such cases. Consequently, the consensus views of experts on the guidelines and related matters and the observational studies that have

examined the frequency with which non-hypervascular lesions are hypervascularized (malignant transformation) and the factors involved in this process are summarized below.

First, the results of a meta-analysis by Suh et al. that summarized prospective and retrospective, observational studies of the frequency with which non-hypervascular lesions are hypervascularized (malignant transformation) showed that the rate of hypervascularization of non-hypervascular lesions detected in the hepatobiliary phase of EOB-MRI was 18% at 1 year, 25% at 2 years, and 30% at 3 years.[7)]

With regard to the strategy for addressing non-hypervascular lesions, a review of the literature on liver biopsy[8)] noted that, although guidelines such as the 2011 guidelines of the American Association for the Study of Liver Diseases (AASLD) recommended biopsy for hepatic lesions that do not show typical contrast enhancement in procedures such as CT and MRI (secondary source 2),[9)] the indications for biopsy are being reduced in recent guidelines in view of its invasiveness and the possibility of sampling error. The 2017 AASLD guidelines (secondary source 3) state that, although 1 to 2-cm nodules in patients with liver cirrhosis that do not show typical contrast enhancement are unlikely to be HCC, either a second imaging examination or follow-up needs to be performed for such nodules.

Nearly all of the reports concerned with the factors related to hypervascularization have been reports of retrospective, observational studies. Two of the articles in the relevant literature have described prospective assessments. The primary objective of these studies was to examine the added diagnostic value of diffusion-weighted imaging[10)] and contrast-enhanced ultrasound,[6)] as indicated in the previous section.

The previously mentioned meta-analysis by Suh et al.[7)] found that the factor most strongly related to hypervascularization was size (≥ 9 to 10 mm) when detected.

Examination of each report showed that they included a mix of investigations of non-hypervascular lesions as a whole and investigations in which lesions were further limited according to the underlying liver disease and MRI signal pattern. In broad terms, factors that have been found to increase risk are lesion size,[11-13)] high signal intensity on T1-weighted and diffusion-weighted images,[10, 13)] past history of HCC,[11, 14)] and high signal intensity on T1-weighted images.[14)] High signal intensity in the hepatobiliary phase of EOB-MRI was reported to be a risk-reducing factor.[12)] Three of these articles are summarized below.

An examination of 633 non-hypervascular lesions that showed high signal intensity in the hepatobiliary phase found that the frequency of hypervascularization was lower than indicated in previous reports.[14)] Hypervascularization was seen in 4% of patients (95% CI, 1.74% to 9.55%) and 0.4% of lesions (95% CI, 0.20% to 0.95%) in 1 year. Multivariate analysis showed the only hypervascularization-related factor to be initial lesion size (continuous value). With the lesions categorized as < 10 mm or ≥ 10 mm in size, a significant difference was seen in non-hypervascularization time ($p = 0.0022$). The 1-year cumulative hypervascularization rate was 0.10% (95% CI, 0.02% to 0.57%) for lesions < 10 mm and 1.31% (95% CI, 0.56% to 3.07%) for lesions ≥ 10 mm.

In a retrospective study of 114 non-hypervascular lesions in 60 patients that did not show high signal intensity on T2-weighted images,[11)] 27 lesions in 21 patients transformed to HCC during the observation period (median duration of observation, 503 days; range, 203 to 1,521 days), and 87 lesions in 47 patients

did not transform to HCC (median duration of observation, 949 days; range, 103 to 254 days). High signal intensity on T1-weighted images [hazard ratio (HR), 2.693; 95% CI, 1.157 to 6.264; p = 0.021] and a past history of HCC (HR = 2.64, p = 0.021) were associated with hypervascularization.

A retrospective investigation by Yang et al. examined 222 non-hypervascular lesions in 97 patients that showed low signal intensity in the hepatobiliary phase of EOB-MRI and did not show high signal intensity on T2-weighted images.[14] A multivariate analysis showed significant relationships for past history of HCC at new onset (HR, 3.493; 95% CI, 1.335 to 9.138; p = 0.011), high signal intensity on T1-weighted images (HR, 2.778; 95% CI, 1.172 to 6.589; p = 0.020), and high signal intensity on diffusion-weighted images (HR, 19.917; 95% CI, 7.050 to 56.271; p = 0.001). In an ROC analysis, the cutoff value for the growth rate (reciprocal of volume-doubling time) was 0.72×10^{-3}/day.

To examine how long a follow-up is necessary and how long the intervals between tests should be, the observation durations in the articles cited here were summarized. The median durations for the 16 articles included in the meta-analysis by Suh et al.[7] ranged from 186 to 886 days, and the measures of central tendency (median for 7 articles, mean for 3 articles) for the duration of observation of non-hypervascular lesions in the other original articles ranged from 167 to 997 days. In the above-mentioned investigation of non-hypervascular lesions that did not show high signal intensity on T2-weighted images,[14] the lesions were observed for a mean of 997 days (range, 137 to 1,804 days). The authors, Yang et al., stated that only 3 lesions were hypervascularized over 3 years, and that all 3 had hypervascularization-related factors. They therefore surmised that, if lesions that lack these factors were observed for 3 years, their risk of malignant transformation would be low.

There is little evidence concerning the optimal intervals for imaging procedures in the follow-up of non-hypervascular lesions, and this subject is not mentioned in the AASLD guidelines (secondary source 2). Japan’s guidelines for the diagnosis and treatment of liver cancer recommend that follow-up using ultrasound or contrast-enhanced CT/MRI be performed every 3 months (secondary source 1).

Supplementary information appears occasionally in the form of reports on the prognosis of patients with non-hypervascular lesions and the risk of HCC occurring at other locations in the liver. The relevant literature is as follows.

In a retrospective investigation by Gyoda et al. of patients who underwent liver resection, 52.2% of non-hypervascular HCC had progressed to classical HCC in year 3 after initial liver resection. In addition, no significant differences were seen after 1 and 3 years between the 36 patients in the group with non-hypervascular nodules and the 75 patients in the group without such nodules with respect to the cumulative incidence rates for classical HCC at different locations from non-hypervascular nodules and non-hypervascular nodules (Group with non-hypervascular nodules: classical HCC, 32.8% at 1 year and 67.1% at 3 years; non-hypervascular nodules, 14.3% at 1 year and 27.5% at 3 years. Group without non-hypervascular nodules: classical HCC, 19.9% at 1 year and 43.4% at 3 years; non-hypervascular nodules, 4.8% at 1 year and 18.1% at 3 years. Classical HCC, p = 0.097; non-hypervascular nodules, p = 0.280). It was concluded that whether non-hypervascular lesions should be resected at the same time as the

primary tumor was unclear based on these findings. Next, no significant differences were seen between HCV-positive patients treated with direct-acting antivirals (DAAs) and those not treated with DAAs with respect to the cumulative hypervascularization rate of non-hypervascular lesions at 12, 18, or 24 months after initial resection. The cumulative hypervascularization rates were 11.8%, 24.2%, and 25.2%, respectively, for the DAA-treated patients and 9.1%, 15.2%, and 24.9% for the DAA-untreated patients ($p = 0.617$).[15] Because the study subjects were patients with relatively advanced disease, selection bias is a concern.

To summarize the above findings, because the 3-year cumulative hypervascularization rate of non-hypervascular lesions was 30%, such lesions should not be neglected. However, clear evidence is lacking with regard to whether non-hypervascular lesions ought to be biopsied and treated. The view of specialists in recent years has been that performing a biopsy when a lesion is first detected is not desirable when its invasiveness is weighed against the prospective benefits, and that either an additional second imaging procedure or follow-up imaging procedure should be performed.

Search keywords and secondary sources

PubMed was searched using the following keywords: hypovascular, hypervascular, hyperenhanced, without early enhancement, without arterial enhancement, lack hypervascular, ultrasonography, ultrasound, hepatitis, liver, liver disease, chronic, and cirrhosis. Of the 28 articles extracted, 12 were cited. In addition, 1 article published after the search and 4 second-hand citations were cited, for a total of 17 articles cited.

In addition, the following were referenced as secondary sources.

1) JSH HCC Guidelines 2017, Revised Version
2) Bruix J et al: Evidence-based diagnosis, staging, and treatment of patients with hepatocellular carcinoma. Gastroenterology 150 (4): 835-853, 2016
3) Heimbach JK et al: AASLD guidelines for the treatment of hepatocellular carcinoma. Hepatology 67 (1): 358-380, 2018

References

1) Kumada T et al: Evolution of hypointense hepatocellular nodules observed only in the hepatobiliary phase of gadoxetate disodium-enhanced MRI. AJR Am J Roentgenol 197 (1): 58-63, 2011
2) Motosugi U et al: Recommendation for terminology: nodules without arterial phase hyperenhancement and with hepatobiliary phase hypointensity in chronic liver disease. J Magn Reson Imaging 48 (5): 1169-1171, 2018
3) Joo I et al: Radiologic-pathologic correlation of hepatobiliary phase hypointense nodules without arterial phase hyperenhancement at gadoxetic acid-enhanced MRI: a multicenter study. Radiology 296 (2): 335-345, 2020
4) Gyoda Y et al: Significance of hypovascular lesions on dynamic computed tomography and/or gadolinium ethoxybenzyl diethylenetriamine pentaacetic acid-enhanced magnetic resonance imaging in patients with hepatocellular carcinoma. J Gastroenterol Hepatol 34 (7): 1242-12348, 2019
5) Mita K et al: Diagnostic sensitivity of imaging modalities for hepatocellular carcinoma smaller than 2 cm. World J Gastroenterol 16 (33): 4187-4192, 2010
6) Kang HJ et al: Additional value of contrast-enhanced ultrasound (CEUS) on arterial phase non-hyperenhancement observations (＞/＝2 cm) of CT/MRI for high-risk patients: focusing on the CT/MRI LI-RADS categories LR-3 and LR-4. Abdom Radiol (NY) 45 (1): 55-63, 2020
7) Suh CH et al: Hypervascular transformation of hypovascular hypointense nodules in the hepatobiliary phase of gadoxetic acid-enhanced MRI: a systematic review and meta-analysis. AJR Am J Roentgenol 209 (4): 781-789, 2017
8) Russo FP et al: When and how should we perform a biopsy for HCC in patients with liver cirrhosis in 2018?: a review. Dig Liver Dis 50 (7): 640-646, 2018

9) Bruix J et al: Management of hepatocellular carcinoma: an update. Hepatology 53 (3): 1020-2, 2011
10) Briani C et al: Non-hypervascular hypointense nodules at gadoxetic acid MRI: hepatocellular carcinoma risk assessment with emphasis on the role of diffusion-weighted imaging. J Gastrointest Cancer 49 (3): 302-310, 2018
11) Kim YS et al: Hypovascular hypointense nodules on hepatobiliary phase without T2 hyperintensity on gadoxetic acid-enhanced MR images in patients with chronic liver disease: long-term outcomes and risk factors for hypervascular transformation. Eur Radiol 26 (10): 3728-3736, 2016
12) Sano K et al: Outcome of hypovascular hepatic nodules with positive uptake of gadoxetic acid in patients with cirrhosis. Eur Radiol 27 (2): 518-525, 2017
13) Cho YK et al: Non-hypervascular hypointense nodules on hepatocyte phase gadoxetic acid-enhanced MR images: transformation of MR hepatobiliary hypointense nodules into hypervascular hepatocellular carcinomas. Gut Liver 12 (1): 79-85, 2018
14) Yang HJ et al: Hypovascular hypointense nodules in hepatobiliary phase without T2 hyperintensity: long-term outcomes and added value of DWI in predicting hypervascular transformation. Clin Imaging 50: 123-129, 2018
15) Toyoda H et al: The impact of HCV eradication by direct-acting antivirals on the transition of precancerous hepatic nodules to HCC: a prospective observational study. Liver Int 39 (3): 448-454, 2019

BQ 37 Which imaging findings are used to diagnose classical (hypervascular) HCC?

Statement

Typical imaging findings for classical (hypervascular) HCC are the following.

Dynamic contrast-enhanced CT: early enhancement in the arterial-dominant phase and washout from the portal venous phase to the equilibrium phase. EOB-MRI: early enhancement in the arterial-dominant phase and washout in the portal venous-dominant phase, low signal intensity from the transitional phase to the hepatobiliary phase.

Perflubutane contrast-enhanced ultrasound: hyperechoic in the arterial-dominant phase, washout in the portal venous-dominant phase, hypoechoic in the Kupffer phase.

Other findings specific to HCC include a capsular structure, mosaic structure, and tumor thrombus. Corona enhancement in the late phase of CT hepatic arteriography (CTHA) is also useful for diagnosis.

Background

In the past, HCC detected in the clinical setting was often advanced HCC (mainly moderately differentiated) that exhibited the properties of hypervascularity on imaging. With advances in diagnostic imaging, small HCCs that did not exhibit hypervascularity (mainly highly differentiated) also came to be detected. To distinguish between these types, the conventional and typical hypervascular HCC is called classical HCC. In the diagnostic imaging of classical (hypervascular) HCC, it is important to evaluate tumor blood flow status by contrast-enhanced CT, MRI, or ultrasonography, and combining this with other findings can provide extremely high diagnostic performance.

Explanation

This BQ was created by consolidating CQ75 (Which tests are useful for diagnosing classical (hypervascular) HCC?) and CQ76 [Are CT during hepatic arteriography (CTHA), CT during arterial portography (CTAP), and angiography recommended as tests to be performed before HCC resection?] from the 2016 edition of these guidelines. Perflubutane (Sonazoid®) contrast-enhanced ultrasound, dynamic contrast-enhanced CT, and Gd-EOB-DTPA (EOB, Primovist®) contrast-enhanced MRI (EOB-MRI) are all useful for diagnosing classical (hypervascular) HCC, and their use is strongly recommended. Of these modalities, EOB-MRI is considered to provide high detection performance in detecting small lesions.[1-6] Because these imaging procedures are already standard approaches, the question was changed from a CQ to a BQ, and the matter of which kinds of imaging findings are important is discussed here.

There are 2 forms of carcinogenic processes for HCC, *de novo* carcinogenesis and multistage carcinogenesis. In the latter case, changes in the status of blood flow in the lesion continually occur during the malignant transformation process.[7-9] As dysplastic nodules become early HCC, portal vein blood flow,

which provides the cells with nutrients, decreases, and it nearly disappears in highly differentiated to moderately differentiated HCC. On the other hand, arterial blood flow increases in highly differentiated to moderately differentiated HCC. Classical (hypervascular) HCC refers to moderately differentiated HCC in which portal vein blood flow has disappeared, and arterial blood flow has increased. Early enhancement on CT or MRI reflects this increase in arterial blood flow. In multistage carcinogenesis, changes also occur in outflow veins. If a peritumoral pseudocapsule forms, the portal vein branches in the pseudocapsule become outflow vessels. Due to flow of contrast medium from the portal vein branches to the surrounding liver parenchyma, strong enhancement (corona enhancement) of the liver parenchyma surrounding the nodule is seen in the late phase of CTHA,[7)] as is washout on CT or MRI. Early enhancement in the arterial-dominant phase and washout after the portal venous-dominant phase on dynamic contrast-enhanced CT, EOB-MRI, or perflubutane contrast-enhanced ultrasound are therefore typical imaging findings in classical (hypervascular) HCC. In addition, corona enhancement on dynamic contrast-enhanced CT/MRI or CTHA is useful for diagnosis.[7, 10)]

The early enhancement on dynamic contrast-enhanced CT/MRI mentioned above refers to the phenomenon whereby the increase in attenuation (or signal intensity) of the tumor is greater than that of the background liver parenchyma. Findings in which the tumors show lower density or signal intensity than the surrounding liver parenchyma before contrast enhancement and iso-density or iso-intensity in the arterial dominant phase are also treated as early enhancement. Imaging must therefore be performed before contrast-enhanced imaging to evaluate early enhancement. Although this is the general view of early enhancement in Japan, it should be noted that, under the LI-RADS system of the American College of Radiology, higher attenuation (higher signal intensity) compared with the liver parenchyma in the arterial phase is defined as arterial phase hyperenhancement (APHE), regardless of the attenuation (signal intensity) before contrast-enhanced imaging. On the other hand, washout refers to relative hypodensity in a nodule compared with the surrounding liver parenchyma in phases such as the portal venous-dominant phase.

In addition, to evaluate early tumor enhancement on dynamic contrast-enhanced CT/MRI, arterial-dominant-phase imaging must be performed with appropriate timing. If it is performed too early, early enhancement cannot be observed because sufficient contrast medium will not have reached the tumor. If early enhancement is not seen even though HCC is suspected, the timing of the imaging should be examined to determine whether it was appropriate.

EOB-MRI cannot evaluate tumor blood flow during the equilibrium phase because the timing of the equilibrium phase of CT or MRI using an extracellular contrast medium corresponds to the transitional phase in EOB-MRI. If washout cannot be verified in the portal venous-dominant phase, a modality such as dynamic contrast-enhanced MRI using an extracellular gadolinium contrast medium or CT is added as necessary.

If rigorous evaluation of the presence or absence of early enhancement is required clinically, CTHA, which can provide the most accurate blood flow information, can be considered. CTHA makes it possible

to evaluate not only early enhancement, but also corona enhancement. Corona enhancement is enhancement seen around a tumor in the late phase of CTHA. With CTHA, it is visualized in nearly all patients with HCC and is very useful for diagnosing microscopic HCC. However, CTHA requires selective catheter insertion into the hepatic artery, making it more invasive than other tests. Consequently, opportunities to perform CTHA for diagnosis alone are limited.

Characteristic gross pathological findings in HCC include capsule formation, an internal mosaic structure, and tumor thrombus of portal and hepatic veins. These gross pathological findings can also be observed by imaging, making such imaging findings useful in the qualitative diagnosis of HCC.

Search keywords and secondary sources

PubMed was searched using the following keywords: hepatocellular carcinoma, sensitivity, specificity, contrast-enhanced, Sonazoid, US, multiphasic, MDCT, CT, gadoxetate, gadoxetic, Gd-EOB-DTPA, Primovist, MR, magnetic resonance, CTHA, CT, and hepatic arteriography.

The following were also referenced as secondary sources.

1) JSH HCC Guidelines 2017
2) Claude B et al: Liver Imaging Reporting and Data System (LI-RADS). American College of Radiology, 2017

References

1) Liu X et al: Gadoxetic acid disodium-enhanced magnetic resonance imaging for the detection of hepatocellular carcinoma: a meta-analysis. PloS One 8 (8): e70896, 2013
2) Chen L et al: Magnetic resonance imaging with gadoxetic acid disodium for the detection of hepatocellular carcinoma: a meta-analysis of 18 studies. Acad Radiol 21 (12): 1603-1613, 2014
3) Junqiang L et al: Gadoxetic acid disodium (Gd-EOBDTPA)-enhanced magnetic resonance imaging for the detection of hepatocellular carcinoma: a meta-analysis. J Magn Reson Imaging 39 (5): 1079-1087, 2014
4) Kierans AS et al: The diagnostic performance of dynamic contrast-enhanced MR imaging for detection of small hepatocellular carcinoma measuring Up to 2 cm: a meta-analysis. Radiology 278 (1): 82-94, 2016
5) Onishi H et al: Hypervascular hepatocellular carcinomas: detection with gadoxetate disodium-enhanced MR imaging and multiphasic multidetector CT. Eur Radiol 22 (4): 845-854, 2012
6) Alaboudy A et al: Usefulness of combination of imaging modalities in the diagnosis of hepatocellular carcinoma using Sonazoid®-enhanced ultrasound, gadolinium diethylene-triamine-pentaacetic acid-enhanced magnetic resonance imaging, and contrast-enhanced computed tomography. Oncology 81 (Suppl 1): 66-72, 2011
7) Ueda K et al: Hypervascular hepatocellular carcinoma: evaluation of hemodynamics with dynamic CT during hepatic arteriography. Radiology 206 (1): 161-166, 1998
8) Ueda K et al: Vascular supply in adenomatous hyperplasia of the liver and hepatocellular carcinoma: a morphometric study. Hum Pathol 23 (6): 619-626, 1992
9) Kitao A et al: Hepatocarcinogenesis: multistep changes of drainage vessels at CT during arterial portography and hepati–arteriography--radiologic-pathologic correlation. Radiology 252 (2): 605-614, 2009
10) Goshima S et al: Gadoxetic acid-enhanced high temporal-resolution hepatic arterial-phase imaging with view-sharing technique: Impact on the LI-RADS category. Eur J Radiol 94: 167-173, 2017

BQ 38 Which imaging examinations are recommended for diagnosing liver tumors in patients with decreased kidney and liver function?

Statement

Non-contrast-enhanced MRI tests, including diffusion-weighted imaging, and ultrasonography, including perflubutane contrast-enhanced imaging, are useful and can be performed safely and are recommended in patients with decreased kidney and liver function. In patients with decreased kidney function, the types of contrast-enhanced CT or MRI that can be considered are EOB-MRI in patients with an estimated glomerular filtration rate (eGFR) of 30 to 60 mL/min/1.73 m^2 and SPIO-contrast-enhanced MRI in those with an eGFR of < 30 mL/min/1.73 m^2. In dialysis patients, SPIO-contrast-enhanced MRI and contrast-enhanced CT can be considered.

There has been insufficient examination of the appropriate selection of tests and contrast media for contrast-enhanced CT/MRI in patients with decreased liver function corresponding to Child-Pugh class C.

Background

The use of iodine and gadolinium contrast media is restricted in patients with decreased kidney function, and enhancement with Gd-EOB-DTPA (EOB, Primovist®) and SPIO (Resovist®) decreases in patients with decreased liver function. Consequently, restrictions on testing and decreased diagnostic performance are concerns in patients with decreased kidney or liver function.

Explanation

The ultrasound contrast medium perflubutane (Sonazoid®)[1)] and the liver-specific MRI contrast medium SPIO[2, 3)] do not affect kidney function and are not known to have increased adverse reactions caused by decreased kidney function. The tests that use these media can therefore be performed normally in patients with decreased kidney function.

Iodine contrast medium administration increases the risk of contrast-induced nephropathy (CIN) in patients with decreased kidney function and an eGFR < 30 mL/min/1.73 m^2, making it difficult to perform contrast-enhanced CT in such patients. With the addition of risk factors such as advanced age and diabetes mellitus associated with chronic kidney disease (CKD), the risk increases even with an eGFR ≥ 30 mL/min/1.73 m^2.

The risk of nephrogenic systemic fibrosis (NSF) increases with the use of gadolinium contrast media in patients with decreased kidney function. Consequently, extracellular gadolinium contrast media and Gd-EOB-DTPA are generally not administered to dialysis patients, patients with CKD and an eGFR < 30 mL/min/1.73 m^2, and patients with acute renal failure. If, after the benefits and risks have been examined, it is concluded that a gadolinium contrast medium must be used, the use of gadodiamide (Omniscan®) or gadopentetate dimeglumine (Magnevist®), for which there have been many reports of NSF, is avoided.

Because Gd-EOB-DTPA is excreted from the liver, as well as the kidneys, it is sometimes thought that it may be superior to an extracellular gadolinium contrast medium. However, Gd-EOB-DTPA clearance actually decreases significantly in dialysis patients, which is known to reduce enhancement of the liver parenchyma.[4] Its use in dialysis patients is therefore not recommended.

There has been insufficient investigation into the selection of the appropriate contrast medium and test for a given eGFR when considering contrast-enhanced CT or MRI in patients with decreased kidney function. Consequently, the recommendations in these guidelines are limited to provisional recommendations. With an eGFR of 30 to 60 mL/min/1.73 m^2, the risk of NSF is not particularly high, and EOB-MRI, which provides high diagnostic performance, is therefore recommended. Because the risk of NSF increases with an eGFR < 30 mL/min/1.73 m^2, there is some doubt about whether to recommend EOB/Primovist® contrast-enhanced MRI or Resovist® contrast-enhanced MRI. However, the package insert for EOB/Primovist® states that administration of the product is to be avoided in such patients, and it is likely to be administered frequently. In light of these considerations, Resovist® contrast-enhanced MRI is recommended in these patients. For dialysis patients, it is recommended that gadolinium contrast media be avoided and that Resovist® contrast-enhanced MRI or contrast-enhanced CT be selected, depending on the circumstances of the facility.

In patients with decreased liver function, enhancement in the hepatobiliary phase of Gd-EOB-DTPA decreases,[5-7] and enhancement in what is referred to as the Kupffer phase of SPIO imaging also decreases.[8] As a result, the worse liver function is based on Child-Pugh class, the greater the decrease in the HCC diagnostic performance of GD-EOB-DTPA.[9] With Child-Pugh class B or C, the contrast between liver parenchyma and HCC has been found to be better with an extracellular gadolinium contrast medium in the equilibrium phase than with Gd-EOB-DTPA in the hepatobiliary phase.[10] There has been insufficient examination of the appropriate selection of contrast-enhanced CT or contrast-enhanced MRI in patients with decreased liver function corresponding to Child-Pugh class C.

Although it cannot outperform contrast-enhanced MRI, diffusion-weighted imaging has been shown to be consistently useful.[11] It may be more important than usual in patients with decreased kidney and liver function. However, its diagnostic performance in HCC decreases in patients with decreased liver function.[9]

Search keywords and secondary sources

PubMed was searched using the following keywords: Pugh, Child score, liver function, ICG, liver failure, contrast media, EOB, gadolinium, SPIO, superparamagnetic iron, iodinated contrast, iodine contrast, Sonazoid, diagnostic imaging, MRI, magnetic resonance, tomography, X-ray computed, computed tomography, computed tomographic, ultrasonography, liver, chronic kidney disease, renal impairment, renal function, diffusion-weighted, DWI, carcinoma, hepatocellular, hepatocellular carcinoma, and hepatocellular carcinomas.

The period searched was through June 2019.

In addition, the following were referenced as secondary sources.

1) JSH HCC Guidelines 2017, Revised Version
2) Japanese Society of Nephrology, Japan Radiological Society, Japanese Circulation Society, Ed.: 2018 Guidelines for Using Iodine Contrast Media in Patients with [Nephropathy]. https://minds.jcqhc.or.jp/n/med/4/med0133/G0001100, 2018
3) Japan Radiological Society, Japanese Society of Nephrology, Ed.: Guidelines for Using Gadolinium Contrast Media in Patients with Nephropathy (2nd edition). Joint Panel on NSF and Gadolinium Contrast Media Use, 2009.

References

1) Binder T et al: NC100100, a new echo contrast agent for the assessment of myoca–ial perfusion--safety and comparison with technetium-99m sestamibi single-photon emission computed tomography in a randomized multicenter study. Clin Cardiol 22: 273-282, 1999
2) Kopp AF et al: MR imaging of the liver with Resovist: safety, efficacy, and pharmacodynamic properties. Radiology 204: 749-756, 1997
3) Reimer P, Balzer T: Ferucarbotran (Resovist): a new clinically approved RES-specific contrast agent for contrast-enhanced MRI of the liver: properties, clinical development, and applications. Eur Radiol 13: 1266-1276, 2003
4) Gschwend S et al.: Pharmacokinetics and imaging properties of Gd-EOB-DTPA in patients with hepatic and renal impairment. Invest Radiol 46: 556-566, 2011
5) Motosugi U et al: Liver parenchymal enhancement of hepatocyte-phase images in Gd-EOB-DTPA-enhanced MR imaging: which biological markers of the liver function affect the enhancement? J Magn Reson Imaging 30: 1042-1046, 2009
6) Katsube T et al: Estimation of liver function using T1 mapping on Gd-EOB-DTPA-enhanced magnetic resonance imaging. Invest Radiol 46: 277-283, 2011
7) Utsunomiya T et al: Possible utility of MRI using Gd-EOB-DTPA for estimating liver functional reserve. J Gastroenterol 47: 470-476, 2012
8) Chung YE et al: Quantification of superparamagnetic iron oxide-mediated signal intensity change in patients with liver cirrhosis using T2 and T2＊ mapping: a preliminary report. J Magn Reson Imaging 31: 1379-1386, 2010
9) Kim AY et al: Detection of hepatocellular carcinoma in gadoxetic acid-enhanced MRI and diffusion-weighted MRI with respect to the severity of liver cirrhosis. Acta Radiol 53: 830-838, 2012
10) Kim SY et al: Comparison of hepatocellular carcinoma conspicuity on hepatobiliary phase images with gadoxetate disodium vs. delayed phase images with extracellular cellular contrast agent. Abdom Radiol (NY) 41: 1522-1531, 2016
11) Park MJ et al: Small hepatocellular carcinomas: improved sensitivity by combining gadoxetic acid-enhanced and diffusion-weighted MR imaging patterns. Radiology 264: 761-770, 2012

BQ 39 When is the use of extracellular gadolinium contrast media and Gd-EOB-DTPA recommended for contrast-enhanced MRI of liver tumors?

Statement

The use of extracellular gadolinium contrast media and Gd-EOB-DTPA is recommended for contrast-enhanced MRI of liver tumors in the cases indicated in the Explanation section.

Background

The preparations currently used in Japan for contrast-enhanced MRI of liver tumors are extracellular gadolinium contrast media, liver-specific contrast media (Gd-EOB-DTPA), and superparamagnetic iron oxide (SPIO) contrast media. Although there has been debate regarding the roles of each of these media in planning and implementing testing in the clinical setting, this has not been examined in RCTs, except in certain conditions, and it has not been addressed in the various previous guidelines. This BQ discusses the matters that ought to be considered in selecting an extracellular gadolinium contrast medium or Gd-EOB-DTPA from among the preparations that can be used in Japan, based on the currently available information and the opinions of specialists.

Explanation

1. Conditions and circumstances for which an extracellular gadolinium contrast medium is recommended more strongly than Gd-EOB-DTPA

An extracellular gadolinium contrast medium is recommended instead of Gd-EOB-DTPA for the following conditions and circumstances.

① The patient has markedly impaired liver function or severe liver cirrhosis

EOB-MRI is unlikely to produce adequate contrast enhancement of the liver parenchyma in the hepatobiliary phase if a condition such as hyperbilirubinemia or severe siderosis in the liver parenchyma is seen. In such cases, use of an extracellular gadolinium contrast medium is considered while taking kidney function into account.[1)]

② The main purpose is diagnosing a hepatic hemangioma

In hepatic hemangioma, pooling is obscure in the transitional and hepatobiliary phases of EOB-MRI, resulting in a tendency for pseudo-washout findings. When hepatic hemangioma needs to be rigorously distinguished from other liver tumors, an extracellular gadolinium contrast medium is recommended. Another concern is that with EOB-MRI, findings of persistent enhancement are obscured due to fibrosis in

conditions such as intrahepatic cholangiocarcinoma. Consequently, an extracellular gadolinium contrast medium is considered when such findings may be useful in diagnosis.[2)]

③ The main purpose is confirming arterial phase enhancement

The gadolinium concentration in Gd-EOB-DTPA is approximately 1/4 that in general extracellular gadolinium contrast media. Therefore, in theory, there may be cases in which tumor enhancement in the arterial phase is indistinct with Gd-EOB-DTPA. In patients for whom evaluation of tumor enhancement in the arterial phase is clinically important, use of an extracellular gadolinium contrast medium is considered.

④ Specificity is considered more important than sensitivity in HCC diagnosis

With dynamic EOB-MRI, the enhancing capsule appearance of HCC in the portal venous and transitional phases may be indistinct due to contrast medium uptake by the liver. In addition, washout may also be seen with conditions such as hemangioma (pseudo-washout). When these findings are important clinically or for diagnostic imaging purposes, use of an extracellular gadolinium contrast medium in repeat or follow-up MRI should also be considered.[3)]

⑤ Transient dyspnea (or transient severe body movement) occurred in the arterial phase with previous EOB-MRI

Breath-holding in the arterial phase may be inadequate. In consideration of the test objectives, the use of an extracellular gadolinium contrast medium is therefore considered.

⑥ Close examination of a blood vessel or abdominal organ other than the liver is necessary

Use of an extracellular gadolinium contrast medium, which has a high gadolinium concentration, is useful in cases, such as for 3D reconstruction of the hepatic artery or portal vein. Use of an extracellular gadolinium contrast medium is also considered when taking into account differences in diagnostic accuracy for liver tumor lesions.

2. Conditions and circumstances for which Gd-EOB-DTPA is recommended more strongly than an extracellular gadolinium contrast medium

Gd-EOB-DTPA is recommended more strongly than an extracellular gadolinium contrast medium for the following conditions and circumstances.

① Diagnosing hypovascular HCC

There are many reports indicating that the use of Gd-EOB-DTPA rather than an extracellular gadolinium contrast medium ought to be considered when the objective is to detect early HCC in patients with chronic hepatitis or liver cirrhosis. However, different study results have also been reported in recent years.[4)]

② Preoperative testing for HCC

To detect microscopic HCC and intrahepatic metastases with high sensitivity, the use of Gd-EOB-DTPA for preoperative MRI in patients with HCC should be considered first.

③ To detect metachronous multiple HCC and recurrence after HCC therapy

The use of Gd-EOB-DTPA, which facilitates detection of microscopic lesions, ought to be considered to detect intrahepatic recurrence in patients who have undergone HCC resection. However, arterial phase enhancement of the site of recurrence may be useful for diagnosing recurrence after localized treatment such as radiofrequency ablation (RFA), and there is no definitive evidence regarding the comparative usefulness of the contrast media.

④ Definitive diagnosis of a pseudolesion was difficult in a previous contrast-enhanced CT or extracellular contrast-enhanced MRI test due to abnormal blood flow

Because a pseudolesion can be verified as such based on Gd-EOB-DTPA uptake, the use of Gd-EOB-DTPA in repeat testing or follow-up MRI ought to be considered.

⑤ Preoperative testing in patients with liver metastasis

Gd-EOB-DTPA enables better visibility of microscopic lesions than extracellular gadolinium contrast media and, therefore, ought to be used in preoperative MRI.

⑥ Differentiating between HCC or hepatocellular adenoma (HCA) and focal nodular hyperplasia (FNH)

In FNH, Gd-EOB-DTPA uptake is often seen in the hepatobiliary phase,[5, 6] which makes Gd-EOB-DTPA more useful than an extracellular gadolinium contrast medium for differential diagnosis.

⑦ Functional information on the biliary system needs to be obtained at the same time as information on a liver tumor

It is possible that a condition such as a biliary fistula can be definitively diagnosed based on the kinetics of Gd-EOB-DTPA, which is excreted in the bile.[7, 8] However, consideration is given to the fact that static and morphological information can also be obtained by MRCP when an extracellular gadolinium contrast medium is used.

Although the advantages of both contrast media are indicated above, there are also reports that describe using both in the same test to optimize these advantages. However, no improvement in diagnostic performance in liver malignancies was seen when Gd-EOB-DTPA was additionally administered after administration of an extracellular contrast medium,[7] and this procedure is not covered by insurance. It is therefore not recommended.

Search keywords and secondary sources

PubMed was searched using the keywords extracellular, hepatobiliary, and magnetic resonance, with the conditions ‘adult’ and ‘human’ specified. The Ichushi and Cochrane Library databases were searched using equivalent keywords. The period searched was through June 2019; hits were obtained for 99 articles. Of these, 15 articles that discussed the different roles of these contrast media in liver tumor diagnosis were referenced.

References

1) Kim SY et al: Comparison of hepatocellular carcinoma conspicuity on hepatobiliary phase images with gadoxetate disodium vs. delayed phase images with extracellular cellular contrast agent. Abdom Radiol 41 (8): 1522-1531, 2016
2) Donato H et al: Liver MRI: from basic protocol to advanced techniques. Eur J Radiol 93: 30-39, 2017
3) Santillan C et al: LI-RADS major features: CT, MRI with extracellular agents, and MRI with hepatobiliary agents. Abdom Radiol (NY) 43 (1): 75-81, 2018
4) Min JH et al: Prospective intraindividual comparison of magnetic resonance imaging with gadoxetic acid and extracellular contrast for diagnosis of hepatocellular carcinomas using the liver imaging reporting and data system. Hepatology 68 (6): 2254-2266, 2018
5) Roux M et al: Differentiating focal nodular hyperplasia from hepatocellular adenoma: Is hepatobiliary phase MRI (HBP-MRI) using linear gadolinium chelates always useful? Abdom Radiol 43 (7): 1670-1681, 2018
6) Tselikas L et al: Impact of hepatobiliary phase liver MRI versus contrast-enhanced ultrasound after an inconclusive extracellular gadolinium-based contrast-enhanced MRI for the diagnosis of benign hepatocellular tumors. Abdom Radiol 42 (3): 825-832, 2017
7) Pahade JK et al: Is there an added value of a hepatobiliary phase with gadoxetate disodium following conventional MRI with an extracellular gadolinium agent in a single imaging session for detection of primary hepatic malignancies? Abdom Radiol 41 (7): 1270-1284, 2016
8) Boraschi P et al: Gadoxetate disodium–enhanced MR cholangiography for evaluation of biliary-enteric anastomoses: added value beyond conventional T2-weighted images. AJR Am J Roentgenol 213 (3): W123-W133, 2019

CQ 13 What are the circumstances in which screening for extrahepatic metastasis of HCC is recommended, and when it is implemented, what are the recommended target organs and imaging examinations?

Recommendation

In patients positive for risk factors for extrahepatic metastasis of HCC (tumor occlusion of portal vein; AFP, > 200 ng/mL; PIVKA-II, ≥ 300 mAU/mL; platelet count, ≤ $1.3 \times 10^5/\mu L$; high level of primary tumor FDG accumulation; < 65 years old), CT, bone scintigraphy, and FDG-PET targeting the lungs, lymph nodes, bone, and adrenals are weakly recommended.

Recommendation strength: 2, strength of evidence: weak (C), agreement rate: 91% (10/11)

CT or MRI to screen for brain metastasis is weakly recommended for patients with an abnormal neurological examination and patients positive for pulmonary metastasis.

Recommendation strength: 2, strength of evidence: weak (C), agreement rate: 91% (10/11)

Background

The circumstances in which screening for extrahepatic metastasis is recommended when treating HCC were examined, along with the target organs and testing methods recommended.

Explanation

The treatment strategy for HCC depends on whether extrahepatic metastasis of HCC is present. If the patient is positive for extrahepatic metastasis, systemic chemotherapy is recommended; if the patient is negative, localized treatment is recommended.[1)] Whether screening for extrahepatic metastasis is necessary is determined based on whether risk factors are present.[2-6)] The lungs, lymph nodes, bone, adrenals, and brain are prioritized as target organs. The risk factors are: age < 65 years; worsening of intrahepatic lesions; tumor occlusion of the portal vein; alpha-fetoprotein (AFP), > 200 ng/mL; protein induced by vitamin K absence of antagonist-II (PIVKA-II), ≥ 300 mAU/mL; platelet count, ≤ $1.3 \times 10^5/\mu L$; and a high level of FDG accumulation in the primary tumor.[2-6)] The frequency of metastasis by metastasis destination is 6% to 29% for the lungs, 5% to 20% for the lymph nodes, 2% to 10% for bone, 1% to 10% for the adrenals, and 0.2% to 0.6% for the brain.[2-5)] The frequency of extrahepatic metastasis at new onset is 1.0% to 2.3%[4, 7)] and it increases to 2% to 24% during subsequent follow-up.[2, 3)]

The standard method used to screen for lung, lymph node, and adrenal metastases is CT. An imaging extent of chest to pelvis can detect most extrahepatic metastasis.

The standard methods used to screen for bone metastases are FDG-PET and bone scintigraphy. Although there is currently insufficient evidence of the superiority of either method, the detection sensitivity of bone scintigraphy has been reported to be somewhat lower.[8)] In addition, the detection sensitivity of FDG-PET

has been reported to be high,[9, 10] and FDG-PET has been found to outperform bone scintigraphy.[11, 12] These findings indicate that, when both tests can be performed, it is appropriate to prioritize FDG-PET. Moreover, the excellent performance of FDG-PET in diagnosing extrahepatic metastasis of HCC, including bone metastasis, provides support for prioritizing FDG-PET in identifying metastasis when unexplained tumor marker elevation is seen.[13] Most HCC bone metastases are osteolytic, and the vertebral bodies account for approximately half of the metastasis destinations.[7] In addition, PET/CT can be used to evaluate the risk of compression fracture and spinal canal stenosis. Consequently, its use further increases the accuracy of metastasis screening. Although there have been case reports describing HCC bone metastasis diagnosis using PET with ^{68}Ga prostate-specific membrane antigen (^{68}Ga-PSMA, not approved in Japan), which is used to diagnose bone metastasis of prostate cancer, whether it is superior to previous tests is unknown.[14]

The standard methods of screening for brain metastasis are contrast-enhanced CT and contrast-enhanced MRI. However, the frequency of HCC brain metastasis is low,[2-5] and a high proportion of patients who are positive have concomitant pulmonary metastasis.[7] It is therefore appropriate to screen patients with symptoms, neurological signs, and pulmonary metastasis.

Search keywords and secondary sources

PubMed was searched using the following keywords: neoplasm staging, risk, neoplasm metastasis, metastases, extrahepatic, brain, cerebral, cerebrum, bone, skeletal, carcinoma, hepatocellular, hepatocellular carcinoma, hepatocellular carcinomas, extrahepatic, positron-emission tomography, bone scan, scintigraphy, and scintigram.

The following references were used as secondary sources.

1) Japan Society of Hepatology: 2009 Evidence-Based Guidelines for Liver Cancer Diagnosis and Treatment. KANEHARA & Co., LTD., 2009.
2) Japan Society of Hepatology: 2013 Evidence-Based Guidelines for Liver Cancer Diagnosis and Treatment. KANEHARA & Co., LTD., 2013.
3) JSH HCC Guidelines 2017, Revised Version, KANEHARA & Co., LTD., 2020.

References

1) Llovet JM et al: SHARP investigators study group: sorafenib in advanced hepatocellular carcinoma. N Engl J Med 359: 378-390, 2008
2) Bae HM et al: Protein induced by vitamin K absence or antagonist-II production is a strong predictive marker for extrahepatic metastases in early hepatocellular carcinoma: a prospective evaluation. BMC Cancer 11: 435, 2011
3) Senthilnathan S et al: Extrahepatic metastases occur in a minority of hepatocellular carcinoma patients treated with locoregional therapies: Analyzing patterns of progression in 285 patients. Hepatology 55: 1432-1442, 2012
4) Uchino K et al: Hepatocellular carcinoma with extrahepatic metastasis: clinical features and prognostic factors. Cancer 117: 4475-4483, 2011
5) Liver Cancer Study Group of Japan: Survey and follow-up study of primary liver cancer in Japan, Report No. 18 (2004 to 2005). Kanzo 51: 460-484, 2010.
6) Lee M et al: 18F-Fluorodeoxyglucose uptake on positron emission tomography/computed tomography is associated with metastasis and epithelial-mesenchymal transition in hepatocellular carcinoma. Clin Exp Metastasis 34: 251-260, 2017
7) Natsuizaka M et al: Clinical features of hepatocellular carcinoma with extrahepatic metastases. J Gastroenterol Hepatol 20: 1781-1787, 2005

8) Chen C et al: High false negative rate of Tc-99m MDP whole-body bone scintigraphy in detecting skeletal metastases for patients with hepatoma. J Formos Med Assoc 111: 140-146, 2012
9) Kim YK et al: Usefulness 18F-FDG positron emission tomography/computed tomography for detecting recurrence of hepatocellular carcinoma in posttransplant patients. Liver Transpl 16: 767-772, 2010
10) Sugiyama M et al: 18F-FDG PET in the detection of extrahepatic metastases from hepatocellular carcinoma. J Gastroenterol 39: 961-968, 2004
11) Lee J et al: Diagnostic value for extrahepatic metastases of hepatocellular carcinoma in positron emission tomography/computed tomography scan. World J Gastroenterol 18: 2979-2987, 2012
12) Seo H et al: 18F-FDG PET/CT in hepatocellular carcinoma: detection of bone metastasis and prediction of prognosis. Nucl Med Commun 36: 226-233, 2015
13) Lin CY et al: 18F-FDG PET or PET/CT for detecting extrahepatic metastases or recurrent hepatocellular carcinoma: a systematic review and meta-analysis. Eur J Radiol 81: 2417-2422, 2012
14) Alipour R et al: 68Ga-PSMA uptake in combined hepatocellular cholangiocarcinoma with skeletal metastases. Clin Nucl Med 42: e452-e453, 2017

FQ 4 How should the efficacy of molecularly-targeted drugs and radiation therapy for HCC be evaluated?

Statement

Although the criteria for evaluating the response to a molecularly-targeted drug for HCC include the modified Response Evaluation Criteria in Solid Tumors (mRECIST), Response Evaluation Criteria in Cancer of the Liver (RECICL), European Association for Study of the Liver (EASL), and Choi criteria, no conclusion has yet been reached regarding which criteria are the most useful for prognosis prediction. Given the current situation, the criteria considered appropriate for each facility should be selected. Moreover, the existing criteria may not be suitable for evaluating the response to radiation therapy.

Background

Liver cancer chemotherapy underwent major changes with the emergence of molecularly-targeted drugs such as sorafenib and lenvatinib. However, it has been noted that, because these drugs occasionally produce tumor necrosis without shrinking the tumor, existing criteria such as the RECIST criteria, which use only lesion size to evaluate the treatment response, would evaluate the local treatment response as poor despite the fact that tumor necrosis was seen, resulting in a discrepancy between the local treatment effect and prognosis. To improve on this point, criteria have been proposed that take into account the fact that the area of poor contrast in the tumor interior is the area of tumor necrosis, such as the mRECIST, EASL, RECICL, and Choi criteria.[1-4)]

Explanation

1. Evaluating the efficacy of molecularly-targeted drugs

Liver cancer-related guidelines recommend evaluating efficacy using criteria that take tumor necrosis into account. In the AASLD consensus statement and the EASL guidelines, combining mRECIST and RECIST version 1.1 is recommended to evaluate local treatment efficacy when systemic treatment is administered (secondary sources 1 and 2). The 2017 guidelines for the diagnosis and treatment of liver cancer recommend using criteria that take tumor necrosis into account, such as the mRECIST, RECICL, and EASL criteria (secondary source 3).

However, evidence that validates the effectiveness of these criteria in evaluating local effects is limited. In examining the relationship between the evaluation of local effects using mRECIST and overall survival, a study comparing nintedanib and sorafenib and a study comparing brivanib and placebo after sorafenib therapy found that the evaluation could be used as a surrogate parameter for overall survival.[5, 6)] Three reports of retrospective investigations that have compared the different criteria have been published.[7-9)] Although clear differences between the criteria were shown, no conclusion has yet been drawn regarding which criteria are the most useful for prognosis prediction. Given the current situation, the criteria

considered appropriate for each facility should be selected from among the mRECIST, RECICL, and EASL criteria, which are recommended in various guidelines, and the newly proposed Choi criteria.

2. Evaluating efficacy following radiation therapy

With regard to radiation therapy for HCC, CQ48 of the 2017 guidelines for the diagnosis and treatment of liver cancer indicates that stereotactic body radiation therapy can be administered (weakly recommended) for a variety of patients with recurrence after local treatment, including patients who do not respond to transarterial chemoembolization (TACE), and for HCC for which other local treatment is difficult. Under current circumstances, radiation therapy is considered a treatment that is selected according to the patient. Studies of radiation therapy for HCC have often used the no-enlargement rate seen with long-term follow-up for local evaluation. This is attributed to the fact that two imaging findings not seen with other treatment methods complicate post-radiation therapy evaluation.

The first such finding is arterial phase enhancement of background liver parenchyma in the irradiation field.[10-14] This complicates the evaluation of viable areas and measurement of lesion size for evaluation criteria that take tumor enhancement into account, such as mRECIST. Such background liver parenchyma enhancement persists for several months, and if the enhancement is nodule-like, it is observed as pseudo-progression, which appears as if it were an enlargement of the tumor enhancement region.[15]

The second finding is that it takes a long time for the tumor enhancement to disappear after treatment. Consequently, there is a risk that treatment efficacy may be underestimated over a short-term clinical course.[14] An investigation by Oldrini et al. that used the mRECIST criteria found that, among lesions that showed a long-term treatment effect, residual tumor enhancement was seen on MRI in 62% of the lesions at 3 months posttreatment and in 19% at 6 months.[16] An investigation using contrast-enhanced ultrasound also found that it took several months for tumor enhancement to disappear.[17] The most recent RECICL criteria (2019 edition) added language indicating that efficacy is evaluated based on the maximum effect seen within 6 months posttreatment. However, in an investigation by Okubo et al., 82% of lesions were evaluated as treatment effect 4 (TE4) by contrast-enhanced CT, but 91% of lesions evaluated as TE3 were locally controlled at 1 year posttreatment. The authors therefore noted that treatment efficacy may be underestimated using the RECICL criteria.[18]

The above considerations indicate that the use of existing criteria, such as the mRECIST, EASL, and RECICL criteria, may not be appropriate for evaluating treatment efficacy after radiation therapy.

3. Overview of plans for possible future studies?

With regard to the evaluation of treatment efficacy following chemotherapy, a study is needed that uses overall survival or localized long-term follow-up observation as the reference standard and examines its relationship to the results of treatment efficacy evaluations based on the various criteria. This can be implemented as a retrospective analysis using existing clinical study data or as a sub-analysis of a study being considered.

For the evaluation of treatment efficacy following radiation therapy, it will be necessary to develop specialized criteria for such therapy. This is needed because of the contrast enhancement of the background liver parenchyma that occurs with treatment, and because it has been noted that a long time is needed for tumor enhancement to disappear after treatment. Information should be comprehensively collected, including information related to posttreatment imaging findings and the formulation and assessment of criteria for evaluating these findings.

Search keywords and secondary sources

PubMed was searched using the following keywords: HCC, chemotherapy, radiation, post-treatment, objective response, response, evaluation, and imaging. Relevant articles were selected from the search results.

With regard to radiation therapy, articles on external radiation beam therapy using X-rays or proton beams were selected. Articles on other treatment methods not commonly used in Japan (e.g., Y-90 transarterial radioembolization) were excluded.

The following references were used as secondary sources.

1) Llovet JM et al: Trial design and endpoints in hepatocellular carcinoma: AASLD consensus conference. Hepatology in press, 2020
2) Galle PR et al: EASL clinical practice guidelines: management of hepatocellular carcinoma. J Hepatol 69: 182-236, 2018
3) JSH HCC Guidelines 2017, Revised Version.

References

1) Lencioni R, Llovet JM: Modified RECIST (mRECIST) assessment for hepatocellular carcinoma. Semin Liver Dis 1: 52-60, 2010
2) Kudo M et al: Response evaluation criteria in cancer of the liver (RECICL 2019 revised version). Kanzo 60: 55-62, 2019
3) Bruix J et al: Clinical management of hepatocellular carcinoma: conclusions of the Barcelona-2000 EASL conference. J Hepatol 35: 421-430, 2001
4) Choi H et al: Correlation of computed tomography and positron emission tomography in patients with metastatic gastrointestinal stromal tumor treated at a single institution with imatinib mesylate: proposal of new computed tomography response criteria. J Clin Oncol 25: 1753-1759, 2007
5) Meyer T et al: mRECIST to predict survival in advanced hepatocellular carcinoma: analysis of two randomised phase II trials comparing nintedanib vs sorafenib. Liver Int 37: 1047-1055, 2017
6) Lencioni R et al: Objective response by mRECIST as a predictor and potential surrogate end-point of overall survival in advanced HCC. J Hepatol 66: 1166-1172, 2017
7) Gavanier M et al: CT imaging findings in patients with advanced hepatocellular carcinoma treated with sorafenib: alternative response criteria (Choi, European Association for the Study of the Liver, and modified Response Evaluation Criteria in Solid Tumor (mRECIST)) versus RECIST 1.1. Eur J Radiol 85: 103-112, 2016
8) Ronot M et al: Alternative response criteria (Choi, European Association for the Study of the Liver, and Modified Response Evaluation Criteria in Solid Tumors［ RECIST］) Versus RECIST 1.1 in patients with advanced hepatocellular carcinoma treated with sorafenib. Oncologist 19: 394-402, 2014
9) Arizumi T et al: Comparison of systems for assessment of post-therapeutic response to sorafenib for hepatocellular carcinoma. J Gastroenterol 49: 1578-1587, 2014
10) Park MJ et al: Stereotactic body radiotherapy-induced arterial hypervascularity of non-tumorous hepatic parenchyma in patients with hepatocellular carcinoma: potential pitfalls in tumor response evaluation on multiphase computed tomography. PLoS One 9: 1-10, 2014
11) Apisarnthanarax S et al: Intensity modulated proton therapy with advanced planning techniques in a challenging hepatocellular carcinoma patient. Cureus 9 (9): e1674, 2017

12) Price TR et al: Evaluation of response after stereotactic body radiotherapy for hepatocellular carcinoma. Cancer 118: 3191-3198, 2012
13) Brook OR et al: CT imaging findings after stereotactic radiotherapy for liver tumors. Gastroenterol Res Pract 2015: 1-8, 2015
14) Lock M et al: Computed tomography imaging assessment of postexternal beam radiation changes of the liver. Futur Oncol 12: 2729-2739, 2016
15) Kellock T et al: Stereotactic body radiation therapy (SBRT) for hepatocellular carcinoma: imaging evaluation post treatment. Br J Radiol 91: 1-6, 2018
16) Oldrini G et al: Tumor response assessment by MRI following stereotactic body radiation therapy for hepatocellular carcinoma. PLoS One 12: 1-12, 2017
17) Shiozawa K et al: Evaluation of contrast-enhanced ultrasonography for hepatocellular carcinoma prior to and following stereotactic body radiation therapy using the Cyberknife® system: a preliminary report. Oncol Lett 11: 208-212, 2016
18) Ohkubo Y et al: Cyberknife, stereotactic body radiation therapy for hepatocellular carcinoma. Kanzo 55: 630-633, 2014

BQ 40 Which imaging examinations are recommended to evaluate the efficacy of TACE in HCC?

Statement

Dynamic CT or dynamic MRI is recommended to evaluate the efficacy of TACE in HCC.

Background

Transcatheter arterial chemoembolization (TACE) for HCC is a treatment that involves injecting an embolizing agent into the arteries that feed a tumor to induce tumor ischemia and necrosis to destroy the tumor. Unlike treatments such as the anticancer chemotherapies generally used for malignancies, no reduction in tumor size is often seen early after treatment, and the use of the RECIST criteria, which are widely used to evaluate treatment efficacy in solid cancers, is therefore often inappropriate. Consequently, treatment efficacy is assessed based on an evaluation of the degree to which the embolizing agent accumulates in the tumor and an evaluation of whether blood flow has disappeared from the tumor site.

Explanation

Features of hypervascular HCC are early enhancement with dynamic CT and dynamic MRI and imaging findings indicating washout. Although early enhancement findings disappear at the site of tumor necrosis following TACE, this is often not accompanied by a reduction in tumor size, particularly immediately after TACE.

Because treatment efficacy evaluation using the RECIST criteria, which are widely used to evaluate treatment efficacy in solid cancers, is based on the amount of change in the tumor diameter following treatment, it is difficult to use the RECIST criteria when evaluating the response to TACE.

With Lipiodol®-TACE, which is performed using an iodized poppy seed oil fatty acid ester (Lipiodol®), an oil-based contrast medium, the area in the tumor where Lipiodol® accumulates is concluded to be in an ischemic state and necrotic. Consequently, if non-contrast CT performed immediately after or 1 month after TACE shows complete Lipiodol® accumulation, a treatment effect can be anticipated. A treatment effect is also likely when the diameters of HCC lesions in which Lipiodol® has accumulated show consistent reduction during TACE follow-up.

However, if Lipiodol® accumulation in the HCC lesions is not uniform in the lesions as a whole, and deficits are seen, tumor necrosis in that region may be inadequate. Moreover, residual or recurrent tumors may be present in the periphery of the site of Lipiodol® accumulation. Consequently, an evaluation is needed of the presence or absence of tumor enhancement using a contrast-enhanced imaging procedure.

Tumor blood flow can be evaluated by dynamic CT or dynamic MRI using a contrast medium or by contrast-enhanced ultrasound.

Dynamic CT permits a more objective evaluation than ultrasound, can be performed with a shorter testing time than MRI, and can be performed at many facilities. It therefore plays a central role in evaluating HCC treatment efficacy. However, strong absorption of Lipiodol® can hinder the detection of tumor enhancement in recurrent lesions, and dynamic MRI becomes necessary when it is difficult to assess whether enhancement is present.

MRI is superior to CT in that it can detect trace amounts of contrast medium with greater sensitivity and is little affected by image modification resulting from Lipiodol® accumulation.[1-3] Moreover, MRI enables blood flow to be evaluated in patients who have an iodine allergy. However, shortcomings of MRI are poor throughput and the fact that the examination takes longer than a CT examination.

The hepatocellular MRI contrast medium Gd-EOB-DTPA (EOB, Primovist®) offers the advantage of enabling lesions to be evaluated from the perspectives of both blood flow and liver function. Consequently, contrast-enhanced MRI performed to evaluate liver tumors has often been switched from contrast-enhanced MRI using a conventional extracellular gadolinium contrast medium to EOB-MRI using Gd-EOB-DTPA.

It should be noted that arterial phase images can be poor with EOB-MRI due to artifacts resulting from transient severe motion (TSM), making it difficult to evaluate tumor enhancement. In addition, Shinagawa et al. reported seeing early enhancement of the peritumoral liver parenchyma and pseudotumors showing low signal intensity in the hepatobiliary phase with EOB-MRI within 1 month after TACE. Caution must therefore be exercised when using EOB-MRI to evaluate the response to HCC therapy with TACE.[4]

Contrast-enhanced ultrasound also enables blood flow at sites of recurrence to be evaluated without the evaluation being affected by Lipiodol® accumulation.[5] Currently, the second-generation ultrasound contrast medium perflubutane (Sonazoid®) is the main contrast medium used. Perflubutane contrast-enhanced ultrasound is superior to CT and MRI with respect to spatial and temporal resolution and is therefore very useful for evaluating the hemodynamics of a single HCC lesion or a small number of such lesions. However, it should be understood that ultrasonography has disadvantages, such as: the presence of dead space; the fact that ultrasound attenuates in deep tissue, making evaluation difficult; and the fact that observing a large number of lesions with a single test is difficult due to problems related to the contrast medium dose and test duration.

Performing TACE using spherical embolization agents has been permitted in Japan since 2014. Because Lipiodol® is not used concurrently in TACE that is performed using a spherical embolization agent, residual tumor blood flow can be evaluated without concern about image modification by Lipiodol®. A method of evaluating the treatment efficacy of TACE using spherical embolization agents will likely be established in the future as cases accumulate.

Search keywords and secondary sources

PubMed was searched using the following keywords, and relevant articles were selected from the search results: HCC, TACE, therapeutic effect, and imaging.

References

1) De Santis M et al: Effects of lipiodol retention on MRI signal intensity from hepatocellular carcinoma and surrounding liver treated by chemoembolization. Eur Radiol 7: 10-16, 1997
2) Hunt SJ et al: Radiologic monitoring of hepatocellular carcinoma tumor viability after transhepatic arterial chemoembolization: estimating the accuracy of contrast-enhanced cross-sectional imaging with histopathologic correlation. J Vasc Interv Radiol 20: 30-38, 2009
3) Murakami T et al: Treatment of hepatocellular carcinoma by chemoembolization: evaluation with 3DFT MR imaging. Am J Roentgenol 160: 295-299,1993
4) Shinagawa Y et al: Pseudolesion of the liver on gadoxetete disodium-enhanced MR images obtained after transarterial chemoembolization for hepatocellular carcinoma: clinicopathologic correlation. Am J Roentogenol 199: 1010-1017, 2012
5) Morimoto M et al: Contrast-enhanced harmonic gray-scale sonographic-histologic correlation of the therapeutic effects of transcatheter arterial chemoembolization in patients with hepatocellular carcinoma. AJR Am J Roentgenol 181: 65-69, 2003

BQ 41 Which imaging examinations are recommended to evaluate the efficacy of RFA in HCC?

Statement

Dynamic CT or dynamic MRI is recommended to evaluate the efficacy of RFA in HCC.

Background

Radiofrequency ablation (RFA), a local treatment for HCC, can destroy tumors by ablating them to induce coagulation necrosis. No reduction in tumor size is seen immediately after RFA therapy, making it difficult to use the RECIST criteria, which are based on size, to evaluate the efficacy of the treatment. To achieve cure, the scope of ablation must include a certain amount of the margin of the periphery rather than just approach the tumor border. Efficacy is therefore evaluated using a contrast medium to determine the scope of ablation, including the tumor.

Explanation

Dynamic CT using iodine contrast media and dynamic MRI using extracellular gadolinium contrast media or hepatocellular contrast media Gd-EOB-DTPA (EOB, Primovist®) do not have dead space and enable more objective blood flow evaluation than ultrasound, making them suitable for evaluating RFA treatment efficacy.

CT systems are installed even in relatively small hospitals, and CT has a short test duration and good throughput, whereas MRI systems are not installed in all hospitals, and MRI has a long test duration and poor throughput. However, treatment efficacy must be evaluated by MRI when the patient is allergic to the iodine contrast media used in CT or when the lesion can be visualized only in the hepatobiliary phase of MRI, particularly EOB-MRI, such as in hypovascular HCC. However, it should be noted that post-RFA HCC shows high signal intensity on T1-weighted images due to the ablation effect, and it may therefore be difficult to assess whether contrast enhancement is present with dynamic contrast-enhanced MRI.[1)]

Perflubutane (Sonazoid®) contrast-enhanced ultrasound is superior to CT and MRI with respect to spatial and temporal resolution and is therefore very useful for evaluating the hemodynamics of a single HCC lesion or a small number of such lesions. However, ultrasonography also has disadvantageous features that make evaluation difficult, such as the presence of dead space and the fact that ultrasound attenuates in deep tissue.

The treatment efficacy of RFA in HCC is ensured by obtaining an adequate safety margin. Although studies by Nakazawa et al. and Kim et al. indicated that a safety margin of approximately ≥ 5 mm should be obtained,[2, 3)] depending on the site where HCC is present (e.g., near a large blood vessel, in the hepatic margin, or other sites where puncture is difficult), obtaining an adequate safety margin may not be technically feasible. Three-dimensional CT (3D CT)[4)] and pre- and post-RFA CT fusion imaging[5)] have

been reported to be useful for evaluating the safety margin. Moreover, CT has been found to enable HCC treatment efficacy to be evaluated immediately after RFA (1 week after).[6)]

Corona enhancement of HCC indicates the outflow tract of tumor blood flow.[7)] This holds important significance for HCC progression, and it is therefore important to consider this the extent of the safety margin.

In a separate case-control study, contrast-enhanced 3D ultrasound using perflubutane was used to evaluate the ablation zone and residual tumors after RFA for HCC, and the results were found to agree well with those obtained with 3D CT.[8)] However, compared with ultrasound, CT and MRI are less operator-dependent, making it easier to objectively assess the change in tumor diameter and whether a safety margin has been obtained.

No reports of large investigations of RFA efficacy evaluation using Gd-EOB-DTPA have been identified. Investigation of this topic is therefore needed.

Search keywords and secondary sources

PubMed was searched using the following keywords, and relevant articles were selected from the search results: HCC, RFA, therapeutic effect, and imaging.

References

1) Khankan AA et al: Hepatocellular carcinoma treated with radio frequency ablation: an early evaluation with magnetic resonance imaging. J Magn Reson Imaging 27: 546-551, 2008
2) Nakazawa T et al: Radiofrequency ablation of hepatocellular carcinoma: correlation between local tumor progression after ablation and ablative margin. AJR Am J Roentgenol 188: 480-488, 2007
3) Kim YS et al: The minimal ablative margin of radiofrequency ablation of hepatocellular carcinoma (＞2 and ＜5 cm) needed to prevent local tumor progression: 3D quantitative assessment using CT image fusion. AJR Am J Roentgenol 195: 758-765, 2010
4) Kim KW et al: Safety margin assessment after radiofrequency ablation of the liver using registration of preprocedure and postprocedure CT images. AJR Am J Roentgenol 196: W565-572, 2011
5) Makino Y et al: Utility of computed tomography fusion imaging for the evaluation of the ablative margin of radiofrequency ablation for hepatocellular carcinoma and the correlation to local tumor progression. Hepatol Res 43: 950-958, 2013
6) Ninomiya T et al: Evaluation of the therapeutic effect using MD-CT immediately after RFA for HCC. Hepatogastroenterology 53: 558-660, 2006
7) Ueda K et al: Hypervascular hepatocellular carcinoma: evaluation of hemodynamics with dynamic CT during hepatic arteriography. Radiology 206: 161-166, 1998
8) Luo W et al: Role of Sonazoid-enhanced three-dimensional ultrasonography in the evaluation of percutaneous radiofrequency ablation of hepatocellular carcinoma. Eur J Radiol 75: 91-97, 2010

BQ 42 Is EOB-MRI recommended for the definitive diagnosis of focal nodular hyperplasia?

Statement

Findings for the hepatobiliary phase of EOB-MRI are useful for the definitive diagnosis of focal nodular hyperplasia (FNH), and EOB-MRI should the first choice when selecting a modality.

Background

FNH manifests as a hypervascular, hyperplastic hepatocellular nodule that typically occurs in normal liver and is considered a reactive lesion that develops in response to abnormal regional blood flow. Although there have been many articles published on methods of diagnostic imaging for FNH, many of these reports use pathology findings or dynamic CT/MRI findings as the gold standard. This suggests that typical dynamic CT/MRI findings are sufficient basis for diagnosis at the clinical level. However, the diagnosis can actually be uncertain in some patients and is often confirmed by a finding of an isointense to high-intensity signal compared with the surrounding liver parenchyma or of a distinctive doughnut-shaped or ring-shaped high-signal area in the hepatobiliary phase of EOB-MRI.

Explanation

The typical imaging findings for FNH are summarized below.

1. Abdominal ultrasound

Although its echogenicity is varied, it is often hypoechoic. Typical findings with Doppler ultrasound and contrast-enhanced ultrasound include visualization of spoke-wheel-shaped vascularization or central vascularization, central scar that is hypoechoic and not contrast-enhanced, enhancement of the nodule as a whole or centrifugal arterial enhancement in the early phase of contrast-enhanced ultrasound, and hyperechoic to isoechoic enhancement in the late phase.[1-3)]

2. Dynamic CT and MRI

On non-contrast CT, FNH shows uniform isodensity or hypodensity internally[4)] and lobularity in the margins.[4, 6)] On MRI, although low signal intensity on T1-weighted images and high signal intensity on T2-weighted images are common, the signal can vary.[6, 7)] On diffusion-weighted imaging, isointense to high-intensity signals are common.[6, 7)] Common findings in dynamic studies are enhancement in the arterial phase[4, 5, 8)] and isodensity compared with the surrounding liver parenchyma from the portal venous phase to the delayed phase.[4, 5, 8)] The main drainage route in FNH is the hepatic veins,[9)] and thus a finding of early venous return is an aid in diagnosis. Central scarring shows hypodensity/low signal intensity in the early phase, contrast enhancement from the late phase onward, and high signal intensity on T2-weighted images.[4, 6)]

3. EOB-MRI

In the hepatobiliary phase of EOB-MRI, FNH shows an isointense to high-intensity signal compared with the surrounding liver parenchyma in most patients (≥ 90%).[10, 11] Central scar shows low signal intensity in the hepatobiliary phase of EOB-MRI.[11] FNH appears as a donut-shaped or ring-shaped high-intensity signal including a central low-intensity that is slightly larger than the pathological central scar.[12, 13]

Although FNH can often be diagnosed by dynamic contrast-enhanced CT/MRI or contrast-enhanced ultrasound, there have been few reports of studies that have performed straightforward comparisons of the diagnostic accuracy of the various diagnostic imaging modalities based on high-level evidence. Bartolotta et al. compared non-contrast-enhanced ultrasound with contrast-enhanced ultrasound and reported that the characteristics findings of FNH (spoke wheel vascularization, central scarring) were more easily seen with contrast-enhanced ultrasound.[2] No studies have compared ultrasound with EOB-MRI, and the superiority of these two modalities therefore cannot be compared. In 2008, Zech et al. reported that the rate at which FNH was diagnosed with certainty was significantly higher with EOB-MRI than with non-contrast-enhanced MRI or dynamic CT (2 of 3 readers).[11] A systematic review published in 2015 confirmed the usefulness of EOB-MRI.[8]

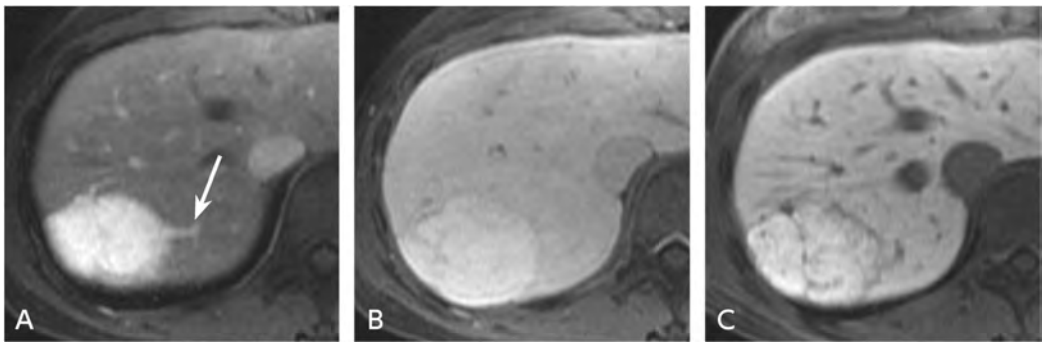

Figure　Focal nodular hyperplasia (woman in her 20s)

A: EOB-MRI, arterial-dominant phase: A 5-cm mass, enhanced in its entirety, is seen in S7/8. Early visualization of a vein (early venous return) is seen near the mass (→)

B: EOB-MRI, transitional phase: The mass shows slightly high signal intensity compared with the surrounding liver.

C: EOB-MRI, hepatobiliary phase: The mass shows higher signal intensity than background liver. Restiform low-intensity signals thought to be scarring are distinct in the interior.

Conditions for consideration in the differential diagnosis of FNH based on imaging include hepatocellular adenoma (HCA), HCC, metastasis, and hepatic angiomyolipoma. Of these, distinguishing FNH from HCA, which, like FNH, is a benign hepatocellular tumor that often occurs in normal liver, is difficult, but important because of differences in its treatment. Treatment of FNH basically involves watchful waiting, whereas surgery is recommended for HCA, particularly when ≥ 5 cm in size or when it increases in size, and in cases such as when it occurs in male patients in view of developments such as complicating intra-abdominal hemorrhage and malignant transformation. Grazioli et al. compared the

frequency of various EOB-MRI findings in 68 FNH lesions and 43 HCA lesions and found that 93% of the HCA lesions (40/43) showed low-intensity signals, whereas 91% of the FNH lesions (62/68) showed isointense to high-intensity signals, which were considered useful findings for distinguishing between the 2 types.[10] In addition, several reports of evidence level 2 have been published,[14, 15] and a systematic review published in 2015 found a high diagnostic rate for the hepatobiliary phase of EOB-MRI in distinguishing between FNH and HCA. However, the number of articles remains small, and it has been suggested that the estimated diagnostic accuracy may be higher than its actual value.[16]

With contrast-enhanced ultrasound, on the other hand, contrast enhancement is known to begin with central vessels in FNH and spread in a centrifugal pattern, which has been shown to be useful for diagnosing FNH and distinguishing it from HCA.[3, 17, 20] Subclassifications of HCA have been proposed and their genetic, pathological, and clinical features elucidated in recent years. In the 2010 WHO classification, 4 subtypes were proposed: hepatocyte nuclear factor 1α-inactivated HCA (H-HCA), inflammatory HCA (I-HCA), β-catenin activated HCA (B-HCA), and unclassified HCA (U-HCA). In the 2019 WHO classification, further refined subclassifications were proposed. Imaging features have also been established for HCA subclassifications,[19-21] with the existence of subtypes that show high signal intensity in the hepatobiliary phase of EOB-MRI reported (some B-HCA and I-HCA).[21] In these cases, greater care needs to be exercised in differentiating from FNH. Points that can be used to differentiate include the fact that arterial phase enhancement is stronger in FNH than in HCA,[10, 13, 22] and that changes such as fatty changes, hemorrhage, and necrosis are rarer in FNH than in adenomas.

Although conventional dynamic CT/MRI and contrast-enhanced ultrasound can also be used to diagnose FNH adequately, the findings from the hepatobiliary phase of EOB-MRI are useful for the definitive diagnosis of FNH. EOB-MRI should therefore be the first choice when selecting a modality in cases where FNH is suspected.

Search keywords and secondary sources

PubMed was searched for the period through June 2019 using the following keywords: focal nodular hyperplasia, Gd-EOB-DTPA, and gadoxetic acid. Hits were obtained for 81 articles. For reference, an additional search was performed using the keywords magnetic resonance imaging, CT, and ultrasound.

In addition, the following were referenced as secondary sources.

1) Bioulac-Sage P et al：Focal nodular hyperplasia and hepatocellular adenoma WHO Classification of Tumours of the digestive system, 5th ed. pp.221-228, IARC, 2019
2) Colombo M et al : EASL clinical practice guidelines on the management of benign liver tumours. J Hepatol 65 : 386-398, 2016

References

1) Piscaglia F et al: Diagnostic features of real-time contrast-enhanced ultrasound in focal nodular hyperplasia of the liver. Ultraschall Med 31: 276-282, 2010
2) Bartolotta TV et al: Hepatic focal nodular hyperplasia: contrast-enhanced ultrasound findings with emphasis on lesion size, depth and liver echogenicity. Eur Radiol 20: 2248-2256, 2010

3) Kong WT et al: Contrast-enhanced ultrasound in combination with color doppler ultrasound can improve the diagnostic performance of focal nodular hyperplasia and hepatocellular adenoma. Ultrasound Med Biol 41: 944-951, 2015
4) Brancatelli G et al: Focal nodular hyperplasia: CT findings with emphasis on multiphasic helical CT in 78 patients. Radiology 219: 61-68, 2001
5) Mathieu D et al: Hepatic adenomas and focal nodular hyperplasia: dynamic CT study. Radiology 160: 53-58, 1986
6) Mortele KJ et al: Focal nodular hyperplasia of the liver: detection and characterization with plain and dynamic-enhanced MRI Abdom Imaging 27: 700-707, 2002
7) Kitao A et al: Differentiation between hepatocellular carcinoma showing hyperintensity on the hepatobiliary phase of gadoxetic acid-enhanced MRI and focal nodular hyperplasia by CT and MRI. AJR Am J Roentgenol 211: 347-357, 2018
8) Suh CH et al: The diagnostic value of Gd-EOB-DTPA-MRI for the diagnosis of focal nodular hyperplasia: a systematic review and meta-analysis Eur Radiol 25: 950-960, 2015
9) Miyayama S et al: Hemodynamics of small hepatic focal nodular hyperplasia: evaluation with single-level dynamic CT during hepatic arteriography. AJR Am J Roentgenol 174: 1567-1569, 2000
10) Grazioli L et al: Hepatocellular adenoma and focal nodular hyperplasia: value of gadoxetic acid-enhanced MR imaging in differential diagnosis. Radiology 262: 520-529, 2012
11) Zech C et al: Diagnostic performance and description of morphological features of focal nodular hyperplasia in Gd-EOB-DTPA-enhanced liver magnetic resonance imaging: results of a multicenter trial. Invest Radiol 43: 504-511, 2008
12) Mohajer K et al: Characterization of hepatic adenoma and focal nodular hyperplasia with gadoxetic acid. J Magn Reson Imaging 36: 686-696, 2012
13) Yoneda N et al: Benign hepatocellular nodules: hepatobiliary phase of gadoxetic acid-enhanced MR imaging based on molecular background. Radiographics 36: 2010-2027, 2016
14) Grieser C et al: Gadoxetic acid enhanced MRI for differentiation of FNH and HCA: a single centre experience. Eur Radiol 24: 1339-48, 2014
15) Bieze M et al: Diagnostic accuracy of MRI in differentiating hepatocellular adenoma from focal nodular hyperplasia: prospective study of the additional value of gadoxetate disodium. AJR Am J Roentgenol 199: 26-34, 2012
16) McInnes MD et al: Focal nodular hyperplasia and hepatocellular adenoma: accuracy of gadoxetic acid-enhanced MR imaging: a systematic review. Radiology 277: 927, 2015
17) Roche V et al: Differentiation of focal nodular hyperplasia from hepatocellular adenomas with low-mecanical-index contrast-enhanced sonography (CEUS): effect of size on diagnostic confidence. Eur Radiol 25: 186-195, 2015
18) Pei XQ et al: Quantitative analysis of contrast-enhanced ultrasonography: differentiating focal nodular hyperplasia from hepatocellular carcinoma. Br J Radiol 86, 2013
19) Laumonier H et al: Hepatocellular adenomas: magnetic resonance imaging features as a function of molecular pathological classification. Hepatology 48: 808-818, 2008
20) van Aalten SM et al: Hepatocellular adenomas: correlation of MR imaging findings with pathologic subtype classification. Radiology 261: 172-181, 2011
21) Ba-Ssalamah A et al: Morphologic and molecular features of hepatocellular adenoma with gadoxetic acid-enhanced MR imaging. Radiology 277: 104-113, 2015
22) Ruppert-Kohlmayr AJ et al: Focal nodular hyperplasia and hepatocellular adenoma of the liver: differentiation with multiphasic helical CT. AJR Am J Roentgenol 176: 1493-1498, 2001

BQ 43 Is dynamic CT recommended for diagnosing mass-forming intrahepatic cholangiocarcinoma?

Statement

Dynamic CT is a useful test for the qualitative diagnosis of lesions and for determining a treatment method, and its use is therefore recommended when mass-forming intrahepatic cholangiocarcinoma is suspected.

Background

Intrahepatic cholangiocarcinoma is broadly classified, based on macroscopic appearance, as the mass-forming type, periductal infiltrating type, and intraductal growth type.[1,2] However, because peripheral intrahepatic cholangiocarcinoma often shows a mass-forming-type morphology, an explanation limited to this type is included.

Explanation

Intrahepatic cholangiocarcinoma shows hypodensity on non-contrast CT, and ring-shaped enhancement is a feature of it in the arterial phase of dynamic CT. The sensitivity of dynamic CT is 60%, with specificity of 65.5%.[3,4] If the tumor diameter is < 3 cm, the early enhancement pattern varies from ring-shaped to uniform.[4, 5] Persistent enhancement, a characteristic finding, is seen in 67% of tumors.[3] It is attributed to an abundant stromal component at the center of the tumor.[5] An accessory finding in approximately 60% of tumors is dilatation of the distal bile duct.[6] Moreover, dynamic CT is useful and widely used for staging intrahepatic cholangiocarcinoma.[5, 7] Its sensitivity and specificity are 89% and 92%, respectively, for portal vein invasion and 84% and 93%, respectively, for hepatic artery invasion,[8] and its diagnostic rate for bile duct invasion is 79.7%.[9]

With regard to the diagnostic performance of contrast-enhanced ultrasound in intrahepatic cholangiocarcinoma, its sensitivity ranges from 60% to 90%, and specificity ranges from 65% to 98%.[10, 11] With regard to the discrimination ability of MRI in HCC, its sensitivity has been found to range from 68.8% to 93.5% and specificity from 86.2% to 97.7%.[12-15] With FDG-PET, sensitivity of 100% and specificity of 85% to 90% have been found for the mass-forming type ≥ 1 cm in size.[16-19] Although FDG-PET is highly useful in diagnosing malignancy, there have been no reports indicating that it is useful for the differential diagnosis of hepatic masses.

Figure　Intrahepatic cholangiocarcinoma (mass-forming type)

A: Non-contrast CT: A tumor lesion with hypodensity is seen in the right hepatic lobe.

B: Dynamic CT, arterial-dominant phase: Ring-shaped enhancement is seen in the tumor margins.

C: Dynamic CT, equilibrium phase: Delayed enhancement is seen in the tumor interior.

Search keywords and secondary sources

PubMed was searched using the following keywords: bile duct cancer, intrahepatic cholangiocarcinoma CT, MRI, and FDG-PET.

References

1) Seo N et al: Cross-sectional imaging of intrahepatic cholangiocarcinoma: development, growth, spread, and prognosis. AJR Am J Roentgenol 209 (2): W64-W75, 2017
2) Chung YE et al: Varying appearances of cholangiocarcinoma: radiologic-pathologic correlation. Radiographics 29 (3): 683-700, 2009
3) Choi SH et al: Intrahepatic cholangiocarcinoma in patients with cirrhosis: differentiation from hepatocellular carcinoma by using gadoxetic acid-enhanced MR imaging and dynamic CT. Radiology 282 (3): 771-781, 2017
4) Kim SJ et al: Peripheral mass-forming cholangiocarcinoma in cirrhotic liver. AJR Am J Roentgenol 189 (6): 1428-1434, 2007
5) Kim SA et al: Intrahepatic mass-forming cholangiocarcinomas: enhancement patterns at multiphasic CT, with special emphasis on arterial enhancement pattern correlation with clinicopathologic findings. Radiology 260 (1): 148-157, 2011
6) Zhao YJ et al: Differentiation of mass-forming intrahepatic cholangiocarcinoma from poorly differentiated hepatocellular carcinoma: based on the multivariate analysis of contrast-enhanced computed tomography findings. Abdom Radiol 41 (5): 978-989, 2016
7) Asayama Y et al: Delayed-phase dynamic CT enhancement as a prognostic factor for mass-forming intrahepatic cholangiocarcinoma. Radiology 238 (1): 150-155, 2006
8) Ruys AT et al: Radiological staging in patients with hilar cholangiocarcinoma: a systematic review and meta-analysis. Br J Radiol 85 (1017): 1255-1262, 2012
9) Ito K et al: The impact of MDCT and endoscopic transpapillary mapping biopsy to predict longitudinal spread of extrahepatic cholangiocarcinoma. JOGS 22 (9): 1528-1537, 2018
10) Chen LD et al: Intrahepatic cholangiocarcinoma and hepatocellular carcinoma: differential diagnosis with contrast-enhanced ultrasound. Eur Radiol 20 (3): 743-753, 2010
11) Furuse J et al: Contrast enhancement patterns of hepatic tumours during the vascular phase using coded harmonic imaging and Levovist to differentiate hepatocellular carcinoma from other focal lesions. Br J Radiol 76 (906): 385-392, 2003
12) Wengert GJ et al: Differentiation of intrahepatic cholangiocellular carcinoma from hepatocellular carcinoma in the cirrhotic liver using contrast-enhanced MR imaging. Acad Radiol 24 (12): 1491-1500, 2017
13) Choi SY et al: Added value of ancillary imaging features for differentiating scirrhous hepatocellular carcinoma from intrahepatic cholangiocarcinoma on gadoxetic acid-enhanced MR imaging. Eur Radiol 28 (6): 2549-2560, 2018

14) Hwang J et al: Capsule, septum, and T2 hyperintense foci for differentiation between large hepatocellular carcinoma (>/＝ 5 cm) and intrahepatic cholangiocarcinoma on gadoxetic acid MRI. Eur Radiol 27 (11): 4581-4590, 2017
15) Kim R et al: Differentiation of intrahepatic mass-forming cholangiocarcinoma from hepatocellular carcinoma on gadoxetic acid-enhanced liver MR imaging. Eur Radiol 26 (6): 1808-1817, 2016
16) Corvera CU et al: 18F-fluorodeoxyglucose positron emission tomography influences management decisions in patients with biliary cancer. J Am Col Surg 206 (1): 57-65, 2008
17) Kim YJ et al: Usefulness of 18F-FDG PET in intrahepatic cholangiocarcinoma. Eur J Nucl Med Mol Imag 30 (11): 1467-1472, 2003
18) Anderson CD et al: Fluorodeoxyglucose PET imaging in the evaluation of gallbladder carcinoma and cholangiocarcinoma. JOGS 8 (1): 90-97, 2004
19) Moon CM et al: Usefulness of 18F-fluorodeoxyglucose positron emission tomography in differential diagnosis and staging of cholangiocarcinomas. J Gastroenterol Hepatol 23 (5): 759-765, 2008

BQ 44 Is EOB-MRI recommended for diagnosing liver metastasis (metastatic liver tumors)?

Statement

EOB-MRI is strongly recommended for diagnosing liver metastasis.

The addition of diffusion-weighted imaging to EOB-MRI has been shown to improve diagnostic performance for lesions < 1 cm in size, and their combined use is therefore recommended.

Hemangioma diagnosis may be difficult with EOB-MRI and therefore requires a comprehensive assessment.

Background

Metastatic liver cancer ("liver metastasis" below) is a disease more frequently encountered than primary liver cancer in routine clinical care. The objectives of diagnostic imaging in this case vary greatly, ranging from the exploratory examination of whether lesions are present used in follow-up to a qualitative diagnosis performed when hepatic lesions are identified and to a diagnostic workup that encompasses the extent and locations of the lesions and is performed in order to select treatment. In recent years, the usefulness of MRI (EOB-MRI) using the liver-specific contrast agent (Gd-EOB-DTPA) in diagnosing liver metastasis has come to be widely recognized.

Explanation

The primary imaging examinations used to diagnose liver metastasis are ultrasound, contrast-enhanced CT, MRI, and FDG-PET. Angiographic CT is not recommended due to its invasiveness. A meta-analysis published in 2002 that examined detection sensitivity in liver metastasis of gastrointestinal cancer, including esophageal cancer, gastric cancer, and colorectal cancer, found sensitivity of 55% for ultrasound, 72% for contrast-enhanced CT, 76% for MRI, and 90% for FDG-PET, with FDG-PET sensitivity being significantly higher than that of the other modalities. At this point, EOB-MRI was not being used clinically and was therefore excluded from the analysis.[1)] As evidence of the high diagnostic performance of EOB-MRI in liver metastasis, a meta-analysis published in 2012 found sensitivity and specificity of 93% and 95%, respectively, and an AUROC of 0.98,[2)] whereas a subsequent meta-analysis in 2018 in colorectal cancer found sensitivity and specificity of 82% and 74% for contrast-enhanced CT, 93% and 87% for EOB-MRI, and 74% and 94% for FDG-PET, respectively, showing superior diagnostic performance with EOB-MRI than with the other imaging examinations.[3)] The use of diffusion-weighted imaging in combination with EOB-MRI will likely increase diagnostic performance. Sensitivity was found to increase to 96% with combined use of diffusion-weighted images as compared with 91% without combined use and to improve from 83% to 91% when only sub-centimeter metastases are indicated to be evaluated.[4)]

Studies of the usefulness of EOB-MRI have often examined liver metastasis in colorectal cancer patients, because patient prognosis can be expected to improve with surgical resection. With the addition of EOB-MRI to contrast-enhanced CT, the treatment plan was found to change for between 19% and 37% of patients,[5-7] and this is the most highly recommended test method for preoperative evaluation, according to the American College of Radiology (ACR) Appropriateness Criteria®. In recent years, preoperative therapy and conversion therapy administered before liver resection following chemotherapy have been widely used for colorectal liver metastasis. EOB-MRI was also found to be effective for the diagnosis of colorectal liver metastasis after chemotherapy, and no difference in diagnostic performance was observed depending on whether chemotherapy was administered.[8] However, performing EOB-MRI for diagnosis of all liver metastases is unreasonable considering the various testing circumstances and cost. It is therefore appropriate to use contrast-enhanced CT, which covers a whole-body check-up, for screening and follow-up imaging examination. An example of tumors other than colorectal cancer for which surgical resection is known to be useful is liver metastasis of neuroendocrine neoplasms. Compared with other sequences or MRI using an extracellular gadolinium contrast agent, the hepatobiliary phase images in EOB-MRI have been found to provide better lesion contrast and identification and a higher rate of interobserver agreement for liver metastases of neuroendocrine neoplasms. However, no studies have compared EOB-MRI with contrast-enhanced CT or FDG-PET.[9, 10] Liver metastasis from pancreatic ductal adenocarcinoma is a disease that is inoperable when it is identified. The detection sensitivity of EOB-MRI for liver metastases from pancreatic ductal adenocarcinoma has been found to be superior to that of contrast-enhanced CT, with patient-based sensitivity of 82% for EOB-MRI and 60% for contrast-enhanced CT and lesion-based sensitivity of 93% for EOB-MRI and 75% for contrast-enhanced CT.[11] EOB-MRI also prevailed in a comparison with MRI using an extracellular gadolinium contrast agent: sensitivity was 95% for EOB-MRI and 84% for extracellular gadolinium contrast-enhanced MRI.[12]

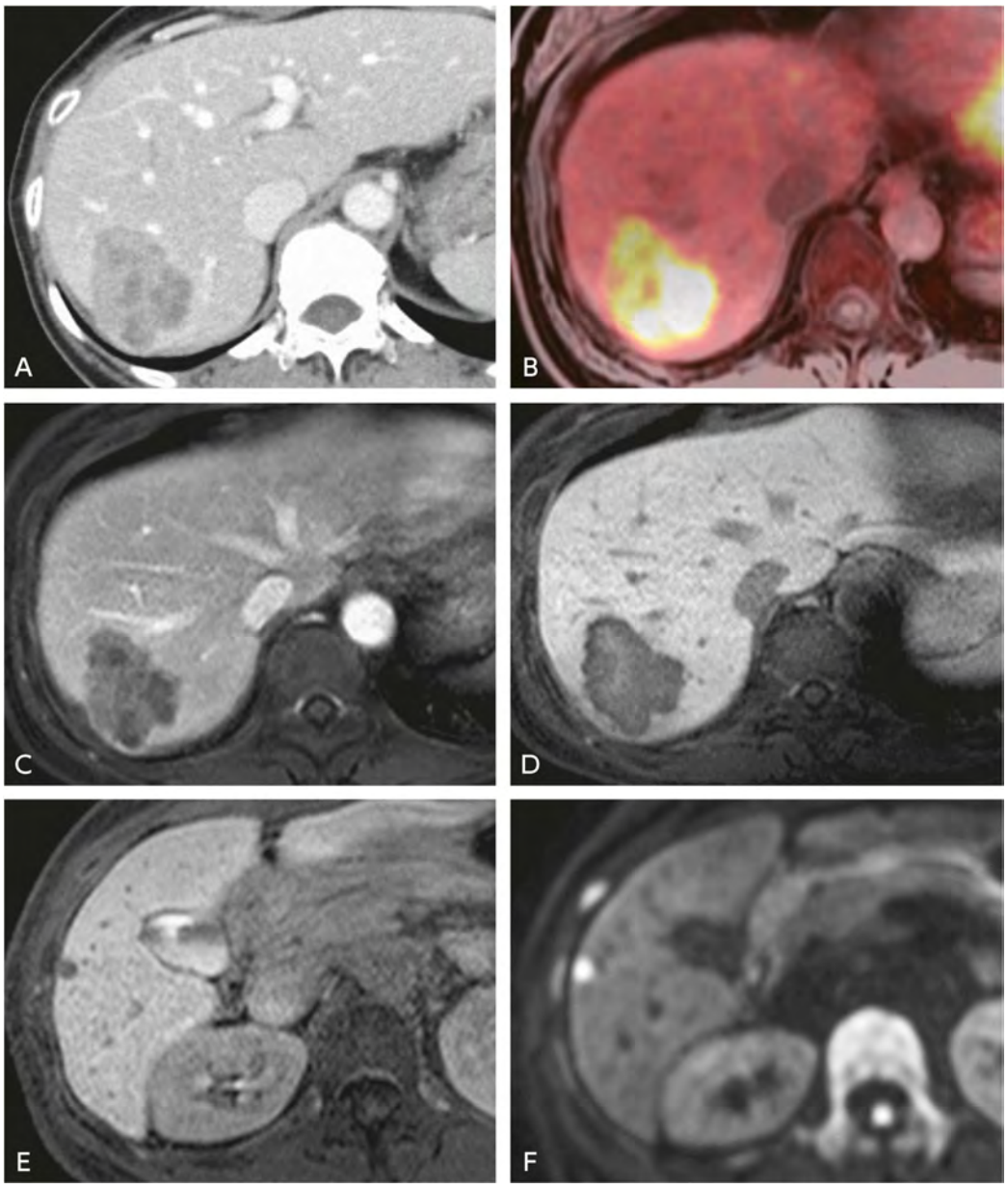

Figure　Liver metastasis of colorectal cancer (woman in her 50s)

A: Contrast-enhanced CT: A lobular, unevenly imaged liver metastasis is seen in liver segment S7.

B: FDG-PET: Increased FDG accumulation seen.

C: EOB-MRI, portal venous phase: As with contrast-enhanced CT, a lobular, unevenly imaged liver metastasis is seen.

D, E: EOB-MRI, hepatobiliary phase: Contrast is good (D), and a 1-cm nodule showing low signal intensity is seen in liver segment S6 (E).

F: MRI, diffusion-weighted imaging: High signal intensity shown, possible microscopic liver metastasis.

As noted previously, although EOB-MRI provides excellent diagnostic performance for liver metastasis, caution is required in diagnosing hemangioma. Because Gd-EOB-DTPA is taken up by hepatocytes beginning approximately 90 seconds after injection of the contrast agent, the concept of an equilibrium phase does not exist for dynamic studies in EOB-MRI. Consequently, the pooling and persistent enhancement in the equilibrium phase images that are useful findings for diagnosing hemangioma may not

be obtainable with EOB-MRI. The lack of pooling and persistent enhancement is highly observed for high-flow hemangiomas and small hemangiomas.[13, 14] To diagnose hemangioma, careful observation for imaging findings such as an area of marginal punctate enhancement in the arterial phase or markedly high signal intensity in T2-weighted images is desirable, along with the combined use of an extracellular gadolinium contrast medium.[5, 15]

Search keywords and secondary sources

PubMed was searched using the following keywords, and further selections were made from the results: liver metastasis, gadoxetic acid, gadoxetate disodium, EOB, and MRI.

In addition, the following was referenced as a secondary source.

1) Kaur H et al: ACR Appropriateness Criteria®: suspected liver metastases. J Am Coll Radiol 14 (5S): S314-S325, 2017

References

1) Kinkel K et al: Detection of hepatic metastases from cancers of the gastrointestinal tract by using noninvasive imaging methods (US, CT, MR imaging, PET): a meta-analysis. Radiology 224 (3): 748-756, 2002
2) Chen L et al: Meta-analysis of gadoxetic acid disodium (Gd-EOB-DTPA)-enhanced magnetic resonance imaging for the detection of liver metastases. PLoS One 7 (11): e48681, 2012
3) Choi SH et al: Diagnostic performance of CT, gadoxetate disodium-enhanced MRI, and PET/CT for the diagnosis of colorectal liver metastasis: systematic review and meta-analysis. J Magn Reson Imaging 47 (5): 1237-1250, 2018
4) Vilgrain V et al: A meta-analysis of diffusion-weighted and gadoxetic acid-enhanced MR imaging for the detection of liver metastases. Eur Radiol 26 (12): 4595-4615, 2016
5) Sofue K et al: Does gadoxetic acid-enhanced 3.0T MRI in addition to 64-detector-row contrast-enhanced CT provide better diagnostic performance and change the therapeutic strategy for the preoperative evaluation of colorectal liver metastases? Eur Radiol 24 (10): 2532-2539, 2014
6) Patel S et al: MRI with gadoxetate disodium for colorectal liver metastasis: is it the new “imaging modality of choice” ? J Gastrointest Surg 18 (12): 2130-2135, 2014
7) Kim HJ et al: Incremental value of liver MR imaging in patients with potentially curable colorectal hepatic metastasis detected at CT: a prospective comparison of diffusion-weighted imaging, gadoxetic acid-enhanced MR imaging, and a combination of both MR techniques. Radiology 274 (3): 712-722, 2015
8) Yu MH et al: Gadoxetic acid-enhanced MRI and diffusion-weighted imaging for the detection of colorectal liver metastases after neoadjuvant chemotherapy. Eur Radiol 25 (8): 2428-2436, 2015
9) Morse B et al: Magnetic resonance imaging of neuroendocrine tumor hepatic metastases: does hepatobiliary phase imaging improve lesion conspicuity and interobserver agreement of lesion measurements? Pancreas 46 (9): 1219-1224, 2017
10) Tirumani SH et al: Value of hepatocellular phase imaging after intravenous gadoxetate disodium for assessing hepatic metastases from gastroenteropancreatic neuroendocrine tumors: comparison with other MRI pulse sequences and with extracellular agent. Abdom Radiol (NY) 43 (9): 2329-2339, 2018
11) Motosugi U et al: Detection of pancreatic carcinoma and liver metastases with gadoxetic acid-enhanced MR imaging: comparison with contrast-enhanced multi-detector row CT. Radiology 260 (2): 446-453, 2011
12) Noda Y et al: Detection of pancreatic ductal adenocarcinoma and liver metastases: comparison of Gd-EOB-DTPA-enhanced MR imaging vs. extracellular contrast materials. Abdom Radiol (NY), 2020［ Epub ahead of print］
13) Goshima S et al: Hepatic hemangioma and metastasis: differentiation with gadoxetate disodium-enhanced 3-T MRI. AJR Am J Roentgenol. 195 (4): 941-946, 2010
14) Tamada T et al: Hepatic hemangiomas: evaluation of enhancement patterns at dynamic MRI with gadoxetate disodium. AJR Am J Roentgenol 196 (4): 824-830, 2011
15) Motosugi U et al: Distinguishing hepatic metastasis from hemangioma using gadoxetic acid-enhanced magnetic resonance maging. Invest Radiol 46 (6): 359-365, 2011

FQ 5 Is contrast-enhanced MRI recommended for distinguishing benign from malignant cystic lesions of the liver?

Statement

Although the discrimination ability of contrast-enhanced MRI with respect to cystic lesions of the liver is limited, and there is a lack of scientific evidence in this regard, it is useful to a certain extent, and its implementation for this purpose can therefore be considered.

Background

Various modalities are considered useful for distinguishing benign from malignant cystic lesions of the liver, such as ultrasound, contrast-enhanced CT, contrast-enhanced MRI, and FDG-PET. Although there have been many previous reports regarding the use of ultrasound, contrast-enhanced CT, and contrast-enhanced MRI, the sample sizes in nearly all of these reports have been small. Consequently, the evidence level is not high. Moreover, there have been very few reports of the usefulness of FDG-PET. This FQ focuses on the ability of contrast-enhanced MRI to distinguish between benign and malignant cystic lesions of the liver.

Explanation

There are a variety of cystic lesions of the liver, including: cysts of the liver parenchyma, such as simple hepatic cysts; congenital hepatic cysts, including Caroli's disease and bile duct-derived cysts; and inflammatory and neoplastic cystic tumors. Malignant cystic tumors of the liver also vary widely and encompass tumors such as: those that arise from cystic lesions; HCC; metastatic liver cancer; and cystic degeneration of solid tumors, such as undifferentiated cancer. Therefore, it is considered inappropriate to lump them together as malignant cystic tumors. Of these types of cystic lesions, this discussion focuses on distinguishing benign from malignant mucinous cystic neoplasms (MCNs) and non-invasive from invasive intraductal papillary neoplasms of the bile duct (IPNB). Although they have often been reported as hepatic biliary cystadenomas/cystadenocarcinomas, these lesions will be consolidated under MCNs in these guidelines.

All contrast-enhanced MRI is useful for detecting the septum and solid portion of an MCN in distinguishing benign from malignant neoplasms. Ultrasound and contrast-enhanced CT are also useful. Although both benign and malignant features are seen with septal enhancement and mural nodules, mural nodules are frequently associated with malignancy, and a papillary solid tumor and nodular thickening of the septum are findings that suggest malignancy (sensitivity, 67% to 100%).[1-6] With any of the modalities, there are limits to the extent to which these findings can detect tumors in accordance with a small solid portion or wall.[7]

In distinguishing non-invasive from invasive IPNB, a tumor diameter of ≥ 2.5 cm on contrast-enhanced MRI, multiplicity, thickening of the bile duct wall, and invasion of surrounding organs are frequent findings in invasive IPNB (Fig.). When these findings are present, the recurrence-free survival rate is low, and multiplicity is a negative prognostic factor for recurrence-free survival.[8)] A histographic analysis of ADC values in diffusion-weighted images found that skewness was useful for distinguishing between non-invasive and invasive IPNB.[9)]

The strengths of MRI are that it is useful for evaluating size and vascular and hepatic invasion and for elucidating internal features such as blood vessels.[5)] There have been almost no reports of EOB-MRI.

Similar to contrast-enhanced MRI, contrast-enhanced CT is useful for evaluating size and vascular and hepatic invasion. However, a strength of contrast-enhanced CT is its excellent spatial resolution, which makes it useful for evaluating size, elucidating anatomical location relationships, and evaluating aspects such as bile duct and blood vessel invasion.[1, 3, 10)] On the other hand, it cannot distinguish between benign and malignant in the presence or absence of calcification, and although the likelihood of malignancy is high with hemorrhage, this is not considered a finding specific to malignancy.[4, 5)]

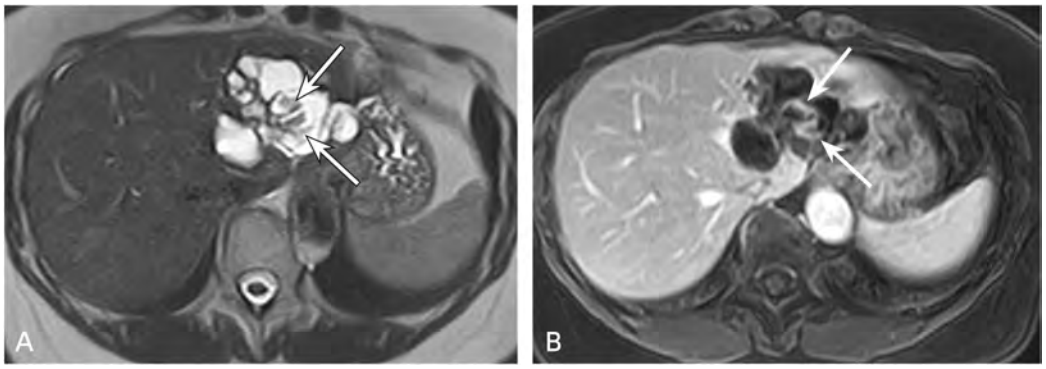

Figure　Patient (woman in her 50s)

A: MRI (single-shot T2-weighted image)

B: Gadolinium contrast-enhanced MRI (fat-suppressed T1-weighted image)

A cystic mass with a maximum size of approximately 6 cm that connects with the dilated bile duct is seen in the lateral segment of the left hepatic lobe. Internally, a papillary solid portion (→) is seen in association with an area of contrast enhancement with a maximum size of 2.3 cm. No tendency for multiplicity or a clear finding of extramural invasion is seen. The findings suggest non-invasive IPNB.

With regard to ultrasonography, a strength of this modality is that it is the optimal test for elucidating the internal aspects of a cyst, such as mucus and the septum.[1, 3)] Ultrasound has also been found to be useful for determining whether mural nodules are present in cystic disease.[11)] In addition, it is useful for diagnosing solid tumors that appear to be cystic lesions on CT or MRI, such as undifferentiated sarcomas.[12)] It has been reported that distinguishing biliary sludge, mucus plugs, and calcification from solid portions can be difficult with ultrasound, and that visualization of solid portions is better with CT.[13-15)] In recent years, contrast-enhanced ultrasonography has also been found to be useful.[16)] In distinguishing benign from malignant MCNs, honeycomb contrast in the arterial phase was found to be common in benign MCNs,

whereas hypoechoicity in the late phase resulting from poor contrast enhancement was reported to be common in malignant cases.[17)]

With FDG-PET, the standard uptake value (SUV) has been reported to be useful in distinguishing non-invasive from invasive IPNB.[18)]

For each modality, the sample sizes in nearly all of the studies have been small, and the evidence is therefore lacking. It would be helpful in the future to conduct investigations that have large sample sizes and that compare the diagnostic performance of the different modalities.

Although all of the modalities are currently limited in their discrimination ability, they each have a different characteristic capacity for discrimination, and combining them for diagnosis is therefore desirable.

Search keywords and secondary sources

Five types of searches of PubMed were performed using the keywords shown below. In the primary search, 2,256 articles were extracted, and 18 were eventually used.

1. liver, cystic tumor, diagnosis, malignant, imaging
2. biliary cystadenocarcinoma, imaging
3. intraductal papillary neoplasm of bile duct, imaging
4. mucinous cystic neoplasm, liver
5. mucin producing, liver

References

1) Choi BI et al: Biliary cystadenoma and cystadenocarcinoma: CT and sonographic findings. Radiology 171 (1): 57-61, 1989
2) Vogt DP et al: Cystadenoma and cystadenocarcinoma of the liver: a single center experience. J Am Coll Surg 200 (5): 727-733, 2005
3) Korobkin M et al: Biliary cystadenoma and cystadenocarcinoma: CT and sonographic findings. AJR Am J Roentgenol 153 (3): 507-511, 1989
4) Buetow PC et al: Biliary cystadenoma and cystadenocarcinoma: clinical-imaging-pathologic correlations with emphasis on the mportance of ovarian stroma. Radiology 196 (3): 805-810, 1995
5) Lewin M et al: Assessment of MRI and MRCP in diagnosis of biliary cystadenoma and cystadenocarcinoma. Eur Radiol 16 (2): 407-413., 2006
6) Xu MY et al: Clinicopathological characteristics and prognostic factors of intrahepatic biliary cystadenocarcinoma. Chin Med J (Engl) 128 (9): 1177-1183, 2015
7) Kokubo T et al: Mucin-hypersecreting intrahepatic biliary neoplasms. Radiology 168 (3): 609-614, 1988
8) Lee S et al: Intraductal papillary neoplasm of the bile duct: assessment of invasive carcinoma and long-term outcomes using RI. J Hepatol 70 (4): 692-699, 2019
9) Jin KP et al: Skewness of apparent diffusion coefficient (ADC) histogram helps predict the invasive potential of intraductal apillary neoplasms of the bile ducts (IPNBs). Abdom Radiol (NY) 44 (1): 95-103, 2019
10) Lee JW et al: CT features of intraductal intrahepatic cholangiocarcinoma. AJR Am J Roentgenol 175 (3): 721-725, 2000
11) Xu HX et al: Imaging features of intrahepatic biliary cystadenoma and cystadenocarcinoma on B-mode and contrast-enhanced ltrasound. Ultraschall Med 33 (7): E241-E249, 2012
12) Buetow PC et al: Undifferentiated (embryonal) sarcoma of the liver: pathologic basis of imaging findings in 28 cases. Radiology 03 (3): 779-783, 1997
13) Lim JH et al: Radiological spectrum of intraductal papillary tumors of the bile ducts. Korean J Radiol 3 (1): 57-63, 2002
14) Han JK, Lee JM: Intrahepatic intraductal cholangiocarcinoma. Abdom Imaging 29 (5): 558-564, 2004
15) Lim JH et al: Intraductal papillary mucinous tumor of the bile ducts. Radiographics. 24 (1): 53-66；discussion -7, 2004
16) Corvino A et al: Diagnostic performance and confidence of contrast-enhanced ultrasound in the differential diagnosis of cystic nd cysticlike liver lesions. AJR Am J Roentgenol. 209 (3): W119-W27, 2017

17) Dong Y et al: Contrast enhanced ultrasound features of hepatic cystadenoma and hepatic cystadenocarcinoma. Scand J Gastroenterol 2 (3): 365-372, 2017
18) Ikeno Y et al: Usefulness of preoperative (18) F-FDG-PET in detecting invasive intraductal papillary neoplasm of the bile duct. nticancer Res 38 (6): 3677-3682, 2018

BQ 45 Which imaging examinations are recommended for determining whether cholecystocholedocholithiasis is present?

Statement

Ultrasound is strongly recommended as an initial test.

If a bile duct stone is suspected, MRI or MRCP is also strongly recommended.

Although CT has lower sensitivity for bile duct stones than MRI/MRCP, its use can also be considered.

Although endoscopic retrograde cholangiopancreatography (ERCP) is not recommended purely for diagnosis, it should be given priority when its use as a treatment is necessary.

Plain radiography is not recommended due to the radiation exposure involved and its low detection performance.

Background

Various diagnostic imaging methods have long been used to detect cholecystolithiasis and bile duct stones. Moreover, many studies have been conducted that have examined and compared the diagnostic performance of the tests. This discussion summarizes these methods and determines a recommendation level for the use of each test in clinical care. Because there have been relatively few reports of intrahepatic bile duct stones, these guidelines focused on choledocholithiasis.

1. Plain radiography

Pigment stones with a high calcium content (calcium bilirubinate stones, black stones) are X-ray-positive calculi, and 15% to 20% of all such stones have sufficient calcification to be recognized by plain radiography.[1)] Although inexpensive, plain radiography is inadequate for diagnosing cholecystocholedocholithiasis and is not recommended due to the radiation exposure involved and its low detection sensitivity.[2, 3)]

2. Ultrasound (US)

This is a safe and inexpensive test with reported accuracy of 93% for cholecystolithiasis.[4)] However, possibly because its diagnostic usefulness is assumed, there have been no recent reports on its use in diagnosis. A meta-analysis of the diagnostic performance of emergency department bedside US in cholecystolithiasis (8 articles, 710 patients) found that its sensitivity was 89.8% (95% CI, 86.4% to 92.5%), and specificity was 88% (95% CI, 83.7% to 91.4%).[5)] Its sensitivity and specificity in choledocholithiasis have been reported to be 25% and 89%, respectively,[6)] and 63% and 95%, respectively.[7)] The Japanese Society of Gastroenterology's guidelines for the diagnosis and treatment of gallstones indicate that US is useful as a primary test for gallstones and recommended it as the initial diagnostic imaging method for determining whether a bile duct stone or cholecystolithiasis is present, although problems remain regarding its detection performance in bile duct stones.

3. CT

A 1987 investigation concerning CT cholecystolithiasis detection rates found sensitivity of 79.1%, specificity of 100%, and accuracy of 89.8%.[8] The diagnostic performance of CT has improved with advances in CT systems. The guidelines for the diagnosis and treatment of gallstones strongly recommend CT as a next test to be performed after US when cholecystolithiasis is suspected. Relatively recent studies of the use of CT reported sensitivity of 65% and specificity of 84% with non-contrast-enhanced CT in bile duct stones[9] and sensitivity of 88.9%, specificity of 92.6%, and accuracy of 90.7% when CT was used with multiplanar reconstruction (MPR) in choledocholithiasis.[10] Non-contrast-enhanced CT is considered the CT standard for determining whether calculi are present. Six articles reported sensitivity of 65% to 100% and specificity of 84% to 100% with CT using drip infusion cholangiography (DIC).[11] However, this is not considered a standard test for cholecystocholedocholithiasis in view of considerations such as adverse reactions to iodine contrast media, radiation exposure, and reduced visualization with hyperbilirubinemia.

4. MRI/MRCP

A meta-analysis of 67 reports (4,711 patients) with appropriate diagnostic criteria found that the sensitivity of MRCP for biliary tract disease was 95%, and specificity was 97%. Sensitivity was 92% for calculi and 88% for malignancies.[12] It was concluded that MRCP is a noninvasive and appropriate test for biliary tract disease. However, although there have been few articles on the diagnosis of cholecystolithiasis with MRCP, as with US, there appears to be no divergence of opinion regarding its usefulness. On the other hand, a comparison of 10 articles on the diagnosis of choledocholithiasis with MRCP found that sensitivity ranged from 80% to 100%, specificity from 83% to 100%, and diagnostic accuracy from 81.3% to ≥ 95%.[13] However, it was reported that the diagnostic performance of MRCP was not high in microliths ≤ 5 mm in size.[14] Two meta-analyses (301 patients and 405 patients) of studies comparing MRCP and endoscopic ultrasound (EUS) both found no significant difference in diagnostic performance between MRCP and EUS.[15, 16] Although it has been reported that there are few cases in which ERCP is avoidable based on information from MRCP,[17] MRI and MRCP are recommended as non-invasive test methods for cholecystocholedocholithiasis in symptomatic patients.

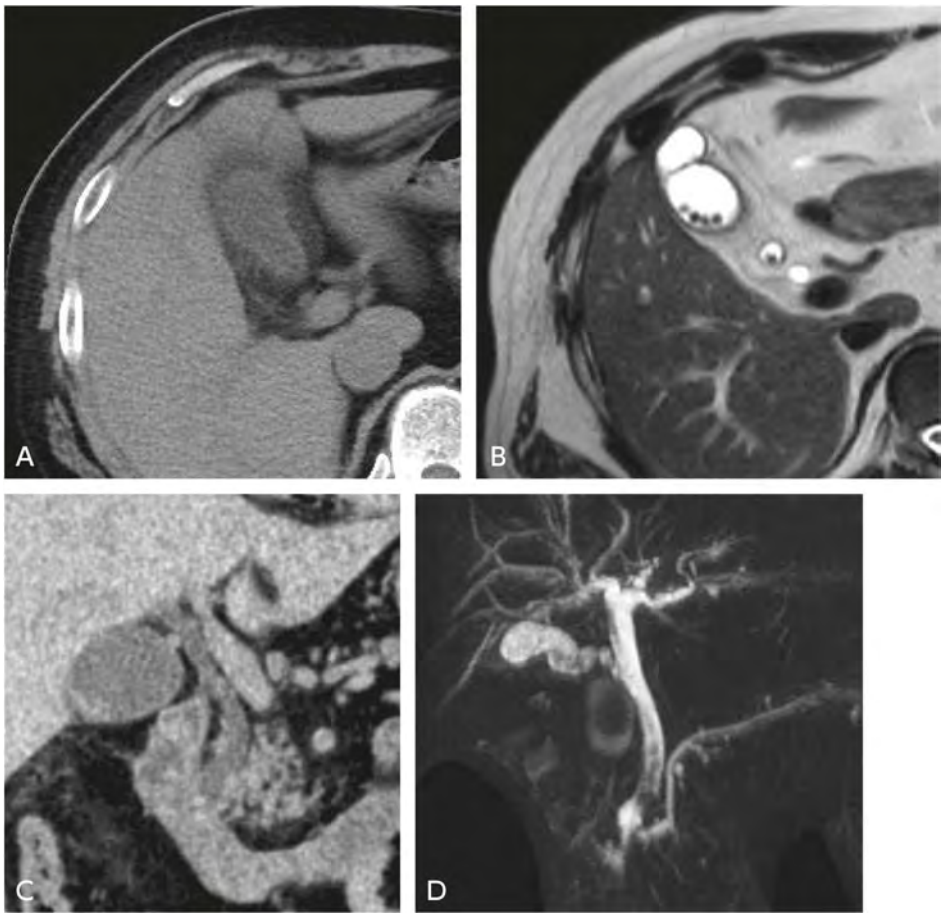

Figure Cholecystolithiasis

A: Non-contrast CT, transverse image, B: MRI, T2-weighted, transverse image, C: Non-contrast CT, coronal image, D: MRCP

In many cases, calculi cannot be visualized even with the improved image quality of the latest CT technology. Calculi in the gallbladder or common bile duct are either indistinct with non-contrast CT (A, C), they are visualized as areas of signal void on T2-weighted imaging (B) and MRCP (D).

5. ERCP

The bile duct stone detection rate of ERCP is high, and as mentioned above, it has been reported that there are few cases in which ERCP can be avoided based on information from MRCP.[17] On the other hand, ERCP carries risks that can by no means be ignored, such as a risk of pancreatitis and cholangitis.[15] Even when it is used only for diagnosis, pancreatitis occurs in 3% to 5% of patients. The mortality rate ranges from 0.2% to 0.5%. Consequently, although ERCP is not recommended purely for diagnosis, it should be given priority when its use as a treatment is necessary. Similarly, high spatial resolution and calculus detection rates have been reported with both EUS and intraductal US. However, because they are invasive tests, they are considered when a diagnosis is not obtained with MDCT or MRI/MRCP.

Search keywords and secondary sources

PubMed was searched using the following keywords: gallstones, cholecystolithiasis, choledocholithiasis detection radiography, abdominal ultrasonography tomography, X-ray computed cholangiopancreatography, magnetic resonance cholangiography, cholangiopancreatography, and endoscopic retrograde.

In addition, the following secondary sources were used as references.

1) Japanese Society of Gastroenterology, Ed.: 2016 Guidelines for the Diagnosis and Treatment of Gallstones, Revised 2nd Edition, Nankodo, 2016.

References

1) Bortoff GA et al: Gallbladder stones: imaging and intervention. Radiographics 20: 751-766, 2000
2) Eisenberg RL et al: Evaluation of plain abdominal radiographs in the diagnosis of abdominal pain. Ann Intern Med 97: 257-261, 982
3) Ahn SH et al: Acute nontraumatic abdominal pain in adult patients: abdominal radiography compared with CT evaluation. Radiology 25: 159-164, 2002
4) Bartrum RJ et al: Ultrasonic and radiographic cholecystography. N Engl J Med 296: 538-541, 1977
5) Ross M et al: Emergency physician-performed ultrasound to diagnose cholelithiasis: a systematic review. Acad Emerg Med 8: 227-235, 2011
6) Gross BH et al: Ultrasonic evaluation of common bile duct stones: prospective comparison with endoscopic retrograde cholangiopancreato raphy. Radiology 146: 471-474, 1983
7) Sugiyama M et al: Endoscopic ultrasonography for diagnosing choledocholithiasis: a prospective comparative study with ultrasonography nd computed tomography. Gastrointest Endosc 45: 143-146, 1997
8) Barakos JA et al: Cholelithiasis: evaluation with CT. Radiology 162: 415-418, 1987
9) Soto JA et al: Diagnosing bile duct stones: comparison of unenhanced helical CT, oral contrast-enhanced CT cholangiography, nd MR cholangiography. AJR Am J Roentgenol 175: 1127-1134, 2000
10) Chung WS et al: Diagnostic accuracy of multidetector-row computed tomography for common bile duct calculi: is it necessary o add non-contrast-enhanced images to contrast-enhanced images? J Comput Assist Tomogr 31: 508-512, 2007
11) Mark DH et al: Evidence-based assessment of diagnostic modalities for common bile duct stones. Gastrointest Endosc 56 (6 uppl): S190-194, 2002
12) Romagnuolo J et al: Magnetic resonance cholangiopancreatography: a meta-analysis of test performance in suspected biliary disease. Ann Intern Med 139: 547-557, 2003
13) Al Samaraee A et al: Preoperative diagnosis of choledocholithiasis: the role of MRCP. Br J Hosp Med (Lond) 70 (6): 339-343, 2009
14) Jendresen MB et al: Preoperative routine magnetic resonance cholangiopancreatography before laparoscopic cholecystectomy: a prospective study. Eur J Surg 168 (12): 690-694, 2002
15) Verma D et al: EUS vs MRCP for detection of choledocholithiasis. Gastrointest Endosc 64: 248-254, 2006
16) Ledro-Cano D: Suspected choledocholithiasis: endoscopic ultrasound or magnetic resonance cholangiopancreatography?: a systematic review. Eur J Gastroenterol Hepatol 19: 1007-1011, 2007
17) Sahai AV et al: The decision-making value of magnetic resonance cholangiopancreatography in patients seen in referral center for suspected biliary and pancreatic disease. Am J Gastroenterol 96: 2074-2080, 2001

BQ 46 Which imaging examinations are recommended if acute cholecystitis is suspected?

Statement

It is strongly recommended that ultrasound be performed initially in patients with suspected acute cholecystitis.

CT and MRI/MRCP are recommended when a definitive diagnosis is difficult based on clinical findings and ultrasonography or when local complications are suspected.

Background

Acute cholecystitis is an inflammatory disease that occurs in the gallbladder. In 85% to 95% of cases, the cause is cholecystolithiasis. Other causes include: aftereffects of surgery, trauma, or burns; long-term intravenous feeding; malignancies; hepatic arterial infusion therapy; diabetes mellitus; collagen disease; medications; infection; and torsion abnormality. A diagnosis of acute cholecystitis is established through a comprehensive assessment based on considerations such as: (1) local signs of inflammation, such as Murphy's sign or mass palpation, spontaneous pain, or tenderness in the right upper quadrant; (2) systemic inflammation findings, such as fever, or white blood cell (WBC) count or C-reactive protein (CRP) elevation; and (3) imaging findings. Diagnostic imaging plays a particularly important role in the diagnosis and severity assessment of acute cholecystitis. Ultrasonography is recommended as the imaging examination to perform initially for reasons such as its low invasiveness, widespread availability, ease of use, and cost-effectiveness. Other imaging examinations used include CT, MRI/MRCP, plain radiography, cholescintigraphy, and drip infusion cholecystocholangiography. The usefulness of ultrasonography in diagnosing acute cholecystitis and comparisons with other imaging examinations are summarized below.

Explanation

1. Usefulness of ultrasonography

Ultrasonography is the best modality for the morphological diagnosis of acute cholecystitis due to its low invasiveness, widespread availability, ease of use, and cost-effectiveness. All of the following guidelines recommend that ultrasonography be performed as the initial imaging examination in patients with suspected acute cholecystitis: the Tokyo Guidelines 2018, European Association for the Study of the Liver (EASL) Clinical Practice Guidelines, National Institute for Health and Care Excellence (NICE) Internal Clinical Guidelines, 2016 World Society of Emergency Surgery (WSES) Guidelines on acute calculous cholecystitis, and the American College of Radiology (ACR) Appropriateness Criteria® (secondary sources 1 to 6). The sensitivity of ultrasonography in diagnosing acute cholecystitis was reported to be 81% (95% CI, 75% to 87%), and specificity was reported to be 83% (95% CI, 73% to 87%).[1)] Ultrasound findings

include maximal abdominal tenderness from pressure of the ultrasound probe over the visualized gallbladder (sonographic Murphy's sign), gallbladder distention (long axis diameter ≥ 8 cm, short axis diameter ≥ 4 cm), gallbladder wall thickening (≥ 4 mm), cholecystolithiasis, debris echo, pericholecystic fluid, a sonolucent layer (hypoechoic layer) in the gallbladder wall, a striated intramural lucency, and an increased Doppler signal (Fig.).[2-7] Combining several findings can increase diagnostic accuracy.[4, 8, 9] Among them, the sonographic Murphy's sign, although of inferior sensitivity, has excellent specificity and is useful by itself for diagnosis. It is considered a more accurate finding when combined with the presence of cholecystolithiasis.[7-9] Although gallbladder wall thickening is also an important finding suggestive of acute cholecystitis, it also has many other causes, such as infection, inflammation, and tumors. It should therefore be combined with other findings, such as the presence of cholecystolithiasis and the sonographic Murphy's sign, for evaluations.[9, 10] In evaluating the severity of acute cholecystitis, attention is paid to pericholecystic abscesses, hepatic abscesses, hypoechoic areas around the gallbladder, intraluminal membranes, irregular thickening of the gallbladder wall, rupture of the gallbladder wall, and intramural/intraluminal gas, which indicates emphysematous cholecystitis.

2. CT

The diagnostic performance of CT is inferior to that of ultrasonography. It is therefore not necessary to perform CT for all patients.[11] It should be performed when definitive diagnosis is difficult based on clinical findings and ultrasonography or when local complications are suspected. Findings include gallbladder distention, gallbladder wall thickening, high-attenuation gallbladder bile, pericholecystic fluid collection, pericholecystic fat stranding, subserosal edema, transient focal enhancement of the liver adjacent to the gallbladder, focal irregularity or defect in an enhanced part of the gallbladder wall, pericholecystic abscesses, and gas in the gallbladder.[12, 13] Enhancement of the liver parenchyma around the gallbladder in the arterial phase can be an important finding in the diagnostic imaging of mild acute cholecystitis that is difficult to definitively diagnose by ultrasonography.[14, 15] CT is superior to ultrasonography and useful for diagnosing local complications such as perforation and abscess.[16, 17] Findings indicating possible gangrenous cholecystitis include intramural/intraluminal gas, intraluminal membranes, pericholecystic abscesses, and focal irregularity or a defect in an enhanced part of the gallbladder wall.[13] Findings useful for distinguishing acute cholecystitis from chronic cholecystitis are gallbladder distention, gallbladder wall thickening, pericholecystic fluid collection, and transient focal enhancement of the liver adjacent to the gallbladder. Combining multiple findings has been reported to increase diagnostic performance.[18]

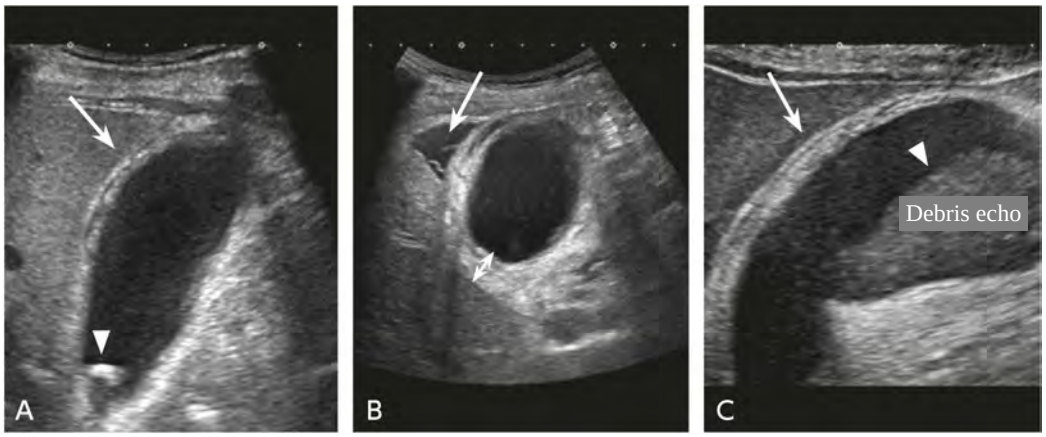

Figure　Acute cholecystitis (ultrasound appearance)

Gallbladder distention, an impacted gallstone (▷), and a sonolucent (hypoechoic) layer in the gallbladder wall (→) are seen (A).
Wall thickening (↔) and pericholecystic fluid collection (→) are seen (B).
Debris echo (▷) and a striated intramural lucency are seen (C).

3. MRI and MRCP

MRI tests provide high-density resolution and are therefore useful for diagnosing acute cholecystitis. Sensitivity of 85% (95% CI, 66% to 95%) and specificity of 81% (95% CI, 69% to 90%) have been reported for MRI, and its diagnostic accuracy is comparable to or better than that of ultrasonography.[1, 19, 20] However, the test requires the patient to remain still, and it cannot be performed in patients who have metal in their body. From the perspectives of test duration and economic considerations, its use is recommended when a definitive diagnosis cannot be obtained based on clinical findings and ultrasonography. Findings include gallbladder distention, wall thickening, mural or mucosal hyperenhancement, pericholecystic fluid collection, a high-signal area in adipose tissue around the gallbladder on T2-weighted images, transient focal enhancement of the liver adjacent to the gallbladder, and gallstones.[20, 21] The finding of a high-signal area in adipose tissue around the gallbladder on T2-weighted images is particularly useful for diagnosis.[20] Detection of stones in the gallbladder neck, cystic duct, and common bile duct with MRI/MRCP is superior to detection by ultrasonography.[19, 22] Increased enhancement of the gallbladder wall and transient focal enhancement of the liver adjacent to the gallbladder are useful for distinguishing acute from chronic cholecystitis.[21, 23]

4. Plain radiography

There are no plain radiography findings specific to acute cholecystitis. However, it can be used to diagnose conditions that need to be distinguished from acute cholecystitis, such as gastrointestinal perforation and intestinal obstruction, which makes it useful for differential diagnosis.

5. Cholescintigraphy

Although ^{99m}Tc-labeled hepatobiliary iminodiacetic acid (HIDA) uptake by the liver and excretion through the common bile duct are visualized with cholescintigraphy, acute cholecystitis can be diagnosed if the gallbladder is not visualized. Morphine-augmented cholescintigraphy, which involves administration of morphine hydrochloride, has a high diagnostic rate.[24] In severe acute cholecystitis, inflammation that extends to the surrounding liver parenchyma is visualized as the rim sign, which is considered a finding of high specificity.[25] Diagnostic sensitivity and specificity for acute cholecystitis were 94% (95% CI, 92% to 96%) and 90% (95% CI, 85% to 93%), respectively, giving cholescintigraphy the highest diagnostic accuracy of all modalities, including ultrasonography.[1] However, its use in acute cholecystitis is limited due to the test duration, level of radiation exposure, and economic considerations.

6. Drip infusion cholangiography, drip infusion cholangiography-CT

Performing plain radiography or CT imaging after intravenous drip infusion of an iodine contrast medium is a technique that can be used for morphological and functional evaluation of the gallbladder. It was previously the only cholangiographic method other than intraoperative cholangiography to be used to diagnose acute cholecystitis and cholecystolithiasis. However, it is now rarely performed because its diagnostic performance in acute cholecystitis is low,[26] superior modalities have emerged, and allergic reactions to the contrast media occur frequently.

Search keywords and secondary sources

PubMed was searched using the following keywords: cholecystitis ultrasonography tomography, X-ray computed magnetic resonance imaging radionuclide imaging cholangiography. The period searched was through June 2019.

In addition, the following secondary sources were used as references.

1) Committee on Guidelines for the Diagnosis and Treatment of Acute Cholangitis, Ed: Guidelines for the Diagnosis and Treatment of Acute Cholecystitis and Acute Cholangitis, 3rd Edition, Igakutosho Shuppan, 2018.
2) Yokoe M et al: Tokyo Guidelines 2018: diagnostic criteria and severity grading of acute cholecystitis (with videos). J Hepatobiliary Pancreat Sci 25 (1): 41-54, 2018
3) European Association for the Study of the Liver: EASL clinical practice guidelines on the prevention, diagnosis and treatment of gallstones. J Hepatol 65 (1): 146-181, 2016
4) Internal Clinical Guidelines Team: National Institute for Health and Care Excellence: clinical guidelines, in gallstone disease: diagnosis and management of cholelithiasis, cholecystitis and choledocholithiasis. National Clinical Guideline Centre, 2014
5) Ansaloni L et al: 2016 WSES guidelines on acute calculous cholecystitis. World J Emerg Surg 11: 25, 2016
6) Peterson CM et al: ACR Appropriateness Criteria®: right upper quadrant pain. J Am Coll Radiol 16: S235-S243, 2019

References

1) Kiewiet JJS et al: A systematic review and meta-analysis of diagnostic performance of imaging in acute cholecystitis. Radiology 264 (3): 708-720, 2012
2) Raghavendra BN et al: Acute cholecystitis: sonographic-pathologic analysis. Am J Roentgenol 137 (2): 327-332, 1981
3) Soyer P et al: Color velocity imaging and power Doppler sonography of the gallbladder wall: a new look at sonographic diagnosis of acute cholecystitis. AJR Am J Roentgenol 171 (1): 183-188, 1998
4) Borzellino G et al: Sonographic diagnosis of acute cholecystitis in patients with symptomatic gallstones. J Clin Ultrasound 44 (3): 152-158, 2016
5) Cohan RH et al: Striated intramural gallbladder lucencies on US studies: predictors of acute cholecystitis. Radiology 164 (1): 31-35, 1987.
6) Laing FC et al: Ultrasonic evaluation of patients with acute right upper quadrant pain. Radiology 140 (2): 449-455, 1982
7) Ralls PW et al: Prospective evaluation of the sonographic Murphy sign in suspected acute cholecystitis. J Clin Ultrasound 10 (3): 113-115, 1982
8) Bree RL: Further observations on the usefulness of the sonographic Murphy sign in the evaluation of suspected acute cholecystitis. J Clin Ultrasound 23: 169-172, 1995
9) Ralls PW et al: Real-time sonography in suspected acute cholecystitis: prospective evaluation of primary and secondary signs. Radiology 155 (3): 767-771, 1985
10) van Breda Vriesman AC et al: Diffuse gallbladder wall thickening: differential diagnosis. AJR Am J Roentgenol 188 (2): 495-501, 2007
11) Harvey RT, Miller WT Jr: Acute biliary disease: initial CT and follow-up US versus initial US and follow-up CT. Radiology 213 (3): 831-836, 1999
12) Fidle J et al: CT evaluation of acute cholecystitis: findings and usefulness in diagnosis. AJR Am J Roentgenol 166 (5): 1085-1088, 1996
13) Bennett GL et al: CT findings in acute gangrenous cholecystitis. AJR Am J Roentgenol 178 (2): 275-281, 2002
14) Kim YK et al: CT findings of mild forms or early manifestations of acute cholecystitis. Clin Imaging 33 (4): 274-280, 2009
15) Ito K et al: Gallbladder disease: appearance of associated transient increased attenuation in the liver at biphasic, contrast-enhanced dynamic CT Radiology 204 (3): 723-728, 1997
16) Terrier F et al: Computed tomography in complicated cholecystitis. J Comput Assist Tomogr 8 (1): 58-62, 1984
17) Kim PN et al: Gallbladder perforation: comparison of US findings with CT. Abdom Imaging 19 (3): 239-242, 1994
18) Yeo DM, Jung SE: Differentiation of acute cholecystitis from chronic cholecystitis: determination of useful multidetector computed tomography findings. Medicine (Baltimore) 97 (33): e11851, 2018
19) Hakansson K et al: MR imaging in clinically suspected acute cholecystitis: a comparison with ultrasonography. Acta Radiol 41 (4): 322-328, 2000
20) Regan F et al: The diagnostic utility of HASTE MRI in the evaluation of acute cholecystitis: half-Fourier acquisition single-shot turbo SE. J Comput Assist Tomogr 22 (4): 638-642, 1998
21) Kaura SH et al: Comparison of CT and MRI findings in the differentiation of acute from chronic cholecystitis. Clin Imaging 37 (4): 687-691, 2013
22) Park MS et al: Acute cholecystitis: comparison of MR cholangiography and US. Radiology 209 (3): 781-785, 1998
23) Altun E et a: Acute cholecystitis: MR findings and differentiation from chronic cholecystitis. Radiology 244 (1): 174-183, 2007
24) Flancbaum L, Alden SM: Morphine cholescintigraphy. Surg Gynecol Obstet 171 (3): 227-232, 1990
25) Bushnell DL et al: The rim sign: association with acute cholecystitis. J Nucl Med 27 (3): 353-356, 1986
26) Eubanks B et al: Current role of intravenous cholangiography. Am J Surg 143 (6): 731-733, 1982

BQ 47 Which imaging examinations are recommended if acute cholangitis is suspected?

Statement

It is recommended that ultrasonography and CT be used in a complementary fashion when acute cholangitis is suspected.

Background

Acute cholangitis is a pathophysiology in which the biliary tract becomes obstructed for any reason, resulting in cholestasis and abnormal bacterial growth. Elevated intraductal pressure causes reflux of infected bile from the bile duct to the veins, resulting in systemic infection. Because the patient's condition may worsen rapidly due to sepsis, acute cholangitis requires a rapid and appropriate response. The diagnostic criteria for acute cholangitis are that the diagnosis is definitive if one item in A, one item in B, and one item in C of the following is seen and that acute cholangitis is suspected if one item in A and one item in either B or C are seen: A, a finding indicating systemic inflammation (fever, inflammatory response on blood tests); B, a finding indicating cholestasis (jaundice, abnormal liver function test); and C, an imaging finding indicating the presence of a bile duct lesion [bile duct dilatation, a cause of cholangitis (e.g., bile duct stenosis, bile duct stone, or a stent)]. That is, diagnostic imaging has major significance in acute cholangitis that can be summarized under 2 categories: determining whether there is a biliary tract occlusion or dilatation; and diagnosing the cause of occlusion. Diagnostic imaging is also useful for evaluating complications such as abscess formation and portal vein thrombosis and distinguishing acute cholangitis from other disorders. Severity is evaluated based on the usual clinical information. Consequently, no diagnostic imaging criteria are used for this purpose.

Explanation

1. Ultrasonography

In patients with suspected acute cholangitis, ultrasonography is the test that should be performed initially, being the best modality in terms of simplicity, low invasiveness, widespread availability, and economy.[1, 2)] Although the test findings include biliary tract dilatation, thickening of the bile duct wall, and biliary tract emphysema, all are nonspecific.[3)] If a bile duct stone is visualized in addition to these findings, it provides stronger evidence for a diagnosis. However, the sensitivity of a diagnosis of choledocholithiasis based on ultrasonography ranges from 25% to 68%, which cannot be considered adequate.[4)] It also has shortcomings such as the fact that the accuracy of an ultrasound test can depend on the skill of the operator and the condition of the patient (e.g., unable to hold breath or remain still, marked intestinal gas, comorbid pneumobilia).[5)]

2. CT

Compared with ultrasonography, CT makes a broader range of diagnoses possible and provides better objectivity. The CT findings in cholangitis are nonspecific findings, such as biliary tract dilatation, biliary tract emphysema, and thickening of the bile duct wall. In addition, inhomogeneous enhancement of the liver as a whole in the arterial phase of dynamic CT has been reported to be indicative of active inflammation (Figs. 1 and 2).[6] Dynamic CT is also useful for determining the cause of a bile duct obstruction, such as a calculus or pancreaticobiliary tumor, and for evaluating whether a complication such as a hepatic abscess or portal vein thrombosis is present (Figs. 1 and 2). Although tests such as non-contrast CT are useful for identifying a stone as the cause of an obstruction,[7] the absorption value of the calculus depends on calcium concentration (calcium phosphate, calcium carbonate) in the calculus. Consequently, the detection sensitivity of CT for bile duct stones is only 25% to 90%.[8, 9]

3. MRI and MRCP

Both MRI and MRCP are also useful for visualizing bile duct stones that cause obstruction[10, 11] and for visualizing malignant disease.[10, 12] Because they can elucidate the biliary system as a whole, they are also useful for guidance during drainage. Although their diagnostic performance in choledocholithiasis is excellent, with sensitivity and specificity both ≥ 90%,[10, 11, 13] decreased sensitivity has been reported for small calculi (≤ 6 mm).[11, 14] They are not first-line tests from the perspectives of widespread availability and simplicity. However, they are suitable for evaluation when the cause of bile duct stenosis cannot be determined by ultrasound or CT. Although it is excellent for evaluating bile duct stenosis caused by obstructions such as bile duct stones or tumors,[15] ERCP is an invasive test performed for treatment (drainage) purposes and is not used solely for diagnosis.

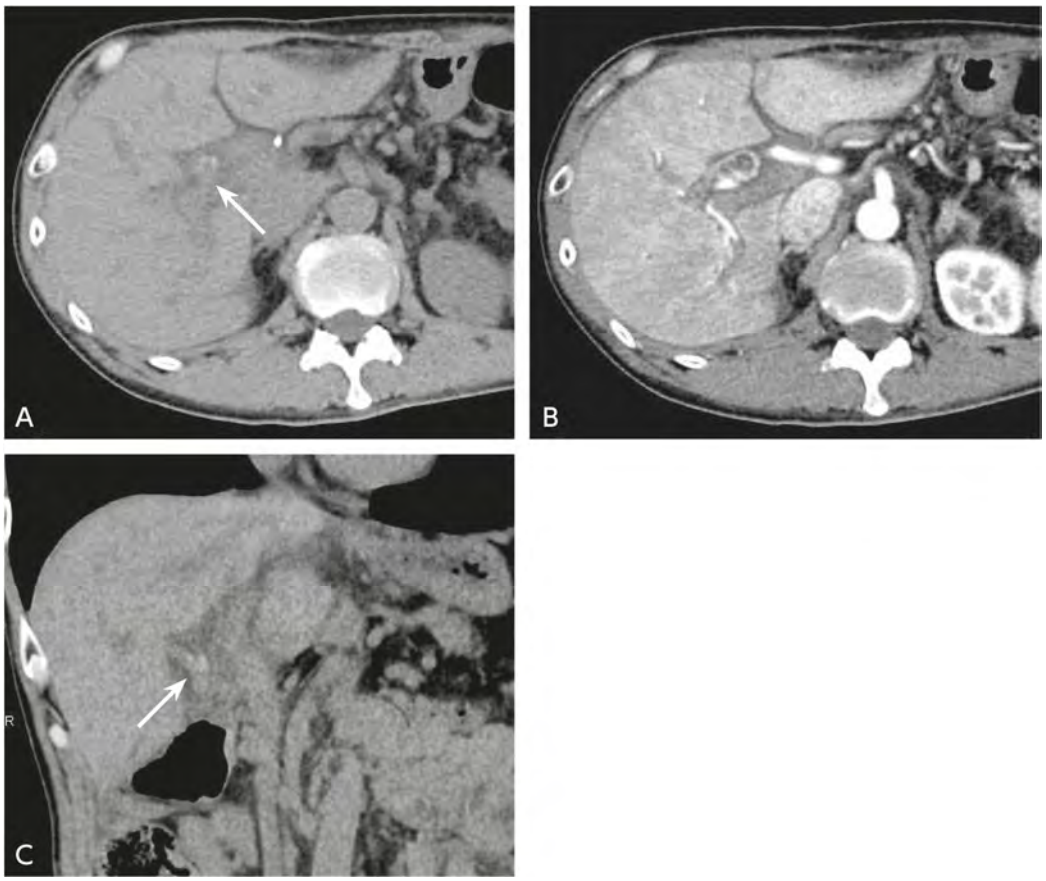

Figure 1. Concomitant bile duct stone impaction and acute cholangitis (man in his 60s)

A: Non-contrast CT, transverse image; B: Contrast-enhanced CT, arterial phase transverse image; C: Non-contrast CT, coronal image

Hyperdense calculi (→) are seen in the bile duct on non-contrast CT. On contrast-enhanced CT, wall thickening and enhancement of the bile duct are seen, with diffuse inhomogeneous enhancement of the liver parenchyma. The findings are suggestive of acute cholangitis.

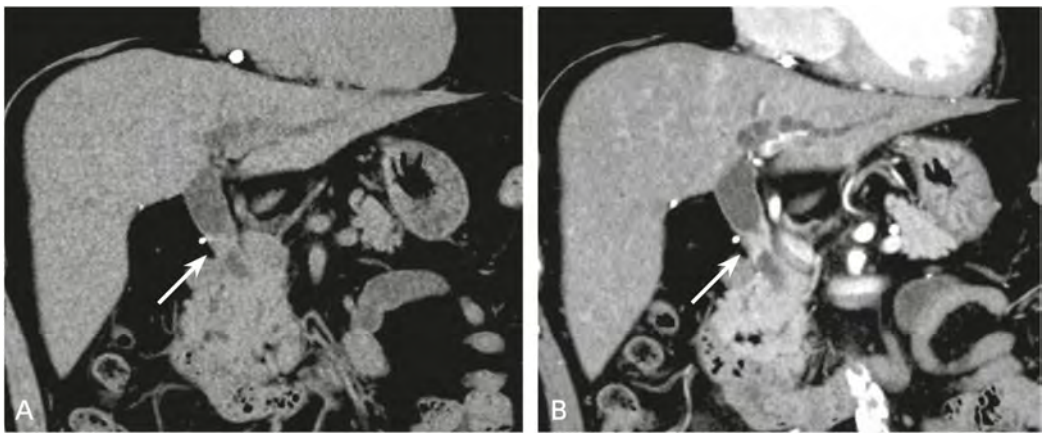

Figure 2. Concomitant bile duct cancer and acute cholangitis (man in his 60s)

A: Non-contrast CT, coronal image; B: Contrast-enhanced CT, arterial phase, coronal image

On non-contrast CT, wall thickening is seen in the distal bile duct, along with distinct contrast enhancement (→). The upstream portion of the bile duct is dilated, and inhomogeneous contrast enhancement is seen in the liver parenchyma, indicating concomitant cholangitis.

Search keywords and secondary sources

PubMed was searched using the following keywords: cholangitis and radiography, ultrasonography computed tomography, magnetic resonance imaging, and endoscopic retrograde cholangiopancreatography.

In addition, the following secondary sources were used as references.

1) Committee for the Revision and Publication of Guidelines for the Diagnosis and Treatment of Acute Cholangitis and Cholecystitis, Ed: 2018 Guidelines for the Diagnosis and Treatment of Acute Cholangitisand Cholecystitis, Igakutosho Shuppan, 2018.
2) Kiriyama S et al: Tokyo Guidelines 2018: diagnostic criteria and severity grading of acute cholangitis (with videos). J Hepatobiliary Pancreat Sci 25: 17-30, 2018

References

1) Rosen CL et al: Ultrasonography by emergency physicians in patients with suspected cholecystitis. Am J Emerg Med 19: 32-36, 2001
2) Kendall JL, Shimp RJ: Performance and interpretation of focused right upper quadrant ultrasound by emergency physicians. The J Emerg Med 21: 7-13, 2001
3) Lameris JS, van Overhagen H: Imaging and intervention in patients with acute right upper quadrant disease. Bailliere's Clin Gastroenterol 9: 21-36, 1995
4) Gandolfi L et al: The role of ultrasound in biliary and pancreatic diseases. Eur J Ultrasound 16: 141-159, 2003
5) Rickes S et al: Impact of the operator's experience on value of high-resolution transabdominal ultrasound in the diagnosis of choledocholithiasis: a prospective comparison using endoscopic retrograde cholangiography as the gold standard. Scand J Gastroenterol 41: 838-843, 2006
6) Arai K et al: Dynamic CT of acute cholangitis: early inhomogeneous enhancement of the liver. AJR Am J Roentgenol 181: 115-118, 2003
7) Balthazar EJ et al: Acute cholangitis: CT evaluation. J Comput Assist Tomogr 17: 283-289, 1993
8) Lee JK et al: Diagnosis of intrahepatic and common duct stones: combined unenhanced and contrast-enhanced helical CT in 1090 patients. Abdom Imaging 31: 425-432, 2006
9) Patel NB et al: Multidetector CT of emergent biliary pathologic conditions. Radiographics 33: 1867-1888, 2013
10) Lomanto D et al: Magnetic resonance-cholangiopancreatography in the diagnosis of biliopancreatic diseases. Am J Surg 174: 33-38, 1997
11) Laokpessi A et al: Value of magnetic resonance cholangiography in the preoperative diagnosis of common bile duct stones. Am J Gastroenterol 96: 2354-2359, 2001
12) Fulcher AS et al: Half-Fourier rare MR cholangiopancreatography: experience in 300 subjects. Radiology 207: 21-32, 1998
13) Verma D et al: EUS vs MRCP for detection of choledocholithiasis. Gastrointest Endosc 64: 248-254, 2006
14) Zidi SH et al: Use of magnetic resonance cholangiography in the diagnosis of choledocholithiasis: prospective comparison with a reference imaging method. Gut 44: 118-122, 1999
15) Lai EC et al: Endoscopic biliary drainage for severe acute cholangitis. N Engl J Med 326: 1582-1586, 1992

J Roentgenol 190: 396-405, 2008

FQ 6 Is contrast-enhanced CT recommended when gallbladder cancer is suspected?

Statement

Although the supporting evidence for its use in distinguishing gallbladder cancer from cholecystitis and in evaluating metastasis cannot be considered sufficient, contrast-enhanced CT is recommended for qualitative diagnosis and determining a treatment strategy when gallbladder cancer is suspected.

Background

When gallbladder wall thickening or a protruding lesion is seen, in addition to benign diseases such as cholecystitis and gallbladder adenomyomatosis, gallbladder cancer should be considered. Transabdominal ultrasonography is generally used as the primary screening test for gallbladder lesions, and contrast-enhanced CT is the most frequently used as the detailed diagnostic imaging method, because it provides high spatial resolution and can be used to evaluate not only the features of gallbladder lesions, but also progression into surrounding tissue. These guidelines show that contrast-enhanced CT is useful for differentiating from benign conditions and determining a treatment strategy when gallbladder cancer is suspected. In addition, it is considered a recommendation grade when comparing contrast-enhanced CT with other imaging modalities such as MRI.

Explanation

With multiphase dynamic contrast-enhanced CT, vascular anatomy and local blood flow can be evaluated, and one can evaluate gallbladder lesions from multiple directions using multiplanar reconstruction. Consequently, good diagnostic accuracy of 84% to 85% has been shown in staging gallbladder cancer with contrast-enhanced CT.[1, 2)] In addition, preoperative vascular mapping has been used by creating 3D CT angiograms. On the other hand, although there has been a somewhat small number of reports on the evaluation of gallbladder cancer using MRI, MRCP is superior for evaluating bile duct invasion and obtaining anatomical information on the bile duct (e.g., pancreaticobiliary maljunction).[3)] Moreover, EOB-MRI has been reported to be useful for evaluating liver invasion[4)] and screening for hepatic metastases.[5)]

The morphology of gallbladder cancer can be mainly classified into the following 3 types: (1) protruding lesions (polypoid lesions); (2) lesions with thickened walls; and (3) massive masses with direct liver invasion. In protruding lesions, a size ≥ 1 cm and morphological features such as having a broad base are important findings suggestive of malignancy, and the additional blood flow evaluation based on multiphase imaging is helpful in the diagnosis. In the case of gallbladder cancer, the difference in the CT numbers in the portal venous and equilibrium phases is small (≤ 10 HU, as a rule) on 3-phase dynamic contrast-enhanced CT (arterial, portal venous, and equilibrium phases) because there is a tendency for

delayed enhancement due to fibrosis in gallbladder cancer, and this is useful as an index for differentiating from benign lesions.[6] Investigations of the differential diagnosis of benign and malignant lesions using diffusion-weighted MRI images reported sensitivity of 78% to 97% and specificity of 78% to 92%.[7, 8] In lesions with thickened walls, early enhancement of the smooth inner layer of the luminal surface is a finding suggestive of chronic cholecystitis, and, on the other hand, the findings of luminal surface irregularity, laminar tearing, and thick inner layer enhancement suggest gallbladder cancer. However, neither CT nor MRI can provide adequate diagnostic performance in distinguishing benign from malignant lesions.[9, 10] In advanced cancers appearing as massive masses, assessing whether there is arterial or portal venous–invasion and evaluating distant metastasis, particularly lymph node and liver metastases, are important for determining a treatment strategy, and for this purpose, CT and MRI are superior to other modalities.[11, 12, 13-15] In particular, contrast-enhanced CT is superior to MRI, because it can rapidly scan extensive areas at one time and elucidate anatomical locations in detail (including blood vessel variations).

Visualization of Rokitansky-Aschoff sinuses (RASs) in the lesion wall by MRCP is useful for differentiating from gallbladder adenomyomatosis.[16] In addition, it has been reported that a similar finding (cotton ball sign) can be identified with high sensitivity by contrast-enhanced CT imaging, and that it is also useful for the differential diagnosis.[17] Diagnosing local invasion depth is important for deciding on an operative procedure and for prognosis prediction. The diagnostic accuracy of invasion depth diagnosis (T-stage classification) using CT has been reported to be between 71% and 93%, indicating relatively high diagnostic performance.[18-21] On contrast-enhanced MRI, delayed enhancement of the base of a protruding gallbladder cancer lesion (subserosal enhancement) has been reported to be an indicator of subserosal invasion (T2).[22] However, for intramural lesions of stage T2 or lower, EUS, which can visualize the layered structure of the gallbladder wall, is the best modality.[9, 12, 23] For lesions of stage T3 or higher that invade beyond the serosa, as in the case of direct liver invasion, CT is superior even to EUS, which has a limited scope of observation. Sensitivity of 80% to 100% and specificity of 81% to 95% have been reported with CT.[9-12, 18, 24] In addition, the diagnostic performance of MRI is nearly equal to that of CT, the sensitivity and specificity of MRI being 67% to 100% and 86% to 100%, respectively.[9, 13-15]

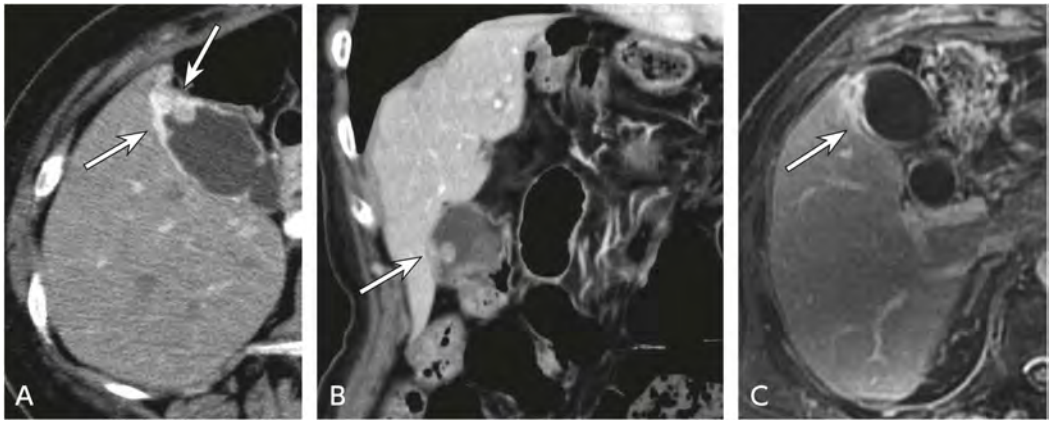

Figure 1. Gallbladder cancer, T2

A: CT, arterial phase; B: CT, portal venous phase, MPR, coronal image; C: EOB-MRI, portal venous phase
An irregularly shaped protruding lesion with a broad base that is showing inhomogeneous enhancement is seen in at the base of the gallbladder. Enhancement of the wall around the base of the protruding lesion (subserosal enhancement, →) is seen on both CT and MRI, suggesting subserosal invasion (T2). In the MPR coronal image, the border with the liver is distinct, and liver invasion can be concluded to be absent.

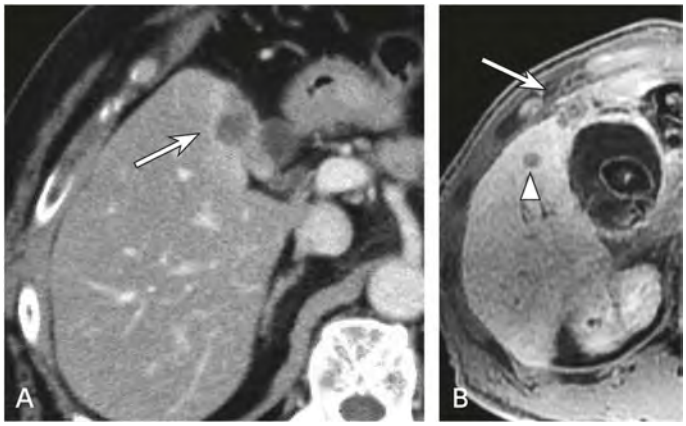

Figure 2. Gallbladder cancer, T3aM1 liver invasion

A: CT, portal venous phase; G: EOB-MRI, hepatobiliary phase, 20 min
An enhanced mass (→) is seen at the base of the gallbladder, mainly at the border, and is invading the liver. Similarly, a mass that is invading the liver is seen in the hepatobiliary phase of EOB-MRI, and hepatic metastasis (▷) showing low signal intensity is also seen nearby.

The sensitivity of MRI for lymph node metastasis has been reported to be 75%, slightly better than that of CT.[25)] However, it is currently diagnosed based only on size (≥ 1 cm) and morphology (round), and diagnostic accuracy is therefore limited to < 80%.[26, 27)]

To summarize, contrast-enhanced CT enables multiplanar reconstruction images to be evaluated, is excellent for gallbladder cancer staging, and is also used for vascular mapping. It is therefore the core test for determining a treatment strategy, including aspects such as an operative procedure, and its use is recommended. Additional information that differs from that obtained with CT can be obtained with MRI. MRI is useful for evaluating the biliary tract using MRI/MRCP and liver metastasis using EOB-MRI, and diffusion-weighted imaging aids in distinguishing benign from malignant lesions. On the other hand, for

intramural lesions (≤ T2) in early-stage gallbladder cancer, contrast-enhanced CT and MRI, whose ability to visualize the layered structure of the wall is limited, are lacking in usefulness. A test that provides high local resolution, such as EUS, is better for diagnosing such lesions. The diagnostic performance of contrast-enhanced CT in evaluating gallbladder cancer is also expected to improve in the future, and continued verification is needed.

Search keywords and secondary sources

PubMed was searched using the following keywords: gallbladder cancer, gallbladder carcinoma, gallbladder malignant, CT, and MRI. The appropriate articles from among the 304 relevant articles identified were included in a hand search.

References

1) Kalra N et al: MDCT in the staging of gallbladder carcinoma. Am J Roentgenol 186: 758-762, 2006
2) Kim SJ et al: Accuracy of preoperative T-staging of gallbladder carcinoma using MDCT. Am J Roentgenol 190: 74-80, 2008
3) Kim JH et al: Preoperative evaluation of gallbladder carcinoma: efficacy of combined use of MR imaging, MR cholangiography, and contrast-enhanced dual-phase three-dimensional MR angiography. J Magn Reson Imaging 16: 676-684, 2002
4) Hwang J et al: Gadoxetic acid-enhanced MRI for T-staging of gallbladder carcinoma: emphasis on liver invasion. Br J Radiol 87 (1033): 20130608, 2014
5) Palmucci S: Focal liver lesions detection and characterization: the advantages of gadoxetic acid-enhanced liver MRI. World J Hepato 6 (7): 477-485, 2014
6) Zhou W et al: Triphasic dynamic contrast-enhanced computed tomography in the differentiation of benign and malignant gallbladder polypoid lesions. J Am Coll Surg 225 (2): 243-248, 2017
7) Ogawa T et al: High b-value diffusion-weighted magnetic resonance imaging for gallbladder lesions: differentiation between benignity and malignancy. J Gastroenterol 47 (12): 1352-1360, 2012
8) Lee NK et al: Diffusion-weighted MRI for differentiation of benign from malignant lesions in the gallbladder. Clin Radiol 69: 78-85, 2014
9) Rodríguez-Fernández A et al: Application of modern imaging methods in diagnosis of gallbladder cancer. J Surg Oncol 93: 650-664, 2006
10) Onoyama H et al: Diagnostic imaging of early gallbladder cancer: retrospective study of 53 cases. World J Surg 23: 708-712, 1999
11) Kumaran V et al: The role of dual-phase helical CT in assessing resectability of carcinoma of the gallbladder. Eur Radiol 12: 1993-1999, 2002
12) Reid KM et al: Diagnosis and surgical management of gallbladder cancer: a review. J Gastrointest Surg 11: 671-681. 2007
13) Schwartz LH et al: Gallbladder carcinoma: findings at MR imaging with MR cholangiopancreatography. J ComputAssist Tomogr 26: 405-410, 2002
14) Kim JH et al: Preoperative evaluation of gallbladder carcinoma: efficacy of combined use of MR imaging, MR cholangiography and contrast-enhanced dual-phase three-dimensional MR angiography. J Magn Reson Imaging. Dec 16: 676-684, 2002
15) Kaza RK et al: Evaluation of gall bladder carcinoma with dynamic magnetic resonance imaging and magnetic resonance cholangiopancreatography Australas Radiol 50: 212-217, 2006
16) Haradome H et al: The pearl necklace sign: an imaging sign of adenomyomatosis of the gallbladder at MR cholangiopancreatography. Radiology 227: 80-88, 2003
17) Yang HK et al: CT diagnosis of gallbladder adenomyomatosis: importance of enhancing mucosal epithelium, the “cotton ball sign” Eur Radiol 28 (9): 3573-3582, 2018
18) Yoshimitsu K et al: Helical CT of the local spread of carcinoma of the gallbladder: evaluation according to the TNM system in patients who underwent surgical resection. AJR Am J Roetngenol 179: 423-428, 2002

19) Kim SJ et al: Accuracy of preoperative T-staging of gallbladder carcinoma using MDCT. AJR Am J Roetngenol 190: 74-80, 2008
20) Kumaran V et al: The role of dual-phase helical CT in assessing resectability of carcinoma of the gallbladder. Eur Radiol 12: 1993-1999, 2002
21) Kim BS et al: Accuracy of CT in local staging of gallbladder carcinoma. Acta Radiol 43: 71-76, 2002
22) Yoshimitsu K et al: Magnetic resonance differentiation between T2 and T1 gallbladder carcinoma: significance of subserosal enhancement on the delayed phase dynamic study. Magn Reson Imaging 30 (6): 854-859, 2012
23) Sadamoto Y et al: Preoperative diagnosis and staging of gallbladder carcinoma by EUS. Gastrointest Endosc 58: 536-541, 2003
24) Li B et al: Computed tomography for assessing resectability of gallbladder carcinoma: a systematic review and meta-analysis. Clin Imaging 37: 327-33, 2013
25) de Savornin Lohman EAJ et al: The diagnostic accuracy of CT and MRI for the detection of lymph node metastases in gallbladder cancer: a systematic review and meta-analysis. Eur J Radiol 110: 156-162, 2019
26) Ohtani T et al: Carcinoma of the gallbladder: CT evaluation of lymphatic spread. Radiology 189: 875-880, 1993
27) Lee SW et al: Clinical usefulness of 18F-FDG PET-CT for patients with gallbladder cancer and cholangiocarcinoma. J Gastroenterol 45: 560-566, 2010

FQ 7 Is contrast-enhanced CT recommended when extrahepatic bile duct cancer is suspected?

Statement

When extrahepatic bile duct cancer is suspected, contrast-enhanced CT is recommended for diagnosis and to evaluate local progression, although the evidence supporting its use to differentiate from cholangitis and evaluate metastasis is inadequate.

Background

When bile duct stenosis is suspected, consideration is given to malignancies, typified by bile duct cancer, and to benign stenosis such as cholangitis and traumatic and postoperative stenosis. However, distinguishing between them is not necessarily easy and currently often relies on cytology. When bile duct cancer is diagnosed, it is clinically important to evaluate whether surgery is indicated. CT is the most frequently used diagnostic imaging modality, and these guidelines show the diagnostic performance of contrast-enhanced CT in diagnosing extrahepatic bile duct cancer and determining operability. In addition, they consider a recommendation grade when comparing contrast-enhanced CT with other imaging modalities such as MRI.

Explanation

Distinguishing benign from malignant bile duct stenosis is not necessarily easy. It is often a struggle to differentiate bile duct cancer from benign stenosis such as traumatic and postoperative stenoses, particularly forms of cholangitis such as primary sclerosing cholangitis and IgG4-related sclerosing cholangitis.[1-3] For bile duct stenosis localized to the hilar or distal bile duct, distinguishing IgG4-related sclerosing cholangitis from bile duct cancer is often clinically problematic.[4] However, there have been few reports on the use of contrast-enhanced CT/MRI in differentiating these conditions. In diagnosing bile duct cancer based on imaging, the detection of tumors, lymph node metastasis, vascular invasion, and remote metastasis is instructive.[5-7] However, it has been reported that when these findings are lacking, tapered, funnel-shaped stenosis of the bile duct is suggestive of IgG4-related sclerosing cholangitis, and abrupt stenosis of the bile duct is suggestive of bile duct cancer (Figs. 1 and 2).[8, 9] However, there is no established view on differentiation between these conditions for imaging findings related to the thickness and contrast enhancement of the bile duct wall.[8-11] The examination above indicates that there is currently little evidence regarding differentiation between bile duct cancer and benign bile duct stenosis based on contrast-enhanced CT, and that further investigation is needed in this area.

On the other hand, MRCP is useful for visualizing the dilated bile duct upstream from a stenosis and is particularly good for visualizing the extent of stenosis and multiple bile duct stenoses.[12, 13] Diagnostic accuracy of ≥ 90% has been reported with MRCP alone in diagnosing primary sclerosing cholangitis,

which is characterized by multifocal bile duct stenoses.[13, 14] However, the diagnostic performance of MRCP alone for the differential diagnosis of bile duct obstruction is not currently considered adequate. Moreover, diffusion-weighted imaging or dynamic study with three-dimensional fat-suppressed T1-weighted imaging has been reported to contribute to the detection and staging of bile duct cancer.[15] However, further investigation is needed regarding the use of MRI to distinguish malignant from benign lesions.

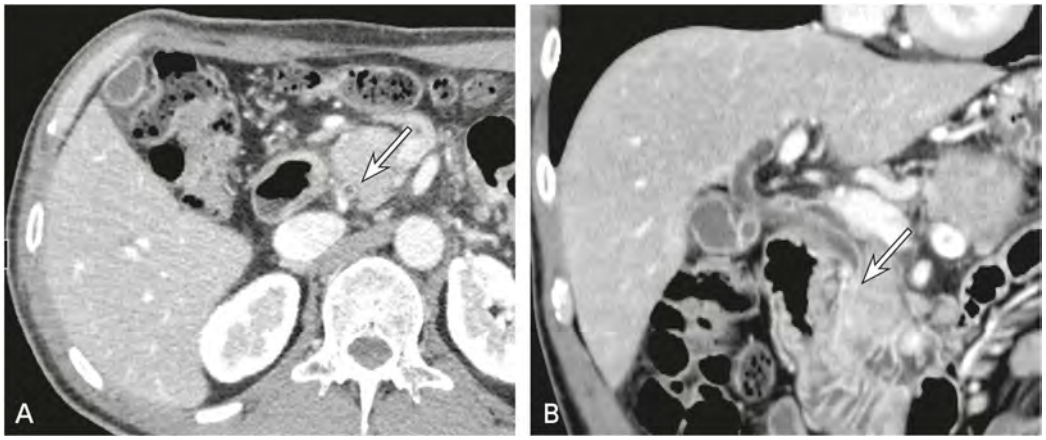

Figure 1. IgG4-related sclerosing cholangitis

A: Contrast-enhanced CT, transverse image: Thickening of the full circumference of the bile duct wall is seen with contrast enhancement (→).

B: Contrast-enhanced CT, coronal image: Funnel-shaped, tapered stenosis is seen from the upper to the lower part of the bile duct (→).

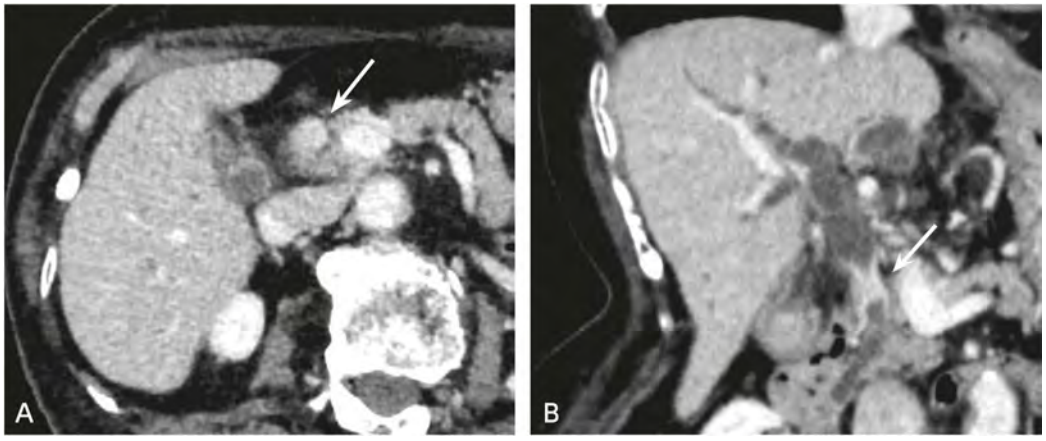

Figure 2. Distal bile duct cancer

A: Contrast-enhanced CT, transverse image: Obstruction and thickening of the full circumference of the bile duct wall are seen with contrast enhancement (→).

B: Contrast-enhanced CT, MPR, coronal image: Abrupt stenosis of the middle and lower bile duct and dilatation of the upstream bile duct are seen (→).

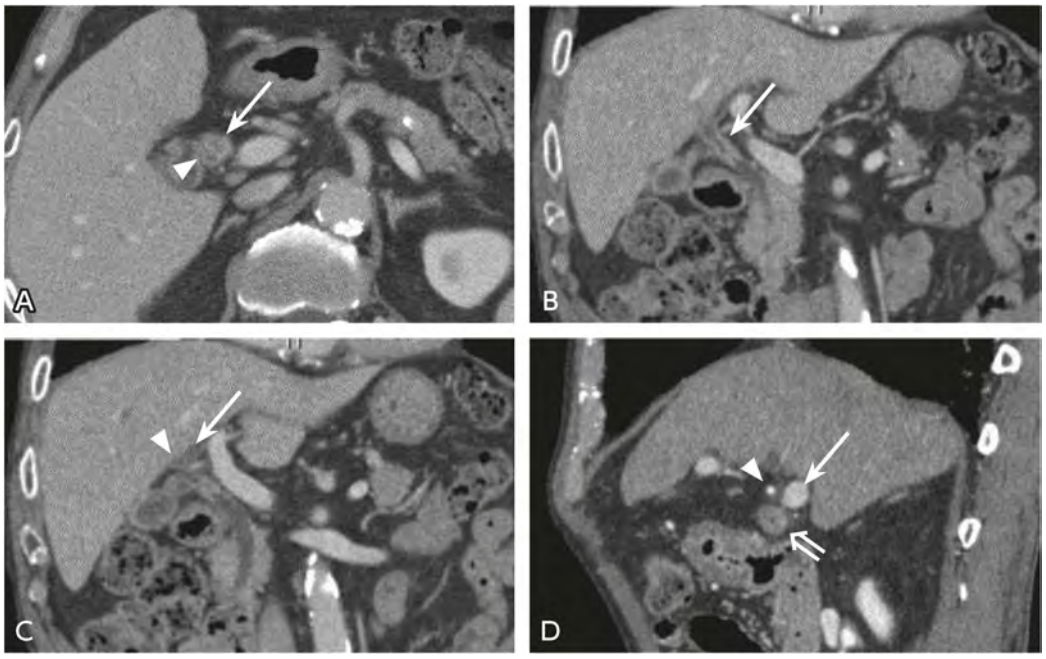

Figure 3. Hilar cholangiocarcinoma

A: Contrast-enhanced CT, transverse image: Wall thickening and enhancement are seen in the common hepatic duct (→) and cystic duct (▷).

B: Contrast-enhanced CT, MPR, coronal image: Wall thickening and enhancement of the common hepatic duct (→) extend caudally, but there are no findings in the downstream portion of the bile duct.

C: Contrast-enhanced CT, MPR, coronal image, 7 ventral slices of B: Neither wall thickening nor enhancement is seen in the left hepatic duct (→) or right hepatic duct (▷).

D: Contrast-enhanced CT, MPR, sagittal image: The wall thickening and enhancement of the common hepatic duct (⇒) are seen to be separated from the right hepatic artery (▷) and portal vein (→).

Contrast-enhanced CT is suitable for obtaining general anatomical information, and it enables the sites of bile duct cancer and the extent of progression into the surrounding areas to be evaluated.[16, 17] Factors considered in judging operability based on imaging include progression along the bile duct, invasion of the hepatic artery and portal vein, the presence or absence of lymph node metastasis, and the presence or absence of distant metastasis. A meta-analysis of these factors found diagnostic accuracy of 86% for progression along the bile duct as determined by contrast-enhanced CT (Fig. 3).[18] Sensitivity and specificity of 83% and 93%, respectively, have been reported for the presence or absence of hepatic artery invasion and 89% and 92%, respectively, for the presence or absence of portal vein invasion. Thus, high diagnostic performance has been found for both. For lymph node invasion, however, specificity was maintained at 88%, but sensitivity decreased to 61%. A meta-analysis by Zhang et al. found that evaluations of operability that took into account the presence or absence of distant metastasis provided sensitivity of 95%, whereas specificity decreased to 69%.[19] The findings suggest that problems remain with the evaluation of microscopic distant metastases, including lymph node invasion and liver metastases. Although MRI/MRCP is considered an alternative to contrast-enhanced CT as a diagnostic imaging method, the meta-analysis by Zhang et al. found that, in evaluations of operability, the sensitivity and specificity of

MRI/MRCP were 94% and 71%, respectively, indicating diagnostic performance equal to that of contrast-enhanced CT.[19] However, there have been few reports on this subject, and investigations that have made comparisons in the same subjects are limited in number.[20, 21] A candidate diagnostic imaging method for supplementing evaluations of lymph node invasion and distant metastasis performed using contrast-enhanced CT is FDG-PET. The sensitivity of FDG-PET for lymph node invasion and distant metastasis (75.9% and 88.3%, respectively) has been reported to be significantly higher than that of contrast-enhanced CT (60.9% and 78.7%, respectively).[20] Consequently, although contrast-enhanced CT shows good diagnostic performance for local progression, its diagnostic performance in evaluating metastasis is limited. The diagnostic performance of contrast-enhanced CT in extrahepatic bile duct cancer is expected to improve with further technological innovation, and continual verification will be required in the future.

Search keywords and secondary sources

PubMed was searched using the following keywords: contrast-enhanced, CT, MRI, MRCP, extrahepatic cholangiocarcinoma, sensitivity, specificity, accuracy, ROC, cholangitis, and human. The period searched was from January 1989 to August 2020, and 519 articles were extracted in the primary screening. After an additional hand search was performed, the 21 articles extracted were examined in the secondary screening.

References

1) Hayashi K et al: Autoimmune sclerosing cholangiopancreatitis with little pancreatic involvements by imaging findings. Hepatogastroenterology 54: 2146-2151, 2007
2) Hamano H et al: Immunoglobulin G4-related lymphoplasmacytic sclerosing cholangitis that mimics infiltrating hilar cholangiocarcinoma: part of a spectrum of autoimmune pancreatitis? Gastrointest Endosc 62: 152-157, 2005
3) Kuroiwa T et al: Bile duct involvement in a case of autoimmune pancreatitis successfully treated with an oral steroid. Dig Dis Sci 47: 1810-1816, 2002
4) Takahiro N et al: Diagnostic procedures for IgG4-related sclerosing cholangitis. J Hepatobiliary Pancreat Sci 18: 127-36, 2011
5) Choi SH et al: Differentiating malignant from benign common bile duct stricture with multiphasic helical CT. Radiology 236: 178-183, 2005
6) Rosch T et al: A prospective comparison of the diagnostic accuracy of ERCP, MRCP, CT, and EUS in biliary strictures. Gastrointest Endosc 55: 870-876, 2002
7) Park MS et al: Differentiation of extrahepatic bile duct cholangiocarcinoma from benign stricture: findings at MRCP versus ERCP. Radiology 233: 234-240, 2004
8) Yata M et al: Comparison of the multidetector-row computed tomography findings of IgG4-related sclerosing cholangitis and extrahepatic cholangiocarcinoma. Clinical Radiology 71: 203-210, 2016
9) Jordan S et al: Differentiating IgG4-related sclerosing cholangiopathy from cholangiocarcinoma using CT and MRI-Experience from a tertiary referring center. Abdom Radiol 44: 2111-2115, 2019
10) Arikawa S et al: Comparison of sclerosing cholangitis with autoimmune panreatitis and infiltrative extrahepatic cholangiocarcinoma: multidetector-row computed tomography findings. Jpn J Radiol 28: 205-213, 2010
11) Maeda E et al: Comparison of CT findings of biliary tract changes with autoimmune panreatitis and extrahepatic bile duct cholangiocarcinoma. Jpn J Radiol 30: 227-234, 2012
12) Lopera JE et al: Malignant hilar and perihilar biliary obstruction: use of MR cholangiography to define the extent of biliary ductal involvement and plan percutaneous interventions. Radiology 220: 90-96, 2001
13) Fulcher AS et al: HASTE MR cholangiography in the evaluation of hilar cholangiocarcinoma. AJR Am J Roentgenol 169: 1501-1505, 1997

14) Textor HJ et al: Three-dimensional magnetic resonance cholangiopancreatography with respiratory triggering in the diagnosis of primary sclerosing cholangitis: comparison with endoscopic retrograde cholangiography. Endoscopy 34: 984-990, 2002
15) Li N et al: MRCP and 3D LAVA imaging of extrahepatic cholangiocarcinoma at 3T MRI. Clin Radiol 67: 579-586, 2012
16) Mortele KJ et al: CT and magnetic resonance imaging in pancreatic and biliary tract malignancies. Gastrointest Endosc 56 (6 S): S206-212, 2002
17) Talamonti MS et al: Staging and surgical management of pancreatic and biliary cancer and inflammation. Radiol Clin North Am 40: 1397-1410, 2002
18) Ruys AT et al: Radiological staging in patients with hilar cholangiocarcinoma: a systematic review and meta-analysis. Br J Radiol 85: 1255-1262, 2012
19) Zhang H et al: Radiological imaging for assessing the respectability of hilar cholangiocarcinoma: a systematic review and meta-analysis. Biomed Res Int 2015: 497942, 2015
20) Kim JY et al: Clinical role of 18F-FDG PET-CT in suspected and potentially operable cholangiocarcinoma: a prospective study compared with conventional imaging. Am J Gastroenterol 103: 1145-1151, 2008
21) Park HS et al: Preoperative evaluation of bile duct cancer: MRI combined with MR cholangiopancreatography versus MDCT with direct cholangiography. AJR Am J Roentgenol 190: 396-405, 2008

BQ 48 Is MRI recommended for diagnosing acute pancreatitis and evaluating its severity?

Statement

MRI is recommended for diagnosing bile duct stones that cause pancreatitis and pancreatic necrosis associated with hemorrhage. It is recommended as an alternative to CT in patients with iodine allergy or renal dysfunction.

Background

In response to the 2012 revision of the Atlanta classification, which reflected the international consensus on acute pancreatitis, the 2015 Guidelines for the Diagnosis and Treatment of Acute Pancreatitis, 4th Edition were published in Japan in 2015 (secondary source 1). The guidelines essentially establish 4 categories of local complications of pancreatitis encompassing the presence or absence of necrosis and a time axis divided at 4 weeks after onset. Detailed references to treatments (particularly endoscopic therapy, interventional radiology, and minimally invasive surgical therapy) are then provided for the categories. In addition to diagnosing acute pancreatitis early, it is important to diagnose its severity early, diagnose the changes in severity over time, and provide interventional treatment early in patients with severe disease. Diagnostic imaging plays a major role in local evaluation of the pancreas and in evaluating systemic complications that arise.

Explanation

MRI is useful for screening for causes of pancreatitis,[1)] diagnosing the nature of fluid accumulations, and selecting treatment.[2, 3)] Serosanguineous fluid accumulations show low signal intensity on T1-weighted images and high signal intensity on T2-weighted images. The necrotic component of fluid accumulations containing mixed necrotic material shows high signal intensity on T1-weighted images and low signal intensity on T2-weighted images. However, because the necrotic component undergoes liquefaction over time, a mixture of low and high signal intensities may become pronounced on T2-weighted images. Moreover, in interstitial edematous pancreatitis, the pancreatic parenchyma shows high signal intensity on T2-weighted images, which is particularly useful for diagnosing pancreatitis in patients with mild pancreatic enlargement. Another advantage of MRI over CT is that MRI does not involve radiation exposure. MRI is contraindicated in patients fitted with devices such as non-compatible pacemakers.

The normal pancreas shows higher signal intensity than the liver on T1-weighted images and near isointensity with the liver on fat-suppressed T2-weighted images, reflecting the high protein content of the acinar cells. In acute edematous pancreatitis, for example, only pancreatic enlargement can be diagnosed by CT; the presence or absence of inflammation (edema) cannot be evaluated. Acute edematous pancreatitis shows low signal intensity on T1-weighted images and high signal intensity on fat-suppressed T2-weighted

images in proportion to the severity of edema, which can shed light on the fact that inflammatory edema has actually occurred in an enlarged pancreas.[4-6] Diagnostic performance is also comparable to that of CT in the diagnosis of peripancreatic fluid collection and thickening of the prerenal fascia.[4, 6]

Although differentiating peripancreatic fat necrosis and fluid collection can pose difficulties with CT, fat necrosis and fluid are clearly distinguishable based on signal intensity with MRI (higher signal intensity for fat necrosis than fluid on T1-weighted images and slightly lower signal intensity for fat necrosis than fluid on T2-weighted images).[4, 6-9] Although hemorrhagic fat necrosis is frequently seen in severe acute pancreatitis, differentiating fat necrosis from simple effusion accumulation is often difficult based solely on CT density. Because fat necrosis of the retroperitoneal space or transverse mesocolon is often associated with hemorrhage, it shows high signal intensity (low signal intensity for effusion) on fat-suppressed T1-weighted images and can therefore be easily diagnosed. Areas of pancreatic necrosis can be visualized as regions of poor contrast enhancement by contrast-enhanced MRI.[8-11] and are often associated with hemorrhage in pancreatic pseudocysts. In the acute phase of hemorrhage, they show hyperdensity on non-contrast CT, enabling diagnosis. However, intracystic hemorrhage changes to hypodensity over time, making the diagnosis of hemorrhage difficult with CT. With MRI, subacute phase hemorrhage, which occurs after at least 1 week, shows high signal intensity on both T1-weighted and T2-weighted images, making diagnosis easy.[12]

MRCP provides high visualizability of gallstones and choledocholithiasis, regardless of the presence or absence of calcification. It should therefore be used aggressively when bile duct stones are not clearly visualized with ultrasound or CT.[13-15] Small gallstones and common bile duct stones can be overlooked when MRCP with MIP alone is used. Consequently, the presence or absence of stones always needs to be determined by consulting the original MRCP images or thin-section T2-weighted images acquired from multiple directions.

Although bile duct stones generally show low signal intensity on T2-weighted images and a variety of signal intensities on T1-weighted images, high signal intensity on T1-weighted images is particularly common in the case of bilirubin stones, which are frequently intrahepatic stones and common bile duct stones. An advantage of MRCP is that, in addition to enabling the diagnosis of stones, it can easily show the overall appearance of the bile and pancreatic ducts.[14, 15] MRCP can also diagnose congenital anomalies that can cause pancreatitis, such as choledochal cysts, pancreaticobiliary maljunction, and pancreas divisum, even without performing ERCP.[16, 17]

Search keywords and secondary sources

PubMed was searched using the following keywords: acute pancreatitis, MRI, and magnetic resonance imaging. The period searched was through June 2019; hits were obtained for 135 articles. An additional hand search was also performed.

In addition, the following were referenced as secondary sources.

1) Committee for the Publication of Guidelines for the Diagnosis and Treatment of Acute Pancreatitis, Ed: 2015 Guidelines for the Diagnosis and Treatment of Acute Pancreatitis, 4th Edition, KANEHARA & Co., LTD., 2015.
2) Research Committee for Intractable Pancreatic Diseases, Program for Intractable Diseases, Ministry of Health, Labour and Welfare Research Grant: Consensus on the diagnosis and treatment of local complications of pancreatitis (e.g., pancreatic pseudocyst, infected walled-off necrosis). Pancreas 29(5): 775-818, 2014.

References

1) Thevenot A et al: Endoscopic ultrasound and magnetic resonance cholangiopancreatography in patients with idiopathic acute pancreatitis. Digest Dis Sci 58: 2361-2368, 2013
2) Shyu JY et al: Necrotizing pancreatitis: diagnosis, imaging, and intervention. Radiographics 34: 1218-1239, 2014
3) Grassedonio E et al: Role of computed tomography and magnetic resonance imaging in local complications of acute pancreatitis. Gland Surg 8 (2): 123-132, 2019
4) Mill er FH et al: MRI of pancreatitis and its complications: part 1, acute pancreatitis. AJR Am J Roentgenol 183: 1637-1644– 2004
5) Ward J et al: T2 - weighted and dynamic MRI in acute pancreatitis: comparison with contrast enhanced CT. Clin Radiol 52: 109 -114, 1997
6) Kim YK et al: Effectiveness of MR imaging for diagnosing the mild forms of acute pancreatitis: comparison with MDCT. J Magn Reson Imaging 24: 1342-1349, 2006
7) Morgan DE et al: Pancreatic fluid collection prior to intervention: evaluation with MR imaging compared with CT and US. Radiology 203: 773-778, 1997
8) Hirota M et al: Visualization of the heterogeneous internal structure of so-called “pancreatic necrosis” by magnetic resonance imaging in acute necrotizing pancreatitis. Pancreas 25: 63-67, 2002
9) Tang MY et al: MR imaging of hemorrhage associated with acute pancreatitis. Pancreatology 18 (4): 363-369, 2018
10) Ward J et al: T2-weighted and dynamic MRI in acute pancreatitis: comparison with contrast enhanced CT. Clin Radiol 52: 109-114, 1997
11) Piironen A et al: Detection of severe acute pancreatitis by contrast-enhanced magnetic resonance imaging. Eur Radiol 10: 354-361, 2000
12) Ikeda O et al: Hemorrhage into pancreatic pseudocyst. Abdom Imaging 32: 370-373, 2007
13) Saifuddin A et al: Comparison of MR and CT scanning in severe acute pancreatitis: initial experiences. Clin Radiol 48: 111-116, 1993
14) Hallal AH et al: Magnetic resonance cholangiopancreatography accurately detects common bile duct stones in resolving gallstone pancreatitis. J Am Coll Surg 200: 869-875, 2005
15) Makary MA et al: The role of magnetic resonance cholangiography in the management of patients with gallstone pancreatitis. Ann Surg 241: 119-124, 2005
16) Hirohashi S et al: Pancreatitis: evaluation with MR cholangiopancreatography in children. Radiology 203: 411-415, 1997
17) Hayashi TY: Ansa pancreatica as a predisposing factor for recurrent acute pancreatitis. World J Gastroenterol 22 (40): 8940-8948, 2016

BQ 49 Is CT recommended for diagnosing chronic pancreatitis?

Statement

CT is useful for diagnosing chronic pancreatitis. To diagnose early chronic pancreatitis, however, careful examination using a modality such as EUS is considered necessary.

Background

In Japan, the Clinical Diagnostic Criteria for chronic pancreatitis have been used in diagnosing chronic pancreatitis. The 2009 revision of the diagnostic criteria, the 2009 chronic pancreatitis Clinical Diagnostic Criteria, incorporated the concept of early chronic pancreatitis (secondary source 1). The revised diagnostic criteria are also referenced in examining the usefulness of CT in diagnosing chronic pancreatitis.

Explanation

Chronic pancreatitis is defined as a pathophysiology in which chronic changes such as irregular fibrosis, cellular infiltration, loss of parenchyma, and tissue granulation occur within the pancreas and, if they progress, are associated with decreased pancreatic exocrine and endocrine secretion. Often irreversible, it is classified as alcoholic or nonalcoholic, depending on the cause. Because they are reversible, autoimmune pancreatitis (AIP) and obstructive pancreatitis are currently handled as separate types of chronic inflammation of the pancreas.

Reports from other countries on the diagnosis of chronic pancreatitis that examined chronic pancreatitis diagnostic rates with CT reported sensitivity ranging from 74% to 91% and specificity ranging from 78% to 98%.[1-3)] Examination by parameter showed sensitivity and specificity of 53% and 94%, respectively, for diffuse calcification of the pancreas and 43% and 88%, respectively, for pancreatolithiasis. Thus, the findings for specificity were high.[4)] CT is therefore considered useful for diagnosis (Fig.), and its usefulness in chronic pancreatitis is reflected in the 2015 Guidelines for the Diagnosis and Treatment of Chronic Pancreatitis, Revised 2nd Edition, the 2014 Guidelines for Endoscopic Treatment of Pancreatolithiasis, and the consensus on the diagnosis and treatment of local complications of pancreatitis (e.g. pancreatic pseudocysts and infected walled-off necrosis; secondary sources 2 to 4).

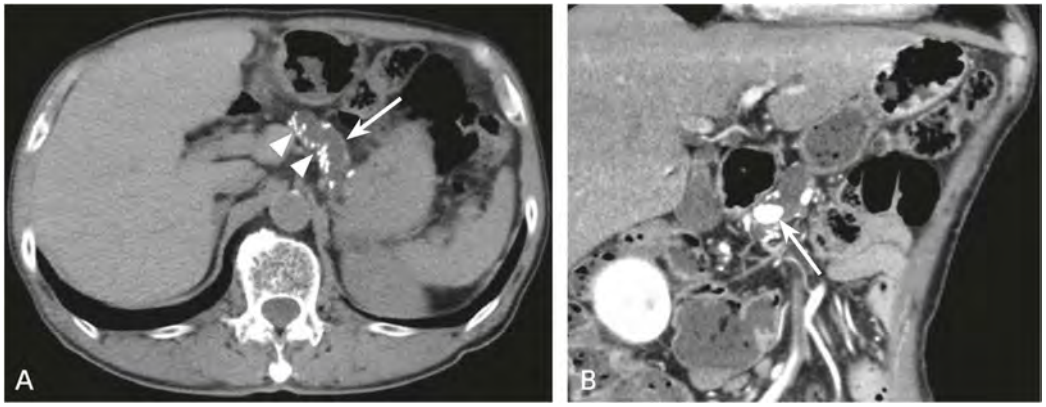

Figure Chronic pancreatitis

A: Non-contrast CT, transverse image: Atrophy of the pancreatic parenchyma and dilatation of the main pancreatic duct are seen (→). Scattered calcification is present in the pancreatic parenchyma (▷).

B: Contrast-enhanced CT, arterial phase, oblique coronal image: Pancreatolithiasis is seen in the main pancreatic duct (→).

Table Imaging findings for early chronic pancreatitis (quoted from secondary source 1)

a. Either a or b is seen.

a. At least 2 of the 7 EUS findings below are seen, including at least 1 of findings (1) to (4).

(1) Lobularity, honeycombing type

(2) Non-honeycombing lobularity

(3) Hyperechoic foci, non-shadowing

(4) Stranding

(5) Cysts

(6) Dilated side branches

(7) Hyperechoic MPD margin

b. Irregular dilatation is seen in 3 or more branch pancreatic ducts in ERCP images.

In addition, the concept of early chronic pancreatitis disease was incorporated into the 2009 chronic pancreatitis Clinical Diagnostic Criteria. In diagnosing early chronic pancreatitis, patients for whom a definitive or near-definitive diagnosis of chronic pancreatitis cannot be obtained and who have least 2 of the following 4 clinical findings are suspected of having chronic pancreatitis: repeated episodes of upper abdominal pain; abnormal blood or urine pancreatic enzyme levels; impaired pancreatic exocrine secretion; and sustained alcohol consumption of 80 g (pure ethanol equivalent) or more per day. For patients with suspected chronic pancreatitis, early (within 3 months) careful examination by EUS or ERCP is recommended, and those with the imaging findings shown in the table are diagnosed with early chronic pancreatitis. The Rosemont classification uses criteria based on EUS, and the CT finding of early chronic pancreatitis is not included in the diagnostic criteria of the current revision (secondary source 1). Reports from other countries have also indicated that CT, compared with EUS and ERCP, in early chronic pancreatitis is not sensitive[5, 6], and its diagnostic performance is not high[7, 8]. The 2009 chronic pancreatitis Clinical Diagnostic Criteria state that, because of the problem of procedural accidents, EUS is first performed for the diagnostic imaging of early chronic pancreatitis, and ERCP is then performed as needed

in symptomatic patients strongly suspected of having pancreatic lesions. Thus, careful examination with a procedure such as EUS is considered necessary for diagnostic imaging of early chronic pancreatitis.

Search keywords and secondary sources

PubMed was searched using the following keywords: chronic pancreatitis, diagnosis, computed tomography, sensitivity, and specificity. The Ichushi and Cochrane Library databases were searched using equivalent keywords. The period searched was from January 1990 to June 2019; hits were obtained for 209 articles. In addition, 2 articles were added with a hand search.

Furthermore, the following were referenced as secondary sources.

1) Research Committee for Intractable Pancreatic Diseases, Ministry of Health, Labour and Welfare, Ed.: 2009 Chronic Pancreatitis Clinical Diagnostic Criteria. Pancreas 24: 645-646, 2009.
2) Japanese Society of Gastroenterology, Ed.: 2015 Guidelines for the Diagnosis and Treatment of Chronic Pancreatitis, Revised 2nd Edition, Nankodo, 2015.
3) Research Committee for Intractable Pancreatic Diseases, Ministry of Health, Labour and Welfare and Japan Pancreas Society, Ed.: 2014 Guidelines for Endoscopic Treatment of Pancreatolithiasis. Pancreas 29(2): 123-147, 2014.
4) Research Committee for Intractable Pancreatic Diseases, Program for Intractable Diseases, Ministry of Health, Labour and Welfare Research Grant, Ed.: Consensus on the diagnosis and treatment of local complications of pancreatitis (e.g., pancreatic pseudocyst, infected walled-off necrosis). Pancreas 29(5): 775-818, 2014.

References

1) Buscail L et al: Endoscopic ultrasonography in chronic pancreatitis: a comparative prospective study with conventional ultrasonography, computed tomography, and ERCP. Pancreas 10: 251-257, 1995
2) Bozkurt T et al: Comparison of pancreatic morphology and exocrine functional impairment in patients with chronic pancreatitis. Gut 35: 1132-1136, 1994
3) Rosch T et al: Modern imaging methods versus clinical assessment in the evaluation of hospital in-patients with suspected pancreatic disease. Am J Gastroenterol 95: 2261-2270, 2000
4) Campisi A et al: Are pancreatic calcifications specific for the diagnosis of chronic pancreatitis?: a multidetector-row CT analysis. Clin Radiol 64: 903-911, 2009
5) Remer EM et al: Imaging of chronic pancreatitis. Radiol Clin North Am 40: 1229-1242, 2002
6) Chong AK et al: Diagnostic performance of EUS for chronic pancreatitis: a comparison with histopathology. Gastrointest Endosc 65: 808-814, 2007
7) Buchler MW et al: A proposal for a new clinical classification of chronic pancreatitis. BMC Gastroenterol 9: 93, 2009
8) Aoun E et al: Rapid evolution from the first episode of acute pancreatitis to chronic pancreatitis in human subjects. JOP 8: 573-578, 2007

BQ 50 Are CT and MRI recommended for diagnosing autoimmune pancreatitis (AIP)?

Statement

CT and MRI are recommended for detecting AIP lesions and screening for extra-pancreatic lesions. Keeping in mind that differentiating from other diseases, particularly pancreatic cancer, is difficult with CT or MRI alone in some patients, it is recommended that histological differentiation by a method such as biopsy under EUS guidance be performed to the extent possible.

Background

AIP is clinically and histologically classified into two subtypes, types 1 and 2; type 1 is overwhelmingly the most frequent type in Japan. Consequently, AIP refers to type 1 AIP below. AIP is known as a pancreatic manifestation of IgG4-related disease that involves systemic organs. Its characteristics include preferential occurrence in middle-aged and elderly men, high serum IgG4 levels, a variety of associated extra-pancreatic lesions, and responsiveness to steroid therapy. Particularly because AIP is responsive to steroid therapy, it is important that it be suspected and diagnosed appropriately.

Explanation

AIP is a systemic, IgG4-related disease that manifests as pancreatic lesions. Its diagnosis requires a comprehensive assessment of clinical, imaging, and pathology findings. Imaging studies in particular are important as the start of diagnosis of the disease, and they play a major role in detecting extra-pancreatic lesions (IgG4-related lesions). Because changes such as cell infiltration, fibrosis, and obliterative phlebitis occur in the affected area in AIP, imaging findings also reflect these changes. Well-known AIP imaging findings that have been reported are sausage-shaped pancreatic enlargement, a capsule-like rim, and diffuse narrowing of the pancreatic duct. The capsule-like rim in particular is a highly specific and important finding, even though it is seen infrequently. With dynamic CT, the affected area is visualized as hypodense compared with normal pancreatic parenchyma in the pancreatic parenchymal phase and shows gradually increasing enhancement through the venous phase.[1-3)] A capsule-like rim similarly consists mainly of fibrillary elements and, therefore, shows a similar gradually increasing enhancement pattern. With MRI, the parenchyma in the affected area shows low signal intensity on T1-weighted images, faint high signal intensity on T2-weighted images, and is associated with slightly decreased diffusion. In addition to changes in the pancreatic parenchyma, the appearance of the pancreatic duct is important for AIP diagnosis. Although the evaluation of pancreatic duct appearance has been limited to evaluation by endoscopic retrograde pancreatography (ERP) in diagnostic criteria in Japan, with advances in MRI systems, particularly the increased availability of 3T systems, the most recent diagnostic criteria (secondary source 1) have added MRCP findings (extensive pancreatic duct non-visualization/narrowing, narrowing “skip”

lesions) for the evaluation of pancreatic duct appearance. Consequently, the importance of MRI in AIP diagnosis is expected to increase further.

AIP is classified as the diffuse, segmental, and focal types according the extent of the affected pancreatic parenchyma. With the diffuse type, which shows lesions in nearly the entire pancreas, AIP can be strongly suspected based on previously reported CT and MRI imaging findings, and it can be diagnosed relatively easily by combining these findings with serum IgG4 levels. In patients with the segmental or focal type, however, it is important to distinguish it from other diseases, particularly pancreatic cancer. Because the treatment and prognosis of the two conditions are entirely different, careful attention must be paid to their differentiation. Their contrast enhancement patterns and MRI signals are similar, particularly with focal-type lesions, making it difficult to distinguish between them based on images. Imaging findings known to be useful for differentiation are the duct-penetrating sign, which indicates penetration through a mass by the pancreatic duct, and homogeneous contrast enhancement in the venous phase, which reflects the limited intralesional necrosis and degeneration in AIP. In addition to these findings, Sugiyama et al. found that intralesional speckled enhancement seen in a mass with dynamic MRI is useful for differentiation.[4-6] Enhancement along a pancreatic duct running through a mass lesion is also seen. In addition to these imaging findings, there are also reports regarding the usefulness of diffusion-weighted imaging.[7-9] All of the imaging findings reported have indicated its usefulness for distinguishing focal AIP from pancreatic cancer. However, the findings are not absolutely conclusive. Given the current situation, in addition to imaging findings, it is important to comprehensively evaluate serum IgG4 levels and the presence or absence of extra-pancreatic lesions. In patients for whom differentiation is difficult, histological differentiation should be performed by biopsy under EUS guidance. To repeat, keeping in mind the fact that AIP is a pancreatic manifestation of IgG4-related disease, it is necessary to be thoroughly familiar with at least the typical features of typical extra-pancreatic lesions (e.g., of the salivary glands, lacrimal glands, bile duct, pancreas, and aorta).[10-13] Contrast-enhanced CT, which permits an extensive area to be screened at one time, is useful for screening for systemic extra-pancreatic lesions, and screening for other organ involvement is required when AIP is suspected.

Search keywords and secondary sources

PubMed was searched using the following keywords: autoimmune pancreatitis, CT, and MRI. The period searched was through June 2019; hits were obtained for 313 articles. An additional hand search was also performed.

In addition, the following were referenced as secondary sources.

1) Japan Pancreas Society/Ministry of Health, Labour and Welfare Research Grant (Research Program for Intractable Disease): Panel on establishing diagnostic criteria and treatment strategies for IgG4-related disease: 2018 Clinical Diagnostic Criteria for Autoimmune Pancreatitis. Pancreas 33(6): 26-97, 2018.

References

1) Irie H et al: Autoimmune pancreatitis: CT and MR characteristics. AJR Am J Roentgenol 170 (5): 1323-1327, 1998
2) Sahani DV et al: Autoimmune pancreatitis: imaging features. Radiology 233 (2): 345-352, 2004
3) Takahashi N et al: Dual-phase CT of autoimmune pancreatitis: a multireader study. AJR Am J Roentgenol 190 (2): 280-286, 2008
4) Ichikawa T et al: Duct-penetrating sign at MRCP: usefulness for differentiating inflammatory pancreatic mass from pancreatic carcinomas. Radiology 221 (1): 107-116, 2001
5) Wakabayashi T et al: Clinical and imaging features of autoimmune pancreatitis with focal pancreatic swelling or mass formation: comparison with so-called tumor-forming pancreatitis and pancreatic carcinoma. Am J Gastroenterol 98 (12): 2679-2687, 2003
6) Sugiyama Y et al: Characteristic magnetic resonance features of focal autoimmune pancreatitis useful for differentiation from pancreatic cancer. Jpn J Radiol 30 (4): 296-309, 2012
7) Kawai Y et al: Autoimmune pancreatitis: assessment of the enhanced duct sign on multiphase contrast-enhanced computed tomography. Eur J Radiol 81 (11): 3055-3060, 2012
8) Furuhashi N et al: Differentiation of focal-type autoimmune pancreatitis from pancreatic carcinoma: assessment by multiphase contrast-enhanced CT. Eur Radiol 25 (5): 1366-1374, 2015
9) Muhi A et al: Mass-forming autoimmune pancreatitis and pancreatic carcinoma: differential diagnosis on the basis of computed tomography and magnetic resonance cholangiopancreatography, and diffusion-weighted imaging findings. J Magn Reson Imaging 35 (4): 827-836, 2012
10) Inoue D et al: IgG4-related disease: dataset of 235 consecutive patients. Medicine (Baltimore) 94 (15): e680, 2015
11) Inoue D et al: Immunoglobulin G4-related lung disease: CT findings with pathologic correlations. Radiology 251 (1): 260-270, 2009
12) Takahashi N et al: Renal involvement in patients with autoimmune pancreatitis: CT and MR imaging findings. Radiology 242 (3): 791-801, 2007
13) Inoue D et al: Immunoglobulin G4-related periaortitis and periarteritis: CT findings in 17 patients. Radiology 261 (2): 625-633, 2011

CQ 14 Is contrast-enhanced MRI recommended for the differential diagnosis of pancreatic masses?

Recommendation

Contrast-enhanced MRI is weakly recommended for the differential diagnosis of pancreatic masses.

Recommendation strength: 2, strength of evidence: weak (C), agreement rate: 100% (8/8)

Background

Pancreatic mass lesions encompass a wide variety of diseases, ranging from malignant tumorous lesions that require treatments such as surgery and chemotherapy, such as pancreatic cancer, neuroendocrine tumors, malignant lymphoma, and solid pseudopapillary neoplasms (SPNs), to diseases for which conservative treatment is selected, such as AIP and mass-forming pancreatitis. In view of the level of invasiveness of surgery for pancreatic disease, qualitative diagnosis by means of non-invasive imaging is important. Although evaluations using contrast-enhanced CT, MRI and EUS play a central role in the differential diagnosis of pancreatic mass lesions, articles showing the usefulness of MRI for evaluating pancreatic mass lesions have been sporadic as MRI imaging systems have improved in recent years. Contrast-enhanced MRI in particular, with its high contrast resolution, is excellent for evaluating the interior characteristics of masses and therefore shows good efficacy for the differential diagnosis of pancreatic masses. For these guidelines, a systematic review was conducted regarding the usefulness of contrast-enhanced MRI in the differential diagnosis of pancreatic mass lesions.

Explanation

This review specified as outcomes the qualitative diagnosis of pancreatic mass lesions, allergic reactions that occur with contrast medium administration, nephropathy associated with contrast medium administration, and test duration, and it identified reference articles using the search criteria indicated below.

In addition to T1-weighted and T2-weighted non-contrast-enhanced MRI, evaluation by diffusion-weighted imaging and MRCP has become feasible in recent years. However, the searches performed for the current review did not yield any articles on a direct comparison of diagnostic performance with non-contrast-enhanced and contrast-enhanced MRI. Moreover, there were no relevant articles on allergic reactions that occur with contrast medium administration, nephropathy associated with contrast medium administration, or test duration within the scope of the search.

An investigation comparing the diagnostic performance of CT and MRI in AIP and pancreatic cancer found that AUC and sensitivity with MRI were both equal to or greater than with CT.[1)] MRI was superior with respect to the visualization of masses and main pancreatic duct stenosis and the detection of homogeneous delayed enhancement in AIP and the visualization of masses and main pancreatic duct

stenosis in pancreatic cancer. Although CT and MRI findings have both been reported to be useful in differentiating from pancreatic cancer, neither modality has been clearly shown to be superior, and findings such as serum IgG4 levels and extra-pancreatic lesions currently need to be comprehensively evaluated.

The 2017 international diagnostic guidelines for intraductal papillary mucinous neoplasms (IPMNs, secondary source 1) recommend resection when CT or MRI findings show high-risk stigmata and thorough examination by EUS and consideration of surgery or follow-up when worrisome features are present. Investigations that compared CT and MRI in evaluating the malignancy grade of IPMNs found CT and MRI to be comparable in detecting findings indicative of malignancy risk, such a high-risk stigmata and worrisome features.[2, 3] However, they found MRI to be useful in detecting enhancement of a thickened cyst wall, which is considered a worrisome feature.[3]

An investigation that compared CT and MRI in the differential diagnosis of solid pancreatic masses ≤ 3 cm in size (127 patients with pancreatic ductal carcinoma, 43 with neuroendocrine tumors, 10 with SPNs, 7 with localized AIP, and 6 with metastatic pancreatic tumors) found that MRI was superior in sensitivity, but that CT and MRI performed comparably in qualitative diagnosis.[4]

An investigation that compared CT and MRI in diagnostic performance for the differential diagnosis of cystic pancreatic masses ≤ 3 cm in size (14 patients with branch-type IPMNs, 12 with mixed-type IPMNs, 6 with MCNs, and 6 with retention cysts or pseudocysts) found that MRI was superior in morphological evaluation, but CT and MRI performed comparably in qualitative diagnosis and in evaluating benign or malignant lesions.[5]

Caution is required regarding the fact that, although infrequent, problems such as anaphylactic shock can occur with the use of contrast media in contrast-enhanced MRI and nephrogenic systemic fibrosis (NSF) with the use of gadolinium contrast media in patients with severe nephropathy.

The findings described above indicate that contrast-enhanced MRI has a discrimination ability that is equal to or slightly better than that of CT for the differential diagnosis of pancreatic masses, and that its diagnostic performance in evaluating the malignancy grade of IPMNs is equal to that of CT and EUS.

Taking these considerations into account, when differentially diagnosing pancreatic masses in routine clinical practice, judgments should be made based on factors such as the radiation exposure and presence or absence of contrast medium allergy and nephropathy of the individual patient. In particular, caution should always be exercised regarding complications resulting from the use of contrast media. It is known that MRI, even with non-contrast-enhanced sequences, can provide useful information for evaluating the internal characteristics of pancreatic mass lesions and an overview of the pancreatic and bile ducts. Consequently, investigations comparing the diagnostic performance of contrast-enhanced and non-contrast-enhanced MRI are anticipated in the future.

Search keywords and secondary references

PubMed was searched using the following keywords: pancreas, pancreatic mass, magnetic resonance imaging, contrast-enhanced, and diagnosis. The period searched was through June 2019; hits were obtained for 234 articles. The primary screening yielded 21 candidate articles, and the full text of 14 of these articles was searched. As a result, 5 articles were used in the review.

In addition, the following was referenced as a secondary source.

1) Tanaka M et al: Revision of international consensus Fukuoka guidelines for the management of IPMN of the pancreas. Pancreatology 17: 738-753, 2017

References

1) Lee S et al: Comparison of diagnostic performance between CT and MRI in differentiating non-diffuse-type autoimmune pancreatitis from pancreatic ductal adenocarcinoma. Eur Radiol 28 (12): 5267-5274, 2018
2) Choi SY et al: Diagnostic performance and imaging features for predicting the malignant potential of intraductal papillary mucinous neoplasm of the pancreas: a comparison of EUS, contrast-enhanced CT and MRI. Abdom Radiol 42 (5): 1449-1458, 2017
3) Kang HJ et al: Assessment of malignant potential in intraductal papillary mucinous neoplasms of the pancreas: comparison between multidetector CT and MR imaging with MR cholangiopancreatography. Radiology 279 (1): 128-139, 2016
4) Choi TW et al: Comparison of multidetector CT and gadobutrol-enhanced MR imaging for evaluation of small, solid pancreatic lesions. Korean J Radiol 17 (4): 509-521, 2016
5) Sainani NI et al: Comparative performance of MDCT and MRI with MR cholangiopancreatography in characterizing small pancreatic cysts. AJR Am J Roentgenol 193 (3): 722-731, 2009

CQ 15 Is diffusion-weighted MRI recommended for diagnosing the benign or malignant nature of pancreatic tumors?

Recommendation

Diffusion-weighted MRI is weakly recommended because ADC values can assist in estimating the malignancy grade of P-NETs.

Recommendation strength: 2, strength of evidence: weak (C), agreement rate: 100% (8/8)

Diffusion-weighted MRI is weakly recommended for IPMNs because examining ADC values and diffusion restriction can assist in diagnosing malignant IPMNs.

Recommendation strength: 2, strength of evidence: weak (C), agreement rate: 100% (8/8)

Background

MRI plays an important role in diagnostic imaging of the abdomen. Because treatment strategies for pancreatic tumors differ greatly depending on whether they are benign or malignant, and the 5-year survival rate for pancreatic cancer is < 10%, accurately distinguishing between malignant pancreatic tumors, typified by pancreatic cancer, and benign tumors is extremely important. Consequently, this discussion focuses on diffusion-weighted MRI and examines whether diffusion-weighted images are useful in the differential diagnosis of benign and malignant pancreatic tumors.

Explanation

For this CQ, examination time (importance, 1 point) and test cost (importance, 3 points) were specified as harmful outcomes, and sensitivity and specificity in diagnosing benign or malignant pancreatic tumors (importance, 9 points) were established as beneficial outcomes. The literature search for this CQ yielded 8 articles that examined pancreatic neuroendocrine tumor (P-NET) grades and 7 articles that examined distinction between benign and malignant IPMNs.

Of the articles that examined P-NET grades, 2 were examined with 3T MRI,[1, 2] 5 were examined with 1.5T MRI,[3-7] and 1 was examined with 1.5T and 3T MRI scanners.[8] Of these 8 articles, 7 reported that ADC values are useful. These included reports showing higher ADC values for grade 1 (G1) tumors than for G2 or G3 tumors (Pereira et al.[5], De Robertis et al.[7], Toshima et al.[8]), a report showing lower ADC values for G3 tumors than for G1 or G2 tumors (Kulali et al.[3]), a report showing significant differences between the ADC values for G1, G2, and G3 tumors (Lotfalizadeh et al.[4]), a report showing a correlation between the ADC value and WHO tumor grade (Kim et al.[1]), and a report showing a significant difference between the ADC values for G1 and G2 tumors (Kim et al.[6]). One of the 8 articles reported finding no significant differences between ADC values, and an article by Hwang et al. reported seeing no significant differences between the ADC values for G1 tumors and those for G2 and G3 tumors.[2] Based on these

findings, the use of ADC values appears to assist in estimating the malignancy grade of P-NETs, and diffusion-weighted MRI is therefore weakly recommended.

Of the articles that examined differentiation between benign and malignant IPMNs, 3 were examined with 3T MRI,[9-11] 3 were examined with 1.5T MRI,[12-14] and 1 was examined with 1.5T and 3T MRI scanners.[15] Six of these 7 articles mentioned ADC values, 4 of which reported significant differences between the ADC values for benign and malignant tumors,[11-14], 2 of the 6 reported finding no significant differences.[9, 15] Four of the 7 articles mentioned diffusion restriction. An article by Kim et al. reported that multivariate analysis showed diffusion restriction to be the only independent imaging parameter that predicted the malignancy of IPMNs.[9] An article by Jang et al. reported that diffusion restriction was seen at a high frequency in the malignant group on visual assessments.[10] Articles by Kang and Ogawa et al. reported finding significantly higher rates of diffusion restriction in malignant IPMNs than in benign IPMNs.[11, 13] Based on these findings, diffusion-weighted MRI is weakly recommended for IPMNs, because examining ADC values and diffusion restriction in areas where tumors are present can assist in diagnosing malignant IPMNs.

Based on the foregoing, diffusion-weighted MRI is weakly recommended for P-NET grading because the use of ADC values can assist in estimating the malignancy grade of P-NETs. In addition, diffusion-weighted MRI is weakly recommended for IPMNs, because examining ADC values and diffusion restriction in areas where tumors are present can assist in diagnosing malignant IPMNs.

Variability in ADC values is seen depending on the type of equipment and facility. Consequently, the use of ADC values in qualitative diagnosis requires an understanding of the reliability and limitations of diffusion coefficients,[16] and this should be considered when the ADC value is used to diagnose benign and malignant tumors.

Although this is only a point for reference, there are discrepancies in the literature regarding differences in ADC values between pancreatic cancer and P-NETs. Whereas Li and Shindo et al. reported significantly lower ADC values in pancreatic cancer than in P-NETs,[17, 18] Guo and De Robertis et al. reported significantly lower ADC values in P-NETs.[19, 20] Wagner et al. reported that ADC values change with the proportions of fibrosis, necrosis, and cell density within the tumors,[21] indicating that the structural components of the cells of pancreatic tumors may affect the changes in ADC values. Consequently, room for debate remains regarding the use of ADC values to distinguish pancreatic cancer from P-NETs.

Search keywords and secondary references

PubMed was searched using the following keywords: pancreatic tumor, diffusion-weighted imaging, magnetic resonance imaging, pancreas, and diagnosis. The Ichushi and Cochrane Library databases were searched using equivalent keywords. The period searched was from January 1990 to June 2019; hits were obtained for 240 articles. In addition, 2 articles were added with a hand search. In the primary screening, 37 articles were extracted, and those whose content was judged unsuitable in the secondary screening were excluded. Ultimately, a qualitative systematic review was conducted using 15 articles.

References

1) Kim M et al: Pancreatic neuroendocrine tumour: correlation of apparent diffusion coefficient or WHO classification with recurrence-free survival. Eur J Radiol 85 (3): 680-687, 2016
2) Hwang EJ et al: Intravoxel incoherent motion diffusion-weighted imaging of pancreatic neuroendocrine tumors: prediction of the histologic grade using pure diffusion coefficient and tumor size. Invest Radiol 49 (6): 396-402, 2014
3) Kulali F et al: Role of diffusion-weighted MR imaging in predicting the grade of nonfunctional pancreatic neuroendocrine tumors. Diagn Interv Imaging 99 (5): 301-309, 2018
4) Lotfalizadeh E et al: Prediction of pancreatic neuroendocrine tumour grade with MR imaging features: added value of diffusion-weighted imaging. European radiology 27 (4): 1748-1759, 2017
5) Pereira JA et al: Pancreatic neuroendocrine tumors: correlation between histogram analysis of apparent diffusion coefficient maps and tumor grade. Abdom Imaging 40 (8): 3122-3128, 2015
6) Kim JH et al: Staging accuracy of MR for pancreatic neuroendocrine tumor and imaging findings according to the tumor grade. Abdom Imaging 38 (5): 1106-1114, 2013
7) De Robertis R et al: Pancreatic neuroendocrine neoplasms: magnetic resonance imaging features according to grade and stage. World J Gastroenterol 23 (2): 275-285, 2017
8) Toshima F et al: Is the combination of MR and CT findings useful in determining the tumor grade of pancreatic neuroendocrine tumors? Jpn J Radio 35 (5): 242-253, 2017
9) Kim M et al: Diagnostic accuracy of diffusion restriction in intraductal papillary mucinous neoplasm of the pancreas in comparison with “high-risk stigmata” of the 2012 international consensus guidelines for prediction of the malignancy and invasiveness. Acta Radiol 58 (10): 1157-1166, 2017
10) Jang KM et al: Value of diffusion-weighted MRI for differentiating malignant from benign intraductal papillary mucinous neoplasms of the pancreas. AJR Am J Roentgenol 203 (5): 992-1000, 2014
11) Kang KM et al: Added value of diffusion-weighted imaging to MR cholangiopancreatography with unenhanced mr imaging for predicting malignancy or invasiveness of intraductal papillary mucinous neoplasm of the pancreas. J Magn Reson Imaging 38 (3): 555-563, 2013
12) Zhang L et al: Value of apparent diffusion coefficient for predicting malignancy of intraductal papillary mucinous neoplasms of the pancreas. Diagn Interv Radiol 22 (4): 308-313, 2016
13) Ogawa T et al: Diffusion-weighted magnetic resonance imaging for evaluating the histological degree of malignancy in patients with intraductal papillary mucinous neoplasm. J Hepatobiliary Pancreat Sci 21 (11): 801-808, 2014
14) Sandrasegaran K et al: Diffusion-weighted imaging in characterization of cystic pancreatic lesions. Clin Radiol 66 (9): 808-814, 2011
15) Hoffman DH et al: Utility of whole-lesion ADC histogram metrics for assessing the malignant potential of pancreatic intraductal papillary mucinous neoplasms (IPMNs). Abdom Radiol (NY) 42 (4): 1222-1228, 2017
16) Sano K et al: Diffusion-weighted MRI in pancreatic disease: Qualitative diagnosis. Journal of Biliary Tract & Pancreas 33 (7): 603-607, 2012
17) Li J et al: Whole-tumor histogram analysis of non-Gaussian distribution DWI parameters to differentiation of pancreatic neuroendocrine tumors from pancreatic ductal adenocarcinomas. Magn Reson Imaging 55: 52-59, 2019
18) Shindo T et al: Histogram analysis of apparent diffusion coefficient in differentiating pancreatic adenocarcinoma and neuroendocrine tumor. Medicine (Baltimore) 95 (4): e257, 2016
19) Guo C et al: Differentiation of pancreatic neuroendocrine carcinoma from pancreatic ductal adenocarcinoma using magnetic resonance imaging: the value of contrast-enhanced and diffusion weighted imaging. Oncotarget 8 (26): 42962-42973, 2017
20) De Robertis R et al: Intravoxel incoherent motion diffusion-weighted MR imaging of solid pancreatic masses: reliability and usefulness for characterization. Abdom Radiol (NY) 44 (1): 131-139, 2019
21) Wagner M et al: Diffusion-weighted MR imaging for the regional characterization of liver tumors. Radiology 264 (2): 464-472, 2012

BQ 51 Is abdominal MRI recommended to detect pancreatic cancer?

Statement

Abdominal MRI and CT are equally useful for detecting pancreatic cancer.

Background

The usefulness of contrast-enhanced MDCT using dynamic imaging to detect pancreatic cancer has been established.[1, 2)] MRI also provides high detection performance of pancreatic cancer, and it is described in detail here.

Explanation

In many patients, pancreatic cancer is already unresectable when it is diagnosed, and this is the main reason for its poor prognosis. When pancreatic cancer is suspected and in high-risk groups, accurate detection or exclusion by diagnostic imaging is desirable.

Among reports from other countries on diagnostic performance in pancreatic cancer,[1-7)] a meta-analysis by Toft et al., considered to be the most reliable (literature search for period from January 2004 to June 2015) that carefully selected 52 original articles (total of 3,567 pancreatic cancer patients), examined the diagnostic performance of MRI and found sensitivity of 93% (95% CI, 88% to 96%), specificity of 89% (95% CI, 82% to 94%), and diagnostic accuracy of 90% (95% CI, 86% to 94%).[1)] With CT, sensitivity was 90% (95% CI, 87% to 93%), specificity was 87% (95% CI, 79% to 93%), and diagnostic accuracy was 89% (95% CI, 85% to 93%), comparable to the values seen for MRI. The report indicated that the diagnostic performance of endoscopic ultrasonography and extracorporeal ultrasonography was also comparable to that of MRI. However, the specificity of PET/CT was a low 70% (95% CI, 54% to 84%), and its diagnostic accuracy was 84% (95% CI, 79% to 89%). It was therefore concluded that PET/CT is inferior to the other imaging modalities.

The most prominent feature of MRI is that it allows for more special imaging techniques than CT. One such technique is diffusion-weighted imaging, which many reports indicated was useful for detecting pancreatic cancer. Takakura et al. reported that an imaging technique that added diffusion-weighted imaging to MRCP resulted in a diagnostic accuracy rate that was comparable to that of 2-phase contrast-enhanced MDCT (MRI, 84%; contrast-enhanced MDCT, 86%), even when not used in combination with contrast-enhanced MRI.[8)] In addition, Park et al. reported that, with the addition of diffusion-weighted imaging to conventional MRI (including gadolinium contrast-enhanced imaging) for small pancreatic cancers ≤ 3 cm in size, the detection sensitivity of two readers (reader 1: 75% to 98%, reader 2: 76% to 96%) improved significantly compared with the normal imaging method.[6)] Moreover, MRCP alone was found to provide high sensitivity and specificity of 84% and 97%, respectively, in

detecting pancreatic cancer, with no significant difference seen compared with the detection performance of ERCP (sensitivity, 70%; specificity, 94%).[7)]

Based on these findings, abdominal MRI is recommended for detecting pancreatic cancer. However, its detection performance is comparable to that of contrast-enhanced MDCT, and the selection of MRI should therefore be considered by taking into account the patient's background and the facility's diagnostic imaging equipment.

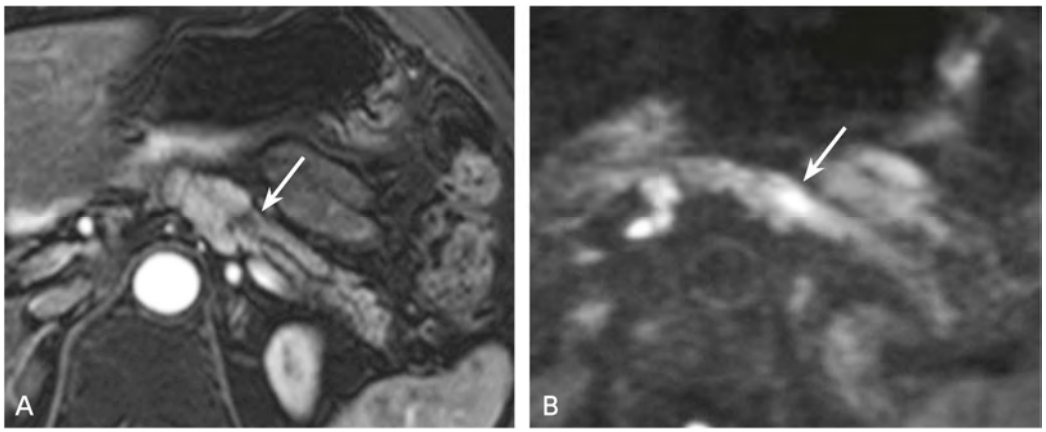

Figure　Pancreatic body cancer

A: Contrast-enhanced MRI, arterial-dominant phase: An area of poor contrast enhancement approximately 1 cm in size (→) is seen in the pancreatic body, along with dilatation of the upstream main pancreatic duct and atrophy of the pancreatic parenchyma. The same lesion showed gradually increasing contrast enhancement with dynamic imaging (not shown).
B: MRI, diffusion-weighted image, b-value = 1,000 s/mm^2: A nodular lesion that appears as a region of high signal intensity (→) is seen in the pancreatic body, consistent with the lesion site indicated by dynamic contrast-enhanced imaging. The finding supports a diagnosis of pancreatic body cancer.

Search keywords and secondary references

PubMed was searched using the following keywords: pancreatic carcinoma, diagnosis, MRI, sensitivity, and specificity. The period searched was from January 1990 to June 2019; hits were obtained for 84 articles. In addition, 5 articles were added with a hand search.

The following were also referenced as secondary sources.

1) Clinical Practice Guidelines for Pancreatic Cancer 2019

References

1) Toft J et al: Imaging modalities in the diagnosis of pancreatic adenocarcinoma: a systematic review and meta-analysis of sensitivity, specificity and diagnostic accuracy. Eur J Radiol 92: 17-23, 2017
2) Treadwell JR, et al: Imaging tests for the diagnosis and staging of pancreatic adenocarcinoma: a meta-analysis. Pancreas 45: 789-95, 2016
3) Rao SX et al: Small solid tumors (＜ or ＝ 2 cm) of the pancreas: relative accuracy and differentiation of CT and MR imaging. Hepatogastroenterology 95: 2261-2270, 2000
4) Motosugi U et al: Detection of pancreatic carcinoma and liver metastases with gadoxetic acid-enhanced MR imaging: comparison with contrast-enhanced multi-detector row CT. Radiology 260: 446-453, 2011
5) Koelbilinger C et al: Gadobenate dimeglumine-enhanced 3.0-T MR imaging versus multiphasic 64-detector row CT: prospective evaluation in patients suspected of having pancreatic cancer. Radiology 259: 757-766, 2011

6) Park MJ et al: Preoperative detection of small pancreatic carcinoma: value of adding diffusion-weighted imaging to conventional MR imaging for improving confidence level. Radiology 273: 433-443, 2014
7) Adamek HE et al: Pancreatic cancer detection with magnetic resonance cholangiopancreatography and endoscopic retrograde cholangiopancreatography: a prospective controlled study. Lancet 65: 808-814, 2000
8) Takakura K et al: Clinical usefulness of diffusion-weighted MR imaging for detection of pancreatic cancer: comparison with enhanced multidetector-row CT. Abdom Imaging 8: 457-462, 2011

BQ 52 Is abdominal MRI recommended to determine pancreatic cancer progression?

Statement

Abdominal MRI is comparably useful to CT for comprehensively determining the progression of pancreatic cancer. However, EOB-MRI is superior for diagnosing hepatic metastasis.

Background

The 2016 diagnostic imaging guidelines strongly recommended MDCT using dynamic imaging to evaluate pancreatic cancer progression. Many reports have indicated that MRI is also useful for determining pancreatic cancer progression, and that is described in detail here.

Explanation

A meta-analysis by Li et al. regarding the detection of vascular invasion to determine pancreatic cancer progression found that the sensitivity and specificity of abdominal MRI were 63% (95% CI, 48% to 77%) and 93% (95% CI, 86% to 98%), respectively.[1)] By comparison, sensitivity and specificity were 73% (95% CI, 67% to 79%) and 95% (95% CI, 93% to 97%), respectively, for CT and 66% (95% CI, 85% to 97%) and 95% (95% CI, 93% to 97%), respectively, for EUS. Thus, CT was found to be superior in terms of sensitivity for vascular invasion. Evaluation by adding multiplanar reconstruction to dynamic MDCT imaging has reported it to be superior to MRI, including contrast-enhanced MRI and MRCP, for determining local progression.[2)] On the other hand, a meta-analysis of vascular invasion assessment by Zhang et al. found no significant differences between MRI and CT. Sensitivity and specificity were 67% (95% CI, 59% to 74%) and 94% (95% CI, 91% to 96%), respectively, for MRI and 71% (95% CI, 64% to 78%) and 92% (95% CI, 89% to 96%), respectively, for CT.[3)] Based on an assessment within the analysis, the report included an additional statement indicating that evaluation by MRA did not contribute to additional information on vascular invasion.

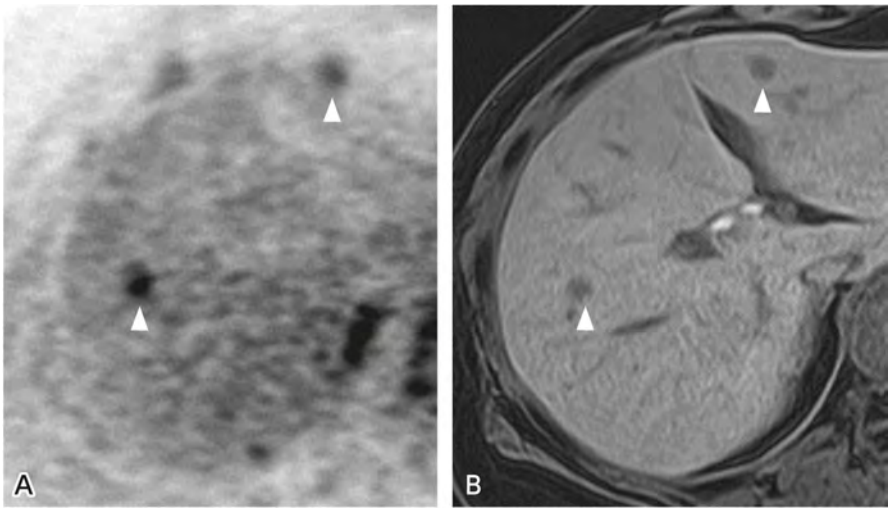

Figure　Multiple hepatic metastases of pancreatic cancer

A: MRI, diffusion-weighted imaging, b-value = 1,000 s/mm^2, reverse contrast image: The presence of high-signal-intense nodules ≤ 1 cm in size (▷) is seen in both liver lobes, suggesting multiple hepatic metastases.
B: EOB-MRI, hepatobiliary phase: Low-signal-intense areas (▷) are seen in the hepatobiliary phase of contrast enhancement, consistent with the high-signal-intense nodules seen with diffusion-weighted imaging. The finding supports a diagnosis of multiple hepatic metastases.

There have been many studies that have evaluated the usefulness of MRI in determining not only local progression, but also the resectability of pancreatic cancer.[4-6] Park et al. compared dynamic contrast-enhanced MRI and MRCP with contrast-enhanced MDCT by specifying the following as criteria for unresectability and found that the two modalities were comparable with respect to diagnostic performance in determining resectability: (1) distant metastasis (liver, peritoneum, abdominal paraaortic lymph nodes); (2) peripancreatic vascular invasion (celiac artery, hepatic artery, superior mesenteric artery); (3) advanced portal vein/superior mesenteric artery invasion; and (4) invasion of surrounding organs (stomach, spleen, colon).[4] Koelblinger et al. obtained similar results for evaluation by 3T MRI and 64-row MDCT (both dynamic imaging).[5]

In recent years, the liver-specific MRI contrast medium Gd-EOB-DTPA has received attention for its use in evaluating hepatic metastasis (Fig.).[7, 8] In addition to having the features of conventional extracellular gadolinium contrast media, it can be used to evaluate the liver parenchyma in the hepatobiliary phase (usually approximately 20 minutes after contrast medium injection) because it is taken up by normal hepatocytes. Motsugi et al. found no difference between EOB-MRI and dynamic contrast-enhanced MDCT with respect to the detection performance of pancreatic cancer, but they reported better sensitivity for hepatic metastases with contrast-enhanced MRI than with contrast-enhanced MDCT.[7] In addition, a meta-analysis by Vreugdenburg et al. found that the sensitivity of EOB-MRI for small metastatic lesions (< 1 cm in diameter) was 2.21-fold greater than that of CT, a significant difference.[8] However, specificity was roughly comparable, that of EOB-MRI being 0.92-fold that of CT. There have also been occasional reports that diffusion-weighted MRI is useful in evaluating pancreatic cancer hepatic metastasis.[9]

These findings indicate that the usefulness of MRI in determining pancreatic cancer progression is comparable to that of MDCT. Abdominal MRI is therefore recommended to determine pancreatic cancer progression. However, its use in combination with MDCT and decisions on when to use one or the other depend on the circumstances of the facility.

Search keywords and secondary references

PubMed was searched using the following keywords: pancreatic cancer, staging, MRI, sensitivity, and specificity. The period searched was from January 1990 to June 2019; hits were obtained for 148 articles. Another 4 articles were added with a hand search.

In addition, the following was referenced as a secondary source.

1) Clinical Practice Guidelines for Pancreatic Cancer 2019

References

1) Li AE et al：Diagnostic accuracy of imaging modalities in the evaluation of vascular invasion in pancreatic adenocarcinoma：a meta-analysis. World J Oncol 4：74-82, 2013
2) Mehmet Erturk S et al：Pancreatic adenocarcinoma：MDCT versus MRI in the detection and assessment of locoregional extension. J Comput Assist Tomogr 30：583-590, 2006
3) Zhang Y et al：Preoperative vascular evaluation with computed tomography and magnetic resonance imaging for pancreatic cancer：a meta-analysis. Pancreatology 12：227-233, 2012
4) Park HS et al：Preoperative evaluation of pancreatic cancer：comparison of gadolinium-enhanced dynamic MRI with MR cholangiopancreatography versus MDCT. J Magn Reson Imaging 30：586-595, 2009
5) Koelblinger C et al：Gadobenate dimeglumine-enhanced 3.0-T MR imaging versus multiphasic 64-detector row CT：prospective evaluation in patients suspected of having pancreatic cancer. Radiology 259：757-766, 2011
6) Bipat S et al：Ultrasonography, computed tomography and magnetic resonance imaging for diagnosis and determining resectability of pancreatic adenocarcinoma：a meta-analysis. J Comput Assist Tomogr 29：438-445, 2005
7) Motosugi U et al：Detection of pancreatic carcinoma and liver metastases with gadoxetic acid-enhanced MR imaging：comparison with contrast-enhanced multi-detector row CT. Radiology 260：446-453, 2011
8) Vreugdenburg TD et al：Comparative diagnostic accuracy of hepatocyte-specific gadoxetic acid（Gd-EOB-DTPA）enhanced MR imaging and contrast enhanced CT for the detection of liver metastases：a systematic review and meta-analysis. Int J Colorectal Dis 31：1739-1749, 2016
9) Holzapfel K et al：Comparison of diffusion-weighted MR imaging and multidetector-row CT in the detection of liver metastases in patients operated for pancreatic cancer. Abdom Imaging 36：179-184, 2011

BQ 53 Are CT and MRI recommended to determine the malignancy grade of P-NETs?

Statement

Contrast-enhanced CT and MRI are useful for evaluating the malignancy grade of P-NETs.

Contrast-enhanced CT and MRI are tests that are widely used to locally diagnose P-NET and screen for hepatic metastasis, and it is recommended that malignancy grade be determined at the same time.

Background

In recent years, the frequency of P-NET detection, particularly the detection of small nonfunctional tumors, has increased with improvements in diagnostic imaging, such as CT and MRI, and the increased availability of histological diagnosis by means such as endoscopic ultrasound-guided aspiration.[1)] The sensitivity of dynamic contrast-enhanced CT and MRI in detecting P-NETs is high, at 82% (95% CI, 67% to 96%) and 79% (95% CI, 54% to 100%), respectively,[2)] and the Guidelines for the Diagnosis and Treatment of Pancreatic and Gastroenteropancreatic Neuroendocrine Neoplasms (NENs), 2nd Edition treat them as tests of recommendation grade A that are useful for locally diagnosing functional and nonfunctional lesions and screening for their metastasis (secondary source 1).

Although neuroendocrine neoplasms are treated as malignancies, their malignancy grades vary widely, from those with a clinical course and prognosis that resemble those of benign neoplasms to highly malignant neoplasms that progress weekly or monthly. In the 4th edition of the 2010 WHO classification of tumors of the digestive system, neuroendocrine neoplasms are classified as grade 1 (G1) and grade 2 neuroendocrine tumors (NETs), which are well differentiated and have a low proliferative capacity, and neuroendocrine carcinomas (NECs), which are poorly differentiated and have a high proliferative capacity (secondary source 2). This classification is very highly correlated with prognosis.[3)] Many studies have examined the relationship between the WHO classification and imaging findings, and CT and MRI have been reported to be useful in evaluating the malignancy grade of P-NETs. This section will provide an overview of the P-NET imaging findings that have been reported to suggest malignancy.

Explanation

Many retrospective, cohort studies and case-control studies have been conducted, and multiple articles have reported that the results of the studies with large sample sizes indicate that the CT and MRI findings suggestive of lesions with high proliferative capacity include the following: (1) large in size; (2) irregular nature of tumor borders; (3) weak contrast enhancement in the arterial phase of dynamic CT (or MRI); (4) weak contrast enhancement in the portal venous phase of dynamic CT (or MRI); (5) inhomogeneous contrast enhancement; (6) vascular invasion present; (7) local invasion present; (8) pancreatic duct (upstream pancreatic duct dilatation) present; (9) mix of cystic or necrotic components present; (10) strong

diffusion restriction; (11) edema of surrounding lymph nodes present; and (12) hepatic metastasis present.[4-11] In addition, studies have also directly analyzed the relationship between imaging findings and prognosis (recurrence-free survival and progression-free survival rates and overall survival rates) and, similar to the findings described above, found that factors such as the following were associated with a poor clinical prognosis: large in size; irregular borders; contrast enhancement (hypovascular, inhomogeneous, gradually increasing); vascular invasion; bile and pancreatic duct dilatation; isointensity to hypointensity on T2-weighted images; lymph node edema; and hepatic metastasis.[5-7, 11-14] In other words, typical P-NETs are often small in size, round or cylindrical with a distinct border, and show marked and homogeneous enhancement in the arterial phase of dynamic CT (early arterial phase to pancreatic parenchymal phase).[15] Those that exhibit these typical findings are likely to be lesions that have a low proliferative capacity and a good prognosis. Conversely, lesions that show atypical imaging findings often pose problems for qualitative diagnosis, particularly differentiation from invasive pancreatic ductal carcinoma, and if they are NENs, they may be lesions with a high proliferative capacity with a poor prognosis.

When the WHO classification of digestive system tumors was revised in 2019, the malignancy grade classification of P-NENs was changed (secondary source 3). Specifically, the 5th edition of the WHO classification further divided NENs with a high proliferative capacity into 2 groups: G3 NETs, which are well-differentiated tumors in the NET category; and neuroendocrine carcinomas (NECs), which are poorly differentiated tumors not in the NET category. NECs and NETs are considered genetically and biologically different tumors, and their treatment strategies and prognoses are completely different. Distinguishing between them is therefore important. Somatostatin receptor scintigraphy is useful for distinguishing between NECs and NETs based on functional imaging. Although G3 NETs have a high proliferative capacity, it has been found that their function is often maintained and that they accumulate frequently, whereas NECs have been reported to accumulate relatively infrequently.[16]

Search keywords and secondary references

PubMed was searched using the following keywords: pancreatic, neuroendocrine, CT, and MRI. The period searched was through June 2019; hits were obtained for 1,222 articles. A hand search was also performed.

In addition, the following were referenced as secondary sources.

1) Committee for the Preparation of the Clinical Practice Guidelines for Gastroenteropancreatic Neuroendocrine Neoplasms (GEP-NENs), 2nd Edition, Japan Neuroendocrine Tumor Society (JNETS), Ed.: Clinical Practice Guidelines for Gastroenteropancreatic Neuroendocrine Neoplasms (GEP-NENs), 2nd Edition, KANEHARA & Co., LTD., 2019.
2) Bosman F et al: WHO classification of tumours of the digestive systems 4th ed. IARC Press, 2010
3) WHO classification of tumours editorial board: WHO classification of tumours: digestive system tumours. 5th ed. IARC Press, 2019

References

1) Ito T et al: Epidemiological trends of pancreatic and gastrointestinal neuroendocrine tumors in Japan: a nationwide survey analysis. J Gastroenterol 50 (1): 58-64, 2015
2) Sundin A et al: ENETS consensus guidelines for the standards of care in neuroendocrine tumors: radiological, nuclear medicine & hybrid imaging. Neuroendocrinology 105 (3): 212-244, 2017
3) Rindi G et al: TNM staging of neoplasms of the endocrine pancreas: results from a large international cohort study. J Natl Cancer Inst 104 (10): 764-777, 2012
4) Kim DW et al: neuroendocrine neoplasms of the pancreas at dynamic enhanced CT: comparison between grade 3 neuroendocrine carcinoma and grade 1/2 neuroendocrine tumor. Eur Radiol 25 (5): 1375-1383, 2015
5) Canellas R et al: Prediction of pancreatic neuroendocrine tumor grade based on CT features and texture analysis. AJR Am J Roentgenol 210 (2): 341-346, 2018
6) Kim JH et al: Pancreatic neuroendocrine tumor (PNET): staging accuracy of MDCT and its diagnostic performance for the differentiation ofP-NET with uncommon CT findings from pancreatic adenocarcinoma. Eur Radiol 26 (5): 1338-1347, 2016
7) Nanno Y et al: Pancreatic duct involvement in well-differentiated neuroendocrine tumors in an independent poor prognostic factor. Ann Surg Oncol 24 (4): 1127-1133, 2017
8) Lotfalizadeh E et al: Prediction of pancreatic neuroendocrine tumour grade with MR imaging features: added value of diffusion-weighted imaging. Eur Radiol 27 (4): 1748-1759, 2017
9) Toshima F et al: Is the combination of MR and CT findings useful in determining the tumor grade of pancreatic neuroendocrine tumors? Jpn J Radiol 35 (5): 242-253, 2017
10) Kang J et al: Association between pathologic grade and multiphase computed tomography enhancement in pancreatic neuroendocrine neoplasm. J Gastroenterol Hepatol doi: 10.1111/jgh.14139, 2018, online ahead of print
11) Canellas R et al: Pancreatic neuroendocrine tumor: correlations between MRI features, tumor biology, and clinical outcome after surgery. J Magn Reson Imaging 47 (2): 425-432, 2018
12) Kim DW et al: Prognostic value of CT findings to predict survival outcome in patientgs with pancreatic neuroendocrine neoplasms: a single institutional study of 161 patients. Eur Radiol 26 (5): 1320-1329, 2016
13) Kim C et al: A comparison of enhancement patterns on dynamic enhanced CT and survival between patients with pancreatic neuroendocrine tumors with and without intratumoral fibrosis. Abdom Radiol 42 (12): 2835-2842, 2017
14) Arai T et al: Contrast-enhancement ratio on multiphase enhanced computed tomography predicts recurrence of pancreatic neuroendocrine tumor after curative resection. Pancreatology 16 (3): 397-402, 2016
15) Sahani DV et al: Gastroenteropancreatic neuroendocrine tumors: role of imaging diagnosis and management. Radiology 266 (1): 38-61, 2013
16) Coriat R et al: Gastroenteropancreatic well-differentiated grade 3 neuroendocrine tumors: review and position statement. Oncologist 21 (10): 1191-1199, 2016

BQ 54 Which imaging examinations are recommended when intestinal obstruction is suspected?

Statement

Plain radiography, ultrasound, and CT are recommended when intestinal obstruction is suspected. However, contrast-enhanced CT is useful for detailed evaluation.

Background

Intestinal obstruction is a condition of impaired intestinal transit caused by mechanical obstructions; ileus is a different condition caused by functional disorders. It is clinically important to diagnose the location, cause, and signs of intestinal ischemia of the intestinal obstruction at an early stage. The diagnosis of intestinal obstruction has been conventionally made based on plain radiography. Currently, ultrasound and CT are widely accepted as standard diagnostic tools. The following is an overview of the efficacy of these diagnostic modalities based on previous diagnostic imaging guidelines and additionally the 2015 clinical practice guidelines for acute abdomen (secondary source 1), supplemented by data from the latest literature, mainly reviews.

Explanation

Plain radiography, which is simple, low cost, and minimally invasive, but allows observation of the entire abdomen as a single test, has been used as a routine test in patients with acute abdomen. Its advantage includes evaluation of intestinal gas patterns associated with intestinal obstruction.[1)] However, pooled data from 4 articles including prospective studies showed that the sensitivity and specificity of plain radiography for intestinal obstruction were 65% and 75%, respectively.[2-5)] The diagnostic performance of ultrasound based on the pooled data from 4 articles showed that the sensitivity and specificity were 92% and 95%, respectively.[2, 3, 6, 7)] The diagnostic performance of CT based on the pooled data from 7 articles showed sensitivity and specificity of 94% (95% CI, 71% to 100%) and 78% (95% CI, 57% to 100%), respectively.[3, 4, 8-12)] According to a small prospective study by Suri et al. testing the diagnostic performance of plain radiography, ultrasound, and CT, CT showed the highest sensitivity (93%) and specificity (100%) in diagnosing intestinal obstruction. CT also showed the best result for identifying the cause of intestinal obstruction (87%), better than both ultrasound (23%) and plain radiography (7%).[3)]

It is important to promptly and accurately diagnose strangulated intestinal obstruction, which generally requires emergent surgery. Contrast-enhanced CT is useful for assessing changes in intestinal wall thickness, intestinal wall contrast enhancement, mesenteric congestion, and ascites. According to the systematic review by Millet et al., contrast enhancement of the intestinal wall and mesenteric fluid accumulation are significantly associated with intestinal ischemia.[13)] A meta-analysis of diagnosis of intestinal ischemia using contrast-enhanced (2-phase) CT showed sensitivity of 93.3% and specificity of

95.9%.[14] Non-contrast CT is desirable when considering a possible diagnosis of intestinal intramural hematomas showing hyperdensity, which may be misdiagnosed as normal intestinal wall enhancement on contrast-enhanced CT alone.[15] In the case of incomplete small bowel obstruction that may not show definite behavior on CT, administration of a water-soluble contrast medium to the small intestine is helpful.[16] It is also useful for evaluating emergent status requiring surgery for an adhesive small bowel obstruction.[17] In evaluating large bowel obstruction, CT is the first choice. However, in the case of large bowel obstruction caused by neoplastic obstruction, volvulus, and intussusception, a barium enema may be indicated. A water-soluble contrast medium should be used for the patient with possible perforation.

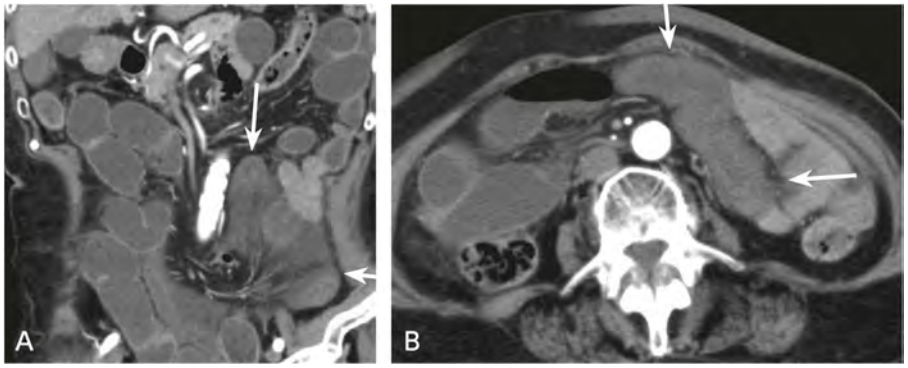

Figure　Strangulated intestinal obstruction

A: Contrast-enhanced CT (coronal image): The small intestine lesion shows closed-loop obstruction (→).
B: Contrast-enhanced CT (transverse image): The closed-loop obstruction shows poor contrast enhancement, which indicates bowel ischemia (→).

Search keywords and secondary references

The following keywords were searched on PubMed: bowel obstruction, CT, ultrasonography, and abdominal radiographs.

In addition, the following was referenced as a secondary source.

1) Committee for the Publication of Clinical Practice Guidelines for Acute Abdomen, Ed.: 2015 Clinical Practice Guidelines for Acute Abdomen. Igaku-Shoin, 2015.

References

1) Eisenberg RL et al: Evaluation of plain abdominal radiographs in the diagnosis of abdominal pain. Ann Surg 197: 464-469, 1983
2) Ogata M et al: Prospective evaluation of abdominal sonography for the diagnosis of bowel obstruction. Ann Surg 223: 237-241, 1996
3) Suri S et al: Comparative evaluation of plain films, ultrasound and CT in the diagnosis of intestinal obstruction. Acta Radiol 40: 422-428, 1999
4) Matsuoka H et al: Preoperative evaluation by magnetic resonance imaging in patients with bowel obstruction. Am J Surg 183: 614-617, 2002
5) Frager D et al: CT of small-bowel obstruction: value in establishing the diagnosis and determining the degree and cause. AJR Am J Roentgenol 162: 37-41, 1994
6) Czechowski J: Conventional radiography and ultrasonography in the diagnosis of small bowel obstruction and strangulation. Acta Radiol 37: 186-189, 1996

7) Schmutz GR et al: Small bowel obstruction: role and contribution of sonography. Eur Radiol 7: 1054-1058, 1997
8) Frager D et al: Detection of intestinal ischemia in patients with acute small-bowel obstruction due to adhesions or hernia: efficacy of CT. AJR Am J Roentgenol 166: 67-71, 1996
9) Balthazar EJ et al: Intestinal ischemia in patients in whom small bowel obstruction is suspected: evaluation of accuracy, limitations, and clinical implications of CT in diagnosis. Radiology 205: 519-522, 1997
10) Obuz F et al: The efficacy of helical CT in the diagnosis of small bowel obstruction. Eur J Radiol 48: 299-304, 2003
11) Peck JJ et al: The role of computed tomography with contrast and small bowel follow-through in management of small bowel obstruction. Am J Surg 177: 375-378, 1999
12) Beall DP et al: Imaging bowel obstruction: a comparison between fast magnetic resonance imaging and helical computed tomography. Clin Radiol 57: 719-724, 2002
13) Millet I et al: Value of CT findings to predict surgical ischemia in small bowel obstruction: a systematic review and meta-analysis. Eur Radiol 25: 1823-1835, 2015
14) Menke J: Diagnostic accuracy of multidetector CT in acute mesenteric ischemia: systematic review and meta-analysis. Radiology 256: 93-101, 2010
15) Furukawa A et al: CT diagnosis of acute mesenteric ischemia from various causes. AJR Am J Roentgenol 192: 408-416, 2009
16) Kendrick ML: Partial small bowel obstruction: clinical issues and recent technical advances. Abdom Imaging 34: 329-334, 2009
17) Branco BC et al: Systematic review and meta-analysis of the diagnostic and therapeutic role of water-soluble contrast agent in adhesive small bowel obstruction. Br J Surg 97: 470-478, 2010

BQ 55 Which imaging examinations are recommended when acute appendicitis is suspected?

Statement

Either ultrasound or CT is recommended as an imaging examination when acute appendicitis is suspected. However, CT provides superior accuracy. Use of a contrast medium in CT is unnecessary.

Background

Acute appendicitis is a type of acute abdomen typically requiring emergent surgery. Its differential diagnosis includes colonic diverticulitis, which should be differentiated to provide appropriate treatment. Ultrasound and CT are commonly used as imaging examinations for acute appendicitis.

Ultrasound is a common examination used for suspected acute abdomen that is easy to access and mobile (can be performed at the bedside), with no radiation exposure. However, the diagnostic performance varies depending on the operator's skill and the patient's condition, such as intestinal gas. CT can cover a broad range of conditions and test objectively with a rapid scan, which is widely used for diagnosing acute abdomen.[1, 2)] The following is an overview of the efficacy of these diagnostic modalities based on previous diagnostic imaging guidelines and, in addition, the 2015 clinical practice guidelines for acute abdomen (secondary source 1), supplemented by data from the latest literature, mainly reviews.

Explanation

Regarding the diagnostic performance of ultrasound in acute appendicitis, a meta-analysis by Terasawa et al. reported sensitivity of 86% (95% CI, 83% to 88%) and specificity of 81% (95% CI, 78% to 84%)[3)]. The meta-analysis by Doria et al. reported sensitivity of 83% (95% CI, 78% to 87%) and specificity of 93% (95% CI, 90% to 96%).[4)] Regarding the diagnostic performance of CT, the meta-analysis by Terasawa et al. reported sensitivity of 94% (95% CI, 91% to 95%) and specificity of 95% (95% CI, 93% to 96%), and the meta-analysis by Doria et al. reported sensitivity of 94% (95% CI, 92% to 95%) and specificity of 94% (95% CI, 94% to 96%). CT showed significantly better sensitivity than ultrasound. However, the diagnostic performance of ultrasound may be higher in Japan than in the reports from Europe and the United States, where the body habitus of the subjects is quite different. CT also has an advantage over ultrasound in diagnosing cases with perforation. Accordingly, CT is recommended as a primary test for adult patients with acute abdomen.

The addition of contrast media increases the sensitivity of CT in diagnosing acute appendicitis.[5)] Another report showed that contrast media improves the detectability of the appendix on CT, though it does not increase the diagnostic accuracy for acute appendicitis.[6)] Contrast-enhanced CT is therefore recommended when the diagnosis is uncertain. In particular, contrast-enhanced CT has an advantage in diagnosing perforated appendicitis.[4)]

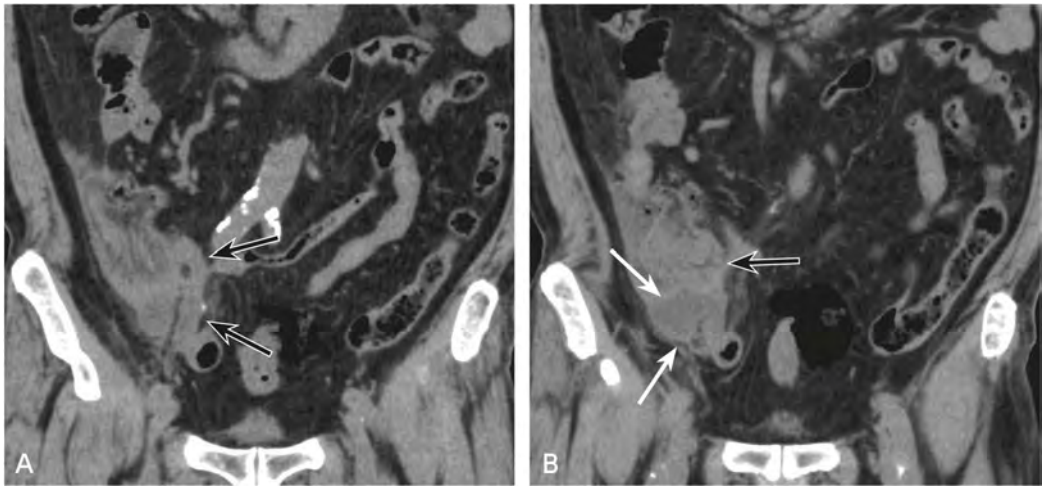

Figure 1. Acute appendicitis

A: Non-contrast CT (coronal image): The CT shows an enlarged appendix (→).

B: Non-contrast CT (coronal image): The right side of the enlarged appendix shows a ruptured appendiceal wall (→) and abscess formation (⇨).

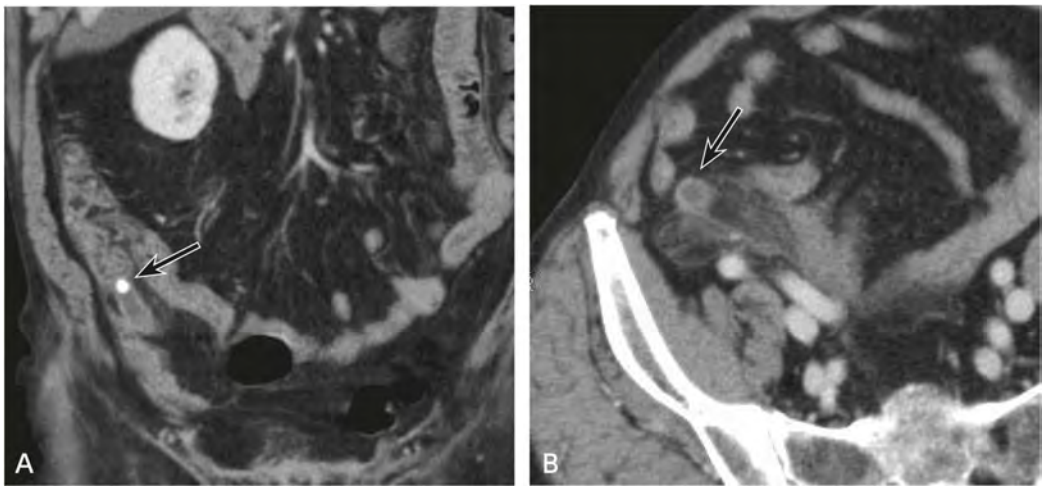

Figure 2. Acute appendicitis

A: Contrast-enhanced CT (coronal image): The CT shows a fecalith in the appendiceal base (→).

B: Contrast-enhanced CT (transverse image): The CT shows an enlarged appendix with increased density of the surrounding adipose tissue (→).

Search keywords and secondary references

The following keywords were searched on PubMed: acute appendicitis, CT, and ultrasonography.

In addition, the following was referenced as a secondary source.

1) Committee for the Publication of Clinical Practice Guidelines for Acute Abdomen, Ed.: 2015 Clinical Practice Guidelines for Acute Abdomen. Igaku-Shoin, 2015.

References

1) Stoker J et al: Imaging patients with acute abdominal pain. Radiology 253: 31-46, 2009
2) van Randen A et al: A comparison of the accuracy of ultrasound and computed tomography in common diagnoses causing acute abdominal pain. Eur Radiol 21: 1535-1545, 2011
3) Terasawa T et al: Systematic review: computed tomography and ultrasonography to detect acute appendicitis in adults and adolescents. Ann Intern Med 141: 537-546, 2004
4) Doria AS et al: US or CT for diagnosis of appendicitis in children and adults?: a meta-analysis. Radiology 241: 83-94, 2006
5) Tamburrini S et al: Acute appendicitis: diagnostic value of nonenhanced CT with selective use of contrast in routine clinical settings. Eur Radiol 17: 2055-2061, 2007
6) Chiu YH et al: Whether intravenous contrast is necessary for CT diagnosis of acute appendicitis in adult ED patients? Acad Radiol 20: 73-78, 2013

BQ 56 Which imaging examinations are recommended when colonic diverticulitis is suspected?

Statement

CT is recommended when colonic diverticulitis is suspected.

Background

Colonic diverticulitis is a common cause of acute abdomen often treated conservatively. It sometimes affects the right-side colon, which mimics acute appendicitis that requires emergent surgery. Ultrasound or CT is commonly used as an imaging examination for colonic diverticulitis.

Ultrasound is a common examination used for suspected acute abdomen that is easy to access and mobile (can be performed at the bedside), with no radiation exposure. However, the diagnostic performance varies depending on the operator's skill and the patient's condition, such as intestinal gas. CT can cover a broad range of conditions and test objectively with a rapid scan, which is widely used for diagnosing acute abdomen.[1, 2)] The following is an overview of the efficacy of these diagnostic modalities based on previous diagnostic imaging guidelines and the guidelines for colonic diverticulosis (diverticular bleeding and diverticulitis), supplemented by data from the latest literature, mainly reviews.

Explanation

According to the pooled data from 4 articles, the diagnostic performance of CT for colonic diverticulitis showed sensitivity of 89%, specificity of 99%, a positive predictive value of 99%, and a negative predictive value of 90%.[3-6)] Pooled data from 4 articles regarding the diagnostic performance of ultrasound showed sensitivity of 91%, specificity of 92%, a positive predictive value of 92%, and a negative predictive value of 91%.[7-10)] A systematic review by Andeweg et al. reported that the sensitivities of ultrasound and CT were 90% and 90%, respectively, and their specificities were 95% and 96%, respectively.[11)]

CT should be used as a standard imaging examination for diagnosing colonic diverticulitis because the severity classification is based on the CT features. However, ultrasound may be used as a first choice for diagnosing colonic diverticulitis because of the reported evidence that ultrasound is useful in diagnosing and evaluating treatment response,[12)] and it shows diagnostic performance similar to CT.[13)] Ultrasound may also be the first choice when there is no CT equipment available, although ultrasound has limitations, including inconsistent results depending on operators, lack of reproducibility, and low sensitivity in diagnosing peritonitis that can be detected on CT.[11, 14)]

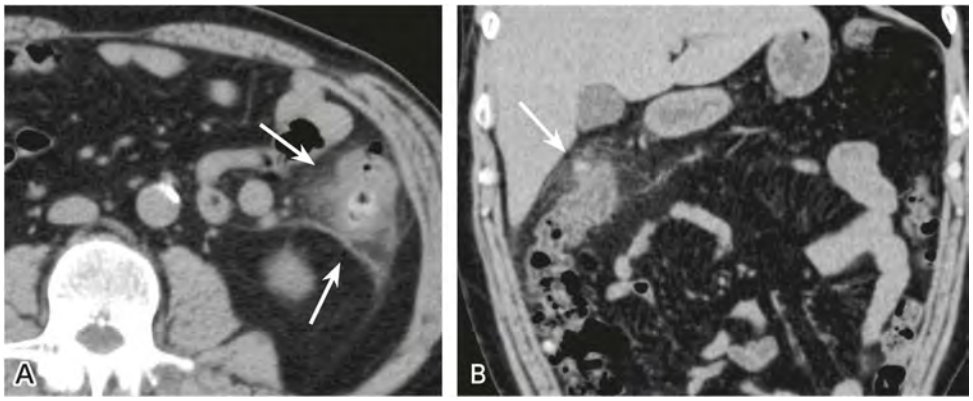

Figure　Colonic diverticulitis

A: Non-contrast CT (transverse image): The CT shows a hyperdense diverticulum in the transverse colon and increased density of surrounding adipose tissue (→).

B: Non-contrast CT (coronal image): A hyperdense diverticulum located in the hepatic flexure seen in figure A (→).

Search keywords and secondary references

The following keywords were searched on PubMed: diverticulitis, CT, and ultrasonography.

The following was referenced as a secondary source.

1) Japanese Gastroenterological Association, Ed.: 2017 Colonic Diverticulosis Guidelines. Japanese Gastroenterological Association, 2017.

References

1) Stoker J et al: Imaging patients with acuteabdominal pain. Radiology 253: 31-46, 2009
2) van Randen A et al: A comparison of the accuracy of ultrasound and computed tomography in common diagnoses causing acute abdominal pain. Eur Radiol 21: 1535-1545, 2011
3) Cho KC et al: Sigmoid diverticulitis: diagnostic role of CT--comparison with barium enema studies. Radiology 176: 111-115, 1990
4) Stefansson T et al: Diverticulitis of the sigmoid colon: a comparison of CT, colonic enema and laparoscopy. Acta Radiol 38: 313-319, 1997
5) Rao PM, Rhea JT. Colonic diverticulitis: evaluation of the arrowhead sign and the inflamed diverticulum for CT diagnosis. Radiology 209: 775-779, 1998
6) Werner A et al: Multi-slice spiral CT in routine diagnosis of suspected acute left-sided colonic diverticulitis: a prospective study of 120 patients. Eur Radiol 13: 2596-2603, 2003
7) Verbanck J et al: Can sonography diagnose acute colonic diverticulitis in patients with acute intestinal inflammation? a prospective study. J Clin Ultrasound 17: 661-666, 1989
8) Hollerweger A et al: Sigmoid diverticulitis: value of transrectal sonography in addition to transabdominal sonography. AJR Am J Roentgenol 175: 1155-1160, 2000
9) Zielke A et al: Prospective evaluation of ultrasonography in acute colonic diverticulitis. Br J Surg 84: 385-388, 1997
10) Schwerk WB et al: Sonography in acute colonic diverticulitis: a prospective study. Dis Colon Rectum 35: 1077-1084, 1992
11) Andeweg CS et al: Toward an evidence-based step-up approach in diagnosing diverticulitis. Scand J Gastroenterol 49: 775-784, 2014
12) Mizuki A et al: The out-patient management of patients with acute mild-to-moderate colonic diverticulitis. Aliment Pharmacol Ther 21: 889-897, 2005
13) King WC et al: Benefits of sonography in diagnosing suspected uncomplicated acute diverticulitis. J Ultrasound Med 34: 53-58, 2015
14) Pradel JA et al: Acute colonic diverticulitis: prospective comparative evaluation with US and CT. Radiology 205: 503-512, 1997

BQ 57 Which imaging examinations are recommended for staging of esophageal cancer?

Statement

Contrast-enhanced CT and PET are recommended for staging of esophageal cancer.

Background

Staging of esophageal cancer is generally undertaken after a definitive diagnosis by endoscopy, including subsequent endoscopic ultrasound (EUS) to estimate invasion depth. (EUS diagnosis for staging is beyond the scope of this article.) Contrast-enhanced CT is widely accepted for assessing TNM elements. MRI is not commonly used. PET may detect lesions that are absent or ill-defined on contrast-enhanced CT. An upper gastrointestinal series using barium sulfate has been conventionally performed in Japan to locate and estimate the invasion depth of esophageal cancer. The following is an overview of the efficacy of these diagnostic modalities based on previous diagnostic imaging guidelines and supplemented by data from the latest literature, mainly reviews.

Explanation

EUS, which provides high resolution, is superior to contrast-enhanced CT for evaluating the invasion depth of superficial cancer. Differentiating among T1, T2, and T3 is difficult for advanced cancer, which is visualized as wall thickening on contrast-enhanced CT. It is clinically important to distinguish between T3 and T4, which invades to extra-esophageal organs, which is a contraindication to surgery. The diagnostic performance of CT for T4 lesions focusing on the fat layer between the tumor and the neighboring organs showed sensitivity ranging from 88% to 100% and specificity from 85% to 100%.[1, 2] Contrast enhancement of the tumor border in the early phase of dynamic contrast-enhanced CT may correspond to adventitial invasion.[3] Recent advances in MDCT which enables production of various 3D images has not yielded additional value for the diagnosis of esophageal cancer. The upper gastrointestinal series using barium sulfate has been conventionally accepted as a method to evaluate invasion depth focusing on lateral deformity in Japan. However, there is no scientific evidence supporting its use for esophageal cancer staging. The advantage of barium sulfate includes diagnosis of location and monitoring esophageal passage, which may be better than endoscopy. (Fig. A, B)

The diagnostic performance of contrast-enhanced CT for lymph node metastasis is not fully reliable. Commonly, the criteria for metastatic nodes are size ≥ 10 mm for intrathoracic and intraperitoneal regions and short-axis diameter ≥ 5 mm for the supraclavicular region,[4, 5] although metastatic nodes may show no enlargement. Using a criterion of ≥ 10 mm yields sensitivity ranging from 30% to 60% and specificity ranging from 60% to 80%.[6, 7]

PET has advantages of providing an overview and examining TNM elements within a single test covering the whole body. PET/CT is an advanced PET fused with CT, which overcomes the low resolution of PET. In the evaluation of primary tumors, early-stage cancer is not detectable with PET, and FDG accumulation has no correlation with invasion depth.[8, 9] PET/CT has a significant advantage over CT in diagnosing lymph node metastasis by detecting FDG accumulation (Fig. C). The sensitivity and specificity of PET for lymph node metastasis have been reported to range from 51% to 65.5% and 84% to 100%, respectively.[10, 11] With regard to distant metastasis, PET can detect unexpected metastasis with an incidence of 5% to 28%.[12]

MRI has not been commonly used for cancer staging because of lower temporal resolution and narrower scanning range than CT and artifacts caused by breathing or heartbeats. Currently, high-resolution T2-weighted imaging has improved lesion detection and diagnosis of invasion depth of esophageal cancer with an accuracy of 81%. The sensitivity and specificity in diagnosing lymph node metastasis have been reported to range from 25% to 62% and from 65% to 78%, respectively.[12]

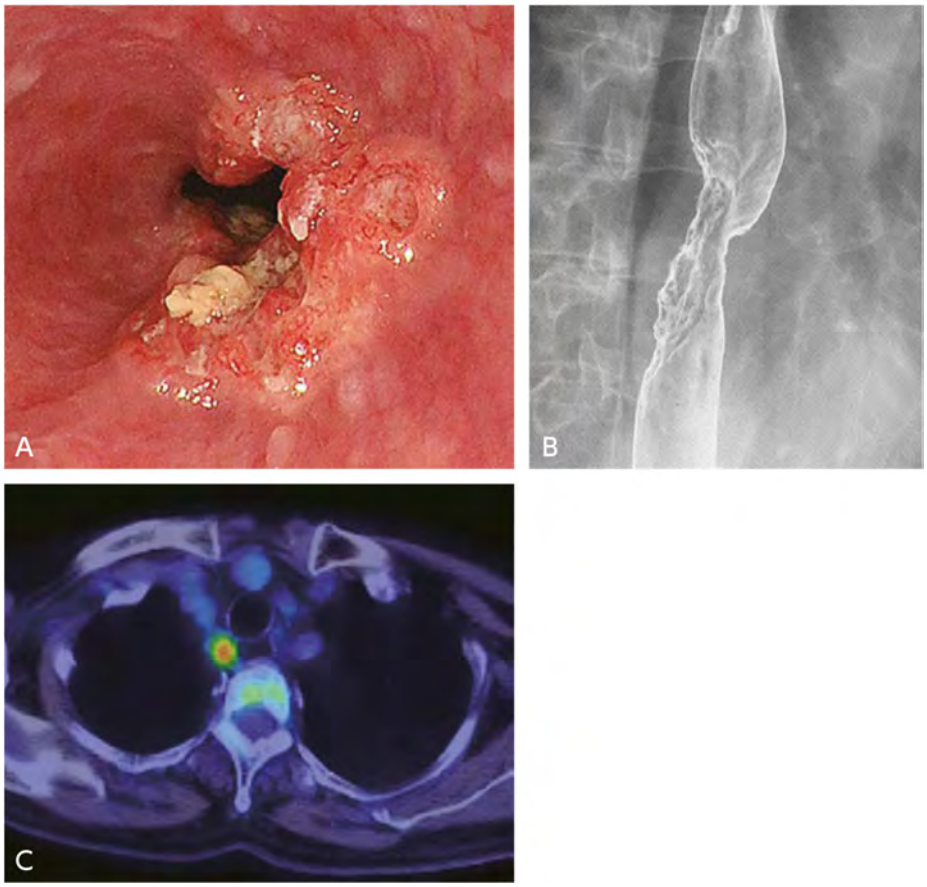

Figure Esophageal cancer

A: Endoscopy: A rough, irregular type 2 lesion forms luminal stenosis.

B: Upper gastrointestinal series: Irregular type 2 tumor located in the middle thoracic esophagus forming luminal stenosis.

C: PET/CT fusion image: A mediastinal lymph node (right recurrent nerve) shows definite FDG accumulation, indicating positive nodal metastasis.

Search keywords and secondary references

In view of the information provided in the diagnostic imaging guidelines 2016, the following keywords were searched on PubMed, limited to articles published since 2016: esophageal cancer, CT, MRI, PET, diagnosis, and staging.

References

1) Picus D et al: Computed tomography in the staging of esophageal carcinoma. Radiology 146: 433-438, 1983
2) Daffner RH et al: CT of the esophagus. II. carcinoma. AJR Am J Roentgenol 133: 1051-1055, 1979
3) Umeoka S et al: Early esophageal rim enhancement: a new sign of esophageal cancer on dynamic CT. Eur J Radiol 82: 459-463, 2013
4) Dorfman RE et al: Upper abdominal lymph nodes: criteria for normal size determined with CT. Radiology 180: 319-322, 1991
5) Fultz PJ et al: Detection and diagnosis of nonpalpable supraclavicular lymph nodes in lung cancer at CT and US. Radiology 222: 245-251, 2002
6) Block MI et al: Improvement in staging of esophageal cancer with the addition of positron emission tomography. Ann Thorac Surg 64: 770-777, 1997
7) Kato H et al: Comparison between positrosn emission tomography and computed tomography in the use of the assessment of esophageal carcinoma. Cancer 94: 921-928, 2002
8) Flamen P et al: Utility of positron emission tomography for the staging of patients with potentially operable esophageal carcinoma. J Clin Oncol 18: 3202-3210, 2000
9) Fukunaga T et al: Evaluation of esophageal cancers using 18F-fluorodeoxyglucose PET. J Nucl Med 39: 1002-1007, 1998
10) van Westreenen HL et al: Systematic review of the staging performance of 18F-fluorodeoxyglucose positron emission tomography in esophageal cancer. J Clin Oncol 22: 3805-3812, 2004
11) Kato H et al: The incremental effect of positron emission tomography on diagnostic accuracy in the initial staging of esophageal carcinoma. Cancer 103: 148-156, 2005
12) van Rossum PSN et al: Imaging of oesophageal cancer with FDG-PET/CT and MRI. Clin Radiol 70: 81-95, 2015

BQ 58 Which imaging examinations are recommended for staging of gastric cancer?

Statement

Contrast-enhanced CT is recommended for staging of gastric cancer.

Background

Staging of gastric cancer is generally undertaken after a definitive diagnosis by endoscopy including subsequent endoscopic ultrasound (EUS) to estimate invasion depth. (EUS diagnosis for staging is beyond the scope of this article.) Contrast-enhanced CT is widely accepted for assessing TNM elements. MRI is not commonly used. PET is also rarely used. An upper gastrointestinal series using barium sulfate has been conventionally performed in Japan to locate and estimate the invasion depth of gastric cancer. The following is an overview of the efficacy of these diagnostic modalities based on previous diagnostic imaging guidelines and supplemented by data from the latest literature, mainly reviews.

Explanation

EUS, which provides high resolution, is superior to contrast-enhanced CT for evaluating the invasion depth of early cancer. Advanced cancer is visualized as wall thickening on contrast-enhanced CT, and the addition of gastric wall distension (created using a foaming agent or water) provides detailed diagnosis. Furthermore, multiplanar reconstruction or 3D images based on MDCT improve diagnostic accuracy for the primary tumor (Fig. A, B).[1-3] Since gastric cancer shows histological diversity, the CT enhancement pattern varies depending on the histological structure of tumors (Fig. C).[4] The CT staging criteria by Chen et al., with diagnostic accuracy of 89%, have been widely accepted.[1] Recently, dual-energy CT has also been used for diagnosing gastric cancer.[5] MRI is specifically useful in differentiating T3 from T4 tumors.[6] An upper gastrointestinal series using barium sulfate, which provides an overview of the entire stomach and locates the tumor, has been conventionally accepted in Japan (Fig. D). It shows a specific advantage over endoscopy in estimating extension and infiltration of diffusely infiltrative gastric cancer. However, there is no scientific evidence supporting the use of upper gastrointestinal series for gastric cancer staging.

CT diagnosis of lymph node metastasis based on size is not fully reliable, although there have been numerous reports showing lymph node metastasis based on size. Chen et al. reported diagnostic accuracy of 78% with node size ≥ 8 mm defined as positive for metastasis.[1] MRI has not been established as clinically useful for diagnosing lymph node metastasis, although diffusion-weighted imaging has added value to increase sensitivity.[7] PET and PET/CT have had limited use for staging of lymph node metastasis because of their low sensitivity, despite the high specificity of greater than 95%. [8]

Gastric cancer metastasizes hematogenously to the liver. It is critically important to diagnose peritoneal dissemination, which is a contraindication to radical resection. Contrast-enhanced CT has been used as a

reliable test for diagnosing distant spread.[9] Ascites is a sign of peritoneal dissemination detected on CT, with sensitivity and specificity of 51% and 97%, respectively.[10] MRI and PET do not show added value in diagnosing distant metastasis.[11, 12]

Search keywords and secondary references

In view of the information provided in the diagnostic imaging guidelines 2016, the following keywords were searched on PubMed limited to articles published since 2016: gastric cancer, CT, MRI, PET, diagnosis, and staging.

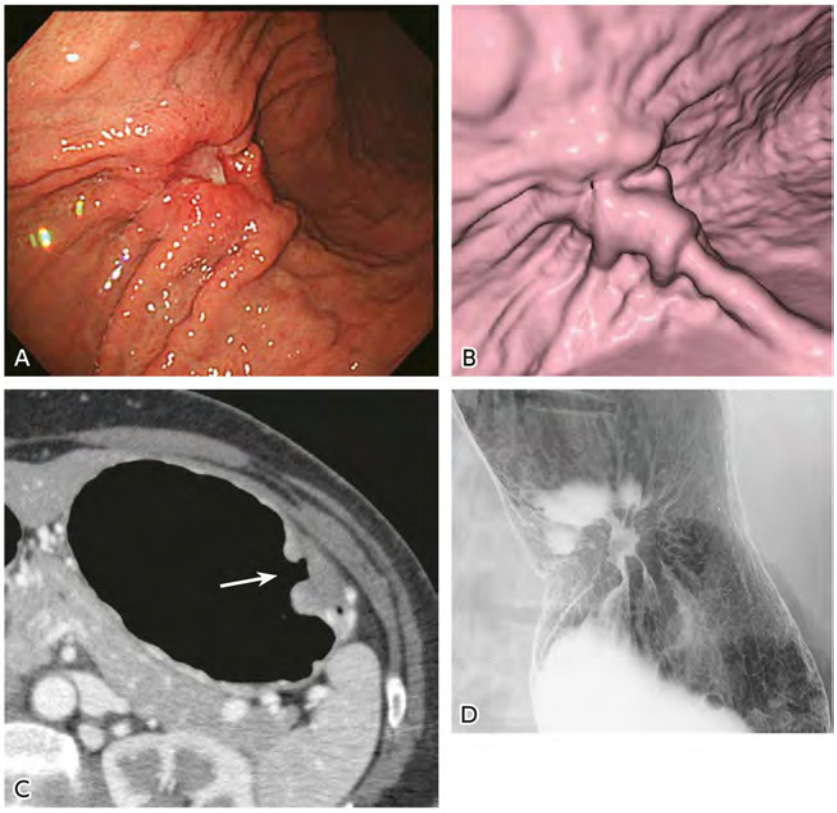

Figure Advanced gastric cancer

A: Endoscopy: A type 3 lesion shows mucosal fold convergence in the greater curvature of the gastric body.
B: 3D CT, gastrography: Virtual endoscopy shows similar findings as optical endoscopy.
C: Contrast-enhanced CT (early phase, transverse image): The lesion shows thickening of the left wall of the stomach (→). Hypodensity in the early phase suggests poorly differentiated adenocarcinoma.
D: Upper gastrointestinal series: The image clearly visualizes a type 3 lesion in the middle gastric body.

References

1) Chen CY et al: Gastric cancer: preoperative local staging with 3D multi-detector row CT-correlation with surgical and histopathologic results. Radiology 242: 472-482, 2007
2) Kim JW et al: Diagnostic performance of 64-section CT using CT gastrography in preoperative T staging of gastric cancer according to 7th edition of AJCC cancer staging manual. Eur Radiol 22: 654-662, 2012
3) Kumano S et al: T staging of gastric cancer: role of multi-detector row CT. Radiology 237: 961-966, 2005

4) Tsurumaru D et al: Diffuse-type gastric cancer: specific enhancement pattern on multiphasic contrast-enhanced compute tomography. Jpn J Radiol 35: 289-295, 2017
5) Shi C et al: Decreased stage migration rate of early gastric cancer with a new reconstruction algorithm using dual-energy CT images: a preliminary study. Eur Radiol 27: 671-680, 2017
6) Huang Z et al: The utility of MRI for pre-operative T and N staging of gastric carcinoma: a systematic review and meta-analysis. Br J Radiol. 88: 1050, 2015
7) Joo I et al: Prospective comparison of 3T MRI with diffusion-weighted imaging and MDCT for the preoperative TNM staging of gastric cancer. J Magn Reson Imaging 41: 814-21, 2015
8) Seevaratnam R et al: How useful is preoperative imaging for tumor, node, metastasis (TNM) staging of gastric cancer?: a meta-analysis. Gastric Cancer 15: 3-18. 2012
9) Lee MH et al: Gastric cancer: imaging and staging with MDCT based on the 7th AJCC guidelines. Abdom Imaging 37: 531-540, 2012
10) Yajima K et al: Clinical and diagnostic significance of preoperative computed tomography findings of ascites in patients with advanced gastric cancer. Am J Surg 192: 185-190, 2006
11) Liu S et al: Added value of diffusion-weighted MR imaging to T2-weighted and dynamic contrast-enhanced MR imaging in T staging of gastric cancer. Clin Imaging 38: 122-128, 2014
12) Kawanaka Y et al: Added value of pretreatment 18F-FDG PET/CT for staging of advanced gastric cancer: comparison with contrast-enhanced MDCT. Eur J Radiol 85: 989-995, 2016

BQ 59 Which imaging examinations are recommended for staging of colorectal cancer?

Statement

Contrast-enhanced CT is recommended for staging of colorectal cancer. MRI is recommended for diagnosing local invasion of rectal cancer. PET is recommended as limited use for diagnosing lymph node and hepatic metastases.

Background

Staging of colorectal cancer is generally undertaken after a definitive diagnosis by endoscopy, including subsequent endoscopic ultrasound (EUS) to estimate invasion depth. (EUS diagnosis for staging is beyond the scope of this article.) Most colorectal cancers are at an advanced stage at the time of diagnosis, whereas early-stage colorectal cancer is very rare. Contrast-enhanced CT is widely accepted for assessing TNM elements. CT colonography (CTC), a CT technique specific to the colorectum, has been generally used as a preoperative test (see BQ 60). Since treatment options for rectal cancer vary depending on local status, MRI, which provides excellent spatial resolution, is suitable for pretreatment evaluation. MRI is also used to examine hepatic metastasis. PET has limited use. A barium enema has been conventionally performed in Japan to locate and estimate invasion depth of colorectal cancer. The following is an overview of the efficacy of these diagnostic modalities based on previous diagnostic imaging guidelines and supplemented by data from the latest literature, mainly reviews.

Explanation

Advanced cancer is visualized as wall thickening on contrast-enhanced CT, and the addition of colorectal wall distension (CTC) provides detailed diagnosis. Diagnosis of invasion depth can be estimated according to lateral deformity based on 3D images, with diagnostic accuracy ranging from 77.6% to 79% (Fig. A, B, C).[1, 2] MRI has a greater diagnostic accuracy than CT in the local diagnosis of rectal cancer, although it depends on the equipment protocol.[3] High-resolution T2-weighted MRI improves lesion detection and local staging (Fig. D).[4] A phased-array coil is commonly used in Japan, whereas a transrectal coil is not common. The sensitivity and specificity of MRI in diagnosing invasion depth of rectal cancer have been reported to be 87% and 75%, respectively.[4] Diffusion-weighted imaging, recently standardized as an MRI sequence, also improves the diagnosis of invasion depth.[5] A barium enema has been conventionally accepted as a method to evaluate invasion depth focusing on lateral deformity in Japan. However, there is no scientific evidence supporting its use for colorectal cancer staging. Recently, the barium enema has been replaced by the air enema image of CTC (see BQ 60).

CT diagnosis of lymph node metastasis based on size is not fully reliable. MRI diagnosis based on size shows sensitivity ranging from 56% to 94% and specificity ranging from 67% to 83%. PET and PET/CT

show superior specificity, ranging from 85% to 95%.[6] PET is also suitable for evaluating hepatic metastasis, with sensitivity and specificity of 93%. Maffione et al. reported that PET results influenced the treatment strategy in 24% of patients with colorectal cancer.[7] More recently, whole-body PET/MRI has enabled highly accurate staging of colorectal cancer.[8, 9]

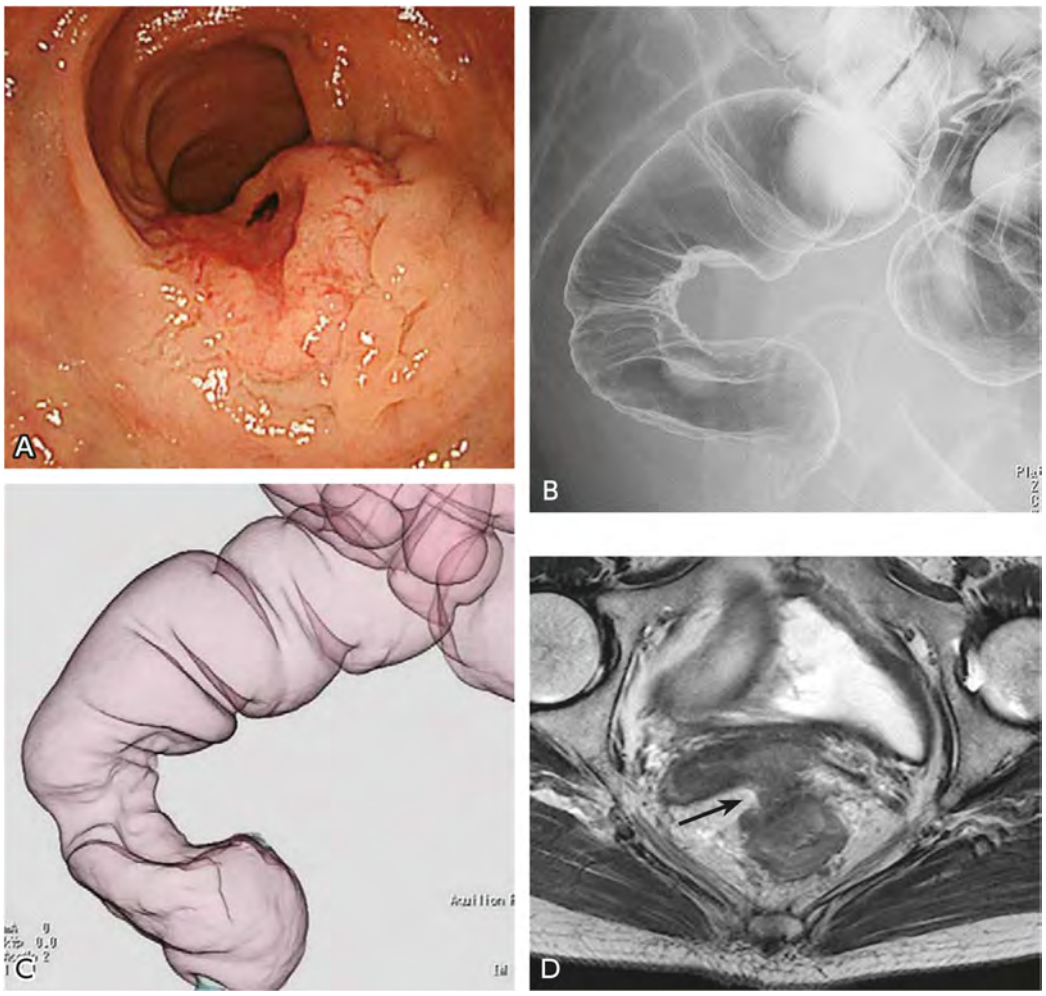

Figure　Advanced rectal cancer

A: Endoscopy: A type 2 ulcerating lesion with a submucosal tumor-like protrusion.

B: Barium enema: The lesion shows deficit-like deformation in the anterior rectal wall, indicating a large tumor with deeper invasion.

C: CTC: The lesion shows similar findings to those seen on barium enema examination.

D: MRI, T2-weighted image: The tumor shows thickening in the anterior rectal wall and invades extensively to the uterus (→).

Search keywords and secondary references

In view of the information provided in the diagnostic imaging guidelines 2016, the following keywords were searched on PubMed limited to articles published since 2016: colorectal cancer, CT, MRI, PET, diagnosis, and staging.

References

1) Nagata K et al: CT air-contrast enema as a preoperative examination for colorectal cancer. Dig Surg 21: 352-358, 2004
2) Utano K et al: Preoperative T staging of colorectal cancer by CT colonography. Dis Colon Rectum 51: 875-881, 2008
3) Mathur P et al: Comparison of CT and MRI in the pre-operative staging of rectal adenocarcinoma and prediction of circumferential resection margin involvement by MRI. Colorectal Dis 5: 396-401, 2003
4) Horvat N et al: MRI of rectal cancer: tumor staging, imaging techniques, and management. Radiographics 39: 367-387, 2019
5) Lu ZH et al: Preoperative diffusion-weighted imaging value of rectal cancer: preoperative T staging and correlations with histological T stage. Clin Imaging 40: 563-568, 2016
6) Jhaveri KS et al: MRI of rectal cancer: an overview and update on recent advances. AJR Am J Roentgenol 205: 42-55, 2015
7) Maffione AM et al: Diagnostic accuracy and impact on management of 18F-FDG PET and PET/CT in colorectal liver metastasis: a meta-analysis and systematic review. Eur J Nucl Med Mol Imaging 42 (1): 152-163, 2015
8) Lee DH et al: Whole-body PET/MRI for colorectal cancer staging: is it the way forward? J Magn Reson Imaging 45: 21-35, 2017
9) Lee SJ et al: Clinical performance of whole-body 18F-FDG PET/Dixon-VIBE, T1-weighted, and T2-weighted MRI protocol in colorectal cancer. Clin Nucl Med 40: 392-398, 2015

BQ 60 Is CT colonography recommended for the local diagnosis of advanced colorectal cancer?

Statement

CT colonography is recommended for the local diagnosis of advanced colorectal cancer.

Background

CT colonography (CTC) is a 3D CT technique specific to the colorectum. A barium enema has been conventionally used in Japan as a preoperative test for colorectal cancer, and in recent years, it has been replaced by CTC. Performing CT immediately after colonoscopy is reasonable for CTC (within one day), and it allows examination of the primary tumor and lymph node and distant metastases with a single test (see BQ 59). In 2012, the revised medical service fees included an additional amount for CTC as a test for patients with suspected colorectal malignancies.

There are no CTC guidelines available in Japan. The present guidelines provide an overview based on the guidelines jointly published by two academic societies, the European Society of Gastrointestinal and Abdominal Radiology and the European Society of Gastrointestinal Endoscopy (secondary source 1), supplemented by data from the latest literature.

Explanation

According to the published data from randomized, controlled studies, multicenter studies, single-center studies, and meta-analyses, CTC showed similar diagnostic accuracy to colonoscopy and superior accuracy to barium enema in detecting colorectal cancer and polyps in symptomatic and asymptomatic patients. According to the SIGGAR studies, the lesion detection rate of CTC was significantly higher than that of barium enema (7.3% vs. 5.6%, $p < 0.039$) and comparable to that of colonoscopy (secondary source 1). Offermans et al. compared CTC and colonoscopy in locating colorectal cancer and found that the error rate was significantly lower with CTC than with endoscopy (13.2% vs. 21.6%, $p < 0.001$).[1)] Kanazawa et al. reported that diagnostic accuracy in the local diagnosis of colorectal cancer was significantly higher with CTC than with endoscopy (98% vs. 90%, $p < 0.05$; Fig. A, B, C).[2)]

Search keywords and secondary references

The following keywords were searched on PubMed for the period since 2016: CT colonography, colorectal cancer, and barium enema.

In addition, the following secondary source was used as a reference.

1) Spada C et al: Clinical indications for computed tomographic colonography: European Society of Gastrointestinal Endoscopy (ESGE) and European Society of Gastrointestinal and Abdominal Radiology (ESGAR) Guideline. Endoscopy 46: 897-915, 2014

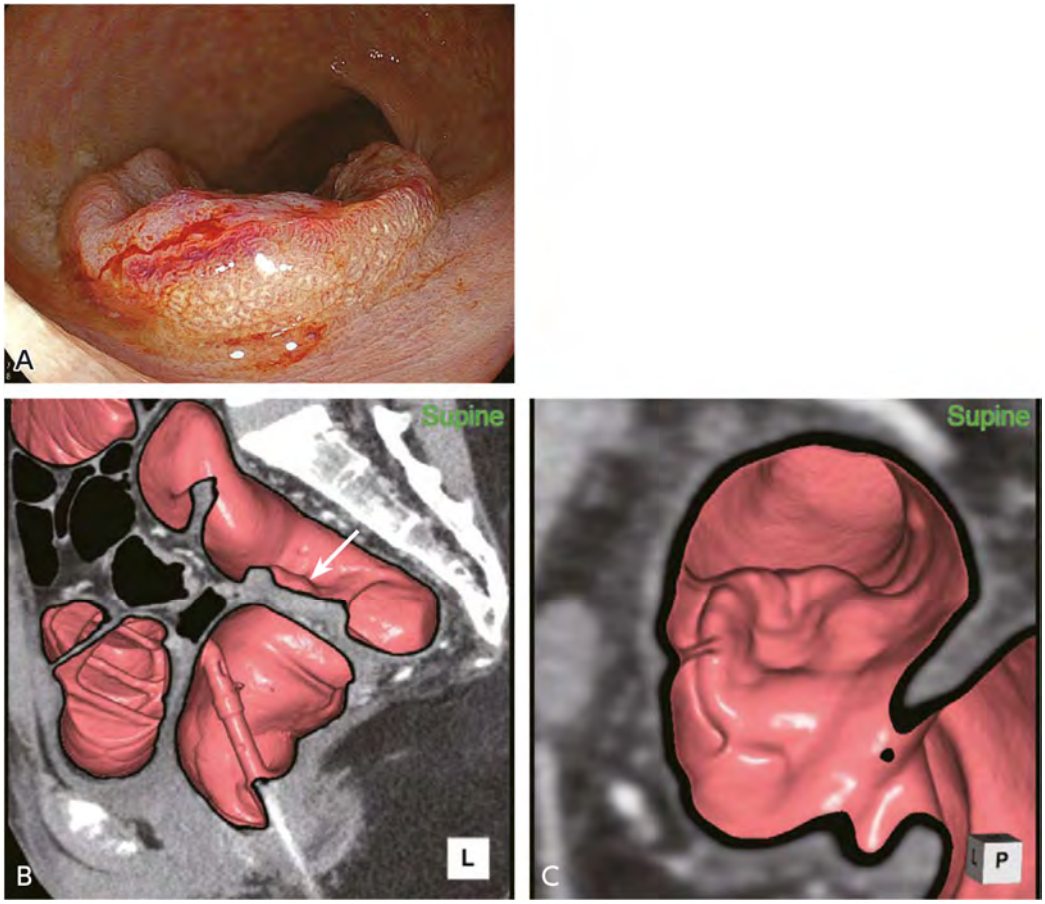

Figure　Advanced rectal cancer

A: Endoscopy: Type 2 advanced rectal cancer.

B: CTC (fusion of virtual colonoscopy and MPR): Type 2 cancer located in the anterior wall of the rectosigmoid segment (RS) of the rectum (→). Anatomical information is clearly visualized on CTC.

C: CTC (fusion of virtual colonoscopy and MPR): The lesion shows findings similar to those seen on colonoscopy.

References

1) Offermans T et al: Preoperative segmental localization of colorectal carcinoma: CT colonography vs. optical colonoscopy. Eur J Surg Oncol 43: 2105-2111, 2017
2) Kanazawa H et al: Combined assessment using optical colonoscopy and computed tomographic colonography improves the determination of tumor location and invasion depth. Asian J Endosc Surg 10: 28-34, 2017

6
Obstetrics and Gynecology

Standard Imaging Methods for Obstetrics and Gynecology

Overview

MRI has been established as a modality of choice for staging uterine cervical and endometrial cancer and for the differential diagnosis of pelvic masses. MRI should not be used for differential diagnosis of atypical genital bleeding, since cytological or histopathological diagnosis of the uterine cervix and endometrium can be easily performed with a Pap smear or biopsy. In Japan, concomitant contrast-enhanced CT is also commonly used for staging diagnosis, including intraperitoneal dissemination and distant metastases. Therefore, the role of MRI in staging gynecological cancer has been limited to local extension On the other hand, adnexal masses are often detected by chance by ultrasound or CT performed in a checkup or to diagnose other diseases. However, when they meet certain conditions (see FQ10), MRI, which is noninvasive and provides excellent diagnostic performance, is recommended for their differential diagnosis. Just before obtaining pelvic MRI, administration of a parasympatholytic agent (scopolamine butylbromide, Buscopan®) is recommended to inhibit intestinal peristalsis.[1)]

The basic procedure for diagnosing gynecological disease is the use of FSE T2-weighted images**.** High-speed imaging sequences such as SSFSE, HASTE, and SSFP should not be substituted because they result in contrast changes. However, these sequences play an important role in fetoplacental imaging, in which inhibiting motion artifacts is the top priority.[2)]

Because it permits post hoc reconstruction in any arbitrary plane, the use of 3D T2-weighted-images enables acquisition of images in planes perpendicular to the uterine body and cervix.[3)] However, tissue contrast is slightly inferior compared with 2D FSE T2-weighted images. It is therefore suitable for use in preoperative examinations in benign conditions such as uterine fibroids. However, it currently should not be used when determining treatment options, such as parametrial invasion of cervical cancer or myometrial invasion of endometrial cancer.

As discussed on page 366, the usefulness of diffusion-weighted images in diagnosing the local extension of endometrial cancer[4)] and cervical cancer[5)] has been established. This is also a useful method for distinguishing between benign and malignant ovarian tumors[6)] and between uterine fibroids and uterine sarcomas.[7)] Consequently, additional diffusion-weighted images from at least 1 plane are essential.

In recent years, 3T systems have also been extensively used for abdominal and pelvic imaging. With regard to performance, the signal-to-noise ratio (SNR) of these systems is better than that of 1.5T systems, which enables thinner slice thicknesses and more detailed images to be obtained. However, tissue contrast in T2-weighted images is better with 1.5T systems. Consequently, in the area of gynecology, clearly depicting the zonal anatomy of the uterus was initially difficult with 3T systems. Recently, however, it has become possible to obtain contrast that compares favorably with that of 1.5T systems, even in the uterus.[8)] There have been reports of the non-inferiority, and superiority in some diseases when using 3T systems compared with 1.5T systems. However, because the wide field of view makes it difficult to maintain the

uniformity of the magnetic field with 3T systems, their use is not recommended for giant uterine and ovarian tumors.

Detailed discussion

1. Endometrial cancer

MRI is used to stage the local extension of endometrial cancer. Myometrial invasion is the most important prognostic factor in endometrial cancer. The types of images used in its diagnosis are T2-weighted images, diffusion-weighted images, T2-weighted and diffusion-weighted fusion images, and contrast-enhanced T1-weighted images, including those obtained by dynamic contrast enhancement. Investigations in recent years have emphasized the usefulness of diffusion-weighted images.[4] To accurately evaluate the depth of myometrial invasion, scanning in planes perpendicular to the long and short axes of the uterus is important.[9] If cervical stromal invasion is seen, it is stage II disease, and extended surgery such as modified radical hysterectomy is recommended, which makes preoperative diagnosis important. Diffusion-weighted images have also been reported to be useful in this setting.[10]

As previously mentioned, concomitant contrast-enhanced CT is also used to diagnose dissemination and distant metastasis. However, fat-suppressed contrast-enhanced T1-weighted images are useful for diagnosing uterine serosal invasion or adnexal extension (stage IIIA), direct invasion to the vesical or rectal mucosa (stage IVA), and intraperitoneal dissemination (stage IVB). If a contrast medium is administered, dynamic contrast enhancement, which provides excellent diagnostic performance with respect to myometrial invasion,[4] should be performed.

○ Standard imaging methods for endometrial cancer (Table 1, Fig. 1)

As mentioned previously, the main role of MRI in Japan as a pretreatment examination for endometrial cancer is to evaluate local extension. MR examination including the following sequences may be sufficient: T2-weighted images parallel to the long and short axes of the uterus, T1-weighted images, diffusion-weighted images, and fat-suppressed contrast-enhanced T1-weighted images that includes dynamic contrast imaging. However, endometrial cancer is often low-risk pathology, i.e. well-differentiated endometrioid carcinoma, and stage IA disease. Therefore, omitting CT can be considered, particularly in young patients. When CT is omitted, a possible option is the addition of transverse imaging perpendicular to the body axis to facilitate the evaluation of lymph node metastases. Selecting sagittal and transverse planes parallel to the long and short axes of the uterus is often difficult for radiation technologists who are not familiar with gynecological examinations. Additional T2-like contrast-enhanced fast sequences, such as HASTE, may be considered to determine the uterine axis. The preferred settings to examine endometrial cancer are an FOV of 25 to 30 cm, slice thickness of 4 to 5 mm for a 1.5T system and 3 to 4 mm for a 3T system, and an interslice gap of approximately 10% to 20%.

Table 1. Examples of sequences for staging endometrial cancer (1.5/3T systems, phased-array coil)

	Imaging Method/Plane	Sequence	Imaging Range	Slice Thickness (mm)		Remarks
				1.5T	3T	
Required	T2-weighted/sagittal	FSE	Uterus/vagina	4 to 5	3 to 4	Parallel to long axis of uterine body
	T1-weighted/sagittal	SE				
	T2-weighted/transverse	FSE	Uterus/adnexa			Perpendicular to long axis of uterine body (short axis of uterine body)
	Diffusion-weighted/transverse or sagittal	EPI or FSE	Same range as T1- and T2-weighted images			Sagittal recommended if cervical stromal invasion suspected ADC map generation with b-value = 800 to 1,500 s/mm^2 required
	Dynamic contrast/transverse or sagittal	2D or 3D GRE		2 to 5	1.5 to 4	Sagittal recommended if cervical stromal invasion suspected Temporal resolution, ≤ 30 seconds, through minimum of 2 minutes
	Fat-suppressed contrast-enhanced T1-weighted images/sagittal					Parallel to long axis of uterine body
	Fat-suppressed contrast-enhanced T1-weighted images/transverse					Perpendicular to long axis of uterine body (short axis of uterine body)
Options for detailed evaluation	Additional survey imaging	SSFSE, HASTE, SSFP, etc.	Whole pelvis	Up to 10		Additional T2 contrast survey imaging to accurately determine the long and short axes of uterus
	T1-weighted/transverse	SE	Uterus/adnexa	4 to 5	3 to 4	Perpendicular to uterine body long axis (uterine body short axis)
	Diffusion-weighted /transverse, sagittal, or coronal	EPI or FSE	Uterus/vagina or uterus/adnexa	4 to 5	3 to 4	Addition of required angles that were not acquired
	Fat-suppressed contrast-enhanced T1-weighted images/coronal	2D or 3D GRE	Uterus/vagina/adnexa	2 to 5	1.5 to 4	Entire pelvic cavity
Options when CT omitted	T2-weighted/transverse or coronal	FSE	Whole pelvis or renal hilus and below	5 to 6		Perpendicular to body axis (normal transverse or coronal plane)
	T1-weighted/transverse or coronal	SE				
	Diffusion-weighted/transverse or coronal	EPI or FSE	Whole pelvis or whole abdomen			

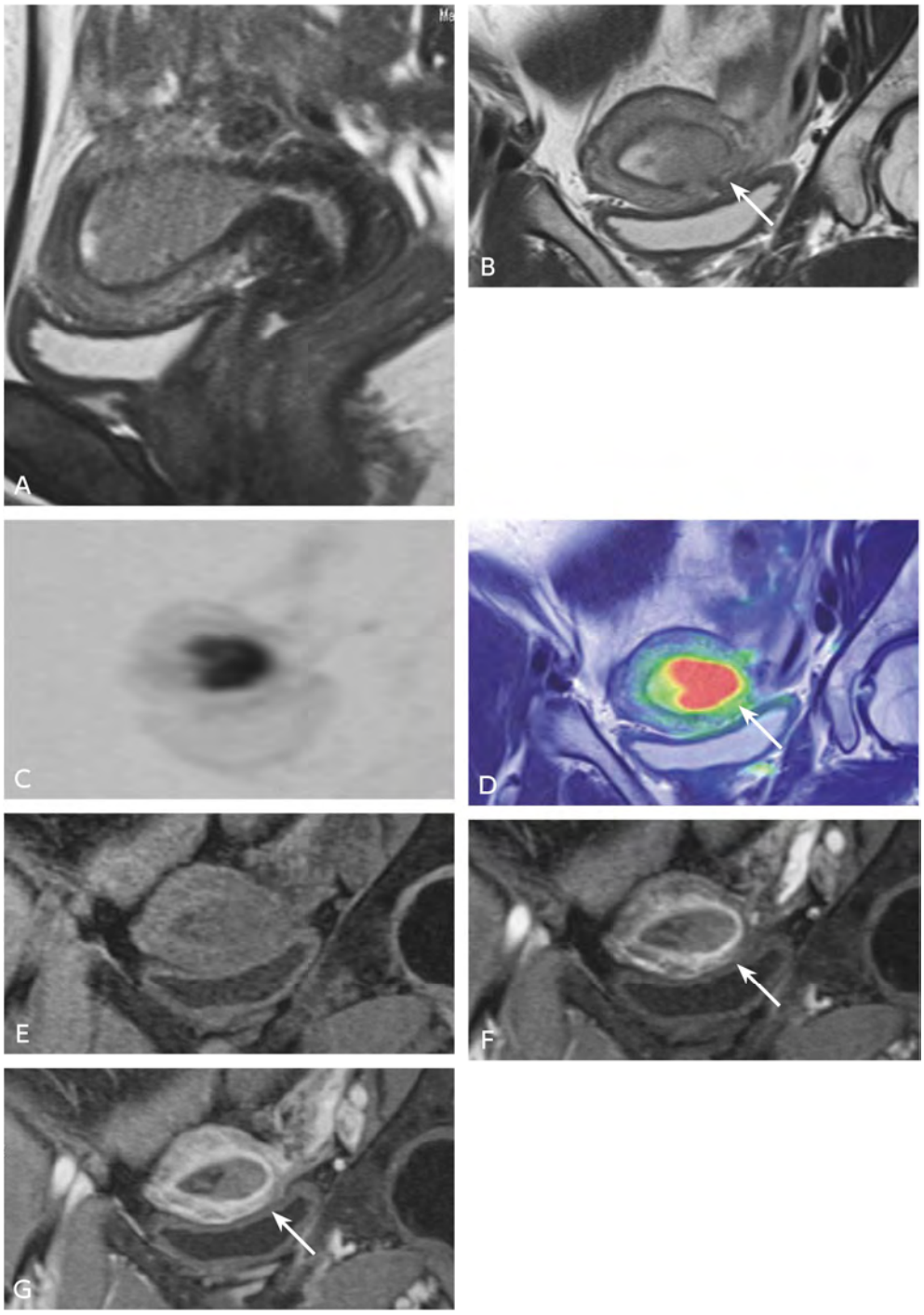

Figure 1. Endometrial cancer (stage IA)

A: sagittal T2-weighted image; B: coronal T2-weighted image; C: coronal diffusion-weighted image; D: coronal T2-/diffusion-weighted fusion image; E: Dynamic contrast-enhanced coronal image, pre-contrast; F: Coronal dynamic contrast-enhanced image, 60 seconds post-contrast; G: coronal fat-suppressed contrast-enhanced T1-weighted image

An exophytic mass that fills the endometrial cavity causes thinning of the junctional zone in the T2-weighted images (→) and is associated with superficial myometrial infiltration. This condition can also be clearly demonstrated on T2-/diffusion-weighted fusion imaging and early-phase dynamic contrast-enhanced imaging.

2. Cervical cancer

As in endometrial cancer, the role of MRI in cervical cancer is to assess local extension and measure tumor diameter. However, invasive cancer, which is an indication for radical hysterectomy, and microinvasive/noninvasive cancer are differentiated histopathologically, and microinvasive (stage IA) and noninvasive cancer are generally not indications for MRI.[11] However, MRI should be aggressively used in the following situations: the results of cytology and histology are inconsistent; an endophytic tumor is suspected on palpation and transvaginal ultrasound without any evidence of macroscopic masses on visual inspection or colposcopy; or histological type indicative of a poor prognosis. MRI can also provide some useful information in differentiating from hyperplastic lesions of the cervix, such as lobular endocervical glandular hyperplasia (LEGH), which is considered a precursor lesion of gastric-type endocervical adenocarcinoma, and Nabothian cysts and tunnel clusters. Gastric-type endocervical adenocarcinoma has a poor prognosis and is common in Japan.

○ Standard imaging methods for cervical cancer (Table 2, Fig. 2)

The basic approach is similar to that for endometrial cancer. Although tumor diameter is an important prognostic factor in cervical cancer, the General Rules for Clinical and Pathological Management of Uterine Cervical Cancer (4th edition) include size in staging the progression for stages IB and IIA exclusively. It therefore requires exact measurement. In particular, subdividing stage IB in the staging of cervical cancer is closely related to determining whether fertility preservation is indicated. T2-weighted images alone or with the addition of diffusion-weighted images are considered sufficient for staging the local extension of cervical cancer.[12] The usefulness of contrast-enhanced examinations has not been established, but there are several reports indicating that dynamic contrast enhancement is useful for visualizing non-invasive cancer and diagnosing parametrial invasion.

3. Myometrial lesions

The established roles played by MRI include qualitative diagnosis (mainly differentiating between fibroids and adenomyosis,[13] and distinguishing benign from malignant lesions) when myometrial lesions are suspected. In the case of fibroids, the roles include determining the number, size, and location of the lesions and predicting and assessing the effectiveness of uterine artery embolization (UAE) treatment.[14] Although MRI is expected to differentiate between fibroids and sarcomas in the clinical setting, a literature search did not provide strong evidence for such use, as discussed in FQ9.

○ Standard imaging methods for suspected myometrial lesions (Table 3)

As previously mentioned, differentiating between fibroids and adenomyosis and determining the size, location, and number of lesions are important for selecting treatment, and T2-weighted images are the basic sequence for this purpose. As in the examination of cervical and endometrial cancer, 3D T2-weighted images are useful despite limited contrast resolution. The multiplanar capability of 3D images clarifies the

relationship of the lesions to the endometrium and peripheral organs after reconstruction.[3] Although relevant evidence is lacking, MR is also useful in differentiating fibroids from sarcomas. In this setting, high signal intensity on T2-weighted images, restricted diffusion, and the presence of transient early enhancement and hemorrhagic necrosis are reported to be signs of malignancy. Therefore, we recommend contrast-enhanced examinations including dynamic contrast enhancement to exclude sarcomas.[7, 15]

4. Recommended MR sequences for diagnosing patients with suspected uterine malformations or with primary amenorrhea

Müllerian duct anomalies (MDAs) such as bicornuate uterus are mainly diagnosed in the reproductive period. To evaluate uterine morphology, T2-weighted images (sagittal and transverse or 3D imaging) with a slice thickness of ≤ 4 mm are required. Since MDAs may appear in combination with unilateral vaginal atresia, the vulva should be included in transverse T2-weighted images. Because an obstructed hemivagina may cause endometriosis, T1-weighted images (with and without fat suppression) are occasionally necessary. Coronal T2-weighted images including the upper abdomen should be added to screening for co-existing urinary tract malformations (unilateral renal agenesis is common). During childhood and adolescence, diagnosing disorders of sexual development is important. MR can provide morphological information about the uterus, vagina, and clitoris. In addition, we should diagnose the morphological characteristics and the location of the gonads. When cryptorchidism is highly suspected, the addition of diffusion-weighted images to fat-suppressed T2-weighted images or STIR covering the inguinal region is helpful, where cryptorchids are highly likely to be located. If there are no uterine or ovarian abnormalities, MRI of the sella turcica is recommended to explore the hypothalamic or pituitary abnormalities in addition to endocrine testing. If congenital adrenal hyperplasia is suspected, it is important investigating the morphology of the adrenals in the coronal plane.

5. Adnexal lesions

The aims of obtaining MRI in evaluating adnexal masses are determining the organ of origin, qualitative diagnosis, and staging (Fig. 3). The standard sequences required for these aims are shown in Table 4. Because ovarian tumors often become very large, the FOV and slice thickness/slice interval need to be flexibly adjusted to include the entire mass. With high-grade serous carcinoma, the most common adnexal malignancies, extensive intraperitoneal dissemination is often already present at onset. As discussed later, distant metastasis, including dissemination, is often diagnosed by contrast-enhanced CT in Japan. However, in patients such as those for whom the use of a contrast medium is contraindicated, diffusion-weighted images can be used to evaluate the abdominal cavity as a whole.

Table 2. Examples of sequences in staging cervical cancer (1.5/3T systems, phased-array coil)

	Imaging Method/Plane	Sequence	Imaging Range	Slice Thickness (mm)		Remarks
				1.5T	3T	
Required	T2-weighted/sagittal	FSE	Uterus/vagina	4 to 5	3 to 4	Parallel to long axis of uterine cervix
	T1-weighted/sagittal	SE				
	T2-weighted/transverse	FSE	Uterus/adnexa			Perpendicular to long axis of uterine cervix
	Diffusion-weighted/transverse or sagittal	EPI or FSE	Same range as T1- and T2-weighted images			Sagittal plane recommended if vaginal invasion is suspected ADC map generation with b-value = 800 to 1,500 s/mm^2 required
Option for detailed evaluation	Additional survey imaging	SSFSE, HASTE, SSFP, etc.	Whole pelvis	Up to 10		Additional T2 contrast survey imaging to accurately determine the long and short axes of uterus
	T1-weighted/transverse	SE	Uterus/adnexa	4 to 5	3 to 4	Perpendicular to long axis of uterine cervix
	Diffusion-weighted/transverse, sagittal, or coronal	EPI or FSE	Uterus/vagina or uterus/adnexa	4 to 5	3 to 4	Any projections are acceptable
	MR urography	2D	Kidney to urinary bladder	30 to 40		
	Dynamic imaging /transverse	2D or 3D GRE	Uterus/vagina	2 to 5	1.5 to 4	Transverse plane recommended for parametrial invasion, sagittal for invasion to the urinary bladder/rectum Temporal resolution ≤ 30 seconds, through minimum of 2 minutes
	Fat-suppressed contrast-enhanced T1-weighted/sagittal		Uterus/vagina			Parallel to long axis of uterine cervix
	Fat-suppressed contrast-enhanced T1-weighted/transverse		Uterus/adnexa			Perpendicular to long axis of uterine cervix
	Fat-suppressed contrast-enhanced T1-weighted/coronal		Uterus/vagina/adnexa	2 to 5	1.5 to 4	Entire pelvic cavity
Options when CT omitted	T2-weighted/transverse or coronal	FSE	Whole pelvis or renal hilus and below	5 to 6		Perpendicular to body axis (normal transverse or coronal plane)
	T1-weighted/transverse or coronal	SE				
	Diffusion-weighted/transverse or coronal	EPI or FSE				

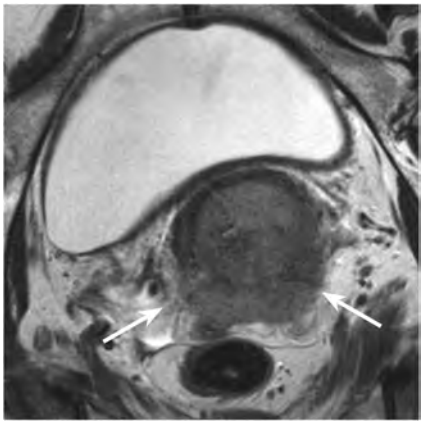

Figure 2. Cervical cancer (stage IIB)

T2-weighted transverse image of the short axis of the cervix: A mass occupying an extensive area of the cervix is penetrating the cervical stroma postero-laterally and protruding into parametrium (→).

Table 3. Examples of sequences for diagnosing myometrial lesions (1.5/3T systems, phased-array coil)

<table>
<tr><th rowspan="2"></th><th rowspan="2">Imaging Method/Plane</th><th rowspan="2">Sequence</th><th rowspan="2">Imaging Range</th><th colspan="2">Slice Thickness (mm)</th><th rowspan="2">Remarks</th></tr>
<tr><th>1.5T</th><th>3T</th></tr>
<tr><td rowspan="4">Required</td><td>T2-weighted/sagittal</td><td>FSE</td><td rowspan="3">Uterus/vagina</td><td rowspan="4">4 to 5</td><td rowspan="4">3 to 4</td><td rowspan="3">Parallel to long axis of uterine body</td></tr>
<tr><td>T1-weighted/sagittal</td><td>SE</td></tr>
<tr><td>Fat-suppressed T1-weighted/sagittal</td><td>SPIR, SPAIR, Dixon, CHESS</td></tr>
<tr><td>T2-weighted/transverse</td><td>FSE</td><td>Uterus/adnexa</td><td>Perpendicular to long axis of uterine body (short axis of uterine body)</td></tr>
<tr><td>Diffusion-weighted/transverse or sagittal</td><td>EPI or FSE</td><td>Same range as T1- and T2-weighted images</td><td>ADC map generation with b-value = 800 to 1,500 s/mm^2 required</td></tr>
<tr><td>Option for detailed evaluation</td><td>Additional survey imaging</td><td>SSFSE, HASTE, SSFP, etc.</td><td>Whole pelvis</td><td colspan="2">Up to 10</td><td>Additional T2 contrast-enhanced survey imaging to accurately determine the long and short axes of uterus</td></tr>
<tr><td rowspan="4">Option to exclude sarcoma/assess whether uterine artery embolization (UAE) indicated</td><td>T1-weighted/transverse</td><td>SE</td><td>Uterus/adnexa</td><td>4 to 5</td><td>3 to 4</td><td>Perpendicular to long axis of uterine body (short axis of uterine body)</td></tr>
<tr><td>Dynamic imaging/ transverse or sagittal</td><td rowspan="3">2D or 3D GRE</td><td>Uterus/vagina/adnexa</td><td rowspan="3">2 to 5</td><td rowspan="3">1.5 to 4</td><td>Temporal resolution 15 to 20 seconds, through minimum of 2 minutes</td></tr>
<tr><td>Fat-suppressed contrast-enhanced T1-weighted /sagittal</td><td>Uterus/vagina</td><td>Parallel to long axis of uterine body</td></tr>
<tr><td>Fat-suppressed contrast T1-weighted/transverse</td><td>Uterus/adnexa</td><td>Perpendicular to long axis of uterine body (short axis of uterine body)</td></tr>
<tr><td>Option to shorten test duration</td><td>3D T2-weighted/sagittal</td><td>Cube, VISTA, SPACE, etc.</td><td>Uterus/vagina</td><td colspan="2">0.6 to 1.2</td><td>Isotropic imaging of whole uterus is required in any direction</td></tr>
</table>

○ Standard imaging methods when an adnexal lesion is suspected (Table 4)

The differential diagnosis of an adnexal mass is performed with the combination of lesion morphology, signal intensity, degree of restricted diffusion, and contrast enhancement. T2-weighted images are important for evaluating the morphological characteristics of masses[16] and elucidating their relationships to other pelvic organs. They should be obtained with FSE sequences to maintain tissue contrast. T1-weighted images and fat-suppressed T1-weighted images are useful for detecting hemorrhage and fat and are

necessary for the differential diagnosis of masses.[6, 16 17] In addition, in-phase GRE imaging and opposed-phase GRE imaging are effective in depicting small amounts of fat and should be added for this purpose. The enhancement pattern in dynamic contrast enhancement and the ADC values in diffusion-weighted images are important for distinguishing between benign and malignant ovarian tumors.[6, 16] With some exceptions (e.g., endometriotic cysts of the ovary without complicating malignancy, simple cysts without mural nodules), these methods are virtually essential. In these instances, the dynamic curve should be visually assessed and an ADC map generated whenever possible.

6. CT imaging to determine the clinical stage of gynecological malignancies

CT is useful for diagnosing lymph node and distant metastases, as well as intraperitoneal dissemination, in gynecological malignancies.

The patients should be scanned from the diaphragm to the inferior border of the pubis. However, the chest is included in the case of an advanced tumor or highly malignant histological subtype that may have metastasized to the chest. Use of an oral contrast medium facilitates the differentiation of gastrointestinal tract and peritoneal lesions. The imaging generally involves pre-contrast and post-contrast single-phase imaging performed 60 to 100 seconds after contrast medium injection. Particularly in ovarian, fallopian tube, and peritoneal cancers (high-grade serous carcinomas), accurately determining the location of disseminated lesions is extremely important. Because coronal and sagittal images generated by MPR are considered superior to standard transverse images for detecting dissemination,[18] it is important to use a thin slice thickness that can generate MPR images, in addition to acquiring images with a standard 5-mm slice thickness.

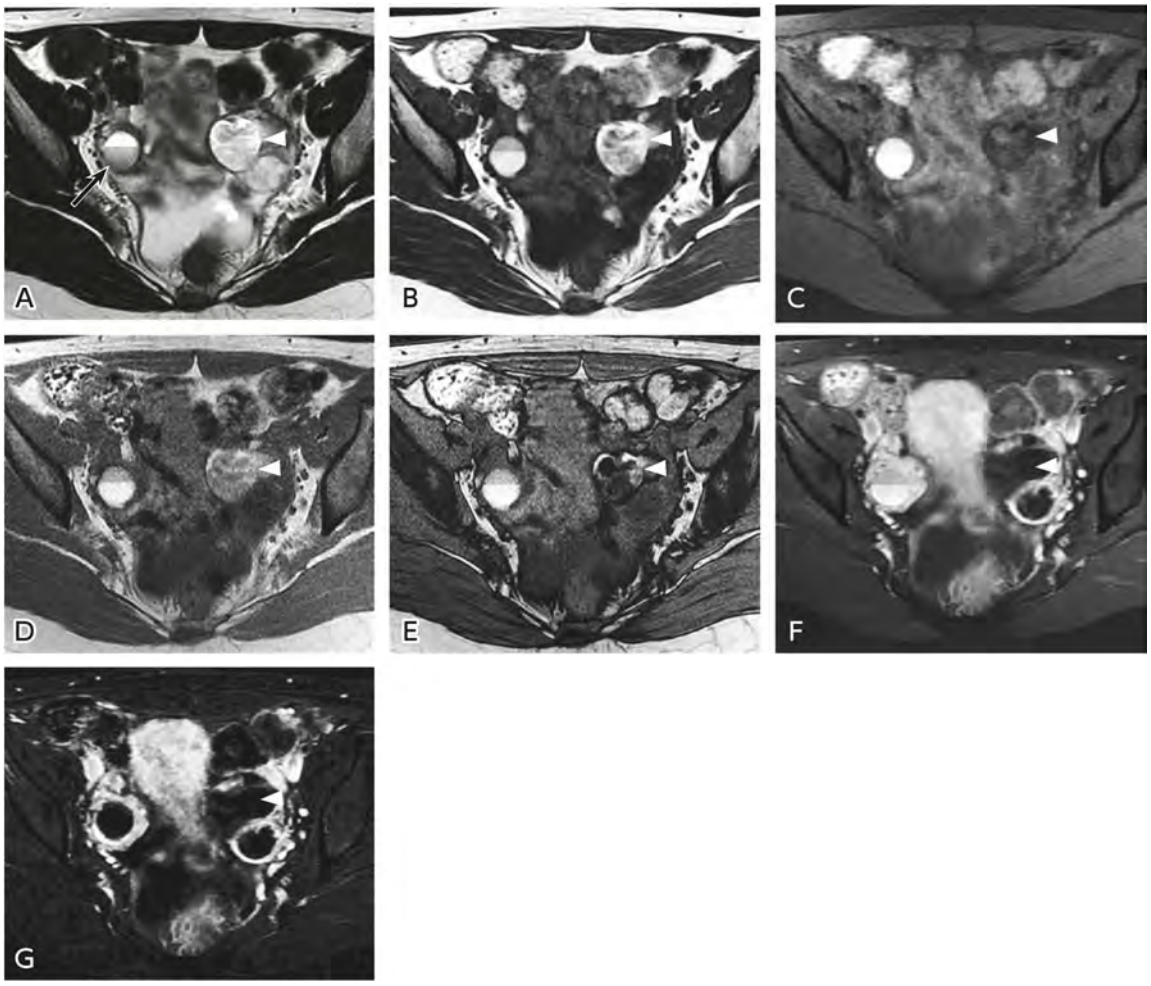

Figure 3. Endometriotic cyst of the right ovary and mature teratoma of the left ovary

A: T2-weighted image; B: T1-weighted image; C: Fat-suppressed T1-weighted image; D: GRE T1-weighted image, in phase; E: GRE T1-weighted image, opposed phase; F: Fat-suppressed T1-weighted image; G: Contrast subtraction image

Formation of a fluid level is seen in a cystic mass in the right ovary (→). A hyperintense region in the dorsal part is not suppressed on the fat-suppressed T1-weighted image, indicating hemorrhagic contents. This region shows slight hypointensity (shading) on the T2-weighted image, suggesting an endometriotic cyst. The existence of the enhanced region is hard to detect on contrast-enhanced T1-weighted images because the contents show hyperintensity before contrast administration. However, no enhanced solid portion is seen on the subtraction image. A cystic mass in the left ovary (▷) that appears as a region of hyperintensity in the T1-weighted images shows a reduced signal on the fat-suppressed T1-weighted image, and a mature teratoma characterized by fat contents is diagnosed. Compared with the in-phase image, the signal reduction in the region interspersed with a fat component is more distinct in the opposed-phase image. However, the region that contains only fat remains hyperintense.

^{18}F-FDG-PET has been found to provide high diagnostic performance in detecting lymph node and distant metastases.[19)] In Japan, ^{18}F-FDG-PET in staging and diagnosing recurrence of gynecological malignancies is covered by national health insurance only when they cannot be definitively diagnosed by other imaging modalities. However, as mentioned in CQ16, many guidelines from Europe and the United States indicate that ^{18}F-FDG-PET/CT should be selected from the outset for high-risk patients.[9, 20)] On the

other hand, there are regional differences in accessibility of not only PET/MRI, but also PET/CT. Given these circumstances, it is currently not recommended as a routinely performed modality.

Table 4. Examples of sequences in diagnosing adnexal mass (1.5/3T systems, phased-array coil)

	Imaging Method/Plane	Sequence	Imaging Range	Slice Thickness (mm)		Remarks
				1.5T	3T	
Required	T2-weighted/sagittal	FSE	Pelvic cavity, including the whole tumor	4 to 8	3 to 6	Slice thickness/interval and FOV depend on tumor diameters
	T1-weighted/transverse	GRE				Both in-phase and opposed-phase imaging
	Fat-suppressed T1-weighted/transverse	SPIR, SPAIR, etc.				
	T2-weighted/transverse	FSE				
	Diffusion weighted/transverse or sagittal	EPI or FSE				ADC map generation with b-value = 800 to 1,500 s/mm^2 required
	Dynamic contrast imaging/ transverse or sagittal	2D or 3D GRE		2 to 8	1.5 to 6	Temporal resolution ≤ 30 seconds, through minimum of 2 minutes
	Fat-suppressed contrast-enhanced T1-weighted/sagittal					
	Fat-suppressed contrast-enhanced T2-weighted/transverse					
Options to shorten test duration	T1-weighted/transverse and fat-suppressed T1-weighted/transverse	3-point DIXON (e.g., LAVA-FLEX, mDIXON)		4 to 8	3 to 6	Imaging with and without fat suppression and in-phase and opposed-phase T1-weighted images can be obtained once using the 3-point Dixon method.
Options for simultaneous evaluation of intraperitoneal dissemination	Fat-suppressed T2-weighted or STIR/coronal	FSE/STIR	From diaphragm to pelvic floor	4 to 8	3 to 6	Can be divided into 2 stacks for upper and lower abdomen
	Diffusion-weighted/coronal	EPI or FSE				
	Fat-suppressed contrast-enhanced T1-weighted/coronal	2D or 3D GRE				

Figure 4. Placenta percreta, 32 weeks of gestation

SSFSE, T2-weighted sagittal image: The inferior part of the anterior uterine wall at the placental attachment site is protruding, and the myometrium in this area is indistinct (▷). Arrow indicates normal myometrium below the placenta.

Table 5. Examples of sequences in placental imaging (1.5T systems, phased-array coil)

	Imaging Method/Plane	Sequence	Imaging Range	Slice Thickness (mm)	Remarks
				1.5T	
Required	T2-weighted/sagittal	SSFSE	Uterus	5 to 10	Parallel to long axis of uterine body
		SSFP			
	T1-weighted/sagittal	SE or GRE			
	T2-weighted/transverse	SSFSE or SSFP			Perpendicular to long axis of uterine body (short axis of uterine body)
Options for detailed evaluation	T2-weighted/coronal	SSFSE, HASTE, SSFP, etc.			In placenta accreta spectrum, the plane perpendicular to the placenta–myometrium interface at the site of suspected adhesion should be added.
	Diffusion-weighted/transverse or sagittal	EPI or FSE			ADC map generation with b-value = 800 to 1,500 s/mm^2 required
	Fat-suppressed T1-weighted/sagittal	SPIR, SPAIR, etc.			Added when diagnosing hemorrhagic lesions such as subchorionic hematomas

7. Placental lesions

Because most placental lesions (e.g., placenta accreta spectrum, uteroplacental circulatory disturbance, placental tumor) are detected by ultrasonography, MRI is often performed when sufficient information is not obtained by ultrasound, or a more precise evaluation is required.[21] Although the use of 1.5T systems is recommended, taking into account factors such as the specific absorption ratio (SAR) and magnetic field, the use of 3T systems is also permitted.[21] Although imaging is performed in the supine position when possible, examinees in late pregnancy may have difficulty maintaining this position due to pressure on the inferior vena cava by the uterus. Consequently, the imaging obtained in the left lateral decubitus position is acceptable.[22] Moreover, the longer the imaging duration, the greater the artifacts caused by fetal movement. The total examination time should therefore be shortened with fast sequences.[21] As sequences with breath-holding such as SSFSE can reduce artifacts, it is worth trying if the patient can hold her breath.

○ Standard methods for antepartum imaging of the placenta (Table 5)

Although recommended sequences are different by suspected condition, placenta accreta spectrum may be the condition that most frequently requires MR. The sequences indicated below are an example for diagnosing placenta accreta spectrum. Specifically, they are SSFSE T2-weighted images and SSFP, which are used to evaluate placental morphology and detect lesions, and T1-weighted images, which are useful for detecting hemorrhage and hematomas near the placenta or in the cervical canal. T1-weighted images are also useful for evaluating the relationship to the surrounding organs based on the presence or absence of interposed fatty tissue.[21] The sagittal plane is the basic plane to diagnose placenta accreta spectrum, because it often occurs in an area of Caesarean section scarring. However, the angle should be changed as needed depending on the site of placental adhesion and the purpose of the imaging.

Secondary source materials used as references

1) Johnson W et al: The value of hyoscine butylbromide in pelvic MRI. Clin Radiol 62: 1087-1093, 2007
2) Kim JA, Narra VR: Magnetic resonance imaging with true fast imaging with steady-state precession and half-Fourier acquisition single-shot turbo spin-echo sequences in cases of suspected placenta accreta. Acta Radiol 45: 692-698, 2004
3) Proscia N et al: MRI of the pelvis in women: 3D versus 2D T2-weighted technique. AJR Am J Roentgenol 195: 254-259, 2010
4) Andreano A et al: MR diffusion imaging for preoperative staging of myometrial invasion in patients with endometrial cancer: a systematic review and meta-analysis. Eur Radiol 24: 1327-1338, 2014
5) Park JJ et al: Parametrial invasion in cervical cancer: fused T2-weighted imaging and high-b-value diffusion-weighted imaging with background body signal suppression at 3 T. Radiology 274: 734-741, 2015
6) Sala E et al: The role of dynamic contrast-enhanced and diffusion weighted magnetic resonance imaging in the female pelvis. Eur J Radiol 76: 367-385, 2010
7) Lakhman Y et al: Differentiation of uterine leiomyosarcoma from atypical leiomyoma: diagnostic accuracy of qualitative MR Imaging features and feasibility of texture analysis. Eur Radiol 27: 2903-2915, 2017
8) Kataoka M et al: MRI of the female pelvis at 3T compared to 1.5T: evaluation on high-resolution T2-weighted and HASTE images. J Magn Reson Imaging 25: 527-534, 2007
9) Nougaret S et al: Endometrial cancer MRI staging: updated guidelines of the European Society of Urogenital Radiology. Eur Radiol, 2018
10) Lin G et al: Endometrial cancer with cervical stromal invasion: diagnostic accuracy of diffusion-weighted and dynamic contrast enhanced MR imaging at 3T. Eur Radiol 27: 1867-1876, 2017
11) Lee SI, Atri M: 2018 FIGO Staging system for uterine cervical cancer: enter cross-sectional imaging. Radiology 292: 15-24, 2019

12) Woo S: Magnetic resonance imaging for detection of parametrial invasion in cervical cancer: an updated systematic review and meta-analysis of the literature between 2012 and 2016. Eur Radiol 28: 530-541, 2018
13) Togashi K et al: Enlarged uterus: differentiation between adenomyosis and leiomyoma with MR imaging. Radiology 171: 531-534, 1989
14) Siddiqui N et al: Uterine artery embolization: pre- and post-procedural evaluation using magnetic resonance imaging. Abdom Imaging 38: 1161-1177, 2013
15) Bi Q et al: Utility of clinical parameters and multiparametric MRI as predictive factors for differentiating uterine sarcoma from atypical leiomyoma. Acad Radiol 25: 993-1002, 2018
16) Thomassin-Naggara I et al: Adnexal masses: development and preliminary validation of an MR imaging scoring system. Radiology 267: 432-443, 2013
17) Sugimura K et al: Pelvic endometriosis: detection and diagnosis with chemical shift MR imaging. Radiology 188: 435-438, 1993
18) Pannu HK et al: Multidetector CT of peritoneal carcinomatosis from ovarian cancer. Radiographics 23: 687-701, 2003
19) Gee MS et al: Identification of distant metastatic disease in uterine cervical and endometrial cancers with FDG PET/CT: analysis from the ACRIN 6671/GOG 0233 multicenter trial. Radiology 287: 176-184, 2018
20) Expert Panel on Women's Imaging and Radiation Oncology-Gynecology: Siegel CL, et al. Pretreatment planning of invasive cancer of the cervix, 2020
21) Jha P C et al: Society of Abdominal Radiology (SAR) and European Society of Urogenital Radiology (ESUR) joint consensus statement for MR imaging of placenta accreta spectrum disorders. Eur Radiol 30: 2604-2615, 2020
22) Leyendecker JR et al: Maternal MRI during and after pregnancy: Leyendecker JR et al (eds): Practical guide to abdominal and pelvic MRI 2nd ed. Lippincott Williams & Wilkins, p171-172, 2010

BQ 61 Does MRI contribute to diagnosing uterine fibroids?

Statement

In patients who cannot be diagnosed by bimanual examination or ultrasound, MRI contributes to qualitative diagnosis and is therefore recommended.

In patients scheduled to undergo invasive uterus-preserving treatment [e.g., myomectomy, UAE, and focused ultrasound surgery (FUS)] MRI is useful for accurately determining the locations, sites, and number of fibroids and is therefore recommended.

Background

Bimanual examination and ultrasonography are the first choices for diagnosing uterine fibroids. However, for patients for whom these methods do not result in a diagnosis, an MRI examination may be ordered. In patients scheduled to undergo invasive uterus-preserving treatment (e.g., myomectomy, UAE, and FUS), MRI is performed to accurately determine the locations, sites, and number of fibroids. This discussion outlines the usefulness of MRI for diagnosing uterine fibroids.

Explanation

The diagnosis of uterine fibroids is made primarily through bimanual examination and the use of transvaginal ultrasonography (TVUS). MRI is not generally performed as a screening examination.[1)] The main circumstances in which MRI is ordered are: ① for detailed examination in patients for whom ultrasound does not provide a diagnosis (particularly when malignancies such as sarcoma cannot be ruled out clinically because a tendency for rapid enlargement is seen or based on pelvic examination findings, for example); and ② for preoperative evaluation of patients scheduled to undergo invasive uterus-preserving treatment (e.g., myomectomy, UAE, and FUS). In a comparison with surgical specimens of submucosal leiomyoma, MRI (sensitivity, 100%; specificity, 91%) provided better results than TVUS (sensitivity, 83%; specificity, 90%) and hysteroscopy (sensitivity, 82%; specificity, 87%).[2)] Multiple investigations of symptomatic fibroids showed that MRI results changed the diagnosis or treatment plan for approximately 20% of patients. Based on these investigations, MRI is recommended to accurately determine the locations, sites, and number of fibroids in patients scheduled to undergo invasive treatment (Fig. 1). In addition, MRI that includes diffusion-weighted imaging is considered useful for predicting and assessing the efficacy of UAE, and MRI-guided FUS (MRgFUS) contributes to intraoperative monitoring and the selection of indicated patients. A 2019 meta-analysis that examined the correlation between ADC values before UAE and the reduction in fibroid size reported that the ADC values were not clearly useful in predicting treatment efficacy.[3)] On the other hand, hormone therapy with gonadotropin-releasing hormone (GnRH) agonists or antagonists is a widely used drug therapy, and it has been reported that good tumor shrinkage is likely with such therapy in fibroids that show hyperintensity on T2-weighted images.[4)]

MRI of typical fibroids shows that they are hypointense masses with distinct borders in T2-weighted images. However, they may be visualized as areas of hyperintensity on T2-weighted images as the result of various types of degeneration or variants, complicating their differentiation from malignancies such as sarcomas.[5, 6] Some fibroids can be diagnosed based on characteristic imaging findings, as in the case of red degeneration and lipoleiomyomas. Referencing diffusion-weighted images and ADC maps is useful for diagnosing leiomyomas that show hyperintensity on T2-weighted images due to severe edema or hydropic degeneration. However, benign cellular leiomyomas have a high cell density that restricts water diffusion, which occasionally makes it difficult to distinguish them from sarcomas (Fig. 2). There have been a number of investigations in recent years regarding the differentiation of fibroids and sarcomas using MRI. The main points regarding differentiation are summarized in the guidelines of the European Society of Urogenital Radiology, and details are provided in FQ9. Both subserosal leiomyomas and benign fibromatous tumors of the ovaries (e.g., fibromas and Brenner tumors) often show hypointensity on T2-weighted images, which occasionally complicates differentiation. MRI visualization of flow voids that continue from the uterine body has been found to be useful for diagnosing subserosal leiomyomas, and analyzing the contrast pattern of dynamic MRI has been reported to be useful for differentiating fibroids and fibromas.[7]

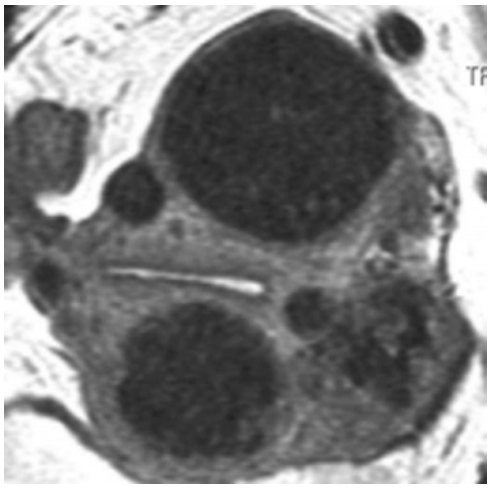

Figure 1. Multiple uterine fibroids

MRI, T2-weighted image: Imaging performed in the uterine body short-axis plane for pre-myomectomy evaluation. Aspects such as the sites and number of fibroids and the distances between the endometrium and fibroids are clearly visualized.

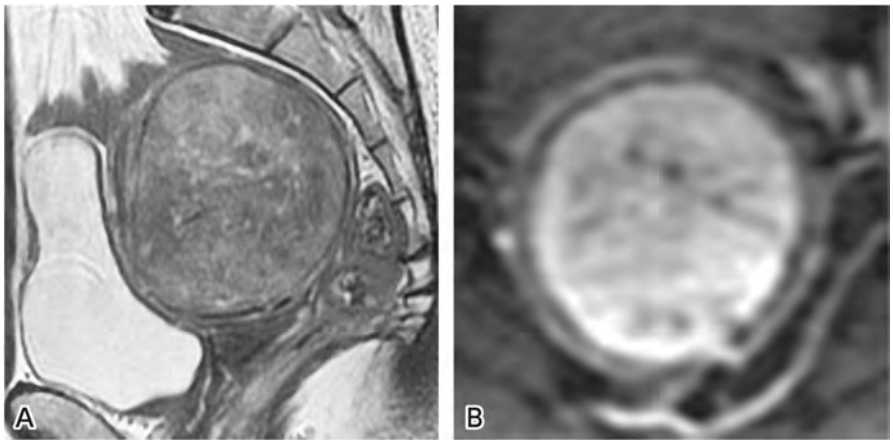

Figure 2. Cellular leiomyoma

A: MRI, T2-weighted sagittal image: An intramyometrial mass showing slight non-homogeneous hyperintensity is seen.
B: MRI, diffusion-weighted image, b-value = 800 s/mm^2: The mass shows hyperintensity and a relatively low ADC (1.08 × 10^{-3} mm^2/s).

Search keywords and secondary sources used as references

PubMed was searched using the following keywords: leiomyoma, myoma, fibroid, uterus, uterine, MRI, and magnetic resonance.

In addition, the following was referenced as a secondary source.

1) Kubik-Huch RA et al: European Society of Urogenital Radiology (ESUR) guidelines: MR imaging of leiomyomas. Eur Radiol 28: 3125-3137, 2018

References

1) Parker WH: The utility of MRI for the surgical treatment of women with uterine fibroid tumors. Am J Obstet Gynecol 206: 31-36, 2012
2) Dueholm M et al: Evaluation of the uterine cavity with magnetic resonance imaging, transvaginal sonography, hysterosonographic examination, and diagnostic hysteroscopy. Fertil Steril 76: 350-357, 2001
3) Dao D et al: The utility of apparent diffusion coefficients for predicting treatment response to uterine arterial embolization for uterine leiomyomas: a systematic review and meta-analysis. Diagn Interv Radiol 25: 157-165, 2019
4) Oguchi O et al: Prediction of histopathologic features and proliferative activity of uterine leiomyoma by magnetic resonance imaging prior to GnRH analogue therapy: correlation between T2-weighted images and effect of GnRH analogue. J Obstet Gynaecol 21: 107-117, 1995
5) Hricak H et al: Uterine leiomyomas: correlation of MR, histopathologic findings, and symptoms. Radiology 158: 385-391, 1986
6) Yamashita Y et al: Hyperintense uterine leiomyoma at T2-weighted MR imaging: differentiation with dynamic enhanced MR imaging and clinical implications. Radiology 189: 721-725, 1993
7) Thomassin-Naggara I et al: Value of dynamic enhanced magnetic resonance imaging for distinguishing between ovarian fibroma and subserous uterine leiomyoma. J Comput Assist Tomogr 31: 236-242, 2007

BQ 62 Is MRI recommended to diagnose adenomyosis?

Statement

MRI is recommended to confirm the diagnosis and clarify complications when transvaginal ultrasound shows abnormal findings in the myometrium that suggest adenomyosis.

Background

Because the symptoms of adenomyosis, such as dysmenorrhea and hypermenorrhea, are nonspecific, it is difficult to confirm the diagnosis based on clinical criteria alone. In routine practice, transvaginal ultrasonography is usually performed first, and MRI is often performed for patients for whom the diagnosis cannot be confirmed by ultrasonography. This discussion summarizes the evidence regarding the usefulness of MRI for diagnosing adenomyosis.

Explanation

The reported sensitivity and specificity for the diagnosis of adenomyosis range from 70% to 86% and 86% to 93%, respectively, for conventional MRI, compared with 65% to 89% and 65% to 98% for transvaginal ultrasonography; thus, no significant difference in diagnostic performance was seen between these modalities.[1-3)] However, a 2010 meta-analysis found that sensitivity and specificity were 77% and 89%, respectively, for MRI and 72% and 81%, respectively, for transvaginal ultrasonography, indicating higher diagnostic performance with MRI.[4)]

In patients with complicating uterine fibroids, who account for approximately 50% of patients with adenomyosis, sensitivity and specificity were 33% and 78%, respectively, for transvaginal ultrasonography and 67% and 82%, respectively, for MRI.[1)] Thus, the diagnostic accuracy of MRI was superior to that of transvaginal ultrasonography. Moreover, in patients with uterine enlargement, MRI was found to provide high diagnostic accuracy in determining whether the cause was fibroids or adenomyosis.[5)]

A frequently reported MRI finding in adenomyosis is diffuse or local thickening of the junctional zone (JZ) in T2-weighted images. This finding reflects smooth muscle hyperplasia associated with ectopic endometrium.[6)] The normal JZ is ≤ 8-mm thick,[7)] and the JZ thickness generally considered the criterion for adenomyosis is ≥ 12 mm. The reported rates of sensitivity and specificity with this criterion range from 63% to 93% and 91% to 96%, respectively.[1, 3)] Also examined as a criterion for evaluating JZ thickening was the ratio of the thickness of the JZ at its thickest site to the thickness of the myometrium as a whole (JZmax/entire myometrium). Using a criterion of ≥ 40%, sensitivity and specificity of 65% and 92.5%, respectively, for adenomyosis were reported.[1)] In addition, there have been numerous reports that the presence of punctiform areas of hyperintensity in the myometrium in T2-weighted images is also a useful finding for diagnosis. This finding reflects cystic ductal dilatation of ectopic endometrium within the lesion[6)] and is highly specific (99%), although it is present in only half of cases (Figs. 1 and 2).[1)]

In recent years, the classification of adenomyosis according to the findings of MRI into 3 subtypes (internal adenomyosis, external adenomyosis, and adenomyoma) has been described.[8] Internal adenomyosis is visualized as JZ thickening, as discussed above. External adenomyosis is visualized in T2-weighted images as hypointense masses with indistinct borders that include microcyst structures that are separate from the JZ and continuous with the uterine serosa. Adenomyoma is a subtype in which masses that are not continuous with either the JZ or the serosal surface form in the myometrium. External adenomyosis is often seen in the posterior wall, and evidence suggests that it is related to deep endometriosis (Fig. 3).[9]

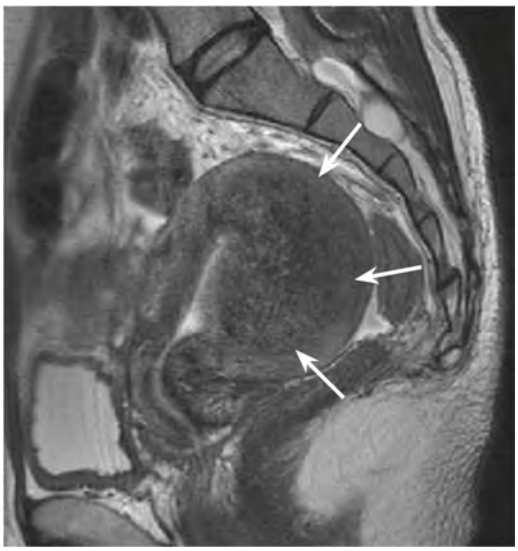

Figure 1. Adenomyosis

MRI, T2-weighted sagittal image: The thickened JZ (→) shows hypointensity on the posterior wall of the uterine body, and the interior includes numerous punctiform areas of hyperintensity. This is a typical image for adenomyosis.

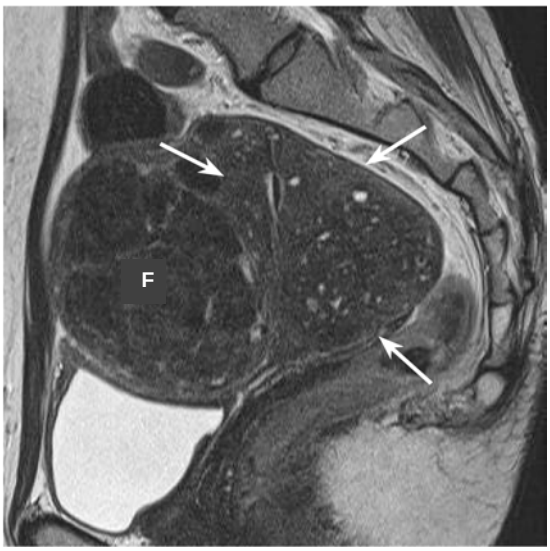

Figure 2. Adenomyosis with complicating fibroids

MRI, T2-weighted sagittal image: Example of concomitant uterine fibroids and adenomyosis. Adenomyosis lesions located predominantly in the posterior wall of the uterine body are visualized as areas of hypointensity with indistinct borders that include punctiform areas of hyperintensity (→). Fibroids are visualized as hypointense masses with distinct borders in the anterior wall (F).

Figure 3. Adenomyosis that is continuous with the uterine serosa (external adenomyosis)

MRI, T2-weighted sagittal image: The lesion is visualized as an area of hypointensity continuous with the serosa on the posterior wall of uterine body (→); it is not continuous with the JZ. The rectum (R) is adherent to the lesion site.

Search keywords and secondary sources used as references

PubMed was searched using the following keywords: MRI, magnetic resonance imaging, and adenomyosis.

References

1) Bazot M et al: Ultrasonography compared with magnetic resonance imaging for the diagnosis of adenomyosis: correlation with histopathology. Hum Reprod 16: 2427-2433, 2001
2) Dueholm M et al: Magnetic resonance imaging and transvaginal ultrasonography for the diagnosis of adenomyosis. Fertil Steril 76: 588-594, 2001
3) Reinhold C et al: Diffuse adenomyosis: comparison of endovaginal US and MR imaging with histopathologic correlation. Radiology 199: 151-158, 1996
4) Champaneria R et al: Ultrasound scan and magnetic resonance imaging for the diagnosis of adenomyosis: systematic review comparing test accuracy. Acta Obstetricia et Gynecologica 89: 1374-1384, 2010
5) Stamatopoulos CP et al: Value of magnetic resonance imaging in diagnosis of adenomyosis and myoma of the uterus. J Minim Invasive Gynecol 19: 620-626, 2012
6) Togashi K et al: Adenomyosis: diagnosis with MR imaging. Radiology 166: 111-114, 1988
7) Kang S et al: Adenomyosis: specificity of 5 mm as the maximum normal uterine junctional zone thickness in MR images. AJR Am J Roentgenol 166: 1145-1150, 1996
8) Bazot M, Darai E: Role of transvaginal sonography and magnetic resonance imaging in the diagnosis of uterine adenomyosis. Fertil Steril 109: 389-397, 2018
9) Kishi Y et al: Four subtypes of adenomyosis assessed by magnetic resonance imaging and their specification. Am J Obstet Gynecol 207: 114.e1-e7, 2012

BQ 63 Is MRI recommended to diagnose and manage ovarian endometriotic cysts?

Statement

MRI is recommended when transvaginal ultrasonography: cannot differentiate ovarian endometriotic cysts from other ovarian tumors; cannot visualize entire lesions; or detects findings suggestive of developing ovarian cancer, such as mural nodules.

FQ 8 Is MRI recommended to diagnose deep infiltrative endometriosis?

Statement

In the diagnosis of deep infiltrative endometriosis by MRI, there are no differences between operators, and MRI provides greater objectivity and better ability to evaluate the spread of lesions than transvaginal ultrasonography.

Background

Endometriosis is a common condition that affects approximately 6% to 10% of women of reproductive age. Its clinical symptoms are variable, including dysmenorrhea, chronic lower abdominal pain, coital pain, dyschezia, and infertility. There are three distinct forms of pelvic endometriosis: ovarian endometriosis, peritoneal endometriosis, and deep infiltrative endometriosis. Deep infiltrative endometriosis is defined as endometriosis infiltrating the peritoneum by more than 5 mm from the surface, whereas peritoneal endometriosis involves the peritoneum superficially. Deep endometriosis is often associated with severe pain.[1)] Deep infiltrative endometriosis is generally found in the uterosacral ligament, posterior vaginal fornix, bowel, and bladder, and pain symptoms relate to the anatomic location of deep infiltrative endometriosis.[2)] Further, endometriosis is associated with ovarian cancer, such as endometrioid carcinoma and clear cell carcinoma.[3-5)]

The primary roles of imaging examinations in diagnosing and managing endometriosis are to characterize ovarian masses, evaluate the extent and localization of endometriosis, and detect cancer arising in ovarian endometriosis. Transvaginal ultrasonography is the first-choice imaging modality in clinical settings, and MRI may be performed as the next step. In this section, we discuss the usefulness of MRI in evaluating and managing ovarian endometriotic cysts and deep infiltrative endometriosis.

Explanation

Transvaginal ultrasonography is the first-line imaging modality to differentiate ovarian endometriotic cysts from other ovarian tumors, with sensitivity and specificity of 83% and 89%, respectively.[6] MRI may be performed as the next step when transvaginal ultrasonography is inconclusive. MRI has a higher sensitivity and specificity for diagnosing ovarian endometriotic cysts (90% and 98%, respectively) than transvaginal ultrasonography.[7] Typical MRI findings include a cystic lesion with hyperintensity on T1-weighted images and hypointensity on T2-weighted images (shading), and multiple hyperintense cysts on T1-weighted images (multiplicity, Fig. 1), which may reflect recurrent hemorrhage. Irregular or angular-shaped cysts, which may reflect adhesion to the surrounding structures, are other characteristic findings of ovarian endometriotic cysts. In addition, discrete, markedly hypointense foci in the cyst on T2-weighted images (T2 dark spot sign) are considered highly specific for endometriotic cysts.[8]

The risk factors for developing ovarian cancer in patients with endometriotic cysts are postmenopausal status and ovarian cyst diameter ≥ 9 cm.[9] If transvaginal ultrasonography detects mural nodules suspicious of ovarian cancer,[4, 5] contrast-enhanced MRI may be useful to distinguish ovarian cancer from pseudo-lesions.[10] Subtraction contrast-enhanced images may be valuable to evaluate the enhancement of mural nodules within hyperintense cysts on T1-weighted images.[6] Other ultrasonographic findings suggesting malignant transformation in endometriotic cysts include increased mass diameter[4] and decreased echogenicity of the cyst content, which may reflect the dilution of hemorrhagic fluid by tumor secretions.[5] If ultrasonography shows these findings, detailed MRI examinations may be performed (see BQ66 regarding differentiation between benign and malignant ovarian tumors).

In investigations of the diagnosis of deep infiltrative endometriosis in the rectum and sigmoid colon, where it occurs preferentially, sensitivity and specificity ranged from 75% to 88% and 98% to 100%, respectively, for MRI and from 33% to 70% and 96% to 100%, respectively, for transvaginal ultrasonography.[11, 12] Thus, MRI showed slightly superior sensitivity. In a recent meta-analysis of involvement of the rectum and sigmoid colon, sensitivity and specificity ranged from 73% to 100% and 50% to 100%, respectively, for MRI and from 73% to 98% and 67% to 100%, respectively, for transvaginal ultrasonography.[13] Thus, MRI and transvaginal ultrasonography were found to have comparable sensitivity and specificity. However, lesions are often missed with transvaginal ultrasonography because the range of observation is limited, and performance is largely dependent on the skill and circumstances of the operator. Japan’s Clinical Practice Guidelines for Less Common Site and Rare Site Endometriosis demonstrate the usefulness of surgical treatment, and MRI plays an important role and allows for objective evaluation of lesion extent and depth for diagnosis of deep infiltrative endometriosis.

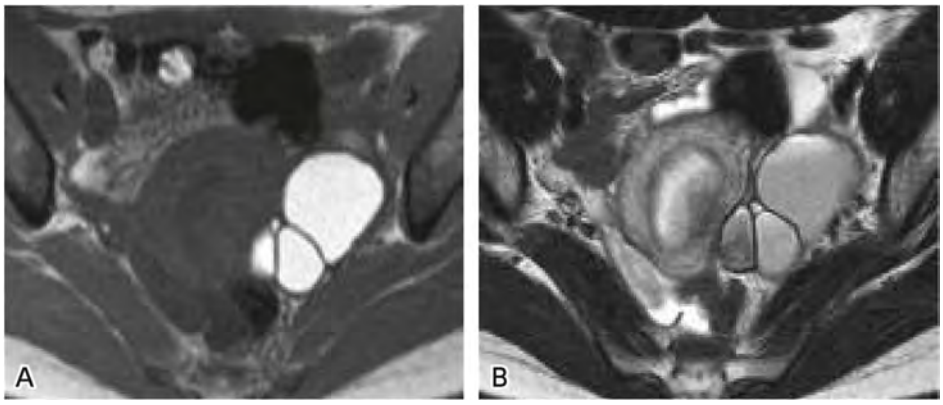

Figure 1. Ovarian endometriotic cysts

A: MRI, T1-weighted image; B: MRI, T2-weighted image: Multilocular cystic masses are seen in the left ovary, showing homogeneous hyperintensity on T1-weighted image (A) and inhomogeneous hypointensity (shading) on T2-weighted image (B).

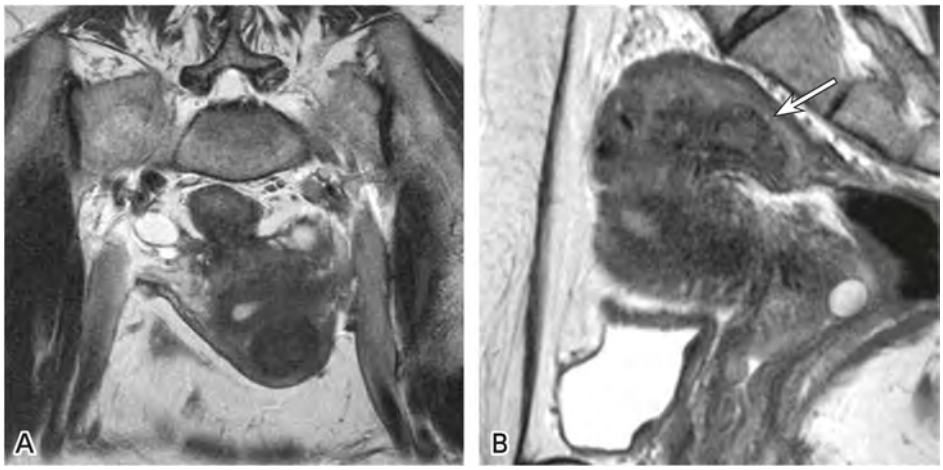

Figure 2. Deep infiltrative endometriosis (patient in her 40s)

A: MRI, T2-weighted oblique coronal image: A lesion with irregular margins that is nearly isointense with the iliacus muscle is present between the rectum and uterus and ovaries and interspersed with small hyperintensity foci. Bilateral ovaries and the rectum are concentrated at the point of the posterior wall of the uterine body.

B: MRI, T2-weighted sagittal image: A mass is present in the border region of the sigmoid colon and rectum (→). A lesion associated with a site of near isointensity with the iliacus muscle is present inferiorly.

Various MRI findings are obtained in deep infiltrative endometriosis. However, in the uterosacral ligament, rectum, and sigmoid colon, sites where deep infiltrative endometriosis occurs preferentially, elevation of the posterior vaginal fornix and contracture of the anterior surfaces of the rectum and sigmoid colon are seen. Moreover, it may result in mass formation, in addition to ovarian adhesion and high signal intensity of the endometrial glands (Fig. 2).[14] Although malignant transformation is known to occur, there have been no definitive reports in this regard, and diagnosis is often challenging.

Search keywords and secondary sources used as references

PubMed was searched for ovarian endometriotic cysts using the following keywords: sensitivity, specificity, endometriosis, diagnosis, and magnetic resonance imaging, and for deep infiltrative endometriosis using the following keywords: MRI and deep infiltrative endometriosis.

In addition, the following were referenced as secondary sources.

1) Japan Society of Obstetrics and Gynecology, Ed.: General Rules for Clinical Management of Endometriosis, Part 2: Diagnosis and Treatment (2nd Edition). KANEHARA & Co., 2010.
2) Panel for the Preparation of Guidelines on Classification, Diagnosis, and Treatment for Multimodal Therapy of Intractable Rare Site Endometriosis, Ed.: Clinical Practice Guidelines for Rare Site Endometriosis. SHINDAN TO CHIRYO SHA, 2018.
3) Bazot M et al: European Society of Urogenital Radiology guidelines: MR imaging of pelvic endometriosis. Eur Radiol 27: 2765-2775, 2017

References

1) Koninckx PR et al: Deep endometriosis: definition, diagnosis, and treatment. Fertil Steril 98 (3): 564-571, 2012
2) Fauconnier A et al: Relation between pain symptoms and the anatomic location of deep infiltrating endometriosis. Fertil Steril 78: 719-726, 2002
3) Pearce CL et al: Association between endometriosis and risk of histological subtypes of ovarian cancer: a pooled analysis of case-control studies. Lancet Oncol 13 (4): 385-394, 2012
4) Taniguchi F et al: Clinical characteristics of patients in Japan with ovarian cancer presumably arising from ovarian endometrioma. Gynecol Obstet Invest 77 (2): 104-110, 2014
5) Testa AC et al: Ovarian cancer arising in endometrioid cysts: ultrasound findings. Ultrasound Obstet Gynecol 38 (1): 99-106, 2011
6) Guerriero S et al: The role of endovaginal ultrasound in differentiating endometriomas from other ovarian cysts. Clin Exp Obstet Gynecol 22: 20-22, 1995
7) Togashi K et al: Endometrial cysts: diagnosis with MR imaging. Radiology 180 (1): 73-78, 1991
8) Corwin MT et al: Differentiation of ovarian endometriomas from hemorrhagic cysts at MR imaging: utility of the T2 dark spot sign. Radiology 271 (1): 126, 2014
9) Kobayashi H et al: Ovarian endometrioma: risks factors of ovarian cancer development. Eur J Obstet Gynecol Reprod Biol 138 (2): 187-193, 2008
10) Tanaka YO et al: Ovarian carcinoma in patients with endometriosis: MR imaging findings. AJR Am J Roentgenol 175 (5): 1423-1430, 2000
11) Bazot M et al: Deep pelvic endometriosis: MR imaging for diagnosis and prediction of extension of disease. Radiology 232: 379-389, 2004
12) Grasso RF et al: Diagnosis of deep infiltrating endometriosis: accuracy of magnetic resonance imaging and transvaginal 3D ultrasonography. Abdom Imaging 35: 716-725, 2010
13) Moura APC et al: Accuracy of transvaginal sonography versus magnetic resonance imaging in the diagnosis of rectosigmoid endometriosis: systematic review and meta-analysis. PLoS One 9 (14): e0214842, 2019
14) Marcal L et al: Deep pelvic endometriosis: MR imaging. Abdom Imaging 35: 708-715, 2010

BQ 64 Is MRI recommended to evaluate the local progression of cervical cancer?

Statement

MRI is strongly recommended to evaluate the local invasion of cervical cancer. Concomitant diffusion-weighted imaging is desirable.

Background

Surgery and chemoradiation therapy are the two pillars of treatment for cervical cancer. The treatment planning is based on the General Rules for Clinical and Pathological Management of Uterine Cervical Cancer (4th Edition) and Guidelines for Treatment of Uterine Cervical Cancer (2017 Edition) in Japan. In The General Rules for Clinical and Pathological Management of Uterine Cervical Cancer, the usefulness of pretreatment diagnostic imaging for staging is noted and recommended. This discussion summarizes the evidence regarding the usefulness of MRI for evaluation of the local invasion of cervical cancer.

Explanation

MRI is widely used in Japan to evaluate invasive cervical cancer (stage IB or higher) before treatment. Moreover, because subclassification based on tumor size was added to the 2018 revised FIGO classification, the role of diagnostic imaging that permits tumor diameter to be objectively measured has become increasingly important.

The usefulness of CT and MRI in staging has been noted since the 1990s. A multicenter meta-analysis found the sensitivity of MRI for parametrial invasion to be higher than that of CT (CT, 55%; MRI, 74%) and their diagnostic performance to detect lymph node metastasis to be comparable.[1)] A recent meta-analysis of the diagnostic performance of MRI with parametrial invasion reported excellent diagnostic performance, with sensitivity and specificity of 76% and 94%, respectively.[2)] A multicenter study of advanced cancer of stage IIb or higher (old classification) conducted from 2000 to 2002 by the American College of Radiology Imaging Network (ACRIN) and Gynecologic Oncology Group (GOG) found that, although the sensitivity of MRI and CT tended to be low (CT, 42%; MRI, 53%), their specificity was high (CT, 82%; MRI, 85%).[3)] Moreover, MRI has shown higher sensitivity than CT for evaluation of invasion to other organs, such as the urinary bladder and rectum,[4)] and is substitutable for cystoscopy, proctoscopy, and excretory urography.[5)] The 2018 revised WHO classification subdivided stage IB into 3 subclassifications (IB1-3) for the purpose of assessing the outcome of radical trachelectomy, a fertility-preserving procedure. Cutoff values of 2 cm and 4 cm are used in determining the subclassification, increasing the importance of tumor diameter measurement.[6)] MRI, which provides excellent tumor tissue contrast, is useful for measuring tumor diameter preoperatively. It is considered even more useful than ultrasonography for this purpose.[7)]

With diffusion-weighted imaging, cervical cancer shows high intensity and a low apparent diffusion coefficient (ADC).[8, 9] Diagnosis using both T2-weighted imaging and diffusion-weighted imaging has been reported to provide higher diagnostic performance than T2-weighted imaging alone for evaluating parametrial invasion.[2, 10]

An adequate consensus has not yet been reached regarding gadolinium contrast-enhanced imaging. For staging, T2-weighted imaging is the basic imaging method, and although improved tumor contrast and diagnostic performance have been reported with contrast-enhanced MRI,[11] its indications are limited. Consequently, its use does not necessarily contribute to improving diagnostic performance.[2]

Search keywords and secondary sources used as references

PubMed was searched using the following keywords: uterine cervical cancer, uterine cervical adenocarcinoma, uterine cervical carcinoma, CT, and MRI.

In addition, the following were referenced as secondary sources.

1) Japan Society of Obstetrics and Gynecology, et al., Ed.: The General Rules for Clinical and Pathological Management of Uterine Cervical cancer: Clinical Edition (4th Edition). KANEHARA & Co., 2020.
2) Japan Society of Gynecologic Oncology, Ed.: 2017 Guidelines for Treatment of Uterine Cervical cancer. KANEHARA & Co., 2017.
3) Balleyguier C et al: Staging of Uterine Cervical cancer With MRI: Guidelines of the European Society of Urogenital Radiology. Eur Radiol 21 (5): 1102-1110, 2011

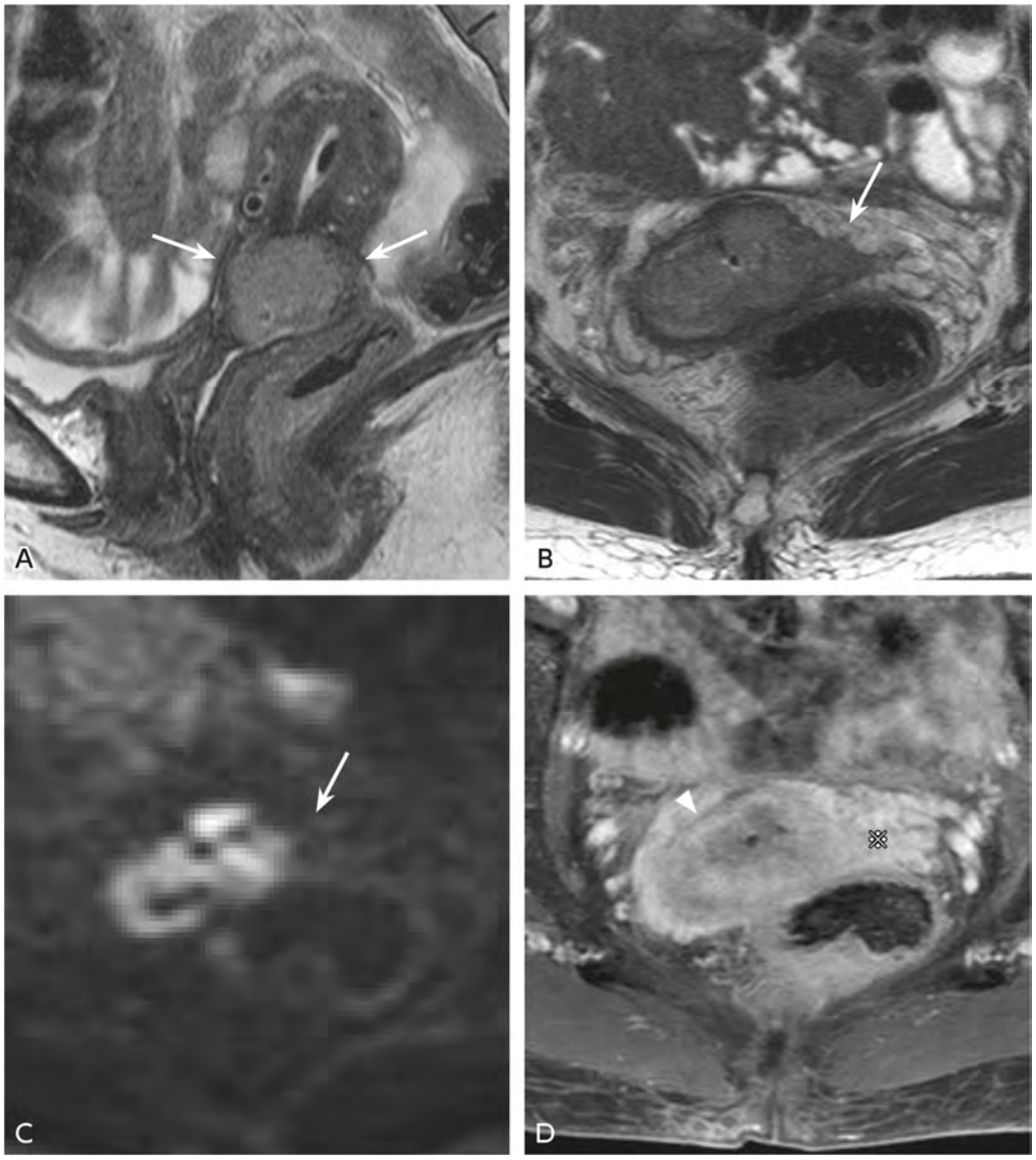

Figure　Cervical cancer, IB1 (pT2a), patient in her 60s

A: MRI, T2-weighted sagittal image: A mass that shows slight high intensity compared with the uterine body myometrium is seen in the cervical area (→).

B: MRI, T2-weighted transverse image: An almost fully circumferential stromal ring is observed. However, the left side is partially indistinct, so that parametrial invasion cannot be excluded (→).

C: MRI, diffusion-weighted imaging, b-value = 800 s/mm^2: The tumor is visualized as high intensity, and no areas of abnormal signal are observed in the left parametrium. (→).

D: MRI, fat-suppressed contrast-enhanced T1-weighted image: The tumor is visualized as a hypointensity lesion (▷). However, venous enhancement in the parametrial tissue is striking (*), making diagnosis of parauterine tissue infiltration difficult.

References

1) Bipat S et al: Computed tomography and magnetic resonance imaging in staging of uterine cervical carcinoma: a systematic review. Gynecol Oncol 91 (1): 59-66, 2003

2) Woo S et al: Magnetic resonance imaging for detection of parametrial invasion in cervical cancer: an updated systematic review and meta-analysis of the literature between 2012 and 2016. Eur Radiol 28 (2): 530-541, 2018

3) Hricak H et al: Role of imaging in pretreatment evaluation of early invasive cervical cancer: results of the intergroup study American College of Radiology Imaging Network 6651-Gynecologic Oncology Group 183. J Clin Oncol 23 (36): 9329-9337, 2005
4) Kim WY et al: Reliability of magnetic resonance imaging for bladder or rectum invasion in cervical cancer. J Reprod Med 56 (11-12): 485-490, 2011
5) Amendola MA et al: Utilization of diagnostic studies in the pretreatment evaluation of invasive cervical cancer in the United States: results of intergroup protocol ACRIN 6651/GOG 183. J Clin Oncol 23 (30): 7454-7459, 2005
6) Lee SI, Atri M: 2018 FIGO staging system for uterine cervical cancer: enter cross-sectional imaging. Radiology 292 (1): 15-24, 2019
7) Epstein E et al: Early-stage cervical cancer: tumor delineation by magnetic resonance imaging and ultrasound: a European multicenter trial. Gynecol Oncol 128 (3): 449-453, 2013
8) Hou B et al: Diagnostic significance of diffusion-weighted MRI in patients with cervical cancer: a meta-analysis. Tumour Biol 35 (12): 11761-11769, 2014
9) Naganawa S et al: Apparent diffusion coefficient in cervical cancer of the uterus: comparison with the normal uterine cervix. Eur Radiol 15 (1): 71-78, 2005
10) Park JJ et al: Parametrial invasion in cervical cancer: fused T2-weighted imaging and high-b-value diffusion-weighted imaging with background body signal suppression at 3 T. Radiology 274 (3): 734-741, 2015
11) Akita A et al: Comparison of T2-weighted and contrast-enhanced T1-weighted MR imaging at 1.5 T for assessing the local extent of cervical carcinoma. Eur Radiol 21 (9): 1850-1857, 2011

BQ 65 Is MRI recommended to evaluate the local progression of endometrial cancer?

Statement

MRI is strongly recommended to preoperatively evaluate the local progression of endometrial cancer. The use of contrast-enhanced MRI is favored. However, if contrast-enhanced examination is difficult, the evaluation can be performed by combined T2-weighted imaging and diffusion-weighted imaging.

Background

The prognosis of endometrial cancer depends on the tissue-type, grade, and stage of the tumor. The treatment plan, including the surgical procedure, varies according to these factors. Diagnostic imaging contributes greatly to preoperative staging. MRI is excellent for evaluating the local progression of tumors. Since deep myometrial invasion (≥ 1/2) is strongly correlated with lymph node metastasis and prognosis, accurate preoperative diagnosis is very important.

Explanation

Japanese guidelines for treatment of uterine body neoplasms recommend that myometrial and cervical stromal invasion should be evaluated by MRI preoperatively (grade A).

MRI is excellent for evaluating the local progression of endometrial cancer, and the guidelines of other countries also recommend MRI for evaluating local tumor extent.

In a 1999 meta-analysis of the preoperative staging of endometrial cancer, Kinkel et al. reported no significant difference among transvaginal ultrasonography (TVUS), CT, and MRI.[1)] The same report showed that contrast-enhanced MRI was useful and significantly better than non-contrast MRI, TVUS, and CT with respect to myometrial invasion.

Many reports have concluded that contrast-enhanced MRI is useful,[2, 3)] and various guidelines recommend it.

Dynamic contrast-enhanced (DCE)-MRI is the basic method. However, the equilibrium phase, during which the contrast between endometrial lesions and the myometrium is high, has been found to be the most suitable for evaluating myometrial invasion.[3, 4)]

Single-phase contrast-enhanced images in the equilibrium phase should be obtained if DCE-MRI is difficult to perform.

The usefulness of diffusion-weighted imaging (DWI) in evaluating deep myometrial invasion has been established.[5)]

A meta-analysis published by Andreano et al. in 2014 reported that there were no significant differences in sensitivity and specificity for evaluating deep myometrial invasion between DWI and DCE-MRI, and the diagnostic accuracy of DWI was at least the same as that of DCE-MRI.

Numerous subsequent meta-analyses also showed DWI to be useful for evaluating deep myometrial invasion.[8, 9)] Because the signal intensity (SI) on DWI is affected by the SI on T2WI, it is recommended that evaluations should be performed by combined DWI and T2WI.

Deng et al. reported that there was no significant difference in sensitivity for evaluating deep myometrial invasion between combined T2WI + DWI and DWI or DCE-MRI.

However, the specificity was significantly higher with combined T2WI and DWI compared with DWI or DCE-MRI, resulting in better diagnostic performance.[8)]

Other studies also reported that combined T2WI and DWI was superior to DCE-MRI alone or combined T2WI and DCE-MRI in evaluating myometrial invasion.[10, 11)]

When a gadolinium contrast medium cannot be used for a reason such as contrast allergy or nephropathy, myometrial invasion can be evaluated by combined T2WI and DWI.[11)]

As for the assessment of cervical stromal invasion (CSI), MRI shows high specificity, but the sensitivity is reportedly low.[12)] A similar result (sensitivity, 50%; specificity, 95%) was shown in a meta-analysis by Bi et al. in 2019.[9).] Because microscopic invasion is difficult to identify on MRI, sensitivity is therefore thought to be low.

There have been few reports showing the usefulness of DWI for evaluating CSI. However, a study that compared combined T2WI + DWI with combined T2WI + DCE-MRI found no significant differences in sensitivity, specificity, or accuracy for evaluating CSI.[11)] Another study reported that the specificity of DWI was higher than that of DCE-MRI, and its accuracy was superior.[13)] These findings suggest that it may also be possible to omit contrast-enhanced MRI for assessing cervical stromal invasion.

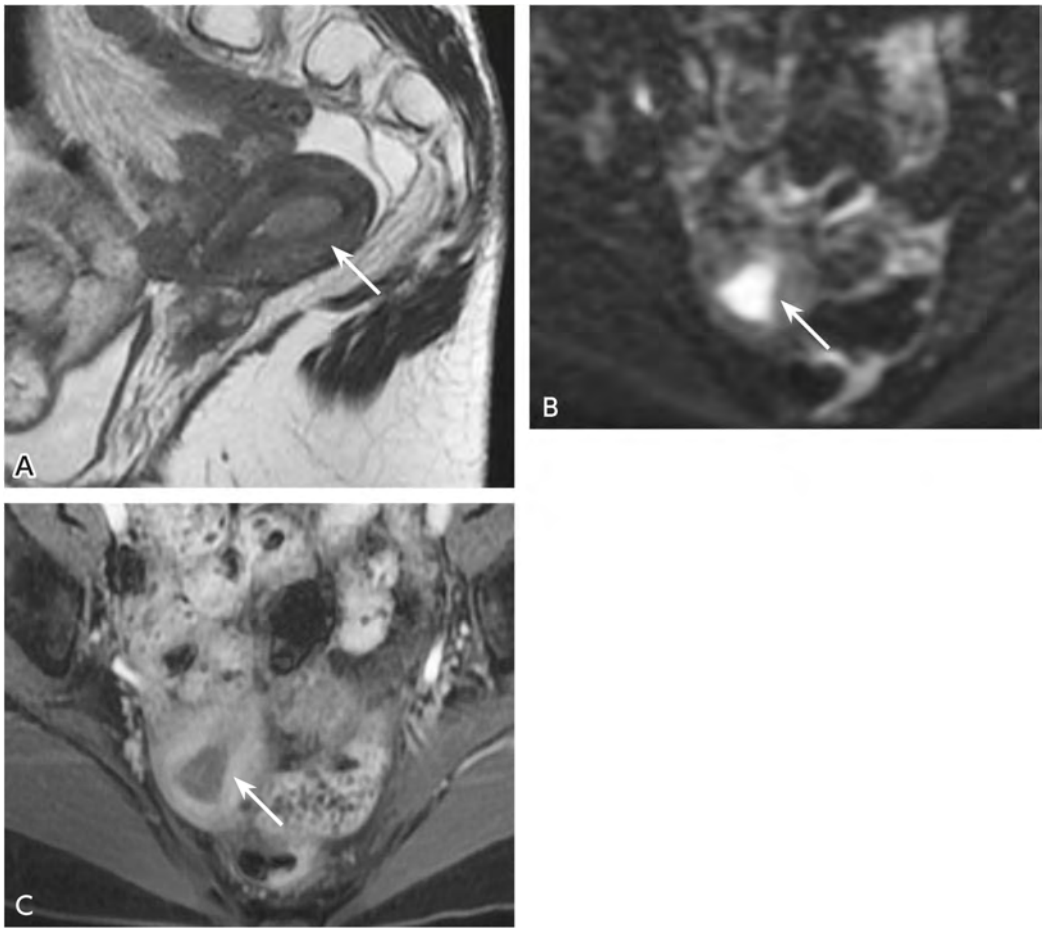

Figure 1. Endometrial cancer/endometrioid carcinoma IA (50s, F)

A: MRI, Sagittal T2WI (T2-weighted sagittal image)
B: MRI, Axial DWI (diffusion-weighted transverse image), b-value = 1,000 s/mm^2
C: DCE-MRI (Dynamic contrast-enhanced MRI) 90s (90 seconds post-contrast)

Compared with the myometrium, endometrial cancer shows hypointensity on T2WI (A) and hyperintensity on DWI (B). The tumor is less enhanced compared with the myometrium (C).
The border between the endometrial cancer and myometrium is clear and smooth on all images, indicating no myometrial invasion

With high-magnetic field MRI (3T), the SNR is high, and it has been reported to be superior to conventional 1.5T MRI for evaluating deep myometrial invasion. However, no significant difference has been found.[6, 8)]

PET/MRI has been reported to be superior to PET/CT for evaluating myometrial and cervical stromal invasion. However, there have been few reports on this topic, and a limited number of facilities can perform these examinations.[14)]

CT has low contrast resolution, and its ability to evaluate local progression is weaker than that of MRI. However, evaluating local progression by CT is considered if there is difficulty performing MRI. Dual-energy CT has been reported to increase the ability to evaluate local progression.[15)]

Its development is expected for use as a substitute for MRI when MRI cannot be performed.

Search keywords and secondary sources used as references

PubMed was searched using the following keywords: computed tomography, CT, magnetic resonance imaging, MRI, positron emission tomography, PET, PET/CT, FDG-PET, ultrasound, ultrasonography, US, uterine body cancer, uterine endometrial cancer, uterine endometrial carcinoma, and staging.

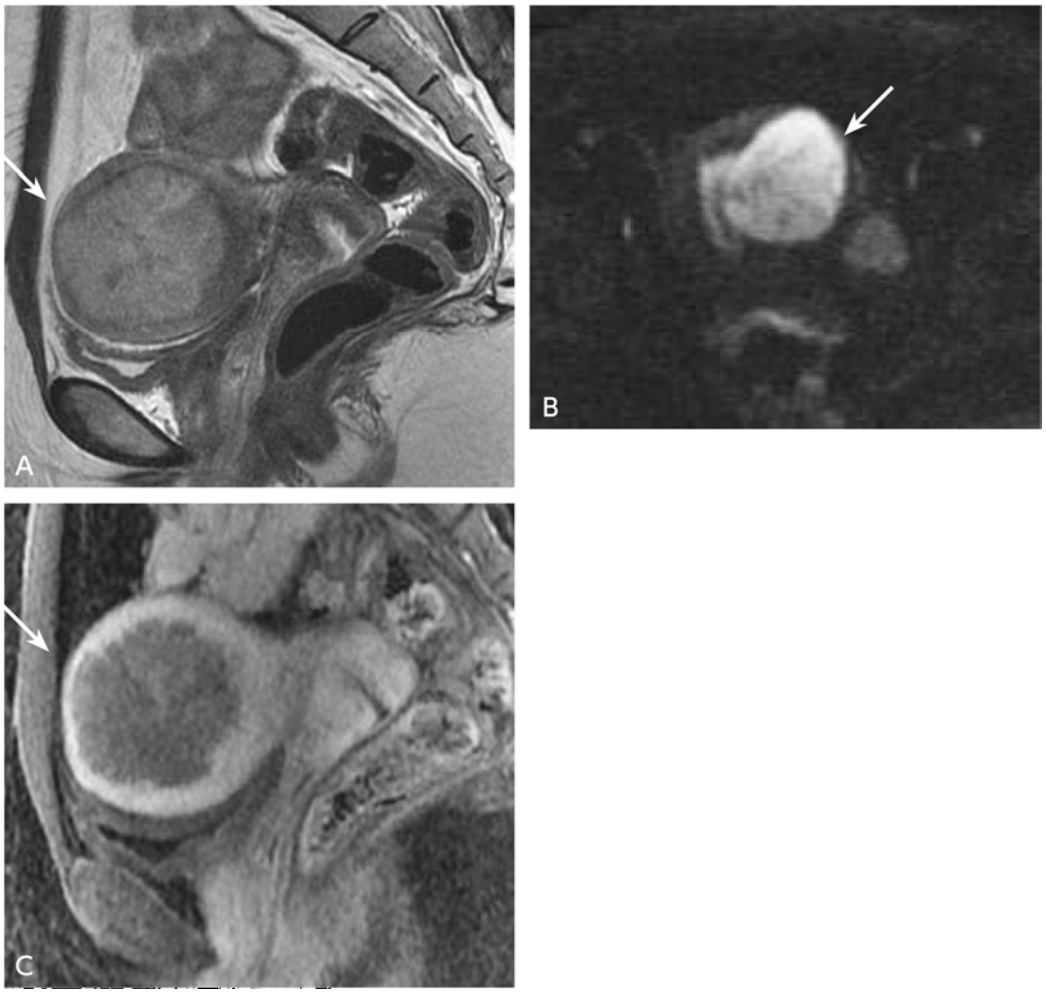

Figure 2. Endometrial cancer/endometrioid carcinoma IB (40s, F)

A: MRI, Sagittal T2WI (T2-weighted sagittal image)

B: MRI, Axial DWI (diffusion-weighted transverse image), b-value = 1,000 s/mm^2

C: DCE-MRI (Dynamic contrast-enhanced MRI) 90s (90 seconds post-contrast)

The border between the endometrial cancer and myometrium is indistinct. Abnormal signal intensity indicating endometrial cancer extends deeply into the myometrium, suggesting deep myometrial invasion. The findings are the same on T2-weighted imaging (A), diffusion-weighted imaging (B), and contrast-enhanced MRI (C).

The following were referenced as secondary sources.

1) Japan Society of Gynecologic Oncology, Ed.: 2017 Guidelines for the treatment of uterine body neoplasm. KANEHARA & Co., 2017.
2) Japan Society of Obstetrics and Gynecology, Japanese Society of Pathology, Ed.: The General Rules for Clinical and Pathological Management of Uterine Corpus Cancer: Pathological Edition (4th Edition). KANEHARA & Co., 2017.
3) Reinhold C et al: ACR Appropriateness Critera®: pretreatment evaluation and follow-up of endometrial cancer. J Am Coll Radiol 17: S472-S486, 2020
4) Nougaret S et al: Endometrial cancer MRI staging: updated guidelines of the European Society of Urogenital Radiology. Eur Radiol 29（2）：792-805, 2019

References

1) Kinkel K et al: Radiologic staging in patients with endometrial cancer: a meta-analysis. Radiology 212: 711-718, 1999
2) Sala E et al: Added value of dynamic contrast-enhanced magnetic resonance imaging in predicting advanced stage disease in patients with endometrial carcinoma. Int J Gynecol Cancer 19: 141-146, 2009
3) Manfredi R et al: Local-regional staging of endometrial carcinoma: role of MR imaging in surgical planning. Radiology 231: 372-378, 2004
4) Park SB et al: Dynamic contrast-enhanced MR imaging of endometrial cancer. optimizing the imaging delay for tumour-myometrium contrast. Eur Radiol 24 (11): 2795-2799, 2014
5) Das SK et al: Usefulness of DWI in preoperative assessment of deep myometrial invasion in patients with endometrial carcinoma: a systematic review and meta-analysis. Cancer Imaging 14: 32, 2014
6) Andreano A et al: MR diffusion imaging for preoperative staging of myometrial invasion in patients with endometrial cancer: a systematic review and meta-analysis. Eur Radiol 24: 1327-1338, 2014
7) Beddy P et al: Evaluation of depth of myometrial invasion and overall staging in endometrial cancer: comparison of diffusion-weighted and dynamic contrast-enhanced MR imaging. Radiology 262 (2): 530-537, 2012
8) Deng L et al: The combination of diffusion- and T2-weighted imaging predicting deep myometrial invasion of endometrial cancer: a systematic review and meta-analysis. J Comput Assist Tomogr 39: 661-673, 2015
9) Bi Q et al: The diagnostic value of MRI for preoperative staging in patients with endometrial cancer: a meta-analysis. Acad Radiol 27: 960-968, 2020
10) Kececi IS et al: Efficacy of diffusion-weighted magnetic resonance imaging in the diagnosis and staging of endometrial tumors. Diagn Interv Imaging 97 (2): 177-186, 2016
11) Bonatti M et al: MRI for local staging of endometrial carcinoma: is endovenous contrast medium administration still needed? Eur J Radiol 84 (2): 208-214, 2015
12) Antonsen SL et al: MRI, PET/CT and ultrasound in the preoperative staging of endometrial cancer: a multicenter prospective comparative study. Gynecol Oncol 128 (2): 300-308, 2013
13) Lin G et al: Endometrial cancer with cervical stromal invasion: diagnostic accuracy of diffusion-weighted and dynamic contrast enhanced MR imaging at 3T. Eur Radiol 27: 1867-1876, 2017
14) Kitajima K et al: Value of fusion of PET and MRI for staging of endometrial cancer: comparison with 18F-FDG contrast-enhanced PET/CT and dynamic contrast-enhanced pelvic MRI. Eur J Radiol 82 (10): 1672-1676, 2013
15) Rizzo S et al: Evaluation of deep myometrial invasion in endometrial cancer patients: is dual-energy CT an option? Radiol Med 123: 13-19, 2018

FQ 9 Which imaging examinations are recommended to diagnose uterine sarcoma?

Statement

MRI is recommended for qualitative diagnosis of uterine sarcoma. However, the level of evidence is not high due to the difficulty of conducting large studies of uterine sarcoma, which is a rare disease. In particular, diagnostic performance is improved by performing diffusion-weighted imaging and generating an ADC map. In addition, contrast-enhanced MRI may contribute to diagnosis.

^{18}F-FDG-PET/CT provides a good diagnostic accuracy rate in the qualitative diagnosis and staging of uterine sarcoma and can potentially assist in its preoperative diagnosis and treatment plan determination.

Background

Although most uterine myometrial masses are uterine fibroids, differentiation from uterine sarcomas is problematic. Although uterine sarcomas are diagnosed histologically following surgery, preoperative diagnostic imaging is required to determine a treatment strategy. This discussion provides an overview concerning MRI, which is usually used for differential diagnosis, and PET/CT, which is currently not covered by national health insurance, but its usefulness is promising. Uterine carcinosarcoma is considered to be metaplasia of endometrial cancer; therefore, uterine carcinosarcoma was excluded from this examination as much as possible.

Explanation

MRI provides good soft tissue contrast and is used to differentiate uterine myometrial masses. Uterine sarcomas are often large, irregularly shaped masses associated with hemorrhage and necrosis, and the diagnostic performance of T1- and T2-weighted imaging, diffusion-weighted imaging, ADC mapping, and contrast-enhanced MRI has been examined.

A uterine myometrial mass with irregular margins and an indistinct border is a finding suggestive of a uterine sarcoma. However, some uterine sarcomas have a distinct border and regular margins on imaging or macroscopically. Consequently, uterine sarcoma cannot be diagnosed based on an assessment of the margins alone.[1, 2)] Hyperintensity on T1-weighted imaging suggests hemorrhage. Although this assists in diagnosis, particularly in the case of leiomyosarcoma, there is no significant difference compared with uterine fibroids.[1-3)] Even when there is no area of hyperintensity on T1-weighted imaging, uterine sarcoma cannot be ruled out. Such areas are also seen on T1-weighted imaging even for uterine fibroids associated with red degeneration or uterine adenomyomas. Although hyperintensity in T2-weighted images is also seen for degenerative leiomyomas and cellular leiomyomas, hyperintensity in T2-weighted images is a finding suggestive of uterine sarcoma, which may not show hypointensity in T2-weighted images mainly.[2, 3)] Diffusion-weighted imaging and ADC mapping can identify areas of high cellularity. In recent years,

ADC measurement has resulted in improved diagnostic performance for uterine sarcoma,[4-6] although the sample sizes used in the investigations were small, and the ADC cutoff values of studies conducted at other facilities cannot be used. Evaluations may be performed visually combining diffusion-weighted images and ADC maps. In contrast-enhanced examinations, uterine sarcoma necrosis and degeneration are visualized as areas of poor contrast enhancement, which is useful for diagnosis.[7] In addition, early contrast enhancement in dynamic studies has been found to contribute to uterine sarcoma diagnosis.[8] Evaluation by multiparametric MRI, which combines several of T2-weighted imaging, diffusion-weighted imaging and ADC values, and dynamic contrast-enhanced MRI, was found to be useful for diagnosing uterine sarcomas, and the use of these methods for comprehensive evaluation is recommended.[9, 10] Although the diagnostic performance of MRI is relatively high for uterine sarcoma, differentiating from uterine fibroid variants such as cellular leiomyomas is difficult with MRI.[4, 5] It should be kept in mind that diagnosis by imaging is difficult in some patients, particularly for patients who wish to preserve fertility.

The main histological subtypes of uterine sarcomas are uterine leiomyosarcomas and endometrial stromal sarcomas, and reports that focus on MRI findings regarding each histological subtype provide useful information for diagnosis. The presence of hemorrhage or necrosis and hypervascularity are clues for the diagnosis of uterine leiomyosarcoma.[2, 8] With endometrial stromal sarcomas, characteristic MRI findings have been described, such as bands of low signal intensity in T2-weighted images of myometrial lesions, infiltration along vessels and ligaments, and cyst formation.[11]

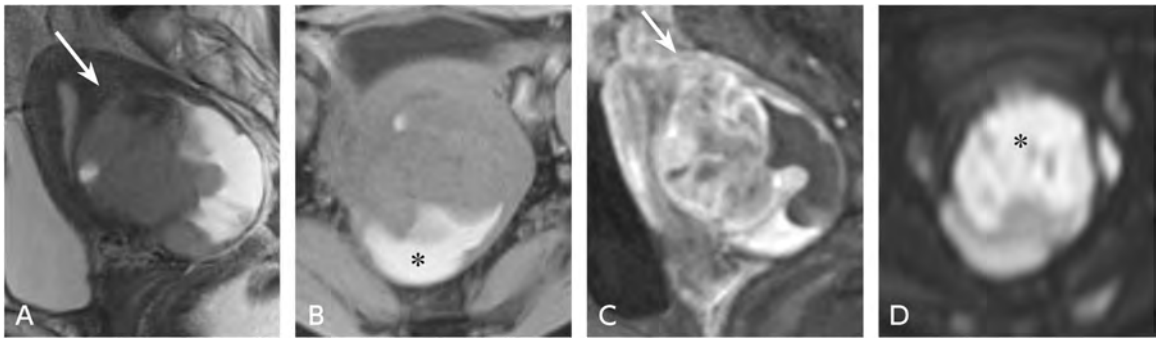

Figure. Woman in her 50s, uterine leiomyosarcoma

A: MRI, T2-weighted sagittal image: An irregularly shaped mass showing non-homogeneous hyperintensity is seen in the myometrium (→).

B: MRI, T1-weighted transverse image: An area of hyperintensity suggestive of hemorrhage is seen (*).

C: Contrast-enhanced MRI, sagittal early-phase image: Early enhancement is seen in the solid portion (→).

D: MRI, diffusion-weighted transverse image, b-value = 800 s/mm^2: The solid portion shows hyperintensity (*) and was hypointense in the ADC map (not shown).

There have been few studies of the diagnostic performance of ^{18}F-FDG-PET/CT with respect to uterine sarcoma, and the studies have had limited sample sizes. However, its usefulness in patients suspected of having uterine sarcomas based on MRI or ultrasonography has been examined. Although FDG shows strong accumulation in uterine sarcomas, it also accumulates in uterine fibroids, and accumulation decreases with age.[12, 13] When ^{18}F-FDG-PET/CT was performed for masses suspected of being uterine

sarcomas based on MRI (masses showing hyperintensity in both T2- and T1-weighted images or in either), the mean maximum standardized uptake value (SUVmax) was higher for uterine sarcomas than for uterine fibroids. Using a cutoff of SUVmax > 7.5, sensitivity and specificity were 80% and 100%, respectively. Moreover, when ^{18}F-FDG-PET/CT was combined with elevated serum lactate dehydrogenase (LDH), sensitivity and sensitivity were 86.6% and 100%, respectively, and false positives could be decreased.[14] For uterine myometrial masses for which rapid enlargement was seen on ultrasonography or MRI, a characteristic pattern of internal accumulation was found to be the hollow ball sign, which indicates a region of decreased accumulation in a uterine sarcoma corresponding to coagulation necrosis in the center of the mass.[15] In a study of uterine sarcoma staging with ^{18}F-FDG-PET/CT, sensitivity, specificity, and the diagnostic accuracy rate were 80%, 100%, and 91%, respectively. However, pulmonary metastases and peritoneal dissemination less than 1 cm in size were FDG-negative, which could result in false-negatives. In that case, however, combining the PET findings with CT findings was found to increase sensitivity.[16] The use of ^{18}F-FDG-PET/CT for the qualitative diagnosis or staging of uterine sarcomas can improve their management, and it has been surmised that ^{18}F-FDG-PET/MRI may serve as a one-stop-shopping type of diagnostic tool in the future.[6]

Search keywords and secondary sources used as references

PubMed was searched using the following keywords: uterine sarcomas, endometrial stromal sarcomas, uterine leiomyosarcomas, diagnostic imaging, MRI, diffusion weighted image, PET, and positron emission tomography.

In addition, the following was referenced as a secondary source.

1) Japan Society of Obstetrics and Gynecology, et al., Ed.: The General Rules for Clinical and Pathological Management of Uterine Corpus Cancer: Pathological Edition (4th Edition). KANEHARA & Co., 2017.

References

1) Cornfeld D et al: MRI appearance of mesenchymal tumors of the uterus. Eur J Radiology 74: 241-249, 2010
2) Li HM et al: Diffusion-weighted imaging or differentiating uterine leiomyosarcoma from degenerated leiomyoma. J Comput Assist Tomogr 41: 599-606, 2017
3) Malek M et al: Investigating the diagnostic value of quantitative parameters based on T2-weighted and contrast-enhanced MRI with psoas muscle and outer myometrium as internal references for differentiating uterine sarcomas from leiomyomas at 3T MRI. Cancer Imaging 19 (1): 20, 2019
4) Tamai K et al: The utility of diffusion-weighted MR imaging for differentiating uterine sarcomas from benign leiomyomas. Eur Radiol 18: 723-730, 2008
5) Sato K et al: Clinical application of diffusion-weighted imaging for preoperative differentiation between uterine leiomyoma and leiomyosarcoma. Am J Obstet Gynecol 368: e1-8, 2014
6) Dubreuil J et al: Diffusion-weighted MRI and 18F-FDG-PET/CT imaging: competition or synergy as diagnostic methods to manage sarcoma of the uterus ?: a systematic review of the literature. Nucl Med Commun 38: 84-90, 2017
7) Lin G et al: Comparison of the diagnostic accuracy of contrast-enhanced MRI and diffusion- weighted MRI in the differentiation between uterine leiomyosarcoma / smooth muscle tumor with uncertain malignant potential and benign leiomyoma. J Magn Reson Imaging 43: 333-342, 2016
8) Goto A et al: Usefulness of Gd-DTPA contrast-enhanced dynamic MRI and serum determination of LDH and its isozymes in the differential diagnosis of leiomyosarcoma from degenerated leiomyoma of the uterus. Int J Gynecol Cancer 12: 354-356, 2002

9) Namimoto T: Combined use of T2-weighted and diffusion-weighted 3-T MR imaging for differentiating uterine sarcomas from benign leiomyomas. Eur Radiol 19: 2756-2764, 2009
10) Bi Q et al: Utility of clinical parameters and multiparametric MRI as predictive factors for differentiating uterine sarcoma from atypical leiomyoma. Acad Radiol 25: 993-1002, 2018
11) Koyama T et al: MR imaging of endometrial stromal sarcoma: correlation with pathologic findings. AJR Am J Roentgenol 173: 767-772, 1999
12) Kitajima K et al: Standardized uptake value of uterine leiomyoma with ^{18}F-FDG PET/CT: variation with age, size, degeneration, and contrast enhancement on MRI. Ann Nucl Med 22: 505-512, 2008
13) Nagamatsu A et al: Use of 18F-fluorodeoxyglucose positron emission tomography for diagnosis of uterine sarcomas. Oncol Rep 23: 1069-1076, 2010
14) Kusunoki S et al: Efficacy of PET/CT to exclude leiomyoma in patients with lesions suspicious for uterine sarcoma on MRI. Taiwanese J Obstet Gynecol 56: 508-513, 2017
15) Ho KC et al: Presurgical identification of uterine smooth muscle malignancies through the characteristic FDG uptake pattern on PET scans. Contrast Media Molecul Imaging 2018: 7890241, 2018
16) Bélissant O et al: Value of ^{18}F-FDG PET/CT imaging in the staging, restaging, monitoring of response to therapy and surveillance of uterine leiomyosarcoma. Nucl Med Commun 39: 652-658, 2018

BQ 66 Is MRI recommended for the qualitative diagnosis of adnexal masses?

Statement

In patients who cannot be diagnosed by ultrasonography, which is the first choice of modalities, MRI contributes to the qualitative diagnosis of adnexal masses and is therefore recommended.

Contrast-enhanced MRI is recommended because it improves diagnostic accuracy for distinguishing between benign and malignant adnexal masses.

Background

An ultrasound examination is the first choice for diagnosing adnexal masses. However, in patients who cannot be diagnosed by ultrasonography, MRI is recommended. This discussion provides an overview regarding the usefulness of MRI for differentiating between benign and malignant adnexal masses.

Explanation

Although the sensitivity, specificity, and AUC of TVUS in distinguishing between benign and malignant adnexal masses are 92%, 89%, and 0.96, respectively,[1)] diagnosing lesions that consist of a mixture of solid and cystic portions is often difficult. MRI is useful for diagnosing patients undiagnosable by ultrasound.[2-5)] A meta-analysis of benign-malignant differentiation using 1.5T MRI published in 2011 showed relatively good diagnostic performance, with values for sensitivity, specificity, and AUC of 92%, 85%, and 0.95, respectively.[6)] The morphological criteria suggestive of malignancy are a large mass diameter (≥ 4 cm), bilaterality, the mass consists mainly of a solid portion, necrosis in the solid portion, the mass is cystic with a wall or septum ≥ 3 mm, and papillary mural nodules. Possible secondary findings include ascites, intraperitoneal dissemination, and lymph node swelling. The morphological findings that are thought to contribute the most to a diagnosis of malignancy are necrosis in the solid portion and mural nodules in a cystic mass.[3, 7)] An examination of signal patterns indicated that a finding of hypointensity in the solid portion of a mass at a level comparable to that of skeletal muscle on T2-weighted imaging suggested a benign fibrotic tumor. Moreover, a finding of hypointensity in the solid portion of a mass on diffusion-weighted imaging, which subsequently became widely available, was found to suggest a benign mass.[8)] On the other hand, hyperintensity of the solid portion on diffusion-weighted imaging suggests a malignant lesion. It should be noted, however, that even for benign lesions, the signal can increase for a lesion with a prolonged T2 value resulting from a change such as edema (T2 shine-through effect). In addition, hyperintensity may be seen in lesions such as thecomas, which have a relatively high cell density, potentially restricting diffusion. Although ADC values tend to be low, in adnexal masses that are malignant tumors, they may also be decreased in benign fibrotic tumors. On the other hand, ADC values tend to be increased in malignant tumors with necrosis or microcysts. Consequently, there is overlap in ADC values

between benign and malignant masses. In meta-analyses of the use of ADC values to differentiate between benign and malignant adnexal masses, a 2016 examination that included both the cystic and solid portions of masses found no significant differences.[9] However, a 2018 investigation that limited its scope to the solid portion of masses suggested that ADC values were useful, with sensitivity, specificity, and AUC values of 91%, 91%, and 0.96, respectively.[10]

In patients for whom benign-malignant differentiation is difficult with non-contrast MRI, including diffusion-weighted imaging, diagnostic accuracy is improved by the use of contrast-enhanced imaging.[3, 11] Consequently, contrast-enhanced MRI is recommended for patients without contraindications. Analysis of the time-intensity curve (TIC) in dynamic MRI has also been used for benign-malignant differentiation. The addition of diffusion-weighted imaging or dynamic MRI to conventional MRI has been found to improve the diagnostic accuracy rate to 95%.[11] Moreover, an effort to standardize diagnostic imaging (ultrasound and MRI) for the differentiation of benign and malignant adnexal masses called the Ovarian-Adnexal Reporting and Data Systems (O-RADS) has been underway since 2015, implemented mainly by the American College of Radiology (ACR). The results of a multicenter study of the MRI version (prospective cohort study), which is based on the scoring system using the characteristics of masses and TIC patterns and the signals of T2-weighted images and diffusion-weighted images of the solid portion of masses, were reported in 2020. When interpreted by skilled radiologists, they showed good diagnostic performance, with sensitivity, specificity, and AUC values of 93%, 91%, and 0.961, respectively.[12]

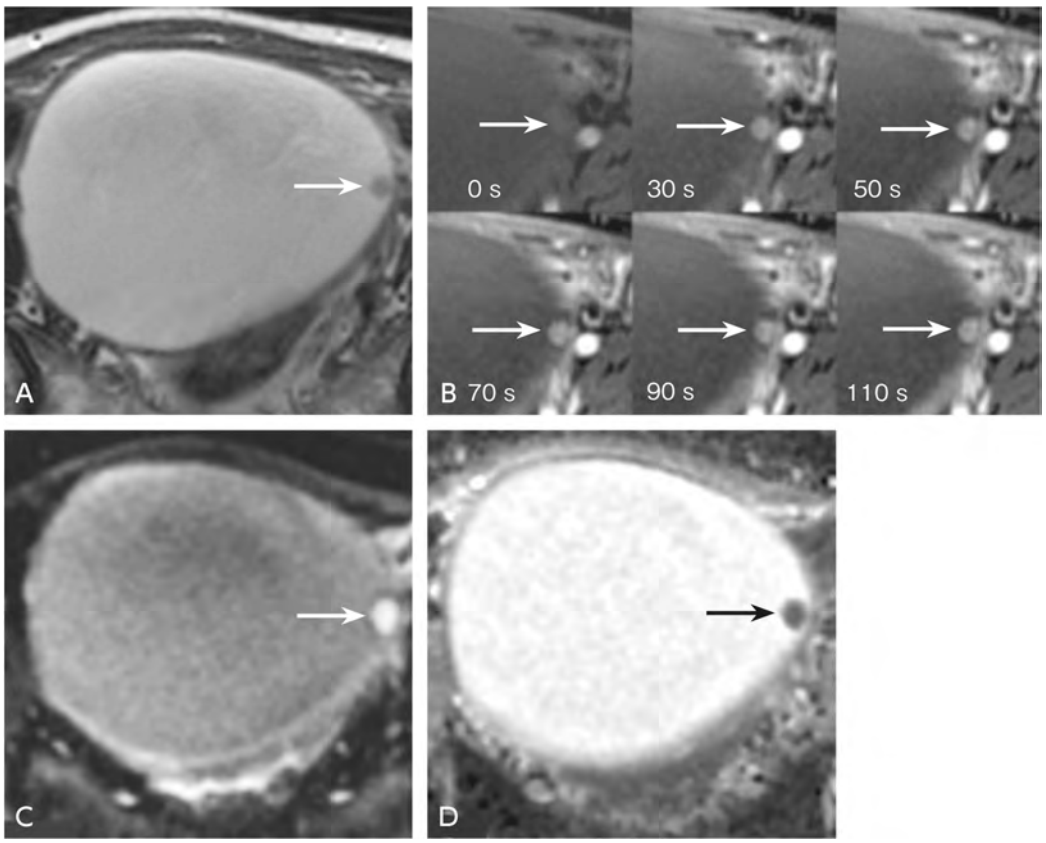

Figure　Ovarian clear cell carcinoma (woman in her 30s)

A: MRI, T2-weighted image: A unicameral cystic mass is seen in the ovary. A mural nodule that shows slight hyperintensity (→) is seen.

B: Dynamic MRI: The nodule shows enhancement that begins in the early phase and continues to the late phase.

C: MRI, diffusion-weighted image, b-value = 800 s/mm^2: The mural nodule shows strong hyperintensity.

D: MRI, ADC map: The mural nodule shows hypointensity.

Search keywords and secondary sources used as references

PubMed was searched using the following keywords, and further selections were made from the results: ovary, ovarian, adnexa, adnexal, and MRI.

In addition, the following was referenced as a secondary source.

1) Forstner R et al: ESUR recommendations for MR imaging of the sonographically indeterminate adnexal mass: an update. Eur Radiol 27: 2248-2257, 2017

References

1) Zhang X et al: Diagnostic accuracy of transvaginal ultrasound examination for assigning a specific diagnosis to adnexal masses: a meta-analysis. Exp Ther Med 20: 265, 2020
2) Yamashita Y et al: Adnexal masses: accuracy of characterization with transvaginal US and precontrast and postcontrast MR imaging. Radiology 194: 557-565, 1995
3) Hricak H et al: Complex adnexal masses: detection and characterization with MR imaging: multivariate analysis. Radiology 214: 39-46, 2000
4) Sohaib SA et al: Characterization of adnexal mass lesions on MR imaging. AJR Am J Roentgenol 180: 1297-1304, 2003
5) Bazot M et al: MR imaging compared with intraoperative frozen-section examination for the diagnosis of adnexal tumors; correlation with final histology. Eur Radiol 16: 2687-2699, 2006
6) Medeiros LR et al: Accuracy of magnetic resonance imaging in ovarian tumor: a systematic quantitative review. Am J Obstet Gynecol 204 (67): e1-10, 2011
7) Stevens SK et al: Ovarian lesions: detection and characterization with gadolinium-enhanced MR imaging at 1.5 T. Radiology 181: 481-488, 1991
8) Thomassin-Naggara I et al: Contribution of diffusion-weighted MR imaging for predicting benignity of complex adnexal masses. Eur Radiol 19: 1544-1552, 2009
9) Kim HJ et al: The value of diffusion-weighted imaging in the differential diagnosis of ovarian lesions: a meta-analysis. PLoS One 11: e0149465, 2016
10) Pi S et al: Utility of DWI with quantitative ADC values in ovarian tumors: a meta-analysis of diagnostic test performance. Acta Radiol 59: 1386-1394, 2018
11) Thomassin-Naggara I et al: Characterization of complex adnexal masses: value of adding perfusion- and diffusion-weighted MR imaging to conventional MR imaging. Radiology 258: 793-803, 2011
12) Thomassin-Naggara I et al: Ovarian-Adnexal Reporting Data System Magnetic Resonance Imaging (O-RADS MRI) score for risk stratification of sonographically indeterminate adnexal masses. JAMA Netw Open 3: e1919896, 2020

FQ 10 Is MRI recommended to diagnose incidental adnexal masses?

Statement

MRI is recommended for simple-appearing cysts larger than 10 cm, masses suspected of being malignant, hemorrhagic cysts in postmenopausal women, and masses with an uncertain diagnosis.

Background

Adnexal masses are frequently detected incidentally on CT or MRI. Although most are benign, they must be managed appropriately because of the high mortality rate of ovarian cancer. This discussion reviews the evidence concerning the types of incidental adnexal masses for which MRI is recommended.

Explanation

The guidelines of the Society of Radiologists in Ultrasound (SRU) advocate managing simple adnexal cysts based on ultrasound, whereas the white paper of the American College of Radiology (ACR) recommends the management of adnexal masses incidentally detected on CT and MRI. The flowchart based on these recommendations is shown in the figure.

The flowchart is based on the morphology and size of adnexal masses and menopausal status.

Morphology of adnexal masses is divided into 3 categories, “simple-appearing cyst”, “mass with characteristic features allowing presumptive diagnosis” and “mass with uncertain diagnosis”.

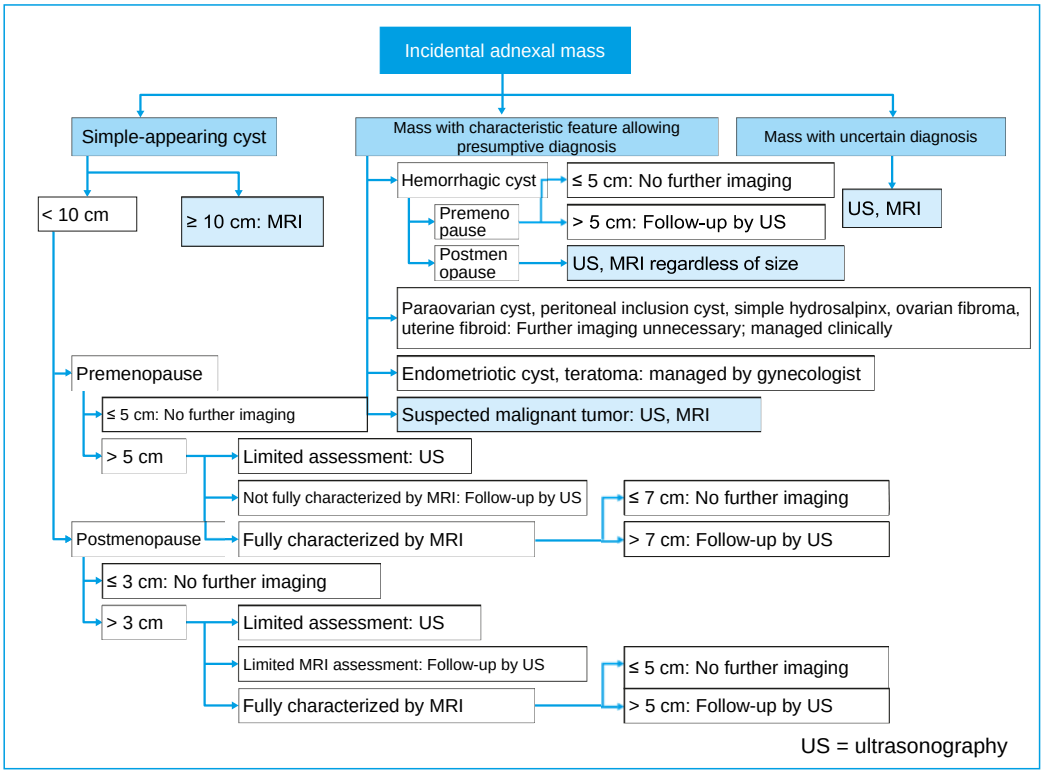

Figure Flow chart for managing incidental adnexal masses (prepared based on secondary source 1, 2)

A simple-appearing cyst is a round or oval anechoic fluid collection with a smooth thin wall and no solid component or septation. Most simple-appearing cysts are functional or non-neoplastic cysts; 14% to 20% of postmenopausal women have simple-appearing cysts, so they are not rare even in the postmenopausal period.[1, 2)] Spontaneous cyst resolution was seen in 82% of premenopausal cases and 44% to 69.4% of postmenopausal cases.[3-5)] Premenopausal cysts ≤ 3 cm in size are considered normal ovarian follicles, and postmenopausal cysts ≤ 1 cm in size are considered normal. Premenopausal cysts ≤ 5 cm in size and postmenopausal cysts ≤ 3 cm in size are mere existence and do not require follow-up. The management of premenopausal cysts > 5 cm and ≤ 7 cm in size and postmenopausal cysts > 3 cm and ≤ 5 cm in size differs according to the degree of certainty in characterizing them as simple-appearing cysts. “Evaluation inadequate” refers to poor image quality or non-contrast-enhanced imaging. “Fully characterized by MRI” refers to an incidental adnexal mass characterized by the following three elements: T2-weighted images; pre- and postcontrast T1-weighted images; and complete anatomic coverage of the mass in at least two image planes. For simple-appearing cysts > 7 cm (premenopausal) and > 5 cm (postmenopausal) sonographic follow-up is recommended. The ACR recommends a follow-up interval of 6 to 12 months. During this period, if the mass is shrinking, no follow-up is required, but if the mass grows, favoring neoplasm, but there is no evidence. For adnexal masses with diameters of 10 cm or larger, characterization by MRI is recommended because ultrasound may have limitations because of the size of the mass.

“Masses with characteristic features allowing presumptive diagnosis” are a group that are characteristic or highly suggestive of particular diagnostic entities by CT and MRI.[5] Most hemorrhagic cysts smaller than 5 cm in premenopausal women are corpus luteum cysts or functional cysts with hemorrhage, so imaging follow-up is not recommended, but for those larger than 5 cm in premenopausal women, sonographic follow-up is recommended. In postmenopausal women, sonographic or MRI follow-up is recommended, regardless of size.

Because endometriotic cysts and teratomas carry a risk of malignant transformation, they should be managed by a gynecologist. Masses suspected of being malignant require further examination by sonography or MRI (see BQ66).

A “mass with uncertain diagnosis” is a mass other than those described above. Ultrasound is required for further characterization, but there may be instances in which MRI is preferred. (see BQ66).

The management of simple-appearing cysts was revised in 2019. A recent study showed no increased risk of malignancy in women with simple-appearing cysts irrespective of cyst size. Unnecessary follow-up is not only a waste of time and money, but it also increases surgical intervention and, thereby, unintended harm.[6-8] Moreover, invasive ovarian serous adenocarcinoma is now known to primarily arise from solid precursors in the fallopian tubes, and simple-appearing cysts are not precursors to ovarian carcinoma.[9] Consequently, the revised recommendations have an increased size threshold for surveillance. It should be noted that this approach is limited to confidently characterized, simple-appearing cysts. If the mass has not been fully characterized, it should be evaluated by ultrasound and MRI. Contrast-enhanced MRI provides high specificity in determining that a mass is benign and should therefore be performed unless contraindicated.[10] Moreover, though the risk of malignancy is considered very low for simple-appearing cysts regardless of their size, their management varies depending on their size. SRU indicates that larger cyst size likely increases the possibility of mischaracterization, but there is no evidence regarding size. The Guideline for Gynecological Practice in Japan (2017 edition) states that, because of the increased risk of torsion with masses > 6 cm in size, regardless of whether the patient is pre- or postmenopausal, they should be managed by a gynecologist. That recommendation is on the basis of limited scientific evidence and depends on the expert’s opinion, so individual management is required to take into account the patient’s circumstances and background.

Search keywords and secondary sources used as references

PubMed was searched using the following keywords, and further selections were made from the results: ovary, ovarian, adnexa, adnexal, incidental, incidentaloma, asymptomatic, US, ultrasound, ultrasonography, CT, computed tomography, MRI, and magnetic resonance imaging.

In addition, the following were referenced as secondary sources.

1) Levine D et al: Simple adnexal cysts: SRU consensus conference update on follow-up and reporting. Radiology 293: 359-371, 2019
2) Patel MD: Management of incidental adnexal findings on CT and MRI: a white paper of the ACR incidental findings committee. J Am Coll Radiol 17: 248-254, 2020
3) Japan Society of Obstetrics and Gynecology and Japan Association of Obstetricians and Gynecologists, Ed.: 2017 Guideline for Gynecological Practice. Japan Society of Obstetrics and Gynecology, 2017.

References

1) Healy DL et al: Ovarian status in healthy postmenopausal women. Menopause 15: 1109-1114, 2008
2) Patel MD et al: Managing incidental findings on abdominal and pelvic CT and MRI, part 1: white paper of the ACR incidental findings committee II on adnexal findings. J Am Coll Raiol 10: 675-681, 2013
3) Borgfeldt. C et al: Transvaginal sonographic ovarian findings in a random sample of women 25-40 years old. Ultrasound Obstet Gynecol 13: 345-350, 1999
4) Modesitt SC et al: Risk of malignancy in unilocular ovarian cystic tumor less than 10 centimeters in diameter. Obstet Gynecol 102: 594-599, 2003
5) Castillo G et al: Natural history of sonographically detected simple unilocular adnexal cysts in asymptomatic postmenopausal women. Gynecol Oncol 92: 965-969, 2004
6) Greenlee RT et al: Prevalence, incidence and natural history of simple ovarian cysts among women over age 55 in a large cancer screening trial. Am J Obstet Gynecol 202: 373 e1-9, 2010
7) Smith-Bindman R et al: Risk of malignant ovarian cancer based on ultrasonography findings in a large unselected population. JAMA Intern Med 179: 71-78, 2019
8) Sharma A et al: Assessing the malignant potential of ovarian inclusion cysts in postmenopausal women within the UK Collaborative Trial of Ovarian cancer Screening (UKCTOCS): a prospective cohort study. BJOG 119: 207-219, 2012
9) Erickson BK et al: The role of the fallopian tube in the origin of ovarian cancer. Am J Obstet Gynecol. 209: 409-414, 2013
10) Anthoulakis C et al: Pelvic MRI as the “golden standard” in the subsequent evaluation of ultrasound-indeterminate adnexal lesions: a systematic review. Gynecol Oncol 132: 661-668, 2014

BQ 67 Is contrast-enhanced CT recommended for evaluating metastases when staging gynecological malignancies?

Statement

Contrast-enhanced CT is recommended because of the wide scanning range, high accessibility, and relatively high diagnostic performance for the staging of gynecological malignancies.

Background

The diagnosis of lymph node metastases and peritoneal dissemination is important in the evaluation of metastases from gynecological malignancies. Accurate diagnosis of these changes provides significant information not only for staging, but also for planning appropriate therapeutic treatment. Contrast-enhanced CT provides a wide scanning range and is particularly readily accessible in Japan. It is widely used to evaluate metastases from gynecological malignancies, and its usefulness for this purpose has been established in routine clinical practice. This discussion provides an overview of the usefulness of contrast-enhanced CT in evaluating metastases of cervical cancer, endometrial cancer, and ovarian cancer, which are common gynecological malignancies.

Explanation

The evaluation of lymph node metastasis is important for the staging of cervical, endometrial, and ovarian cancer. In particular, lymph node metastasis can be diagnosed by imaging according to the revised classification of the International Federation of Gynecological and Obstetrics (FIGO, secondary source 1) and the Japanese General Rules for Clinical Management (secondary source 2) of Cervical Cancer (stage IIIC).

Contrast-enhanced CT plays a certain role in the diagnosis of lymph node metastases of cervical cancer. A meta-analysis demonstrated that CT yielded a sensitivity and specificity of 50% and 92%, respectively, in evaluating lymph node metastases of cervical cancer, but its diagnostic performance was significantly lower than that of FDG-PET (“PET” below) and PET/CT.[1)] On the other hand, a more recent meta-analysis showed a sensitivity and specificity of 59% and 91%, respectively, with no significant differences compared with PET and PET/CT.[2)] A recent large, multicenter, controlled study found that the sensitivity and specificity of contrast-enhanced CT for lymph node metastases were 77% and 63%, respectively, which did not differ significantly from the results for PET/CT (sensitivity, 81%; specificity, 69%).[3)] The positivity criteria for lymph nodes in that study were as follows: A lymph node was considered positive on CT if the short axis was > 8 mm for a node with a short axis more than half the length of the long axis, and > 10 mm for a node with a short axis less than half the length of the long axis.

Regarding endometrial cancer, a meta-analysis revealed that the sensitivity and specificity of CT for lymph node metastases were 45% and 88%, respectively (no analysis for PET/CT).[4)] A recent meta-analysis

found that the sensitivity and specificity of CT were 44% and 93%, respectively.[5] The sensitivity and specificity of PET/CT were 67% and 91%, respectively, but no information about significant differences was provided. A large, multicenter, comparative study showed that the sensitivity and specificity of contrast-enhanced CT were 54% and 85%, respectively (same diagnostic criteria as used in reference 3), with no significant differences compared with the results for PET/CT (sensitivity, 63%; specificity, 83%).[6]

With regard to the lymph node metastases of ovarian cancer, a meta-analysis reported diagnosis with a sensitivity and specificity of 42.6% and 95%, respectively; the sensitivity and specificity of PET and PET/CT were 73.2% and 96.7%, respectively, with the sensitivity being significantly higher than that of CT.[7]

In view of these results, as well as the fact that CT is a readily accessible modality, contrast-enhanced CT is recommended particularly to evaluate lymph node metastases of cervical and endometrial cancer.

Peritoneal dissemination is observed mainly in ovarian cancer, and many of the articles about peritoneal dissemination involved investigations of ovarian cancer. Consequently, the following discussion concerns ovarian cancer. In a multicenter study of ovarian cancer staging, the sensitivity and specificity of CT for detecting peritoneal dissemination were 92% and 82%, respectively, on a per-patient basis. However, the detection performance of CT was poor for small lesions $\leq$ 2 cm in size.[8] The sensitivity and specificity on a per-site basis were 65% and 82%, respectively. Meanwhile, the sensitivity for dissemination to the serosa of the small intestine and colon was poor, at 17% and 45%, respectively.[9] Although peritoneal dissemination in several sites is not easily detected on contrast-enhanced CT, the use of contrast-enhanced CT is recommended to evaluate peritoneal dissemination because current CT examinations are usually performed using MDCT, which provides a wide scanning range and facilitates the generation of reconstructed sagittal and coronal images. In Europe and the United States, contrast-enhanced CT for the evaluation of peritoneal dissemination is often performed using an oral contrast medium. Because oral contrast media are not widely used in Japan, it should be noted that the diagnostic performance may actually be even lower in Japan than the reported diagnostic performance.

Diffusion-weighted MR imaging has been found to be useful and even superior to contrast-enhanced CT and PET/CT for detecting peritoneal dissemination and distant metastases.[9] It therefore needs to be discussed as an imaging method to consider when evaluating peritoneal dissemination and distant metastases.

Because remote metastasis such as pulmonary metastasis occurs with these gynecological cancers, CT scan from the chest to the pelvic region is increasingly being performed in routine clinical practice. Although it is difficult to stipulate scan ranges for contrast-enhanced CT, the ACR Appropriateness Criteria® indicate that chest CT may be appropriate for cervical cancer beyond stage IB (secondary source 3) and is also usually appropriate for endometrial cancer in high-risk groups (secondary source 4). For staging ovarian cancer, the guidelines indicate that imaging of both the abdominopelvic region and the area from the chest to the pelvic region is usually appropriate (secondary source 5). For endometrial cancer, the recommendation grades of the ACR Appropriateness Criteria® differ depending on the preoperative risk of

metastasis. Perhaps in Japan as well, rather than uniformly performing preoperative examinations, stratification according to risk level should be considered.

Search keywords and secondary sources used as references

PubMed was searched using the following keywords: gynecology, cervical cancer, endometrial cancer, ovarian cancer, metastasis, lymph nodes, peritoneal dissemination, staging, and CT.

In addition, the following were referenced as secondary sources.

1) Bhatla N et al: Cancer of the cervix uteri. Int J Gynecol Obstet 143 S2: 22-36, 2018
2) Japan Society of Obstetrics and Gynecology, et al., Ed.: The General Rules for Clinical and Pathological Management of Uterine Cervical Cancer: Clinical Edition (4th Edition). KANEHARA & Co., 2020.
3) Siegel CL et al: ACR Appropriateness Criteria®: pretreatment planning of invasive cancer of the cervix. J Am Coll Radiol 9: 395-402, 2012
4) Reinhold C et al: ACR Appropriateness Criteria®: pretreatment evaluation and follow up of endometrial cancer. J Am Coll Radiol 17: S472-S486, 2020
5) Kang SK et al: ACR Appropriateness Criteria®: staging and follow-up of ovarian cancer. J Am Coll Radiol 15: S198-S207, 2020

References

1) Choi HJ et al: Diagnostic performance of computer tomography, magnetic resonance imaging, and positron emission tomography or positron emission tomography/computer tomography for detection of metastatic lymph nodes in patients with cervical cancer: meta-analysis. Cancer Sci 101: 1471-1479, 2010
2) Liu B et al: A comprehensive comparison of CT, MRI, positron emission tomography or positron emission tomography/CT, and diffusion weighted imaging-MRI for detecting the lymph nodes metastases in patients with cervical cancer: a meta-analysis based on 67 studies. Gynecol Obstet Invest 82: 209-222, 2017
3) Atri M et al: Utility of PET-CT to evaluate retroperitoneal lymph node metastasis in advanced cervical cancer: Results of ACRIN6671/GOG0233 trial. Gynecol Oncol 142: 413-419, 2016
4) Selman TJ et al: A systematic review of tests for lymph node status in primary endometrial cancer. BMC Women's Health 8: 8, 2008
5) Reijnen C et al: Diagnostic accuracy of clinical biomarkers for preoperative prediction of lymph node metastasis in endometrial carcinoma: a systematic review and meta-analysis. Oncologist 9: e880-e890, 2019
6) Atri M et al: Utility of PET/CT to evaluate retroperitoneal lymph node metastasis in high-risk endometrial cancer: results of ACRIN 6671/GOG 0233 trial. Radiology 283: 450-459, 2017
7) Yuan Y et al: Computer tomography, magnetic resonance imaging, and positron emission tomography or positron emission tomography/computer tomography for detection of metastatic lymph nodes in patients with ovarian cancer: a meta-analysis. Eur J Radiol 81: 1002-1006, 2012
8) Tempany CM et al: Staging of advanced ovarian cancer: comparison of imaging modalities: report from the radio logical diagnostic oncology group. Radiology 215: 761-767, 2000
9) Michielsen K et al: Whole-body MRI with diffusion-weighted sequence for staging of patients with suspected ovarian cancer: a clinical feasibility study in comparison to CT and FDG-PET/CT. Eur Radiol 24: 889-901, 2014

CQ 16 Is the addition of FDG-PET/CT to diagnostic CT with IV contrast recommended for staging or re-staging in gynecological malignancies?

Recommendation

The addition of FDG-PET/CT to contrast-enhanced CT has the advantage of improving diagnostic accuracy, but radiation exposure needs to be considered. It is known that FDG-PET/CT is a minimally invasive procedure without marked adverse events, sometimes providing clinically relevant additional information for therapeutic strategies. Therefore, the addition of FDG-PET/CT to diagnostic CT with IV contrast is weakly recommended for detecting metastatic or recurrent lesions.

Recommendation strength: 2, strength of evidence: weak (C), agreement rate: 94% (17/18)

Background

In Japan, CT with IV contrast is routinely performed to detect lymph node metastases, intraperitoneal dissemination, and distant metastases for initial staging or re-staging after treatment for gynecological malignancies. The efficacy of contrast-enhanced CT has already been established in routine clinical practice, and the clinical usefulness of FDG-PET/CT has also been reported (Figure). To examine whether the addition of FDG-PET/CT has an add-on effect compared with contrast-enhanced CT alone and to determine a recommendation grade, this topic was specified as a CQ, and a systematic review was conducted. The subject of the review was diagnostic accuracy in screening for lymph node metastases, intraperitoneal dissemination, and distant metastases in the initial staging and re-staging after treatment of typical gynecological malignancies, such as ovarian cancer, cervical cancer, and endometrial cancer.

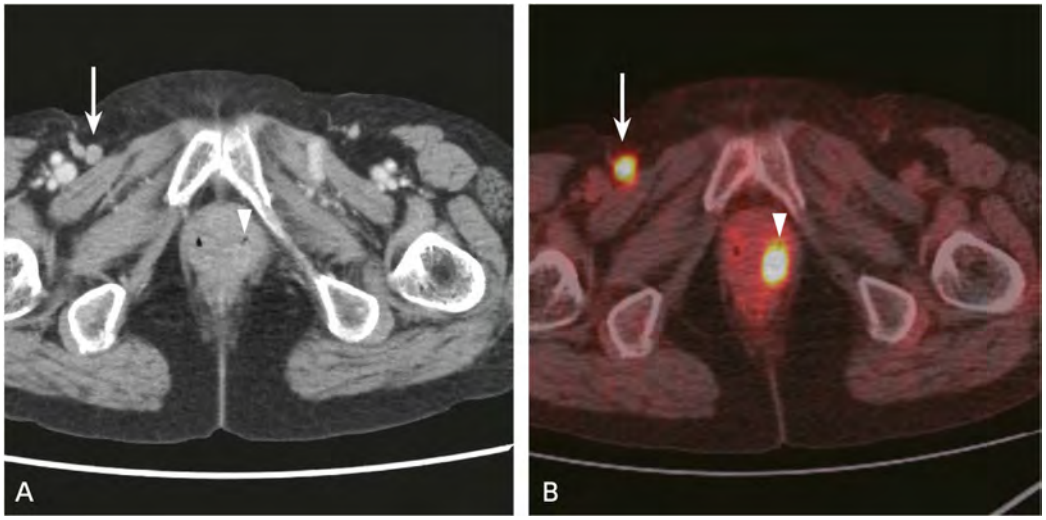

Figure　A postoperative case of endometrial cancer where FDG-PET/CT shows a nodal metastasis and local recurrence, for which contrast-enhanced CT provided inconclusive findings.

A: Contrast-enhanced CT; B: FDG-PET/CT

The patient was a woman in her 70s. Focal intense uptake is seen in a right inguinal lymph node (B →) and to the left side of the vaginal stump (B ▷), suggesting nodal metastasis and local recurrence, respectively. Neither had been identified on prior contrast-enhanced CT because the right inguinal node was < 1 cm in diameter (A →), and contrast of the recurrent tumor was weak (A ▷). The former lesion later enlarged, indicating a nodal metastasis, and the latter was histologically confirmed to be a recurrence.

Explanation

A literature search was conducted using the keywords indicated below, and articles were extracted in primary and secondary screenings. For ovarian cancer, one report of a nonrandomized, controlled study[1)] and 18 reports of observational studies (all cross-sectional studies)[2-19)] were extracted. Concerning cervical and endometrial cancers, two reports of nonrandomized, controlled studies[20, 21)] and three reports of observational studies (all cross-sectional studies)[22-24)] were extracted. These reports were then used in a qualitative systematic review. The plan was to compare two groups of studies, Group (A), in which assessments were performed with contrast-enhanced CT alone, and Group (B), in which assessments were performed with contrast-enhanced CT plus FDG-PET/CT. Studies of assessments by PET/CT alone (contrast-enhanced CT not included) were also included in Group (B). In addition, in evaluating the combination of contrast-enhanced CT and FDG-PET/CT in Group (B), whether fused images between contrast-enhanced CT and FDG-PET were available was not considered important. In the systematic review, the following aspects were considered first as outcomes: initial diagnostic performance (sensitivity, specificity, and accuracy), the contribution to the treatment plan, and the reduction in unnecessary tests (healthcare economics and patient burden). However, since there was a limited amount of articles demonstrating the contribution of treatment plans and the avoidance of unnecessary tests, only diagnostic performance was evaluated as an outcome.

The extracted studies on ovarian cancer were inconsistent in terms of population and methods because some focused on detecting only peritoneal metastasis, nodal metastasis, and recurrence. Overall, the diagnostic accuracy rate ranged from 56.9% to 96.7% for contrast-enhanced CT alone [pooled accuracy, 82.4% (95% CI, 80.3% to 84.2%)] and from 63.8% to 97.1% for contrast-enhanced CT plus FDG-PET/CT [pooled accuracy, 92.2% (95% CI, 90.7% to 93.5%)]. The diagnostic accuracy of contrast-enhanced CT plus FDG-PET/CT tended to be higher than that of contrast-enhanced CT alone. In most studies that performed statistical analyses (5/6), the diagnostic accuracy of contrast-enhanced CT plus FDG-PET/CT was statistically significantly superior.

The extracted studies of cervical and endometrial cancers, like those of ovarian cancer, were also inconsistent in populations and methods. Two studies were for cervical cancer plus endometrial cancer, two examined cervical cancer alone, and one examined endometrial cancer alone. The overall sample size for each type of cancer was small. In addition, the articles that examined both cervical and endometrial cancers were from the same hospital in Japan, suggesting possible bias. The diagnostic accuracy ranged from 77.8% to 87.0% [pooled accuracy, 81.3% (95% CI, 77.0% to 86.8%)] for CT alone and from 82.9% to 95.0% [pooled accuracy, 87.8% (95% CI, 89.3% to 96.3%)] for contrast-enhanced CT plus FDG-PET/CT. In studies with statistical analysis (3/5), the diagnostic accuracy or AUC of contrast-enhanced CT plus FDG-PET/CT was found to be statistically significantly superior. Thus, the studies showed that, as a method of improving accuracy in diagnosing metastases and recurrence of ovarian, cervical, and endometrial cancers, adding FDG-PET/CT to contrast-enhanced CT is clinically significant.

On the other hand, both contrast-enhanced CT and FDG-PET/CT are examinations associated with radiation exposure and relatively higher medical cost. Moreover, the availability of FDG-PET/CT examinations differs among regions. Therefore, performing PET/CT examinations for all cases everywhere is challenging. Nevertheless, the 2018 edition of the FIGO classification (secondary source 5) and Japan's General Rules for Clinical and Pathological Management of Uterine Cervical Cancer (4th edition, secondary source 6) indicate that cervical cancer metastases can be assessed by diagnostic imaging (stage IIICr). Consequently, the number of opportunities for detailed examination that includes FDG-PET/CT to improve diagnostic accuracy may increase.

The above considerations indicate that adding FDG-PET/CT to contrast-enhanced CT is helpful to a certain extent for increasing diagnostic accuracy in staging and re-staging for ovarian, cervical, and endometrial cancers, based on some investigations, although their evidence level was not very high. It is, therefore, weakly recommended in response to this CQ.

Search keywords and secondary sources used as references

PubMed was searched using the following keywords: FDG, CT, enhanced CT, cervical cancer, endometrial cancer, ovarian cancer, gynecological malignancies, sensitivity specificity, and uterine cancer.

In addition, the following were referenced as secondary sources.

1) Siegel CL et al: ACR Appropriateness Criteria®: pretreatment planning of invasive cancer of the cervix. J Am Coll Radiol 9: 395-402, 2012
2) Kang SK et al: ACR Appropriateness Criteria®: staging and follow-up of ovarian cancer. J Am Coll Radiol 15: S198-S207, 2018
3) Reinhold C et al: ACR Appropriateness Criteria®: pretreatment evaluation and follow-Up of endometrial cancer. J Am Coll Radiol 17: S472-S486, 2020
4) Survey of Medical Institutions [2017 Survey of Medical Institutions (static and dynamic surveys), Ministry of Health, Labour and Welfare]
5) Bhatla N et al: FIGO cancer report 2018: cancer of the cervix uteri. Int J Gynaecol Obstet 143 (S2): 22-36, 2018
6) Japan Society of Obstetrics and Gynecology, et al., Ed.: The General Rules for Clinical and Pathological Management of Uterine Cervical Cancer: Clinical Edition (4th Edition). KANEHARA & Co., 2020.

References

1) Hynninen J et al: A prospective comparison of integrated FDG-PET/contrast-enhanced CT and contrast-enhanced CT for pretreatment imaging of advanced epithelial ovarian cancer. Gynecol Oncol 131 (2): 389-394, 2013
2) Rubini G et al: Role of 18F-FDG PET/CT in diagnosing peritoneal carcinomatosis in the re-staging of patient with ovarian cancer as compared to contrast enhanced CT and tumor marker Ca-125. Rev Esp Med Nucl Imagen Mol 33 (1): 22-27, 2014
3) Kim HW et al: Peritoneal carcinomatosis in patients with ovarian cancer: enhanced CT versus 18F-FDG PET/CT. Clin Nucl Med 38 (2): 93-97, 2013
4) Kitajima K et al: Performance of integrated FDG-PET/contrast-enhanced CT in the diagnosis of recurrent ovarian cancer: comparison with integrated FDG-PET/non-contrast-enhanced CT and enhanced CT. Eur J Nucl Med Mol Imaging 35 (8): 1439-1448, 2008
5) Tawakol A et al: Diagnostic performance of 18F-FDG PET/contrast-enhanced CT versus contrast-enhanced CT alone for post-treatment detection of ovarian malignancy. Nucl Med Commun 37 (5): 453-460, 2016
6) Kitajima K et al: Diagnostic accuracy of integrated FDG-PET/contrast-enhanced CT in staging ovarian cancer: comparison with enhanced CT. Eur J Nucl Med Mol Imaging 35 (10): 1912-1920, 2008
7) Sari O et al: The role of FDG-PET/CT in ovarian cancer patients with high tumor markers or suspicious lesion on contrast-enhanced CT in evaluation of recurrence and/or in determination of intraabdominal metastases. Rev Esp Med Nucl Imagen Mol 31 (1): 3-8, 2012
8) Lee YJ et al: Diagnostic value of integrated ^{18}F-fluoro-2-deoxyglucose positron emission tomography/computed tomography in recurrent epithelial ovarian cancer: accuracy of patient selection for secondary cytoreduction in 134 patients. J Gynecol Oncol 29 (3): e36, 2018
9) Nasu K et al: Impact of positron emission tomography/computed tomography in the management of patients with epithelial ovarian carcinoma after treatment. Arch Gynecol Obstet 283 (5): 1121-1126, 2011
10) Mangili G et al: Integrated PET/CT as a first-line re-staging modality in patients with suspected recurrence of ovarian cancer. Eur J Nucl Med Mol Imaging 34 (5): 658-666, 2007
11) Gadducci A et al: Positron emission tomography/computed tomography in platinum-sensitive recurrent ovarian cancer: a single-center Italian study. Anticancer Res 40 (4): 2191-2197, 2020
12) Bhosale P et al: Clinical utility of positron emission tomography/computed tomography in the evaluation of suspected recurrent ovarian cancer in the setting of normal CA-125 levels. Int J Gynecol Cancer 20 (6): 936-944, 2010
13) Schmidt S et al: Peritoneal carcinomatosis in primary ovarian cancer staging: comparison between MDCT, MRI, and 18F-FDG PET/CT. Clin Nucl Med 40 (5): 371-327, 2015
14) Bilici A et al: Clinical value of FDG PET/CT in the diagnosis of suspected recurrent ovarian cancer: is there an impact of FDG PET/CT on patient management? Eur J Nucl Med Mol Imaging 37 (7): 1259-1269, 2010
15) Cho SM et al: Usefulness of FDG PET for assessment of early recurrent epithelial ovarian cancer. AJR Am J Roentgenol 179 (2): 391-395, 2002
16) Sala E et al: Recurrent ovarian cancer: use of contrast-enhanced CT and PET/CT to accurately localize tumor recurrence and to predict patients' survival. Radiology 257 (1): 125-134, 2010
17) Lopez-Lopez V et al: Use of (18) F-FDG PET/CT in the preoperative evaluation of patients diagnosed with peritoneal carcinomatosis of ovarian origin, candidates to cytoreduction and hipec: a pending issue. Eur J Radiol 85 (10): 1824-1828, 2016

18) Abdelhafez Y et al: Role of 18F-FDG PET/CT in the detection of ovarian cancer recurrence in the setting of normal tumor markers. Egypt J Radiol Nucl Med 47: 1787-1794, 2016
19) Michielsen K et al: Whole-body MRI with diffusion-weighted sequence for staging of patients with suspected ovarian cancer: a clinical feasibility study in comparison to CT and FDG-PET/CT. Eur Radiol 24 (4): 889-901, 2014
20) Atri M et al: Utility of PET-CT to evaluate retroperitoneal lymph node metastasis in advanced cervical cancer: results of ACRIN6671/GOG0233 trial. Gynecol Oncol 142 (3): 413-419, 2016
21) Atri M et al: Utility of PET/CT to evaluate retroperitoneal lymph node metastasis in high-risk endometrial cancer: results of ACRIN 6671/GOG 0233 trial. Radiology 283 (2): 450-459, 2017
22) Kitajima K et al: Performance of integrated FDG-PET/contrast-enhanced CT in the diagnosis of recurrent uterine cancer: comparison with PET and enhanced CT. Eur J Nucl Med Mol Imaging 36 (3): 362-372, 2009
23) Kitajima K et al: Low-dose non-enhanced CT versus full-dose contrast-enhanced CT in integrated PET/CT studies for the diagnosis of uterine cancer recurrence. Eur J Nucl Med Mol Imaging 37 (8): 1490-1498, 2010
24) Jung W et al: Value of imaging study in predicting pelvic lymph node metastases of uterine cervical cancer. Radiat Oncol J 35 (4): 340-348, 2017
25) Meads C et al: Positron emission tomography/computerised tomography imaging in detecting and managing recurrent cervical cancer: systematic review of evidence, elicitation of subjective probabilities and economic modelling. Health Technol Assess 17 (12): 1-323, 2013

FQ 11 Does CT or MRI during pregnancy affect the fetus?

Statement

With appropriate control of the imaging range, frequency, and parameters, radiation exposure with CT does not increase the incidence of fetal malformations. Although it slightly increases the frequency of pediatric cancer, the carcinogenic risk is low at the individual level. There have been no reports indicating that non-contrast MRI is harmful for fetuses.

FQ 12 Does contrast medium administration affect the fetus?

Statement

There have been no reports indicating that iodine contrast media for CT are harmful for fetuses. Gadolinium contrast media for MRI may increase the incidence of stillbirth, neonatal mortality, and postnatal inflammatory skin symptoms. CT or MRI, including contrast-enhanced imaging, can be performed if required to determine a treatment plan, there is no safer alternative, and it cannot be deferred until after the end of pregnancy. Contrast-enhanced MRI requires greater caution in determining whether it is indicated.

FQ 13 Is it possible to breast-feed after contrast medium administration?

Statement

There have been no reports of harm to infants resulting from breast-feeding after contrast medium administration. Consequently, unless there is a special reason, there is no need to restrict breast-feeding.

Background

The need may arise to perform CT or MRI during pregnancy, and CT or MRI may be performed without knowledge of a pregnancy. In addition, there may be situations that require that a decision be made during pregnancy or breast-feeding regarding an indication for contrast medium use. This discussion provides an overview regarding the safety of CT, MRI, and contrast medium use during pregnancy and breast-feeding.

Explanation

The effects of radiation on a fetus during pregnancy depend on the timing and dose of exposure. They are divided into deterministic effects with a threshold for impairment (e.g., malformation, mental retardation) and stochastic effects without a threshold (e.g., carcinogenic risk, genetic disorders). If the embryo is exposed to radiation 1 to 2 weeks after fertilization, it will either miscarry or be completely restored, and there is no risk of malformation. If exposure occurs during the organogenesis period between 4 and 10 weeks of pregnancy, the likelihood of teratogenicity increases. If it occurs during the period of brain formation between 10 and 27 weeks (particularly through 17 weeks), the likelihood of a central nervous system disorder increases. However, the threshold is considered to be 100 mGy, and the International Commission on Radiological Protection (ICRP) says that exposure of < 100 mGy should not be considered a reason for pregnancy termination. To ensure safety, the Guideline for Obstetrical Practice in Japan and the guidelines of the American College of Obstetricians and Gynecologists (ACOG) indicate that the permissible dose is 50 mGy. The level of fetal radiation exposure with CT is determined by the imaging range, frequency, and parameters. Under normal conditions, the exposure dose of a single CT imaging procedure does not reach 50 mGy and, therefore, does not result in deterministic effects. However, with multiple abdominopelvic CT imaging procedures (plain and contrast-enhanced CT or multiphase CT), the dose may exceed 50 mGy. Consequently, unless steps are taken to sufficiently reduce exposure, multiple procedures should be avoided. With regard to carcinogenic risk, the incidence of pediatric cancer may increase up to 2-fold even with low-dose exposure.[1-3)] Because spontaneous cancer incidence is inherently very low, carcinogenic risk at the level of the individual has always been low. However, because stochastic effects are proportional to the exposure dose, effort should be made to reduce exposure as much as possible.

There have been no reports indicating that MRI performed using systems of ≤ 3T is harmful to a fetus at any stage of pregnancy,[4, 5)] and the position of the ACR is that MRI can be performed at any stage. However, the Guideline for Obstetrical Practice in Japan indicates that MRI should be performed during or after the 14th week of pregnancy, and safety concerns have been expressed regarding the use of 3T systems.[4)] Thus, adequate consensus has not been reached regarding the safety of testing during the 1st trimester and the use of 3T systems. Consequently, consideration should be given to avoiding such testing when possible.

An adverse event resulting from administration of iodinated contrast agents during pregnancy is neonatal hypothyroidism in neonates following amniotic fluid imaging performed using oil-soluble iodinated contrast agents, which was reported in the 1970s. However, there have been no reports of adverse events with transvenous administration of nonionized iodinated contrast agents.[6, 7)] The European Society of Urogenital Radiology (ESUR) recommends that a thyroid function test be performed in neonates within 1 week after birth if an iodinated contrast agent is used during pregnancy. In Japan, however, this is an item included in the mass screening of neonates and therefore requires no special care.

Adverse events of gadolinium contrast media administration reported in 2016 with contrast-enhanced MRI performed at any stage of pregnancy were increases in the incidence of stillbirth, neonatal mortality, and postnatal rheumatoid skin rash and inflammatory skin symptoms.[4] However, objections have been raised about this study. For example, it has been noted that the relationship to skin disease was significant only in the 1st trimester, that the number of stillbirths and neonatal deaths was small (7 of 397 patients), that the control group consisted of patients who did not undergo MRI rather than patients who underwent non-contrast MRI, and that a linear chelating agent that was distributed during the first half of the study period may have caused the adverse events. Whether macrocyclic chelating agents carry a similar risk is not known. The ACR and ESUR have not designated their use as contraindicated.

As indicated above, effects sufficiently harmful to designate CT and MRI (including the use of contrast media) contraindicated during pregnancy have not been demonstrated. However, the long-term safety of such testing has not been established, and whether it is indicated depends on the degree to which it is needed. That is, after the procedure is explained to the patient, it can be performed if it is necessary to determine a treatment plan, there is no safer alternative, and it cannot be deferred until after the end of pregnancy. It should be explained that miscarriage or preterm labor (15%), malformation (3%), developmental disability (4%), and mental retardation (1%) can occur with no relationship to the test. Examples of indications for (contrast-enhanced) CT are pulmonary thromboembolism and trauma. Although MRI is recommended for acute abdomen, CT is permitted for institutions or time periods in which MRI scanning and interpretation are not available. A common indication for contrast-enhanced MRI is to evaluate malignancies detected during pregnancy. However, a more cautious approach to determining whether it is indicated is required, one that takes the estimated risk into account.

When a contrast agent is administered during breast-feeding, it is absorbed from the intestine of the neonate via the mother’s milk at a level of < 0.01% in the case of an iodinated contrast agent and < 0.0004% in the case of a gadolinium contrast agent. There have been no reports of adverse effects on neonates, and the ACR, ESUR, and Japan Radiological Society have expressed the view that breast-feeding after contrast imaging is likely safe. On the other hand, the package inserts for iodinated and gadolinium contrast agents indicate that breast-feeding should be avoided for a certain period after an agent is administered, which contradicts the position of the academic societies. Theoretically, the possibility of an event such as an allergic reaction cannot be excluded, even with a trace amount of contrast agent. If the patient wishes to restrict breast-feeding after the situation is explained, she is instructed to express and discard breast milk for 24 hours.

Search keywords and secondary sources used as references

PubMed was searched using the following keywords: pregnancy, lactation, CT, MRI, contrast medium, gadolinium, and iodine. Animal studies and observational studies without a control group were excluded.

In addition, the following were referenced as secondary sources.

1) Japan Society of Obstetrics and Gynecology, Japan Association of Obstetricians and Gynecologists, Ed.: Guideline for Obstetrical Practice in Japan 2017. Japan Society of Obstetrics and Gynecology, 2017.
2) ACR committee on drugs and contrast media: ACR manual on contrast media 2020. American College of Radiology, 2020
3) ESUR contrast media safety committee: ESUR guidelines on contrast agents version10.0. European Society of Urogenital Radiology, 2018
4) ACOG committee on obstetric practice: ACOG committee opinion No.723: guidelines for diagnostic imaging during pregnancy and lactation. Obstet Gynecol 130 (4): e210-e216, 2017
5) Wang PI et al: Imaging of pregnant and lactating patients: part 1, evidence-based review and recommendations. AJR Am J Roentgenol 198: 778-784, 2012
6) Wang PI et al: Imaging of pregnant and lactating patients: part 2, evidence-based review and recommendations. AJR Am J Roentgenol 198: 785-792, 2012
7) Masselli G et al: Acute abdominal and pelvic pain in pregnancy: ESUR recommendations. Eur Radiol 23: 3485-3500, 2013
8) Expert panel on MR safety: ACR guidance document on MR safe practices: 2013. J Magn Reson Imaging 37: 531-543, 2013

References

1) Schulze-Rath R et al: Are pre- or postnatal diagnostic X-rays a risk factor for childhood cancer?: a systematic review. Radiat Environ Biophys 47: 301-312, 2008
2) Rajaraman P et al: Early life exposure to diagnostic radiation and ultrasound scans and risk of childhood cancer: case-control study. BMJ 342: d472, 2011
3) Ray JG et al: Major radiodiagnostic imaging in pregnancy and the risk of childhood malignancy: a population-based cohort study in Ontario. PLoS Med 7: e1000337, 2010
4) Ray JG et al: Association between MRI exposure during pregnancy and fetal and childhood outcomes. JAMA 316: 952-961, 2016
5) Chartier AL et al: The safety of maternal and fetal MRI at 3T. AJR Am J Roentgenol 213: 1170-1173, 2019
6) Rajaram S et al: Effect of antenatal iodinated contrast agent on neonatal thyroid function. Br J Radiol 85: e238-242, 2012
7) Kochi MH et al: Effect in utero exposure of iodinated intravenous contrast on neonatal thyroid function. J Comput Assist Tomogr 36: 165-169, 2012

FQ 14 Which imaging examinations are recommended to diagnose acute abdomen in pregnant women?

Statement

Ultrasonography should be performed first to diagnose acute abdomen in pregnant women.
If diagnosis by ultrasonography is difficult, non-contrast MRI is recommended.
CT is considered if diagnosis by ultrasonography and non-contrast MRI proves difficult, MRI cannot be performed, or the advantages of CT outweigh those of MRI. Contrast-enhanced imaging can be performed as needed (see FQ12)

Background

Appendicitis is the most frequent cause of acute abdomen during pregnancy, and diagnostic imaging is often relied upon for its diagnosis. If appendix perforation and panperitonitis occur concomitantly in a pregnant woman, problems such as miscarriage or preterm labor and maternal septicemia increase. Consequently, early diagnosis and treatment are required.

There is no debate regarding the fact that ultrasonography (US) is the first choice for diagnostic imaging of acute abdomen in pregnant women. This discussion provides an overview regarding the safety of CT and MRI as imaging examinations to be performed after US if definitive diagnosis by US proves difficult.

Explanation

The main guidelines are in agreement regarding the order of priority for diagnostic imaging examinations of acute abdomen in pregnant women. US is the first choice, and non-contrast MRI is the second choice if diagnosis by US proves difficult. In addition to this general rule, CT that takes radiation exposure into account can be performed if diagnosis by MRI proves difficult or MRI is difficult to perform due to problems related to factors such as time or the MRI emergency system.

Unlike non-pregnant women, white blood cell count elevation, and nausea and vomiting are frequently seen in pregnant women under normal circumstances, making it difficult to judge whether these findings are abnormal. Moreover, assessing abdominal findings becomes difficult as pregnancy progresses. Organ displacement resulting from exclusion by the enlarging uterus also complicates the diagnosis of acute abdomen in pregnant women. That is why diagnostic imaging plays an important role in acute abdomen during pregnancy.

Although the types of acute abdomen in pregnant women vary, they are broadly divided into 2 categories: gynecological and non-gynecological acute abdomen. Gynecological disease is often diagnosed at the US stage when the gynecologist strongly suspects acute abdomen based on the clinical and US findings. If further testing is needed in addition to US, selecting MRI is appropriate in view of its diagnostic performance. Non-gynecological disease can also often be diagnosed by US alone when a lesion

is easily identified by US despite anatomical displacement, or characteristic findings are seen on blood collection or urinalysis. In that case, no additional imaging examinations are needed. Appendicitis, which is frequently present in acute abdomen in pregnant women and for which the diagnostic performance of US decreases as pregnancy progresses, tends to require additional imaging examinations due to the possibility that it will require rapid treatment intervention.

Accurate diagnosis of appendicitis in pregnant women is important because of the complications that result from false-negatives and false-positives. Fetal mortality rates in pregnant women with appendicitis were found to increase to 5%, 20%, and 35.7% in patients without perforation, patients with perforation, and patients with complicating peritonitis, respectively.[1)] Delays in diagnosis resulting from false-negatives can have serious consequences. On the other hand, the frequency of negative appendectomy resulting from false-positives is higher in pregnant women (23% to 37%) than in non-pregnant women (14% to 18%), and negative appendectomy is considered a risk factor for preterm delivery (10% to 26%) and fetal death (3% to 7.3%).[2)] These findings show that false-negatives and false-positives should be avoided in diagnosing appendicitis in pregnant women. Moreover, they demonstrate the importance of imaging examinations that permit accurate and rapid diagnosis.

In prospective studies of the performance of US in diagnosing appendicitis in pregnant women, sensitivity and specificity in the 1st, 2nd, and 3rd trimesters of 92% and 66.7%, 63.7% and 75%, and 50% and 100%, respectively, were reported by Kazemini et al.,[3)] whereas sensitivity and specificity of 40% and 100%, 33% and 100%, and 0% and 100%, respectively, were reported by Butala et al.[4)] Thus, the reports show that diagnosing appendicitis by US is often difficult in acute abdomen in pregnant women, and that this tendency is particularly strong in late pregnancy, when the size of the uterus increases.

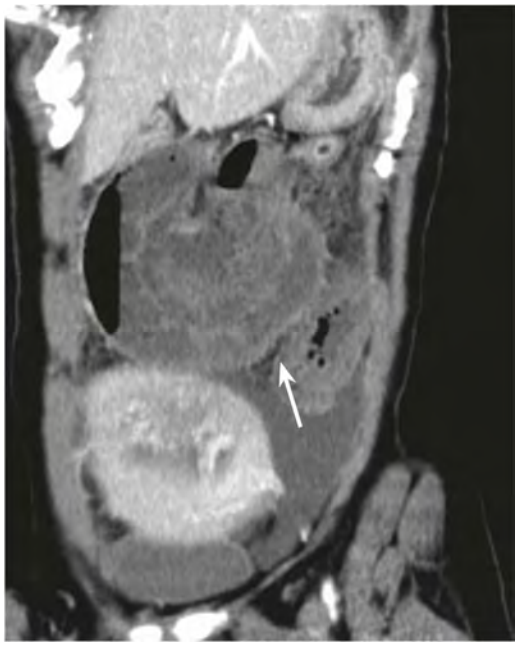

Figure　Strangulated intestinal obstruction in a pregnant woman (at 17 weeks of pregnancy)

Contrast-enhanced CT, MPR, oblique coronal image: The small intestine forms a closed loop, the wall in that area is thickened, and contrast enhancement is weak (→). Strangulated intestinal obstruction was diagnosed, surgery was planned, and the small intestine was partially resected.

In screening for the causes of acute abdomen in pregnant women, MRI has been found to be useful for many conditions. In addition to acute appendicitis, diagnosis of the following conditions is considered feasible with MRI: gastrointestinal disease (inflammatory bowel disease, diverticulitis, ileus), hepatobiliary disease (gallstones, choledocholithiasis, acute cholecystitis, pancreatitis, HELLP syndrome, acute fatty liver), urological disease (physiological hydronephrosis, ureteral calculus), vascular disease (venous thrombosis), and gynecological disease (uterine fibroids, ovarian masses and torsion).[5] Baron et al. reported sensitivity and specificity of 91% and 88%, respectively, for MRI and 85% and 90% for CT in acute abdomen in pregnant women, excluding that resulting from trauma; thus, the diagnostic performance of the 2 modalities was comparable.[6] Reports of the diagnosis of appendicitis by MRI that show high diagnostic performance have increased. A meta-analysis by Blumenfeld et al. reported sensitivity and specificity of 90.5% and 98.6%, respectively.[7] Non-contrast MRI is therefore recommended for acute abdomen in pregnant women when diagnosis by US is difficult.

However, the use of CT is permitted under certain circumstances due to the limited availability of emergency MRI in Japan. A questionnaire survey of radiology departments at general hospitals in the United States (85 institutions responded) found that 63 institutions (74%) had a written policy of using diagnostic imaging in pregnant women. Moreover, the proportion that prioritized the use of MRI and CT to diagnose appendicitis in the 1st, 2nd, and 3rd trimesters was 39% and 32%, 38% and 48%, and 29% and 58%, respectively.[8] Thus, MRI tended to be selected in early pregnancy and CT in late pregnancy. Moreover, CT can be considered if the patient has sustained serious trauma; if gastrointestinal perforation,

intestinal disease associated with strangulation, or thrombosis with a complicating pulmonary embolism is suspected; or if differential diagnosis is inconclusive and extensive imaging is required. To summarize, CT is considered if diagnosis by US and non-contrast MRI proves difficult, MRI cannot be performed, or CT is more advantageous than MRI. In such cases, contrast-enhanced imaging can be performed if necessary. If it is clear that contrast-enhanced CT would provide high diagnostic performance, it is recommended that non-contrast CT be omitted to reduce radiation exposure and that contrast-enhanced CT alone be performed. Reduction of radiation exposure by CT techniques such as low-dose CT should be aggressively applied clinically.

Search keywords and secondary sources used as references

PubMed was searched using the following keywords: acute abdominal pain, US, MR, CT, pregnancy, and appendicitis.

In addition, the following were referenced as secondary sources.

1) Bhosale PR et al: ACR Appropriateness Criteria®: acute pelvic pain in the reproductive age group. Ultrasound Q 32 (2): 108-115, 2016
2) Garcia EM et al: ACR Appropriateness Criteria®: right lower quadrant pain-suspected appendicitis. J Am Coll Radiol 15: S373-S387, 2018
3) Masselli G et al: Acute abdominal and pelvic pain in pregnancy: ESUR recommendations. Eur Radiol 23 (12): 3485-3500, 2013

References

1) Walker HG et al: Laparoscopic appendicectomy in pregnancy: a systematic review of the published evidence. Int J Surg 12 (11): 1235-1241, 2014
2) Aggenbach L et al: Impact of appendicitis during pregnancy: no delay in accurate diagnosis and treatment. Int J Surg 15: 84-89, 2015
3) Kazemini A et al: Accuracy of ultrasonography in diagnosing acute appendicitis during pregnancy based on surgical findings. Med J Islam Repub Iran. 31: 48-52, 2017
4) Butala P et al: Surgical management of acute right lower-quadrant pain in pregnancy: a prospective cohort study. J Am Coll Surg 211: 490-494, 2010
5) Spalluto LB et al: MR imaging evaluation of abdominal pain during pregnancy: appendicitis and other nonobstetric causes. Radiographics 32: 317-334, 2012
6) Baron KT et al: Comparing the diagnostic performance of MRI versus CT in the evaluation of acute nontraumatic abdominal pain during pregnancy. Emerg Radiol 19 (6): 519-525, 2012
7) Blumenfeld YJ et al: MR imaging in cases of antenatal suspected appendicitis: a meta-analysis. J Matern Fetal Neonatal Med 24 (3): 485-488, 2011
8) Jaffe TA et al: Practice patterns in imaging of the pregnant patient with abdominal pain: a survey of academic centers. AJR Am J Roentgenol 189: 1128-1134, 2007

FQ 15 Is MRI recommended to diagnose abnormalities of the placenta and umbilical cord?

Statement

MRI is recommended to diagnose abnormalities of the placenta and umbilical cord if sufficient information cannot be obtained by US or a more detailed evaluation is needed.

Background

US is usually performed periodically in the medical examinations of pregnant women. Consequently, most placental lesions and umbilical cord abnormalities are detected by US. Disorders of the placenta and umbilical cord were broadly divided into the following types, and the indication and the usefulness of MRI for each type were examined and are explained below: ① placenta accreta spectrum, ② placental abruption, ③ placental tumor, and ④ vasa previa.

Explanation

1. Placenta accreta spectrum

A 2013 meta-analysis regarding the diagnostic performance of US and MRI for placenta accreta spectrum reported sensitivity and specificity of 83% and 95%, respectively, for US and 82% and 88%, respectively, for MRI, with no significant differences between the two modalities.[1)] A 2018 meta-analysis also showed high diagnostic performance for MRI, with sensitivity ranging from 86.5% to 100% and specificity from 96.8% to 98.8%.[2)] Although MRI is inferior to US with respect to simplicity and spatial resolution, it is highly objective, and it is useful in patients with posterior placental wall adhesion, which is difficult to reach with US. It has been found to contribute to improved diagnostic performance when diagnosis is difficult with US.[3, 4)] However, the diagnostic performance of MRI can depend on the experience of the interpreting radiologist.[5)] MRI findings suggestive of placenta accreta spectrum are myometrial thinning of the uteroplacental interface, intraplacental dark bands in T2-weighted images, an intraplacental expanded flow void, protrusion of the placenta toward the urinary bladder, and interruption of the urinary bladder wall adjoining the placenta.[6-9)]

2. Placental abruption

Treatment must often be started quickly, and diagnosis is largely based on clinical findings. Although US is convenient, its sensitivity has been reported to be low, ranging from 24% to 53%.[10, 11)] MRI has been found to provide higher detection performance than US (sensitivity, 100%) and excellent visualization of the location and size of the retroplacental hematomas that occur with placental abruption.[11-13)] Moreover, because hematomas often appear as hyperintensities in T1-weighted images, they can be diagnosed

relatively easily regardless of the experience of the interpreting radiologist.[12] MRI is selected when US is negative, but excluding placental abruption is clinically important.

3. Placental tumor

With the exception of trophoblastic disease, hemangiomas are the most common placental tumors. Although tumors such as teratomas have also been reported, they are exceedingly rare. Case reports regarding the usefulness of MRI for these placental tumors are seen only sporadically. Review articles have shown that MRI is indicated when diagnosis by US is difficult.[14, 15]

4. Vasa previa

High diagnostic performance has been reported for color Doppler imaging, with sensitivity of 100% and specificity ranging from 99.0% to 99.8%.[16, 17] In patients with a succenturiate lobed placenta, which is a risk factor for vasa previa, MRI has been reported to be useful for the isolation and evaluation of succenturiate (accessory) placental lobes, the internal os, and blood vessels.[18, 19] Consequently, the ACR Appropriateness Criteria® state that, although US alone is usually adequate for diagnosing vasa previa, MRI may be indicated in some cases.

Search keywords and secondary sources used as references

PubMed was searched using the keywords indicated below for each type of disorder. Placenta accreta spectrum: MRI, ultrasound, invasive placenta, and placenta accreta; placental abruption: MRI, ultrasound, placenta, placental abruption, bleeding, and hemorrhage; placental tumor: MRI, ultrasound, placenta, placental, neoplasm, tumor, chorioangioma, and hemangioma; vasa previa: MRI, ultrasound, placenta, placental, and vasa previa.

In addition, the following were referenced as secondary sources.

1) Podrasky AE et al: ACR Appropriateness Criteria®: second and third trimester bleeding. Ultrasound Q 29: 293-301, 2013
2) Jauniaux E et al: Vasa praevia: diagnosis and management: green-top guideline No.27b. BJOG. 126 (1): e49-e61, 2019
3) Jha P et al: Society of Abdominal Radiology (SAR) and European Society of Urogenital Radiology (ESUR) joint consensus statement for MR imaging of placenta accreta spectrum disorders. Eur Radiol 30 (5): 2604-2615, 2020
4) Masselli G et al: Acute abdominal and pelvic pain in pregnancy: ESUR recommendations. Eur Radiol 23: 3485-3500, 2013
5) Jauniaux E et al: FIGO consensus guidelines on placenta accreta spectrum disorders: prenatal diagnosis and screening. Int J Gynaecol Obstet 140: 274-280, 2018

References

1) Meng X et al: Comparing the diagnostic value of ultrasound and magnetic resonance imaging for placenta accreta: a systematic review and meta-analysis. Ultrasound Med Biol 39: 1958-1965, 2013
2) Familiari A et al: Diagnostic accuracy of magnetic resonance imaging in detecting the severity of abnormal invasive placenta: a systematic review and meta-analysis. Acta Obstet Gynecol Scand 97: 507-520, 2018
3) Budorick NE et al: Another look at ultrasound and magnetic resonance imaging for diagnosis of placenta accreta. J Matern Fetal Neonatal Med 24: 1-6, 2016
4) Warshak CR et al: Accuracy of ultrasonography and magnetic resonance imaging in the diagnosis of placenta accreta. Obstet Gynecol 108: 573-581, 2006

5) Millischer AE et al: Magnetic resonance imaging for abnormally invasive placenta: the added value of intravenous gadolinium injection. BJOG 124: 88-95, 2017
6) Lax A et al: The value of specific MRI features in the evaluation of suspected placental invasion. Magn Reson Imaging 25: 87-93, 2007
7) Derman AY et al: MRI of placenta accreta: a new imaging perspective. AJR Am J Roentgenol 197: 1514-1521, 2011
8) Ueno Y et al: Novel MRI finding for diagnosis of invasive placenta praevia: evaluation of findings for 65 patients using clinical and histopathological correlations. Eur Radiol 24: 881-888, 2014
9) Bour L et al: Suspected invasive placenta: evaluation with magnetic resonance imaging. Eur Radiol 24: 3150-3160, 2014
10) Glantz C et al: Clinical utility of sonography in the diagnosis and treatment of placental abruption. J Ultrasound Med 21: 837-840, 2002
11) Masselli G et al: MR imaging in the evaluation of placental abruption: correlation with sonographic findings. Radiology 259: 222-230, 2011
12) Nguyen D et al: Imaging of the placenta with pathologic correlation. Semin Ultrasound CT MR 33: 65-77, 2012
13) Masselli G et al: Magnetic resonance imaging of clinically stable late pregnancy bleeding: beyond ultrasound. Eur Radiol 21: 1841-1849, 2011
14) Masselli G et al: MR imaging of the placenta: what a radiologist should know. Abdom Imaging 38: 573-587, 2013
15) Elsayes KM et al: Imaging of the placenta: a multimodality pictorial review. Radiographics 29: 1371-1391, 2009
16) Ruiter L et al: Systematic review of accuracy of ultrasound in the diagnosis of vasa previa. Ultrasound Obstet Gynecol 45: 516-522, 2015
17) Rebarber A et al: Natural history of vasa previa across gestation using a screening protocol. J Ultrasound Med 33: 141-147, 2014
18) Kikuchi A et al: Clinical significances of magnetic resonance imaging in prenatal diagnosis of vasa previa in a woman with bilobed placentas. J Obstet Gynaecol Res 37: 75-78, 2011
19) Oyelese Y et al: Magnetic resonance imaging of vasa praevia. BJOG 110: 1127-1128, 2003

7
Uroradiology

Standard Protocols for the Urinary Tract

Kidneys

Renal tumors are often identified on ultrasound examinations or on CT examinations incidentally. Dynamic CT using MDCT enables to characterize and stage the renal lesions, and to provide the anatomical information for blood vessels, and urinary systems in a single examination. In addition, it is used to evaluate lymph node and distant metastasis.

If contrast-enhanced CT is contraindicated such as due to iodine allergy, the primary lesion is diagnosed by MRI. Bone scintigraphy is performed if bone metastasis is suspected. PET might be useful for evaluating recurrence.

In dynamic contrast-enhanced study with either CT or MRI, the following four phases are observed following rapid contrast medium injection (3 to 5 mL/s).

① Arterial phase

This is the period from approximately 20 to 30 s after the start of contrast medium administration, when the renal artery is strongly enhanced. It is useful for evaluating 3D arterial images.

② Corticomedullary phase

This is the period from 30 to 70 s after the start of contrast medium administration, when mainly the renal cortex is enhanced. Imaging in the early corticomedullary phase (30 to 40 s) enables the renal arteries and veins to be assessed. This phase is advantageous when evaluation of the arteries and veins is required or when tumor vascularity is evaluated.

③ Nephrographic phase

This is the period from 80 to 130 s after the start of contrast medium administration, when the renal cortex and medulla are comparably enhanced and the renal parenchyma shows uniform attenuation. This is the best phase for lesion detection and staging.

④ Excretory phase

This is the period beginning 180 s after the start of contrast medium administration, during which the contrast medium is excreted and the urinary tract is visualized. This phase is suitable for evaluating tumor invasion into the renal pelvis.

In clinical practice, the phases required to meet the objectives of the examination are selected from among the 4 described above.

1. When a tumorous lesion is suspected

① CT

The following phases are usually acquired when a renal tumor is suspected.[1)]

(1) Non-contrast

(2) Corticomedullary phase (~ 30 to 40 s after the start of contrast medium administration, Fig. 1A)

(3) Nephrographic phase (~ 100 s after the start of contrast medium administration)

(4) Excretory phase (~ 180 s after the start of contrast medium administration)

Both characterization and staging can be accomplished. Non-contrast CT is important for differentiating benign tumors, i.e. diagnosing angiomyolipomas.

Approximately 100 mL of a non-ionic contrast medium is administered in 30 s. An injection rate of ≥ 3 mL/s is suitable for obtaining good arterial images. Because the contrast arrival time to the aorta varies in individuals, bolus tracking should be used.

The scanning range should completely cover the both kidneys. When chest imaging is used for screening pulmonary metastasis, good enhancement of the blood vessels in the chest is maintained in the nephrographic phase, which facilitates the evaluation of lymph nodes that attach to the blood vessels. However, the imaging can be performed in any phase.

In general, a 5-mm-slice thickness is applied. For small lesions, thinner slice reconstruction, of approximately 3-mm thickness, would be applied. Thin-slice images are required to obtain MPR images such as coronal and sagittal plane images. When evaluating the vascular anatomy preoperatively, 3D CTA images should be generated using a slice thickness of approximately 1 mm.

Non-contrast CT and nephrographic phase CT alone are sufficient for follow-up (including the chest).

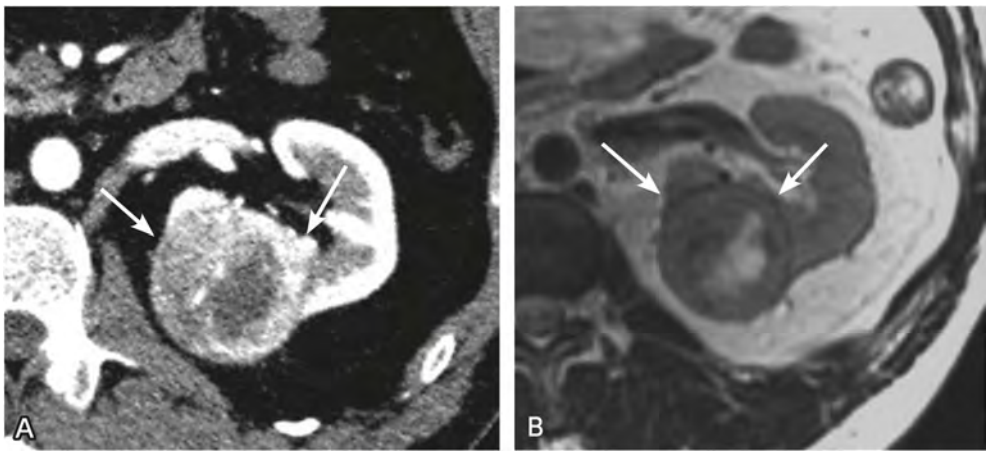

Figure 1. Left renal cell carcinoma (RCC)

A: Dynamic CT, corticomedullary phase, 35 s after contrast medium administration: Inhomogeneous strong enhancement (→) indicated abundant tumor blood flow.

B: MRI, T2-weighted transverse image: a pseudocapsule is seen around the tumor (→).

Table 1. Examples of RCC sequences (phased-array coil)

Imaging Method	Sequence	1.5T		3T		Other
		TE/TR	Slice thickness	TE/TR	Slice thickness	
(1) T2-weighted imaging/transverse, coronal	Breath-hold FSE	Approx. 3000/100 ms (ETL approx. 12)	4 to 8 mm	Approx. 3000/90 ms (ETL approx. 20 to 24)	3 to 8 mm	
	Respiratory-gated FSE	R-R interval /approx. 90 ms	4 to 8 mm	R-R interval /approx. 90 ms	3 to 8 mm	
	Breath-hold heavy T2-weighted	∞ /approx. 80 ms	4 to 8 mm	∞ /approx. 80 ms	3 to 8 mm	
(2) Pre-contrast T1-weighted imaging	3D GRE	4 to 5 /approx. 1.2 to 2 ms	4 to 8 mm	4 to 5 /approx. 1.2 to 2 ms	3 to 8 mm	Imaging times: 30, 60 to 90, and 150 to 180 s after injection
(3) Dynamic MRI	3D GRE	4 to 5 /approx. 1.2 to 2 ms (FA approx. 12 to 15°)	4 to 8 mm	4 to 5 /approx. 1.2 to 2 ms (FA approx. 12 to 15°)	3 to 8 mm	
(4) Diffusion-weighted imaging	Respiratory-gated 2D-EPI	R-R interval /approx. 100 ms	4 to 8 mm	R-R interval /approx. 100 ms	3 to 8 mm	b-value = 0, 750 to 1,000 s/mm^2

② MRI

The following types of imaging are usually used when performing an MRI evaluation.[2)]

(1) T2-weighted imaging (transverse and coronal)

(2) Pre-contrast T1-weighted imaging

(3) Dynamic MRI using a contrast medium

(4) Diffusion-weighted imaging

Both characterization and staging can be performed with this protocol.

The imaging range sufficiently covers both kidneys. The slice thickness is approximately 3 to 8 mm. The recommended parameters are shown in Table 1. As in-phase and opposed-phase imaging enables detection of a mixture of water and fat, tumors with intracellular lipid, such as clear cell carcinomas, can be diagnosed. T2-weighted imaging is useful for detecting pseudocapsules in renal cell carcinoma (Fig. 1B). In addition, several reports show that diffusion-weighted imaging is useful for differentiating benign from and malignant lesions, and for determining the aggressiveness of cancer.[3)]

2. When an infectious lesion is suspected

Since CT is standard modality of choice, MRI is rarely applied. The following phases of CT imaging are usually performed.

① Non-contrast

② Post-contrast imaging (70 to 90 s after the start of contrast medium administration)

The contrast injection rate should be ≥ 2 mL/s. The imaging range sufficiently covers the kidneys. A 5 mm-thick reconstruction is usually applied.

Some literature recommends post-contrast tri-phasic dynamic study as shown below.[4)]

① Non-contrast

② Corticomedullary phase (30 s after the start of contrast medium administration)

③ Nephrographic phase (70 to 90 s after the start of contrast medium administration)

④ Excretory phase (5 min after the start of contrast medium administration)

However, the nephrographic phase is considered superior to the corticomedullary and excretory phases for detecting lesions and evaluating its spread.[5] In view of the radiation exposure, pre-contrast and tri-phasic post-contrast studies are hardly implemented. It is appropriate to perform pre-contrast and the nephrographic phase CT, adding excretory-phase imaging only if urinary tract obstruction is suspected.[5]

Imaging methods for the upper urinary tract

In the evaluation of the upper urinary tract, CT is the modality of choice for lesion detection, determining invasion depth, and screening for lymph node and distant metastases. MDCT (≥ 16-row CT) enables this information to be obtained with a single examination. CT urography, pre- and post-contrast excretory-phase imaging with thin slice, is widely used to evaluate the urinary tract.[6, 7] MRI may be used in cases where a contrast medium is contraindicated, such as in cases with iodine allergy.

1. When urolithiasis is suspected

When painful hematuria is present, and imaging is performed to detect urinary stones, non-contrast CT imaging is performed from the upper pole of the kidney to the pelvic floor using a slice thickness of 3 to 5 mm and pitch of 1 to 1.5.

Low-dose imaging provides sufficient diagnostic performance for detecting urinary stones. Consequently, imaging that reduces radiation exposure as much as possible is performed.

2. When a tumor is suspected

① CT

The following imaging (CT urography protocol) is performed, when screening for upper urinary tract tumor; such as when there is painless hematuria (in elderly persons), past history of urothelial neoplasia, or bladder cancer.[6, 7]

(1) Non-contrast CT

(2) Nephrographic phase (~ 100 s after the start of contrast medium administration)

(3) Excretory phase (~ 8 min after the start of contrast medium administration, Fig. 2)

Similar to the urolithiasis protocol, non-contrast CT imaging is performed first and covers the area from the upper pole of the kidney to the inferior margin of the pubic bone. A contrast medium is then administered. Because visualization of the urinary tract in the excretory phase tends to be dose-dependent, a dose of approximately 600 mgI/mL/kg BW (body weight (kg) × 2 mL for 300 mgI/mL agent) is recommended. The contrast medium is administered in approximately 30 s, and the entire kidneys are scanned approximately 100 s after the start of contrast injection (nephrographic phase). Approximately 8 to

10 min after the start of contrast medium administration, excretory phase images are acquired from the upper pole of the kidney to the inferior margin of the pubic bone. In cases of screening for metastasis in the chest, the nephrographic phase image is suitable for evaluating the hilar lymph nodes. However, any phase is acceptable for evaluating the lung. Urinary bladder tumors can be visualized as filling defects by having the patient urinate once after nephrographic phase imaging, waiting approximately 40 min, and then performing excretory phase imaging approximately 45 min after urination. This enables excretory-phase imaging to be performed with the whole urinary bladder filled with homogeneous contrast medium.[7)]

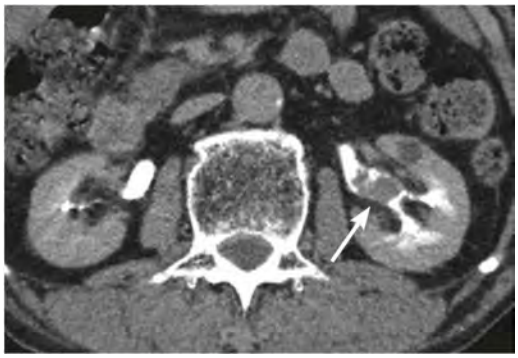

Figure 2. Left renal pelvic cancer

Dynamic CT, excretory phase, 8 min after contrast medium administration: A tumor is seen in the left renal pelvis (→).

Table 2. Examples of ureteral cancer sequences (phased-array coil)

Imaging Method	Sequence	1.5T		3T		Other
		TE/TR	Slice thickness	TE/TR	Slice thickness	
(1) T2-weighted/transverse and coronal	Breath-hold FSE	Approx. 3,000/90 ms (ETL approx. 15)	4 to 8 mm	Approx. 3,000/90 ms (ETL approx. 20 to 24)	3 to 8 mm	
	Respiratory-gated FSE	R-R interval/approx. 90 ms	4 to 8 mm	R-R interval/approx. 90 ms	3 to 8 mm	
	Breath-hold heavy T2-weighted	Infinite/approx. 80 ms	4 to 8 mm	Infinite/approx. 80 ms	3 to 8 mm	
(2) Pre-contrast T1-weighted	3D GRE	4 to 5/approx. 1.2 to 2 ms	4 to 8 mm	4 to 5/approx. 1.2 to 2 ms	3 to 8 mm	
(3) Post-contrast, fat-suppressed, T1-weighted/transverse and coronal	3D GRE	4 to 5/approx. 1.2 to 2 ms (FA approx. 12 to 15°)	4 to 8 mm	4 to 5/approx. 1.2 to 2 ms (FA approx. 12 to 15°)	3 to 8 mm	
(4) Diffusion-weighted imaging	Respiratory-gated 2D-EPI	R-R interval/100 ms	4 to 8 mm	R-R interval/100 ms	3 to 8 mm	b-value = 0, 750 to 1,000 s/mm^2
(5) MR urography	Projection					
	Fat-suppressed RARE	≥ 4,000/approx. 1,250 ms	4 to 80 mm	≥ 6,000/ approx. 1,200 ms	4 to 80 mm	
	Multislice					
	Fat-suppressed heavy T2-weighted	Infinite/approx. 80 ms	4 to 5 mm	Infinite/approx. 80 ms	4 to 5 mm	
	Respiratory-gated FSE	R-R interval/100 ms		R-R interval/100 ms		

Thin slices provide better performance for detecting small lesions. Reconstruction using a slice thickness of ≤ 3 mm is therefore recommended. MPR images, such as excretory-phase, thin-slice, coronal images, are generated as needed.

To improve urinary tract visualization, oral hydration with water before and after contrast medium administration is desirable.

This imaging method enables both lesion detection and staging to be performed.

② MRI

If upper urinary tract tumor is the main target disease, the following imaging methods are implemented.

(1) T2-weighted imaging (transverse and coronal)
(2) Pre-contrast T1-weighted imaging
(3) Post-contrast, fat-suppressed, T1-weighted imaging (transverse and coronal)
(4) Diffusion-weighted imaging
(5) MR urography

Of these, diffusion-weighted imaging is also highly useful for detecting lesions, distinguishing between benign and malignant lesions, and staging.[8, 9)]

The imaging range for the above is the entire abdomen, including both kidneys, using a slice thickness of approximately 3 to 8 mm. There are two types of MR urography based on the slice thickness used; projection imaging with a single thick-slice slab or, multislice imaging with reconstruction of the multiple slices acquired. The imaging is performed under breath-hold. The parameters recommended for each imaging method are shown in Table 2.

The urinary bladder[10, 11)]

MRI is used for the local staging of bladder cancer. CT is used mainly to evaluate lymph nodes and distant metastases and local recurrence. Although cystoscopy is used to detect bladder cancer, CT urography is also used on the bladder to evaluate the urinary tract as a whole.

1. CT

The following types of CT imaging are selected and combined depending on the purpose of the imaging: non-contrast CT, arterial phase (20 to 30 s after contrast medium administration), corticomedullary phase (30 to 70 s after contrast medium administration), nephrographic phase (80 to 130 s after contrast medium administration), and excretory phase (beginning 8 min after contrast medium administration). For the contrast medium, 100 mL of a nonionized iodinated contrast agent is administered at a rate of 2 to 3 mL/s. If arterial phase vascular images are to be reconstructed, the contrast medium is administered at a rate of approximately 4 mL/s. Non-contrast CT plus contrast-enhanced CT that includes the excretory phase with a thin-slice (1 to 2 mm) is called CT urography.[12)] Commonly used CT urography protocols are single-bolus technique, in which contrast medium is administered once and imaging is performed 3 times (non-contrast

CT, nephrographic phase, and excretory phase), and split-bolus technique, in which contrast medium administration is divided into two times and imaging is performed twice (plain and mixed nephrographic phase/excretory phase).[12] Because imaging is performed once fewer with the split-bolus technique compared with single-bolus, radiation exposure is proportionally reduced with split-bolus imaging. In a mixed nephrographic/excretory phase with split-bolus imaging, the kidneys show equivalent enhancement as the nephrographic phase and the urinary tract is filled with excreted contrast medium as the excretory phase. The single-bolus technique is chosen for high-risk patients with urothelial carcinoma. Contrast enhancement of bladder cancer tumors is the greatest from the late corticomedullary phase to the early nephrographic phase.[13] With thin-slice imaging, almost all bladder cancer larger than 5 mm are detectable.[14] As thin-slice imaging over a relatively extensive range is required, a scanner with ≥ 16 rows is desirable although a 64-row scanner is not necessary.

2. MRI

Imaging is performed in accordance with the Vesical Imaging-Reporting and Data System (VI-RADS), a standardized imaging method[15] (Table 3). However, the imaging parameters shown are strictly examples and can be appropriately adjusted to suit the specifications of a specific MRI system. MRI of the bladder is performed before transurethral resection of a bladder tumor. The expansion and thickness of the bladder wall vary depending on the amount of urine that has accumulated. For high-quality local staging, the bladder wall should be in a moderately expanded state. In many patients, appropriate bladder distension can be obtained by having the patient urinate once 1 hour before the examination, then drink approximately 500 mL of water before the examination, and refrain from urinating until the examination is completed.

The imaging range includes the entire bladder and the prostatic urethra. The basic imaging plane is the transverse plane, with sagittal or coronal plane imaging added. The optimal plane for determining the invasion depth of bladder cancer is theoretically the plane perpendicular to the bladder wall at the tumor base. However, if multiple bladder cancers are present, or if lesions are present along an extensive area of the wall, imaging in the optimal plane for all of the lesions is difficult due to time restrictions. Moreover, image quality is poor with oblique diffusion-weighted imaging. A slice thickness of approximately 3 to 4 mm is appropriate for T2- and diffusion-weighted imaging. Diffusion-weighted imaging is performed using the EPI method with fat suppression. The imaging is performed using b-values of 0 and 1,000 s/mm^2. For contrast-enhanced imaging, dynamic imaging is performed using an injector. The contrast medium dose is 0.1 mmol/kg, injected at a rate of 1.5 to 2.0 mL/s, with a saline chaser. Imaging is performed before contrast medium administration and 5 or 6 times at 30-s intervals beginning from 30 s after contrast medium administration. It is performed as high-speed GRE T1-weighted imaging in 2D or 3D. The preferred plane is the sagittal plane, which can minimize the number of slices. However, if the sagittal plane is parallel to the bladder wall at the base of the lesion to be evaluated (e.g., if the tumor is on the lateral wall), transverse or coronal imaging is performed. Reconstruction can be performed after the examination for any arbitrary plane if volume data are obtained by 3D imaging. Reconstructing T2- and

diffusion-weighted images in the same plane facilitates comparison during interpretation. Although not essential, a magnetic field strength of 3T, as compared with 1.5T, provides a better signal-to-noise ratio and spatial resolution and permits high-speed imaging, enabling images of suitable quality for diagnosis to be obtained.

Table 3. Examples of bladder cancer sequences (phased-array coil)

	T2-Weighted Imaging	Diffusion-Weighted Imaging	Dynamic MRI
1.5T			
TR (ms)	5,000	4,500	3.3
TE (ms)	80	88	1.2
FA (degree)	90	90	
FOV (cm)	23	27	35
Matrix	256 × 189 to 256	128 × 109	256 × 214
Slice thickness (mm)	4	4	1
Slice interval (mm)	0 to 0.4	0 to 0.4	0
	1 to 2	10 to 15	1
b-value (s/mm^2)	–	0, 800 to 1,000	–
3T			
TR (ms)	4,690	2,500 to 5,300	3.8
TE (ms)	119	61	1.2
FA (degree)	90	90	15
FOV (cm)	23	32	27
Matrix	400 × 256 to 320	128 × 128	192 × 192
Slice thickness (mm)	3 to 4	3 to 4	1
Slice interval (mm)	0 to 0.4	0.3 to 0.4	0
	2 to 3	4 to 10	1
b-value (s/mm^2)		0, 800 to 1,000 (up to 2,000)	

Imaging methods for the prostate gland

MRI, which provides excellent tissue contrast, is suitable for local assessment of the prostate gland. MRI has traditionally been used for local staging after malignancy is proved by prostate biopsy. However, it was found that when MRI is performed after prostate biopsy, the intraprostatic signal is altered by hemorrhage due to biopsy, complicating cancer diagnosis. Consequently, MRI is now increasingly performed prior to biopsy to detect clinically significant prostate cancer. However, depending on the prefecture, pre-biopsy MRI may not be approved for medical fee reimbursement. The effect of bleeding can be reduced by allowing at least 8 weeks after prostate biopsy before performing a local evaluation by MRI.[16)]

Table 4. Examples of prostate cancer sequences (for both 3T and 1.5T systems, phased-array coil)

Imaging Method	Sequence	TR/TE	Slice Thickness	Other
(1) T2-weighted/transverse	FSE	Approx. 4,000 ms/ approx. 100 ms	3 mm	The FOV is 12 to 20 cm. Imaging is performed without gaps. The entire prostate is imaged, including the seminal vesicles.
(2) T1-weighted	FSE or GRE	FSE: approx. 400 to 700 ms/10 ms; GRE: approx. 4 ms/approx. 2 ms	3 to 4 mm	Same range as diffusion-weighted and dynamic contrast imaging. Can be performed with or without fat suppression.
(3) Diffusion-weighted	SE-EPI Concurrent fat suppression with STIR or CHESS	≥ 3,000 ms/ ≤ 90 ms	≤ 4 mm	ADC map generated with FOV of 16 to 22 cm and 2 b-values of 0 to 100 and 800 to 1,000 s/mm^2. Diffusion-weighted images with high b-values (b-values > 1400 s/mm^2) can be acquired by actual imaging or with computed DWI instead.
(4) T2-weighted/coronal or sagittal	FSE	Approx. 4,000 ms/ approx. 100 ms	3 mm	The prostate is set to be slightly caudal to the center of the FOV.
(5) Dynamic MRI, transverse plane	3D GRE Concomitant fat suppression	< 100 ms/ < 5 ms	3 mm	Temporal resolution of < 15 s is preferable, and observations are carried out through 2 min after contrast medium injection.

DWI: diffusion-weighted image

There has been large variability between facilities and radiologists with respect to imaging and image interpretation performed to detect prostate cancer. The Prostate Imaging-Reporting and Data System (PI-RADS), which was designed to standardize these procedures, was proposed in 2012, and versions 2[17] and 2.1[18] were published in 2015 and 2019, respectively. Awareness of PI-RADS is increasing in Japan. Based on the standardized imaging methods indicated by PI-RADS, example parameters for each imaging method are shown in Table 4. The parameters should be optimized by the individual institutions.

1. Preparation before an MRI examination: To obtain better images

Before an MRI examination, the patient is asked to evacuate the bowel to reduce intrarectal gas and residue, which can degrade images.

If an antispasmodic (glucagon, scopolamine butylbromide) can be used, it can reduce motion artifacts resulting from intestinal peristalsis. However, cost and adverse reactions need to be considered.

2. Magnetic field strength

Although appropriate parameters can be obtained with either a 3T or 1.5T system, imaging with a 3T system is recommended. Imaging is performed using a 1.5T system if image quality degradation is a concern due to metal artifacts from implantable devices; such as bilateral total hip replacement. Prostate MRI using a low magnetic field of < 1.5T is not recommended.

3. Signal receiving coil

Given suitable imaging conditions, appropriate images can be obtained using a phased-array coil. The use of a transrectal coil is therefore unnecessary, particularly in view of the invasiveness of such coils.

4. Prostate MRI protocol

T1-weighted, T2-weighted (≥ 2 imaging planes), diffusion-weighted, and dynamic contrast-enhanced study constitute the basic protocol. T2-weighted, diffusion-weighted, and dynamic contrast-enhanced study are particularly important for diagnosis (Fig. 3).

① T2-weighted imaging

T2-weighted imaging is performed using FSE in the transverse plane and at least 1 other plane (coronal or sagittal). A slice thickness of 3 mm without interslice gap is recommended. 3D acquisition can be used as an adjunct to 2D images. 3D acquisition with isotropic voxels enables detailed anatomical structures to be visualized and is useful for distinguishing true lesions from pseudolesions due to partial volume effects. It should be noted, however, that the soft tissue contrast of 3D images is not the same as 2D-images, and that the contrast may be inferior to that of 2D T2-weighted imaging.

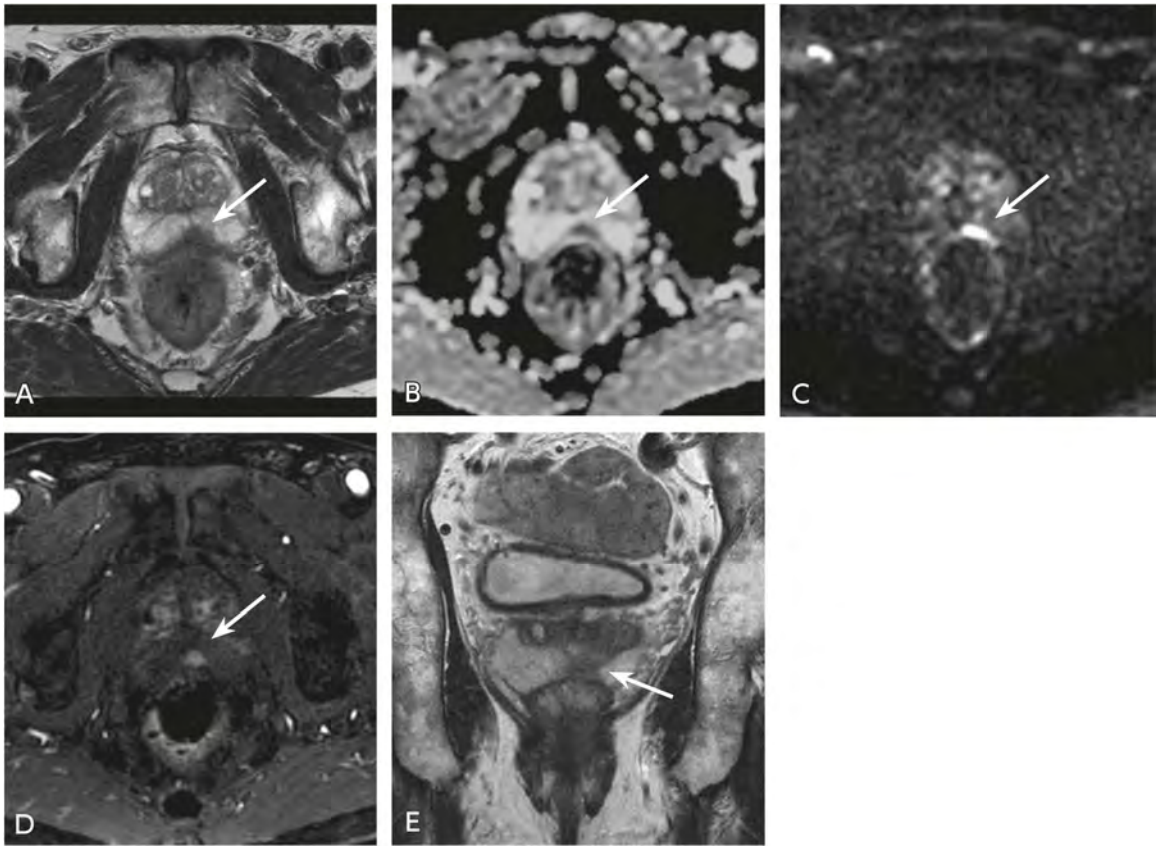

Figure 3. MRI of prostate cancer (T2a)

A: T2-weighted transverse image; B: ADC map; C: Diffusion-weighted image (b-value = 2,000 s/mm^2);
D: Dynamic contrast image, early phase; E: T2-weighted coronal image
The patient was a man in his 70s. A 10-mm nodule is seen in the margin of the left lobe of the prostate gland. The nodule shows hypointensity in the T2-weighted image (A) and ADC map (B) and early enhancement in the dynamic contrast image (C). The findings are suggestive of prostate cancer. In the T2-weighted coronal image, an area of hypointensity is seen extending caudally from the center region (D). The findings in the dynamic contrast image and T2-weighted coronal image facilitate differentiation of the normal central region from the cancer. It should be noted that intrarectal gas can distort diffusion-weighted images and make it difficult to evaluate the dorsal portion of the prostate.

② Diffusion-weighted imaging

For diffusion-weighted imaging, SE-EPI (with fat suppression) and normal breathing are recommended. Matching of slice location and slice thickness of T2-weighted imaging facilitates diagnosis. Diffusion-weighted imaging with a high b-value (b-value > 1,400 s/mm^2) and ADC map are required. The ADC map must be generated from a low b-value (0 to 100 s/mm^2) and an intermediate b-value (800 to 1,000 s/mm^2). Consequently, if there is a limitation with respect to time or another factor, one possible approach is to acquire imaging with only low and intermediate b-values and compute DWI with a high b-value.

③ T1-weighted imaging

Transverse plane images are acquired using SE and GRE. Fat suppression may or may not be used. Hemorrhage in the prostate gland or the seminal vesicle can be detected. The imaging range can be the

same as with diffusion-weighted and dynamic contrast-enhanced study. However, because high spatial resolution is not necessary for T1-weighted images as T2-weighted imaging, it can be modified to reduce the acquisition time or to increase the imaging range. In at least 1 plane, the area from the inferior margin of the prostate to the common iliac bifurcation is included in the imaging range, and the lymph nodes present at the cranial end of the prostate are evaluated.

④ Dynamic contrast imaging

For dynamic contrast imaging, fat-suppressed GRE T1-weighted imaging is performed. A 3D sequence (e.g., VIBE, LAVA, THRIVE) is recommended. An FOV that includes the prostate and seminal vesicles in their entirety is selected. Spatial resolution should be ≤ 2 mm × 2 mm and temporal resolution < 15 s. Observation is carried out for 2 min after contrast medium injection. If any signal change such as post-biopsy hemorrhage is seen as hyperintensity on T1-weighted imaging before contrast-enhanced imaging, subtraction images facilitate determination of the presence or absence of contrast enhancement.

Metastasis could be found if the prostate specific antigen (PSA) level is ≥ 10 ng/mL or the Gleason score for cancer tissue obtained by biopsy is ≥ 8. Consequently, in addition to prostate MRI, which is a local evaluation, CT is performed for whole-body metastasis screening, and bone scintigraphy is performed to assess bone metastasis.

Imaging methods for the testicles and scrotum

Testicular and scrotal lesions are broadly classified as those associated with acute symptoms referred to as acute scrotum and those not associated with such symptoms. The former type includes testicular torsion, testicular infarction, acute epididymo-orchitis, and testicular rupture. The latter includes tumor, granuloma, and testicular microlithiasis. Many testicular tumors are detected due to irregular nodular swelling found by self-examination. More than 90% of testicular tumors are malignant germ cell tumors that occur in relatively young men between the ages of approximately 15 and 45 years. The other types of tumors include sex cord-stromal tumors, malignant lymphoma, leukemia, and metastatic tumors.

Ultrasonography is the first choice of diagnostic imaging modalities for testicular and scrotal lesions, with Doppler ultrasonography used concomitantly to evaluate blood flow. Ultrasonography is also the first choice for acute scrotum. However, difficulty may be encountered in evaluating testicular blood flow by ultrasonography, and dynamic MRI using a contrast medium is added in that case. If a tumorous lesion is suspected, MRI can be used to identify intratumoral hemorrhage, necrosis, and the fatty component, and to sensitively evaluate structures such as septal structures. Ultrasonography and MRI can be used in combination for purposes such as differentiating between benign and malignant lesions, inferring the histopathological-type of tumors, and evaluating aspects such as local progression. To diagnose the distant metastasis of tumorous lesions, evaluation by CT, MRI, or radioisotope inspection (RI, PET) is performed.

1. MRI of testicular and scrotal lesions[19)]

Because of the small size of the imaging target, high-resolution imaging is necessary. An MR scanner of 1.5T or higher should be used.

A 3T scanner, which provides a better SNR than 1.5T, should be used if possible. However, scientific evidence that 3T systems are more useful is lacking. The receiver coil used is a surface or phased-array coil, each of which has a high SNR and enables high-resolution imaging.

The field-of-view (FOV) includes the bilateral scrotum, and the transverse and coronal plane imaging indicated below is performed with a small FOV and thin slice thickness (FOV: approximately 15 to 20 cm; slice thickness: approximately 3 to 5 mm; slice gap: minimum).

T1- and T2-weighted imaging are standard. In the case of tumorous lesions, fat-suppressed T1-weighted imaging or dual echo T1-weighted imaging is added to detect the fatty component occasionally seen in germ cell tumors. For acute scrotum, $T2^{*}$-weighted imaging, which sensitively detects the intratesticular hemorrhage seen with testicular torsion, is added as needed.

Diffusion-weighted imaging is recommended because it reflects the pathological background of lesions. The imaging is performed with b-values of at least 0 s/mm^2 and 800 to 1,000 s/mm^2, and an ADC map is generated. Lesions such as epidermoid cysts and seminomas and malignant lymphomas, which have high cellularity, show particularly marked hyperintensity in diffusion-weighted images, which is useful for differentiation (Fig. 4).

Dynamic contrast MRI is an important imaging method for acute scrotum in particular. Using 3D GRE T1-weighted imaging, a gadolinium contrast medium is rapidly injected intravenously, and imaging is performed approximately 30 s to 1 min later. This is done repeatedly, and the contrast enhancement of areas such as the testicles and epididymis is assessed (Fig. 5). Imaging should be performed until 8 min after injection to assess washout from tumorous lesions. If visually assessing contrast enhancement is difficult, subtraction images are generated, and time-signal intensity curves are plotted for the testicles and lesions. In the case of a tumorous lesion, dynamic contrast MRI can be omitted, and aspects such as the internal structure and extent of progression can be evaluated with normal pre- and post-contrast T1-weighted imaging alone (or fat-suppressed contrast T1-weighted imaging).

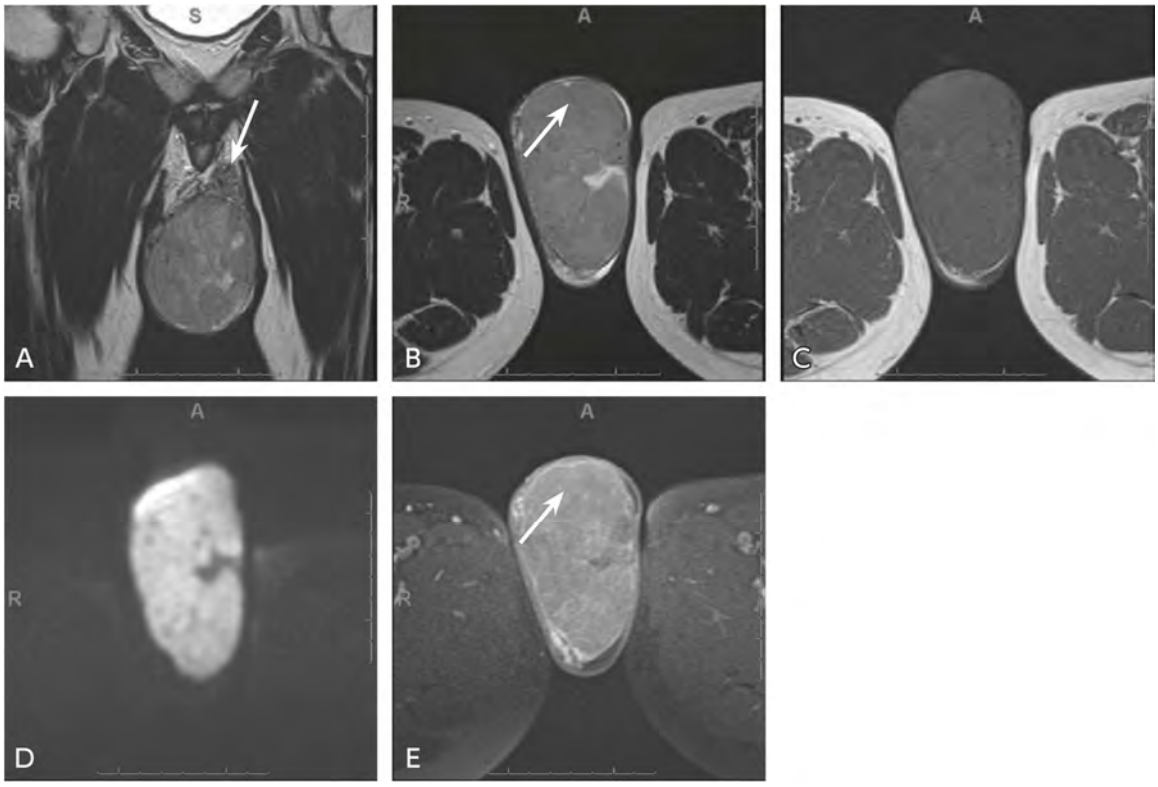

Figure 4. MRI of a malignant testicular tumor

A: T2-weighted coronal image; B: T2-weighted transverse image; C: T1-weighted image; D: Diffusion-weighted image; E: Post-contrast image

The left testis is enlarged and replaced by a tumor of moderate signal intensity in the T2-weighted images. The interior is relatively homogeneous and shows a signal of moderate intensity in the T2-weighted images and marked hyperintensity in the diffusion-weighted image. Extension to the spermatic cord is visualized in the coronal T2-weighted image (A →). In addition, a restiform structure that shows hypointensity on T2-weighted imaging (B →) is seen in the interior, with increased contrast enhancement of this structure seen (E →). The findings reflect fibrous septa, and a seminoma is strongly suspected.

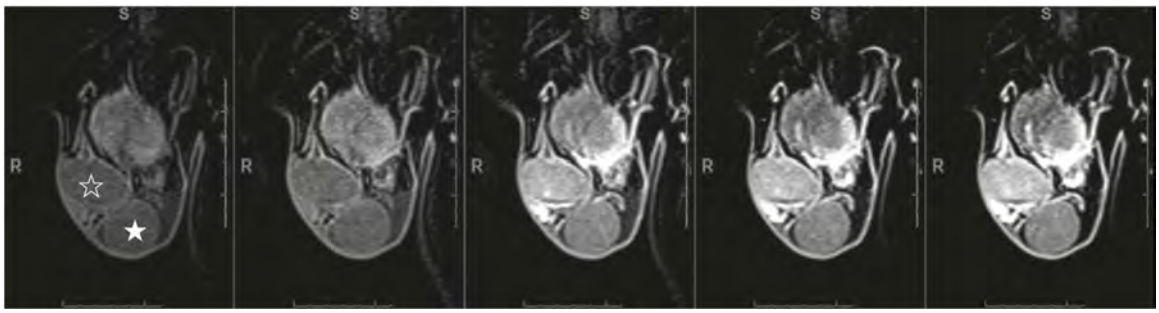

Figure 5. MRI of acute scrotum

Testicular torsion was suspected but could not be confirmed by ultrasonography, and the patient underwent MRI.

Dynamic contrast MRI: No abnormalities could be identified on T1- and T2-weighted imaging (not shown). With dynamic contrast MRI, enhancement was poorer in the left testis (★) than in the right (☆). The patient underwent orchidopexy for incomplete testicular torsion, which was cured without testicular necrosis.

2. Malignant testicular tumor staging and diagnosis of recurrence

Malignant testicular tumors tend to metastasize to the lymph nodes and lungs. With regard to lymph node metastasis, tumors that arise in the left testis metastasize to the lateral side of the aorta near the left renal vein. Right testicular tumors progress from the pericaval lymph nodes at the height of the 2nd lumbar vertebra to the thoracic duct and metastasize to the left supraclavicular lymph nodes and lungs. Infiltration of the epididymis by the primary tumor increases the risk of metastasis to the inguinal lymph nodes. Hematogenous metastasis often occurs in the late stage of the disease. However, choriocarcinoma metastasizes to the lungs early and may also metastasize to the brain, bone, and liver. Contrast-enhanced CT, which enables high-speed, extensive imaging using thin slices, is useful for evaluating such lymph node and pulmonary metastases.

For the contrast medium, a 300 mgI/mL nonionic contrast agent is administered at an injection rate of 2 to 3 mL/s. The volume administered is either approximately 100 mL or approximately 2 mL per kilogram of the patient's weight. The timing of the imaging is approximately 50 to 60 s after the start of contrast medium administration. The area imaged is from the supraclavicular fossa to the inguinal region. Reconstruction using a slice thickness of $\leq$ 5 mm is recommended. Although the cutoff value for lymph node enlargement is generally a short-axis diameter of 10 mm, a short-axis diameter of approximately 6 mm and the use of thin slices are necessary to evaluate lymph node metastases of testicular tumors.[20)]

As necessary, bone scintigraphy is performed to evaluate bone metastasis, and contrast-enhanced MRI is performed to evaluate brain metastasis. In addition, FDG-PET has been reported to be useful for lymph node, pulmonary, and bone metastases. However, as indicated for BQ76, there is inadequate scientific evidence to recommend PET alone.

The frequency of recurrence varies according to factors such as the stage, histopathological type, and recurrence risk classification, and the timing for performing each type of imaging examination for posttreatment follow-up also varies. In this regard, the European Association of Urology (EAU) guidelines[21)] and the National Comprehensive Cancer Network (NCCN) Clinical Practice Guidelines in Oncology[22)] are instructive.

Secondary source materials used as references

1) Sheth S et al: Current concepts in the diagnosis and management of renal cell carcinoma: role of multidetector CT and three-dimensional CT. Radiographics 21: S237-254, 2001
2) Pedrosa I et al: MR imaging of renal masses: correlation with findings at surgery and pathologic analysis. Radiographics 28: 985-1003, 2008
3) Vendrami CL et al: Differentiation of solid renal tumors with multiparametric MR imaging. Radiographics 37: 2026-2042, 2017
4) Urban BA et al: Tailored helical CT evaluation of acute abdomen. Radiographics 20: 725-749, 2000
5) Stunell H et al: Imaging of acute pyelonephritis in the adult. Eur Radiol 17: 1820-1828, 2007
6) Van Der Molen AJ et al: CT urography: definition, indications and techniques: a guideline for clinical practice. Eur Radiol 18: 4-17, 2008
7) Jinzaki M et al: Role of computed tomography urography in the clinical evaluation of upper tract urothelial carcinoma. Int J Urol 23: 284-298, 2016
8) Akita H et al: Performance of diffusion-weighted MRI post-CT urography for the diagnosis of upper tract urothelial carcinoma: Comparison with selective urine cytology sampling. Clin Imaging 52: 208-215, 2018

9) Akita H et al: Preoperative T categorization and prediction of histopathologic grading of urothelial carcinoma in renal pelvis using diffusion-weighted MRI. AJR Am J Roentgenol 197: 1130-1136, 2011
10) Japan Radiological Society, Ed.: Diagnostic Imaging Guidelines 2016. KANEHARA & Co., 2016.
11) Japanese Urological Association, Ed.: 2019 Clinical Practice Guidelines for Bladder Cancer. Igakutosho Shuppan, 2019.
12) Sudakoff GS et al: Multidetector computerized tomography urography as the primary imaging modality for detecting urinary tract neoplasms in patients with asymptomatic hematuria. J Urol 179: 862-867, 2008
13) Kim JK et al: Bladder cancer: analysis of multi-detector row helical CT enhancement pattern and accuracy in tumor detection and perivesical staging. Radiology 231: 725-731, 2004
14) Jinzaki M et al: Detection of bladder tumors with dynamic contrast-enhanced MDCT. AJR Am J Roentgenol 188: 913-918, 2007
15) Panebianco V et al: Multiparametric magnetic resonance imaging for bladder cancer: development of VI-RADS (Vesical Imaging-Reporting and Data System). Eur Urol 74: 294-306, 2018
16) Qayyum A et al: Organ-confined prostate cancer: effect of prior transrectal biopsy on endorectal MRI and MR spectroscopic imaging. AJR Am J Roentgenol 183: 1079-1083, 2004
17) Weinreb JC et al: PI-RADS (Prostate Imaging-Reporting and Data System) version 2. Eur Urol 69: 16-40, 2015
18) Turkbey B et al: PI-RADS (Prostate Imaging-Reporting and Data System) version 2.1. Eur Urol 76: 340-351, 2019
19) Tsili AC et al: MRI of the scrotum: recommendations of the ESUR scrotal and penile imaging working froup. Eur Radiol 28: 31-43, 2018
20) Hilton S et al: CT detection of retroperitoneal lymph node metastases in patients with clinical stage I testicular non seminomatous germ cell cancer: assessment of size and distribution criteria. AJR Am J Roentgenol 169: 521-525, 1997
21) Albers P et al: Guidelines on testicular cancer: 2015 Update. Eur Urol 68: 1054-68, 2015
22) Gilligan T et al: NCCN clinical practice guidelines in oncology: testicular cancer version 2. J Natl Compr Canc Netw 17: 1529-1554, 2019

BQ 68 Is DMSA scintigraphy recommended to detect renal scarring?

Statement

DMSA scintigraphy is useful and recommended for detecting renal scarring.

Background

Repeated recurrence of pyelonephritis due to vesicoureteral reflux or upper urinary tract infection is known to result in impairment and scarring of the renal parenchyma. Scarring can also occur as a result of conditions such as asymptomatic congenital hydronephrosis. Extensive scarring can cause decreased kidney function, resulting in conditions such as proteinuria, hypertension, and renal failure. Consequently, early detection is required. To detect renal scarring, ultrasonography and dimercaptosuccinic acid (DMSA) are often used. For this BQ, the usefulness of renal scarring detection by DMSA scintigraphy was examined.

Explanation

Farghaly et al. performed DMSA planar imaging and SPECT imaging in 190 patients with conditions such as vesicoureteral reflux. Of the 200 examinations performed, scarring was detected in 95 planar imaging examinations and 100 SPECT examinations.[1)]

Temiz et al. compared the results of DMSA scintigraphy and ultrasonography in 62 pediatric patients (mean age, 5 years; range, 6 months to 15 years) with vesicoureteral reflux. Although DMSA scintigraphy detected scarring in 55%, the detection rate was 38% with ultrasonography. Moreover, DMSA scintigraphy was able to identify scarring in 35% of kidneys deemed normal by ultrasonography.[2)]

Brenner et al. compared DMSA planar images and SPECT images of 40 patients (37 of whom were children). They found no significant difference in the number of scars detected by the 2 methods.[3)]

Moorthy et al. examined the kidneys of 930 children who underwent ultrasonography and DMSA examinations on the same day. They found that, although ultrasonography provided high specificity in detecting renal scarring, its sensitivity and positive and negative predictive values were low. They concluded that ultrasonography cannot substitute for DMSA examination.[4)]

Moreover, DMSA scintigraphy can enable quantitation by expressing the rate of renal tracer uptake as a percentage, providing a useful index for the evaluation and follow-up of renal function.

Search keywords and secondary sources used as references

PubMed was searched using the following keywords: renal, scar, DMSA, and detection. Four articles were selected from the results.

1) Farghaly HRS, Mohamed Sayed MH: Technetium-99m dimercaptosuccinic acid scan in evaluation of renal cortical scarring: Is it mandatory to do single photon emission computerized tomography? Indian J Nucl Med 30 (1): 26-30, 2015

2) Temiz Y et al: The efficacy of Tc99m dimercaptosuccinic acid (Tc-DMSA) scintigraphy and ultrasonography in detecting renal scars in children with primary vesicoureteral reflux (VUR). Int Urol Nephrol 38 (1): 149-152, 2006
3) Brenner M et al: Comparison of 99mTc-DMSA dual-head SPECT versus high-resolution parallel-hole planar imaging for the detection of renal cortical defects. AJR Am J Roentgenol 193 (2): 333-337, 2009
4) Moorthy I et al: Ultrasonography in the evaluation of renal scarring using DMSA scan as the gold standard. Pediatr Nephrol 19 (2): 153-156, 2004

BQ 69 Is contrast-enhanced CT recommended to evaluate solid renal masses?

Statement

Contrast-enhanced CT is strongly recommended to determine whether a renal mass is solid.

Dynamic CT is recommended because it can identify clear cell renal cell carcinomas, which account for 70% to 80% of renal cell carcinomas (RCCs), and because benign disease, for which surgery is omitted, can be suspected if enhancement of the mass is homogeneous.

Background

Diagnosis of a solid renal tumor involves first determining that it is a solid mass. Next, benign masses are differentiated from malignant ones. Based on disease frequency, it is important to differentiate renal cell carcinoma (RCC) from renal angiomyolipoma (AML) and oncocytoma. In the case of a malignancy, information on tissue-type should also be provided. For the purpose of molecularly targeted therapy, it is also now important to differentiate between clear cell renal cell carcinoma and other tissue-types. The following discussion provides an overview regarding the usefulness of contrast-enhanced CT for identifying solid renal masses, differentiating benign from malignant masses, and diagnosing the subtype of a mass.

Explanation

Characterizing a mass as solid or cystic involves performing not only non-contrast CT, but also contrast-enhanced CT imaging, and observing the presence or absence of contrast enhancement is very important. In the past, a mass was judged to be solid when an increase in the CT number of ≥ 10 HU was seen from pre- to post-contrast.[1)] However, since the emergence of helical CT, in view of the pseudoenhancement effect, an increase in the CT number of ≥ 20 HU has been considered to indicate contrast enhancement.[2)] Moreover, characterizing masses ≤ 10 mm in size is difficult with a slice thickness of 5 mm. However, imaging with thin slices of approximately 3 mm markedly improves the characterization of 5 to 10 mm masses.[3)] If a cyst is strongly suspected at the non-contrast CT stage, normal contrast-enhanced CT (nephrographic phase) is adequate. However, if a solid mass is suspected, dynamic CT is recommended to differentiate a benign mass from a malignant mass.

Because the proportion of resected masses that are benign is 46.3% for those < 1 cm in size and approximately 20% for those 2 to 4 cm in size, rigorously distinguishing malignant tumors from others is particularly important for preoperatively evaluating small-diameter tumors.[4)] AML can often be diagnosed by detecting the fat concentrations (< -10 HU) with non-contrast CT. This is referred to as classic AML. Non-contrast CT is more accurate than contrast-enhanced CT for detecting fat concentrations.[5)] In comparison, the homogeneity and contrast pattern of contrast-enhanced CT are useful for differentiating

fat-poor AML[6], which accounts for approximately 5% of AMLs, from RCC.[7] First, masses that show non-homogeneous marked enhancement in the corticomedullary phase of dynamic CT can be almost definitively determined to be clear cell renal cell carcinomas, i.e., malignant (Fig. 1).[8-10] However, few fat-poor AMLs show early-phase enhancement. Rather, many show homogeneous mild to moderate enhancement (Fig. 2).[6, 7, 11, 12] In addition, hyperdensity (≥ 45 HU) compared with the renal parenchyma[6, 7, 13, 14] and tumors with a higher long-axis diameter/short-axis diameter ratio on non-contrast CT are common.[13] Oncocytomas, although known for central scarring, show homogeneity on contrast-enhanced CT if small in size. The contrast pattern of oncocytomas resembles that of chromophobe renal cell carcinomas, which tends to be homogeneous, which poses a problem for their differentiation. Segmental enhancement inversion (tumor more strongly enhanced in the early phase of contrast than in the late phase; converse true for the interstitium) has been proposed as a characteristic finding of oncocytomas. However, this finding has also been reported for chromophobe renal cell carcinomas. Consequently, differentiating oncocytomas from chromophobe renal cell carcinomas remains difficult. In addition, benign tumors such as leiomyomas and metanephric adenomas also show hyperintensity on non-contrast CT and homogeneity on contrast-enhanced CT. Hyperdensity and homogeneous contrast on non-contrast CT (hyperattenuating homogeneously enhancing masses) are useful clues that suggest a possibly benign mass.[6, 7, 11] However, malignancies such as papillary renal cell carcinomas also have this appearance, and a definitive determination by biopsy is therefore recommended.[6, 7, 11]

Figure 1. Clear cell renal cell carcinoma

Contrast-enhanced CT, corticomedullary phase: A non-homogeneously enhancing mass is seen in the left kidney (→), a finding indicative of clear cell renal cell carcinoma.

Figure 2. Fat-poor AML

Contrast-enhanced CT, corticomedullary phase: A homogeneous and hypovascular solid mass is seen in the right kidney (→). The mass is a fat-poor AML.

Dynamic CT is also useful for diagnosing RCC subtypes. The 3 main RCC tissue types are the clear cell, chromophobe, and papillary types. Clear cell renal cell carcinomas undergo non-homogeneous enhancement in the corticomedullary phase and decreased enhancement in the nephrographic and early

excretory phases.[8-10] Chromophobe renal cell carcinomas show moderate homogeneous contrast enhancement in the corticomedullary phase and decreased enhancement subsequently.[8-10] Papillary renal cell carcinomas often undergo only slight contrast enhancement in the corticomedullary phase and gradual homogeneous enhancement.[8-10] These differences in contrast patterns reflect intratumoral angiogenesis,[8] and the 3 main tissue types can be mutually differentiated. It should be noted, however, that oncocytomas show similar enhancement pattern with clear cell renal cell carcinomas and chromophobe renal cell carcinomas[8-10, 15-17], and that metanephric adenomas resemble papillary renal cell carcinomas.[8]

Search keywords and secondary sources used as references

PubMed was searched using the following keywords: renal, tumor, CT, assessment, characteristics, differentiation, pathologic correlation, renal cell carcinoma, and angiomyolipoma.

In addition, the following was referenced as a secondary source.

1) Wang ZJ et al: ACR Appropriateness Criteria®: clinical condition indeterminate renal masses. J Am Coll Radiol 17: S415-S428, 2020

References

1) Bosniak MA: The small (less than or equal to 3.0 cm) renal parenchymal tumor: detection, diagnosis, and controversies. Radiology 179: 307-317, 1991
2) Curry NS: Small renal masses (lesions smaller than 3 cm): imaging evaluation and management. AJR Am J Roentgenol 164: 355-362, 1995
3) Jinzaki M et al: Evaluation of small (＜/＝3 cm) renal masses with MDCT: benefits of thin overlapping reconstructions. AJR Am J Roentgenol 183: 223-228, 2004
4) Frank I et al: Solid renal tumors: an analysis of pathological features related to tumor size. J Urol 170: 2217-2220, 2003
5) Davenport MS et al: Diagnosis of renal angiomyolipoma with hounsfield unit thresholds: effect of size of region of interest and nephrographic phase imaging. Radiology 260: 158-165, 2011
6) Jinzaki M et al: Angiomyolipoma: imaging findings in lesions with minimal fat. Radiology 205: 497-502, 1997
7) Jinzaki M et al: Renal angiomyolipoma: a radiological classification and update on recent developments in diagnosis and management. Abdom Imaging 39: 588-604, 2014
8) Jinzaki M et al: Double-phase helical CT of small renal parenchymal neoplasms: correlation with pathologic findings and tumor angiogenesis. J Comput Assist Tomogr 24: 835-842, 2000
9) Zhang J et al: Solid renal cortical tumors: differentiation with CT. Radiology 144: 494-504, 2007
10) Pierorazio PM et al: Multiphasic enhancement patterns of small renal masses (≤ 4 cm) on preoperative computed tomography: utility for distinguishing subtypes of renal cell carcinoma, angiomyolipoma, and oncocytoma. Urology 81: 1265-1271, 2013
11) Silverman SG et al: Hyperattenuating renal masses: etiologies, pathogenesis, and imaging evaluation. Radiographics 27: 1131-1143, 2007
12) Yang CW et al: Are there useful CT features to differentiate renal cell carcinoma from lipid-poor renal angiomyolipoma? AJR Am J Roentgenol 201: 1017-1028, 2013
13) Woo S et al: Angiomyolipoma with minimal fat and non-clear cell renal cell carcinoma: differentiation on MDCT using classification and regression tree analysis-based algorithm. Acta Radiol 55: 1258-1269, 2014
14) Schieda N et al: Unenhanced CT for the diagnosis of minimal-fat renal angiomyolipoma. AJR Am J Roentgenol 203: 1236-1241, 2014
15) Kim JI et al: Segmental enhancement inversion at biphasic multidetector CT: characteristic finding of small renal oncocytoma. Radiology. 252: 441-448, 2009
16) Schieda N et al: Diagnostic accuracy of segmental enhancement inversion for the diagnosis of renal oncocytoma using biphasic computed tomography (CT) and multiphase contrast-enhanced magnetic resonance imaging (MRI). Eur Radiol 24: 2787-2794, 2014
17) Choudhary S et al: Renal oncocytoma: CT features cannot reliably distinguish oncocytoma from other renal neoplasms. Clin Radiol 64: 517-522, 2009

FQ 16 In which cases is MRI recommended to differentiate renal mass lesions?

Statement

MRI is useful when determining whether a lesion is benign or malignant is difficult with CT and when differentiating RCC subtypes. MRI is also used when contrast-enhanced CT cannot be performed due to circumstances such as pregnancy, decreased renal function, or allergy to iodinated contrast media.

Background

Recently, the frequency with which small renal masses ≤ 4 cm in diameter are detected incidentally on ultrasonography and CT has increased. Because it is known that the frequency of benign masses increases among those ≤ 4 cm in diameter, differentiating benign from malignant masses is critical.[1)] Multiparametric MRI (mpMRI) is a concept that involves analyzing image data as qualitative, semi-quantitative, and quantitative biomarkers. The data are for images such as T1-weighted images (chemical shift images: in-phase and opposed-phase images), T2-weighted images, diffusion-weighted images, and dynamic contrast images.[2)] In fact, mpMRI of renal mass lesions is considered useful for the qualitative diagnosis of lesions (benign-malignant differentiation), as well as their detection, and for differentiating RCC subtypes.[1)]

Explanation

The most common type of small solid renal mass for which surgery is performed is malignant RCC (~ 80%). The main subtypes are the clear cell, papillary, and chromophobe types, with frequencies of 75%, 10%, and 5%, respectively. The clear cell type has a poor prognosis.[2)] The diagnostic accuracy rate of CT in diagnosing solid renal masses as RCC is ≥ 90%.[3)] Consequently, a general treatment strategy can be determined using CT examinations in nearly all cases. On the other hand, the frequency of benign tumors has been reported to be 46.3% for those < 1 cm in size and 20% for those 2 to 4 cm in size, the main tumors being renal AMLs and oncocytomas.[4)] As background, the frequency of identified benign masses is lower in Asian, including Japanese, populations than in European and American populations. This is because oncocytomas are less frequent in the Asian population, and angiomyolipomas account for a relatively large number.[5, 6)] Ninety-five percent of AMLs are classic AMLs, in which the fat component of the mass can be detected by CT (CT number < -10 HU). However, approximately 5% are fat-poor AMLs, in which fat cannot be detected. Consequently, differentiating AMLs from RCCs by CT alone is often difficult.[7)] Oncocytomas have characteristic findings, such as early-phase contrast enhancement that ranges from moderate to hypervascular,[8)] central scarring, and segmental enhancement inversion. However, these findings are also seen with RCC,[9)] making diagnosis by CT alone difficult. Consequently, it is expected that

the addition of MRI for indeterminate renal masses to assess them as benign or malignant on CT could improve differentiation accuracy.[1)]

First, tumors that show post-contrast homogeneous enhancement on CT may be benign. Of these, those that show hyperdensity comparable to that of skeletal muscle on non-contrast CT and hypointensity on T2-weighted images are strongly suspected of being fat-poor AMLs (hyperattenuating type).[7, 10)] Such tumors often show low values in ADC maps, early-phase contrast enhancement, and late-phase washout.[10)] For tumors that show attenuation comparable to that of the renal parenchyma and mild-to-moderate, homogeneous early-phase contrast enhancement on non-contrast CT, a fat-poor AML (iso-attenuating type) is suspected if the tumor shows a lower signal on T1-weighted opposed-phase images than on in-phase images.[7)] However, although an examination of the use of mpMRI for renal masses with central scarring seen by CT showed that it may be possible to use MRI to exclude oncocytoma,[11)] it is difficult to diagnose actively on MRI. In addition, differentiating homogeneous oncocytomas from renal cell carcinoma is also considered difficult even with the use of mpMRI.[1)]

Furthermore, mpMRI may be useful for diagnosing RCC subtypes. If a tumor shows attenuation comparable to that of the renal parenchyma on non-contrast CT, mild early-phase contrast enhancement, and gradually increasing late-phase enhancement, papillary renal cell carcinoma is most commonly suspected based on frequency. With the addition of MRI in this case, a low signal in T2-weighted images is suggestive of papillary renal cell carcinoma,[10)] and a moderate-to-high signal indicates a possible mucinous tubular and spindle cell carcinoma.[11)] Papillary renal cell carcinomas often show a decreased signal on in-phase T1-weighted images compared with opposed-phase T1-weighted images due to intratumoral hemorrhage.[12)] In comparison, due to intracellular lipids, clear cell renal cell carcinomas show a lower signal on opposed-phase T1-weighted images than on in-phase images, a non-homogeneous high signal in T2-weighted images, and early-phase non-homogeneous enhancement.[1)]

CT is readily accessible and less expensive than MRI, and a single CT examination can provide information for the qualitative diagnosis of renal masses and staging over an extensive area and on structures such as the renal artery and vein and ureter. Consequently, as the first-choice examination, CT is highly useful. Another advantage of CT is that it is suitable for use in elderly individuals and patients who cannot tolerate a long examination duration or breath-hold examination.[14)] MRI, on the other hand, does not involve exposure to ionizing radiation, and it can visualize lesions with tissue contrast superior to that of CT. The diagnostic performance of MRI for detecting lesions that require surgery and locally staging RCC compares favorably with CT. However, many facilities have busy MRI examination schedules, and few can perform emergency examinations. In addition, due to considerations such as the somewhat higher fees for MRI than for CT and the long duration of MRI examinations, MRI is performed as an adjunct subsequent to CT. However, MRI is the first examination used in circumstances where contrast-enhanced CT cannot be performed, as in pregnancy, decreased renal function, or allergy to iodinated contrast media.[15)]

Although CT plays the central role in the diagnostic imaging of solid renal masses, MRI may be useful for differentiating benign from malignant masses and diagnosing renal cell carcinoma subtypes when used as an adjunctive examination. It can also aid in determining a treatment plan.

Search keywords and secondary sources used as references

PubMed was searched using the following keywords: renal tumors, renal cell carcinoma, oncocytoma, angiomyolipoma, and MRI. The period searched was through June 2019.

In addition, the following were referenced as secondary sources.

1) Japan Radiological Society, Ed.: Diagnostic Imaging Guidelines 2016. KANEHARA & Co., 2016.
2) Heilbrun ME et al: ACR Appropriateness Criteria®: indeterminate renal mass. J Am Coll Radiol 12: 333-341, 2015

References

1) Vendrami CL et al: Differentiation of solid renal tumors with multiparametric MR imaging. Radiographics 37: 2026-2042, 2017
2) Kay FU et al: Imaging of solid renal masses. Radiol Clin North Am 55: 243-258, 2017
3) Kim EY et al: Clinico-radio-pathologic features of a solitary solid renal mass at MDCT examination. Acta Radiol 51: 1143-1148, 2010
4) Frank I et al: Solid renal tumors: an analysis of pathological features related to tumor size. J Urol 170: 2217-2220, 2003
5) Fujii Y et al: Incidence of benign pathologic lesions at partial nephrectomy for presumed RCC renal masses: Japanese dual-center experience with 176 consecutive patients. Urology 72 (3): 598-602, 2008
6) Fujii Y et al: Benign lesions at surgery for presumed renal cell carcinoma: an Asian perspective. Int J Urol 17 (6): 500, 2010
7) Jinzaki M et al: Renal angiomyolipoma: a radiological classification and update on recent developments in diagnosis and management. Abdom Imaging 39: 588-604, 2014
8) Cornelis F et al: Routinely performed multiparametric magnetic resonance imaging helps to differentiate common subtypes of renal tumours. Eur Radiol 24: 1068-1080, 2014
9) Rosenkrantz AB et al: MRI Features of renal oncocytoma and chromophobe renal cell carcinoma. AJR Am J Roentgenol 195: W421-427, 2010
10) Lim RS et al: Renal angiomyolipoma without visible fat: can we make the diagnosis using CT and MRI? Eur Radiol 28: 542-553, 2018
11) Cornelis F et al: Combined late gadolinium-enhanced and double-echo chemical-shift MRI help to differentiate renal oncocytomas with high central T2 signal intensity from renal cell carcinomas. AJR Am J Roentgenol 200: 830-838, 2013
12) Chiarello MA et al: Diagnostic accuracy of MRI for detection of papillary renal cell carcinoma: a systematic review and meta-analysis. AJR Am J Roentgenol 211: 812-821, 2018
13) Cornelis F et al: CT and MR imaging features of mucinous tubular and spindle cell carcinoma of the kidneys: a multi-institutional review. Eur Radiol 27: 1087-1095, 2017
14) Krishna S et al: CT imaging of solid renal masses: pitfalls and solutions. Clin Radiol 72: 708-721, 2017 15) Allen BC et al: Characterizing solid renal neoplasms with MRI in adults. Abdom Imaging 39: 358-387, 2014
15) Allen BC et al: Characterizing solid renal neoplasms with MRI in adults. Abdom Imaging 39: 358-387, 2014

BQ 70 Which imaging examinations are recommended for staging renal cancer?

Statement

Contrast-enhanced CT is strongly recommended. MRI is the alternative modality for patients who cannot undergo contrast-enhanced CT. MRI may be useful if determining the presence or absence of perirenal fat invasion, intravenous tumor thrombus, and venous mural infiltration of tumor thrombus is difficult with CT.

Chest CT is recommended if there is a risk of pulmonary metastasis due to a very large primary tumor or locally advanced disease. Chest radiography is recommended if the risk of pulmonary metastasis is low.

Bone scintigraphy is not recommended as a routine examination. It can be considered if bone metastasis is clinically suspected.

PET has been reported to be useful for metastasis screening and diagnosing recurrence during follow-up. However, its significance as a routine examination has not been established.

Background

Preoperative staging of renal cancer is essential for formulating a treatment plan. As indicated in The General Rule for Clinical and Pathological Studies on Renal Cell Carcinoma, the modality that plays the central role in this is CT. Evidence regarding the usefulness of incorporating MRI, bone scintigraphy, and PET is also reviewed.

Explanation

1. CT

In a prospective study of imaging methods, the staging capability of CT was significantly greater with combined 3-phase imaging (plain, corticomedullary phase, and nephrographic phase: diagnostic accuracy rate, 91%) than with combined 2-phase imaging (plain and corticomedullary phase or plain and nephrographic phase: diagnostic accuracy rate, 82% and 86%, respectively).[1)] Dynamic contrast CT is considered useful both for the qualitative diagnosis of masses and for staging.

The biggest factor that has reduced the staging capability for the T stage of renal cancers has been low diagnostic performance for perirenal and renal sinus fat invasion (differentiation of T1/T2 and T3a).[1-5)] CT findings of perirenal fat invasion include the following: renal fascial thickening, thickening of the bridging septa, fluid accumulation, left-right asymmetrical dilatation and irregularity of the peritumoral blood vessels and blood vessels in Gerota's fascia, the presence of tumorous nodules in the tumor margins and perirenal fatty space, and contrast enhancement of those nodules.[6, 7)] The General Rule for Clinical and Pathological Studies on Renal Cell Carcinoma indicates that outward protrusion from the renal contour

resulting in rupture of the lateral cortex and nodules ≥ 1 cm in size that are continuous with tumors in perirenal fatty tissue should be evaluated. However, difficulty may be encountered in differentiating tumor infiltration and benign changes in fatty tissue resulting from conditions such as inflammation. The reported sensitivity and specificity of CT for perirenal fat invasion ranged from 84% to 100% and from 56% to 93%, respectively.[7-9] The diagnostic performance of 16- and 64-row MDCT with respect to renal sinus fat invasion has also been examined. However, the positive predictive value has been found to be low, ranging from 48.9% to 56.3%, even when coronal reconstructed images were combined.[10] An investigation by Kim et al. found that CT findings that were predictors of renal sinus fat invasion were tumor diameter (≥ 5 cm), poor contrast of the lesioned kidney, irregular tumor margin, and lymph node metastasis.[10] Clinically, total nephrectomy is indicated for T1, T2, and T3a, with the exception of some T1a patients for whom partial nephrectomy is indicated. Consequently, accurate preoperative diagnosis of perirenal and renal sinus fat invasion is not of great importance. However, because arteries, veins, and lymph ducts are present in abundance in renal sinus fat, systemic metastasis is a possibility, and renal sinus fat invasion has been found to be a prognostic factor for recurrence-free survival and cancer-specific survival.[11]

The diagnostic performance of CT with respect to intravenous tumor thrombus has been found to improve with the use of multiplanar reconstruction images, with sensitivity and specificity of 93% and 80%, respectively, which have been reported as measures of its detection performance.[12] CT has been found to be capable of identifying the extent of tumor thrombus with accuracy of 84%, with the exception of the segmental veins.[13]

Although the diagnostic criteria used for lymph node metastasis are generally a short-axis diameter ≥ 1 cm with loss of the horseshoe shape, the diagnostic performance of these criteria is inadequate. Diagnostic accuracy rates of 74% to 78% have been reported for the evaluation of lymph node metastasis by 4- to 64-row MDCT.[5, 8] Because microscopic infiltration cannot be assessed, the false-negative rate is approximately 10%. The false-positive rate has ranged from 3% to 43% due to reactive lymph node enlargement. An imaging finding other than enlargement is a low attenuation area resulting from central necrosis, and non-homogeneous contrast enhancement is a CT finding with a high positive predictive value.[14] If lymph node metastasis affects the clinical determination of a treatment plan, CT-guided biopsy/aspiration may be performed. Because the lung is the organ that is the most common site of distant RCC metastasis, chest CT is also performed. However, it has been reported that chest CT can be omitted in the absence of symptoms and abnormal test data in stages cT1a and cN0.[15]

2. MRI

MRI results in no radiation exposure and provides good tissue contrast. It is generally used when CT cannot be performed due to circumstances such as pregnancy or serious allergy to contrast media. MRI is useful when CT contrast enhancement is unevaluable, such as in the case of a hemorrhagic lesion. The diagnostic performance of MRI with respect to T staging and tumor thrombus has been reported to be roughly equal to that of 4-row MDCT.[2, 12] However, MDCT permits imaging to be performed over a wide

area in a short time, and it can be used to diagnose distant metastasis. Consequently, MRI has a limited role in staging.

A case in which MRI is useful is in assessing the feasibility of nephron-sparing surgery (differentiating T1a and T3a). Specifically, the combination of pseudocapsule rupture and changes in the peripheral fatty tissue in T2-weighted images yields high diagnostic performance (diagnostic accuracy rate, 91%) with respect to perirenal fat infiltration.[16] Moreover, MRI sequences such as true FISP are useful when assessing intravenous tumor thrombus is difficult with CT. MRI findings such as those concerned with embolus texture analysis and characteristics of the venous wall are useful for assessing venous wall invasion by tumor thrombus.[17, 18]

3. Bone scintigraphy

The reports to date have indicated that bone scintigraphy can be performed in circumstances where bone metastasis is strongly suspected, such as in the presence of bone pain. However, they indicate that it is of little value as a routine examination for staging.[19-23] In a retrospective study of 205 patients with pathologically demonstrated RCC, bone metastasis was present in 34 patients (17%), and sensitivity and specificity of 94% and 86%, respectively, were seen in an examination of the diagnostic performance of bone scintigraphy. However, its positive predictive value was a low 57%. Moreover, the bone metastasis rate in patients with stage T1-3aN0M0 disease and no bone pain was ≤ 5%. It was therefore concluded that bone scintigraphy is not recommended in such cases.[19]

Uchida et al. compared FDG-PET and bone scintigraphy in 227 patients with bone metastasis, including 21 patients with renal cancer. They reported that the lesion detection rate for osteolytic bone metastases was significantly lower with bone scintigraphy (19 lesions) than with FDG-PET (41 lesions).[24] In view of the fact that nearly all renal cancer bone metastases are osteolytic metastases, the sensitivity of bone scintigraphy cannot be considered high. Bone scintigraphy is not recommended as a routine examination for staging renal cancer. Its use is appropriate in patients for whom bone metastasis is strongly suspected, such as those in whom the degree of primary tumor progression is high and the likelihood of metastasis is also high and in those with bone pain or hematological abnormalities.

4. PET

PET (PET/CT) is currently covered by national health insurance in Japan for all malignancies except early gastric cancer if staging or the definitive diagnosis of metastasis and recurrence cannot be performed with another test or diagnostic imaging modality. In the case of renal cancer, an examination of the metastasis detection performance of FDG-PET/CT showed its sensitivity, specificity, and diagnostic accuracy rate to be 89.5%, 83.3%, and 85.7%, respectively, findings comparable to but not superior to those of conventional examinations.[25] Because of its advantages, however, it is recommended when diagnosis is difficult with conventional examinations. The advantages are the ability to perform whole-body screening with a single examination, and the fact that it can avoid renal dysfunction and allergy problems resulting

from the use of a contrast medium. FDG uptake in RCC is known to be low, and increased diagnostic accuracy is anticipated in the future with the use of other tracers instead of FDG.

Search keywords and secondary sources used as references

PubMed was searched using the following keywords: renal cell carcinoma, preoperative, staging, CT, MRI, bone scintigraphy, positron emission tomography, and chest CT.

In addition, the following were referenced as secondary sources.

1) Japanese Urological Association, Japanese Society of Pathology, and Japan Radiological Society, Ed.: The General Rule for Clinical and Pathological Studies on Renal Cell Carcinoma (5th Edition). Medical Review, 2020.
2) Japanese Urological Association, Ed.: 2017 Clinical Practice Guidelines for Renal Cancer. Medical Review, 2017.
3) Vikram R et al: ACR Appropriateness Criteria®: renal cell carcinoma staging. J Am Coll Radiol 13: 518-525, 2016

References

1) Kopka L et al: Dual-phase helical CT of the kidney: value of the corticomedullary and nephrographic phase for evaluation of renal lesions and preoperative staging of renal cell carcinoma. AJR Am J Roentogenol 169: 1573-1578, 1997
2) Hallscheidt PJ et al: Diagnostic accuracy of staging renal cell carcinomas using multidetector-row computed tomography and magnetic resonance imaging: a prospective study with histopathologic correlation. J Comput Assist Tomogr 28: 333-339, 2004
3) Roberts WW et al: Pathological stage does not alter the prognosis for renal lesions determined to be stage T1 by computerized tomography. J Urol 173: 713-715, 2005
4) Hallscheidt PJ et al: Multislice computed tomography in planning nephron-sparing surgery in a prospective study with 76 patients: comparison of radiological and histopathological findings in the infiltration of renal structures. J Comput Assist Tomogr 30: 869-874, 2006
5) Türkvatan A et al: Preoperative staging of renal cell carcinoma with multidetector CT. Diagn Interv Radiol 15: 22-30, 2009
6) Tsili AC et al: Perinephric fat invasion on renal cell carcinoma: evaluation with multidetector computed tomography-multivariate analysis. JCAT 36: 450-457, 2013
7) Hedgire SS et al: Preoperative evaluation of perinephric fat invasion in patients with renal cell carcinoma: correlation with pathological findings. Clinical Imaging 37: 91-96, 2013
8) Catalano C et al: High-resolution multidetector CT in the preoperative evaluation of patients with renal cell carcinoma. AJR Am J Roentgenol 180: 1271-1277, 2003
9) Bolster F et al: Renal cell carcinoma: accuracy of multidetector computed tomography in the assessment of renal sinus fat invasion. J Comput Assist Tomogr 40 (6): 851–855, 2016
10) Kim C et al: Diagnostic value of multidetector computed tomography for renal sinus fat invasion in renal cell carcinoma patients. Eur J Radiol 83: 914-918, 2014
11) Kresowik TP et al: Combined renal sinus fat and perinephric fat renal cell carcinoma invasion has a worse prognosis than either alone. J Urol 184: 48-52, 2010
12) Hallscheidt PJ et al: Preoperative staging of renal cell carcinoma with inferior vena cava thrombus using multidetector CT and MRI: prospective study with histopathological correlation. J Comput Assist Tomogr 29: 64-68, 2005
13) Guzzo TJ et al: The accuracy of multidetector computerized tomography for evaluating tumor thrombus in patients with renal cell carcinoma. J Urol 181: 486-460, 2009
14) Tsili AC et al: Advanced of multidetector computed tomography in the characterization and staging renal cell carcinoma. World J Radiol 7: 110-127, 2015.
15) Larcher A et al: When to perform preoperative chest computed tomography for renal cancer staging. BJU Int 20: 490-496, 2017
16) Roy C Sr et al: Significance of the pseudocapsule on MRI of renal neoplasms and its potential application for local staging: a retrospective study. AJR Am J Roentgenol 184: 113-120, 2005
17) Adams LC et al: Renal cell carcinoma with venous extension: prediction of inferior vena cava wall invasion by MRI. Cancer Imaging 18: 17, 2018
18) Alayed A et al: Diagnostic accuracy of MRI for detecting inferior vena cava wall invasion in renal cell carcinoma tumor thrombus using quantitative and subjective analysis. AJR Am J Roentgenol: 212: 562–569, 2019
19) Koga S et al: The diagnostic value of bone scan in patients with renal cell carcinoma. J Urol 166: 2126-2128, 2001

20) Rosen PR et al: Bone scintigraphy in the initial staging of patients with renal-cell carcinoma: concise communication. J Nucl Med 25: 289-291, 1984
21) Campbell RJ et al: Staging of renal cell carcinoma: cost-effectiveness of routine preoperative bone scans. Urology 25: 326-329, 1985
22) Blacher E et al: Value of routine radionuclide bone scans in renal cell carcinoma. Urology 26: 432-434, 1985
23) Staudenherz A et al: Is there a diagnostic role for bone scanning of patients with a high pretest probability for metastatic renal cell carcinoma? Cancer 85: 153-155, 1999
24) Uchida K et al: F-FDG PET/CT for diagnosis of osteosclerotic and osteolytic vertebral metastatic lesions: comparison with bone scintigraphy. Asian Spine J 7: 96-103, 2013
25) Park JW et al: Significance of 18F-fluorodeoxyglucose positron-emission tomography/computed tomography for the postoperative surveillance of advanced renal cell carcinoma. BJU Int 103: 615-619, 2009

BQ 71 Is CT recommended when a urothelial tumor of the upper urinary tract is suspected?

Statement

CT urography, which involves imaging in the excretory phase of contrast-enhanced CT, is recommended for patients in the high-risk group who are suspected of having an upper urinary tract urothelial tumor. The high-risk group includes patients with a history of urothelial tumors and middle-aged and elderly patients with macroscopic hematuria.

Background

The characteristics of urothelial carcinoma are multiple simultaneous occurrences and a high rate of recurrence. Its diagnosis requires detailed examination of the urinary tract as a whole, including the renal pelvis, ureter, and bladder. Although bladder tumors can be diagnosed by cystoscopy, upper urinary tract urothelial tumors are difficult to diagnose. CT urography is becoming widely used for the detailed examination of upper urinary tract tumors, and the evidence regarding its usefulness and issues is reviewed below.

Explanation

Intravenous urography has long been the first choice as an imaging modality for simple screening of the urinary tract as a whole, and CT urography using MDCT, which involves excretory phase imaging after contrast medium administration, has been reported to be useful. Maximum-intensity projection (MIP) or volume rendering (VR) enables intravenous urography-like pyelograms to be easily generated. CT urography also allows detailed observation of urinary tract and non-urinary tract lesions in normal high-resolution transverse images. In Europe and the United States, CT urography has rapidly become widely used, and intravenous urography is now rarely performed. The detection sensitivity of CT urography for upper urinary tract urothelial tumor has been reported to be very high, ranging from 91% to 97%.[1-3] An article that compared CT urography and intravenous urography with respect to the diagnostic results for upper urinary tract urothelial carcinoma in patients with hematuria reported sensitivity, specificity, and diagnostic accuracy of intravenous urography ranging from 75% to 80%, 81% to 86%, and 81% to 85%, respectively and those of CT urography ranging from 94% to 96%, 95% to 100%, and 94% to 99%, thus, the results for CT urography were superior to those for intravenous urography.[4, 5] The guidelines of the American College of Radiology give intravenous urography scores of 1, 2, and 3 points (the lowest rank out of 9 points) and CT urography scores of 7, 8, and 9 points (the highest rank) as a method for examining patients with hematuria (secondary source 1). The guidelines of the European Association of Urology and the Japanese Urological Association also strongly recommend CT urography to diagnose upper urinary tract tumors (secondary sources 2 and 3).

However, a problem with CT urography is that the radiation exposure involved in a single examination is 2 to 3 times higher than the radiation exposure with intravenous urography (~ 15 to 30 mSv with CT urography and 5 to 10 mSv with intravenous urography, according to previous reports). Consequently, the guidelines of the European Society of Urogenital Radiology recommend that the indication for CT urography be limited to patients aged ≥ 40 years with macroscopic hematuria, who are more likely to have urothelial carcinomas (secondary source 4). The use of the iterative reconstruction method and low-tube-voltage imaging is being widely implemented clinically to reduce the radiation exposure that has impeded widespread CT urography use.[6, 8)] The use of low-tube-voltage imaging and dual-energy CT are also being widely adopted to reduce the contrast medium dose without reducing image quality. 8,9) In groups at high risk of upper urinary tract tumors, 3-phase imaging involving plain imaging, either corticomedullary- or nephrographic-phase imaging, and excretory phase imaging is generally performed, however, debate continues in this regard.[10)]

Search keywords and secondary sources used as references

PubMed was searched using the following keywords: urothelial tumor, CT, and CT urography.

In addition, the following were referenced as secondary sources.

1) Wolfman DJ et al: ACR Appropriateness Criteria®: hematuria. J Am Coll Radiol 17: S138-S147, 2020
2) Rouprêt M et al: European Association of Urology guidelines on upper urinary tract urothelial carcinomas: 2020 update. Eur Urol 79 (1): 62-79, 2021
3) Oya M et al: Evidenced-based clinical practice guideline for upper tract urothelial carcinoma (summary--Japanese Urological Association, 2014 edition). Int J Urol 22 (1): 3-13, 2015 (replace this reference to English version identical to Japanese Guideline.
4) Van Der Molen AJ et al: CT urography: definition, indications and techniques: a guideline for clinical practice. Eur Radiol 18: 4-17, 2008

References

1) Cowan NC et al: Multidetector computed tomography urography for diagnosing upper urinary tract urothelial tumour. BJU International 99: 1363-1370, 2007
2) Chlapoutakis K et al: Performance of computed tomographic urography in diagnosis of upper urinary tract urothelial carcinoma, in patients presenting with hematuria: systematic review and meta-analysis. Eur J Radiol 73: 334-338, 2010
3) Wang LJ et al: Diagnostic accuracy of transitional cell carcinoma on multidetector computerized tomography urography in patients with gross hematuria. J Urol 181: 524-531, 2009
4) Wang LJ et al: Multidetector computerized tomography urography is more accurate than excretory urography for diagnosing transitional cell carcinoma of the upper urinary tract in adults with hematuria. J Urol 183: 48-55, 2010
5) Jinzaki M et al: Comparison of CT urography and excretory urography in the detection and localization of urothelial carcinoma of the upper urinary tract. AJR Am J Roentgenol 196: 1102-1109, 2011
6) Juri H et al: Low-dose computed tomographic urography using adaptive iterative dose reduction 3-dimensional: comparison with routine-dose computed tomography with filtered back projection. J Comput Assist Tomogr 37: 426-431, 2013
7) Kim SH et al: Comparison of full- and half-dose image reconstruction with filtered back projection or sinogram-affirmed iterative reconstruction in dual-source single-energy MDCT urography. AJR Am J Roentgenol 211: 641-648, 2018
8) Kim SY et al: Low-tube-voltage CT urography using low-concentration-iodine contrast media and iterative reconstruction: a multi-institutional randomized controlled trial for comparison with conventional CT urography. Korean J Radiol 19: 1119-1129, 2018
9) Shuman WP et al: Dual-energy CT urography with 50% reduced iodine dose versus single-energy CT urography with standard iodine dose. AJR Am J Roentgenol 212: 117-123, 2019
10) Fojecki G et al: Consultation on UTUC, Stockholm 2018 aspects of diagnosis of upper tract urothelial carcinoma. World J Urol 37: 22712278, 2019

BQ 72 Is MRI recommended to determine the invasion depth of bladder cancer?

Statement

MRI is recommended before transurethral resection of a bladder tumor if cystoscopy indicates possible muscle-invasive bladder cancer.

Background

In bladder cancer, the treatment plan and survival vary depending on invasion depth. The presence or absence of muscle invasion is particularly important for assessing the suitability of bladder-sparing treatment. Invasion depth determination that uses the high contrast resolution of MRI is considered reliable.

Explanation

Muscle invasion of bladder cancer is definitively determined by the pathological diagnosis of specimens resected in the transurethral resection of a bladder tumor (TUR-BT). However, underestimation is also known to occur not infrequently with pathological diagnosis.[1, 2)] MRI is normally omitted if small pedunculated lesions are observed by cystoscopy, and the likelihood of non-muscle invasive bladder cancer is high. MRI is performed for staging before TURBT for lesions for which muscle-invasive cancer cannot be ruled out by cystoscopy. The Vesical Imaging-Reporting and Data System (VI-RADS), which describes standard MRI imaging and diagnostic methods, was published in 2018 against a background of widespread MRI diagnosis of bladder cancer. The purpose of VI-RADS is to predict the muscle invasion of incipient or recurrent bladder cancer. MRI is performed before TURBT to avoid postoperative reactive change of the TURBT and to determine the VI-RADS morphological category. T2-weighted, diffusion-weighted, and dynamic contrast enhanced MRI are performed. Anatomical information is obtained with T2-weighted imaging. With diffusion-weighted and dynamic contrast imaging, contrast between tumors and normal tissue is high. Diffusion-weighted images and dynamic contrast-enhanced MRI play a central role in predicting muscle invasion. Prediction of the likelihood of muscle invasion is made according to the categorization table (Table). As the category number increases, the likelihood of muscle invasion increases. If the quality of the diffusion-weighted images is good, the category on diffusion-weighted imaging is adopted as the final determination. If the quality of the diffusion-weighted images is inadequate, the category on dynamic contrast imaging is adopted as the final determination. A meta-analysis found that, with the use of VI-RADS, sensitivity and specificity for muscle invasion were 0.83 (95% CI, 0.70 to 0.90) and 0.90 (95% CI, 0.83 to 0.95), respectively.[3)] Good interobserver agreement rates (kappa coefficients) ranging from 0.81 to 0.90 were reported. The reported prevalence of muscle-invasive cancer by category was 0% for category 1, 19% for category 2, 44% for category 3, 90% for category 4, and 94% for category 5 (investigation with 50% prevalence of muscle-invasive bladder cancer in all patients).[4)] At present, the

fact that the use of TURBT and pathological diagnosis is the general rule for diagnosing muscle invasion remains unchanged. However, MRI is expected to be a tool that complements their use. Moreover, the ability of CT to differentiate muscle-invasive cancer from non-muscle-invasive cancer is weak.

Table. Categories of the Vesical Imaging-Reporting and Data System (VI-RADS, prepared based on secondary source 2)

Category	T2-Weighted Imaging (structural category: SC)	Diffusion-Weighted Imaging (DW category)	Dynamic MRI (CE category)
1	Uninterrupted low SI line representing the integrity of muscularis propria (lesion <1 cm; exophytic tumor with or without stalk and/or thickened inner layer)	Muscularis propria with intermediate continuous SI on DWI (lesion <1 cm, hyperintense on DWI and hypointense on ADC, with or without stalk and/or low SI thickened inner layer on DWI)	No early enhancement of the muscularis propria (lesions corresponding to SC 1 findings)
2	Uninterrupted low SI line representing the integrity of muscularis propria (lesion >1 cm; exophytic tumor with stalk and/or high SI thickened inner layer, when present, or sessile/broad-based tumor with high SI thickened inner layer, when present)	Muscularis propria with continuous intermediate SI on DWI (lesion >1 cm, hyperintense on DWI and hypointense on ADC, with low SI stalk and/or low SI thickened inner layer on DWI, or broad-based/sessile tumor with low/intermediate SI thickened inner layer on DWI)	No early enhancement of muscularis propria with early enhancement of inner layer (lesions corresponding to SC 2 findings)
3	Lack of category 2 findings with associated presence of an exophytic tumor without stalk, or sessile/broad-based tumor without high SI thickened inner layer but with no clear disruption of low SI muscularis propria	Lack of category 2 findings (lesions corresponding to T2 category 3 findings) but with no clear disruption of low SI muscularis propria.	Lack of category 2 findings (lesions corresponding to SC category 3 findings) but with no clear disruption of low SI muscularis propria
4	Interruption of low SI line suggesting extension of the intermediate SI tumor tissue to muscularis propria	High SI tumor on DWI and low SI tumor on ADC extending focally to muscularis propria.	Tumor early enhancement extends focally to muscularis propria
5	Extension of intermediate SI tumor to extravesical fat, representing the invasion of the entire bladder wall and extravesical tissues	High SI tumor on DWI and low SI tumor on ADC extending to the entire bladder wall and extravesical fat.	Tumor early enhancement extends to the entire bladder wall and to extravesical fat

SI: signal intensity

Panebianco V et al: Multiparametric magnetic resonance imaging for bladder cancer: development of VI-RADS (Vesical Imaging-Reporting And Data System). Eur Urol 74: 294-306, 2018

Search keywords and secondary sources used as references

PubMed was searched using the following keywords: magnetic resonance imaging, urinary bladder neoplasms, and neoplasm staging.

In addition, the following were referenced as secondary sources.

1) Japanese Urological Association, Ed.: 2019 Clinical Practice Guidelines for Bladder Cancer. Igakutosho Shuppan, 2019.
2) Panebianco V et al: Multiparametric magnetic resonance imaging for bladder cancer: development of VI-RADS (Vesical Imaging-Reporting And Data System). Eur Urol 74: 294-306, 2018

References

1) Cumberbatch MGK et al: Repeat transurethral resection in non-muscle-invasive bladder cancer: a systematic review. Eur Urol 73: 925-933, 2018
2) Naselli A et al: Role of restaging transurethral resection for T1 non-muscle invasive bladder cancer: a systematic review and meta-analysis. Eur Urol Focus 4: 558-567, 2018
3) Woo S et al: Diagnostic performance of vesical imaging reporting and data system for the prediction of muscle-invasive bladder cancer: a systematic review and meta-analysis. Eur Urol Oncol 3: 306-315, 2020
4) Ueno Y et al: Diagnostic accuracy and interobserver agreement for the Vesical Imaging-Reporting and Data System for muscle-invasive bladder cancer: a multireader validation study. Eur Urol 76: 54-56, 2019

CQ 17 Is omitting contrast-enhanced MRI recommended when MRI is performed to detect clinically significant prostate cancer in patients with incipient disease?

Recommendation

Omitting contrast-enhanced MRI is weakly recommended for MRI examinations performed to detect clinically significant prostate cancer. This applies only to facilities capable of all of the following: 3T-MRI imaging under appropriate conditions, image evaluation by a radiologist with extensive experience interpreting prostate MRI, and pathological diagnosis by biopsy guided by location information obtained with MRI.

Recommendation strength: 2, strength of evidence: weak (C), agreement rate: 87% (13/15)

Background

Prostate cancer is a malignancy that affects approximately 90,000 people in Japan. It is classified as either clinically significant (CS) cancer that requires therapeutic intervention or clinically insignificant/not clinically significant (NCS) cancer with little need for intervention. There have been numerous recent reports that prostate MRI can efficiently detect CS cancer, and its role as a pre-biopsy examination has come to be regarded as important. The initial version of the Prostate Imaging Reporting and Data System (PI-RADS), which describes standard MRI examination and diagnostic methods for prostate cancer, indicated that it is diagnosed by multiparametric MRI (mpMRI), which combines T2-weighted, diffusion-weighted, and dynamic contrast-enhanced imaging (secondary source 1). Beginning from version 2, however, PI-RADS has indicated that the role of dynamic contrast-enhanced imaging is limited (secondary sources 2 and 3). Since then, there has been increased reporting of the usefulness of biparametric MRI (bpMRI), which omits dynamic contrast-enhanced imaging and uses only T2-weighted and diffusion-weighted imaging. Because bpMRI does not involve the use of a contrast medium, reductions in examination time and cost and a decrease in the workload of medical staff can be expected, and there is no need for concern about adverse reactions to a contrast medium. On the other hand, there is apprehension about lower detection performance with bpMRI than with mpMRI in CS cancers.

For the present discussion, the question of whether omitting contrast-enhanced MRI is recommended when MRI examination is performed to detect incipient CS cancer was raised as a CQ, and a qualitative systematic review was conducted regarding bpMRI and mpMRI.

Explanation

For this systematic review, a decrease in CS cancer detection performance was specified as an adverse outcome. A literature search for studies that compared the diagnostic performance of bpMRI and mpMRI was performed using the keywords indicated below and yielded 9 relevant articles.[1-9)] All 9 articles were reports of cross-sectional studies. In all but 1 of the articles on MRI, 3T systems were used. In all of the articles, the image evaluations were performed by radiologists with abundant experience in interpreting prostate MRI. For the MRI evaluation method, criteria basically in accordance with PI-RADS or original diagnostic criteria such as a Likert scale were adopted. In nearly all of the articles, pathological diagnosis involved either total prostatectomy or targeted biopsy guided by location information obtained with MRI. Although there is no internationally uniform definition of CS cancer, the definition used in the 9 articles was similar to that adopted clinically (Table). The 9 articles had a low risk of bias and low indirectness.

The sensitivity, specificity, and diagnostic accuracy rate for CS cancer ranged from 53% to 96%, 15% to 93%, and 42% to 89%, respectively, with bpMRI and from 52% to 95%, 16% to 93%, and 42% to 88% for mpMRI. Thus, the diagnostic performance of bpMRI and mpMRI was roughly equal.[1-9)] In 3 articles, an ROC analysis was performed. AUC ranged from 0.68 to 0.81 with bpMRI and from 0.71 to 0.79 with mpMRI. Thus, no difference was seen between the 2 methods.[2, 4, 7)] One article that used a PI-RADS (version 2) category of 4 or higher as the criterion for a positive finding reported a trade-off between sensitivity and specificity, with significantly lower sensitivity (63% vs. 80%) and significantly higher specificity (72% to 45%) seen with bpMRI than with mpMRI. Thus, the results showed that the number of false-negative lesions increased if a contrast medium was not used (adverse outcome).[2)] However, the diagnostic accuracy rate (66% vs. 71%) and AUC (0.81 vs. 0.79) were similar for the 2 methods.[2)]

Table. Definition of clinically significant prostate cancer used in the 9 articles extracted in the systematic review

Definition	Reference No.
Lesion with GS ≥ 7	1), 3), 9)
Lesion with GS ≥ 7 and/or tumor volume ≥ 0.5 mL and/or lesion with extracapsular extension	2)
Lesion with GS ≥ 7 and/or lesion with extracapsular extension	4)
Lesion with GS ≥ 7 and/or lesion with tumor length ≥ 5 mm	5)
Lesion with intermediate to high risk (NCCN guidelines*)	6)
Lesion with GS ≥ 7 and/or lesion with tumor volume ≥ 5 mL	7)
GS 6 lesion with more than 3 positive cores by biopsy and/or GS 6 lesion that occupies ≥ 50% of biopsy length or lesion with GS ≥ 7	8)

GS: Gleason score, NCCN: National Comprehensive Cancer Network

* Prostate cancer risk classification from NCCN guidelines (version 2.2014)
low risk: PSA (prostate specific antigen) ≤ 10 ng/mL, GS ≤ 6, and T1-T2a
intermediate risk: PSA=10-20 ng/mL, GS 7, and T2b
high risk: PSA > 20 ng/mL, and/or GS ≥ 8, and/or T2c-T3a

Based on the above findings, the conclusion of this systematic review was that bpMRI and mpMRI are comparable in diagnostic performance.

Although no systematic review was conducted for measures other than diagnostic performance, it is self-evident that omitting contrast-enhanced MRI shortens the examination time, reduces the cost burden, and eliminates the risk of contrast medium adverse reactions for the patient. For medical staff, it eliminates the need to interview the patient about contrast media, secure a route for contrast medium administration, and address adverse reactions. It also shortens the length of imaging performed by the radiological technologist, reducing the workload of medical staff. A bpMRI examination that omits contrast-enhanced MRI is therefore weakly recommended to detect CS cancer. This applies only to facilities capable of all of the following: 3T-MRI imaging under appropriate conditions, image evaluation by a radiologist with extensive experience interpreting prostate MRI, and pathological diagnosis by biopsy guided by location information obtained with MRI. Conversely, evaluation by mpMRI that includes contrast-enhanced MRI is preferable at facilities that cannot meet the above preconditions. This is due to concern about lower detection performance with bpMRI than with mpMRI in CS cancer. In performing bpMRI examinations, hyoscine butylbromide needs to be administered before the examination to reduce motion artifacts caused by gastrointestinal peristalsis. In addition, imaging acquisition techniques that are in accordance with PI-RADS should be determined, such as high-spatial-resolution T2-weighted imaging and high b-value (≥ 1,400 s/mm^2) diffusion-weighted imaging (secondary sources 2 and 3). Moreover, because the subjects assessed in this systematic review were patients with clinically suspected CS cancer, these recommendations do not apply to prostate cancer screening. They also do not apply to patients with a higher than normal risk for prostate cancer, such as those with a family history of prostate cancer and those with prior negative biopsy and elevated PSA levels, due to concern about the major detriment that would result from a bpMRI false-negative. In addition, the diagnostic performance of bpMRI and mpMRI for detecting post-treatment recurrent tumors and staging (extracapsular extension, seminal vesicle invasion) has not been shown to be comparable, and contrast-enhanced examinations are therefore added as needed.

Search keywords and secondary sources used as references

PubMed was searched using the following keywords: prostate neoplasms, prostate cancer, clinically significant cancer, magnetic resonance imaging, multiparametric MRI, biparametric MRI, abbreviated MRI, and Prostate Imaging Reporting and Data System (PI-RADS).

In addition, the following were referenced as secondary sources.

1) Barentsz JO et al: ESUR prostate MR guidelines 2012. Eur Radiol 22: 746-757, 2012
2) Weinreb JC et al: PI-RADS Prostate Imaging - Reporting and Data System 2015, Version 2. Eur Urol 69: 16-40, 2016
3) Turkbey B et al: Prostate Imaging Reporting and Data System Version 2.1: 2019 Update of Prostate Imaging Reporting and Data System Version 2. Eur Urol 76: 340-351, 2019

References

1) van der Leest M et al: High diagnostic performance of short magnetic resonance imaging protocols for prostate cancer detection in biopsy-naive men: the next step in magnetic resonance imaging accessibility. Eur Urol 76: 574-581, 2019
2) Choi MH et al: Prebiopsy biparametric MRI for clinically significant prostate cancer detection with PI-RADS version 2: a multicenter study. AJR Am J Roentgenol 212: 839-846, 2019
3) Mussi TC, et al: Comparison between multiparametric MRI with and without post - contrast sequences for clinically significant prostate cancer detection. Int Braz J Urol 44: 1129-1138, 2018
4) Di Campli E et al: Diagnostic accuracy of biparametric vs multiparametric MRI in clinically significant prostate cancer: comparison between readers with different experience. Eur J Radiol 101: 17-23, 2018
5) Lee DH et al: Comparison of multiparametric and biparametric MRI in first round cognitive targeted prostate biopsy in patients with PSA levels under 10 ng/mL. Yonsei Med J 58: 994-999, 2017
6) Kuhl CK et al: Abbreviated biparametric prostate MR imaging in men with elevated prostate-specific antigen. Radiology 285: 493-505, 2017
7) Barth BK et al: Detection of clinically significant prostate cancer: short dual-pulse sequence versus standard multiparametric MR imaging: a multireader study. Radiology 284: 725-736, 2017
8) Mussi TC et al: Are dynamic contrast-enhanced images necessary for prostate cancer detection on multiparametric magnetic resonance imaging? Clin Genitourin Cancer 15: e447-e454, 2017
9) Thestrup KC et al: Biparametric versus multiparametric MRI in the diagnosis of prostate cancer. Acta Radiol Open 5: 2058460116663046, 2016

BQ 73 Is MRI recommended for the local staging of prostate cancer?

Statement

MRI is recommended to evaluate extracapsular and seminal vesicle invasion in prostate cancer of intermediate or high risk.

(Note: With a body surface coil, a ≥ 1.5T system needs to be used, and the imaging conditions must be optimized.)

Background

Prostate cancer is increasing, making it important to standardize the diagnostic imaging methods. Although MRI is considered a reliable diagnostic imaging method for the local staging of prostate cancer, it is not performed for all patients. Whether MRI is useful for the local staging of prostate cancer (extracapsular invasion, seminal vesicle invasion) and the circumstances in which its usefulness increases are examined below.

Explanation

MRI is considered the most reliable diagnostic imaging method for the local staging of prostate cancer. The Prostate Imaging and Reporting and Data System (PI-RADS) has been widely adopted in recent years to decrease the variability in MRI diagnostic performance that occurs depending on the experience of the reader and to standardize imaging and interpretation methods. However, its main objective is cancer detection, and a specific scoring method for local staging has not been established (secondary source 2). Many investigations that have examined MRI diagnostic performance with respect to extracapsular extension have used transrectal coils. Recently, however, more investigations have used a 3T-MRI system without using a transrectal coil. High-resolution T2-weighted imaging is necessary to accurately evaluate extracapsular extension and neurovascular bundle and seminal vesicle invasion. However, a 3T-MRI system is advantageous because it enables thin-slice, high-spatial-resolution imaging to be performed using a body surface coil.

Reliable T2-weighted imaging findings for extracapsular extension include the following: ① changes in the prostate contour (local protrusion and asymmetry), ② morphological changes in the adjacent neurovascular bundles (left-right asymmetry), ③ rupture of the capsular structure, ④ obliteration of rectoprostatic angle, and ⑤ direct invasion to the neurovascular bundles. These findings are not all given the same weight. Findings ① and ② are indirect findings, whereas ④ and ⑤, which directly indicate an extraprostatic mass, are more strongly suggestive of extracapsular extension. Finding ⑥, the tumor contact length with the prostatic capsule, has been designated a predictor of extracapsular invasion. A contact length of ≥ 6 mm is suggestive of slight extracapsular invasion, and a contact length of ≥ 10 mm is suggestive of unambiguous extracapsular invasion.[1)] Reports vary regarding the diagnostic performance of

T2-weighted imaging with respect to extracapsular extension. Sensitivity, specificity, and diagnostic accuracy have been found to range from 22% to 82%, 70% to 100%, and 61% to 84%, respectively.[2-17] In a meta-analysis by de Rooij et al. that compiled data on the diagnostic performance of MRI in staging, the pooled sensitivity and specificity for extracapsular extension were 57% (95% CI, 49% to 64%) and 91% (95% CI, 88% to 93%), respectively.[18] Diagnostic performance is also determined by whether the evaluation can be performed in the plane orthogonal to the surface where the tumor and capsule are in contact.

Although T2-weighted imaging plays the central role in evaluating extracapsular extension, the certainty of extracapsular extension is increased by the addition of diffusion-weighted imaging.[19] However, whether adding an evaluation of extracapsular extension by dynamic contrast imaging to T2-weighted imaging is meaningful depends, in part, on the experience of the reader.[13, 20]

Findings in T2-weighted images for seminal vesicle invasion include the localized or diffuse elimination of the botryoidal internal structure of the seminal vesicle due to a hypointense mass, localized thickening of the seminal vesicle wall and septum, and elimination of the angle between the prostate and seminal vesicle.[21] Reports on diagnostic performance with respect to seminal vesicle invasion have indicated sensitivity, specificity, and diagnostic accuracy ranging from 23% to 100%, 75% to 100%, and 76% to 97%, respectively.[3-6, 8-10, 14-17] A meta-analysis regarding seminal vesicle invasion showed sensitivity of 51% without the use of a transrectal coil and 59% with transrectal coil use for T2-weighted imaging.[18] With the addition of diffusion-weighted or dynamic contrast imaging, sensitivity increased from 53% to 64%.[18]

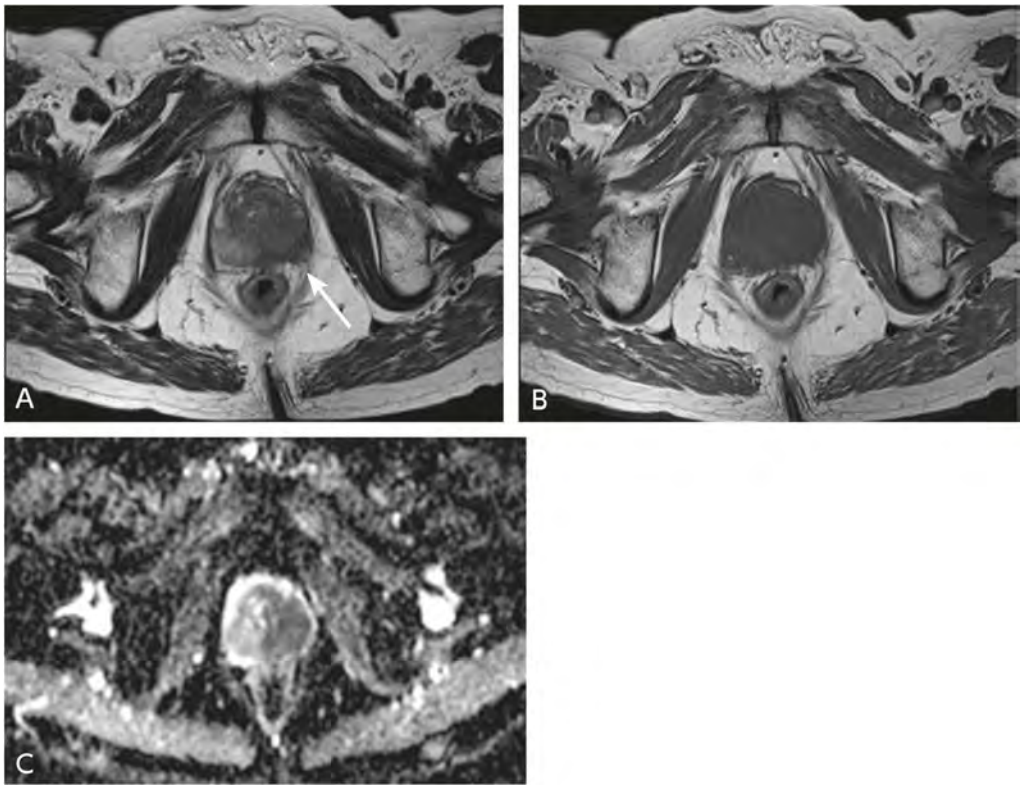

Figure. Prostate cancer (patient with PSA of 22 ng/mL)

A: MRI, T2-weighted image; B: MRI, T1-weighted image; C: MRI, ADC map, b-value = 1,000 s/mm^2
The left border area has changed to hypointense in the T2-weighted image, and this extends to the transitional area. Cancer is therefore suspected. The contour of the left dorsal region is spiny and shows a signal similar to that of the main lesion. Extracapsular invasion is suspected (→). The T1-weighted image clearly shows the disturbance of the contour. The ADC map clearly shows the intraprostatic tumor distribution, but it cannot indicate extracapsular progression in detail.

In the diagnosis and treatment of prostate cancer, appropriate treatment is selected by taking into account the risk classification, which combines the clinical stage, prostate-specific antigen (PSA) level, Gleason score, and the amount of cancer tissue in the biopsy needle. In Europe and the United States, it is also widely recognized that, when an imaging examination is performed, the examination is selected by taking into account the risk of the tumor. This is also indicated in guidelines [European Association of Urology (EAU) 2020, secondary source 3; American College of Radiology (ACR) 2017, secondary source 4]. A retrospective investigation found that MRI diagnostic performance with respect to extraprostatic extension was poor in low-risk patients, but good in patients at moderate or greater risk. However, the variation in specificity between risk levels was small.[8)] Patients with a PSA level > 10 mg/mL or Gleason score > 7 on biopsy are considered to be at moderate or greater risk, and evaluating extracapsular and seminal vesicle invasion by MRI has merit in such cases.

In Japan, diagnosis is often performed by imaging using a body surface coil, such as a pelvic phased-array coil. Imaging with an integrated system that uses both a body surface coil and a transrectal coil improves staging compared with imaging using a body surface coil alone.[14)] However, transrectal coil

use has not been widely adopted in Japan. Even if only a body surface coil is used, no large difference in staging capability is seen if a ≥ 1.5T MRI system is used and imaging is performed after the elimination of rectal gas, which reduces image quality, with a thin slice thickness of approximately 4 mm and good spatial resolution.[17] The most recent version of PI-RADS, version 2.1, indicates that the use of a transrectal coil is not required (secondary source 2).

Multiparametric MRI combines T2-weighted imaging, which has customarily been used to show morphological images, with functional imaging methods such as diffusion-weighted imaging or dynamic contrast imaging. Although its impact does not extend to cancer detection, mpMRI may improve pretreatment staging by incorporating information such as clinical data, tumor volume, and the length of the area of contact between a tumor and the prostatic capsule.[11, 22-24]

Search keywords and secondary sources used as references

PubMed was searched using the following keywords: prostate cancer, staging, and MRI.

In addition, the following were referenced as secondary sources.

1) Japan Radiological Society, Ed.: Diagnostic Imaging Guidelines 2016. KANEHARA & Co., 2016.
2) Turkbey B et al: Prostate Imaging Reporting and Data System Version 2.1: 2019 update of Prostate Imaging Reporting and Data System Version 2. Eur Urol 76: 340-351, 2019
3) Mottet N et al: EAU guidelines on prostate cancer. European Association of Urology, 2020
4) Coakley FV et al: ACR Appropriateness Criteria®: prostate cancer-pretreatment detection, surveillance, and staging. J Am Coll Radiol 14: S245-S257, 2017

References

1) Rosenkrantz AB et al: Length of capsular contact for diagnosing extraprostatic extension on prostate MRI: assessment at an optimal threshold. J Magn Reson Imaging 43: 990-997, 2016
2) Yu KK et al: Detection of extracapsular extension of prostate carcinoma with endorectal and phased-array coil MR imaging: multivariate feature analysis. Radiology 202: 697-702, 1997
3) Sanchez-Chapado M et al: Comparison of digital rectal examination, transrectal ultrasonography, and multicoil magnetic resonance imaging for preoperative evaluation of prostate cancer. Eur Urol 32: 140-149, 1997
4) Presti JC Jr et al: Local staging of prostatic carcinoma: comparison of transrectal sonography and endorectal MR imaging. Am J Roentgenol 166: 103-108, 1996
5) Cornud F et al: Local staging of prostate cancer by endorectal MRI using fast spin-echo sequences: prospective correlation with pathological findings after radical prostatectomy. Br J Urol 77: 843-850, 1996
6) Perrotti M et al: Endo-rectal coil magnetic resonance imaging in clinically localized prostate cancer: is it accurate? J Urol 156: 106-109, 1996
7) Ogura K et al: Dynamic endorectal magnetic resonance imaging for local staging and detection of neurovascular bundle involvement of prostate cancer: correlation with histopathologic results. Urology 57: 721-726, 2001
8) Allen DJ et al: Does body-coil magnetic-resonance imaging have a role in the preoperative staging of patients with clinically localized prostate cancer? BJU Int 94: 534-538, 2004
9) Nakashima J et al: Endorectal MRI for prediction of tumor site, tumor size, and local extension of prostate cancer. Urology 64: 101-105, 2004
10) Chelsky MJ et al: Use of endorectal surface coil magnetic resonance imaging for local staging of prostate cancer. J Urol: 150: 391-395, 1993
11) Wang L et al: Prostate cancer: incremental value of endorectal MR imaging findings for prediction of extracapsular extension. Radiology 232: 133-139, 2004
12) Brassell SA et al: Correlation of endorectal coil magnetic resonance imaging of the prostate with pathologic stage. World J Urol 22: 289-292, 2004

13) Fütterer JJ et al: Staging prostate cancer with dynamic contrast-enhanced endorectal MR imaging prior to radical prostatectomy: experienced versus less experienced readers. Radiology 237: 541-549, 2005
14) Fütterer JJ et al: Prostate cancer: comparison of local staging accuracy of pelvic phased-array coil alone versus integrated endorectal–pelvic phased-array coils. Local staging accuracy of prostate cancer using endorectal coil MR imaging. Eur Radiol 17: 1055-1065, 2007
15) Chandra RV et al: Endorectal magnetic resonance imaging staging of prostate cancer. ANZ J Surg 77: 860-865, 2007
16) Park BK et al: Comparison of phased-array 3.0-T and endorectal 1.5-T magnetic resonance imaging in the evaluation of local staging accuracy for prostate cancer. J Comput Assist Tomogr 31: 534-538, 2007
17) Lee SH et al: Is endorectal coil necessary for the staging of clinically localized prostate cancer?: comparison of non-endorectal versus endorectal MR imaging. World J Urol 28: 667-672, 2010
18) de Rooij M et al: Accuracy of magnetic resonance imaging for local staging of prostate cancer: a diagnostic meta-analysis. Eur Urol 70: 233-245, 2016
19) Woo S et al: Extracapsular extension in prostate cancer: added value of diffusion-weighted MRI in patients with equivocal findings on T2-weighted imaging. AJR Am J Roentgenol 204: W168-175, 2015
20) Bloch BN et al: Prediction of prostate cancer extracapsular extension with high spatial resolution dynamic contrast-enhanced 3-T MRI. Eur Radiol 22: 2201–2210, 2012.
21) Roethke M et al: Seminal vesicle invasion: accuracy and analysis of infiltration patterns with high-spatial resolution T2-weighted sequences on endorectal magnetic resonance imaging. Urol Int 92: 294-299, 2014
22) Schieda N et al: MRI assessment of pathological stage and surgical margins in anterior prostate cancer (APC) using subjective and quantitative analysis. J Magn Reson Imaging 45: 1296-1303, 2017
23) Lim C et al: Evaluation of apparent diffusion coefficient and MR volumetry as independent associative factors for extra-prostatic extension (EPE) in prostatic carcinoma. J Magn Reson Imaging 43: 726-736, 2016
24) Baco E et al: Predictive value of magnetic resonance imaging determined tumor contact length for extracapsular extension of prostate cancer. J Urol 193: 466, 2015

BQ 74 Is bone scintigraphy recommended for prostate cancer staging and posttreatment follow-up?

Statement

The use of bone scintigraphy should be avoided in low-risk patients (PSA ≤ 10 ng/mL, Gleason score ≤ 7) because of the low positivity rate. However, it is useful in patients with symptoms suggestive of bone metastasis and posttreatment PSA-recurrent patients.

Background

Following the lymph nodes, bone is the second most common organ for prostate cancer metastasis. Bone scintigraphy is a nuclear medicine examination that uses a ^{99m}Tc-labeled phosphate compound (methylene diphosphonate, hydroxymethylene diphosphonate). Its benefit is that it enables sensitive whole-body screening for bone lesions. Although it has long been used in prostate cancer care, the routine use of bone scintigraphy for staging and posttreatment follow-up poses problems from the perspectives of radiation exposure and cost. Recently, computer-aided diagnosis (CAD) has been introduced to bone scintigraphy, and there have been sporadic reports indicating that it is useful for improving diagnostic performance and predicting prognosis. This section reviews the relatively recent literature dealing with bone scintigraphy in prostate cancer and summarizes how it is used.

Explanation

In a meta-analysis that compared the diagnostic performance of choline-PET/CT (not covered by national health insurance in Japan), MRI, and bone scintigraphy with respect to bone metastasis in prostate cancer, an analysis of 11 articles on a per-patient basis showed that the sensitivity and specificity of bone scintigraphy were 79% and 82%, respectively, and that the diagnostic performance of bone scintigraphy was inferior to that of choline-PET/CT and MRI.[1)]

Rather than diagnostic performance, many recent studies of bone scintigraphy in prostate cancer have examined the positivity rate of bone scintigraphy according to patient characteristics (e.g., serum PSA level, Gleason score, T stage of the primary tumor).[2-9)] A position that reflects these observations and is common to the guidelines of urology societies in Japan, Europe, and the United States is that patients with a PSA level of ≤ 10 ng/mL and Gleason score ≤ 7 who are asymptomatic are at low risk of metastasis, and that bone scintigraphy for staging is not recommended for such patients. However, it may be meaningful for identifying lesion locations in patients such as those with symptoms suggestive of bone lesions and posttreatment PSA-recurrent patients (particularly patients with a high PSA doubling rate). Several reports describe improved diagnostic performance with respect to bone metastasis when SPECT or SPECT/CT is added to bone scintigraphy.[10-12)] However, the prolonged imaging duration and, in the case of SPECT/CT, CT radiation exposure, pose problems for these methods. Rather than being routinely added, SPECT or

SPECT/CT imaging should be performed when findings difficult to assess by planar imaging are obtained, and the imaging should be restricted to a localized area.

With regard to the diagnostic performance of CAD, many articles indicate that its sensitivity and specificity both exceed 80%.[13-15] It should be noted, however, that CAD basically just separates lesions according to the likelihood that they are benign or malignant based on pattern recognition, and it in no way reflects factors such as patient characteristics and findings from other imaging examinations. The bone scan index (BSI), which uses CAD to quantify the degree of whole-body abnormal bone uptake, has been reported to be an index that predicts treatment efficacy and an independent prognosis predictor (reflecting patient prognosis).[16,17] BSI is an objective index of posttreatment decreased uptake, and it is considered particularly useful for evaluating the condition of certain patients, such as those with diffuse bone metastases.

Search keywords and secondary sources used as references

PubMed was used to search the literature with the following keywords: prostate cancer, bone metastasis, bone scan, and bone scintigraphy. The period searched was from 2015 to June 2019, and 1 new article (reference 17) was used in the review. Consequently, including the 16 articles cited in the 2016 edition of the guidelines (CQ147), a total of 17 articles were cited.

In addition, the following were referenced as secondary sources.

1) Japanese Urological Association, Ed.: 2016 Clinical Practice Guidelines for Prostate Cancer. Medical Review, 2016.
2) Mottet N et al: EAU guidelines on prostate cancer. European Association Urology, 2020

References

1) Shen G et al: Comparison of choline-PET/CT, MRI, SPECT, and bone scintigraphy in the diagnosis of bone metastases in patients with prostate cancer: a meta-analysis. Skeletal Radiol 43: 1503-1513, 2014
2) Zacho HD et al: Prospective multicenter study of bone scintigraphy in consecutive patients with newly diagnosed prostate cancer. Clin Nucl Med 39: 26-31, 2014
3) Tanaka N et al: Bone scan can be spared in asymptomatic prostate cancer patients with PSA of ≤ 20 ng/ml and Gleason score of ≤ 6 at the initial stage of diagnosis. Jpn J Clin Oncol 41: 1209-1213, 2011
4) Lee SH et al: Is it suitable to eliminate bone scan for prostate cancer patients with PSA ≤ 20 ng/ml? World J Urol 30: 265- 269, 2012
5) Palvolgyi R et al: Bone scan overuse in staging of prostate cancer: an analysis of a veterans affairs cohort. Urology 77: 1330-1337, 2011
6) Briganti A et al: When to perform bone scan in patients with newly diagnosed prostate cancer: external validation of the currently available guidelines and proposal of a novel risk stratification tool. Eur Urol 57: 551-558, 2010
7) Hirobe M et al: Bone scanning: who needs it among patients with newly diagnosed prostate cancer? Jpn J Clin Oncol 37: 788-792, 2007
8) Ishizuka O et al: Prostate-specific antigen, Gleason sum and clinical T stage for predicting the need for radionuclide bone scan for prostate cancer patients in Japan. Int J Urol 12: 728-732, 2005
9) Yap BK et al: Are serial bone scan useful for the follow-up of clinically localized, low to intermediate grade prostate cancer managed with watchful observation alone? BJU Int 91: 613-617, 2003
10) McLoughlin LC et al: The improved accuracy of planar bone scintigraphy by adding single photon emission computed tomography (SPECT-CT) to detect skeletal metastases from prostate cancer. Ir J Med Sci 185: 101-105, 2016
11) Helyar V et al: The added value of multislice SPECT/CT in patients with equivocal bony metastasis from carcinoma of the prostate. Eur J Nucl Med Mol Imaging 37: 706-713, 2010
12) Even-Sapir E et al: The detection of bone metastases in patients with high-risk prostate cancer: ^{99m}Tc-MDP planar bone scintigraphy, single- and multi-field-of-view SPECT, ^{18}F-fluoride PET, and ^{18}F-fluoride PET/CT. J Nucl Med 47: 287-297, 2006

13) Koizumi M et al: Evaluation of a computer-assisted diagnosis system, BONENAVI version 2, for bone scintigraphy in cancer patients in a routine clinical setting. Ann Nucl Med 29: 138-148, 2015
14) Takahashi Y et al: Assessment of bone scans in advanced prostate carcinoma using fully automated and semi-automated bone scan index methods. Ann Nucl Med 26: 586-593, 2012
15) Sadik M et al: Improved classification of planar whole-body bone scans using a computer-assisted diagnosis system: a multicenter, multiple-reader, multiple-case study. J Nucl Med 50: 368-375, 2009
16) Mitsui Y et al: Prediction of survival benefit using an automated bone scan index in patients with castration-resistant prostate cancer. BJU Int 110: E628-E634, 2012
17) Zacho HD et al: Bone scan index is an independent predictor of time to castration-resistant prostate cancer in newly diagnosed prostate cancer: a prospective study. Urology 108: 135-141, 2017

BQ 75 Which imaging examinations are recommended for staging testicular tumors?

Statement

There is strong evidence that CT is useful for this purpose, and it is therefore recommended. There is no adequate scientific basis for recommending PET.

Background

Because most testicular tumors are testicular germ cell tumors, where simply “testicular tumors” is used below it refers to testicular germ cell tumors. With recent advances in chemotherapy, the cure rate for testicular tumors has become very high. According to a 2006 report, the 5-year survival rate was 94% for the good-risk group based on the classification of the International Germ Cell Cancer Collaborative Group, 83% for the intermediate-risk group, and 71% for the poor-risk group.[1)] One of the most important factors in achieving a high cure rate is accurate staging. The staging classification of the Japanese Urological Association is determined by the location and size of metastases. Based on these considerations, imaging examinations for staging testicular tumor—specifically CT and PET—were examined.

Explanation

CT is an examination that is necessary for staging testicular tumors. It is strongly recommended for this purpose in the representative guidelines for Europe and the United States, such as those of the American College of Radiology (ACR) and European Association of Urology (EAU), as well as the Japanese Urological Association (secondary sources 1 to 3). The most frequent sites of testicular tumor metastases are the retroperitoneal lymph nodes. Therefore, the entire abdomen should always be scanned. Although the diagnosis of retroperitoneal lymph node metastasis by CT (Fig.) basically involves the use of size criteria, sensitivity and specificity largely depend on the cutoff value used. Hilton et al. reported that when a cutoff of 10 mm was used, specificity was 100%, but sensitivity was only 37%.[2)] Lowering this to 4 mm improved sensitivity to 93%, but specificity was 58%. To strike a balance between sensitivity and specificity, Hudolin et al. proposed a cutoff of 7 to 8 mm.[3)] Moreover, lymph node length in the craniocaudal direction has been found to be correlated with metastasis,[4)] and MPR in coronal as well as transverse imaging planes, is useful. Diagnosis based on size has limitations, such as the fact that changes such as inflammatory swelling result in false positives, in addition to the fact that small metastases result in false negatives. However, diagnostic performance can be improved to some extent by understanding lymph flow anatomy. That is, with a right testicular tumor, the primary landing zone is the infrarenal inter-aortocaval lymph nodes, followed by the paracaval, the precaval, and preaortic lymph nodes. With a left testicular tumor, on the other hand, the primary landing zone is the infrarenal paraaortic lymph nodes, followed by the inter-aortocaval and the preaortic lymph nodes. Particular attention is needed if the lymph nodes at these sites are conspicuous.

For pulmonary metastasis detection, chest CT is more sensitive than plain chest radiography. However, it often produces false positives for lung lesions ≤ 10 mm in size. With stage I seminomas, it may be possible to omit chest CT if there are no abnormalities on chest radiography.[5)] Chest CT is considered excellent for detecting mediastinal lymph node metastasis, although there have been few reports in this regard.

No firm conclusion has been reached regarding the usefulness of adding FDG-PET for staging. PET performed to stage nonseminomas has been reported to provide significantly better sensitivity and negative predictive value than CT.[6, 7)] However, a 2007 prospective, multicenter study examined 111 patients who were positive for stage I vascular invasive nonseminomas. Of these, 87 were found to be negative by PET and underwent follow-up without treatment. During a median follow-up period of 12 months, recurrence was seen in 33 of these 87 patients, and the study was terminated early. Moreover, 37% had a recurrence within 1 year. These findings indicate non-treatment follow-up cannot be performed based on a negative PET finding.[8)] A possible explanation for PET false negatives during initial staging is the presence of small lesions (< 0.5 cm or < 1 cm) and mature teratomas.[9)] On the other hand, the literature regarding the role of PET in staging seminomas is insufficient. Based on the above considerations, it was concluded that there is no clear basis for recommending PET for staging.

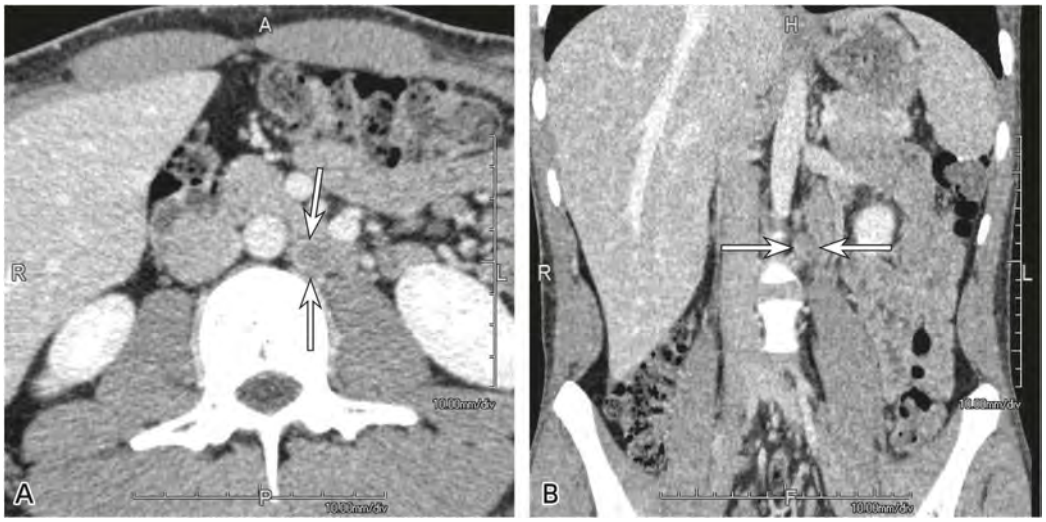

Figure. Patient who underwent high orchiectomy for a left testicular tumor

A: Contrast-enhanced CT, transverse image; B: Contrast-enhanced CT, coronal image
Enlarged paraaortic lymph node: 10 mm × 14 mm in the transverse image with craniocaudal length of 17 mm in the coronal image. Metastasis suspected (A, B →). Diagnosed as a stage IIA nonseminoma.

Search keywords and secondary sources used as references

PubMed was searched using the following keywords: testicular neoplasms, seminoma, nonseminoma, CT, and PET.

In addition, the following were referenced as secondary sources.

1) Japanese Urological Association, Ed.: 2015 Clinical Practice Guidelines for Testicular Tumors. KANEHARA & Co., 2015.
2) Yacoub JH et al: ACR Appropriateness Criteria®: staging of testicular malignancy. J Am Coll Radiol 13 (10), 1203-1209, 2016
3) Laguna MP et al: EAU guidelines on testicular cancer 2020. European Association of Urology, 2020

References

1) van Dijk MR et al: Survival of non-seminomatous germ cell cancer patients according to the IGCC classification: an update based on meta-analysis. Eur J Cancer 42: 820-826, 2006.
2) Hilton S et al: CT detection of retroperitoneal lymph node metastases in patients with clinical stage I testicular nonseminomatous germ cell cancer: assessment of size and distribution criteria. AJR Am J Roentgenol 169: 521-525, 1997
3) Hudolin T et al: Correlation between retroperitoneal lymph node size and presence of metastases in nonseminomatous germ cell tumors. Int J Surg Pathol 20: 15-18, 2012
4) Howard SA et al: Craniocaudal retroperitoneal node length as a risk factor for relapse from clinical stage I testicular germ cell tumor. AJR Am J Roentgenol 203: W415-420, 2014
5) Horan G et al: CT of the chest can hinder the management of seminoma of the testis: it detects irrelevant abnormalities. Br J Cancer 96: 882-885, 2007
6) de Wit M et al: [18F]-FDG-PET in clinical stage I/II non-seminomatous germ cell tumours: results of the German multicentretrial. Ann Oncol 19: 1619-1623, 2008
7) Lassen U et al: Whole-body FDG-PET in patients with stage I non-seminomatous germ cell tumours. Eur J Nucl Med Mol Imaging 30: 396-402, 2003
8) Huddart RA et al: ^{18}fluorodeoxyglucose positron emission tomography in the prediction of relapse in patients with high-risk, clinical stage I nonseminomatous germ cell tumors: preliminary report of MRC trial TE22: the NCRI Testis Tumour Clinical Study Group. J Clin Oncol 25: 3090-3095, 2007
9) De Santis M et al: The role of positron emission tomography in germ cell cancer. World J Urol 22: 41-46, 2004

BQ 76 Which imaging examinations are recommended for the posttreatment evaluation of a testicular tumor?

Statement

CT is recommended for evaluation after chemotherapy for a testicular tumor.

FDG-PET has a high negative predictive value in evaluating the viability of residual masses (particularly for masses ≥ 3 cm in size) after chemotherapy for seminomas and can therefore contribute to determining a treatment strategy. There is insufficient scientific evidence regarding the posttreatment evaluation of nonseminomas by FDG-PET, and it is therefore not recommended for this purpose.

Background

Recent advances in chemotherapy have led to striking improvement in the cure rate for advanced testicular tumors with metastasis. However, there is debate regarding the treatment strategy to adopt when residual masses are seen after chemotherapy. Residual masses are often only necrotic tissue and scar tissue containing no viable tumor cells, and retroperitoneal lymph node dissection (RPLND) is a highly invasive surgical procedure. Consequently, much is expected of residual mass evaluation by diagnostic imaging. This discussion provides an overview of the diagnostic imaging used for the post-chemotherapy evaluation of testicular tumors associated with metastasis, addressing seminomas and nonseminomas separately.

Explanation

Radical high orchiectomy is performed for testicular tumors without metastasis, with chemotherapy and radiation therapy added as necessary. To check for recurrence, periodic follow-up (surveillance) involving tumor marker measurement and abdominal CT is strongly recommended in multiple guidelines promulgated in other countries.

For metastatic seminomas, chemotherapy is performed in addition to high orchiectomy. It is also strongly recommended that tumor marker measurement and abdominal CT be performed for post-chemotherapy evaluation. Although residual masses are seen in 55% to 80% of patients after chemotherapy, many of these masses consist of necrotic or fibrous tissue. The conventional method used to assess the activity of residual masses has been to use a cutoff of 3 cm for the maximum diameter of a mass on CT. In reality, however, only 11-37% of residual masses ≥ 3 cm are found to be viable lesions.[1)]

FDG-PET has been reported to provide strong capability for evaluating the viability of residual masses after seminoma chemotherapy, particularly for masses ≥ 3 cm in size.[2-5)] Moreover, several international guidelines recommend FDG-PET for evaluating residual masses after seminoma chemotherapy. On the other hand, it has occasionally been reported that FDG-PET produces many false positives.[6-9)] In a systematic review published in 2014, pooled analysis results showed that the sensitivity, specificity, positive predictive value, and negative predictive value of FDG-PET were 78%, 86%, 58%, and 94%,

respectively.[10] The negative predictive values that have been reported for FDG-PET have been high, generally ≥ 90%.[1, 2, 4-7] Consequently, if a patient is negative on FDG-PET performed ≥ 6 weeks after chemotherapy, the likelihood of a viable tumor is considered low even if the diameter of a residual mass is ≥ 3 cm, and additional treatment may be avoided. The reported positive predictive values have varied widely depending on the report, ranging from 23% to 100%. In a study of 90 patients positive for residual masses on FDG-PET that was published in 2018, the positive predictive value was low, at 23%, and it was 22% for patients with masses ≥ 3 cm in diameter.[9] Caution is therefore required when aggressively performing additional treatment based only on a positive FDG-PET/CT finding. The most recent guidelines of the European Association of Urology (EAU) recommend follow-up by FDG-PET or CT if there is no enlargement of the mass.

In a prospective, multicenter study of 641 patients with nonseminomatous testicular tumors that was published in 2000, the proportion of patients with masses that consisted only of postoperative necrotic tissue increased as the diameter of the residual mass, as measured on post-chemotherapy CT, decreased and as the reduction rate increased.[11] However, 28% of the patients had a viable residual tumor (teratoma or carcinoma) if the diameter of the residual mass was ≤ 9 mm, and 20% had a viable residual tumor if the rate of diameter reduction was ≥ 85%. In addition, a 2003 report indicated that, when retroperitoneal lymph node dissection (RPLND) was performed in 87 patients with residual tumors ≤ 20 mm in diameter after treatment with bleomycin, etoposide, and cisplatin (BEP), viable tumors were seen in 33%.[12] It can therefore be concluded that, with nonseminomas, the likelihood of a viable residual mass is relatively high even if the diameter of the post-chemotherapy mass is small.

With regard to FDG-PET evaluation after chemotherapy for nonseminomas, a prospective, multicenter study in which the results for all of the patients were confirmed histologically was conducted in 2008. It found the sensitivity, specificity, positive predictive value, and negative predictive value of FDG-PET to be 70%, 48%, 59%, and 51%, respectively, and its diagnostic accuracy rate to be 56%. The diagnostic accuracy rate was 55% for CT and 56% for tumor marker measurement. Thus, the results indicated that the addition of FDG-PET to CT and tumor marker measurement does not provide additional information for postoperative tissue prediction.[13] Another study identified the problem of residual mature teratomas resulting in false negatives with FDG-PET,[14] and use of FDG-PET is not recommended in the guidelines from other countries.

Search keywords and secondary sources used as references

PubMed was searched using the following keywords, and further selections were made from the selected articles: testicular, testis, germ cell tumor, tumor, cancer, carcinoma, seminoma, nonseminoma, CT, and PET.

In addition, the following were referenced as secondary sources.

1) Laguna MP et al: EAU guidelines on testicular cancer 2020. European Association of Urology, 2020
2) Gilligan T et al: NCCN Guidelines®: testicular cancer ver 2. 2021. National Comprehensive Cancer Network, 2021

References

1) Bachner M et al: 2-^{18}fluoro-deoxy-D-glucose positron emission tomography (FDG-PET) for postchemotherapy seminoma residual lesions: a retrospective validation of the SEMPET trial. Ann Oncol 23: 59-64, 2012
2) De Santis M et al: Predictive impact of 2-^{18}fluoro-2-deoxy-D-glucose positron emission tomography for residual postchemotherapy masses in patients with bulky seminoma. J Clin Oncol 19: 3740-3744, 2001
3) Becherer A et al: FDG PET is superior to CT in the prediction of viable tumour in post-chemotherapy seminoma residuals. Eur J Radiol 54: 284-288, 2005
4) Ambrosini V et al: 18F-FDG PET/CT impact on testicular tumours clinical management. Eur J Nucl Med Mol Imaging 41: 668-673, 2014
5) De Santis M et al: 2-^{18}fluoro-deoxy-D-glucose positron emission tomography is a reliable predictor for viable tumor in postchemotherapy seminoma: an update of the prospective multicentric SEMPET trial. J Clin Oncol 22: 1034-1039, 2004
6) Hinz S et al: The role of positron emission tomography in the evaluation of residual masses after chemotherapy for advanced stage seminoma. J Urol 179: 936-940, 2008
7) Siekiera J et al: Can we rely on PET in the follow-up of advanced seminoma patients? Urol Int 88: 405-409, 2012
8) Decoene J et al: False-positive fluorodeoxyglucose positron emission tomography results after chemotherapy in patients with metastatic seminoma. Urol Oncol 33: 23.e15-23.e21, 2015
9) Cathomas R et al: Questioning the value of fluorodeoxyglucose positron emission tomography for residual lesions after chemo- therapy for metastatic seminoma: results of an International Global Germ Cell Cancer Group registry. J Clin Oncol 36: 3381-3387, 2018
10) Treglia G et al: Diagnostic performance of fluorine-18-fluorodeoxyglucose positron emission tomography in the postchemotherapy management of patients with seminoma: systematic review and meta-analysis. Biomed Res Int 2014: 852681, 2014
11) Steyerberg EW et al: Retroperitoneal metastases in testicular cancer: role of CT measurements of residual masses in decision making for resection after chemotherapy. Radiology 215: 437-444, 2000
12) Oldenburg J et al: Postchemotherapy retroperitoneal surgery remains necessary in patients with nonseminomatous testicular cancer and minimal residual tumor masses. J Clin Oncol 21: 3310-3317, 2003
13) Oechsle K et al: ［18F］Fluorodeoxyglucose positron emission tomography in non seminomatous germ cell tumors after chemotherapy: the German multicenter positron emission tomography study group. J Clin Oncol 26: 5930-5935, 2008
14) De Santis M et al: The role of positron emission tomography in germ cell cancer. World J Urol 22: 41-46, 2004

BQ 77 Which imaging examinations are recommended to diagnose adrenal adenomas?

Statement

Non-contrast CT and dynamic contrast-enhanced CT are strongly recommended.

Chemical shift MRI is more sensitive than non-contrast CT and is recommended.

Background

In recent years, with the development and widespread adoption of diagnostic imaging, mass lesions in the adrenals have frequently been detected by chance (incidentalomas) in imaging examinations performed for other purposes. Adrenal incidentalomas have been reported in 5% of CT examinations.[1, 2] Approximately 75% of adrenal incidentalomas are adrenal adenomas.[2] Diagnosing adrenal adenomas is therefore important for the differential diagnosis of adrenal masses. This discussion provides an overview regarding CT and chemical shift MRI, which are commonly used to diagnose adrenal adenomas.

Explanation

Two main approaches are taken to diagnosing adrenal adenomas by CT and MRI based on the presence or absence of lipids and the contrast enhancement pattern. Adenomas show lower attenuation than metastatic tumors on non-contrast CT due to the abundant presence of intracellular lipids. A meta-analysis showed that when a mean intratumoral CT number of < 10 HU was considered indicative of adenoma, sensitivity and specificity were 71% and 98%, respectively.[3] This diagnostic criterion was also adopted for the ACR Appropriateness Criteria® (secondary source 1). Using the mean CT number of < 10 HU as the diagnostic criterion enables approximately 70% of adenomas to be diagnosed with non-contrast CT.[3] In examinations of methods other than using the mean CT number, when CT numbers of all the pixels in a mass were analyzed using histograms, and masses in which ≥ 10% of the pixels had a CT number of < 0 HU or the 10th percentile of the CT numbers (mean CT number - [1.282 × standard deviation]) was < 0 HU were considered adenomas, sensitivity ranged from 84% to 91%.[4-6] If these methods can be used to diagnose adenomas by non-contrast CT, additional imaging examinations are unnecessary.[7]

Adrenal adenomas have the characteristics of medullary tumors, which have little fibrous compared with metastatic tumors, and the contrast-enhanced washout rate is high. The contrast-enhanced washout rate with the use of dynamic contrast-enhanced CT is quantitatively measured as follows: ① with pre-contrast CT: (early-phase CT number - late-phase CT number) / (early-phase CT number - pre-contrast CT number); and ② without pre-contrast CT: (early-phase CT number - late-phase CT number) / (early-phase CT number). Using images acquired 1 min (early phase) and 15 min after contrast injection (late phase), diagnostic performance with respect to masses that could not be diagnosed as adrenal adenomas (mean CT number of < 10 HU) by pre-contrast CT showed ① sensitivity and specificity of 86% and 92%, respectively,

when non-contrast CT was performed (washout rate > 60%) and ② sensitivity and specificity ranging from 77% to 82% and 89% to 92%, respectively, when pre-contrast CT was not performed (washout rate > 40%).[8, 9)]

For lipid detection, chemical shift MRI is more sensitive than CT and is particularly superior for detecting small quantities of lipids. The presence of lipids is suggested and adenoma can be diagnosed when the signal drop is seen in opposed-phase imaging compared with in-phase imaging.[10, 11)] For quantitative evaluation, the following methods are used to calculate the tumor signal intensity index and the tumor-to-spleen signal intensity ratio: ① tumor signal intensity index: tumor signal intensity on in phase - tumor signal intensity on opposed phase) / tumor signal intensity on in phase, and ② tumor-to-spleen signal intensity ratio: tumor-to-spleen signal intensity on opposed phase / tumor-to-spleen signal intensity on in phase. When the tumor signal intensity index is ≥ 16.5%, or the tumor-to-spleen signal intensity ratio is ≤ 71%, sensitivity and specificity range from 81% to 100% and 94% to 100%, respectively, enabling diagnosis.[1, 5, 12)] A meta-analysis found no difference in the diagnostic performance of qualitative and quantitative evaluations.[13)] When a cutoff of 20% was used for the tumor signal intensity index, sensitivity and specificity with respect to masses that could not be diagnosed as adrenal adenomas (mean CT number of > 10 HU) by non-contrast CT were 67% and 100%, respectively.[14)] Moreover, the diagnostic performance of chemical shift MRI was higher than that of CT histogram analysis.[15)] An investigation that compared the diagnostic performance of chemical shift MRI and dynamic contrast-enhanced CT in masses that could not be diagnosed as adrenal adenomas by non-contrast CT (mean CT number > 10 HU) found dynamic contrast-enhanced CT to be useful, with diagnostic accuracy of 88.1% (sensitivity, 91.7%; specificity, 74.8%) for dynamic contrast-enhanced CT and 73.6% (sensitivity, 67.1%; specificity, 88.7%) for chemical shift MRI.[16)] Consequently, although chemical shift MRI has diagnostic performance limitations in masses that cannot be diagnosed by non-contrast CT,[14, 17)] as is the case for non-contrast CT, it is recommended as a noninvasive examination with high specificity.

With all of the diagnostic methods that use the lipid detection and contrast enhancement patterns described above, there are false positives for neoplasms such as adrenocortical carcinoma, clear cell renal cell carcinoma, hepatocellular carcinoma, and pheochromocytoma.[18-21)] Attention is therefore also paid to clinical information such as past history, tumor size, and enlargement trends.

With regard to diffusion-weighted imaging, it has been reported that, in adrenal masses that are difficult to diagnose by chemical shift MRI, lesions with an apparent diffusion coefficient (ADC) of > 1.50 ± 10^{-3} mm^2/s are highly likely to be adenomas.[22)] However, the converse results, where ADC values of adenomas were lower than those of malignant tumors, have also been reported,[23)] as have results showing no significant difference between the ADC values of adenomas and metastatic tumors.[24)] Consequently, no conclusion has been reached in this regard.

Search keywords and secondary sources used as references

PubMed was searched using the following keywords, and further selections were made from the results: adrenal, adrenocortical, adenoma, mass, tumor, incidentaloma, pheochromocytoma, imaging, metastasis, computed tomography, magnetic resonance imaging, and positron emission tomography.

In addition, the following was referenced as a secondary source.

1) Choyke PL et al: ACR Appropriateness Criteria®: incidentally discovered adrenal mass. J Am Coll Radiol 3: 498-504, 2006

References

1) Boland GW et al: Incidental adrenal lesions: principles, techniques, and algorithms for imaging characterization. Radiology 249: 756-775, 2008
2) Song JH et al: The incidental adrenal mass on CT: prevalence of adrenal disease in 1,049 consecutive adrenal masses in patients with no known malignancy. AJR Am J Roentgenol 190: 1163-1168, 2008
3) Boland GW et al: Characterization of adrenal masses using unenhanced CT: an analysis of the CT literature. AJR Am J Roentgenol 171: 201-204, 1998
4) Ho LM et al: Lipid-poor adenomas on unenhanced CT: does histogram analysis increase sensitivity compared with a mean attenuation threshold? AJR Am J Roentgenol 191: 234-238, 2008
5) Halefoglu AM et al: Differentiation of adrenal adenomas from nonadenomas using CT histogram analysis method: a prospective study. Eur J Radiol 73: 643-651, 2010
6) Rocha TO et al: Histogram analysis of adrenal lesions with a single measurement for 10th percentile: feasibility and incremental value for diagnosing adenomas. AJR Am J Roentgenol 211: 1227-1233, 2018
7) Garrett RW et al: Adrenal incidentalomas: clinical controversies and modified recommendations. AJR Am J Roentgenol 206: 1170-1178, 2016
8) Caoili E M et al: Adrenal masses: characterization with combined unenhanced and delayed enhanced CT. Radiology 222: 629-633, 2002
9) Marty M et al: Diagnostic accuracy of computed tomography to identify adenomas among adrenal incidentalomas in an endocrinological population. Eur J Endocrinol 178: 439-446, 2018
10) Korobkin M et al: Characterization of adrenal masses with chemical shift and gadolinium-enhanced MR imaging. Radiology 197: 411-418, 1995
11) Mitchell DG et al: Benign adrenocortical masses: diagnosis with chemical shift MR imaging. Radiology 185: 345-351, 1992
12) Fujiyoshi F et al: Characterization of adrenal tumors by chemical shift fast low-angle shot MR imaging: comparison of four methods of quantitative evaluation. AJR Am J Roentgenol 180: 1649-1657, 2003
13) Platzek I et al: Chemical shift imaging for evaluation of adrenal masses: a systematic review and meta-analysis. Eur Radiol 29: 806-817, 2019
14) Haider MA et al: Chemical shift MR imaging of hyperattenuating (> 10 HU) adrenal masses: does it still have a role? Radiology 231: 711-716, 2004
15) Jhaveri KS et al: Comparison of CT histogram analysis and chemical shift MRI in the characterization of indeterminate adrenal nodules. AJR Am J Roentgenol 187: 1303-1308, 2006
16) Koo H J et al: The value of 15-minute delayed contrast-enhanced CT to differentiate hyperattenuating adrenal masses compared with chemical shift MR imaging. Eur Radiol 24: 1410-1420, 2014
17) Park BK et al: Comparison of delayed enhanced CT and chemical shift MR for evaluating hyperattenuating incidental adrenal masses. Radiology 243: 760-765, 2007
18) Patel J et al: Can established CT attenuation and washout criteria for adrenal adenoma accurately exclude pheochromocytoma? AJR Am J Roentgenol 201: 122-127, 2013
19) Choi YA et al: Evaluation of adrenal metastases from renal cell carcinoma and hepatocellular carcinoma: use of delayed contrast-enhanced CT. Radiology 266: 514-520, 2013
20) Heye S et al: Adrenocortical carcinoma with fat inclusion: case report. Abdom Imaging 30: 641-643, 2005
21) Moosavi B et al: Intracellular lipid in clear cell renal cell carcinoma tumor thrombus and metastases detected by chemical shift (in and opposed phase) MRI: radiologic-pathologic correlation. Acta Radiol 57: 241-248, 2016
22) Sandrasegaran K et al: Characterization of adrenal masses with diffusion-weighted imaging. AJR Am J Roentgenol 197: 132-138, 2011
23) Song J1 et al: Utility of chemical shift and diffusion-weighted imaging in characterization of hyperattenuating adrenal lesions at 3.0T. Eur J Radiol 81: 2137-2143, 2012

24) Tsushima Y et al: Diagnostic utility of diffusion-weighted MR imaging and apparent diffusion coefficient value for the diagnosis of adrenal tumors. J Magn Reson Imaging 29: 112-117, 2009

8
Breast

Standard Imaging Methods for Breast

Introduction

In nearly all cases, the reason for diagnostic imaging of the breast region is breast cancer, and the purpose is to detect and diagnose it and evaluate its progression. Because the purpose varies according to the method used, the discussion is organized by method.

X-ray mammography (Fig. 1)

X-ray mammography (“mammography” below) is the most basic type of diagnostic imaging of the breast region and has long been used. It is currently used not only to diagnose breast disease, but also for breast cancer screening. Diagnostic mammography is the type discussed here. Mammography is indicated when breast disease is suspected. However, because its ability to detect masses is low in dense breasts, its use in young individuals and those in the lactation period requires consideration. Because imaging is performed with the breast compressed, another diagnostic method is considered if compression is not possible or advisable. Breast imaging systems that meet the specifications established by the Japan Radiological Society are used. They are used with detectors for breast imaging. The types of detectors used are: film-screen detectors, used in analog devices; imaging plate (IP) detectors, used in computed radiography (CR); and flat-panel detectors (FPDs), used for digital radiography (DR). Imaging is performed with a dose of ≤ 3 mGy per image. With digital mammography, imaging conditions that can be used to estimate the total radiation dose are specified (July 2005 Japan Radiological Society recommendation). The standard imaging views are the mediolateral oblique (MLO) and craniocaudal (CC) views.

1. Criteria for good images

① Mediolateral oblique (MLO) view (Fig. 1A)

(1) Left and right mammograms are symmetrical.
(2) The nipple is imaged in profile.
(3) The pectoralis major is shown up to the nipple level.
(4) The retromammary fat space is well visualized.
(5) The tissue of the thoracoabdominal wall of the inframammary area is included, and the inframammary fold is extended.
(6) There are no breast folds.

② Craniocaudal (CC) view (Fig. 1B)

(1) Left and right mammograms are symmetrical.

(2) The medial mammary tissue must always be visualized, and the lateral part included as much as possible.
(3) The chest wall is included to a deep level. (If possible, a part of the pectoralis major is displayed.)
(4) The nipple is imaged in profile.
(5) There are no breast folds.

2. Additional imaging

Additional imaging is performed as necessary. The main types of additional imaging are the following.

① Exaggerated craniocaudal (XCC) view

Performed when a lesion is in a lateral area and is not seen with the normal CC view.

② 90-degree lateral [mediolateral (ML) or lateromedial (LM)] view

Performed to accurately understand the vertical spatial relationship between a lesion and the nipple.

③ Magnified view (M)

Performed to evaluate calcification morphology in detail.

④ Spot compression imaging

Performed to eliminate local overlap.

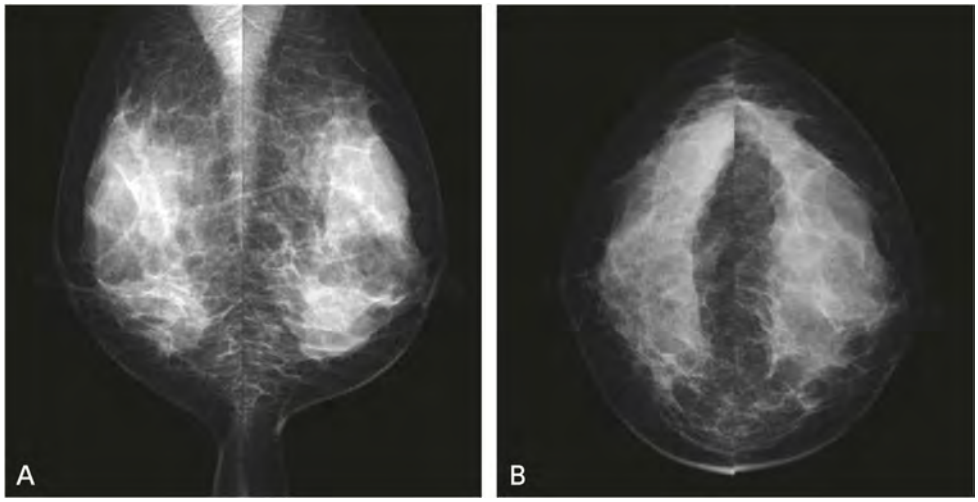

Figure 1. Normal breast (mammogram)

A: MLO view, B: CC view

Digital breast tomosynthesis (DBT, Fig. 2)

DBT is imaging technology that reconstructs cross-sections of arbitrary height from tomographic imaging performed once. With the breast compressed, the X-ray tube is moved to various limited angles (-theta to +theta) in relation to the detector, and tomograms are reconstructed from projection images obtained by multiple image acquisitions. In this way, images with little overlap are reconstructed.

Depending on the system, factors such as the angles to which the X-ray tube is moved, number of irradiations, imaging duration, and method of reconstruction vary greatly, as does the image quality obtained.

As with 2D mammography, the imaging views used are the MLO and CC views.

The method of breast compression is the same as for 2D imaging. However, the imaging method varies according to the system used. With some systems, 2D and DBT imaging can be performed simultaneously. With others, DBT imaging must be performed after 2D imaging.

Breast ultrasonography (Fig. 3)

Ultrasonography is widely used to diagnose breast disease. Because radiation is not used, it can be applied to any patient suspected of having a breast disease. However, it is inferior to mammography with respect to its ability to visualize calcification. In addition, it is often performed to detect and diagnose lesions simultaneously in real time. Consequently, the system settings and performance of the examiner affect diagnostic ability. The systems generally used are hand-held, real-time systems, and fully digital systems that can perform imaging processing by means such as tissue harmonics and spatial compounding are becoming widely used. The use of a high-frequency probe designed for the body surface is required. The gain, dynamic range, and focus are adjusted so that the characteristics of a lesion can be correctly determined. A basic test involves examination of the whole breast bilaterally. If malignancy is suspected, the lymph nodes are also examined. If a lesion is detected, the image is recorded. The basic approach is to record static images (Fig. 3). However, video can also be saved as necessary. For solid masses, imaging is performed in at least 2 views, and measurements are then performed. For lesions that do not form obvious masses, several typical cross-sections should be recorded, along with images of the same region of the contralateral breast. If breast cancer is suspected, the involvement of the surrounding tissue is evaluated, particularly the presence or absence of pectoralis major or skin invasion or intraductal foci.

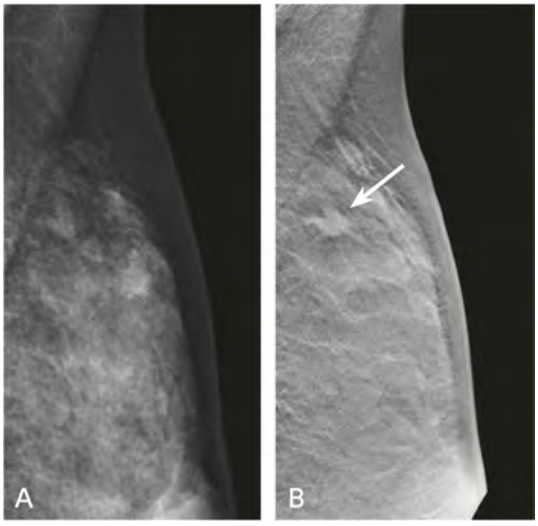

Figure 2. Invasive ductal carcinoma of the left breast

A: 2D mammogram, left MLO view: No obvious abnormality can be identified.
B: Tomosynthesis slice image: An irregularly shaped mass is clearly visualized in the left upper (U) region.

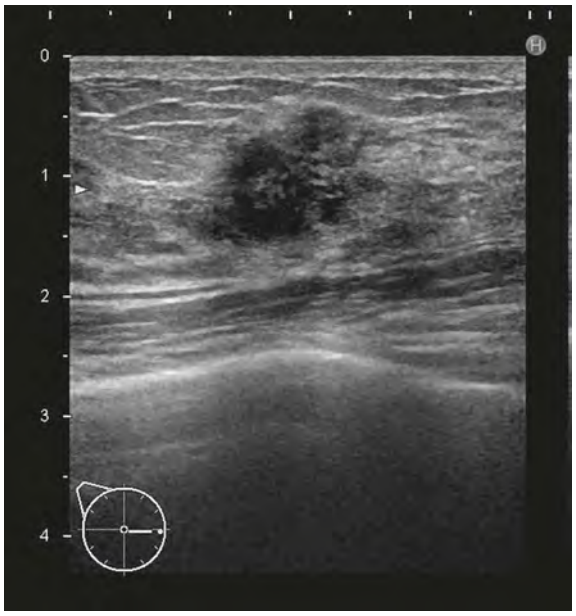

Figure 3. Invasive ductal carcinoma of the right breast

Ultrasonography shows an irregularly shaped hypoechoic mass with indistinct margin, posterior echo attenuation, and interruption of the anterior border.

MRI (Fig. 4)

Breast cancer is a tumor with relatively abundant blood flow that shows strong early enhancement and is distinctly visualized on contrast-enhanced MRI using gadolinium contrast media. Consequently, dynamic MRI is useful for diagnosing breast cancer.[1-4)] With diffusion-weighted imaging, breast cancer can be visualized without the use of contrast media. However, the detectability of breast cancer does not surpass the detectability provided by dynamic MRI, and contrast studies are therefore essential for the careful investigation of breast cancer.[5)]

It is recommended that imaging be performed 7 to 14 days after the start of menstruation.[3)] Outside of this period, particularly during the latter half of the menstrual cycle, mammary fibroglandular tissue enhancement increases. This increases the risk of masking the enhancement of breast cancer and thereby obscuring it (false negative) or producing a finding that can be mistaken for breast cancer (false positive).[1, 3, 4)] However, if necessary, imaging in the third week of the menstrual cycle may be considered, although it may not yield good results.[3)] The treatment schedule should not be delayed in order to perform MRI at the optimal time.

Using a dedicated breast coil, imaging of both breasts simultaneously should be performed beginning from the early phase of contrast-enhanced imaging. This is so that latent minute breast cancer in the contralateral breast is not overlooked.[1, 2, 4)] Moreover, left-right symmetry of mammary fibroglandular

tissue enhancement is commonly seen. Consequently, comparing the left and right breasts aids in distinguishing between breast cancer and mammary fibroglandular tissue enhancement.[1)]

To obtain good image quality, a 1.5T or 3T MRI system should be used.[2-5)] The following types of imaging are recommended. A basic imaging plane at many facilities is the transverse plane.

① Fat-suppressed T2-weighted imaging
② T1-weighted imaging
③ Diffusion-weighted imaging
④ Dynamic MRI
⑤ Contrast-enhanced fat-suppressed T1-weighted imaging

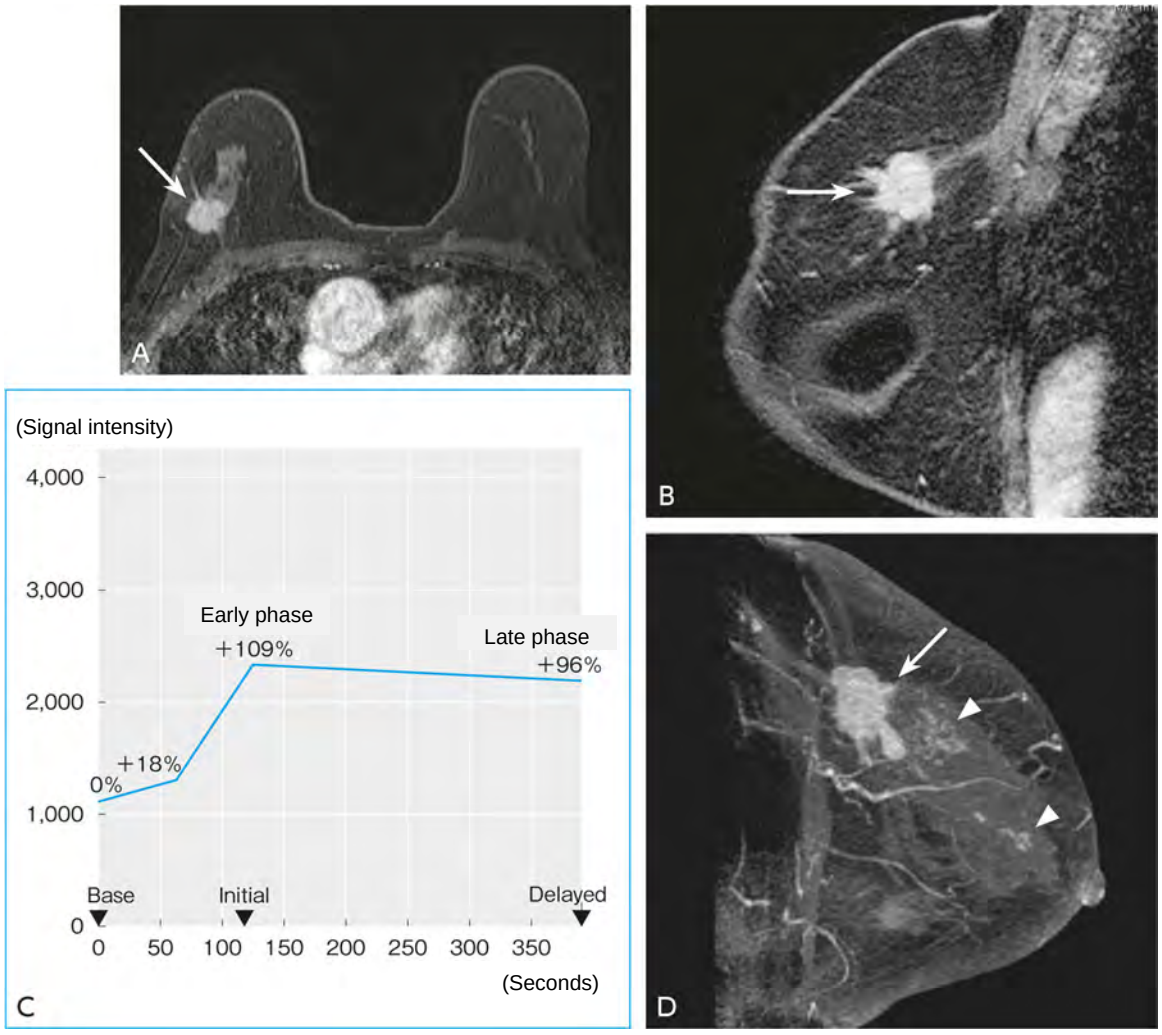

Figure 4. Breast cancer of the right breast (woman in her 70s)

A: Dynamic MRI, early-phase axial image
B: Contrast-enhanced MRI (fat-suppressed, T1-weighted, high-resolution sagittal image acquired between the early and late phases of dynamic MRI)
C: Time-intensity curve analysis
D: MIP image of B

A spiculated, irregularly shaped mass (→) is seen in the periphery of C area of the right breast on the early-phase image of dynamic MRI (A) and the contrast-enhanced fat-suppressed T1-weighted image (B). The time-intensity curve analysis (C) shows that the mass demonstrates a fast-washout kinetic pattern. Total mastectomy was performed (in accordance with the patient's wishes, preoperative chemotherapy was not performed), and invasive ductal carcinoma (scirrhous type, HER2-enriched) was proven pathologically. Non-mass enhancement (▷) extending towards the nipple seen on the MIP image (D) was proven to be extensive intraductal spread on pathological examination.

Breast cancer often shows isointensity to fibroglandular tissue and is indistinct on fat-suppressed T2-weighted images. Lesions such as cysts, fibroadenomas, and mucinous carcinomas are often clearly visualized as masses of high signal intensity due to the presence of abundant fluid.[1, 2, 6] Invasive ductal carcinoma is occasionally associated with edema in the surrounding area, which is visualized as a high signal intensity area.

On T1-weighted images, breast cancer often shows isointensity with fibroglandular tissue and is indistinct. Lipoma and hamartoma have fat tissue in the mass, which shows high signal intensity on T1-weighted images and low signal intensity on fat-suppressed T1-weighted images (precontrast images). Lesions such as complex cysts and duct ectasia, which have proteinaceous or hemorrhagic content, often show high signal intensity on T1-weighted and fat-suppressed T1-weighted images.[1)]

Table 1. Examples of breast MRI sequences (1.5T system, dedicated breast coil)

Imaging method	Sequence	TR/TE (ms)	Slice thickness (mm)	Notes
① T2-weighted / axial	FSE with fat suppression	3,000-5,000 / 80-100	4	
② T1-weighted / axial	Fast 3D-GRE	5-10 / minimum-in phase (flip angle, 10-20°)	1-2	
③ Diffusion-weighted / axial	Single-shot EPI with fat suppression	3,000-5,000 / minimum	4	b-value = 0, 800*-1,000 s/mm^2
④ Dynamic MRI / axial	Fast 3D-GRE with fat suppression	5-10 / minimum-in phase (flip angle, 10-20°)	1-2	Subtraction images are useful if fat suppression is not used
⑤ Contrast-enhanced T1-weighted / sagittal	Fast 3D-GRE with fat suppression	5-10 / minimum-in phase (flip angle, 10-20°)	1-2	Between early and late phase or after late phase Imaging at other cross-sectional planes High spatial resolution imaging

* b-value = 800 s/mm^2 is recommended by the working group of the European Society of Breast Imaging[5)]

On diffusion-weighted images, breast cancer, especially invasive ductal carcinoma, often shows high signal intensity and is clearly depicted. On the other hand, ductal carcinoma in situ, intraductal spread, and small or markedly fibrous invasive ductal carcinoma are often invisible or poorly depicted on diffusion-weighted images, and their detectability is limited. Benign lesions such as cysts and fibroadenomas that show marked high signal intensity on T2-weighted images often show high signal intensity and findings confused with breast cancer on diffusion-weighted images.[5)] Measuring ADC values

makes it possible to quantitatively evaluate the diffusion of tumors. The ADC values decrease in breast cancer and increase in benign tumors, and they are therefore used to distinguish between benign and malignant tumors.[1, 5] For measurement of ADC values, it is recommended that a small ROI (≥ 3 pixels) be set in the area with the lowest value (black) in the lesion on the ADC map, while avoiding areas of necrosis and of poor enhancement indicated by dynamic MRI.[5]

On dynamic MRI, invasive ductal carcinoma is often visualized as a mass, and ductal carcinoma in situ and intraductal spread are visualized as non-mass enhancement. The diagnosis is made by analyzing their shapes, margins, internal enhancement characteristics, and distribution pattern. For this approach, it is desirable to image with fat suppression technique [4] and a spatial resolution with pixel size of 1 mm × 1 mm or less and slice thickness of 2.5-3 mm or less.[2, 4] Because peak enhancement of breast cancer occurs within 2 minutes after intravenous injection of contrast media, the early phase, the period from 1 to 2 minutes after injection, is best for tumor visualization. Although tumors can be depicted even in the late phase, 2 minutes or later after injection, tumor conspicuity is decreased because tumor enhancement weakens, and fibroglandular tissue enhancement strengthens.[2]

Breast cancer is strongly enhanced in the early phase and tends to show gradually decreasing enhancement in the late phase. In contrast, benign tumors and lesions often show weak enhancement in the early phase and gradually increasing enhancement in the late phase. Based on this idea of the contrast enhancement pattern, benign and malignant tumors are discriminated by time-intensity curve analysis.[1] Time-intensity curve analysis requires imaging at least 3 times: precontrast, early phase to evaluate peak tumor enhancement, and late phase to observe the changes of tumor enhancement over time after the peak. It is also considered important that imaging be performed with high temporal resolution by acquiring images for 1 to 2 minutes in each phase. An imaging time exceeding 2 minutes may risk missing the peak of tumor enhancement in the early phase, which leads to overlooking washout in the late phase.[2]

To obtain information to augment dynamic MRI, additional contrast-enhanced T1-weighted imaging at different cross-sections or higher spatial resolution is performed between early and late phase imaging or after late phase imaging in many institutions. The MIP image is highly useful post-processing for evaluating the extent of a tumor. It is also helpful for evaluating fibroglandular tissue enhancement and detecting unexpected lesions. Accurate evaluation of enhancement in lesions that shows high signal intensity originally before contrast media administration is difficult. For such lesions, generating and viewing subtraction images obtained by subtracting the precontrast image from the postcontrast image is recommended to confirm the presence or absence of enhancement.[1]

The Breast Imaging Reporting and Data System (BI-RADS) MRI of the American College of Radiology defines the lexicon to be used for findings when interpreting breast MRI, and this has now become the de facto global standard. It is recommended that interpretation reports are prepared in accordance with BI-RADS MRI.[1]

MDCT (Fig. 5)

MDCT is now mainly used for preoperatively staging of breast cancer and detection of postoperative recurrence and metastasis. MDCT was previously used in Japan to diagnose the extent of breast cancer in the breast. However, MRI is the best modality with respect to the problem of radiation exposure and the ability to diagnose breast cancer extent. It is therefore now recommended that the preferred method for diagnosing the spread of breast cancer in the breast is MRI. Consequently, MDCT is considered for patients who cannot undergo MRI, such as those with internal metal objects or claustrophobia and those for whom MRI contrast media are contraindicated.[7)] The usefulness of CT in distinguishing benign from malignant breast disease has not been established, and it is therefore not recommended for this purpose alone.[8)]

Nearly all of the reports indicating that MDCT is useful in breast disease have been reports of single-center studies, and the imaging methods used have varied between centers. An optimal MDCT imaging method has not yet been established.

1. Imaging methods

① Body position during imaging

The primary purpose of CT is to simultaneously evaluate lymph node metastasis and distant metastasis to areas such as the lungs. Consequently, the basic position for imaging is supine. However, to simulate surgery, CT imaging is also performed in a position that approximates the position during surgery.[9, 10)]

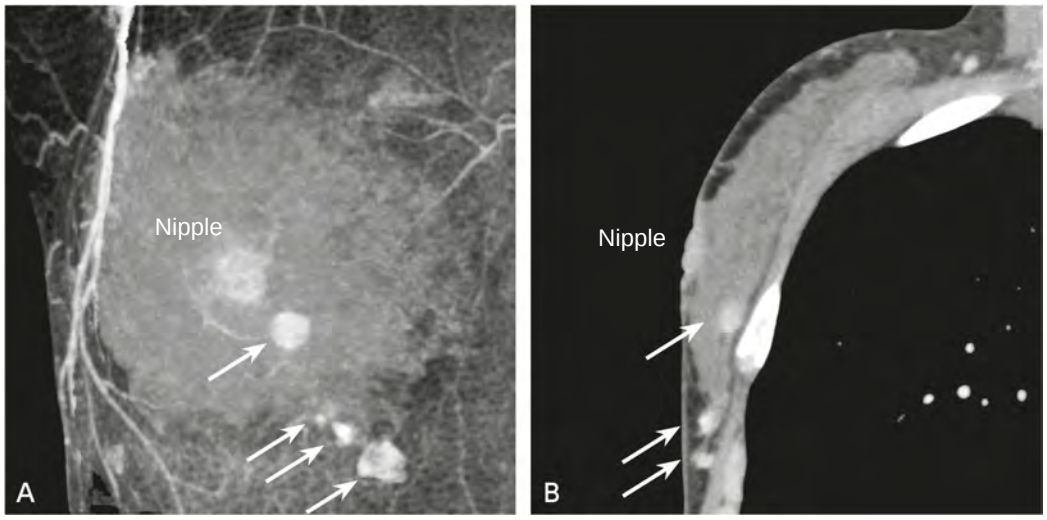

Figure 5. Invasive ductal carcinoma of the right breast

A: Contrast-enhanced CT, MIP image; B: Contrast-enhanced CT, oblique MPR image shows the relationship between the nipple and distal nodules. Numerous linearly distributed nodules are shown in the inner-lower part of the right breast. The relative locations of the nipple and lesions are clear.

② Imaging conditions

Imaging conditions that provide optimal images need to be specified based on a thorough understanding of the performance of the CT system being used at the facility. It is also important to select a protocol intended to reduce radiation exposure by means such as using CT automatic exposure control (CT-AEC) or iterative image reconstruction.

③ Contrast media

Because the ability to detect breast cancer on non-contrast CT is weak, use of a contrast medium is essential. Although intravenous injection of iodine contrast media at a concentration of 300 mg I/mL and injection rate of 2 to 3 mL/s is commonly reported, high concentrations (370 to 400 mg I/ml) of contrast media are also used.[11, 12] However, there have been almost no reports concerned with the optimal contrast medium injection dose and method of injection.

④ Timing of imaging

Many reports indicate that imaging for the early phase of contrast-enhanced imaging begins 60 to 90 seconds after the start of contrast medium injection, and that late-phase imaging is performed from 3 to 5 minutes after injection. As indicated in BI-RADS-MRI, it is recommended that early-phase imaging be performed within 2 minutes of injection, when breast cancer is most enhanced.[1)] Delayed-phase imaging is also important to evaluate intraductal lesions, which have a delayed contrast peak. Delayed-phase imaging also enables the time-concentration curve to be evaluated. However, the usefulness of the time-concentration curve for distinguishing malignant from benign lesions with CT has not been established.

2. Interpretation method

MPR and MIP images should be prepared to diagnose the spread of breast cancer in the breast by multidirectional observation (Fig. 5). Although no diagnostic criteria have been established, it is recommended that the findings be evaluated and a final assessment (categorization) determined in conformance with BI-RADS-MRI.

Secondary source materials used as references

1) Morris EA et al: ACR BI-RADS® atlas, breast imaging reporting and data system, 5th ed. American College of Radiology, 2013
2) Mann RM et al: Breast MRI: guidelines from the European Society of Breast Imaging. Eur Radiol 18: 1307-1318, 2008
3) Mann RM et al: Breast MRI: EUSOBI recommendations for women's information. Eur Radiol 25: 3669-3678, 2015
4) American College of Radiology: ACR practice parameter for the performance of contrast-enhanced magnetic resonance imaging (MRI) of the breast. https://www.acr.org/-/media/ACR/Files/Practice-Parameters/mr-contrast-breast.pdf American College of Radiology, 2018
5) Baltzer P et al: Diffusion-weighted imaging of the breast: a consensus and mission statement from the EUSOBI international breast diffusion-weighted imaging working group. Eur Radiol 30: 1436-1450, 2020
6) Kuhl CK et al: Do T2-weighted pulse sequences help with the differential diagnosis of enhancing lesions in dynamic breast MRI? J Magn Reson Imaging 9: 187-196, 1999
7) The Japanese Breast Cancer Society, Ed.: 2011 Evidence-Based Breast Cancer Clinical Practice Guidelines: (2) Epidemiology and Diagnosis. KANEHARA & Co., pp 140-141, 2011.

8) The Japanese Breast Cancer Society, Ed.: 2011 Evidence-Based Breast Cancer Clinical Practice Guidelines: (2) Epidemiology and Diagnosis. KANEHARA & Co., pp 144-145, 2011.
9) Doihara H et al: Clinical significance of multidetector-row computed tomography in breast surgery. Breast J 12 (5 Suppl 2): S204-S209, 2006
10) Harada-Shoji N et al: Usefulness of lesion image mapping with multidetector-row helical computed tomography using a dedicated skin marker in breast-conserving surgery. Eur Radiol 19: 868-874, 2009
11) Uematsu T et al: Comparison of magnetic resonance imaging, multidetector row computed tomography, ultrasonography, and mammography for tumor extension of breast cancer. Breast cancer Res Treat 112: 461-474, 2008
12) Kang DK et al: Clinical application of multidetector row computed tomography in patient with breast cancer. J Comput Assist Tomogr 32: 583-598, 2008

FQ 17 Is contrast-enhanced MRI recommended for the qualitative diagnosis of microcalcification without abnormal findings on ultrasonography?

Statement

Contrast-enhanced MRI can be considered to assist in selecting a diagnostic strategy.

Background

Microcalcification detected by mammography screening is an important sign that is suggestive of noninvasive carcinoma. The positive predictive value (PPV) of microcalcification of categories 3 and 4 of the BI-RADS system of the American College of Radiology (ACR) has ranged widely, from 0% to 19% and 20% to 65.8%, respectively. However, many reported PPVs of microcalcification on mammography have been ≤ 30%.[1-7)] These results indicate that biopsy results for microcalcification are often benign. It has therefore been argued that stricter criteria for microcalcification biopsy ought to be established.

To avoid unnecessary biopsies, the usefulness of contrast-enhanced MRI to determine whether biopsy is indicated for microcalcification has been investigated in recent years. In Japan, stereotactic vacuum-assisted breast biopsy (SVAB) or tomosynthesis-guided vacuum-assisted breast biopsy (TVAB) is generally indicated for microcalcification without abnormal findings on ultrasonography. Although there have been several reports from Japan regarding the usefulness of contrast-enhanced MRI for qualitative diagnosis of microcalcifications without abnormal findings on ultrasonography, the evidence is still insufficient. Consequently, this was examined as an FQ.

Explanation

Reports regarding the usefulness of contrast-enhanced MRI in microcalcification have been published since 1996.[8, 9)] After 2000, the diagnostic performance of contrast-enhanced MRI improved with technological developments, an example being simultaneous bilateral dynamic imaging, and the recognition of background parenchymal enhancement.[3, 4, 10-25)] Moreover, due to the changes in the diagnostic strategy with the introduction of SVAB, reports recommending contrast-enhanced MRI for the qualitative diagnosis of microcalcification increased.

In a meta-analysis including 20 published studies, a finding of contrast enhancement of a microcalcification on contrast-enhanced MRI was found to be associated with the diagnosis of malignancy with high sensitivity (87%)[26)] and specificity of 81%. The sensitivity and specificity of contrast-enhanced MRI in microcalcification based on BI-RADS category were as follows: 57% and 32%, respectively, for BI-RADS category 3 microcalcifications; 92% and 82%, respectively, for category 4; and 95% and 66%, respectively, for category 5. Thus, the improvement in diagnostic performance that resulted from the addition of contrast-enhanced MRI was particularly marked for BI-RADS category 4 microcalcifications,

suggesting that, though it cannot be an alternative for biopsy, contrast-enhanced MRI is useful for excluding malignancy.

However, 6 of the studies examined in the above-mentioned meta-analysis included patients with other mammographic abnormalities in addition to microcalcifications.[11-13, 19, 21, 24)] Moreover, the meta-analysis did not indicate whether there were abnormal findings on ultrasonography. The studies that clearly indicate "without abnormal findings on ultrasonography" were mainly from Japan. The sensitivity and specificity of contrast-enhanced MRI in these studies ranged from 79% to 100% and from 78% to 95%, respectively.[3, 10, 18, 20, 27)] The studies varied regarding whether they included BI-RADS category 3 microcalcifications and whether the diagnostic criterion for malignancy on contrast-enhanced MRI was contrast enhancement or a BI-RADS-MRI category of ≥ 4. No consistent tendency can be identified with respect to the qualitative diagnostic performance of contrast-enhanced MRI in the condition of microcalcification without abnormal findings on ultrasonography.

In recent years, overdiagnosis has come to be considered problematic in breast cancer management. Overdiagnosis is the detection and diagnosis of cancer that does not affect the prognosis of the patient. Early-stage breast cancer that is low-grade and noninvasive carcinoma is highly likely to result in overdiagnosis.[28, 29)] In the above-mentioned meta-analysis, the false-negative rate of contrast-enhanced MRI in the qualitative diagnosis of microcalcification was approximately 10%. However, in nearly all of these cases, the carcinoma was noninvasive. When invasive or microinvasive cancer was investigated, the negative predictive value of contrast-enhanced MRI was a very high 99%.[26)] In noninvasive carcinoma, the detection rate with contrast-enhanced MRI has been reported to be high for high-grade noninvasive carcinoma, regardless of BI-RADS category of microcalcification, and many of the false-negatives have been found to be low-grade noninvasive carcinoma.[27)] To avoid overdiagnosis and overtreatment of low-grade noninvasive carcinoma, the option of active surveillance by imaging is permitted for microcalcification without abnormal contrast-enhanced MRI findings.

As a prospect for the future, the different roles of contrast-enhanced MRI may be clarified to determine the indication for biopsy according to the subdivided categories based on the microcalcification characteristics or patient background characteristics, such as whether the patient is in a high-risk group. There is little evidence from Europe and the United States concerning the usefulness of contrast-enhanced MRI performed based on ultrasonography findings. Data should therefore be accumulated and analyzed in Japan. In addition, depending on the results of clinical trials of non-resection of low-grade noninvasive carcinoma,[30, 31)] greater significance may be placed on the role of contrast-enhanced MRI. However, contrast-enhanced MRI is also associated with the problem of cost, and evidence needs to be accumulated to consider the balance between adverse effects and benefits.

In conclusion, contrast-enhanced MRI is not an alternative for SVAB or TVAB for diagnosing microcalcification without abnormal findings on ultrasonography. However, it may assist in selecting a diagnostic strategy, and its use can therefore be considered.

Search keywords and secondary sources used as references

PubMed was searched using the following keywords: breast neoplasm, breast, calcinosis, calcification, mammography, ultrasonography, magnetic resonance imaging, biopsy, needle, image-guided biopsy, diagnosis, diagnostic imaging, carcinoma, intraductal, and noninvasive.

In addition, the following was referenced as a secondary source.

1) The Japanese Breast Cancer Society Clinical Practice Guidelines for Breast Cancer 2018.

References

1) Kettritz U et al: Stereotactic vacuum-assisted breast biopsy in 2874 patients: a multicenter study. Cancer 100: 245-251, 2004
2) Rominger M et al: Breast microcalcifications as type descriptors to stratify risk of malignancy: a systematic review and meta-analysis of 10665 cases with special focus on round/punctate microcalcifications. Rofo 184: 1144-1152, 2012
3) Uematsu T et al: Dynamic contrast-enhanced MR imaging in screening detected microcalcification lesions of the breast: is there any value? Breast cancer Res Treat 103: 269-281, 2007
4) Jiang Y et al: Evaluation of the role of dynamic contrast-enhanced MR imaging for patients with BI-RADS 3-4 microcalcifications. PLoS One 9: e99669, 2014
5) Liberman L et al: The breast imaging reporting and data system: positive predictive value of mammographic features and final assessment categories. AJR Am J Roentgenol 171: 35-40, 1998
6) Mendez A et al: Evaluation of Breast Imaging Reporting and Data System Category 3 mammograms and the use of stereotactic vacuum-assisted breast biopsy in a nonacademic community practice. Cancer 100: 710-714, 2004
7) Orel SG et al: BI-RADS categorization as a predictor of malignancy. Radiology 211: 845-850, 1999
8) Gilles R et al: Clustered breast microcalcifications: evaluation by dynamic contrast-enhanced subtraction MRI. J Comput Assist Tomogr 20: 9-14, 1996
9) Westerhof JP et al: MR imaging of mammographically detected clustered microcalcifications: is there any value? Radiology 207: 675-681, 1998
10) Nakahara H et al: Three-dimensional MR imaging of mammographically detected suspicious microcalcifications. Breast cancer 8: 116-124, 2001
11) Trecate G et al: Breast microcalcifications studied with 3D contrast-enhanced high-field magnetic resonance imaging: more accuracy in the diagnosis of breast cancer. Tumori 88: 224-233, 2002
12) Bluemke DA et al: Magnetic resonance imaging of the breast prior to biopsy. JAMA 292: 2735-2742, 2004
13) Bazzocchi M et al: Contrast-enhanced breast MRI in patients with suspicious microcalcifications on mammography: results of a multicenter trial. AJR Am J Roentgenol 186: 1723-1732, 2006
14) Kneeshaw PJ et al: Differentiation of benign from malignant breast disease associated with screening detected microcalcifications using dynamic contrast enhanced magnetic resonance imaging. Breast 15: 29-38, 2006
15) Cilotti A et al: Contrast-enhanced MR imaging in patients with BI-RADS 3-5 microcalcifications. Radiol Med 112: 272-286, 2007
16) Zhu J et al: Diagnostic accuracy of high-resolution MRI using a microscopy coil for patients with presumed DCIS following mammography screening. J Magn Reson Imaging 25: 96-103, 2007
17) Houserkova D et al: The value of dynamic contrast enhanced breast MRI in mammographically detected BI-RADS 5 microcalcifications. Biomed Pap Med Fac Univ Palacky Olomouc Czech Repub 152: 107-115, 2008
18) Akita A et al: The clinical value of bilateral breast MR imaging: is it worth performing on patients showing suspicious microcalcifications on mammography? Eur Radiol 19: 2089-2096, 2009
19) Fiaschetti V et al: 3-5 BI-RADS microcalcifications: correlation between MRI and histological findings. ISRN Oncol 2011: 643890, 2011
20) Kikuchi M et al: Usefulness of MRI of microcalcification lesions to determine the indication for stereotactic mammotome biopsy. Anticancer Res 34: 6749-6753, 2014
21) Li E et al: A comparative study of the diagnostic value of contrast-enhanced breast MR imaging and mammography on patients with BI-RADS 3-5 microcalcifications. PLoS One 9: e111217, 2014
22) Linda A et al: Role of magnetic resonance imaging in probably benign (BI-RADS category 3) microcalcifications of the breast. Radiol Med (Torino) 119: 393-399, 2014
23) Stehouwer BL et al: 3-T breast magnetic resonance imaging in patients with suspicious microcalcifications on mammography. Eur Radiol 24: 603-609, 2014
24) Brnic D et al: MRI and comparison mammography: a worthy diagnostic alliance for breast microcalcifications? Acta Radiol 57: 413-421, 2016

25) Strobel K et al: Assessment of BI-RADS category 4 lesions detected with screening mammography and screening US: utility of MR imaging. Radiology 274: 343-351, 2015
26) Bennani-Baiti B et al: MR Imaging for diagnosis of malignancy in mammographic microcalcifications: a systematic review and meta-analysis. Radiology 283: 692-701, 2017
27) Shimauchi A et al: Breast MRI as a problem-solving study in the evaluation of BI-RADS categories 3 and 4 microcalcifications: is it worth performing? Acad Radiol 25: 288-296, 2018
28) Sunders ME et al: Continued observation of the natural history of low-grade ductal carcinoma in situ reaffirms proclivity for local recurrence even after more than 30 years of follow-up. Mod Pathol 28: 662-669, 2015
29) Sagara Y et al: Survival benefit of breast surgery for low-grade ductal carcinoma in situ: a population-based cohort study. JAMA Surg 150: 739-745, 2015
30) Francis A et al: Addressing overtreatment of screen detected DCIS; the LORIS trial. Eur J Cancer 51: 2296-2303, 2015
31) Kanbayashi C et al: Current approach and future perspective for ductal carcinoma in situ of the breast. Jpn J Clin Oncol 47: 671-677, 2017

FQ 18 Is investigation recommended for incidental breast lesions detected by CT performed for non-breast disease?

Statement

Investigation of incidental breast lesions can be considered.

Background

Incidental breast lesions are occasionally discovered during CT for non-breast disease. These may include malignancies such as breast cancer. Consequently, watchful waiting is required at a minimum, and, depending on the case, investigation with another modality may also be necessary.

Explanation

The incidental discovery of a breast lesion by chest or cardiac CT is occasionally encountered. The reported detection rates of incidental findings range widely, from 0.63%[1)] to 7.6%.[2)] However, imaging conditions, such as whether a contrast medium was used and slice thickness, varied, as were the periods when the studies were conducted, indicating that differences in the systems used may have played a major role in the variability. Whereas observations were performed using a contrast medium and slice thickness of 1 mm in 1 study, the imaging conditions used in the other were not specified. With cardiac CT[3)] and non-contrast-enhanced, low-dose CT for lung cancer screening, which has become common in recent years,[4)] detection rates are fairly low.

The rate of malignancy of detected lesions also ranges widely, from 9% to 60%.[5)] Round to oval shape, distinct borders, and weak enhancement are findings suggestive of a benign lesion. Large size, irregular or lobular shape, spiculation, strong enhancement, and the presence of enlarged axillary lymph nodes are considered suggestive of a malignant lesion.[5-15)] Non-mass enhancement with contrast-enhanced CT has also been found to be suggestive of malignancy.[11)]

The probability of a detected lesion being malignant has been found to be higher in older individuals than in younger individuals.[11, 14, 16)] However, the absence of an age difference with respect to the distribution of malignant and benign lesions has also been reported.[5, 8)] The distributions of the test subjects may have affected the results.

With regard to the management of incidental findings, if previously acquired images of the lesions are available for comparison, it is recommended that lesions that have enlarged and newly developed lesions be actively investigated.[4)] If the above-described CT findings suggestive of a benign lesion are obtained, watchful waiting is an option. However, an article that evaluated the economic considerations concluded that investigating such incidental breast lesions detected by CT results in less of a financial burden than a screening program for detecting primary breast cancer.[17)] Consequently, such lesions can be investigated.

As mentioned above, although studies have been conducted of incidental breast lesions found on CT, there has been large variability in the lesions examined and the imaging methods and types of imaging used. Further evidence is awaited.

Search keywords and secondary sources used as references

PubMed was searched for the period from 1992 through May 2020 using the following keywords: chest CT, cardiac CT, breast neoplasm, and incidental. Hits were obtained for 53 articles. Sixteen articles were extracted during screening. Of these, 17 were reviewed, including 1 article designated as a reference.

References

1) Healey TT et al: Cancer yield of incidental breast lesions detected on chest computed tomography. J Comput Assist Tomogr 42 (3): 453-456, 2018
2) Hussain A et al: The incidence and outcome of incidental breast lesions detected by computed tomography. Ann R Coll Surg Engl 92 (2): 124-126, 2010
3) Flor N et al: Malignant incidental extracardiac findings on cardiac CT: systematic review and meta-analysis. AJR Am J Roentgenol 201 (3): 555-564, 2013
4) Godoy MCB et al: Extrapulmonary neoplasms in lung cancer screening. Transl Lung Cancer Res 7 (3): 368-375, 2018
5) Taira N et al: Contrast-enhanced CT evaluation of clinically and mammographically occult multiple breast tumors in women with unilateral early breast cancer. Jpn J Clin Oncol 38 (6): 419-425, 2008
6) Yi JG et al: Chest CT of incidental breast lesions. J Thorac Imaging 23 (2): 148-155, 2008
7) Bach AG et al: Comparison between incidental malignant and benign breast lesions detected by computed tomography: a systematic review. J Med Imaging Radiat Oncol 57 (5): 529-533, 2013
8) Lin YP et al: Differentiation of malignant and benign incidental breast lesions detected by chest multidetector-row computed tomography: Added value of quantitative enhancement analysis. PLoS One 11 (4): e0154569, 2016
9) Monzawa S et al: Incidental detection of clinically unexpected breast lesions by computed tomography. Acta Radiol 54 (4): 374-379, 2013
10) Krug KB et al: Focal breast lesions in clinical CT examinations of the chest: a retrospective analysis. Rofo 189 (10): 977- 989, 2017
11) Lin WC et al: Incidentally detected enhancing breast lesions on chest computed tomography. Korean J Radiol 12 (1): 44-51, 2011
12) Porter G et al: Incidental breast masses detected by computed tomography: are any imaging features predictive of malignancy? Clin Radiol 64 (5): 529-533, 2009
13) Gossner J: Intramammary findings on CT of the chest: a review of normal anatomy and possible findings. Pol J Radiol 81: 415-421, 2016
14) Choi YJ et al: Incidental breast lesions on chest CT: clinical significance and differential features requiring referral. J Korean Soc Radiol 79 (6): 303-310, 2018
15) Falomo E et al: Incidence and outcomes of incidental breast lesions detected on cross-sectional imaging examinations. Breast J 24 (5): 743-748, 2018
16) Moyle P et al: Incidental breast lesions detected on CT: what is their significance? Br J Radiol 83 (987): 233-240, 2010
17) Schramm D et al: Costs associated with evaluation of incidental breast lesions identified on computed tomography. Br J Radiol 89 (1059): 20140847, 2016

CQ 18 Is contrast-enhanced breast MRI recommended to determine a treatment strategy before breast cancer surgery?

Recommendation

Contrast-enhanced breast MRI is weakly recommended to determine a treatment strategy before breast cancer surgery.

Recommendation strength: 2, strength of evidence: moderate (B), agreement rate: 100% (10/10)

Background

Contrast-enhanced breast MRI is highly sensitive for breast cancer and widely used clinically. In Japan, contrast-enhanced breast MRI is commonly performed to diagnose the extent of lesions preoperatively in patients definitively diagnosed with breast cancer. It often assists in determining the local surgical procedure. The Clinical Practice Guidelines for Breast Cancer 2018 of the Japanese Breast Cancer Society weakly recommend contrast-enhanced breast MRI to select a treatment strategy before breast cancer surgery.

However, it has been noted that the specificity of contrast-enhanced breast MRI for breast cancer is relatively low compared with its high sensitivity, and the false-positive rate for MRI-detected lesions is high. It has therefore been noted that performing contrast-enhanced breast MRI before breast cancer surgery may increase the likelihood of total mastectomy for early-stage breast cancer. Consequently, the uniform use of contrast-enhanced breast MRI before breast cancer surgery is a subject of debate in Europe and the United States.

Based on these considerations, the usefulness of contrast-enhanced breast MRI for selecting a treatment strategy before breast cancer surgery was evaluated for this CQ. The evaluation took into account, in addition to the accuracy of contrast-enhanced breast MRI in diagnosing breast cancer extent, factors such as the false-positive rate for MRI-detected lesions, the relationship between preoperative MRI and total mastectomy, and the reduction in the rate of postoperative local recurrence.

Explanation

As a newly considered beneficial outcome related to breast cancer surgery, the present qualitative systematic review examined the decrease in the rate of repeat breast cancer surgery, with the increase in total mastectomy examined as an adverse outcome. These outcomes were examined in addition to the outcomes used for this CQ in the Clinical Practice Guidelines for Breast Cancer 2018: the reduction in the local recurrence rate, improvement in the accuracy of diagnosis of breast cancer extent, increased sensitivity for breast cancer, and the reduction in the recurrence rate of the contralateral breast.

Beneficial outcomes related to the initial surgery for preoperative contrast-enhanced breast MRI that were examined in the qualitative systematic review were improvement in the accuracy of diagnosis of

breast cancer extent, reduction in the rate of repeat surgery, and increased sensitivity for breast cancer. Adverse outcomes examined were increases in the false-positive rate and total mastectomy.

Ten articles on case-control studies were used to examine the improvement in the accuracy of diagnosis of breast cancer extent.[1-10] Although the studies that were compiled used different criteria, they generally showed contrast-enhanced MRI to be superior to mammography and ultrasonography for diagnosing breast cancer extent. Specifically, the concordance rates of contrast-enhanced MRI with postoperative pathology were higher than those of other modalities.[1, 2] Moreover, the diagnostic accuracy of MRI (66% to 98%) was higher than that of mammography and ultrasonography (52% to 56%).[3-5] On the other hand, the overall trend was for MRI to underestimate tumor extent less often than mammography, but to overestimate it more often.[2, 5, 6, 8, 10]

With regard to the rate of repeat surgery after initial breast cancer surgery, the articles referenced as a whole, particularly the report of a 2010 randomized, controlled study (COMICE study),[11] reported no significant differences between the groups that underwent MRI (1.6% to 29%) and those that did not (3.3% to 45%).[11-20] However, in 2 cohort studies reported in articles newly included in the present review in which propensity score matching was performed (patients with invasive lobular carcinoma were the subjects of 1 study), significantly lower repeat surgery rates were found in the groups that underwent preoperative MRI than in the groups that did not.[19, 20]

With regard to increased sensitivity for breast cancer, the current qualitative systematic review examined the increase in the ability to detect additional malignancies provided by preoperative MRI of the ipsilateral and contralateral breasts.[13, 16, 20-22] The reference standards were the true positive rate for MRI-detected lesions that underwent additional biopsy and the true positive rate including postoperative pathology results. Thus, variability was seen between the reports. However, additional malignancies were seen in the breast with known breast cancer detected by preoperative MRI in 7.3% to 22% of patients, and contralateral breast cancer was detected in 1.9% to 5.7% of patients.

However, in the articles included in the current review as a whole, MRI-detected lesions were seen in 15.2% to 40% of patients, with false-positive rates ranging from 34% to 66%.[13, 16, 17, 20-27] The addition of preoperative MRI detects a certain amount of additional breast cancer not identifiable by mammography or ultrasonography in the ipsilateral and contralateral breasts (increased breast cancer sensitivity: beneficial outcome). At the same time, however, it is certain to increase false positives (increased false positives: adverse outcome).

With regard to the increase in total mastectomy as initial surgery, the rates of total mastectomy in the articles examined in the present review as a whole were 7.1% to 42.9% in the groups that underwent preoperative MRI and 0% to 47.9% in the groups that did not.[11, 13, 16-21, 28] Specifically, in 2 relatively old cohort studies,[13, 21] in addition to the COMICE study,[11] the rate was significantly higher in the groups that underwent preoperative MRI than in the groups that did not. However, in the relatively new studies added to this review (1 randomized, controlled study,[17] 5 cohort studies,[18-21, 28]) no significant differences in the total mastectomy rate were seen between these groups.

Next, a qualitative, systematic review regarding decreases in the local recurrence rate and contralateral breast recurrence rate was conducted. These measures were considered beneficial outcomes of the addition of preoperative contrast-enhanced breast MRI that was related to prognosis following initial surgery. In the referenced articles as a whole,[11-15, 19, 21, 23, 28-32] the local recurrence rates after breast cancer surgery tended to be lower in the groups that underwent MRI before breast cancer surgery (0.3% to 6.1%) than in those that did not (1% to 9%). However, the differences were significant in 3 of 13 studies, indicating uncertainty that the local recurrence rate was reduced in the preoperative MRI groups.

Four cohort studies and four case-control studies were used to examine the decrease in the rate of contralateral breast cancer recurrence.[13, 14, 19, 20, 29-31, 33] Although these included studies with short follow-up periods, the contralateral breast recurrence rates in the studies used in this review as a whole were 1% to 3.2% in the group that underwent preoperative MRI and 1.3% to 21.7% in those that did not. Thus, some articles reported high rates of contralateral breast recurrence in the groups that did not undergo MRI. However, significant differences were seen in 3 of the 8 studies, indicating uncertainty that the contralateral breast cancer recurrence rate was reduced in the groups that underwent preoperative MRI.

Based on these findings, it is unclear whether preoperative breast MRI produces the beneficial outcomes considered the most important, i.e., reductions in the rates of local recurrence and repeat surgery. Moreover, the false-positive rate, considered the most important adverse outcome, was high, and the possibility that this was related to increased total mastectomy cannot be ruled out. Consequently, it cannot be said with certainty that the benefits of preoperative breast MRI outweigh the adverse effects.

However, the data from the 2010 COMICE study, which examined the relationship between breast MRI performed before breast cancer surgery and breast cancer surgery, are old. Moreover, subsequent to that study, MRI diagnostic criteria were standardized, and accuracy controls and methods of managing MRI-identified lesions, including MRI-guided biopsy, underwent refinement. As a result, the findings of that study are removed from current clinical practice. Consequently, points that should be considered are that the newer controlled studies that were included in the present review for the first time reported that the repeat-surgery rate was reduced in the groups that underwent preoperative MRI, and that the use of MRI was not associated with increased total mastectomy. In studies other than randomized, controlled studies, it has been noted that preoperative breast MRI tends to be performed in high-risk patients, such as those who are younger or have dense breasts or invasive lobular carcinoma. The most recent cohort studies, which performed propensity score matching, found that repeat-surgery rates were significantly lower in groups that underwent MRI. With regard to increased total mastectomy, the newer controlled studies that were included in the present review noted that the use of MRI may not lead to an increase because of the appropriate evaluation of MRI-detected lesions and determination of a treatment strategy to manage such lesions (through the use of MRI-guided biopsy or multidisciplinary team conferences for multidisciplinary decisions on procedures).

Based on the current review, no definitive associations were found between preoperative MRI and reductions in the rates of postoperative local and contralateral breast recurrence. Whether additional

postoperative treatment (local radiation therapy or postoperative adjuvant therapy) was administered was a more significant factor than whether MRI was performed. Moreover, contrast-enhanced breast MRI showed high sensitivity for breast cancer, which was specified as another beneficial outcome for this CQ. It is clear that contrast-enhanced breast MRI was able to detect ipsilateral and contralateral breast cancer that could not be identified by mammography or ultrasonography. The accuracy of breast MRI in diagnosing breast cancer extent is higher than that of mammography or ultrasonography. Consequently, it may assist in determining whether a new breast cancer surgical procedure (e.g., nipple- or skin-sparing total mastectomy) is indicated. Such procedures are based on breast reconstruction, which is increasing in recent years and requires more accurate diagnosis of breast cancer extent. In determining the strength of the recommendation for Japan, the number of MRI units and the low cost of MRI in Japan (healthcare environment that facilitates MRI use) should be taken into account.

Based on the above considerations, contrast-enhanced breast MRI is weakly recommended to select a treatment strategy before breast cancer surgery. To detect contralateral breast cancer, bilateral imaging using a breast-specific coil is necessary. Moreover, consideration should be given to the adverse effects of MRI, and the appropriate evaluation and management of MRI-detected lesions are required. The treatment strategy, including aspects such as the surgical procedure to be used, should be determined in a multidisciplinary fashion by a multidisciplinary team conference.

Search keywords and secondary sources used as references

As in the case of CQ 6 of secondary source 2, the Clinical Practice Guidelines for Breast Cancer, PubMed was searched using the following keywords: breast neoplasms, magnetic resonance imaging, neoplasm recurrence, local, false positive reactions, neoplasm invasiveness, preoperative period, preoperative care, neoplasm staging, diagnosis, and diagnostic imaging. The period searched was from the date of the search performed for the above-mentioned guidelines (December 2016) to June 2019; hits were obtained for 184 articles. The Ichushi and Cochrane Library databases were also searched using the same keywords. In the secondary screening, 5 articles were extracted, and 5 articles were added with a hand search. A qualitative, systematic review was performed of these articles together with those used for the above-mentioned CQ 6.

In addition, the following were referenced as secondary sources.

1) The Japanese Breast Cancer Society Clinical Practice Guidelines for Breast Cancer 2018.
2) The Japanese Breast Cancer Society Clinical Practice Guidelines for Breast Cancer 2018.

References

1) Amano G et al: Correlation of three-dimensional magnetic resonance imaging with precise histopathological map concerning carcinoma extension in the breast. Breast cancer Res Treat 60: 43-55, 2000
2) Nori J et al: : Role of preoperative breast MRI in ductal carcinoma in situ for prediction of the presence and assessment of the extent of occult invasive component. Breast J 20: 243-248, 2014
3) Esserman L et al: : Utility of magnetic resonance imaging in the management of breast cancer: evidence for improved preoperative staging. J Clin Oncol17: 110-119, 1999
4) Uematsu T et al: Comparison of magnetic resonance imaging, multidetector row computed tomography, ultrasonography, and mammography for tumor extension of breast cancer. Breast cancer Res Treat 112: 461-474, 2008
5) Proulx F et al: Value of pre-operative breast MRI for the size assessment of ductal carcinoma in situ. Br J Radiol89: 20150543, 2016
6) Boetes C et al: Breast tumors: comparative accuracy of MR imaging relative to mammography and US for demonstrating extent. Radiology 197: 743-747, 1995
7) Menell JH et al: Determination of the presence and extent of pure ductal carcinoma in situ by mammography and magnetic resonance imaging. Breast J 11: 382-390, 2005
8) van der Velden APS et al: The value of magnetic resonance imaging in diagnosis and size assessment of in situ and small invasive breast carcinoma. Am J Surg 192: 172-178, 2006
9) Santamaria G et al: Preoperative MRI of pure intraductal breast carcinoma-a valuable adjunct to mammography in assessing cancer extent. Breast 17: 186-194, 2008
10) Koh J et al: Assessing sizes of breast cancers that show non-mass enhancement on MRI based on inter-observer variability and comparison with pathology size. Acta Radiol 60: 1102-1109, 2019
11) Turnbull L et al: Comparative effectiveness of MRI in breast cancer (COMICE) trial: a randomized controlled trial. Lancet 375: 563-571, 2010
12) Hwang N et al: Magnetic resonance imaging in the planning of initial lumpectomy for invasive breast carcinoma: its effect on ipsilateral breast tumor recurrence after breast-conservation therapy. Ann Surg Oncol 16: 3000-3009, 2009
13) Ko ES et al: Analysis of the effect of breast magnetic resonance imaging on the outcome in women undergoing breast conservation surgery with radiation therapy. J Surg Oncol 107: 815-821, 2013
14) Sung JS et al: Preoperative breast MRI for early-stage breast cancer: effect on surgical and long-term outcomes. AJR Am J Roentgenol 202: 1376-1382, 2014
15) Gervais MK et al: Preoperative MRI of the breast and ipsilateral breast tumor recurrence: long-term follow up. J Surg Oncol 115: 231-237, 2017
16) Brück N et al: Preoperative magnetic resonance imaging in patients with stage I invasive ductal breast cancer: a prospective randomized study. Scand J Surg 107: 14-22, 2018
17) Balleyguier C et al: Preoperative breast magnetic resonance imaging in women with local ductal carcinoma in situ to optimize surgical outcomes: results from the randomized phase III trial IRCIS. J Clin Oncol 37: 885-892, 2019
18) Ozanne EM et al: Locoregional treatment of breast cancer in women with and without preoperative magnetic resonance imaging. Am J Surg 213: 132-139, 2017
19) Choi WJ et al: Long-term survival outcomes of primary breast cancer in women with or without preoperative magnetic resonance imaging: a matched cohort study. Clin Oncol (R Coll Radiol) 29: 653-661, 2017
20) Ha SM et al: Breast MR imaging before surgery: outcomes in patients with invasive lobular carcinoma by using propensity score matching. Radiology 287: 771-777, 2018
21) Miller BT et al: The influence of preoperative MRI on breast cancer treatment. Ann Surg Oncol 19: 536-540, 2012
22) Karlsson A et al: The accuracy of incremental pre-operative breast MRI findings: concordance with histopathology in the Swedish randomized multicenter POMB trial. Eur J Radiol 114: 185-191, 2019
23) Hill MV et al: Relationship of breast MRI to recurrence rates in patients undergoing breast-conservation treatment. Breast cancer Res Treat 163: 615-622, 2017
24) Yabuuchi H et al: Incidentally detected lesions on contrast-enhanced MR imaging in candidates for breast-conserving therapy: correlation between MR findings and histological diagnosis. J Magn Reson Imaging 23: 486-492, 2006
25) Tozaki M et al: Magnetic resonance-guided vacuum-assisted breast biopsy: results in 100 Japanese women. Jpn J Radiol 28: 527-533, 2010
26) Nakano S et al: Impact of real-time virtual sonography, a coordinated sonography and MRI system that uses an image fusion technique, on the sonographic evaluation of MRI-detected lesions of the breast in second-look sonography. Breast cancer Res Treat 134: 1179-1188, 2012
27) Uematsu T et al: Real-time virtual sonography examination and biopsy for suspicious breast lesions identified on MRI alone. Eur Radiol 26: 1064-1072, 2016

28) Ha SM et al: Long-term survival outcomes in invasive lobular carcinoma patients with and without preoperative MR imaging: a matched cohort study. Eur Radiol 29: 2526-2534, 2019
29) Fischer U et al: The influence of preoperative MRI of the breasts on recurrence rate in patients with breast cancer. Eur Radiol 14: 1725-31, 2004
30) Solin LJ et al: Relationship of breast magnetic resonance imaging to outcome after breast-conservation treatment with radiation for women with early-stage invasive breast carcinoma or ductal carcinoma in situ. J Clin Oncol 26: 386-91, 2008
31) Yi A et al: Breast cancer recurrence in patients with newly diagnosed breast cancer without and with preoperative MR imaging: a matched cohort study. Radiology 276: 695-705, 2015
32) Ryu J et al: Preoperative magnetic resonance imaging and survival outcomes in T1-2 breast cancer patients who receive breast-conserving therapy. J Breast cancer 19: 423-428, 2016
33) Kim JY et al: Unilateral breast cancer: screening of contralateral breast by using preoperative MR imaging reduces incidence of metachronous cancer. Radiology 267: 57-66, 2013

FQ 19 Which imaging examinations are recommended to evaluate the axillary lymph nodes before breast cancer surgery?

Statement

Ultrasonography is recommended for the preoperative evaluation of the axillary lymph nodes.

There is an insufficient scientific basis for using CT, MRI, or FDG-PET (PET/CT) for the sole purpose of preoperatively evaluating axillary lymph node metastasis.

Background

The presence or absence of axillary lymph node metastasis is important for staging and considering a treatment strategy. However, there are currently limitations to its evaluation by diagnostic imaging, and pathological evaluation is therefore considered necessary. Patients who undergo axillary lymph node dissection may experience impairment of the upper extremity and shoulder joint (restricted joint range of motion, upper extremity edema, sensory impairment, pain) of the operative side. Consequently, methods that are minimally invasive have come to be selected. Currently, standard treatment for breast cancer that is clinically negative for axillary lymph node metastasis is to omit axillary lymph node dissection if sentinel lymph node (SLN) biopsy is negative for metastasis. As of recently, axillary lymph node dissection may be omitted even in patients positive for SLN metastasis if the patients undergo radiation therapy. Under such circumstances, appropriate evaluation of the axillary lymph nodes is necessary to determine whether SLN biopsy is indicated.

Explanation

This question was examined by performing a literature search using the keywords indicated below, with survival rate improvement, false positives, sensitivity, overevaluation of microscopic metastasis, and cost-effectiveness as outcomes. There were no articles on survival rate improvement with diagnostic imaging or cost-effectiveness.

SLN biopsy is currently the standard treatment for primary breast cancer considered clinically negative for axillary lymph node metastasis (N0; secondary source 1). Generally, a blue dye or radioisotope is injected into the breast and enters a lymph duct. The first lymph node it reaches is identified as the SLN and resected. If the SLN is positive for metastasis based on an intraoperative rapid pathology examination, axillary lymph node dissection is performed to level II. However, since the results of the ACOSOG Z0011 study were reported, there has been debate regarding whether axillary lymph node dissection can be omitted even if metastasis to the SLN is seen.[1)] The NCCN guidelines (secondary source 2) indicate that SLN biopsy is indicated if metastasis is suspected in up to 2 lymph nodes based on imaging studies. If 1 or 2 SLNs are metastasis-positive, they recommend that axillary lymph node dissection be omitted and breast-conserving surgery and radiation therapy be performed. Consequently, under the current

circumstances, the question of how to use diagnostic imaging can no longer be considered by simply comparing the diagnostic performance of each modality.

Ultrasonography is noninvasive, and its use is recommended to evaluate the axillary region, as well as for the widely performed preoperative breast evaluations. An examination of the diagnostic performance of ultrasonography reported sensitivity of 49% to 87% and specificity of 55% to 94%.[2] Improvement in diagnostic performance has been reported by combining size (short-axis diameter > 5 mm considered positive) and morphological criteria (findings of round shape, hypoechoic pattern, cortical thickening, disappearance of the hilum, and lobularity) and blood flow information obtained by modalities such as color Doppler imaging.[3] For lymph nodes suspected of involvement based on ultrasonography, confirmation by ultrasound-guided axillary lymph node biopsy (cytology and histology) is recommended.[4] In a systematic review of 6 studies in 4,271 patients who underwent diagnosis by ultrasound-guided biopsy, axillary lymph node metastasis was seen is ≤ 2 nodes in 78.9% of patients who were negative for metastasis by ultrasound-guided biopsy and 43.2% of patients who were positive for metastasis. It was therefore concluded that, even in patients who are positive on ultrasound-guided biopsy, axillary lymph node dissection may be unnecessary in roughly half.[5] Thus, it has recently become necessary to consider whether SLN biopsy is indicated based not only on an assessment of whether lymph node metastasis has occurred, but also on whether it has occurred in 2 or fewer nodes.

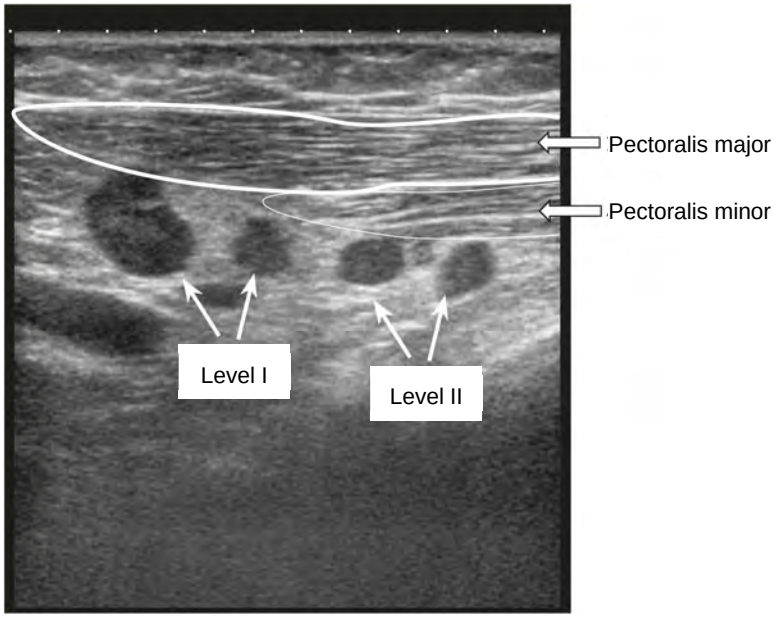

Figure. Ultrasonography performed for preoperative staging of breast cancer

Enlarged lymph nodes are seen in right axillary region levels I and II. Metastasis was suspected based on morphology, and malignancy was diagnosed by aspiration biopsy cytology. Axillary lymph node dissection was performed, and metastasis was confirmed histopathologically.

MRI is commonly performed to diagnose breast disease, with MRI of the axillary region performed as secondary imaging.[3] Examination of the diagnostic performance of MRI in the axillary lymph nodes in a recent meta-analysis showed sensitivity of 48% to 62% (pooled sensitivity, 55%) and specificity of 82% to 89% (pooled specificity, 86%).[6] Compared with ultrasonography, MRI is viewed as enabling more objective evaluation with little operator dependence.[3] However, it cannot be said that appropriate methods of imaging and diagnosis have been established at this point. Consequently, the imaging range does not always adequately include the axillary region.

FDG-PET/CT may be performed to evaluate the axillary lymph nodes together with whole-body metastasis screening. In a meta-analysis, its sensitivity and specificity were found to range from 47% to 63% (pooled sensitivity, 56%) and from 87% to 93% (pooled specificity, 91%), respectively.[6] Although technological innovations such as system improvements and the 3D time-of-flight (TOF) method are thought to have improved the ability to detect lesions, detecting small lymph node metastases (< 5 mm in diameter or patients with microscopic metastasis) is particularly difficult.[7]

With CT, the axillary region may be evaluated at the same time as screening for chest lesions or metastasis to areas including the abdomen. CT can provide more objective data than ultrasonography. However, an examination of diagnostic performance using previous reports showed sensitivity ranging from 60% to 78% and specificity ranging from 76% to 97%.[8-10] Thus, CT cannot be considered effective in its diagnostic performance.[3]

The above findings indicate that axillary lymph node diagnosis based on diagnostic imaging has limitations and cannot substitute for SLN biopsy. The use of ultrasonography to preoperatively evaluate the axillary lymph nodes is recommended in view of considerations such as exposure to radiation and contrast media and because it can be performed noninvasively and used in interventions.

Search keywords and secondary sources used as references

PubMed was searched using the following keywords: breast cancer, axillary lymph node, ultrasound, ultrasonography, MRI, CT, and PET/CT.

In addition, the following were referenced as secondary sources.

1) The Japanese Breast Cancer Society Clinical Practice Guidelines for Breast Cancer 2018.
2) Gradishar WJ et al: NCCN Guidelines®: Breast Cancer Ver 7. 2021. National Comprehensive Cancer Network, 2021

References

1) Giuliano AE et al: Axillary dissection vs no axillary dissection in women with invasive breast cancer and sentinel node metastasis: a randomized clinical trial. JAMA 305: 569-575, 2011
2) Alvarez S et al: Role of sonography in the diagnosis of axillary lymph node metastases in breast cancer: a systematic review. AJR Am J Roentgenol 186: 1342-1348, 2006
3) Chang JM et al: Axillary nodal evaluation in breast cancer: state of the art. Radiology 295: 500-515, 2020
4) Houssami N et al: Preoperative ultrasound-guided needle biopsy of axillary nodes in invasive breast cancer: meta-analysis of its accuracy and utility in staging the axilla. Ann Surg 254: 243-251, 2011
5) Ahmed M et al: Meta-analysis of tumour burden in pre-operative axillary ultrasound positive and negative breast cancer patients. Breast cancer Res Treat 166: 329-336, 2017

6) Zhang X et al: PET/CT and MRI for identifying axillary lymph node metastases in breast cancer patients: systematic review and meta-analysis. J Magn Reson Imaging 52: 1840-1851, 2020
7) Mori M et al: Diagnostic performance of time-of-flight PET/CT for evaluating nodal metastasis of the axilla in breast cancer. Nucl Med Commun 40: 958-964, 2019
8) Uematsu T et al: In vitro high-resolution helical CT of small axillary lymph nodes in patients with breast cancer: correlation of CT and histology. AJR Am J Roentgenol 176: 1069-1074, 2001
9) Shien T et al: Evaluation of axillary status in patients with breast cancer using thin-section CT. Int J Clin Oncol 13: 314-319, 2008
10) Ogasawara Y et al: Multidetector-row computed tomography for the preoperative evaluation of axillary nodal status in patients with breast cancer. Surg Today 38: 104-108, 2008

FQ 20 Is whole-body screening by CT, PET, or PET/CT recommended before breast cancer surgery?

Statement

In primary breast cancer of stage I or II, which shows no signs of metastasis, whole-body screening by CT, PET, or PET/CT before breast cancer surgery is generally not recommended. However, in stage II disease, whole-body screening by PET or PET/CT is considered depending on the breast cancer subtype, tumor grade, and patient background. Whole-body screening by CT, PET, or PET/CT is essentially recommended in stage III disease.

Background

In the previous guidelines, whole-body screening before primary breast cancer surgery was recommended in disease of stage III or higher. However, it was not recommended in stage I or II disease, which has a low rate of distant metastasis (secondary sources 1 to 4).

In the General Rules for Clinical and Pathological Recording of Breast Cancer (18th edition, secondary source 5), the clinical staging classification used is the anatomic stage classification based on the TNM classification conforming to the TNM Classification of Malignant Tumours of the Union for International Cancer Control (eighth edition, UICC; secondary source 6). Recently, however, the treatment strategy for breast cancer has been determined using the breast cancer subtype based on biomarkers, as well as the clinical stage. In addition, the American Joint Committee on Cancer (AJCC) staging manual (8th edition, secondary source 7) incorporated the prognostic stage, which combines the tumor grade and subtype classification with the anatomic stage classification, and this has been used since January 2018 in the United States.

With regard to whole-body screening before primary breast cancer surgery, there is also a need in Japan to consider not only the clinical stage, which has conventionally been used, but also the breast cancer subtype, tumor grade, and patient background. Consequently, the usefulness of such screening by CT, PET, or PET/CT was examined based on the currently available evidence.

Explanation

Whole-body screening by diagnostic imaging before breast cancer surgery is often performed to screen for distant metastasis, which may result in a change in the treatment plan. In The Diagnostic Imaging Guidelines 2016 (secondary source 4), preoperative screening for distant metastasis by CT, PET, or PET/CT was not recommended in stage I or II breast cancer if there were no clinical findings strongly suggestive of metastasis. There was a lack of scientific evidence for such use. There was scientific evidence for its use in stage III breast cancer, and it was therefore recommended in that case. Moreover, the Japanese

Breast Cancer Society Clinical Practice Guidelines for Breast Cancer 2018 weakly recommend that preoperative whole-body screening by CT, PET, or PET/CT not be performed in stage I or II breast cancer.

A review of several studies showed that distant metastasis was found in 2.6% of the patients who underwent examinations in stage I or II.[1-8)] The proportion with distant metastasis was 0.4% for stage I, 6.9% for stage II, 5.3% for stage IIA, and 10.9% for stage IIB. Thus, the frequency of distant metastasis was low in patients with stage I breast cancer, indicating that preoperative whole-body screening is not very useful in these patients.

An examination by modality found that CT (chest and abdomen) was more useful than chest radiography and liver ultrasonography for detecting pulmonary or liver metastasis, although CT false-positives were common in stages I and II.[9)] False positives on chest CT have been reported to occur frequently in stage I and II breast cancer, resulting in additional imaging examinations and increased radiation exposure and cost.[10)] Consequently, the usefulness of CT in stage I and II disease is considered low.

With PET and PET/CT, the ratio of false positives to true positives has been found to increase as the stage of disease decreases.[11)] Consequently, whole-body screening with PET and PET/CT is not recommended for stage I disease.[12-15)] For diagnosing axillary lymph node metastasis, sentinel node biopsy (SNB) is the gold standard, and PET and PET/CT cannot substitute for it.[14, 16)] Previous guidelines from Japan, Europe, and the United States do not recommend whole-body screening by PET and PET/CT in stage II disease (secondary sources 1 to 4). However, a systematic review found that, with the addition of PET and PET/CT to conventional diagnostic imaging to classify patients with stage II breast cancer, the distant metastasis detection rate increased from 1.2% to between 3.3% and 34.3%.[1)] The results of several other studies also suggested that PET and PET/CT are useful for detecting distant metastasis in stage II breast cancer.[3, 4, 14-18)] Moreover, PET and PET/CT were reported to result in a change of treatment plan in 8% to 18% of stage II patients.[19)] In stage II breast cancer, many studies have found PET and PET/CT to be useful in patients positive for axillary lymph node metastasis and in stage IIB disease.[3, 4, 14-16)] However, evidence for this is lacking. Further evaluation in large, multicenter studies is considered necessary to evaluate the role of PET and PET/CT in patients with stage II disease and disease in the stage IIA and IIB subgroups to elucidate the clinical stages in which PET and PET/CT can be systematically performed in a cost-effective manner.[11, 13, 15, 19)] In stage III or locally advanced breast cancer, numerous studies have reported that PET and PET/CT were useful, detecting distant metastasis and changing the treatment plan in 10% to 29% of patients.[1, 13-16, 20)] The sensitivity of PET and PET/CT in detecting distant metastasis has ranged from 78% to 100%, which is higher than the 37% to 78.6% sensitivity of non-metabolic imaging examinations that reflect morphological and anatomical changes, such as conventional ultrasonography and CT.[1)] The diagnostic accuracy of PET and PET/CT in bone metastasis may be higher than that of bone scintigraphy.[2, 16)] Another advantage of PET and PET/CT is that it can be used to examine not only the chest, abdomen, and bones, but also the extra-axillary lymph nodes in a single examination.[11, 14, 15)] However, evidence regarding its cost-effectiveness is lacking.[13)]

Whether the clinical stage alone should be considered when examining whether preoperative whole-body screening is needed is also a subject of debate. In a study by Riedl et al. of 134 patients aged < 40 years with stage I to IIIC breast cancer, stage IV lesions were seen by PET or PET/CT in 10% of patients with asymptomatic stage I or II disease, with distant metastasis seen in 17% of patients with stage IIB disease.[4)] Compared with elderly breast cancer patients, patients < 40 years old are more likely to have higher biological malignancy or metastasis.[14)] Early detection of distant metastasis may be helpful in changing the survival rate or treatment of such patients. In breast cancer patients < 40 years old, whole-body screening by PET or PET/CT may be beneficial even in stage I or II breast cancer (particularly stage IIB). Studies have suggested that it may be particularly useful if high-risk disease is involved.[4, 13)]

Studies of subtypes have found that, in patients with stage II breast cancer, those negative for hormone receptors, HER2-positive younger patients, and HER2-positive or triple-negative patients undergo diagnostic imaging more frequently for clinical staging.[21, 22)] With regard to distant metastasis detection in patients with stage II breast cancer, bone and liver metastases are often detected with the luminal B (HER2-positive) and HER2-positive subtypes, and bone, liver, and pulmonary metastases are often detected with the basal-like subtype. Screening for metastasis in these subtypes has been found to be helpful.[12)] However, the finding of no significant differences in the metastasis detection rate between the hormone-receptor positive, HER2-positive, and triple-negative subtypes has also been reported.[22, 23)]

Whether whole-body screening is needed in stage II (particularly stage IIB) breast cancer and whether patient background such as subtype, patient age, and high-risk disease need to be taken into account remain subjects of considerable debate. Large, prospective, adequately planned, multicenter studies are therefore needed. Moreover, studies based on prognostic staging classification are likely to increase in number in the future.

Finding distant metastasis through preoperative whole-body screening with CT, PET, or PET/CT would result in a change of treatment plan that could avoid unnecessary surgery. If no metastasis is found, such screening could alleviate the patient’s anxiety. However, within the scope of the literature search, there were no reports relevant to improving overall survival time. Moreover, although radiation exposure increases with screening, within the scope of the literature search, there were no articles that presented evidence regarding the risk versus benefit of the increased exposure. With regard to increased cost, such screening is likely much less expensive in Japan than in Europe and the United States. However, there were no articles that presented evidence regarding its cost-effectiveness.

Based on the above considerations, whole-body screening is currently not recommended before breast cancer surgery in stage I or II primary breast cancer without signs of metastasis. However, depending on patient background such as the cancer subtype, tumor grade, the patient’s age, and breast cancer risk, whole-body screening may be considered.

Search keywords and secondary sources used as references

PubMed was searched using the following keywords: breast neoplasms, preoperative period, preoperative care, diagnosis, diagnostic imaging, neoplasm staging, metastasis, CT, and PET. The period searched was through June 2019; hits were obtained for 354 articles. Although a hand search was also performed, there were no articles that examined the usefulness of preoperative whole-body screening based on prognostic staging classification.

In addition, the following were referenced as secondary sources.

1) The Japanese Breast Cancer Society Clinical Practice Guidelines for Breast Cancer 2018 4th Edition
2) The Japanese Breast Cancer Society Clinical Practice Guidelines for Breast Cancer 2018, Supplement 2019.
3) William J et al: NCCN Guidelines®: breast cancer Ver 5. 2020. National Comprehensive Cancer Network, 2020
4) Japan Radiological Society, Ed.: Diagnostic Imaging Guidelines 2016. KANEHARA & Co., 2016.
5) Japanese Breast Cancer Society, Ed.: General Rules for Clinical and Pathological Recording of Breast Cancer (18th edition). KANEHARA & Co., 2018.
6) UICC Japanese Joint Committee on TNM Classification, translation: TNM Classification of Malignant Tumours (eighth edition), Japanese version. KANEHARA & Co., 2017.
7) Amin MB et al: American Joint Committee on Cancer (AJCC) staging manual 8th edition. Spriger, 2017

References

1) Brennan ME et al: Evaluation of the evidence on staging imaging for detection of asymptomatic distant metastases in newly diagnosed breast cancer. The Breast 21: 112-123, 2012
2) Riegger C et al: Whole-body FDG PET/CT is more accurate than conventional imaging for staging primary breast cancer patients. Eur J Nucl Med Mol Imaging 39: 852-863, 2012
3) Bernsdorf M et al: Preoperative PET/CT in early-stage breast cancer. Ann of Oncol 23: 2277-2282, 2012
4) Riedl CC et al: Retrospective analysis of 18F-FDG PET/CT for staging asymptomatic breast cancer patients younger than 40 years. J Nucl Med 55: 1578-1583, 2014
5) Cochet A et al: 18F-FDG PET/CT provides powerful prognostic stratification in the primary staging of large breast cancer when compared with conventional explorations. Eur J Nucl Med Mol Imaging 41: 428-437, 2014
6) Schirrmeister H et al: Fluorine-18 2-deoxy-2-fluoro-D-glucose PET in the preoperative staging of breast cancer: comparison with the standard staging procedures. Eur J Nucl Med 28: 351-358, 2001
7) Groheux D et al: Effect of 18F-FDG PET/CT imaging in patients with clinical Stage Ⅱ and Ⅲ breast cancer. J Radial Oncol Biol Phys 71: 695-704, 2008
8) Jeong YJ et al: Additional value of F-18FDG PET/CT for initial staging in breast cancer with clinically negative axillary nodes. Breast cancer Res Treat 145: 137-142, 2014
9) Hyeyoung K et al: The value of preoperative staging chest computed tomography to detect asymptomatic lung and liver metastasis in patients with primary breast carcinoma. Breast cancer Res Treat 126: 637-641, 2011
10) Dull B et al: Overuse of chest CT in patients with stage I and II breast cancer: an opportunity to increase guidelines compliance at an NCCN member institution. J Natl Compr Canc Netw 15: 783-789, 2017
11) Groheux D et al: Should FDG PET/CT be used for the initial staging of breast cancer? Eur J Nucl Med Mol Imaging 36: 1539- 1542, 2009
12) Chen X et al: Baseline staging tests based on molecular subtype is necessary for newly diagnosed breast cancer. J Exp Clin Cancer Res 33: 28, 2014
13) Aroztegui AC et al: 18F-FDG PET/CT in breast cancer: Evidence-based recommendations in initial staging. Tumour Biol 39 (10): 1-23, 2017
14) Groheux D et al: Performance of FDG PET/CT in the clinical management of breast cancer. Radiology 266: 389-405, 2013
15) Groheux D et al: 18F-FDG PET/CT for staging and restaging of breast cancer. J Nucl Med 57: 17S-26S, 2016
16) Paydary K et al: The evolving role of FDG-PET/CT in the diagnosis, staging, and treatment of breast cancer. Mol Imaging Biol 21: 1-10, 2019
17) Evangelista L et al: Diagnostic and prognostic impact of fluorine-18 fluorodeoxyglucose PET/CT in preoperative and postoperative setting of breast cancer patients. Nucl Med Commun 38: 537-545, 2017
18) Nursal GN et al: Is PET/CT necessary in the management of early breast cancer? Clin Nucl Med 41: 362-3675, 2016

19) Krammer J et al: 18F-FDG PET/CT for initial staging in breast cancer patients: is there a relevant impact on treatment planning compared to conventional staging modalities? Eur Radiol 25: 2460-2469, 2015
20) Yararbas U et al: The value of 18F-FDG PET/CT imaging in breast cancer staging. Bosn J Basic Med Sci 18: 72-79, 2018
21) Linkugel A et al: Staging studies have limited utility for newly diagnosed stage I-II breast cancer. J Surg Res 196: 33-38, 2015
22) Bychkovsky BL et al: Imaging in the evaluation and followup of early and advanced breast cancer: when, why, and how often? Breast 31: 318-324, 2017
23) Srour KM et al: Overuse of preoperative staging of patients undergoing neoadjuvant chemotherapy for breast cancer. Ann Surg Oncol 26: 3289-3294, 2019

FQ 21 Which breast imaging surveillance is recommended for the ipsilateral or contralateral breast of women treated with breast-conserving surgery?

Statement

For the early detection of ipsilateral local recurrence and contralateral breast cancer after breast-conserving surgery, periodic ultrasonography should be performed in addition to annual mammography. MRI is recommended only in patients with mammography-negative dense breasts at the initial examination and should be performed for patients who understand its disadvantages, such as adverse reactions to the contrast medium, high cost, and increased recall and biopsy rates.

Background

Routine mammography for ipsilateral local recurrence and contralateral breast cancer after breast-conserving surgery (BCS) has been reported to improve prognosis, and postoperative annual mammography is strongly recommended.[1)] However, other imaging examinations were performed experimentally as routine examination after BCS, but the scientific evidence was insufficient, and there is currently no standardization of the methods and interval.

For this FQ, we examined the usefulness of some imaging examinations (tomosynthesis, ultrasonography, MRI, CT) in periodic follow-up for ipsilateral local recurrence and contralateral breast cancer after BCS. Mammography was excluded from this study because mammography is recommended every 1 or 2 years after BCS (secondary source 1) according to other countries' guidelines, and it is performed at many facilities in Japan. Moreover, in patients with hereditary breast and ovarian cancer syndrome, a group at high risk of breast cancer, bilateral or contralateral risk-reduction mastectomy has been found not only to reduce the risk of breast cancer, but also to improve overall survival. However, surveillance by breast MRI is recommended for patients who have not undergone risk-reduction mastectomy, and it has been covered by national health insurance since April 2020 (secondary source 2). Because surveillance by annual mammography and contrast-enhanced MRI is recommended for high-risk groups, these modalities were excluded from the present study.

Explanation

A report from South Korea, an Asian country like Japan, showed that ipsilateral local recurrence detected on mammography often presented with calcification (21.2%), whereas contralateral breast cancer was often detected by masses (51.3%).[2)] There was no significant difference in the presence of no detectable lesions on mammography: 39% for ipsilateral local recurrences and 40% for contralateral breast cancers. The reasons for this, in the case of ipsilateral local recurrence, were related to dense breasts, changes in mammary tissue due to postoperative scarring and positioning due to breast deformity, and in the case of

contralateral breast cancer, to poor delineation of the primary breast cancer[3]. Recently, tomosynthesis has been reported to be useful for mammography-negative dense breasts.[4] In a comparison of mammography alone and mammography plus tomosynthesis after surgery or radiation therapy, the addition of tomosynthesis to mammography reduced the false-positive rate from 6.9% to 4.9% and increased the cancer detection rate from 4.9% to 6.9%[5]. On the other hand, the false-positive rate of tomosynthesis vs ultrasonography for women with dense breasts on screening mammography, like that for lesions difficult to detect, was not significantly different, but the cancer detection rate was significantly higher with ultrasonography than with tomosynthesis, at 7.1/1,000 tests and 4.0/1,000 tests, respectively.[6] The combination of mammography and tomosynthesis is considered more useful than mammography alone for periodic follow-up of ipsilateral local recurrence and contralateral breast cancer after BCS. However, the screening data show that the combination of mammography and ultrasonography is better. Moreover, because radiation exposure increases with the combined use of tomosynthesis, the use of ultrasonography in combination with mammography is given priority. In addition, The Japanese Breast Cancer Society Clinical Practice Guidelines for Breast Cancer indicate that the use of ultrasonography is useful for the early diagnosis of local recurrence after BCS, especially for luminal type breast cancer, and they recommend the combined use of other modalities for other histological subtypes of breast cancer (secondary source 3).

In a study that compared the diagnostic performance of mammography and MRI for local recurrence after BCS, the sensitivity, specificity, recall rate, and PPV3* (mammography vs. MRI) were 70.3% vs. 61.4%, 88.5% vs. 88.2%, 12.2% vs. 12.6%, and 30.5% vs. 19.5%, respectively. The false-positive rate, the rate of biopsy within 1 year, and the cancer detection rate for mammography vs MRI were 3.5 vs. 6.8/1,000 tests, 4.0% vs. 10.1%, and 8.2 vs. 10.8/1,000 tests, respectively, all higher for MRI[7]. The differences in the cancer detection rate and the rate of biopsy within 1 year were significant, indicating that MRI is useful for recurrence detection. In a cohort study of women ≤ 50 years of age who had undergone BCS, the cancer detection rate of mammography, ultrasonography, and MRI alone was 4.4, 5.2, and 7.3/1,000 tests, respectively. Thus, diagnostic performances of ultrasonography and of MRI were higher than for mammography, but increases in the recall and biopsy rates were also seen. Moreover, when ultrasonography or MRI was combined with mammography, the cancer detection rate was 6.8 and 8.2/1,000 tests, respectively, both higher than that of mammography alone, and that of the combined MRI group was higher than that of the combined ultrasound group. Although the detection rate of early breast cancer improved by combined use of these modalities, the disadvantages of combined use of ultrasound and MRI were the recall rate of 13.0% vs. 13.8%, the biopsy rate of 1.4% vs 2.7%, and PPV3* of 37.9% vs 28.6%, respectively, with the disadvantages increasing in the MRI group[8].

With regard to contralateral breast cancer, an MRI surveillance study of 322 postoperative breast cancer patients showed a 20% reduction in the risk of contralateral invasive breast cancer (to detect noninvasive cancer). On multivariate analysis of the useful factors on MRI, it was significantly more useful in patients with breast cancer that was difficult to detect at initial diagnosis, such as patients with dense breasts ($p <$

0.0007) or those with mammography-negative breast cancer ($p < 0.0001$), regardless of the histological type of breast cancer at initial onset.[9)]

For the early detection of ipsilateral local recurrence and contralateral breast cancer after BCS, mammography combined with ultrasonography or MRI is more useful than mammography alone, and mammography combined with MRI is superior to mammography combined with ultrasonography. However, the combined use of MRI is accompanied by increased disadvantages, as indicated by increased recall and biopsy rates. Consequently, the use of MRI for surveillance is permitted if the patient first adequately understands its disadvantages, such as the side effects of contrast media, the high cost, and increases in the recall and biopsy rates. Ultrasonography, on the other hand, as compared with other modalities, results in little exposure to radiation and pharmaceutical preparations and is inexpensive even if used frequently. It permits frequent follow-up of suspicious lesions without necessarily performing biopsies, with little disadvantage for the patient. In conclusion, periodic follow-up should be performed by ultrasonography in addition to mammography for the early detection of ipsilateral local recurrence and contralateral breast cancer after BCS. The use of MRI is permitted if the patient understands the disadvantages associated with the examination.

Non-contrast CT has a low detection rate of ipsilateral local recurrence and contralateral breast cancer, and it is not recommended for postoperative surveillance of breast cancer. For contrast-enhanced CT, there are no new reports of detection of local recurrence alone, but rather of postoperative systemic surveillance. The use of contrast media is necessary to detect breast lesions on CT examination, but the side effects of contrast media and associated radiation exposure are considered disadvantageous for patients. Therefore, CT is not recommended for the early detection of ipsilateral local recurrence or contralateral breast cancer after BCS.

* PPV3: The value obtained by dividing the number of breast cancer findings by the number of patients with BI-RADS categories 4 and 5 final assessments (diagnostic category) who underwent tissue biopsy (cytology), (= the number of breast cancer/number of biopsies).

Search keywords and secondary sources used as references

PubMed was searched using the following keywords: breast-conserving therapy, ipsilateral breast recurrent cancer, contralateral recurrent breast cancer, mammography, ultrasound, ultrasonography, MRI, CT, local recurrence, recurrence, high-risk group, and BRCA1/2.

In addition, the following were referenced as secondary sources.

1) Japanese Breast Cancer Society, translation supervision: NCCN Guidelines®: breast cancer Ver 7. 2021. National Comprehensive Cancer Network, 2021.
2) HBOC Clinical Practice Working Group Rules Committee, Future Directions Committee, Japanese Breast Cancer Society: Manual on Health-Insurance Covered Treatment of Hereditary Breast and Ovarian Cancer Syndrome. Japanese Breast Cancer Society, 2020.
3) The Japanese Breast Cancer Society Clinical Practice Guidelines for Breast Cancer 2018.

References

1) Paszat LF et al: Annual surveillance mammography after early-stage breast cancer and breast cancer mortality. Curr Oncol 23 (6): e538-e545, 2016
2) Yoon GY et al: Recurrent and second breast cancer detected on follow-up mammography and breast ultrasound after breast-conserving surgery: imaging finding and clinicopathologic factors. J Korea Soc Radiol 74 (1): 15-21, 2016
3) Yeom YK et al: Screening mammography for second breast cancers in women with history of early-stage breast cancer: factors and causes associated with non-defection. BMC Med Imaging 19 (2): 1-9, 2019
4) Skaane P et al: Comparison of digital mammography alone and digital mammography plus tomosynthesis in a population-based screening program. Radiology 267: 47-56, 2013
5) Sia J et al: A prospective study comparing digital breast tomosynthesis with digital mammography in surveillance after breast cancer treatment. Eur J Cancer 61: 122–127, 2016
6) Calabrese TM et al: Adjunct screening with tomosynthesis or ultrasound in women with mammography-negative dense breasts: interim report of a prospective comparative trial. J Clin Oncol 34: 1882-1888, 2016
7) Wernli KJ et al: Surveillance breast MRI and mammography: comparison in women with a personal history of breast cancer. Radiology 292: 311–318, 2019
8) Cho N et al: Breast cancer screening with mammography plus ultrasonography or magnetic resonance imaging in women 50 years or younger at diagnosis and treated with breast conservation therapy. JAMA Oncol 3 (11): 1495-1502, 2017
9) Hegde JV et al: Predictors associated with MRI surveillance screening in women with a personal history of unilateral breast cancer but without a genetic predisposition for future contralateral breast cancer. Breast cancer Res Treat 166: 145-156, 2017

FQ 22 Is whole-body imaging recommended for periodic surveillance after surgery for anatomic stage I and II breast cancer?

Statement

Essentially, it is recommended that periodic whole-body imaging not be performed after surgery for anatomic stage I and II breast cancer. However, the method of surveillance should be determined for each patient by taking into account the breast cancer subtype along with the anatomic stage.

Background

Multiple guidelines from Japan and other countries recommend not performing whole-body imaging for periodic surveillance after breast cancer surgery. However, in clinical practice, more than a few facilities do perform whole-body imaging after such surgery. The studies that provided the basis for the guidelines were designed and conducted in the 1980s.[1-3] Since then, the clinical environment in which breast cancer treatment, metastasis, and recurrence occur has changed greatly as a result of advances in drug therapy and diagnostic imaging. This FQ was examined based on the current evidence concerning whether whole-body imaging is recommended for the postoperative periodic surveillance of anatomic stage I and II breast cancer, which is considered unlikely to recur.

Explanation

Two prospective studies that compared surveillance consisting only of periodic examination and mammography after breast cancer surgery and surveillance that also involved various imaging and blood tests (intensive surveillance) showed no improvement in the survival rate with intensive surveillance.[1-3] Moreover, a meta-analysis of these studies found no difference in the survival rate or recurrence-free survival rate, and a subgroup analysis by age, tumor diameter, and lymph node metastasis status also showed no significant differences.[4]

Based on these results, the guidelines of the American Society of Clinical Oncology (ASCO), National Comprehensive Cancer Network (NCCN), European Society for Medical Oncology (ESMO), and European School of Oncology (ESO) recommend periodic patient interviews, clinical breast examinations, and mammography for the surveillance of asymptomatic patients after breast cancer surgery. They do not recommend periodic chest radiography, bone scintigraphy, ultrasonography, CT, or PET/CT to detect distant metastasis. The purpose of surveillance after breast cancer surgery is to detect local recurrence or contralateral breast cancer early, rather than to find asymptomatic distant metastasis.

However, the studies that provided the basis for this approach were designed and conducted in the 1980s. Since then, major advances have been achieved in drug therapy and diagnostic imaging, and the survival rates for metastatic and recurrent breast cancer have improved. Particularly in the case of oligometastasis, as compared with multiple metastases, localized treatment such as surgery has been found to be useful for

improving prognosis.[5] Consequently, the significance of early detection of distant metastasis may change in the future.[6]

Moreover, it has recently been shown that the risk of recurrence varies according to the breast cancer subtype, which is classified based on biomarkers. The most recent edition of the American Joint Committee on Cancer (AJCC) staging manual, the 8th edition, incorporated a prognostic stage, which combines the tumor grade and subtype classification, into the anatomic stage based on the previous TMN classification for breast cancer staging. The prognostic stage has been reported to enable more accurate staging with respect to survival and prognosis than the anatomic stage.[7, 8] In breast cancer subtypes with a high risk of recurrence and breast cancer with an advanced prognostic stage, better treatment efficacy and quality of life (QOL) improvement are likely if metastasis is detected and treatment started at a stage when the tumor load is small, such as in oligometastasis, even in asymptomatic patients. Consequently, periodic whole-body imaging after breast cancer surgery is acceptable if it is in accordance with the patient's wishes.

However, there have been no reports of studies that have examined the effectiveness of intensive surveillance after breast cancer surgery according to subtype or based on prognostic stage. Its effectiveness with respect to the survival rate and QOL in breast cancer with a high risk of recurrence has also not been demonstrated. In Japan, a prospective, clinical study of the usefulness of intensive surveillance using imaging examinations for a group at high risk of recurrence based on the breast cancer subtype and lymph node metastasis has begun, and the results of the analysis are awaited.[9]

From the perspective of healthcare costs, the cost of testing increases with intensive surveillance. Periodic intensive testing is unlikely to be cost-effective for breast cancer with a low risk of metastasis or recurrence. Moreover, the increase in radiation exposure that results from CT, bone scintigraphy, and PET/CT is a type of risk. Adverse reactions such as allergic reactions to contrast media represent another type of risk. Furthermore, intensive testing increases the risk of false-positive lesions and may increase the psychological burden on the patient unnecessarily and increase unnecessary invasive testing.

The effectiveness of periodic whole-body imaging to detect distant metastasis after surgery for anatomic stage I and II breast cancer has not been demonstrated. Consequently, it is basically recommended that periodic whole-body imaging not be performed. However, the method of surveillance should be determined for each patient by taking into account the breast cancer subtype along with the anatomic stage.

Search keywords and secondary sources used as references

PubMed was searched using the following keywords: breast neoplasm, neoplasm staging, tomography, X-ray computed, postoperative period, postoperative care, mastectomy, follow-up studies, prognosis, neoplasm metastasis, diagnostic imaging, receptor, ErbB-2, receptor, and estrogen. The period searched was through June 2019; hits were obtained for 343 articles. Although a hand search was also performed, there were no articles that examined the effectiveness of intensive surveillance after breast cancer surgery based on cancer subtype or prognostic stage.

In addition, the following were referenced as secondary sources.

1) The Japanese Breast Cancer Society Clinical Practice Guidelines for Breast Cancer 2018.
2) The Japanese Breast Cancer Society Clinical Practice Guidelines for Breast Cancer 2018, Supplement 2019.
3) Hortobagyi GN et al: American Joint Committee on Cancer (AJCC) cancer staging manual 8th ed. Springer, 589-636, 2017

References

1) Ghezzi P et al: Impact of follow-up testing on survival and health-related quality of life in breast cancer patients: a multicenter randomized controlled trial. The GIVIO Investigators. JAMA 271: 1587-1592, 1994
2) Rosselli Del Turco M et al: Intensive diagnostic follow-up after treatment of primary breast cancer: a randomized trial, National Research Council Project on Breast cancer follow-up. JAMA 271: 1593-1597, 1994
3) Palli D et al: Intensive vs clinical follow-up after treatment of primary breast cancer: 10-year update of a randomized trial, National Research Council Project on Breast cancer Follow-up. JAMA 281 (17): 1586, 1999
4) Moschetti I et al: Follow-up strategies for women treated for early breast cancer. Cochrane Database Syst Re (v 5): CD001768, 2016
5) Pagani O et al: International guidelines for management of metastatic breast cancer: can metastatic breast cancer be cured? J Natl Cancer Inst 7; 102 (7): 456-463, 2010
6) Puglisi F et al: Follow-up of patients with early breast cancer: is it time to rewrite the story? Crit Rev Oncol Hematol. 91 (2): 130-141, 2014
7) Mittendorf EA et al: Bioscore: a staging system for breast cancer patients that reflects the prognostic significance of underlying tumor biology. Ann Surg Oncol 24 (12): 3502-3509, 2017
8) Weiss A et al: Validation study of the American Joint Committee on Cancer eighth edition prognostic stage compared with the anatomic stage in breast cancer. JAMA Oncol 4 (2): 203-209, 2018
9) Hojo T et al: Intensive vs. standard post-operative surveillance in high-risk breast cancer patients (INSPIRE): Japan Clinical Oncology Group Study JCOG1204. Jpn J Clin Oncol 45 (10): 983-986, 2015

9
Musculoskeletal

Standard Imaging Methods for Musculoskeletal Resions

A Spinal imaging methods

Overview

Conventional radiography is the first modality of choice if a lesion of the spine or spinal cord is suspected. MRI or CT is then performed to identify the lesion and determine its cause. MRI provides more information than CT and is therefore normally given priority. CT is performed if a detailed bone evaluation is required, and myelography and discography are also performed as necessary.

Detailed discussion

1. Conventional radiography

The standard imaging method includes imaging with 2 different projections, the anteroposterior and lateral projections. Both oblique views are added if foraminal stenosis or spondylolysis is suspected, for imaging with a total of 4 views. To evaluate spinal instability, as in the case of atlantoaxial subluxation and spondylolisthesis, imaging with the lateral views of anteflexion and retroflexion is added. Imaging with the open-mouth odontoid anteroposterior projection is added to evaluate odontoid fracture caused by cervical trauma, atlantoaxial destruction resulting from rheumatoid arthritis, and atlantoaxial rotatory fixation, which occurs preferentially in children.

2. Myelography and discography

Myelography is performed to evaluate spinal canal stenosis and spinal cord/nerve root sheath compression of various causes. Discography is performed for the morphological evaluation of intervertebral disks and for functional diagnosis by inducing or reproducing intervertebral disc pain. They are also performed in combination with CT (CT myelography, CT discography). The use of myelography and discography is becoming limited as MRI becomes more widely used.

3. CT

CT is performed to visualize fracture lines and calcification and ossification changes, such as ossification of the posterior longitudinal ligament, and intervertebral and intravertebral gas. It is also performed to evaluate spinal canal stenosis. The acquired slice thickness should be the thinnest possible for the system (≤ 1 mm). The 3 standard planes in which MPR images are generated are the transverse, sagittal, and coronal planes. Other planes are added as necessary. Three-dimensional imaging using the surface rendering shaded surface display (SSD) and the VR method is useful for showing complex structures in 3D. It is used when there is a need to understand 3D spatial relationships, such as in the case of atlantoaxial subluxation or

odontoid fracture. Because CT has a complementary relationship to MRI, their mutual strengths and weaknesses should be determined and used.

4. MRI

① Body position during imaging and coil used

Imaging is performed with the patient in the supine position. If the patient has scoliosis, the body axis is kept as straight as possible. When imaging of the cervical spine is performed, to avoid artifacts resulting from swallowing or cerebrospinal fluid and blood vessel pulsation, dentures are removed to minimize swallowing and neck movement. Although a phased array coil for the spine is used, use of a dedicated coil is not necessary with systems equipped with an in-table coil.

② Imaging sequences and planes

There are 2 standard imaging planes, the sagittal and transverse planes. For sagittal imaging, an imaging range that adequately includes the bilateral intervertebral foramina is set. T2-weighted sagittal imaging makes it easy to obtain an overview of the anatomy and lesions, and this is the imaging performed initially. T1-weighted sagittal imaging is useful for visualizing bone marrow lesions, lesions that show hyperintensity on T1-weighted images (e.g., hematomas, lipomas), and perineural cysts and for evaluating fat in the vertebral canal. With transverse imaging, the imaging cross-section selected varies according to the clinical signs and disease. In degenerative spinal disease, it is recommended that imaging at the intervertebral level and 3 slices above and below be selected. If a spinal cord or spinal canal lesion is suspected, the appropriate lesion levels are selected. If they are extensive, 1 cross-section each at the vertebral body and intervertebral levels should be selected. T2-weighted transverse imaging and $T2^*$-weighted transverse imaging are useful for evaluating spinal canal stenosis and the interior of the spinal canal. Compared with $T2^*$-weighted imaging, T2-weighted imaging has higher bone marrow lesion detection sensitivity and is less susceptible to magnetic susceptibility artifacts. However, a disadvantage of T2-weighted imaging is its susceptibility to artifacts caused by cerebrospinal fluid and blood vessel pulsation. Consequently, for imaging of the cervical and thoracic spine in degenerative spinal disease, $T2^*$-weighted imaging is recommended instead of T2-weighted imaging. If evaluation of the signal intensity of the lesion itself or of a spinal cord lesion is necessary, or the patient has metal implants, T2-weighted imaging is preferable. It should be noted, however, that $T2^*$-weighted imaging may overestimate spinal canal stenosis. T2-weighted imaging is recommended for transverse imaging of the lumbar spine. T1-weighted transverse imaging is useful when it is difficult to differentiate intervertebral disc herniation from the surrounding structures with T2- and $T2^*$-weighted imaging. It is also useful for seeing the relationship between a severely displaced intervertebral disc and the nerve root. Coronal imaging is useful for evaluating paraspinal lesions and the physical relationship between the nerve root, a protruding intervertebral disk, vertebral osteophytes, and a tumor. Fat-suppressed T2-weighted imaging and short-TI inversion recovery (STIR) imaging are excellent for detecting bone marrow lesions and perispinal lesions.

However, STIR imaging is even less susceptible to artifacts caused by metal than T2-weighted imaging, and it can provide stable fat suppression in areas where the magnetic field is non-uniform, such as the cervical and thoracic spine. For MR myelography, 2D and 3D methods are available. However, the 3D method, which provides good temporal resolution and contrast, is more widely used. MR myelography is used as an equivalent test to regular myelography, which is highly invasive. It enables good images of the lumbar spine to be obtained. However, in the cervical and thoracic spine, the subarachnoid space is narrow, and the images are susceptible to degradation caused by artifacts of cerebrospinal fluid pulsation and of magnetic field non-uniformity.

Table 1. Recommended parameters for MRI

Field of view (FOV)	Cervical and thoracic spine: 20 to 34 cm
	Lumbar spine: 16 to 20 cm
Slice thickness	Cervical spine: 3 to 4 mm
	Thoracic and lumbar spine: 4 to 5 mm
Matrix	256 to 512 ×132 to 270

Although the imaging parameters vary depending on the MR system, the important recommended parameters are shown in Table 1.

③ Standard imaging methods

The standard imaging methods must provide the ability to evaluate the bone marrow, intervertebral disks, spinal canal interior, and spinal cord. If a hematoma or tumorous lesion (e.g., tumor, cysts) is detected, the ability to perform qualitative diagnosis to some degree is necessary. The combination of sagittal and transverse imaging described above is recommended. The following are examples.

(1) Cervical spine (Fig. 1), thoracic spine

Sagittal imaging: T1-weighted imaging, T2-weighted imaging, and fat-suppressed T2-weighted or STIR imaging

Transverse imaging: T1-weighted imaging and $T2^*$-weighted or T2-weighted imaging

(2) Lumbar spine (Fig. 2)

Sagittal imaging: T1-weighted imaging, T2-weighted imaging, and fat-suppressed T2-weighted or STIR imaging

Transverse imaging: T1-weighted imaging, T2-weighted imaging

For cervical and thoracic spine transverse imaging, $T2^*$-weighted imaging is recommended in principle rather than T2-weighted imaging. However, if it is necessary to evaluate the signal intensity of the lesion itself or a spinal cord lesion, T2-weighted imaging should be performed. In investigating trauma, $T2^*$-weighted imaging is considered useful for detecting spinal cord injury (hemorrhage). Sagittal

T2*-weighted imaging should be added to the standard imaging method, and the transverse T2-weighted imaging should be changed to T2*-weighted imaging.

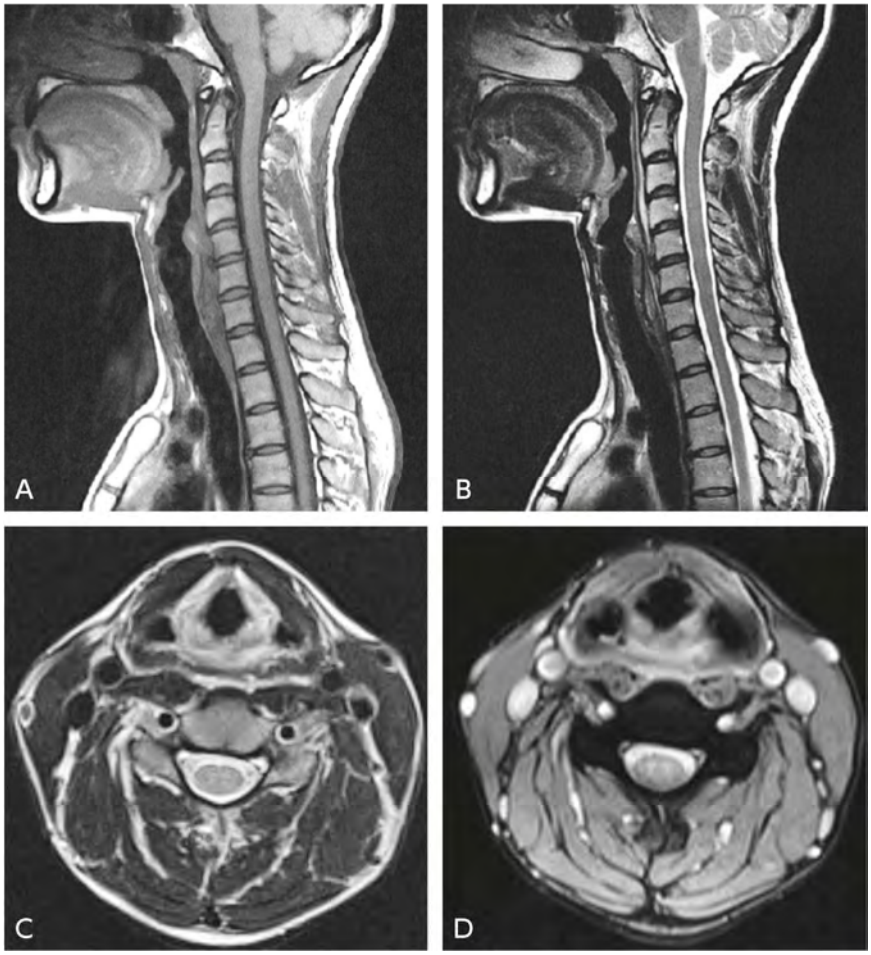

Figure 1. Cervical spine MRI

A: T1-weighted sagittal image, B: T2-weighted sagittal image, C: T2-weighted transverse image
D: T2*-weighted transverse image

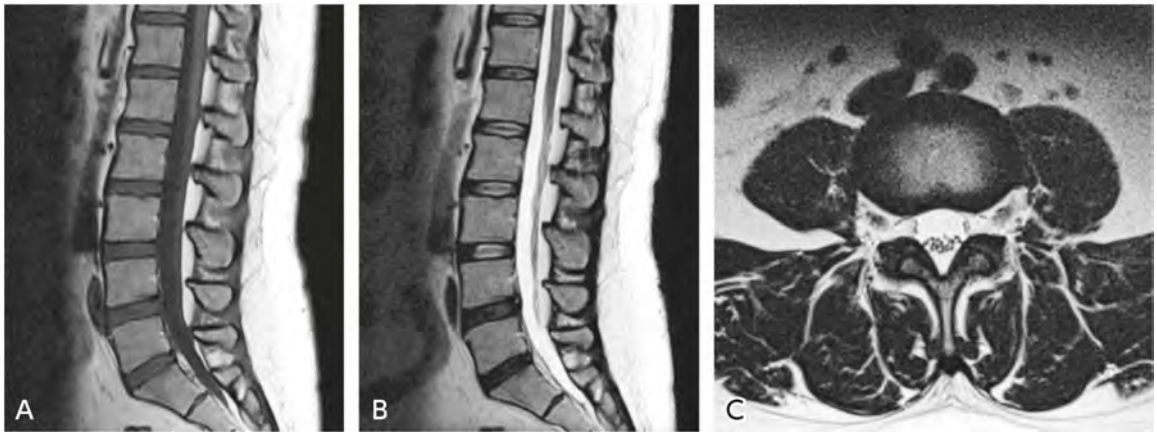

Figure 2. Lumbar spine MRI

A: T1-weighted sagittal image, B: T2-weighted sagittal image, C: T2-weighted transverse image

B Joint imaging methods

Overview

Conventional radiography remains the standard modality for diagnostic imaging of the joints. Although arthrography was previously performed for close investigation, its use has become limited with advances in imaging systems and their increased availability, and opportunities to use MRI in particular have increased. With MRI of the joints, it is considered necessary to evaluate small structures, and particular attention must be paid to the imaging range and cross-section selected and to the resolution. Unlike other areas, proton density-weighted imaging is commonly used for the joints. However, this imaging method is susceptible to image degradation resulting from blurring artifacts. To reduce this, a relatively short echo train length should be selected. The imaging methods for the various joints are described below.

Shoulder joint imaging methods

1. Conventional radiography

The standard imaging method involves imaging with 2 views, the anteroposterior and transverse views. Anteroposterior projection imaging is normally performed in the neutral position. Imaging with internal and external rotation is added as necessary. The lateral view of the scapula (Y view) is suitable for observing the inferior surface of the acromion. Imaging with this view is performed when diagnosing a rotator cuff tear or subacromial impingement. The internally rotated anteroposterior projection and flexion/semiaxial view (Stryker notch view) are useful for visualizing depressed fractures (Hill-Sachs lesions) of the posterolateral area of the humeral head, which occur with recurrent shoulder dislocation or subluxation. Imaging with the arm elevated (zero position) and with the upper arm hanging downward and under downward stress is useful for diagnosing joint laxity and loose shoulder. Imaging of the bicipital groove is performed to evaluate osteophyte protuberance and narrowing of the bicipital groove when long head of the biceps tendon injury and inflammation are suspected.

2. Arthrography

With the emergence of MRI, the use of contrast-enhanced imaging of the joint capsule and bursa to diagnose lesions of the soft tissue such as the rotator cuff and glenoid labrum has become limited. However, arthrography has advantages, such as permitting dynamic observations for investigating the cause of pain on movement, which is difficult with normal MRI, and it can be performed together with treatment for conditions such as joint distension (reduction of intra-articular pressure). Arthrography may also be performed in combination with CT and MRI (CT arthrography, MR arthrography).

3. CT

CT is performed for purposes such as evaluating bone fractures and visualizing joint mice and calcification. The acquired slice thickness should be the thinnest possible for the system (≤ 1 mm). The 3 standard planes in which MPR images are generated are the transverse, oblique sagittal parallel to the glenoid fossa, and oblique coronal perpendicular to the oblique sagittal. Other planes are added as necessary. For bone fractures, CT plays an ancillary role to conventional radiography and can be used to evaluate aspects such as the presence or absence of fracture lines, the number and location of bone fragments, the direction of displacement, and the condition of the joint surface. Three-dimensional images generated using the SSD and VR methods are suitable for determining the nature of bone fractures and dislocations. They are useful for purposes such as the preoperative planning of fracture reduction, osteosynthesis, and functional reconstructive surgery. CT arthrography may be performed to evaluate intra-articular structures such as the glenoid labrum and joint-side rotator cuff.

4. MRI

① Body position during imaging and coil used

The body position during imaging is supine, with the arms in an unstrained, natural, neutral to mildly externally rotated position and the palms of the hands facing the trunk. However, it should be noted that external rotation of the arms may cause pain. Material such as sponge is used to reduce artifacts caused by movement, and the shoulder joint is held in place with a shoulder coil (e.g., phased-array coil or flex coil). A device such as a bust band is used to address respiratory movement. Because the shoulder joint is located laterally on the body and away from the center of the gantry, some means of positioning and increasing the static magnetic field uniformity needs to be devised.

② Imaging sequences and plan

Although T2-weighted imaging is useful for evaluating the rotator cuff, its sensitivity in detecting glenoid labrum lesions is low. $T2^*$-weighted imaging is useful for evaluating the glenoid labrum. However, because false lesions can appear even in a normal glenoid labrum due to the magic angle effect, caution is required in such evaluations. Moreover, bone marrow lesions are indistinct with these imaging methods. Fat-suppressed, $T2^*$-weighted imaging and STIR imaging enable lesions to be visualized in soft tissue, including the rotator cuff, and bone marrow with high sensitivity. Proton density-weighted imaging is useful for evaluating the rotator cuff and glenoid labrum. However, false lesions can also appear in the rotator cuff with this modality due to the magic angle effect, and caution is therefore required in such evaluations. Although T1-weighted imaging provides little information, it is useful for evaluating the bone marrow and incidental abnormal findings, such as hematomas and tumorous lesions (e.g., tumors and cysts).

Table 2. Recommended parameters for MRI

Field of view (FOV)	15 to 18 cm
Slice thickness	3 to 4 mm
Matrix	256 × 230
Echo train length for proton density-weighted imaging	4 to 6

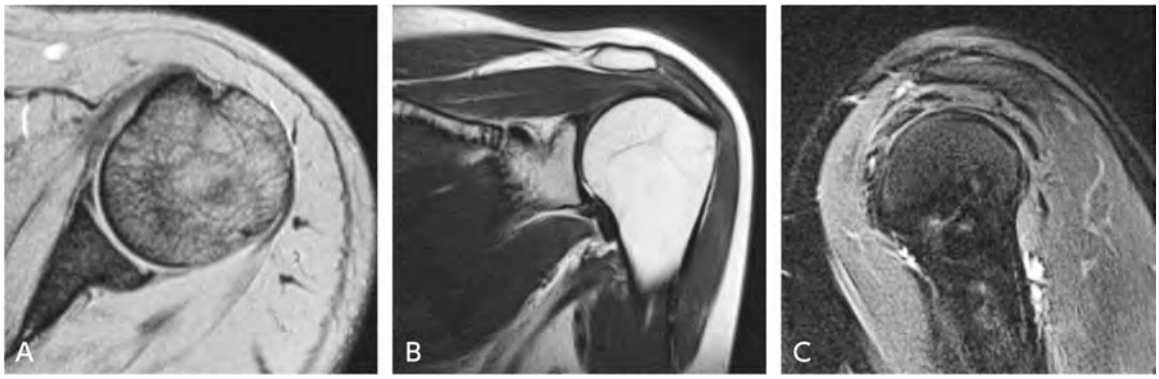

Figure 3. Shoulder joint MRI

A: T2*-weighted transverse image, B: T2-weighted oblique coronal image, C: Fat-suppressed, T2-weighted oblique sagittal image

There are 3 standard imaging planes, the transverse, oblique coronal, and oblique sagittal planes. Transverse imaging is performed perpendicular to the glenoid fossa (or trunk axis) and humerus (or trunk axis) and includes the area from the acromioclavicular ligament to the subscapularis muscle. Oblique coronal imaging is performed parallel to the supraspinatus muscle and includes the area from the infraspinatus muscle to the subscapularis muscle. For oblique sagittal imaging, imaging perpendicular to the glenoid fossa is specified and includes the area from the deltoid muscle to the center of the scapula. In abduction and external rotation, oblique transverse imaging is performed from the coronal scout parallel to the long-axis of the humerus. Oblique coronal and oblique sagittal imaging are added as appropriate. The imaging views useful for the shoulder's essential components/structures are as follows: oblique coronal and oblique sagittal imaging for the rotator cuff, oblique sagittal and oblique coronal imaging for the intra-articular long head of the biceps tendon, transverse imaging for the bicipital groove, oblique sagittal and transverse imaging for the glenohumeral ligaments and rotator cuff interval, and transverse and oblique coronal imaging for the glenoid labrum. The 3 standard imaging views are added complementarily for diagnosis.

Although the imaging parameters vary depending on the MR system, the important recommended parameters are shown in Table 2.

③ Standard imaging method

The standard imaging methods must permit evaluation of the bone marrow and the stabilizing mechanism, including the rotator cuff, the long head of the biceps tendon, and the glenoid labrum. T2-weighted imaging and T2*-weighted imaging are considered fundamental, and fat-suppressed,

T2-weighted imaging from at least 1 plane is desirable. T1-weighted imaging is considered for bone marrow evaluation and when a hematoma or tumorous lesion is present and should be performed from 1 plane. The imaging methods to be used are determined based on the above considerations. Examples are shown below (Fig. 3).

Oblique coronal imaging: T1-weighted imaging, T2-weighted imaging, or fat-suppressed, T2-weighted imaging*

Oblique sagittal imaging: T2-weighted imaging or fat-suppressed, T2-weighted imaging*

(*Combination of oblique coronal, T2-weighted imaging and oblique sagittal, fat-suppressed, T2-weighted imaging or oblique coronal, fat-suppressed, T2-weighted imaging and oblique sagittal, T2-weighted imaging)

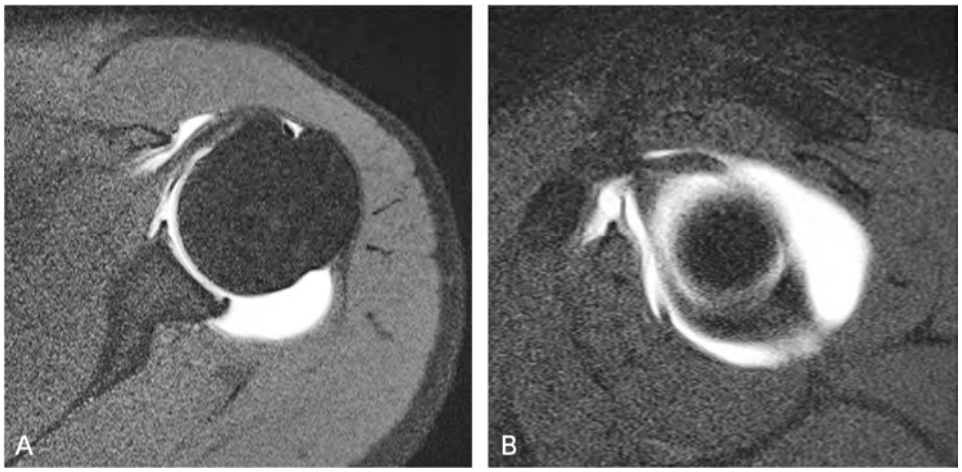

Figure 4. Shoulder joint (direct MR arthrography)

A: Fat-suppressed T1-weighted transverse image, B: Fat-suppressed T1-weighted oblique sagittal image

④ MR arthrography

MR arthrography is used to evaluate injury to intra-articular structures such as the glenoid labrum, long head of the biceps tendon/labrum complex, glenohumeral ligaments, and joint-side rotator cuff. MR arthrography encompasses direct MR arthrography, wherein imaging is performed after a diluted solution of contrast medium is injected into the joint, and indirect MR arthrography, wherein imaging is performed with an exercise load applied after intravenous administration. In direct MR arthrography, imaging is performed after 10 to 20 mL of gadolinium contrast medium diluted 100-fold to 250-fold with physiological saline are injected into the joint (Fig. 4). Although it is invasive, it provides adequate expansion of the joint capsule. Indirect MR arthrography, although minimally invasive, has disadvantages, such as the need for an exercise load, inadequate expansion of the joint capsule, and hindrance of the evaluation by soft tissue contrast enhancement. Direct MR arthrography is more commonly performed.

Fat-suppressed, T1-weighted imaging is performed from the 3 standard angles, with imaging in external rotation and abduction added as appropriate. However, this position may induce pain and cannot be used for all patients. Injury to intra-articular structures can be evaluated based on contrast medium leakage and infiltration. To differentiate between intra- and extra-articular fluid accumulations, additional fat-suppressed, T2-weighted imaging should be performed for any plane.

⑤ Intra-articular contrast medium administration

Currently, only 1 iodine contrast medium is approved for intra-articular administration in Japan. The package inserts for gadolinium contrast media do not mention intra-articular administration. The intra-articular administration of gadolinium contrast media is widely accepted not only in Japan, but throughout the world. However, when performing MR arthrography, such use must be clearly explained to the patient in advance and the patient's consent obtained.

Elbow joint imaging methods

1. Conventional radiography

The standard imaging method includes imaging with 2 different projections, the anteroposterior and lateral projections. Anteroposterior projection imaging should be obtained with the elbow extended. Lateral view imaging is performed with elbow flexion at 90 degrees. In both views, the forearm is in a neutral position with respect to rotation. Oblique projection is useful for detecting bone fractures that are hard to discern, particularly fractures of the radial head, the coronoid process of the ulna, and the lateral epicondyle in children. For osteochondritis dissecans of the humeral capitulum, anteroposterior projection with flexion of 45 degrees provides better visualization of lesions than normal anteroposterior projection. Osteophyte formation and ulnar groove deformation in cubital tunnel syndrome are observed by ulnar groove projection. Valgus/varus stress radiography is performed to evaluate instability resulting from injury of the medial and lateral collateral ligaments. Comparison by imaging of the unaffected side is useful in the case of trauma in a child when assessment is uncertain. However, caution is required with respect to increased radiation exposure.

2. Arthrography

Because MRI has improved demonstration of the structural components of the joint, the use of arthrography is limited. In the case of a partial rupture of the medial collateral ligament, penetration of contrast medium into the ruptured area is seen on CT or MR arthrography, and detection of ligament injury is better than with noncontrast tests.

3. CT

CT is often performed to determine the presence or absence of a fracture in acute trauma, the condition of the joint surface, displaced bone fragments, and to conduct a detailed investigation of loose bodies or

osteophytes that could restrict the range of motion of the joint. MPR images of the joint surface are generated in 3 planes, transverse, sagittal, and coronal. However, to permit high-resolution image reconstruction from all angles, the slice thickness selected is the minimum for the system used (≤ 1 mm). In this case, a reconstruction slice thickness of 2 mm is selected. VR imaging is useful for purposes such as preoperative simulation. However, depending on the setting of the threshold it can be difficult to visualize small fractures and loose bodies. Consequently, it is used to complement MPR.

4. MRI

① Body position during imaging and coil used

Imaging is performed in the supine position with the elbow extended and the arm lowered. For good visualization of the collateral ligaments, forearm rotation in relation to the upper arm is minimized. If the patient is physically large, the elbow joint may be at the edge of the gantry and outside the center of the static magnetic field, resulting in poor image quality. In this case, the patient is tilted so that the elbow joint moves closer to the center. Although there is a method that involves having the patient raise the imaged arm while in the prone position, this places a burden on the shoulder joint, making the imaging susceptible to artifacts caused by movement. It is important to confirm that the subject is in a position that allows him or her to remain still, and that the test can be performed comfortably.

A round or rectangular coil and a coil for the hand and elbow are used. When examining intra-articular structures in detail, a small round coil or coil for the hand and elbow that is 7 to 8 cm in diameter is used to increase spatial resolution.

② Imaging sequences and planes

The imaging sequences vary depending on the target structure. If the target is a ligament, $T2^*$-weighted imaging, fat-suppressed, T2-weighted imaging or STIR imaging, and proton density-weighted imaging are suitable. For detailed examination of the common tendons of the extensor and flexor muscles, T2-weighted imaging and fat-suppressed, T2-weighted imaging or STIR imaging are useful. For detection of bone injury, STIR imaging and fat-suppressed, T2-weighted imaging are highly sensitive, and T1-weighted imaging is excellent for evaluating fracture lines and intra-articular hematomas. For evaluating articular cartilage, fat-suppressed, proton density-weighted imaging, 3D, fat-suppressed, GRE-T1-weighted imaging, and 3D GRE with water-selective sequence are useful. When imaging the elbow joint, the area being imaged is at the edge of the magnetic field. Consequently, STIR imaging often provides better fat suppression than fat-suppressed, T2-weighted imaging.

There are 3 standard imaging planes, the transverse, coronal, and sagittal planes. For transverse imaging, the area from the distal metaphysis of the humerus to the radial tuberosity is imaged. Coronal imaging is set to be performed parallel to a straight line from the medial epicondyle to the lateral epicondyle or a straight line across the anterior border, as seen in a transverse image acquired at the level of the distal metaphysis of the humerus (Fig. 5). The sagittal plane is the plane perpendicular to the coronal plane.

Although the imaging parameters vary depending on the MR system, the recommended parameters are shown in Table 3. During 3D data acquisition by GRE, a slice thickness of ≤2 mm can be selected, allowing images of higher spatial resolution to be obtained.

③ Standard imaging methods

It is important that the standard imaging methods enable the lateral collateral ligament, tendon origins, and bone marrow to be evaluated. Coronal imaging is useful for evaluating the lateral collateral ligament and tendon origins. Transverse imaging is performed to evaluate soft tissue, particularly muscle. STIR and fat-suppressed, T2-weighted imaging are useful for evaluating various structures. At a minimum, coronal and transverse imaging should be performed. T1-weighted imaging is useful for evaluating bone marrow, hematomas, and tumorous lesions. Coronal or sagittal T1-weighted imaging is recommended. The imaging duration is approximately 30 minutes. The imaging methods to be used are determined based on the above considerations. Examples are shown below.

Coronal imaging: $T2^*$-weighted imaging, fat-suppressed, T2-weighted or STIR imaging, and proton density-weighted imaging

Sagittal imaging: T1-weighted imaging and fat-suppressed, T2-weighted or STIR imaging

Transverse imaging: STIR imaging

Figure 5. Elbow joint MRI

A: T1-weighted transverse imaging, B: $T2^*$-weighted coronal imaging

Table 3 Recommended parameters for MRI

Field of view (FOV)	10 to 14 cm
Slice thickness	3 to 4 mm
Matrix	256 × 230～204
Echo train length for proton density-weighted imaging	4 to 6

If detailed demonstration of the articular cartilage is required, sagittal, fat-suppressed, proton density-weighted imaging, 3D, fat-suppressed, GRE-T1-weighted imaging, or 3D GRE with water-selective sequence imaging can be added. $T2^*$-weighted imaging is useful for detecting small loose bodies in patients with restricted range of motion, as in the case of a throwing injury or locking.

Hand and wrist joint imaging methods

1. Conventional radiography

The standard imaging views for conventional radiography of the hand and wrist joint are the anteroposterior and lateral views, with other imaging methods added as necessary. For example, scaphoid fractures frequently occur in the waist of the scaphoid bone, and the anteroposterior projection of ulnar flexion, which enables the scaphoid bone to be evaluated along its long axis, is useful in this case. In addition, the oblique view with pronation of 45 degrees to 60 degrees clearly shows fractures between the center of the bone and its distal end. Fractures of the uncinate process of the hamate bone are diagnosed by carpal tunnel imaging. In evaluating carpal instability, accurate lateral view imaging in the neutral position is necessary to measure the scapholunate angle (normally 30 degrees to 60 degrees).

2. Arthrography

Arthrography is used to evaluate the triangular fibrocartilage and the scapholunate and lunotriquetral ligaments. Imaging of 3 compartments, the radiocarpal joint, distal radioulnar joint, and middle carpal joint, is considered the standard imaging method. However, imaging of the radiocarpal joint alone has been shown to provide equal diagnostic performance. Problems with arthrography are that it is of limited usefulness for evaluating radial carpal pain, accurately identifying sites of ligament damage with it is difficult, and it provides no information on the severity of damage. In addition, false positives (degenerative changes can produce a positive test) and false negatives (ligament injury without intercompartmental communication cannot be diagnosed) are problematic.

3. CT

CT is performed to diagnose microscopic and complicated bone fractures and to perform detailed evaluations, such as the evaluation of bone fracture healing. A slice thickness of approximately 1 mm is desirable. Multiplanar reconstruction imaging is very useful for these evaluations. It enables images to be generated not only in the transverse, sagittal, and coronal planes, but in planes that suit the purpose of the testing. Three-dimensional reconstruction imaging (SSD or VR) is used to elucidate the locations of lesion sites in three dimensions.

4. MRI

MRI permits detailed evaluation of the structure of the complex bone and soft tissue of the carpal region and fingers. The recent development of high magnetic fields and coil technology has made it possible to

visualize structures such as ligaments, tendons, and nerves clearer than before and contributed to improved diagnostic accuracy.

① Body position during imaging and coil used

If one hand is being imaged, imaging is performed with the patient prone and the hand raised above the head and fixed in place (“superman” position). If this position is difficult for the patient to maintain, imaging is performed with the patient supine, the elbow extended, and the hand fixed in place alongside the body. To image the hand as close as possible to the center of the MRI table, a lateral position may be used. Although the use of a small round coil is standard, a suitable coil is selected for imaging of the entire hand or both hands.

② Imaging sequences and planes

The main imaging sequences used are T1-, T2-, and $T2^{*}$-weighted imaging and proton density-weighted imaging. Fat suppression is concurrently used as appropriate. Because STIR imaging provides uniform fat suppression, the 3D-GRE method, which is frequently used for the same purpose as fat-suppressed, T2-weighted imaging, is advantageous for visualizing fine structures and evaluating the blooming that occurs in relation to hemorrhage. Post-contrast, fat-suppressed, T1-weighted imaging may provide useful information for evaluating tumors, tumor-like conditions, and infectious diseases such as rheumatoid arthritis and infection. When the imaged site is definable, imaging is performed with a coil such as a small round coil and the FOV narrowed to approximately 6 cm. The slice thickness used is approximately 2 to 3 mm for 2D imaging and approximately 1 mm for 3D imaging, with a matrix size of $\geq 256 \times 256$. Diffusion-weighted imaging is not generally used.

Evaluation by transverse imaging is the standard evaluation for rupture of an extensor or flexor tendon. Sagittal imaging is useful for evaluating long-axis views. In the case of collateral ligament injury, the imaging plane must be correctly set to the coronal plane suitable for the joint, and particular caution is required to determine the position in the case of thumb collateral ligament injury (Fig. 6). For intercarpal ligament or triangular fibrocartilage complex (TFCC) injury, coronal plane imaging is standard, with sagittal imaging used complementarily. Two-dimensional or 3D-GRE sequences are added. Carpal fracture is evaluated by transverse, coronal, and sagittal imaging. Transverse imaging is useful for hamate fractures.

Figure 6. Thumb MRI

A: T1-weighted transverse imaging, B: Fat-suppressed, T2-weighted coronal imaging
Correctly specifying coronal imaging for the metacarpophalangeal (MP) joint facilitates collateral ligament injury (→) diagnosis.

For detailed examination of rheumatoid arthritis, both hands should be imaged simultaneously when possible. However, there is no consensus on the appropriate limb position for imaging. If there are equipment (coil) limitations, only 1 hand is included in the imaging range. In any event, firm immobilization of the hand and the subject's cooperation are essential to minimize body movement artifacts. T1-weighted imaging is useful for evaluating destructive changes, fat-suppressed, T2-weighted imaging and STIR imaging are useful for evaluating bone marrow edema, and post-contrast, fat-suppressed, T1-weighted imaging is useful for evaluating synovitis. Dynamic contrast-enhanced MRI, while not essential, is useful for characterization, including determining the status of a condition. The selection of the imaging sequence is also an important factor in obtaining good image quality. Imaging in the coronal plane is standard, with transverse plane imaging added as appropriate.

Hip joint imaging methods

1. Conventional radiography

The standard imaging method involves imaging from 2 views, the anteroposterior projection and the lateral view of the femur of the hip being examined. The anteroposterior projection imaging is performed with the hip extended and the leg slightly internally rotated. With the leg internally rotated, the femoral neck faces frontward, making superimposition of the greater and lesser trochanters unlikely. The lateral view of the femur is useful for evaluating femoral neck fractures, femoral head osteonecrosis, Perthes' disease, and slipped femoral capital epiphysis. In adults, anteroposterior projection imaging is performed with flexion of 90 degrees and abduction of 45 degrees. Oblique view imaging is performed with the pelvis inclined 45 degrees toward the hip being examined, flexion of 90 degrees, and abduction of 45 degrees

(Lauenstein view or a modified version of it). Axial view imaging is performed with the asymptomatic hip in flexion and the hip being examined in extension. Transverse view imaging can also be performed if a factor such as pain makes flexion and abduction of the hip being examined difficult. In children, imaging in the frog-leg view is common. Anteroposterior projection imaging with adduction or abduction is used as dynamic imaging to evaluate the fit of the acetabulum and femoral head.

2. Arthrography

Arthrography is performed mainly to evaluate the articular cartilage, acetabular lip, and joint mice. Concomitant CT or MRI (CT and MR arthrography) is useful for their detailed evaluation. However, because arthrography is invasive, its indications are limited.

3. CT

CT is performed for purposes such as evaluating bone fractures (evaluation of fracture morphology, bone fragment displacement, and condition of articular surface; visualization of small bone fragments) and visualizing joint mice and calcification. The acquired slice thickness should be the thinnest possible for the system (≤ 1 mm). The 3 standard planes in which MPR images are generated are the transverse, sagittal, and coronal planes. Other planes are added as necessary. Three-dimensional images generated using the SSD and VR methods are useful for determining the nature of bone fractures and dislocations in 3D. In osteoarthritis and femoral head osteonecrosis, CT may be used for a preoperative simulation of joint replacement surgery, as well as for evaluating bone morphology.

4. MRI

① Body position during imaging and coil used

MRI is normally performed in the supine position using a body coil and includes the bilateral hip joints. Use of a phased-array coil enables images with a high SNR to be obtained. A local coil is used if detailed evaluation of structures such as the acetabular lip and articular cartilage is required for only 1 hip joint.

② Imaging sequences and planes

T1-weighted imaging is useful for evaluating the bone marrow and incidental abnormal findings, such as hematomas and tumorous lesions (e.g., tumors and cysts). Proton density-weighted imaging and $T2^*$-weighted imaging are suitable for evaluating the acetabular lip. However, bone marrow lesions are indistinct with these modalities. T2-weighted imaging has low visualization sensitivity for the acetabular lip, and bone marrow lesions are indistinct with this modality. However, it is useful for visualizing joint fluid accumulation and fracture lines. Fat-suppressed, T2-weighted imaging and STIR imaging enable lesions to be visualized in soft tissue and bone marrow with high sensitivity.

The following modalities are useful for evaluating articular cartilage: proton density-weighted imaging, fat-suppressed, proton density-weighted imaging, T2-weighted imaging, and 3D, fat-suppressed,

GRE-T1-weighted imaging or 3D selective water excitation GRE-T1 weighted imaging. Three-dimensional, fat-suppressed, GRE-T1-weighted imaging, and 3D selective water excitation, GRE-T1-weighted imaging enable thin MPR images to be generated in any arbitrary plane, making these modalities suitable for detailed evaluation of the morphology and thickness of the articular cartilage.

Table 4. Recommended parameters for MRI

Field of view (FOV)	Bilateral: 32 to 40 cm Unilateral: 14 to 18 cm
Slice thickness	3 to 4 mm
Matrix	256 × 230 to 256
Echo train length for proton density-weighted imaging	4 to 6

There are 3 standard imaging planes, the coronal, sagittal, and transverse planes. The most standard of these is the coronal plane. Coronal and transverse imaging enable left-right comparisons, and coronal imaging can be used to evaluate the pelvis as a whole. Sagittal imaging is suitable for evaluating the anterior and posterior of the epiphysis and acetabulum.

Although the imaging parameters vary depending on the MR system, the important recommended parameters are shown in Table 4.

③ Standard imaging methods

The standard imaging methods must provide the ability to evaluate the bone marrow, including that of the femoral head, the acetabular lip, and the articular cartilage. Fat-suppressed, proton density-weighted imaging is useful for evaluating various structures and should be performed in the coronal plane. T1-weighted imaging is considered for bone marrow evaluation and when a hematoma or tumorous lesion is present. It should be performed in the coronal plane. Fat-suppressed, T2-weighted imaging and STIR imaging enable lesions to be visualized in soft tissue and bone marrow with high sensitivity. Imaging from 1 or more angles is recommended with these modalities. T2-weighted imaging should also be performed from 1 or more angles.

The imaging sequences to be used are determined based on the above considerations. Examples (Fig. 7) are shown below.

Coronal imaging: T1-weighted imaging, T2-weighted imaging, fat-suppressed, proton density-weighted imaging

Sagittal imaging: T2-weighted imaging

Transverse imaging: Fat-suppressed, T2-weighted or STIR imaging

If femoral head osteonecrosis is suspected, or the imaging is performed to examine it in detail, sagittal T2-weighted imaging should be changed to T1-weighted imaging.

Knee joint imaging methods

1. Conventional radiography

The standard imaging method includes imaging with 2 different projections, the anteroposterior and lateral projections. Anteroposterior projection imaging is performed in extension with the leg slightly inwardly rotated. Lateral view imaging is performed with flexion of 30 degrees. Patellar axial view imaging (skyline view) is added to evaluate the patellofemoral joint. Axial dynamic imaging, in which the patellar axial view imaging is performed with flexion of 30, 60, and 90 degrees, is useful for evaluating the fit of the articular surface of the patellofemoral joint. Standing anteroposterior projection imaging enables the thickness of the articular cartilage of the femoral neck joint to be visualized as the width of the joint cleft, making it useful for evaluating the thickness of the cartilage. Imaging should be performed with the patient standing on the one leg that is being examined. If this is difficult, however, imaging is performed with the patient standing on both legs. Anteroposterior projection imaging in flexion (intercondylar fossa view) is useful for visualizing osteochondritis dissecans, joint mice, and avulsion fractures at cruciate ligament insertion sites. Valgus/varus stress radiography is performed to evaluate instability resulting from medial and lateral collateral ligament injuries. Anterior/posterior drawer radiography is performed to evaluate instability resulting from anterior cruciate ligament injury/posterior cruciate ligament injury.

2. Arthrography

Because arthrography is invasive and requires skill to perform, it is being replaced by MRI. Arthrography may also be performed in combination with CT and MRI (CT arthrography, MR arthrography) to evaluate the articular cartilage and visualize joint mice.

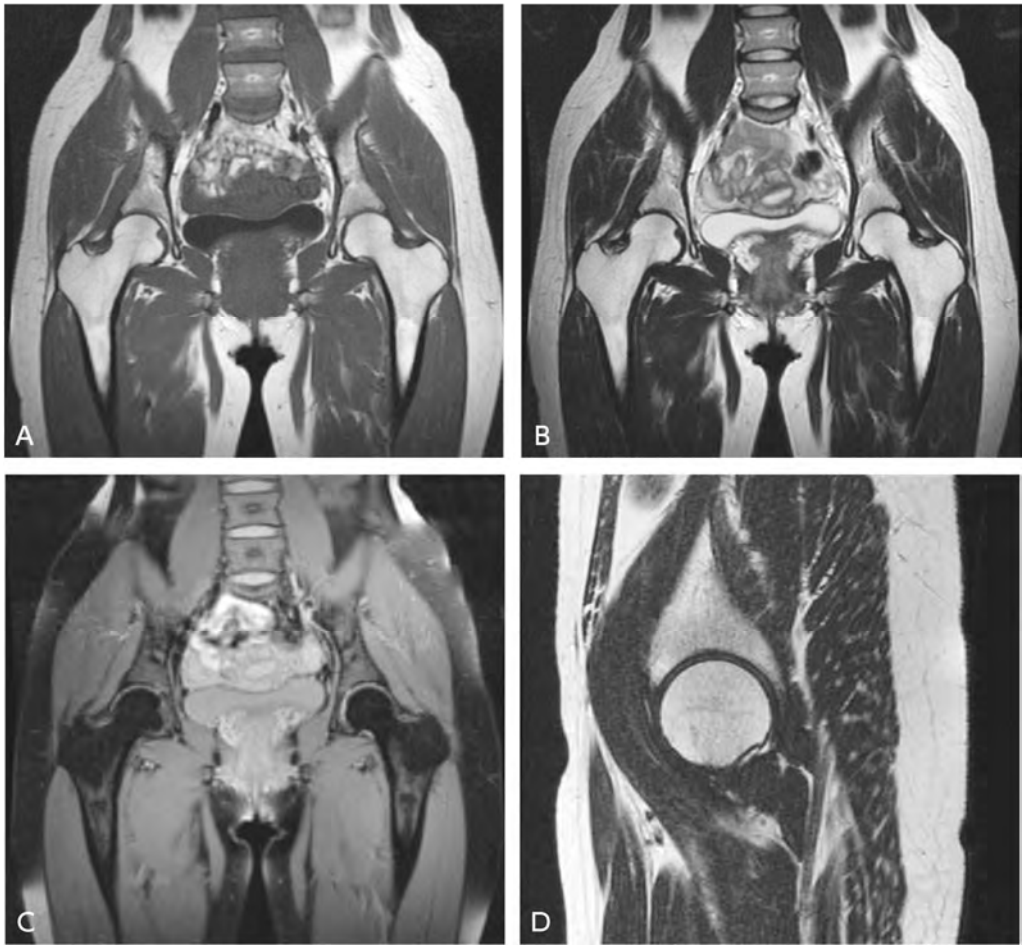

Figure 7. Hip joint MRI

A: T1-weighted coronal image, B: T2-weighted coronal image, C: Fat-suppressed, proton density-weighted, coronal image
D: T2-weighted sagittal image

3. CT

CT is performed for purposes such as evaluating bone fractures (evaluation of fracture morphology, bone fragment displacement, and condition of articular surface; visualization of small bone fragments), evaluating osteochondral injury, and visualizing joint mice and calcification. The acquired slice thickness should be the thinnest possible for the system (≤ 1 mm). The 3 standard planes in which MPR images are generated are the transverse, sagittal, and coronal planes. Other planes are added as necessary. Fracture lines are distinctly visualized in a plane perpendicular to the fracture line. Three-dimensional images generated using the SSD and VR methods are useful for determining the nature of bone fractures and dislocations in 3D.

4. MRI

① Body position during imaging and coil used

Imaging in slight flexion rather than full extension is recommended to distinctly visualize the anterior cruciate ligament. To avoid torsion on the cruciate ligaments and lateral collateral ligament, excessive

internal rotation and external rotation are avoided, and imaging is performed in a comfortable position with the leg in slight external rotation. A cylindrical knee coil is used.

② Imaging sequences and planes

Although T2-weighted imaging is useful for evaluating tendons and ligaments, its sensitivity in detecting meniscal injury is low. Proton density-weighted imaging is suitable for evaluating the menisci, tendons, and ligaments. However, false lesions can appear in normal tendons and ligaments that are at a 55-degree angle with respect to the static magnetic field due to the magic angle effect, and caution is therefore required in such evaluations. $T2^*$-weighted imaging is useful for evaluating the menisci. Its sensitivity in visualizing meniscal injury is higher than that of proton density-weighted imaging. Three-dimensional, $T2^*$-weighted imaging enables MPR images to be generated in thin planes and any arbitrary plane, making it excellent for visualizing small ruptures and evaluating rupture morphology. Bone marrow lesions are indistinct with T2-weighted, proton-weighted, and $T2^*$-weighted imaging. Fat-suppressed, T2-weighted imaging and STIR imaging enable lesions to be visualized in bone marrow and soft tissue, including tendons and ligaments, with high sensitivity. Although T1-weighted imaging provides little information, it is useful for evaluating the bone marrow and incidental abnormal findings, such as hematomas and tumorous lesions (e.g., tumors and cysts).

Table 5. Recommended parameters for MRI

Field of vision (FOV)	12 to 16 cm
Slice thickness	3 to 4 mm†
Matrix	256 × 230 to 256
Echo train length for proton density-weighted imaging	4 to 6

† ≤ 1 mm for 3D $T2^*$-weighted imaging

The imaging sequences useful for evaluating articular cartilage with general MR systems are proton density-weighted imaging, fat-suppressed, proton density-weighted imaging, T2-weighted imaging, 3D, fat-suppressed, GRE-T1-weighted imaging, and 3D selective water excitation, GRE-T1 weighted imaging. Three-dimensional, fat-suppressed, GRE-T1-weighted imaging, and 3D selective water excitation, GRE-T1-weighted imaging enable thin MPR images to be generated in any arbitrary plane, making these sequences suitable for detailed evaluation of the morphology and thickness of the articular cartilage. They are also used to evaluate the volume of the articular cartilage. In addition, sequences such as delayed gadolinium-enhanced magnetic resonance imaging of cartilage (dGEMRIC), T2 mapping, and T1 rho mapping have been proposed to evaluate qualitative changes in cartilage (collagen degeneration and decreased proteoglycans), the MR systems that can perform these imaging sequences are limited, and their clinical usefulness has not been established.

There are 3 standard imaging planes, the sagittal, coronal, and transverse planes. The menisci are evaluated in the sagittal and coronal planes, tendons and ligaments in the 3 standard planes, the articular cartilage of the femorotibial articulation in the sagittal and coronal planes, and the articular cartilage of the

patellofemoral joint in the sagittal and transverse planes. Although the imaging parameters vary depending on the MR system, the important recommended parameters are shown in Table 5.

③ Standard imaging methods

Most knee joint MRI is performed to closely examine internal derangement and trauma of the knee. The standard imaging methods must provide the ability to evaluate the menisci, ligaments, articular cartilage, and bone marrow. Sagittal T2-weighted imaging and proton density-weighted imaging elucidate the anatomy of the intra-articular structures, and one of them should therefore be performed. Fat-suppressed, proton density-weighted imaging is suitable for evaluating various structures, and its use in any plane is recommended. However, its sensitivity in detecting meniscal tears is slightly lower than that of $T2^{*}$-weighted imaging. It is recommended that at least $T2^{*}$-weighted imaging in either the sagittal or coronal plane and fat-suppressed, proton density-weighted imaging from 1 or more angles be performed. T1-weighted imaging is considered for bone marrow evaluation and when a hematoma or tumorous lesion is present. It should be performed from 1 angle. The imaging sequences to be used are determined based on the above considerations. Examples are shown below.

(1) Example 1 (Fig. 8)

Sagittal imaging: T2- and $T2^{*}$-weighted imaging†

Coronal imaging: T1-weighted and fat-suppressed, proton density-weighted imaging

Transverse imaging: Fat-suppressed, proton density-weighted imaging

(2) Example 2

Sagittal imaging: T1- and proton density-weighted imaging

Coronal imaging: $T2^{*}$-weighted imaging* and fat-suppressed, T2-weighted or STIR imaging

Transverse imaging: Fat-suppressed, proton density-weighted imaging

(† $T2^{*}$-weighted imaging performed in 3D and MPR image generation that includes the sagittal and coronal planes is preferable)

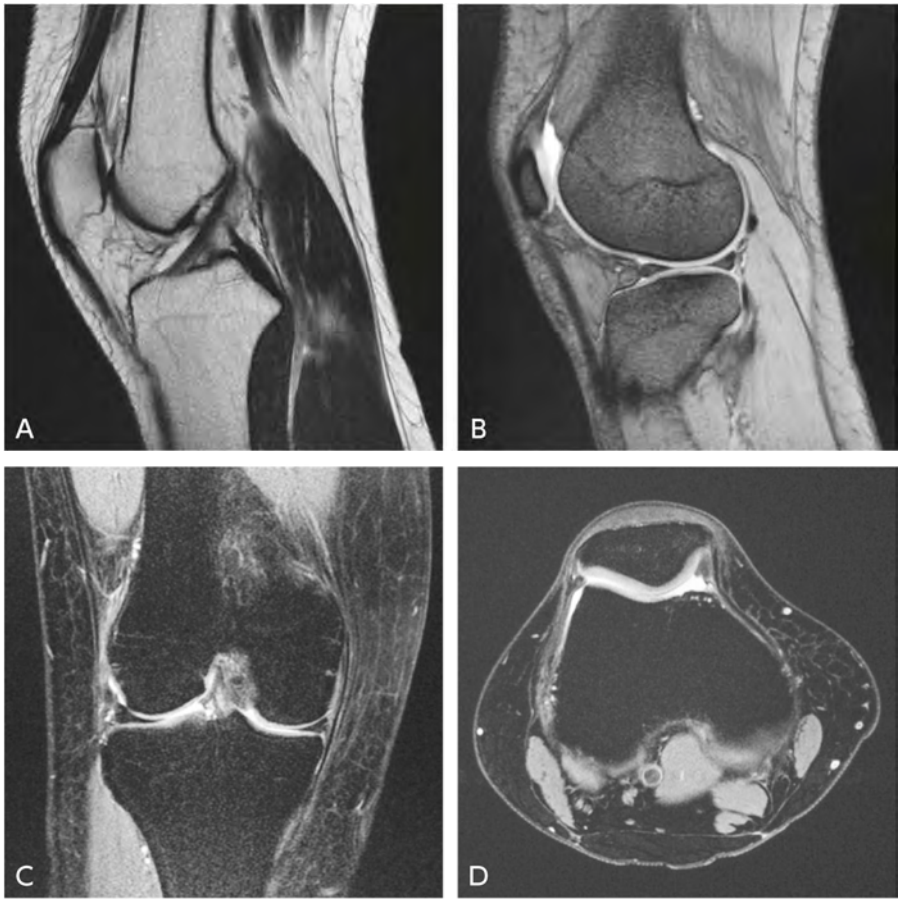

Figure 8. Knee joint MRI

A: T1-weighted sagittal image, B: T2*-weighted sagittal image, C: Fat-suppressed, proton density-weighted coronal image
D: Fat-suppressed, proton density-weighted transverse image

The addition of sagittal fat-suppressed, T2-weighted imaging or STIR imaging is recommended if anterior knee pain is present or extensor mechanism impairment is suspected. If a detailed evaluation of the articular cartilage is required, 3D, fat-suppressed, GRE-T1-weighted imaging and 3D selective water excitation, GRE-T1-weighted imaging can be added.

Ankle joint imaging methods

1. Conventional radiography

The standard examination consists of 3 views, the anteroposterior projection, the anteroposterior projection with internal rotation (mortise view), and the lateral view. In the anteroposterior projection, the lateral aspect of the talus and the fibular lateral malleolus are superimposed. However, in the anteroposterior projection with the leg internally rotated 20 degrees, the articular surfaces of the talus, medial malleolus, and lateral malleolus are depicted. The oblique view is also useful for fractures. The dorsiflexion and plantar flexion lateral views and weight-bearing anteroposterior and lateral views are useful for evaluating the articular surface and joint space of the talocrural joint. Stress imaging is performed

to evaluate instability resulting from lateral ligament injury. In anterior drawer radiography, lateral imaging is performed while the subject holds the leg firmly in place with one hand with the ankle in plantar flexion of 20 degrees, grasps the forefoot with the other hand, and pulls it anteriorly. In inversion stress imaging, anteroposterior projection imaging is performed with the foot joint in plantar flexion of approximately 20 degrees and forcibly inverted. The talar tilt angle is then evaluated.

2. Arthrography

Arthrography may be performed for evaluation before and after surgery for osteochondral injury of the trochlea tali. CT or MR arthrography is then subsequently performed. For detailed examination of joint mice, contrast medium and air are injected for double contrast.

3. CT

CT is performed for purposes such as: determining the presence or absence of a fracture difficult to diagnose by conventional radiography, such as bone fragment displacement associated with a fracture or Lisfranc joint injury; determining the presence or absence of loose bodies; osteochondral injury evaluation; and postoperative evaluation. MPR images are generated in 3 planes, transverse, sagittal, and coronal, relative to the articular surface. To enable image reconstruction at high resolution from any angle, the acquired slice thickness specified is the minimum for the system used (≤1 mm). Reconstructed images orthogonal to the target articular surface should be generated for observation using a workstation. A plane orthogonal to the fracture line is useful for diagnosing fracture healing. VR images provide an overall view of fractures and are useful for determining the course of a tendon. If a surgical fixation material is present, the effect of metal artifacts can be reduced by acquiring thin slices, using a soft tissue algorithm for the reconstruction filter, and performing observations with a wide window width. Depending on the CT system used, it may be possible to use metal artifact-reduction technology.

4. MRI

① Body position during imaging and coil used

With the patient in the supine position, the foot is placed in a natural position (normally plantar flexion of approximately 20 degrees), and the ankle joint is held in place with towels or packing material. It is important that the foot position be comfortable to avoid movement artifacts. For the local coil, cylindrical knee coils or head coils are used, as well as ankle coils. If a 2-channel flexible coil is used, it is attached to the medial and lateral sides of the ankle joint.

② Imaging sequences and planes

The imaging sequences and planes vary depending on the target structure. If the target is a ligament or tendon, proton density-weighted, T2-weighted, fat-suppressed T2-weighted, or STIR imaging is performed. If the target is the bone marrow, T1-weighted, fat-suppressed T2-weighted, or STIR imaging is used. For

detailed examination of the articular cartilage, T2-weighted imaging, fat-suppressed, proton density-weighted imaging, 3D, fat-suppressed, GRE-T1-weighted imaging, and 3D GRE with water-selective sequence are useful.

The 3 standard imaging planes for the ankle joint, the sagittal, coronal, and transverse planes, are selected centering on the talocrural joint. Coronal imaging provides good visualization of the ankle mortise and is useful for evaluating the articular surface when the coronal plane is perpendicular to the surface of the distal tibiofibular syndesmosis in transverse imaging at the level of the distal tibiofibular syndesmosis (Fig. 9). If transverse imaging is specified relative to the axis of the lower leg (body axis), the plane may change depending on the degree of ankle plantar flexion. To improve reproducibility, transverse imaging is specified so that it parallels the articular surface of the posterior subtalar joint with the smallest inclination in sagittal imaging (Fig. 10).

Although the imaging parameters vary depending on the MR system, the important recommended parameters are shown in Table 6.

③ Standard imaging methods

(1) Joint sprain

Transverse and coronal imaging: Proton density-weighted and T2-weighted imaging

Sagittal imaging: Fat-suppressed, T2-weighted or STIR imaging

(2) Ankle joint swelling and pain

Sagittal or coronal imaging: T1-weighted, T2-weighted, and fat-suppressed, T2-weighted or STIR imaging

(3) Achilles tendon swelling and pain

The imaging range includes the area from the calcaneal insertion of the Achilles tendon to the muscle tendon junction.

Sagittal imaging: T1-weighted, T2-weighted, and fat-suppressed, T2-weighted or STIR imaging

Transverse imaging: T2-weighted and fat-suppressed, T2-weighted or STIR imaging

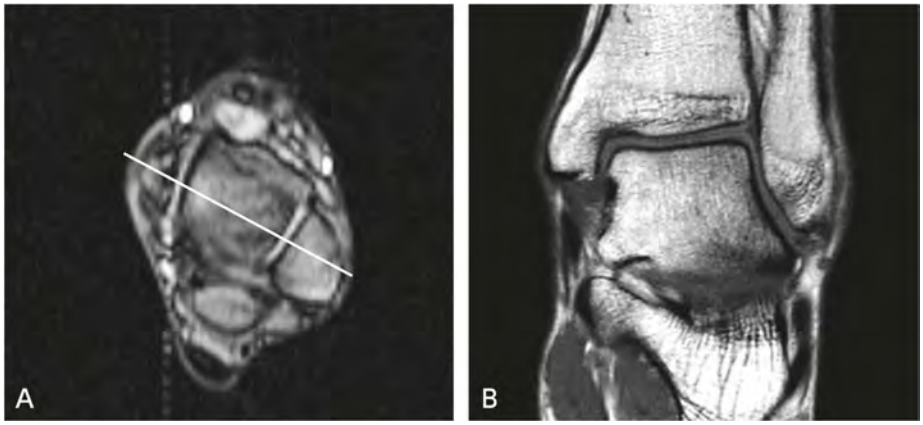

Figure 9. Ankle joint MRI

A: T1-weighted transverse image, B: T1-weighted coronal image

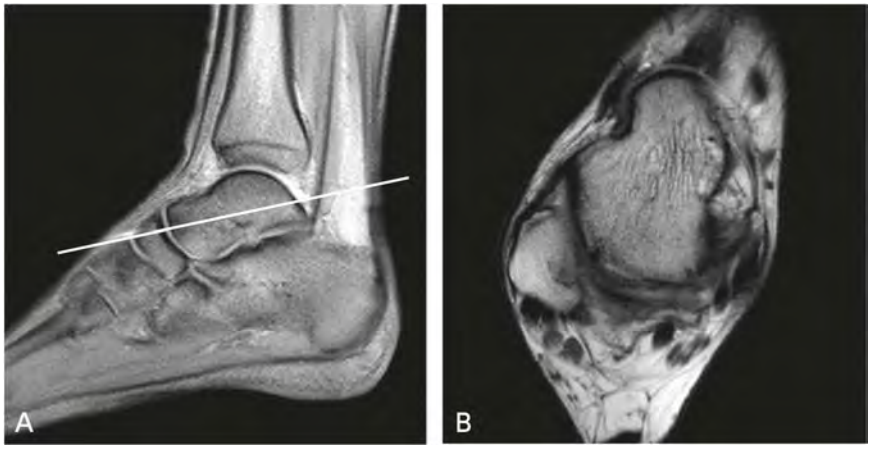

Figure 10. Ankle joint MRI

A: T1-weighted sagittal image, B: T2-weighted oblique transverse image

Table 6 Recommended parameters for MRI

Field of view (FOV)	10 to 15 cm
Slice thickness	3 to 4 mm
Matrix	256 × 204 to 230
Echo train length for proton density-weighted imaging	4 to 6

(4) Plantar pain and swelling

Coronal or sagittal imaging: T1-weighted, T2-weighted, and fat-suppressed, T2-weighted or STIR imaging

(5) Entrapment neuropathy such as plantar numbness

Oblique coronal imaging perpendicular to the posterior subtalar joint: T1-weighted, T2-weighted, and fat-suppressed, T2-weighted or STIR imaging

Sagittal or transverse imaging: Fat-suppressed, T2-weighted or STIR imaging

C Imaging methods for bone and soft tissue tumors and tumor-like lesions

Overview

Conventional radiography provides high diagnostic value in the diagnosis of bone tumors and tumor-like lesions. It should be the first imaging examination performed for this purpose. MRI is excellent for detecting lesions and evaluating local invasion and is often performed following conventional radiography. The modality that plays the central role in the diagnostic imaging of soft tissue neoplasms and tumor-like lesions is MRI, which provides excellent contrast resolution. Conventional radiography is not as useful for diagnosing these lesions as it is for diagnosing bone tumors and tumor-like lesions. However, calcification and ossification patterns in lesions and changes in adjacent bones offer clues for diagnosis. It is therefore useful to perform conventional radiography first. CT is not often aggressively used for tumors or tumor-like lesions in either bone or soft tissue. However, it is suitable for evaluating sites with anatomically complex bone structure and excellent for detecting microscopic ossification and calcification and analyzing the bone cortex in detail.

Detailed discussion

1. Conventional radiography

Conventional radiography is generally performed in the anterior-posterior (frontal) and lateral views (Fig. 11). It is used to analyze the sites and distribution of lesions, their internal and marginal characteristics, and calcified substrates and to evaluate bone cortex changes, periosteal reactions, and soft tissue changes. Imaging from any arbitrary angle can be added as necessary.

2. CT

Thin-section CT is useful for evaluating the bone cortex and ossification/calcification in lesions. Images are acquired with the thinnest possible slice thickness, and MPR images suitable for the evaluation are generated. Thin-section CT is also suitable for detecting small niduses of osteoid osteomas. CT angiography is useful for evaluating vascular anatomy and vascular tumor invasion before and after surgery.

3. MRI

① Body position during imaging and coil used

For the limbs, which are off-center, a body position should be found that places the site being imaged as close to the center of the magnetic field as possible. The optimal coil is selected according to the lesion site and size. For malignancies, the imaging range and coil need to be determined by also taking into account the evaluation of skip lesions and regional lymph nodes. Use of a local coil is appropriate for small subcutaneous lesions of the hands and feet. For tumors of the anterior chest wall, imaging may be performed in the prone position or a bust band used to reduce respiratory artifacts.

② Imaging sequences and planes

SE T1- and T2-weighted imaging is performed to accurately evaluate the internal characteristics of tissue. Fat suppression is used to ① detect adipose tissue, ② improve visualization of edema and inflammation, and ③ increase gadolinium contrast medium enhancement.

The methods of fat-suppressed imaging are: non-selective fat suppression (STIR), which uses the difference in the relaxation times of water and fat; selective fat suppression (chemical shift-selective, CHESS), which uses the difference in the resonance frequencies of water and fat; and water-fat separation (water excitation, Dixon), which uses the difference in the phase dispersions of water and fat. Non-selective and water-fat separation fat-suppression methods are robust against magnetic field non-uniformity and provide stable fat suppression even for sites with complex morphologies, such as the hands and feet. With non-selective fat suppression, tissues with T1 values near that of fat (e.g., hematomas and tissues enhanced by contrast media) are also suppressed. Consequently, contrast-enhanced MRI cannot be used concomitantly. Selective fat suppression involves selectively suppressing only the fat signal by applying frequency-selective excitation pulses that match the resonant frequency of fat protons. It provides good fat suppression. However, it is susceptible to non-uniform fat suppression resulting from magnetic field non-uniformity and therefore requires high static magnetic field uniformity. This limits its imaging range.

With $T2^*$-weighted imaging, magnetic susceptibility is strongly reflected in the images, expanding the signal void. It can therefore sensitively detect hemosiderosis in conditions and lesions such as giant cell tumors of the bone, pigmented villonodular synovitis, and hematomas. Like hemosiderin, ossification/calcification, collagen fibers, and amyloid deposits show hypointensity on T2-weighted imaging. Consequently, $T2^*$-weighted imaging is added when they need to be differentiated from hemosiderin. Diffusion-weighted imaging is a method that emphasizes proton diffusion. In addition to the qualitative diagnosis of lesions including small round cell tumors such as malignant lymphomas, epidermal cysts, and abscesses, it holds promise for preventing the oversight of skip lesions and enlarged lymph nodes.

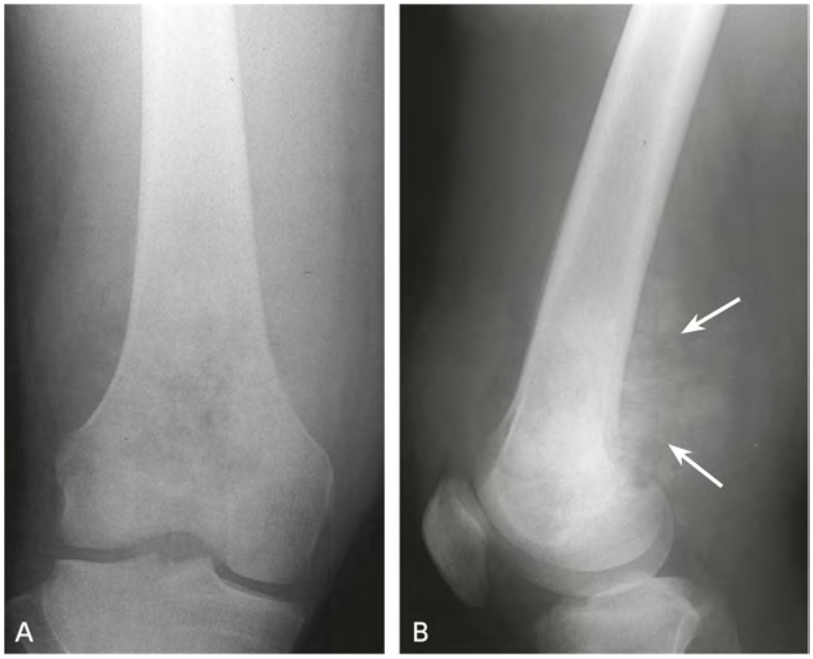

Figure 11. Conventional radiography of osteosarcoma

A: Knee joint, anteroposterior projection; B: Knee joint, lateral view
An osteolytic lesion with indistinct borders is seen in the distal metaphysis of the right femur. Cloud-like calcifications that show bone formation are irregularly mixed in the lesion. In the lateral view, a radial periosteal reaction and soft tissue calcification (→) are seen.

Contrast-enhanced MRI is used for purposes such as differentiating between cystic and solid lesions, identifying appropriate sites for biopsy, determining the presence or absence of inflammatory lesions, and evaluating tumor necrosis after treatment. Dynamic MRI involves rapidly injecting contrast medium intravenously and repeatedly imaging in the same plane. It enables the hemodynamics of tumors to be evaluated and is useful for purposes such as diagnosing highly vascular lesions and distinguishing between residual tumors and post-treatment changes (e.g., edema and fibrosis). MRA can be used to visually identify tumor-associated blood vessels. MRA images can be generated by performing dynamic MRI as a 3D-GRE sequence. They facilitate the visualization of tumor-associated blood vessels and the visual understanding of anatomical spatial relationships.

There are 2 standard imaging planes, along the long and short axes of lesions. In general, transverse and sagittal or transverse and coronal imaging is performed. Transverse imaging is often useful for evaluating invasion of neurovascular bundles in malignancies. The FOV and slice thickness are determined by taking into account the extent of the lesions and the somatotype of the subject. The number of averaged samples and the acquisition matrix are selected so that the SNR is not problematic. The concomitant use of a multichannel coil and parallel imaging can shorten imaging time while maintaining the SNR and is effective when extensive imaging is required.

③ Standard imaging methods

The standard sequences are SE T1- and T2-weighted imaging. Fat suppression should be used concomitantly for at least 1 plane. In addition, diffusion-weighted imaging can be performed in a relatively short time, and its addition is recommended (Fig. 12). The above-mentioned benefits of contrast testing are taken into account in deciding whether it is indicated and whether to perform normal contrast-enhanced MRI or dynamic MRI (Fig. 12). The imaging sequences to be used are determined based on the above considerations. Examples are shown below in Table 7.

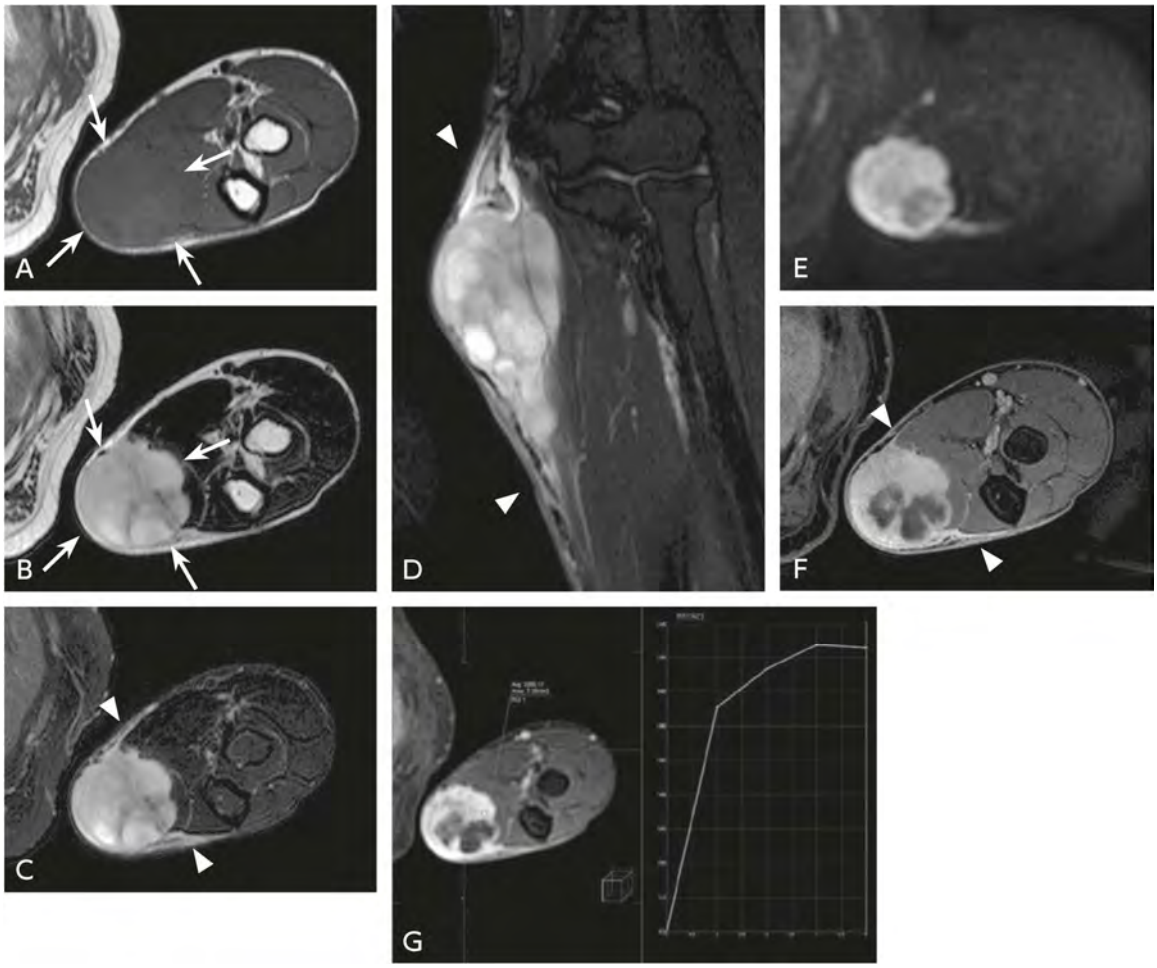

Figure 12. MRI of myxofibrosarcoma

A: T1-weighted transverse image, B: T1-weighted transverse image, C: Fat-suppressed, T2-weighted transverse image, D: Fat-suppressed, T2-weighted sagittal image, E: Diffusion-weighted image (b-value = 1,000 s/mm^2),
F: Fat-suppressed, contrast-enhanced MRI transverse image, G: Dynamic MRI transverse image, optional
A subcutaneous mass with indistinct borders is seen on the medial left upper arm (→). The mass is isointense with muscle in T1-weighted images and shows somewhat non-uniform hyperintensity in T2-weighted images (→). In fat-suppressed, T2-weighted images, hyperintense areas are seen along the fascia transversely and craniocaudally to the tumor (▷). On diffusion-weighted imaging, the mass shows hyperintensity and an ADC value of 1.7×10^{-3} mm/s (ADC map not shown). In the fat-suppressed, contrast-enhanced MRI image, a strongly enhanced solid portion and a weakly enhanced area of degeneration and a necrotic portion are seen. The area along the fascia is also enhanced, and tumor progression (“tail sign”) is seen (▷). Dynamic MRI shows a highly vascular tumor that is enhanced relatively early, which is consistent with findings for myxofibrosarcoma.

4. Nuclear medicine tests

① PET and PET and PET/CT

The radiotracer used for PET is a glucose analog called ^{18}F-FDG. For 2D data acquisition, 185 to 444 MBq (3 to 7 MBq/kg) of FDG are administered intravenously; for 3D data acquisition, 111 to 259 MBq (2 to 5 MBq/kg) are administered. The dose is increased or decreased as appropriate depending on the system used for imaging and the age and body weight of the patient. Sixty to 90 minutes after administration, a PET or PET/CT system is used to perform whole-body emission and transmission scans (in the case of PET) or CT imaging (in the case of PET/CT). In many malignancies, glucose transporter and hexokinase activity are increased, and phosphatase activity is extremely low. Consequently, high levels of FDG accumulate. FDG accumulation in malignancies is also increased more than 1 hour after administration, but it often decreases in benign disease. Consequently, addition of late-phase (2 hours after administration) imaging may aid in distinguishing malignant from benign conditions.

Table 7. Examples of sequences for bone and soft tissue tumors and tumor-like lesions

Imaging Method	Sequence	TR/TE	Other
T2-weighted/transverse	FSE	Approximately ≥ 3,000 ms/100 ms	Imaging slice thickness and FOV changed as appropriate depending on lesion
T1-weighted/transverse	FSE or SE	400 to 750/10 to 12 ms	Imaging slice thickness and FOV changed as appropriate depending on lesion
T2*-weighted (optional)	2D GRE	400 to 600/15 to 20 ms, FA 30°	Added if hemosiderosis suspected
T1-weighted coronal/sagittal	FSE or SE	400 to 750/10 to 12 ms	Imaging slice thickness and FOV changed as appropriate depending on lesion
Fat-suppressed, T2-weighted/ coronal/sagittal	FSE	Approximately ≥ 3,000 ms/100 ms	With the STIR and Dixon methods, good fat suppression is obtained even in areas of magnetic field non-uniformity.
Diffusion-weighted	SE-EPI	5,000 to 6,000/shortest time, ms	b-values of 0 and 1,000 s/mm^2 selected to prepare ADC map
Dynamic MRI (optional)	3D-GRE or 2D-GRE	4 to 5/1.2 to 2 ms or 400/shortest time, ms	Imaging times: 30, 60, 120, and 210 seconds after injection
Gd T1-weighted/transverse, coronal, sagittal	FSE or SE	Approximately 400 to 750/12 ms	Concomitant fat suppression performed for at least 1 angle

② Bone scintigraphy

The radiopharmaceuticals used for bone scintigraphy include ^{99m}Tc-methylene diphosphonate (MDP) and ^{99m}Tc-hydroxymethylene diphosphonate (HMDP). Imaging is performed beginning 2 to 3 hours after intravenous injection and after urination immediately before the test. The use of a low-energy, high-resolution collimator is recommended for the gamma camera used in imaging. Whole-body anterior and posterior views are depicted using a WL setting suitable for bone and soft tissue. If an abnormality is suspected, oblique and expanded acquisition and SPECT or SPECT/CT imaging are performed.

Secondary source materials used as references

1) Uetani M: Diagnostic Imaging of Bone and Soft Tissue, 2nd Edition. Shujunsha, 2010.
2) Fukuda K: MRI of the Joints, 2nd Edition. Medical Science International, 2013.
3) Yamashita Y: Findings of the examination of routine MRI imaging standardization, a research project of the Japanese Society for Magnetic Resonance in Medicine, 1st Report: spine, spinal cord, and mammary gland. Japanese Journal of Magnetic Resonance in Medicine 28: 196-209, 2008.
4) Ross JS et al：Diagnostic imaging spine 1st ed. Amirsys/Elsevier Saunders, 2004
5) Sugimura K: MRI of Bone and Soft Tissue. Medical View, 2000.
6) Schulte-Altedorneburg G: MR arthrography: pharmacology, efficacy and safety in clinical trials. Skeletal Radiol 32: 1-12, 2003
7) Horio S: How to Take and View Plain Radiographs of Bones and Joints, 8th Edition, 2010.
8) Sashi R: MRI of the Shoulder, 2nd Edition. Medical View, 2011.
9) Takahara M et al: Natural progression of osteochondritis dissecans of the humeral capitellum: initial observations. Radiology 216: 207-212, 2000
10) Yanagawa N: Standardization for X-ray CT imaging. Japan Radiological Society, 2010.
11) Timmerman LA et al: Preoperative evaluation of the ulnar collateral ligament by magnetic resonance imaging and computed tomography arthrography: evaluation in 25 baseball players with surgical confirmation. Am J Sports Med 22: 26-31, 1994
12) Uetani M, et al.: Main Points of Bone and Soft Tissue Diagnostic Imaging. Medical View, 2006.
13) Stoller DW: Magnetic resonance imaging in orthopaedics and sports medicine, 3rded. Lippincott Williams & Wilkins, 2007
14) Potter HG et al: High resolution non contrast MRI of the hip. J Magn Reson Imaging 31: 268-278, 2010
15) Niitsu M: Knee MRI, 2nd Edition. Igaku Shoin, 2009.
16) Rogers LF: The ankle, radiology of skeletal trauma 3rded. Churchill Livingstone, 1992
17) Brandser EA et al: contribution of individual projections alone and in combination for radiographic detection of ankle fractures. AJR Am J Roentgenol 174: 1691-1697, 2000
18) Buckwalter KA: Musculoskeletal imaging with multi slice CT. AJR Am J Roentgenol 176: 979-986, 2001
19) Fujimoto H: New Main Points of Bone and Soft Tissue Diagnostic Imaging. Medical View, 2014.
20) Ehara S: Handbook of Bone Trauma Diagnostic Imaging. Medical Science International, 2012.
21) Committee on Bone and Soft Tissue Tumors, Japanese Orthopaedic Association, Ed.: General Rules for Clinical and Pathological Studies on Malignant Bone Tumors, 4th Edition. KANEHARA & Co., 2015.
22) Committee on Bone and Soft Tissue Tumors, Japanese Orthopaedic Association, Ed.: General Rules for Clinical and Pathological Studies on Malignant Soft Tissue Tumors, 3rd Edition. KANEHARA & Co., 2002.
23) Japanese Society of Nuclear Medicine, Ed.: FDG PET and PET/CT Diagnostic Guidelines. Japanese Society of Nuclear Medicine, 2018.
24) Japanese Society of Nuclear Medicine, Ed.: Nuclear Medicine Diagnostic Guidelines. Japanese Society of Nuclear Medicine, 2008.

BQ 78 Is MRI recommended for diagnosing cervical spondylotic myelopathy?

Statement

MRI is useful and recommended for identifying lesion sites, evaluating pathological changes, and predicting prognosis. However, spinal cord compression factors cannot be adequately evaluated with MRI alone. It should therefore be performed in combination with conventional radiography or CT.

Background

MRI has become an essential imaging modality for the diagnosis of cervical spine disease. Its usefulness in diagnosing cervical spondylotic myelopathy was examined.

Explanation

Numerous studies have compared the performance of MRI (Fig.) and other diagnostic imaging modalities in diagnosing cervical spondylotic myelopathy or have examined the correlation between MRI findings and neurological findings or MRI findings and posttreatment prognosis. In an investigation of 26 patients with cervical radiculopathy or cervical myelopathy, Larsson et al. found that MRI together with conventional radiography was suitable as the first line of testing for the diagnosis of cervical spondylotic myelopathy. However, they reported that differentiating between bony and soft tissue spinal cord compression factors was difficult with MRI alone.[1)] Sengupta et al. compared surgical findings and image interpretation results for 41 patients with cervical spondylosis who underwent surgery and also concluded that differentiating between spinal cord compression factors was difficult with MRI.[2)] On the other hand, Nagata et al. analyzed 115 cases of cervical spondylotic myelopathy and found that the severity of spinal cord compression seen on T1-weighted, sagittal MRI images was correlated with myelography findings and clinical severity based on the cervical spondylosis treatment outcome criteria of the Japanese Orthopaedic Association (JOA score).[3)] They therefore concluded that MRI is useful for diagnosis and postoperative evaluation. Bucciero et al. calculated the ratio of the anteroposterior diameter of the spinal cord to the transverse diameter (anteroposterior compression ratio, APCR) in transverse MRI images of 35 patients with cervical spondylotic myelopathy who underwent surgery.[4)] They found that, if the ratio was ≥ 40%, the neurological findings were mild. In patients with a ratio ≥ 10%, the neurological findings indicated a serious condition, and no postoperative improvement was seen. Based on an investigation of 37 patients who underwent surgery, Chung et al. reported that spinal cord compression severity in transverse images was related to postoperative prognosis.[5)] In addition, Wada et al. found that, based on the postoperative outcomes of 50 patients who underwent surgery, the spinal cord cross-sectional area at the site of greatest compression was most highly correlated with prognosis.[6)] Moreover, they found that the area was ≤ 40 mm^2 in many patients whose postoperative improvement rate was poor. Thus, in terms of its ability to directly

visualize spinal cord compression, the usefulness of MRI for diagnosing cervical spondylotic myelopathy, evaluating its pathology, and predicting postoperative prognosis has been demonstrated. However, diagnosis by visual assessment has limitations, particularly the poor interobserver agreement rates that have been reported.[2, 7)]

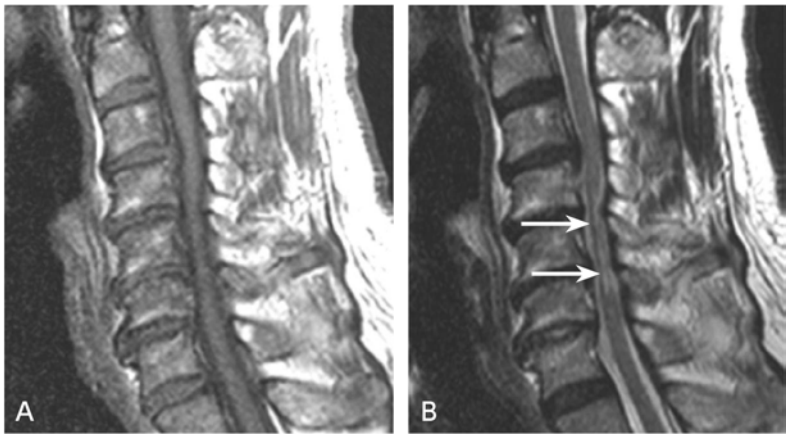

Figure Cervical spondylotic myelopathy

A: MRI, T1-weighted sagittal image; B: MRI, T2-weighted sagittal image
Pronounced intervertebral disc degeneration and proliferative changes in the uncovertebral joints are seen at the C3/4 to C6/7 level. The cervical spinal cord is compressed and flattened, and areas of intraspinal hyperintensity are seen between multiple vertebrae in the T2-weighted image (→).

In cervical spondylotic myelopathy, in addition to morphological changes such as spinal cord compression and flattening, areas of abnormal intraspinal hyperintensity are often seen, particularly on T2-weighted images ("T2 hyperintensity areas" below). This finding is thought to reflect a reversible or irreversible pathological condition.[8)] Although many studies have examined its diagnostic significance, their conclusions have varied. Chung et al. examined 37 patients with cervical spondylotic myelopathy who underwent surgery and reported that T2 hyperintensity areas were not related to postoperative outcome.[5)] Based on an investigation of 52 patients with cervical spondylotic myelopathy who received conservative therapy, Matsumoto et al. concluded that T2 hyperintensity areas were not related to clinical severity or treatment outcome.[9)] However, Chen et al. classified T2 hyperintensity areas as type 1 (indistinct borders with faint hyperintensity) and type 2 (distinct borders with marked hyperintensity) in 64 patients with cervical spondylotic myelopathy who underwent surgery and found that, whereas the prognosis of those with type 1 was similar to that of patients without T2 hyperintensity areas, the prognosis of those with type 2 was poor.[10)] Based on an analysis of the prognosis of 146 patients who underwent surgery, Suri et al. reported that the prognosis was poor if an area of abnormal hyperintensity was seen in T1- or T2-weighted images.[11)] Moreover, in an investigation in 64 patients who underwent surgery, Chatley et al. found that patients with T2 hyperintensity areas in 2 or more vertebral bodies had a poor prognosis.[12)] A similar finding was also described in the report by Wada et al.[6)]

Other studies have examined the diagnostic usefulness of contrast-enhanced MRI. In an investigation of the relationship between preoperative contrast-enhanced, T1-weighted images and clinical symptoms of 683 patients with cervical spondylotic myelopathy who underwent surgery, Ozawa et al. found no significant difference in preoperative JOA scores between a group with intraspinal enhancement and a group without such enhancement.[13] However, postoperative JOA scores were significantly higher in the group without enhancement.

Although MRI is useful for identifying lesion sites, evaluating pathological changes, and predicting prognosis in the diagnosis of cervical spondylotic myelopathy, evaluating spinal cord compression factors with MRI alone is difficult. It should therefore be used in combination with conventional radiography or CT. However, problems remain, such as the fact that the findings lack objectivity (poor interobserver agreement rate) and the fact that no clear conclusion has been reached regarding the significance of T2 hyperintensity areas.

In addition to these typical imaging methods, methods such as diffusion tensor imaging (DTI) are used for diagnosis. To answer the question of whether these methods contribute usefully to early diagnosis and prognosis prediction, further standardization of imaging methods and accumulation of clinical cases are needed.[14] The images normally obtained with MRI are obtained with the patient in the supine position and still, which makes it difficult to evaluate the various dynamic factors involved in spinal cord compression. To solve this problem, the additional use of dynamic/kinetic MRI by means of a device such as an open MRI system has been found to be useful.[15]

Search keywords and secondary sources used as references

PubMed was searched using the following keywords: cervical spondylosis, cervical spondylotic myelopathy, and MRI.

In addition, the following was referenced as a secondary source.

1) The Japanese Orthopaedic Association Clinical Practice Guidelines Committee, Cervical Spondylotic Myelopathy Formulation Committee, Ed.: 2015 Clinical Practice Guidelines for Cervical Spondylotic Myelopathy. Nankodo, 2015.

References

1) Larsson EM et al: Comparison of myelography, CT myelography and magnetic resonance imaging in cervical spondylosis and disk herniation: pre- and postoperative findings. Acta Radiol 30: 233-239, 1989
2) Sengupta DK et al: The value of MR imaging in differentiating between hard and soft cervical disc disease: a comparison with intraoperative findings. Eur Spine J 8: 199-204, 1999
3) Nagata K et al: Clinical value of magnetic resonance imaging for cervical myelopathy. Spine 15: 1088-1096, 1990
4) Bucciero A et al: Cord diameters and their significance in prognostication and decisions about management of cervical spondylotic myelopathy. J Neurosurg Sci 37: 223-228, 1993
5) Chung SS et al: Factors affecting the surgical results of expansive laminoplasty for cervical spondylotic myelopathy. Int Orthop 26: 334-338, 2002
6) Wada E et al: Can intramedullary signal change on magnetic resonance imaging predict surgical outcome in cervical spondylotic myelopathy? Spine 24: 455-461, 1999
7) Cook C et al: Observer agreement of spine stenosis on magnetic resonance imaging analysis of patients with cervical spine myelopathy. J Manipulative Physiol Ther 31: 271-276, 2008

8) Bucciero A et al: MR signal enhancement in cervical spondylotic myelopathy. Correlation with surgical results in 35 cases. J Neurosurg Sci 37: 217-222, 1993
9) Matsumoto M et al: Increased signal intensity of the spinal cord on magnetic resonance images in cervical compressive myelopathy. Does it predict the outcome of conservative treatment? Spine 25: 677-682, 2000
10) Chen CJ et al: Intramedullary high signal intensity on T2-weighted MR images in cervical spondylotic myelopathy: prediction of prognosis with type of intensity. Radiology 221: 789-794, 2001
11) Suri A et al: Effect of intramedullary signal changes on the surgical outcome of patients with cervical spondylotic myelopathy. Spine 3: 33-45, 2003
12) Chatley A et al: Effect of spinal cord signal intensity changes on clinical outcome after surgery for cervical spondylotic myelopathy. J Neurosurg Spine 11: 562-567, 2009
13) Ozawa H et al: Clinical significance of intramedullary Gd-DTPA enhancement in cervical myelopathy. Spinal Cord 48: 415-422, 2010
14) Martin AR et al: Translating state-of-the-art spinal cord MRI techniques to clinical use: a systematic review of clinical studies utilizing DTI, MT, MWF, MRS, and fMRI. Neuroimage Clin 10: 192-238, 2015
15) Kolcun JP, et al: The role of dynamic magnetic resonance imaging in cervical spondylotic myelopathy. Asian Spine J 11: 1008-1015, 2017

BQ 79 Is MRI recommended for diagnosing lumbar disc herniation?

Statement

Non-contrast MRI is useful and recommended for diagnosing lumbar disc herniation. Contrast-enhanced MRI may be useful for the follow-up of intervertebral disc herniation, differentiation from tumors, and diagnosis of postoperative recurrence. Consequently, its use can be considered. There is no scientific evidence that MR myelography should be used in addition to non-contrast MRI, and its use is therefore not recommended.

Background

MRI is minimally invasive and results in no radiation exposure, and it has become an essential diagnostic imaging modality for diagnosing lumbar spine disease. The usefulness of plain and contrast-enhanced MRI and MR myelography in diagnosing lumbar disc herniation was examined.

Explanation

Studies have compared the performance of non-contrast MRI (Fig.) and other diagnostic imaging modalities in diagnosing lumbar disc herniation. Janssen et al. compared non-contrast MRI, myelography, and CT myelography in 60 patients who underwent surgery for suspected intervertebral disc herniation and found that the diagnostic accuracy rate was 96% for non-contrast MRI, 81% for myelography, 57% for CT myelography, and 84% for the combination of myelography and CT myelography.[1)] Thus, the diagnostic accuracy rate was the highest with non-contrast MRI. On the other hand, Thornbury et al. compared non-contrast MRI, CT, and CT myelography in 95 patients with lumbar pain (56 underwent surgery) and found no significant differences in their diagnostic performance.[2)] Szypryt et al. compared non-contrast MRI and myelography in 30 patients who underwent surgery for suspected intervertebral disc herniation and found that the diagnostic accuracy rate was 88% for non-contrast MRI and 75% for myelography. Thus, non-contrast MRI was found to be slightly superior.[3)] The fact that non-contrast MRI shows diagnostic performance comparable or superior to that of other diagnostic imaging modalities, combined with the fact that it results in no radiation exposure and is minimally invasive, makes it the most highly recommended modality.

With regard to the usefulness of non-contrast MRI in evaluating radiculopathy, studies have examined the relationship between nerve root sheath morphology, compression severity, and intervertebral disc herniation. Gorbachova et al. examined non-contrast MRI in 96 patients and reported finding no relationship between the short-axis diameter of the nerve root sheath and the presence or absence of intervertebral disc herniation.[4)] On the other hand, Pfirrmann et al. found that the severity of nerve root compression (4-step classification) resulting from intervertebral disc herniation was well correlated with non-contrast MRI and intraoperative findings for 94 nerve roots examined by surgery.[5)] Although there have been studies showing correlations between leg pain and the severity of nerve root compression and

intervertebral disc herniation, no studies have showed consistency between pain sites and non-contrast MRI findings.[6, 7] In a recent study, Mostofi et al. examined the medical records of 241 patients diagnosed with lumbar disc herniation and found that 27 of these patients (11.20%) had hernia findings on the symptomatic side and contralateral side.[8]

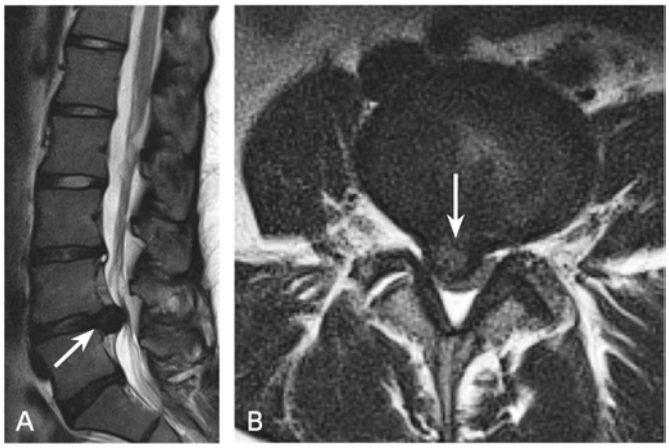

Figure. Lumbar disc herniation

A: MRI, T2-weighted sagittal image; B: MRI, T2-weighted transverse image, L4/5 level Herniation of the intervertebral disc at the L4/5 level is seen extruding posteriorly and slightly to the right (→), resulting in spinal canal stenosis.

Some studies have shown contrast MRI to be useful for the follow-up of intervertebral disc herniation. Komori et al. examined the contrast-enhanced MRI images of 48 patients with unilateral nerve root symptoms and reported that intervertebral disc herniation that showed ring-shaped contrast enhancement was susceptible to resorption.[9] Autio et al. examined the contrast-enhanced MRI images of 160 patients with unilateral sciatic neuralgia and found that thick ring-shaped enhancement of an intervertebral disc herniation, a higher degree of herniation displacement, and being aged 41 to 50 years were related to the hernia resorption rate.[10] Although the findings of detached intervertebral disc herniation are often confusingly similar to tumor findings, contrast-enhanced MRI has been reported to be useful for distinguishing such hernias from tumors.[11, 12] In addition, Hueftle et al. compared the MRI and pathological findings of 17 patients with failed back surgery syndrome who underwent surgery and found that early contrast-enhanced MRI images, obtained within 10 minutes after contrast administration, were useful for differentiating between epidural fibrosis and the recurrence of intervertebral disc herniation.[13] Amador et al. performed contrast-enhanced MRI in 72 patients diagnosed with intervertebral disc herniation by CT performed for acute lumbar sciatic neuralgia and examined whether the presence or absence of contrast enhancement was useful for predicting hernia disappearance 1 year later. Although hernias without contrast enhancement tended to remain, no significant correlation was seen between the contrast pattern and hernia disappearance.[14] Contrast-enhanced MRI is normally not needed to diagnose intervertebral disc herniation. However, it may be useful for follow-up, differentiating from tumors, and diagnosing postoperative recurrence.

MR myelography is excellent for visualizing the subarachnoid space and nerve root and ganglion morphology and is used as a substitute for myelography. Aota et al. examined 83 patients diagnosed with intervertebral disc herniation by MRI and found that swelling and deformation of the nerve roots and dorsal root ganglia were distinctly visualized, and that the severity of these changes and leg pain severity were well correlated.[15] On the other hand, Pui et al. examined 72 patients diagnosed with intervertebral disc herniation of the cervical or lumbar spine by MRI and found that adding MR myelography to non-contrast MRI did not improve diagnostic performance with respect to hernias.[16] O'Connell et al. examined 207 patients with lumbar pain or spinal radicular symptoms and concluded that adding MR myelography to non-contrast MRI did not yield much additional information.[17] Wilmink concluded that, although MR myelography is useful for elucidating the relationship between sciatic neuralgia and the appearance of nerve root compression caused by a change such as intervertebral disc herniation, it is not an imaging method that can replace non-contrast MRI.[18] Based on these findings, there is no evidence indicating that MR myelography should be added to non-contrast MRI, and the use of MR myelography is therefore not recommended.

Search keywords and secondary sources used as references

PubMed was searched using the following keywords: back pain, sciatica, disk herniation, and MRI.

In addition, the following was referenced as a secondary source.

1) Japanese Orthopaedic Association and Japanese Society for Spine Surgery and Related Research, Ed.: Clinical Practice Guidelines for Lumbar Disc Herniation, Revised 2nd Edition. Nankodo Co., 2011.

References

1) Janssen ME et al: Lumbar herniated disk disease: comparison of MRI, myelography, and post-myelographic CT scan with surgical findings. Orthopedics 17: 121-127, 1994
2) Thornbury JR et al: Disk-caused nerve compression in patients with acute low-back pain: diagnosis with MR, CT myelography, and plain CT. Radiology 186: 731-738, 1993
3) Szypryt EP et al: Diagnosis of lumbar disc protrusion: a comparison between magnetic resonance imaging and radiculography. J Bone Joint Surg Br 70: 717-722, 1988
4) Gorbachova TA et al: Nerve root sleeve diameters at normal segments and at segments with proximate disc disease: MRI evaluation. Skeletal Radiol 31: 511-515, 2002
5) Pfirrmann CWA et al: MR image-based grading of lumbar nerve root compromise due to disk herniation: reliability study with surgical correlation. Radiology 230: 583-588, 2004
6) Porchet F et al: Relationship between severity of lumbar disc disease and disability scores in sciatica patients. Neurosurgery 50: 1253-1259, 2002
7) Beattie PF et al: Associations between patient report of symptoms and anatomic impairment visible on lumbar magnetic resonance imaging. Spine 25: 819-828, 2000
8) Mostofi K et al: Reliability of the path of the sciatic nerve, congruence between patients' history and medical imaging evidence of disc herniation and its role in surgical decision making. Asian Spine J 9: 200-204, 2015
9) Komori H et al: Contrast-enhanced magnetic resonance imaging in conservative management of lumbar disc herniation. Spine 23: 67-73, 1998
10) Autio RA et al: Determinants of spontaneous resorption of intervertebral disc herniations. Spine 31: 1247-1252, 2006
11) Aydin MV et al: Intradural disc mimicking: a spinal tumor lesion. Spinal Cord 42: 52-54, 2004
12) Lee JS et al: Intradural disc herniation at L5-S1 mimicking an intradural extramedullary spinal tumor: a case report. J Korean Med Sci 21: 778-780, 2006
13) Hueftle MG et al: Lumbar spine: postoperative MR imaging with Gd-DTPA. Radiology 167: 817-824, 1988

14) Amador AR et al: Natural history of lumbar disc hernias: does gadolinium enhancement have any prognostic value ? Radiologia 55: 398-407, 2013
15) Aota Y et al: Dorsal root ganglia morphologic features in patients with herniation of the nucleus pulposus. Spine 26: 2125- 2132, 2001
16) Pui MH et al: Value of magnetic resonance myelography in the diagnosis of disc herniation and spinal stenosis. Australas Radiol 44: 281-284, 2000
17) O'Connell MJ et al: The value of routine MR myelography at MRI of the lumbar spine. Acta Radiol 44: 665-672, 2003
18) Wilmink JT: MR myelography in patients with lumbosacral radicular pain: diagnostic value and technique. Neuroradiol J 24: 570-576, 2011

BQ 80 Is hand and wrist joint MRI recommended for diagnosing rheumatoid arthritis (RA)?

Statement

Hand and wrist joint MRI is useful and recommended. It is preferably used in combination with contrast-enhanced imaging and should be performed together with an examination by a rheumatologist and serological testing.

Background

The findings of joint MRI in RA include synovial thickening, bone marrow edema, bone erosion, synovial fluid accumulation, and tenosynovitis. However, the specificity of these findings is weak, and similar findings may be obtained in other inflammatory joint diseases. The 2010-ACR/EULAR criteria emphasize the distribution of subjective and objective findings such as joint pain and swelling and the number of affected joints (secondary source 1) and do not include items related to joint MRI. The usefulness of hand and wrist joint MRI in diagnosing RA was examined.

Explanation

Why is hand and wrist MRI a subject of debate even though RA is a systemic disorder that affects a variety of joints and organs? One answer is that the hand and wrist joints are sites where RA occurs preferentially, and bone erosion can be more easily observed in these joints than in larger joints.[1)] In addition, the changes that occur in joints throughout the body can to a certain extent be understood by evaluating the hand and wrist joints, according to an investigation of whole-body MRI.[2)]

The standard imaging methods used are T1-weighted, fat-suppressed, T2-weighted (or STIR imaging), and post-contrast, fat-suppressed, T1-weighted imaging. Contrast-enhanced imaging is not always essential for evaluating bone erosion and bone marrow edema. However, the use of fat-suppressed, T2-weighted imaging (or STIR imaging) to evaluate synovitis and tenosynovitis can result in underestimation or overestimation, and contrast-enhanced imaging is therefore essential for their accurate evaluation.[3, 4)] Imaging of both hands is preferable if possible.[5)]

Several cohort studies have examined the usefulness of hand and wrist joint MRI (Fig.) in diagnosing RA. Some studies have found hand and wrist joint MRI to not be useful for distinguishing between early RA and other inflammatory joint diseases.[6, 7)] On the other hand, Sugimoto et al. found that, in 48 patients with suspected early RA, supplementing the 1987-ACR criteria with MRI diagnostic criteria (secondary source 2, bilateral hand joints, metacarpophalangeal joint, and proximal interphalangeal joint contrast enhancement) improved the diagnostic sensitivity and accuracy rates, with the rates of diagnostic sensitivity, specificity, and accuracy changing from 77%, 91%, and 83%, respectively, to 96%, 86%, and 94%, respectively.[8)] In an investigation of MRI of the bilateral hand joints and serum markers in 129 patients

with unclassified arthritis, Tamai et al. found that the combination of bone marrow edema visualized by MRI and anti-CCP antibody positivity was useful for diagnosing RA.[9)]

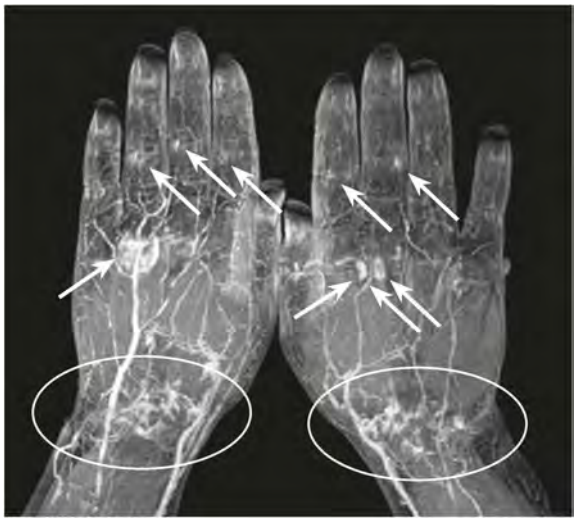

Figure RA

MRI of both hands, fat-suppressed, contrast-enhanced, T1-weighted imaging, MIP image: Multiple areas of abnormal enhancement are seen in the bilateral carpal regions (circled areas) and finger joints (→), findings indicative of polyarthritis.

According to a meta-analysis by Suter et al., the diagnostic performance of hand and wrist joint MRI in early RA varies greatly depending on the MRI diagnostic criteria used, with sensitivity ranging from 20% to 100% and specificity from 0% to 100%.[10)] Although it is difficult to characterize the diagnostic performance of hand and wrist MRI based on those results, an examination of the details shows that sensitivity and specificity were relatively high for the combination of synovitis, bone marrow edema, and bone erosion, and that specificity tended to be high and sensitivity low only for bone marrow edema and bone erosion. Hand and wrist joint MRI should therefore be used in combination with contrast-enhanced imaging to visualize synovitis. Moreover, specificity can be improved by keeping in mind that a few arthritis findings can be observed even in healthy individuals, particularly elderly individuals.[11)]

For the diagnosis of RA, hand and wrist joint MRI is preferably performed in combination with contrast-enhanced imaging, and interpretation should take into account the normal ranges for findings. Moreover, rather than a diagnosis based on MRI alone, an evaluation that combines MRI with an examination by a rheumatologist and serological testing is recommended.

Search keywords and secondary sources used as references

PubMed was searched using the following keywords: hand, wrist, rheumatoid arthritis, diagnosis, and MRI.

In addition, the following were referenced as secondary sources.

1) Aletaha D et al: 2010 Rheumatoid arthritis classification criteria: an American College of Rheumatology/European League Against Rheumatism collaborative initiative. Arthritis Rheum 62 (9): 2569-2581, 2010
2) Arnet FC et al: The American Rheumatism Association 1987 revised criteria for the classification of rheumatoid arthritis. Arthritis Rheum 31: 315-324, 1988

References

1) Rubin DA: MRI and ultrasound of the hands and wrists in rheumatoid arthritis: imaging findings. Skeletal Radiol 48 (5): 677-695, 2019
2) Kamishima T et al: Contrast-enhanced whole-body joint MRI in patients with unclassified arthritis who develop early rheumatoid arthritis within 2 years: feasibility study and correlation with MRI findings of the hands. AJR Am J Roentgenol 195 (4): W287-W292, 2010
3) Stomp W et al: Aiming for a simpler early arthritis MRI protocol: can Gd contrast administration be eliminated? Eur Radiol 25 (5): 1520-1527, 2015
4) Aoki T et al: Diagnosis of early-stage rheumatoid arthritis: usefulness of unenhanced and gadolinium-enhanced MR images at 3T. Clin Imaging 37 (2): 348-353, 2013
5) Mo YQ et al: Magnetic resonance imaging of bilateral hands is more optimal than MRI of unilateral hands for rheumatoid arthritis. J Rheumatol 45 (7): 895-904, 2018
6) Boutry N et al: MR imaging findings in hands in early rheumatoid arthritis: comparison with those in systemic lupus erythematosus and primary Sjogren syndrome. Radiology 236 (2): 593-600, 2005
7) Duer-Jensen A et al: Bone edema on magnetic resonance imaging is an independent predictor of rheumatoid arthritis development in patients with early undifferentiated arthritis. Arthritis Rheum 63 (8): 2192-2202, 2011
8) Sugimoto H et al: Early-stage rheumatoid arthritis: prospective study of the effectiveness of MR imaging for diagnosis. Radiology 216 (2): 569-575, 2000
9) Tamai M et al: A prediction rule for disease outcome in patients with undifferentiated arthritis using magnetic resonance imaging of the wrists and finger joints and serologic autoantibodies. Arthritis Rheum 61 (6): 772-778, 2009
10) Suter LG ey al: Role of magnetic resonance imaging in the diagnosis and prognosis of rheumatoid arthritis. Arthritis Care Res (Hoboken) 63 (5): 675-688, 2011
11) Boer AC et al: Using a reference when defining an abnormal MRI reduces false-positive MRI results-a longitudinal study in two cohorts at risk for rheumatoid arthritis. Rheumatology 56 (10): 1700-1706, 2017

CQ 19 Is MR arthrography recommended for diagnosing rotator cuff injury?

Recommendation

Although there are reports indicating that the diagnostic performance of MR arthrography in evaluating subscapularis tendon rupture and the postoperative shoulder rotator cuff is superior to that of non-contrast MRI, nearly all of the reports as a whole indicate that the sensitivity and specificity of MR arthrography and non-contrast MRI are comparable in the diagnosis of rotator cuff injury. It is therefore weakly recommended that MR arthrography not be performed in view of its invasiveness.

Recommendation strength: 3, strength of evidence: weak (C), agreement rate: 100% (9/9)

Background

MRI is known to be useful for diagnosing rotator cuff injury. However, whether MR arthrography, which is invasive, is necessary for diagnosis is not yet known. Consequently, the need for MR arthrography was examined.

Explanation

There have been 6 meta-analysis articles[1-6)] and 2 articles[7, 8)] describing cross-sectional studies of the diagnostic performance of MRI, including MR arthrography and non-contrast MRI, in rotator cuff injury. A systematic review of these articles was conducted. The sensitivity and specificity reported were as follows. The sensitivity and specificity of non-contrast MRI ranged from 77% to 96% and from 81% to 100%, respectively.[1-6)] The sensitivity and specificity of MR arthrography ranged from 77% to 100% and from 92% to 100%, respectively.[1-6)] These results indicate that the diagnostic performance of MR arthrography and non-contrast MRI is comparable.

A systematic review by Lenza et al. found that sensitivity and specificity in the diagnosis of full-thickness (complete) rotator cuff tear were 94% and 93%, respectively, for non-contrast MRI and 94% and 92%, respectively, for MR arthrography.[1)] No statistically significant differences were seen. In a meta-analysis by de Jesus et al., sensitivity and specificity in the diagnosis of partial and full-thickness rotator cuff tears were 87.0% and 81.7%, respectively, for non-contrast MRI (Fig. A) and 92.3% and 94.5%, respectively, for MR arthrography (Fig. B).[2)] The area under the curve (AUC) in the ROC analysis was 0.935 for MR arthrography and 0.878 for non-contrast MRI. In a meta-analysis by Dinnes et al., sensitivity and specificity in the diagnosis of full-thickness tears were 89% and 93%, respectively, for non-contrast MRI and 95% and 93%, respectively, for MR arthrography.[3)] However, the diagnostic performance of both was low for partial (incomplete) tears.

In a meta-analysis by McGarvey et al. of studies that used recent MRI systems that were limited exclusively to 3T-MRI, sensitivity and specificity for full-thickness tears were 95.7% and 99.0%,

respectively, for non-contrast MRI and 96.5% and 97.8%, respectively, for MR arthrography.[4] Thus, the diagnostic performance of the 2 methods was comparable. However, sensitivity and specificity for diagnostic performance in partial tears were 80.5% and 100%, respectively, for non-contrast MRI versus 86.5% and 95.2%, respectively, for MR arthrography, indicating that MR arthrography was more sensitive than non-contrast MRI, and non-contrast MRI was more specific than MR arthrography, the differences being significant. With regard to diagnostic performance in subscapularis tendon rupture, that of MR arthrography tends to be superior to that of non-contrast MRI overall. In a meta-analysis by Huang et al. of diagnostic performance in partial bursal surface tears, the sensitivity, specificity, and AUC were 77%, 96%, and 0.82, respectively, for non-contrast MRI and 77%, 98%, and 0.88, respectively, for MR arthrography, indicating that the diagnostic performance of the 2 methods was comparable.[5] With regard to diagnostic performance in rotator cuff tears, Roy et al. reported that sensitivity and specificity were both 90% with both non-contrast MRI and MR arthrography, indicating comparable diagnostic performance for both.[6]

For rotator cuff tear evaluation in the postoperative shoulder, Magee et al. reported sensitivity and specificity of 84% and 100%, respectively, with non-contrast MRI and 100% and 100%, respectively, with MR arthrography.[7, 8] Thus, the diagnostic performance of MR arthrography was higher.

The above findings indicate that, although some reports show that MR arthrography provides superior diagnostic performance in subscapularis tendon injury and postoperative rotator cuff tear, nearly all of the reports indicate that the performance of non-contrast MRI and MR arthrography is basically comparable in the diagnosis of rotator cuff injury. Although there were no reports of adverse reactions to contrast media with MR arthrography, it is weakly recommended that MR arthrography not be performed in view of its invasiveness.

Figure　Rotator cuff tear

A: MRI of a full-thickness rotator cuff tear, fat-suppressed, proton density-weighted, oblique coronal image: A continuous interruption and defect are seen through the full thickness of the superior rotator cuff (→). The glenohumeral joint and subacromial bursa communicate through this site.

B: MR arthrography of a partial rotator cuff tear, fat-suppressed, T1-weighted, oblique coronal image: Contrast medium influx is seen on the articular surface at the greater tubercle insertion of the superior rotator cuff (→).

Search keywords and secondary sources used as references

PubMed, the Ichushi, and Cochrane Library databases were searched using the following keywords: rotator cuff injury, rotator cuff tear, MRI, MR arthrography, humans, human, sensitivity, specificity, and ROC. The period searched was from January 2016 to July 2020, and hits were obtained for 110 articles. Two articles were extracted in the secondary screening. In addition, 3 articles were added with a hand search. A qualitative systematic review of these articles was conducted.

In addition, the following was referenced as a secondary source.

1) Japan Radiological Society, Ed.: Diagnostic Imaging Guidelines 2016. KANEHARA & Co., 2016.

References

1) Lenza M et al: Magnetic resonance imaging, magnetic resonance arthrography and ultrasonography for assessing rotator cuff tears in people with shoulder pain for whom surgery is being considered. Cochrane Detabase Syst Rev 24: 9, 2013
2) de Jesus JO et al: Accuracy of MRI, MR arthrography, and ultrasound in the diagnosis of rotator cuff tears: a meta-analysis. AJR Am J Roentgenol 192: 1701-1707, 2009
3) Dinnes J et al: The effectiveness of diagnostic tests for the assessment of shoulder pain due to soft tissue disorders: a systematic review. Health Technol Assess 7: 1-166, 2003
4) McGarvey C et al: Diagnosis of rotator cuff tears using 3-tesla MRI versus 3-tesla MRA: a systematic review and meta-analysis. Skeletal Radiol 45 (2): 251-261, 2016
5) Huang T et al: Diagnostic accuracy of MRA and MRI for the bursal-sided partial-thickness rotator cuff tears: a meta-analysis. J Orthop Surg Res 14 (1): 436, 2019
6) Roy JS et al: Diagnostic accuracy of ultrasonography, MRI and MR arthrography in the characterisation of rotator cuff disorders: a systematic review and meta-analysis. Br J Sports Med 49 (20): 1316-1328, 2015
7) Magee T: Imaging of the post-operative shoulder: does injection of iodinated contrast in addition to MR contrast during arthrography improve diagnostic accuracy and patient throughput? Skeletal Radiol 47 (9): 1253-1261, 2018
8) Magee T: Utility of pre- and post-MR arthrogram imaging of the shoulder: effect on patient care. Br J Radiol 89 (1062): 20160028, 2016

CQ 20 Is MR arthrography recommended for diagnosing a glenoid labrum tear?

Recommendation

MR arthrography is weakly recommended for diagnosing a glenoid labrum tear.

Recommendation strength: 2, strength of evidence: weak (C), agreement rate: 89% (8/9)

Background

MRI is a widely used and useful test for diagnosing shoulder joint diseases, and the use of non-contrast MRI for this purpose is recommended. MR arthrography includes direct MR arthrography, in which observations are performed after a contrast medium is administered in the joint and the joint capsule has been relaxed, and indirect MR arthrography, in which a contrast medium is administered intravenously. Although there is evidence suggesting that MR arthrography may provide higher diagnostic performance than non-contrast MRI for glenoid labrum lesions, its use is not uniformly recommended. This CQ discusses the usefulness of MR arthrography in diagnosing glenoid labrum tears.

Explanation

There have been 1 cohort study,[1)] 2 cross-sectional studies,[2, 3)] and 3 meta-analyses[4-6)] that examined the diagnostic performance of MR arthrography and non-contrast MRI in glenoid labrum tear, using shoulder arthroscopy as the reference standard. A qualitative systematic review of the articles describing these studies was conducted. Three types of glenoid labrum injuries (superior labrum anterior and posterior (SLAP) lesions[1-6)], anterior glenoid labrum lesions[2-4)], and posterior glenoid labrum lesions) were evaluated respectively[2-4)]

Aspects of the studies, such as the magnetic fields of the MRI systems used and the patient groups examined, varied. In particular, variability in the diagnostic performance of non-contrast MRI was seen with low magnetic field systems and 3T-MRI. Nearly all of the reports showed that MR arthrography provided better sensitivity for all of these types of glenoid labrum tears (MR arthrography, 80% to 100%; non-contrast MRI, 23% to 98%), whereas the specificity of the 2 methods was roughly comparable (MR arthrography, 81% to 100%; non-contrast MRI, 88% to 100%).[1-6)]

In studies that compared the diagnostic performance of direct and indirect MR arthrography with that of non-contrast MRI in SLAP lesions, sensitivity ranged from 80.4% to 85% with direct MR arthrography, 74.2% to 78% with indirect MR arthrography, and 63% to 83% with non-contrast MRI, whereas specificity ranged from 90.7% to 94%, 61% to 66.5%, and 87.2% to 99%, respectively.[4, 5)] Thus, the diagnostic performance of indirect MR arthrography was inferior with respect to both sensitivity and specificity. This is likely attributable in large part to factors such as inadequate expansion of the joint capsule and interpretation interference by soft tissue contrast enhancement with indirect MR arthrography.

Figure 1. SLAP lesion

MRI, fat-suppressed, T2-weighted, oblique coronal image: A hyperintense region is seen at the attachment of the superior glenoid labrum (→).

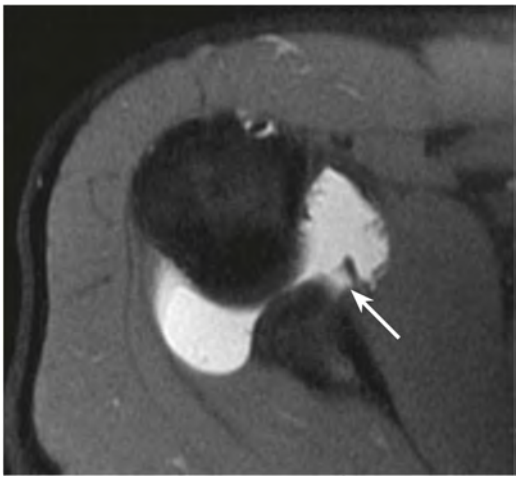

Figure 2. Anterior glenoid labrum detachment resulting from anterior shoulder dislocation (Bankart lesion)

Direct MR arthrography, fat-suppressed, T1-weighted, transverse image: Contrast medium influx is seen near the inner border of the anterior glenoid labrum (→).

With regard to abduction and external rotation (ABER), sensitivity and specificity for anterior glenoid labrum tear were 83% and 99%, respectively, with non-contrast MRI, 87% and 99%, respectively, with MR arthrography (regardless of whether it was contrast-enhanced imaging), and 94% and 94%, respectively, with MR arthrography in ABER. Sensitivity and specificity for SLAP lesions were 83% and 99%, respectively, with non-contrast MRI, 84% and 92%, respectively, with MR arthrography (regardless of whether it was contrast-enhanced imaging), and 100% and 100%, respectively, with MR arthrography in ABER.[4)] Thus, sensitivity improved with ABER. With regard to diagnostic performance improvements resulting from the addition of ABER, it should be noted that it was not always added in the reports that were examined, and that it was added only for patients in whom instability was seen clinically in some of the included reports.

In the postoperative shoulder, symptoms suggestive of recurrence are seen in approximately 20% of patients, and differentiation of the glenoid labrum that has undergone postoperative changes and recurrence is difficult. Magee compared sensitivity and specificity in the postoperative shoulder and reported sensitivity and specificity for SLAP lesions of 100% and 97%, respectively, with MR arthrography and 71% and 100%, respectively, with non-contrast MRI. For the anterior glenoid labrum lesion, sensitivity and specificity were 100% and 100%, respectively, with MR arthrography and 80% and 100%, respectively, with non-contrast MRI. For the posterior glenoid labrum, sensitivity and specificity were 100% and 98%, respectively, with MR arthrography and 81% and 100%, respectively, with non-contrast MRI.[2)] Thus, MR arthrography was found to be useful. However, 22 patients in this study who could not be evaluated by MR arthrography or non-contrast MRI due to metal artifacts were instead evaluated by CT arthrography and

excluded from the analysis. It should be noted that this was considered to result in sensitivity and specificity that were higher than those in the previous studies.

In a study that evaluated the effectiveness of MR arthrography in patient care, the sensitivity of MR arthrography and non-contrast MRI was 96% to 98% and 81% to 83%, respectively, for SLAP lesions, 94% to 97% and 74% to 77%, respectively, for anterior glenoid labrum lesions, and 91% to 97% and 76% to 82%, respectively, for posterior glenoid labrum lesions, showing that MR arthrography is superior to non-contrast MRI. The specificity of MR arthrography and non-contrast MRI was 100% for all 3 types of lesions.[3)] Abnormalities were seen by MR arthrography in 18 of the 48 patients (37%) with normal findings on non-contrast MRI, and additional findings were obtained by MR arthrography in only 3 of the 42 patients (6%) with abnormalities seen on non-contrast MRI. These additional findings were lesions that were clinically identifiable by arthroscopy, suggesting that additional MR arthrography may not be necessary for patients with abnormalities seen on non-contrast MRI.

MR arthrography, particularly direct MR arthrography, is invasive and time-consuming and has problems such as patient discomfort before and after the procedure, risk of infection, and cost. However, there is weak evidence that it is superior to non-contrast MRI for evaluating glenoid labrum tears, and its use is therefore weakly recommended.

Search keywords and secondary sources used as references

PubMed was searched using the following keywords: shoulder, labrum, labral, injury, tear, MR arthrography, MRI, humans, human, sensitivity, specificity, and ROC. The period searched was from January 2016 to July 2020; hits were obtained for 40 articles. The Ichushi and Cochrane Library databases were also searched using the same keywords. Six articles were extracted in the secondary screening, and a qualitative systematic review of the articles was conducted.

In addition, the following was referenced as a secondary source.

1) Japan Radiological Society, Ed.: Diagnostic Imaging Guidelines 2016. KANEHARA & Co., 2016.

References

1) Berth A et al: Magnetic resonance-guided direct shoulder arthrography for the detection of superior labrum anterior-posterior lesions using an open 1.0-T MRI scanner. Pol J Radiol 84: e251-e257, 2019
2) Magee T: Imaging of the post-operative shoulder: does injection of iodinated contrast in addition to MR contrast during arthrography improve diagnostic accuracy and patient throughput? Skeletal Radiol 47 (9): 1253-1261, 2018
3) Magee T: Utility of pre- and post-MR arthrogram imaging of the shoulder: effect on patient care. Br J Radiol 89 (1062): 20160028, 2016
4) Ajuied A et al: Diagnosis of glenoid labral tears using 3-tesla MRI vs. 3-tesla MRA: a systematic review and meta-analysis. Arch Orthop Trauma Surg 138 (5): 699-709, 2018
5) Symanski JS et al: Diagnosis of superior labrum anterior-to-posterior tears by using MR imaging and MR arthrography: a systematic review and meta-analysis. Radiology 285 (1): 101-113, 2017
6) Arirachakaran A et al: A systematic review and meta-analysis of diagnostic test of MRA versus MRI for detection superior labrum anterior to posterior lesions type II-VII. Skeletal Radiol 46 (2): 149-160, 2017

BQ 81 Are conventional radiography, bone scintigraphy, and MRI recommended for diagnosing idiopathic osteonecrosis of the femoral head?

Statement

Conventional radiography, bone scintigraphy, and MRI are standard imaging examinations included among the diagnostic criteria and staging and disease classification of the working group of the Specific Disease Investigation Committee under the auspices of the Japanese Ministry of Health, Labour and Welfare of idiopathic osteonecrosis of the femoral head, and their use for diagnosing idiopathic osteonecrosis of the femoral head is recommended.

CQ 21 Is CT recommended for diagnosing idiopathic osteonecrosis of the femoral head?

Recommendation

CT cannot be considered superior to MRI or bone scintigraphy for diagnosing idiopathic osteonecrosis of the femoral head. However, there is weak evidence indicating that CT is superior for evaluating subchondral fractures, an important factor for staging. Its use is therefore weakly recommended.
Recommendation strength: 2, strength of evidence: D (very weak), agreement rate: 100% (10/10)

Background

Idiopathic osteonecrosis of the femoral head is recognized as a designated intractable disease by the Ministry of Health, Labour and Welfare. Because histological examination of biopsy samples is not 100% accurate, multiple approaches to diagnosis are needed, including diagnostic imaging. Staging and disease classification play major roles in clinical findings, treatment selection, and prognosis prediction; diagnosis incorporating them is also important.

In Japan, the diagnostic criteria and staging and disease classification of the working group of the Specific Disease Investigation Committee under the auspices of the Japanese Ministry of Health, Labour and Welfare's of idiopathic osteonecrosis of the femoral head have been authorized by the Japanese Orthopaedic Association and are widely used (secondary source 1). The diagnostic criteria incorporate conventional radiography, bone scintigraphy, MRI, and histology findings; staging classification uses conventional radiography findings; and disease classification uses conventional radiography and MRI findings (secondary source 1). Internationally, although there is a staging classification, there are no international diagnostic criteria, and the staging classification serves in this role. The frequently used

staging classification of the Association Research Circulation Osseous (ARCO) incorporates findings from conventional radiography, CT, bone scintigraphy, and MRI (secondary source 2).

The basis of the BQ statement and CQ recommendation grade for each imaging examination used to diagnose idiopathic osteonecrosis of the femoral head is explained below.

Explanation

There have been 8 articles reporting cross-sectional studies of the diagnostic performance of each type of imaging examination in idiopathic osteonecrosis of the femoral head and 1 meta-analysis of the diagnostic performance of MRI.[1-9)] A systematic review of these articles was conducted. The reference standards used in the studies were varied and included histological examination of biopsy specimens, intramedullary pressure, and 1 or several different imaging examinations. There were few studies of conventional radiography or CT. Consequently, a meta-analysis could not be performed. However, both sensitivity and specificity were found to be lower with conventional radiography than with the other imaging examinations. Conventional radiography sensitivity and specificity were 57% and 77%, respectively.[1)] CT sensitivity was 70.6% in 1 study[2)] and 92.7% in another.[3)] Bone scintigraphy sensitivity and specificity ranged from 60% to 91.3% and 79% to 100%, respectively.[1-6)] MRI (Fig.) sensitivity and specificity ranged from 50% to 100% and 71% to 100%, respectively.[1, 3-5, 7)]

Mitchell et al. compared the diagnostic performance of MRI, CT, and bone scintigraphy in an ROC analysis and reported that MRI provided the highest accuracy for early diagnosis.[8)] In a meta-analysis of the diagnostic performance of MRI in early idiopathic osteonecrosis of the femoral head by Zhang et al., sensitivity and specificity were both high, at 93.0% (95% CI, 92.0% to 94.0%) and 91.0% (95% CI, 89.0% to 93.0%), respectively, indicating that the diagnostic performance of MRI was high.[9)] In 2 studies that compared bone scintigraphy combined with SPECT and MRI, sensitivity was higher with bone scintigraphy (91% and 100%) than with MRI (87% and 66%).[4, 7)]

Figure　Idiopathic osteonecrosis of the femoral head

A: MRI, T1-weighted coronal image; B: MRI, T2-weighted sagittal image: Osteonecrosis is present in the anterosuperior area of the left femoral head, and band-like hypointensity suggestive of a necrotic border is seen (⇨). Linear hypointensity parallel to the articular surface is seen in the subchondral region of the anterosuperior area of the femoral head (▷), a finding indicative of subchondral fracture. This is accompanied by a hypointense region indicating bone marrow edema in the periphery of the necrosis (→).

C: CT, MPR, coronal image; D: CT, MPR, sagittal image: Subchondral fracture in the anterosuperior femoral head is identified as linear sclerotic changes (▷). Linear sclerotic changes are seen on the border with the osteonecrosis (⇨).

On the other hand, in a multicenter study of diagnostic performance in idiopathic osteonecrosis of the femoral head, Sugano et al. reported very high diagnostic performance (sensitivity of 91% and specificity of 99%) by combining any 2 of 5 criteria identified for conventional radiography, bone scintigraphy, MRI, and histology.[1)]

The above findings indicate that the diagnostic performance of bone scintigraphy combined with SPECT and MRI is high, and combining multiple tests is considered desirable. However, these studies have various problems that should be considered. These include the fact that they use a variety of reference standards, the MRI magnetic field strengths and imaging methods used vary, and many of the reports are old, and the performance of the imaging systems used differed from that of current systems.

With regard to staging, there were 5 articles reporting cross-sectional studies of the usefulness of imaging examinations,[10-14] and a systematic review of these articles was conducted. Lee et al. reported that the stage increased with the use of CT and MRI as compared with conventional radiography in 4 of 15 hip joints with idiopathic osteonecrosis of the femoral head.[10] In a comparison of staging according to the ARCO classification with the use of conventional radiography and MRI, Zibis et al. found that the sensitivity and specificity of conventional radiography using MRI as the reference standard were 88% and 90.5%, respectively, for stage II, 79.2% and 82%, respectively, for stage III, and 76% and 100%, respectively, for stage IV.[11] Moreover, the agreement rate between MRI and conventional radiography was 80.6% for staging, 71.2% for the location of the osteonecrotic lesion, 67.1% for the size of the osteonecrotic lesion, 79.2% for the presence of collapse of the articular surface, and 56.3% for degree of collapse.

Subchondral fracture in necrotic bone and collapse of the articular surface are important factors in staging. Sensitivity and specificity of 71% and 97%, respectively, were reported for conventional radiography in the evaluation of subchondral fracture, using CT as the reference standard.[12] Sensitivity of 38% and 92.9% and specificity of 100% and 28.6% were reported in 2 studies of MRI.[12, 13] Meier et al. compared the diagnostic performance of CT and MRI with respect to the presence and severity of subchondral fracture and collapse of the articular surface in ARCO classification stage III patients, using histology as the reference standard.[14] The detection rate for subchondral fracture was higher with CT (CT, 100%; MRI, 51%), and the extent of subchondral fracture and the severity of collapse could be evaluated more accurately with CT. CT was therefore reported to be superior to MRI for staging. Thus, although the evidence is weak, it indicates that CT is superior to conventional radiography and MRI for evaluating subchondral fractures in necrotic bone and the collapse of the articular surface. CT has also been used in preoperative planning in recent years.

Although the performance of conventional radiography in diagnosing idiopathic osteonecrosis of the femoral head is not very high, it is an imaging examination that results in little radiation exposure and permits inexpensive screening. High diagnostic performance is seen with MRI and bone scintigraphy combined with SPECT. Consequently, they are considered the standard imaging examinations. The diagnostic performance of CT cannot be considered superior to that of MRI or bone scintigraphy combined with SPECT, and CT results in radiation exposure. However, there is weak evidence that it is superior to those modalities for evaluating subchondral fracture in necrotic bone and collapse of the articular surface, which are important factors for staging. Its use is therefore weakly recommended.

Search keywords and secondary sources used as references

PubMed and the Cochrane Library database were searched for the period from 2016 to 2019 using the following keywords: femoral head, osteonecrosis, necrosis, radiography, bone scintigraphy, bone scan, CT, MRI, human, humans, sensitivity, specificity, and ROC. Although hits were obtained for 110 articles, only 1 article was extracted in secondary screening. Another 13 articles that provided evidence regarding the usefulness of imaging examinations in diagnosing idiopathic osteonecrosis of the femoral head were also included in the review. These were among the articles cited in the Diagnostic Imaging Guidelines 2016 for the CQ, “What types of diagnostic imaging are recommended for diagnosing femoral head osteonecrosis?”

In addition, the following were referenced as secondary sources.

1) The Japanese Orthopaedic Association; Ministry of Health, Labour and Welfare panel on the designated intractable disease idiopathic osteonecrosis of the femoral head; The Japanese Orthopaedic Association Panel on Clinical Practice Guidelines, Committee to Formulate Clinical Practice Guidelines for idiopathic osteonecrosis of the femoral head: 2019 Clinical Practice Guidelines for idiopathic osteonecrosis of the femoral head. Nankodo, 2019.
2) Yoon BH et al: The 2019 Revised Version of Association Research Circulation Osseous Staging System of Osteonecrosis of the Femoral Head. J Arthroplasty 35: 933-940, 2020
3) Japan Radiological Society, Ed.: Diagnostic Imaging Guidelines 2016. KANEHARA & Co., 2016.

References

1) Sugano N et al: Diagnostic criteria for non-traumatic osteonecrosis of the femoral head: a multicentre study. J Bone Joint Surg Br 81: 590-595, 1999
2) Coleman BG et al: Radiographically negative avascular necrosis: detection with MR imaging. Radiology 168: 525-528, 1988
3) Thickman D et al: Magnetic resonance imaging of avascular necrosis of the femoral head. Skeletal Radiol 15: 133-140, 1986
4) Stulberg BN et al: Multimodality approach to osteonecrosis of the femoral head. Clin Orthop Relat Res 240: 181-193, 1989
5) Markisz JA et al: Segmental patterns of avascular necrosis of the femoral heads: early detection with MR imaging. Radiology 162: 717-720, 1987
6) Lee EJ et al: Incidence and radio-uptake patterns of femoral head avascular osteonecrosis at 1 year after renal transplantation: a prospective study with planar bone scintigraphy. Nucl Med Commun 27: 919-924, 2006
7) Ryu JS et al: Bone SPECT is more sensitive than MRI in the detection of early osteonecrosis of the femoral head after renal transplantation. J Nucl Med 43: 1006-1011, 2002
8) Mitchell DG et al: Avascular necrosis of the hip: comparison of MR, CT, and scintigraphy. AJR Am J Roentgenol 147: 67-71, 1986
9) Zhang YZ et al: Accuracy of MRI diagnosis of early osteonecrosis of the femoral head: a meta-analysis and systematic review. J Orthop Surg Res 13: 167, 2018
10) Lee MJ et al: A comparison of modern imaging modalities in osteonecrosis of the femoral head. Clin Radiol 42: 427-432, 1990
11) Zibis AH et al: The role of MR imaging in staging femoral head osteonecrosis. Eur J Radiol 63: 3-9, 2007.
12) Stevens K et al: Subchondral fractures in osteonecrosis of the femoral head: comparison of radiography, CT, and MR imaging. AJR Am J Roentgenol 180: 363-368, 2003
13) Yeh LR et al: Diagnostic performance of MR imaging in the assessment of subchondral fractures in avascular necrosis of the femoral head. Skeletal Radiol 38: 559-564, 2009
14) Meier R et al: Bone marrow oedema on MR imaging indicates ARCO stage 3 disease in patients with AVN of the femoral head. Eur Radiol 24: 2271-2278, 2014

BQ 82 Is MRI recommended for diagnosing meniscal and cruciate ligament injuries of the knee joint?

Statement

MRI is useful and recommended for diagnosing meniscal and cruciate ligament injuries of the knee joint. However, it should not be performed alone, but rather in combination with an examination by an orthopedist that includes history-taking.

Background

There are many opportunities to use MRI to diagnose injuries of the menisci and cruciate ligaments, which are intra-articular structures. However, diagnosis based on manual testing by an orthopedist is also established, and some orthopedists think there is little need for MRI. Moreover, although the most reliable diagnostic method is arthroscopy, it is highly invasive and expensive compared with MRI. MRI should therefore be used for diagnosis instead of arthroscopy, if possible. The usefulness of MRI for diagnosing meniscal and cruciate ligament injuries is discussed below.

Explanation

Numerous cross-sectional studies have examined the performance of MRI in diagnosing meniscal and cruciate ligament injuries of the knee joint, using arthroscopy as the reference standard (Figs. 1 and 2). In a meta-analysis by Oei et al., MRI sensitivity and specificity were 93.3% (95% CI, 91.7% to 95.0%) and 88.4% (95% CI, 85.4% to 91.4%), respectively, for medial meniscal tears; 79.3% (95% CI, 74.3% to 84.2%) and 95.7% (95% CI, 94.6% to 96.8%), respectively, for lateral meniscal tears; 94.4% (95% CI, 92.3% to 96.6%) and 94.3% (95% CI, 92.7% to 95.9%), respectively, for anterior cruciate ligament tears; and 91.0% (95% CI, 83.2% to 98.7%) and 99.4% (95% CI, 98.9% to 99.9%), respectively, for posterior cruciate ligament tears.[1)] In a meta-analysis by Crawford et al., sensitivity, specificity, and the diagnostic accuracy rate were 91.4%, 81.1%, and 86.3%, respectively, for medial meniscal tears; 76.0%, 93.3%, and 88.8%, respectively, for lateral meniscal tears; and 86.5%, 95.2%, and 93.4%, respectively, for anterior cruciate ligament tears.[2)] In a meta-analysis by Phelan et al., MRI sensitivity and specificity were 89% (95% CI, 83% to 94%) and 88% (95% CI, 82% to 93%), respectively, for medial meniscal tears; 78% (95% CI, 66% to 87%) and 95% (95% CI, 91% to 97%), respectively, for lateral meniscal tears; and 87% (95% CI, 77% to 94%) and 93% (95% CI, 91% to 96%), respectively, for anterior cruciate ligament tears.[3)] Although MRI shows high diagnostic performance in meniscal and cruciate ligament injuries, its lowest sensitivity is for lateral meniscal tears. Consequently, when interpreting MRI, the lowest criterion for the presence of a tear in the lateral meniscus should be specified. The MRI systems used in the reports varied widely, from 0.1T to 1.5T. However, reports show that there are no differences in diagnostic performance depending on the magnetic field strengths of the systems.[4-6)]

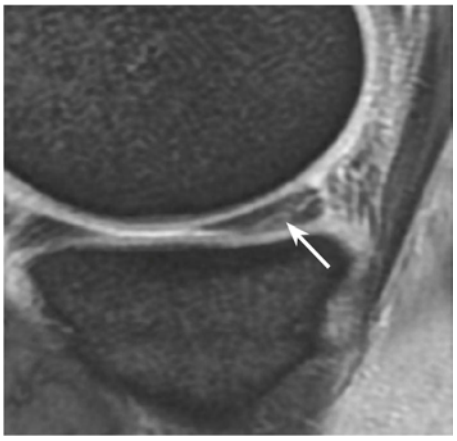

Figure 1. Horizontal tear of the medial meniscus

MRI, $T2^*$-weighted sagittal image: A linear hyperintensity is seen extending to the inferior surface of the posterior horn of the medial meniscus (→).

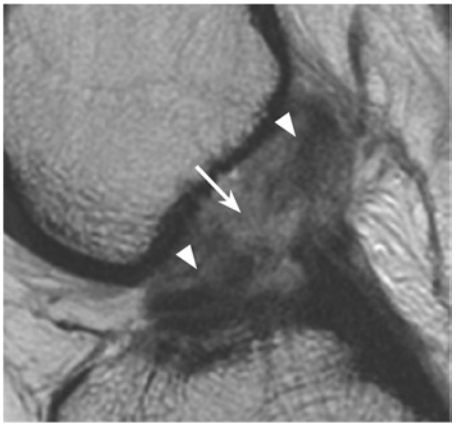

Figure 2. Complete tear of the anterior cruciate ligament

MRI, T2-weighted sagittal image: There is no continuity at the center of the anterior cruciate ligament (→), and swelling, hyperintensity, and deflection of the fragments are seen (▷).

Numerous cross-sectional studies have also examined the usefulness of manual testing in diagnosing meniscal and cruciate ligament injuries of the knee joint, using arthroscopy as the reference standard. Meta-analyses of these studies showed variability in the diagnostic performance of the various manual tests.[7, 8] However, in investigations regarding typical manual tests, a meta-analysis by Hegedus et al. of the McMurray test for meniscal injury showed sensitivity of 70.5% and specificity of 71.1%,[7] and a meta-analysis by Van Eck et al. of the Lachman test without anesthesia for diagnosing anterior cruciate ligament injury showed sensitivity and specificity of 81% each.[8] However, the shortcomings of arthroscopy include the fact that it is dependent on the skill of the operator; that some locations are difficult to observe, such as the margins and posterior segment of the meniscus; and that only the surface of intra-articular structures can be observed. It should therefore be kept in mind that arthroscopy is less than perfect as a reference standard.

Several cross-sectional studies have used arthroscopy as the reference standard in comparing the diagnostic performance of MRI with clinical findings obtained in examinations by orthopedists that included history-taking. However, the subjects in nearly all of these studies have been patients with suspected meniscal or ligament injuries based on clinical findings. Although there are reports indicating that the diagnostic performance of clinical findings is comparable to or higher than that of MRI,[9-13] there are also reports indicating that the diagnostic performance of MRI is higher than that of clinical findings,[14, 15] making it difficult to draw conclusions. However, after the orthopedist has examined the patient, the evaluation generally combines MRI with clinical findings rather than being based on MRI alone. Several cross-sectional studies examined whether diagnostic arthroscopy can be obviated by performing MRI in patients with suspected meniscal or ligament injuries based on clinical findings obtained in an examination

by an orthopedist. The results indicated that arthroscopy was reduced by 27.3% to 51.4% with the use of MRI.[16-18)]

MRI is useful for diagnosing meniscal and cruciate ligament injury and is recommended as a standard imaging examination for this purpose. However, it should preferably not be performed alone, but rather in combination with an examination by an orthopedist that includes history-taking.

Search keywords and secondary sources used as references

PubMed was searched for the period since 2012 using the following keywords: knee, meniscus injury, meniscus tear, ligament injury, ligament tear, MRI, and arthroscopy.

References

1) Oei EH et al: MR imaging of the menisci and cruciate ligaments: a systematic review. Radiology 226: 837-848, 2003
2) Crawford R, et al: Magnetic resonance imaging versus arthroscopy in the diagnosis of knee pathology, concentrating on meniscal lesions and ACL tears: a systematic review. Br Med Bull 84: 5-23, 2007
3) Phelan N et al: A systematic review and meta-analysis of the diagnostic accuracy of MRI for suspected ACL and meniscal tears of the knee. Knee Surg Sports Traumatol Arthrosc 24: 1525-1539, 2016
4) Vellet AD et al: Anterior cruciate ligament tear: prospective evaluation of diagnostic accuracy of middle- and high-fieldstrength MR imaging at 1.5T and 0.5T. Radiology 197: 826-830, 1995
5) Cotton A: MR imaging of the knee at 0.2T and 0.5T: correlation with surgery. AJR Am J Roentgenol 174: 1093-1097, 2000
6) Cheng Q, et al: Comparison of 1.5- and 3.0-T magnetic resonance imaging for evaluating lesions of the knee: a systematic review and meta-analysis (PRISMA-compliant article). Medicine 97: 38, 2018
7) Hegedus EJ et al: Physical examination tests for assessing a torn meniscus in the knee: a systematic review with meta-analysis. J Orthop Sports Phys Ther 37: 541-550, 2007
8) Van Eck CF et al: Methods to diagnose acute anterior cruciate ligament rupture: a meta-analysis of physical examinations with and without anaesthesia. Knee Surg Sports Traumatol Arthrosc 21: 1895-1903, 2013
9) Brooks S et al: Accuracy of clinical diagnosis in the knee arthroscopy. Ann R Coll Surg Engl 84: 265-268, 2002
10) Ryzewicz M et al: The diagnosis of meniscus tears: the role of MRI and clinical examination. Clin Orthop Relat Res 455: 123-133, 2007
11) Madhusudhan TR at al: Clinical examination, MRI and arthroscopy in meniscal and ligamentous knee Injuries: a prospective study. J Orthop Surg Res 3: 19, 2008
12) Rayan F et al: Clinical, MRI, and arthroscopic correlation in meniscal and anterior cruciate ligament injuries. Int Orthop 33: 129-132, 2009
13) Yan R et al: Predicted probability of meniscus tears: comparing history and physical examination with MRI. Swiss Med Wkly 141: w13314, 2011
14) Navali AM et al: Arthroscopic evaluation of the accuracy of clinical examination versus MRI in diagnosing meniscus tears and cruciate ligament ruptures. Arch Iran Med 16: 229-232, 2013
15) Munk B et al: Clinical magnetic resonance imaging and arthroscopic findings in knees: a comparative prospective study of meniscus anterior cruciate ligament and cartilage lesions. Arthroscopy 14: 171-175, 1998
16) Ruwe PA et al: Can MR imaging effectively replace diagnostic arthroscopy ? Radiology 183: 335-339, 1992
17) Bui-Mansfield LT et al: Potential cost saving of MR imaging obtained before arthroscopy of the knee. AJR Am J Roentgenol 168: 913-918, 1997
18) Vincken PW et al: Effectiveness of MR imaging in selection of patients for arthroscopy of the knee. Radiology 223: 739-746, 2002

BQ 83 Is MRI recommended for diagnosing bone tumors and tumor-like lesions?

Statement

The first imaging examination that should be performed is conventional radiography. MRI is useful for detecting lesions and evaluating pathological changes and local invasion. It is therefore recommended when a malignancy is suspected based on conventional radiography or when a treatment plan cannot be determined.

Background

Although conventional radiography is the first imaging examination performed to evaluate bone tumors and tumor-like lesions, the opportunities to use MRI are numerous. The usefulness of MRI for diagnosing bone tumors and tumor-like lesions and its indications were examined.

Explanation

Although various imaging examinations are used to diagnose bone tumors and tumor-like lesions, conventional radiography (Fig.) is the least expensive and most accessible test that can detect lesions and be used to analyze their histological characteristics, and it can be performed at any facility. Typical cases of benign lesions can often be diagnosed by conventional radiography alone; there is little need to add other imaging examinations in such cases, except when invasive treatment is considered.[1, 2)] However, evaluation of flat bones may be difficult with conventional radiography alone. Ma et al. compared the diagnostic performance of MRI (Fig.) alone and MRI combined with conventional radiography in distinguishing benign from malignant bone tumors and tumor-like lesions in 51 patients. They found that the sensitivity of both methods was very good for malignant lesions, with no difference in sensitivity between them.[3)] However, with MRI alone, there was a tendency to overestimate benign lesions as malignant lesions, whereas evaluation with the combination of conventional radiography and MRI improved specificity by 20% and diagnostic accuracy by 18%.

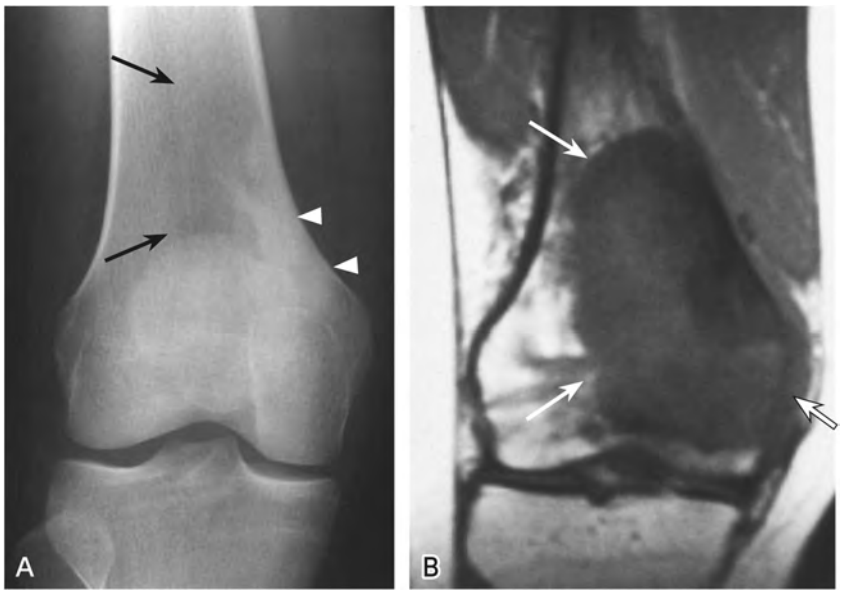

Figure Osteosarcoma

A: Plain radiograph, anteroposterior projection: An osteolytic lesion with indistinct borders is seen in the distal metaphysis of the right femur (→). Cloud-like calcification is seen inside the lesion (▷).

B: MRI, T1-weighted coronal image: An eccentric hypointense lesion is seen extending from the metaphysis to the epiphysis (⇨). The extent of the lesion's progression is clearer than in the plain radiograph.

Some studies have compared the performance of MRI and other diagnostic imaging modalities in determining the extent of bone tumors and tumor-like lesions. Hogeboom et al. compared CT and MRI in evaluating infiltration in 25 patients with bone tumors and tumor-like lesions. They reported that MRI was superior to CT in 25% of patients with bone marrow infiltration, 31% of patients with bone and soft tissue infiltration, and 36.4% of patients with joint infiltration.[4)] In evaluating cortical bone destruction, however, CT was found to be useful and superior to MRI in 13.6% of the same group of patients. Zimmer et al. evaluated infiltration in 52 patients with bone tumors and tumor-like lesions and reported that MRI was superior to CT in 33% of patients with bone marrow infiltration and 38% of those with soft tissue invasion.[5)] Bloem et al. compared MRI with CT and angiography in local staging of 56 patients with malignant bone tumors. They reported diagnostic sensitivity of 100% for MRI, 33% for CT, and 83% for angiography and specificity of 98% for MRI, 93% for CT, and 71% for angiography.[6)] The investigators concluded that MRI was comparable to angiography for evaluating neurovascular infiltration and that MRI should be selected for the local staging of malignant bone tumors. Frank et al. compared the lesion detection performance of MRI and bone scintigraphy in 106 patients with clinically suspected malignant bone tumors and found the detection sensitivity of MRI to be significantly higher than that of bone scintigraphy.[7)]

With regard to internal characterization, MRI, with its high contrast resolution, has been reported to be useful in a variety of diseases.[8-12)] MRI can be used to infer the pathologies, such as fat, blood/hemosiderin, cartilage matrix, mucoid matrix, collagen fibers, and cysts, and it is useful for the qualitative diagnosis of

lesions. Mori et al. compared the diagnostic performance of MRI combined with conventional radiography and contrast-enhanced CT alone in 32 patients with bone tumors and tumor-like lesions. They reported that, although CT was superior for evaluating cortical bone destruction and calcification in lesions, the combination of MRI and conventional radiography was superior for analyzing the histological characteristics of lesions in 56% of the patients.[13)]

In the diagnosis of bone tumors and tumor-like lesions, MRI is useful for detecting lesions and evaluating pathological changes, and it is particularly good for evaluating local infiltration. However, CT is useful for evaluating cortical bone and calcification in lesions. For screening, conventional radiography is suitable, and MRI is recommended when a malignant tumor is suspected based on conventional radiography or when a treatment plan cannot be determined. When evaluating MRI, conventional radiography should be used as a reference.

Search keywords and secondary sources used as references

PubMed was searched using the following keywords: bone tumor and MRI.

In addition, the following were referenced as secondary sources.

1) Bestic JM et al: ACR Appropriateness Criteria®: primary bone tumors J Am Coll Radiol 17: S226-S238, 2020
2) Committee on Bone and Soft Tissue Tumors, Japanese Orthopaedic Association, Ed.: General Rules for Clinical and Pathological Studies on Malignant Bone Tumors, 4th Edition. KANEHARA & Co., 2015.

References

1) Sundaram M et al: Computed tomography or magnetic resonance for evaluating the solitary tumor or tumor-like lesion of bone? Skeletal Radiol 17: 393-401, 1988
2) Griffiths HJ et al: The use of MRI in the diagnosis of benign and malignant bone and soft tissue tumours. Australas Radiol 37: 35-39, 1993
3) Ma LD et al: Differentiation of benign and malignant musculoskeletal tumors: potential pitfalls with MR imaging. Radiographics 15: 349-366, 1995
4) Hogeboom WR et al: MRI or CT in the preoperative diagnosis of bone tumours. Eur J Surg Oncol 18: 67-72, 1992
5) Zimmer WD et al: Bone tumors: magnetic resonance imaging versus computed tomography. Radiology 155: 709-718, 1985
6) Bloem JL et al: Radiologic staging of primary bone sarcoma: MR imaging, scintigraphy, angiography, and CT correlated with pathologic examination. Radiology 169: 805-810, 1988
7) Frank JA et al: Detection of malignant bone tumors: MR imaging vs scintigraphy. AJR Am J Roentgenol 155: 1043-1048, 1990
8) Aoki J et al: MR findings indicative of hemosiderin in giant-cell tumor of bone: frequency, cause, and diagnostic significance. AJR Am J Roentgenol 166: 145-148, 1996
9) Cohen EK et al: Hyaline cartilage-origin bone and soft-tissue neoplasms: MR appearance and histologic correlation. Radiology 167: 477-481, 1988
10) Frick MA et al: Imaging findings in desmoplastic fibroma of bone: distinctive T2 characteristics. AJR Am J Roentgenol 184: 1762-1768, 2005
11) Murphey MD et al: Telangiectatic osteosarcoma: radiologicpathologic comparison. Radiology 229: 545-553, 2003
12) Campbell RS et al: Intraosseous lipoma: report of 35 new cases and a review of the literature. Skeletal Radiol 32: 209-222, 2003
13) Mori T et al: Three-dimensional images of contrast-enhanced MDCT for preoperative assessment of musculoskeletal masses: comparison with MRI and plain radiographs. Radiation Med 23: 398-406, 2005

CQ 22 Is contrast-enhanced MRI recommended for diagnosing soft tissue neoplasms and tumor-like lesions?

Recommendation

Although there is not a strong need for routine contrast-enhanced MRI, dynamic contrast-enhanced MRI is in some cases useful for distinguishing benign from malignant lesions, and contrast-enhanced MRI is therefore weakly recommended.

Recommendation strength: 2, strength of evidence: weak (C), agreement rate: 89% (8/9)

Background

MRI is a diagnostic imaging modality that plays the central role in diagnosing soft tissue neoplasms and tumor-like lesions. The Japan Radiological Society's Diagnostic Imaging Guidelines 2016 indicate that non-contrast MRI is useful for distinguishing benign from malignant lesions and for the qualitative diagnosis of benign masses, and they recommend that it be used in combination with clinical findings and conventional radiography. Contrast-enhanced MRI, on the other hand, has been said not to be useful for characterization because many solid tumors undergo enhancement over time. Consequently, opinions differ regarding the uniform use of contrast-enhanced MRI.[1, 2)]

This CQ discusses the usefulness of contrast-enhanced MRI for the qualitative diagnosis of soft tissue neoplasms and tumor-like lesions, the differentiation of benign and malignant lesions, and the histological diagnosis of the malignancy of soft tissue sarcomas.

Explanation

Contrast-enhanced MRI is used to differentiate between cysts and solid tumors for cyst-like soft tissue neoplasms and tumor-like lesions that show hyperintensity in T2-weighted images. Because diagnosing cysts is difficult, contrast-enhanced MRI is particularly useful when a lesion occurs at a site other than in the periphery of a joint, where cysts occur preferentially, and when a lesion shows non-uniform hyperintensity in T2-weighted images.[2, 3)] If a thick septum or nodule with contrast enhancement is seen in a lipoma, an atypical lipomatous tumor or well-differentiated liposarcoma is suspected.[4)] Dynamic contrast-enhanced MRI, which involves rapidly injecting contrast medium intravenously and repeatedly imaging in the same plane, is useful for internal characterization of components such as highly vascular components, which undergo enhancement early, and fibrous components, which undergo gradual enhancement, and thereby contributes to qualitative diagnosis.[5)]

With regard to the differentiation of benign and malignant lesions, van Rijswijk et al. conducted an investigation in 140 patients with soft tissue neoplasms or tumor-like lesions (benign in 67 patients, malignant in 73 patients) and reported sensitivity and specificity of 69% and 73%, respectively, with non-contrast MRI alone and 74% and 78%, respectively, with the addition of contrast-enhanced MRI.[6)]

With the further addition of dynamic contrast-enhanced MRI, sensitivity and specificity were 82% and 78%, respectively, the best results obtained. On the other hand, in an investigation in 39 patients with soft tissue neoplasms or tumor-like lesions (benign in 27 patients, malignant in 12 patients) by Grande et al., the addition of contrast-enhanced MRI to non-contrast MRI did not improve the diagnostic accuracy rate (decreased from 66% to 59%), but the addition of dynamic contrast-enhanced MRI improved it to 76%.[7] As the above findings indicate, there is still no established view regarding improvement in the ability to distinguish benign from malignant lesions with the addition of contrast-enhanced MRI to non-contrast MRI. However, sensitivity and specificity ranging from 64% to 96% and from 58% to 80%, respectively, were reported when tumors that underwent early-phase enhancement in dynamic contrast-enhanced MRI were considered malignant, indicating that dynamic contrast-enhanced MRI is to some extent useful for differentiating between benign and malignant lesions (Fig.).[5-9] Although variability was seen in the results, this was likely attributable to the sample sizes and the types of patients included in the studies. In addition, differences in the definition of early enhancement, the strength of the MRI magnetic field, and the MRI imaging parameters used should be considered. Because abnormal angiogenesis is often seen histopathologically in malignancies, the possibility of malignancy must be kept in mind for masses that undergo early enhancement in dynamic contrast-enhanced MRI. However, early enhancement in dynamic contrast-enhanced MRI is also seen in benign tumors and tumor-like lesions that undergo early enhancement, such as hemangiomas, glomus tumors, and acute myositis ossificans. It is therefore important to first exclude early-enhancing benign lesions by conventional radiography or non-contrast MRI, in addition to clinical information, and then focus on early enhancement in dynamic contrast-enhanced MRI.

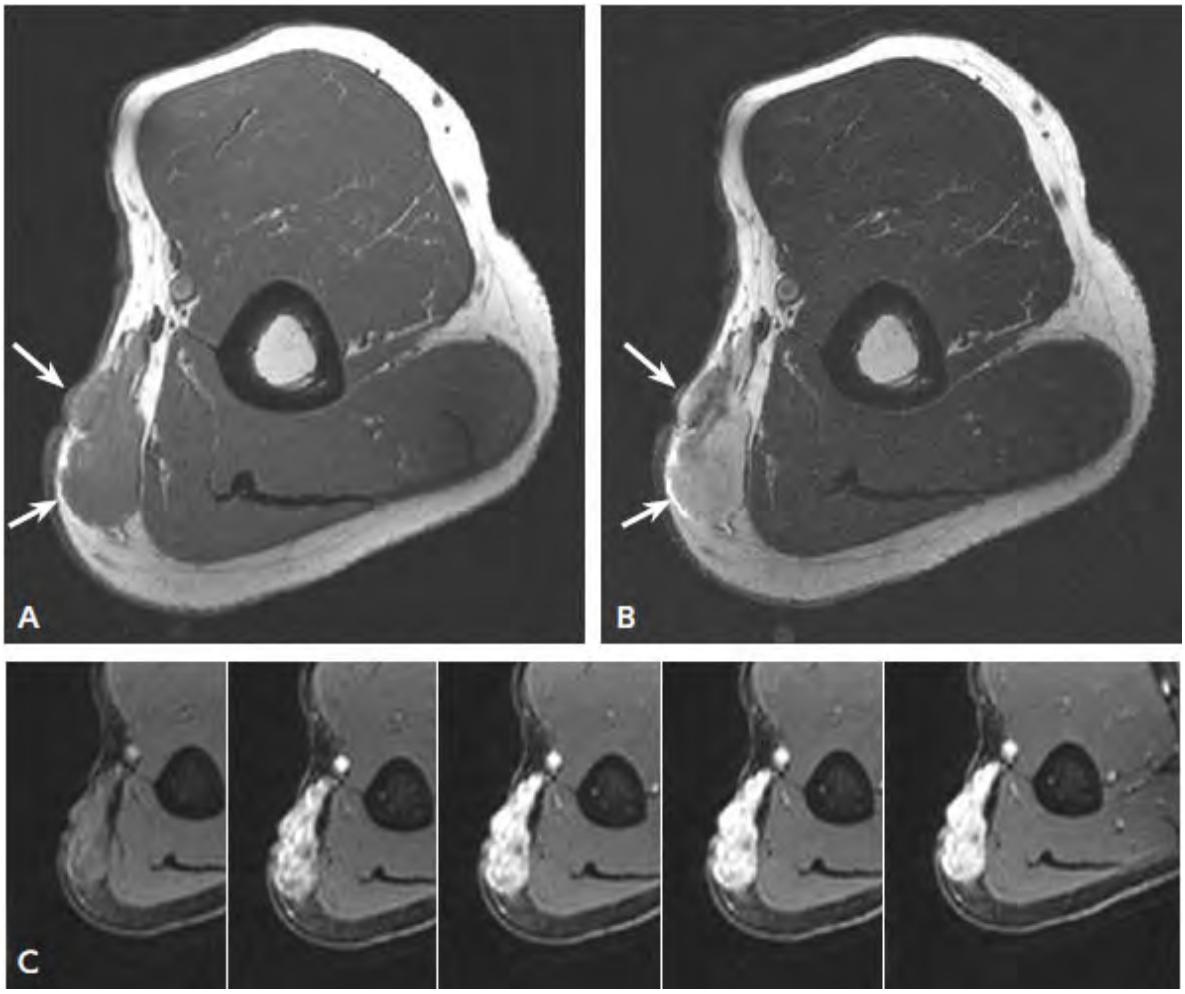

Figure Myxofibrosarcoma

A: MRI, T1-weighted image; B: MRI, T2-weighted image; C: Dynamic contrast-enhanced MRI
A subcutaneous mass with irregular margins is seen in the left brachial region (→). It is seen as isointensity compared with muscle on the T1-weighted image and as hyperintensity on the T2-weighted image. In dynamic contrast-enhanced MRI, the mass shows rapid initial enhancement, followed by sustained late enhancement.

With regard to the histological diagnosis of the malignancy of soft tissue sarcomas, Zhao et al. examined the MRI findings of 95 patients with soft tissue sarcomas and found that, when tumors that showed peritumoral enhancement were considered, the high-grade group (grades 2 and 3), sensitivity and specificity were 91% and 57%, respectively.[10] A multivariate analysis of 130 patients with soft tissue sarcoma by Crombé et al. showed that peritumoral enhancement, intratumoral necrosis, and heterogeneity of ≥ 50% in T2-weighted images were findings suggestive of high malignancy (grade 3). They reported that combining any 2 of these findings resulted in sensitivity and specificity of 75% and 64.2%, respectively.[11] In investigations in which the signals from tissues were imaged at high temporal resolution after contrast medium administration, and perfusion MRI was used to quantitatively analyze perfusion (hemodynamics at the capillary level), the transfer rate constant for leakage of the contrast medium into the extracellular space

(K^{trans}) was significantly higher in the high-grade group (grades 2 and 3) than in the low-grade group (grade 1).[12, 13)]

These findings indicate that contrast-enhanced MRI is useful for differentiating between cystic and solid tumors. Early enhancement in dynamic contrast-enhanced MRI is in some cases useful for differentiating benign from malignant tumors. Peritumoral enhancement may be useful in the histological diagnosis of the malignancy of soft tissue sarcomas. Contrast-enhanced MRI is weakly recommended for diagnosing soft tissue neoplasms and tumor-like lesions.

Search keywords and secondary sources used as references

PubMed and the Cochrane Library database were searched for the period from 2016 to 2019 using the following keywords, and selections were made from among 212 articles: soft tissue tumor, soft tissue tumor-like lesion, conventional MRI, contrast-enhanced MRI, dynamic contrast-enhanced MRI, sensitivity, and specificity. In the secondary screening, 10 articles were extracted, and 6 articles were added with a hand search.

In addition, the following was referenced as a secondary source.

1) Japan Radiological Society, Ed.: Diagnostic Imaging Guidelines 2016. KANEHARA & Co., 2016.

References

1) May DA et al: MR imaging of musculoskeletal tumors and tumor mimickers with intravenous gadolinium: experience with 242 patients. Skeletal Radiol 26: 2-15, 1997
2) Kransdorf MJ et al: The use of gadolinium in the MR evaluation of soft tissue tumors. Semin Ultrasound CT MR 18: 251-268, 1997
3) Ma LD et al: Differentiation of benign from malignant musculoskeletal lesions using MR imaging: pitfalls in MR evaluation of lesions with a cystic appearance. AJR Am J Roentgenol 170: 1251-1258, 1998
4) Panzarella MJ et al: Predictive value of gadolinium enhancement in differentiating ALT/WD liposarcomas from benign fatty tumors. Skeletal Radiol 34: 272-278, 2005
5) van der Woude HJ et al: Musculoskeletal tumors: does fast dynamic contrast-enhanced subtraction MR imaging contribute to the characterization? Radiology 208: 821-828, 1998
6) van Rijswijk CS et al: Soft-tissue tumors: value of static and dynamic gadopentetate dimeglumine-enhanced MR imaging in prediction of malignancy. Radiology 233: 493-502, 2004
7) Del Grande F et al: Characterization of indeterminate soft tissue masses referred for biopsy: What is the added value of contrast imaging at 3.0 tesla? J Magn Reson Imaging 45: 390-400, 2017
8) Tuncbilek N et al: Dynamic contrast enhanced MRI in the differential diagnosis of soft tissue tumors. Eur J Radiol 53: 500-505, 2005
9) Barile A et al: Musculoskeletal tumours: preliminary experience with perfusion MRI. Radiol Med 112: 550-561, 2007
10) Zhao F et al: Can MR imaging be used to predict tumor grade in soft-tissue sarcoma? Radiology 272: 192-201, 2014
11) Crombé A et al: Soft-tissue sarcomas: assessment of MRI features correlating with histologic grade and patient outcome. Radiology 291: 710-721, 2019
12) Li X et al: Soft tissue sarcoma: can dynamic contrast-enhanced (DCE) MRI be used to predict the histological grade? Skeletal Radiol 49: 1829-1838, 2020
13) Gondim Teixeira PA et al: Perfusion MR imaging at 3-tesla: can it predict tumor grade and histologic necrosis rate of musculoskeletal sarcoma? Diagn Interv Imaging 99: 473-481, 2018

10
Pediatric

Standard Pediatric Imaging Methods

Overview

1. Introduction

Thoughtless imaging examinations should not be made in the evaluation of children, who have long lives ahead and represent the future. Thoughtless and inappropriate examinations occur as a result of improper justification and optimization. The basic approaches and procedures for the diagnostic imaging of children are discussed in the overview at the beginning of these guidelines (p. 32 to 35), and the reader is encouraged to refer to them. Although they are essentially the same as for adults, justification and optimization must be implemented with particular rigor for children.

Because pediatric diagnostic imaging covers all of the organs, further detailed discussion of each examination modality by patient age and disease type would far exceed the scope of the preface to the pediatrics section. Consequently, this section discusses basic approaches in general terms.

2. Justification of imaging examinations: best examination first!

Justification starts with an examination of whether an examination is truly necessary. A requirement is that the risk associated with factors such as the invasiveness of an examination be less than the benefit it contributes to diagnosis and treatment. Even if an examination is found to meet this requirement, it is essential that the examination most suitable for the purpose of examination be performed first. Another important consideration in justification is examining whether a procedure that does not involve radiation exposure, such as ultrasonography or MRI, can provide diagnostic performance comparable to that of one that does involve radiation exposure, such as CT, and be used instead of the latter. This is the process involved in the justification of pediatric diagnostic imaging. It is synonymous with performing the best examination first.

Detailed discussion

1. Optimization of pediatric CT: not more nor less

The optimization of pediatric radiography is based on the as-low-as-reasonably-achievable (ALARA)[1)] principle. The most important type of optimization in pediatric diagnostic imaging is the optimization of CT, which can be performed often and in a short time, but is associated with radiation exposure. The point that should be emphasized most is that pediatric CT is fundamentally single-phase imaging. One should not be bound to the bygone rule that non-contrast CT combined with contrast-enhanced CT is the standard. Modern CT systems, which represent marked advances in technology, enable lung fields, bone, and calcification all to be evaluated by contrast-enhanced CT alone. Non-contrast CT is of course sufficient for evaluating the lung fields, airways, and bony structures, including the middle and inner ear. If a truncal

tumor or inflammatory disease is suspected, the use of single-phase contrast-enhanced CT is the overriding rule. Non-contrast CT alone is the rule for emergency cranial CT for conditions such as status epilepticus and consciousness disturbance. MRI is indicated if there are no findings on CT and neurological symptoms persist. However, if MRI cannot be performed, non-contrast CT is repeated. Only in special cases (e.g., there is reason to suspect a condition such as vascular malformation) is contrast-enhanced CT performed without non-contrast CT. The indications for multiphase contrast-enhanced imaging are very limited to cases where information on the arteries is needed, such as before surgery and with severe trauma.

With regard to CT imaging conditions, the lowest dose that can provide the necessary information is generally used. Moreover, multiple protocols specific to children, separate from the protocols used for adults, must be prepared depending on the performance of the system used, the body size of the patient, and the purpose of the examination. Of course, losing diagnostic information by using a radiation dose so low that the required information cannot be obtained would defeat the purpose of the examination. Consequently, a dose that is not too high or too low should be selected by applying specialized knowledge and collaborating with radiological technologists.

Preparing pediatric CT protocols that are varied and appropriate for the body sizes and circumstances of the patients and generally involve single-phase imaging is the essence of pediatric CT optimization, and the principle of "not more nor less" should be applied. Diagnostic reference levels, which serve as standards for reviewing doses used at your facility, are provided in the Overview section at the beginning of these guidelines (p. 33).

2. Optimization of Pediatric MRI

MRI involves no radiation exposure, provides excellent density resolution, and involves little need for contrast medium administration. It should therefore be the procedure that is most used for children. Because the examination time is long, however, it requires appropriate restraint or sedation for children who cannot remain motionless. With regard to sedation measures, a system that can respond to emergencies is essential. Such a system should be established based on the MRI sedation recommendations issued by the relevant academic societies (first edition published in May 2013, revised editions published in February and April 2020).[2)]

Many children are physically small, and their respiratory and heart rates are higher than those of adults. Moreover, many very difficult situations are often encountered in MRI that cannot be addressed with an adult protocol, such as the usually difficult breath-hold examination. To overcome these difficulties, k-space sampling techniques, such as radial sampling, which suppresses artifacts caused by movements of the rib cage, diaphragm, and heartbeat, respiratory gating using techniques such as navigator echo, and body motion correction methods using techniques such as PROPELLER/BLADE need to be tailored to the various sequences and imaging angles and optimized for the system used. In addition, diffusion-weighted imaging and the ADC values it yields often provide useful information on body and pathological tissues,

and pathophysiology, whether in the central nervous system, trunk, or bone and soft tissue. Its routine use is therefore recommended.

Physiological signal changes in the brain (myelinization) and bone marrow (change from red to yellow marrow) occur from the neonatal period through childhood, necessitating measures to tailor sequences to those changes. Because the volume of fluid in the brain is large in premature infants and neonates, it is difficult to establish contrast with the cerebrospinal fluid. It is therefore necessary to specify a longer effective TE (≥ 120 at a minimum) than for adults and older children when performing FSE T2-weighted imaging, particularly with 1.5T systems. When evaluating the brains of premature infants, diagnosis should be undertaken based on the corrected age in weeks or months (the chronological age added to the gestational age at birth).[3)]

A gadolinium contrast medium should be used after thoroughly examining whether its use will provide additional information. With MRI of the central nervous system (CNS), sites of failure of the blood-brain barrier undergo contrast enhancement just as with iodinated contrast agent-enhanced CT. However, for non-CNS examinations, MRI, which fundamentally provides excellent tissue contrast, lacks the significant anatomical contrast seen with CT contrast agents. Consequently, the additional information obtained with contrast medium administration is limited. Therefore, examinations for tumors or inflammation in the CNS, trunk, bone, or soft tissue for a purpose such as evaluating posttreatment efficacy should not be automatically performed using a contrast medium without proper justification. Rather, its indication should be rigorously determined by considering the effects of tissue accumulation of free gadolinium, particularly in children. It has been reported that, when the findings of a plain examination were normal, the use of a gadolinium contrast medium in the brain detected imaging abnormalities in just 0.3% of cases, indicating that it did not provide additional clinical information.[4)]

3. Optimization of pediatric ultrasonography

Ultrasonography is even more useful for diagnosis in children, who are physically small and have very little subcutaneous and visceral fat, than it is in adults. The small size of children enables deep areas to be observed even with the use of a high-frequency probe. The resulting spatial resolution provides images overwhelmingly superior to those obtained by modalities such as CT. Special measures or training are needed to perform ultrasonography in children who are uncooperative. However, because ultrasonography does not involve radiation exposure and is not invasive, there is no reason not to try it.

Moreover, sites where ultrasonography is used in children but cannot be considered in adults include the mediastinal organs such as the thymus (probe placed in the intercostal area near the sternum or over the sternum) and, from the neonatal period to infancy, the intracranial region and spine using the fontanel and cranial sutures as acoustic windows (observed from between vertebrae in the case of direct scanning from the dorsum or if ossification has advanced). These are useful for screening for changes such as dimples.

4. Optimization for pediatric nuclear medicine

Nuclear medicine is a useful modality for obtaining information that cannot be obtained with other imaging procedures. Because it involves radiation exposure, however, the question of whether it is indicated needs to be carefully examined. For example, it is not an exaggeration to say that an examination such as gallium-67 (^{67}Ga) scintigraphy is a thing of the past and far from the first choice of examination methods for a fever of unknown origin. Optimization is performed according to the ALARA principle.[1)] It is recommended that pediatric nuclear medicine examinations be performed, and dose and indication determined based on the consensus guidelines for the proper implementation of pediatric nuclear medicine examinations and by referring to the nuclear medicine section of these guidelines.[5)]

Summary: The role of the diagnostic radiologist

In addition to the high carcinogenic risk of radiation exposure in children, the effects of agents such as contrast media (e.g., adverse reactions to cumulative effects and their consequences) need to be considered in the context of the long remaining life expectancy of children, which can be 60 to 80 years or longer. Pediatric imaging procedures therefore should be carefully selected based on the judgement of specialists and performed using the most appropriate method in a way that is minimally invasive and avoids the loss of important diagnostic information. This is where diagnostic radiologists can best show their capabilities as a specialist, and also an area where their active involvement that uses their specialized knowledge makes a direct contribution to children, with whom the future rests.

Secondary source materials used as references

1) Multidisciplinary conference organized by the Society of Pediatric Radiology: The ALARA (as low as reasonably achievable) concept in pediatric CT intelligent dose reduction. Pediatr Radiol 32: 217-313, 2001
2) Japan Pediatric Society, Japanese Society of Pediatric Anesthesiology, Japanese Society of Pediatric Radiology: Joint Recommendations on Sedation During MRI. Journal of the Japan Pediatric Society 124(4): 771-805, 2020
3) Aida N: A Key to Brain MRI Interpretation (3rd Edition): Important Points and Normal Images. Gakken Medical Shujunsha. pp.316-323, 2012
4) Dunger D et al: Do we need gadolinium-based contrast medium for brain magnetic resonance imaging in children? Pediatr Radiol 48: 858-846, 2018
5) Study Panel on the Proper Implementation of Pediatric Nuclear Medicine Tests, Japanese Society of Nuclear Medicine: Consensus Guidelines for the Proper Implementation of Pediatric Nuclear Medicine Tests. Japanese Society of Nuclear Medicine, 2013

BQ 84 In which cases is CT recommended for minor head trauma in children?

Statement

With minor head trauma in children, the risk of intracranial injury is evaluated using criteria such as the PECARN criteria for cranial CT indications, the CHALICE rule, and the CATCH rule. If the risk is low, CT should not be performed.

Background

Pediatric trauma, typified by head contusion, is a condition often seen in emergency outpatient care. In nearly all cases, it is mild and can be addressed by watchful waiting alone. Abnormal CT findings are rare, and cases that result in surgery are even rarer. Decisions must be made regarding whether CT is needed for a mild head injury and whether it is indicated in view of the risk associated with radiation exposure.

Explanation

An increasing number of studies have examined how to predict the risk of intracranial injury in minor head trauma in children and narrow the indications for CT. However, the findings have varied, and there is no standard view on the types of cases in which CT should be performed.[1-8)] The following 3 sets of criteria are supported by high-level evidence.[9, 10)]

The cranial CT indication criteria of the Pediatric Emergency Care Applied Research Network (PECARN) (Table 1) are used to assess whether CT is recommended based on considerations such as the Glasgow Coma Scale (GCS) score and consciousness status, with patients stratified as aged < 2 years or 2 to 18 years.[11, 12)] Severely impaired patients with a GCS score ≤ 13 are not considered suitable for CT.

The children’s head injury algorithm for the prediction of important clinical events (CHALICE rule) (Table 2) is used for patients with head trauma who are aged 2 to 16 years. Based on the diagnostic imaging guidelines of the United States and the clinical guidelines of the United Kingdom, the rule is widely used clinically.

The Canadian assessment of tomography for childhood head injury (CATCH rule) is used for children aged 0 to 16 years with a GCS score of 13 to 15 within 24 hours after injury and abnormal clinical symptoms (the CATCH2 rule, which has additional items, was released in 2018).[13)] It was found to be highly sensitive in a large, multicenter cohort study (Table 3).

In the clinical setting, whether CT is indicated should be assessed by selecting from among those rules based on the circumstances. However, the judgement of the patient's primary care physician, wishes of the patient's family, and circumstances at the relevant facility also need to be given adequate consideration.

In 2019, the Recommendations and Guidelines for CT Imaging Criteria in Pediatric Head Injury were released by the Japanese Society of Child Neurology, Japanese Society for Pediatric Neurosurgery,

Japanese Society of Emergency Pediatrics, and Japanese Society of Pediatric Radiology. They cover topics such as the previously mentioned rules, figures, and tables, and the points to keep in mind when using them, along with measures to reduce radiation exposure during CT imaging. In addition, it provides examples of written explanations for families who are sent home after it is determined that CT is unnecessary based on the criteria. It is therefore a document that should be used for reference.

Table 1. PECARN cranial CT indication criteria

(Indications for CT tests in GCS 14 - 15 head injury)

< 2 years old
・GCS = 14, altered consciousness, or palpable skull fracture
・Subcutaneous hematoma other than of the forehead, loss of consciousness for ≥ 5 seconds, dangerous mechanism of injury, or parents consider appearance to be different from usual
≥ 2 years old
・GCS = 14, altered consciousness, or basal skull fracture finding
・Loss of consciousness, vomiting, dangerous mechanism of injury, or intense headache

CT not recommended if above are not applicable

Table 2. CHALICE rule

・Loss of consciousness for ≥ 5 minutes
・Amnesia for ≥ 5 minutes
・Somnolence
・Vomiting ≥ 3 times
・Abuse suspected
・Convulsion in a patient with no past history of epilepsy
・GCS < 14. GCS < 15 if < 1 year old
・Compound fracture, suspected depressed fracture, or bulging anterior fontanel
・Basal skull fracture finding (otorrhagia, raccoon eyes, cerebrospinal fluid leak, Battle sign)
・Neurological abnormality
・Subcutaneous hematoma or bruise ≥ 5 cm in child < 1 year old
・Dangerous mechanism of injury, e.g., high-speed trauma [traffic accident occurring at or greater than a certain speed (64 km/hour), fall from a height of ≥ 3 m, collision with an object moving at high speed]

Detailed examination by CT required if any of the above are applicable

Table 3. CATCH and CATCH2 rules (CT test indications for mild head injury and consciousness level GCS 13 - 15 on examination)

(1) GCS score < 15 points at 2 hours post-trauma
(2) Compound or depressed fracture suspected
(3) Worsening headache
(4) Agitated state on examination
(5) Basal skull fracture suspected
(6) Large hematoma in scalp
(7) High-energy trauma
[(8) Vomiting ≥ 4 times]

Cranial CT recommended if any of the 7 items is present [8 items, including (8), for CATCH2 rule]

Search keywords and secondary sources used as references

PubMed was searched using the following keywords: children, minor head injury, trauma, and CT.

In addition, the following were referenced as secondary sources.

1) Medina L et al (eds.): Evidence-based imaging in pediatrics. Springer, 2010
2) Kuppermann N et al: Identification of children at very low risk of clinically-important brain injuries after head trauma: a prospective cohort study. Lancet 374: 1160-1170, 2009
3) Dunning J et al: Derivation of the children's head injury algorithm for the prediction of important clinical events decision rule for head injury in children. Arch Dis Child 91: 885-891, 2006
4) Osmond MH et al: CATCH: a clinical decision rule for the use of computed tomography in children with minor head injury. CMAJ 182: 341-348, 2010
5) Japanese Society of Child Neurology, et. al, Ed.: Recommendations and Guidelines for CT Imaging Criteria in Pediatric Head Injury. Japanese Society of Child Neurology, 2019

References

1) Greenes DS, Schutzman SA: Clinical indicators of intracranial injury in head-injured infants. Pediatrics 104: 861-867, 1999
2) Palchak MJ et al: A decision rule for identifying children at low risk for brain injuries after blunt head trauma. Ann Emerg Med 42: 492-506, 2003
3) Haydel MJ, Shembekar AD: Prediction of intracranial injury in children aged five years and older with loss of consciousness after minor head injury due to nontrivial mechanisms. Ann Emerg Med 42: 507-514, 2003
4) Oman JA et al: Performance of a decision rule to predict need for computed tomography among children with blunt head trauma. Pediatrics 117: e238-246, 2006
5) Boran BO et al: Evaluation of mild head injury in a pediatric population. Pediatr Neurosurg 42: 203-207, 2006
6) Atabaki SM et al: A clinical decision rule for cranial computed tomography in minor pediatric head trauma. Arch Pediatr Adolesc Med 162: 439-445, 2008
7) Dunning J et al: A meta-analysis of variables that predict significant intracranial injury in minor head trauma. Arch Dis Child 89: 653-659, 2004
8) Maguire JL et al: Should a head-injured child receive a head CT scan?: a systematic review of clinical prediction rules. Pediatrics 124: e145-154, 2009
9) Babl FE et al: Accuracy of PECARN, CATCH, and CHALICE head injury decision rules in children: a prospective cohort study. Lancet 389: 2393-2402, 2017
10) Mastrangelo M, Midulla F: Minor head trauma in the pediatric emergency department: decision making nodes. Curr Pediatr Rev 13: 92-99, 2017
11) Pickering A et al: Clinical decision rules for children with minor head injury: a systematic review. Arch Dis Child 96: 414-421, 011
12) Mihindu E et al: Computed tomography of the head in children with mild traumatic brain injury. Am Surg 80: 841-843, 2014
13) Osmond MH et al: Validation and refinement of a clinical decision rule for the use of computed tomography in children with minor head injury in the emergency department. CMAJ 190: 816-822, 2018

BQ 85 Is neuroimaging recommended for a suspected febrile seizure?

Statement

Because it does not involve radiation exposure and provides even higher detection performance than CT, MRI is recommended as an imaging examination in complex febrile seizures, frequent seizures, and seizures associated with neurological deficits. However, in patients who require sedation, the risk associated with sedation is taken into account in deciding whether to perform MRI.

If simple febrile seizure is definitively diagnosed clinically, there is little need for diagnostic imaging (CT/MRI). However, a congenital metabolic abnormality or autoimmune disease may be involved in the background as an underlying disease. Consequently, cranial MRI can be considered for detailed examination if complex febrile seizure is still a possibility, or there are frequent seizures or seizures associated with neurologic deficit symptoms. Cranial CT is a meaningful test to perform before lumbar puncture and can be considered for this purpose.

Background

According to the guidelines for the management of febrile seizures and the febrile seizure clinical practice guidelines of the Japanese Society of Child Neurology, febrile seizure is a seizure disorder (includes convulsive and nonconvulsive seizures) typically associated with fever of ≥ 38 °C that occurs mainly in infants at 6 to 60 months postpartum. It refers to seizures that occur in the absence of central nervous system infections such as meningitis, metabolic disease, or other obvious causes of seizures. It excludes seizures in individuals with a history of epilepsy.

More than 90% of children with a history of febrile seizure do not subsequently develop epilepsy. It is basically considered a transient, benign condition. However, it is important to differentiate it from conditions such as encephalopathy and encephalitis, which require immediate and aggressive treatment, and organic abnormalities must also be excluded if seizures occur repeatedly. Whether diagnostic imaging should be performed if febrile seizure is suspected and the important conditions from which it should be differentiated were examined.

Explanation

Febrile seizure is the most frequently encountered convulsive disease of childhood. Its prevalence in Japan has been reported to be 7% to 8%, slightly higher than in Europe and the United States (2% to 5%). The convulsive seizures associated with febrile seizure are typically generalized seizures, such as generalized tonic-clonic seizures. Febrile seizures that are generalized seizures lasting less than 15 minutes that do not occur repeatedly within 24 hours are termed simple febrile seizures. Those with at least 1 of the following 3 characteristics are termed complex febrile seizures: ① has elements of focal seizures (partial

seizures); ② seizure lasts longer than 15 minutes; and ③ usually occurs multiple times within 24 hours during a single febrile episode.

The rate of recurrence of febrile seizures is approximately 30%. Risk factors are ① either parent has a past history of febrile seizure, ② onset at < 1 year of age, ③ brief intervals between febrile episodes (≤ roughly 1 hour), and ④ temperature ≤ 39 °C during seizures. Although the incidence of subsequent epilepsy is low, risk factors for subsequently developing epilepsy include ① the presence of a neurological abnormality before the onset of febrile seizures, ② a family history of epilepsy in a parent or sibling, ③ complex febrile seizure, and ④ brief intervals between febrile episodes (≤ roughly 1 hour). Complex febrile seizures are a risk factor for epilepsy.

No reports based on strong evidence were found that recommend diagnostic imaging (CT or MRI) for children with simple febrile seizures. The American Academy of Pediatrics recommends against CT or MRI for simple febrile seizures. However, abnormal imaging findings may be seen with complex febrile seizures.[1, 2)]

Conditions that must be differentiated from febrile seizure include: forms of encephalitis and meningitis, such as bacterial and viral encephalitis and meningitis and tuberculous meningitis; subdural empyema, extradural empyema/subdural abscess, extradural abscess; brain abscess; and acute encephalopathy. Clinical findings are often difficult to obtain because the patients are children, and diagnostic imaging therefore plays more than a minor role. Although their frequency is lower than that of febrile seizure, early diagnosis and treatment of these conditions are important because delays in their diagnosis and treatment result in a poorer overall prognosis and functional prognosis.

Although the above-mentioned guidelines indicate that lumbar puncture is not a procedure that should be performed routinely, they indicate that it should be performed aggressively if encephalitis or meningitis is suspected. Consequently, diagnostic imaging is also meaningful to a certain extent as a means of excluding an intracranial space-occupying lesion, which is a contraindication for lumbar puncture.

MRI is recommended as an imaging examination because it involves no radiation exposure and detects lesions more sensitively than even CT. However, the risk associated with sedation should be considered in patients that require it, and a system adequate to support MRI sedation should be implemented based on the joint recommendations. Acute-phase CT is useful as a convenient method of ruling out an intracranial space-occupying lesion and increased intracranial pressure.

Acute encephalopathy is a disease in which a convulsion or a sudden consciousness disturbance is seen in the acute phase of a viral infection associated with high fever.[3)] The pathogenic virus and clinicopathological classification do not correspond in a 1-to-1 fashion. That is, a specific viral infection can produce a variety of clinicopathological features and, conversely, a variety of viruses can present with the same clinicopathological features. Moreover, acute encephalopathy may occur in disorders other than infection, such as: congenital metabolic abnormalities; nonviral infections such as bacterial infections, cat-scratch disease, and Q fever; and autoimmune disorders.[3-7)] In incipient disease without consciousness disturbance, differentiating between acute encephalopathy with biphasic seizures and late reduced diffusion

(AESD) and febrile seizures is difficult. Identifying subcortical hyperintensity (bright tree appearance) in diffusion-weighted images on day 4 to 5 after onset facilitates diagnosis.[3] What are termed reversible lesions of the corpus callosum splenium appear in a variety of pathophysiologies, including after drug administration. Lesions in acute encephalopathy are known to be reversible if the lesion distribution is limited to white matter that extends to the corpus callosal splenium and Rolando's area. [8, 9]

In the chronic phase, hippocampal atrophy was found on MRI in 6 of 15 patients with complex febrile seizures, although the evidence level for this finding is not high.[10] The risk of developing epilepsy has been reported to be high in patients with complex febrile seizures. Diagnostic imaging is also therefore regarded as having a specific role in detailed examination in the chronic phase, such was when seizures occur repeatedly.[11]

Search keywords and secondary sources used as references

PubMed was searched using the following keywords: febrile seizure, CT, and MRI.

In addition, the following were referenced as secondary sources.

1) Fukuyama Y, et al.: Guidelines for the management of febrile seizures. Japanese Journal of Pediatrics 49:207-215, 1996
2) Seki T: Febrile seizures—Recent findings and new management guidelines. New Developments in Child Neurology 26:139-152, 1997
3) Japanese Society of Child Neurology, Ed.: 2015 Clinical Practice Guidelines for Febrile Seizures. SHINDAN TO CHIRYO SHA, 2015
4) Subcommittee on Febrile Seizures, American Academy of Pediatrics: Neurodiagnostic evaluation of the child with a simple febrile seizure. Pediatrics 127: 389-394, 2011
5) Japan Pediatric Society, et al.: Joint Recommendations on Sedation During MRI. Journal of the Japan Pediatric Society 124(4):771-805, 2020

References

1) Takanashi J et al: Diffusion MRI abnormalities after prolonged febrile seizures with encephalopathy. Neurology 66: 1304- 1309, 2006
2) Rasool A et al: Role of electroencephalogram and neuroimaging in first onset afebrile and complex febrile seizures in children from Kashmir. J Pediatr Neurosci 7: 9-15, 2012
3) Takanashi J et al: Excitotoxicity in acute encephalopathy with biphasic seizures and late reduced diffusion. AJNR Am J Neuro Radiol 30: 132- 135, 2009
4) Kubota H et al: Q fever encephalitis with cytokine profiles in serum and cerebrospinal fluid. Pedatr Infect Dis J 20: 318-319, 2001
5) Ogura K et al: MR signal changes in a child with cat scratch disease encephalopathy and status epilepticls. Eur Neurol 51: 109-110, 2004
6) Mizuguchi M: Acute necrotizing encephalopathy of childhood: a novel form of acute encephalopathy prevalent in Japan and Taiwan. Brain Dev 19: 81-92, 1997
7) Tada H et al: Clinically mild encephalitis/encephalopathy with a reversible splenial lesion. Neurology 63: 1854-1858, 2004
8) Maeda M et al: Reversible splenial lesion with restricted diffusion in a wide spectrum of diseases and conditions. J Neuroradiol 33: 229-236, 2006
9) Takanashi J et al: Differences in the time course of splenial and white matter lesions in clinically mild encephalitis /encephalopathy with a reversible splenial lesion (MERS). J Neurol Sci 292: 24-27, 2010
10) VanLandingham KE et al: Magnetic resonance imaging evidence of hippocampal injury after prolonged focal febrile convulsions. Ann Neurol 43: 413-426, 1998
11) Neligan A et al: Long-term risk of developing epilepsy after febrile seizures: a prospective cohort study. Neurology 78: 1166-1170, 2012

BQ 86 Is skeletal survey by plain radiography recommended to identify child abuse?

Statement

Skeletal survey of the bones is an established means of identifying bone injury in children under 2 years of age who have experienced physical abuse.

FQ 23 Is chest CT recommended for diagnosing rib fracture for child abuse?

Statement

Although rib fracture in an infant is a finding strongly suggestive of abuse, diagnosing bone fractures in the acute phase is difficult with plain radiography. By comparison, CT provides high sensitivity in the acute and subacute phases and for bone fractures in the process of healing. In circumstances where abuse is suspected, chest CT using an appropriate radiation dose is weakly recommended if rib fracture is not clearly seen on initial skeletal survey.

Explanation

1. Plain radiography for identifying child abuse

Bone fracture is common in cases of physical abuse ("abuse" below), following skin and soft tissue injury in frequency.[1)] The first choice of imaging for evaluating bone fracture is plain radiography ("XR" below). Because physically abused young children cannot describe their own symptoms, the clinical diagnosis of bone fracture is difficult, and it is not unusual to detect latent bone fractures by XR in such patients.

A background pathophysiology (conditions that predispose the patient to bone fracture, such as rickets and osteogenesis imperfecta) may also be involved in bone fractures in children. However, if the cause of bone fracture is abuse, overlooking this places the life of the child in serious danger. Skeletal survey is a test method that comprehensively images the whole body to detect latent bone fractures when abuse is suspected. Latent bone fractures have been reported to be detected by skeletal survey in 11% to 34% of children suspected of having experienced abuse.[1-3)] Consequently, the appropriate use of skeletal survey is important.

With the skeletal survey typically performed in the United Kingdom and United States, standard imaging consists of cranial imaging from 2 angles, imaging of the bones of the extremities from 1 to 2 angles, and imaging of the bones of the trunk from 2 angles. Reference examples of skeletal surveys based on secondary sources 1 and 2 are shown in the table. There is no categorically established method of skeletal

survey. Consequently, the method used must be determined by each facility. The details of the imaging are explained below.

① Classification according to age

Approximately 90% of abused children are < 2 years old, and more than 80% of those with bone fractures due to abuse are < 18 months old.[1, 4] The proportion of patients examined for bone fractures at hospitals who were found to have experienced abuse was 20% to 25% for those < 1 year old and 6 to 7% for those between 1 and 2 years old.[2] Because age is inversely related to the risk of bone fracture, it is recommended that a skeletal survey be performed for all patients < 2 years old and according to the circumstances of the individual for those 2 to 5 years old.

② Both oblique views of the chest

The likelihood of abuse is high with rib fractures with no clear mechanism of injury.[4] However, the ribs overlap with the cardiac and mediastinal shadows in the normal frontal view of the chest, making it difficult to diagnose bone fractures with little deviation. Sensitivity and specificity in detecting bone fractures increase with the addition of both oblique views, resulting in imaging from 4 angles, as compared with the 2 angles of the frontal and lateral chest views.[5] Consequently, including both oblique views in the skeletal survey is recommended.

Even combining the above-mentioned 4 types of chest imaging, diagnosing rib fractures by XR may be difficult. Evaluation by chest CT has been suggested in such cases.

Table. Skeletal survey

		RCR-RCPCH (2017), secondary source 1	ACR-SPR (2017), secondary source 2	Skeletal survey reference examples
Skeletal survey	Cranium	Frontal AP Lateral	Frontal AP Lateral	Frontal AP (**1) Lateral
	Chest	Frontal AP (to the shoulders)* Both obliques (ribs)*	Frontal AP*, lateral (includes ribs, thoracic vertebrae, upper lumbar vertebrae) Both obliques (ribs)*	Frontal AP*, lateral (thoracic vertebrae) Both obliques (ribs)*
	Abdomen, pelvis	Frontal AP (abdomen to pelvis)	Frontal AP (middle lumbar vertebrae to pelvis)	Frontal AP (abdomen to pelvis)
	Spine	Lateral (cervical vertebrae to lumbosacral vertebrae) < 1 year old: imaging performed once ≥ 1 year old: imaging divided into multiple procedures	Frontal AP, lateral (cervical vertebrae) Lateral (lumbosacral vertebrae)	Lateral (cervical vertebrae) Lateral (lumbosacral vertebrae)
	Upper extremities	Young children (small children): Frontal AP (upper arm to forearm)* Lateral (elbow, wrist) Older children: Frontal AP (upper arm; shoulder to elbow, forearm; elbow to wrist)* Lateral (elbow, wrist)	Bilateral upper arm AP* Bilateral forearm AP*	Bilateral upper arm AP* (**2, 3) Bilateral forearm AP*
	Lower extremities	Young children (small children): Frontal AP (hip to ankle)* Lateral (Knee, ankle) Ankle mortise AP view Older children: Frontal AP (femur, lower leg)* Frontal AP (knee, ankle) Lateral (knee, ankle)	Bilateral femur AP* Bilateral lower leg AP*	Bilateral femur AP (hip)* (**2, 3) Bilateral lower leg AP*
	Hands and feet	Bilateral hand PA Bilateral foot PA	Bilateral hand PA* Bilateral foot PA or AP*	Bilateral hand PA* Bilateral foot PA*
Follow-up skeletal survey (FUSS)	Imaging performed 11 to 14 days later Initial imaging performed within 28 days FUSS imaging is performed for the sites indicated with *, in addition to sites where the initial skeletal survey showed or were suggestive of abnormalities.		FUSS is performed for the sites indicated with * approximately 2 weeks after the initial imaging.	FUSS is performed for the sites indicated with * approximately 2 weeks after the initial imaging.

** 1: Cranial XR unnecessary when cranial CT performed.

** 2: In small children, imaging can be performed at the same time from the upper arm to the forearm and from the femur to the lower leg.

** 3: Lateral view added if bone fractures suspected based on frontal view of arms and legs.

③ Long bones lateral view

Although the addition of a lateral view of the long bones does not affect the detection of diaphyseal fractures, it has been found to improve sensitivity in detecting metaphyseal fractures.[6] Because metaphyseal fractures in infants are highly specific to abuse, the addition of a lateral view is recommended if the frontal view is suggestive of a lesion.

④ Imaging of the spine, pelvis, hands, and feet

The view has been expressed that these sites should not be included in a skeletal survey because fracture frequency is low at these sites and in view of the radiation exposure involved.[1] However, another report indicated that the frequency of bone fracture was 5.5% at these sites in children who were suspected of experiencing abuse and underwent a skeletal survey, and it also indicated there were cases in which bone fracture was seen at only these sites.[7] This suggests that there is a high risk of overlooking abuse if these sites are excluded. Including them in a skeletal survey is therefore recommended.

⑤ Head

When a patient is examined, cranial CT may be performed before the skeletal survey to evaluate head injury. CT is highly sensitive in detecting bone fractures, and it is recommended that multiplanar imaging be performed in addition to transverse imaging. In addition, the use of 3D reconstruction imaging facilitates differentiation from normal structures such as sutures and vascular grooves.[8, 9] Consequently, in patients who undergo cranial CT, generating multiplanar and 3D reconstruction images can substitute for cranial XR.

⑥ FUSS

The repair of bone fracture progresses in 1 to 2 weeks after injury, and union occurs in approximately 2 months. At 10 to 14 days after injury, aspects of the healing process such as the periosteal reaction and soft callus are seen on XR. This can contribute to improvement in the lesion detection rate, evaluation of suspicious lesions, and estimates of the time of injury.[1, 2] Bone fractures in the healing process were seen with a FUSS in 9% to 12% of infants whose initial skeletal survey findings were negative. Consequently, if suspicion of abuse remains, a FUSS is recommended approximately 2 weeks after the initial skeletal survey.

However, methods that limit a FUSS to specific sites to avoid unnecessary radiation exposure have been proposed, and the cranium is excluded from a FUSS in the United Kingdom and the United States (because evaluating the process of cranial repair is difficult with XR). Moreover, it was found that if the initial skeletal survey findings for the spine and pelvis were negative, excluding them from the FUSS did not impede treatment.[10] Consequently, exclusion from the FUSS can be considered.

2. Chest CT for rib fractures resulting from child abuse

Rib fractures in infants that have no clear mechanism of injury are strongly suggestive of abuse.[4] An oblique view of the rib cage is therefore added in the skeletal survey to improve bone fracture detection sensitivity. However, diagnosing acute bone fractures with little deviation in infants is difficult with XR. They often cannot be diagnosed with XR due to decreased lung field permeability and overlap with the cardiac shadow and mediastinal structures.

By comparison, some reports indicated that chest CT provides higher detection sensitivity for rib fractures than XR in the acute phase and during the healing process.[11-15] In investigations that compared post-mortem images with autopsy data, sensitivity for rib fractures ranged from 14% to 46% with XR and from 45% to 85% with CT.[11, 12] CT was also found to provide higher detection sensitivity than XR in surviving patients.[13-15]

Generating CT multiplanar and 3D reconstructed images facilitates the identification of lesion location and is useful for detecting bone fractures of the scapula and vertebrae.[15]

However, although the diagnostic performance of CT is high, it poses problems such as radiation exposure and sedation. Although bone fractures may also be newly identified with a FUSS, early chest CT can be considered if abuse is suspected, in view of the dramatic effect that a definitive diagnosis of rib fracture has on a child's vital prognosis. When CT is performed, the radiation dose should be reduced to a level that still ensures diagnostic quality.

Search keywords and secondary sources used as references

PubMed was searched using the following keywords: abuse, fracture, skeletal survey, bone survey, non-accidental injury, rib, and CT.

In addition, the following were referenced as secondary sources.

1) The Royal College of Radiologists and The Society and College of Radiographers: The radiological investigations of suspected physical abuse in children, 2017
2) Wootton-Gorges SL et al: ACR Appropriateness Criteria®: suspected physical abuse-child. J Am Coll Radiol 14: S338-S349, 2017

References

1) Karmazyn B et al: The prevalence of uncommon fractures on skeletal surveys performed to evaluate for suspected abuse in 930 children: should practice guidelines change? AJR Am J Roentgennol 197: W159-W163, 2011
2) Wood JN et al: Development of guidelines for skeletal survey in young children with fractures. Pediatrics 134: 45-53, 2014
3) Duffy SO et al: Use of skeletal surveys to evaluate for physical abuse: analysis of 703 consecutive skeletal surveys. Pediatrics 127: e47-e52, 2011
4) Kemp AM et al: Patterns of skeletal fractures in child abuse: systematic review. BMJ 337: a1518, 2008
5) Marine MB et al: Is the new ACR-SPR practice guideline for addition of oblique views of the ribs to the skeletal surveys for child abuse justified? AJR Am J Roentgenol 202: 868-871, 2014
6) Karmazyn B et al: Long bone fracture detection in suspected child abuse: contribution of lateral views. Pediatr Radiol 42: 463-469, 2012
7) Kleinman PK et al: Yield of radiographic skeletal surveys for detection of hand, foot, and spine fractures in suspected child abuse. AJR Am J Roentgenol 200: 641-644, 2013
8) Prabhu SP et al: Three-dimensional skull models as a problem-solving tool in suspected child abuse. Pediatr Radiol 43: 575-581, 2013

9) Culotta PA et al: Performance of computed tomography of the head to evaluate for skull fractures in infants with suspected non-accidental trauma. Pediatr Radiol 47: 74-81, 2017
10) Harper NS et al: The utility of follow-up skeletal surveys in child abuse. Pediatrics 131: e672-e678, 2013
11) Shelmerdine SC et al: Chest radiographs versus CT for the detection of rib fractures in children (DRIFT): a diagnostic accuracy observational study. Lancet Child Adolesc Health 2: 802-811, 2018
12) Hong TS et al: Value of postmortem thoracic CT over radiography in imaging of pediatric rib fractures. Pediatr Radiol 41: 736-748, 2011
13) Sanchez TR et al: Characteristics of rib fractures in child abuse: the role of low-dose chest computed tomography. Pediatr Emerg Care 34: 81-83, 2018
14) Sanchez TR et al: CT of the chest in suspected child abuse using submillisievert radiation dose. Pediatr Radiol 45: 1072- 1076, 2015
15) Wootton-Gorges SL et al: Comparison of computed tomography and chest radiography in the detection of rib fractures in abused infants. Child Abuse Negl 32: 659-663, 2008

BQ 87 In which cases is fetal MRI recommended?

Statement

Fetal MRI is recommended when a lesion of the head, head and neck, or trunk (excluding the heart) is suspected. However, the imaging and interpretation should be performed by a radiology technologist and diagnostic radiologist with as much experience as possible.

Background

Fetal MRI is useful for diagnosing fetal diseases and provides information beneficial for perinatal management and counseling parents. However, ultrasound is the standard test for fetal screening. MRI is performed when ultrasound shows an abnormality of the fetus and further information is needed, when evaluation by ultrasound is insufficient for reasons such as maternal obesity or oligohydramnios, and when no abnormalities are seen by ultrasound but a fetal abnormality is considered likely. To determine whether it is indicated, information is needed regarding how useful MRI is and the conditions and disorders that are good indications for fetal MRI. Consequently, these were the topics examined.

Explanation

Detailed examination of fetal malformations and masses accounts for many of the indications for fetal MRI. Moreover, as fetal therapy develops and its indications expand, evaluation by fetal MRI is becoming important. The gestational week at which diagnosis is possible depends on the disorder. However, it has been shown that no adverse events are seen in the fetus even when typical 1.5T non-contrast MRI is performed from the 1st trimester.[1)]

There have been several reports comparing the diagnostic performance of ultrasound and MRI. Ultrasound was found to be superior in 4%, MRI in 39% (of which, MRI contributed to a change of diagnosis in 56%, to new findings in 31%, and to confirmation of the diagnosis in 13%), and the 2 modalities were found to be comparable in 57%.[2)] A review by Bekker et al. found that MRI provided additional information useful for diagnosis in 23% to 100% of patients and changed fetal care in 13% to 39%.[3)] Examination by anatomical region showed that the addition of MRI to ultrasound contributed significantly to diagnosis in the central nervous system, urogenital tract, gastrointestinal tract, and chest.[2)] Abnormalities in these regions are therefore good indications for MRI. However, MRI was not shown to be useful for the skeletal system (limbs), face, and heart.[2)]

Typical indications for fetal MRI are shown in the table below. In addition, indications for each anatomical region are described in the following.

1. Head (central nervous system), spine, and spinal cord

Cerebral ventriculomegaly, brain parenchymal malformation (e.g., callosal dysgenesis, cortical dysplasia, and posterior fossa malformation), and destructive changes of the brain parenchyma (e.g., hemorrhage, infarction, and inflammation) are good indications. In addition, twin-to-twin transfusion syndrome is associated with a high risk of intracranial complications and therefore necessitates an intracranial evaluation.

In a prospective study by Goncalves et al., MRI was found to be superior to ultrasound for diagnosing central nervous system conditions, and MRI added information related to prognosis and counseling to that obtained by ultrasound in 22.2% of patients. Therefore, central nervous system evaluation is the best indication for fetal MRI.[4)]

A review by Jarvis et al. regarding cases in which brain malformation was suspected found that the MRI diagnostic accuracy rate was 91%, which was 16% higher than that evaluated with ultrasound alone.[5)] In 55% of the patients, the MRI and ultrasound findings were concordant for the correct diagnosis. In 15%, the information obtained with MRI added to that obtained with ultrasound. In 19%, an erroneous ultrasound diagnosis was corrected based on MRI.[5)] In addition, MRI resulted in a change in the counseling provided to the parents or in perinatal management in 41.9%.[5)] In addition, it has been reported that additional findings were obtained by MRI in 55% of patients.[2)] Another report showed that, among patients with an abnormality on ultrasound, the counseling the parents received changed based on MRI in 49.6%, the diagnosis changed in 31.7%, and perinatal management changed in 18.6%.[6)]

Table Typical indications for fetal MRI

Indication: Major Category		Indication: Minor Category
Head	Malformation	e.g., cerebral ventriculomegaly, callosal dysgenesis, holoprosencephaly, posterior fossa malformation, cortical dysplasia, and cephalocele (encephalocele, meningocele)
	Vascular disorder	vascular malformation, hydranencephaly, cerebral infarction, cerebral hemorrhage, complication of monochorionic twin pregnancy
Spine and spinal cord	Tumor (mass)	sacrococcygeal teratoma
	Malformation	neural tube defect (e.g., myelomeningocele),vertebral body malformation
Head and neck	Tumor (mass)	vascular malformation (venous malformation, lymphatic malformation (LM)), teratoma, goiter
	Malformation	facial cleft, gnathoschisis
Chest	Tumor (mass), malformation	congenital lung anomalies(congenital pulmonary airway malformation (CPAM), pulmonary sequestration, bronchial atresia, congenital lobar emphysema), congenital diaphragmatic hernia, mediastinal mass (teratoma, vascular malformation, thymic mass), esophageal atresia
	Other	pulmonary hypoplasia (evaluation of lung volume and signal intensity resulting from congenital diaphragmatic hernia, oligohydramnios, tumor, skeletal dysplasia, etc.), pleural effusion, pericardial effusion
Abdomen, pelvis, and retroperitoneum	Tumor (mass)	Abdominopelvic tumor, cyst (e.g., hemangioma, neuroblastoma, sacrococcygeal teratoma, suprarenal mass, renal mass, ovarian cyst)
	Malformation	e.g., urinary tract malformation (e.g., renal malformation, lower urinary tract obstruction, cloacal malformation, bladder exstrophy), intestinal tract malformation (anorectal malformation, intestinal atresia), abdominal wall abnormality (gastroschisis, omphalocele)
	Other	meconium peritonitis; fetal ascites, such as chylous ascites
Monochorionic twin complications		1 fetal death, conjoined twins

Not all disorders could be covered, and the usefulness of MRI varies between individual patients. The indications for MRI are therefore not limited to these.
(Prepared based on secondary source 2)

2. Head and neck

Evaluation of masses such as vascular malformations (lymphatic malformation (LM), venous malformations), teratomas, and goiters is common. Differentiating goiters from other masses is facilitated by characteristic hyperintensity in T1-weighted images. In evaluating masses, not only qualitative diagnosis but also evaluating the presence or absence of airway narrowing is important for determining perinatal management that includes ex utero intrapartum treatment (EXIT; a procedure in which the fetus is treated by placing the mother under general anesthesia, laparotomy is performed, the exposed uterus is incised, and blood circulation is maintained in the umbilical cord while maintaining the airway). An investigation by Poutamo et al. found that MRI provided information useful for diagnosis or the exclusion of lesions in 6 of 8 patients with head and neck lesions.[7)]

As mentioned previously, there are also reports that MRI was not useful for evaluating the face. On the other hand, the diagnostic accuracy rate for orofacial cleft was found to be 59% with ultrasound and 92% with MRI.[8)]

3. Chest

Congenital diaphragmatic hernia and congenital lung anomalies are the main indications. Evaluations for complicating pulmonary hypoplasia and hydrops fetalis are also performed. Adding MRI to ultrasound was found to provide additional information for lesions of the chest in 38% to 44% of patients.[2, 9] In congenital lung anomalies, MRI was found to be superior to ultrasound for visualizing abnormal blood vessels from the systemic circulation.[10]

MRI was not found to be useful with respect to fetal heart malformations, with ultrasound reported to be superior for their diagnosis.[2]

4. Abdomen, pelvis, and retroperitoneum

Abdominal masses and malformations (e.g., urinary tract malformation, gastrointestinal obstruction, gastroschisis) are the main changes evaluated. Meconium shows hyperintensity in T1-weighted images beginning from approximately 20 weeks, making it useful for evaluating the intestine. Adding MRI to ultrasound has been reported to provide additional information on abdominal gastrointestinal lesions in 38% of patients and on urogenital tract lesions in 29% of patients.[2]

Search keywords and secondary sources used as references

PubMed was searched using the following keywords: magnetic resonance imaging, and fetus.

In addition, the following were referenced as secondary sources.

1) American College of Radiology: ACR-SPR practice parameter for the safe and optimal performance of fetal magnetic resonance imaging (MRI), 2015
2) Patenatude Y et al: The use of magnetic resonance imaging in the obstetric patien (t SOGC CLINICAL PRACTICE GUIDELINE). J Obstet Gynaecol Can 36: 349-363, 2014
3) Prayer D et al: ISUOG practice guidelines: performance of fetal magnetic resonance imaging. Ultrasound Obstet Gynecol 49: 671-680, 2017

References

1) Ray JG et al: Association between MRI exposure during pregnancy and fetal and childhood outcomes. JAMA 316(9): 952-961, 2016
2) Kul S et al: Contribution of MRI to ultrasound in the diagnosis of fetal anomalies. J Magn Reson Imaging 35(4): 882-890, 2012
3) Bekker MN, van Vugt JM: The role of magnetic resonance imaging in prenatal diagnosis of fetal anomalies. Eur J Obstet Gynecol Reprod Biol 96(2): 173-178, 2001
4) Gonçalves LF et al: Diagnostic accuracy of ultrasonography and magnetic resonance imaging for the detection of fetal anomalies: a blinded case-control study. Ultrasound Obstet Gynecol 48(2): 185-92, 2016
5) Jarvis D et al: A systematic review and meta-analysis to determine the contribution of mr imaging to the diagnosis of foetal brain abnormalities In Utero. Eur Radiol 27(6): 2367-2380, 2017
6) Levine D et al: Fast MR imaging of fetal central nervous system abnormalities. Radiology 229(1): 51-61, 2003
7) Poutamo J et al: Magnetic resonance imaging supplements ultrasonographic imaging of the posterior fossa, pharynx and neck in malformed fetuses. Ultrasound Obstet Gynecol 13(5): 327-334, 1999
8) Zheng W et al: The prenatal diagnosis and classification of cleft palate: the role and value of magnetic resonance imaging. Eur Radiol 29(10): 5600-5606, 2019
9) Levine D et al: Fetal thoracic abnormalities: MR imaging. Radiology 228(2): 379-388, 2003
10) Mon RA et al: Diagnostic accuracy of imaging studies in congenital lung malformations. Arch Dis Child Fetal Neonatal Ed 104(4): F372-F377, 2019

BQ 88 Which imaging examinations are recommended when retinoblastoma is suspected?

Statement

MRI, which involves no radiation exposure and provides excellent tissue resolution, is recommended. Although CT provides high detection performance with respect to calcification and is useful for diagnosis on initial examination, it is associated with radiation exposure and is therefore not always necessary. Posttreatment follow-up and periodic CT are not recommended.

Explanation

Retinoblastoma is the most common childhood intraocular tumor and occurs unilaterally in 2/3 of patients and bilaterally in 1/3, according to a report published in Japan.[1)] Left-right and male-female differences are unclear.[1)] Approximately 90% of retinoblastoma cases are diagnosed by 3 years of age and approximately 40% by 1 year of age.[1)] The initial diagnosis is performed by fundoscopy and ocular ultrasound. MRI and CT are used to more definitively determine whether there has been local progression and confirm the diagnosis.[2-11)]

In developed countries, nearly all intraocular lesions are detected while in a localized state. Consequently, the main objectives of treatment are to preserve the eye and visual function rather than to save the patient's life. Treatments such as laser and radiation therapy are selected for early lesions. Invasion of the optic nerve, choroid, and sclera is related to the presence or absence of distant metastasis. However, from the perspective of preserving visual function and based on the risk of metastasis associated with the manipulation, pathological findings cannot be obtained for all patients.[12)] For lesions that are not limited to within the eyeball and pose a high risk of metastasis, eye enucleation is considered, and multimodal treatment that includes chemotherapy is selected. Given this context, the use of MRI, which provides excellent tissue resolution, is encouraged to evaluate the risk of metastasis.

MRI can be used to evaluate metastasis-related factors such as pathological optic nerve and choroid invasion. Aspects related to these factors are evaluated. These include: the volume, long-axis diameter, morphology, and location of the tumor; enlargement and contrast enhancement of the optic nerve; and the signal intensity and degree of diffusion restriction in T2-weighted images.[2-6, 8, 11)] Optic nerve invasion is suspected if the tumor is large, the lesion covers the optic nerve, or the optic nerve is enlarged and shows contrast enhancement. However, none of these findings can be used to diagnose invasion with 100% certainty. Consequently, the findings are considered in combination to evaluate the risk of metastasis comprehensively (Figs. 1 and 2). In a study by de Jong et al. (370 patients), the minimum tumor volume and long-axis diameter that resulted in optic nerve invasion and apparent choroid invasion were 0.59 cm^3 and 13.90 mm and 0.19 cm^3 and 8.15 mm, respectively.[2)]

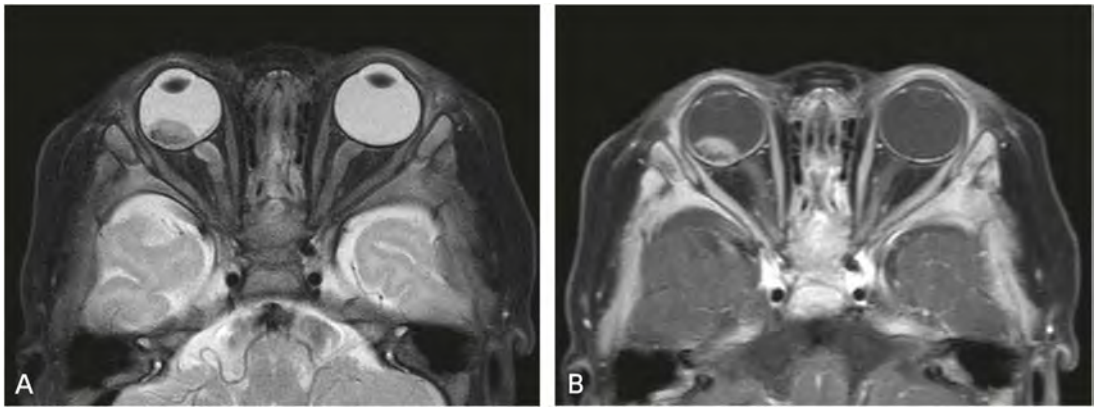

Figure 1. Patient without optic nerve invasion

A: MRI, fat-suppressed T2-weighted transverse image: A right intraocular tumor is seen. The long-axis diameter was measured at approximately 11 mm, but the tumor volume was 0.33 cm^3.
B: Gadolinium contrast-enhanced MRI, fat-suppressed contrast-enhanced T1-weighted transverse image: No optic nerve or extraocular invasion is seen.
Based on these findings, the risk of metastasis was judged to be low. Eyeball enucleation was selected, and there was judged to be no optic nerve invasion.

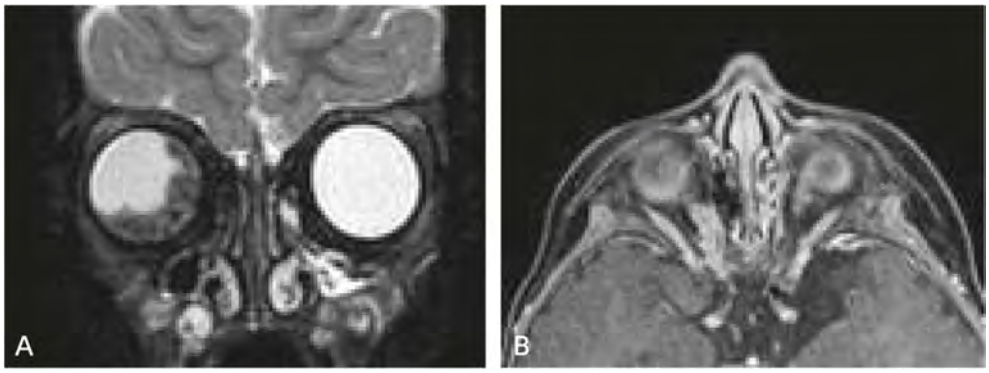

Figure 2. Patient with optic nerve invasion

A: MRI, fat-suppressed T2-weighted coronal image: A right intraocular tumor with a long-axis diameter of 22 mm is seen.
B: Gadolinium contrast-enhanced MRI, fat-suppressed contrast-enhanced T1-weighted transverse image: Increased contrast enhancement and enlargement of the right optic nerve are seen.
Based on these findings, there was judged to be extraocular extension and a high risk of metastasis. Eyeball enucleation was performed, optic nerve invasion observed, and aftertreatment implemented.

Few cases of retinoblastoma are associated with metastasis on initial examination, and nearly all can be evaluated for the presence or absence of optic nerve invasion by fundoscopy. Consequently, whole-body screening on initial examination is not necessary in all patients.[13)]

Screening for calcification is important for diagnosing retinoblastoma.[10)] However, calcification has been reported to be visualized by MRI in ≥ 90% of cases, and CT is therefore not always necessary.[4)]

Search keywords and secondary sources used as references

PubMed was searched using the following keywords: retinoblastoma, MRI, and CT.

In addition, the following were referenced as secondary sources.

1) Japanese Society of Pediatric Hematology/Oncology, Ed.: 2016 Practical Guidelines for Pediatric Cancer, 2nd Edition. KANEHARA & Co., 2016

References

1) Committee for the National Registry of Retinoblastoma: The national registry of retinoblastoma in Japan (1983-2014). Jpn J Ophthalmol 62: 409-423, 2018
2) de Jong MC et al: Diagnostic accuracy of intraocular tumor size measured with MR imaging in the prediction of postlaminar optic nerve invasion and massive choroidal invasion of retinoblastoma. Radiology 279: 817-826, 2016
3) Li Z et al: Diagnosis of postlaminar optic nerve invasion in retinoblastoma with MRI features. J Magn Resonance Imaging 51(4): 1045-1052, 2020
4) Lemke AJ et al: Retinoblastoma - MR appearance using a surface coil in comparison with histopathological results. Eur Radiol 17: 49-60, 2007
5) Kim U et al: Accuracy of preoperative imaging in predicting optic nerve invasion in retinoblastoma: a retrospective study. Ind J Ophthalmol 67: 2019-2022, 2019
6) Hiasat JG et al: The predictive value of magnetic resonance imaging of retinoblastoma for the likelihood of high-risk pathologic features. Eur J Ophthalmol 29: 262-268, 2019
7) de Jong MC et al: Diagnostic performance of magnetic resonance imaging and computed tomography for advanced retinoblastoma: a systematic review and meta-analysis. Ophthalmology 121: 1109-1118, 2014
8) Cui Y et al: Correlation between conventional MR imaging combined with diffusion-weighted imaging and histopathologic findings in eyes primarily enucleated for advanced retinoblastoma: a retrospective study. Eur Radiol 28: 620-629, 2018
9) Chawla B et al: Magnetic resonance imaging for tumor restaging after chemotherapy in retinoblastoma with optic nerve invasion. Ophthalmic Genet 39: 584-588, 2018
10) Arrigg PG et al: Computed tomography in the diagnosis of retinoblastoma. Br J Ophthalmol 67: 588-591, 1983
11) Kim JW et al: Clinical significance of optic nerve enhancement on magnetic resonance imaging in enucleated retinoblastoma patients. Ophthalmol Retina 1: 369-374, 2017
12) Shields CL et al: Vitrectomy in eyes with unsuspected retinoblastoma. Ophthalmology 107: 2250-2255, 2000
13) Chantada G et al: Results of a prospective study for the treatment of retinoblastoma. Cancer 100: 834-842, 2004

BQ 89 Which imaging examinations are recommended to diagnose and stage neuroblastomas?

Statement

CT and MRI are useful and recommended for diagnosing masses suspected of being neuroblastomas. ^{123}I-MIBG scintigraphy is useful for staging neuroblastomas, and its use with CT or MRI for a comprehensive evaluation is strongly recommended.

Background

Neuroblastoma is a commonly seen pediatric cancer, following leukemia and brain tumors in frequency. According to the registry of the Research Project on Specific Pediatric Chronic Diseases, approximately 320 children are newly affected by neuroblastoma each year in Japan. Approximately half of cases occur before 1 year of age and approximately 80% by 3 years of age. It occurs in the sympathetic ganglia of the trunk and the adrenal medulla. Approximately half of neuroblastomas occur in the adrenal glands, followed by areas such as the extra-adrenal retroperitoneum (25%), chest (16%), neck (3%), and pelvis (3%). Metastasis is seen at the time of diagnosis in approximately 70% of cases, occurring preferentially in the bone marrow (70%), bone (55%), and regional lymph nodes (30%). Metastasis is also seen in areas such as the liver; distant lymph nodes, such as the supraclavicular lymph nodes; and skin. Its prognosis is strongly correlated with age at the time of diagnosis, clinical stage, and biological factors, and it is a cancer known to show diversity.

The treatment strategy is generally selected according to risk classification.[1)] The risk classification is assessed by evaluating a combination of clinical factors, such as age at the time of diagnosis, disease stage, and tissue classification, along with biological factors, such as MYCN gene amplification and tumor cell ploidy. The International Neuroblastoma Staging Risk Group Staging System (INRGSS), proposed in 2009, is based on diagnostic imaging performed before the start of treatment. Consequently, diagnostic imaging plays a major role in neuroblastoma staging.

Explanation

1. Diagnosis and staging

Neuroblastomas are often first detected due to abdominal distension or palpation of an abdominal mass. It is also not unusual for them to be diagnosed based on metastatic lesion symptoms (e.g., bone or joint pain). Ultrasonography is selected to establish the presence of an abdominal tumor. It is easy to perform and involves no radiation exposure.

CT and MRI are excellent for evaluating the localization and extent of tumors and are also useful for staging. Their use is therefore recommended.[2)] They are useful for evaluating the presence or absence of invasion of major blood vessels and adjacent organs and extension into the spinal canal. In addition, they

are useful for determining a treatment strategy that includes surgical resection. CT and MRI are also useful for evaluating the presence or absence and extent of lymph node metastasis and the presence or absence of bone marrow, bone, and liver metastases and for staging. In a multicenter, prospective study by Siegel et al., the diagnostic performance of contrast-enhanced CT and MRI in neuroblastoma with distant metastasis was 81% and 83%, respectively, the difference being nonsignificant. The positive and negative predictive values with respect to detection performance in lymph node metastasis were 20% and 95%, respectively, for CT and 19% and 99%, respectively, for MRI. The positive and negative predictive values with respect to tumor extent were 73% and 83%, respectively, for CT and 81% and 79%, respectively, for MRI.[2)] CT and MRI are regarded as equally useful for evaluating primary lesions and local invasion.

With regard to neuroblastoma staging, the International Neuroblastoma Risk Group (INRG) proposed an international preoperative staging system based on imaging findings in 2009, and its use has grown (Table 1). Under this new classification system, surgical risk is evaluated based on imaging findings (image-defined risk factors, IDRFs). Localized tumors are classified as L1 and L2 based on the presence or absence of IDRFs and M and MS based on the type of distant metastasis. Items checked for IDRFs of the abdominopelvic region are shown in Table 2. In addition, diagnostic imaging is used to evaluate 20 checked items, such as the presence or absence and extent of extension into the trachea and spinal canal and the presence or absence of major organ invasion. The IDRF evaluation is an important index for determining a treatment strategy, and evaluation in multiple planes is useful.

Table 1. International Neuroblastoma Risk Group Staging System

Stage	Description
L1	A localized tumor confined to one body compartment without IDRF (image-defined risk factor)
L2	A localized tumor with at least one IDRF
M	Distant metastasis (excluding MS)
MS	< 18 months of age with metastasis confined to skin, liver, and/or bone marrow bone marrow metastasis: tumor cells in bone marrow < 10% of nucleated cells and MIBG scintigraphy negative

IDRF = image-defined risk factor, prepared from secondary source 1

Table 2. IDRFs for the abdominopelvic region

Anatomic Region	Description
Multiple body compartments	Ipsilateral tumor extension within ≥ 2 compartments (e.g., chest and abdomen, abdomen and pelvis)
Abdomen and pelvis	Tumor infiltrating porta hepatis or hepatoduodenal ligament Tumor encasing branches of superior mesenteric artery at mesenteric root Tumor encasing celiac artery and/or superior mesenteric artery root Tumor invading one or both renal pedicles Tumor encasing aorta and/or inferior vena cava Tumor encasing iliac vessels Pelvic tumor crossing sciatic notch
Intraspinal tumor extension	Intraspinal tumor extension (any level) provided that ≥ 1/3 of spinal canal in the axial plane is invaded, the perimedullary leptomeningeal spaces are not visible, or spinal cord intensity is abnormal
Infiltration of adjacent organs and structures	Infiltration of the pericardium, diaphragm, kidney, liver, duodenum, pancreas, and mesentery

Prepared from secondary source 1

As a method of tumor scintigraphy with neuroblastoma-specific uptake, ^{123}I-MIBG scintigraphy ("MIBG scintigraphy" below) is useful for evaluating primary and metastatic lesions.[3, 4)] In an examination of the diagnostic performance of MIBG scintigraphy by Vik et al., sensitivity and specificity of 88% and 83%, respectively, were reported. The causes of false positives were found to be the effects of physiological uptake by organs and structures such as the heart, salivary gland, brown fat, lacrimal gland, liver, and urinary bladder. The causes of false negatives were found to include tumor cell maturity and intratumoral necrosis and cystic changes.[5)] MIBG scintigraphy requires that imaging be performed 24 hours after radionuclide administration. Its diagnostic performance is improved by including SPECT in addition to planar imaging.[5)] SPECT/CT further improves resolution and is therefore useful not only at the time of diagnosis, but also when evaluating treatment efficacy.[6, 7)]

The sensitivity and specificity of bone scintigraphy in evaluating bone metastasis were found to be 70% to 78% and 51%, respectively. Thus, the diagnostic performance of bone scintigraphy was lower than that of MIBG scintigraphy and MRI. However, bone scintigraphy is recommended to evaluate skeletal system metastasis in patients negative on MIBG scintigraphy.[7)] Because the liver shows strong physiological uptake with MIBG scintigraphy, ultrasonography, CT, or MRI is needed to evaluate liver metastasis.[1, 8)] Moreover, when it is difficult to interpret abnormal uptake with MIBG scintigraphy at a site where metastasis may have occurred, another modality must be added to assess whether there is metastasis.

The number of reports comparing ^{18}F-FDG PET ("PET" below) and MIBG scintigraphy has increased in recent years.[7-9)] Although PET provides excellent visualization of small lesions, it has been found to be inferior to MIBG scintigraphy in overall diagnostic performance, including the diagnosis of metastatic lesions.[8,9)] PET involves higher levels of radiation exposure than MIBG scintigraphy, which is highly tumor-specific, and it produces many false positives and false negatives. Its use is therefore limited to special cases, such as patients negative on MIBG scintigraphy.

Based on the above considerations, contrast-enhanced CT or MRI is recommended for the local evaluation of neuroblastomas, and MIBG scintigraphy, in addition to CT and MRI, is strongly recommended to evaluate distant metastasis.

2. Selection of CT and MRI

A disadvantage of CT is that it generally requires the use of a contrast agent and is associated with radiation exposure. However, its advantages are that it enables the entire trunk to be evaluated in a short time and can be performed relatively easily at any facility. MRI, because of its high tissue resolution, does not require the use of a contrast agent. However, its shortcomings are that it is noisy, its tests take a long time, its imaging range is limited, and it often requires sedation for even longer than CT. Moreover, contrast-enhanced CT is superior for preoperatively evaluating blood vessels, whereas MRI is superior for evaluating tumors that extend to the central nervous system or spinal canal. Performing both CT and MRI is more useful for diagnosis. However, the modality should be selected according to the condition of the affected child and the circumstances of the facility.

Search keywords and secondary sources used as references

PubMed was searched using the following keywords: neuroblastoma and diagnostic imaging.

In addition, the following were referenced as secondary sources.

1) Brisse HJ et al: Guidelines for imaging and staging of neuroblastic tumors: consensus report from The International Neuroblastoma Risk Group project. Radiology 261: 243-257, 2011
2) Bar-Sever Z et al: Guideline on nuclear medicine imaging in neuroblastoma. Eur J Nucl Med Mol Imaging 45: 2009-2024, 2018
3) Monclair T et al: The International Neuroblastoma Risk Group (INRG) Staging System: an INRG task force report. J Clin Oncol 27: 298-303, 2009

References

1) Brodeur GM: Neuroblastoma: biological insights into a clinical enigma. Nat Rev Cancer 3: 203-216, 2003
2) Siegel MJ et al: Staging of neuroblastoma at Imaging: report of the Radiology Diagnostic Oncology Group. Radiology 223: 168-175, 2002
3) Matthay KK et al: Criteria for evaluation of disease extent by 123I-metaiodobenzylguanidine scans in neuroblastoma: a report for the International Neuroblastoma Risk Group (ONRG) Task Force. British Journal of Cancer 102: 1319-1326, 2010
4) Fendler WP et al: High 123I-MIBG uptake in neuroblastic tumours indicates unfavorable histopathology. Eur J Nucl Med Mol Imaging 40: 1701-1710, 2013
5) Vik TA et al: 123I-mIBG scintigraphy in patients with known or suspcted neuroblastoma: results from a prospective multicenter trial. Pediatr Blood Cancer 52: 784-790, 2009
6) Rozovsky K et al: Added Value of SPECT/CT for correlation for MIBG scintigraphy and diagnostic CT in neuroblastoma and pheochromocytoma. AJR Am J Roentgenol 190: 1085-1090, 2008
7) Mueller WP et al: Nuclear medicine and multimodality imaging of pediatric neuroblastoma. Pediatr Radiol 43: 418-427, 2013
8) Sharp SE et al: 123I-MIBG scintigraphy and 18F-FDG PET in neuroblastoma. J Nucl Med 50: 1237-1243, 2009
9) Papathanasiou ND et al: 18F-FDG PET/CT and 123I-metaiodo- benzylguanidine imaging in high-risk neuroblastoma: diagnostic comparison and survival analysis. J Nucl Med 52: 519-525, 2011

BQ 90 Is MIBG scintigraphy recommended for the posttreatment follow-up of neuroblastomas?

Statement

MIBG scintigraphy is useful and recommended for the follow-up of neuroblastomas.

Background

Neuroblastomas are fetal tumors that arise from the sympathetic nervous system. They can occur anywhere from the base of the skull to the pelvis. Neuroblastomas are the most common extracranial tumors that occur between the ages of 1 and 4 years. Neuroblastomas are the cause of approximately 15% of cancer deaths in young children. They account for 7% to 10% of pediatric cancers, peak in their occurrence at < 2 years of age, and 90% are diagnosed by 5 years of age. Metastasis is seen at the time of diagnosis in approximately 70% of patients with neuroblastomas. However, the prognosis is strongly correlated with age at diagnosis, disease stage, and biological factors.[1-3] The evaluation of distant metastasis by MIBG scintigraphy has been reported to be correlated with prognosis in neuroblastoma.[4] Although MIBG scintigraphy is already being widely used in Japan for patients with neuroblastomas, its usefulness in posttreatment follow-up was examined.

Explanation

Using ^{123}I-MIBG planar imaging and SPECT for the posttreatment follow-up of 40 patients, Okuyama et al. visualized 10 of 11 recurrent tumors in 8 patients (91%) Of these 10, no elevation of tumor markers was seen in 3 patients.[5] In an investigation of 11 patients with neuroblastoma, Rozovsky et al. reported that recurrence was detected in 5 patients with whole-body imaging and SPECT, but in only 2 patients with diagnostic CT. They suggested that contrast-enhanced CT can be omitted in the absence of MIBG SPECT/CT findings.[6]

Search keywords and secondary sources used as references

PubMed was searched using the following keywords: neuroblastoma, MIBG, scintigraphy, and follow. Four articles were selected from the results.

References

1) Brodeur GM et al: Revisions of the international criteria for neuroblastoma diagnosis, staging, and response to treatment. J Clin Oncol 11(8): 1466-1477, 1993
2) Shimada H et al: International neuroblastoma pathology classification for prognostic evaluation of patients with peripheral neuroblastic tumors: a report from the Children's Cancer Group. Cancer 92(9): 2451-2461, 2001
3) Bown N et al: Gain of chromosome arm 17q and adverse outcome in patients with neuroblastoma. N Engl J Med 340(25): 1954-1961, 1999

4) Schmidt M et al: The prognostic impact of functional imaging with (123) I-MIBG in patients with stage 4 neuroblastoma ＞1 year of age on a high-risk treatment protocol: results of the German Neuroblastoma Trial NB97. Eur J Cancer 44(11): 1552-1558, 2008
5) Okuyama C et al: Utility of follow-up studies using meta-[123 I] iodobenzylguanidine scintigraphy for detecting recurrent neuroblastoma. Nucl Med Commun 23(7): 663-672, 2002
6) Rozovsky K et al: Added value of SPECT/CT for correlation of MIBG scintigraphy and diagnostic CT in neuroblastoma and pheochromocytoma. AJR Am J Roentgenol 190(4): 1085-1090, 2008

11
Nuclear Medicine and Hematology

BQ 91 Is FDG-PET recommended to stage malignant lymphoma and diagnose its recurrence?

Statement

PET is recommended for staging highly FDG-avid malignant lymphoma tissue types. Screening for recurrence with FDG-PET is recommended when recurrence is suspected based on evidence such as clinical symptoms and laboratory test findings.

Background

A characteristic of malignant lymphoma is that it occurs throughout the body. Determining the extent of malignant lymphoma lesions and staging them is necessary to determine a treatment strategy and prognosis. Previously, ^{68}-Ga scintigraphy was used for detailed examinations of the whole body. In recent years, however, it has been replaced by ^{18}F-FDG-PET, which is superior both in sensitivity and specificity. Moreover, with the development of and advances in CT and fusion PET/CT systems, diagnostic accuracy has improved dramatically, and ^{18}F-FDG-PET/CT examinations ("FDG-PET" below) have come into mainstream use. FDG-PET is used to evaluate treatment efficacy in many histologic subtypes of malignant lymphoma, and staging by PET also plays a role as a pretreatment evaluation.

Explanations

Malignant lymphoma is classified as Hodgkin lymphoma and non-Hodgkin lymphoma, and non-Hodgkin lymphoma is further classified as low-, intermediate-, and high-grade lymphoma. To stage malignant lymphoma, the Ann Arbor classification system is used. The system emphasizes involvement of both the upper and lower sides of the diaphragm and extranodal involvement.

Malignant lymphoma shows a wide range of FDG uptake depending on the tissue type. Hodgkin lymphoma and intermediate- and high-grade lymphomas show high FDG uptake. Consequently, the detection performance of PET for nodal and extranodal lesions is high in these types of lymphomas.[1)] In malignant lymphomas with high FDG uptake, PET sensitivity was found to be ≥ 90%, and the stage was changed as a result of PET in 10% to 30% of patients.[2, 3)] In a study that compared PET/CT and contrast-enhanced CT, sensitivity for nodal lesions was 94% and 88%, respectively, and specificity was 100% and 86%, respectively. Sensitivity for extranodal lesions was 88% and 50%, respectively, and specificity was 100% and 90%, respectively.[4)]

The Lugano classification (2014), a revised version of the Ann Arbor classification, was created at the 2014 International Conference on Malignant Lymphoma.[5)] Under the Lugano classification system (2014), staging is performed by PET before treatment if PET is used to assess treatment efficacy in malignant lymphoma with high FDG uptake. It was found that, because PET provides high performance in detecting

bone marrow infiltration in Hodgkin lymphoma and diffuse large B-cell lymphoma, bone marrow biopsy can be omitted if FDG-PET is performed.[6)]

The usefulness of PET in staging tissue types with low FDG avidity (chronic lymphocytic leukemia/small lymphocytic lymphoma, lymphoplasmacytoid lymphoma, mycosis fungoides, nodal marginal zone B-cell) is not well defined. PET is therefore not recommended for these tissue types, and their staging is performed using contrast-enhanced CT.[6)] Evaluation by MRI is recommended in primary lymphoma of the central nervous system.[5)] In primary gastrointestinal malignant lymphoma, the main lesions are extranodal lesions. Consequently, they often diverge from the Ann Arbor classification, and a classification for primary gastrointestinal malignant lymphoma, established at the International Conference on Malignant Lymphoma, is used in addition to the Ann Arbor classification.

For the posttreatment follow-up and evaluation of malignant lymphoma, determinations are made clinically by appropriate history-taking, physical findings, blood counts, biochemical test results, and imaging examinations. In 50% to 80% of patients who show clinical signs during posttreatment follow-up, the signs are associated with recurrence.[7)] Approximately 80% of recurrence takes place at sites where the lesions were initially located.[6)] It is thought that many facilities perform CT as an imaging examination to screen for the recurrence of malignant lymphoma. However, there is no evidence that periodic imaging examinations, including FDG-PET, are useful for this purpose, and they are not recommended.[8-10)]

Periodic screening for recurrence with FDG-PET has a false-positive rate of > 20%, resulting in unnecessary tests and biopsies and patient anxiety. FDG-PET should be performed if recurrence is suspected based on factors such as clinical symptoms and test findings.

Search keywords and secondary sources used as references

In relation to malignant lymphoma staging, PubMed was searched using the following keywords: malignant lymphoma, FDG PET, and staging. In relation to diagnosing malignant lymphoma recurrence, PubMed was searched using the following keywords: malignant lymphoma, FDG PET, relapse, and surveillance.

In addition, the following were referenced as secondary sources.

1) Japan Society of Hematology, Ed.: Practical Guidelines for Hematological Malignancies, 2018 Revised Version. KANEHARA & Co., 2020
2) Cheson BD et al: Revised response criteria for malignant lymphoma. J Clin Oncol 25(5): 579-586, 2007
3) Carbone PP et al: Report of the committee on Hodgkin's disease staging classification. Cancer Res 31(11): 1860-1861, 1971
4) Rosenberg SA: Validity of the Ann Arbor staging classification for the non-Hodgkin's lymphomas. Cancer Treat Rep 61: 1023-1027, 1977
5) Cheson BD et al: Recommendations for initial evaluation, staging, and response assessment of Hodgkin and non-Hodgkin lymphoma: the Lugano classification. J Clin Oncol 32(27): 3059-3068, 2014
6) Rohatiner A et al: Report on a workshop convened to discuss the pathological and staging classifications of gastrointestinal tract lymphoma. Ann Oncol 5(5): 397-400, 1994

References

1) Cheson BD: Role of functional imaging in the management of lymphoma. J Clin Oncol 29: 1844-1854, 2011
2) Weiler-Sagie M et al: ^{18}F-FDG avidity in lymphoma readdressed: a study of 766 patients. J Nucl Med 51(1): 25-30, 2010
3) Isasi CR et al: A meta analysis of 18F-2-deoxy-2-fluoro-D-glucosepositron emission tomography in the staging and restaging of patients with lymphoma. Cancer 104: 1066-1074, 2005
4) Schaefer NG et al: Non-Hodgkin lymphoma and Hodgkin disease: coregistered FDG PET and CT at staging and restaging-do we need contrast-enhanced CT? Radiology 232: 823-829, 2004
5) Barrington SF et al: Role of imaging in the staging and response assessment of lymphoma: consensus of the International Conference on Malignant Lymphomas Imaging Working Group. J Clin Oncol 20；32(27): 3048-3058, 2014
6) Kostakoglu L et al: Current role of FDG PET/CT in lymphoma. Eur J Nucl Med Mol Imaging 41(5): 1004-1027, 2014
7) Weeks JC et al: Value of follow-up procedures in patients with large-cell lymphoma who achieve a complete remission. J Clin Oncol 9: 1196-1203, 1991
8) Jerusalem G et al: Early detection of relapse by whole-body positron emission tomography in the follow-up of patients with Hodgkin's disease. Ann Oncol 14: 123-130, 2003
9) Zinzani PL et al: Role of [18F]fluorodeoxyglucose positron emission tomography scan in the follow-up of lymphoma. J Clin Oncol 27: 1781-1787, 2009
10) Hiniker SM et al: Value of surveillance studies for patients with stage I to II diffuse large B-cell lymphoma in the rituximab era. Int J Radiat Oncol Biol Phys 92: 99-106, 2015

BQ 92 Is FDG-PET recommended to assess treatment efficacy for malignant lymphoma?

Statement

The use of FDG-PET to assess treatment efficacy when treatment is completed is recommended for malignant lymphomas of FDG-avid tissue types (e.g., diffuse large B-cell lymphoma, follicular lymphoma, Hodgkin lymphoma).

Background

Chemotherapy is the main treatment selected for malignant lymphoma, with surgery, radiation therapy, and radioimmunotherapy performed according to the circumstances. FDG-PET, which is considered excellent for evaluating lesion activity, is used to assess treatment efficacy, and a consensus on its usefulness has been published based on the accumulated data.[1, 2)]

Explanation

In assessing treatment efficacy for malignant lymphoma, ^{68}-Ga scintigraphy was previously used to evaluate lesion activity, in addition to the use of CT to observe the size of the lesion. FDG-PET (PET/CT) began to be used instead of ^{68}-Ga scintigraphy in the early 2000s, and numerous reports regarding its usefulness were published. The role of FDG-PET in treatment efficacy assessment was clarified by the International Harmonization Project Criteria, which were compiled by Cheson et al. in 2007. PET has since come to play a central role in assessing the efficacy of malignant lymphoma treatment. Various investigations were subsequently conducted,[1-7)] and the Lugano classification, a revised version of the 2007 criteria, was published in 2014.

The Lugano classification involves visual assessment on a 5-point scale. If FDG uptake in the area of the lesion is equal to or lower than that in the liver (score, ≤ 3), there is considered to be no active lesion (negative) in malignant lymphoma with standard therapy. This visual assessment is widely used at present. The 2007 criteria specified the mediastinal blood pool as background. However, due to the large number of posttreatment false positives, the criteria were modified after an international conference in 2009.[5, 6, 8-11)] In malignant lymphoma of FDG-avid tissue types (i.e., many lymphomas, such as diffuse large B-cell lymphoma, follicular lymphoma, Hodgkin lymphoma), this classification is used to assess treatment efficacy at treatment completion. However, if no FDG uptake is seen before treatment, CT is used to assess treatment efficacy.[2)] Efficacy assessment using a quantitative index such as the standardized uptake value (SUV) supplements visual assessment. However, it is not necessarily required because the accumulated data are still insufficient, and there is large variability between systems and facilities.

In view of factors such as inflammation associated with treatment, treatment efficacy should be assessed at least 3 weeks after treatment completion and, ideally, 6 to 8 weeks after completion and beyond. Immune

checkpoint inhibitors have also been used to treat malignant lymphoma in recent years. However, because of the pronounced inflammatory response associated with the treatment, caution is needed with respect to false positives. If the progressive metabolic disease assessment is indeterminate with the Lugano classification, retesting is performed after 12 weeks.[12)]

Particularly in Europe, several investigations have recently been conducted on interim PET, whereby the treatment response is assessed early after the start of treatment, often after 2 cycles of chemotherapy, using FDG-PET's sensitivity to lesion activity. Interim PET determines the subsequent treatment strategy. Although there have been reports regarding the usefulness of this approach, no consistent assessment has been established, and it should not be adopted for routine clinical practice. In diffuse large B-cell lymphoma, a negative interim PET finding may indicate a good prognosis, but a positive finding does not necessarily suggest a poor prognosis.[9)] In advanced-stage Hodgkin lymphoma, on the other hand, negative and positive interim PET findings have both been found to be useful for determining the prognosis.[13)] A clinical study of the advisability of using the results of interim PET for treatment intervention is currently underway.

Search keywords and secondary sources used as references

PubMed was searched using the following keywords: lymphoma, PET, and response.

In addition, the following were referenced as secondary sources.

1) Cheson BD et al: Revised response criteria for malignant lymphoma. J Clin Oncol 25: 579-586, 2007
2) Cheson BD et al: Recommendations for initial evaluation, staging, and response assessment of Hodgkin and non-Hodgkin lym- phoma: the Lugano classification. J Clin Oncol 32: 3059-3068, 2014
3) Juweid ME et al: Use of positron emission tomography for response assessment of lymphoma: consensus of the imaging subcommittee of International Harmonization Project in Lymphoma. J Clin Oncol 25: 571-578, 2007
4) Barrington SF et al: Role of imaging in the staging and response assessment of lymphoma: consensus of the International Conference on Malignant Lymphomas Imaging Working Group. J Clin Oncol 32: 3048-3058, 2014

References

1) Cerci JJ et al: Cost effectiveness of positron emission tomography in patients with Hodgkin’s lymphoma in unconfirmed complete remission or partial remission after first-line therapy. J Clin Oncol 28: 1415-1421, 2010
2) Barnes JA et al: End-of-treatment but not interim PET scan predicts outcome in nonbulky limited-stage Hodgkin’s lymphoma. Ann Oncol 22: 910-915, 2011
3) Spaepen K et al: Prognostic value of positron emission tomography (PET) with fluorine-18 fluorodeoxyglucose ([18F]FDG) after first-line chemotherapy in non-Hodgkin’s lymphoma: Is [18F]FDG-PET a valid alternative to conventional diagnostic methods? J Clin Oncol 19: 414-419, 2001
4) Micallef IN et al: Epratuzumab with rituximab, cyclophosphamide, doxorubicin, vincristine, and prednisone chemotherapy in patients with previously untreated diffuse large B-cell lymphoma. Blood 118: 4053-4061, 2011
5) Pregno P et al: Interim 18-FDG-PET/CT failed to predict the outcome in diffuse large B-cell lymphoma patients treated at the diagnosis with rituximab-CHOP. Blood 119: 2066-2073, 2012
6) Trotman J et al: Positron emission tomography-computed tomography (PET-CT) after induction therapy is highly predictive of patient outcome in follicular lymphoma: analysis of PET-CT in a subset of PRIMA trial participants. J Clin Oncol 29: 3194-3200, 2011
7) Dupuis J et al: Impact of [18F]fluorodeoxyglucose positron emission tomography response evaluation in patients with high-tumor burden follicular lymphoma treated with immunochemotherapy: a prospective study from the Groupe d’Etudes des Lymphomes de l’Adulte and GOELAMS. J Clin Oncol 30: 4317-4322, 2012
8) Meignan M et al: Report on the first international workshop on interim-PET-scan in lymphoma. Leuk Lymphoma 50: 1257-1260, 2009

9) Mamot C et al: Final results of a prospective evaluation of the predictive value of interim positron emission tomography in patients with diffuse large B-cell lymphoma treated with R-CHOP-14 (SAKK 38/07). J Clin Oncol 33: 2523-2529, 2015
10) Martelli M et al: [18F]fluorodeoxyglucose positron emission tomography predicts survival after chemoimmunotherapy for primary mediastinal large B-cell lymphoma: results of the International Extranodal Lymphoma Study Group IELSG-26 study. J Clin Oncol 32: 1769-1775, 2014
11) Biggi A et al: International validation study for interim PET in ABVD-treated, advanced-stage Hodgkin lymphoma: interpretation criteria and concordance rate among reviewers. J Nucl Med 54: 683-690, 2013
12) Cheson BD et al: Refinement of the Lugano classification lymphoma response criteria in the era of immunomodulatory therapy. Blood 128: 2489-2496, 2016
13) Gallamini A et al: Early interim 2-[18F]fluoro-2-deoxy-D-glucose positron emission tomography is prognostically superior to international prognostic score in advanced-stage Hodgkin's lymphoma: a report from a joint Italian-Danish study. J Clin Oncol 25: 3746-3752, 2007

CQ 23 Is the addition of FDG-PET/CT or PET recommended to evaluate the activity of multiple myeloma (MM) after treatment?

Recommendation

The addition of FDG-PET/CT or PET is weakly recommended to evaluate the activity of MM after treatment.

Recommendation strength: 2, strength of evidence: weak (C), agreement rate: 100% (8/8)

Background

In MM, the presence or absence and number of lesions seen on MRI are prognostic factors. Consequently, whole-body or total spinal/pelvic MRI has become the gold standard for the imaging evaluation of MM. Several studies that compared performance in detecting bone lesions in newly diagnosed MM (NDMM) showed the detection performance of MRI to be superior to that of modalities such as whole-body CT, plain radiography, bone scintigraphy, and FDG-PET/CT.[1)] In previously treated MM (PTMM), FDG-PET/CT has been found to be useful for predicting prognosis,[2)] evaluating minimal residual disease (MRD), and evaluating extraosseous lesions.[3)] However, few controlled studies have examined whether the addition of FDG-PET/CT or PET to MRI, the usual test, is effective in PTMM. Consequently, although MRI is generally used for the follow-up of PTMM in Japan, there is insufficient evidence that it improves the patients' prognosis and quality of life (QOL).

Explanation

A literature search was conducted for this CQ and, after the primary and secondary screenings, a qualitative systematic review of 5 cohort study articles[3-8)] and 1 case series study article[9)] was performed. An active lesion detection index was calculated as the diagnostic odds ratio (DOR) when MRI alone was used to evaluate active lesions in PTMM and when FDG-PET/CT or PET was added. The pooled value was 5.98 (95% CI, 2.99 to 12.0; $p < 0.001$), indicating that the DOR was significantly higher with the addition of FDG-PET/CT or PET and that the addition is useful for evaluating active MM lesions after treatment.[10)]

Points common to each of the reports were that pretreatment abnormal signals were prolonged, and that there was an overwhelmingly high number of false positives in MRI. Evaluating metabolic changes with FDG-PET/CT or PET enabled treatment efficacy and recurrent lesions to be evaluated more accurately. However, because FDG-PET/CT and PET involve radiation exposure, although at low levels, they cannot be performed for every evaluation in all patients with PTMM. No reports examining the risks and benefits of such evaluations were found in the searched literature, and this remains a topic to be addressed in the future.

Although MRI is used to evaluate PTMM bone lesions in Japan, the background described above indicates that the addition of FDG-PET/CT or PET enables treatment efficacy and recurrence to be assessed more accurately. Consequently, their use can be considered.

Search keywords and secondary sources used as references

PubMed was searched using the following keywords: multiple myeloma, previously treated multiple myeloma, FDG PET, and MRI.

In addition, the following were referenced as secondary sources.

1) Durie BG et al: International uniform response criteria for multiple myeloma. Leukemia 20(12): 2220, 2006
2) Rajkumar SV et al: International Myeloma Working Group updated criteria for the diagnosis of multiple myeloma,. Lancet Oncol 15(12): e538-e548, 2014
3) Hillengass J et al: International Myeloma Working Group consensus recommendations on imaging in monoclonal plasma cell disorders. Lancet Oncol 20(6): e302-e312, 2019
4) The National Institute for Health and Care Excellence Myeloma: diagnosis and management, 2016

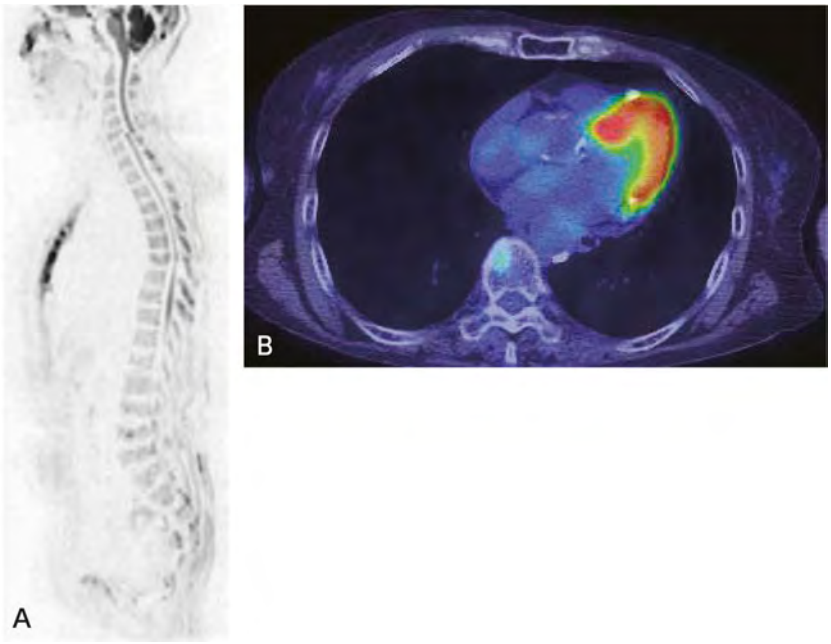

Figure. Evaluation of MM activity after treatment with FDG-PET/CT

The patient was a woman in her 60s. She had previously been treated for secretory multiple myeloma. A detailed examination was performed due to an elevated level of M protein in the blood.
A: FDG-PET/CT: There are no abnormal findings, and no abnormal signal is seen in the bone marrow of the vertebral bodies.
B: FDG-PET/CT fusion image: Abnormal uptake is seen in the 9th thoracic vertebra, indicating a recurrent lesion.

References

1) Fonti R et al: ^{18}F-FDG PET/CT, ^{99m}Tc-MIBI, and MRI in evaluation of patients with multiple myeloma. J Nucl Med 49(2): 195-200, 2008
2) Bartel TB et al: F18-fluorodeoxyglucose positron emission tomography in the context of other imaging techniques and prognostic factors in multiple myeloma. Blood 114(10): 2068-2076, 2009
3) Lu YY et al: FDG PET or PET/CT for detecting intramedullary and extramedullary lesions in multiple myeloma: a systematic review and meta-analysis. Clin Nucl Med 37(9): 833-837, 2012
4) Cascini GL et al: Whole-body MRI and PET/CT in multiple myeloma patients during staging and after treatment: personal experience in a longitudinal study. Radiol Med 118(6): 930-948, 2013
5) Derlin T et al: Comparative diagnostic performance of ^{18}F-FDG PET/CT versus whole-body MRI for determination of remission status in multiple myeloma after stem cell transplantation. Eur Radiol 23(2): 570-578, 2013
6) Zamagni E et al: A prospective comparison of ^{18}F-fluorodeoxyglucose positron emission tomography-computed tomography, magnetic resonance imaging and whole-body planar radiographs in the assessment of bone disease in newly diagnosed multiple myeloma. Haematologica 92(1): 50-55, 2007
7) Basha MAA et al: Diagnostic performance of ^{18}F-FDG PET/CT and whole-body MRI before and early after treatment of multiple myeloma: a prospective comparative study. Jpn J Radiol 36(6): 382-393, 2018
8) Moreau P et al: Prospective evaluation of magnetic resonance imaging and [^{18}F]fluorodeoxyglucose positron emission tomography-computed tomography at diagnosis and before maintenance therapy in symptomaticp patients with multiple myeloma included in the IFM/DFCI 2009 trial: results of the IMAJEM study, J Clin Oncol 35(25): 2911-2918, 2017
9) Spinnato P et al: Contrast enhanced MRI and ^{18}F-FDG PET-CT in the assessment of multiple myeloma: a comparison of results in different phases of the disease. Eur J Radiol 81(12): 4013-4018, 2012
10) Yokoyama K et al: Comparison of MRI and FDG-PET/CT for treatment response assessment in multiple myeloma: a meta-analysis (in press)

Index

Brenner tumor
bronchial asthma
bronchial atresia
bronchiectasis
bronchiolitis obliterans syndrome
bronchogenic cyst
Buerger's disease

C

callosal dysgenesis
cardiac amyloidosis
cardiac sarcoidosis
cardiomyopathy
Caroli's disease
cat-scratch disease
cavernous angioma
cellular leiomyoma
central nervous system infection
cerebral amyloid angiopathy
cerebral aneurysm
cerebral contusion
cerebral infarction
cerebral ventriculomegaly
cerebrospinal fluid leak
cervical cancer
cervical spondylotic myelopathy
Chlamydophila pneumoniae pneumonia
cholangiocellular carcinoma
cholangitis
cholecystitis
cholecystolithiasis
choledochal cyst
choledocholithiasis
cholesteatoma
cholesterol embolism
chromophobe renal cell carcinoma
chronic cholecystitis
chronic coronary artery disease
chronic headache
chronic heart failure
chronic hepatitis
chronic hepatitis B
chronic hepatitis C
chronic interstitial pneumonia
chronic kidney disease (CKD)
chronic liver disease
chronic lower abdominal pain
chronic lymphocytic leukemia
chronic nephropathy
chronic obstructive pulmonary disease (COPD)
chronic otitis media
chronic pancreatitis
chronic pulmonary thromboembolism
chronic sinusitis
chronic subdural hematoma
chronic thromboembolic pulmonary hypertension
chylous ascites
classical hepatocellular carcinoma
clear cell carcinoma
clear cell carcinoma
clear cell renal cell carcinoma
cloacal malformation
cluster headache
cognitive dysfunction
collagen disease
collagen vascular disease
collateral ligament injury
colonic diverticulitis
colonic diverticulosis
colorectal cancer
colorectal malignant tumor
community-acquired pneumonia
complex febrile seizure
complication of central venous puncture
compression fracture
conductive hearing loss
congenital adrenal hyperplasia
congenital diaphragmatic hernia
congenital hearing disorder
congenital heart disease
congenital hepatic cyst
congenital hydronephrosis
congenital lobar emphysema
congenital pulmonary airway malformation (CPAM)
conjoined twins
contrast-induced nephropathy (CIN)
convulsion
coronary artery aneurysm
coronary artery malformation
Coronavirus disease-19 (COVID-19)

D

E

F

G

gangrenous cholecystitis
gastric cancer
gastric-type endocervical adenocarcinoma
gastroenteropancreatic neuroendocrine neoplasm (NEN)
gastrointestinal perforation
gastroschisis
germ cell tumor
giant cell arteritis
giant cell tumor of bone
glenoid labrum tear
glioma
glomus tumor
glottic cancer
gnathoschisis
goiter

H

head and neck squamous cell carcinoma
heart valve disease
HELLP syndrome
hemangioma
hemorrhagic stroke
hemosiderosis
hepatic angiomyolipoma
hepatic hemangioma
hepatitis B
hepatitis C
hepatocellular adenoma (HCA)
hereditary breast and ovarian cancer syndrome
herpes simplex encephalitis
high-grade serous carcinoma
hilar cholangiocarcinoma
hippocampal (amygdaloid) sclerosis
Hodgkin's lymphoma
holoprosencephaly
hydranencephaly
hydrops fetalis
hyperbilirubinemia
hypersensitivity pneumonia
hypersensitivity pneumonitis
hypertensive cardiac hypertrophy
hypertensive heart
hypertensive heart disease
hypertrophic cardiomyopathy
hypervascular hepatocellular carcinoma
hypopharyngeal cancer
hypovascular hepatocellular carcinoma
hypovascular well-differentiated hepatocellular carcinoma

I

idiopathic interstitial pneumonia
idiopathic osteonecrosis of the femoral head
idiopathic pulmonary fibrosis (IPF)
IgG4-related disease
IgG4-related sclerosing cholangitis
ileus
impending rupture of aortic aneurysm
increased intracranial pressure
infected aneurysm
infected walled-off necrosis
inflammatory abdominal aortic aneurysm
inflammatory aortic aneurysm
inflammatory bowel disease
influenza virus pneumonia
inner ear disorder
intermediate-grade lymphoma
interstitial edematous pancreatitis
interstitial pneumonia
intervertebral disc herniation
intestinal atresia
intestinal intramural hematoma
intestinal obstruction
intestinal obstruction
intestinal perforation
intestinal tract malformation
intracerebral hemorrhage
intracranial hemorrhage
intracranial mass
intracranial neoplasm
intraductal papillary mucinous neoplasm (IPMN)
Intraductal papillary neoplasm of the bile duct (IPNB)
intrahepatic bile duct stone
intrahepatic cholangiocarcinoma
intrahepatic cholangiocellular carcinoma
intraorbital foreign body
intravenous tumor thrombus
intraventricular hemorrhage
intussusception

J

K

L

M

mycosis
mycosis fungoides
mycotic infection
myelomeningocele
myocardial damage
myocardial infarction
myocardial ischemia
myocarditis
myositis ossificans
myxofibrosarcoma

N

nabothian cyst
nasopharyngeal cancer
nasopharyngeal tumor
neonatal hypothyroidism
nephrogenic systemic fibrosis (NSF)
nephropathy
neural tube defect
neuroblastoma
Neuroendocrine carcinoma (NEC)
Neuroendocrine tumor (NET)
neurofibroma
Neuromyelitis optica (NMO)
nodal marginal zone lymphoma
non-fibrotic (subacute) hypersensitivity pneumonitis
nonhemorrhagic stroke
non-Hodgkin's lymphoma
noninvasive thymoma
non-small cell lung cancer
nonspecific interstitial pneumonia (NSIP)
non-traumatic acute headache
non-traumatic subarachnoid hemorrhage
non-vascular intracranial disorder

O

obliterative phlebitis
obstructive jaundice
obstructive pancreatitis
obstructive pulmonary disease
obstructive respiratory disorder
odontogenic maxillary sinusitis
odontoid fracture
old lacunar infarct
oligohydramnios
oncocytoma
optic neuritis
oral cavity cancer
orbital cellulitis
organizing pneumonia (OP)
oropharyngeal cancer
ossification of posterior longitudinal ligament
osteoarthritis
osteoblastic bone metastasis
osteoblastic metastasis
osteochondritis dissecans
osteogenesis imperfecta
osteomyelitis
osteosarcoma
ovarian cancer
ovarian clear cell carcinoma
ovarian cyst
ovarian endometriosis
ovarian endometriotic cyst
ovarian tumor

P

painful hematuria
painless hematuria
Pancoast tumor
pancreas divisum
pancreatic body cancer
pancreatic cancer
pancreatic ductal carcinoma
pancreatic head cancer
pancreatic neuroendocrine tumor (P-NET)
pancreatic pseudocyst
pancreatic tail cancer
pancreatitis
panperitonitis
papillary renal cell carcinoma
papilloma
paraganglioma
Parkinson's disease
parotid mass
parotid tumor
partial small bowel obstruction
pediatric cancer
perforated appendicitis
pericardial effusion
peripheral intrahepatic cholangiocarcinoma

peritoneal endometriosis
peritonitis
Perthes' disease
pharyngeal cancer
pheochromocytoma
physiological hydronephrosis
pigmented villonodular synovitis
pituitary adenoma
placenta accreta spectrum
placenta percreta
placental abruption
placental tumor
pleomorphic adenoma
pleural mesothelioma
pneumobilia
pneumococcal pneumonia
pneumoconiosis
polymyositis (PM)
posterior cruciate ligament injury
posterior fossa malformation
posterior mediastinal tumor
postobstructive pneumonia
postoperative rotator cuff tear
primary amenorrhea
primary headache
primary intraaxial brain tumor
primary lung cancer
primary sclerosing cholangitis
primary Sjögren's syndrome (pSjS)
progressive benign pleural disease
prostate cancer
pseudoaneurysm
pulmonary apical tumor
pulmonary edema
pulmonary embolism
pulmonary fibrosis
pulmonary hypoplasia
pulmonary metastasis
pulmonary sequestration
pulmonary thromboembolism
pyelonephritis

Q

Q fever

R

radiological and medical service
rectal cancer
renal cancer
renal cell carcinoma (RCC)
renal dysfunction
renal malformation
renal pelvic cancer
renal scarring
renal tumor
renal angiomyolipoma (AML)
retinoblastoma
retropharyngeal abscess
reversible cerebral vasoconstriction syndrome (RCVS)
rheumatoid arthritis (RA)
rheumatoid skin rash
rib fracture
rickets
rotator cuff injury
rotator cuff tear

S

sacrococcygeal teratoma
salivary gland tumor
scaphoid fracture
schwannoma
secretory multiple myeloma
seminoma
sepsis
sex cord-stromal tumor
shoulder dislocation
sialoadenitis
silicosis
simple febrile seizure
sinonasal tumor
sinusitis
skull fracture
slipped femoral capital epiphysis
small cell lung carcinoma
small lymphocytic lymphoma
small round cell tumor
soft tissue neoplasm
soft tissue sarcoma
Solid pseudopapillary neoplasm (SPN)
spinal canal stenosis

spinal cord injury
spinal cord ischemia
spondylolisthesis
spondylolysis
steatohepatitis
strangulated intestinal obstruction
stroke
subarachnoid hemorrhage
subdural abscess
subdural empyema
subdural hematoma
subdural hematoma
submucosal leiomyoma
subscapularis tendon injury
subscapularis tendon rupture
subserosal leiomyoma
symptomatic cerebral hemorrhage
synovitis
syphilitic aortitis
systemic lupus erythematosus (SLE)
systemic sclerosis (SSc)

T

Takayasu's arteritis
temporal arteritis
temporal lobe epilepsy
tenosynovitis
tension headache
teratoma
testicular germ cell tumor
testicular infarction
testicular microlithiasis
testicular rupture
testicular torsion
testicular tumor
thecoma
thoracic aortic aneurysm
thoracic descendign aortic aneurysm
thoracoabdominal aortic aneurysm
thromboangiitis obliterans
throwing injury
thunderclap headache
thymic carcinoma
thymic epithelial tumor
thymic hyperplasia
thymoma
thyroid cancer
thyroid tumor
tongue cancer
transient ischemic attack
traumatic subarachnoid hemorrhage
triangular fibrocartilage complex (TFCC) injury
trigeminal autonomic cephalalgia
tuberculoma
tuberculosis
tuberculous meningitis
tuberculous pleuritis
tunnel cluster
twin-to-twin transfusion syndrome

U

ulcerative colitis
unilateral autonomic symptom
unstable angina
upper urinary tract infection
upper urinary tract tumor
ureteral calculus
ureteral cancer
ureteropelvic cancer
urinary calculus
urinary tract malformation
urothelial carcinoma
urothelial neoplasm
usual interstitial pneumonia (UIP)
uterine leiomyoma
uterine leiomyosarcoma
uterine malformation
uterine sarcoma
uteroplacental circulatory disturbance

V

vasa previa
vascular Behçet's disease
vascular dementia
vascular malformation
vasculitis
vasospastic angina
venous malformation
venous thromboembolism
venous thrombosis
vertebral body malformation

vesicoureteral reflux
viral pneumonia
volvulus

W

Warthin’s tumor
well-differentiated hepatocellular carcinoma
well-differentiated liposarcoma
well-differentiated thyroid carcinoma